Compare and contrast the Midwater and Otter Trawl of the Longfin smelt San Francisco Bay Study

Acuña, Shawn and Fullerton, Dave

Metropolitan Water District of Southern California

THE METROPOLITAN WATER DISTRICT OF SOUTHERN CALIFORNIA

Acknowledgements

- DFW: Randy Baxter, Mike Aiken, Pat Coulston, Carl Wilcox
- DWR: Ted Sommer, Louise Conrad, Paul Helliker
- PWA: Dave Fullerton, Terry Erlewine, Chuck Hanson
- UCD: Jim Hobbs
- UMES: Paulinus Chigbu
- ICF: Lenny Grimaldo
- USGS: Fred Feyrer, Jon Burau

San Francisco Bay Study

- Established in 1980
- Many sites and 7 regions:
  - South Bay, Central Bay, San Pablo Bay, Suisun Bay, West Delta, Sac River and SJ River
- Two trawls
  - Midwater Trawl
  - Otter Trawl
- Recent divergence

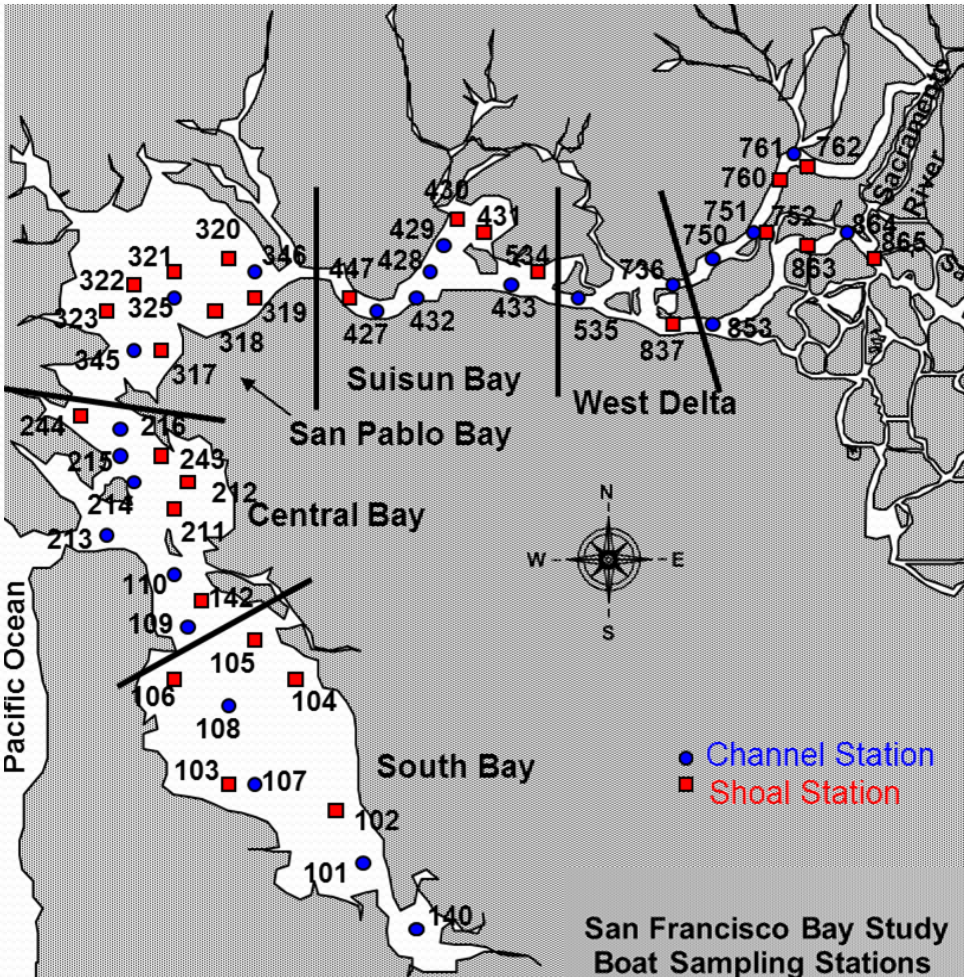

CPUE for Otter Trawl and Midwater Trawl

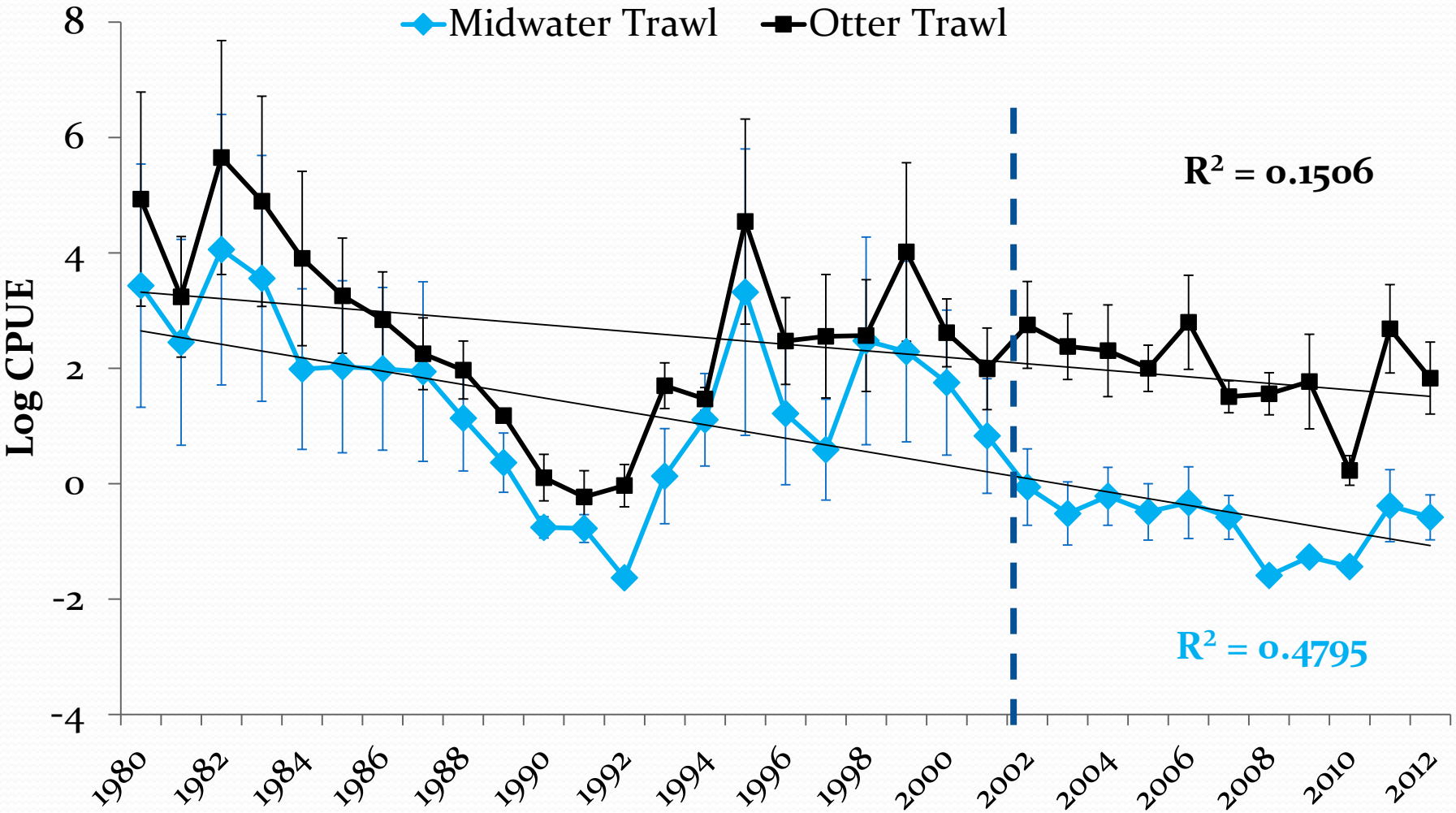

Probability of MW if caught in OT

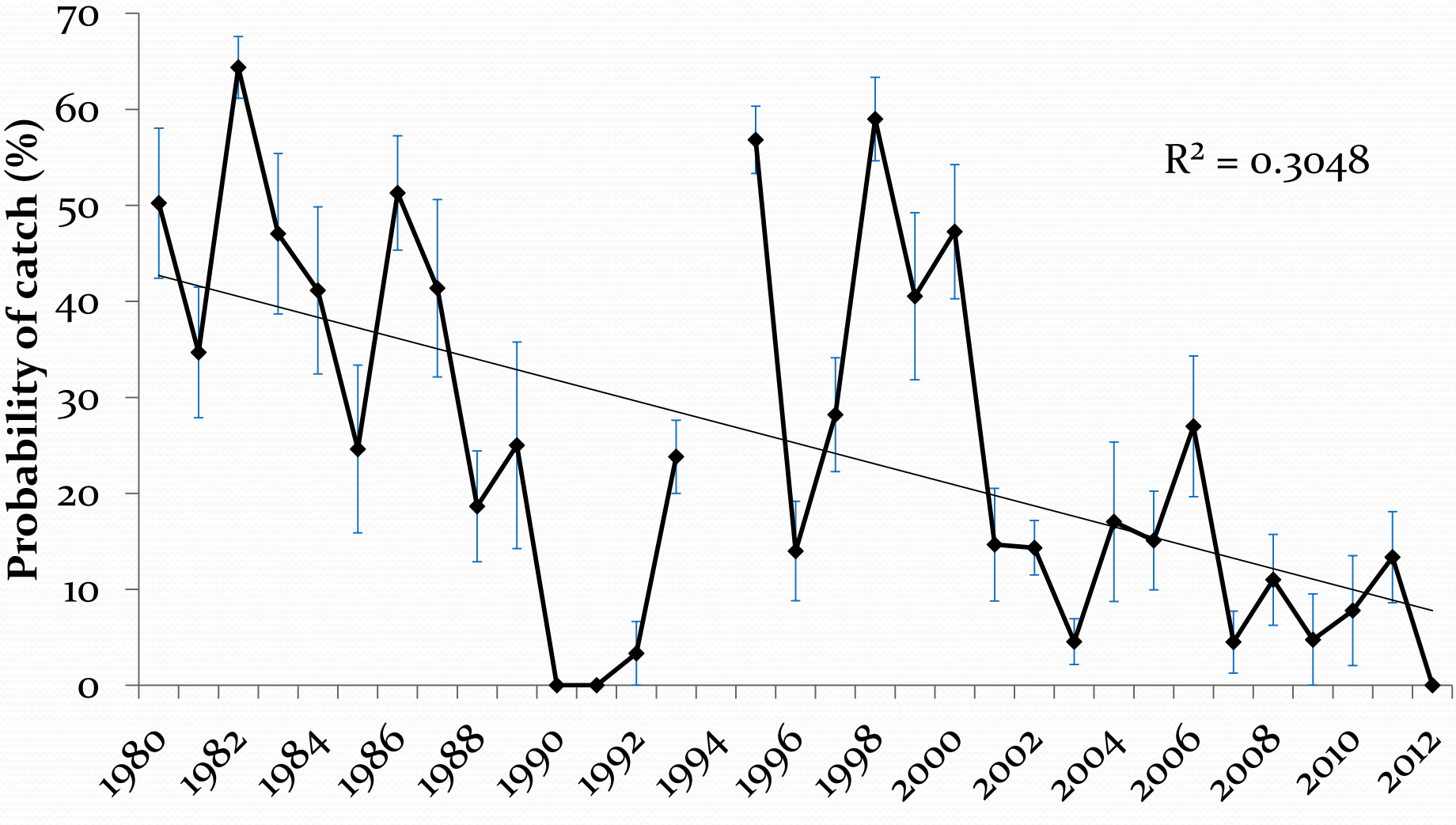

Presence/absence

- Set up presence/absence; presence =1, absence = 0
- Both trawls for age 0 fish
- 4 scenarios
  - M(0):O(1) -> Otter Trawl only
  - M(1):O(0) -> Midwater Trawl only
  - M(1):O(1) -> Both trawls
  - M(0):O(0) -> Neither trawl
- Examined different parameters: Secchi, salinity, depth, temperature

Secchi Depth and Water Depth

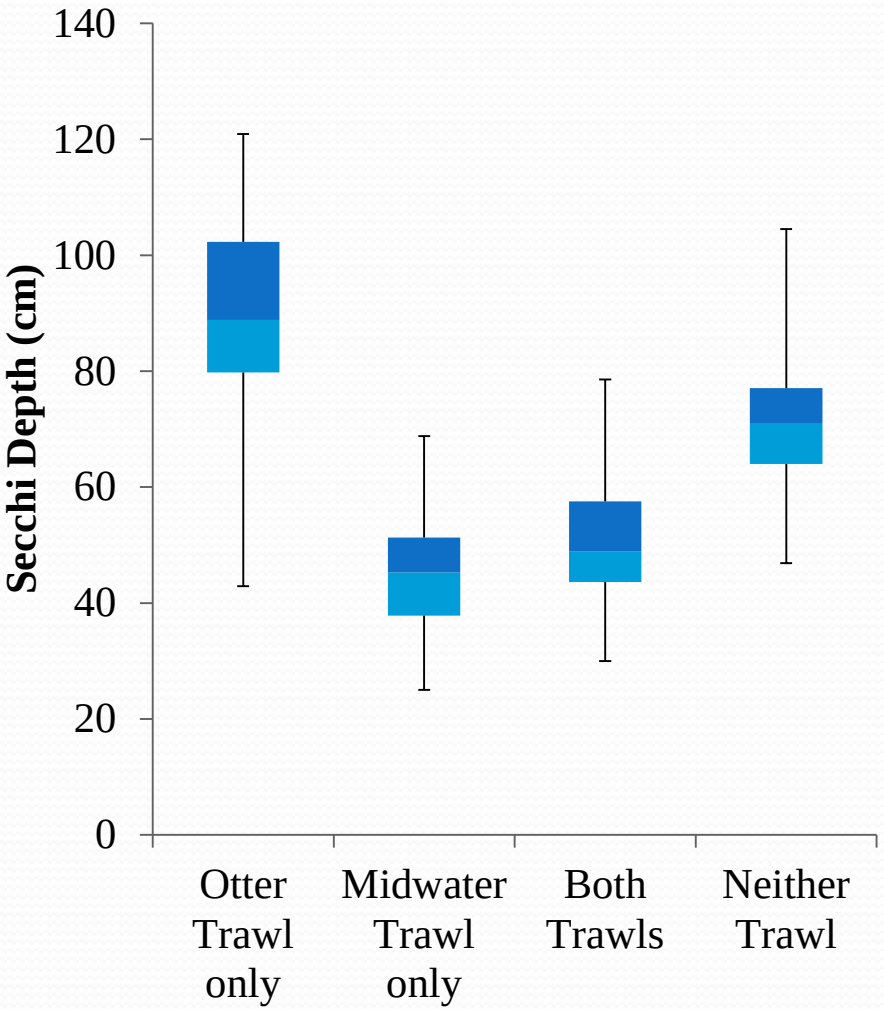

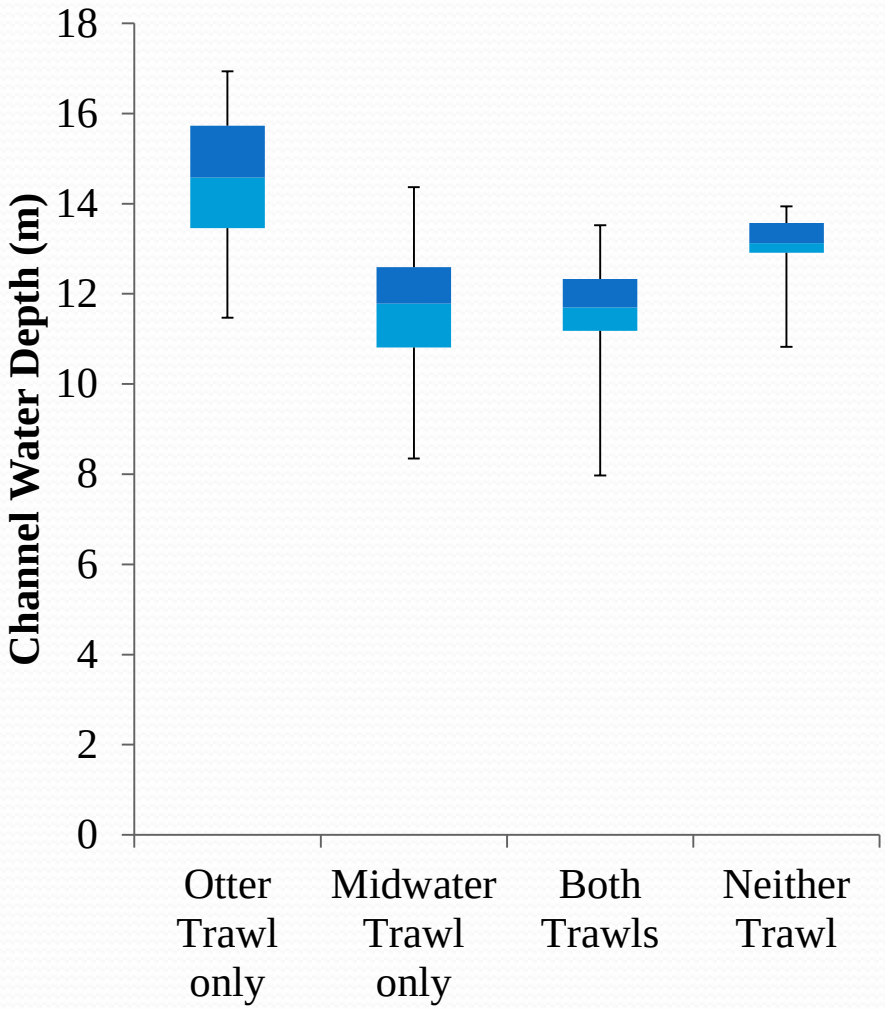

Does the vertical distribution and/or gear avoidance affect the Midwater Trawl/Otter Trawl catch frequency ratio?

Gear avoidance

- Secchi depth/MW
- Increases in Secchi depth
  - Increased water clarity
- Increase potential to detect MW Trawl
- Results in lower catch

Secchi Depth

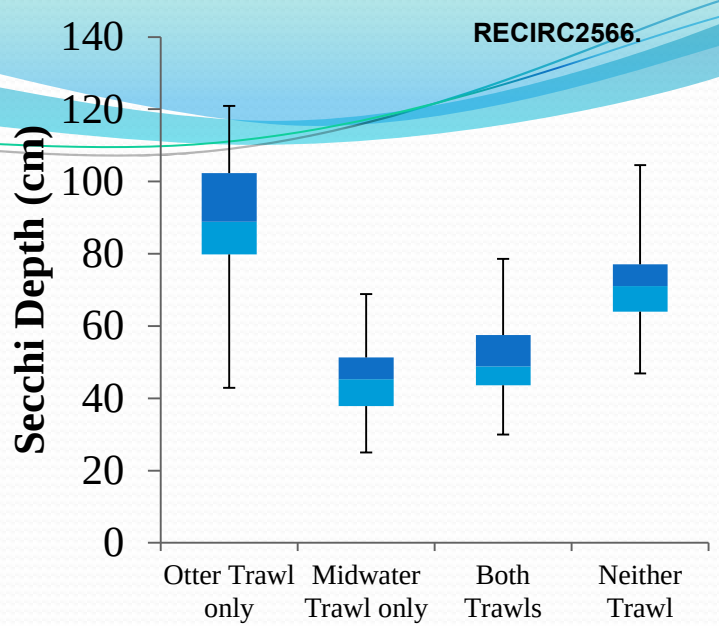

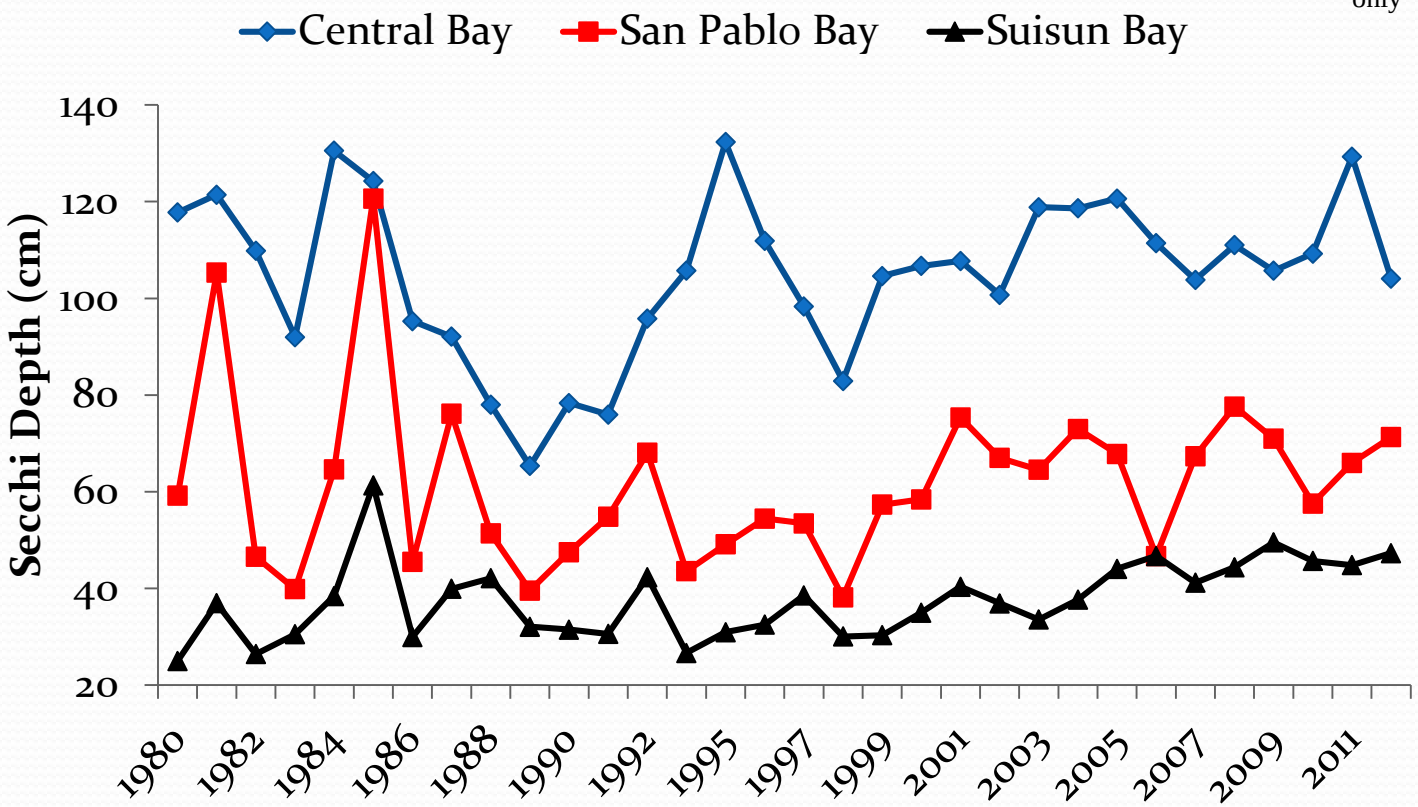

Vertical Distribution

- LFS stratification
- Time at depth
  - MW is a 12 minute trawl
  - Deeper station →less time at each depth stratum
- Depth Coverage
  - MW trawl covers ~11 m
  - Ave Channel Depth >11 m

Quinn et al 2012

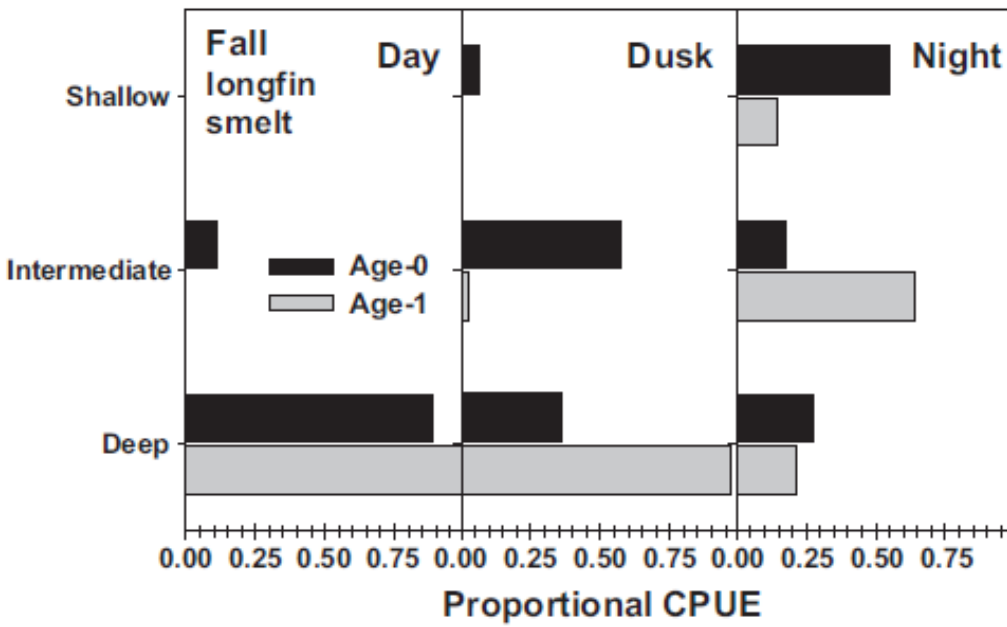

MW coverage

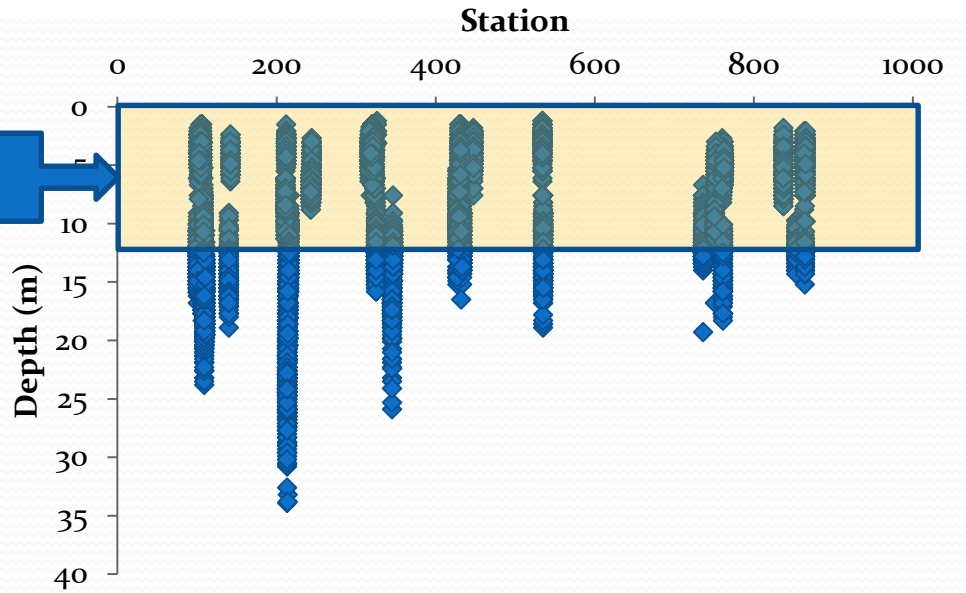

CPUE and Depth in the Channel sites

Midwater CPUE

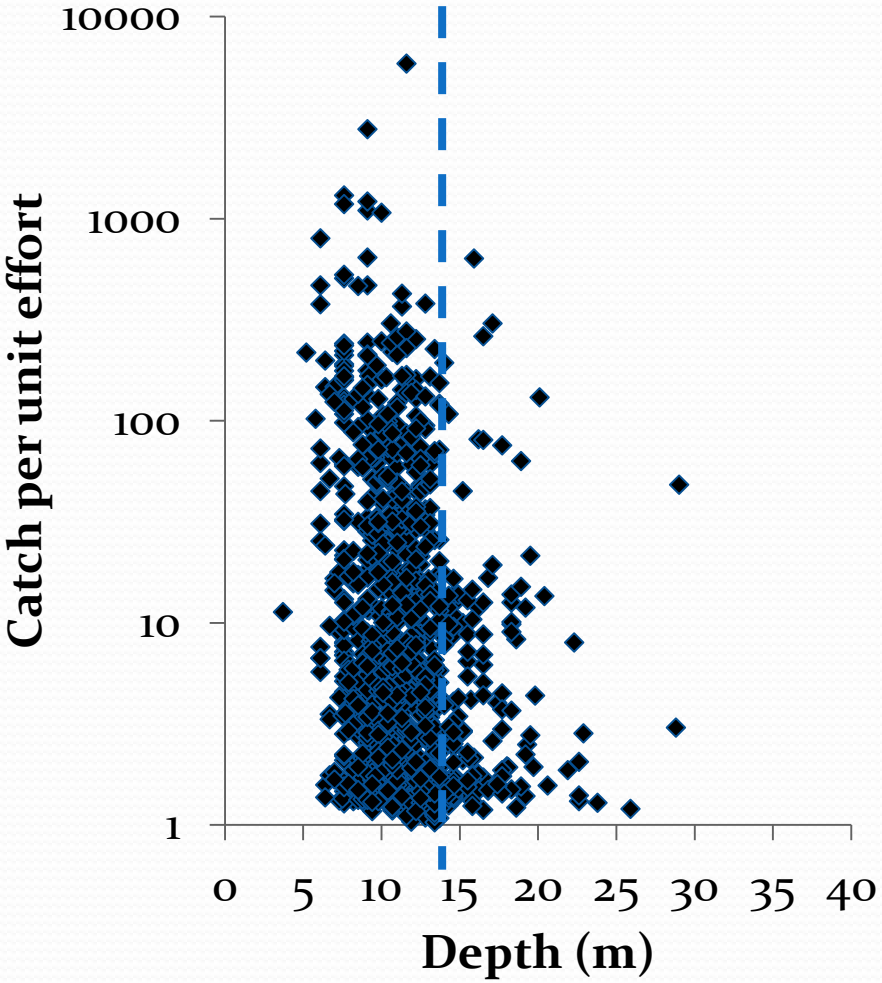

Otter trawl CPUE

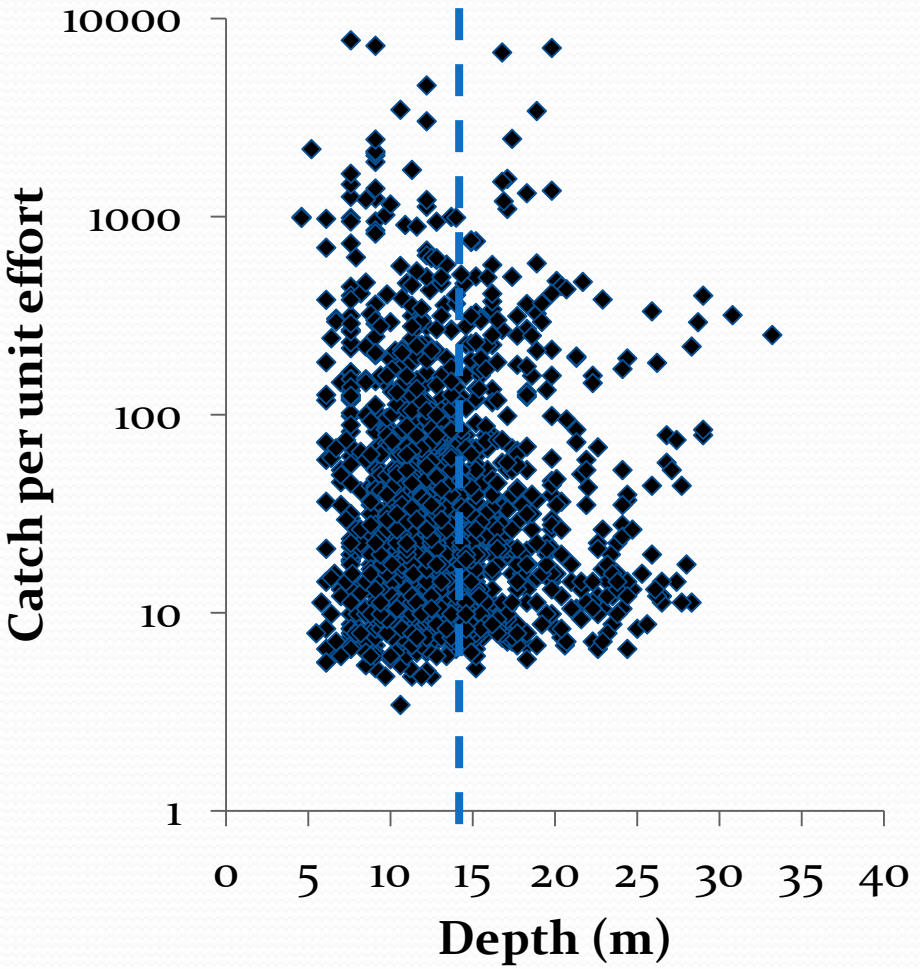

Depth from 1980-2012

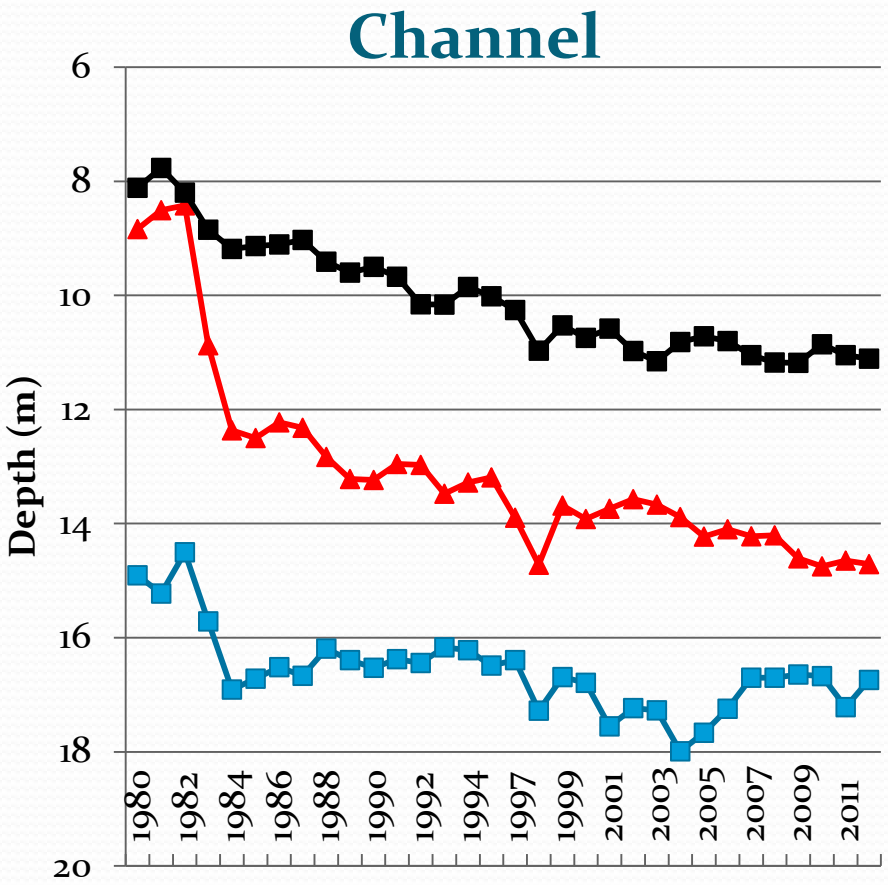

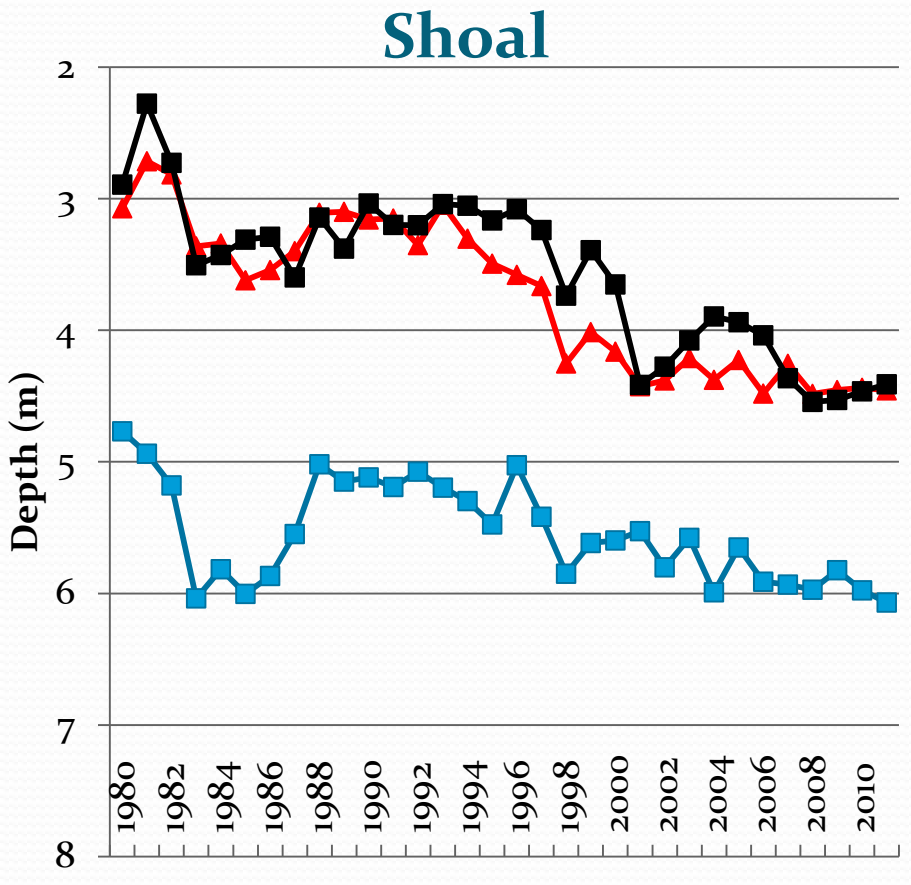

Central Bay San Pablo Bay Suisun Bay

Summary

- Divergence in the two trawls
  - CPUE
  - MW/OT, 'false' zeros
- Presence/absence analysis
  - Secchi Depth
  - Water Depth
- Conceptual model
  - Gear avoidance
  - Vertical distribution

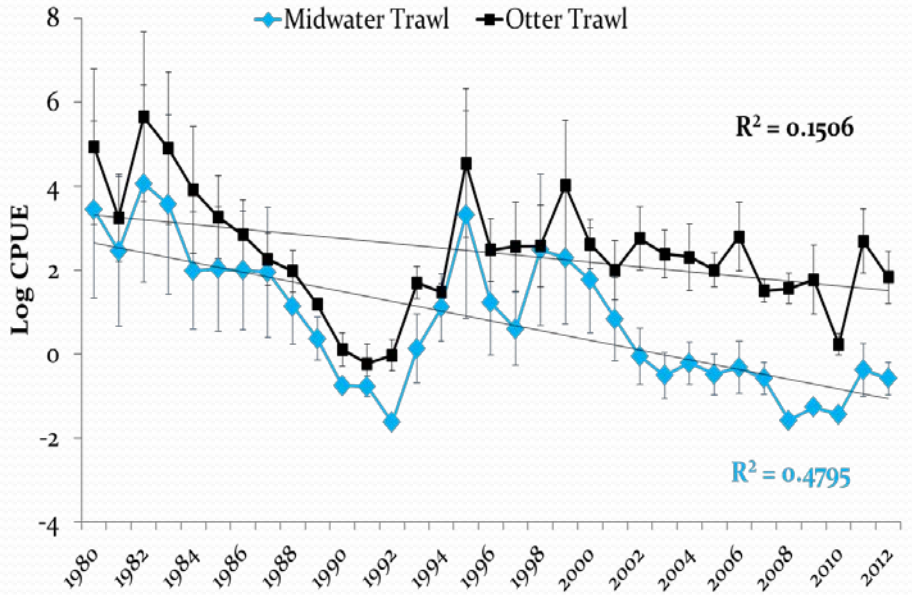

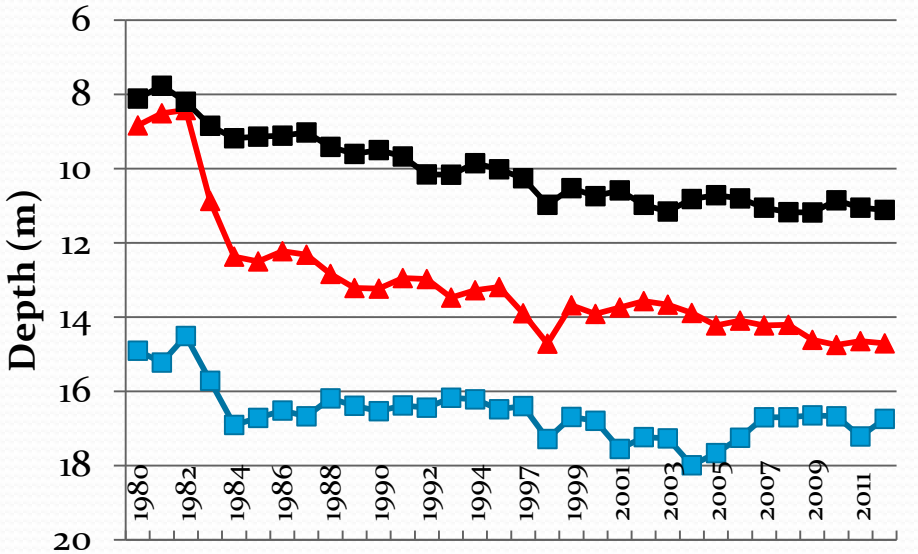

Future Studies

Vertical Distribution Habitat Study:

- Stratified depth trawling
- Smelt Cam
- Day/night trawl

Statistical analysis:

- GAM
- Occupancy model

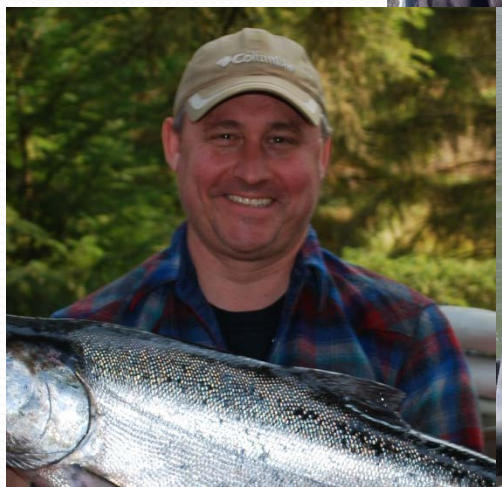


Thank you

Independent Review Panel (IRP) Report for the 2014 Long-term Operations Biological Opinions (LOBO) Annual Science Review

A report to the
Delta Science Program

Prepared by

Dr. James J. Anderson – University of Washington
Dr. James A. Gore (Panel Chair) – University of Tampa
Dr. Ronald T. Kneib (Lead Author) – RTK Consulting Services & University of Georgia (Senior Research Scientist Emeritus)
Dr. Nancy E. Monsen – Stanford University (Visiting Scholar, Department of Civil and Environmental Engineering, Environmental Fluid Mechanics Laboratory)
Dr. John M. Nestler – Fisheries and Environmental Services & USACE Engineer Research and Development Center (Retired)
Dr. John Van Sickle – U.S. Environmental Protection Agency, Western Ecology Division (Retired)

December 2014

Delta Stewardship Council
Delta Science Program

Scope and Intent of Review: This report presents findings and opinions of the Independent Review Panel (IRP) assembled by the Delta Science Program to inform the National Marine Fisheries Service (NMFS) and the U.S. Fish & Wildlife Service (USFWS) as to the efficacy of water operations and certain regulatory actions prescribed by their respective Long-term Operations Biological Opinions' (LOBO) Reasonable and Prudent Alternative Actions (RPAs) as applied from October 1, 2013 through September 30, 2014 (Water Year 2014).

This year's annual review focused primarily on: (1) implementation of NMFS's RPAs associated with modified Delta Cross Channel (DCC) Gate opening criteria in the Drought Operations Plan, (2) proposed modifications to the Juvenile Production Estimate (JPE) calculation and use/application of data from acoustically-tagged Chinook Salmon releases, (3) proposed calculations for Cumulative Salvage Index values used in estimating take of adult Delta Smelt under the USFWS Old and Middle River flow RPAs, and (4) general implementation of RPA actions under dry year conditions based on prior IRP concerns about RPA implementation under such conditions.

After reviewing a required set of written documents (Appendix 1), the IRP convened at a public workshop in Sacramento, CA on 6-7 November 2014. The first day of the 2-day workshop included agency presentations and provided a forum for the IRP to consider information on water operations, activities, and findings related to RPA Actions as implemented in the critically dry 2014 water year. On the second day, the IRP deliberated in a private session beginning at 8:00 a.m. in order to prepare and present their initial findings at the public workshop at 2:00 p.m., after which there was an opportunity for agency representatives, members of the public, and the IRP members to comment and otherwise exchange impressions and information. Subsequent IRP communication and deliberations were conducted via email and conference calls in the course of drafting this final report.

EXECUTIVE SUMMARY

The 2014 LOBO IRP recognizes that the critically dry 2014 water year (WY) compounded the usual challenges and constraints faced by all of the agencies charged with seeking to balance existing commitments and mandated coequal goals of (1) providing a reliable water supply for California, and (2) protecting, restoring and enhancing the Delta environment, associated Central Valley ecosystems and the threatened or endangered species dependent on those systems.

Concerns regarding the capacity to achieve specific RPA targets under dry conditions have been expressed in previous IRP reports (Anderson et al. 2010 to 2013), along with the prediction that some physical targets may not be routinely achievable. After five years of operating under the RPA actions, observations are now available for water years ranging from wet to critically dry. The 2014 WY extended a trend of beginning the WY with less reservoir storage than the previous year and ending with even lower levels of water reserves entering the subsequent WY. Even those with senior water rights recognized the need to voluntarily postpone or forego delivery of water allotments. Much of the shortfall in surface water availability may have been offset by increased pumping of groundwater resources. California has only recently passed legislation that recognizes the connection between above-ground and below-ground sources of water and the Department of Water Resources will begin prioritizing basins and monitoring groundwater beginning in 2015.

The first of four charges to the LOBO IRP in 2014 involved the operation of the Delta Cross Channel (DCC) gates to protect both water quality in the southern Delta and emigrating salmon smolts. The effectiveness of gate closures intended to deter entrainment of emigrating smolts into the interior Delta via the DCC cannot be assessed at this time because the passage of smolts is not routinely monitored in the DCC downstream of the gates. Even if there were adequate fish monitoring downstream of the DCC gates, smolts can be drawn into the interior Delta downriver at the junction with Georgiana Slough, where tidal effects can have a strong influence on hydrodynamics that may increase entrainment. A complex diurnal/tidal DCC gate operation plan, which was not used in WY 2014 but proposed for possible application in the near future, was based on observations of diel and tidally-influenced smolt migration behavior. The plan would result in short-term pulses of freshwater directed toward the interior and southern Delta. Currently, it was unclear if the addition of this level of complexity to DCC gate operations would achieve either greater protection for protected species or the expected benefits to water quality in the southern Delta. Nonetheless, this is an example of the

type of thinking that previous LOBO IRPs have encouraged. That is, to link fish behavior and survival to water operations and RPA Actions.

The Juvenile Production Estimate (JPE), which is used to set allowable take of winter-run Chinook Salmon smolts at the CVP/SWP pumping facilities, was another issue considered by the 2014 LOBO panel. A combination of extreme environmental conditions and a transitional approach to the estimation of juvenile survival from spawning grounds downriver to the Delta contributed additional uncertainty to the JPE in WY 2014. In the present report, the panel makes suggestions for reducing the substantial uncertainty in future estimates of JPE by applying a proportional hazards approach to statistically modeling survival rates as a function of environmental conditions, and considering using a form of “trickle releases” rather than batch releases of acoustically tagged winter-run Chinook Salmon as a means of improving the statistical modeling of smolt survival. The continued use of late fall-run Chinook Salmon as surrogates for winter-run Chinook in future acoustic tagging studies is discouraged. Not only are the late-fall run fish larger, but they exhibit a much shorter migration travel time than winter-run fish that may interrupt their migration in response to changes in flow and turbidity. The panel encourages further analysis of the effects of environmental condition on all early life stages of winter-run Chinook Salmon.

An interim approach to calculating the Cumulative Salvage Index (CSI) for use in the estimation of allowable incidental take of Delta Smelt at the State and federal pumping facilities was proposed as an alternative to the method currently used by the U.S. Fish & Wildlife Service. There is substantial uncertainty associated with both methods of calculating CSI and when this uncertainty is considered, values generated by each method are not statistically distinguishable. Consequently, the panel had no basis to recommend replacement of the current method with an interim approach. Both methods should soon be superseded by a Delta Smelt life history model that may lead to a more realistic estimate of the at-risk population size of Delta Smelt and improve the future calculation of allowable take for this species.

The 2014 WY was the third consecutive year of dry conditions and between April and mid-November 2014 water resources were managed under a collaborative State and federal Drought Operations Plan. California has experienced longer periods between wet years in the recent past (e.g., 2000-2004 and 1987-1992), and so it is prudent to recognize that real-time resource management must include the flexibility to adjust to a “new normal” set of expectations with the realization that there may be even more protracted periods of drought than expected from the historical climatic record.

The panel remained encouraged by signs of movement toward the application of research aimed at linking the survival and behavior of fishes to water operations, but clear, quantifiable associations between specific RPA actions and population-level responses in species targeted for protection remain elusive. The LOBO IRP continues to encourage the development of methods that will explicitly link the success or failure of achieving desired temperatures, flows, and other physical targets to the biological/ecological responses of the listed species. As the IRP has noted before, this is the only way that the intended goals (e.g., protection of listed species) of RPA Actions can be assessed in a scientific context.

Table of Contents

INTRODUCTION

Surface water resources of California's Central Valley flow through a highly-engineered storage/delivery system that has developed to meet the needs of farms, industry, and millions of people residing within municipal districts within this watershed. Added to the complex infrastructure and landscape alterations is an equally complex suite of rules governing the distribution of water, which affect flows and water quality of riverine and deltaic ecosystems associated with California's Central Valley. These and other anthropogenic alterations over time have been accompanied by substantive changes in aquatic flora and fauna, including a persistent decline in native fishes. Some of these species have been afforded protection under the Endangered Species Act (ESA) and government agencies have been charged with developing ways of protecting these populations from further jeopardy associated directly or indirectly with water operation projects in the region.

Drought conditions have persisted in the Central Valley for the past three years and water reserves have been steadily declining with each passing year, making the coequal goals increasingly difficult to achieve. Ground water resources have been seriously depleted because California has been relatively slow to formally recognize the connection between surface and ground water resources.

Water operations are currently conducted to meet the coequal goals of providing a reliable water supply to California and ecosystem restoration and enhancement, including the protection of endangered species. Ultimately, the ability to meet this mandate appears to rest largely on adjusting existing water operations in a region where precipitation is highly variable in both space and time. This constrains the options for meeting the aforementioned coequal goals largely to modifications in water operations that amount to serial adjustments in reservoir releases and export pumping from the system so as to avoid jeopardizing protected fish populations while continuing to ensure the availability of water for other human uses.

***Background on the LOBO RPA review process*:** NOAA's National Marine Fisheries Service (NMFS) and the U.S. Fish and Wildlife Service (USFWS) have each issued Biological Opinions on long-term operations of the Central Valley Project (CVP) and State Water Project (SWP, hereinafter CVP/SWP; Long-term Operations Biological Opinions) that include Reasonable and Prudent Alternatives (RPA) designed to alleviate jeopardy to listed species and adverse modification of critical habitat. NMFS' Opinion requires the U.S. Bureau of Reclamation (USBR) and NMFS to host a workshop no later than November 30 of each year to review the prior water year's operations and to determine whether any measures prescribed in the RPA should be altered in light of new information (NMFS' OCAP Opinion, section 11.2.1.2, starting on page 583).

Amendments to the RPA must be consistent with the underlying analysis and conclusions of the Biological Opinions and must not limit the effectiveness of the RPA in avoiding jeopardy to the ESA listed species or result in adverse modification of critical habitat.

The purpose of this annual review of the Long-term Operations Biological Opinions (LOBO) is to inform NMFS and USFWS as to the effectiveness of operations and regulatory actions prescribed by their respective RPAs in the 2014 Water Year, and to make recommendations/review proposals for changes to implementation of actions consistent with the purpose of the RPA.

Since the Long-term Operations Biological Opinions were issued, NMFS, USFWS, USBR, U.S. Geological Survey (USGS), California Department of Fish and Wildlife (CDFW) and the Department of Water Resources (DWR) have been performing scientific research and monitoring in concordance with the implementation of the RPAs. Technical teams and/or working groups, including the geographic divisions specified in the NMFS' Long-term Operations Biological Opinion, have summarized their data and results following implementation of the RPA Actions within technical reports. The data and summary of findings related to the implementation of the RPAs provide the context for scientific review regarding the effectiveness of the RPA Actions for minimizing the effects of water operations on ESA listed species and critical habitat related to the operations of the CVP/SWP. A subset of these technical reports, some of which included responses to IRP recommendations offered in previous years, was presented for consideration by the 2014 LOBO IRP (see Appendix 1).

General charge and scope for the 2014 LOBO IRP: Annual reviews prior to 2012 considered all of the RPA Actions but in subsequent years, the panel's charge has focused on a subset of the operations and RPAs.

This year's (2014) annual review included:

(1) Modified Delta Cross Channel Gate opening criteria as described in Attachment G of the Central Valley Project (CVP) and State Water Project (SWP) Drought Operations Plan and Operational Forecast, April 1, 2014 through November 15, 2014;

(2) Modifications to the winter-run Chinook Salmon Juvenile Production Estimate calculation and use/application of survival data from acoustically-tagged Chinook Salmon releases;

(3) A proposal for calculating Cumulative Salvage Index values used for estimating take likely to occur under the USFWS Old and Middle River flow RPA for adult Delta Smelt; and

(4) A general consideration of RPA actions under dry year conditions based on questions and concerns expressed in prior annual science reviews.

As in previous years, the specific scope of the 2014 LOBO review was defined by questions posed to the 2014 IRP by the agencies and technical teams/task groups that presented materials for review. This IRP report addresses each of the questions posed from a scientific perspective, and provides additional observations, opinions and recommendations where, in the panel's opinion, they seemed potentially useful to agency staff for consideration, especially in regard to near real-time decision making.

***Acknowledgments*:** The members of the IRP appreciate and acknowledge the efforts of the agency and technical team representatives and contractors who responded to questions and suggestions made by previous IRPs, prepared the written materials, and delivered the workshop presentations on which this report is based. Each year we are cognizant that much of the material has to be compiled, analyzed, and organized in a relatively short time. We also recognize that government agency personnel faced additional pressures resulting from a critically dry 2014 Water Year, continuing government budget uncertainties, and a partial federal government shutdown early in the water year. Despite the many competing demands on the workshop participants, the materials were presented professionally, concisely, and on schedule. The panel wishes to express a special thanks to Peter Goodwin (Lead Scientist) and the entire staff of the Delta Science Program for providing the organization and logistical support to facilitate our task. In particular, Lindsay Correa (Senior Environmental Scientist), as usual, expertly attended to a wide variety of technical and provisional details in support of the IRP's efforts before, during and following the workshop. Title page photo credit: http://jonjost.files.wordpress.com/2010/10/sacramento-delta-copy.jpg

LOBO IRP COMMENTS ON RPA ACTIONS IN WATER YEAR 2014

General comments and observations

The 2014 LOBO IRP was asked to read a number of technical team reports that described RPA actions that were not highlighted at the 2014 workshop in Sacramento. These reports contained team responses to previous (2012 LOO) panel comments, and the IRP was generally gratified to know that many of the concerns of previous panels were recognized and some were being addressed.

The agencies and technical teams appear to be gradually shifting their perspective from short-term reactionary (crisis management) to a more long-term anticipatory view. The relevance of several categories of forecasting analysis and models (from climate change to computational fluid dynamics modeling) are increasingly applied as important management tools in the region. Hopefully, this trend continues to help address the many emerging management challenges associated with the “new normal” condition of reduced water availability.

It was obvious that progress on some types of projects (e.g., gravel augmentations in Clear Creek, the Lower American River, and the Stanislaus River) is a source of pride in accomplishment for the technical teams. The IRP does not intend to diminish these valuable contributions to habitat improvement in any way. With that said, the IRP would be remiss if it did not point out that the ultimate success of such projects is inextricably tied to other aspects of the overall plan. For example, improvements in the structural value of spawning habitat (i.e., suitable gravel for redds) will have little realized benefit to salmonid populations if appropriate water temperatures and flows cannot be maintained within redds and juvenile rearing habitats to support improved survival of fry and smolts. The critically dry conditions in WY 2014 presented a real challenge in this regard and temperature and flow targets could not be met. Also, some projects affecting cold-water delivery capacity seem to be on long-term hold (e.g., Oak Bottom Temperature Control Curtain (OBTCC) at Whiskeytown Lake).

These delays clearly affect progress in other areas. For example, according to the Clear Creek Technical Team Report, the Spring Creek Temperature Control Curtain (SCTCC) was replaced but its effectiveness has not been tested because it was designed to operate in unison with the OBTCC and separate tests of effectiveness were deemed to have no useful purpose. So while claiming success toward meeting an RPA Action (i.e., replacement of the SCTCC), there is no basis on which to judge the effectiveness in terms of the intended purpose of the Action. Connecting the effects to the larger issue of maintaining temperature targets in Clear Creek to improve the survival of salmonid early life stages seems an even less attainable expectation. This harks back to the recommendations of previous panels which consistently encouraged progress toward demonstrable connections between biological responses of the protected species and the RPAs.

Modified Delta Cross Channel (DCC) Gate Opening Criteria per Attachment G in the Drought Operations Plan

RPA Actions IV.1.1 and IV.1.2 include modifications in the operation of the Delta Cross Channel Gate (DCC) to reduce the exposure risk of emigrating spring- and winter-run Chinook Salmon yearlings to mortality associated with water operations in the interior Delta. However, multi-year drought conditions prior to, and including, the critically dry 2014 WY resulted in a decision to modify RPA Actions involving the DCC to balance fish protection with the need for maintaining Delta water quality standards mandated by Water Right Decision 1641 (December 1999). Some modifications to the DCC operation were applied in the 2014 WY and others proposed for continued use during drought conditions in the future. These modifications involved a series of triggers based on combinations of water quality conditions within the Delta and the anticipated or actual presence of juvenile winter-run and spring-run Chinook as well as steelhead based on catch indices from the Knight's Landing rotary screw trap, Sacramento trawl, and beach seine collections, which are all located upstream of the DCC gates. Additional operational complexity using a diurnal schedule to open and close the DCC gates during ebb tides was proposed based on recent studies of diurnal/tidal movement patterns of young emigrating salmonids, but was not applied in WY 2014.

Whether or not relatively brief periods of DCC Gate openings under drought conditions would provide enough freshwater to have the desired effect on water quality in the interior Delta remains on open question. Also, the numbers of salmonids (or green sturgeon) that pass through the DCC or enter the interior Delta via Georgiana Slough are not directly monitored. Consequently, it remains unclear as to whether the modified DCC Gate operations will achieve the water quality and salmonid protection objectives intended.

Daytime, diurnal (ebb-only) operation of the DCC is a new criterion that was proposed for future operations under continued drought conditions, and it may be important to analyze the benefits of this modification. The rationale for the diurnal/tidal operation of the gates is based on three key field observations:

(1) Recent salmonid tagging studies (e.g., Chapman et al. 2013; Steel et al. 2013; and other references cited in Attachment G of the Revised DCC Gate Triggers Matrix for April 1 through November 15, 2014) have shown that most migrating smolts travel past the DCC Gate at night and have a positive response to high-velocity flows.

(2) Hydrodynamic field experiments (Burau 2014) have shown that the junction of the Sacramento River and the DCC is a confluence point during flood tides, directing all Sacramento source water around the junction into the DCC during flood tides.

(3) Field observations and numerical modeling studies (e.g., Monsen et al. 2007) confirm that electrical conductivity levels decrease at key stations in the central Delta when the DCC remains open continuously for multiple days.

The Delta Operations for Salmonids and Sturgeon Group (DOSS) made a reasonable argument for developing this operating criterion based on their current understanding of the science. However, other hydrodynamic factors, such as those supported by field observations in the Mokelumne system (Gleichauf et al. in press), may need to be considered. The net benefit of short-term diurnal/tidal gate openings may not be as significant as currently anticipated for the electrical conductivity criteria at interior Delta stations.

The intended benefit of opening the DCC gates is that freshwater from the Sacramento will be diverted into the Mokelumne system and travel through that system toward the San Joaquin and the interior Delta. It is assumed that this pulse of water will be capable of preventing additional saltwater intrusion on the San Joaquin stem of the Delta. This assumption is based on experience of pump operators and other studies that have shown that when the DCC remains opened for multiple days, better water quality in the central Delta is the end result.

When the DCC gate is continuously open, flow in the North Mokelumne is driven by the head difference between the Sacramento and San Joaquin rivers. Therefore, there is a net flow downstream through the Mokelumne system towards the interior Delta. This net flow when DCC remains open was observed by Gleichauf et al. (in press) during 2012 field experiments at the junction of Georgiana Slough and the Mokelumne.

When the DCC gate is closed, flow in the North Mokelumne is driven by the head difference between the east-side streams and the San Joaquin River. Because there is a very minimal flow in the east-side streams, the North Mokelumne River can experience tidal flows when the DCC is closed (Gleichauf et al. in press)

When the DCC gate is pulsed open and closed, the head diffference that will drive flow in the Mokelumne will alternate. When the gate is open, the head difference between the Sacramento and the San Joaquin will drive the flow. When the gate is closed, tidal conditions will likely occur in the Mokelumne. As a result the “freshette” that enters the Mokelumne through the DCC gates will likely tidally slosh and may disperse in the Mokelumne until the next freshette enters the next day when the DCC is re-opened. Therefore, the travel time of the Sacramento sourced water through the Mokelumne to the central Delta will be much longer than would would normally occur when the DCC

gate is continuously open. Depending on how long this operation is used, the benefit of reducing salinity in the central Delta may or may not be achieved.

At the LOBO Workshop on November 6, 2014 in Sacramento, Barbara Byrne presented a clear and detailed explanation of NMFS challenges to develop decision triggers to close the Delta Cross Channel in order to prevent the entrainment of juvenile salmonids into the southern Delta where smolts are subject to increased mortality risk during outmigration. Several potentially conflicting objectives and constraints on operation of the Delta Cross Channel (DCC) were recognized based on information provided to the IRP (i.e., Attachment G REVISED DCC GATE TRIGGERS MATRIX, as well as presentations and discussions at the LOBO 2014 workshop).

Freshwater flows diverted through the DCC are required to reduce salinity in the interior Delta, but flows are also needed to reduce salinity in the Sacramento River (presumably to move X2 westward toward the estuary). At the same time, there is a need to discourage the outmigration of salmonid smolts via the DCC to reduce entrainment into the interior Delta and associated mortality risk due to water operations.

In addition to the potentially conflicting needs associated with the volume and routing of freshwater flows, there are constraints on the operational flexibility of the DCC gates associated with public access and mechanical limitations. The boating public routinely uses the DCC to move between the Sacramento River and the interior and southern Delta. Under present operations, anticipated gate openings and closings are disseminated as a public service announcement. Short-term, unannounced gate operations may strand boaters on the wrong side of closed gates causing boater inconvenience and potential safety issues. Mechanical constraints permit the DCC gates to be operated in either fully closed or fully open positions, and there is some concern regarding the potential for mechanical failure of the gates if frequency of operation exceeds design parameters.

Biological triggers requiring gate closures focus on the portion of the system extending from Knights Landing to the DCC and currently do not consider the presence of emigrating salmonids downstream of the DCC. Sampling of smolts is restricted to stations upstream of the DCC in order to provide for an early warning trigger because average smolt travel time from Knights Landings to the DCC is approximately 2.5 days. However, sampling is not conducted at the entrance to the DCC or routinely downstream of the DCC gates. Consequently, it is difficult to determine the effectiveness of the DCC gate closures in protecting smolts from entrainment risks in the interior Delta.

There are several reasons that neither the Sacramento Trawl Catch Index (STCI) nor the Sacramento Beach Seine Index (SBCI) are useful in providing a high degree of protection for salmonids or other species of interest lingering near the DCC. For example, fish movement is typically episodic and appears to be associated with environmental cues such as flow, temperature, daylight duration, or tidal dynamics. Episodic events (e.g., many zeros or low numbers and occasional high numbers) are difficult to accurately sample with a regular, but infrequent sampling schedule relative to the time scale inherent to the episodic event. The frequency of sampling with beach seines and trawls is implied to be daily when the DCC gates are open. Unless these samples are timed to coincide with conditions that trigger fish movements, there is considerable risk of the datasets including false negatives that compromise the protection the catch indices were intended to provide.

Most of the catch indices' triggers are small in magnitude ranging from the capture of one to five fish and it is unclear how the catch relates to the number of fish actually present in the sampling area. Such small numbers complicate the challenge of accurately protecting emigrants by gate closures at the DCC.

It may be possible to operate the gates to better protect emigrating salmonid smolts if passage for boat traffic were not considered as a purpose equal in importance to emigrant protection. Perhaps other provisions for recreational boat passage could be integrated into the DCC facilities as they have been in other parts of the Delta (e.g., the small boat lock at the Suisun Marsh Salinity Control gates).

The IRP encourages efforts to increase operational flexibility of the DCC gates. However, operational changes within tidal and diel cycles will have impacts on fish and salinity distributions throughout the Delta, some of which may be unanticipated and perhaps even detrimental.

The addition of fish sampling stations downstream of the DCC gates would improve estimates of the efficacy of DCC gate operations for fish protection. Fish should be sampled south of the entrance to the DCC and within the channel to ensure that episodic events are not missed by the DCC gate closure triggers. In any case, the catch data will be difficult to interpret because of the complex movements of salmon over tidal and diel cycles. The IRP suggests that a first step in tracking the movements of fish in the vicinity of the DCC would be to expand the acoustic tag sampling with the goal of tracking fish movements between DCC and Georgianna Slough over the relevant temporal cycles.

Proposed Modifications to the Juvenile Production Estimate (JPE) Calculation and Use/Application of Data from Acoustically-Tagged Chinook Salmon Releases

The Juvenile Production Estimate (JPE) for winter-run Chinook Salmon (WRCS) is used to set the allowable take of WRCS at the CVP/SWP pumps during the juvenile migration. It is therefore estimated prior to the migration and is based on spawner carcass surveys and survivals of the juveniles over their life stages prior to entering the Delta where they are susceptible to entrainment in the pumps. The analysis presented below was extracted from the primary material in the Juvenile Production Estimates Calculation Report (JPECR 2014), the background material, and the presentations of Stuart and Oppenheim at the IPR 2014 workshop.

The approach to estimating JPE has not been consistent from year to year and is without an accurate benchmark of survival. The process seems largely based on the ever-changing “best judgment” of those serving collectively in the DOSS work group. The method of calculating the JPE was in transition in 2014 due to the first-time use of acoustic tagged WRCS to estimate survival. In addition, the migration occurred during the third year of an ongoing drought, which may have resulted in anomalous fish migration behavior and survival in the current WY. This new information and extreme conditions increased the uncertainty on the estimates of JPE and illustrated the need for a better understanding of how environmental conditions (e.g., flow, temperature, and turbidity) affect fish behavior and survival.

The methodology for estimating the JPE in the 2014 migration season began with a simple budget (spreadsheet) model based on carcass surveys in the upper Sacramento River to estimate total Adult Escapement (AE). This was expanded to the number of viable eggs per adult (E) and then adjusted downward by a prediction of the survival (S1) of fish to Red Bluff Diversion Dam (RBDD) and a prediction of survival (S2) from RBDD to a location defined as the top of the Delta. The formula is JPE = AE*E*S1*S2. The allowable take at the pumps was then set at x percent of the number of fish at the top of the Delta using the formula, Take = x*JPE/100, where x = 2% for wild WRCS.

The JPE uses predicted survivals S1 and S2 calculated from historical direct and surrogate measures. In the 2014 WY, S1 was calculated as the mean of the time series of the ratios of juveniles passing RBDD (the Juvenile Production Index, JPI) divided by the adult carcass survey adjusted for fecundity data and pre-spawning mortality. In past years, S2 was calculated by surrogate measures based on survival of late fall-run Chinook Salmon (LFCS). In 2014, S2 was replaced with survival estimated from a

weighted mixture of four years of acoustic tagged survival estimates from LFCS and one year estimated from acoustic tagged WRCS. The weighting was agreed upon in a working group and the total survival in the JPE was lowered 6% (0.078 to 0.073) compared to the method used in previous years.

The validity of the JPE was based on the assumption that the 2014 WY environment was similar to that of earlier dry years in which the LFCS studies were conducted. However, WY 2014 was an anomalous year. At the end of migration in 2014, the JPI data revealed a very low estimate of S1. Also, the weighted mixture of acoustic tagged LFCS and WRCS likely biased the estimate of S2. Both factors would result in a significantly overestimated JPE for 2014, as is illustrated in Table 1 below. Scenario 1 in Table 1 essentially recreates the information used in producing the JPE for 2014. Scenario 2 illustrates the JPE if only the WRCS survival were used to estimate S2. Scenario 3 uses the S1 calculated from the JPI for 2014 and S2 from Scenario 2. The table suggests that the JPE estimated for the 2014 drought year could have been overestimated by up to a factor of three. However, even at this level the actual take (338 WRCS) would be only 4% of the Annual Take Limit. Thus, even if the JPE were significantly overestimated in WY 2014, the run was not likely endangered by water export operations.

Table 1. Calculations of JPE using three scenarios. Numbers based on Attachment 1 of "Juvenile Production Estimate (JPE) Calculation and Use/Application of Survival Data from Acoustically-tagged Chinook Salmon Releases prepared for the 2014 Annual Science Panel Review Workshop".

	Scenario	Adult Escape (AE)	Viable egg per Adult (E)	Viable egg estimate	Survival to RBDD (S1)	Juveniles passing RBDD	Survival RBDD to Delta (S2)	Juveniles to Delta (JPE)	Annual Take Limit
1	NOAA method	5,958	2,755	16,411,348	0.27	4,431,064	0.27	1,196,387	23,928
2	Use WR S2	5,958	2,755	16,411,348	0.27	4,431,064	**0.16** [A]	708,970	14,179
3	Use JPI & WR S2	5,958	2,755	16,411,348	0.15 [C]	**2,485,787** [B]	**0.16**	397,726	7,955

A. WRCS acoustic tag estimated survival for 2013.
B. JPI for 2014 based on real-time rotary screw trap catch at RBDD.
C. Calculated S1 based on JPI and viable egg estimate.

Issues with S2: Survival from RBDD to Delta

There were several reasons that S2 determined using LFCS was likely biased high. First, LFCS smolts were 1.8 times the length of the WRCS smolts. Second, the LFCS smolts moved through the river below RBDD approximately a month sooner than the WRCS fish. Third, the WY 2014 flow was lower than flows in which the LFCS and WRCS survivals were measured. Conventional understanding suggests that all three factors (smolt size, travel time, and flow) would contribute to overestimates of JPE: big fish survive better than small fish, faster migration increases fish survival, and fish migrating in higher flows should survive better than fish migrating in lower flows. Thus, all factors suggest S2 was overestimated in 2014.

The panel found no compelling justification for including LFCS in estimates of S2 other than to maintain continuity with earlier tagging studies when LFCS were used as surrogates for estimating S2 in WRCS. However, it also seemed plausible that using S2 derived from WRCS studies conducted in low flow years would overestimate the JPE in high flows years. Several approaches aimed at adjusting S2 for flow year were discussed by the Winter-run Sub-team (Attachment 4 Winter-run Sub-team final call 12-19-13 in the JPE Calculation Report [JPECR] 2014) but the methods yielded unrealistically low estimates of S2. Given the limitations of data and theory, the panel outlines below two possible approaches and encourages the Winter-run Sub-team to include these among other future considerations.

Approach 1–Match flow method: In the next few years, when the JPE will be calculated with limited WRCS survival data, it is reasonable to use S2 estimates that best match S2 values associated with years having similar flow conditions.

Approach 2–Mechanistic method: As a companion to simply selecting results from similar water years, it may be possible to derive S2 based on mechanisms. The approach is based on the observation from the WRCS acoustic tag study in 2013 that smolts may interrupt their downstream migration in low flow conditions. Under this hypothesis juvenile migration survival will need to be described in two parts: an active migration part and a holdover part. For illustration, assume survival is distance dependent in active migration and time dependent in holdover behavior. Then survival is:

$$S2(X, T_{hold}) = S_{active}(X) S_{hold}\left(T_{hold}\right) = \exp\left(aX + bT_{hold}\right)$$

where X is distance traveled in active migration and T_{hold} is the duration of the holdover part of the migration. Note this equation is different from one in which prey actively migrate and predators may exhibit stationary and roaming foraging (Anderson et al. 2005).

The regression technique for estimating the coefficients in the above equation depends on the available data. The following method outlines a statistically rudimentary approach in which the active migration coefficient, a, is calculated by simply removing the holdover portion of the data and estimating the coefficient in the regression:

$$\log S_{active}\left(X\right) = a_0 + aX$$

where a_0 is a nuisance parameter. The coefficient for holdover part of the migration is estimated in a similar manner with:

$$\log S_{hold}\left(T_{hold}\right) = b_0 + bT_{hold}$$

The next step is to identify environmental conditions that induce fish holdover behavior. If the duration of holdover were a function of flow and otherwise fish move at a fixed velocity then the holdover behavior could be estimated with data on the total travel time of fish. The regression requires a functional form of the relationship between holdover duration and the controlling variables. Finding a suitable form of the relationship is problematic, but one possible approach begins with a graphical analysis plotting total travel time T_x over distance x, (e.g., RBDD to Interstate 80), against likely controlling variables (e.g., flow, turbidity, etc.) For example, assume holdover duration decreases exponentially with flow (F) such that fish exhibit diminishing holdover behavior as flow increases. Then the holdover duration might fit the equation:

$$T_{total} = T_{active} + T_{hold} = T_{active} + \alpha e^{\beta F}$$

where T_{total} and T_{active} are the durations of the total migration and the active portion of the migration. While in this example the flow vs. holdover relationship is determined separately from the survival elements, the two components could be determined with multiple linear or multiple nonlinear techniques if sufficient data were available.

Juvenile tagging to support the statistical modeling of survival S2

Acoustic tagging is a promising method for addressing a number of questions related to fish movement and behavior, but acoustic telemetry monitoring has a number of limitations, including technological issues with the reliability of detection under conditions of varying noise interference, water depth, turbulence, water quality, etc. (Donaldson et al. 2014). The application of acoustic tagging to estimate fish survival in variable environments is especially challenging, but improvements in modeling approaches are beginning to resolve some of the problems (e.g., Perry et al. 2010). The panel was not provided with much specific information on the potential contributions to uncertainty in estimates of juvenile salmonid survival that could be traced to technological or experimental design limitations of the acoustic tagging program, so those concerns are not explicitly considered in the following discussion.

There is very substantial uncertainty in JPE due to uncertainty in estimates of S1 and S2. This may motivate NMFS to increase their efforts to statistically model survival rates as a function of temperature, flow, and other factors. The approach is known as analysis of survival under proportional hazards. The analytical tools are available in the R statistical language or as standalone packages. For example, the SURPH model from the University of Washington (http://www.cbr.washington.edu/analysis/apps/surph/):

> **Survival Under Proportional Hazards**
>
> SURPH is an analytical tool for estimating survival using release-recapture data as a function of environmental and experimental effects. These effects may apply to a population (such as ambient temperature) or an individual (such as body length). SURPH provides flexible modeling capability for selecting the most parsimonious models, and diagnostic reports and graphs for analyzing data and selected models. Hypothesis testing can be done with Likelihood Ratio Test, AIC, or Analysis of Deviance.
> **Current Version:**
> SURPH 3.5.2

Discussion of the value of the proportional hazards approach

The standard approach for estimating survival is to release a large batch of tagged juveniles (either acoustic or coded-wire tags) upstream, and then record the proportion that are ultimately detected or recovered as they exit the Delta. If survival rate estimates are available from a large number of such batch releases, it is possible to statistically model the survival rate as a function of environmental covariates. An example is shown in Figure 7 of Cramer Fish Sciences (CFS) (2014).

However, it takes many batch-release experiments to accumulate enough data for such modeling. Tagged-fish releases could make much more efficient use of their data if individual tagged fish, rather than individual batches of fish, could supply independent replicates for modeling. The individual-fish approach to modeling is impractical for batch releases, however, because all tagged fish in the same batch will experience nearly identical environmental conditions (flow, temperature, etc.) during their passage to the Delta. This means that individual fish within one batch cannot be used as independent replicates.

Perhaps a more efficient tag-release strategy, for the purpose of statistical modeling of survival rates, would be to release tagged fish in a small, steady stream over time, instead of all together in a large batch. This “trickle-release” strategy would yield a broader representation of covariate values during a single migration season. It also would greatly increase sample sizes for modeling because individual fish, not batches, would serve as independent replicates. Because individual fish (i.e., tags) can be identified, one can statistically summarize the environmental conditions experienced by each fish that was eventually detected at Chipps Island, over the time period between its upstream release and its downstream detection. Tagged fish that were not detected downstream could be assumed, perhaps unrealistically, to have the same average transit time as the detected fish, so that one could also estimate the environmental factors experienced by individual non-detected fish. The detected (“present”) and non-detected (“absent”) individual fish could then serve as replicates in a binary logistic regression model that predicts the probability of presence (that is, the survival probability) for individual fish, as a function of their environmental covariates experienced during outmigration.

Note that the trickle-release strategy can also be used in the same way as a single batch release, namely to estimate a single, net survival proportion based on counting the “detects” and “non-detects” from many released fish. However, a trickle-release estimate based on N released fish should be more reliable than the estimate obtained by releasing those same N fish in a single batch. That is because the transit and survival “events” that comprise the trickle-release estimate are more spread out over time than they would be for a batch release, thus better representing the range of conditions experienced by all juveniles during the full season of outmigration.

The panel recognizes that logistical and practical factors, such as the availability of captured juveniles, would constrain any proposed trickle-release strategy. The JPE team may wish to consider ways of loosening these constraints and look into a trickle-release strategy in order to rapidly improve the statistical modeling of survival.

Issues with S1: Survival egg to RBDD

The first survival component of the JPE (i.e., the survival prior to reaching RBDD), S1, was found to be biased low for 2014. S1 was estimated at 0.27, but based on the JPI the survival was 0.16 (Table 1). This bias resulted in an overestimate of the JPE (compare Scenario 1 to 2 in Table 1).

In considering Egg to Fry Survival (Attachment 3 of JPECR 2014) the panel concluded that the ratio of the S1 calculated from the JPI ($S1_{JPI}$) and S1 used in the JPE ($S1_{JPE}$) was highly uncertain (Figure 1). Ideally, the ratio would be 1 and, because the ratio directly reflects bias in the JPE, the panel concludes that JPE, just from S1 alone, is highly uncertain. The panel also noted that the ratio in 2014 was 0.59, which was the third lowest of the record.

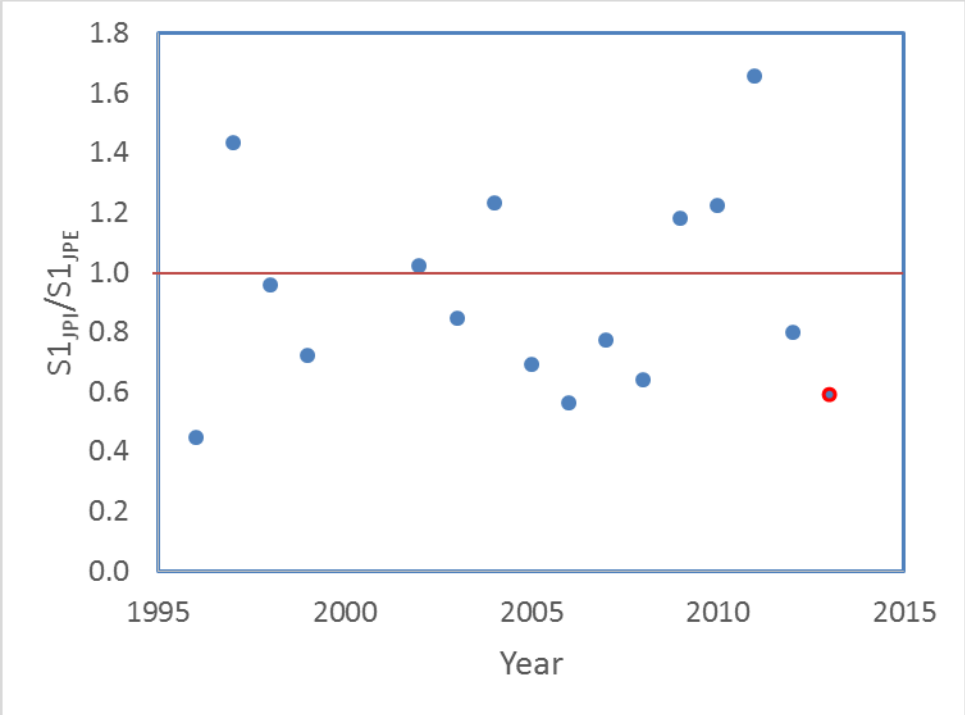

Figure 1. Ratio of S1 calculated from JPI to the corresponding value of S1 used in calculating the JPE. The ratio can be interpreted as a measure of the adjustment in JPE for errors in S1. The 2014 ratio (in red) indicates, that from errors in S1 alone, the JPE was 59% of the reported estimate. Data from Egg to Fry Survival in Attachment 3 of JPECR (2014).

Recommendations on JPE

The current overall conclusion on JPE is that the method of calculating JPE results in a highly uncertain value and has weak support in data and theory. Some of these problems can be resolved with future research, but the challenges in improving JPE estimates are considerable. Therefore, the panel suggests applying the precautionary principle when estimating the JPE until additional data is acquired on survivals of WRCS. To assist in developing an improved JPE the panel suggests the following incomplete list of actions:

1. Derive and report JPE by alternative methods (e.g., NOAA current model, the Cramer Fish Science Sacramento River Winter Chinook Salmon Juvenile Production Model (CFS 2014), and other methods as modified with suggestions for S1 and S2 estimations).

2. Make separate estimates, with confidence intervals, of S1, S2, and JPE from each method.

3. To develop better estimates of S1 (egg to RBDD) the panel suggests conducting retrospective analysis of models using the existing data (1996-2014) from the smolt carcass surveys, JPI, and environmental monitoring. The analysis could include both statistical (multinomial regressions) and mechanistic (e.g., CFS WRCS juvenile production model) approaches. The panel is not aware that either NOAA or CFS conducted a retrospective analysis of their methods using available data.

4. Commit resources to developing improved estimates of WRCS survival below RBDD (i.e., S2). The panel concluded that neither the data nor theory is sufficient to reliably estimate S2 survival at the present time. Approach 1 outlined above is likely to provide the most conservative estimated of S2. Additionally, the panel encourages estimating survivals using alternative methods such as outlined in Approach 2 above.

5. Explore the trickle release strategy combined with proportional hazards approach for estimating survivals and identifying the controlling environmental covariates.

Proposed Alternative Method to Calculate Cumulative Salvage Index Values Used for Estimating Take Likely to Occur Under the USFWS Old and Middle River Flow RPA for Adult Delta Smelt

Issues with the method used to determine incidental take of adult Delta Smelt have persisted for years. Most of the issues involve the accuracy of estimates of (1) Delta Smelt population sizes and (2) mortality associated with water operations. In this year's review, the IRP was asked to consider an alternative method of calculating a Cumulative Salvage Index (CSI) for Delta Smelt proposed by the Metropolitan Water District and to comment as to it whether it should be used to temporarily replace the method currently being applied by the USFWS. Even if there were a reasonable basis to consider one method of calculating CSI superior over the other, both are based on some measure of historical salvage, which has never been associated with any reliable estimate of Delta Smelt population size. If CSI is considered independent of population size, its application in the calculation of allowable incidental take must be dependent on a reliable estimate of population size, which has remained elusive. The lack of an accurate at-risk population estimate for Delta Smelt is a larger issue than the value of CSI in determining a reasonable level of incidental take, but the charge presented to the panel in 2014 was to consider alternative methods of calculating CSI.

The cumulative salvage index (CSI) for Delta Smelt in a historical water year *t* is the ratio between the cumulative salvage (CS) of smelt at the water-project pumping stations during December-March of that year, and the Fall Midwater Trawl Index ($FMWT_{t-1}$) from the previous year. The USFWS averaged the three CSI values for years 2006-2008 to determine the allowable incidental take (ITL) of smelt for the projects during any upcoming year. They set ITL equal to this average CSI (= 8.63) multiplied by the ($FMWT_{t-1}$) value for the upcoming year.

The "Proposed Alternative Method…" document (PAM) argues that the three years selected for averaging the CSI do not adequately represent years with high entrainment risk to smelt from first-flush events. The PAM argument appears to be that salvage during 2006-2008 did not capture the full CSI variability that could be expected due to non-anthropogenic factors (i.e., first flushes) that are beyond the control of flow management, where flow is measured by OMR.

The PAM suggests that a broader range of realistic CSI values can be obtained from a linear regression model that predicts CSI from two predictors: i) OMR flow, and ii) an inadequately-defined Secchi depth variable as a surrogate for turbidity, known to strongly influence smelt movement. The PAM describes how the regression model, which predicts log(CSI), was fitted to CSI, OMR, and Secchi data from n = 18 years

between 1993 and 2012 (1997-98 were omitted). The PAM then assumes scenarios of how the historical OMR flows for those 18 years would have been altered, if RPA controls on OMR had been implemented in some years. These altered flows are then inserted back into the model, along with the observed Secchi values from those years, to predict new CSI values that might have been observed historically, if the RPA controls on flow had been implemented (Figure 12, PAM).

The PAM interpretation of these predictions is very brief and unclear (Sec. 4, PAM). By implication, their point seems to be that, even if the RPA controls on OMR had been implemented during those 18 years, one would still have seen values of CSI that were much larger in many years than the 8.63 average from 2006-2008. Thus, the PAM believes that CSI = 8.63 defines an unrealistically low multiplier for estimating the expected smelt salvage, given the natural variation in factors other than OMR flow that determine smelt entrainment.

The final PAM document, as reviewed by the panel, stops short of stating exactly how their historical predictions from the CSI regression might be used to set an alternative, higher CSI threshold that would increase the ITL. However, that is clearly the purpose of PAM's regression model, as seen in an earlier draft of the PAM and in written responses to that draft from K. Newman and the NRDC, all of which were available to the panel.

In the Charge questions, the IRP was asked to evaluate the "scientific robustness" of the PAM's proposed regression model, its assumptions, and its predictions.

***Prediction uncertainty of the regression model*.**

The panel supports the basic concept behind the PAM effort, namely, to use modeling to extend the years of historical data that inform an ITL determination assuming, of course, that the current Delta Smelt population size is within the range of historical population sizes. The panel did not find the PAM's modeling method to be a sufficient advance over the current ITL-setting method to warrant a recommendation that USFWS switch to the PAM approach. The substantial statistical uncertainties surrounding both methods is sufficient justification for the reluctance to support a change in approach.

Although the PAM's regression model's fit was "very good" (p. 13, PAM) with $R^2 = 0.75$, individual predictions of CSI from the model are highly uncertain, due to the effects of back-transforming from the log(CSI) scale. This prediction uncertainty can be illustrated by first refitting the regression model (their Eq. 1), using the data in Table 1 of PAM, and then using the model to predict CSI for the 18 historical years of Tables 1 and 2 (PAM).

Like the PAM predictions in their Table 3, our predictions assumed the PAM Scenario 1 (Table 2) for altered OMR, and used historical observed Secchi values. However, we also computed 95% confidence intervals (CI's) on predicted CSI for each year (Neter et al. 1983). See Fig. 2 below.

The PAM argues that model predictions of CSI (red X's on the plot in Fig. 2) represent levels of CSI that one might expect to see in the future if RPA controls on flow are implemented. However, the CI's on these predictions are quite wide. In 16 of 18 years, the CIs cover the (2006-2008) mean value of 8.63, which is currently used by USFWS as the most likely future value of CSI under RPA controls on flow.

The mean value of 8.63 itself also has a wide CI [0, 25] based on being an average from CSI values from only three years. Note that the CI [0, 25] covers the regression model's point predictions in all but one historical year. In short, there is no significant difference between the mean value from the USFWS's "representative" years, and the regression model predictions when both are interpreted as likely values of future CSI under RPA controls.

Given these uncertainties, the panel was not persuaded that the PAM regression model produces more accurate predictions of the CSI levels one might expect to see in the future as compared with the 2006-2008 mean of 8.63. We do not recommend switching to the regression model for setting an ITL, especially because both models should soon be superseded for that purpose by a smelt life cycle model that would presumably also account for uncertainty in estimates of population size. Neither the draft PAM proposal nor the current USFWS implementation of the 8.63 multiplier account for CSI prediction uncertainty (Fig. 1) in their use of CSI to determine an ITL. Future ITL determinations, however they are calculated, will be more scientifically credible if they do account for such uncertainties.

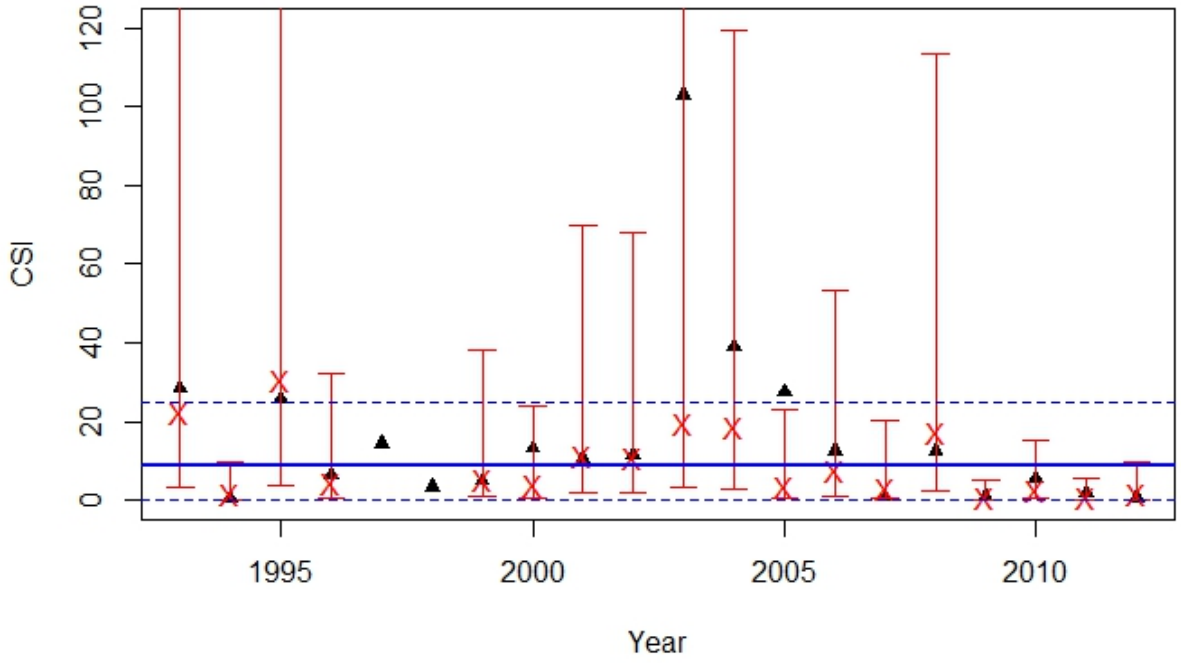

Figure 2. PAM regression model predictions of smelt CSI (red X's) and their 95% prediction intervals (red error bars), for 18 historical years (1993-2012), under PAM Scenario 1 of altered OMR flows. Black triangles are observed values of CSI. The solid blue line is mean CSI = 8.63, which is the multiplier currently used for the ITL. Dashed blue lines are the 95% CI on the estimated mean of 8.63.

The modeled response of CSI to river flow.

In their workshop presentations, the PAM authors noted that their regression approach to estimating CSIs, as well as the 3-year mean CSI, will be superseded by a more complex and realistic, process-based smelt model within a few years. It is the panel's understanding that the goal is to develop a spatially-explicit life cycle model of Delta Smelt that simulates population distributions throughout the Delta, as a function of freshwater inflows and withdrawals, sediment regimes, temperature, and other factors. Such a model would be valuable for a generally improved understanding of smelt population dynamics. However, our focus here is on how such a life cycle model might be used to better manage flow near the pumping projects, thus reducing entrainment and smelt loss.

The PAM's regression model reveals challenges that will arise when the more complex life cycle model is applied to the flow management problem. One such challenge is to

make assumptions about the independence of a model's driving variables. The PAM report made regression model predictions only for the 18 historical years whose data was used to develop the model. To make the predictions, the PAM authors used the observed values of Secchi depth measurements for those years, but they altered the observed OMR values from those years under two scenarios of hypothetical flow management. These decisions assume that OMR and Secchi measurements can vary independently of each other, and the PAM (p.13) argues for this independence because their Secchi variable was measured in the Sacramento River, at some distance from the water projects. In his comments on the draft PAM report, K. Newman reported an apparent nonlinear relationship between Secchi and negative OMR values in the 18-year record, thus challenging PAM's independence assumption. Newman's apparent relationship is suggestive, but cannot be resolved without additional data.

The PAM's strategy of predicting only for the 18 historical years, using their observed Secchi values and altering their observed OMR flows, seems to imply that these Secchi and OMR values are specifically linked to particular years and hence are linked to each other, which is inconsistent with the PAM's independence assumption. Thus, although PAM's historical predictions are an interesting exercise, we could not recommend using the observed Secchi values from specific historical years, along with their paired, scenario- adjusted OMR values from corresponding years, is not recommended for predicting likely future values of CSI.

Instead, the panel suggests using a Monte Carlo approach to predict likely future values of CSI. This approach would repeatedly choose random, independent values of Secchi and OMR from their respective distributions, which could be estimated from the 18-year record. The random (OMR, Secchi) pairs would then be inserted into the regression model, to repeatedly predict CSI. Likely future values of CSI would then be described by the resulting distribution of predicted CSI values, which could be summarized by its mean, variance, and shape (probably lognormal). This approach recognizes that Secchi and OMR in a future year are highly unlikely to be identical to the values from some historical year, and it is also consistent with the PAM's independence assumption.

The Monte Carlo approach attempts to characterize the response of the regression model to OMR and Secchi in a more general fashion. For example, the relative effects of these two predictor variables can be compared by their standardized regression coefficients, which are computed by multiplying each coefficient in Eq. 2 of PAM by the standard deviation of its predictor variable and dividing by the standard deviation of log(CSI), as estimated from the model-fitting data (Neter et al. 1983). The standardized coefficients of Secchi and OMR are -0.76 and -0.36, respectively. This means that an increase in Secchi of one standard deviation is predicted by the model to result in a

change of -0.76 standard deviation units in log(CSI). A similar interpretation applies for the standardized OMR coefficient. Thus, in standard deviation units, a given change in the Secchi value has about twice the effect on log(CSI) as does an equivalent change in OMR flow.

The secondary importance of OMR as a controller of CSI can also be demonstrated by plotting the regression model's predictions of CSI versus OMR, while fixing Secchi at lower (25%ile), median (50%ile) and higher (75%ile) values of its observed historical distribution (Fig. 3). The plot shows that the predicted value of CSI at any level of OMR flow depends strongly on what one assumes for a Secchi value.

In short, any application of the regression model to limit salvage through OMR flow management (that is, setting an ITL) requires one to also make quantitative assumptions about turbidity (i.e., Secchi) levels in a future year. The above analysis shows that these assumed levels of Secchi will play a dominant role in determining the ITL.

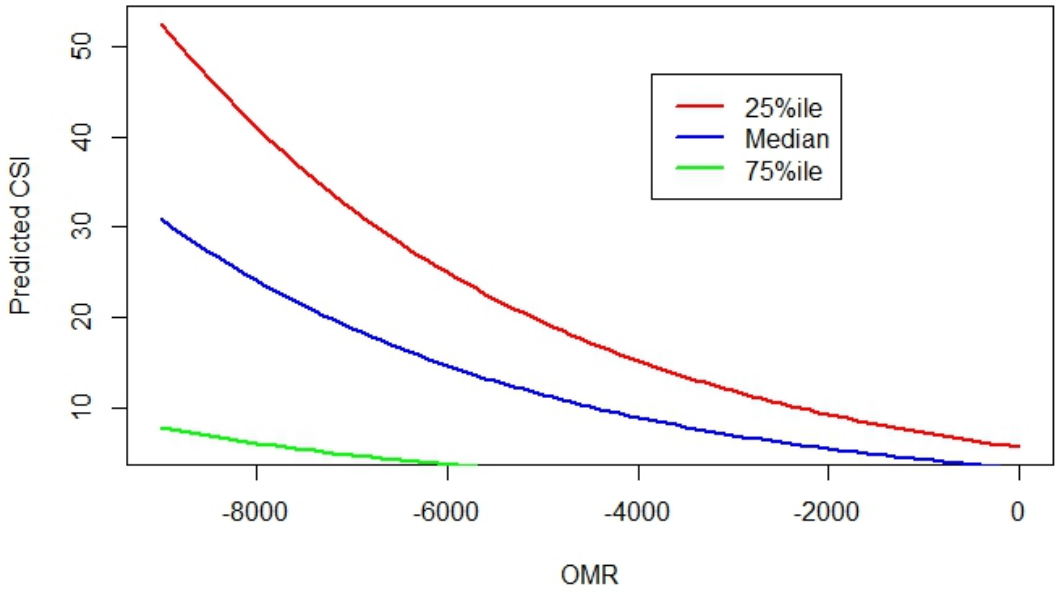

Figure 3. PAM regression model predictions of CSI versus OMR flow, with Secchi held fixed at its 25th, 50th, and 75th percentiles.

The above analysis has implications for the ongoing development of the smelt life-cycle model, and its planned role in setting an ITL. The historical data and our PAM model analysis suggest that river flow, as indexed by OMR or other flow variable(s), will be a

relatively weak predictor of cumulative smelt salvage in any realistic model. This conjecture is consistent with the well-known, process-based effects of turbidity on smelt dynamics. We expect that turbidity, along with other factors, will exert a strong control on the overall level and changes in smelt salvage that could be expected from any managed flow regime.

To use the life cycle model in a forecasting mode, as is needed for setting an ITL for a future year, values of these other factors must be projected or assumed for the future. This process will add considerable uncertainty to any future projections of flow effects on CSI. As model complexity increases, so will the cumulative effort and uncertainty of making such assumptions and projections. Hence, the panel advises the life cycle model development team to think in advance about the challenges of using their model in a strict forecasting mode to help set ITLs for Delta Smelt. Hopefully, these considerations will influence the level of realism and complexity that the life cycle modelers will attempt to represent.

General Consideration of RPA Actions Under Dry Year Conditions

With a third year of increasing drought severity, participating agencies were faced with a series of experimental and operational challenges. There must be careful consideration of hydrologic events in the future and what impacts might be foreseen on operations and concurrent monitoring and research opportunities.

In its annual report on Drought Operations and Forecasts, DWR suggests that:

"… the forecasted carryover storage of approximately one million acre-feet in Lake Oroville by the end of water year 2014 (September 30, 2014) will be sufficient to meet human health and safety needs in 2015 (projected as 260,000 af) and other project purposes, including maintaining Delta salinity control. This level of storage should be sufficient under a conservative 90% exceedance hydrologic assumption for water year 2015, while still meeting regulatory and contractual commitments."

This plan does not propose a reserve for the following year, 2016, in the event that the drought is not relieved. Presumably this forecast is based upon a historical record that indicates a likely return to wetter conditions. However, another consideration must be made; that this drought may be the leading edge of a climate change event of indeterminate intensity and duration. Therefore, it behooves DWR and other agencies to consider alternative targets and strategies.

The importance of accurate forecasting tools is highlighted by the recent series of dry water years with the possibility that this trend will continue into the future. Different tools

are used to optimize reservoir operation to meet downstream temperature targets over short- versus long-time periods. Both categories of tools are needed to ensure that a dam is operated to maximize benefit to target biota. Short-time period tools address questions such as, “what blend of reservoir water by depth and temperature is required to meet a downstream temperature target based on daily or weekly forecast meteorological conditions?” Such a tool is expected to give relatively accurate forecasts (~1.0^{O} C) because it can be supported with reasonably accurate meteorological forecasts. It can be used to adjust daily-weekly operation in near real-time. Long-time period tools address questions such as, “what blend of reservoir water by depth and temperature is required to meet a downstream water temperature target (i.e., the temperature control point) requirement over an annual cycle or other extended time period?” Such a tool cannot be as accurate as the short-term operations tool because it must employ input data synthesized over the annual cycle. Consequently, in long-term operations, a particularly critical time period (e.g., hottest and driest year in the period of record) is analyzed to determine the most downstream point in the river so that a downstream target can be reliably met. It makes little sense to operate to an overly ambitious, downstream target early in the water year and then retreat later in the season to a temperature control point closer to the dam because of a shortage of cold water storage. Worse yet, it is possible to deplete cold water storage or for reservoir water levels to be reduced to a point where it cannot be discharged using the water withdrawal system of the dam as happened this past year at Shasta Dam.

Efforts are underway to build a sophisticated temperature monitoring/modeling system for the Upper Sacramento River to improve the short time period management of river water temperature. This should allow USBR to better manage the cold water resource. However, the existing legacy water quality model upon which the long time period release patterns are based continues to be HEC-5Q, for which neither a user-manual nor calibration report are available. In the original formulation of HEC-5Q, a 1-D (vertical) reservoir stratification model (all that was available at the time of development of HEC-5Q) was used to forecast reservoir stratification patterns. Unfortunately, a 1-D formulation to simulate reservoir stratification is usually inadequate because most reservoirs are inherently 2-D (longitudinal and vertical). Based on satellite imagery, Shasta Lake is clearly a 2-D system. Use of a 1-D model for reservoir simulation requires that model parameters be manipulated (i.e., values are used outside of recommended ranges) to force the model to simulate a condition for which it was not designed. Inappropriate use of a 1-D model for an application that is inherently 2-D affects model accuracy. A more accurate formulation (e.g., CE-QUALW2) should be used to replace HEC-5Q. From the Sacramento River Temperature Task Group Report of WY 2014, it is clear that USBR continues to use HEC-5Q with no apparent movement towards use of an alternate model. The continued use of HEC-5Q will severely limit the

ability of USBR to manage water to meet the co-equal goals, particularly to perform scenario analysis over an annual cycle to evaluate the existing carry over storage and develop reasonable downstream temperature control points.

During presentations by USBR, the panel was informed that water levels within Shasta Lake were lowered below the level of the opening to the Temperature Control Device. This device was designed to release shallow water in the spring and early summer and deep water in the late summer and early fall (Higgs and Vermeyen 1999). Information on the water stratification pattern upstream of the dam and how the stratification pattern related to the elevation of the other release ports was not presented. Consequently, it is not possible to make a complete assessment of how extremely low forebay water levels affected the ability of the outlets to blend water to meet downstream water temperature targets. It might be useful to investigate reservoir destratification techniques to determine if they could be useful to bring colder, deeper water closer to the surface at the elevation of the lowest port of the Temperature Control Device. These well-established techniques were originally developed to mix warmer, oxygenated surface water with deep oxygen-depleted water to improve the water quality of hypolimnetic (deep) releases. In the case of Shasta Dam, these same reservoir destratification techniques could be used to solve the inverse problem of bringing deeper colder water to the elevation of the lower ports on the Temperature Control Device.

One consideration might be including an end-of-year storage target as part of the in-season management. Currently, operations focus upon water quality and temperature targets throughout the year but do not include an end-of-year storage target.

As has been mentioned in previous reports, it is becoming evident that the possibility of long-term changes in weather pattern must be considered for research and management purposes. Normal oscillations in both Pacific and Atlantic oscillations, including the Atlantic Multidecadal Oscillation (AMO), the Pacific Decadal Oscillation (PDO), and the El Niño Southern Oscillation (ENSO), have been shown to have dramatic effects on agricultural production (Maxwell et al. 2013), river flow patterns (Kelly and Gore 2008), and a series of landscape effects that drive ecosystem function in river ecosystems (Gaiser et al. 2009; Johnson et al. 2013;Sheldon and Burd 2013; Keellings and Waylen 2014; Olin et al. 2014). These far-reaching changes suggest that many new challenges to management and research must include predictable changes in these oscillations, but also with climate change, the possibility of dampening or alteration of the oscillations which might influence temperature and water quality targets for management (Olin et al. 2014).

The potential impact of long-term climate change will necessitate some creative analysis of various scenarios for future research and management decisions. Although there are a wide variety of potential impacts, there is considerable potential for significant changes in water availability and allocations in the next 100 years. Cayan et al. (2008) have demonstrated that, depending upon a variety of carbon-dioxide levels, water availability [as snow water equivalents] can be significant to future decisions (Table 2).

Table 2. Changes in April 1 snow water equivalents for the San Joaquin, Sacramento, and parts of the Trinity drainages (adapted from Cayan et al. 2008).

ELEVATION	MEAN 1961-1990 (Km^3)	2005-2034	2035-2064	2070-2099
1000 – 2000 m	4.0	-13 to -48%	-26 to -68%	-60 to -93%
2000 – 3000 m	6.5	+12 to -33%	-08 to -36%	-25 to – 79%
3000 – 4000 m	2.49	+19 to -13%	-02 to -16%	-02 to -55%
All Elevations	13.0	+06 to -29%	+0.12 to -42%	-32 to -79%

With these potential changes, it is imperative that various scenarios of flow loss be conducted in order to determine long-term management, research, and monitoring strategies. At a minimum, a time-series analysis of historical records [accounting for decadal or multi-decadal patterns] with 20%, 30%, and 40% losses should be examined. These losses, then, can be used to determine critical months for alteration of management and monitoring schedules.

We are gratified that the Clear Creek Technical Team continues to complete its PHABSIM analysis, as reported this past year. Although there has been considerable effort to demonstrate that RIVER2D provides more accurate habitat assessments than IFG4, for example, the ultimate output still remains a relationship between habitat availability and daily, weekly, or monthly discharge. These outputs present an opportunity for a new project to analyze the ultimate gain or loss in habitat under reduced flow scenarios. A relationship between habitat and discharge under flow reduction scenarios can be created from the model output. Time-series analysis, through TSLIB or other exceedance programs, should be based upon frequency and duration of habitat events rather than the discharges associated with those values. These graphical presentations can create the decisions necessary to create more effective management and monitoring strategies. See example in Figure 4.

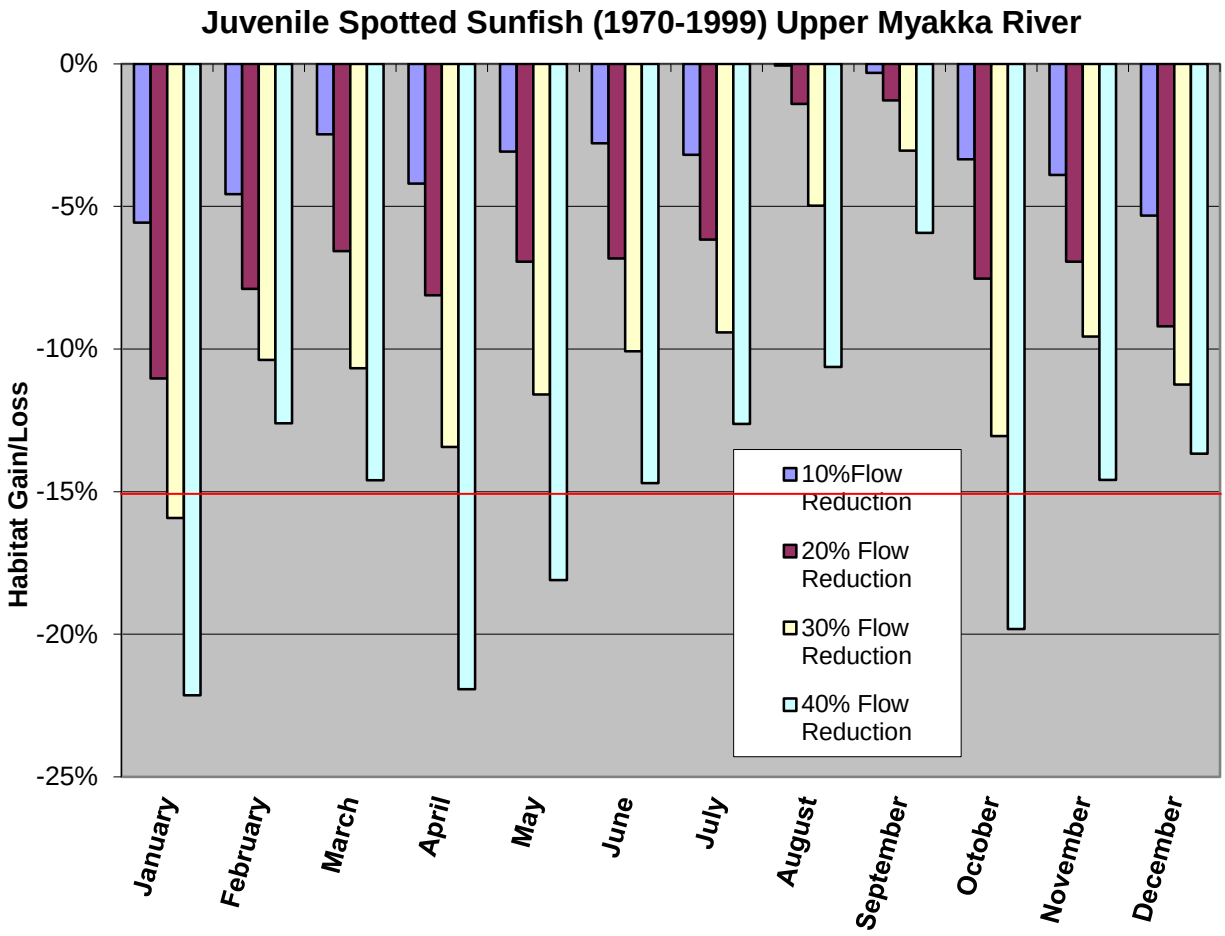

Figure 4. An estimate of habitat gain or loss during the AMO dry period on the Myakka River. If a 15% habitat loss cannot be exceeded, this model predicts that a 20% flow reduction is acceptable in January but in September even a 40% flow reduction does not significantly impact juvenile spotted sunfish. This analysis is repeated for a suite of target fish and macroinvertebrates.

The panel recognizes that water operation actions are driven by a set of mandated rules and that the agency personnel manning reservoir operations may not have the authority to take actions outside of the framework of these rules. However, it would appear that additional flexibility (altered rules) could be authorized by the appropriate agency management under critically dry conditions such as occurred in WY 2014 in order to conserve scarce water resources.

IRP RESPONSES TO QUESTIONS DEFININGTHE SCOPE OF THE 2014 LOBO ANNUAL REVIEW

Responses of 2014 IRP to questions regarding modified Delta Cross Channel (DCC) Gate opening criteria per Attachment G in the Drought Operations Plan

1) **Is using the upstream trigger at Knights Landing protective of 95% of the juvenile population monitoring for downstream emigrating fish given their travel time to the DCC?**

The question presumes that the size of the juvenile population at risk is known (i.e., 95% of what number?) However, the panel is unaware of any information that provides an accurate estimate of population size and so is unable to provide an answer. To answer the question even in terms of relative population size requires some quantitative measure of the population at Knights Landing and a site in the Sacramento River downstream of the DCC for comparison.

In any case, it seems highly unlikely that protection of 95% of the juvenile population could ever be demonstrated. The 95% confidence interval around any estimate of 95% of the juvenile population size would likely be so large as to be meaningless.

2) **Are the localized triggers of the Sacramento trawl and area beach seines protective of 95% of fish lingering in the area of the DCC?**

See answer to Question 1 above. In addition, the uncertainty of the estimates of population size made using either the trawl or beach seine data would have to be known as well. Given that these methods provide essentially an instantaneous snapshot of catch at discrete locations, the accuracy of these methods is likely considerably less than that of the Knights Landing rotary screw trap, which samples a location continuously for an extended period of time. It seems unlikely that any method currently in use could provide the information necessary to answer either Question 1 or 2.

3) **Are there other (possibly more sensitive) recommended methods or other station locations, both upstream and downstream of the DCC, for use as the basis for a DCC trigger in the future?**

The time delay of approximately two days currently required to close the Delta Cross Channel should be shortened, if possible. Sampling locations that are closer than two-days travel time to the DCC gates would improve the ability to predict fish arrival times

at the DCC gates, but would require a more rapid response time for gate closure, which may be impractical.

4) **What studies or methods would you recommend to evaluate the effectiveness of the DCC gate operations?**

The question of DCC operations effectiveness involves both fish diversion and Delta water quality since DCC operations must consider both criteria.

Considerations for studying operations for fish passage effectiveness

The April 2014 Delta Science Program workshop entitled, “Interior Delta Flows and Related Stressors” is of direct relevance to improving the effectiveness of fish diversion at the DCC. In particular, the workshop presentation by Jon Burau (USGS/Sacramento) on the hydrodynamic field studies at the junction of the Sacramento River with Georgiana Slough and the Delta Cross Channel appear relevant to improving the operational effectiveness of the DCC.

This presentation, described a 2008 acoustic telemetry study that has relevance to the operations of the DCC over diel and tidal cycles. Three findings were relevant to the effective DCC operations:

Based on the Burau (2014) presentation, the IRP suggests testing the hypothesis that an effective DCC operation is to open the gates on the ebb tides during the day. Further studies of the behavior of acoustically tagged fish in the DCC over diel and tidal cycles may be required to evaluate this hypothesis.

a. a majority of the fish arrived at night at the DCC**.**

b. with DCC gates open fish may be drawn into the interior Delta with the convergence of velocity streamlines on the flood tide

c. with DCC gates closed fish can be drawn into the interior Delta by the convergence of velocity streaklines into Georgiana slough

Considerations for studying operations for water quality effectiveness

Studies also suggest that tidally coordinated DCC operations would be effective for improving Delta water quality (i.e., low interior Delta salinity). The issues to consider here are the primary assumptions that opening the DCC gates, especially if operations include a diurnal/tidal component, will allow sufficient freshwater flows through the Mokelumne system to significantly reduce salinity in the interior Delta.

The benefit of opening the DCC gates is assumed to be that freshwater from the Sacramento will be diverted into the Mokelumne system and flow towards the San Joaquin and the interior Delta. It is further assumed that these pulses of water will be capable of preventing additional saltwater intrusion on the San Joaquin stem of the Delta. These assumptions are based on the collective experience of pump operators and studies that have shown that when the DCC is open continually for multiple days, the end result is better water quality in the interior Delta.

Therefore, there is a continuous net flow downstream through the Mokelumne system towards the central Delta. This net flow on the North Mokelumne River when DCC gates are open was observed during 2012 field experiments at the junction of Georgiana Slough and the Mokelumne River by Gleichauf et al. (in press) who observed that the river was tidal when the DCC was closed. Depending on how long this operation is used, the expected benefit for salinity in the central Delta may or may not be realized.

Balancing the needs of water quality and fish protection are important enough to justify further analysis of the water quality benefit that will result from this modified DCC gate operation. A hydrodynamic modeling analysis and associated salinity transport modeling should be done to analyze whether improvements in water quality in the central Delta justifies this operation. The simulation should use the observed Sacramento and San Joaquin inflow, Clifton Court Forebay gate operations, and State and federal facility pump operations for WY 2014. The operation of the DCC should be modeled in three conditions. In the first condition, model the DCC operations with the actual gate operations in 2014. In the second condition, model the proposed pulsed open and closed operation. In the third simulation, model the period with the DCC set open for the entire period when the DCC pulse flow was modeled in the second simulation. From this modeling exercise, the travel time of the Sacramento River freshette to the interior Delta water quality stations can be calculated and compared to the travel time when the DCC remains continually open.

Responses of 2014 IRP to questions regarding proposed modifications to the juvenile production estimate (JPE) calculation and use/application of data from acoustically-tagged Chinook Salmon releases

1) **How important is it to eliminate overlap in survival terms vs. potentially not including the survival rate of the fry life history stage?**

Given the considerable uncertainty and variability in the survival estimates used to calculate JPE, the adjustment for the fry life history stage outlined in the presentation for the overlap in the survival terms is not warranted. The current two-term model based on S1 and S2 is of sufficient complexity.

Eliminating the overlap in survival stages reduces bias in the final JPE. The downside is that there is no longer a distinct survival term for fry, which might be biologically less realistic. However, for the narrow but important purpose of making an unbiased JPE, the panel suggests using a model that is structured primarily by the data that can be collected, rather than by biological realism. If the data required for a good estimate of fry survival is currently unobtainable, then the best option may be to exclude a fry survival term from the JPE calculator. In short, the panel supports the current approach in which survivals are defined in terms of data collection sites not by specific life stages.

The panel also noted that the anomalous conditions in 2014 illustrate that fish migration behavior cannot be simply defined by distinct life stages in which well-defined transitions from fry to smolt stages occur at specific times and locations. Winter-run Chinook Salmon migrate through the river system over a protracted period of time at different sizes. Examples of the anomalous conditions in 2014 include:

- The migration was characterized by an extended period of rearing at upriver locations, higher percentage of smolt-sized fish passing the RBDD, a distinct response of fish to a precipitation and turbidity event, and shorter Delta residence time (Stuart IRP Presentation 2014).

- Fish passed RBDD later than in other years but passed Chipps Island earlier. Additionally, the passage date is quite variable; 50% passage at Knights Landing varied by four months over a 7-year observation record.

- The CFS Juvenile Production Simulation model did not capture the unusual conditions in this drought year and therefore the JPE based on numbers from carcass surveys is highly uncertain. The CFW model significantly under-predicts

the uncertainties (Jones and Bergman 2010) and could not account for the discrepancy.

2) **How should the missing life-stages (i.e., fry-to-smolt) and the gap in juvenile rearing from Red Bluff Diversion Dam (RBDD) to Salt Creek (approximately 2.5 RM downstream of RBDD) be accounted for in the current JPE methodology?**

Not accounting for mortality in the 2.5 RM reach between RBDD and Salt Creek is not significant compared to survival to Tower Bridge, a distance of approximately 370 RM. Using the WRCS to characterize the survival per RM, then ignoring the 2.5 RM reach would increase survival from 13.8% to 14%. This level of change is insignificant compared to other forms of uncertainty and bias.

Accounting for the fry-to-smolt survival stage appears problematic because when and where a fry becomes a smolt is not measurable.

3) **Hatchery origin juvenile winter-run have shown a unique life-history strategy not seen in other runs, in that they hold upstream in dry years for 30-50 days. How should this behavior be incorporated into the JPE?**

The panel was unable to provide advice on this difficult problem. However, a similar problem has been studied concerning the migration of Snake River sub-yearling fall Chinook. In that system initiation of migration was highly variable and involved temperature and growth rate thresholds. See the MS thesis: Widener, D. *Migration and bioenergetics of juvenile Snake River fall Chinook salmon*. 2012. Available from: http://www.cbr.washington.edu/sites/default/files/papers/widener_thesis.pdf

4) **The weighting for the JPE brood year 2013 was 50% for the 5 years of late fall-run acoustic tag data, and 50% for the one year of winter-run acoustic tag data.**

    a. **The late fall-run acoustic tag data included data from various water year types, and the year of winter-run acoustic tag survival was conducted in a dry water year. How should water year type be considered and factored into the weighting in any given water year?**

See section *Issues with S2: Survival from RBDD to Delta* above for possible approaches.

    b. **What should the weighting be between late fall-run and winter-run acoustic tag data with each additional year of winter-run acoustic tag data? At what**

point (how many years of winter-run acoustic tag data) should we not consider the late fall-run acoustic tag data to develop the winter-run JPE?

Use of late fall-run acoustic studies to estimate winter-run JPE is not encouraged until sufficient data are available to compare WRCS and LFCS survival and migration properties.

Furthermore, it is unrealistic to calculate any sort of average survival rate, regardless of the weighting scheme, and then assume that it is an accurate single estimate for next year's survival. Instead, the panel suggests that when sufficient WRCS survival data become available the JPE be estimated using Monte Carlo methods in which the terms in the JPE are repeatedly and randomly selected from individual historical years of survival rates and other vital rate parameters.

5) **What additional studies or methods would you recommend to improve the accuracy of the JPE in the future?**

Develop Monte Carlo methods to estimate a distribution of likely future JPE values from the spreadsheet model, rather than a single point estimate of JPE. Alternatively, replace the spreadsheet calculator with some version of the Cramer Fish Sciences model (CFS 2014). Future tagging studies may wish to consider using trickle releases, rather than large batch releases in order to facilitate survival-rate modeling.

Some possible methods for estimating the survival terms in the JPE are discussed in the JPE Section of the 2014 IRP report.

6) **Given that approximately 4.43 million fry were estimated to pass RBDD from the JPE calculator, but only 1.78 million fry were estimated to pass RBDD based on U.S. Fish and Wildlife Service's rotary screw trapping, how should these conflicting data be interpreted?**

The discrepancy can be largely explained by the variability in the model's egg-to-fry survival parameter (see Fig. 1). If one considers the multiplicative effect of uncertainty in the egg production rate, it is surprising that the discrepancy isn't actually much larger. The estimate of S1 used in the calculation of JPE from carcass surveys is highly uncertain. See JPE Section "*Issues with S1*" and "*Recommendations on JPE"* above.

Responses of 2014 IPR to questions regarding the proposal for calculating cumulative salvage index values used for estimating take likely to occur under the USFWS Old and Middle River flow RPA for adult Delta Smelt

1) **Is the proposed calculation more scientifically robust than the method, based on cumulative salvage index (CSI) values from 2006-2008, that is currently used to estimate incidental take?**

The meaning of "scientifically robust" is unclear. Predictions from the regression method and the current method do not significantly differ due to their high uncertainties. Thus, there is no objective basis upon which to recommend switching from the current method to the regression method for purposes of setting an ITL.

2) **Is the proposed calculation more scientifically robust than the RPA of (in) accounting for the effects of variable physical and biological conditions on incidental take that may be expected in the future?**

The proposed regression model does account for one additional environmental factor (turbidity, as indexed by the Secchi measurement), and so may be more realistic than the current method. However, this increased realism adds the burden of making future projections of Secchi, if the proposed model is used to estimate future expected take. Also, there is no connection to the size of the Delta Smelt population at risk. As the smelt population approaches zero, relationship between salvage and environmental variables such as turbidity or flows should not be expected to match historical correlations that may have held when smelt were more abundant.

3) **Is it scientifically appropriate to use model-adjusted OMR values but historical turbidity values to adjust historical salvage values, as is done in the proposal?**

This action is appropriate, as long as you assume that OMR and Secchi are independent, which is a questionable assumption. However, even if this independence is true, the use of only the 18 historical CSI predictions to determine an ITL is unrealistic because it understates the true variability of likely future CSI values.

4) **Are there additional aspects of the proposed calculation of CVP/SWP salvage of adult Delta Smelt that could be refined?**

Yes. Seriously consider the uncertainty in any such calculations and the subsequent effect on allowable take.

5) **Are there alternative methods or studies that would improve future estimates of take?**

The panel understands that a smelt life cycle model is currently under development, for making future estimates of take. We encourage that effort and suggest that it incorporate estimates of model uncertainty.

One of the key metrics in this proposed calculation is OMR flow, a daily, tidally-averaged index. This metric is also being considered in other future calculations of entrainment. What is missing in the discussion of entrainment at the export facilities, in general, is the recognition that the export facilities are located in the tidal zone of the South Delta and that flows around those facilities cannot be simplified to daily, tidally-averaged flows when considering entrainment issues. Entrainment is a tidal timescale problem.

Responses of 2014 IPR to questions regarding the general implementation of the RPA Actions under dry year conditions based on prior science review questions about RPA implementation

1) **Were the scientific indicators, study designs, methods, and implementation procedures used appropriate for evaluating the effectiveness of the RPA actions under dry conditions? Are there other approaches that may be more appropriate under dry conditions?**

The effectiveness of RPA Actions as measured in terms of biological responses has remained elusive under all conditions. Certainly, some actions and triggers were altered as a result of limited available water resources in this critically dry water year, but there were no outstanding biological metrics that could be used to evaluate effectiveness of the actions in terms of population benefits in the present or subsequent year.

2) **How can implementation of RPA actions be adjusted to more effectively meet their objectives under dry conditions?**

As previous IRP reports have noted consistently, effectiveness must be tied to biological response metrics, which continue to be associated with so much uncertainty that it has not been possible for the panel to provide a satisfactory response to this question in any water year type, at least thus far.

REFERENCES

Anderson, J.J., R.T. Kneib, S.A. Luthy and P.E. Smith. 2010. Report of the 2010 Independent Review Panel (IRP) on the Reasonable and Prudent Alternative (RPA) Actions Affecting the Operations Criteria and Plan (OCAP) for State/Federal Water Operations. Prepared for: Delta Stewardship Council, Delta Science Program. December 9, 2010. 39 p.

Anderson, J.J., J.A., Gore, R.T. Kneib, M.S. Lorang and J. Van Sickle. 2011. Report of the 2011 Independent Review Panel (IRP) on the Implementation of Reasonable and Prudent Alternative (RPA) Actions Affecting the Operations Criteria And Plan (OCAP) for State/Federal Water Operations. Final report submitted to the Delta Stewardship Council, Delta Science Program. December 9, 2011, 47 p.

Anderson, J.J., J.A., Gore, R.T. Kneib, M.S. Lorang and J. Van Sickle. 2012. Report of the 2012 Delta Science Program Independent Review Panel (IRP) on the Long-term Operations Opinions (LOO) Annual Review. Final report submitted to the Delta Stewardship Council, Delta Science Program. December 1, 2012, 54 p.

Anderson, J.J., J.A. Gore, R.T. Kneib, M.S. Lorang, J.M. Nestler and J. Van Sickle. 2013. Report of the 2013 Delta Science Program Independent Review Panel (IRP) on the Long-term Operations Biological Opinions (LOBO) Annual Review. Final report submitted to the Delta Stewardship Council, Delta Science Program. December 7, 2013, 59 p.

Burau, J.R. 2014. Presentation: Understanding Juvinile Salmon Entrainment at Junctions. Delta Science Workshop on the Interior Delta Flows and Related Stressors, April 16, 2014, https://www.youtube.com/watch?v=RNldBDqL3rc&index=7&list=PLqTHCliW1HhrNF3c81L_k9Ml7VLcoJ4j2

Cramer Fish Sciences (CFS). 2014. A Revised Sacramento River Winter Chinook Salmon Juvenile Production Model. Prepared by Kristopher Jones, Paul Bergman, and Brad Cavallo for the National Oceanic and Atmospheric Administration, Sacramento, CA. 21 p.

Cayan, D.R., E.P. Maurer, M.D. Dettinger, M. Tyree and K. Hayhoe. 2008. Climate change scenarios for the California region. *Climatic Change* 87 (Supple 1): S21-S42.

Chapman, E.D., A.R. Hearn, C.J. Michel, A.J. Ammann, S.T. Lindley, M.J. Thomas, P.T. Sandstrom, G.B. Singer, M.L. Peterson, R.B. MacFarlane and A.P. Klimley.2013. Diel movements of out-migrating Chinook salmon (*Oncorhynchus tshawytscha*) and steelhead trout (*Oncorhynchus mykiss*) smolts in the Sacramento/San Joaquin watershed. *Environmental Biology of Fishes* 96: 273-286.

Donaldson, M.R., S.G. Hinch, C.D. Suski, A.T. Fisk, M.R. Heupel and S.J. Cooke. 2014. Making connections in aquatic ecosystems with acoustic telemetry monitoring. *Frontiers in Ecology and the Environment* 12(10): 565-573; doi: 10.1890/130283.

Gaiser, E.E., N.D. Deyrup, R.W. Bachmann, L.E. Battoe, and H.M. Swain. 2009. Multi-decadal climate oscillations detected in a transparency record from a subtropical Florida lake. *Limnol. Oceanogr.* 54: 2228-2232.

Gleichauf, K. P. Wolfram, N.E. Monsen, O. Fringer, and S.G. Monismith. Accepted. In press. Dispersion Mechanisms of a Tidal River Junction in the Sacramento-San Joaquin Delta, California *San Francisco Estuary and Watershed Science*

Johnson, N.T., C.J. Martinez, G.A. Kiker, and S. Leitman. 2013. Pacific and Atlantic sea surface temperature influences on streamflow in the Apalachicola-Chattahoochee-Flint river basin. *Journal of Hydrology* DOI 10.1016/jhydrol.2013.03.005

Jones and Bergman (2010) A Revised Sacramento River Winter Chinook Salmon Juvenile Production Model. Cramer Fish Sciences.

Higgs, J. A., T. B. Vermeyen. 1999. Shasta temperature control device CFD modeling study. Bureau of Reclamation, Technical Service Center, Water Resources Research Laboratory. http://www.usbr.gov/pmts/hydraulics_lab/pubs/PAP/PAP-0845.pdf accessed on 2 December 2014.

Keellings, D., and P. Waylen. 2014. Investigating teleconnection drivers of bivariate heat waves in Florida using extreme value analysis. *Climate Dynamics* DOI 10.1007/s00382-014-2345-8.

Kelly, M.H. and J.A. Gore. 2008. Florida river flow patterns and the Atlantic Multidecadal Oscillation. River Research and Applications 24: 598-616.

Maxwell, J.T., P.A. Knapp, and J.T. Ortegren. 2013. Influence of the Atlantic Multidecadal Oscillation on tupelo honey production from AD 1800 to 2010. *Agriculture and Forest Meteorology* 174/175: 129-134.

Maxwell, J.T., P.A. Knapp, and J.T. Ortegren. 2013. Influence of the Atlantic Multidecadal Oscillation on tupelo honey production from AD 1800 to 2010. *Agriculture and Forest Meteorology* 174-175: 129-134.

Monismith, S.G., M. Fabrizio, M. Healey, J. Nestler, K. Rose, J. Van Sickle. 2014. Workshop on the Interior Delta Flows and Related Stressors Panel Summary Report. http://deltacouncil.ca.gov/sites/default/files/documents/files/Int-Flows-and-Related-Stressors-Report.pdf

Monsen, N. E., J.E. Cloern and J. R. Burau. 2007. Effects of Flow Diversions on Water and Habitat Quality: Examples form California's Highly Manipulated Sacramento-San Joaquin Delta. *San Francisco Estuary and Watershed Science* 11 (3): http://repositories.cdlib.org/jmie/sfews/vol5/iss3/art2.

Mood, A.M., F.A. Graybill, and D.C. Boes. 1974. Introduction to the theory of statistics (3rd ed.) McGraw-Hill, NY.

Morgan-King, T. L. and D. H. Schoellhamer. 2013. Suspended-Sediment Flux and Retention in a Backwater Tidal Slough Complex near the Landward Boundary of an Estuary. *Estuaries and Coasts* 36 (2):300-318. doi: 10.1007/s12237-012-9574-z.

Murphy, D. D. and S. A. Hamilton. 2013. Eastward Migration or Marshward Dispersal: Exercising Survey Data to Elicit an Understanding of Seasonal Movement of Delta Smelt. *San Francisco Estuary and Watershed Science* 11 (3): http://escholarship.org/uc/item/4jf862qz.

Nestler, J. M., Pompeu, P. S., Goodwin, R. A., Smith, D. L., Silva, L. G. M., Baigún, C. R. M. and Oldani, N. O. 2012. The river machine: A template for fish movement and habitat, fluvial geomorphology, fluid dynamics and biogeochemical cycling. *River Research and Applications*, 28: 490–503. doi: 10.1002/rra.1567

Neter, J., W. Wasserman and M.H. Kutner. 1983. Applied linear regression models. Richard D. Irwin publishers, Homewood IL.

Olin, J.A., P.W. Stevens, S.A. Rush, N.E. Hussey, and A.T. Fisk. 2014. Loss of seasonal variability in nekton community structure in a tidal river: Evidence for homogenization in a flow-altered system. *Hydrobiologia* DOI 10.1007/s10750-014-2083-2.

Perry, R.W., J.R. Skalski, P.L. Brandes et al. 2010. Estimating survival and migration route probabilities of juvenile Chinook salmon in the Sacramento-San Joaquin River Delta. *North American Journal of Fisheries Management* 30: 142-156.

Sheldon, J.E. and A.B. Burd. 2013. Alternating effects of climate drivers on Altamaha River discharge to coastal Georgia, USA. *Estuaries and Coasts* DOI 10.1007/s12237-013-9715-z.

Steel, A.E., P.T. Sandstrom, P.L. Brandes and A.P. Klimley. 2013. Migratory route selection by juvenile Chinook salmon at the Delta Cross Channel, and the role of water velocity and individual movement patterns. *Environmental Biology of Fishes* (Special Issue) 96:215-224.

APPENDIX 1 – Materials for 2014 IRP Review

Review Materials Available to the 2014 LOBO Independent Review Panel

I. The following documents were provided in electronic format as required reading by the IRP prior to the 2-day workshop in Sacramento, CA on 6-7 November 2014:

1) Attachment G of the CVP and SWP Drought Operations Plan and Operational Forecast, April 1, 2014 through November 15, 2014

2) Juvenile Production Estimate (JPE) Calculation and Use/Application of Survival Data from Acoustically-tagged Chinook Salmon Releases Report

3) Proposal for Calculating Cumulative Salvage Index Values Used For Estimating Take Likely to Occur under the USFWS Old and Middle River Flow RPA for Adult Delta Smelt prepared by Metropolitan Water District

4) Sacramento River Temperature Task Group (SRTTG) Annual Report of Activities

5) Clear Creek Technical Team (CCTT) Annual Report of Activities

6) American River Group (ARG) Annual Report of Activities

7) Stanislaus Operations Group (SOG) Annual Report of Activities

8) Delta Operations for Salmonids and Sturgeon Group (DOSS) Annual Report of Activities

II. The following additional reports were made available in electronic format for supplemental use in providing historical context for the IRP:

1) Interagency Fish Passage Steering Committee (IFPSC) Annual Report of Activities
2) The Smelt Working Group (SWG) Annual Report of Activities
3) Water Year 2014 Winter Run Chinook Drought Operations Assessment
4) RPA Summary Matrix of the NMFS and USFWS Long-term Operations BiOps RPAs
5) Central Valley Project and State Water Project Drought Operations Plan and Operational Forecast, April 1, 2014 through November 15, 2014

6) Proposal for a Revised ITL and Expected Take for Adult Delta Smelt Metropolitan Water District July 29, 2014 Draft
7) DRAFT Comments on “Proposal for a revised ITL and expected take for adult Delta Smelt” (Ken Newman, August 21, 2014)
8) Proposed Response to Ken Newman Comments on Proposed ITL Method Paper (David Fullerton, September 8, 2014)
9) USFWS Biological Opinion Sections for ITL

III. ***The following additional materials were made available following the Workshop in Sacramento at the request of the IRP for supplemental use of the IRP***:

- PowerPoint Presentations from the LOBO Workshop (held November 6, 2014 in Sacramento, CA)
- Public Comments on Proposal to Revise the Delta Smelt CSI and Adult ITL Calculation (Natural Resources Defense Council and The Bay Institute, October 24, 2014)

Additional background information from the Science Program website was also available, including reports from previous IRPs.

Report of the 2012 Delta Science Program Independent Review Panel (IRP) on the Long-term Operations Opinions (LOO) Annual Review

Prepared for: **Delta Science Program**

December 1, 2012

Panel Members:

James J. Anderson, Ph.D., University of Washington
James A Gore, Ph.D., (Panel Chair) University of Tampa
Ronald T. Kneib, Ph.D., (Lead Author), RTK Consulting Services & Univ. of GA (Senior Research Scientist Emeritus)
Mark S. Lorang, Ph.D., University of Montana
John M. Nestler, Ph.D., Fisheries and Environmental Services & USACE Engineer Research and Development Center (Retired)[1]
John Van Sickle, Ph.D., U.S. Environmental Protection Agency Western Ecology Division (Retired)

Scope and Intent of Review: This report represents findings and opinions of the Independent Review Panel (IRP) assembled by the Delta Science Program to inform the National Marine Fisheries Service (NMFS) and the U.S. Fish & Wildlife Service (USFWS) as to the efficacy of the water operations and regulatory actions prescribed by their respective Long-term Operations Opinions' (LOO) Reasonable and Prudent Alternative Actions (RPAs) as applied from October 1, 2011 through September, 30 2012 (Water Year 2012). This year's annual review focused primarily on implementation of NMFS's RPAs for Clear Creek (RPA Actions I.1.1 – I.1.6) and the Spring 2012 Delta Operations joint stipulation agreement for water operations and fisheries that was required to be executed in water year 2012 in lieu of NMFS's RPA Action IV.2.1.

After reviewing a required set of written documents (Appendix 1), the IRP convened at a public workshop in Sacramento, CA on 31 October - 1 November 2012. The first day of the 2-day workshop provided a forum for the IRP to consider updated information and new research findings and to discuss issues related to the application of RPA actions. On the second day the IRP deliberated in a private session beginning at 8:30 a.m. in order to prepare and present their initial findings at the public workshop at 2:00 p.m., after which there was an opportunity for agency representatives, members of the public and the IRP to comment and otherwise exchange impressions and information.

[1] Dr. Nestler will provide advice to the Panel on subjects relative to his expertise on eco-hydraulics and coupled hydrodynamics and fish behavior modeling. He is not tasked with written assignments for the report development.

Subsequent IRP communication and deliberations were conducted via email and conference call in the course of drafting this final report.

EXECUTIVE SUMMARY

The review panel appreciates the unique challenges and constraints faced by all of the agencies attempting to balance existing commitments and mandated coequal goals of (1) providing a reliable water supply for California and (2) protecting, restoring and enhancing the Delta ecosystem from which water resources are derived for a multitude of human uses. We continue to commend all of the agencies charged with this daunting task for their efforts to date as they strive to cooperate and integrate activities directed at achieving this goal within the context of persistent change in environmental and socioeconomic conditions.

The dry 2012 water year presented a greater challenge to achieving specific RPA targets than was the case in the previous year and confirmed concerns expressed in Anderson et al. (2011) that some physical targets may not be routinely achievable. After three years of operating under the RPA actions, observations are available for a small sampling of both wet and dry years. Although it still remains too early to make definitive assessments of long-term effects on listed species populations, signs linking specific RPA actions to improved conditions remain elusive. Nonetheless, as noted by the two previous OCAP IRPs, the current LOO IRP emphasizes the continued need to explicitly link the success or failure of meeting physical targets prescribed in the RPAs to the biological/ecological responses of the listed species.

The IRP was encouraged by a perceived movement toward research aimed at measuring the survival and behavior of fishes within a spatially-explicit landscape relevant to water operations. Inclusion of more ecological and behavioral responses of the fish populations or life stages targeted by the RPA actions continues to be recommended as multiple years of observations become available.

The regular evaluation of goals and objectives is as much a part of an adaptive management strategy as are decisions to alter actions when justified by novel observations and response data that deviate from expectations. It is not too soon to step back and consider whether the intentions of habitat restoration efforts are tracking toward expected outcomes. If positive effects on listed species are not detectable following a series of “good” water years in the future, concerns about the detectability of effects under less favorable conditions will persist.

Findings from recent research reported at the 2012 LOO Workshop corroborated previous expectations of nonconformity in behavior of salmonid smolts and passive particles within the context of water flows and routing through the Delta. Consequently,

the application of passive particle models as a means of adjusting water operations to protect out-migrating salmonid smolts in real-time is not recommended. The IPR encourages a shift in the water management paradigm to include a more fish centric behaviorally and ecologically based perspective.

The IRP appreciated the opportunity to concentrate on a focal subset of RPA actions this year but wondered about progress, biological responses and consequences in applying the many other prescribed actions within the watersheds. The inclusion of maps for geographic orientation to the portion of the system under discussion was helpful to a degree and appreciated, but still fell short of expectations.

Finally, the time allotted at the workshop for panel deliberations (5.0-5.5 hrs) on the second day was again much appreciated and provided adequate time for the IRP members to organize thoughts and reach some consensus prior to presenting preliminary findings in the afternoon. We continue to encourage a similar time allotment for deliberation by future panels.

Table of Contents

INTRODUCTION

The Sacramento-San Joaquin watersheds and Delta comprise a complex system of distributaries, reservoirs, human-engineered channels, levees and a mix of agricultural and urban areas that have replaced former wetlands and floodplains. Significant structural alterations of the ecosystem date back to the mid-nineteenth century. Many of the anthropogenic changes in the Delta and its upstream tributaries were designed to store, redirect and convey water to meet human demands within the region, with little consideration for other biotic components of the ecosystem.

The chronic multi-decadal alteration of the natural ecosystem associated with meeting the demands of an increasing human population within and beyond the Central Valley watersheds have contributed to profound changes in the system's aquatic fauna, including a persistent decline in certain species of native fishes. Consequently, some of these jeopardized species have been afforded protection under the Endangered Species Act (ESA).

Within the historical context of engineered water resource management, formal legislative recognition that water and other habitats should be managed to restore and enhance the ecosystem as a coequal goal with providing a reliable water supply to California (Delta Reform Act) represents an ambitious and novel conceptual approach to water management within the region. Ultimately, the ability to meet this mandate appears to rest largely on adjusting existing water operations within the context and constraints of a system developed and engineered to primarily achieve one of these goals. If an appropriate combination of localized spatial and temporal deliveries of water cannot be found to maintain or restore the necessary ecological conditions to support the desirable species populations, the most feasible alternative may be to accept the ecosystem components that are sustainable within the constraints and limitations imposed by historical uses of the available limited resources.

***Background on the LOO RPA review process*:** NOAA's National Marine Fisheries Service (NMFS) and the U.S. Fish and Wildlife Service (USFWS) have each issued Biological Opinions on long-term operations of the Central Valley Project (CVP) and State Water Project (SWP, hereinafter CVP/SWP; Long-term Operations Opinions) that include Reasonable and Prudent Alternatives (RPA) designed to alleviate jeopardy to listed species and adverse modification of critical habitat. NMFS' Opinion requires the U.S. Bureau of Reclamation (USBR) and NMFS to host a workshop no later than November 30 of each year to review the prior water year's operations and to determine whether any measures prescribed in the RPA should be altered in light of new information (NMFS' OCAP Opinion, section 11.2.1.2, starting on page 583). Amendments to the RPA must be consistent with the underlying analysis and

conclusions of the Biological Opinions and must not limit the effectiveness of the RPA in avoiding jeopardy to the ESA listed species or result in adverse modification of critical habitat.

The purpose of both Long-term Operations Opinions (LOO) is to present the responsible agency's biological opinion on whether USBR's and DWR's long-term operations of the CVP/SWP are likely to jeopardize the continued existence or adversely modify the designated critical habitat for the ESA listed species under each agency's jurisdiction. Because both Long-term Operations Opinions concluded that the long term operations of the CVP/SWP are likely to jeopardize the continued existence or adversely modify designated critical habitats, the USFWS and NMFS prescribed RPAs to minimize CVP/SWP operations related effects to the level where these effects do not appreciably reduce the likelihood of jeopardizing the continued existence of ESA listed species or adversely modifying critical habitat. The RPA in NMFS' Long-term Operations Opinion (2009 RPA with 2011 amendments) includes both broad and geographic division specific RPA Actions. The RPA Actions in both Long-term Operations Opinions provide specific objectives, scientific rationales, and implementing procedures.

Since the Long-term Operations Opinions were issued, NMFS, USFWS, USBR, U.S. Geological Survey (USGS), California Department of Fish and Game (CDFG) and the DWR have been performing scientific research and monitoring in concordance with the implementation of the RPAs. Technical teams and/or working groups, including the geographic divisions specified in the NMFS' Long-term Operations Opinion, have summarized their data and results following implementation of the RPA Actions within technical reports. The data and summary of findings related to the implementation of the RPAs provide the context for scientific review regarding the effectiveness of the RPA Actions for minimizing the effects of water operations on ESA listed species and critical habitat related to the operations of the CVP/SWP. However, not all technical reports were included in the official review materials to be considered by the 2012 LOO IRP (see Appendix 1).

In January 2012, Public Water Agencies (PWA), State of California and Federal agencies filed a joint stipulation regarding project operations during April and May 2012 in the litigation relating to NMFS' Long-term Operations Opinion. The parties stipulated that if a rock barrier were installed at the head of Old River, the CVP/SWP would operate within an adaptive range of Old and Middle River flows in lieu of operating to the inflow:export ratio specified in RPA Action IV.2.1 of NMFS' Long-term Operations Opinion.

At the request of USFWS and NMFS, the Delta Science Program (DSP) employed the services of an independent science review panel to assist NMFS and USBR in reviewing the effectiveness of the implementation of NMFS Long-term Operations Opinion RPA and documents associated with the implementation of the joint stipulation. The role of the Independent Review Panel (IRP) is to provide a technical review to the agencies involved in implementing NMFS' Long-term Operations Opinion RPA.

The intent of the annual review is to inform National Marine Fisheries Service (NMFS) and U.S. Fish and Wildlife Service (USFWS) as to the efficacy of the prior year's water operations and regulatory actions prescribed by their respective Reasonable and Prudent Alternatives (RPAs), with the goal of developing lessons learned, incorporating new science, and making appropriate scientifically justified adjustments **to the RPAs or their implementation** to support water year 2013 real-time decision making.

General scope and charge to the 2012 LOO IRP: The previous two annual reviews have considered all of the RPA Actions but this year's panel charge focused on a subset of the RPAs primarily related to water operations and populations of Chinook salmon (*Oncorhynchus tshawytscha*) and Central Valley steelhead (*Oncorhynchus mykiss*) within portions of the San Joaquin and Sacramento watersheds and Delta.

This year's annual review deals with the implementation of NMFS' Long-term Operations Opinion's Clear Creek RPA Actions (I.1.1 – I.1.6) and the Spring 2012 Delta Operations in lieu of NMFS' RPA Action IV.2.1 per joint stipulation (Spring 2012 Delta Operations) for operations and fisheries for water year 2012 (October 1, 2011 through September 30, 2012) and considers:

(1) Whether implementation of the Clear Creek RPA actions met the intended purposes of the actions;

(2) The agency's responses to and implementation of independent review panel recommendations from the prior year's Long-term Operations Opinion Annual Review on the Clear Creek RPA actions;

(3) Study designs, methods, and implementation procedures used; and

(4) Recommendations for adjustments to implementation of the RPA Actions or Suite of Actions for meeting their objectives.

Five questions (some multi-part) were posed to the 2012 IRP panel and defined the scope of the panel's charge. This report addresses each of the questions posed and provides additional observations and opinions where they seemed relevant and potentially useful from a scientific perspective.

***Acknowledgements*:** The members of the IRP appreciate and acknowledge the efforts of the agency and technical team representatives and contractors who prepared the written materials and delivered the workshop presentations that were the basis for this report. We recognize that much of the material had to be compiled, analyzed and organized in a relatively short time. Despite the many competing demands on the workshop participants, the materials were presented professionally, concisely, on schedule and often were responsive to the previous IRP's recommendations for format changes. The panel wishes to express a special thanks to the Delta Science Program, Peter Goodwin (Lead Scientist), Sam Harader (Program Manager) and the entire staff for providing the organization and logistical support to facilitate our task. In particular, Lindsay Correa (Environmental Scientist), as usual, expertly attended to a wide variety of technical and provisional details in support of the IRP's efforts before, during and following the workshop.

LOO IRP COMMENTS ON RPA ACTIONS IN WATER YEAR 2012

General comments and observations

Some of the NMFS RPA actions and Joint Stipulation commitments have yet to be implemented or completed and so the 2012 IRP is unable to develop an opinion as to whether or not they have or will meet their intended purpose. These include:

(1) Action I.1.2. Channel Maintenance Flows from re-operation of the Whiskeytown Glory Hole spills to include mean daily spills of 3250 cfs for one day to occur 7 times in a 10-yr period. This action was targeted for implementation in winter 2013 and will likely be delayed until 2014, so once again was not implemented and cannot be evaluated.

(2) Action I.1.3. Spawning Gravel Augmentation was once again performed but there was little information available to evaluate whether it is meeting the intended purpose. The written report from the Clear Creek Technical Team (CCTT) contained a note to "[insert section here]" that may have been intended to provide salmonid or macroinvertebrate responses to the RPA. During the LOO 2012 workshop in Sacramento the CCTT indicated that the data were not currently available.

(3) Action I.1.4. Replacement of Spring Creek Temperature Control Curtain in Whiskeytown Lake. This action was completed by the Bureau of Reclamation in June 2011, but there was no test of its effectiveness that would allow an evaluation of the intended purpose of the action. Furthermore, the intended effect of the curtain was to lower water temperatures delivered to the Sacramento River and not necessarily Clear Creek, which was the focus of this year's annual review.

(4) Action I.1.6. Adaptively Manage to Habitat Suitability/IFIM Study Results. Although the IFIM Study is completed, results were not provided for evaluation, so the IRP is unable to formulate an opinion this year.

(5) In the Joint Stipulation Order (Case 1:09-CV-01053-LJO-DLB, Document 660, filed 01/19/12, p 6 and 7 of 11), DWR committed to developing a study for a pilot predator removal and control program to be submitted to NMFS and CA-DFG for review and comment and "if a rock barrier is installed (at the head of Old River), a predator monitoring study will evaluate predation associated with the installation and operation of the rock barrier". At the workshop there was some verbal mention of these activities having been carried out, but no data were provided to the IRP for evaluation.

Hydrographic analysis

Annual planning and decisions on water operations are based, in part, on qualitative categories (e.g., wet, above normal, below normal, dry and critical) of water availability derived from indices of unimpaired runoff measured during two periods within the year, with an adjustment for the previous year's conditions. However, the approach provides little room for forecasting conditions in an upcoming water year, except perhaps for an implicit expectation of a relatively dry year (i.e., 60% of the WY categories are less than "normal"). The ability to plan for alternative decisions on water use based on predicted near-term climate conditions (e.g., global patterns in sea water temperatures driving El Niño-Southern Oscillation events) would contribute to the improvement of real-time responses required to meet the intentions of RPA Actions.

Given the wealth of annual flow records available to various technical groups, it is almost imperative that a more concise analysis of rainfall patterns and overarching landscape-level climatic patterns be accomplished in order to create the most effective adaptive management strategy. One of the goals of restoring the system will be to recreate or simulate previously existing hydrographic cues; that is, an effective benchmark period must be created. In most cases, the previous 20 to 40 years are not useful tools. . The effect of climatic change and other phenomena make this arbitrary period an inappropriate target which sets target flows. With increasing observations of linkage between long-term oscillations in oceanic temperature and/or changes in climatic trends *(*e.g., Werritty 2002, Hannaford and Marsh 2006, and Maurer et al. 2004), it is increasingly important to understand regional runoff patterns so that an effective benchmark target can be identified (Kelly and Gore 2008). Maurer (2007) and Cayan et al. (2008) have done extensive modeling of potential climate change scenarios and could offer insights into changes in runoff that might affect management decisions. The IRP suggests that a review of annual flow records to detect any predictable patterns influenced by the Pacific Oscillation as well as proposed scenarios for climate change in California will be useful exercises to "fine-tune" future management options.

IRP responses to questions defining the charge and scope of the 2012 LOO annual review

The 2012 Annual Review focused on NMFS' Long-term Operations Opinion's Clear Creek RPA Actions (I.1.1 – I.1.6) and the Spring 2012 Delta Operations:

Implementation of actions

1) **How well did implementation of the Clear Creek RPA Actions and Spring 2012 Delta Operations meet the intended purposes of the actions?**

Clear Creek RPA Actions

There were six Clear Creek RPA Actions to consider this year, but some were not conducted (e.g., Action I.1.2, Channel Maintenance Flows) or the information necessary to determine whether the intended purposes were met was sparse or lacking.

Spring attraction flows (Action I.1.1) provided pulses of 400 and 800 cfs from Whiskeytown Lake instead of the minimum of two 600 cfs pulses described in the RPA Action. The intention of this action is to attract adult spring-run Chinook holding in the Sacramento River into Clear Creek. Although the pulses moved gravel downstream (a stated secondary purpose), the CCTT report (Page 5, para. 4) opined that fish monitoring results were inconclusive - just as they were in 2010 - due to low adult counts. The IRP agrees that the 2012 counts were disappointingly low. However, one can still statistically evaluate the effects of pulses on the counts. In 2012, nine fish were seen before the first pulse, 13 after the first pulse, and 39 after the second. If the pulses had had no effect, then one would expect these 61 fish to have been equally distributed among the three surveys, with about 61/3 = 20 fish seen in each survey. However, a chi-squared goodness of fit test (Zar 2010) rejects this equal-distribution null hypothesis ($P<0.001$, chi-squared = 26.1, df=2). Thus, there is evidence for a nonrandom difference in counts between the surveys, presumably (but not necessarily) due to the pulse flows. This same test, using "exact" P-values, can also be applied to the even-lower counts of 2010 and 2011.

Channel maintenance flows (Action I.1.2) were not performed and were once again delayed until 2014. Discharges of about 3000 cfs were common events in the past and discharges above 5000 cfs are most likely required to establish geomorphic threshold crossing events. A one day spike of 3,250 cfs will not complete much in the form of geomorphic work other than water some rocks and result in negative ecological impacts to Clear Creek. Small pulses of 400 to 800 cfs have stage increases of 0.5 - 1 ft at the confined location of the Igo gauging station. These would barely be measurable

differences in terms of stage along the floodplain sites where most of the spawning and rearing habitat exists.

Spawning gravel augmentation (Action I.1.3) was intended to enhance and maintain previously degraded spawning habitat for spring-run Chinook and CV Steelhead. In 2011, 10,000 tons of gravel was placed at 5 sites in Clear Creek. Again there was no reliable metric to determine whether or not these augmentations are replacing or enhancing the quality of the spawning habitat for the targeted salmonid species or other fish and macroinvertebrate assemblages. Despite this lack of reliable metrics to gauge success, there is a clear intention to continue the spawning gravel augmentation project, with a concern expressed about the future source of gravel. The current plan is to use mine tailings that will be washed to remove the finer sediments containing mercury and potentially other contaminants and use a retention pond to permanently isolate those contaminants from the watershed. It is unclear how the quality of spawning habitat might be affected.

Replacement of the Spring Creek Temperature Control Curtain (SCTCC) (Action I.1.4) was intended to reduce adverse impacts of project operations on water temperatures for listed salmonids in the Sacramento River. The USBR replaced the SCTCC in Whiskeytown Lake on schedule in June 2011 at a cost of $3 million. However, unidentified “technical problems” with monitoring equipment apparently precluded pre-project monitoring to evaluate the effectiveness of this action. Effects, if any, of the SCTCC on temperatures in Clear Creek were not considered. However, in connection with the discussion on this temperature curtain, the IRP was informed that the Oak Bottom temperature control curtain (OBTCC) in Whiskeytown Lake was also damaged and in need of replacement or repair. While the agencies involved seemed to agree that the OBTCC should be replaced, no plan was advanced to test its effectiveness in meeting the intention of this action. It is unclear how the effectiveness of these temperature control curtains on water temperatures will be determined in either the Sacramento River or in Clear Creek.

Thermal Stress Reduction (Action I.1.5) was intended to improve conditions in Clear Creek for over-summering steelhead and spring-run Chinook during holding, spawning and embryo incubation. Seasonal temperature target maxima in Clear Creek at the USGS Igo gauge (about 6.5 miles downstream of Whiskeytown Dam) were set at 60° F during June 1 to September 15, and 56° F during September 15 to October 31. Thus far during 2009-2012, the temperature target was achieved consistently during the June to mid-September period, but frequently failed to be met during mid-September to October. In 2012, the temperature during this period exceeded the target maxima 69% of the time. During 2009-2011, temperatures exceeded the target 38% to 72% of the

time. In prior years (2001-2008) temperatures at the Igo gauge exceeded the temperature target during September and October only 7% of the time. Once again there was mixed success in meeting the physical targets set by this RPA Action and no biological response data on which to base an opinion as to the intended effects on salmonids.

The Clear Creek Technical Team (CCTT) put forth a complex hypothesis that involved potential impacts of an interaction involving the Oak Bottom and Spring Creek temperature control curtains and the effects of “power-peaking” at generating stations above Whiskeytown Lake as a possible explanation for the failure to meet the conditions of Action I.1.5 during mid-September to October in recent years. There seemed to be agreement among the agencies that the Oak Bottom Temperature Control Curtain (OBTCC) was in need of replacement but there was no consensus regarding the role of power-peaking in current conditions.

There was a paucity of hard evidence provided to the IRP on which to form an opinion as to the scientific soundness of alternative hypotheses to explain the temperature observations at the Igo gauge.

Adaptively Manage to Habitat Suitability/IFIM Study Results (Action I.1.6) was intended to improve habitat conditions for spring-run Chinook and steelhead by adaptive management of flow conditions that favor salmonid survival. This Action is associated with what is perhaps the least definable objective. Also the IFIM Study which began in 2004 has been completed but reports on the findings were not available to the 2012 IRP. Consequently, there is no basis on which to develop an opinion as to the effectiveness of this RPA Action at this time.

Spring 2012 Delta Operations

There were three objectives to the Spring 2012 Joint Stipulation agreement:

(a) to provide for minimum protection of out-migrating juvenile steelhead by managing flow conditions in the Delta in a manner expected to allow salmonids to successfully exit the Delta;

(b) to increase water exports consistent with the protection mentioned in (1) above;

(c) to generate real-time tracking information in order to better understand how pumping rates, flows in Old & Middle Rivers, and juvenile steelhead migrations relate to one another.

The agreement called for installing a rock barrier at the head of Old River and managing flows in Old & Middle Rivers within an adaptive range of -1250 to -3500 cfs during April and -1250 to -5000 cfs during May. A predation study associated with the rock barrier was also required as part of a predator control study. The rock barrier was not completely impermeable and had several open culverts through which water and fish could pass into Old River.

In terms of meeting the intended purpose of the joint stipulation, increased water exports (a portion of Objective b) was achieved. Exports were ca. 57,000 acre ft greater than would have occurred under the NMFS RPA Action IV.2.1 (inflow:export ratio). The water provision side of the stipulation was achieved. While this was described as a "modest" increase in water supply, its significance should be considered within the context of the 2012 water year (WY) being categorized as "critical" and only upgraded to "dry" near the middle of May and the end of the joint stipulation period. NMFS determined that no further adjustments were needed as a result of the change in WY classification.

As for meeting the intended purpose of the biological portion of the agreement (protection of juvenile steelhead and clarification of the relationships between fish migration and inflows/exports), the IRP was unable to determine the level of success or failure for several reasons including the following.

The decision to install a rock barrier at Head of Old River (HORB) was based upon an assumption that it would not enhance predation on salmonid smolts; a previously tested non-physical barrier (bubble curtain) was shown to enhance the risk of predation mortality on smolts, which was the primary reason given for not using that approach.

Estimates of mortality used in setting the triggers for the number of tagged smolts that could be entrained by water operations depended on the assumption that the HORB did not enhance predation risk. Although testing that assumption was one of the conditions of the Joint Stipulation agreement, the 2012 IRP was not informed as to the outcome of any study to test predation associated with the rock barrier.

Furthermore, findings of the 2011 VAMP acoustic tag study, which estimated route-specific survival rates of tagged Chinook smolts, found that the highest survival rate through the Delta was via Old River. Most (64%) of the tagged smolts surviving to Chipps Island did so via artificial transport from the CVP holding tank. The HORB was intended to inhibit migration of smolts via Old River (the shortest route to the CVP holding tank) and as a consequence enhanced negative OMR flows, which may have

encouraged higher smolt entrainment into the southern Delta via alternative routes. Data presented by the VAMP study showed that forcing smolts through the Delta by blocking the entrance to Old River decreased survival, presumably due to predation through the central Delta region.

The Spring 2012 plan for water operations focused on characterizing smolt movement with mean project operations, OMR flows, pump exports and I/E ratio. The plan appeared to be based upon the assumption that fish movements and survival would be correlated with measures of mean flow. However studies cited in the Tech Memo demonstrated weak correlations between smolt movement and particle tracking model studies and between project operations, OMR flows and smolt movement and survival. Studies available in the literature and many published in the region have demonstrated that fish movement across a wide range of taxa exhibit behavioral response to tidal oscillations. These behaviors facilitate either the retention of species in the Delta, or upstream/downstream movements necessary to complete their life cycles. The importance of tidal dynamics on smolt migration and interactions with predators and pumps received limited attention in the 2012 operations. When it was addressed it was in the context of tidal effects on passive particle movements.

It was emphasized by the 2010 OCAP IRP (Anderson et al. 2010, p 24) and confirmed by the Acoustic Tag Study conducted in April-May 2012 that steelhead smolts do not behave like passive particles and it was simply inappropriate to rely on the PTM to direct water operations intended to protect out-migrating juvenile steelhead. The effects on steelhead smolt survival could not be determined and this action cannot be described as providing any level of protection for steelhead.

The IRP believes that discerning behavioral responses of smolts and predators to tidal oscillations is crucial for understanding variation in salmonid survival within the Delta, and abundant information is available on the significance of tidal factors. Consequently, the IRP concludes that the best available information was not used in planning the 2012 Delta Operations.

2011 IRP recommended adjustments for Clear Creek Actions

2) **Where the 2011 Independent Review Panel made recommended adjustments to implementation of the Clear Creek RPA Actions,**
    a) **Were the adjustments made?**
    b) **How well did these adjustments improve the effectiveness of implementing the actions?**

The Clear Creek technical Team (CCTT) report and presentation frequently acknowledged the suggestions of the 2011 IRP. The recommended suggestion

regarding gravel size in the spawning gravel augmentation program were followed but there were no biological response data upon which to base an opinion regarding whether or not this suggestion improved effectiveness of the action.

Although the CCTT agreed with the 2011 IRP's suggestion for improved temperature and flow modeling in the system, especially for Whiskeytown Lake, this has yet to be undertaken.

Also, the IRP suggestion to give a more natural hydrograph shape to the pulse release flows was not done. The 2012 IRP reiterates these last two suggestions.

Effectiveness of coordinating real-time operations with CCTT input

3) **How effective was the process for coordinating real-time operations with the Clear Creek technical team analyses and input as presented in NMFS' Long-term Operations Opinion [NMFS' 2009 RPA with 2011 amendments (pages 8-9)]?**

The CCTT Report lists topics associated with coordinated long-term operations on eight dates between December 15, 2011 and September 20, 2012 but there appeared to be no real-time operation effects related to analysis and input. However, there appeared to have been at least two incidents relevant to the implementation of actions. These were (a) a week-long period (June 3-11, 2012) during which warmer than intended water was released from Whiskeytown Lake due to an upper release gate being "inadvertently" left open, and (b) operations at the Redding power station which apparently is not under the control of USBR. The presentations from the CCTT and USBR made at the workshop in Sacramento on October 31, 2012 along with subsequent discussions with the IRP suggested that there may be a need for improved coordination between real-time operations and some of the RPA Actions intended to benefit salmonid populations in Clear Creek.

Indicators, study designs, methods and implementation procedures

4) **(a) Were the scientific indicators, study designs, methods, and implementation procedures used appropriate for evaluating the effectiveness of the Clear Creek RPA Actions and the Spring 2012 Delta operations?**

The approach in the Tech Memo was clearly articulated. Whether it was supported by the best available science prior to the study is less clear. In general, there can be little certainty as to the effectiveness of the indicators, study designs, methods and

implementation procedures without reliable and accurate measures of biological responses.

Clear Creek RPA Actions

In general, the CCTT report tended to consider progress toward meeting RPA Action targets as a measure of success, which could be appropriate for actions intended to follow some expected trajectory over time (e.g., multi-year projects) but most actions are not defined in that manner.

A list of restoration goals have been created by the CCTT, but these goals must be continuously reviewed as studies are completed or different goals and endpoints are identified. These goals cannot remain static and the IRP urges the CCTT to review these goals annually to determine if the objectives and endpoints remain realistic. “River restoration” has been variously defined in the literature over the past three decades, ranging from “the complete structural and functional return to a pre-disturbance state” (Cairns 1991) to something less than ideal [“a return to an ecosystem which closely resembles unstressed surrounding areas”] (Gore 1985). Four overall targets can be identified (modified from Brookes and Shields [1996]):

Target	Definition	Management Approach
Full Restoration	Complete functional and structural return to an identified pre-disturbance conditions	Direct intervention, natural recovery, or enhanced recovery
Rehabilitation	Partial return to an identified pre-disturbance condition	Direct intervention or enhanced recovery
Enhancement	Any improvement in physical or biological quality	Mainly direct intervention
Creation	Development of a resource that did not previously exist, including “naturalization’ which creates a configuration of contemporary magnitudes and rates of riverine processes	Direct intervention

Gore and Shields (1995) argue that rehabilitation is probably the most likely obtainable target, yet the most expensive, while creation or abandonment of the project, is least expensive but most manageable. Targets continually shift in this broad spectrum of possibilities and the CCTT should consider modifying these targets as a component of their adaptive management strategy.

One of the goals of this project is the completion of the IFIM studies in order to create an adaptive management strategy. The successful completion of this study should allow the analysis of the appropriateness of other activities such as gravel augmentation and the achievement of restoration goals. It is imperative that the results of IFIM studies be reported. An adaptive management plan provides the flexibility that allows managers to respond to future change. These strategies must adapt to the actual results of the Clear Creek restoration plan as it progresses, yet one of the fundamental tools for the development of these strategies, after 16 years of restoration planning and work remains incomplete. The location, duration, and availability of habitat (as expressed as weighted usable area in PHABSIM or other habitat simulations]) over time under various operational scenarios can become a valuable planning tool.

Ultimately, completion of the IFIM study will require the correct choice of index period; that is, the previous historical records that best replicate natural hydrographs in the region, assuming that restoration of the hydrograph is, indeed, an acceptable restoration target. The choice of index period can be important as it must include a target condition prior to alteration *and* include the effects of regular climatic changes such as the Pacific Oscillation (see comparable work by Kelly and Gore, 2008, in the Southeastern US) and the effect of changing land use in PHABSIM predictions (Casper et al. 2011). For example, with changes in the Atlantic Multidecadal Oscillation, PHABSIM predicts a significant change in both fish and macroinvertebrate communities with each cycle (Warren and Nagid 2009) with shifts in dominant functional feeding groups and species composition, among macroinvertebrates, and top carnivores in the fish community. Such modeling results allow the focus of management strategies to shift as natural hydrographic conditions change.

During the CCTT presentation and later discussions at the workshop in Sacramento, it appeared that the team did not yet have an effective way to assess the effect of the temperature control curtains on temperatures of water releases from the reservoir into either the Sacramento River or Clear Creek. Also, there was a greater emphasis on relatively small (a few degrees) decreases in the temperature of the water released from Whiskeytown Lake rather than on stream water temperature when it reached targeted reach boundaries such as the Igo gauge, approximately 6.5 miles downstream or the lower reaches of Clear Creek approximately 12 miles from the dam.

Gravel augmentation has been a very active restoration activity in Clear Creek since 1996 (150,000 tons) and is planned to be continued into the future ($4.5 million). At this point there is insufficient data to support the ecological effectiveness of the gravel augmentation activities. It appears that two related responses follow this restoration

activity. Spawning increases a couple percentage points and then just as rapidly declines (Fig. 9 CCTT 2012 report).

The CCTT 2012 report alludes to physical monitoring since 1996 and Figure 10 and 11 in that report show that pulse flows since 2009 have moved gravel in the Dog Gulch site just below Whiskeytown Dam, but there was less movement of gravel in the Peltier site just downstream. The IRP was unable to determine the type of data that were collected to distinguish the spread of gravel from the existing stream bed or how the magnitude of movement was assessed.

Spawning seems to occur very near the channel banks which may be a species preference or it could be that these areas had less gravel. At the 2012 LOO workshop, it was indicated that the channel was deeper at the edges as a result of how the gravel was placed and perhaps how the river flow encountered the gravel deposits. However, this only underscores the need to step back and quantitatively evaluate a set of metrics aimed at testing the restoration goals.

An independent 2005 review specifically of gravel augmentation practices in the Central Valley listed 20 unanswered questions concerning gravel augmentation practices (Lave et al. 2005.). One of the largest data gaps for Clear Creek, and most likely for the other sites, is linking threshold entrainment to discharge and routing/deposition of gravel through Clear Creek system.

The long-term future source of material for the gravel augmentation activities will come from mining tailings and hence there may be a potential to introduce additional mercury contamination to the system. The direct transfer of mercury - and other metals from sediments - through the aquatic food chain is a concern wherever past mining is prominent, such as in the Clear Creek basin. Fine sediments contain the higher levels of mercury then gravel and the fine bed sediments of Clear Creek have been shown to contain mercury levels 2 to 10 times natural background levels (Moore 2002).

Gravel augmentation seems to encourage spawning and hence the excavation of redds. There is also an expectation that gravel augmentation will result in favorable alterations of channel morphology. Both small- and large-scale morphological changes to the bed can result in an increased flow of hyporheic water through the surface sediment. Merz et al. (2004) reported on the possible benefits of gravel augmentation on spawning bed enhancement showing that it increases survival and growth of Chinook salmon embryos in the Mokelumne River. Other authors have shown the exchange of hyporheic water enhances the formation of riffle complexes with measurable impacts in terms of moderating riverbed water temperature (Grant et al. 2006a, b, Hanna et al. 2009). Brown et al. (2007) showed that spatial variation in sediment source resulting from flood

transport of mine tailings along with temporal changes in hydrology, combine to dictate the role of the hyporheic zone in the transport and retention of arsenic.

In the lower reaches of Clear Creek bed sediments have mercury concentrations that are already above background levels and high flows that scour the bed reintroduce fine sediments into the flow. This coupled with gravel augmentation could be enhancing geomorphic change that in turn enhances hyporheic water flow through sites that encourage spawning soon after mobilization of the gravel. If so, gravel augmentation and flushing flows could be encouraging spawning in gravels where intra-gravel flow contaminated fines passed through incubating salmon embryos. The total net effect on salmon reproduction from the restoration activities of gravel augmentation coupled with flooding is unknown but it is not unlikely that gravel augmentation to encourage salmon spawning in an already highly contaminated creek bed could adding an additional layer of stress detrimental to the survival of the very species it is trying to help.

Indeed, Moore (2002) in discussing Clear Creek specifically states:

> *"Understanding the distribution of such widespread contamination is essential to river restoration, especially where dredging, filling, excavation, floodplain construction and changing sediment dynamics may lead to remobilization of contaminants from the riverbed/floodplain, making them more bioavailable. Specific river restoration efforts can also be stymied by bed-sediment contamination, especially those designed to increase/recreate fish spawning habitat. An example is the dependence of some salmonids on areas of upwelling through a gravel bed. If the bed is contaminated with mercury or other heavy metals, geochemical reactions within the bed can release contaminants to the water that irrigates fish eggs. This increased metal loading can decrease reproduction and productivity at spawning sites."*

The IRP recognizes that the plan is to wash the gravel used in the augmentation and remove the more heavily contaminated fine sediments, storing them in containment areas. However, this commits one or all of the agencies involved to the perpetual obligation of preventing the concentrated contaminants from entering the watershed.

The CCTT Report also included speculation about what may be learned through the use of both video and sonar. There are many "may"s here. The IRP suggests that CCTT members posit some specific, realistic outcomes from these two monitoring sources and think through exactly what conclusions could be drawn before investing substantial financial resources in video and sonar monitoring programs.

Spring 2012 Delta Operations

The study design for real-time operations using acoustic tagging material was inadequate to develop real-time operations. The operations were based on the arrival of fish at specific points in the inner Delta which were adjusted over the season because the fish arrived at the target points earlier than expected.

The general project operations have been managed in terms of the mean flows in OMR and in the San Joaquin River. This has been the fundamental approach for operations of the system for years but has resulted in inadequate protection for fishes. In part, this is because attempts to understand the movement and survival of fish through the Delta to date have not considered effects of tides, which are the dominant control on flow velocities and mean direction of flow.

Delta survival of steelhead, and especially Chinook, was extremely low based on tagging studies. Characterizations of survival in terms of river km or mean flow are inadequate because the rapid travel time and complex routing of fish through different reaches cannot be explained by these mean measures. The IRP suggests the travel, routing and survival of fish through the system needs to account for migrant behavior and the behaviors of the predators in response to the strong tidal influences in the Delta (see Appendix A2.2: Selective Tidal-Stream Transport).

The acoustic tagging experiment also had logistic and possibly methodological difficulties from the start, so reliability of the results is questionable for reasons that will be explained subsequently. Second, when difficulties were encountered, there was an attempt to use an “adaptive management” approach in real-time that only seemed to complicate the situation. Adaptive management requires that something be learned before adjustments are made, it was not intended to simply take another course when things are not going as intended in real time. There were two substantial examples of this:

(1) When the acoustic tagging study could not begin on April 1, the Particle Tracking Model (PTM) was substituted as a means of providing input into decisions regarding water operations for the purpose of protecting juvenile steelhead. As mentioned earlier, there was no means of determining whether or not this approach provided even minimal protection for out-migrating smolts.

(2) The original plan for the acoustic tag study was to run water operations in a manner that allowed OMR flows in the range of -1250 to -3500 cfs in April and -1250 to -5000 cfs in May. However, when the tagging study had logistical difficulties that delayed its start for 2 weeks a series of decisions was made that altered the experimental design.

After the first release of tagged smolts on April 16, when OMR flows of -3500 cfs were planned the number of tags entrained in the south Delta exceeded the trigger within 4 days and after a delay of 2 more days OMR flows were reduced to -1250 cfs through April 30. At this point, a decision was made to raise the trigger and switch the experimental treatment level to OMR flows of -5000 cfs instead of the -1250 cfs planned for May 1-15. Two days after release of the second group of tagged smolts the trigger was once again exceeded and, because of other constraints on water operations, flows were reduced to -1250 cfs for the remainder of the period (May 8-12) following a 5 day delay. The response was to raise the trigger once again and schedule operations to flows of -5000 cfs for the finally period as originally planned. Five days after the final release of tagged smolts, the highest trigger was exceeded and flows were reduced to -1250 cfs during May 23-28. Consequently, the apparent attempt at real-time "adaptive management" during this experiment resulted in a substantial alteration of the original experimental design that weakened the test for effects of flow on steelhead smolt survival and routing as follows:

Time Period	Original Plan	As Conducted – Spring 2012
April 1-15	-1250 cfs for 14 days	-1800 cfs Apr 1-7; -2500 cfs Apr 8-14; No Tags
April 16-30	-3500 cfs for 14 days	-2446 cfs for 7 days
May 1-15	-1250 cfs for 14 days	-2933 cfs for 7 days
May 16-31	-5000 cfs for 14 days	-5193 cfs for 7 days

Note that the changes implemented did not allow for any measurement of tagged smolt survival and routing under the lowest OMR flows (-1250 cfs) and the intermediate flow treatment level (-3500 cfs) was not achieved. Instead, two of the flow treatment levels were so similar (-2446 cfs and -2933 cfs) as to be functionally identical and there was no minimum flow regime included in the experiment as conducted. However, this did not seem to deter reaching the conclusion that there was no relationship between OMR flows and smolt entrainment to the interior Delta. This is too broad a conclusion to draw from the altered experimental design. It remains entirely possible that entrainment is related to OMR flows within any range between -2446 cfs and >0 cfs and becomes asymptotic at some threshold level of negative OMR flow.

Also, many of the study's initial conclusions are not adequately supported by the analyses because they fail to make use of statistical testing or confidence intervals. The analyses should be redone with greater statistical rigor, where possible. It is possible to test for evidence of a flow effect within the range of flow levels tested using the available data. We suggest recoding release groups 1 and 2 as "intermediate" OMR flow, and group 3 as "high" OMR flow. Then Groups 1 and 2 can be considered as independent replicates (n=2) of an "intermediate" flow treatment level, with Group 3 providing the only replicate (n=1) of a "high" flow treatment level.

Methodological issues with the acoustic tag study on steelhead smolts conducted under the 2012 Joint Stipulation Agreement.

The IRP recognizes that there were logistical, meterological and other difficulties beyond the control of the Department of Water Resources and their collaborators and contractors in conducting the Spring 2012 acoustic tag study. The LOO IRP also acknowledges that previous OCAP IRPs have consistently recommended studies to link biological responses and the physical targets in the RPA Actions. The attempt to move in this direction with the acoustic tag study was commendable and the following comments should not be interpreted as a criticism of those who attempted it.
As with most experiments, the credibility and reliability of the findings depends substantially on whether or not assumptions are reasonable or tested. The following were assumptions stated in the workshop presentation by Kevin Clark as applying to the Spring 2012 acoustic tag study:

(1) Tag detection probability at each location is high (>80%) and similar to the 2010 VAMP findings.

(2) Detection probability may vary among receiver arrays but not between release groups within arrays.

(3) No predator detection filter was required (i.e., all detections were assumed to be live steelhead, not tags carried by predators that had consumed tagged smolts).

(4) OMR flow differences between Group 3 and Groups 1 + 2 were sufficient to test the hypothesis that flows affect fish behavior.

(5) Sentinel hatchery steelhead and wild steelhead smolts behave similarly.

(6) Hatchery smolts released in the tidal portion of the San Joaquin River behave like river-run steelhead.

As to the first and second assumptions, the two studies used very different acoustic tags and receivers. The Joint Stipulation Study used VEMCO tags (V5) which transmit at 180KHz and VAMP uses Hydroacoustic Technology Model 795Lm tags which transmit at 307KHz. Both frequencies are suitable for use in freshwater but the detectable signal range of tags transmitting above 100KHz tends to be degraded with increasing salinity, turbidity, boat noise, etc. There was no mention of range tests conducted on the field arrays to verify this assumption. In tidal environments, one can also expect detection range to be affected by tidal movement and may differ at high and

low tides (for a good example see Pautzke 2008). These assumptions can and should be tested. If environmental variation within the Delta affected the detection range of the receivers that resulted in a systemic bias, it could result in reduced tag detections being incorrectly perceived as mortality. When detection probabilities are < 100% and are not properly accounted for, survival estimates are expected to be biased lower (Drenner et al. 2012).

The third assumption conflicts with observations from the VAMP acoustic tagging studies (Vogel 2010, 2011) which now attempts to apply a predator filter that accounts for a considerable number of tag detections.

The fourth assumption was considered earlier. The two points representing treatment level flows in this experiment are relatively high and so the findings only apply to OMR flows that are more negative than -2446 cfs. There is a large range of flows more positive than this value within which a relationship between flow and smolt behavior could still exist. This is a severe limitation on the findings of the Joint Stipulation Study.

The fifth and sixth assumptions are unlikely true, as several studies have demonstrated differences in the behavior and survival of out-migrating wild and hatchery salmonid smolts (e.g., Chittenden et al. 2008; also see reviews by Melnychuk et al. 2010 and Drenner et al. 2012).

Several other potentially important assumptions were not mentioned. Among these were that: (a) tagging does not affect survival, (b) there was little or no mortality from handling, (c) tag expulsion was minimal, (d) the tag burden (weight of tag:weight of smolt) was appropriate and similar across groups, and (e) that tags did not affect swimming performance or predator avoidance.

In a recent review of tagging studies to examine the behavior and survival of salmonids, it was noted that only 10.6% of studies reported in the 207 papers assessed tagging and handling effects and only about a third of the studies even acknowledged them (Drenner et al. 2012). Given that one of the logistical challenges mentioned in the joint stipulation study was a paucity of experienced personnel available to implant acoustic tags, this could have been a potentially important source of mortality and tag loss in this study. Given the constraints to conduct the study in Spring 2012 under difficult circumstances, it may be impractical to expect such an assumption to be rigorously tested, but lacking evidence to substantiate this and other assumptions provides reason to doubt the accuracy of the findings.

Information on the size of smolts used in each group was not provided, but VEMCO V5 acoustic tags weigh an average of 0.65 g. Ideally, tag burdens of no more than 2% are recommended for most species, and burdens in excess of ca. 5% are generally not recommend for salmonid smolts (e.g., Adams et al. 1998), suggesting that appropriate smolt sizes for V5 acoustic tags would be > 13 g. There have been very few studies assessing the effects of tag burdens on the behavior and survival of salmonids (Drenner et al. 2012). However, early short-term swimming performance and higher predation rates have been associated with juvenile Chinook salmon carrying surgically-implanted transmitters for radio telemetry (Adams et al. 1998).

Statistical issues with the acoustic tag study on steelhead smolts conducted under the 2012 Joint Stipulation Agreement.

Data analysis issues were not specifically addressed in the charge to the 2012 LOO IRP but the IRP believed it was necessary to comment on this aspect of the recent studies because statistical rigor is crucial for objectively interpreting apparent patterns in the results. For example, Figure 5 in the "Status Report for 2012 Acoustic Telemetry Stipulation Study" shows cumulative detections at different receiver arrays. Cumulative distributions can exaggerate differences between time series counts. In the upper panel, the green and blue curves appear quite different, and yet the time series differ only by a few fish on days 2 and 3. Because the counts are low, it is important to place confidence intervals on these curves, before claiming they differ. In addition, with low sample sizes, it is more realistic to plot cumulative counts as a stair-step rather than a smooth curve.

These same comments apply to the cumulative count figures in the PowerPoint presentation (e.g., slide 31, 37, 39) given on this topic at the workshop in Sacramento on October 31, 2012. Because of low counts, the confidence intervals on the curves in these figures will likely all overlap substantially.

It would also have been useful to place confidence intervals on the estimated proportions in Figure 6 in the same Status Report, and in all other figures that display similar estimates (Zar 2010). To test whether proportions differed across the three junctions, the IRP suggests fitting a logistic regression model with probability of entering the interior Delta as the response variable, and junction and flow level as the explanatory variables. Recoding groups 1 and 2 together as "Intermediate flows", and group 3 as "Higher flow", it would be possible to test for the hypothesized difference between the 2 flow levels and reach a supportable conclusion, at least within the range of flows observed.

The boxplots in Figure 11 of the Status Report on the 2012 Acoustic Telemetry Study are unclear with respect to the sources of variation represented. The IRP was unable to determine the sample sizes in each case, but if small (n < 10), then boxplots can be misleading, and perhaps the data should just be plotted as distinct points. Also, this figure includes data from earlier releases ("six year release groups"), then release group ID's 1, 2, 3 and their relation to flow have no clear meaning.

At the top of p. 18 of the Status Report, "a generalized linear model with binomial error structure" was applied to tag detections at receiver array 9 compared to either array 12 or 14. The IRP did not understand exactly what was being tested by this model.

The 2011 VAMP acoustic tagging study of Chinook salmon smolts.

The 2012 IRP recognizes that evaluating the Vernalis Adaptive Management Program (VAMP) studies was not specifically within this year's charge. However, during the workshop in Sacramento (October 31, 2012) the IRP was presented an update from Rebecca Buchanan on the findings of the 2011 VAMP Acoustic Tagging Study which estimated survival of hatchery-reared acoustically tagged Chinook salmon smolts along different potential emigration routes from Mossdale to Chipps Island. Within the context of the workshop, it was difficult to avoid making comparisons between the VAMP and Joint Stipulation Acoustic Tagging Studies given the similarities in the intentions and objectives of the research projects.

The VAMP findings were that overall survival along all routes combined was less than 2% in 2011 and that survival was greater through the southern Delta than through the mainstem of the San Joaquin River. Also, plots of findings from three years of the VAMP acoustic tag study (2008, 2010 and 2011) suggested that higher river flows at Vernalis resulted in lower survival of smolts along the San Joaquin River route. These results contrast with those from earlier coded wire tag (CWT) mark-recapture estimates (analysis by Newman) which have been the basis of the NMFS Biological Opinion on salmonids and to provide the rationale for RPA Actions involving water operations in the Delta (see Report on Spring 2012 Delta Operations in lieu of Action IV.2.1 per Joint Stipulation).

In the VAMP 2011 tagging study, detailed route-specific survival rates tended to decrease in down-river segments and were greatest along the Old River route leading to the CVP tank from which tagged smolts were transported by truck to Chipps Island. The findings, if reliable, suggest that transport from collection facilities associated with water operations provides the best survival chances for Chinook salmon smolts in the San Joaquin watershed. Moreover, it suggests that the use of rock and/or other barriers

at the head of Old River on the San Joaquin River that force smolts into the Delta interior where survival is less than 2% should be reconsidered. Indeed, it seems plausible from findings of recent acoustic tagging studies that higher smolt survival will be achieved through encouraging migration down Old River and towards the CVP tank.

The IRP is unaware of any current measure of smolt survival subsequent to transport and release at Chipps Island, but studies conducted in the Columbia River watershed have suggested that there was little evidence of “delayed” mortality associated with transport induced stress in spring Chinook smolts (Rechisky et al. 2012). The same study also suggested that survival to adulthood could still be impaired by early ocean entry as a result of transport. In the 2011 VAMP acoustic study, transported smolts reached Chipps Island in less than half the time (average of 2.6 days, n=24) as those taking an unassisted river route (average 6.3 days, n=8), so route-specific consequences for survival to adulthood remain uncertain.

The VAMP acoustic tagging program has been conducted annually since 2008 and so these studies have an experience advantage over the Spring 2012 Joint Stipulation Study (i.e., less likely to have experienced surgically-related sources of mortality and tag expulsion due to skill levels of personnel), but nonetheless are subject to many of the same criticisms regarding certain key assumptions, especially those related to array-specific detection probabilities under different environmental conditions. In fact, the use of HTI Model 795Lm acoustic tags, which transmit at a frequency of 307KHz would be expected to have an even smaller detection range in the tidal estuary than the VEMCO tags (180 KHz) used in the Joint Stipulation Study. Unless there have been array-specific range tests conducted across the entire environmental gradient that were not available to the IRP, there is reason to doubt the claim of high detection probabilities for every route and river segments between arrays, especially in tidal environments where salinity and perhaps turbidity are greater than in the freshwater reaches. A first step in addressing this issue would be to focus range detection tests on arrays associated with areas identified as mortality “hotspots” where survival was considered to be at or near zero.

There are a few other considerations that complicate comparisons between the VAMP acoustic tag studies and the CWT studies analyzed by Newman (2008). Perhaps the most important difference is that CWT studies depend on actual recaptures of tagged smolts so survival of individuals to the recapture point is a certainty. Acoustic tag studies – with the exception of smolts transported from the CVP tank – track tags and not smolts. The tags could be transported within predators that consumed smolts or could go undetected by a given receiver array due to imperfect detection probabilities.

Although there are filters that can be applied to adjust for these discrepancies, these are still estimates associated with a level of uncertainty.

Another difference between the CWT and acoustic tag studies is the route endpoint which was Jersey Point for the CWT studies and Chipps Island (over 10 miles farther down-estuary) for the VAMP acoustic tag studies. If smolt survival was low between Jersey Point and Chipps Island, it would help explain the difference in survival among the studies. However, the 2011 VAMP data are not consistent with this hypothesis given that smolt survival within that segment was estimated to be about 69% (see slide 22 in PowerPoint presentation by Buchanan et al., LOO Annual Review, October 31, 2012). Alternatively, differences may be due to inter-annual variation in smolt survival, which is known to be highly variable in other systems (e.g., Chittenden et al. 2010).

In any case, substantial uncertainties remain regarding the effects of water operations on the survival and behavior of out-migrating salmonid smolts. Conflicting findings of different studies and methodological issues associated with the approaches used to evaluate survival and routing behavior of out-migrating salmonid smolts have not yet provided a clear path to suggest that fine-tuning water operations will provide a successful means of maintaining or restoring salmonid populations that migrate through the southern Delta.

Clear Creek Technical Team Report specific questions

Were the approaches used to develop the recommended actions to reduce water temperatures scientifically appropriate?

The CCTT report provided a number of suggestions aimed at reducing water temperatures in discharges from the Whiskeytown Reservoir. The presumed effects of replacing the Oak Bottom Temperature Control Curtain (OBTCC) and power peaking on Clear Creek temperatures (Fig. 16 in the CCTT Report) were largely speculative and need to be verified through modeling, analysis of existing temperature data and controlled experiments, if possible.

Releases of colder water from lower in the reservoir as temperatures warm in the summer seems to be a common sense recommendation but still requires some verification with respect to the available volume of cooler bottom water in storage and how far downstream the intended effects on temperature are likely to extend under different climatic conditions, ranging from sunny and hot to cloudy and cooler.

What recommended adjustments to actions and implementation procedures for reducing water temperatures might be scientifically appropriate for the next year, while maintaining equal or greater protection for fish?

Any of the suggestions "might be" scientifically appropriate but require some objective testing to be certain. The IRP suggests that CCTT consider options for assessing the potential temperature-specific pools of water available, through modeling and real-time monitoring within Whiskeytown Reservoir and upstream.

Given that there seems to be consensus among the agencies in favor of repair/replacement of the OBTCC, the 2012 LOO IRP can see no reason to object but would strongly recommend that this action be conditioned on an evaluation of effectiveness that includes measurements before and after installation of a replacement curtain.

Spring 2012 Delta Operations specific questions

Was the approach to real-time operations, including the use of a rock barrier at the Head of Old River (HORB) and acoustic tagged fish for triggering real-time decisions, while providing equal or greater protection to out-migrating steelhead smolts under RPA Action IV.2.1, clearly articulated and supported by best available science in the NMFS February Tech Memo and supporting documentation?

The approach was clearly articulated in the February Tech Memo and supporting documentation but there was little basis for assessing the effects of the HORB on the intention of providing equal or greater protection for out-migrating smolts.

Survival models played a prominent role in decisions about the rock barrier and Old River flows, as evidenced in materials provided to the IRP. The models are also the kernel of the "HORB and survival exploration tool" spreadsheet. However, none of the material reviewed by the IRP discussed the uncertainties of these models, apart from the statement that survival estimates may be somewhat too high for present-day conditions (Report on Spring 2012 Delta Operations, Appendix D, pg. 3). Because of their management importance, the IRP believes it is critical to quantify and communicate the uncertainties of these models.

In addition, the IRP traced the constant survival estimates (flat lines in Figure 2 of the Report on Spring 2012 Delta Operations) back to the Newman (2008) report. However, the IRP could not locate the figure's flow-dependent survival equations in that report,

nor could we find the idea of estimating a weighted average (mixed model) of the flow-dependent and flow-independent models.

In Appendix C (Summary of expected benefits of the Spring 2012 Delta Operations Report), the interpretation of relative survival in OMR vs. San Joaquin was unclear. Smolt survival was apparently lower (again, no uncertainty estimates) in the San Joaquin in 2009-2010, with an acoustic barrier in place. And San Joaquin survival in 2008 was higher when no barrier was in place. Nevertheless, a rock barrier (HORB) was installed at the Head of Old River in 2012,"… based on a preponderance of the data". What data constitutes "a preponderance" of evidence is unclear. Perhaps all comparable through-Delta survival estimates, from all years, should be tabulated and presented with key environmental conditions (barrier presence, flows, tagging method, etc.), to reveal the true variation in survival estimates and possible reasons for that variation.

There were several reasons one could reasonably speculate that the effects of the HORB were detrimental to survival of smolts. Given that the VAMP acoustic tag study results have indicated that Chinook smolt survival through the Delta is substantially greater when smolts are transported to Chipps Island from the CVP holding tank, routing smolts via the shortest river segments to the holding tank would seem the best option for protecting out-migrating salmonid smolts.

The HORB inhibits passage along one of the shortest routes to the holding tanks from the upper San Joaquin watershed. Also, the HORB increases negative Old and Middle River flows and potential opportunities for smolts to become entrained along routes in the southern Delta, where survival is considerably lower.

Also, it has simply been assumed that the HORB does not result in enhanced predation mortality on smolts as was shown to occur with the non-physical barrier tested in previous years. All of the calculations and recalculations of route-specific mortality on acoustic tagged smolts that resulted in increasing the number of entrained smolts required to trigger real-time decisions for adjusting water operations were all based on the assumption that the HORB was not associated with increased mortality from predators or other factors. Lacking evidence to the contrary, it is difficult to conclude that the HORB provided equal or greater protection for smolts.

Finally, even after the triggers for tagged smolts were exceeded, there were frequently substantial lags of several days before pumping operations were reduced. Taken together, it is difficult to conclude that the approach taken in the Spring 2012 operations provided even minimal protection for out-migrating smolts. Negative effects of such

artificial stresses may have even enhanced the higher natural mortality expected in a dry (or critical) water years such as 2012.

Were the weekly adjustments made consistent with the Tech Memo and supported by the available data and information, while providing necessary protections?

Weekly adjustments to operations appeared to be made within the season because the rapid movement of fish into the Delta was unexpected.

Is the overall approach of using acoustically tagged fish to adjust weekly operations scientifically supportable?

It was not clear to the IRP how water operations coordinated on the movement of acoustically tagged fish was protecting the passage of smolts. The study found that fish entrainment into the inner Delta was not related to pumping operations, suggesting that weekly adjustment of operations by fish movement is not scientifically supportable.

Were the scientific indicators (e.g., fish behavior or drivers of habitat conditions) used appropriate for evaluating the effectiveness of the Spring 2012 Delta Operations?

The lack of a relationship between fish movement and particle tracking model results and the lack of relationships between OMR inflows/exports and smolt movement/survival suggest that these were insensitive indicators for evaluating effectiveness of Delta operations on salmonids in Spring 2012.

Were the scientific indicators and methods used for classifying and detecting "smolt-type" vs. "predator-type" tags in real time appropriate for informing the Spring 2012 Delta Operations?

The Joint Stipulation study using acoustic tag did not determine if detected tags represented smolts or predators that had recently consumed tagged smolts. The approach to determining behavior relative to the tidal component may provide some classification regime. The 2012 IRP also noted that estimated survival - even without adjusting for predators (i.e., assuming no predation of observed tags) - was so low that the run may not be sustainable. Thus, although the classification of tag status is important, especially for identifying smolt movement patterns, the results may be of limited value in evaluating the impact of Delta operations on salmon and steelhead.

How well did the particle tracking model predict fish behavior relative to acoustically tagged data?

The acoustic tracking data as analyzed provide little information of fish behavior. However information in the tidal component of the particles may provide an approach to interpreting fish behavior. See Appendix 2 at the end of this report.

What are the most important analyses to complete for the 2012 data set? What scientific methods for analyzing voluminous response data (e.g., tag detections throughout the acoustic receiver array) and treatment conditions data (e.g., magnitude and direction of flow near specific receivers) might be more appropriate for evaluating the effectiveness of the Spring 2012 Delta Operations?

The question assumes that the 2012 data set is sufficiently reliable and contains important information extractable by analysis.

An important analysis is to evaluate survival and routing relative to Delta hydraulics including the mean and tidal flow components on a reach specific basis. See Appendices 2.1 and 2.2.

What scientific indicators and methods used for classifying and detecting "smolt-type" vs. "predator-type" tags in real time might be more appropriate for informing the Spring 2012 Delta Operations?

How to detect smolt-type vs. predator-type behavior is a subset to the larger issue of how tides affect predatory-prey interactions in the river and Delta. See Appendix 2.3 for further discussion.

What adjustments to the particle tracking models, as informed by the acoustically tagged fish studies, might be more effective for predicting fish behavior and informing future acoustic study design?

Information on mean and oscillatory (tidal) components of the flow over reaches and at reach junctions are likely to provide important information predator-prey and migration behavior as influenced by tides. See Appendices 2.3 and 2.4. However, the 2012 IRP reiterates the suggestion of the 2010 OCAP IRP that rather than making adjustments to the PTMs, a behavioral model for how species in the Delta respond to their local environment should be developed from first principles.

How should the experimental design be adjusted in future years to test key habitat drivers of smolt behavior and survival, and support weekly operational decision making?

Behavior-based fish movement modeling is gaining increasing acceptance as a potentially important tool in water and living resource management in the Bay-Delta and Sacramento River. Despite its potential, behavioral modeling is still a relatively new and

developing technology whose optimum future use will depend on decisions made in the near-term. The IRP believes that actions need to be taken soon to help ensure that this technology contributes to future difficult management decisions.

Fish movement modeling and its many possible derivatives such as time-dependent or distant-dependent mortality forecasting should be considered in its broadest context. A useful way to understand fish movement modeling is to relate it to Computational Fluid Dynamics (CFD) modeling. CFD modeling is used to develop a virtual representation of a flow field which is then input to mathematical algorithms that attempt to capture sensory acquisition, sensory processing, and cognition.

Time varying, multi-dimensional CFD codes may be many thousands of lines long so that their connection to a behavioral model may be difficult and time-consuming. It is important for the region to formulate and address the strategic questions inherent in using fish movement models to address the many pressing questions faced by the region. Poor decisions made without fully understanding either the full range of possible modeling approaches, or before the full range of tentative uses are identified, can result in future performance or application challenges.

An effective way of addressing this would be through a series of technology workshops in which uncertainties in the optimum development and application of fish movement models can be identified and discussed. These workshops should include experts in fish movement modeling at different scales, fish tagging experts to answer questions about collection, calibration and validation of data, CFD modelers to answer questions concerning optimum hydraulic modeling, regional living resource experts to identify and refine potential applications, and living resource managers to describe important management questions that must be addressed. Each workshop should produce a guidance document that can be used to strategically develop behavioral modeling with specific application to the Bay-Delta watersheds.

The results of tagging studies to date (through the 2012 study), show little correlation between operations and fish movement, and so do not currently support using salmon to manage operations on a weekly basis. In Appendices 2.1 to 2.4 the IRP presents hypotheses on how migration and survival may be influenced by tidal oscillations in the river and Delta. If ongoing or future research identifies significant mechanisms affecting fish on tidal cycles, then managers might consider adjusting Delta operations on this scale. However, considerable work will be required to evaluate this hypothesis, and if supported, to design a tidally-based management program.

The 2012 IRP also raises the question of whether salmon populations are sustainable in the San Joaquin River (Appendix 2.5). While the IRP realizes that the Biological Opinion for the operations of the SWP and CVP is not charged with addressing the viability of the run, the IRP believes the question eventually needs to be addressed in this or another process.

5) How should multi-year data sets on NMFS' Long-term Operations Opinion RPA Action implementation be used to improve future implementation of the Clear Creek RPA Actions?

The hydrologic system that is used to control the flow of water in Clear Creek below Whiskeytown reservior is extremely complex, involving 3 reservoirs two tunnels, flow and temperature demands in the Trinity, Sacramento Rivers and power production for the City of Redding. In addition, water management in this river system must contribute to meething the co-equal goals of providing a reliable supply of water for human needs and provide for healthy ecosystem functioning. Componding the physical complexity is the high level of interagency involvement, communication and data sharing required to operate the system at peak potential. Moreover, decisions need to be made based on forecasting water supply months ahead of time.

Because of this complexity in system structure, opertational demands and interannual climate variation, it would be useful to develop an expert decision system to assist in making operational decisions on how water is routed through the system

Existing physical water routing models based on Computational Fluid Dynamics (CFD) could be developed in such a way as to link the hydrologic system of reservoirs, tunnels and river outflows to climate modeling and prediction output. This would allow for better strategic planning and action rather than relying primarily on reactive operation. One suggestion is to seek the input of an expert in this type of modeling to help guide an initial phase of investigation into models and feasibility.

A major problem addressed by the 2011 OCAP IRP (Anderson et al. 2011) was the need to enhance communication and data sharing through a common web-based clearing house along with easily accessible monitoring data to assess and ensure regulatory compliance. This same message has been voiced by all agencies, consultants, participipating scienctists, academic institutions and other review panels (Lave et al. 2005.). However, no progress in this direction seems to have been made. What is needed is a web-based collaboration tool that can buid multidisciplinary collaboration, centralize data and information, including development of robust yet easy to use search and display tools, that communicate complex information from large-scale modeling results and network sensors in a way that allows various stakeholders to view

decisions and their effects. These tools exist and can be applied to resolve not only issues related to Clear Creek but the whole Central Valley system.

The IRP suggests that the Delta Science Program could facilitate a workshop where industry and academic leaders in this field can present their approaches and potential solutions to the agency partners. Perhaps the Clear Creek working group could provide a test bed model to start building such a web-based collaboration tool.

Another significant need for the Clear Creek group and restoration effort is that of an independent synthesis of all the restoration work and systems management to date. There has been 16 years of restoration effort in Clear Creek below Whiskeytown reservoir without an apparent synoptic review of that work. Instead, the CCTT continues to emphasize perpetual spawning gravel augmentation and changes to the timing and magnitude of reservoir releases without an objective assessment of what has been accomplished to date.

Temperature control in Clear Creek is directly related to the manner in which water flow is managed within the Trinity-Whiskeytown reservoir complex. A temperature control curtain has been replaced in Whiskeytown reservoir near the Spring Creek Tunnel intake and is expected to force more cold water toward that outflow. However, there has not been any data to corroborate that assumption. It is not known how this repair action has or could impact temperature control actions in Clear Creek through operation of the upper and lower intake gates at the Glory Hole intake tower. However, water temperature measured at the Whiskeytown outflow while water intake was shifted between the upper and lower intakes indicates that changes in water temperature outflow can be achieved (Figs. 6 and 16 of the CCTT 2012 report). Indeed, even a mix of water (refered to as middle gate) from both intakes shows an immediate change in water temperature that brackets the entire temperature regime from May to November measured over the past 12 years (Fig. 16, CCTT 2012 report). This suggests that water temperatures in Clear Creek can be controlled to benefit spring-run Chinook and steelhead, but it remains to be seen how far downriver temperature reductions can be maintained.

What is not clear from the CCTT 2012 report is how to assess the potential to achieve this in different water years and whether cooler temperatures in Clear Creek can be extended below the Igo gauging station throughout the summer.

Two planned pulsed flows of 400 cfs and 800 cfs from Whiskeytown reservoir were released in May and June of 2012 with the intent of attracting spring-run Chinook salmon into the upper reaches above Igo. Snorkel data conducted before and after the

pulsed flows showed that Chinook salmon moved upstream but it was unclear that they did so in response to the pulsed flows. Reaching such a conclusion would require comparable snorkel surveys without pulsed flows, which could not be done simultaneously.

The 2012 LOO IRP reiterates the suggestion of the 2011 OCAP IRP that if pulsed flows are going to be released they should follow a more gradual rising limb with a longer smooth falling limb.

REFERENCES

Adams, N.S., D.W. Rondorf, S.D. Evans, J.E. Kelly and R.W. Perry. 1998. Effects of surgically and gastrically implanted radio transmitters on swimming performance and predator avoidance of juvenile Chinook salmon (*Oncorhynchus tshawytscha*). Canadian Journal of Fisheries and Aquatic Sciences 55:781-787.

Anderson, J. J., E. Gurarie, and R. W. Zabel. 2005. Mean free-path length theory of predator-prey interactions: Application to juvenile salmon migration. Ecological Modelling 186:196-211.

Anderson, J.J., R.T. Kneib, S.A. Luthy and P.E. Smith. 2010. Report of the 2010 Independent Review Panel (IRP) on the Reasonable and Prudent Alternative (RPA) Actions Affecting the Operations Criteria and Plan (OCAP) for State/Federal Water Operations. Prepared for: Delta Stewardship Council, Delta Science Program. December 9, 2010. 39 p.

Anderson, J.J., J,A, Gore, R.T. Kneib, M.S. Lorang and J. Van Sickle. 2011. Report *of the 2011 Independent Review Panel (IRP) on the Implementation of Reasonable and Prudent Alternative (RPA) Actions Affecting the Operations Criteria And Plan (OCAP) for State/Federal Water Operations*. Final report submitted to the Delta Stewardship Council (report can be found on the Delta Science Program web page: http://deltacouncil.ca.gov/event-detail/3877).

Bennett, W. A., W. J. Kimmerer, and J. R. Burau. 2002. Plasticity in vertical migration by native and exotic estuarine fishes in a dynamic low-salinity zone. Limnology and Oceanography 47:1496-1507.

Brookes, A. and F.D. Shields, Jr. 1996. *River Channel Restoration. Guiding Principles for Sustainable Projects.* Wiley, Chichester.

Brown, B. V., H. M. Valett, and M. E. Schreiber (2007), Arsenic transport in groundwater, surface water, and the hyporheic zone of a mine-influenced stream-aquifer system, Water Resources Research 43, W11404, doi:10.1029/2006WR005687

Cairns, J. 1991. The status of the theoretical and applied science of restoration ecology. *The Environmental Professional* 13: 186-194.

Casper, A.F., B. Dixon, J. Earls and J.A. Gore. 2011. Linking a spatially explicit watershed model (SWAT) with an in-stream fish habitat model (PHABSIM): A case study of setting minimum flows and levels from a low gradient, sub-tropical river. *River Research and Applications* 27: 269-282.

Cayan, D.R., E.P. Maurer, M.D. Dettinger, M. Tyree and K. Hayhoe. 2008. Climate change scenarios for the California region. *Climatic Change* 87 (Suppl 1): S21-

S42.

Chittenden, C.M., M.C. Melnychuk, D.W. Welch and R.S. McKinley. 2010. An investigation into the poor survival of an endangered coho salmon population. PLoS ONE 5(5):e10869. Doi:10.1371/journal.pone.0010869.

Chittenden, C.M., S. Sura, K.G. Butterworth, K.F. Cubitt, N. Plantalech Manel-La, S. Balfry, F. Økland and R.S. McKinley. 2008. Riverine, estuarine and marine migratory behavior and physiology of wild and hatchery-reared coho salmon *Oncorhynchus kisutch* (Walbaum) smolts decending the Campbell River, BC, Canada. Journal of Fish Biology 72:614-628.

Clements, S., T. Stahl, and C. B. Schreck. 2012. A comparison of the behavior and survival of juvenile coho salmon (*Oncorhynchus kisutch*) and steelhead trout *(O. mykiss*) in a small estuary system. Aquaculture 362–363:148-157.

Drenner, S.M., T.D. Clark, C.K. Whitney, E.G. Martins, S.J. Cooke and S.G. Hinch. 2012. A synthesis of tagging studies examining the behavior and survival of anadromous salmonids in marine environments. PLoS ONE 7(3): e31311. Doi: 10.1371/journal.pone.0031311.

Gibson, R. N. 2003. Go with the flow: tidal migration in marine animals. Hydrobiologia 503:153-161.

Gore, J.A. (Ed.) 1985. *The Restoration of Rivers and Streams*. *Theory and Experience*. Butterworth Publ., Inc., Boston, MA. 280 p.

Gore, J.A. and F.D. Shields, Jr. 1995. Can large rivers be restored? *BioScience* 45: 142-152.

Grant, G.E., R. Haggerty, S. Lewis, B. Burkholder and P. Wampler. 2006a. Potential effects of gravel augmentation on temperature in the Clackamas River, Oregon. Report to Portland General Electric, Portland, Oregon, dated June 1, 2006, 10 p.

Grant, G., B. Burkholder, A. Jefferson, S. Lewis and R. Haggerty. 2006b. Hyporheic flow, temperature anamolies, and gravel augmentation: preliminary findings of a field investigation on the Clackamas River, Oregon. Report to Portland General Electric, Portland, Oregon, dated December 6, 2006, 20 p.

Hanna, D.M., I.A. Malcolm and C. Bradley. 2009. Seasonal hyporheic temperature dynamics over riffle bedforms. Hydrological Processes 23(15):2178-2194.

Hannaford, J. and T. Marsh. 2006. An assessment of trend in UK runoff and low flows using a network of undisturbed catchments. *International Journal of Climatology* 26: 1237-1253.

Hedger, R. D., I. Uglem, E. B. Thorstad, B. Finstad, C. M. Chittenden, P. Arechavala-Lopez, A. J. Jensen, R. Nilsen, and F. Økland. 2011. Behaviour of Atlantic cod, a marine fish predator, during Atlantic salmon post-smolt migration. ICES Journal of Marine Science: Journal du Conseil 68:2152-2162.

Kelly, M.H. and J.A. Gore. 2008. Florida river flow patterns and the Atlantic Multidecadal Oscillation. River Research and Applications 24: 598-616.

Kimmerer, W., J. Burau, and W. Bennett. 2002. Persistence of tidally-oriented vertical migration by zooplankton in a temperate estuary. Estuaries and Coasts 25:359-371.

Lave, R.,Harve, S. McBain, D. Reiser, L. Rempel and L. Sklar (2005). Key uncertainties in gravel augmentation: geomorphological, and biological research needs for effective river restoration. Report for the CALFED Rivers, Rocks and Restoration Workshop in July of 2004

Lima, S. L. 2002. Putting predators back into behavioral predator–prey interactions. Trends in Ecology and Evolution 17:70-75.

Maurer, E.P. 2007. Uncertainty in hydrologic impacts of climate change in the Sierra Nevada, California, under two emission scenarios. *Climatic Change* 82: 309-325.

Maurer, E.P., D.P. Lettenmaier and N.J. Mantua. 2004. Variability and potential sources of predictability of North American runoff. *Water Resources Research* 40(9): W09306, DOI: 10.1029/2003WR002789.

Melnychuk, M.C., D.W. Welch and C.J. Walters. 2010. Spatio-temporal migration patterns of Pacific salmon smolts in rivers and coastal marine waters. PLoS ONE 5(9): e12916. Doi: 10.1371/journal.pone.0012916.

Mesick, C. 2001. The effects of San Joaquin River flows and Delta export rates during October on the number of adult San Joaquin Chinook salmon that stray. Contributions to the Biology of Central Valley Salmonids 2:139-161.

Merz, J.E., J.D. Setka, G.B. Pasternack and J.M. Wheaton. 2004. Predicting benefits of spawning habitat rehabilitation to salmonid (*Oncorhynchus* spp.) fry production in a regulated California river. Canadian Journal of Fisheries and Aquatic Sciences 61:1433-1446.

Moore, J.N. 2002. *Trace metals in sediments from mine-impacted rivers: Clear Creek, California project*. Final Report for Award No. 02-WRAG-001. 33 p.

Moore, A., E. C. E. Potter, N. J. Milner, and S. Bamber. 1995. The migratory behaviour of wild Atlantic salmon (*Salmo salar*) smolts in the estuary of the River Conwy, North Wales. Canadian Journal of Fisheries and Aquatic Sciences 52:1923-1935.

Newman, K.B. 2008. An evaluation of four Sacramento-San Joaquin River Delta juvenile salmon survival studies. Project Report for CalFed Science Program Project number SCI-06-G06-299.

Pautzke, S.M. 2008. Distribution of migratory striped bass in Plum Island Estuary, Massachusetts. M.S. Thesis, University of Massachusetts, Amherst, 105 p.

Poff, N. L., J. D. Allan, M. A. Palmer, D. D. Hart, B. D. Richter, A. H. Arthington, J. L. Meyer, K. H. Rogers and J. A. Stanford. 2003. River flows and water wars: Emerging science for environmental decision making. Frontiers in Ecology and the Environment 1(6):298–306.

Rechisky, E.L., D.W. Welch, A.D. Porter, M.C. Jacobs-Scott, P.M. Winchell and J.L. McKern. 2012. Estuarine and early-marine survival of transported and in-river migrant Snake River spring Chinook salmon smolts. Scientific Reports 2:448. Doi: 10.1038/srep00448.

Vogel, D.A. 2010. Evaluation of acoustic-tagged juvenile Chinook salmon movements in the Sacramento-San Joaquin Delta during the 2009 Vernalis Adaptive Management Program. 72 p.

Vogel, D.A. 2011. Evaluation of acoustic-tagged juvenile Chinook salmon movements in the Sacramento-San Joaquin Delta during the 2010 Vernalis Adaptive Management Program. 72 p.

Warren, G.L. and E.J. Nagid. 2009. Habitat Selection by Stream Indicator Biota: Development of Biological Tools for the Implementation of Protective Minimum Flows for Florida Stream Ecosystems. Florida Fish and Wildlife Conservation Commission, FWRI Library Code: F2195-05-08-F.

Wells, J. T. 1995. Chapter 6 Tide-Dominated Estuaries and Tidal Rivers. Pages 179-205 *In* G. M. E. Perillo, editor. Developments in Sedimentology. Elsevier.

Werritty, A. 2002. Living with uncertainty: climate change, river flows and water resource management in Scotland. *Science of the Total Environment* 294: 29-40.

Zar, J.H. 2010. Biostatistical analysis, 5th ed. Pearson,– Prentice-Hall, Upper Saddle River, New Jersey, 960 p.

APPENDIX 1 – Materials for IRP Review

Review Materials Available to the 2012 LOO Independent Review Panel

I. The following documents were provided in electronic format as required reading by the IRP prior to the 2-day workshop in Sacramento, CA on 31 October -1 November 2012:

1) Draft 2012 Clear Creek Technical Team Report for the Coordinated Long-Term Operation BiOp Integrated Annual Review

2) Spring 2012 Delta Operations in lieu of NMFS' RPA Action IV.2.1 per joint stipulation
    - Appendix A: Joint stipulation
    - Appendix B: RPA Action IV.2.1
    - Appendix C: Summary of expected benefits from alternative operations
    - Appendix D: NMFS Technical Memorandum issued March 16, 2012
    - Appendix E: Tabular summary of Spring 2012 operations and cumulative tag detection data
    - Appendix F: NMFS Determination for Operations per Joint Stipulation During April 1-7, 2012
    - Appendix G: NMFS Determination for Operations per Joint Stipulation During April 8-14, 2012
    - Appendix H: NMFS Determination on April 12, 2012
    - Appendix I: NMFS Determination on April 27, 2012
    - Appendix J: NMFS Determination on May 4, 2012
    - Appendix K: NMFS determination on May 11, 2012
    - Appendix L: Water supply impacts of operations under Joint Stipulation relative to RPA Action
    - Head of Old River Barrier and survival exploration tool

3) Preliminary Report (Phase 1 Analyses) for the 2012 Acoustic Telemetry Stipulation Study

II. The following additional reports were made available in electronic format for supplemental use in providing historical context for the IRP:

- Smelt Working Group (SWG) Annual Report on the Implementation of the Delta Smelt Biological Opinion on the Coordinated Operations of the Central Valley Project and State Water Project ("OCAP" Biological Opinion) Water Year 2012
- Sacramento River Temperature Task Group (SRTTG) Annual Report of Activities
- American River Group (ARG) Annual Report of Activities

- Stanislaus Operations Group (SOG) Annual Report of Activities
- Delta Operations for Salmonids and Sturgeon Group (DOSS) Annual Report of Activities
- Report of the 2011 Independent Review Panel (IRP) on the Implementation of Reasonable and Prudent Alternative (RPA) Action Affecting the Operations Criteria And Plan (OCAP) for State/Federal Water Operations (December 9, 2011)
- Federal Agencies' Detailed Response to the 2011 Independent Review Panel's Report (June 20, 2012)
- Report of the 2010 Independent Review Panel (IRP) on the Reasonable and Prudent Alternative (RPA) Actions Affecting the Operations Criteria and Plan (OCAP) for the State/Federal Water Operations
- Joint Department of Commerce and Department of the Interior Response to the Independent Review Panel's (IRP) 2010 Report of the Reasonable and Prudent Alternative (RPA) Actions Affecting the Operations Criteria and Plan (OCAP) for the State/Federal Water Operations
- NMFS' 2009 RPA with 2011 amendments
- USFWS Biological Opinion on the Long-Term Operational Criteria and Plan (OCAP) for coordination of the Central Valley Project and State Water Project (pages 279-282 and 329-356)
- RPA Summary Matrix of the NMFS and USFWS Long-term Operations Opinions RPAs
- National Academy of Science's March 19, 2010, report
- VAMP peer review report
- State Water Board's Delta Flows Recommendations Report
- NMFS RPA, Appendix 2-B, Task 4: Green Sturgeon Research
- 2011 OCAP Review Materials, Background Information and Presentations (http://deltacouncil.ca.gov/science-program/2011-ocap-review-materials-background-information-and-presentations)
- 2010 OCAP Annual Review Materials and Presentations (http://deltacouncil.ca.gov/events/science-program-workshop/workshop-ocap-integrated-annual-review)

APPENDIX 2 – Framework for Addressing Salmonid Issues

Framework for addressing effect of Old and Middle River flows on reach-scale survival rate

A2.1: XT Survival Model

The current paradigm for characterizing movement of smolts through the Delta reaches relies on mean flow to characterize the movement and routing of fish. The tagging studies in 2012 and earlier years clearly indicate that this characterization is inadequate. Below is a mechanistic approach to consider smolt movement, routing and survival through the Delta in terms of the dynamics of encounters of predators and smolts as based on the XT survival model (Anderson et al. 2005).

The underlying equation characterizes survival in terms of both the distance traveled *x* and the time *t* to travel through a reach. The concept is that if smolt (prey) mortality over a distance is the result of predators then survival depends on both the mean travel time and the relative random velocity between the predator and smolt. Survival is

$$S = \exp\left(-\frac{x}{\lambda}\sqrt{1+\left(\frac{\omega}{U}\right)^2} \right) \quad (1)$$

where ω is the root mean-squared (rms) random component of velocity of the predator relative to the smolt, *U* is the mean velocity of the smolt through a river reach and *x* is the reach distance. The final term λ is the mean free-path length a smolt travels before a predation event and is defined

$$\lambda = \frac{1}{\pi r^2 \rho} \quad (2)$$

where ρ is the predator density per unit volume, and *r* is the predator-smolt interaction distance that on the average results in a predation event. The interaction distance *r* depends on the visual field of the predator and therefore depends on light levels and turbidity.

Because in Equation (1) survival depends on the ratio of two velocities to understand what controls survival, an understanding of the velocities is important. To illustrate their nature assume that the predators are territorial while smolts move with the water and exhibit selective tidal-stream transport (discussed in A2.2). Then the random predator-

prey velocity ω is essentially the mean tidal velocity and the smolt velocity *U* is the reach length divided by the smolt's mean travel time through the reach. When $U/\omega > 1$, the mean smolt velocity is large compared to the tidal velocity so a predator gets only one chance at a passing smolt. However, when $U/\omega < 1$ the tidal velocity is larger than the mean smolt velocity and the tidal flow can bring the smolt into the predator's territory multiple times.

Figure A2.1 illustrates how smolt velocity and tides interact. Based on Equation (1), *x* and λ are constant for a reach so the shape of the survival curve depends only on U/ω. When U/ω is large, survival approaches its maximum value $S_{\max} = \exp(-x/\lambda)$ which depends only on reach distance, predator density and the capture distance, but not on either the smolt velocity or the tidal velocity. When U/ω drops below 1, (i.e., the tides become important) survival precipitously declines. Note that in total smolt survival depends on five variables, not simply smolt mean velocity. Furthermore, survival does not directly relate to particle velocity *V.* In other words, smolt velocity is only one of five variables affecting survival and the impact of particle movement on smolt survival is ambiguous.

The current operation schemes focus on controlling particle travel time which is controlled through project exports, the E/I ratio, and OMR flow. The 2012 stipulation study examined the survival and movement of acoustically-tagged steelhead in relation to project exports and OMR flows. The study demonstrated that under the conditions examined, fish travel time was not related to particle movement nor was route selection of the fish related to Delta operations. While the study to manage Delta operations considered smolt survival, with its focus on fish travel time, it did not consider other factors that control survival through reaches. In particular, smolt survival depends on the relative predator-smolt encounter velocities, as outlined above, and routing. Below we consider factors that determine fish migration velocity (Appendix 2.2), predator-smolt encounter velocities (Appendix 2.3) and fish routing (Appendix 2.4).

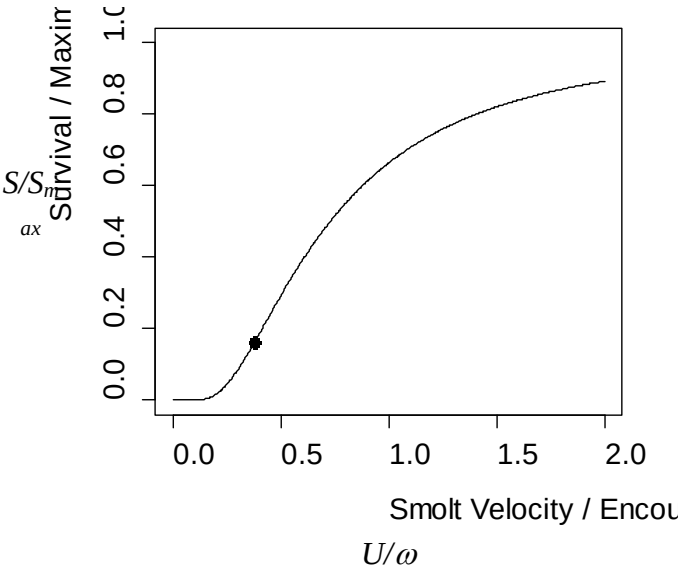

Figure A2.1. Relative reach survival depends on the ratio of the mean smolt migration velocity U to the relative predator encounter velocity ω. Maximum survival S_{max} depends on reach length x and mean free-path length before a predator encounter λ . Estimate of relative survival of fall Chinook from San Joaquin River to Chipps Island denoted by (●).

A2.2: Selective Tidal-Stream Transport (STST)

The stipulation study using acoustically tagged steelhead smolts clearly demonstrated particle and fish movements were poorly correlated. For example, calculated with hydraulic models, particles take 20 to 40 days to move through the Delta while observations on fish passage time are typically 10 days and can be less (Figure A2.2). It is well known that fish and zooplankton perform vertical migrations over the tidal cycle to remain in the Delta (e.g., Bennett et al. 2002, Kimmerer et al. 2002). Additionally many fish species (Gibson 2003), including salmon smolts (Moore et al. 1995) exhibit selective tidal-stream transport (STST) during migration. Here we illustrate the feasibility that salmon and steelhead smolts use STST to move quickly through the Delta.

In selective tidal-stream transport (STST) an animal moves in and out of low velocity regions of the water column on selective parts of the tidal cycle to facilitate upstream or downstream movement. To speed downstream migration salmon smolts move into the higher velocity surface layer on ebb tides and lower velocity near shore regions on flood tides (Clements et al. 2012).

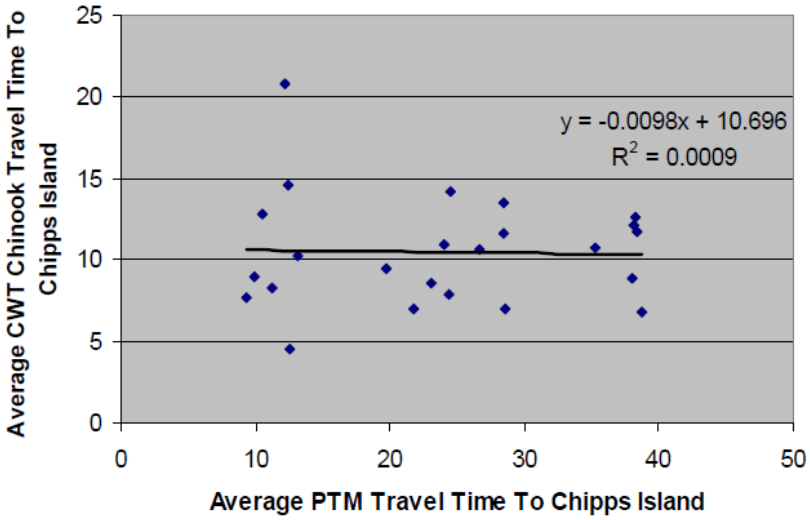

Figure A2.2. Release CWT Chinook salmon in the lower San Joaquin River and the associated Particle Model arrival time to Chipps Island in (LOO Annual Review 2012) Appendix H page H-24).

To demonstrate the feasibility that smolts use STST migrating through the Delta, assume the fish move with the ebb tide and hold in low velocity areas during the flood tide. The resulting across-ground velocity of a smolt can be expressed

$$U = V + \varphi v \qquad (3)$$

where V is the mean particle velocity experienced by the smolt, v is the rms tidal velocity and φ measures the contribution of STST behavior to migration. In the simplest view, φ is a measure of the fraction of the tidal cycle that smolts hide in low velocity regions. If $\varphi = 0.5$ then the smolts effectively hide in low velocity areas during the entire flood tide and drift downstream during the ebb tide. Values less than 0.5 indicate tidal selective movement occurs during only part of flood tide or that the smolts move into low velocity, but not zero-velocity areas on the flood tide. Figure A2.3 illustrates an idealized behavior where a smolt moves into a zero-velocity region during 3 hrs about the peak flood tide. Additionally, if STST is estimated over multiple reaches, φ represents an average of reach properties and behavioral responses.

Thus, Equation (3) hypothesizes that the difference between the observed smolt velocity and the mean particle velocity can be explained by the smolt STST behavior. To evaluate this hypothesis consider the difference in the estimated travel time of particles and CWT smolts traveling from the Lower San Joaquin River to Chipps Island (Figure A2.2) which gives T_{smolt} = 10 d, T_{ptm}= 25 d. Assuming the distance traveled by the smolts is approximately 2 x10^5 ft, then the average fish and particle velocities over the reach are $U = T_{smolt}/x$ = 0.23 ft/s and $V = T_{ptm}/x$ = 0.11 ft/s. Measurements of water

velocity including tidal and mean flow indicate a typical maximum tidal velocity of 1 ft/s (Figure A2.4) which gives a rms tidal velocity of v = 0.7 ft/s. Then arranging Equation (3) to give $\varphi = (U - V)/v$ the STST index is φ = 0.17.

In other words the travel time of fish through the San Joaquin River can be explained by the fish exhibiting a moderate amount of selective tidal-stream transport.

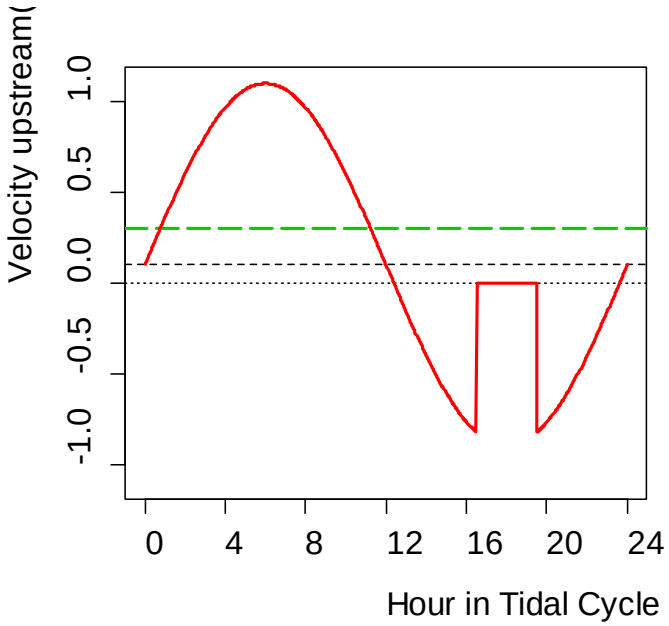

Figure A2.3. Illustration of selective tidal-stream transport. The reach water velocity is composed of a tidal component and residual (- - -) from the mean river flow. Smolt velocity (——) follows the water velocity until upstream velocity exceeds a threshold triggering fish to move into a low velocity area. The average smolt velocity over the tidal cycle (— — —) exceeds the average water velocity (- - - -).

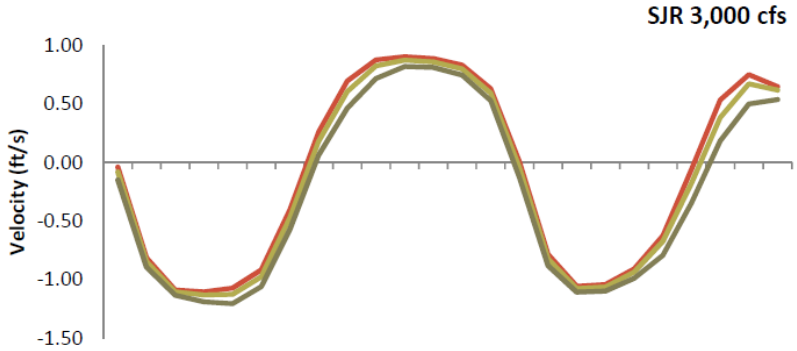

Figure A.2.4. Instantaneous average velocity values across 24 channel segments from the mouth of Middle River to Export facilities. Velocity data for each channel were taken from a single day (May 7, 2007) (LOO Annual Review 92012) Appendix A, page D-50).

Discussion of STST behavior.

The parameter φ quantifies STST behavior over the Delta and the correlation of φ with environmental conditions should provide insight to the mechanisms controlling fish migration behavior. For example, we might hypothesize that fish are able to detect the direction downstream by asymmetric changes in the environmental properties over a tidal cycle. The signal may include asymmetric patterns in the vertical or temporal distributions of turbidity and micro turbulence. For example, turbulence should be highest on the flood tide, possibly triggering movement into a low velocity region. Furthermore, in tidal rivers and estuaries the flood tide may move through progressively smaller cross-sectional areas causing the tidal currents to become progressively more asymmetric in both speed and direction (Wells 1995), which could facilitate detection of the tidal signal. Furthermore, if asymmetry in the channel configuration alters the signal triggering behavior then the complexity of the Delta may result in complex STST behavior. For example, fish moving from the San Joaquin River into Franks Tract may first experience a strong signal of tidal direction but once inside the track where the channel widens the signal may virtually disappear. With heterogeneity in STST signal strength we expect φ to vary over reaches and flow conditions.

Action.

The IRP suggests researchers evaluate the relationships of φ with differing environmental and hydraulic properties of the reaches. As a null hypothesis to the STST behavior, assume fish swim downstream independent of tidal conditions. In this case there would be no correlation of φ with Delta geometry. Note that the null hypothesis is also biologically possible if salmon navigate using the geomagnetic signals that indication location. However, even if fish use geomagnetic navigation they may do so in the context of STST behavior.

A2.3: Predator-Smolt Encounters

Equation (1) proposes that the importance of the downstream velocity of the smolts in determining their migration survival depends on the encounter velocity of the smolts to predators. Furthermore, the probability of encounters and predation events is expected to change over tidal and diel cycles and depend on the avoidance strategy of the smolts and the search strategy of the predators. While numerous studies have documented STST behavior, the panel is unaware of specific studies exploring predator-prey interactions in STST conditions. In a general sense, the smolt STST strategy is to move out of the Delta and avoid predators while the predator STST strategy is to remain in the Delta and encounter prey. Competing predator and prey strategies have been viewed

as a predator-prey shell game that depends on the ability of the predator to adjust its strategy to the temporal flux of prey (Lima 2002). A recent study suggests a type of shell game may occur in Atlantic cod foraging on Atlantic salmon during their post-smolt estuary migration (Hedger et al. 2011). The cod exhibited a more focused foraging distribution during the smolt outmigration, but their distribution was not influenced by the tides, i.e. they held station against the tides. Delta predators may use a similar mechanism. We illustrate the implications of such strategies in the example below that combines the XT survival model and the STST hypothesis.

We begin by defining the random encounter velocity between predator and prey (Anderson et al. 2005) as

$$\omega = \sqrt{u_{smolt}^2 + u_{pred}^2} \tag{4}$$

where u_{smolt} and u_{pred} are the rms random velocities of smolts and predators respectively. With STST behavior, relating smolt rms random velocity to acoustic tag observations may be problematic since in the model part of the tidally-correlated movement of the smolts is attributed to the mean movement. However, approximations of the rms random velocities can be developed based on assumptions of the behavior of predators and smolts. Assume that predators hold station during the ebb tide such that smolts pass through a gauntlet of predators, while on the flood tide the smolts are stationary and the predators move with the flow searching for prey. Assume the combined effect of these two strategies depends on STST behavior and the rms tidal velocity, which we take as a surrogate for the random search velocity of the predators. Then, the random predator-smolt encounter velocity might be expressed $\omega = (1-\varphi)v$ and the ratio of mean smolt migration velocity to the predator-smolt random encounter velocity is

$$\frac{U}{\omega} = \left(\frac{V}{v} + \varphi\right) \Big/ \left(1-\varphi\right) \tag{5}$$

Using the example for travel time of CWT Chinook from the lower San Joaquin River to Chipps Island gives $U/\omega = 0.38$.. Including Equation (5) in Equation (1), survival over the reach is on the order of 16% of the maximum survival, S_{max} (Figure A2.1). If the maximum observed survival through the Delta is on the order of S_{max} = 20% then survival should be 3%, which is about what was observed in 2012.

The salient point is the XT predation model and selective tidal transport hypothesis together provide a mechanistic explanation for both the observed rapid movement and low survival of smolts in the Delta.

If smolts and predators exhibit distinct behavioral patterns relative to the direction and velocity of the water currents over tidal cycles then classification of smolt and predatory-type tags may require correlations of tag movement with the proximal water velocities. Distinct behavior patterns may be most evident on peak flow or slack water periods.

Action.

Much information is known about the behavior of organisms on tidal oscillations, but little is known about the effects of tidal oscillations on predator-prey interactions. The panel suggests that prior to additional field work in this area a workshop be held bringing experts together on tidal physics, foraging ecology and predator-prey theory. The panel suggests a mix of local, national and international experts comprise the workshop membership.

A2.4: Fish Routing

The 2012 joint stipulation study found that movement into the inner Delta appeared independent of the OMR flow which suggests that route selection is influenced by proximal conditions at the junctions of the channels. We hypothesize that routing is determined mainly by the response of the fish to the flow field as structured by the channel shape and the flow, which is comprised of the pure tidal flow and the residual flow generated by river flow and pump operations. Thus, it is reasonable to hypothesize that the behavioral factors that produce STST are also important in route selection at reach junctions.

The IRP proposes studying route selection at two spatial-temporal scales: a *reach scale* involving the asymmetric patterns of hydrodynamics of the tidal cycle and a *junction scale* that considers the flow structure over the scales directly perceived by fish during the passage through junctions. Frameworks for studying entrainment at reach and junction scales need to be based on working hypotheses of how hydraulic and behavioral factors interact to determine routing. Examples of reach and junction scale hypotheses are briefly outlined below. These are not intended to be complete or necessarily correct; their purpose is to illustrate general approaches and levels of detail that may be needed in designing analyses and frameworks at each scale. The panel encourages this two-pronged approach as a way to derive a working understanding of fish routing mechanisms while developing analysis that can draw on the existing, coarser scale data available through CWT and the finer scale acoustic tagging studies. As an aside, the panel suggests that mechanisms of STST and route selection in salmon will also have value for understanding the movement of resident Delta fish such as delta smelt and longfin smelt.

Reach scale analysis framework.

As an example of a reach scale routing hypothesis begin with the assumption that if smolt STST occurs in reaches it also occurs in junctions. Based on the STST hypothesis detailed in Appendix 2.2 smolts exhibit asymmetric behavior to selectively move downstream by moving into low velocity regions when triggered by signals indicating a flood tide. Note also, that reversal of OMR flows may disrupt and confuse this signal. The strength of the STST should be reach specific and might be quantified by φ (Equation 2) characterizing the fraction of a tidal cycle over which fish seek lower velocity regions. For a working hypothesis, assume that routing at a reach junction depends on the reach-specific φ, the junction hydrodynamic *v*, and the junction geometry, expressed here as cross-sectional area *A* (Figure A2.5). Then an equation expressing the fraction *f* of fish routed through reach 1 might be written

$$f_1 = \frac{\varphi_1 v_1 A_1}{\varphi_1 v_1 A_1 + \varphi_2 v_2 A_2} \qquad (6)$$

and fraction passing through reach 2 becomes $f_2 = 1 - f_1$. The important feature of this framework is that routing involves three factors, behavioral, hydraulic and geometric properties. The challenge is to formulate measures that are mechanistically meaningful and measurable. Three trial hypotheses/analyses (developed in conversation with R. Buchanan) are outlined below:

Hypothesis 1: assume φ_i from reaches Equation (3) applies to Equation (6) and the $\varphi_i A_i$ is the junction volume transport averaged over a tidal cycle.

Hypothesis 2: assume reach-specific φ_i and v_i represent rms velocities.

Hypothesis 3: assume φ_i is junction-specific and must be characterized by correlating fish and water movements with the junction.

Again, these approaches are presented to illustrate an approach for conducting analyses based on underlying transport mechanisms.

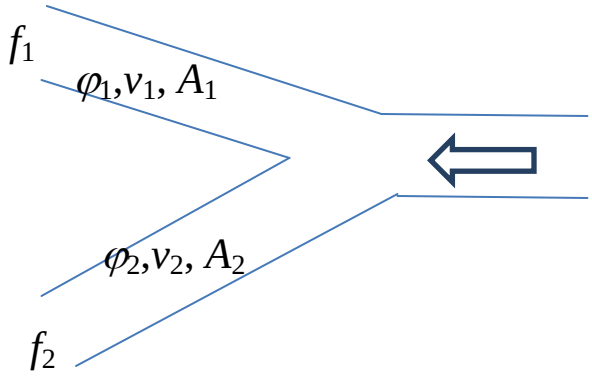

Figure A2.5. Reach routing model based on STST behavior and tidal dynamics.

Junction scale analysis framework.

An alternative, higher resolution, approach is available through the melding of computational fluid dynamics models with models of the rheotactic response of fish. Such studies are being carried out in the Sacramento River by David Smith of the Army Corps of Engineers Cognitive Ecology and Ecohydraulics Research group el.erdc.usace.army.mil/emrrp/nfs/index.html. A description of ecohydraulics to study fish routing derived from the research groups follows:

> The Eulerian–Lagrangian–agent Method (ELAM) provides a framework to analyze fish habitat occupancy as a function of environmental change. We create a 'virtual reality' of the environment and then analyze/forecast habitat occupancy as a function of discharge, channel morphology, habitat complexity, and water quality using a fish habitat selection algorithm coupled to a particle–tracking model (PTM). We model the cognition, adaptation, and learning of fishes along with their physiological sensory capabilities instead of using habitat suitability criteria or reach–scale habitat classification (e.g., pool, riffle, run, shear zone, etc). Reach–scale habitat occupancy patterns are resolved from responses to physical and chemical stimulus at the microhabitat scale. Thus, we can forecast fish response to changes in river channel morphology derived from hydrographic manipulation or construction of engineered structures. Traditional habitat suitability criteria and reach–scale habitat classifications limit flexibility and the level of fidelity that can be used in analysis of a restoration project. The ELAM approach is a "plug–and–play" tool that supports management decisions in a theoretically– and mathematically–rigorous manner (el.erdc.usace.army.mil/emrrp/nfs/fishhabitat.html).

For further discussion, see the response to question “How should the experimental design be adjusted in future years to test key habitat drivers of smolt behavior and survival, and support weekly operational decision making?”

A2.5: Is the San Joaquin River a salmon sink?

The low Delta passage survival of fall-run Chinook and steelhead on the order of 1-3%, begs the question as to whether the San Joaquin River can support salmon populations in the future or whether it is a sink habitat receiving adult Chinook from other Central Valley rivers. The high stray rate of the hatchery raised fall Chinook (e.g., Mesick 2001) may suggest natural production in the system is not being maintained or will not be in the future with increased Central Valley warming by climate change. The IRP recommends that this possibility be consider through an analysis of source-sink population dynamics of the Sacramento/San Joaquin populations.

Report of the 2013 Independent Review Panel (IRP) on the Long-term Operations Biological Opinions (LOBO) Annual Review

Prepared for: **Delta Science Program**

December 7, 2013

Panel Members:

James J. Anderson, Ph.D., University of Washington
James A. Gore, Ph.D., (Panel Chair) University of Tampa
Ronald T. Kneib, Ph.D., (Lead Author), RTK Consulting Services & University of Georgia (Senior Research Scientist Emeritus)
Mark S. Lorang, Ph.D., University of Montana
John M. Nestler, Ph.D., Fisheries and Environmental Services & USACE Engineer Research and Development Center (Retired)
John Van Sickle, Ph.D., U.S. Environmental Protection Agency Western Ecology Division (Retired)

Scope and Intent of Review: This report represents findings and opinions of the Independent Review Panel (IRP) assembled by the Delta Science Program to inform the National Marine Fisheries Service (NMFS) and the U.S. Fish & Wildlife Service (USFWS) as to the efficacy of water operations and certain regulatory actions prescribed by their respective Long-term Operations Biological Opinions' (LOBO) Reasonable and Prudent Alternative Actions (RPAs) as applied from October 1, 2012 through September 30, 2013 (Water Year 2013).

This year's annual review focused primarily on: (1) implementation of NMFS's RPAs for Shasta Operations in connection with the activities of the Sacramento River Temperature Task Group (RPA Actions I.2.1 – I.2.4), (2) new approaches to loss estimation of Chinook salmon, steelhead and green sturgeon at the Skinner Delta Fish Protective Facility and Tracy Fish Collection Facility (NMFS Opinion Term and Condition 2a), and (3) the USFWS RPAs related to Water Operations in connection with protection of delta smelt from December through June of the 2013 Water Year (RPA Action 1).

The federal government shutdown in early October 2013 affected the timely provision to the IRP of an official written report on Water Operations related to protection of delta smelt, and so comments and recommendations on this aspect of the original charge to the panel was amended to be at the discretion of the IRP; the IRP included comments and recommendations on delta smelt in its 2013 report.

After reviewing a required set of written documents (Appendix 1), the IRP convened at a public workshop in Sacramento, CA on 6-7 November 2013. The first day of the 2-day workshop provided a forum for the IRP to consider information on water operations, activities and findings related to RPA Actions related to Shasta Operations and effects on aspects of the early life history of winter-run Chinook salmon in the Sacramento River, the development of loss equations for listed anadromous fishes associated with Delta Water Operations, and a retrospective consideration of Delta Water Operations as related to delta smelt protective actions early in the 2013 Water Year (WY). On the second day the IRP deliberated in a private session beginning at 8:30 a.m. in order to prepare and present their initial findings at the public workshop at 2:00 p.m., after which there was an opportunity for agency representatives, members of the public and the IRP members to comment and otherwise exchange impressions and information. Subsequent IRP communication and deliberations were conducted via email and conference calls in the course of drafting this final report.

EXECUTIVE SUMMARY

The review panel recognizes the unique challenges and constraints faced by all of the agencies attempting to balance existing commitments and mandated coequal goals of (1) providing a reliable water supply for California and (2) protecting, restoring and enhancing the Delta environment and associated Central Valley ecosystems. The agencies charged with this daunting task continue to cooperate and integrate activities, at least to some degree, but polarity of focus remains evident. Perhaps this is to be expected in an environment where so much is at stake, socio-economic pressure is intense, and so little is precisely predictable.

The dry 2013 water year (WY) presented an even greater challenge to achieving specific RPA targets than was the case in 2012 and confirmed concerns expressed in previous IRP reports (Anderson et al. 2010, 2011, 2012) that some physical targets may not be routinely achievable. After four years of operating under the RPA actions, observations are available for a small sampling of both wet and dry years. The 2013 WY began with the promise of a wet or normal year but ended dry with low reservoir storage due largely to a sparse snowpack and one of the driest January-May periods in the past 90 years.

Although it still remains too early to make definitive assessments of long-term effects on listed species populations, signs linking specific RPA actions to improved conditions remain elusive. A science review panel is not required to confirm or refute that prescribed physical/numerical targets such as temperature compliance points and incidental take are met in any given year. Rather, as noted by all of the previous OCAP/LOO IRPs, the current LOBO IRP emphasizes the continued need to explicitly link the success or failure of meeting physical targets prescribed in the RPA Actions to the biological/ecological responses of the listed species. This is the only way that the intended goals (e.g., protection of listed species) of RPA Actions can be assessed in a scientific context.

The IRP was encouraged by a perceived continued movement toward research aimed at linking the survival and behavior of fishes to water operations on the Sacramento River as well as at the Delta Pumping Facilities. Inclusion of more ecological and behavioral responses of the fish populations or life stages targeted by the RPA actions continues to be recommended as multiple years of observations become available to support a more comprehensive evaluation of the co-equal goals. Despite recent efforts to improve loss estimates from water operations in the Delta, the IRP remains concerned with the assumptions and statistical approaches applied in the evaluation of

listed fish species loss estimates associated with the pumping facilities. In particular, direct and indirect losses due to entrainment into the pumping facilities and the variance estimates associated with those losses may be substantially underestimated, and are not well-connected to population size estimates. Given that loss estimates are essential for establishing levels of incidental take, accurate estimates of losses relative to the size of the at-risk populations would certainly be worth the effort required to obtain them.

As noted in previous years, the regular evaluation of realistic goals and objectives is as much a part of an adaptive management strategy as are decisions to alter actions when justified by novel observations and response data that deviate from expectations. The dry 2013 WY provided another opportunity to consider how it is not too soon to step back and consider whether the intentions of habitat restoration efforts are tracking toward expected outcomes. If effects of water operations and protective actions on populations of listed species are not detectable following a series of either “good” or “bad” water years in the future, concerns about whether or not fine-tuning of water operations can contribute substantively to the survival of native species will persist.

The IRP again appreciated the opportunity to concentrate on a focal subset of RPA actions this year but noted some concerns about progress, biological responses and consequences in applying the many other prescribed actions within the watersheds. Promised improvements intended to reduce fish losses at the pumps, expand spawning and rearing habitat, preserve cool water reservoir storage and advance temperature model development are reportedly progressing but remain behind schedule.

Table of Contents

INTRODUCTION

Historically, the challenge of meeting water needs for much of California's growing human population has been met by engineering water storage and delivery systems that have profoundly changed the landscape and flow regimes of riverine and deltaic ecosystems associated with California's Central Valley. These and other anthropogenic alterations over time have been accompanied by profound changes in aquatic flora and fauna, including a persistent decline in native fishes. Consequently, some species have been afforded protection under the Endangered Species Act (ESA) and government agencies have been charged with developing ways of protecting these populations from further jeopardy associated directly or indirectly with water operation projects in the region.

Recent formal legislative recognition that water and other habitats should be managed to restore and enhance the ecosystem as a coequal goal with providing a reliable water supply to California (Delta Reform Act) provided an ambitious and novel conceptual approach to water management within the region. Ultimately, the ability to meet this mandate appears to rest largely on adjusting existing water operations within the context and constraints of a system developed and engineered to primarily achieve one of these goals – a reliable water supply in a region where precipitation is highly variable in both space and time. This constrains the options for meeting the aforementioned co-equal goals largely to modifications in water operations that amount to frequent serial adjustments in reservoir releases and export pumping from the system so as to avoid jeopardizing protected fish populations while continuing to ensure the availability of water for other human uses.

***Background on the LOBO RPA review process*:** NOAA's National Marine Fisheries Service (NMFS) and the U.S. Fish and Wildlife Service (USFWS) have each issued Biological Opinions on long-term operations of the Central Valley Project (CVP) and State Water Project (SWP, hereinafter CVP/SWP; Long-term Operations Biological Opinions) that include Reasonable and Prudent Alternatives (RPA) designed to alleviate jeopardy to listed species and adverse modification of critical habitat. NMFS' Opinion requires the U.S. Bureau of Reclamation (USBR) and NMFS to host a workshop no later than November 30 of each year to review the prior water year's operations and to determine whether any measures prescribed in the RPA should be altered in light of new information (NMFS' OCAP Opinion, section 11.2.1.2, starting on page 583). Amendments to the RPA must be consistent with the underlying analysis and conclusions of the Biological Opinions and must not limit the effectiveness of the RPA in avoiding jeopardy to the ESA listed species or result in adverse modification of critical habitat.

The purpose of this annual review of the Long-term Operations Biological Opinions (LOBO) is to inform NMFS and USFWS as to the effectiveness of operations and regulatory actions prescribed by their respective RPAs in the 2013 Water Year.

Since the Long-term Operations Opinions were issued, NMFS, USFWS, USBR, U.S. Geological Survey (USGS), California Department of Fish and Wildlife (CDFW) and the Department of Water Resources (DWR) have been performing scientific research and monitoring in concordance with the implementation of the RPAs. Technical teams and/or working groups, including the geographic divisions specified in the NMFS' Long-term Operations Opinion, have summarized their data and results following implementation of the RPA Actions within technical reports. The data and summary of findings related to the implementation of the RPAs provide the context for scientific review regarding the effectiveness of the RPA Actions for minimizing the effects of water operations on ESA listed species and critical habitat related to the operations of the CVP/SWP. A subset of these technical reports was presented for consideration by the 2013 LOBO IRP (see Appendix 1).

General charge and scope for the 2013 LOBO IRP: Annual reviews prior to 2012 considered all of the RPA Actions but in 2013, as in the previous year, the panel's charge focused on a subset of the operations and RPAs.

This year's annual review included:

(1) Temperature management opportunities and constraints in WY 2013 as assessed by the Sacramento River Temperature Task Group (SRTTG);

(2) Proposed modifications to Term and Condition 2a of the NMFS Long-term Operations BiOp, which required USBR to develop alternative methods for the quantification of incidental take of listed salmonid species and green sturgeon at the Federal and State export facilities;

(3) A retrospective analysis of water operations and delta smelt protective actions taken in WY 2013.

The specific scope of the 2013 LOBO review was defined by questions posed to the 2013 IRP by the technical teams/task groups that presented materials for review. This IRP report addresses each of the questions posed from a scientific perspective, and provides additional observations, opinions and recommendations where, in the panel's opinion, they seemed potentially useful to agency staff for consideration in real-time decision making.

***Acknowledgements*:** The members of the IRP appreciate and acknowledge the efforts of the agency and technical team representatives and contractors who prepared the written materials and delivered the workshop presentations on which this report is based. Each year we are cognizant that much of the material has to be compiled, analyzed and organized in a relatively short time, and that this year the federal government shutdown in October 2013 was a particularly difficult challenge for the federal agencies involved. Despite the many competing demands on the workshop participants, the materials were presented professionally, concisely, and largely on schedule. The panel wishes to express a special thanks to the Delta Science Program management and the entire staff for providing the organization and logistical support to facilitate our task. In particular, Lindsay Correa (Senior Environmental Scientist), as usual, expertly attended to a wide variety of technical and provisional details in support of the IRP's efforts before, during and following the workshop. Similarly, George Isaac ably assisted us through a number of administrative issues.

LOBO IRP COMMENTS ON RPA ACTIONS IN WATER YEAR 2013

General comments and observations

The IRP begins this annual review with a familiar mantra to encourage the development of scientifically defensible connections between satisfying the conditions of specific physical or numerical targets prescribed in the RPAs and ecological responses in the listed species populations. Meeting prescribed targets such as temperature control points within specific river reaches and prescribed levels of incidental take is not the same as succeeding in the intended overarching purpose of the RPAs. An annual science panel is not required to confirm whether or not prescribed targets are achieved but rather if achieving those targets can reasonably be expected to address the intended purpose of reducing or eliminating jeopardy to listed species associated with annual water operations. This requires a demonstrable connection between biological responses of the protected species and the RPAs. The 2013 panel's intent is not to suggest that previous IRP statements to the same effect have gone unheeded, but rather as a reminder to encourage the continued movement we have seen in this direction.

At the workshop in Sacramento, the panel was presented with a brochure that briefly described the California Data Exchange Center and Flood Emergency Response Program. Presumably, this was offered in response to previous IRP recommendations (Anderson et al., 2011, 2012) to develop of a web-based collaborative tool that encouraged multidisciplinary collaboration and a centralized data source for real-time management of water resources as applied to the LOBO objectives. The purpose of the program is to provide reservoir operations staff secure and rapid access to data from

remote sensors and instrumentation that feeds into forecasting models intended to coordinate reservoir operations prior to and during flood emergencies. It was not surprising that such a system is in place, but it is unclear how easily it could be adapted to the purposes the previous IRPs envisioned.

Hydrologic summary of the 2013 Water Year (WY)

The 2013 WY presented a forecasting challenge for water operations in that precipitation early in the year held out a false promise of water availability later in the year. The early season precipitation was followed by the driest January to May period on record for the past 90 years. Although total precipitation for the WY was nominally less than 10% below average, it was the distribution of precipitation that presented the challenge for water management. Snowpack in the mountains did not persist much beyond April and there were early demands for irrigation water from some users with senior water rights.

Given the wealth of annual flow records available to various technical groups, it is important to have and use the results of a comprehensive analysis of rainfall patterns coupled to regional and global climatic patterns. Such an analysis should identify precipitation-related conditions under which regional aquatic biota have evolved and which also help to identify reservoir release patterns that can be used as part of an adaptive management strategy favoring the survival of those species [see, for example, recent studies conducted in the eastern United States; Maxwell et al. 2013, Sheldon and Burd 2013, and Sherwood and Greening 2013]. One requirement for restoring or maintaining habitat quality will be to recreate or simulate previously existing hydrographic cues important to the survival of listed species. A first step is to establish a relevant benchmark that characterizes important cyclic phenomena. These cycles may not be apparent simply by looking at random blocks of a certain number of years, but rather by viewing historical running averages of various lengths in order to detect predictable cycles of wet/dry periods. With increasing observations of linkage between long-term oscillations in oceanic temperature and/or changes in climatic trends (e.g., Werritty 2002, Hannaford and Marsh 2006, and Maurer *et al.* 2004), it is increasingly important to understand regional runoff patterns (Kelly and Gore 2008). Maurer (2007) and Cayan *et al.* (2008) have done extensive modeling of potential climate change scenarios and could offer insights into changes in runoff that might affect management decisions.

The IRP suggests that a review of annual flow records to detect any predictable patterns influenced by the Pacific Decadal Oscillation (PDO) as well as consideration of proposed scenarios for climate change in California will be useful exercises to “fine-tune” future management options. This objective can be easily accomplished [and may

have already been completed] through analysis of running averages of monthly flow records over 10, 20, 30 and 50 year periods in order to detect oscillations that drive long-term forecasts of water availability. It is likely, for example, that 10-year oscillations will parallel the PDO and longer oscillations may reflect more complex phenomena but will allow the development of wet-period and dry-period forecasting and management strategies.

The very dry 2013 hydrologic year, particularly following on the heels of a previously dry year in 2012, is an opportunity to refine long-term forecasting and management strategies, as the inclusion of these years will result in a downward trend in estimates of available water and a more realistic expectation of achieving the co-equal goals of water supply and resource protection under less than optimal conditions.

The analysis of data describing physical habitat characteristics important in sustaining populations of ESA target species in this very dry year also presents an excellent opportunity to identify marginal habitats that may be limiting the successful recovery of these species, and how the characteristics of those habitats are affected by RPA actions.

Sacramento River Temperature Task Group 2013 Technical Report for the Long-Term Operations BiOps

As in previous dry years, when temperature compliance points (TCP) could not be met downstream, they were moved upstream. This year was no exception and the TCP of 56º F was moved upstream to Airport Road Bridge, where there is no temperature monitoring station to verify that the TCP is even being met. A surrogate station at Balls Ferry is used to estimate water temperature at Airport Road. Riverine temperatures are monitored in one dimension longitudinally at discrete points, which does not account for spatial variation in temperature along a cross-section of the river, with depth, or due to springs (hyporheic flows from the streambed or adjacent upland) or various levels of shade provided by riparian vegetation in off channel habitats. Monitoring the spatial variation in water temperature could provide useful, even essential, information for water management aimed at maintaining or improving survival of salmonid early life stages. Given the apparent difficulty with achieving TCPs between Balls Ferry and Bend Bridge, there appears to be a need to reconsider requirements for TCPs farther downriver of Clear Creek, particularly where there is little overlap with the location of salmonid spawning sites and early life stages. The fact that the vast majority of salmon redds are located upriver of Balls Ferry only serves to support a focus on what can be accomplished in terms of water operations to maintain suitable spawning and early

rearing habitat in areas that are being used by fish. Cold water storage that is conserved rather than released in unsuccessful attempts to extend TCPs farther down river than necessary to insure survival of developing embryos and alevins where redds are located, can be used to improve survival of juveniles during the summer months by reducing both temperature stress and the risk of stranding; that is, it may be a useful exercise to determine the location of the TCP by the downstream extent of a predetermined majority of potentially successful redds in both main-stem and secondary channels. See Appendix 3 for details of a heuristic model that should help to demonstrate this point.

The IRP suggests that the question of changing compliance points from a daily average temperature to a 7-day average daily maximum (7DADM) needs to be evaluated in the context of how it affects the location of the TCP as well as survival of salmonid early life stages. The current management scheme, based on daily average temperature, is potentially suboptimal because the location of the TCP is too far downstream, which then reduces the water available to address other mortality processes, e.g. redd dewatering and juvenile stranding (See Appendix 3). If the 7DADM metric effectively moves the TCP farther downstream (relative to the current average temperature location) and so requiring additional water, then the standard could be detrimental to both total fish survival and flexibility of Shasta operations. Alternatively, if the TCPs are allowed to change locations based on the availability of cold water resources, changing them from a daily average temperature to a 7DADM could even result in the TCP moving upstream. Therefore, until a model is developed and applied to consider tradeoffs in water allocations the IPR believes the effects of the temperature standard on fish is uncertain.

As noted by previous OCAP and LOO panels, decisions to augment or constrain water releases need to consider the coupling of hydrology and biology, including spatio-temporal impacts on adult selection of redd locations as well as survival of egg through early juvenile life stages. Some of these relevant issues are discussed in Appendix 5.

The Effect of TCD Hydraulic Operational Criteria on Storage of Cold Water

Constraints on Shasta operations that affected the use of the cold water resource within the reservoir were evident in WY 2013. According to the technical report:

“Because of the low storage and elevation at Shasta Reservoir this water year, Shasta Temperature Control Device (TCD) operational criteria limited Reclamation’s flexibility with the TCD gate configurations. This reduced the temperature operation efficiency for a period in June 2013. In June, Reclamation was required to open all the middle shutters sooner than desired to meet hydraulic operational criteria. This was based on

the Shasta TCD operation manual, which states at water surface elevation 1010 feet, all middle gates are to be open to maintain proper submergence of the penstock intakes."

We note that operations to meet temperature criteria in June of 2013 (page 9) could not be optimized because of these operational restrictions. It may be useful to evaluate the likelihood of critical depletions more than 30 days in advance so that water deliveries can be scheduled over a longer time period and hence avoid the hydraulic operational criteria that have the net effect of forcing the inefficient use of cold water storage. In this recommendation, we assume that the need to invoke this operational criteria decreases with reductions in powerhouse discharge.

Use of HEC-5Q for Long Term Temperature Forecasts

The IRP understands that the quantity of cold water storage primarily in Shasta Reservoir, but also in Trinity and Whiskeytown Reservoirs determines the downstream extent of Sacramento River habitat that meets the temperature requirements of early life history stages of fall and winter-run Chinook salmon. Effective use of the cold water resource over an annual operational cycle to maximize survival benefits for fish requires accurate predictions and monitoring of: (a) reservoir stratification dynamics, (b) selective withdrawal characteristics of the reservoir outlets, and (c) water temperature dynamics of the upper river. The IRP was informed at the LOBO workshop that HEC-5Q was used to develop water flow and temperature management scenarios for consideration. HEC-5Q is a standard modeling tool developed by the Corps of Engineers to evaluate alternative operational plans. It can be used for short-term optimization (optimum blending of water from different reservoir strata to meet an immediate downstream temperature target) when combined with selective withdrawal capability. It can also be used for long-term optimization (i.e., determine release quantity and water temperatures to optimize reservoir storage) to meet long-term downstream temperature criteria. We have several comments related to the use of HEC-5Q to support water temperature management in the Sacramento River.

First, as with all models, there are tradeoffs between model accuracy and run-time. Models useful for optimization must be relatively simple to minimize the time required for multiple runs to converge on an optimal operation given a specific optimization function. We assume that the need for reduced run-time factored into the decision to use this model. However, some of the attributes of HEC-5Q that make it useful for long term operational optimization also increase the error of its predictions. While calibration details for the modeling were not provided, based on experience and expertise represented on the IRP, there are multiple sources of uncertainty that may affect the accuracy of the forecasts by as much as 2-3º C. Increased error in model forecasts increase the risk that incorrect water management decisions may be made. In the case

of the HEC-5Q application, we note three attributes of the HEC-5Q application that likely affect forecast accuracy:

- The model was updated with meteorological conditions at 6-hour time-steps instead of 1-hr or even 3-hr updates. While longer time periods between updates will likely not affect prediction accuracy of reservoir stratification, they will likely affect the accuracy of river temperature predictions, particularly at lower flows or during high temperatures when salmon early life stages are most susceptible to temperature effects.

- The reservoir dynamics were simulated with a 1-D representation (vertical) whereas stratification and water quality dynamics within reservoirs are typically 2-D (longitudinal and vertical) although situations may occur were a full 3-D representation may be required. As a consequence, calibration parameters in a 1-D model must be adjusted to ranges outside of values that have physical meaning to "force" the 1-D model to calibrate to reality that is usually at least 2-D, if not 3-D. The amount of error associated with use of a 1-D model to simulate a reservoir depends upon the extent to which the 1-D assumption is violated.

- The river was simulated with a 1-D representation (longitudinal). This is likely the smallest source of error and may be negligible depending upon how the temperature calibration was performed. For example, if the riverine part of the HEC-5Q model was calibrated to accurately simulate low flow, summer time conditions then the simulations may be of acceptable accuracy. However, if the model was calibrated to minimize residuals (i.e., differences between predicted and observed water temperatures) over an annual cycle then the simulation accuracy may be reduced for the time periods that are most critical to salmon early life stages. In addition, the report mentions a number of ungaged and unmonitored tributaries downstream of Keswick Dam that may seasonally affect water temperature. The methods used to synthesize tributary flow and temperature should be reviewed to optimize forecast accuracy.

Next, while there is nothing inherently wrong with HEC-5Q we note that it is an older legacy model that, to our knowledge has not been updated for more than a decade. For purposes addressed in this review, a more current model such as CE-QUAL-W2 or a dedicated temperature model that can be run to support real-time operations (CE-QUAL-W2 can also be used for this purpose) may be more appropriate. Interestingly, CE-QUAL-W2 has been applied to Shasta Dam and the IRP wondered why it was not used to support management decisions that are based on downstream temperature and stage dynamics.

There seems to be suboptimal communication between field survey teams monitoring redd dewatering and juvenile stranding and group members who simulate water temperatures. Model selection and calibration should be coordinated within the SRTTG such that future temperature modeling and forecasting are configured, calibrated and optimized to accurately predict temperatures at TCPs located at different distances downstream of Keswick dam during critical salmon early life stages or alternatively to identify a TCP based on the distributions of redds.

Temperature modelers may wish to calibrate to extreme values/conditions in the Sacramento River instead of using standard methods to reduce deviations (differences between measurements versus predictions) over an annual cycle. That is, the ability to simulate temperatures around 40^{O} F is less important than the ability to accurately simulate temperatures around 55^{O} F. This can be done easily during calibration by weighting more heavily (e.g., doubling them) residuals associated with critical time periods when temperatures approach detrimental levels.

Another question of interest is also affected by the details of model calibration. The LOBO workshop presentation by Brycen Swart (NOAA Fisheries) included temperature measurements summarized as average daily water temperature versus a seven day running average of daily maximums (7DADM). There is typically about a 2^{O} F difference between the two temperature statistics which is likely consistent with the expected error in the river water temperature predictions from HEC-5Q. The selection of an acceptable maximum temperature measure that avoids deleterious effects on early salmon life stages, while minimizing demands on water resources, should include input from river water temperature modelers to ensure model accuracy during the months and flow conditions considered to be most critical to salmon survival.

The IRP noted that the extensive water temperature data collected by the California Department of Fish and Wildlife (CDFW) in connection with monitoring salmon redds did not appear to be integrated into the temperature modeling studies conducted by the BoR. It would have been useful to compare the measured temperatures obtained by the CDFW during redd dewatering/stranding studies to the predictions made by HEC-5Q to get a better idea of the differences between predicted and observed water temperatures.

NMFS seemed most interested in how water releases affected seasonal variation in water depth as it pertains to redd dewatering and juvenile stranding. HEC-5Q (or a future model) can output both stage and depth. The IRP considered ways that the output of both stage and discharge estimates could be coupled to survival of early life

stages associated with dewatering/stranding of redds and juveniles (see Appendix 3 of this report).

Better Integrating Long-term Forecast Simulations with Real-Time Operations

Reservoir operations currently appear to be based on relatively long-term simulations derived from data and hydrologic models from the U.S. Army Corps of Engineers Hydrologic Engineering Center (HEC) but many of the issues addressed by the Sacramento River Temperature Task Group (SRTTG) require short-term remedies using real-time operations at Shasta, Trinity, and Whiskeytown Reservoirs. The SRTTG seems to be largely operating in a reactive adjustment mode as a means of meeting RPA targets. For example, TCPs in any given year are reset depending on the availability of cold water storage in reservoirs, but ultimately are expected to meet 10-year running average expectations at multiple riverine locations (Clear Creek, Balls Ferry, Jelly's Ferry and Bend Bridge). In WY 2013, a 56º F TCP was set at Airport Road Bridge, where there is no RPA requirement to meet any 10-year running average success criterion. The SRTTG annually recommends a TCP point that, given available cold water storage, is feasible for the longest river reach that could provide salmonid spawning habitat regardless of where active spawning is occurring. Long-term forecast simulations were apparently inadequate to support more strategic use of the cold water resource during the dry 2013 WY, if in fact there even were a more effective way of managing reservoir operations. Inter-annual variability in the seasonal amount and spatial distribution of precipitation in the region presents a serious forecasting challenge.

It appears that the real-time operations needs of the SRTTG and the long-term forecasting of USBR are not well interfaced, and perhaps there is an opportunity here to collaborate on development of an integrated long-term forecasting and real-time operations capability. For example, the present *ad hoc* temperature monitoring system does not include a station at Airport Road Bridge. This could easily be remedied and such collaboration would increase the accuracy of temperature forecasts and provide increased lead time prior to water crisis situations thereby potentially increasing the efficiency with which the cold water resource can be managed to enhance survival of salmonids as suggested in Appendix 3 of this report.

Critical elements of an improved real-time monitoring system would include at least: (a) one or more automatic temperature profilers within Shasta Reservoir to describe temperature stratification patterns near the dam; (b) real-time temperature reporting sondes located at points within the Sacramento River channel and significant tributary mouths; (c) real-time calibrated reporting stage monitors, and (d) a dedicated high

resolution temperature forecasting model that can be used in near-real time to forecast and evaluate downstream temperatures, stages, and discharges based on different scenarios of dam releases, release temperatures, and range of anticipated meteorological conditions. The real time model, coupled with reporting temperature and stage monitors, will help ensure that the cold water resource within the three reservoirs is used as efficiently as possible to protect fish and allow flexibility in water operations.

Establishing a real-time modeling capability requires additional information. For example, transects of channel and flood plain morphology at key locations at known spawning habitats should be surveyed if such information does not presently exist. Annually collected low flow light detection and ranging (Lidar) data for the reaches below Keswick dam to Red Bluff diversion dam (see Fig. 1 in Revnak and Killam 2013) could be used to develop a Digital Elevation Model (DEM) to feed into existing hydraulic models. The DEM in conjunction with stage-discharge and temperature relationships could be used to evaluate the likelihood of stranding and dewatering over all discharge regimes and as spatial distribution of spawning and rearing change from year to year.

In addition, the IRP supports continued and expanded monitoring of redd dewatering and juvenile stranding and suggests that the teams place temperature/water level sensors in redds and important juvenile rearing habitats. This will allow a retrospective analysis of modeling and application of water flows intended to benefit the species of interest over their riverine life cycle stages. Then the important question of how many fish benefit from the water management can be addressed so that informed decisions can be made to maximize protection of salmon redds and low flow juvenile salmon habitat. With this type of assessment informed decisions about moving TCP can be made in keeping with RPAs, which are aimed at protecting fish not simply meeting TCP goals.

Consideration of River Water Temperature Dynamics

In general, the SRTTG seems to consider river water temperatures in a simplistic way as though water temperatures are laterally and vertically homogeneous within the river corridor. It would be desirable to measure the spatial variability of temperature and water level relative to critical spawning and rearing habitat, including secondary channels (see Appendix 5). Future temperature dynamics studies within the river corridor should include monitoring temperatures in the main channel, secondary channels, hyporheic (within the gravel) zones, secondary channels, and tributaries.

Loss Estimation for Listed Anadromous Species

The technical team (TT) uses Jahn's (2011) simple model to estimate fish loss*:*

$$K = G\text{-}H = H/S\text{-}H$$

where *K* =loss, *G*=entrainment, *S*=survival proportion, and *H*=salvage.

Given that entrainment cannot be measured directly, there appears to be no other means of estimating loss except from observed (expanded) salvage and an assumed survival rate, even though this may compromise the accuracy of the total loss estimate if entrainment (or losses associated with it) are large or highly variable. Setting the entrainment issue aside for now, the IRP also had several concerns with the implementation of the loss model and with estimates of its uncertainty:

a) characterizing *S* as a fixed parameter leads to underestimates of total loss,

b) characterizing the uncertainty of *S, H, G, and K* by standard errors understates their true variability,

c) Equations 8 and 9 of Jahn's (2011) error propagation method are incorrect, and

d) Jahn's (2011) model fails to account for probable losses associated with zero salvage, further negatively biasing its loss estimates.

See Appendix 2 for a more detailed explanation of the concerns and some recommendations for resolving these issues. Appendix 2 includes several suggested ways to reduce the bias of the loss estimates and increase the realism of their uncertainties, including: a) modeling *S* to realistically vary over short time scales (daily, weekly), b) estimating annual loss as the sum of daily losses, c) treating *G* and *K* as random variables whose uncertainties are estimated via Monte Carlo simulation rather than closed-form error propagation, and d) using a Bayesian method to estimate the probable losses associated with zero salvage. Finally, we suggest statistical strategies for making RPA-triggering decisions based on daily loss estimates, in the face of high uncertainties in those estimates.

Delta Water Operations and Delta Smelt Protective Actions

The seasonal distribution of precipitation in the Central Valley watersheds in WY 2013 resulted in a distinct “first flush” event, which has not been as discretely discernible in previous years. The Smelt Working Group (SWG) thus had some information to alert them to a potential trigger for spawning migration that could place some portion of the pre-spawn adult delta smelt population in a location that would make them susceptible to entrainment into the pumping facilities. By mid-December delta smelt were appearing in salvage and the USFWS determined that OMR flows should be constrained under RPA Action 1. This was the first time that Action 1 had been applied to protect pre-spawn delta smelt and when negative OMR flows were reduced, the number of salvaged delta smelt declined, totaling 86 between December 12 and January 1. The continued presence of delta smelt in the central and south Delta led to the implementation of continued – albeit more relaxed - constraints under subsequent RPA Action 2 in January, which was associated with another 146 delta smelt in expanded salvage, for a total of 232 by February 2, 2013. This level of take remained below the revised allowable incidental take value of 362 for WY 2013.

Recent efforts to understand the population dynamics of delta smelt using an individual-based modeling approach (Rose et al. 2013a, b) have suggested that multiple factors (e.g., temperature, stage-dependent growth rates, entrainment into water operations, etc.) are important in determining the inter-annual abundance of this species in the estuary but the importance of key factors may vary among years (i.e., wet versus dry). However, Rose et al. 2013a also cautioned that their model was not designed to forecast future delta smelt population abundance.

The IRP continues to believe that discerning behavioral responses of delta smelt to tidal oscillations (e.g., Feyrer et al. 2013) and perhaps associated turbidity changes is crucial for understanding delta smelt movements and spatial dispersion, which has potential consequences for affecting the level of fish entrainment at the Delta pumping facilities. Reliance on salvage to estimate delta smelt mortality associated with water operations remains a concern of the IRP. New information about potential losses associated with entrainment at the pumping facilities (e.g., Castillo et al. 2012) suggest that the determination of allowable incidental take even from extended salvage estimates may underestimate actual facility impacts on this species.

The IRP also continues to believe that the use of particle tracking models may not adequately capture the behavioral responses of delta smelt to important migration cues. Reliance on turbidity measures associated with discrete “first flush” events to predict delta smelt migration is risky because these events vary in intensity and annual

occurrence. Furthermore, delta smelt tend to be distributed within the water column during incoming tides and move to the bottom and shallow channel edges during ebb tides (Feyrer et al. 2013) as a means of maintaining their position within the estuary.

Lacking convincing evidence to the contrary, it seems counter-intuitive that an annual species such as the delta smelt would have evolved to depend for its survival on temporally unreliable environmental cues to trigger migrations associated with crucial life cycle events such as spawning or selection of nursery locations. Perhaps turbidity cues are more obvious to the smelt than to human observers, but the smelt are not making decisions about water operations.

See Appendix 4 for a discussion of delta smelt behavior and a potential approach for developing preemptive actions to reduce entrainment.

IRP RESPONSESTO QUESTIONS DEFININGTHE SCOPE OF THE 2013 LOBO ANNUAL REVIEW

Responses to questions regarding Sacramento River Temperature Task Group 2013 specific questions

1) **How well did implementation of the RPA actions meet the intended purpose of the actions?**

When the intended purpose of an RPA action is to meet a very discrete objective, it is relatively easy to decide if the intended purpose is met. For example, Action I.2.2.A requires USBR to convene a group to consider a range of fall actions if the end of September storage is 2.4 MAF or above. This was the case in WY 2013, so this action met its intended purpose in WY 2013. Other examples are not so clear, especially when only certain portions of the intended purpose are either met or not achieved. For instance, part of Action 1.2.4, which deals with the development and implementation of a Keswick release schedule, requires that USBR fund an independent modeler to report on temperature management and recommend refinements by March 2010. This has yet to occur, so the intended purpose of this portion of Action 1.2.4 has not been met.

Determining the successful implementation of other aspects of Action 1.2.4 may depend on whether one perceives the intended purpose of the actions as meeting a physical target or having a desirable biological effect on salmonid populations. It continues to be difficult, if not impossible in dry years (such as WY 2013), to meet TCPs as one moves farther downriver, but based on modeling water temperatures and using a surrogate monitoring station at Balls Ferry, it appears that an average daily temperature of 56º F

can be maintained at Airport Road Bridge. However, this has yet to be demonstrated with *in situ* measurements.

TCPs are also intended to be measured on the basis of a 10-year running average at multiple locations, but this is only the fourth year they have been in place. Thus, it is not possible to determine if TCPs are even meeting their intended site-specific targets. One complication with using Airport Road Bridge is that it was not one of the original locations specified in the RPAs and there is no temperature monitoring station at that location, which will make it difficult to include in a 10-year running average. Finally, the link between RPA actions and survival of salmonid early life stages remains elusive, but see Appendix 3 of this report.

Aspects of other RPA actions (e.g. I.2.3.A) were clearly the result of compromises that seemed to favor water operations over the requirements of the fish populations, at least as viewed by the fish agencies. While the fish agencies expressed a desire to maintain Keswick releases at 4500 cfs to avoid dewatering redds and stranding juvenile Chinook salmon, releases were ramped down from December through mid-February to 3800 cfs. While this was 550 cfs higher than desired by USBR, it was 1250 cfs lower than what the fish agencies considered necessary for salmonid protection. In such an instance, it is impossible to make an assessment as to whether or not the intended purpose of an RPA action was met.

2) **How effective was the process for coordinating real-time operations with the technical team's analyses and input as presented in the NMFS' Long-term Operations BiOps?**

Six meetings were convened to discuss cold water reserves that could be allotted to maintain TCPs and desirable river stage levels in the Sacramento River. However, there is little evidence to suggest any of the operations had a significant positive or detrimental effect on Sacramento Chinook populations (dewatering of some redds notwithstanding), nor was any evidence presented on how water transfers from Trinity to Shasta Lakes might be affecting salmonids in the Trinity River. Consequently, the IRP was unable to provide an objective answer to this question. Meetings were held, technical teams provided input and USBR made water operation decisions that were affected by considerations extrinsic to those that were part of the process to which the question pertains.

3) **Were the scientific indicators, study designs, methods and implementation procedures used appropriate for evaluating the effectiveness of the RPA actions? Are there other approaches that may be more appropriate to use?**

No. Spatial variation in water temperature and river stage needs to be better addressed within the context of impacts on salmonid spawning habitat and early life stage impacts of water operations. Deployment of water level loggers and temperature probes in spatial arrangements that are relevant for addressing the question of how flow regulation impacts fish is seemingly a requisite first step. Modeling alone may not solve the problem without accurate on the ground measurements.

Currently the ability to meet the TCPs is a central measure of the effectiveness of the RPA Action I.2.1. The IRP postulates that a more effective measure might be developed by integrating information on the spatial/temporal distributions of salmon during critical freshwater life stages into the TCP decision. Instead of meeting a TCP, consider a model-derived estimate of salmonid freshwater survival. As demonstrated in Appendix 3, such a measure might improve fish survival and flexibility in storage water operations. The IRP understands moving away from the current TCP measure would affect reservoir operations. Given the implications, the IRP suggests that NOAA form a working group to consider this issue.

4) **How can implementation of RPA actions I.2.1. – I.2.4. be adjusted to more effectively meet their objectives?**

Aquatic biota key to local geophysical dynamics and geospatial complexity. These factors are not reflected in the RPA actions, with the result that the river corridor of the upper Sacramento River is treated as a homogeneous system. By default, management actions are restricted to adjusting flow and release rates in attempts to meet a TCP based on storage of cold water in the upstream reservoirs. Substantial opportunities for salmon recovery and conservation may be realized by considering geophysical dynamics and geospatial complexity. For example, 29 of 45 redds pictured in Revnak and Killam (2013, Appendix D) were located in secondary channels. Environmental conditions (particularly temperatures) in the secondary channels can be substantially different than those in the main channel. Also, substantial numbers of juvenile Chinook were either stranded or in jeopardy of stranding in secondary channels and marginal riverine habitats. Although total juvenile abundance was not monitored, these shallow marginal habitats and secondary channels are certainly used by juvenile salmon. NMFS should consider adjusting RPA actions 1.2.1 - 1.2.4 so that redd location and juvenile abundance are better related to temporal and spatial patterns in habitat quality (e.g., water temperature, depth, and velocity pattern) at the scale salmon life stages respond to their environments (see Appendix 5).

In the SRTTG report and presentation at the LOBO workshop in Sacramento, there was a proposal to change the nature of the temperature compliance points from daily

average values to 7DADM. There may be good biological justification for considering this depending on how sensitive early life stages are to brief exposures to suboptimal, or even lethal, temperatures. There is some evidence that the 7DADM may better protect salmon early life stages from negative effects of temperature spikes than does an average daily temperature TCP. However, the specific temperature of a TCP based on daily maxima was not suggested. If the intent is to use the same value (56º F), the effect of using the 7DADM would be to move the current TCP (daily average temperature) downriver at considerable cost in cold water resources with little improvement in early life stage survival if the distribution of redds continues to remain upriver of Airport Road Bridge. Alternatively, if the intent is to set a higher temperature (i.e., > 56º F) for a daily maximum-based TCP, there may be little or no effect on location of the current TCP, or it could even move upstream. In any case, it is important to consider inter-annual variation in cold water storage and the trade-offs associated with adopting a 7DADM TCP (or a different duration of running average) as the preferred maximum thermal threshold for insuring survival of salmon early life stages. These trade-offs are considered by the IRP in Appendix 3 of this report.

Responses of 2013 IRP to questions regarding Chinook, steelhead and green sturgeon loss estimation at the Delta Pumping facilities

1) **Are the technical work team's proposed equations for estimating loss supported by current science?**

Mostly. However, the direct application of the equations to annual salvage creates a bias. Overlooking the losses associated with inserted zeros creates additional bias in the loss estimates. Additional modeling research may be needed to devise the most accurate (least biased) loss estimates.

2) **Are the technical work team's proposed equations for estimating annual loss confidence intervals scientifically appropriate?**

No. Uncertainty has been modeled in terms of standard errors (SE) of fixed parameters. This approach greatly understates the true uncertainty. Also, an error propagation method was used to estimate the SE of loss from the SEs of survival and salvage. Two of Jahn's (2011) equations (8 and 9) for this propagation are incorrect. The IRP proposes modeling salvage, survival, entrainment and loss as random variables, and estimating the mean and standard deviation of daily and annual losses via Monte Carlo simulation instead of closed-form error propagation.

3) **Which, if any, of the proposed terms in the technical work team's equations introduce the greatest uncertainty? How might these formulations be improved in the future?**

The greatest uncertainty is due to the survival proportion, and to the lack of direct measures of entrainment. The IRP suggests additional research to better characterize whole-facility survival, as a function of season, flow, temperature and other relevant factors. Appendix 2 of the present review report includes a Bayesian model for loss estimation which has the ability to incorporate independent knowledge about entrainment, if and when such knowledge becomes available.

4) **Which, if any, data inputs in the technical work team's equations are likely to reduce accuracy in their estimates?**

The current assumptions about zero data values for salvage leads to a negative bias in daily and annual loss estimation. Appendix 2 suggests a correction for this bias. The unrealistic assumption of a single, fixed value for survival creates an additional negative bias for annual loss.

5) **Are ongoing studies sufficient to gather data needed to calibrate coefficients and terms in the loss equations? What changes to ongoing studies or recommendations for future studies are needed to gather data to measure coefficients and values in the equations' terms?**

The concept of coefficients that can be calibrated, and of model parameters with standard errors, is not a realistic framework for modeling survival rate, entrainment, and loss. Realistically, these quantities vary widely and unpredictably over time. The IRP suggests viewing these quantities as random variables and modeling their distributions, as is done by Cramer Fish Sciences (2013). A careful synthesis of previous mark-recapture experiments that estimate whole-facility survival (e.g., Clark et al. 2009), along with additional novel experiments, may be the most effective path to estimate survival distributions and to model the effects of factors that control survival. In addition, research aimed at directly measuring entrainment is encouraged. Even if resulting measurements are crude, they can increase the accuracy of loss estimates via the Bayesian model described in Appendix 2.

6) **Given the importance of the hypothesized relationship between water velocity and facility efficiency for salmonid salvage, what scientific study designs and methods might be appropriate to investigate how this relationship could be incorporated into whole facility survival estimates?**

Given the limited potential to manipulate exports for the purposes of conducting controlled experiments aimed at establishing a relationship between water velocity and whole facility survival rates, controlled flume studies may provide a portion of the

answer. However, it will be difficult to simulate realistic conditions that capture all of the variables that determine whole facility survival. For example, the effects of predator fields associated with the facilities would be particularly difficult to simulate. In order to accurately determine whole facility survival rates, it is important to determine whether or not there is even a relationship between salmonid salvage and entrainment survival (mortality). Perhaps this could be addressed with carefully designed mark-recapture experiments conducted over multiple but relatively short-term periods of controlled water export pumping that would not interfere with total exports. For example, low and high water velocity runs could be alternated in experimental runs such that average weekly (or monthly) exports were unaffected while monitoring the recapture (in salvage and escapement – i.e., *sensu* fish overcoming the influence of entrainment flows and migrating out of the area) of marked fish released at the point where they would be initially entrained into the pumping facilities.

7) **What additional studies should be seasonally, annually, or semiannually completed to increase the accuracy of estimates of loss for green sturgeon?**

So little is known about the life-history of the green sturgeon that any studies shedding light on this species' responses to physical habitat variables (velocity, depth, substrate, cover, and complex hydraulics), particularly during its early life stages are likely to be useful.

8) **How well is the genetic information used in the technical work team's equation for estimating loss of winter run Chinook?**

With the information provided, it is difficult to determine the effectiveness of the genetic information.

9) **What sampling design provides the most accurate approach for characterizing the presence of genetic winter run Chinook salmon occurring inside and outside the Delta model winter-run size category?**

The IRP was not provided with alternative approaches to consider and is reluctant to suggest novel sampling designs at this time. However, the ability to separate cohorts associated with different salmon runs from overlapping size distributions seems to be at the core of this issue. There are algorithms and software packages that may assist in separating these cohorts with an assignable probability of goodness of fit (e.g., legacy software MIX Program v. 3.1, and the more current mixdist; for details see http://ms.mcmaster.ca/peter/mix/mix31.html and http://cran.r-project.org/web/packages/mixdist/mixdist.pdf). In practice, fitting mixed distributions can be more of an art than a science, but the more information that one has at the start, the better the chances of successfully distinguishing cohorts among mixed size

distributions. In this regard, the genetic information available on winter-run Chinook salmon could be applied in retrospective analyses to test the accuracy of this approach.

Responses to questions regarding the retrospective analysis of water operations and delta smelt protective actions taken during December – June of WY 2013

1) **How well did implementation of RPA Action 1 meet the intended purpose of the Action?**

The information necessary to answer this question is incomplete. The outcome in the absence of the Action cannot be determined. The answer also depends on the intended purpose of the Action.

If the intent was to prevent exceedence of the allowable incidental take of delta smelt, then the answer is a qualified “maybe” because incidental take was not exceeded. However, this conclusion should be viewed in light of observations from previous years when incidental take limits also were not exceeded even though Action 1 was not implemented. Take limits were not exceeded in any of the past four water years and Action 1 was not implemented in three of the four years. Consequently, there is no apparent association between the implementation of Action 1 and whether or not the calculated allowable incidental take is exceeded. What might have happened if Action 1 was not implemented in WY 2013 is simply conjecture.

If the intent of Action 1 is to protect the delta smelt population from impacts of water pumping operations, there is little on which to base a judgment. Incidental take is calculated from historical delta smelt salvage (Cumulative Salvage Index, CSI) and no clear relationship has been demonstrated between salvage and total mortality of pre-spawn adults attributable to pumping operations. For example, if recent studies (e.g., Castillo et al. 2012) are any indication, entrainment mortality may be substantially greater than previously envisioned. That is, salvaged delta smelt may represent a very small percentage of actual “take” (loss) associated with water operations. Also, allowable incidental take is calculated using a measure of estimated relative population size (i.e., the Fall Midwater Trawl Index) that may not be reliable. The Fall Midwater Trawl was not designed to collect delta smelt and any assumed relationship between the abundance index based on those collections and the actual size of the smelt population is questionable at best. This is interesting in light of the fact that larger salvage values in the past can determine the current allowable take limits. For example, this year the allowable take of adult delta smelt (not including losses other than extended salvage) was originally calculated as 305, but an error discovered in the value for salvage in the 2006 WY resulted in a revised allowable take value of 362, an

increase of nearly 20% based on a revised single value of salvage from seven years ago.

2) **How can implementation of RPA Action 1 be adjusted to more effectively meet its objectives?**

Without knowing the effectiveness of RPA Action 1 (see answer to the previous question) it is difficult to suggest a means of improving effectiveness. At the LOBO Workshop in Sacramento this year, earlier implementation of Action 1 was proposed as a means of providing preemptive protection for delta smelt while at the same time allowing for greater subsequent water exports; essentially, the proposal was to increase efficiency of delta smelt protection. The IRP agrees, in concept, that a more aggressive and preemptive implementation of Action 1 is worth developing. See Appendix 4 for a discussion of delta smelt behavior and movements that the IRP offers as straw-man guidance in the development of an improved implementation procedure for Action 1 that may provide more preemptive protection for pre-spawning adults.

REFERENCES

Anderson, J., A. Blumberg, P. Goodwin, S. Monismith and C. Simenstad. 2009. Science Review of the Two Gates Project. edited by Clifford N Dahm and Lauren Hastings.

Anderson, J.J., R.T. Kneib, S.A. Luthy and P.E. Smith. 2010. Report of the 2010 Independent Review Panel (IRP) on the Reasonable and Prudent Alternative (RPA) Actions Affecting the Operations Criteria and Plan (OCAP) for State/Federal Water Operations. Prepared for: Delta Stewardship Council, Delta Science Program. December 9, 2010. 39 p.

Anderson, J.J., J.A., Gore, R.T. Kneib, M.S. Lorang and J. Van Sickle. 2011. Report of the 2011 Independent Review Panel (IRP) on the Implementation of Reasonable and Prudent Alternative (RPA) Actions Affecting the Operations Criteria And Plan (OCAP) for State/Federal Water Operations. Final report submitted to the Delta Stewardship Council, Delta Science Program. December 9, 2011, 47 p.

Anderson, J.J., J.A., Gore, R.T. Kneib, M.S. Lorang and J. Van Sickle. 2012. Report of the 2012 Delta Science Program Independent Review Panel (IRP) on the Long-term Operations Opinions (LOO) Annual Review. Final report submitted to the Delta Stewardship Council, Delta Science Program. December 1, 2012, 54 p.

Bennett, W. A., W. J. Kimmerer, and J. R. Burau. 2002. Plasticity in vertical migration by native and exotic estuarine fishes in a dynamic low-salinity zone. *Limnology and Oceanography* 47:1496-1507.

Cramer Fish Sciences (CFS). 2013. Alternative Loss Calculation: Sensitivity Analysis. Cramer Fish Science, Gresham Oregon. Prepared for Department of Water Resources, Division of Environmental Services. 45 p.

Castillo, G., J. Morinaka, J. Lindberg, R. Fujimura, B. Baskerville-Bridges, J. Hobbs, G. Tigan and L. Ellison. 2012. Pre-screen loss and fish facility efficiency for delta smelt at the South Delta's State Water Project, California. *San Francisco Estuary and Watershed Science* 10(4): http://www.escholarship.org/uc/item/28m595k4.

Cayan, D.R., E.P. Maurer, M.D. Dettinger, M. Tyree and K. Hayhoe. 2008. Climate change scenarios for the California region. *Climatic Change* 87 (Supple 1): S21-S42.

Chagnaud, B. P., C. Brucker, M. H. Hofmann and H. Bleckmann. 2008. Measuring flow velocity and flow direction by spatial and temporal analysis of flow fluctuations. *Journal of Neuroscience* 28 (17):4479-4487. doi: Doi 10.1523/Jneurosci.4959-07.2008.

Clark, K.W, D. Bowen, R.B. Mayfield, K.P. Zehfuss, J.D. Taplin, and C.H. Hanson. 2009. Quantification of Pre-screen Loss of Juvenile Steelhead in Clifton Court Forebay. Department of Water Resources The Natural Resources Agency, Sacramento California.

Feyrer, F., K. Newman, M. Nobriga, and T. Sommer. 2011. Modeling the Effects of Future Outflow on the Abiotic Habitat of an Imperiled Estuarine Fish. *Estuaries and Coasts* 34 (1):120-128. doi: 10.1007/s12237-010-9343-9.

Feyrer F., D. Portz, D. Odum, K.B. Newman, T. Sommer, et al. (2013) SmeltCam: Underwater Video Codend for Trawled Nets with an Application to the Distribution of the Imperiled Delta Smelt. *PLoS ONE* 8(7): e67829. doi:10.1371/journal.pone.0067829.

Ganju, N. K. and D. H. Schoellhamer. 2008. Chapter 24 Lateral variability of the estuarine turbidity maximum in a tidal strait. In: *Proceedings in Marine Science*, edited by Hiroyuki Yamanishi Jeremy Spearman Tetsuya Kusuda and Z. Gailani Joseph, 339-355. Elsevier.

Goodwin, R. A., J. M. Nestler, J. J. Anderson, L. J. Weber and D. P. Loucks. 2006. Forecasting 3-D fish movement behavior using a Eulerian-Lagrangian-agent method (ELAM). *Ecological Modelling* 192 (1-2):197-223. doi: 10.1016/j.ecolmodel.2005.08.004.

Hannaford, J. and T. Marsh. 2006. An assessment of trend in UK runoff and low flows using a network of undisturbed catchments. *International Journal of Climatology* 26: 1237-1253.

Hasenbein, M., L. M. Komoroske, R. E. Connon, J. Geist and N. A. Fangue. 2013. Turbidity and Salinity Affect Feeding Performance and Physiological Stress in the Endangered Delta Smelt. *Integrative and Comparative Biology* 53 (4):620-634. doi: 10.1093/icb/ict082.

Hauer, F. R. and M.S. Lorang. 2004. River regulation, decline of ecological resources, and potential for restoration in an arid lands river in the western USA. *Aquatic Sciences* 66: 1-14.

Hilton, W. A, A. Johnson and W. Kimmerer. 2013. Feeding Ecology of Delta Smelt During a Seasonal Pulse of Turbidity. http://digitalcommons.calpoly.edu/star/217/

Hobbs, J. A., W. A. Bennett and J. E. Burton. 2006. Assessing nursery habitat quality for native smelts (Osmeridae) in the low-salinity zone of the San Francisco estuary. *Journal of Fish Biology* 69 (3):907-922. doi: 10.1111/j.1095-8649.2006.01176.x.

Jahn, A. 2011. An Alternative Technique to Quantify the Incidental Take of Listed Anadromous Fishes at the Federal and State Water Export Facilities in the San Francisco Bay-Delta Estuary. Kier Associates, Ukiah California. Prepared for National Marine Fisheries Service, Central Valley Office.

Jones, N. L., J. K. Thompson and S. G. Monismith. 2008. A note on the effect of wind waves on vertical mixing in Franks Tract, Sacramento-San Joaquin Delta, California. *San Francisco Estuary and Watershed Science* 6 (2): Article 4.

Kelly, M.H. and J.A. Gore. 2008. Florida river flow patterns and the Atlantic Multidecadal Oscillation. *River Research and Applications* 24: 598-616.

Lorang, M.S., Hauer, F.R., Whited, D.C., and Matson, P.L., 2013. Using airborne remote-sensing imagery to assess flow releases from a dam in order to maximize re-naturalization of a regulated gravel-bed river, *in* De Graff, J.V., and Evans, J.E., eds., *The Challenges of Dam Removal and River Restoration: Geological Society of America Reviews in Engineering Geology*, v. XXI, p. 117–132, doi:10.1130/2013.4021(10).

Maurer, E.P. 2007. Uncertainty in hydrologic impacts of climate change in the Sierra Nevada, California, under two emission scenarios. *Climatic Change* 82: 309-325.

Maurer, E.P., D.P. Lettenmaier and N.J. Mantua. 2004. Variability and potential sources of predictability of North American runoff. *Water Resources Research* 40(9): W09306, DOI: 10.1029/2003WR002789.

Maxwell, J.T., P.A. Knapp, and J.T. Ortegren. 2013. Influence of the Atlantic Multidecadal Oscillation on tupelo honey production from AD 1800 to 2010. *Agriculture and Forest Meteorology* 174-175: 129-134.

Mood, A.M., F.A. Graybill, and D.C. Boes. 1974. Introduction to the theory of statistics (3rd ed.) McGraw-Hill, NY.

Morgan-King, T. L. and D. H. Schoellhamer. 2013. Suspended-Sediment Flux and Retention in a Backwater Tidal Slough Complex near the Landward Boundary of an Estuary. *Estuaries and Coasts* 36 (2):300-318. doi: 10.1007/s12237-012-9574-z.

Murphy, D. D. and S. A. Hamilton. 2013. Eastward Migration or Marshward Dispersal: Exercising Survey Data to Elicit an Understanding of Seasonal Movement of Delta Smelt. *San Francisco Estuary and Watershed Science* 11 (3): http://escholarship.org/uc/item/4jf862qz.

Nestler, J. M., Pompeu, P. S., Goodwin, R. A., Smith, D. L., Silva, L. G. M., Baigún, C. R. M. and Oldani, N. O. 2012. The river machine: A template for fish movement

and habitat, fluvial geomorphology, fluid dynamics and biogeochemical cycling. *River Research and Applications*, 28: 490–503. doi: 10.1002/rra.1567

Revnak R. and D. Killam. 2013. Redd dewatering and juvenile stranding in the upper Sacramento River Year 2012-2013. *Red Bluff Fisheries Office Technical Report* No. 01-2013. 45 p.

Rice, J.A. 1988. Mathematical statistics and data analysis. Wadsworth and Brooks/Cole, Pacific Grove, CA.

Rippeth, T. P., N. R. Fisher and J. H. Simpson. 2001. The cycle of turbulent dissipation in the presence of tidal straining. *Journal of Physical Oceanography* 31 (8):2458-2471.

Rose, K.A., W.J. Kimmerer, K.P. Edwards and W.A. Bennett. 2013a. Individual-based modeling of delta smelt population dynamics in the upper San Francisco Estuary: I. Model description and baseline results. *Transactions of the American Fisheries Society* 142: 1238-1259.

Rose, K.A., W.J. Kimmerer, K.P. Edwards and W.A. Bennett. 2013b. Individual-based modeling of delta smelt population dynamics in the upper San Francisco Estuary: II. Alternative baselines and good versus bad years. *Transactions of the American Fisheries Society* 142: 1260-1272.

Shchepetkin, A. F. and J. C. McWilliams. 2005. The regional oceanic modeling system (ROMS): a split-explicit, free-surface, topography-following-coordinate oceanic model. *Ocean Modelling* 9 (4):347-404. doi: http://dx.doi.org/10.1016/j.ocemod.2004.08.002.

Sheldon, J.E. and A.B. Burd. 2013. Alternating effects of climate drivers on Altamaha River discharge to coastal Georgia, USA. *Estuaries and Coasts* DOI 10.1007/s12237-013-9715-z.

Sherwood, E.T. and H.S. Greening. 2013. Potential impacts and management implications of climate change on Tampa Bay Estuary critical coastal habitats. *Environmental Management* DOI 10.1007/s00267-013-0179-5.

Sommer, T. and F. Mejia. 2013. A Place to Call Home: A Synthesis of Delta Smelt Habitat in the Upper San Francisco Estuary. *San Francisco Estuary and Watershed Science* 11 (2): http://www.escholarship.org/uc/item/32c8t244.

Sommer, T., F. H. Mejia, M. L. Nobriga, F. Feyrer and L. Grimaldo. 2011. The Spawning Migration of Delta Smelt in the Upper San Francisco Estuary. *San Francisco Estuary and Watershed Science* 9 (2): http://www.escholarship.org/uc/item/86m0g5sz .

Stanford, J.S., M.S. Lorang and F.R. Hauer. 2005. The shifting habitat mosaic of river ecosystems. *Verhandlungen des Internationalen Verein Limnologie* 29: 123-136.

Stanford, J. A., J. V. Ward, W. J. Liss, C. A. Frissell, R. N. Williams, J. A. Lichatowich, and C. C. Coutant. 1996. A general protocol for restoration of regulated rivers. *Regulated Rivers* 12:391–414.

Tockner K., M. Push, D.Borchardt and M.S. Lorang. 2010. Multiple stressors in coupled river-floodplain ecosystems. *Freshwater Biology* 55 (Suppl. 1):135–151.

Vincik, R. F. and J. M. Julienne. 2012. Occurrence of delta smelt (*Hypomesus transpacificus*) in the lower Sacramento River near Knights Landing, *California. California Fish and Game* 98 (3):171-174.

Werritty, A. 2002. Living with uncertainty: climate change, river flows and water resource management in Scotland. *Science of the Total Environment* 294: 29-40.

APPENDIX 1 – Materials for 2013 IRP Review

Review Materials Available to the 2013 LOBO Independent Review Panel

I. The following documents were provided in electronic format as required reading by the IRP prior to the 2-day workshop in Sacramento, CA on 6-7 November 2013:

1) Sacramento River Temperature Task Group 2013 Technical Report for the Long-Term Operations BiOps Annual Science Review

2) Chinook, Steelhead, and Green Sturgeon Loss Estimation for Skinner Delta Fish Protective Facility and Tracy Fish

II. The following document was provided to the IRP with a delay resulting from the federal government shutdown in early October 2013 and, as a consequence, it was left to the discretion of the 2013 IRP to address in the annual review:

1) Retrospective Analysis of Water Operations and Delta Smelt Protective Actions Taken in Early Water Year 2013

III. ***The following additional reports were made available in electronic format for supplemental use in providing historical context for the IRP***:

- Jahn, A. 2011. An Alternative Technique to Quantify the Incidental Take of Listed Anadromous Fishes at the Federal and State Water Export Facilities in the San Francisco Bay-Delta Estuary. Kier Associates, Ukiah California. Prepared for National Marine Fisheries Service, Central Valley Office. (http://www.kierassociates.net/Kier%20Assoc_OIA%20TO%203062_Incidental%20take%20at%20the%20Delta%20pumps_final.pdf)
- American River Group (ARG) Annual Report of Activities
- Stanislaus Operations Group (SOG) Annual Report of Activities
- Delta Operations for Salmonids and Sturgeon Group (DOSS) Annual Report of Activities
- Interagency Fish Passage Steering Committee (IFPSC) Annual Report of Activities
- The Smelt Working Group (SWG) 2013 Annual Report of Activities

Additional background information from the Science Program website was also available, including the RPA Summary Matrix of the NMFS and USFWS Long-term Operations BiOps RPAs and reports for previous IRPs.

APPENDIX 2 – Accuracy and Precision of Loss Estimates for Chinook Salmon, Steelhead and Green Sturgeon at the Skinner and Tracy Fish Facilities

The draft (Sept. 30, 2013) of this loss estimation report (hereafter "LER") describes an approach for estimating annual loss, and its uncertainty, of anadromous fish species at the two pumping facilities.

To estimate annual loss and its uncertainty, LER used the general loss model of Jahn (2011), with some changes in values of model parameters. The IRP has several statistical concerns and suggestions related to the Jahn (2011) approach, as detailed below. As a result of these concerns we believe that the underlying statistical model for loss estimation requires further research and development.

Jahn's (2011) simplified model for estimating loss:

For a single species and one pumping facility, Jahn's (2011) loss model is:

$$K = G - H = H/S - H \qquad (1)$$

where:

K = Total number of fish lost over a time period.

H = Total expanded salvage over the period, equal to the sum of the 2-hourly expanded salvages within the period.

$G = H/S$ = Total number of fish entering the facility ("entrained"), whose survivors were salvaged during the period.

S = Survival proportion for the period, defined here as the proportion of entrained fish that navigate the facility and enter the holding tanks alive during the salvage period.

Comments on loss estimation:

1. **Equation 7 of Jahn (2011) has an unrealistic assumption**

Jahn's (2011) Equation 7 (hereafter Equation J-7) estimates the standard error of G (hereafter, SE(G)), as a function of S, H and their standard errors. Equation J-7 is an application of a widely-used error propagation method, often called the "delta method" (Rice 1988).

The IRP has two principal concerns about Jahn's (2011) interpretation of Equation J-7:

a) Equation J-7 gives an approximate, not an exact, estimate of SE(*G*). The approximation can be poor, especially for a highly nonlinear function like *G* = *H/S*, unless random values of *S* vary closely around their mean value.

b) Jahn (2011) assumes that the covariance between *H* and *S* is 0, hence his omission of the covariance term from Equation J-7. Jahn (2011) makes this assumption because there is no obvious way to estimate the covariance. However, salvage is the causal result of survival operating on entrainment, that is, *H*= *G***S*. Thus, there must be a sizeable, positive covariance between *H* and *S*. Setting this covariance to zero will result in the estimated SE(*G*) being too large, as Jahn (2011) notes. Although this strategy is conservative from a policy perspective, it is nevertheless unrealistic and merits further research.

2. **Equation J-8 is incorrect.**

The correct expression is (Rice 1988, p. 124):

$$SE(K) = \sqrt{\big(SE(G)\big)^2 + \big(SE(H)\big)^2 - 2COV(G,H)} \qquad (2)$$

Thus, the correct value of SE(*K*) is probably larger than the incorrect estimate given by Equation (J-8). Again, there is no estimate for the covariance, COV(G,H). However, since *G*= *H/S*, one would certainly expect *G* to covary positively with its numerator, H. Thus, it is unrealistic to assume that COV(*G,H*) = 0.

The unknown covariance in Equation 2 can be avoided by applying the error propagation method to the full loss expression, that is, to *K* = (*H/S* – *H*). From the formula for the approximate variance of any function of two random variables (Rice, 1988, p. 146), we can derive

$$SE(K) \approx \sqrt{\frac{(1-S)^2}{S^2}\big(SE(H)\big)^2 + \frac{H^2}{S^4}\big(SE(S)\big)^2 - 2\frac{H(1-S)}{S^3}COV(H,S)} \qquad (3)$$

Equation 3 replaces the incorrect, 2-step estimate of Equations J-7 and J-8. As the "≈" indicates, the error propagation method gives only an approximate estimate of SE(*K*).

Equation 3 still contains the unknown, and non-negligible, covariance, COV(*H,S*). However, as Jahn (2011) did with Equation J-7, setting this covariance equal to 0 gives a conservative (largest possible) estimate for SE(*K*). If the technical team continues

using the error propagation method to estimate SE(*K*), then it seems appropriate to abandon Equations J-7 and J-8, in favor of Equation 3, while making some reasonable assumption about the value of COV(*H,S*). Below, we suggest how to estimate the uncertainty of annual loss without using the error propagation method.

3. **Equation J-9 is incorrect.**

The correct formula is (Rice, 1988, p. 124):

$$SE(K_{total}) = \sqrt{\left(SE(K_1)\right)^2 + \left(SE(K_2)\right)^2 + 2COV(K_1, K_2)} \quad (4)$$

In this case, it may be reasonable to assume that COV(K_1,K_2) = 0, signifying that loss estimates from the two pumping facilities are mutually independent. Equation 4, rather than Equation J-9, should be used to calculate the SE of the total loss estimate. Below, we suggest an alternative approach for estimating K_{total} and its uncertainty.

4. **Time scale for loss estimation.**

Jahn's (2011) approach applies Equation 1 to estimate the total annual loss, and its uncertainty, as follows: First, accumulate daily (or 2-hour) estimates of expanded salvage over the year, to estimate total annual salvage (*H*). This *H* estimate, along with a single value of *S*, are inserted into Equation 1 to yield a point estimate of total annual loss. Jahn (2011) then uses Equations J-7 to J-9 to estimate the SE of annual loss, based on the point estimates of *H* and *S* and their SE's.

However, the technical team also applies Equation 1 to daily salvage, thus estimating daily loss in real time, as described in CFS (2013). The daily loss estimate can potentially trigger an RPA action.

As an alternative to Jahn's (2011) approach, daily loss estimates could be summed over the year to estimate annual loss. An annual sum of daily loss estimates will be more accurate than Jahn's approach, for two reasons. First, a daily loss estimate more accurately represents the loss "process" experienced by individual fish, which spend only a few days to a few weeks moving through a pumping facility (e.g., Clark et al. 2009, Table 16). Second, daily loss estimates enable one to model *S* more realistically, as a random variable with substantial variation over time. With the present LER approach, summed daily losses will exactly equal their annual loss estimate, because the daily and annual estimates use the same, single value of *S*. However, if *S* is more realistically assumed to vary on a daily basis, then the two approaches will generally yield quite different annual loss estimates.

To demonstrate this, we carried out a Monte Carlo simulation using the framework of CFS (2013), in which daily salvage and daily survival proportion are modeled as random variables:

A. Expanded salvage statistics from Table (J-12) were rescaled to model daily salvage as a negative binomial random variable, with mean and standard deviation (not standard error) of 0.94 and 2.51 fish, respectively. It was assumed that the Table (J-12) data extended over 180 days (the actual period length is unclear from the table).

B. Survival proportion for any week was modeled as a normally-distributed random variable, with mean = 0.33 (Jahn's (p.20) high estimate)) and standard deviation (not standard error) of 0.10 (Clark et al. 2009, Table 12).

C. We generated 100 data sets, each with 180 daily values of salvage and survival proportion, by taking independent random samples from the distributions in A and B.

D. For each data set, the total 180-day loss was estimated in two ways:

a) The 180 daily salvages were summed to estimate whole-period salvage. Then Equation 1 was applied, with *S* = sample mean of the 180 daily survival proportions. This simulates Jahn's (2011) approach, yielding an estimate of total loss over 180 days.

b) The 180 daily losses were estimated by applying Equation 1 to the random daily values of salvage and survival proportion. Daily losses were then summed over 180 days to estimate total loss.

Results: Figure A2.1 below plots the 100 pairs of estimates of the total 180-day loss. A single point on the plot shows 2 estimates (a and b) derived from exactly the same set of 180 daily salvage values and 180 daily survival proportions. The straight line is the 1-1 line.

As the plot suggests, the annual sum of daily losses usually exceeded the Jahn-model loss. In fact, this occurred for 93 of 100 synthetic data sets, and by a mean exceedance of 142 fish. The annual sum of daily losses also had greater variability (SD=323 fish) over the 100 data sets than did annual loss from the Jahn model (SD=68 fish).

For each data set, the total salvage (180-day sum of daily salvage) was identical for both estimation methods. Thus, the differences in Figure A2.1 are due entirely to the effect of allowing *S* to vary daily, rather than assume a single mean value of *S* for the 180-day period. The negative bias in the Jahn estimate, relative to the summed-daily-

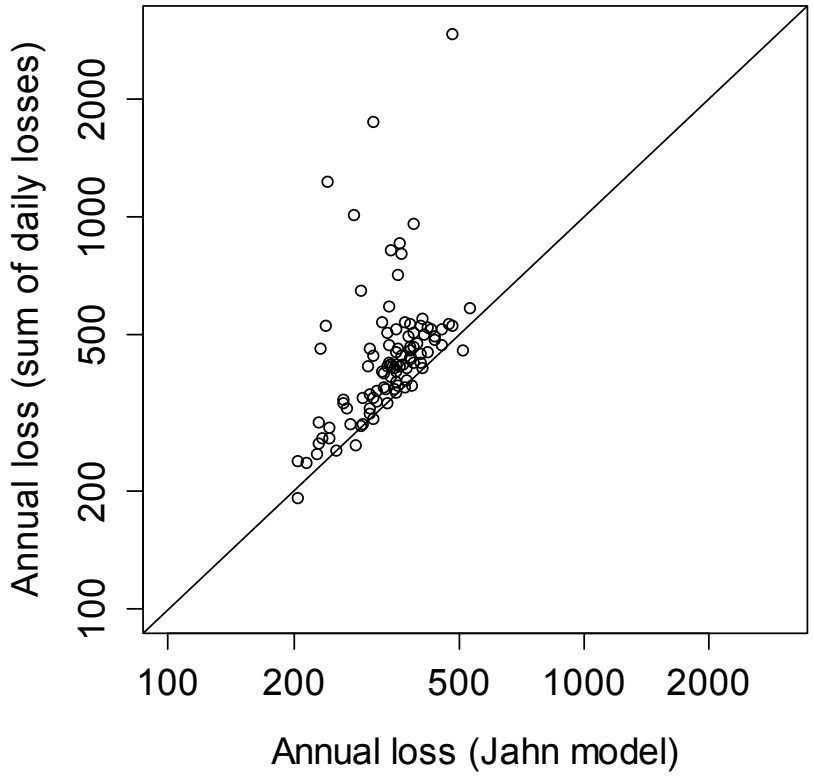

Figure A2.1. Plot of annual loss calculated as sum of daily loss estimates versus annual loss estimated from the Jahn model

loss estimate, can also be theoretically predicted from the nonlinear role of *S* in Equation 1 (Jensen inequality: Mood et al. 1974). Thus, a pattern somewhat like Figure A2.1 will be seen regardless of the particular distributions and the shorter time scale (daily, weekly, monthly) that is used to model survival and salvage.

Figure A2.1 does not reveal which of the annual loss estimates (Jahn model versus summed daily loss) is closest to the true annual loss. However, summed losses from shorter time periods (daily? weekly? biweekly?) should be more accurate than Jahn's whole-period loss estimate for the reasons given above.

5. **The Jahn (2011) model does not account for probable losses associated with zero observed salvage.**

Jahn (2011, p.8-9) inserts zero-count values of salvage into the raw 2-hour-sample data set for selected 2-hr sampling periods, during which fish might well have entered the

facility, based on factors like season, flow, and recent nonzero salvage. This seems to be a sensible approach. However, Jahn assumes that these inserted zeros do not contribute to the annual or daily loss estimates. We believe that this approach overlooks the probable fish loss that is associated with zero observed salvage, resulting in underestimates of loss.

Suppose a particular 2-hr sampling period has zero salvage (H=0). According to Equation 1, $G = H/S$. Thus, the Jahn (2011) approach also assumes that a zero salvage estimate for the period is the result of zero entrainment (G=0) associated with that period. And, it is true that if G=0, then H must be 0. However, it is also possible that some small, nonzero number of fish could have been entrained (G>0), and all of them were ultimately lost, resulting in H=0 for the period.

For example suppose G = 3 fish are entrained, and assume that S = 0.20, that is, 20% of entrained fish survive. For a small number of fish, S is more accurately interpreted as a survival probability, that is, each entrained fish has a 20% probability of surviving. Assuming independence of individual fish, the probability that none of the 3 fish survives is equal to the probability that all 3 are lost, which is given by:

$$\text{Prob (0 survivors)} = (1-S)^3 = 0.8^3 = 0.51 \qquad (5)$$

In other words, there is about a 50% chance that all 3 entrained fish will be lost, resulting in a salvage of 0 fish. Jahn's model fails to account for this possible loss.

One might argue that Jahn (2011) accounts for the zero-salvage probable losses by allowing them to contribute to an increased standard error in annual salvage, and hence to an increased standard error of annual loss (SE(K)). However, Jahn (2011) uses SE(K) to construct a two-sided, symmetric confidence interval around the point estimate of K. But in reality, the zero-salvage probable losses create a one-sided bias -- their omission can only create an underestimate of annual and daily losses.

We can estimate the probable loss associated with zero salvage. Equation 5 is an example of calculating Pr(H=0 | G=3), the conditional probability of obtaining zero salvage, given that 3 fish were entrained. However, we now need to calculate the conditional probability that 3 fish were entrained, given that the observed salvage was zero, that is, Pr(G=3 | H=0). From Bayes Theorem, we get:

$$Pr(G = m \mid H = 0) = \frac{Pr(H=0|G=m)Pr(G=m)}{\Sigma_j Pr(H=0|G=j)Pr(G=j)} \qquad (6)$$

These probabilities can be calculated for entrainment values of m = 0,1, 2, … fish . Then the probabilities can be used to calculate the mean and variance of the number of

entrained fish, given that zero salvage was observed. In Equation 6, Pr(H=0 | G=m) = $(1\text{-}S)^m$. In Equation 6, Pr(G = m) is the prior probability that m fish were entrained. Without a basis for estimating these priors, a standard approach is to assume they are equal. Under this assumption, Pr(G = m) = Pr(G=j), so these terms cancel out of the numerator and the denominator of Equation 6, leaving:

$$Pr(G = m \mid H = 0) = \frac{(1-S)^m}{\Sigma_j (1-S)^j} \qquad , m = 0,1,2\ldots \tag{7}$$

For m greater than about 30 fish, these probabilities are negligible, so we only calculate the first 31 probabilities (including that for m = 0).

Once the probabilities of Equation 7 are calculated, the expected number (mean) of entrained fish, given zero salvage, is calculated as:

$$\text{Mean}(G \mid H=0) = \Sigma_m \, m \, \Pr(G=m \mid H=0) \tag{8}$$

A similar equation can be written for the conditional variance of G, given that H=0.

Equations 7 and 8 were calculated using an assumed survival proportion (probability) of S = 0.1, then the calculation was repeated for S = 0.2, and again for S = 0.3. This yielded expected entrainments of 7.8, 4.0, and 2.3 fish, respectively. In other words, every 2-hr period of inserted-zero salvage results from an average of between 2.3 and 7.7 fish becoming entrained and then lost, assuming survival rates in the range 0.1 – 0.3.

These expected losses are not accounted for by the Jahn estimates, and they could add up to many fish on an annual basis. The IRP recommends that the mean value of this probable loss be calculated for all inserted-zero salvages in the data set, and added to daily and annual loss estimates.

Finally, we note that the Bayesian approach (Equations 6-8) can just as easily be used to estimate loss from nonzero salvage values. That is, one can use Equations 7 and 8 to calculate the mean and variance of entrainment, G, given any value for salvage. Then $K = G - H$. Replacing G=H/S with the probability calculations of Equations 6-8 avoids possible discretization errors, when H is a small number of fish. In addition, the Bayesian method allows for improved accuracy, if future research or monitoring can provide direct estimates of entrainment, that is, of Pr(G = m). The IRP suggests that the technical team explore the use of the Bayesian method, via Monte Carlo simulation (see below), to estimate all daily and annual losses, and their variances.

6. Statistical modeling framework for loss estimation

The IRP strongly suggests changing the statistical framework for estimating daily and annual loss. The current framework assumes that annual survival proportion, salvage, and loss can be modeled as single-valued parameters, with their uncertainties characterized by SE's. This framework may seriously understate the true uncertainty of estimated loss, because it understates the true uncertainty in survival proportions. Survival uncertainty is more accurately represented by Table 5, for example, in which Chinook survival proportions were observed to vary by a factor of 60 over 8 mark-recapture trials. In another experiment (Table J-6), Chinook survival rates through CVP louvers varied by a factor of 10 across replicate mark-recapture trials conducted within a two-week period. We believe that these magnitudes of variability, rather than the SE of mean survival, should be represented in the uncertainty of loss estimates. Moreover, in some cases, Jahn (2011) is driven to stating placeholder values, and /or guestimates (Table J-4; "high", "medium", "low"), for survival rates, because the true survival rates are so very uncertain. The assignment of SE's to such speculative survival rates is not credible, because the SE's do not represent the high uncertainty that prompted the speculation in the first place.

We suggest that survival proportion, and hence loss, instead be modeled on a short time scale (daily?) as random variables. The CFS (2013) report gives examples of how to model the probability distributions of these random variables. Daily loss, and hence annual loss estimated by the sum of daily losses, would also be random variables characterized by their estimated means and standard deviations. This strategy can incorporate the realistic variability of survival proportion that is observed in mark-recapture experiments. We believe that the random-variable framework would provide more accurate estimates of loss and its uncertainty.

7. Computing the annual loss and its uncertainty

If the technical team pursues these suggestions, then the computation of annual loss and its uncertainty is no longer so simple. For example, we have suggested that survival rates and loss be modeled on a daily basis, as random variables, with daily loss then summed over the year. In addition, loss-estimation factors such as prescreen and louver components of survival, cleaning adjustments, Chinook ESU classification, and serial correlation of salvage all have their own uncertainties to contribute. Finally, the probable zero-count losses should be added to daily and annual losses.

With these added complexities, it becomes impractical, and perhaps impossible, to estimate the standard deviation of loss using closed-form error propagation (e.g., Equation 3).

For this reason, the IRP suggests using Monte Carlo simulation to estimate daily and annual loss and its uncertainty. For a single day, the observed salvage could be taken at face value, as a number known without error. Then randomly select 100 values of S from its assumed probability distribution. For each *S*-value, calculate *G* from *G*=*H*/*S*, or else calculate the conditional mean of *G* from the Bayes equations. Next, add any zero-salvage corrections to the *G* values. Finally, inserting the 100 *G*-values into Equation 1 gives 100 estimates of daily loss, *K*. This yields a probability distribution of *K* for the day, whose mean and variance can be calculated. Summing the means and variances of loss for the year gives the statistics of the annual loss distribution. From such statistics, one can construct approximate confidence intervals or exceedance probabilities for daily and annual losses.

The above scheme assumes that daily expanded salvage is known without error. An option would be to obtain the daily salvage from a measurement error model, which would have the same intent as Jahn's Equations J-4 to J-6

A well-conceived and well-documented Monte Carlo script would offer a flexible computing environment for exploring a broad spectrum of quantitative scenarios about the numerous factors that contribute to fish losses. The script(s) developed for CFS (2013) would probably be a good starting point.

Finally, the major challenge of a Monte Carlo approach is how to represent the causal dependence of salvage on survival in a random-variable context, in other words, how to model the covariance between these two variables. This problem pervades the application of Equation 1 or of Equations 6-8, whether one uses closed-form estimates (Jahn 2011) or Monte Carlo estimates for uncertainty.

8. Making an RPA-triggering decision, based on highly-uncertain daily losses

During the Nov. 6-7 panel meetings, the technical team requested advice on interpreting higher, more-realistic variances of daily losses, such as those seen in CFS (2013) and in our simulation scenarios (Comment 4). Specifically, how can a highly-uncertain daily loss estimate be meaningfully compared to an RPA- triggering threshold?

To illustrate the problem, suppose that an RPA is supposed to be triggered if the daily loss exceeds 15 fish. And suppose that the expanded salvage on a certain day is 12 fish. Monte Carlo application of Equation 1 to this salvage value, using the random survival assumptions of Comment 4, yields an estimated loss distribution with a mean of 31 fish and standard deviation (SD) of 21 fish. This high SD, relative to the mean, is due to our assumption of high daily variability in the survival rate. Now, suppose that we

calculate a 2-sided, 90% confidence interval (CI) around the “best” point estimate of loss (the mean), yielding 31 ± 1.64*21 = [-3, 65] fish (assuming Normality). This CI extends far below the trigger level of 15 fish, indicating that the true loss might not have exceeded the trigger, even though the mean estimated loss (31 fish) is more than double the trigger level. With such a wide CI, it is very difficult to decide whether the trigger was exceeded.

Two possible strategies for making a sensible trigger-exceedance decision in the face of such high uncertainty are:

a) Make the trigger-exceedance decision based on a 7-day moving average of daily loss, rather than an individual daily loss. The 7-day moving average has a standard deviation equal to SD/√7, which implies that CI width will be reduced by a factor of √7 = 2.6. This increased precision may be adequate to develop a more useful CI for estimated loss. The moving average smooths out any apparent daily spikes in loss, but such spikes are highly questionable anyway, because of the high variance in estimated loss..

b) Use a one-sided (rather than two-sided) confidence interval, and relax the confidence level. As before, assume that a day’s loss is normally distributed with mean = 31 and SD= 21. The trigger decision depends only how small the true loss might be, not on how large it might be. Thus, we can construct a 1-sided, lower confidence bound for the true loss, and compare this bound to the trigger level. Reducing the confidence level will also help shrink the lower bound towards the mean. For example, a lower one-sided 75% confidence bound for loss is given by 31 – (0.67*21) = 17 fish. In other words, we can be 75% confident that the true loss was at least 17 fish. Because this exceeds the trigger of 15 fish, the RPA could be activated. The key strategic idea here is the need for managers to tolerate a reduced level of confidence (e.g., 75% rather than 90% or 95%) in decision rules, due to realistically high uncertainties.

APPENDIX 3 – Forecasting storage water release for temperature control and limit stranding and dewatering

The IRP was asked to answer the question, “What other tools are available to help forecast and manage storage and releases levels so we are not annually running into the issue of dewatering redds and stranding juveniles?” The short answer is that models are available or can be developed to predict the effect of storage water decisions on fish survival.

We suggest that both simple and detailed models are useful for management. Heuristic models that illustrate interactions of processes in terms non-dimensional parameters are useful for demonstrating the nature of the water allocation tradeoffs. Detailed models calibrated to the existing system and linked to physical models are needed to characterize the interaction of management actions and fish survival. The development of management models will involve considerable effort and require a team approach. However, a simple model that illustrates the processes can be relatively straightforward. Below we develop a simple or heuristic model to illustrate the system variables. Surprisingly, simple models may also have value in actual management as tools to inform managers that ultimately must make decisions based on judgments.

Heuristic Optimal Temperature Compliance Point Model (hOTCP)

This example model illustrates the approach of expressing the tradeoff storage water releases for cooling redds vs. releases for stage control to limit dewatering of eggs and stranding of juveniles. Currently the water storage is allocated to maintain a temperature control point in the Sacramento River during egg incubation stages. The model example illustrates the tradeoff of allocating storage water for egg and juvenile stages.

The model is intended to illustrate overall survival benefits that can be achieved during the egg vs. juvenile stages using available cold water storage in a trade-off to control temperature benefiting egg/embryo survival early on and later to reduce stranding during the juvenile stage. However, the concept is applicable for simultaneous actions involving temperature and stage controls to address redd dewatering as well as juvenile stranding.

For this illustration assume the effect of water releases on the survival of eggs and juveniles are independent. Then including a survival term for the background survival independent of reservoir operations, the total survival from egg through the juvenile stage is

$$S_{total} = S_{egg} S_{juv} S_{other} \tag{3.1}$$

Assume all redds upstream of the temperature compliance point (TCP) have 100% survival and redds below the TCP have 0% survival. This assumption is allowed because other mortality effects are captured in S_{other}. For a more realistic representation of temperature, the effect of temperature on mortality can be included but the essential dynamic should not be significantly different from eq. 3.1.

Assume the density of redds decreases exponentially with distance x from the face of Keswick Dam as

$$\rho(x) = \frac{1}{\lambda} \exp\left(-\lambda x\right) \tag{3.2}$$

where λ expresses the shape of the distribution of redds along the river. Note that the function fits well the observed distribution of redds. The survival of eggs in the river that depends on reservoir releases is a function of distance downstream as

$$S_{egg}(x) = \int_0^x \rho(x')dx' = 1 - \exp\left(-\lambda x\right) \tag{3.3}$$

where x is a distance equal to or less than the maximum temperature compliance point (TCP) defined as x_0. Typically x_0 is forecast prior to the beginning of the season and represents the maximum distance downstream at which temperature can be maintained below the critical maximum required to insure egg survival during incubation season.

Define the total preseason forecast of storage volume available for fish as v_0 and assume the maximum TCP location has a linear relationship with v_0 as

$$x_0 = \alpha v_0 \tag{3.4}$$

Here the relationship between TCP and volume is highly simplified but the form represents the basic property that more water is required to maintain a TCP further downstream. Because we assume the volume of water used and TCP location are linearly related in this model, the relationship between storage volume v_x and another TCP further upriver can be expressed as

$$x = \alpha v_x \,. \tag{3.5}$$

Having simplified egg survival as either 0 or 100% we can disregard egg incubation time and variations in storage water during incubation, so water storage after incubation can be described as

$$v_1 = v_0 - v_x = v_0\left(1 - \frac{x}{x_0}\right) \tag{3.6}$$

This remaining volume v_1 is thus available for other uses independent of temperature control. For our example, assume the remaining fish storage water is allocated for stage control to avoid juvenile stranding. The volume could also be allocated during the incubation period to minimize redd dewatering.

The more water available for river stage control, the less mortality from river stage effects. However, because of the nonlinear properties of flow and river elevation, the effect of storage volume decreases with volume amount. We can capture the general diminishing effect of additional flow on river elevation with an exponential function as

$$S_{juv} = 1 - \mu e^{-\beta v_1} \tag{3.7}$$

where μ is the maximum juvenile mortality if no storage water releases were available to target stranding and dewatering events and β characterizes the efficiency of water releases on reducing dewatering and stranding. Note that a brief analysis of the relationship between spawning and dewatering flows for fall-run Chinook salmon (Appendix B, Table B1 in Sacramento River Temperature Task Group 2013 Technical Report) indicates that an exponential relationship describes the impact of flow reduction on dewatering. Because both dewatering and stranding are processes driven by flow effects on river stage, we expect that eq. 3.7 is adequate for representing the effect of flow on stage-dependent mortality processes.

Combining the above equations the total survival over the two life stages is

$$S_{total}(x) = \left(1 - e^{-\lambda x}\right)\left(1 - \mu e^{-\beta v_0 (1 - x/x_0)}\right) S_{other} \tag{3.8}$$

where $x \le x_0$.

We simplify the equation first by normalizing the compliance point x to the distance of maximum temperature compliance x_0 giving

$$y = x/x_0 \tag{3.9}$$

such that y has the range $0 \le y \le 1$. Next, combine the parameters. The extent to which the available volume of storage water is capable of protecting the population of redds can be characterized as

$$a = \lambda \alpha v_0 . \tag{3.10}$$

That is, increasing the parameter *a* by an increase in any of the component terms increases the protection of the redds. For example, a larger λ implies the redd distribution is closer to Keswick dam so less storage water is required to cool the egg distribution. A larger v_0 implies more water is available to cool the redds. Note that *a* is a non-dimensional coefficient that can be estimated by fitting the distribution of redds scaled to the maximum temperature compliance point x_0. That is, in principle *a* can be estimated from the redd distribution, the amount of storage water available and the hydraulic properties of the system.

The second term defines the extent to which storage water can protect redds and juveniles from dewatering and stranding. It is defined as

$$b = \beta v_0 . \tag{3.11}$$

In principle *b* can be characterized from information on the hydraulic properties of the system and the location of redds and juveniles. An increase in *b* can be achieved by any combination of increased efficiency (β) and available coldwater storage (v_0). The IRP suggests that the efficiency term might be estimated from currently available information such as is illustrated in Appendix B, Table B1 in Sacramento River Temperature Task Group 2013 Technical Report.

With these non-dimensional parameters the total survival as a function of the TCP at distance *y* is

$$S_{total}(y) = S_{egg} S_{juv} = \left(1 - e^{-ay}\right)\left(1 - \mu e^{-b(1-y)}\right) S_{other} \tag{3.12}$$

Note that the value of S_{other} is not important because it does vary with storage reservoir operations.

The distance of the TCP that yields the optimum total survival is defined by $dS(y)/dy = 0$ giving

$$\frac{dS_{total}(y)}{dy} = \frac{ae^{b}}{\mu} - be^{(a+b)y_*} + \left(b - a\right)e^{by_*} = 0 \tag{3.13}$$

Note in Fig. A3.1 the total survival of eggs quickly approaches the asymptote of 100% survival and essentially tracks the cumulative distribution of redds downstream of Keswick Dam. Water not allocated for temperature control is allocated for stage control to reduce egg dewatering and juvenile stranding. Therefore S_{juv} is greatest when $y = 0$ and decreases progressively with increasing y because water not allocated to temperature control is allocated for stage control. The curvature of the total survival

curve to the right of the optimum depends on the effectiveness of storage water for stage control activities.

Eq. 3.13 may be useful for management if it identifies the optimal distance for the temperature control point that balances survival of eggs and the survival of juveniles. Furthermore, the optimum allocation of storage water for temperature control is

$$v^* = y^* v_0 . \tag{3.14}$$

The salient point is that the optimum TCP and volume of water allocated for temperature control is likely to be generally less than the volume of water that is used under the current RPA. Figure A3.1 illustrates this point by applying the model to WY 2013 in which the location of the TCP was set at Airport Road, which gives x_0 ~ river mile 17.

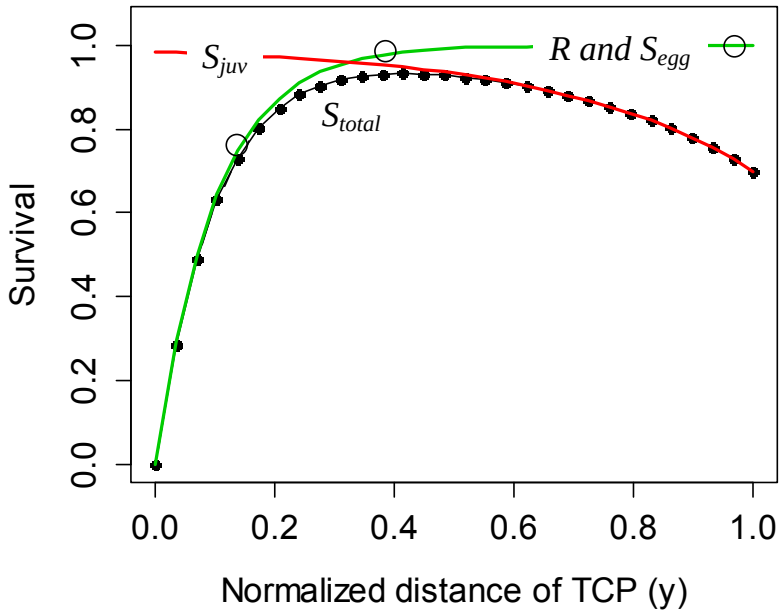

Fig. A3.1. Model output showing relationship between egg (S_{egg}), juvenile (S_{juv}) and total survival as a function of temperature compliance points (y) based on eq. 3.12. The large circles depict cumulative redd density R at the normalized TCP location. Optimum TCP is y^*= 0.41 for this scenario.

We estimated the parameter *a* using the redd density information for winter run Chinook from Table 2 in Sacramento River Temperature Task Group Annual Report of Activities 2013. From eq. (3.3) the cumulative distribution of percent redd vs. distance is

$$\mathrm{R}(y) = 1 - \exp(-ay) . \tag{3.14}$$

where $R(y)$ is the cumulative redd distribution as a function of normalized distance y. Knowing the distribution $R(y)$ we estimate the parameter giving a = 10 for WY 2013. We have no estimate of parameter b but in principle it is straightforward because its components can be estimated; v_0 is simply the total amount of storage water available for fish and β be estimated from river stage information and juvenile distributions.

Analysis indicates that the shape of survival vs. the TCP location is sensitive to the parameter *a,* but is less sensitive to *b* (Fig. A3.2). However, it is important to note that the survival over a range of TCP locations is relatively flat with any selected value of *b* such that the optimum TCP is relatively insensitive to *b* even though the optimum TCP location is sensitive to changes in *a*. Fortunately, *a* potentially can be estimated with some confidence while for *b*, an accurate estimate is not as critical for finding the optimal TCP location.

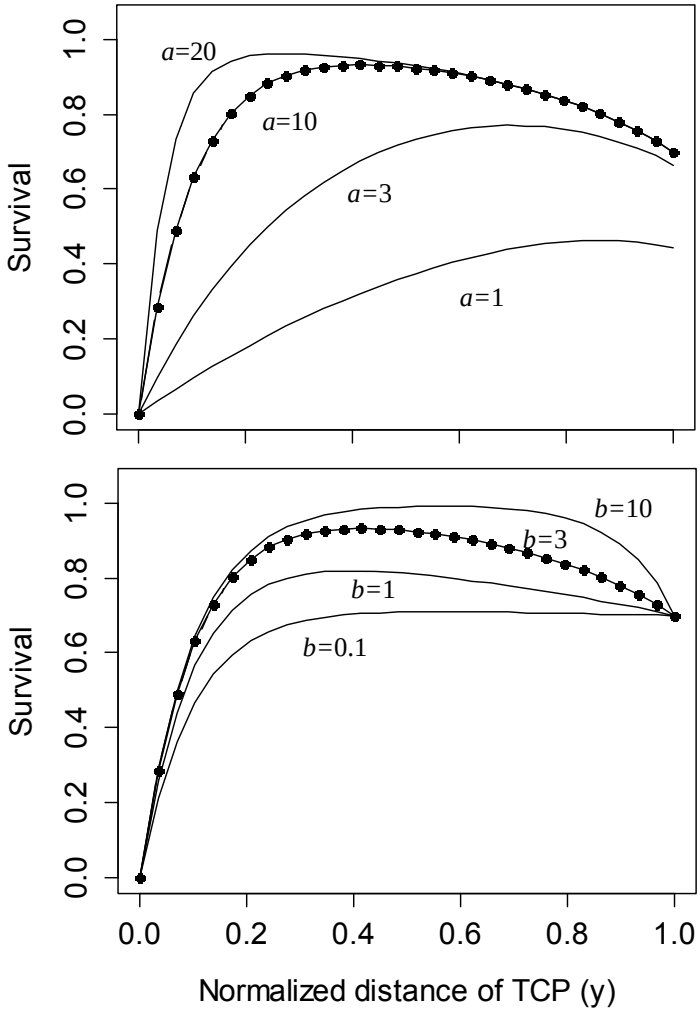

Fig. A3.2. Sensitivity of survival (S_{total}) with TCP distance *y* for differing values of *a* and *b* where base parameter values are sane as in Fig. A3.1.

For WY 2013 we assume b = 3 and μ = 0.3 then solving eq. (3.13) using the *uniroot* function in the R statistical package, the normalized optimum TCP location is y^* = 0.41. Thus, based on the Airport Road TCP (~ river mile 17) used in 2013 the model indicates the optimum TCP was at river mile 7. An exploration of the sensitivity of y* to variations of μ and b will give a measure of the uncertainty in the optimum. The salient points of this analysis are that it is feasible to estimate a TCP that optimizes survival across the two life stages and the optimum is likely to require less water than is used to meet the current TCP. Thus, it is possible the RPA can be adjusted to increase both fish survival and water operations flexibility.

Management - Optimal Temperature Compliance Point Model

A management model to forecast water release impacts could be developed in the basic framework of the heuristic model, but include spatial and temporal distributions of fish, river temperature and stage. The relationship between water releases, river stages and temperature would be input from a hydraulic model. The redd distribution could be characterized by redd survey information, not the distribution parameter λ in the heuristic model. The management could also use realistic temperature survival and growth models to characterize emergence timing and survival of eggs.

If detailed information were available on the distributions and environmental characteristics of redds and juvenile nursery grounds then management of a TCP location could be replaced by a management that optimizes survival across fish sites. The sites would include individual redds and juvenile habitats. Storage water releases would then seek to optimize the survival across the sum of sites and therefore the fish population itself.

Conclusions of Model Analysis

The heuristic model developed here illustrates that higher fish survival and greater flexibility in reservoir operations might be obtained by using a forecast model that accounts for the tradeoff of water allocations for different mortality processes and life stages. The model suggests that survival may be increased about 10%, which is moderate. However, the model also suggests that this improvement in survival might be attained with 50% less water than is currently used in maintaining TCPs defined by the RPA. Such a saving of storage water would be substantial for water years in which the location of the TCP extends significantly downstream of the majority of the redds. The IRP has in past reviews encouraged further integration of water operations with biology, and the model presented here illustrates the potential benefits of such an approach.

Appendix 4 - Delta smelt movements relevant to implementation of RPA Action 1

The underlying motivation for a preemptive Action as posed to the IRP in Question 2 involving RPA Action 1 is to reduce pumping flows prior to the fish entering the Old and Middle River environment, thus allowing the pre-spawning migrants to pass into the western and northern regions of the Delta without being drawn into the negative flow of the OMR. Developing an effective preemptive action requires understanding the behavior of delta smelt to their environmental cues during the migration. Below we address this issue, discussing alternative theories of delta smelt migration as based on the past and recent publications on delta smelt.

A working hypothesis of delta smelt movement

Delta smelt live in low salinity zones of the estuary and migrate upstream to spawn (Sommer et al. 2011). Previously it was believed that the fish migrated between the western and eastern portions of the delta. However, recent studies suggest that the life cycle is more complex. The adult population appears mostly as diffuse loci in and adjacent to the northern Delta's open waters from which individuals undertake landward movements to spawn (Murphy and Hamilton 2013). While the centroid of the adult population is located near the X2 low-salinity boundary (Feyrer et al. 2011) delta smelt are also found in Liberty Island, Yolo Bypass (Sommer and Mejia 2013) and as far north as Knights Landing (Vincik and Julienne 2012). The historical population distribution included the eastern and southern regions of the delta but currently these areas are largely without delta smelt (Murphy and Hamilton 2013).

Salinity and turbidity are key environmental variables that affect distribution of delta smelt, but the relative significance of these variables has been under debate in the literature (Sommer and Mejia 2013). Other variables have been identified as important including tidal velocity (Sommer et al. 2011), which correlates with other properties such as turbulence (Rippeth et al. 2001). How delta smelt respond to environmental variables is critical to developing a preemptive Action 1 to divert the movement of delta smelt in the OMR during their pre-spawning migration. Here we develop a straw-man or working hypothesis on the important variables to consider in designing an Action. We begin with a discussion of models or theories of delta smelt movement.

Two basic models have been proposed for how environmental variables affect delta smelt migration. One model identifies kinesis in which a fish moves with random and directed movements along a water property gradient, e.g., salinity. The rate of movement depends on the differential between an optimal salinity and the fish's local

salinity. Residence of delta smelt in the X2 region is achieved by setting the optimal salinity at the X2 salinity. Movement toward freshwater in the landward pre-spawning migration is produced by lowering the optimal salinity for pre-spawning adults (Rose et al. 2013a). In essence, to switch between X2 residence and pre-spawning migration the optimal salinity level is changed and the delta smelt swims toward lower salinity water upstream. The model describes the general life cycle distribution of delta smelt and was implemented in an individual based model to explore processes controlling population levels (Rose et al. 2013a). However, it was not strictly intended to be an accurate representation of the mechanisms of migration. The IRP suggests the concept of kinesis is not conceptually wrong, but it must be applied over the small scale at which delta smelt perceive their environment, not at the large scale on which it has been applied previously.

A second model describes movement in terms of tidal surfing, or tidally mediated migration, in which upstream movement is achieved by the smelt moving into higher velocity regions of the water column during the flood tide and lower velocity regions during the ebb tide. This model has more biological realism than the kinesis model and can reproduce the distributions and movement rates of delta smelt, but as currently applied (Sommer et al. 2011) it does not address the mechanisms controlling the tidal cycle movements between high and low velocities. More important, the tidal surfing model is mute on how a fish distinguishes between ebb and flood tides – an essential ability for tidal surfing. While knowing how fish distinguish and respond to hydrodynamic properties has scientific appeal, the knowledge is important for developing delta smelt protection since any action can only modify the hydrodynamics and thus the link to fish behavior is essential.

While both models can reproduce delta smelt distributions, the mechanisms are different and designing a preemptive Action 1 based on an incorrect model of delta smelt behavior may neither produce desired results nor be cost effective. However, the selection of which model is more realistic is not difficult because the kinesis model, as previously applied, has been largely rejected. A plan proposed in 2009 to divert delta smelt from the Central Delta with a gating system in the central delta (Two-Gates project www.usbr.gov/mp/2gates/docs/index.html) was based on delta smelt kinesis to salinity and turbidity fields. However, a review of the plan identified significant problems with the kinesis movement model (Anderson et al. 2009) and the project was eventually withdrawn (www.c-win.org/two-gates-project-expedient-delta-conveyance.html).

In contrast, recent studies provide clear support for the tidal surfing model. A SmeltCam, which visually identifies free moving fish, revealed that in the lower Sacramento River in November 2012 delta smelt were dispersed over the water column

during the flood tide and in the lower velocity regions near the bottom and side channels on the ebb time (Feyrer et al. 2013). The authors noted that the conditions were associated with the upstream migration of delta smelt to areas where spawning ultimately occurs during spring. The study essentially documented the fine-scale delta smelt distribution prior to the ‘‘first flush’’ and their upstream migration. Other studies have also documented delta smelt asymmetric behavior over tidal cycles. The pre-spawning migration velocity of delta smelt can be produced in a model with particles moving from the upper to the lower 10% of the water column between the flood and ebb tides (Sommer et al. 2011). In Suisun Bay, delta smelt feed predominantly on the flood tide in the day (Hobbs et al. 2006). To maintain residence in the dynamic low salinity zone of the western delta other species exhibit vertical migrations that are coordinated with the tides (Bennett et al. 2002). Thus, solid evidence (in the San Francisco Bay Delta system and many studies elsewhere not discussed) supports a model of tidally coordinated movement and indicates that tidal surfing is sufficient to produce the observed migration velocities and distributions of adult delta smelt and other species.

However, the tidal surfing model by itself does not describe how an animal coordinates movement with the tide. Perhaps the parsimonious perspective is to assume that delta smelt seek to maintain position in a favorable local environment, e.g., they seek a range of turbidity (small-scale kinesis), which because of estuary hydrodynamics occurs mostly on flood tides. Some support for this mechanism comes from (Hasenbein et al. 2013) who observed that delta smelt feeding performance was highest between 12 and 120 NTU and diminished otherwise. Also, higher levels of salinity stressed delta smelt. If delta smelt seek a favorable turbidity range when available, do not respond to turbidity when the level is low, and avoid higher levels of salinity, then a relatively simple correlation of small-scale distributions of turbidity and salinity with velocity profiles may be sufficient to explain movement behavior of delta smelt.

If delta smelt seek local regions of optimal turbidity then understanding movement in a tidal system reduces to correlating the optimal attraction regions with tidal velocities. Here studies indicate that turbidity levels are highest on the flood tides in the Carquinez Strait connecting San Pablo and Suisun Bay (Ganju and Schoellhamer 2008), in the Sacramento River above the confluence with the San Joaquin (Feyrer et al. 2013) and in channels of Cache slough in the northern Delta (Morgan-King and Schoellhamer 2013). These are all areas with significant delta smelt populations.

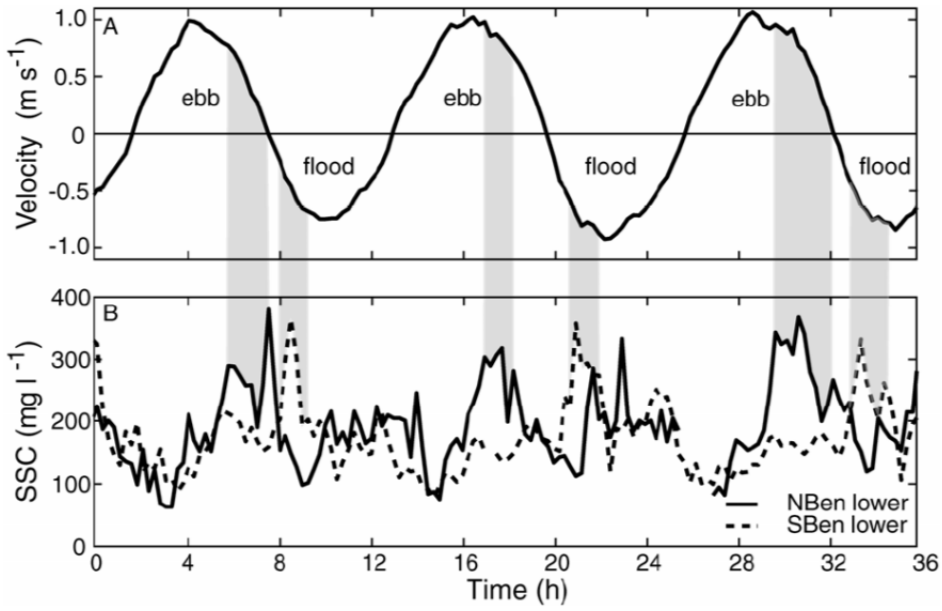

Figure A4.1. Water velocity and suspended sediment concentration (SSC) in Carquinez Strait and Suisun Bay. Carquinez Strait connects San Pablo Bay and Suisun Bay. Grizzly and Honker Bays are shallow areas of Suisun Bay. Sites NBen and SBen are located on piers of the I-680 Bridge. Depth is referenced to mean lower low water [from Ganju and Schoellhamer 2008].

Fig. A4.1 illustrates the asymmetrical patterns in turbidity across a tidal cycle in Carquinez Strait. In general, the pattern varies spatially, with flow and sediment availability such that the correlations of flood and high turbidity are expected to increase and decrease depending on conditions. Under the hypothesis that tidal surfing requires a high flood tide/turbidity correlation, then the propensity for movement against the mean flow will vary according to the estuarine physics. The flood/turbidity correlation is likely to be strongest in the western Delta and backwater sloughs because of tidal asymmetry in these environments (Morgan-King and Schoellhamer 2013). Strong tidal asymmetry and a high flood/turbidity correlation also would be expected during first flush events. In regions with low correlations, delta smelt movements should be more random. Furthermore, when turbidity throughout the water column is below the threshold for attraction, we expect that delta smelt would not seek higher velocity regions on either flood or ebb tides. Again, their movements would become random and we expect the net movement of the delta smelt would follow the mean flow.

While we frame the hypothesis in terms of tidal-scale changes in turbidity, we suggest the underlying mechanisms act at the scale of the fish's immediate environment. At the perceptive scale of the fish, optimal turbidity may occur in the low velocity regions near shore and bottom on the ebb tide, while on the flood tide the optimal turbidity is associated with higher velocities, which generally occur throughout the water column. Also note that the mechanism may involve asymmetric patterns of small-scale

turbulence over the tidal cycle. Fish can detect micro-turbulence in the water column (Chagnaud et al. 2008) and because turbulence induces resuspension of sediment, turbidity and turbulence may both appear to have an effect on delta smelt movement.

In summary, our working hypothesis is that tidal surfing behavior results because over the tidal cycle delta smelt seek water with intermediate turbidity, which depending on the asymmetry of the tidal cycle, tends to be in low velocity regions on the ebb tide and high velocity regions on the flood tide. Furthermore, the strength of tidal asymmetry varies spatially and seasonally so that delta smelt movements are expected to vary spatially and seasonally in a similar manner to the variability in tidal asymmetry.

As was indicated at the LOBO workshop, the USFWS seeks to fine-tune actions to protect delta smelt. The IRP realizes that considerable progress has been made in understanding delta smelt movement, but suggests that the best possible protection program requires explicit consideration of the small-scale physical properties to which fish respond. Below is a brief description of a straw-man program to test the hypothesis that delta smelt exhibit taxis to abiotic attraction zones that form and dissipate over the tidal cycle resulting in dispersion, retention or upstream tidal surfing depending on the bathymetry and flow of the local environment.

Program Hypothesis: By altering tidal asymmetry in critical channels and times, delta smelt movement towards pumps can be reduced.

Program Elements:

1. Characterize delta smelt responses (feeding, predator avoidance, taxis) to abiotic factors and identify an envelope of attraction, plausibly defined by ranges of turbidity, salinity and light levels. Example work: Hilton et al. (2013) and Hasenbein et al. (2013).
2. Characterize delta smelt distribution over tidal cycles. Example work: Feyrer et al. (2013), Bennett et al. (2002).
3. Characterize attraction envelope location and velocity properties over tidal cycles. Example work: Shchepetkin and McWilliams (2005), Ganju and Schoellhamer (2008; Morgan-King and Schoellhamer (2013), Jones et al. (2008).
4. Model delta smelt movement by linking behavior, attraction envelope and hydrodynamics. Example Goodwin et al. 2006, ROMs and DSM2 hydrodynamic models.
5. Using the model, identify hydraulic conditions that initiate upstream delta smelt movement and develop actions to disrupt delta smelt movement into inner delta.

Appendix 5 – Additional considerations- secondary channels of the Sacramento River

Most redds and stranding sites are associated with either secondary channels or smaller scale features (e.g., margins and geomorphically complex features of the main channel; Figs. A5.1 and A5.2). Secondary channels may be one of the most important options for river restoration because they appear to be a potentially important habitat resource for conservation and recovery of fall- and winter-run Chinook.

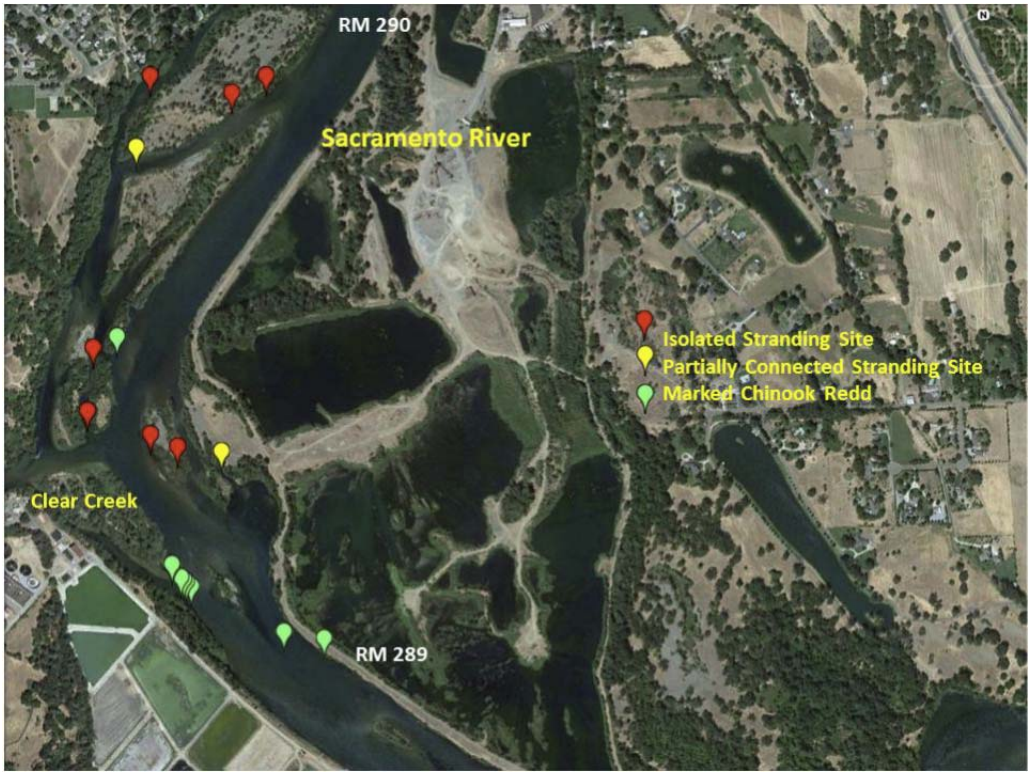

Figure A5.1. Strong association of stranding sites and redds with secondary channels in Sacramento River near Clear Creek. From Appendix D of Revnak and Killam (2013 RBFO Technical Report No. 01-2013).

Figure A5.2. Strong association of stranding sites and redds with secondary channels in Sacramento River near Highway 44 Bridge. From Appendix D of Revnak and Killam (2013 RBFO Technical Report No. 01-2013).

Existing and recently formed secondary channels should be identified and described by hydrogeomorphic variables such as average depth, width, length, and substrate type. Secondary channels so described can be sorted over a range of flows important to different salmon life stages. A description of their persistence should also be noted to address potentially important management issues. For example, have there been changes in the secondary channels through time, particularly since the closure of Shasta and Keswick Dams?

The IRP noted the presence of at least 8-9 secondary channels and more may be identified with a rigorous census that could even detect channels recently abandoned either from channel migration or avulsion processes. At least two important general categories of secondary channels can be identified – fully connected (both ends connect to the Sacramento River throughout the hydrograph) and partially connected (connected at the lower end only under low flows) – although other categories may also be discovered. Secondary channels that become disconnected at the upstream end and then become spring brooks because channel-bed elevation intercepts the top layer of the unconfined groundwater table may be particularly important juvenile rearing habitat (Stanford et al 2005,). Hyporheic water inputs are important in many rivers of the arid western U.S. because warm river water that flows from the open surface main channel into the underlying bed sediments is cooled before remerging as surface flow in the form of a spring brook (Hauer and Lorang 2004). Secondary channels that intercept

both hyporheic and regional groundwaters may be particularly valuable cool water refugia for salmon during times when cold water storage in Shasta Dam is limited. Partially connected secondary channels may be the cool water temperature refugia of last resort for salmonid early life stages under stressful temperature conditions.

Secondary channels are typically highly dynamic hydrogeomorphic features that can experience more dramatic hydrologic changes (fully wetted to dry conditions) than the main channel (Hauer and Lorang 2004, Lorang et al. 2013). The rates of change will likely not be constant. They will depend upon patterns of in-channel sediment dynamics, bank erosion, interaction with large woody debris, fluctuating water levels, succession of riparian vegetation and hydrologic events that cross geomorphic threshold levels (i.e., those discharges that mobilize and transport sediment) and do so for a sufficient duration to accomplish geomorphic work (i.e., cut-and-fill alluviation channel migration and avulsion) (Lorang et al. 2013, Nestler et al. 2012). The existing geomorphic complexity and inferred temporal dynamics suggest that future side-channel management plans must be carefully considered and developed.

As a precautionary note, channel modifications made by means other than natural processes may have major unintended consequences (Stanford et al. 1996). The diversity and productivity of salmonid rivers depends on maintaining a “shifting mosaic of habitat” (Stanford et al. 2005). For example bank erosion is often viewed negatively especially if mobilized sediments bury redds immediately downstream. However, those sediments are also key elements for the creation of new gravel bars that support the rejuvenation of riparian vegetation. Caution must be exercised when in-channel modifications are made to enhance production of single species because such actions may add a suite of stressors to other species which can result in a feedback loop to indirectly affect the species of concern (Tockner et al. 2010). The net effect of a single species focus is to reduce the diversity and persistence of the aquatic community as a whole (Tockner et al. 2010). In-channel modifications will only be successful through careful consideration of how they may affect natural first order hydrogeomorphic drivers for biogeochemical processes which are secondary response variables and hence tertiary drivers of food web dynamics within the river ecosystem. Simply having potential habitat visible from an aerial photo or mapped from the ground does not insure successful juvenile production unless that habitat structure provides the necessary habitat quality.

If secondary channels are recognized as important elements in future strategic efforts to protect and enhance salmonid populations in the Sacramento River, they should be incorporated as part of a holistic adaptive management approach that explicitly focuses on the geophysical processes that shape the dynamic abiotic and biotic structure of the

entire riverine ecosystem at multiple spatial and temporal scales. One of the most efficient ways to promote desirable ecosystem structure and functionality is to allow natural processes to self-maintain (Stanford et al. 1996).

Adaptive Management of Secondary Channels

Program-level restoration of secondary channels to serve as temperature refugia for salmonid early life stages may face difficult technical challenges and management issues. The SRTTG could take a formal collaborative adaptive management (AM) approach to restoration and conservation of secondary channels and similar small-scale habitat features in the Upper Sacramento River. An AM approach should include development of goals and objectives, guiding principles (e.g., self-maintenance), and conceptual models that describe how secondary channels contribute to salmon conservation and recovery. The conceptual models should be of sufficient detail and completeness that critical sources of uncertainty can be identified. These sources of uncertainty can then become the foci of studies that systematically improve the efficacy of management plans.

Estuaries and Coasts
DOI 10.1007/s12237-014-9877-3

Riders on the Storm: Selective Tidal Movements Facilitate the Spawning Migration of Threatened Delta Smelt in the San Francisco Estuary

W. A. Bennett · J.R. Burau

Received: 5 May 2014 / Revised: 13 August 2014 / Accepted: 26 August 2014

Abstract Migration strategies in estuarine fishes typically include behavioral adaptations for reducing energetic costs and mortality during travel to optimize reproductive success. The influence of tidal currents and water turbidity on individual movement behavior were investigated during the spawning migration of the threatened delta smelt, *Hypomesus transpacificus*, in the northern San Francisco Estuary, California, USA. Water current velocities and turbidity levels were measured concurrently with delta smelt occurrence at sites in the lower Sacramento River and San Joaquin River as turbidity increased due to first-flush winter rainstorms in January and December 2010. The presence/absence of fish at the shoal-channel interface and near the shoreline was quantified hourly over complete tidal cycles. Delta smelt were caught consistently at the shoal-channel interface during flood tides and near the shoreline during ebb tides in the turbid Sacramento River, but were rare in the clearer San Joaquin River. The apparent selective tidal movements by delta smelt would facilitate either maintaining position or moving upriver on flood tides, and minimizing advection down-estuary on ebb tides. These movements also may reflect responses to lateral gradients in water turbidity created by temporal lags in tidal velocities between the near-shore and mid-channel habitats. This migration strategy can minimize the energy spent swimming against strong river and tidal currents, as well as predation risks by remaining in turbid water. Selection pressure on individuals to remain in turbid water may underlie population-level observations suggesting that turbidity is a key habitat feature and cue initiating the delta smelt spawning migration.

Keywords Selective tidal movements · Tidal currents · Turbidity · Migration · Endangered species · San Francisco Estuary

Communicated by Judy Grassle

W. A. Bennett (✉)
Center for Watershed Sciences, Bodega Marine Laboratory, University of California, Davis, P.O Box 247, Bodega Bay, CA 94923, USA
e-mail: wabennett@ucdavis.edu

J. Burau
California Water Science Center, U.S. Geological Survey, 6000 J Street, Sacramento, CA 95819-6129, USA

Introduction

Migration is a widespread life history strategy that optimizes the use of spatial and temporal variability in habitat quality to increase reproductive success and fitness of individuals (Dingle 1996). Characterizing this fascinating and complex phenomenon involves perspectives at various levels of biological organization, such that migration is most readily defined by the behavior of individuals, but then only fully understood in terms of population outcomes or consequences (Roff 1992; Dingle 1996). For fishes in estuarine and river systems, recent work has focused on quantifying cost/benefit trade-offs underlying the evolution of migration strategies. For any specific strategy to persist, the potential benefits (e.g., foraging and reproductive success) must outweigh the substantial costs in time and metabolic energy expended, as well as the added risks of mortality (e.g., predation) during migration (Jonsson and Jonsson 1993; Bronmark et al. 2008; Chapman et al. 2013). Theoretical and empirical studies (Roff 1988; Jorgensen et al. 2008) suggest migrants ameliorate costs through adaptive responses in various traits, including ecological (Schaffer and Elson 1975; Jonsson and Jonsson 2006), morphological (Crossin et al. 2004; Jonsson and Jonsson 2006), and behavioral (Hinch and Rand 2000;

Published online: 23 September 2014

McElroy et al. 2012; Keefer et al. 2013). Accordingly, selection pressure to conserve energy for reproduction is more likely to be stronger on smaller or long-distance migrants and when spawning occurs soon after migrating (Kinnison et al. 2001; Crossin et al. 2004; Jonsson and Jonsson 2006).

Behavioral responses used by fishes to optimize cost/benefit trade-offs are often triggered by external cues and can include individual assessments of body condition and maturity level, as well as strategies for swimming against strong river and tidal currents (Brodersen et al. 2008a, b; Forsythe et al. 2012). Typically, external cues signal optimal times and routes for traveling that minimize predation risks and promote reproductive success. Thus, cues initiating migration are often somewhat predictable, including annual and monthly lunar cycles (Forsythe et al. 2012), seasonal water temperatures (Quinn and Adams 1996; Dahl et al. 2004), as well as tidal currents and river outflows (Anderson and Beer 2009; Forsythe et al. 2012). For many species, the energetic costs of swimming are tremendous. Atlantic salmon (*Salmo salar*) have been estimated to lose between 60 and 70 % of their energy reserves during migration and spawning (Jonsson et al. 1997), whereas sockeye salmon (*Onchorynchus nerka*) can use up to 84 % of their total energy reserves for swimming (Hinch and Rand 1998). This suggests that there is strong selection pressure to adjust travel speeds and distances, as well as position in tidal currents to conserve energy for reproduction. For example, sockeye salmon travel upriver in narrow bands near the shoreline where current speeds are lower than mid-channel (Hinch and Rand 2000), and Pallid sturgeon (*Scaphirhynchus albus*) appear to zigzag across river channels taking advantage of weaker currents on the inside of river bends as they migrate (McElroy et al. 2012).

In the present study, we investigate the effect of tidal currents and water quality variables (e.g., turbidity) on the individual movement behaviors used during the spawning migration by the threatened delta smelt, *H. transpacificus*, endemic to the northern San Francisco Estuary (SFE), California, USA. (Fig. 1). This small (<90 mm) semi-anadromous species is primarily an annual with a few individuals living to spawn in a second spring. Delta smelt was abundant historically, but declined dramatically over the last three decades, such that it is now protected under the California state and federal Endangered Species Act (ESA, USFWS 1993). Relatively little is known about spawning and reproduction in nature; adhesive embryos spawned by delta smelt have never been found (Moyle et al. 1992; Bennett 2005). Spawning in most years occurs primarily in the upper freshwater portions of the northern Delta during spring (March–June), with larvae and juveniles dispersing and rearing in the tidal freshwater to the low-salinity zone (<12) of the system (Fig. 1). This region expands to encompass Suisun Bay in years with moderate to high freshwater outflow and contracts in dry, or drought, conditions to include only the Delta (Bennett 2005, Fig. 1). During fall (September–November), maturing adults reside primarily in the low-salinity zone which also maintains elevated water turbidity relative to elsewhere due to wind-wave resuspension occurring over two large shallow (<3 m) sub-embayments, Grizzly and Honker Bays (Ruhl et al. 2001, Fig. 1).

Delta smelt undertake an annual spawning migration that appears to begin immediately following the arrival of turbid water from land runoff mobilized by the first major winter (December–February) rainstorm, the so-called first flush (Bergamaschi et al. 2001; Grimaldo et al. 2009; Sommer et al. 2011). The sudden increase in turbidity may reduce predation risks, signaling the optimal time for traveling upriver (about 15–20 km) to spawning habitat in the northern Delta (Grimaldo et al. 2009; Sommer et al. 2011). Although turbidity is a readily apparent cue associated with the delta smelt migration, other potentially co-occurring and interactive processes also may be involved (Rakowitz et al. 2008).

Our objectives were to (1) evaluate individual movement behavior in relation to the prevailing hydrodynamics at tidal time scales to understand how this small pelagic fish is able to travel upriver against strong river and tidal flows (ca. 1,800 m^3 s^{-1}) and (2) explore if processes observed at the individual and tidal scales can help to explain the apparent roles of turbidity as a habitat feature (Feyrer et al. 2007) and a cue for the spawning migration at the population level (Grimaldo et al. 2009; Sommer et al. 2011). Here, we distinguish *movements* as those made by individuals over a few meters at tidal time scales, and *migration* as a distributional shift occurring annually over kilometers and months at the population level. Our study occurred in two consecutive winters, integrating monitoring of hydrodynamics, water turbidity, salinity, and temperature, concurrently with sampling for fish. Understanding how individual behaviors interact with tidal currents and water quality is essential to gain insight into the processes promoting pelagic habitat for estuarine species and the evolution of migration.

Methods

Study Area

The Delta region of the SFE is composed of a complicated network of tidally forced channels and canals that is considered one of the most highly altered terminal floodplain ecosystems (Lund et al. 2010, Fig. 1). The Delta is used primarily to transfer freshwater from the Sacramento River in the north and San Joaquin River in the south to central and southern California via canals of the State Water Project and Central Valley Project (Lund et al. 2010, Fig. 1). The diverted freshwater supports production of about one half of the fruits and vegetables in the USA and provides drinking water for about 25 million Californians. Water-exporting operations, however,

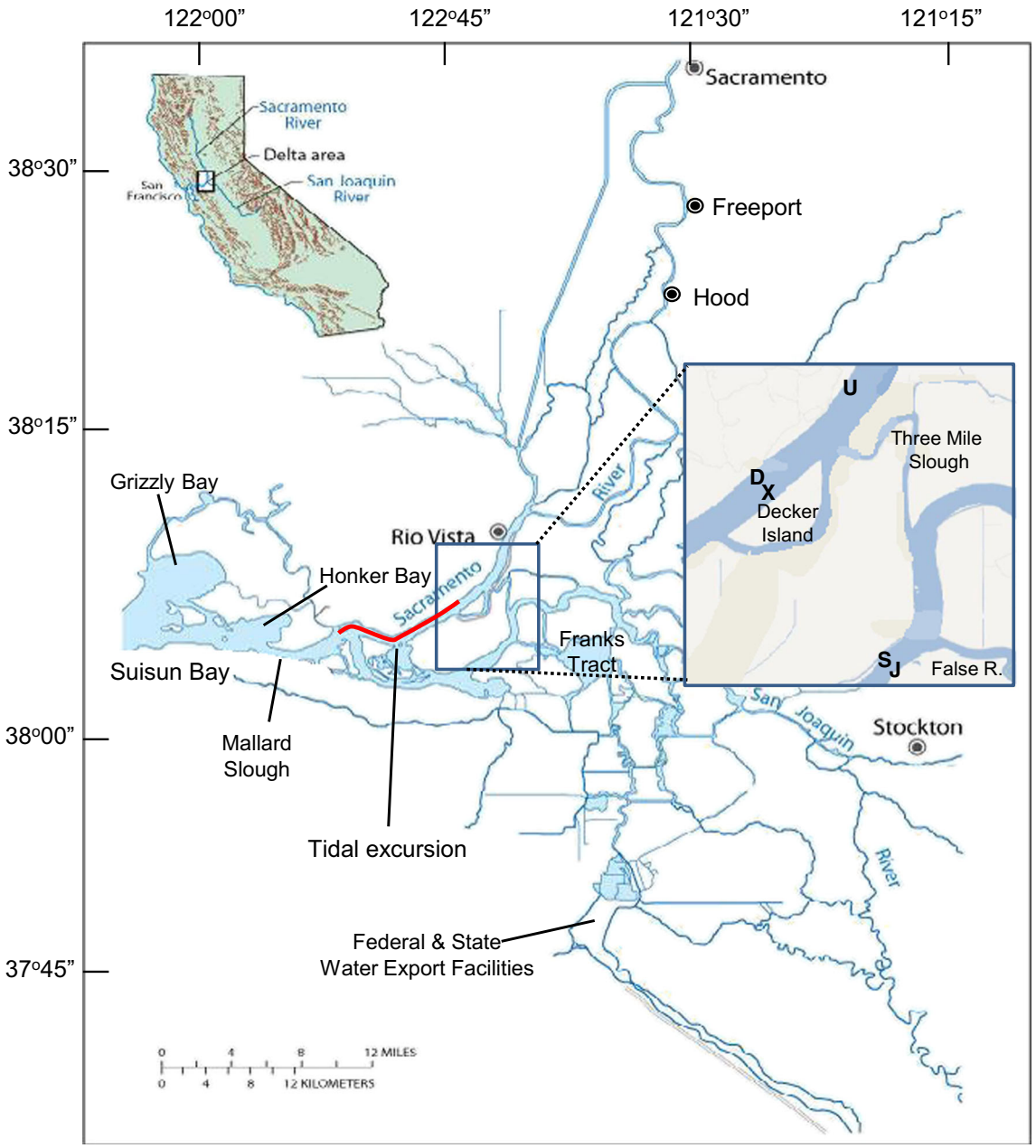

Fig. 1 Map of study area in the lower Sacramento River and San Joaquin River in the northern San Francisco Estuary, CA, USA. *Letters* show location of sampling stations and typical tidal excursion (*thick line*)

also kill large numbers of fish, including delta smelt (Kimmerer 2008; Grimaldo et al. 2009). ESA regulations intended to minimize entrainment mortality of delta smelt often restrict water-exporting operations and interfere with allocations of freshwater throughout California, which has unfortunately intensified controversy and litigation focusing on this imperiled species.

Study Design

Our study was conducted in the lower Sacramento River and San Joaquin River, two potential migration routes for delta smelt in the western Delta (Fig. 1). While the Sacramento River is likely the primary route, in some years, individuals enter the San Joaquin River and travel through the central Delta, which increases the chance of entrainment in the water export facilities (Grimaldo et al. 2009). Our fieldwork coincided with the first major winter storms producing the first flush and occurred on January 27–28, 2010 and then December 21, 2010 to January 1, 2011. Sampling integrated continuous monitoring of hydrodynamics, water turbidity, salinity, and temperature, concurrently with sampling for fish to quantify the pelagic microhabitat typically used by delta smelt at tidal time scales. Based on velocity measurements

taken at this location using a horizontal acoustic Doppler profiler (Burau, unplublished data), we decided to sample hourly at fixed locations. This would enable sampling of 8–12 km of river water and fish habitat as it moved past our position by strong tidal currents (ca. 85 cm s^{-1}) over a complete tidal cycle, depending on the spring/neap lunar phase (Fig. 1).

During the January 2010 study, hereafter referred to as the Pilot Study, sampling occurred only near Decker Island in the lower Sacramento River (D, Fig. 1), whereas during the following winter (December 2010), sampling alternated daily between sites in the Sacramento River and those near Jersey Point in the San Joaquin River (Fig. 1). The bathymetry in this reach of the Sacramento River is relatively prismatic (i.e., uniform in cross section) within about 18 km of our sampling location, because it was completely man-made by dredging during the late 1800s for flood control. Thus, because this reach of the river is wide (ca. 900 m), relatively shallow (ca. 10 m), and prismatic, it has very weak lateral mixing and other potential complicating hydrodynamic factors; particles released in this region tend to return to their original release point on subsequent tide (Fischer et al. 1979; Nidzieko et al. 2009). This facilitates separating behavioral responses from hydrodynamic influences on responses of fish to changes in tidal current direction and water clarity. In contrast, the hydrodynamics at the San Joaquin location are more complex, with water mixed by secondary currents in nearby bends and exchanging with side channels such that it can come from different regions of the Delta (Fig. 1).

In the Sacramento River, we chose our sampling sites along the northwestern side of the river just inside the channel marker buoys, where tidal fronts regularly occur at the shoal-channel interface (Fig. 1). Our rationale was based on the well-documented observation that a variety of pelagic organisms, including small fishes, tend to exploit open-water habitat by aggregating at tidal fronts (Owen 1981; Maravelias and Reid 1997; Marchand et al. 1999). A horizontal acoustic Doppler current profiler (H-ADCP, ChannelMaster, Teledyne RD Instruments) calibrated using the index velocity method (Ruhl and Simpson 2005; Coz et al. 2008) was deployed from a channel marker and continuously monitored river discharge and tidal current velocity distribution at mid-depth; electrical conductivity, temperature, and turbidity were also measured using a 6,600 V2-4 MultiSonde (YSI, Inc.) and available in real-time throughout the study via a RavenXTV CDMA Sierra Wireless Cellular Modem (Campbell Scientific, Inc.). Additional water current velocity and turbidity data (e.g., used in Fig. 2) collected by the U.S. Geological Survey were measured as part of the Interagency Ecological Program's continuous monitoring program (http://www.water.ca.gov/iep/).

Overall, sampling for fish occurred hourly over 12–16 h, to encompass complete tidal cycles which varied in duration

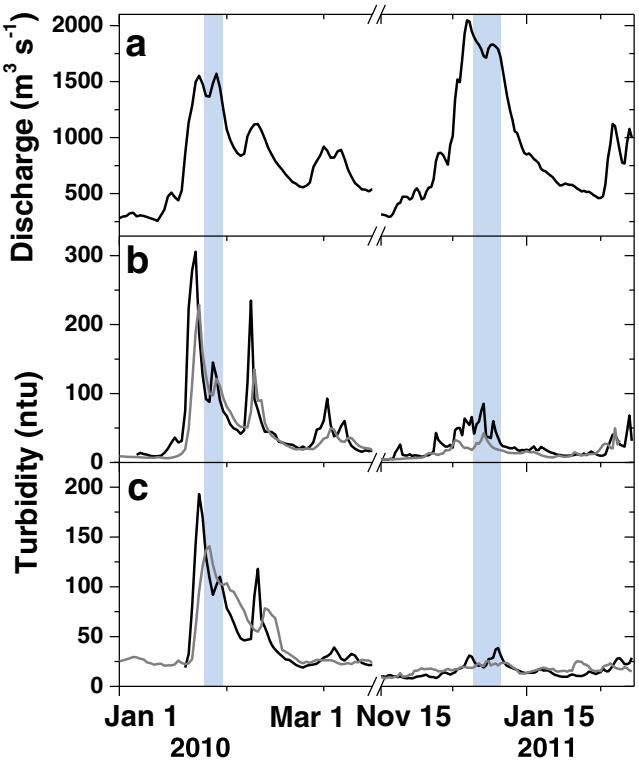

Fig. 2 Sacramento River flow (*a*) and turbidity levels at Freeport (*black line*) and Rio Vista (*gray line*) (*b*), as well as Decker Island (*black*) and Mallard Slough (*gray*) in the lower San Joaquin River (*c*) from January 2010 to March 2011. *Vertical shading* shows both study periods

with the magnitudes of river flow and the tides. Each day of sampling required several field crews working concurrently at different locations and began at the top of the hour nearest time of slack water estimated using the real-time data from the hydrodynamic instruments. Fish were sampled in the upper 4 m of the water column using Kodiak trawls, which involves towing a 7.6×1.8-m net with mesh that tapers from 50 mm at the mouth to 6 mm at the cod end. This presents a cross-sectional area of about 14 m^2 when the net is stretched between two boats running in parallel. During each winter study, a crew with a Kodiak trawl sampled hourly at station D near Decker Island in the lower Sacramento River (Fig. 1). In the December 2010 study, another crew also sampled concurrently with a 15.2×1.2-m beach seine with a 3-mm mesh along the adjacent shoreline at station D, with an additional Kodiak trawl and beach seine crews also sampling immediately upriver, near Three Mile Slough (station U, Fig. 1). Station U was located about one third of the distance of the maximum tidal excursion from station D (Fig. 1). If delta smelt were caught at station D during the flood tide, we might expect to detect them at station U after a few hours if fish were moving upriver with the incoming tide. The crew sampling at station U alternated hourly with station X, located mid-channel directly offshore from station D to assess the extent to which delta smelt were distributed laterally (Fig. 1).

Table 1 Numbers of fish caught in Kodiak trawl and beach or purse seines in the Sacramento and San Joaquin Rivers on January 27–28, 2010 (1/10) and from December 21, 2010 to January 1, 2011 (12/10–1/11)

Species	Sacramento River			San Joaquin River		
	Kodiak Trawl 1/1012/10-1/11		Beach Seine	Kodiak Trawl	Purse seine	Total
Delta smelt *Hypomesus transpacificus*[a]	225	479	176	3	0	883
Threadfin shad *Dorosoma petenense*	73	359	182	38	13	665
Chinook salmon *Oncorhyncus tshawytscha*[a]	129	237	1,594	13	5	1,978
Mississippi silverside *Menidia beryllina*	35	151	821	5	55	1,067
Pacific lamprey *Lampetra tridentata*[a]	7	59	0	0	0	66
Longfin smelt *Spirinchus thaleichthys*[a]	20	48	7	0	0	75
American shad *Alosa sapidissima*	6	27	0	15	0	48
Bluegill *Lepomis macrochirus*	5	9	8	7	1	30
River lamprey *Lampetra ayresi*[a]	1	11	0	0	0	12
Tule perch *Hysterocarpus traski*[a]	1	1	20	4	62	88
Striped bass *Morone saxatilis*	2	3	639	0	293	937
Splittail *Pogonichthys macrolepidotus*[a]	13	4	59	0	24	100
Sacramento pikeminnow *Ptychocheilus grandis*[a]	15	0	26	1	1	43
Yellowfin goby (*Acanthogobius flavimanus*)	0	3	21	2	8	34
Wakasagi *Hypomesus nipponensis*	3	3	17	0	1	24
Bigscale logperch *Percina macrolepida*	0	0	1	0	46	47
Hitch *Lavinia exilicauda*[a]	0	0	12	0	11	23
Redear sunfish *Lepomis microlophis*	0	0	4	0	3	7
Shimofuri goby *Tridentiger bifasciatus*	2	3	7	0	0	12
Rainbow trout *Oncorhynchus mykiss*[a]	7	2	0	0	0	9
Largemouth bass *Micropterus salmoides*	0	1	0	1	2	4

Only Kodiak trawls were used during the 1/10 sampling

[a] Denote 513 native species

Every other day during the December 2010 study, we sampled in the San Joaquin River with a Kodiak trawl crew that alternating hourly between station S, at the shoal-channel interface, and station J, located on the opposite side of the main channel (Fig. 1). These two locations were chosen so that we sampled water that exchanged into different regions of the central Delta. For example, on ebb tides, water at station S is transported from the San Joaquin River, whereas at station J, water arrives from the southern Delta via the False River (Fig. 1). Thus, by sampling laterally at this single location, we could compare and contrast two distinct routes of potential fish transport, assuming fish move with the water. If delta smelt were detected at station J, the prevailing hydrodynamics associated with dispersive mixing in Franks Tract would substantially increase the probability for these fish to become vulnerable to the major water export facilities in the south Delta (Fig. 1). At station S, a separate crew used a 30-m purse seine with a 5-mm mesh to sample near the shoreline because of the logistical difficulties associated using a beach seine at this location.

Given that both delta smelt and winter run Chinook salmon, *Oncorhynchus tshawytscha*, co-occurred in our study area and are both protected under the federal ESA, strict fish-take limits were imposed with catch reported daily to the regulatory agencies. Although delta smelt occur in very low densities, we closely monitored catch and adjusted sampling effort (tow durations) in real time to avoid excessive take of these species. Thus, we tailored sampling to reliably detect delta smelt presence/absence rather than quantify overall density. All fish caught during sampling were first identified and measured for length. The majority of juvenile Chinook salmon were then released immediately unharmed, as were other fishes in the catch. About 30 % of the delta smelt in the catch appeared unharmed and were swimming normally after capture, thus were also released. Although fewer individuals of this fragile species survived relative to others, the proportion released was higher than anticipated and likely due to reducing trawl durations from 15 to 10 min. The remaining delta smelt were then coded and individually rolled up in aluminum foil and placed into a dewar containing liquid nitrogen and archived. Hydrodynamic and delta smelt catch data were initially explored using various graphical techniques. Generalized linear modeling (GLM) was then used to evaluate an apparent association between tidal current direction and delta smelt catch.

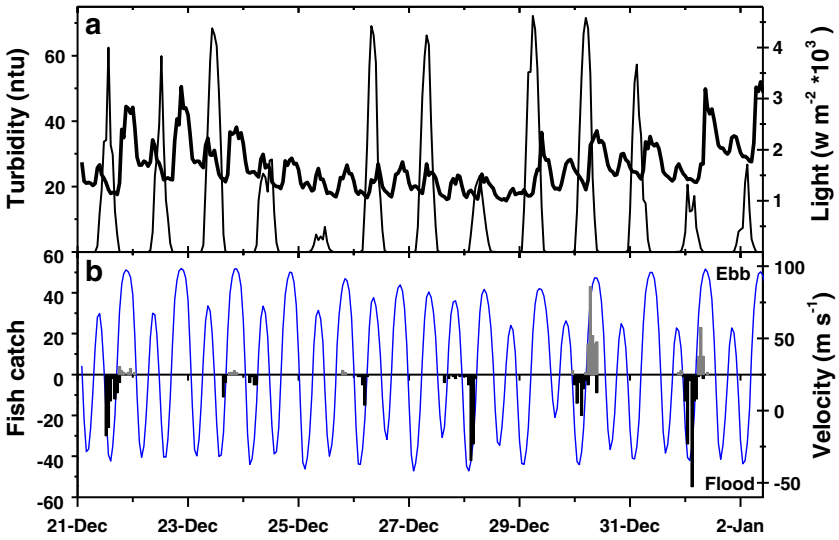

Fig. 3 Trends in turbidity (*thick line*) and light intensity (*a*) with delta smelt catch at shoal-channel margin (*dark bars*) and near the shoreline (*gray bars*) in relation to tidal and river flows (*b*), from the December 2010 field sampling in the Sacramento River. Negative water velocity represents flood tides

Results

Physical Conditions

Patterns of rainfall, river discharge, and turbidity differed substantially between the two winter study periods (Fig. 2). During the 2009–2010 winter of the Pilot Study, river flows were relatively low, peaking at only about 1,557 m^3 s^{-1} (Fig. 2(a)), but were apparently sufficient to mobilize higher levels of turbidity (~350 nephelometric turbidity units (NTU) at Freeport, Fig. 2(b)) than those observed in the following winter season. After the December 2010 "first flush" rainstorm, however, turbidity levels were far lower than anticipated (~50–80 NTU) at our Sacramento River study area and did not increase in the San Joaquin River (Fig. 2(b, c)). This was surprising given that flows in the Sacramento River peaked at 2,124 m^3 s^{-1} (Fig. 2). These unusually low turbidity levels likely resulted from intentional releases of relatively clear water from reservoirs in the upper watershed to accommodate the large volumes of runoff projected from this storm. The reservoir releases were substantial, constituting 30–80 % of the flow in the Sacramento River during December–January, whereas they typically only make up about 10 % of the river flow. As a result, the slight increases in turbidity observed in the lower Sacramento River were derived from turbid water extending upriver on flood tides to our study area from Suisun Bay, given that the highest levels occurred primarily during flood tides.

Table 2 Results of alternative generalized linear models associating delta smelt occurrence with environmental conditions at the shoal-channel margin versus the near the shoreline, including *z*-statistics, probabilities of significance, and Akaike Information Criteria (AIC)

Model	Variable					
	Velocity (CMS)	Turbidity (NTU)	Hour (h)	Year	CMS×NTU	AIC
Channel margin						
CMS	−5.78***					127
NTU		−3.98***				153
CMS+NTU	−5.09***	−2.39*				122
CMS+NTU+h	−4.37***	−2.41*	−0.813			124
CMS+NTU+Year	−4.15***	−2.41*		1.16		123
CMS+NTU+CMS×NTU	−2.59**	−2.09*			1.19	123
Shoreline						
CMS	4.24***					76
NTU		3.96***				92
CMS+NTU	3.22**	0.36				78
CMS+h	3.82***		1.03			77

*p<0.05; **p<0.01; ***p<0.001

Fish Catch

Overall, 21 fish species were collected during the two winter sampling periods, with catch composition varying greatly between the Sacramento River and San Joaquin River, as well as in the Kodiak trawls versus the beach or purse seines (Table 1). Pelagic species, such as delta smelt and threadfin shad, *Dorosoma petenense*, were most abundant in the Kodiak trawls, whereas juvenile Chinook salmon and Mississippi silversides, *Menidia beryllina*, dominated the catch in the shoreline sampling. During the Pilot Study, 225 delta smelt and 129 juvenile Chinook salmon were caught in the Pilot Study, with 655 and 1,831 of each species respectively caught during the December 2010 sampling period. Juvenile Chinook salmon and Mississippi silversides, *M. beryllina*, dominated the catch in the shoreline sampling. In contrast, only 3 delta smelt and 18 juvenile Chinook salmon were caught at the San Joaquin River locations (Table 1).

Delta smelt were caught fairly consistently by focusing our sampling near the shoal-channel interface during both the Pilot Study and the December 2010 study period. At this location (D, Fig. 1), 82 % of net tows occurring on flood tides detected delta smelt relative to 67 % of samples taken nearby at the mid-channel station (X, Fig. 1). The higher detection of delta smelt at the interface facilitated identifying a clear tidal signal in the catch time series, such that during flood tides, delta smelt were caught almost exclusively in the Kodiak trawls, whereas on ebb tides, they were primarily caught in the beach seines at the shoreline stations (Fig. 3). Delta smelt catch in the Kodiak trawls was also somewhat higher when turbidity levels were elevated and in the morning (Fig. 3).

Generalized linear models with a binomial error distribution and a logit link function (i.e., logistic regression) were used to associate delta smelt occurrence (i.e., presence/absence) in the Kodiak trawls and beach seines with tidal velocity, water turbidity, time of day, and calendar year sampled as predictor variables (Table 2). Overall, variability in water temperatures and specific conductance was low, averaging 10 °C (range=1.8 °C) and 116 μS cm^{-1} (range=149 μS cm^{-1}), respectively. In preliminary analyses, both factors were not significant predictors, thus were not included in the final analyses. For the Kodiak trawl samples, the optimal model explaining fish occurrence included water current velocity ($t=-5.36$, $df=90$, $P<0.0001$) and turbidity ($t=-5.36$, $df=90$, $P<0.0001$), whereas for the beach seine samples, only current velocity ($t=4.24$, $df=90$, $P<0.0001$) was retained as a significant predictor (Table 2). Hour of the day and winter sampled as well as an interaction term with velocity and turbidity were not significant (Table 2). The best-fit models for fish presence/absence by gear type exhibit inverse relationships with water current velocity; during flood tides, probabilities of occurrence increased on flood tides in the Kodiak trawls and during ebb tides in the beach seines (Fig. 4a). While the flood-ebb tidal asymmetry in delta smelt occurrence was also apparent during the nighttime, the overall catch was much lower. Cumulative frequency distributions of fish catch over time indicate that more delta smelt were caught in the Kodiak trawls before mid-day, whereas they more frequently appeared in the beach seines later in the afternoon and evening (Fig. 4b).

Discussion

Our results from two sampling periods in consecutive years indicate that during winter, delta smelt aggregate near frontal zones at the shoal-channel interface moving laterally into the shoals on ebb tides and back into the channel on flood tides. For a small pelagic fish attempting to migrate upriver against strong river flows and tidal currents, this behavioral strategy would facilitate either maintaining position or moving upriver during flood tides, whereas on ebb tides, it would help to minimize advection down-estuary. Delta smelt have been shown to prefer modest swimming velocities and a discontinuous stroke and glide behavior in the laboratory, prompting Swanson et al. (1998) to suggest that selective tidal stream transport would be likely employed during the spawning migration. Sommer et al. (2011) using a particle-tracking

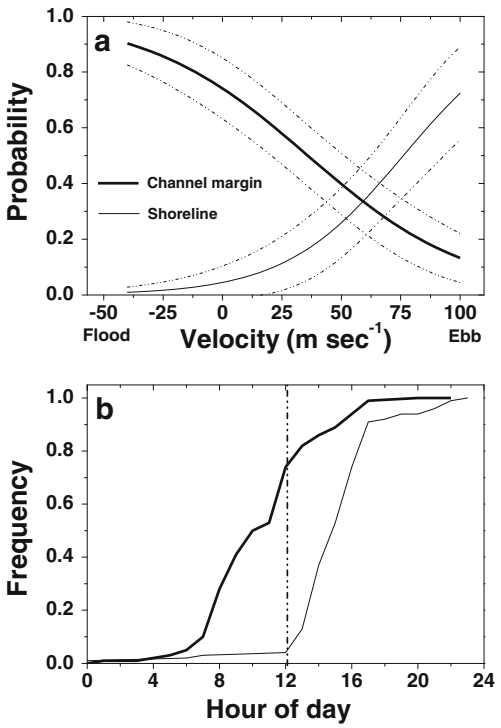

Fig. 4 Generalized linear model fits of delta smelt occurrence to tidal velocity (**a**) and cumulative distributions of catch relative to sampling hour of the day (**b**) at the shoal-channel margin (*thick line*) and near the shoreline (*thin line*) with 95 % confidence limits, respectively, from the December 2010 field sampling in the Sacramento River

model showed that moving upriver was only plausible if fish exhibited tidally selective vertical movements; simulating lateral migration was not possible with their one-dimensional vertically averaged model. Indeed, given the small body size, observed swimming behaviors, and extreme flow velocities typically observed on ebb tides during storms (>1,500 $m^3 s^{-1}$), it is unlikely that vertical tidal movements would facilitate migration. Although fewer delta smelt were caught during the night, the same tidal asymmetry was evident in the catch. Delta smelt are visual foragers, thus are more highly aggregated nearer the surface during the daytime (Hobbs et al. 2006). Lower catch at night is likely due to these fish being more dispersed throughout the water column in darkness, a pattern also observed for larval smelt in the low-salinity zone (Bennett et al. 2002). Such higher dispersion is sufficient to lower catch efficiency of the Kodiak trawl net at night which samples only the upper portion of the water column.

These results also indicate the effectiveness of tuning our sampling routine closely to the scales of the processes in question. Standard monitoring surveys that sample monthly across a fixed sample grid, irrespective of the tides, may be useful for detecting trends in distribution or abundance over many years, but they are hampered by considerable observational bias due to tidal aliasing and are thus not sufficient for addressing finer-scale or process-oriented questions. By focusing our sampling close to the shoal-channel interface, we detected (caught) delta smelt in 82 % (station D, Fig. 1) of net tows during flood tides, whereas detections declined to 67 % at the nearby mid-channel station (X, Fig. 1). Moreover, improving our understanding of how these fish interact with the tides also provides key information on the microhabitat preferences and behaviors essential for adapting monitoring programs, and management options for delta smelt and other pelagic fishes in tidally dominated systems.

The apparent selective tidal movements may also be in response to lateral turbidity gradients that can develop near slack water (Yu et al. 2012). In the shoals, shallow depths and slower tidal currents due to increased friction with the shoreline substantially reduces momentum, such that currents switch direction in the shallows before changing in the center of the river channel (by as much as about an hour) where it is deeper and currents are stronger. This temporal asynchrony in tidal timing, in the presence of a prominent along-channel turbidity gradient in the Sacramento River, can produce lateral turbidity gradients near slack water (Fig. 5). When the turbidity source for the along-channel gradient switches from down-estuary in Suisun Bay before the first flush to upriver in the Delta afterwards, inverse patterns in these lateral turbidity gradients are produced with respect to the tides (Fig. 5). Before first flush, as the ebb tide begins, relatively clear water moves downriver along the shoals before it appears in the channel (Fig. 5(a)); on the flood, the reverse occurs with water of higher turbidity moving upriver near shore before the channel (Fig. 5(b)). Thus, if fish attempt to remain with turbid water, they are likely to move upriver near the shoals first and then in the channel as the flood develops, but then travel back down-estuary on the ebb, because clearer water arrives in the shoals first which discourages lateral movement. After first flush,

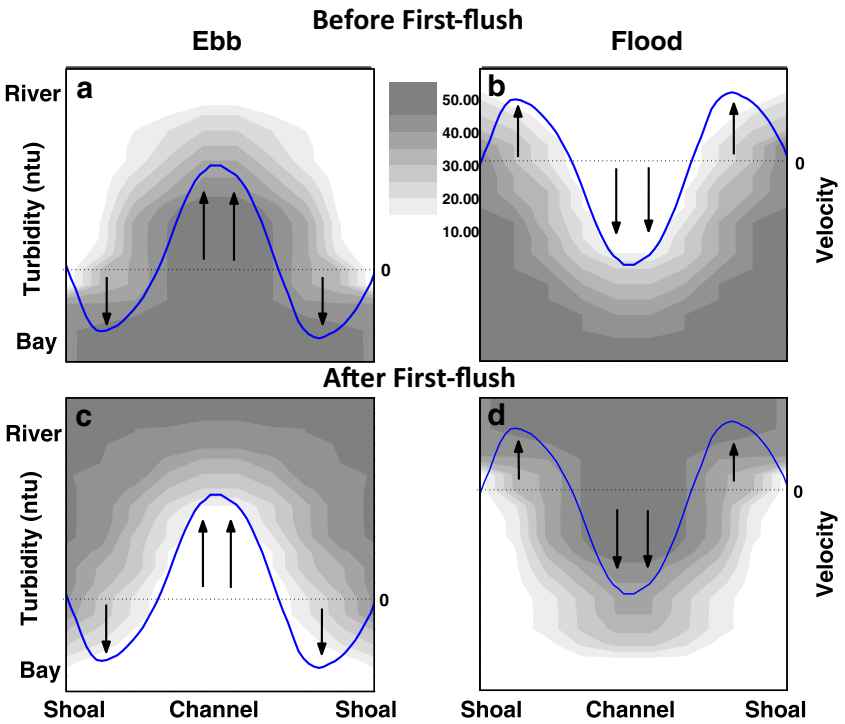

Fig. 5 Conceptual diagram showing how cross-channel gradients in water turbidity (*shaded*) develop from temporal asynchronies in near-shore versus mid-channel tidal velocities near slack water (*line*, *vector arrows*), as well as how these gradient patterns reverse when the source of turbidity along-channel switches from down-estuary to upriver, before (**a**, **b**) and after (**c**, **d**) the first-flush winter rainstorm

the turbidity source is from upriver, which then reverses both the along-channel and lateral gradients (Fig. 5(c, d)). Now, as the flood tide begins, water in the channel remains turbid while clearer water from down-estuary arrives in the shoals first which discourages onshore movements by fish such that they remain in the turbid channel and move upriver with the tide (Fig. 5(d)). Thus, after the first flush, the coherence of lateral turbidity gradient and tidal current allows fish to greatly reduce the energy needed to swim upriver, even if they are only attempting to remain in turbid water as the tide changes direction.

Our results, thus far, cannot distinguish the relative importance of turbidity versus changing tidal direction as cues for moving laterally or for the spawning migration. Selective tidal movements are a common strategy among marine and estuarine organisms (e.g., review by Forward and Tankersley 2001); however, little is known concerning if or how individuals detect tidal currents and direction (Chapman et al. 2013), with the possible exception of blue crab (*Callinectes sapidus*) larvae (Forward et al. 2003). Related strategies for migrating have been reported for sockeye salmon (Hinch and Rand 2000) and Pallid sturgeon (McElroy et al. 2012). For delta smelt with a primarily annual life cycle, the advantages of moving laterally are likely to vary greatly given the high interannual variability in freshwater outflows. Extremely high outflow in wet years can weaken or completely overwhelm the flood tidal signal in the Sacramento River and thus preclude or impair maturation and the reproductive output of spawning individuals (Kinnison et al. 2001; Bronmark et al. 2008). In such years, fish may choose to reproduce in suboptimal habitat or migrate up the San Joaquin River which has lower outflows, but this increases potential mortality by moving fish toward the water export facilities (Grimaldo et al. 2009). Nonetheless, there is likely strong selection pressure to use both cues for moving laterally, such that adaptive responses to turbid water by individuals may underlie observations at the population level suggesting that it is a cue for the spawning migration (Grimaldo et al. 2009). When considered in the cost-benefit trade-off proposed by Bronmark et al. (2008), turbidity may sufficiently reduce predation risks relative to potential growth and reproductive benefits, tipping the balance in favor of migrating. Understanding these processes may facilitate development of management tools using turbidity to reduce entrainment impacts not only on imperiled species, such as delta smelt, but also on others occurring in highly dynamic systems subjected to human interventions and future changes in climate.

Acknowledgments We would like to thank the many biologists and technicians for the field assistance with the California Water Science Center and Columbia River Research Laboratory of the U.S. Geological Survey, U.S. Fish and Wildlife Service, Interagency Ecological Program for the San Francisco Estuary, California Department of Fish and Game, and University of California, Davis. For the help with ESA permission and compliance, we thank E. Gleason (USFWS) and D. Hampton (U.S. National Marine Fisheries Service). Considerable help with planning and logistics was provided by N. Adams, G. Rutz, and V. Orsini (CRRL), J. Adib-Samii and R. Baxter (CDFG), Larry Brown and D. Schoellhamer (USGS), J. Netto (USFWS), L. Grimaldo (USBR), A. Mueller-Solger (IEP), and T. Sommer (California Department of Water Resources). We thank B. McElroy and an anonymous reviewer for the helpful comments. Funding was provided by E. Van Nieuwenhuyse and M. Chotkowski, U.S. Bureau of Reclamation and facilitated by A. Castle and D. Nawi, U.S. Department of the Interior.

References

Anderson, J.J., and W.N. Beer. 2009. Oceanic, riverine, and genetic influences on spring Chinook salmon migration timing. *Ecological Applications* 19: 1989–2003.

Bennett, W.A. 2005. Critical assessment of the delta smelt population in the San Francisco Estuary, California. *San Francisco Estuary and Watershed Science*. Available at http://repositories.cdlib.org/jmie/sfews/vol3/iss2/art1/. Accessed 2 Sep 2008.

Bennett, W.A., W.J. Kimmerer, and J.R. Burau. 2002. Plasticity in vertical migration by native and exotic estuarine fishes in a dynamic low-salinity zone. *Limnology and Oceanography* 47: 1496–1507.

Bergamaschi, B.A., K.M. Kuivila, and M.S. Fram. 2001. Pesticides associated with suspended sediments entering San Francisco Bay following the first major storm of water year 1996. *Estuaries* 24: 368–380.

Brodersen, J., P.A. Nilsson, J. Ammitzboll, L.-A. Hansson, C. Skov, and C. Bronmark. 2008a. Optimal swimming speed in heads currents and effects on distance movement of winter-migrating fish. *PloS One* 3(5): e2156. doi:10.1371/journal.pone.0002156.

Brodersen, J., P.A. Nilsson, L.A. Hansson, C. Skov, and C. Bronmark. 2008b. Condition-dependent individual decision-making determines cyprinid partial migration. *Ecology* 89: 1195–1200.

Bronmark, C., C. Skov, J. Brodersen, P.A. Nilsson, and L.A. Hansson. 2008. Seasonal migration determined by a tradeoff between predator avoidance and growth. *PLoS ONE* 3: e1957.

Chapman, B.B., A. Eriksen, H. Baktoft, J. Brodersen, P.A. Nilsson, K. Hulthen, C. Bronmark, L.A. Hansson, P. Gronkjaer, and C. Skov. 2013. A foraging cost of migration for a partially migratory cyprinid fish. *PLoS ONE* 8: e61223.

Coz, J.L., G. Pierrefeu, and A. Paquier. 2008. Evaluation of river discharges monitored by a fixed side-looking Doppler profiler. *Water Resources Research* 44: W00D09. doi:10.1029/2008WR006967.

Crossin, G.T., S.G. Hinch, A.P. Farrell, D.A. Higgs, A.G. Lotto, J.D. Oakes, and M.C. Healey. 2004. Energetics and morphology of sockeye salmon: Effects of upriver migratory distance and elevation. *Journal of Fish Biology* 65: 788–810.

Dahl, J., J. Dannewitz, L. Karlsson, E. Petersson, A. Lof, and B. Ragnarsson. 2004. The timing of spawning migration: Implications of environmental variation, life history, and sex. *Canadian Journal of Zoology* 82: 1864–1870.

Dingle, H. 1996. *Migration: The biology of life on the move*. New York: Oxford University Press.

Feyrer, F., M.L. Nobriga, and T.R. Sommer. 2007. Multi-decadal trends for three declining fish species: Habitat patterns and mechanisms in the San Francisco estuary, California. U.S.A. *Canadian Journal of Fisheries and Aquatic Sciences* 64: 723–734.

Fischer, H.B., E.J. List, R.C.Y. Koh, J. Imberger, and N.H. Brooks. 1979. *Mixing in inland and coastal waters*. San Diego, CA: Academic.

Forsythe, P.S., K.T. Scribner, J.A. Crossman, A. Ragavendran, E.A. Baker, C. Davis, and K.K. Smith. 2012. Environmental and lunar cues are predictive of the timing of river entry and spawning-site arrival in the lake sturgeon *Acipenser fulvescens*. *Journal of Fish Biology* 81: 35–53.

Forward, R.B., and R.A. Tankersley. 2001. Selective tidal stream transport of marine animals. *Oceanography and Marine Biology* 39: 305–353.

Forward, R.B., R.A. Tankersley, and J.M. Welch. 2003. Selective tidal-stream transport of the blue crab *Callinectes sapidus*: An overview. *Bulletin of Marine Science* 72: 347–365.

Grimaldo, L.F., P.B. Moyle, T. Sommer, N. Van Ark, G. Jones, E. Holland, P. Smith, and B. Herbold. 2009. The effects of large-scale water diversions in a freshwater tidal estuary: Can fish losses be managed? *North American Journal of Fisheries Management* 29: 1253–1270.

Hobbs, J.A., W.A. Bennett, and J. Burton-Hobbs. 2006. Assessing nursery habitat quality for native fishes in the low-salinity zone of the San Francisco estuary, California. *Journal of Fish Biology* 69: 907–922.

Hinch, S., and P. Rand. 1998. Swim speeds and energy use of upriver-migrating sockeye salmon (*Oncorhynchus nerka*): Role of local environment and fish characteristics. *Canadian Journal of Fisheries and Aquatic Sciences* 55: 1821–1831.

Hinch, S., and P. Rand. 2000. Optimal swimming speeds and forward-assisted propulsion: Energy-conserving behaviors of upriver-migrating adult salmon. *Canadian Journal of Fisheries and Aquatic Sciences* 57: 2470–2478.

Jonsson, B., and N. Jonsson. 1993. Partial migration: Niche shift versus sexual maturation in fishes. *Reviews in Fish Biology and Fisheries* 3: 348–365.

Jonsson, B., and N. Jonsson. 2006. Life-history effects of migratory costs in anadromous brown trout. *Journal of Fish Biology* 69: 860–869.

Jonsson, N., B. Jonsson, and L.P. Hansen. 1997. Changes in proximate composition and estimates of energetic costs during upstream migration and spawning in Atlantic salmon *Salmo salar*. *Journal of Animal Ecology* 66: 425–436.

Jorgensen, C., E.S. Dunlop, A.F. Opdal, and O. Fiksen. 2008. The evolution of spawning migrations: State dependence and fishing-induced changes. *Ecology* 89: 3436–3448.

Keefer, M.L., C.C. Caudill, C.A. Perry, and M.L. Moser. 2013. Context-dependent diel behavior of upstream-migrating anadromous fishes. *Environmental Biology of Fishes* 96: 691–700.

Kimmerer, W.J. 2008. Losses of Sacramento River Chinook salmon and delta smelt to entrainment in water diversions in the Sacramento – San Joaquin Delta. *San Francisco Estuary Watershed Science*. Available at http://repositories.cdlib.org/jmie/sfews/vol6/iss2/art2/. Accessed 13 Oct 2008.

Kinnison, M., M. Unwin, A. Hendry, and T. Quinn. 2001. Migratory costs and the evolution of egg size and number in introduced and indigenous salmon populations. *Evolution* 55: 1656–1667.

Lund, J., E. Hanak, W. Fleenor, W.A. Bennett, R. Howitt, J. Mount, and P. Moyle. 2010. *Comparing futures for the Sacramento-San Joaquin Delta*. Berkeley: University of California Press.

Maravelias, C.D., and D.G. Reid. 1997. Identifying the effects of oceanographic features and zooplankton on prespawning herring abundance using generalized additive models. *Marine Ecology Progress Series* 147: 1–9.

Marchand, C., Y. Simard, and Y. Gratton. 1999. Concentration of capelin (*mallotus villosus*) in tidal upwelling fronts at the head of the Laurentian channel in the St. Lawrence estuary. *Canadian Journal of Fisheries and Aquatic Sciences* 56: 1832–1848.

McElroy, B., A. DeLonay, and R. Jacobson. 2012. Optimum swimming pathways of fish spawning migrations in rivers. *Ecology* 93: 29–34.

Moyle, P.B., B. Herbold, D.E. Stevens, and L.W. Miller. 1992. Life history of delta smelt in the Sacramento–San Joaquin Estuary, California. *Transactions of the American Fisheries Society* 121: 67–77.

Nidzieko, N.J., J.L. Hench, and S.G. Monismith. 2009. Lateral circulation in well-mixed and stratified flows with curvature. *Journal of Physical Oceanography* 39: 831–851.

Owen, R.W. 1981. Fronts and eddies in the sea: Mechanisms, interactions and biological effects. In *Analysis of marine ecosystems*, ed. A.R. Longhurst, 197–233. New York: Academic.

Quinn, T.P., and D.J. Adams. 1996. Environmental changes affecting the migratory timing of American shad and sockeye salmon. *Ecology* 77: 1151–1162.

Rakowitz, G., B. Berger, J. Kubecka, and H. Keckeis. 2008. Functional role of environmental stimuli for the spawning migration in Danube nase *Chondrostoma nasus* (L.). *Ecology of Freshwater Fish* 17: 502–514.

Roff, D.A. 1988. The evolution of migration and some life history parameters in marine fishes. *Environmental Biology of Fishes* 22: 133–146.

Roff, D.A. 1992. *The evolution of life histories*. London: Chapman and Hall.

Ruhl, C. A., M.R. Simpson. 2005. Computation of Discharge Using the Index-velocity Method in Tidally Affected Areas, U.S. Geological Survey Scientific Investigations Report. 2005–5004. Available at http://pubs.usgs.gov/sir/2005/5004/. Accessed 10 Jan 2013.

Ruhl, C.A., D.H. Schoellhamer, R.P. Stumpf, and C.L. Lindsay. 2001. Use of remote sensing images of San Francisco Bay to analyze suspended-sediment concentrations. *Estuarine, Coastal and Shelf Science* 53: 801–812.

Schaffer, W.M., and P.F. Elson. 1975. The adaptive significance of variation in life history among local populations of Atlantic salmon in North America. *Ecology* 56: 577–590.

Sommer, T., F. Mejia, M. Nobriga, F. Feyrer, and L. Grimaldo. 2011. The spawning migration of delta smelt in the upper San Francisco Estuary. *San Francisco Estuary and Watershed Science*. Available at http://repositories.cdlib.org/jmie/sfews/vol9/iss2/art2/. Accessed 1 Sep 2011.

Swanson, C., P.S. Young, and J.J. Cech. 1998. Swimming performance of delta smelt: maximum performance, and behavioral and kinematic limitations on swimming at submaximal velocities. *Journal of Experimental Biology* 201: 333–345.

Yu, Q., Y.P. Wang, B. Flemming, and S. Gao. 2012. Tide-induced suspended sediment transport: depth-averaged concentrations and horizontal residual fluxes. *Continental Shelf Research* 34: 53–63.

SFCWA
State & Federal Contractors Water Agency

DELTA SMELT EFFECTIVE POPULATION SIZE PRELIMINARY REPORT

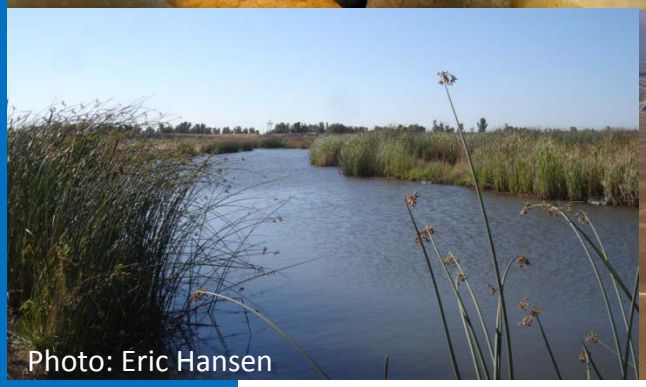

Photo: Eric Hansen

Photo: CDWR

Prepared for:

State & Federal Contractors Water Agency
1121 L Street, Suite 806
Sacramento, CA 95814

Prepared by:

Blankenship Ph.D.
Gregg Schumer
Jesse Wiesenfeld M.S.
Cramer Fish Sciences – Genidaqs
3300 Industrial Way, Suite 100
West Sacramento, CA 95691

September 2015

CRAMER FISH SCIENCES
An Employee Owned Consulting Company

GENIDAQS℠
aquatic species sampling, simplified

TABLE OF CONTENTS

List of Figures

List of Tables

EXECUTIVE SUMMARY

Present monitoring programs were not designed to derive population estimates of Delta Smelt. Thus, estimating Delta Smelt annual population size (N) has proven challenging due to difficulties in estimating gear efficiencies and sampling in all potentially occupied habitats. Additionally, reliance on an abundance index has hindered the ability to evaluate the role that water exports may play in Delta Smelt population dynamics. There is an alternative to using an abundance index for assessing Delta Smelt population status. The ongoing activities of regulators and stakeholders provide information and biological material on which genetic measures can be made. From a conservation and population recovery stand point, the effective population size (N_e) is a critical metric to know over time, as there are agreed upon thresholds where genetic impact (long term viability) would be minimized – the so called 50/500 rule. Further, the N_e is measurable, which would provide credible and useful information for assessing impacts of water operations to Delta smelt. Calculating this alternative population size measure will increase the information content produced from current monitoring activities, adding value without increasing "take". Additionally, scientifically defensible population size measures could directly inform deliberations about water operation impacts on Delta smelt and population recovery performance measures.

Information regarding Delta smelt N_e is limited, which was stated as a critical information gap in review of Delta smelt Long-term Operations Opinions Reasonable and Prudent Alternatives. The information that does exist regarding total Delta smelt N_e shows N_e has recently approached the threshold where long-term population persistence could be impacted (N_e ~ 1000). This project calculated the N_e of Delta smelt from existing tissue collections from 2011-2014 year classes.

Genidaqs obtained tissues samples from existing material collected from ongoing IEP activities that encounter Delta Smelt (e.g., mid-water trawls, kodiak trawls, tow-nets, gear-efficiency studies). Genidaqs has in its possession approximately 2,740 Delta Smelt tissues samples. We do not have an exact number because we believe a small number of tissues are likely misidentified as Delta Smelt. We have had to assume for this analysis the IEP metadata to be correct. Nevertheless, the collection likely comprises most of the available wild Delta Smelt tissues intercepted between 2011 and 2015.

Population genetic analyses were performed on N=995, N=534, N=678, and N=421 tissues from year classes 2011, 2012, 2013, and 2014, respectively. Results were consistent with statistical expectations for population samples. In other words, there was no evidence of genetic data artifacts and collections appeared to be from single populations. Further, there was no evidence of genetic differences among year classes.

Effective population sizes were estimated for each year class (i.e., single collection) using the linkage disequilibrium data (Waples and Do 2008; 2010). The effective population size was also estimated using observed variance in allele frequencies over time (i.e., multi-collection) (Pollack 1983; Waples 1989). Allele frequency data were compared between year classes 2011 and 2014. Effective population size estimation algorithms were implemented in NeEstimator v2.01

(Do et al. 2013). For this initial reporting of results, a conservative hypothesis test was used to interpret effective size results. Specifically, was there any evidence suggesting the genetic effective size of Delta Smelt is below 1000 (i.e., H~~O~~$_0$: N_e is greater than 1000)? For N_e estimates generated on year classes 2011-2014, the lower bound of the 95% confidence interval was 5134, 1840, 3921, and 4193, respectively. At this time, there is no population genetic evidence supporting the acceptance of the alternative hypothesis that N_e of Delta Smelt is below 1000. The N_e for Delta Smelt – as of 2014 year class – appears to be above the threshold where quantitative genetic diversity is expected to be lost each generation through genetic drift (i.e., Ne > 500).

Despite the positive result that the Delta Smelt gene pool is expected to retain quantitative genetic diversity at its present size (i.e., > 500), a cautionary note is required. The resiliency of Delta Smelt is low because the species occupies a restricted~~tion~~ geographic range and largely has an annual reproductive cycle. The effective size could decrease quite rapidly (~years) and take millennia to recover, which would negatively impact the long-term viability (extinction risk) of the species.

Nevertheless, the implication of the present information is that a large number of Delta Smelt remain in the San Francisco Estuary system. The disparity between Delta Smelt abundance indices and N_e is a concern as it may indicate existing monitoring programs will have difficulty adequately representing Delta Smelt abundance, distribution or habitat needs.

INTRODUCTION

From a conservation and population recovery stand point, N_e is a critical metric regarding population status and is useful for assessing impacts of water operations to Delta Smelt. The size at which a population functions genetically is N_e. For example, i) the loss of each generation's genetic diversity is a function of N_e, ii) the level of genetic variability within a population (over an evolutionary timescale) is determined by the product of N_e and mutation, and iii) the spread of favorable genes within a population is determined by the product of N_e and selection. Information regarding Delta smelt N_e is limited, which was stated as a critical information gap by the IRP review of Delta smelt OCAP Reasonable and Prudent Alternatives. The information that does exist regarding total Delta smelt N_e was reported within Katie Fisch's Ph.D. dissertation and subsequent publication (Fisch et al. 2011). These data show N_e has recently approached the threshold where long-term population persistence could be impacted (N_e ~ 1000).

While new methods are being developed that link Delta smelt abundance indices with favorable habitat, N_e can immediately inform risk and water operations assessment. There are conventions for population size thresholds at which genetic impact would be minimized, the so called 50/500 rule (Franklin, 1980; Franklin and Frankham 1998; Frankham et al. 2014). An $N_e \geq 50$ would prevent an unacceptable rate of inbreeding for a short time, while $N_e \geq 500$ is required to maintain long term genetic variability. Therefore, estimating N_e can be an important tool for assessing the genetic vulnerability of an endangered species. Additionally, an agreed upon target for N_e could serve as a threshold for management action (example N_e = 500). Documenting N_e would credibly demonstrate whether the Delta smelt population remains above or below the established threshold. This type of target threshold could be used to establish criteria for gauging population level impacts and bring some reason to recovery planning. Further, N_e estimates would provide an early warning capability for observing threats to viability (i.e., loss of genetic diversity through inbreeding), as low N_e to N ratios suggest that populations may become vulnerable to genetic stochasticity prior to any indication apparent from census estimates (Hauser et al. 2002).

Genetic methods can be used to calculate N_e by measuring genetic indices affected by N_e. The fundamental concept is that genetic diversity will be more stable over time in a population with a large N_e than a population with small N_e, with the mathematical relationship defined between the genetic diversity measures and underlying N_e. Jargon surrounds the descriptions of genetic estimators, but the most common categories are inbreeding effective size ($N_{e\,(I)}$) and variance effective size ($N_{e\,(v)}$) (reviewed by Wang, 2005). The salient differences between the two categories are that $N_{e\,(I)}$ deals with loss of diversity and inbreeding (prior to reproduction) and variance effective size ($N_{e\,(v)}$) deals with the random loss of alleles (following reproduction). In fish, the most common methods are $N_{e\,(v)}$ in form. The present study uses a variance estimator, sampling a year class of juveniles post-reproduction. The linkage disequilibrium method estimates Ne within a single cohort sample using the observed magnitude of chance associations of alleles between loci (Hill 1981; Waples 2006). The temporal method uses a

standardized variance (F) of allele frequencies – comparing two time points – to estimate N_e (Nei and Tajima, 1981; Waples, 1989).

The number of Delta Smelt individuals, in the form of an index, is estimated annually. Yet, there is debate surrounding the accuracy of sampling methods in characterizing the true population size and how an abundance index should be used to inform water operations. The effective population size can be quantified from existing monitoring activities, has established scientifically defensible thresholds, and directly relates to recovery planning and population viability. This project calculated the N_e of Delta Smelt from existing tissue collections from 2011-14 year classes.

METHODS

Field Collections

Delta Smelt were captured by CDFW personnel during IEP Summer Townet (TNS), Fall Mid-water Trawl (FMWT), and Spring Kodiak Trawl (SKT). Additional tissue samples were obtained from gear efficiency studies (mid-water trawls, kodiak trawls, tow-nets) and collection of brood stock for Fish Culture and Conservation Facility.

For material transported to Swee Teh's laboratory (UCD), fish were frozen (whole) in liquid nitrogen and then transferred to ultra-cold freezers. Whole fish were thawed to conduct an unrelated analysis, and at that time a fin clips were taken from each fish. Fin tissue samples were placed in 100% ethanol and refrozen (-80^{o}C). If fin tissues were sampled directly, these tissues were stored directly into 100% ethanol.

Laboratory Processing

DNA was extracted and isolated from each Delta Smelt tissue using DNAEasy (Qiagen).

Genotypes were composed of 12 STR (microsatellite) loci Htr104a, Htr127a, Htr115a, Htr120a, Htr116a, Htr114a, Htr119a, Htr131a, Htr103a, Htr126a, Htr117a, Htr109a (Fisch et al 2009). Polymerase Chain Reaction protocols used followed Fisch et al. (2009) or alterations communicated to us by UC Davis Genome Variation Lab. Fragments were visualized on 3730 automated capillary sequencer (Applied Biosystems). Trace files were analyzed using Geneious v8 software, with marker binsets derived from previously genotyped individuals provided to us by UC Davis Genome Variation Lab. All individuals were "scored" independently by two people. All observed discrepancies were reconciled prior to final data export. Duplicate genotypes were searched for and removed. Individuals with genotypes composed of a minimum of eight loci were retained for genetic analysis.

Genetic Analysis

Population genetic analyses were performed on N=995, N=534, N=678, and N=421 tissues from year classes 2011, 2012, 2013, and 2014, respectively. Both within and among collection genetic diversity was evaluated. The following standard population genetic tests were performed to determine whether genotype data were of sufficient quality for analysis:

1. Observed heterozygosity was calculated following (Hedrick 1983). This is a basic quantification of genetic diversity and a comparison between observed and expected heterozygosity provides an indication of population data quality. Heterozygosity estimates were high, as ~84% of observations contained alternate (i.e., non-identical) alleles (Table 1-1).
2. For each locus and collection Hardy-Weinberg equilibrium was assessed using an exact test following a modified version of the (Guo and Thompson 1992) Markov-chain random walk algorithm (Markov chain length: 1000000 steps; Significance level = 0.05). Genetic data will deviate from equilibrium if multiple populations are unknowingly combined into a single collection for analysis or genetic markers provide anomalous genotypes. Little to no statistical deviations from equilibrium expectations were observed. Meaning collections consisted of single populations (no subdivisions required) and genotype data were of sufficient quality for analysis (Table 1-1).
3. Intra-collection pairwise linkage disequilibrium was estimated following (Slatkin and Excoffier 1996) permutation test (Number of permutations: 16000; Number of initial conditions for EM: 5; Significance level = 0.05). Linkage disequilibrium is the non-random association of alleles between loci in gametes. Correlations among alleles at different genetic markers could occur by chance in finite (small; unstable) populations, if sampling was not representative of entire population, or if markers provide anomalous genotypes. Observed linkage disequilibrium was quite low (data not shown), suggesting genetic data was derived from a representative sample from a large population. There is a mathematical relationship between linkage disequilibrium and effective population size.
4. To determine whether allele frequency distributions from collections were statistically equivalent (i.e., samples drawn from same underlying distribution), an exact test was used following a Markov-chain procedure described by Raymond and Rousset (1995) (Markov chain length: 100000 steps; Significance level = 0.05). Population genetic analysis starts from the presumption that there is a single population sample, and genetic data are only divided into finer partitions if there is evidence supporting a need to do so. Equilibrium tests (#2 and #3 above) showed within year class subdivisions were not warranted. Comparing allele frequencies between collections quantified differentiation among year classes. There is no differentiation among year classes (Table 1-2). Meaning the population is large enough that stochastic reproductive processes (genetic drift) are not apparent, and genetic characteristics (allele frequencies) have remained stable over time.
5. Tests for departures from Hardy-Weinberg and linkage equilibrium, and allele frequency comparisons were implemented using ARLEQUIN 3.5 software (Excoffier et al. 2007).

Table 1-1. Sample summary. Delta Smelt tissues analyzed by year class, observed heterozygosity, mean number of alleles per locus (MNA), and number of loci deviating from Hardy-Weinberg equilibrium expectations (Bonferroni correction α=0.05) (HWE).

Year Class	Sample Size	Observed Hz	MNA	HWE
2011	995	0.8430	26.00	0
2012	534	0.8360	24.58	1
2013	678	0.8361	24.83	1
2014	421	0.8463	23.75	0

Table 1-2. Year class differentiation summary. For each pairwise comparison of allele frequency variation non-differentiation exact p-values are shown (α = 0.05).

	2011	2012	2013	2014
2011	-			
2012	1.00000	-		
2013	1.00000	1.00000	-	
2014	1.00000	1.00000	1.00000	-

Effective population size was estimated for each year class (i.e., single collection) using the linkage disequilibrium data (Waples and Do 2008; 2010). The analysis assumes linkage disequilibrium arises exclusively from genetic drift to estimate N_e (i.e., neutral unlinked loci in randomly mating population) (Hill 1981). Alleles below a frequency of 0.5 were screened out (i.e., P_{crit}=0.5). Effective population size was also estimated using observed variance in allele frequencies over time (i.e., multi-collection) (Pollak, 1983; Waples 1989). Allele frequency data were compared between year classes 2011 and 2014. Alleles below a frequency of 0.5 were screened out (i.e., P_{crit}=0.5). Effective population size estimation algorithms were implemented in NeEstimator v2.01 (Do et al. 2014).

The correlation coefficients are quite small for each year class analyzed; resulting in corresponding estimates of effective population size being quite large (Table 1-3). For the 2014 year class calculation based on linkage disequilibrium (i.e., single sample) and both temporal method calculations, the N_e estimates were infinity. Meaning there is no evidence for genetic data variation being the result of genetic drift (i.e., a finite number of parents), all variation can be explained by sampling error (Waples and Do 2010). For N_e estimates generated on year classes 2011-2014, the lower bound of the 95% confidence interval was 5134, 1840, 3921, and

4193, respectively. At this time, there is no population genetic evidence supporting the hypothesis that N_e of Delta Smelt is below 1000. The N_e for Delta Smelt – as of 2014 year class – appears to be above the threshold where quantitative genetic diversity is expected to be lost each generation through genetic drift (i.e., Ne > 500).

Table 1-3. Effective population size estimates.

Year Class	Mean Samples	r^2	Ne	CI Low	CI High
2011	978.6	0.001035	32138	5134	Infinite
2012	521.7	0.002008	4200	1840	Infinite
2013	664.9	0.001517	56379	3921	Infinite
2014	385.2	0.002526	Infinite	4193	Infinite
Temporal Methods: A comparison between 2011 and 2014 year classes					
Pollak			Infinite	1827	Infinite
Nei/Tajima			Infinite	1987	Infinite

CONCLUSIONS

- Consistent with prior years, samples we analyzed were representative of a single population and no problems with the data were detected.
- The implication of the present information is that a large number of Delta Smelt remain in the San Francisco Estuary system.
- The trend in Delta Smelt N_e – as of the 2014 year class – is above the threshold where quantitative genetic diversity is expected to be lost each generation through genetic drift (i.e., $N_e > 500$).
- The disparity between Delta Smelt abundance indices and N_e is a concern as it may indicate existing monitoring programs will have difficulty adequately representing Delta Smelt abundance, distribution or habitat needs.
- Despite the positive result that the Delta Smelt gene pool is expected to retain quantitative genetic diversity at its present size, the resiliency of Delta Smelt is low because the species occupies a restricted geographic range and largely has an annual reproductive cycle.
- The Delta smelt effective population size could decrease quite rapidly (~years) and take millennia to recover, which would negatively impact the long-term viability (extinction risk) of the species. Nevertheless,

RECOMMENDATIONS

- Continue to estimate Delta smelt N_e (sufficient numbers of Delta smelt samples are expected to be available) despite declining catch from existing monitoring programs.
- Support development and implementation of alternative sampling methods that can provide critical data to inform effective management and recovery strategies for delta smelt.

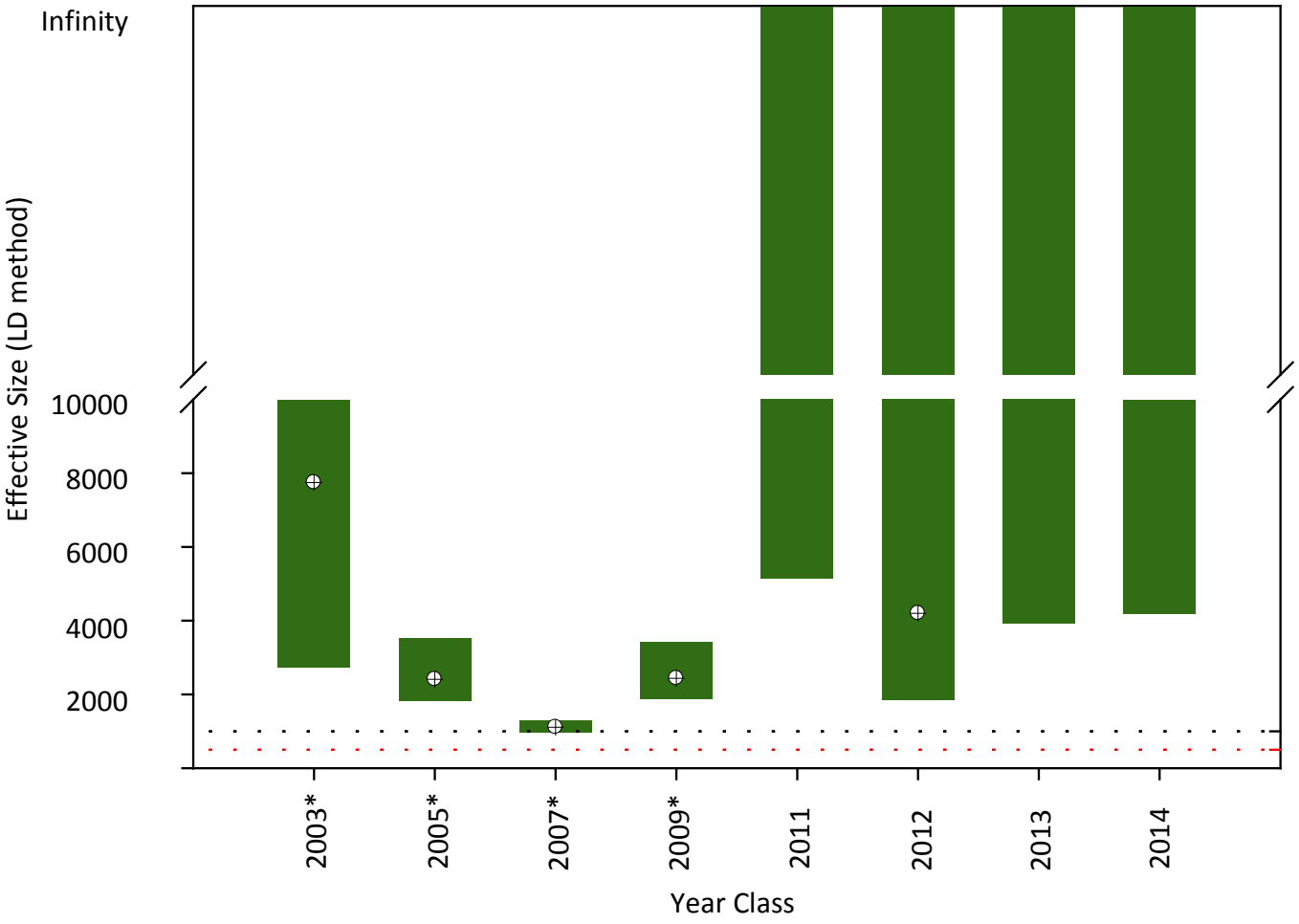

Figure 1. Combined chart of effective size estimates from year classes 2003, 2005, 2007, 2009 (*Fisch et al. 2011) and the current study, year classes 2011-2014. The cross-hatched circle is the point estimate reported for that year class. The black dotted line represents N_e=1000 and the red dotted line represents N_e=500.

REFERENCES

Do, C., R.S. Waples, D. Peel, G.M. Macbeth, B.J. Tillett, and J.R. Ovenden. 2014. NeEstimator v2: re-implementation of software for the estimation of contemporary effective population size (Ne) from genetic data. Mol. Ecol. Resour. 14(1): 209–214.

Excoffier, L., G. Laval, and S. Schneider. 2007. Arlequin (version 3.0): An integrated software package for population genetics data analysis. Evol. Bioinforma. Online 1: 47–50.

Fisch, K.M., J.M. Henderson, R.S. Burton, and B. May. 2011. Population genetics and conservation implications for the endangered delta smelt in the San Francisco Bay-Delta. Conserv. Genet. 12(6): 1421–1434.

Fisch, K.M., J.L. Petersen, M.R. Baerwald, J.K. Pedroia, and B. May. 2009. Characterization of 24 microsatellite loci in delta smelt, Hypomesus transpacificus, and their cross-species amplification in two other smelt species of the Osmeridae family. Mol. Ecol. Resour. 9(1): 405–408.

Frankham, R., C.J.A. Bradshaw, and B.W. Brook. 2014. Genetics in conservation management: Revised recommendations for the 50/500 rules, Red List criteria and population viability analyses. Biol. Conserv. 170: 56–63.

Franklin, I.R. 1980. Evolutionary change in small populations. p. 135–150. *In* Conservation Biology An Evolutionary-Ecological Perspective. eds Soule ME, Wilcox BA. Sinauer, Sunderland, Massachusetts.

Franklin, I.R., and R. Frankham. 1998. How large must populations be to retain evolutionary potential? Anim. Conserv. 1(01): 69–70.

Guo, S.W., and E.A. Thompson. 1992. Performing the Exact Test of Hardy-Weinberg Proportion for Multiple Alleles. Biometrics 48(2): 361–372.

Hauser, L., G.J. Adcock, P.J. Smith, J.H.B. Ramírez, and G.R. Carvalho. 2002. Loss of microsatellite diversity and low effective population size in an overexploited population of New Zealand snapper (Pagrus auratus). Proc. Natl. Acad. Sci. 99(18): 11742–11747.

Hedrick, P.W. 1983. Genetics of populations. Science Books International, Boston.

Nei, M., and F. Tajima. 1981. Genetic drift and estimation of effective population size. Genetics 98: 625–640.

Pollak, E. 1983. A NEW METHOD FOR ESTIMATING THE EFFECTIVE POPULATION SIZE FROM ALLELE FREQUENCY CHANGES. Genetics 104: 531–548.

Raymond, M., and F. Rousset. 1995. Genepop (Version 1.2) - Population Genetics Software For Exact Tests and Ecumenicism. J. Hered. 86: 248–249.

Slatkin, M., and L. Excoffier. 1996. Heredity - Abstract of article: Testing for linkage disequilibrium in genotypic data using the Expectation-Maximization algorithm. Heredity 76(4): 377–383.

Wang, J. 2005. Estimation of effective population sizes from data on genetic markers. Philos. Trans. R. Soc. B Biol. Sci. 360(1459): 1395–1409.

Waples, R.S. 1989. A generalized approach for estimating effective population size from temporal changes in allele frequency. Genetics 121: 379–391.

Waples, R.S., and C. Do. 2008. ldne: a program for estimating effective population size from data on linkage disequilibrium. Mol. Ecol. Resour. 8(4): 753–756.

Waples, R.S., and C. Do. 2010. Linkage disequilibrium estimates of contemporary Ne using highly variable genetic markers: a largely untapped resource for applied conservation and evolution. Evol. Appl. 3(3): 244–262.

OCAP 2012 Steelhead Tagging Study: Statistical Methods and Results

Prepared for:

Joshua Israel
U.S. Bureau of Reclamation
Sacramento, CA

Prepared by:

Rebecca Buchanan
Columbia Basin Research
School of Aquatic and Fishery Sciences
University of Washington
Seattle, WA

18 December 2014

Introduction

A total of 1,435 acoustic-tagged steelhead were released into the San Joaquin River at Durham Ferry in April and May of 2012: 477 in early April, 478 in early May, and 480 in mid-May. Acoustic tags were detectable on hydrophones located at 26 stations throughout the lower San Joaquin River and Delta to Chipps Island (i.e., Mallard Slough).

Statistical Methods

Data Processing for Survival Analysis

The University of Washington received the database of tagging and release data from the US Fish and Wildlife Service. The tagging database included the date and time of tag activation and tagging surgery for each tagged steelhead released in 2012, as well as the name of the surgeon (i.e., tagger), and the date and time of release of the tagged fish to the river. Fish size (length and weight), tag size, and any notes about fish condition were included, as well as the survival status of the fish at the time of release. Tag serial number and three unique tagging codes were provided for each tag, representing codes for various types of signal coding. Tagging data were summarized according to release group and tagger, and were cross-checked with Pat Brandes (USFWS) and Josh Israel (USBR) for quality control.

Acoustic tag detection data collected at individual monitoring sites (Table 1) were transferred to the US Geological Survey (USGS) in Sacramento, California. A multiple-step process was used to identify and verify detections of fish in the data files and produce summaries of detection data suitable for converting to tag detection histories. Detections were classified as valid if two or more pings were recorded within a 30 minute time frame on the hydrophones comprising a detection site from any of the three tag codes associated with the tag. The University of Washington received the primary database of autoprocessed detection data from the USGS. These data included the date, time, location, and tag codes and serial number of each valid detection of the acoustic steelhead tags on the fixed site receivers. The tag serial number indicated the acoustic tag ID, and were used to identify tag activation time, tag release time, and release group from the tagging database.

The autoprocessed database was cleaned to remove obviously invalid detections. The University of Washington identified potentially invalid detections based on unreasonable travel times or unlikely transitions between detections, and queried the USGS processor about any discrepancies. All corrections were noted and made to the database. All subsequent analysis was based on this cleaned database.

The information for each tag in the database included the date and time of the beginning and end of each detection event when a tag was detected. Unique detection events were distinguished by detection on a separate hydrophone or by a time delay of 30 minutes between repeated hits on the same receiver. Separate events were also distinguished by unique signal coding schemes (e.g., PPM vs. hybrid PPM/HR). The cleaned detection event data were converted to detections denoting the beginning and end of receiver "visits," with consecutive visits to a receiver separated either by a gap of 12 hours or more between detections on the receiver, or by detection on a different receiver. Detections from receivers in dual or redundant arrays were pooled for this purpose, as were detections using different tag coding schemes.

Distinguishing between Detections of Salmon and Predators

The possibility of predatory fish eating tagged study fish and then moving past one or more fixed site receivers complicated analysis of the detection data. The steelhead survival model depended on the assumption that all detections of the acoustic tags represented live juvenile steelhead, rather than a mix of live steelhead and predators that temporarily had a steelhead tag in their gut. Without removing the detections that came from predators, the survival model would produce potentially biased estimates of survival of actively migrating juvenile steelhead through the Delta. The size of the bias would depend on the amount of predation by predatory fish and the spatial distribution of the predatory fish after eating the tagged steelhead. In order to minimize bias, the detection data were filtered for predator detections, and detections assumed to come from predators were identified.

The predator filter used for analysis of the 2012 data was based on the predator filter designed and used in the analysis of the 2011 data (Buchanan 2013). That predator filter in turn was based on predator analyses presented by Vogel (2010, 2011), as well as conversations with fisheries biologists familiar with the San Joaquin River and Delta regions. The filter was applied to all detections of all tags. Two data sets were then constructed: the full data set including all detections, including those classified as coming from predators (i.e., "predator-type"), and the reduced data set, restricted to those detections classified as coming from live steelhead smolts (i.e., "smolt-type"). The survival model was fit to both data sets separately. The results from the analysis of the reduced "smolt-type" data set are presented as the final results of the 2012 OCAP tagging study. Results from analysis of the full data set including "predator-type" detections were used to indicate the degree of uncertainty in survival estimates arising from the predator decision process.

The predator filter used for steelhead tagging data must account for both the possibility of extended rearing by steelhead in the Delta before eventual outmigration, and the possibility of residualization. These possibilities mean that some steelhead may have long residence or transition times, or they may move upstream either with or against the flow. Nevertheless, it was assumed that steelhead could not move against very high flow, and that their upstream excursions would be limited after entering the Delta at the head of Old River. Maximum residence times and transition times were imposed for most regions of the Delta, even allowing for extended rearing.

Even with these flexible criteria for steelhead, it was impossible to perfectly distinguish between a residualizing or extended rearing steelhead and a resident predator. A truly residualizing steelhead that is classified as a predator should not bias the overall estimate of successfully leaving the Delta at Chipps Island, because a residualizing steelhead would not be detected at Chipps Island. However, the case of a steelhead exhibiting extended rearing or delayed migration before finally outmigrating past Chipps Island is more complicated. Such a steelhead may be classified as a predator based on long residence times, long transition times, atypical movements within the Delta, or a combination of all three. Such a classification would negatively bias the overall estimate of true survival out of the Delta for steelhead. On the other hand, the survival model assumes common survival and detection probabilities for all steelhead, and thus is implicitly designed for actively migrating steelhead. With that understanding, the "survival" parameter estimated by the survival model is more properly interpreted as the joint probability of migration and survival, and its complement includes both mortality and extended rearing or residualization. The possibility of classifying steelhead with extended rearing times in the Delta as predators does not bias the survival model under this interpretation of the model parameters, and in fact is more likely to improve model performance (i.e., fit) with these non-actively migrating steelhead detections removed. In short, it was necessary either to limit survival analysis to actively migrating steelhead, or to assume that all detections came from steelhead. The first approach used the outcome of the predator filter described here for analysis. The second approach used all detection data.

The predator filter was based on assumed behavioral differences between actively migrating steelhead smolts and predators such as striped bass and white catfish. All detections were considered when implementing the filter, including detections from acoustic receivers that were not otherwise used in the survival model. As part of the decision process, environmental data including river flow, river stage, and water velocity were examined from several points throughout the Delta (Table 2), as

available, downloaded from the California Data Exchange Center website (http://cdec.water.ca.gov/selectQuery.html) and the California Water Data Library (www.water.ca.gov/waterdatalibrary/) on 27 September 2013. Environmental data were reviewed for quality, and obvious errors were omitted.

For each tag detection, several steps were performed to determine if it should be classified as predator or steelhead. Initially, all detections were assumed to be of live smolts. A tag was classified as a predator upon the first exhibition of predator-type behavior, with the acknowledged uncertainty that the steelhead smolt may actually have been eaten sometime before the first obvious predator-type detection. Once a detection was classified as coming from a predator, all subsequent detections of that tag were likewise classified as predator detections. The assignment of predator status to a detection was made conservatively, with doubtful detections classified as coming from live steelhead.

A tag could be given a predator classification at a detection site on either arrival or departure from the site. A tag classified as being in a predator because of long travel time or movement against the flow was generally given a predator classification upon arrival at the detection site. On the other hand, a tag classified as being in a predator because of long residence time was given a predator classification upon departure from the detection site. Because the survival analysis estimated survival within reaches between sites, rather than survival during detection at a site, the predator classifications on departure from a site did not result in removal of the detection at that site from the reduced data set. However, all subsequent detections were removed from the reduced data set.

Criteria for distinguishing between steelhead detections and predator detections were partially based on observed behavior of tags in fish that were assumed to have been transported from the holding tanks at either the State Water Project (SWP) or the Central Valley Project (CVP) to release sites in the lower San Joaquin River or Sacramento River, upstream of Chipps Island, under the assumption that such tags must have been in steelhead smolts rather than in steelhead predators. Tags assumed to have been transported from either SWP or CVP were used to identify the range of possible steelhead movement through the rest of the Delta. This was most helpful for detection sites in the western portion of the study area. This method mirrors that used for the 2011 predator filter (Buchanan 2013).

Acoustic receivers were stationed inside the holding tanks at CVP, and tags that were observed in the holding tanks and then next observed at either Chipps Island (i.e., Mallard Island), Jersey Point, or False River were assumed to have been transported. Acoustic receivers were not placed in the holding

tanks at SWP, and so fish transported from SWP were identified with less certainty. It was assumed that tags were transported from SWP if they were detected either inside or outside the radial gates at the entrance to the Clifton Court Forebay (CCFB; the final receivers encountered before the SWP holding tank) and next detected at either Chipps Island, Jersey Point, or False River. This group may include tagged fish that migrated from the CCFB entrance to the Jersey Point/False River/Chipps Island area inriver, evading detection at the multiple Old River and Middle River receivers north of the CCFB. While this pathway was possible, it was deemed less likely than the SWP transport pathway for fish with no detections between CCFB and the downstream sites (Jersey Point, etc.).

The predator filter used various criteria that addressed several spatial and temporal scales and fit under several categories (see Buchanan 2013 for more details): fish speed, residence time, upstream transitions, other unexpected transitions, travel time since release, and movements against flow. The criteria used in the 2011 study were updated to reflect river conditions and observed tag detection patterns in 2012 (Table 3). The predator scoring and classification method used for the 2011 study was used again for the 2012 study, resulting in tags being classified as in either a predator or a smolt upon arrival at and departure from a given receiver site and visit; for more details, see Buchanan 2013. All detections of a tag subsequent to its first predator designation were classified as coming from a predator, as well.

The criteria used in the predator filter were spatially explicit, with different limits defined for different receivers and transitions (Table 3). The overall approach to various regions is described here.

DFU, DFD = Durham Ferry Upstream (A0) and Durham Ferry Downstream (A2): ignore flow and velocity measures, allow long residence and transition times and multiple visits.

BCA, MOS, and HOR = Banta Carbona (A3), Mossdale (A4), and Head of Old River (B0): allow longer residence time if next transition is directed downstream; may have extra visits at BCA if arrival flow is low.

SJL = San Joaquin River near Lathrop (A5): allow longer travel time if low flow during transition; upstream transitions from Stockton sites are not allowed.

ORE = Old River East (B1): allow longer residence time if arrive at low velocity.

SJG = San Joaquin River at Garwood Bridge (A6): repeat visits or transitions from upstream require arrival flow/velocity to be opposite direction from flow/velocity on previous departure.

SJNB = San Joaquin River at Navy Bridge Drive (A7): fast transitions moving downstream require positive water velocity.

MAC = MacDonald Island (A8): allow more flexibility (longer residence time, transition time) if transition water velocity was low and positive for downstream transitions, or low and negative for upstream transitions.

MFE/MFW = Medford Island (A9): allow more flexibility (longer residence time, transition time) if transition water velocity was low and positive for downstream transitions, or low and negative for upstream transitions; transitions from interior Delta sites (B3, B4, C2, C3) must have departed interior Delta sites with very low or positive flow/velocity; transitions from Radial Gates (D) not allowed.

TCE/TCW = Turner Cut (F1): should not move against flow.

ORS = Old River South (B2): allow longer transition times from ORE if mean water velocity during transition was low.

MRH = Middle River Head (C1): shorter residence times than ORS; repeat visits are not allowed.

MR4 = Middle River at Highway 4 (C2): should not move against flow on repeat visits; should arrive on negative/low water velocity if arriving from San Joaquin (Stockton); should not have left water export facilities against high pumping (E1) or reservoir inflow (D).

MRE = Middle River at Empire Cut (C3): should not move against flow on repeat visits or on transitions from San Joaquin or Old River.

CVP = Central Valley Project (E1): allow multiple visits; transitions from downstream Old River should not have departed Old River site against flow or arrived during low pumping.

CVPtank = Central Valley Project holding tank (E2): assume that steelhead can leave tank and return (personal communication, Brent Bridges, USBR).

OR4 = Old River at Highway 4 (B3): allow many visits; should not arrive against flow or water velocity.

OLD = Old River near Empire Cut (B4): should not move against flow on repeat visits or on transitions from Turner Cut or Old River.

RGU/RGD = Radial Gates (D1, D2 = D):

- Assume steelhead smolts can move from D2 back to D1
- No distinction between near-field and mid-field visit (i.e., gap in detection does not define new visit)
- Residence time may include time spent in river between first arrival at RG and final departure from RG (with no detection elsewhere during "visit")
- Maximum residence time = 80 hours (3.3 days), accounting for gaps in detection, unless:
- if detected at D2 before D1:
    - if the large majority (>80%) of residence time was spent inside CCFB (i.e., at D2, allowing for gaps in detection), then maximum combined residence time = 336 hours (14 days); these tags appear to have spent long time inside CCFB before returning to Old River, look like predators
    - otherwise maximum combined residence time = 800 hours (33 days); these tags spent some time in CCFB, then returned to the entrance channel or river, and eventually returned to radial gates; allow longer residence time than those that spent most of visit inside CCFB.

JPE/JPW and FRE/FRW = Jersey Point (G1) and False River (H1): no flow/velocity restrictions; allowed for transition from Threemile Slough (TMS/TMN)

TMS/TMN = Threemile Slough (T1): should not move against flow on departing from interior Delta or San Joaquin River sites

In addition, detections in the San Joaquin River after previous entry to the Interior Delta (e.g., Old and Middle River sites or export facilities) from Stockton or sites farther downstream in the San Joaquin River were generally not allowed. The exception was at MacDonald Island (A8) and Turner Cut (F1). Detections at sites other than CVP (E1) and the radial gates (D1/D2) after arriving at either CVP or the radial gates from the lower San Joaquin River were not allowed. These restrictions were based on the assumption that juvenile steelhead that leave the lower San Joaquin River for the Interior Delta are not expected to return to the San Joaquin River, and those that leave the lower San Joaquin River for the

water export facilities are not expected to subsequently leave the facilities other than through salvage and transport. Maximum travel times were imposed on transitions in the Interior Delta and at the facilities for steelhead observed leaving the lower San Joaquin River for these regions.

Constructing Detection Histories

For each tag, the detection data summarized on the "visit" scale were converted to a detection history (i.e., capture history) that indicated the chronological sequence of detections on the fixed site receivers throughout the study area. In cases in which a tag was observed passing a particular receiver or river junction multiple times, the detection history represented the final route of the tagged fish past the receiver or river junction. Detections from the receivers comprising certain dual arrays were pooled, thereby converting the dual arrays to redundant arrays: the San Joaquin River near Mossdale Bridge (MOS), Lathrop (SJL), and Garwood Bridge (SJG); Old River East near the head of Old River (ORE); the Central Valley Project trash racks (CVP); and the radial gates just outside of Clifton Court Forebay (RGU). For some release groups, a better model fit was found by pooling detections from dual arrays into redundant arrays at the Durham Ferry Downstream site (D2), MacDonald Island (A8), Old River South (ORS), and/or Jersey Point (G1). Unlike in the 2011 analysis (Buchanan 2013), the status of the radial gates (opened or closed) upon detection at the receivers just outside the radial gates (RGU) was not included in the detection history because the sparseness of the detection data at this site precluded incorporating gate status into the survival model.

Survival Model

A two-part multi-state statistical release-recapture model was developed and used to estimate perceived steelhead smolt survival and migration route parameters throughout the study area. The release-recapture model is a slightly simplified version of the model used in the 2011 steelhead analysis (Buchanan 2013), and similar to the model developed by Perry et al. (2010) and the model developed for the 2009 – 2011 VAMP studies (SJRGA 2010, 2011, 2013). Figure 1 shows the layout of the receivers using both descriptive labels for site names and the code names used in the survival model (Table 1). The survival model represents movement and perceived survival throughout the study area to the primary exit point at Chipps Island (i.e., Mallard Island) (Figure 2, Figure 3). Individual receivers comprising dual arrays were identified separately, using "a" and "b" to represent the upstream and downstream receivers, respectively. Most sites used in 2012 were also used in 2011, although some site names changed, and some sites were added and others removed from 2011 (Figure 1,Table 1). The Paradise Cut sites from 2011 were not used in 2012 because flows were too low for fish to enter

Paradise Cut. Additional detection sites were installed in 2012 in the San Joaquin River just upstream of the head of Old River (HOR = B0), and in Old and Middle rivers north of Highway 4 (OLD = B4 and MRE = C3). Some sites were omitted from the survival model, but all were used in the predator filter.

The statistical model depended on the assumption that all tagged steelhead in the study area were actively migrating, and that any residualization occurred upstream of the Durham Ferry release site. If, on the contrary, tagged steelhead residualized downstream of Durham Ferry, and especially within the study area (downstream of the Mossdale receiver, A4), then the multi-state statistical release-recapture model estimated perceived survival rather than survival, where perceived survival is the joint probability of migrating and surviving. The complement of perceived survival includes both the probability of mortality and the probability of halting migration to rear or residualize. Unless otherwise specified, references to "survival" below should be interpreted to mean "perceived survival."

Fish moving through the Delta toward Chipps Island may have used any of several routes. The two primary routes modeled were the San Joaquin River route (Route A) and the Old River route (Route B). Route A followed the San Joaquin River past the distributary point with Old River near the town of Lathrop, CA and past the city of Stockton, CA. Downstream of Stockton, fish in the San Joaquin River route (route A) may have remained in the San Joaquin River past its confluence with the Sacramento River and on to Chipps Island. Alternatively, fish in Route A may have exited the San Joaquin River for the interior Delta at any of several places downstream of Stockton, including Turner Cut, Columbia Cut (just upstream of Medford Island), and the confluence of the San Joaquin River with either Old River or Middle River, at Mandeville Island. Of these four exit points from the San Joaquin River between Stockton and Jersey Point, only Turner Cut was monitored and assigned a route name (F, a subroute of route A). Fish that entered the interior Delta from any of these exit points may have either moved north through the interior Delta and reached Chipps Island by returning to the San Joaquin River and passing Jersey Point and the junction with False River, or they may have moved south through the interior Delta to the state or federal water export facilities, where they may have been salvaged and trucked to release points on the San Joaquin or Sacramento rivers just upstream of Chipps Island. All of these possibilities were included in both subroute F and route A.

For fish that entered Old River at its distributary point on the San Joaquin River just upstream of Lathrop, CA (route B) , there were several pathways available to Chipps Island. These fish may have migrated to Chipps Island either by moving northward in either the Old or Middle rivers through the interior Delta, or they may have moved to the state or federal water export facilities to be salvaged and

trucked. The Middle River route (subroute C) was monitored and contained within Route B. Passage through the State Water Project via Clifton Court Forebay was monitored at the entrance to the forebay and assigned a route (subroute D). Likewise, passage through the federal Central Valley Project was monitored at the entrance trashracks and in the facility holding tank and assigned a route (subroute E). Subroutes D and E were both contained in subroutes C (Middle River) and F (Turner Cut), as well as in primary routes A (San Joaquin River) and B (Old River). All routes and subroutes included multiple unmonitored pathways for passing through the Delta to Chipps Island.

Several exit points from the San Joaquin River were monitored and given route names for convenience, although they did not determine unique routes to Chipps Island. The first exit point encountered was False River, located off the San Joaquin River just upstream of Jersey Point. Fish entering False River from the San Joaquin River entered the interior Delta at that point, and would not be expected to reach Chipps Island without subsequent detection in another route. Thus, False River was considered an exit point of the study area, rather than a waypoint on the route to Chipps Island. It was given a route name (H) for convenience. Likewise, Jersey Point and Chipps Island were not included in unique routes. Jersey Point was included in many of the previously named routes (in particular, routes A and B, and subroutes C and F), whereas Chipps Island (the final exit point) was included in all previously named routes and subroutes except route H. Thus, Jersey Point and Chipps Island were given their own route name (G). Three additional sets of receivers located in Old River (Route B) and Middle River (Subroute C) north of Highway 4 and in Threemile Slough (Route T) were not used in the survival model. The routes, subroutes, and study area exit points are summarized as follows:

A = San Joaquin River: survival

B = Old River: survival

C = Middle River: survival

D = State Water Project: survival

E = Central Valley Project: survival

F = Turner Cut: survival

G = Jersey Point, Chipps Island: survival, exit point

H = False River: exit point

T = Threemile Slough: not used in survival model

The release-recapture model used parameters that denote the probability of detection (P_{hi}), route entrainment (ψ_{hl}), perceived steelhead survival (the joint probability of migrating and surviving; S_{hi}), and transition probabilities equivalent to the joint probability of movement and survival ($\phi_{kj,hi}$) (Figure 2, Figure 3, Table A1). Unique detection probabilities were estimated for the individual receivers in a dual array: P_{hia} represented the detection probability of the upstream array at station *i* in route *h*, and P_{hib} represented the detection probability of the downstream array.

The model parameters are:

P_{hi} = detection probability: probability of detection at telemetry station *i* within route *h*, conditional on surviving to station *i*, where *i* = *ia*, *ib* for the upstream, downstream receivers in a dual array, respectively.

S_{hi} = perceived survival probability: joint probability of migration and survival from telemetry station *i* to *i*+1 within route *h*, conditional on surviving to station *i*.

ψ_{hl} = route entrainment probability: probability of a fish entering route *h* at junction *l* (*l* =1, 2), conditional on fish surviving to junction *l*.

$\phi_{kj,hi}$ = transition probability: joint probability of migration, route entrainment, and survival; the probability of migrating, surviving, and moving from station *j* in route *k* to station *i* in route *h*, conditional on survival to station *j* in route *k*.

The sparse detection data at the receivers outside the Clifton Court Forebay (site D1, RGU) did not allow classification of transitions by status of the radial gates (open or closed) upon tag arrival at D1. This was a change from the 2011 survival model.

The full survival model used detections at sites B1 (ORE), B2 (ORS), and C1 (MRH) to estimate survival between the head of Old River and the head of Middle River $\left(S_{B1}\right)$, the probability of remaining in Old River at the head of Middle River $\left(\psi_{B2}\right)$, and the probability of entering Middle River at its head

$(\psi_{C2} = 1 - \psi_{B2})$. Only three tags were detected at the C1 site indicating entry to Middle River: one tag was later observed upstream of the head of Old River, and so its C1 detection was not used in the survival model, and the other two tags (both from the third release group) were classified as in predators before reaching MRH. Thus, for all results for tags deemed to be in smolts, and for most cases in general, no detections at C1 were available to be used in the survival model. In these cases, it was not possible to separately estimate the survival parameter S_{B1} and route entrainment probability ψ_{B2}, but instead only their product was estimable: $\phi_{B1,B2} = S_{B1}\psi_{B2}$. Under the assumption that no fish passed the C1 receivers without detection, then in these cases $\psi_{B2} = 1$ and $\phi_{B1,B2} = S_{B1}$. However, there was no way to test that assumption. For the single release group in which predator-type detections at C1 were available for use in the survival model, detections at C1 were too sparse and were omitted from analysis. In this case (third release group), it is acknowledged that $\phi_{B1,B2} < S_{B1}$.

A variation on the parameter naming convention was used for parameters representing the transition probability to the junction of False River with the San Joaquin River, just upstream of Jersey Point (Figure 1). This river junction marks the distinction between routes G and H, so transition probabilities to this junction are named $\phi_{kj,GH}$ for the joint probability of surviving and moving from station *j* in route *k* to the False River junction. Fish may arrive at the junction either from the San Joaquin River or from the interior Delta. The complex tidal forces present in this region prevent distinguishing between smolts using False River as an exit from the San Joaquin and smolts using False River as an entrance to the San Joaquin from Frank's Tract. Regardless of which approach the fish used to reach this junction, the $\phi_{kj,GH}$ parameter (e.g. $\phi_{A9,GH}$ or $\phi_{C2,GH}$) is the transition probability to the junction of False River with the San Joaquin River via any route; ψ_{G1} is the probability of moving downstream toward Jersey Point from the junction; and $\psi_{H1} = 1 - \psi_{G1}$ is the probability of exiting (or re-exiting) the San Joaquin River to False River from the junction (Figure 2).

For fish that exited the San Joaquin River for the interior Delta downstream of Stockton, CA, the parameters $\phi_{B3,D1}$, $\phi_{B3,E1}$, $\phi_{C2,D1}$, and $\phi_{C2,E1}$ represent the joint probabilities of moving from either site B3 or C2 toward to the export facilities and surviving. Similar parameters were not estimated for fish that reached the B3 or C2 sites via Old River within Route B, but rather transition to the export facilities within route B was estimated directly from the head of Middle River (sites B2 and C1) using

parameters $\phi_{B2,D1}$, $\phi_{B2,E1}$, $\phi_{C1,D1}$, and $\phi_{C1,E1}$. Both routes A and B were used to estimate northward transition probabilities from sites B3 and C2 in the interior Delta to the junction with Jersey Point and False River: $\phi_{B3,GH}$ and $\phi_{C2,GH}$. Likewise, both routes A and B were used to estimate transitions at or within the export facility sites (i.e., $\phi_{D1,D2}$ and $\phi_{E1,E2}$), as well as transition probabilities from the interior receivers at these sites to Chipps Island (i.e., $\phi_{D2,G2}$ and $\phi_{E2,G2}$).

For fish that reached the interior receivers at the State Water Project (D2) or the Central Valley Project (E2), the parameters $\phi_{D2,G2}$ and $\phi_{E2,G2}$, respectively, represent the joint probability of migrating and surviving to Chipps Island, including survival during and after collection and transport (Figure 2). Some salvaged and transported smolts were released in the San Joaquin River upstream of Jersey Point and Chipps Island, and others were released in the Sacramento River upstream of the confluence with the San Joaquin River. Because salvaged fish released in the Sacramento River moved toward Chipps Island without passing Jersey Point and the False River junction, it was not possible to estimate the transition probability to Chipps Island via Jersey Point for salvaged fish. Thus, only the overall probability of making the transition to Chipps Island was estimated for fish passing through the water export facilities.

Because of the complexity of routing in the vicinity of MacDonald Island (referred to as "Channel Markers" in previous reports [Buchanan 2013, SJRGA 2010, 2011, 2013]) on the San Joaquin River, Turner Cut, and Medford Island, and the possibility of reaching the interior Delta via either route A or route B, the full survival model that represented all routes was decomposed into two submodels for analysis, as in the 2011 analysis (Buchanan 2013). Submodel I modeled the overall migration from release at Durham Ferry to arrival at Chipps Island without modeling the specific routing from the lower San Joaquin River (i.e., from the Turner Cut Junction) through the interior Delta to Chipps Island, although it included detailed subroutes in route B for fish that entered Old River at its upstream junction with the San Joaquin River (Figure 2). In Submodel I, transitions from MacDonald Island (A8) and Turner Cut (F1) to Chipps Island were interpreted as survival probabilities ($S_{A8,G2}$ and $S_{F1,G2}$) because they represented all possible pathways from these sites to Chipps Island. Submodel II, on the other hand, focused entirely on Route A, and used a virtual release of tagged fish detected at the San Joaquin River receiver array near Lathrop, CA , (A5, SJL) to model the detailed routing from the lower San Joaquin River near MacDonald Island and Turner Cut through or around the interior Delta to Jersey Point and

Chipps Island (Figure 3). Submodel II included the Medford Island detection site (A9), which was omitted from Submodel I because of complex routing in that region.

The two submodels I and II were fit concurrently using common detection probabilities at certain shared receivers: B3 (OR4), C2 (MR4), D1 (RGU), D2 (RGD), E1 (CVP), E2 (CVP holding tank), G1 (JPE/JPW), and H1 (FRE/FRW). While submodels I and II both modeled detections at these receivers, actual detections modeled at these receivers came from different tagged fish in the two submodels, with detections coming from Route B fish in Submodel I and from Route A fish in Submodel II. Detections at all other sites included in Submodel II either included the same fish as in Submodel I (i.e., sites SJG [A6], SJNB [A7], MAC [A8], TCE/TCW [F1], and MAE/MAW [G2]), or else were unique to Submodel II (i.e., site MFE/MFW [A9]); detection probabilities at these sites were estimated separately for submodels I (if included) and II to avoid "double-counting" tags used in both submodels. In the previous year of this study (Buchanan 2013), unique transition parameters through the water export facility sites (i.e., $\phi_{D1,D2}$, $\phi_{D2,G2}$, $\phi_{E1E2,}$, and $\phi_{E2,G2}$) were estimated for Submodels I and II, under the assumption that fish that arrive outside the CVP or the Clifton Court Forebay coming from the head of Old River might have a different likelihood of reaching the interior receivers than fish that came from the lower San Joaquin River. Because of the sparse detection data at these sites in 2012, the models were fit first using unique parameters for the two submodels, and then using common transition parameters for the two submodels. The significance of submodel-specific (i.e., route-specific) effects on these four transition parameters was assessed using a Likelihood Ratio Test (α=0.05; Sokal and Rohlf, 1995); results were reported from the most parsimonious model that fit the data.

In addition to the model parameters, derived performance metrics measuring migration route probabilities and survival were estimated as functions of the model parameters. Both route entrainment and route-specific survival were estimated for the two primary routes determined by routing at the head of Old River (routes A and B). Route entrainment and route-specific survival were also estimated for the major subroutes of routes A and B. These subroutes were identified by a two-letter code, where the first letter indicates routing used at the head of Old River (A or B), and the second letter indicates routing used at the next river junction encountered: A or F at the Turner Cut Junction, and B or C at the head of Middle River. Thus, the route entrainment probabilities for the subroutes were:

$\psi_{AA} = \psi_{A1}\psi_{A2}$: probability of remaining in the San Joaquin River past both the head of Old River and the Turner Cut Junction,

$\psi_{AF} = \psi_{A1}\psi_{F2}$: probability of remaining in the San Joaquin River past the head of Old River, and exiting to the interior Delta at Turner Cut,

$\psi_{BB} = \psi_{B1}\psi_{B2}$: probability of entering Old River at the head of Old River, and remaining in Old River past the head of Middle River,

$\psi_{BC} = \psi_{B1}\psi_{C2}$: probability of entering Old River at the head of Old River, and entering Middle River at the head of Middle River,

where $\psi_{B1} = 1 - \psi_{A1}$, $\psi_{F2} = 1 - \psi_{A2}$, and $\psi_{C2} = 1 - \psi_{B2}$. In cases with no detections in Middle River near its head (site C1, MRH), the estimates of route selection in the B and C subroutes (ψ_{BB} and ψ_{BC}) depend on the assumption that no fish actually entered Middle River without detection (i.e., $\psi_{B2} = 1$ and $\psi_{C2} = 0$).

The probability of surviving from the entrance of the Delta near Mossdale Bridge (site A4, MOS) through an entire migration pathway to Chipps Island was estimated as the product of survival probabilities that trace that pathway:

$S_{AA} = S_{A4}S_{A5}S_{A6}S_{A7}S_{A8,G2}$: Delta survival for fish that remained in the San Joaquin River past the head of Old River and Turner Cut,

$S_{AF} = S_{A4}S_{A5}S_{A6}S_{A7}S_{F1,G2}$: Delta survival for fish that entered Turner Cut from the San Joaquin River,

$S_{BB} = S_{A4}S_{B1}S_{B2,G2}$: Delta survival for fish that entered Old River at its head, and remained in Old River past the head of Middle River,

$S_{BC} = S_{A4}S_{B1}S_{C1,G2}$: Delta survival for fish that entered Old River at its head, and entered Middle River at its head.

In cases where no tags were detected at the Middle River site near its head (MRH, site C1), the parameter S_{B1} in S_{BB} was replaced by $\phi_{B1,B2}$ under the assumption that $\psi_{B2}=1$, and the parameter S_{BC} is not estimable.

The parameters $S_{A8,G2}$ and $S_{F1,G2}$ represent the probability of getting to Chipps Island (i.e., Mallard Island, site MAE/MAW) from sites A8 and F1, respectively. Both parameters represent multiple pathways around or through the Delta to Chipps Island (Figure 1). Fish that were detected at the A8 receivers (MacDonald Island) may have remained in the San Joaquin River all the way to Chipps Island, or they may have entered the interior Delta downstream of Turner Cut. Fish that entered the interior Delta either at Turner Cut or farther downstream may have migrated through the interior Delta to Chipps Island via Frank's Tract or Fisherman's Cut, False River, and Jersey Point; returned to the San Joaquin River via its downstream confluence with either Old or Middle River at Mandeville Island; or gone through salvage and trucking from the water export facilities. All such routes are represented in the $S_{A8,G2}$ and $S_{F1,G2}$ parameters, which were estimated directly using Submodel I.

Survival probabilities $S_{B2,G2}$ and $S_{C1,G2}$ represented survival of fish to Chipps Island that remained in the Old River at B2 (ORS), or entered the Middle River at C1 (MRS), respectively. Fish in both these routes may have subsequently been salvaged and trucked from the water export facilities, or have migrated through the interior Delta to Jersey Point and on to Chipps Island (Figure 1). Because there were many unmonitored river junctions within the "reach" between sites B2 or C1 and Chipps Island, it was impossible to separate the probability of taking a specific pathway from the probability of survival along that pathway. Thus, only the joint probability of movement and survival could be estimated to the next receivers along a route (i.e., the $\phi_{kj,hi}$ parameters defined above and in Figure 2). However, the overall survival probability from B2 ($S_{B2,G2}$) or C1 ($S_{C1,G2}$) to Chipps Island was defined by summing products of the $\phi_{kj,hi}$ parameters:

$$S_{B2,G2}=\phi_{B2,D1}\phi_{D1,D2}\phi_{D2,G2}+\phi_{B2,E1}\phi_{E1,E2}\phi_{E2,G2}+\left(\phi_{B2,B3}\phi_{B3,GH}+\phi_{B2,C2}\phi_{C2,GH}\right)\psi_{G1}\phi_{G1,G2}$$

$$S_{C1,G2}=\phi_{C1,D1}\phi_{D1,D2}\phi_{D2,G2}+\phi_{C1,E1}\phi_{E1,E2}\phi_{E2,G2}+\left(\phi_{C1,B3}\phi_{B3,GH}+\phi_{C1,C2}\phi_{C2,GH}\right)\psi_{G1}\phi_{G1,G2}$$

The parameter $S_{C1,G2}$ is not estimable in cases with no detections at C1.

Fish in the Old River route that successfully bypassed the water export facilities and reached the receivers in Old River or Middle River near Highway 4 (sites B3 or C2, respectively) may have used any of several subsequent routes to reach Chipps Island. In particular, they may have remained in Old or Middle rivers until they rejoined the San Joaquin downstream of Medford Island, and then migrated in the San Joaquin, or they may have passed through Frank's Tract and False River or Fisherman's Cut to rejoin the San Joaquin River. As described above, these routes were all included in the transition probabilities $\phi_{B3,GH}$ and $\phi_{C2,GH}$, representing the probability of moving from site B3 or C2, respectively, to the False River junction with the San Joaquin.

Both route entrainment and route-specific survival were estimated on the large routing scale, as well, focusing on routing only at the head of Old River. The route entrainment parameters were defined as:

$\psi_A = \psi_{A1}$: probability of remaining in the San Joaquin River at the head of Old River

$\psi_B = \psi_{B1}$: probability of entering Old River at the head of Old River.

The probability of surviving from the entrance of the Delta (site A4, MOS) through an entire large-scale migration pathway to Chipps Island was defined as a function of the finer-scale route-specific survival probabilities and route-entrainment probabilities:

$S_A = \psi_{A2} S_{AA} + \psi_{F2} S_{AF}$: Delta survival (from Mossdale to Chipps Island) for fish that remained in the San Joaquin River at the head of Old River, and

$S_B = \psi_{B2} S_{BB} + \psi_{C2} S_{BC}$: Delta survival for fish that entered Old River at the head of Old River.

In cases with no detections at site C1 (MRH, Middle River at its head), the Old River survival probability through the delta is simply $S_B = S_{BB}$, which already includes the parameter ψ_{B2} (assumed to be 1). Using the estimated migration route probabilities and route-specific survival for these two primary routes (A and B), survival of the population from A4 (Mossdale) to Chipps Island was estimated as:

$$S_{Total} = \psi_A S_A + \psi_B S_B .$$

Survival was also estimated from Mossdale to the Jersey Point/False River junction, both by route and overall. Survival through this region ("Mid-Delta" or MD) was estimated only for fish that

migrated entirely inriver, without being trucked from either of the water export facilities. Thus, the route-specific Mid-Delta survival for the large-scale San Joaquin River and Old River routes was defined as follows:

$S_{A(MD)} = \psi_{A2} S_{AA(MD)} + \psi_{F2} S_{AF(MD)}$: Mid-Delta survival for fish that remained in the San Joaquin River past the head of Old River, and

$S_{B(MD)} = \psi_{B2} S_{BB(MD)} + \psi_{C2} S_{BC(MD)}$: Mid-Delta survival for fish that entered Old River at its head, where

$$S_{AA(MD)} = S_{A4} S_{A5} S_{A6} S_{A7} \left[\phi_{A8,GH} + \phi_{A8,A9}\phi_{A9,GH} + \left(\phi_{A8,B3} + \phi_{A8,A9}\phi_{A9,B3} \right) \phi_{B3,GH} + \left(\phi_{A8,C2} + \phi_{A8,A9}\phi_{A9,C2} \right) \phi_{C2,GH} \right],$$

$$S_{AF(MD)} = S_{A4} S_{A5} S_{A6} S_{A7} \left[\phi_{F1,GH} + \phi_{F1,B3}\phi_{B3,GH} + \phi_{F1,C2}\phi_{C2,GH} \right],$$

$$S_{BB(MD)} = S_{A4} S_{B1} \left(\phi_{B2,B3}\phi_{B3,GH} + \phi_{B2,C2}\phi_{C2,GH} \right), \text{ and}$$

$$S_{BC(MD)} = S_{A4} S_{B1} \left(\phi_{C1,B3}\phi_{B3,GH} + \phi_{C1,C2}\phi_{C2,GH} \right).$$

In cases with no detections in Middle River near its head (site C1, MRH), the B subroute Mid-Delta survival probability is estimated as $S_{BB(MD)} = S_{A4}\phi_{B1,B2} \left(\phi_{B2,B3}\phi_{B3,GH} + \phi_{B2,C2}\phi_{C2,GH} \right)$. In such cases, the subroute C survival probability $S_{BC(MD)}$ is unestimable, because no tags are observed taking that route.

Total Mid-Delta survival (i.e., from Mossdale to the Jersey Point/False River junction) was defined as $S_{Total(MD)} = \psi_A S_{A(MD)} + \psi_B S_{B(MD)}$. Mid-Delta survival was estimated only for those release groups with sufficient tag detections to model transitions through the entire south Delta and lower San Joaquin River and to the Jersey Point/False River junction.

Survival was also estimated through the southern portions of the Delta ("Southern Delta" or SD), both within each primary route and overall:

$$S_{A(SD)} = S_{A4} S_{A5} S_{A6} S_{A7}, \text{ and}$$

$$S_{B(SD)} = S_{A4} S_{B1} \left(\psi_{B2} S_{B2(SD)} + \psi_{C2} S_{C1(SD)} \right),$$

where $S_{B2(SD)}$ and $S_{C1(SD)}$ are defined as:

$$S_{B2(SD)} = \phi_{B2,B3} + \phi_{B2,C2} + \phi_{B2,D1} + \phi_{B2,E1}, \text{ and}$$

$$S_{C1(SD)} = \phi_{C1,B3} + \phi_{C1,C2} + \phi_{C1,D1} + \phi_{C1,E1}.$$

In cases with no detections in Middle River near its head (site C1), Southern Delta survival within route B is defined as

$$S_{B(SD)} = S_{A4}\phi_{B1,B2}S_{B2(SD)}.$$

Total survival through the Southern Delta was defined as:

$$S_{Total(SD)} = \psi_A S_{A(SD)} + \psi_B S_{B(SD)}.$$

The probability of reaching Mossdale from the release point at Durham Ferry, $\phi_{A1,A4}$, was defined as the product of the intervening reach survival probabilities:

$$\phi_{A1,A4} = \phi_{A1,A2}S_{A2}S_{A3}.$$

This measure reflects a combination of mortality and residualization upstream of Old River.

Individual detection histories (i.e., capture histories) were constructed for each tag as described above. More details and examples of detection history construction and model parameterization are available in Buchanan 2013. Under the assumptions of common survival, route entrainment, and detection probabilities and independent detections among the tagged fish in each release group, the likelihood function for the survival model for each release group is a multinomial likelihood with individual cells denoting each possible capture history.

Parameter Estimation

The multinomial likelihood model described above was fit numerically to the observed set of detection histories according to the principle of maximum likelihood using Program USER software, developed at the University of Washington (Lady et al. 2009). Point estimates and standard errors were computed for each parameter. Standard errors of derived performance measures were estimated using the delta method (Seber 2002: 7-9). Sparse data prevented some parameters from being freely

estimated for some release groups. Transition, survival, and detection probabilities were fixed to 1.0 or 0.0 in the USER model as appropriate, based on the observed detections. The model was fit separately for each release group. For each release group, the complete data set that included possible detections from predatory fish was analyzed separately from the reduced data set restricted to detections classified as steelhead smolt detections. Population-level estimates of parameters and performance measures, representing all three release groups, were estimated as weighted averages of the release-specific estimates, using weights proportional to release size.

For each release group, the significance of route (A or B) on estimates of transition probabilities at the Central Valley Project and the radial gates at Clifton Court Forebay to Chipps Island (i.e., $\phi_{D1,D2}$, $\phi_{D2.G2}$, $\phi_{E1,E2}$, and $\phi_{E2,G2}$) were tested using a Likelihood Ratio Test (α=0.05; Sokal and Rohlf, 1995). In the event that the effect of route on these parameter estimates and model fit was negligible, common transition probabilities through these regions were used in the two submodels representing the different routes. Otherwise, unique transitions based on route through these facilities were estimated. For each model, goodness-of-fit was assessed visually using Anscombe residuals (McCullagh and Nelder 1989). The sensitivity of parameter and performance metric estimates to inclusion of detection histories with large absolute values of Anscombe residuals was examined for each release group individually.

For each release group, the effect of primary route (San Joaquin River or Old River) on estimates of survival to Chipps Island was tested with a two-sided *Z*-test on the log scale:

$$\mathrm{Z} = \frac{\ln\left(\hat{S}_A\right) - \ln\left(\hat{S}_B\right)}{\sqrt{\hat{V}}},$$

where

$$V = \frac{Var\left(\hat{S}_A\right)}{\hat{S}_A} + \frac{Var\left(\hat{S}_B\right)}{\hat{S}_B} - \frac{2Cov\left(\hat{S}_A, \hat{S}_B\right)}{\hat{S}_A \hat{S}_B}.$$

The parameter *V* was estimated using Program USER. Survival estimates to Jersey Point and False River (i.e., $S_{A(MD)}$ and $S_{B(MD)}$) were also compared in this way. Also tested was whether tagged steelhead smolts showed a preference for the San Joaquin River route using a one-sided *Z*-test with the test statistic:

$$Z = \frac{\hat{\psi}_A - 0.5}{SE\left(\hat{\psi}_A\right)}.$$

Statistical significance was tested at the 5% level (α=0.05).

Analysis of Tag Failure

The first of two tag-life studies began on April 5, 2012 with the last failure recorded on June 25, 2012. The second tag-life study began on May 24, 2012, and the last tag failure was recorded on August 20, 2012. A single tag in the May study was omitted from analysis because it was malfunctioning at the time of tag activation. This left data on 48 tags from the April study, and 44 tags from May study.

Observed tag survival was modeled using the 4-parameter vitality curve (Li and Anderson, 2009). In both tag-life studies, the majority of the tags failed on day 80, with only a few premature failures. Because of the concurrent failure of so many tags, it was necessary to right-censor the failure times at day 80 for both studies in order to adequately fit the tag-survival model. Despite having censored the failure times, a good fit to the tag-failure data was achieved. Stratifying by tag-life study (April or May) versus pooling across studies was assessed using the Akaike Information Criterion (AIC; Burnham and Anderson 2002).

The fitted tag survival model was used to adjust estimated fish survival and transition probabilities for premature tag failure using methods adapted from Townsend et al. (2006). In Townsend et al. (2006), the probability of tag survival through a reach is estimated based on the average observed travel time of tagged fish through that reach. For this study, travel time and the probability of tag survival to Chipps Island were estimated separately for the different routes (e.g., San Joaquin route vs. Old River route). Subroutes using truck transport were handled separately from subroutes using only inriver travel. Standard errors of the tag-adjusted fish survival and transition probabilities were estimated using the inverse Hessian matrix of the fitted joint fish-tag survival model. The additional uncertainty introduced by variability in tag survival parameters was not estimated, with the result that standard errors may have been slightly low. In previous studies, however, variability in tag-survival parameters has been observed to contribute little to the uncertainty in the fish survival estimates when compared with other, modeled sources of variability (Townsend et al., 2006); thus, the resulting bias in the standard errors was expected to be small.

Analysis of Tagger Effects

Tagger effects were analyzed in several ways. The simplest method used contingency tests of independence on the number of tag detections at key detection sites throughout the study area. Specifically, a lack of independence (i.e., heterogeneity) between the detections distribution and tagger was tested using a chi-squared test (α=0.05; Sokal and Rohlf, 1995). Detections from those downstream sites with sparse data across all taggers were omitted for this test in order to achieve adequate cell counts, and the chi-squared test was performed via Monte Carlo simulations to accommodate remaining low cell counts.

Lack of independence may be caused by differences in survival, route entrainment, or detection probabilities. A second method visually compared estimates of cumulative survival throughout the study area among taggers. A third method used Analysis of Variance to test for a tagger effect on individual reach survival estimates, and an F-test to test for a tagger effect on cumulative survival throughout each major route (routes A and B). Tagger effects on estimates of individual parameters were also assessed using an F-test. Finally, the nonparametric Kruskal-Wallis rank sum test (Sokal and Rohlf 1995, ch. 13) was used to test for whether one or more taggers performed consistently poorer than others, based on individual reach survival or transition probabilities through key reaches. In the event that survival was different for a particular tagger, the model was refit to the pooled release groups without tags from the tagger in question, and the difference in survival estimates due to the tagger was tested using a two-sided Z-test on the lognormal scale. The reduced data set (without predator detections), pooled over release groups, was used for these analyses.

Analysis of Travel Time

Travel time was measured from release at Durham Ferry to each detection site. Travel time was also measured through each reach for tags detected at the beginning and end of the reach, and summarized across all tags with observations. Travel time between two sites was defined as the time delay between the last detection at the first site and the first detection at the second site. In cases where the tagged fish was observed to make multiple visits to a site, the final visit was used for travel time calculations. When possible, travel times were measured separately for different routes through the study area. The harmonic mean was used to summarize travel times.

Route Entrainment Analysis

A physical barrier was installed at the head of Old River in 2012. The barrier was designed to keep fish from entering Old River, but included culverts that allowed limited fish passage. Only 58 of the

1,435 (4%) tags released in juvenile steelhead in 2012 were detected entering the Old River route in 2012, while 776 (54% of 1,435) were detected in the San Joaquin River route. Because of the barrier and the low number of tags detected in the Old River route, no effort was made to relate route entrainment at the head of Old River to hydrologic conditions in 2012. A route entrainment analysis was performed for the Turner Cut junction instead.

The effects of variability in hydrologic conditions on route entrainment at the junction of Turner Cut with the San Joaquin River were explored using statistical generalized linear models (GLMs) with a binomial error structure and logit link (McCullagh and Nelder, 1989). The acoustic tags used in this analysis were restricted to those detected at either of the acoustic receiver dual arrays located just downstream of the Turner Cut junction: site MAC (model code A8) or site TCE/TCW (code F1). Tags were further restricted to those whose final pass of the Turner Cut junction came from either upstream sites or from the opposite leg of the junction; tags whose final pass of the junction came either from downstream sites (e.g., MFE/MFW) or from a previous visit to the same receivers (e.g., multiple visits to the MAC receivers) were excluded from this analysis. Tags were restricted in this way in order to limit the delay between initial arrival at the junction, when hydrologic covariates were measured, and the tagged fish's final route selection at the junction. Only one steelhead was observed moving from one junction leg to the other (i.e., from Turner Cut to the San Joaquin at MacDonald Island). Predator-type detections were also excluded. Detections from a total of 505 tags were used in this analysis: 169, 208, and 124 from release groups 1, 2, and 3, respectively.

Hydrologic conditions were represented in several ways, primarily total river flow (discharge), water velocity, and river stage. These measures were available at 15-minute intervals from the TRN gaging station in Turner Cut, maintained by the USGS (Table 2). The Turner Cut acoustic receivers (TCE and TCW) were located 0.15 – 0.30 km past the TRN station in Turner Cut. No gaging station was available in the San Joaquin River close to the MAC receivers. The closest stations were PRI (13 km downstream from the junction), and SJG (18 km upstream from the junction) (Table 2). These stations were considered too far distant from the MAC receivers to provide measures of flow, velocity, and river stage sufficiently accurate for describing localized conditions at the Turner Cut junction for the route entrainment analysis. Thus, while measures of hydrologic conditions were available in Turner Cut, measures of flow proportion into Turner Cut were not available.

Additionally, there was no measure of river conditions available just upstream of the junction that might inform about the environment as the fish approached the junction. Instead, gaging data

from the SJG gaging station (18 km upstream of the junction) were used as a surrogate for conditions upstream of the junction. Because of the distance between the SJG station and the Turner Cut junction, and the fact that the San Joaquin River becomes considerably wider between the SJG station and the junction, conditions at SJG were used only as an index of average conditions during the time when the fish was in this reach. In particular, no measure of tidal stage or flow direction was used at SJG. Instead, the analysis used the average magnitude (measured as the root mean square, RMS) of flow and velocity at SJG during the tag transition from the time of tag departure from the SJG acoustic receiver (model code A6) to the time of estimated arrival at the Turner Cut junction.

Conditions at the TRN gaging station were measured at the estimated time of arrival at the Turner Cut junction. The location (named TCJ for Turner Cut Junction) used to indicate arrival at the junction was located in the San Joaquin River 1.23 km from the TCE receiver and 2.89 km upstream of the MACU receiver. Time of arrival at TCJ $\left(t_i\right)$ was estimated for tag i by a linear interpolation from the observed travel time from the SJNB or SJG acoustic receivers upstream to detection on either the MAC or TCE/TCW receivers just downstream of the junction. Linear interpolation is based on the first-order assumption of constant movement during the transition from the previous site. In a tidal area, it is likely that movement was not actually constant during the transition, but in the absence of more precise spatiotemporal tag detection data, the linear interpolation may nevertheless provide the best estimate of arrival time.

The TRN gaging station typically recorded flow, velocity, and river stage measurements every 15 minutes. Some observations were missing during the time period when tagged steelhead were passing the junction. Linear interpolation was used to estimate the flow, velocity, and river stage conditions at the estimated time of tag arrival at TCJ:

$$x_i = w_i x_{t_{1(i)}} + (1 - w_i) x_{t_{2(i)}}$$

where $x_{t_{1(i)}}$ and $x_{t_{2(i)}}$ are the two observations of metric x (x = Q [flow], V [velocity], or C [stage]) at the TRN gaging station nearest in time to the time t_i of tag i arrival such that $t_{1(i)} \le t_i \le t_{2(i)}$. The weights w_i were defined as

$$w_i = \frac{t_{2(i)} - t_i}{t_{2(i)} - t_{1(i)}},$$

and resulted in weighting x_i toward the closest flow, velocity, or stage observation.

In cases with a short time delay between consecutive flow and velocity observations (i.e., $t_{2(i)} - t_{1(i)} \leq 60$ minutes), the change in conditions between the two time points was used to represent the tidal stage (Perry 2010):

$$\Delta x_i = x_{t_{2(i)}} - x_{t_{1(i)}}$$

for $x = Q, V,$ or C, and tag i.

Negative flow measured at the TRN gaging station was interpreted as river flow being directed into the interior Delta, away from the San Joaquin River (Cavallo et al. 2013). Flow reversal (i.e., negative flow at TRN) was represented by the indicator variable U (Perry 2010):

$$U_i = \begin{cases} 1, & for\ Q_i < 0 \\ 0, & for\ Q_i \geq 0 \end{cases}$$

Prevailing flow and velocity conditions in the reach from the SJG acoustic receiver to arrival at the Turner Cut junction were represented by the root mean square (RMS) of the time series of observed conditions measured at the SJG gaging station during the estimated duration of the transition:

$$x_{RMS(i)} = \sqrt{\frac{1}{n_i} \sum_{j=T_{1(i)}}^{T_{2(i)}} x_j^2}$$

where x_j = observed covariate x at time j at the SJG gaging station $(x = Q \text{ or } V)$, $T_{1(i)}$ = closest observation time of covariate x to the final detection of tag i on the SJG acoustic receivers, and $T_{2(i)}$ = closest observation time of covariate x to the estimated time of arrival of tag i at TCJ. If the time delay between either $T_{1(i)}$ and final detection of tag i on the SJG acoustic receivers, or $T_{2(i)}$ and estimated time of arrival of tag i at TCJ, was greater than 1 hour, then no measure of covariate x from the SJG gaging station was used for tag i.

Daily export rate for day of arrival of tag i at TCJ was measured at the Central Valley Project (E_{iCVP}) and State Water Project (E_{iSWP}) (data downloaded from DayFlow on November 5, 2013). Fork

length at tagging L_i and release group RG_i were also considered. Finally, arrival time (day vs. night) at the Turner Cut Junction site (TCJ) was measured based on whether the tagged steelhead first arrived at TCJ between sunrise and sunset $\left(day_i\right)$.

All continuous covariates were standardized, i.e.,

$$\tilde{x}_{ij} = \frac{x_{ij} - \overline{x}_j}{s(x_j)}$$

for the observation x of covariate j from tag i. The indicator variables U, RG, and day were not standardized.

The form of the generalized linear model was

$$\ln\left(\frac{\psi_{iA}}{\psi_{iF}}\right) = \beta_0 + \beta_1\left(\tilde{x}_{i1}\right) + \beta_2\left(\tilde{x}_{i2}\right) + \cdots + \beta_p\left(\tilde{x}_{ip}\right)$$

where $\tilde{x}_{i1}, \tilde{x}_{i2}, \ldots, \tilde{x}_{ip}$ are the observed values of standardized covariates for tag i (covariates 1, 2, …, *p*, see below), ψ_{iA} is the predicted probability that the fish with tag i selected route A (San Joaquin River route), and $\psi_{iF} = 1 - \psi_{iA}$ (F = Turner Cut route). Route choice for tag i was determined based on detection of tag i at either site A8 (route A) or site F1 (route F). Estimated detection probabilities for the three release groups were 0.97 – 1.00 for site A8 and 0.58 – 1.00 for site F1 (Appendix Table A2). The estimated detection probability at site F1 was 0.58 for the first release group (April), and 1.00 for the latter two release groups (May). If tag detections at site F1 from the first release group were missing completely at random, then these missing detections should not bias results from the route entrainment analysis because the analysis is restricted to those tags that had detections at F1 (or A8). However, if detections from F1 were missing because of a factor that may also have influenced route choice at the Turner Cut junction, then the missing detections produced by low detectability may bias results of this analysis. Thus, the analysis was performed both with and without tag detections from the first release group.

Single-variate regression was performed first, and covariates were ranked by P-values from the appropriate F-test (McCullagh and Nelder 1989). Covariates found to be significant alone $(\alpha = 0.05)$ were then analyzed together in a series of multivariate regression models. Because of high correlation

between flow and velocity measured from the same site, and to a lesser extent, correlation between flow or velocity and river stage, the covariates flow, velocity, and river stage were analyzed in separate models. The exception was that the flow index in the reach from SJG to TCJ (Q_{SJG}) was included in the river stage model. Exports at CVP and SWP had low correlation over the time period in question, so CVP and SWP exports were considered in the same models. The general forms of the three multivariate models were:

Flow model: $Q_{TRN} + Q_{SJG} + \Delta Q_{TRN} + U + day + E_{CVP} + E_{SWP} + L + RG$

Velocity model: $V_{TRN} + V_{SJG} + \Delta V_{TRN} + U + day + E_{CVP} + E_{SWP} + L + RG$

Stage model: $C_{TRN} + Q_{SJG} + \Delta C_{TRN} + U + day + E_{CVP} + E_{SWP} + L + RG.$

Backwards selection with F-tests was used to find the most parsimonious model in each category (flow, velocity, and stage) that explained the most variation in the data (McCullagh and Nelder 1989). Main effects and two-way interaction effects were considered. The model that resulted from the backwards selection process in each category (flow, velocity, or stage) was compared using an F-test to the full model from that category to ensure that all significant main effects were included. AIC was used to select among the flow, velocity, and stage models. Model fit was assessed by grouping data into discrete classes according to the independent covariate, and comparing predicted and observed frequencies of route entrainment into the San Joaquin using the Pearson chi-squared test (Sokal and Rohlf 1995).

Survival through Facilities

A supplemental analysis was performed to estimate the probability of survival of tagged fish from the interior receivers at the water export facilities through salvage to release on the San Joaquin or Sacramento rivers. Overall salvage survival from the interior receivers at site $k2$, $S_{k2(salvage)}$ $(k = D, E)$, was defined as

$$S_{k2(salvage)} = \phi_{k2,GH} + \phi_{k2,G2},$$

where $\phi_{k2,G2}$ is as defined above, and $\phi_{k2,GH}$ is the joint probability of surviving from site $k2$ to the Jersey Point/False River junction and not going on to Chipps Island. The subset of detection histories

that included detection at site $k2$ $(k = D, E)$ were used for this analysis. Detections from the full data set were used to estimate the detection probability at sites G1, G2, and H1, although only data from tags detected at either D2 or E2 were used to estimate salvage survival. Profile likelihood was used to estimate the 95% confidence intervals for both $S_{D2(salvage)}$ and $S_{E2(salvage)}$.

Results

Detections of Acoustic-Tagged Fish

There were 1,435 tags released in juvenile steelhead at Durham Ferry in 2012. Of these, 1,187 (83%) were detected on one or more receivers either upstream or downstream of the release site (Table 4), including any predator-type detections. A total of 1,104 tags (77%) were detected at least once downstream of the release site, and 840 (59%) were detected in the study area from Mossdale to Chipps Island (Table 4). A smaller proportion of the last release group (39%) was detected in the study area than of the earlier release groups (67% - 70%).

Overall, there were 776 tags detected on one or more receivers in the San Joaquin River route downstream of the head of Old River (Table 4). In general, tag detections decreased within each migration route as distance from the release point increased. Of these 776 tags, 776 were detected on the receivers near Lathrop, CA; 724 were detected on one or both of the receivers near Stockton, CA (SJG or SJNB); 606 were detected on the receivers in the San Joaquin River near MacDonald Island or in Turner Cut; and 326 were detected at Medford Island (Table 5). Not all of the 776 tags detected in the San Joaquin River downstream of the head of Old River were assigned to that route for the survival model, because some were subsequently detected in the Old River route or upstream of Old River. Overall, 751 tags were assigned to the San Joaquin River route for the survival model (Table 4). Of these 751 tags, 138 were observed exiting the San Joaquin River at Turner Cut, 183 were observed at the Old or Middle River receivers near Empire Cut, 94 were observed at the Old or Middle River receivers near Highway 4, and 68 were observed at the water export facilities receivers (including the radial gates at the entrance to the Clifton Court Forebay) (Table 5, Table 6). A total of 297 San Joaquin River route tags were detected at the Jersey Point/False River receivers, including 112 detections on the False River receivers (Table 5). However, the majority of the tags detected at False River were later detected either at Jersey Point or Chipps Island, and so only 10 San Joaquin River tags were used in the survival model at

False River (Table 6). A total of 252 San Joaquin River route tags were eventually detected at Chipps Island, including predator-type detections (Table 5).

Only 58 tags were detected in the Old River route (Table 4). All 58 of these tags were detected at the Old River East receivers near the head of Old River, while 51 were detected near the head of Middle River, and 32 were detected either at the receivers at the water export facilities, or at the Old or Middle River receivers near Highway 4 in the interior Delta (Table 4, Table 5). Only 3 tags were detected on the Middle River receivers near the head of Middle River. Also, only 3 of the tags detected in the Old River route were ever detected at the receivers in the Old and Middle rivers near Empire Cut (omitting a single tag that was eventually detected at Durham Ferry after detection in the northern Middle River), and only 1 of these 3 tags entered the Old River route via the head of Old River. Similarly, few tags appear to have reached either the Old River receivers (6 tags) or the Middle River receivers (2 tags) at Highway 4 via the Old River route (Table 5).

Some of the 58 tags detected in the Old River route were assigned to a different route for the survival model because they were subsequently detected in the San Joaquin River after their Old River route detections. In all, 48 tags were assigned to the Old River route at the head of Old River based on the full sequence of tag detections (Table 4). Of these 48 tags, 22 were detected at the CVP trashracks, although only 15 of these CVP detections were used in the survival model because the others were later detected either at the radial gates or farther north in Old or Middle rivers (Table 5, Table 6). No Old River route tags were detected at the Jersey Point/False River receivers; while some tags were observed to reach the Jersey Point/False River junction coming from the northern Old and Middle river receivers, these tags had all remained in the San Joaquin River at the head of Old River, and entered the interior Delta downstream of the city of Stockton, CA. Of the 48 tags assigned to the Old River route at the head of Old River, 4 were detected at Chipps Island, including predator-type detections (Table 5, Table 6).

In addition to the Old and Middle river receivers located near Empire Cut, the Threemile Slough receivers recorded detections of tags but were purposely omitted from the survival model. Fifty-two (52) tags were detected on the Threemile Slough receivers: 37 tags came directly from the San Joaquin River receivers (MacDonald and Medford islands), 13 from Jersey Point or False River, and 1 each from Turner Cut and the Old River receiver near Empire Cut.

The predator filter used to distinguish between detections of juvenile steelhead and detections of predatory fish that had eaten the tagged steelhead classified 265 of the 1,435 tags (18%) released as

being detected in a predator at some point during the study (Table 7). Of the 840 tags detected in the study area (i.e., at Mossdale or points downstream), 122 tags (15%) were classified as being in a predator, although some had been identified as a predator before entering the study area. A total of 103 tags (12%) were classified as a predator within the study area. The region upstream of Mossdale had a larger percentage of tags classified as in a predator at some point, with 181 of 781 tags (23%) detected in that region classified as in a predator. Nineteen of those 181 tags were classified as a predator downstream of Mossdale, and then returned to the upstream regions (Table 7).

Within the study area, the detection sites with the largest number of first-time predator-type detections were Garwood Bridge (14 of 724, 2%), Navy Drive Bridge (11 of 693, 2%), and the CVP trashracks (10 of 76, 13%) (Table 7). Most predator classifications were assigned to tags on arrival at the detection site in question because of unexpected travel time and unexpected transitions between detection sites, with the result that predator-type detections at those sites were removed from the survival model. Predator classifications on departure from a detection site were typically because of long residence times, and were most prevalent at Garwood Bridge, Navy Drive Bridge, and the receivers at the Clifton Court Forebay radial gates entrance channel.

When the detections classified as coming from predators were removed from the detection data, somewhat fewer detections were available for survival analysis (Table 8, Table 9, and Table 10). With the predator-type detections removed, 1,045 of the 1,435 (73%) tags released were detected downstream of the release site, and 821 (57% of those released) were detected in the study area from Mossdale to Chipps Island (Table 8). The final release group had a lower percentage (37%) of total tags subsequently detected within the study area than the earlier release groups (65% to 70%). The final release group also had the lowest percentage of tags detected anywhere after release (70% vs. 79% - 88% for previous releases).

Many more steelhead were observed using the San Joaquin River route at the head of Old River (759) than the Old River route (42) (Table 8). As observed from the full data set including the predator-type detections, the reduced data set with only steelhead-type detections showed that the majority of the tags detected at the receivers in the western and northern portions of the study area, including the water export facilities, Jersey Point, and Chipps Island, used the San Joaquin River route at the head of Old River rather than the Old River route (Table 9). No tagged steelhead from the Old River route were detected at the Old and Middle river receivers near Empire Cut (OLD and MRE, respectively), although 50 tagged steelhead from the San Joaquin River route were detected at OLD, and 175 were detected at

MRE (Table 9). Thus, using a barrier to keep steelhead out of Old River at its head does not necessarily prevent them from entering the interior Delta farther downstream. While there were more San Joaquin River route steelhead detected at the receivers near the export facilities than Old River route steelhead, the differences between routes was not as marked at those locations at the northern Old and Middle river receivers. Of the 42 steelhead assigned to the Old River route at the head of Old River, 12 were detected at the radial gates receivers and 18 were detected at the Central Valley Project. Only 3 of the Old River route steelhead were eventually detected at Chipps Island (Table 9). At most sites in the San Joaquin River route, considerably fewer steelhead were detected from the third release group (mid-May) than from either of the first two release groups (Table 9). For the Old River route, however, detection counts were similar between the second and third release groups, and tended to be lower than for the first release group (early April) (Table 8). Detection counts used in the survival model follow a similar pattern (Table 10).

Tag-Survival Model and Tag-Life Adjustments

The Akaike Information Criterion (AIC) indicated that pooling data from both tag-life studies (AIC = 8.9) was preferable to stratifying by study month (AIC = 17.6). Thus, a single tag survival model was fitted and used to adjust fish survival estimates for premature tag failure. The estimated mean time to failure from the pooled data was 77.7 days ($\widehat{SE} = 10.8$ days) (Figure 4).

The complete set of detection data, including any detections that may have come from predators, contained some detections that occurred after the tags began dying, although before the precipitous drop in tag survival at day 80 (Figure 5, Figure 6). The sites with the latest detections were the Durham Ferry site located just downstream of the release site, Banta Carbona, the San Joaquin River receiver near Medford Island, and the CVP holding tank. Some of these late-arriving detections may have come from predators, or from residualizing steelhead. Tag-life corrections were made to survival estimates to account for the premature tag failure observed in the tag-life studies. All estimates of reach survival for the acoustic tags were greater than 0.97 (out of a possible range of 0 – 1), and cumulative tag survival to Chipps Island was estimated at 0.98 or above with or without predator-type detections. Thus, there was very little effect of either premature tag failure or corrections for tag failure on the estimates of steelhead reach survival.

Tagger Effects

Fish in the release groups were fairly evenly distributed across tagger, with 11-14 more fish tagged by taggers C or D than by taggers A or B in each release group (Table 11). For each tagger, the number tagged was distributed evenly across the three release groups. A chi-squared test found no evidence of lack of independence of tagger across release groups (χ^2 =0.0184, df=6, P=1.0000). The distribution of tags detected at various key detection sites was well-distributed across taggers and showed no evidence of a tagger effect on survival, route entrainment, or detection probabilities at these sites (χ^2 =36.7316, df=39, P=0.5738; Table 12).

Estimates of cumulative survival throughout the San Joaquin River route to Chipps Island showed similar patterns of survival across all taggers. Although taggers A and C had consistently higher cumulative survival through much of the San Joaquin River route, there was no significant difference in overall survival to Chipps Island among taggers (Figure 7). Analysis of variance found no effect of tagger on reach survival (P=0.6649). Larger differences in cumulative survival by tagger were observed in the Old River route, with tagger B showing relatively low survival to the South Delta exit points in the Old River route (Figure 8) compared to the other taggers. However, there was no effect of tagger on cumulative survival via the Old River route either to the South Delta exits points (P=0.7735) or to Chipps Island (P=0.6840). Rank tests found no evidence of consistent differences in reach survival across fish from different taggers either upstream of the Head of Old River (P=0.9932), or in either the San Joaquin River route (P=0.9932) or the Old River route (P=0.9363).

Survival and Route Entrainment Probabilities

For each release group, likelihood ratio tests indicated that transition probabilities through the Central Valley Project and Clifton Court Forebay did not significantly depend on the route taken to those sites (i.e., the San Joaquin River route versus the Old River route) ($P \geq 0.4005$ without the predator-type detections, and $P \geq 0.2301$ with the predator-type detections). Thus, common transition probabilities through those regions were estimated, regardless of route.

Some parameters were unable to be estimated because of sparse data. In particular, only 3 tags were detected at the receiver at the head of Middle River (MRH, model code C1). Two of these were classified as a predator prior to arrival at site C1, and they were both last observed at site C1. The third tag was observed making over 20 visits to site C1, and finally ended its detection history at Banta Carbona; because it was classified as a predator on after departure from its first visit to C1, the first C1

detection was available to be used in analysis excluding the predator-type detections. However, having only 1-3 detections at C1 made estimation of detection probabilities at that site impossible and/or estimation of transition probabilities from that site intractable. Thus, no detections of C1 were actually used in the analysis for any release group. This prevented estimation of all transition parameters starting at C1: $\phi_{C1,B3}$, $\phi_{C1,C2}$, $\phi_{C1,D1}$, and $\phi_{C1,E1}$. It was also necessary to combine the survival probability from ORE (site B1) to the Middle River junction with Old River $\left(S_{B1}\right)$ and the route entrainment probability into Old River at that junction $\left(\psi_{B2}\right)$ to yield the transition probability $\phi_{B1,B2} = S_{B1}\psi_{B2}$. This transition probability may be interpreted as equal to the survival parameter from the head of Old River to the head of Middle River only under the assumption that no fish actually entered Middle River (i.e., $\psi_{B2} = 1$). In the absence of Middle River detections and under the assumption that the Middle River receivers were actually working, this may be a reasonable assumption. In cases such as the first release group using steelhead-type detections and the third release group using all detections (steelhead-type and predator-type), in which there were detections at Middle River but too few to estimate parameters there, it must be noted that estimates of $\phi_{B1,B2}$ are minimum estimates of survival from the head of Old River to the head of Middle River.

There were very few tags observed moving to the Jersey Point and False River receivers from the northern Old and Middle River receivers (i.e., those near Highway 4, OR4 [B3] and MR4 [C2]). Of the fish coming from the Old River route at the head of Old River, none were observed moving from the Highway 4 receivers to Jersey Point and False River, and of the fish coming from the San Joaquin River route, only 4 tags were observed moving to Jersey Point and False River from OR4, and none from MR4. Thus, estimates of $\phi_{B3,GH}$ and $\phi_{C2,GH}$ were both 0 for Old River route fish, and $\phi_{C2,GH}$ was also estimated at 0 for San Joaquin River route fish. Furthermore, no estimates of $\phi_{G1,G2}$ or ψ_{G1} were available for Old River route fish.

In some cases, detections were available at a particular site but were too sparse to include the site in the model. There were too few detections at the False River receivers (site H1) from the first and second release groups to estimate the detection probability at that site. Site H1 was omitted from the model in these cases, and the parameters $\phi_{x,G1} = \phi_{x,GH}\psi_{G1}$ were estimated for *x* = A8, A9, B3, C2, and F1. In many cases analysis of model residuals showed that incorporating certain detection sites or the

full dual array at certain sites in the model reduced the quality of the model fit to the data. In such cases as these where it was possible to simplify the data structure and still attain useful and valid parameter estimates, the problematic sites were either omitted (e.g., site A2 at Durham Ferry Downstream for the second and third release groups) or detections from the dual array were pooled (e.g., site A8 at MacDonald Island for the second release group) to improve model fit. In cases where site A2 was removed, the model used the composite parameter $\phi_{A1,A3} = \phi_{A1,A2} S_{A2}$ in place of $\phi_{A1,A2}$ and S_{A2}.

Using only those detections classified as coming from juvenile steelhead and excluding the predator-type detections, the estimates of total survival from Mossdale to the receivers at Chipps Island, S_{total}, ranged from 0.26 ($\widehat{SE} = 0.02$) for the first release group (released in early April) to 0.35 ($\widehat{SE} =$ 0.03) for the second release group (released in early May) (Table 13). The overall population estimate for all fish in the tagging study was 0.32 ($\widehat{SE} = 0.02$). Estimates of the probability of remaining in the San Joaquin River at the junction with Old River $\left(\psi_A = \psi_{A1}\right)$ were very high, ranging from 0.92 ($\widehat{SE} =$ 0.02) for the third release group to 0.97 ($\widehat{SE} = 0.01$) for the second release group; the population estimate was 0.94 ($\widehat{SE} = 0.01$) (Table 13). For each release group, there was a significant preference for the San Joaquin River route (P<0.0001 for each group). Estimates of survival from Mossdale to Chipps Island via the San Joaquin River route $\left(S_A\right)$ ranged from 0.28 ($\widehat{SE} = 0.03$) for the early April release group to 0.36 ($\widehat{SE} = 0.04$) for the mid-May release group; the overall population estimate was 0.33 ($\widehat{SE} = 0.03$). In the Old River route, estimates of survival from Mossdale to Chipps Island were considerably lower, ranging from 0.05 ($\widehat{SE}$ = 0.03) for the mid-May release group, to 0.10 ($\widehat{SE}$ =0.07) for the early May release group; the overall population estimate was 0.07 ($\widehat{SE}$ =0.03) (Table 13). For all release groups, the estimate of survival to Chipps Island was significantly higher in the San Joaquin River route than in the Old River route (P≤0.0405).

Survival was estimated to the Jersey Point/False River junction for fish that did not pass through the holding tanks at the CVP or the SWP. This survival measure $\left(S_{total(MD)}\right)$ had estimates ranging from 0.32 ($\widehat{SE} = 0.03$) for the early April release group to 0.46 ($\widehat{SE} = 0.03$) for the early May release group,

averaging 0.41 ($\widehat{SE} = 0.02$) over all release groups. All of the tagged steelhead observed at the Jersey Point/False River junction came via the San Joaquin River route; none had taken the Old River route at the head of Old River. Many of the Old River route fish were observed at the receivers closest to the salvage facilities at Central Valley Project (i.e., the holding tank) and the State Water Project (i.e., the radial gates receivers); the survivors of these fish would not have contributed to survival to Jersey Point/False River. Because $S_{total(MD)}$ does not reflect survival to downstream regions via salvage, it is not necessarily indicative of overall survival to Chipps Island $\left(S_{total}\right)$. In all, very few tags were observed leaving the San Joaquin River for False River (Table 10, and $\hat{\psi}_{H1}$ in Table A2 in Appendix).

Survival was estimated through the South Delta ($S_{A(SD)}$, $S_{B(SD)}$, and $S_{total(SD)}$) for all release groups. The "South Delta" region corresponded to the region studied for Chinook salmon survival in the 2009 VAMP study (SJRGA 2010). Estimates of survival in the San Joaquin River from Mossdale to MacDonald Island (MAC) or Turner Cut (TCE/TCW) $\left(S_{A(SD)}\right)$ ranged from 0.78 ($\widehat{SE} = 0.04$) for the first release group to 0.89 ($\widehat{SE} = 0.03$) for the last release group, yielding a population estimate of 0.83 ($\widehat{SE} = 0.02$) (Table 13). In the Old River route, estimated survival from Mossdale to the entrances of the water export facilities (CVP, RGU) or the northern Old River and Middle River receivers near Highway 4 (OR4, MR4) $\left(S_{B(SD)}\right)$ ranged from 0.23 ($\widehat{SE} = 0.11$) for the last release group to 0.80 ($\widehat{SE} = 0.08$) for the first release group; the population-level estimate was 0.55 ($\widehat{SE} = 0.07$) (Table 13). The larger standard errors on the Old River route estimates reflect the relatively small numbers of fish using the Old River route in 2012 compared to the San Joaquin River route. Total estimated survival through the entire South Delta region $\left(S_{total(SD)}\right)$ ranged from 0.78 ($\widehat{SE} = 0.04$) for the first release group to 0.84 ($\widehat{SE} = 0.03$) for the last release group, yielding a population estimate of 0.81 ($\widehat{SE} = 0.02$) over all three release groups (Table 13).

Including predator-type detections in the analysis produced little change in the estimates of survival on any of the spatial scales considered, including survival to Chipps Island, survival to the Jersey Point/False River region, or survival through the South Delta (Table 13, Table 14). The largest difference was in estimates of survival through the South Delta region in the Old River route, which increased from 0.80 ($\widehat{SE} = 0.08$) without the predator-type detections for the April release group to 0.89 ($\widehat{SE} = 0.07$)

with the predator-type detections (Table 13, Table 14). The increase may be due to the typically high density of predators at the CVP trashracks and radial gates. Overall survival to Chipps Island showed essentially no change (difference ≤ 0.01) when predator-type detections were included (Table 14). Survival from Mossdale to the Jersey Point/False River region (without salvaged fish) showed similarly negligible changes when predator-type detections were included. The small effect of removing the predator detections on survival estimates over the larger spatial scales may reflect limitations of the spatial range of the predators, or similarities in behavior between steelhead and the predatory fish targeted in the predator filter (Table 13, Table 14).

Travel Time

For tags classified as being in steelhead, average travel time through the system from release at Durham Ferry to Chipps Island was 9.41 days ($\widehat{SE} = 0.25$ days) (Table 15a). Travel time to Chipps Island tended to decrease for later release groups: the first release group (early April) took an average of 13.64 days ($\widehat{SE} = 0.51$), while the final release group (mid-May) took an average of 7.93 days ($\widehat{SE} = 0.37$) (Table 15a). The large majority of tags reaching Chipps Island came via the San Joaquin River route; the 3 tags that got to Chipps Island via the Old River route had a slightly longer travel time (average = 13.00 days; $\widehat{SE} = 2.57$ days). While most tags that were observed at Chipps Island arrived within 15 days of release at Durham Ferry, there were several tags that took longer, and 4 tags that took 25 – 40 days to get to Chipps Island. All of the very slow tags had remained in the San Joaquin River at the head of Old River.

Travel time from release to Mossdale Bridge receivers averaged approximately 2 – 3 days throughout the study, and travel time to the Turner Cut junction receivers (i.e., at Turner Cut and MacDonald Island) averaged approximately 5 – 8 days over all release groups (Table 15a). Travel time from release to the receivers near or at the water export facilities (Central Valley Project and Clifton Court Forebay radial gates) tended to be longer for fish taking the San Joaquin River route rather than the Old River route. This pattern was not consistent throughout the season, however; Old River route fish from the final release group took considerably longer than their counterparts in the San Joaquin River route (Table 15a). However, few fish took the Old River route at the head of Old River, and so the results for the Old River route may be skewed by the small sample size. Pooled over all three release groups, there was little difference in total travel time to the radial gate receivers at the Clifton Court Forebay by route (approximately 9 – 10 days), and San Joaquin River route fish took approximately 2

extra days to reach the Central Valley Project than Old River route fish (Table 15a). Very few fish reached the receivers in the interior Delta (i.e., Middle River and Old River receivers near Highway 4) via the Old River route, and they tended to take just over two weeks from the release at Durham Ferry. Most fish that were observed at those receivers came from the San Joaquin River route, and took an average of 9 – 10 days from Durham Ferry, averaged over all release groups. Fish from the first release group tended to have longer travel times to the Highway 4 receivers (12 – 13 days) than fish from later release groups (7 – 9 days) (Table 15). All fish observed at the Jersey Point or False River receivers came via the San Joaquin River route, and average travel times were approximately 7 – 8 days (averaged over all releases). The first release group generally took longer to reach these receivers (12 days) than fish released later (6 – 8 days) (Table 15a).

Including detections from tags classified as predators tended to lengthen average travel times, but the general pattern across routes and release groups stayed the same (Table 15b). The average travel time from release to Chipps Island via all routes, including the predator-type detections, was 9.52 days ($SE = 0.26$ days) (Table 15b). Increases in travel time with the predator-type detections reflect the travel time criteria in the predator filter, which assumes that predatory fish may move more slowly through the study area than migrating steelhead. Travel time increases may also reflect multiple visits to a site by a predator, because the measured travel time reflects time from release to the start of the final visit to the site.

Average travel time through reaches for tags classified as being in steelhead ranged from 0.01-0.09 days (20 – 130 minutes) from the entrance channel receivers at the Clifton Court Forebay (RGU) to the interior forebay receivers (RGD) to over 5 days from the head of Old River (ORE) to the head of Middle River (MRH) and from Old River South (ORS) to Old River near Highway 4 (OR4) (Table 16a). However, of those tags classified as a steelhead, only one tag was observed moving from ORE to MRH and only two tags moving from ORS to OR4. The “reach” from the exterior to the interior radial gate receivers (RGU to RGD) was the shortest, so it is not surprising that it would have the shortest travel time, as well. However, travel time did not always reflect travel distance. For example, average travel time from Lathrop (SJL) to Garwood Bridge (SJG) was approximately 0.76 days through a distance of about 18 rkm, while average travel time from the Old River South receivers (ORS) to the Central Valley Project trashrack receivers (CVP) was 2.93 days, also through a distance of approximately 18 rkm. Travel times within the San Joaquin River tended to be shorter than travel times that involved the interior Delta. For example, the average travel time from the MacDonald Island receivers to the Jersey

Point/False River receivers (~26 rkm) was 1.61 ($\widehat{SE} = 0.05$) days, while the average travel time from the MacDonald Island receivers to the receivers in Old River near Highway 4 (~27 rkm) was 3.73 ($\widehat{SE} = 0.36$) days (Table 16a). The comparable distances but widely different travel times suggest that travel in the interior Delta may be prolonged by the complexity of the routing and hydrologic environment in that region.

Reach travel times tended to be longer in the first release group than in the later groups, although this was not consistent throughout the study area. This was most apparent in the San Joaquin River reaches, in particular from the Navy Drive Bridge (SJNB) to MacDonald Island and Turner Cut, and from MacDonald or Medford islands to points downstream (Table 16a). Including the predator detections tended to increase reach travel times, although not consistently across all reaches and release groups (Table 16b).

Route Entrainment Analysis

River flow (discharge) at the TRN gaging station in Turner Cut ranged from -4,646 cfs to 3,363 cfs (average = -1,117 cfs) during the estimated arrival time of the tagged steelhead at the Turner Cut junction location (TCJ) in 2012. Water velocity in Turner Cut was highly correlated with river flow (r=0.999), and velocity values ranged from -0.8 ft/s to 0.7 ft/s (average = -0.2 ft/s). The flow in Turner Cut was negative (i.e., directed to the interior Delta) upon arrival at TCJ of approximately 65% (326 of 505) tags in this analysis. River stage measured in Turner Cut was moderately correlated with both river flow and velocity (r=-0.73), and ranged from 6.7 ft to 11.3 ft (average = 9.2 ft). Changes in river stage in the 15-minute observation period containing the arrival of the tagged steelhead to the Turner Cut junction (TCJ) ranged from -0.2 ft to 0.2 ft (average = 0 ft). Changes in river stage were not correlated with stage (r=-0.08). The index of river flow in the reach from Stockton to Turner Cut was uncorrelated with flow and velocity in Turner Cut upon arrival at TCJ (r=0.14), and only moderately correlated with river stage at Turner Cut (r=-0.30). The flow index in the Stockton-Turner Cut reach ranged from 765 cfs to 4,018 cfs (average = 2,702 cfs).

The daily export rate at CVP ranged from 821 cfs to 4,263 cfs (average = 1,048 cfs), with exports generally low early in the study and peaking in mid-May. The daily export rate at the State Water Project (SWP) ranged from 507 cfs to 3,699 cfs (average = 1,604 cfs). SWP exports were more variable than CVP exports but also peaked in mid-May. Exports from CVP and SWP were uncorrelated (r=-0.06).

Neither CVP nor SWP exports was correlated with either flow (r=0.07 for CVP, r=-0.08 for SWP) or river stage (r=-0.22 for CVP, r=0.01 for SWP) in Turner Cut.

The single-variate analyses using all three release groups found significant effects (α=5%) of several covariates on the probability of remaining in the San Joaquin River at Turner Cut: river stage and change in river stage at TRN, change in flow and velocity at TRN, release group, exports at CVP, fork length at tagging, and reverse flow at TRN (Table 17). Exports at SWP and total flow and velocity at TRN were significant at the 10% level (Table 17). When tags were limited to the second and third release group, which passed Turner Cut during periods of high detection probability at all receivers in the region, the effects of fork length and reverse flow at TRN were no longer significant at the 5% level, although fork length was significant at the 10% level (Table 18). SWP exports, flow, and velocity in Turner Cut were no longer significant at the 10% level without the first release group. The fact that flow and velocity at TRN were (marginally) significant only when the first release group was included, during a time of deficient detection probability at the Turner Cut acoustic receivers, suggests that the effects of flow and velocity were confounded with the effects of non-detection at site F1. This may produce a bias in the results. For example, if the detection probability at the F1 receivers was lower during periods of high flow through Turner Cut during the first release group, then the regression model might indicate an effect of increased flow on the route entrainment probability when in fact the effect was only on the detection probability. For this reason, further results are limited to the second and third release groups, for which detection probabilities were high at all acoustic receivers downstream of the Turner Cut junction.

When limited to the second and third release groups, the single-variate regression models found significant effects on the probability entering Turner Cut of change in flow and velocity at TRN ($P<0.0001$ for both), river stage and change in river stage at TRN ($P<0.0001$ for both), release group ($P=0.0087$), and CVP exports ($P=0.0093$). Fork length was significant at the 10% level, but not the 5% level ($P=0.0866$). Neither of the measures of river conditions in the reach from SJG to the Turner Cut junction was significant ($P \geq 0.3324$), nor was the direction of flow in Turner Cut ($P=0.3678$) or SWP exports ($P=0.3892$). Arrival during daylight was non-significant ($P=0.7659$). As mentioned above, neither flow nor velocity at TRN was significant ($P \geq 0.8370$) when restricted to the later release groups (Table 18).

Several covariates had strong effects based on the single-variate models (Table 18). However, while the single-variate models may suggest possible relationships, confounding among the

independent covariates and the possibility of a causal relationship with an unobserved factor both make it impossible to conclude that changes in any of the significant single-variate measures directly produce changes in the route entrainment at Turner Cut. Multiple regression may shed more light on which covariates are worthy of further study, but causal relationships will not be discernable.

Multiple regression using data from the second and third release groups found significant effects of river stage and change in river stage at the TRN gaging station, as well as changes in flow and velocity at the TRN station (Table 19). Release group was also significant for each of the flow, velocity, and stage models ($P \leq 0.0038$), reflecting a difference in the underlying propensity to enter Turner Cut for the mid-May release group relative to the early May release group. Exports at CVP were significant ($P = 0.0008$) for the flow and velocity models but not for the stage model (Table 19). All three models (flow, velocity, and stage) adequately fit the data ($P>0.99$), but the stage model accounted for more variation in route entrainment than either flow ($\Delta\text{AIC}=5.2$) or water velocity ($\Delta\text{AIC}=5.4$) (Table 19).

The stage model predicted the probability of entering Turner Cut from its junction with the San Joaquin River according to:

$\psi_F = \left[1+\exp\left(-3.55+0.54C_{TRN}-4.76\Delta C_{TRN}\right)\right]^{-1}$ for fish from the second release group, and

$\psi_F = \left[1+\exp\left(-4.35+0.54C_{TRN}-4.76\Delta C_{TRN}\right)\right]^{-1}$ for fish from the third release group,

where C_{TRN} and ΔC_{TRN} represent the river stage and 15-minute change in river stage upon tag arrival at the Turner Cut junction. If ΔC_{TRN} is interpreted as a partial indicator of the tidal cycle in Turner Cut, this model of route entrainment indicates that at a given point in the tidal cycle, steelhead that arrive at a higher river stage have a lower probability of entering Turner Cut than fish that arrive at a lower river stage (Figure 9). Although river stage and river discharge (flow) are moderately correlated in Turner Cut such that higher river stages are associated with negative river flows ($r=-0.73$), river flow was not significantly correlated with the probability of entering Turner Cut ($P= 0.8370$ from a single-variate model, Table 18). This suggests that it is the tidal component of river stage, rather than the inflow component, that may be influencing entry into Turner Cut. This route entrainment model suggests that for a given level of river stage, steelhead that arrive on an ebb tide ($\Delta C_{TRN}<0$) are less likely to enter Turner Cut than fish that arrive on a flood tide ($\Delta C_{TRN}>0$) (Figure 10). However, the actual modeled

probability of entry into Turner Cut depends on the level of river stage upon arrival at the junction (cf. Figure 10 vs. Figure 11). Overall, steelhead from the third release group were more likely to enter Turner Cut than those from the second release group.

Survival through Facilities

Survival through the water export facilities was estimated as the overall probability of reaching either Chipps Island, Jersey Point, or False River after being last detected in the CVP holding tank (model code E2, for the federal facility) or the interior receivers at the radial gates at the entrance to Clifton Court Forebay (site RGU, code D2, for the closest receiver to the state facility). Thus, survival for the federal facility is conditional on being entrained in the holding tank, while survival for the state facility is conditional on entering (and not leaving) the Clifton Court Forebay, and includes survival through the Forebay to the holding tanks. Results are reported for the individual release groups, and also for the full set of data from all three release groups combined (population estimate).

Estimated survival from the CVP holding tanks to Chipps Island ranged from 0.50 ($\widehat{SE} = 0.18$) for the second release group (early May), with a 95% profile likelihood interval of (0.19, 0.81), to 0.68 ($\widehat{SE} = 0.28$) (95% CI = (0.16, 0.99)) for the third release group (mid-May). The population estimate, found from pooling across release groups, was 0.57 ($\widehat{SE} = 0.12$) (95% CI = (0.33, 0.79)) (Table 20). For the state facility, estimated survival from the radial gates to Chipps Island, Jersey Point, and False River ranged from 0 for the first release group (April) to 0.30 ($\widehat{SE} = 0.15$) (95% CI = (0.09, 0.62)) for the third release group. The population estimate for the state facility was 0.17 ($\widehat{SE} = 0.08$), with a 95% confidence interval of (0.06, 0.36) (Table 20).

References

Buchanan, R. 2013. OCAP 2011 Steelhead Tagging Study: Statistical Methods and Results. Prepared for Bureau of Reclamation, Bay Delta Office, Sacramento CA. August 9, 2013. 110 p.

Burnham, K. P., and D. R. Anderson (2002). Model selection and multimodel inference: A practical information-theoretic approach. 2nd edition. Springer. New York, NY. 488 pp.

Cavallo, B., P. Gaskill, and J. Melgo (2013). Investigating the influence of tides, inflows, and exports on sub-daily flow in the Sacramento-San Joaquin Delta. Cramer Fish Sciences Report. 64 pp. Available online at: http://www.fishsciences.net/reports/2013/Cavallo_et_al_Delta_Flow_Report.pdf.

Lady, J. M., and J. R. Skalski (2009). USER 4: User-Specified Estimation Routine. School of Aquatic and Fishery Sciences. University of Washington. Available from http://www.cbr.washington.edu/paramest/user/.

Li, T., and J. J. Anderson (2009). The Vitality model: A Way to understand population survival and demographic heterogeneity. Theoretical Population Biology 76: 118-131.

McCullagh, P., and J. Nelder (1989). Generalized linear models. 2nd edition. Chapman and Hall, London.

Perry, R. W., J. R. Skalski, P. L. Brandes, P. T. Sandstrom, A. P. Klimley, A. Ammann, and B. MacFarlane (2010). Estimating survival and migration route probabilities of juvenile Chinook salmon in the Sacramento-San Joaquin River Delta. North American Journal of Fisheries Management 30: 142-156.

San Joaquin River Group Authority (2010). 2009 Annual Technical Report: On Implementation and Monitoring of the San Joaquin River Agreement and the Vernalis Adaptive Management Plan (VAMP). Prepared for the California Water Resources Control Board.

San Joaquin River Group Authority (2011). 2010 Annual Technical Report: On Implementation and Monitoring of the San Joaquin River Agreement and the Vernalis Adaptive Management Plan (VAMP). Prepared for the California Water Resources Control Board.

San Joaquin River Group Authority (2013). 2011 Annual Technical Report: On Implementation and Monitoring of the San Joaquin River Agreement and the Vernalis Adaptive Management Plan (VAMP). Prepared for the California Water Resources Control Board.

Seber, G. A. F. (2002). The estimation of animal abundance. Second edition. Blackburn Press, Caldwell, New Jersey.

Sokal, R. R., and Rohlf, F. J. (1995). Biometry, 3rd ed. W.H. Freeman and Co., New York, NY, USA.

Townsend, R. L., J. R. Skalski, P. Dillingham, and T. W. Steig (2006). Correcting Bias in Survival Estimation Resulting from Tag Failure in Acoustic and Radiotelemetry Studies. Journal of Agricultural, Biological, and Environmental Statistics 11: 183-196.

Vogel, D. A. (2010). Evaluation of acoustic-tagged juvenile Chinook salmon movements in the Sacramento-San Joaquin delta during the 2009 Vernalis Adaptive Management Program. Technical Report for San Joaquin River Group Authority. 72 p. Available http://www.sjrg.org/technicalreport/ (accessed 13 December 2011).

Vogel, D. A. (2011). Evaluation of acoustic-tagged juvenile Chinook salmon and predatory fish movements in the Sacramento-San Joaquin Delta during the 2010 Vernalis Adaptive Management Program. Technical report for San Joaquin River Group Authority. Available http://www.sjrg.org/technicalreport/ (accessed 13 December 2011).

Figures

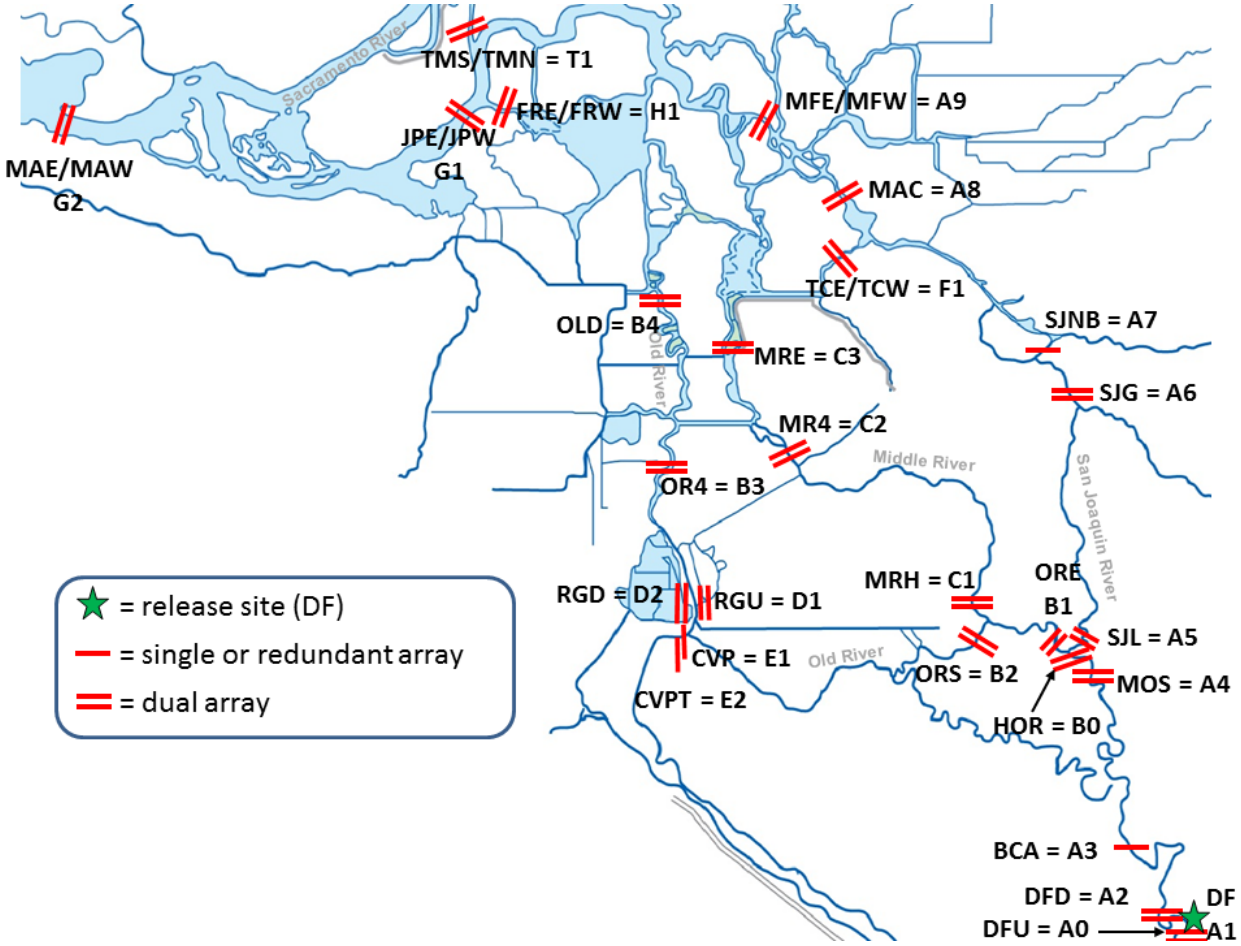

Figure 1. Locations of acoustic receivers and release site used in the 2012 OCAP steelhead study, with site code names (3- or 4-letter code) and model code (letter and number string). Site A1 is the release site at Durham Ferry. Sites B0, B4, C3, and T1 were excluded from the survival model.

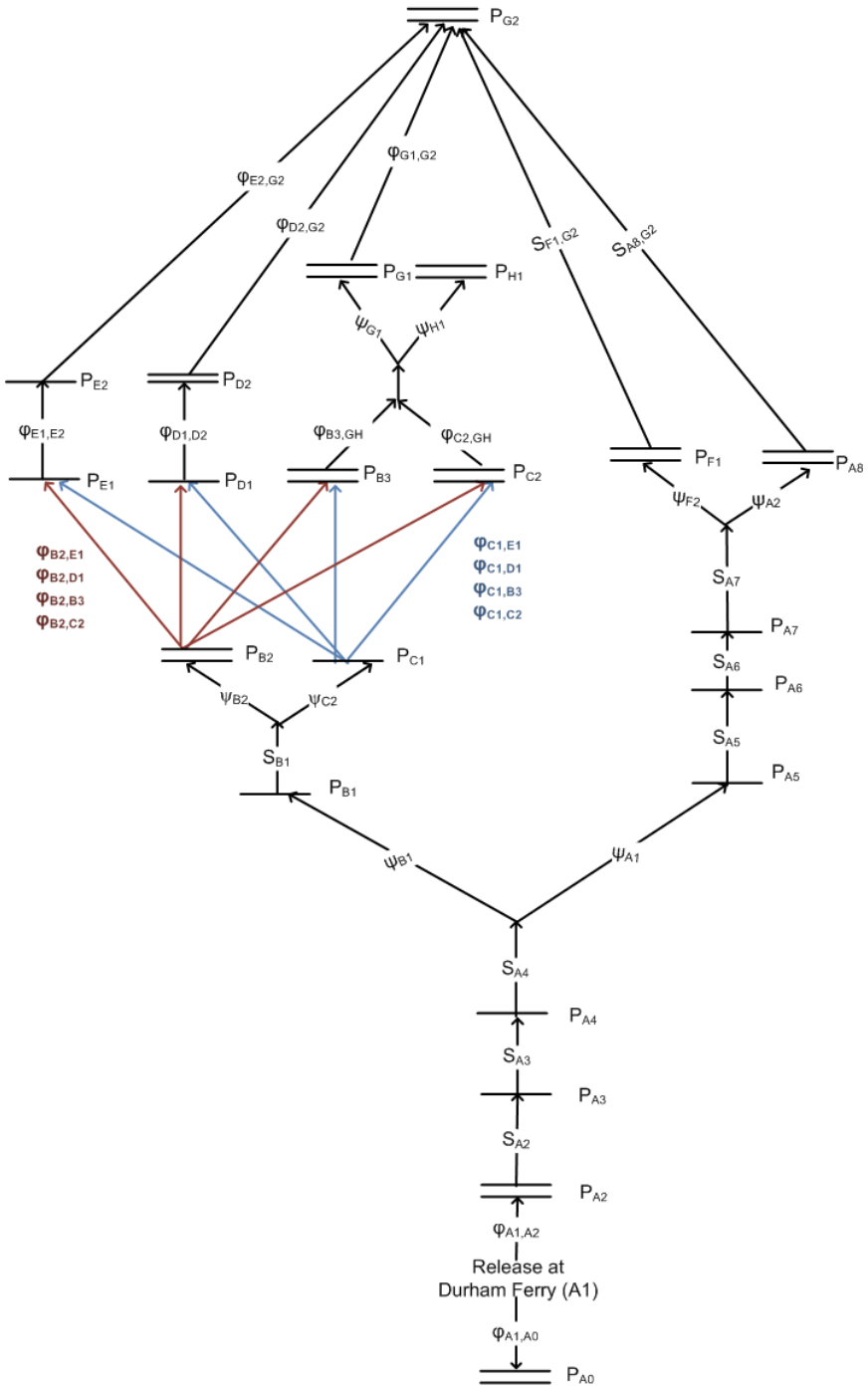

Figure 2. Schematic of 2012 mark-recapture Submodel I with estimable parameters. Single lines denote single-array or redundant double-line telemetry stations, and double lines denote dual-array telemetry stations. Names of telemetry stations correspond to site labels in Figure 1. Migration pathways to sites B3 (OR4), C2 (MR4), D1 (RGU), and E1 (CVP) are color-coded by departure site.

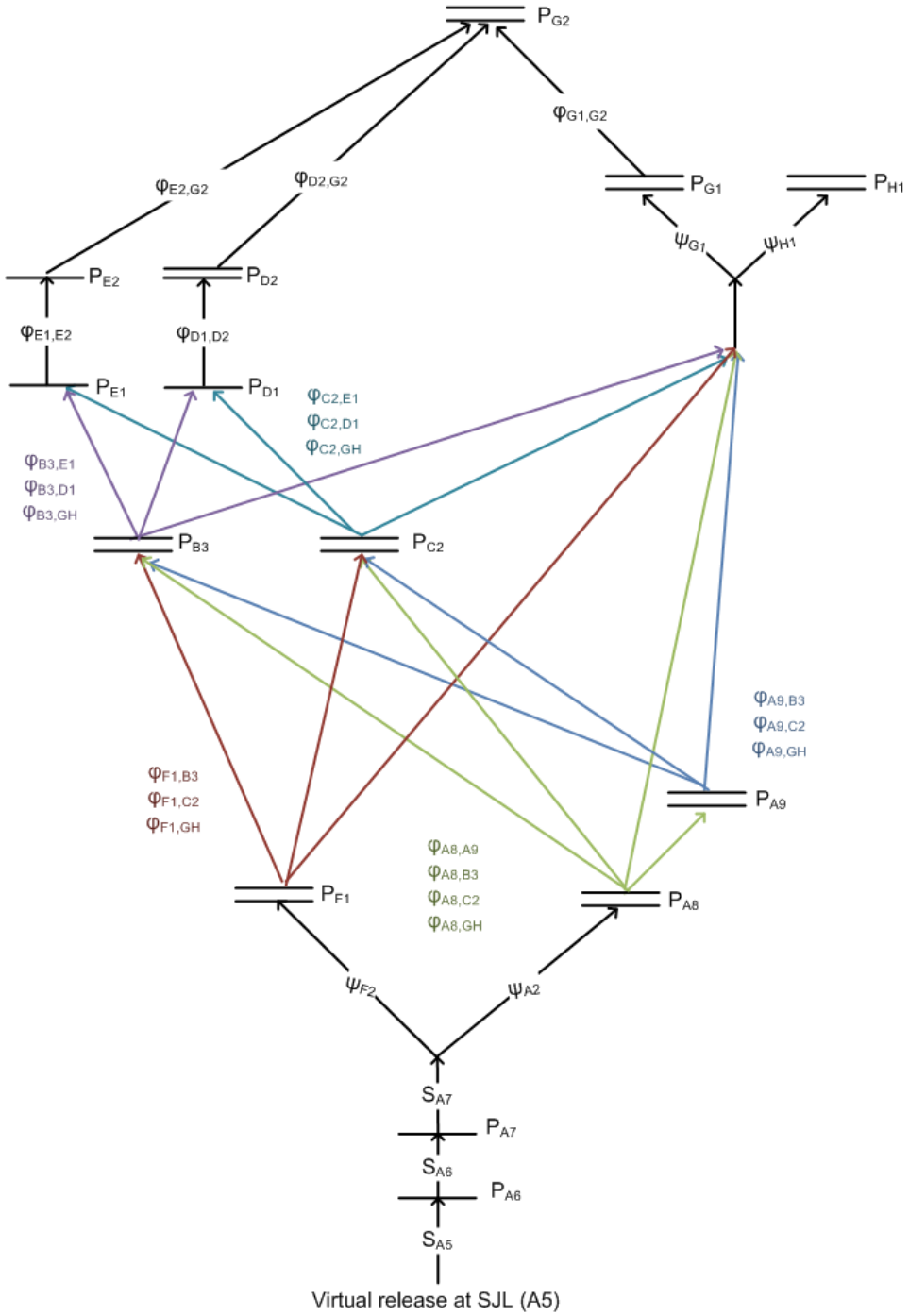

Figure 3. Schematic of 2012 mark-recapture Submodel II with estimable parameters. Single lines denote single-array or redundant double-line telemetry stations, and double lines denote dual-array telemetry stations. Names of telemetry stations correspond to site labels in Figure 1. Migration pathways to sites B3 (OR4), C2 (MR4), D1 (RGU), and E1 (CVP) are color-coded by departure site.

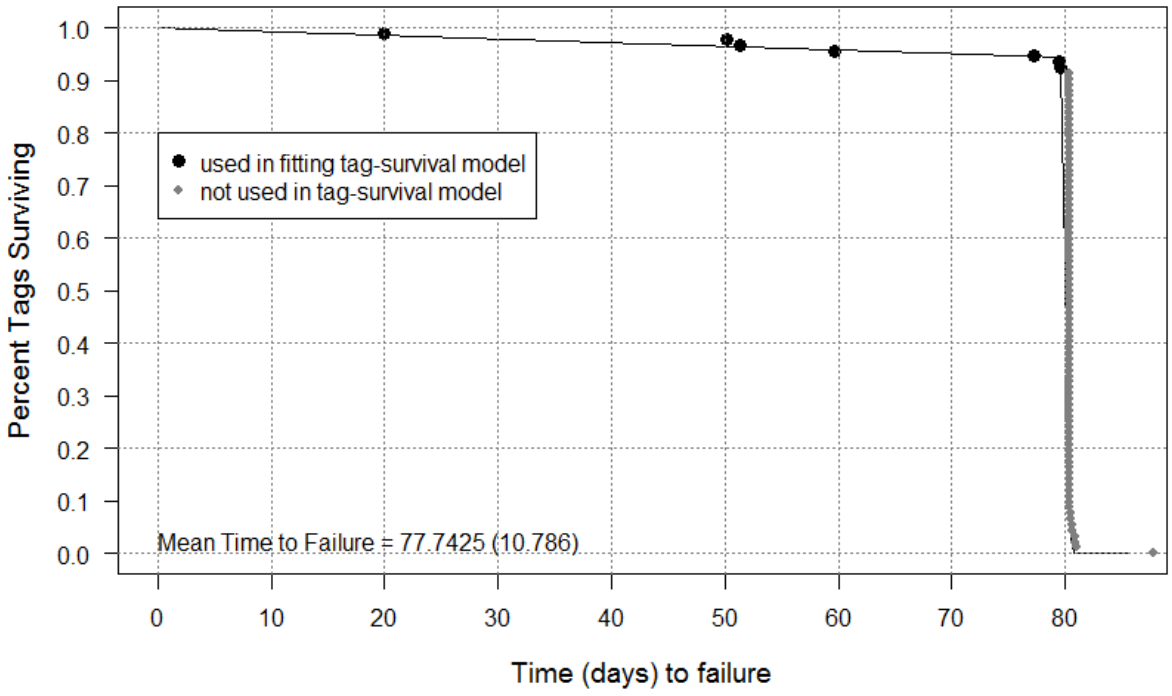

Figure 4. Observed tag failure times from the 2012 tag-life studies, pooled over the April and May studies, and fitted four-parameter vitality curve. Failure times were censored at day 80 to improve fit of the model.

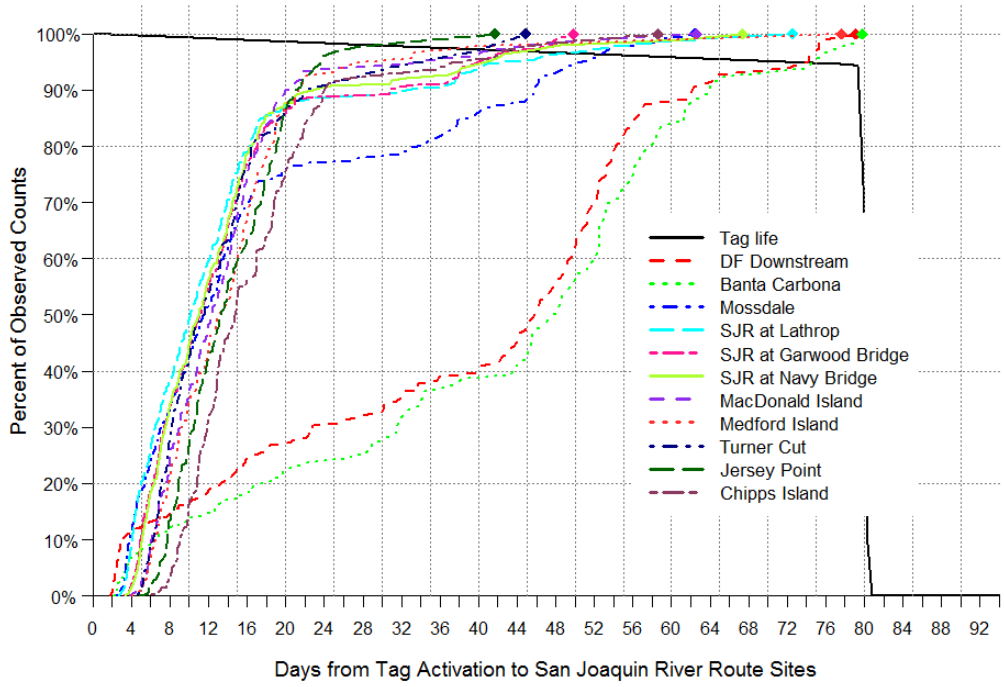

Figure 5. Four-parameter vitality survivorship curve for tag life, and the cumulative arrival timing of acoustic-tagged juvenile steelhead at receivers in the San Joaquin River route to Chipps Island in 2012, including detections that may have come from predators.

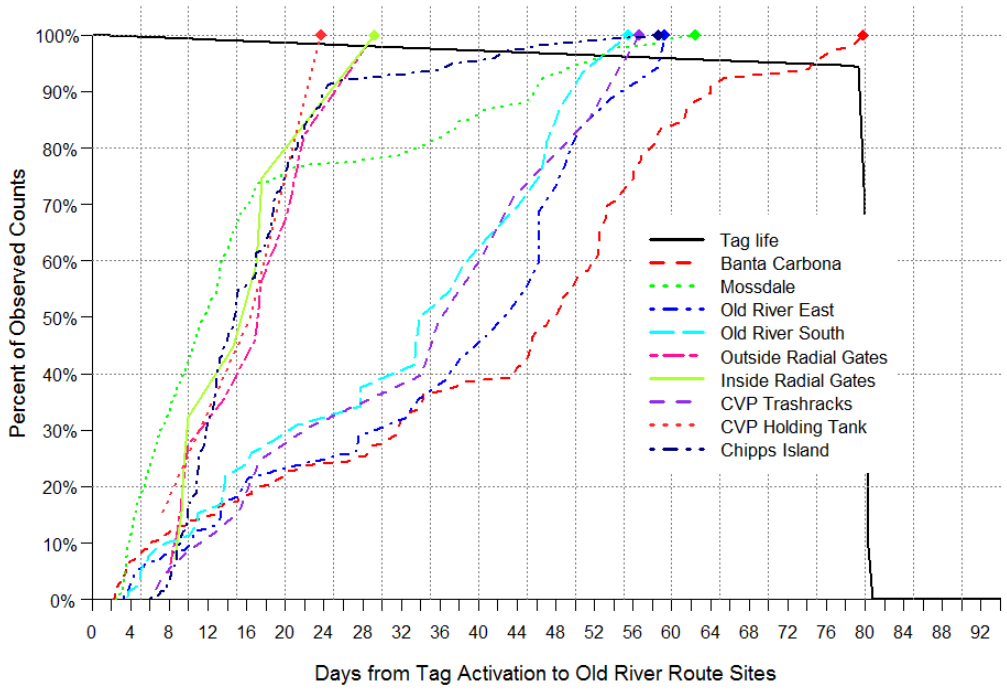

Figure 6. Four-parameter vitality survivorship curve for tag life, and the cumulative arrival timing of acoustic-tagged juvenile steelhead at receivers in the Old River route to Chipps Island in 2012, including detections that may have come from predators.

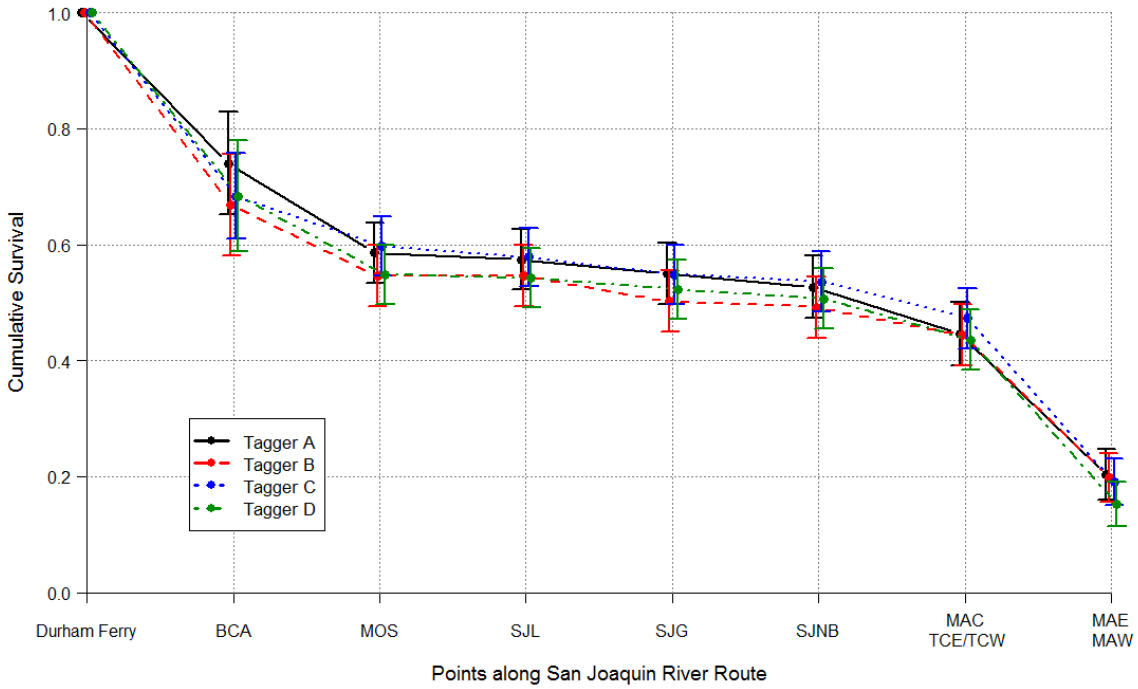

Figure 7. Cumulative survival from release at Durham Ferry to various points along the San Joaquin River route to Chipps Island, by tagger. Error bars are 95% confidence intervals.

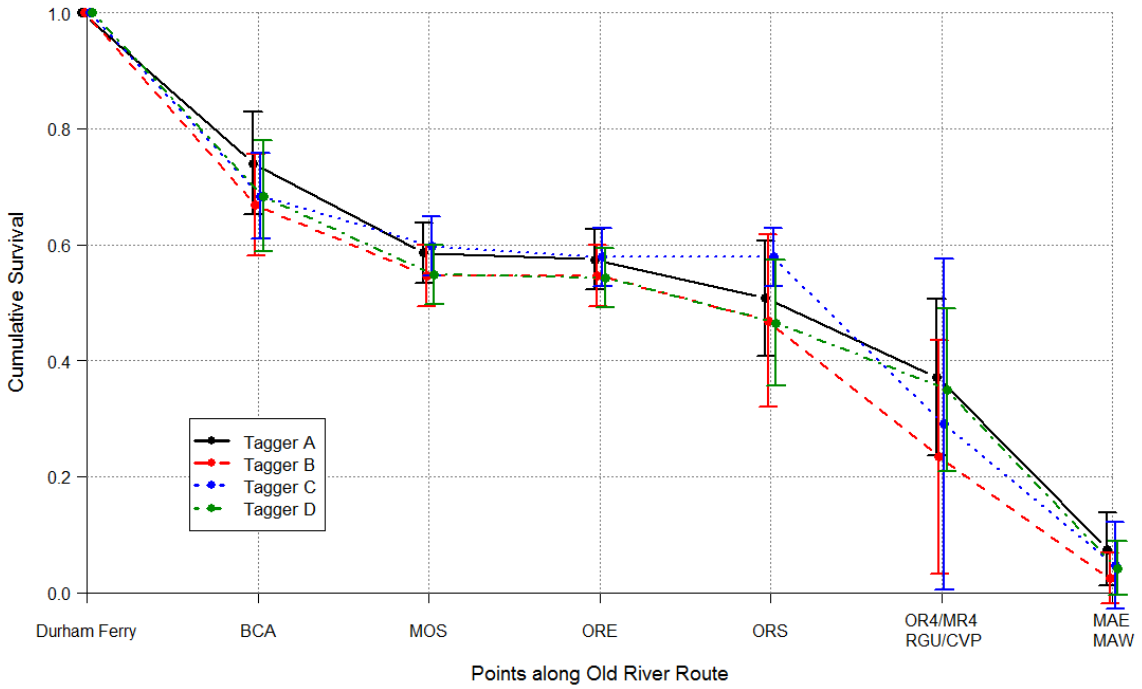

Figure 8. Cumulative survival from release at Durham Ferry to various points along the Old River route to Chipps Island, by tagger. Error bars are 95% confidence intervals.

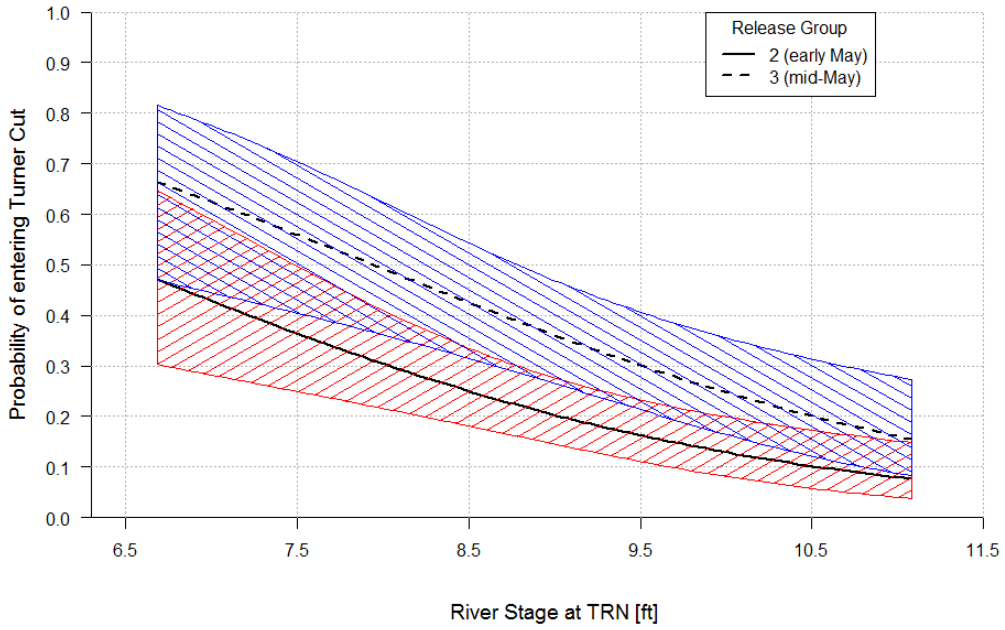

Figure 9. Fitted probability of entering Turner Cut at its junction with the San Joaquin River versus river stage measured at the TRN gaging station in Turner Cut, for change in stage (ΔC_{TRN}) = 0 ft/s, with 95% confidence bands, in 2012.

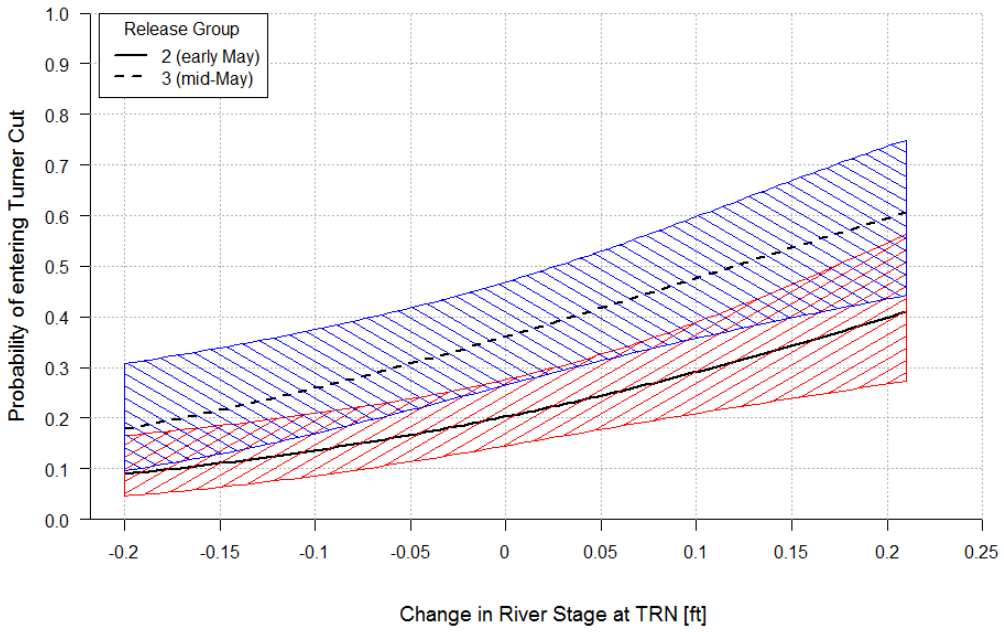

Figure 10. Fitted probability of entering Turner Cut at its junction with the San Joaquin River versus 15-minute change in river stage (ΔC_{TRN}) measured at the TRN gaging station in Turner Cut, for stage = 9 ft on arrival at the junction, with 95% confidence bands, in 2012.

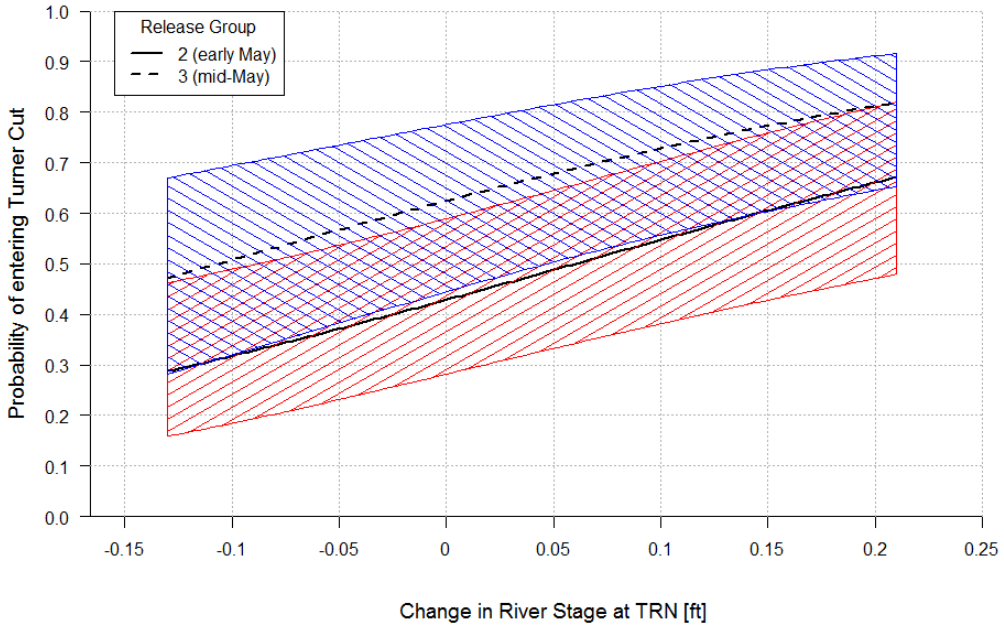

Figure 11. Fitted probability of entering Turner Cut at its junction with the San Joaquin River versus 15-minute change in river stage (ΔC_{TRN}) measured at the TRN gaging station in Turner Cut, for stage = 7 ft on arrival at the junction, with 95% confidence bands, in 2012.

RECIRC2566.

Tables

Table 1. Names and descriptions of receivers and hydrophones used in the 2012 steelhead tagging study, with receiver codes used in Figure 1, the survival model (Figures 2, 3), and in data processing by the United States Geological Survey (USGS). The release site was located at Durham Ferry.

Individual Receiver Name and Description	Hydrophone Location		Receiver Code	Survival Model Code	Data Processing Code
	Latitude (°N)	Longitude (°W)			
San Joaquin River near Durham Ferry upstream of the release site, upstream node	37.685806	121.256500	DFU1	A0a	300856
San Joaquin River near Durham Ferry upstream of the release site, downstream node	37.686444	121.256806	DFU2	A0b	300857
San Joaquin River near Durham Ferry; release site (no acoustic hydrophone located here)	37.687011	121.263448	DF	A1	
San Joaquin River near Durham Ferry downstream of the release site, upstream node	37.688222	121.276139	DFD1	A2a	300858
San Joaquin River near Durham Ferry downstream of the release site, downstream node	37.688333	121.276139	DFD2	A2b	300859
San Joaquin River near Banta Carbona	37.727722	121.298917	BCA	A3	300860
San Joaquin River near Mossdale Bridge, upstream node	37.792194	121.307278	MOSU	A4a	300861
San Joaquin River near Mossdale Bridge, downstream node	37.792356	121.307369	MOSD	A4b	300862
San Joaquin River upstream of Head of Old River, upstream node (not used in survival model)	37.805528	121.320000	HORU	B0a	300863
San Joaquin River upstream of Head of Old River, downstream node (not used in survival model)	37.805000	121.321306	HORD	B0b	300864
San Joaquin River near Lathrop, upstream	37.810875[a]	121.322500[a]	SJLU	A5a	300869/300870
San Joaquin River near Lathrop, downstream	37.810807[a]	121.321269[a]	SJLD	A5b	300871/300872
San Joaquin River near Garwood Bridge, upstream	37.934972	121.329333	SJGU	A6a	300877
San Joaquin River near Garwood Bridge, downstream	37.935194	121.329833	SJGD	A6b	300878
San Joaquin River at Stockton Navy Drive Bridge	37.946806	121.339583	SJNB	A7	300879
San Joaquin River at MacDonald Island, upstream	38.018022[a]	121.462758[a]	MACU	A8a	300899/300901
San Joaquin River at MacDonald Island, downstream	38.023877[a]	121.465916[a]	MACD	A8b	300900/300902
San Joaquin River near Medford Island, east	38.053134[a]	121.510815[a]	MFE	A9a	300903/300904
San Joaquin River near Medford Island, west	38.053773[a]	121.513315[a]	MFW	A9b	300905/300906
Old River East, near junction with San Joaquin, upstream	37.811653[a]	121.335486[a]	OREU	B1a	300865/300866

a = Average latitude and longitude given for sites with multiple hydrophones or for sites with multiple locations throughout the study

Table 1. (Continued)

Individual Receiver Name and Description	Hydrophone Location		Receiver Code	Survival Model Code	Data Processing Code
	Latitude (°N)	Longitude (°W)			
Old River East, near junction with San Joaquin, downstream	37.812284[a]	121.335558[a]	ORED	B1b	300867/300868
Old River South, upstream	37.819583	121.378111	ORSU	B2a	300873
Old River South, downstream	37.820028	121.378889	ORSD	B2b	300874
Old River at Highway 4, upstream	37.893864[a]	121.567083[a]	OR4U	B3a	300882/300883
Old River at Highway 4, downstream	37.895125[a]	121.566403[a]	OR4D	B3b	300884/300885
Old River near Empire Cut, upstream receiver (not used in survival model)	37.967125[a]	121.574514[a]	OLDU	B4a	450022
Old River near Empire Cut, downstream receiver (not used in survival model)	37.967375[a]	121.574389[a]	OLDD	B4b	450023
Middle River Head, upstream	37.824744	121.380056	MRHU	C1a	300875
Middle River Head, downstream	37.824889	121.380417	MRHD	C1b	300876
Middle River at Highway 4, upstream	37.895750	121.493861	MR4U	C2a	300881
Middle River at Highway 4, downstream	37.896222	121.492417	MR4D	C2b	300880
Middle River at Empire Cut, upstream receiver (not used in survival model)	37.941685[a]	121.533250[a]	MREU	C3a	300898/450021
Middle River at Empire Cut, downstream receiver (not used in survival model)	37.942861[a]	121.532370[a]	MRED	C3b	300897/450030
Radial Gate at Clifton Court Forebay, upstream (in entrance channel to forebay), array 1	37.830086	121.556594	RGU1	D1a	300888
Radial Gate at Clifton Court Forebay, upstream, array 2	37.829606	121.556989	RGU2	D1b	300889
Radial Gate at Clifton Court Forebay, downstream (inside forebay), array 1 in dual array	37.830147[a]	121.557528[a]	RGD1	D2a	300890/300892/ 460009/460011
Radial Gate at Clifton Court Forebay, downstream, array 2 in dual array	37.829822[a]	121.557900[a]	RGD2	D2b	300891/460010
Central Valley Project trashracks, upstream	37.816900[a]	121.558459[a]	CVPU	E1a	300894/460012
Central Valley Project trashracks, downstream	37.816647	121.558981	CVPD	E1b	300895
Central Valley Project holding tank (all holding tanks pooled)	37.815844	121.559128	CVPtank	E2	300896
Turner Cut, east (closer to San Joaquin)	37.991694	121.455389	TCE	F1a	300887
Turner Cut, west (farther from San Joaquin)	37.990472	121.456278	TCW	F1b	300886
San Joaquin River at Jersey Point, east (upstream)	38.056351[a]	121.686535[a]	JPE	G1a	300915 - 300922
San Joaquin River at Jersey Point, west (downstream)	38.055167[a]	121.688070[a]	JPW	G1b	300923 - 300930

a = Average latitude and longitude given for sites with multiple hydrophones or for sites with multiple locations throughout the study

Table 1. (Continued)

Individual Receiver Name and Description	Hydrophone Location		Receiver Code	Survival Model Code	Data Processing Code
	Latitude (°N)	Longitude (°W)			
False River, west (closer to San Joaquin)	38.056834[a]	121.671403[a]	FRW	H1a	300913/300914
False River, east (farther from San Joaquin)	38.057118[a]	121.669673[a]	FRE	H1b	300911/300912
Chipps Island (aka Mallard Island), east (upstream)	38.048772[a]	121.931198[a]	MAE	G2a	300931 - 300942
Chipps Island (aka Mallard Island), west (downstream)	38.049275[a]	121.933839[a]	MAW	G2b	300943, 300979 - 300983, 300985 - 300990
Threemile Slough, south (not used in survival model)	38.107771[a]	121.684042[a]	TMS	T1a	300909/300910
Threemile Slough, north (not used in survival model)	38.111556[a]	121.682826[a]	TMN	T1b	300907/300908

a = Average latitude and longitude given for sites with multiple hydrophones or for sites with multiple locations throughout the study

Table 2. Environmental monitoring sites used in predator decision rule and route entrainment analysis. Database = CDEC (http://cdec.water.ca.gov/) or Water Library (http://www.water.ca.gov/waterdatalibrary/).

Environmental Monitoring Site			Detection Site	Data Available					Database
Site Name	Latitude (°N)	Longitude (°W)		River Flow	Water Velocity	River Stage	Pumping	Reservoir Inflow	
CLC	37.8298	121.5574	RGU, RGD	No	No	No	No	Yes	CDEC
FAL	38.0555	121.6672	FRE/FRW	Yes	Yes	Yes	No	No	CDEC
GLC	37.8201	121.4497	ORS	Yes	Yes	Yes	No	No	CDEC
MAL	38.0428	121.9201	MAE/MAW	No	No	Yes	No	No	CDEC
MDM	37.9425	121.534	MR4, MRE	Yes	Yes	Yes	No	No	CDEC[a]
MSD	37.7860	121.3060	HOR, MOS	Yes	Yes	Yes	No	No	Water Library
ODM	37.8101	121.5419	CVP	Yes	Yes	Yes	No	No	CDEC
OH1	37.8080	121.3290	ORE	Yes	Yes	Yes	No	No	CDEC
OH4	37.8900	121.5697	OR4	Yes	Yes	Yes	No	No	CDEC
ORI	37.8280	121.5526	RGU, RGD	Yes	Yes	No	No	No	Water Library
PRI	38.0593	121.5575	MAC, MFE/MFW	Yes	Yes	Yes	No	No	CDEC
RMID040	37.8350	121.3838	MRH	No	No	Yes	No	No	Water Library
ROLD040	37.8286	121.5531	RGU, RGD	No	No	Yes	No	No	Water Library
SJG	37.9351	121.3295	SJG, SJNB	Yes	Yes	Yes	No	No	CDEC
SJJ	38.0520	121.6891	JPE/JPW	Yes	Yes	Yes	No	No	CDEC
SJL	37.8100	121.3230	SJL	Yes	Yes	Yes	No	No	Water Library
TRN	37.9927	121.4541	TCE/TCW	Yes	Yes	Yes	No	No	CDEC
TRP	37.8165	121.5596	CVP	No	No	No	Yes	No	CDEC
TSL	38.1004	121.6866	TMS/TMN	Yes	Yes	Yes	No	No	CDEC
VNS	37.6670	121.2670	DFU, DFD, BCA	Yes	No	Yes	No	No	CDEC
WCI	37.8316	121.5541	RGU, RGD	Yes	Yes	No	No	No	Water Library

a = California Water Library was used for river stage

Table 3a. Cutoff values used in predator filter in 2012. Observed values past cutoff or unmet conditions indicate a predator. See Table 3b for Flow, Water Velocity, Extra Conditions, and Comment. Footnotes refer to both this table and Table 3b.

Detection Site	Previous Site	Residence Time[a] (hr)			Migration Rate[c, d] (km/hr)		BLPS (Magnitude)	No. of Visits	No. of Cumulative Upstream Forays
		Near Field	Mid-field	Interior Delta/Facilities[b]					
		Maximum	Maximum	Maximum	Minimum	Maximum	Maximum	Maximum	Maximum
DFU	DF	500	1,000		0	4		1	0
	DFU, DFD, BCA	500	1,000		0	4		3	2
DFD	DF	500	1,000		0	4.5		1	0
	DFU, DFD	500	1,000		0	4.5		10 (15[g])	0 (2[g])
	BCA	500	1,000		0.2	4		3	2
BCA	DF	20 (1000[g])	40 (1000[g])		0	4.5	4	1	0
	DFU, DFD	20 (1000[g])	40 (1000[g])		0.1	4.5	4	3	0
	BCA	60 (1000[g])	350 (1000[g])					8	1
	MOS	1	2		0.1	4	4	2	2
MOS	DFU	50 (100[g])	100 (200[g])		0.1	6	4.5	2 (1[g])	0
	DF, DFD	50 (100[g])	100 (200[g])		0.1	6	4.5	1	0
	BCA	50 (100[g])	100 (200[g])		0	6	4.5	2	0
	MOS	25	250					3	1
	HOR	50	100		0.1	6	4.5	2	1
SJL	MOS, HOR	24	48		0.2 (0.1[g])	6	4.5	2	0
	SJL	2	236 (86[g])					2	1
	ORE	1	2		0.4	6		0	0
	SJG	0.1	10		1.5	4	4.5	2	0
SJG	SJL	30	60		0.2	6	4.5	1	0
	SJG	15	89					5	1

a = Near-field residence time includes up to 12 hours missing between detections, while mid-field residence time includes entire time lag between first and last detections without intervening detections elsewhere

b = Interior Delta residence time (Facilities residence time in parentheses) after leaving first site in Interior Delta (or Facilities, respectively)

c = Approximate migration rate calculated on most direct pathway

d = Missing values for transitions to and from same site: travel times must be 12 to 24 hours, unless otherwise specified under "Extra conditions"

g = See comments for alternate criteria

Table 3a. (Continued)

Detection Site	Previous Site	Residence Time[a] (hr)			Migration Rate[c, d] (km/hr)		BLPS (Magnitude)	No. of Visits	No. of Cumulative Upstream Forays
		Near Field	Mid-field	Interior Delta/Facilities[b]					
		Maximum	Maximum	Maximum	Minimum	Maximum	Maximum	Maximum	Maximum
SJG	SJNB	10	20		0.2	4	4.5	2	3
SJNB	SJG	30	60		0.03 (0.13[g])	6	4.5	1	0
	SJNB	15	135					2	4
	MAC, TCE/TCW	6	12		1.3 (1.1[g])	4	4.5	2	4
MAC	SJG, SJNB	30 (20[g])	70 (40[g])		0.1 (0.4[g])	6	4.5	1	0
	MAC	30 (15[g])	500					3	4
	MFE/MFW	15	30		0.5	4	4.5	3	4
	TCE/TCW	15	30		0.1	6		3	1
	MRE	15	30		0.1	4.5		1	1
MFE/MFW	SJG, SJNB, MAC, TCE/TCW	35 (20[g])	70 (40[g])		0.1 (0.4[g])	6	4.5	1	0
	MFE/MFW	10	150					2	4
	MRE	35	70		0.1	4.5		1	0
	OLD	10	20		0.1	4.5		0	0
	JPE/JPW, TMN/TMS	10	20		1.9	4	4.5	1	0
HOR	MOS	12 (100[g])	24 (200[g])		0	6	4.5	2	0
	HOR	12	250					2	1
	SJL, ORE	5	10		0.1 (0.2[g])	6	4.5	2	1
ORE	HOR	15 (10[g])	30 (20[g])		0.1	6	4.5	1	0
	ORE	3	88					3	1
	SJL	3	6		0.4	6		1	1
	ORS, MRH	1	2		0.3	4	4.5	0	0

a = Near-field residence time includes up to 12 hours missing between detections, while mid-field residence time includes entire time lag between first and last detections without intervening detections elsewhere

b = Interior Delta residence time (Facilities residence time in parentheses) after leaving first site in Interior Delta (or Facilities, respectively)

c = Approximate migration rate calculated on most direct pathway

d = Missing values for transitions to and from same site: travel times must be 12 to 24 hours, unless otherwise specified under "Extra conditions"

g = See comments for alternate criteria

Table 3a. (Continued)

Detection Site	Previous Site	Residence Time[a] (hr)			Migration Rate[c, d] (km/hr)		BLPS (Magnitude)	No. of Visits	No. of Cumulative Upstream Forays
		Near Field	Mid-field	Interior Delta/Facilities[b]					
		Maximum	Maximum	Maximum	Minimum	Maximum	Maximum	Maximum	Maximum
ORS	ORE	12	24		0.02 (0.06[g])	6	4.5	1	0
	ORS	12	220					8	1
	MRH	12	24		0.2	6		1	0
	RGU, CVP	12	24		0.3	4	4.5	2	1 (2[g])
OR4	ORS	100	200	120 (10)	0.2	4.5	4	2	0
	RGU	100	200	120 (10)	0	4.5	4	15	4
	CVP	100	200	120 (10)	0.1	4.5	4	15	4
	OR4	100	700	120 (10)				15	4
	OLD, MRE	30	60	120 (10)	0.1 (0[g])	4 (4.5[g])	4 (NA[g])	15	4
	MR4	100	200	120 (10)	0.1	4.5		4	4
OLD	SJNB	100	200		0.2	4.5		1	0
	MAC, MFE/MFW	100	200		0.1	4.5		1	0
	OR4	100	200	120 (10)	0.1	4.5	4	2	0
	OLD	100	700	120 (10)				4	0
	MRE	100	200	120 (10)	0.1	4.5		1	0
	TCE/TCW	100	200		0.1	4.5		1	0
MRH	ORE	10	20		0.03	6		1	0
	ORS	1	2		0.2	6		1	1
	MRH	1	22					0	0
MR4	ORS	15	30	120 (10)	0.1	4.5	4	1	0
	OR4, OLD	15	30	120 (10)	0.1	4.5	NA (4[g])	1	0 (1[g])

a = Near-field residence time includes up to 12 hours missing between detections, while mid-field residence time includes entire time lag between first and last detections without intervening detections elsewhere

b = Interior Delta residence time (Facilities residence time in parentheses) after leaving first site in Interior Delta (or Facilities, respectively)

c = Approximate migration rate calculated on most direct pathway

d = Missing values for transitions to and from same site: travel times must be 12 to 24 hours, unless otherwise specified under "Extra conditions"

g = See comments for alternate criteria

Table 3a. (Continued)

Detection Site	Previous Site	Residence Time[a] (hr)			Migration Rate[c, d] (km/hr)		BLPS (Magnitude)	No. of Visits	No. of Cumulative Upstream Forays
		Near Field	Mid-field	Interior Delta/Facilities[b]					
		Maximum	Maximum	Maximum	Minimum	Maximum	Maximum	Maximum	Maximum
	MR4	10	75	120 (10)				2	0
	MRE	15	30	120 (10)	0.1	4	4	1	1
	RGU	15	30	120 (10)	0.1	4.5		1	0
	CVP	15	30	120 (10)	0.1	4.5		1	0
	TCE/TCW	15	30		0.1	4.5		1	0
MRE	SJL, SJG, SJNB	50	100		0.2 (0.3[g])	4.5		1	0
	MAC, MFE/MFW	50	100		0.1	4.5		1	0
	OR4, OLD	30	60	120 (10)	0.1	4.5		1	0
	MR4	50	100	120 (10)	0.1	4.5	4	1	0
	MRE	30	160	120 (10)				4	0
	TCE/TCW	50	100		0.1	4.5		1	0
	TMN/TMS	30	60	120 (10)	0.2	4	4	1	1
RGU/RGD	ORS	80 (336[i]; 800[ij])		120 (100)	0.08	4.5	4	1	0
	CVP	80 (336[i]; 800[ij])		120 (100)	0.02	4.5	4	2	0
	OR4	80 (336[i]; 800[ij])		120 (100)	0	4	4	2	2
	MR4	10 (336[i])[k]		120 (100)	0.06	4.5		1	0
CVP	ORS	150		300	120 (100)	0.2	4.5	4	1
	CVP	100		510	180 (100)				4

a = Near-field residence time includes up to 12 hours missing between detections, while mid-field residence time includes entire time lag between first and last detections without intervening detections elsewhere

b = Interior Delta residence time (Facilities residence time in parentheses) after leaving first site in Interior Delta (or Facilities, respectively)

c = Approximate migration rate calculated on most direct pathway

d = Missing values for transitions to and from same site: travel times must be 12 to 24 hours, unless otherwise specified under "Extra conditions"

g = See comments for alternate criteria

i = If returned to Old River from Clifton Court Forebay and most detections were at RGU (not RGD)

j = If known presence at gates < 80 hours, or if present at RGU < 80% of total residence time before returning to Old River

k = Maximum residence time is 100 hours if known presence at gates < 10 hours, or 800 hours if present at RGU < 80% of total residence time before returning to Old River

Table 3a. (Continued)

Detection Site	Previous Site	Residence Time[a] (hr)			Migration Rate[c, d] (km/hr)		BLPS (Magnitude)	No. of Visits	No. of Cumulative Upstream Forays
		Near Field	Mid-field	Interior Delta/Facilities[b]					
		Maximum	Maximum	Maximum	Minimum	Maximum	Maximum	Maximum	Maximum
CVP	RGU	100 (150[g])	200 (300[g])	180 (100)	0	4	4	10 (1[g])	9 (3[g])
	OR4	100 (150[g])	200 (300[g])	180 (100)	0.1	4	4	10 (1[g])	9 (3[g])
	MR4	150	300	180 (100)	0.1	4.5		1	0
CVPtank	CVP	20	150	120 (10)	0	NA		2	3
TCE/TCW	SJNB	12	24		0.1	6	4.5	1	0
	TCE/TCW	12	106					3	4
	MAC	12	24		0.2	6		1	4
	MRE	12	24		0.2	4.5		1	4
JPE/JPW	MAC, MFE/MFW, TCE/TCW, OLD	40	80		0.2	4.5	4	1	0
	TMN/TMS	40	80		0.2	4.5	4	2	4
	CVPtank	40	80		0.2	3.4	4.5	1	0
	RGU	40	80		0	0.8	4.5	1	0
	JPE/JPW	20	80					3	0
	FRE/FRW	20	80		0.1	7		3	4
MAE/MAW	MAC, MFE/MFW, TCE/TCW, MRE	40	200		0.2	7		1	0
	CVP, CVPtank	40	200		0.2	3		1	0
	RGU/RGD	40	200		0	2		1	0
	JPE/JPW, FRE/FRW, TMN/TMS	40	200		0.2	7		2	0
	MAE/MAW	40	160					2	0
FRE/FRW	SJNB	30	80		0.2	4.5	4	1	0

a = Near-field residence time includes up to 12 hours missing between detections, while mid-field residence time includes entire time lag between first and last detections without intervening detections elsewhere

b = Interior Delta residence time (Facilities residence time in parentheses) after leaving first site in Interior Delta (or Facilities, respectively)

c = Approximate migration rate calculated on most direct pathway

d = Missing values for transitions to and from same site: travel times must be 12 to 24 hours, unless otherwise specified under "Extra conditions"

g = See comments for alternate criteria

Table 3a. (Continued)

Detection Site	Previous Site	Residence Time[a] (hr)			Migration Rate[c, d] (km/hr)		BLPS (Magnitude)	No. of Visits	No. of Cumulative Upstream Forays
		Near Field	Mid-field	Interior Delta/Facilities[b]					
		Maximum	Maximum	Maximum	Minimum	Maximum	Maximum	Maximum	Maximum
FRE/FRW	MAC, MFE/MFW, TCE/TCW, OR4, OLD, MRE	30	80		0.1	4.5	4	1	0
	TMN/TMS	30	80		0.2	4.5	4	1	0
	JPE/JPW	30	80		0.1	7		2	0
	FRE/FRW	10	80					3	0
TMN/TMS	MAC, MFE/MFW	20	100		0.2	4.5	4	1	0
	TCE/TCW	20	100		0.2	4.5	4	1	0
	OLD	20	100		0.2	4.5	4	1	0
	TMN/TMS	10	64					2	0
	JPE/JPW, FRE/FRW	20	100		0.2	4.5	4	2	4
	MAE/MAW	20	100		0.2	4.5	4	1	4

a = Near-field residence time includes up to 12 hours missing between detections, while mid-field residence time includes entire time lag between first and last detections without intervening detections elsewhere

b = Interior Delta residence time (Facilities residence time in parentheses) after leaving first site in Interior Delta (or Facilities, respectively)

c = Approximate migration rate calculated on most direct pathway

d = Missing values for transitions to and from same site: travel times must be 12 to 24 hours, unless otherwise specified under "Extra conditions"

g = See comments for alternate criteria

Table 3b. Cutoff values used in predator filter in 2012. Observed values past cutoff or unmet conditions indicate a predator. Footnotes, Extra Conditions and Comment refer to both this table and Table 3a.

		Flow[e] (cfs)		Water Velocity[e] (ft/sec)			Extra Conditions	Comment
Detection Site	Previous Site	At arrival	At departure[f]	At arrival	At departure[f]	Average during transition		
DFU	DF							
	DFU, DFD, BCA						Travel time < 600 hours from DFU	
DFD	DF						Transition from MOS not allowed	
	DFU, DFD						Travel time < 400 from DFD	Alternate values if coming from DFD
	BCA							
BCA	DF							Alternate values if next transition is downstream
	DFU, DFD						If coming from DFU: Maximum of 1 visit if next transition is downstream; Travel time < 200	Alternate values if next transition is downstream
	BCA	<12000					Maximum of 3 visits if arrival flow > 12000 cfs; Travel time < 200 (500[g])	Alternate values and known presence in detection range < 30 hours if next transition is downstream
	MOS		<5000					
MOS	DFU							Alternate values if next transition is downstream
	DF, DFD	>11000					Allow 2 visits, no minimum migration rate if arrival flow < 11000 cfs	Alternate values if next transition is downstream
	BCA	<11000					Allow 1 visit if arrival flow > 11000 cfs	Alternate values if next transition is downstream
	MOS	<14000				<2.7	Travel time < 35	
	HOR	<14000				<3		
SJL	MOS, HOR							Alternate value if coming from HOR

e = Flow or velocity condition, if any, must be violated for predator classification

f = Condition at departure from previous site

g = See comments for alternate criteria

Table 3b. (Continued)

Detection Site	Previous Site	Flow[e] (cfs) At arrival	Flow[e] (cfs) At departure[f]	Water Velocity[e] (ft/sec) At arrival	Water Velocity[e] (ft/sec) At departure[f]	Water Velocity[e] (ft/sec) Average during transition	Extra Conditions	Comment
SJL	MOS, HOR							Alternate value if coming from HOR
	SJL					<1.9	Travel time < 200 (50[g])	Alternate values if average transition water velocity outside range
	ORE							Not allowed because of barrier
	SJG					<1		Not allowed
SJG	SJL						Known presence in detection range < 12	
	SJG	<1000 (>-1000)[h]	>-1000 (<1000)[h]	<0.5 (>-0.5)[h]	>-0.5 (<0.5)[h]	<0.8	Known presence in detection range < 9	
	SJNB	<3500	<3500	<1.1	<1.1	<1.1	Known presence in detection range < 6	
SJNB	SJG	<2000 (>2000)[h]	<0.7 (>0.5)[h]				Maximum migration rate is 2 if average water velocity < -0.15 and arrival flow < 2000; known presence in detection range < 12	Alternate values for alternate flow, velocity conditions
	SJNB						Travel time < 50; known presence in detection range < 9	
	MAC, TCE/TCW							Alternate value if coming from TCE/TCW
MAC	SJG, SJNB					-0.1 to 0.4		Alternate values if average transition water velocity outside range; alternate minimum migration rate = 0.5 if coming from SJG
MAC	MAC					<0.1	Travel time < 60	Alternate values if average transition water velocity outside range

e = Flow or velocity condition, if any, must be violated for predator classification

f = Condition at departure from previous site

g = See comments for alternate criteria

h = High flow/velocity on departure requires low values on arrival (and vice versa)

Table 3b. (Continued)

Detection Site	Previous Site	Flow[e] (cfs)		Water Velocity[e] (ft/sec)			Extra Conditions	Comment
		At arrival	At departure[f]	At arrival	At departure[f]	Average during transition		
MAC	MFE/MFW			-0.8 to 0.8			Known presence in detection range < 15 (8[g])	Alternate values if arrival water velocity outside range
	TCE/TCW							
	MRE							
MFE/MFW	SJG, SJNB, MAC, TCE/TCW					-0.1 to 0.4	Maximum of 2 visits if coming from MAC	Alternate values if average transition water velocity outside range
	MFE/MFW						Travel time < 60	
	MRE		>-1500		>-0.1			
	OLD		>-1500		>-0.5			Not allowed
	JPE/JPW, TMN/TMS	<5000		<0.1		<0.1		Not allowed
HOR	MOS	<11000					Travel time < 700; 1 visit allowed and travel time < 200 if arrival flow outside range	Alternate values if next transition is downstream
	HOR	<14000				<2.7	Travel time < 35	
	SJL, ORE	<14000				<2.7 (3[g])		Alternate values if coming from ORE
ORE	HOR			<0.8				Alternate values if arrival water velocity outside range
	ORE						Travel time < 60	
	SJL	>500						
	ORS, MRH	<3000						Not allowed because of barrier
ORS	ORE					<1.8		Alternate value if average transition water velocity outside range
	ORS						Travel time < 200	
	MRH							

e = Flow or velocity condition, if any, must be violated for predator classification

f = Condition at departure from previous site

g = See comments for alternate criteria

Table 3b. (Continued)

Detection Site	Previous Site	Flow[e] (cfs)		Water Velocity[e] (ft/sec)			Extra Conditions	Comment
		At arrival	At departure[f]	At arrival	At departure[f]	Average during transition		
ORS	RGU, CVP					<1.5	Not allowed if came from lower SJR	Alternate value if coming from CVP
OR4	ORS	>-1500		>-0.5				
	RGU	>-1500		>-0.5			CCFB inflow < 3000 cfs on departure[f]	
	CVP	>-1500	>-1000	>-0.5	>-0.6		CVP pumping < 1500 cfs on departure[f]	
	OR4	<1500 (>-1500)[h]	>-1500 (<1500)[h]	<0.5 (>-0.5)[h]	>-0.5 (<0.5)[h]		Travel time < 500	
	OLD, MRE	<1500	NA (<1500[g])	<0.5	NA (<0.1[g])		Known presence in detection range < 10 hours	Alternate values if coming from MRE
	MR4							
OLD	SJNB							
	MAC, MFE/MFW							
	OR4	>-2000	>-1500	>-0.1	>-0.5			
	OLD	<1500 (>-1500)[h]	>-1500 (<1500)[h]	<0.5 (>-0.5)[h]	>-0.5 (<0.5)[h]		Travel time < 500	
	MRE							
	TCE/TCW		<200		<0.05			
MRH	ORE						Transition from MRH not allowed	
	ORS							
	MRH						Travel time < 15	Not allowed
MR4	ORS							
	OR4, OLD	<0 (2500[g])		<0 (0.25[g])				Alternate values if coming from OLD

e = Flow or velocity condition, if any, must be violated for predator classification

f = Condition at departure from previous site

g = See comments for alternate criteria

h = High flow/velocity on departure requires low values on arrival (and vice versa)

Table 3b. (Continued)

Detection Site	Previous Site	Flow[e] (cfs)		Water Velocity[e] (ft/sec)			Extra Conditions	Comment
		At arrival	At departure[f]	At arrival	At departure[f]	Average during transition		
MR4	MR4	<-5500 (>-6000)[h]	>-6000 (<-5500)[h]	<-0.5 (>-0.5)[h]	>-0.5 (<-0.5)[h]		Travel time < 30	
	MRE	<2500	<1500	<0.25	<0.1	<0.1		
	RGU						CCFB inflow < 3000 cfs on departure[f]	
	CVP						CVP pumping < 4000 cfs on departure[f]	
	TCE/TCW			<0.15	<0.1			
MRE	SJL, SJG, SJNB	<1500		<0.1			No previous entry to Interior Delta from lower SJR if coming from SJL	Alternate value if coming from SJL
	MAC, MFE/MFW	<1500		<0.1				
	OR4, OLD	>-1500 (NA[g])	>-1500 (NA[g])	>-0.1 (NA[g])	>-0.5 (NA[g])		Known presence in detection range < 10 hours	Alternate values of coming from OLD
	MR4	>-1500		>-0.1		>0		
	MRE	<1500 (>-1500)[h]	>-1500 (<1500)[h]	<0.1 (>-0.1)[h]	>-0.1 (<0.1)[h]		Travel time < 100	
	TCE/TCW	<1500	<200	<0.1	<0.05			
	TMN/TMS	<1500		<0.1		<0.25	Known presence in detection range < 10 hours	
RGU/RGD	ORS							
	CVP		>-1000		>-0.6		CVP pumping < 4000 cfs at departure[f]	
	OR4		<2000		<0.8			
	MR4							
CVP	ORS							
	CVP						CVP pumping > 1500 cfs on arrival; travel time < 100	

e = Flow or velocity condition, if any, must be violated for predator classification

f = Condition at departure from previous site

g = See comments for alternate criteria

h = High flow/velocity on departure requires low values on arrival (and vice versa)

Table 3b. (Continued)

Detection Site	Previous Site	Flow[e] (cfs)		Water Velocity[e] (ft/sec)			Extra Conditions	Comment
		At arrival	At departure[f]	At arrival	At departure[f]	Average during transition		
CVP	RGU	<3000		<1.5			Travel time < 200	Alternate values if came via lower SJR
	OR4	<3000	<2000	<1.5	<0.8		CVP pumping > 1500 cfs on arrival	Alternate values if came from lower SJR
	MR4							
CVPtank	CVP						Travel time < 100	
TCE/TCW	SJNB			<0.1				
	TCE/TCW	<1500 (>-1500)[h]	>-1500 (<1500)[h]	<0.3 (>-0.3)[h]	>-0.3 (<0.3)[h]		Travel time < 60	
	MAC			<0.1		<0.1		
	MRE	>-500	>-1000	>-0.1	>-0.1	>-0.2		
JPE/JPW	MAC, MFE/MFW, TCE/TCW, OLD							
	TMN/TMS							
	CVPtank						Maximum travel time is 2 from CVPtank	Trucking release sites are downstream of JPE/JPW
	RGU						Maximum travel time is 300 from RGU	Trucking release sites are downstream of JPE/JPW
	JPE/JPW						Travel time < 50	
	FRE/FRW							
MAE/MAW	MAC, MFE/MFW, TCE/TCW, MRE						Not allowed if prior entry to Interior Delta from lower SJR	
	CVP, CVPtank							
	RGU/RGD							
	JPE/JPW, FRE/FRW, TMN/TMS							
	MAE/MAW						Travel time < 40	

e = Flow or velocity condition, if any, must be violated for predator classification

f = Condition at departure from previous site

h = High flow/velocity on departure requires low values on arrival (and vice versa)

Table 3b. (Continued)

Detection Site	Previous Site	Flow[e] (cfs) At arrival	Flow[e] (cfs) At departure[f]	Water Velocity[e] (ft/sec) At arrival	Water Velocity[e] (ft/sec) At departure[f]	Water Velocity[e] (ft/sec) Average during transition	Extra Conditions	Comment
FRE/FRW	SJNB						Not allowed if prior entry to Interior Delta from lower SJR	
	MAC, MFE/MFW, TCE/TCW, OR4, OLD, MRE							
	TMN/TMS							
	JPE/JPW							
	FRE/FRW							
TMN/TMS	MAC, MFE/MFW		>-50000		> -1		Not allowed if prior transition to facilities from lower SJR	
	TCE/TCW						Not allowed if prior transition to facilities from lower SJR	
	OLD		> 0		> 0		Not allowed if prior transition to facilities from lower SJR	
	TMN/TMS	<0 (>0)[h]	>0 (<0)[h]	<0 (>0)[h]	>0 (<0)[h]			
	JPE/JPW, FRE/FRW							
	MAE/MAW							

e = Flow or velocity condition, if any, must be violated for predator classification

f = Condition at departure from previous site

h = High flow/velocity on departure requires low values on arrival (and vice versa)

Table 4. Number of tags from each release group that were detected after release in 2012, including predator-type detections and detections omitted from the survival analysis.

Release Group	1	2	3	Total
Number Released	477	478	480	1,435
Number Detected	425	392	370	1,187
Number Detected Downstream	408	372	324	1,104
Number Detected Upstream of Study Area	323	144	314	781
Number Detected in Study Area	333	318	189	840
Number Detected in San Joaquin River Route	306	306	164	776
Number Detected in Old River Route	21	11	26	58
Number Assigned to San Joaquin River Route	304	297	150	751
Number Assigned to Old River Route	20	11	17	48

Table 5. Number of tags observed from each release group at each detection site in 2012, including predator-type detections. Routes (SJR = San Joaquin River, OR = Old River) represent route assignment at the head of Old River. Pooled counts are summed over all receivers in array and all routes. Route could not be identified for some tags.

Detection Site	Site Code	Survival Model Code	Release Group			Total
			1	2	3	
Release site at Durham Ferry			477	478	480	1,435
Durham Ferry Upstream	DFU	A0	32	35	152	219
Durham Ferry Downstream	DFD	A2	288	84	159	531
Banta Carbona	BCA	A3	71	52	178	301
Mossdale	MOS	A4	333	318	189	840
Head of Old River	HOR	B0	332	313	177	822
Lathrop	SJL	A5	306	306	164	776
Garwood Bridge	SJG	A6	288	286	150	724
Navy Drive Bridge	SJNB	A7	273	278	142	693
MacDonald Island Upstream	MACU	A8a	198	197	94	489
MacDonald Island Downstream	MACD	A8b	194	188	89	471
MacDonald Island	MAC	A8	202	198	96	496
Medford Island East	MFE	A9a	125	130	67	322
Medford Island West	MFW	A9b	121	131	68	320
Medford Island (Pooled)	MFE/MFW	A9	126	132	68	326
Turner Cut East	TCE	F1a	25	64	54	143
Turner Cut West	TCW	F1b	14	61	56	131
Turner Cut (Pooled)	TCE/TCW	F1	32	64	56	152
Old River East	ORE	B1	21	11	26	58
Old River South Upstream	ORSU	B2a	21	10	18	49
Old River South Downstream	ORSD	B2b	21	3	0	24
Old River South (Pooled)	ORS	B2	21	10	18	49
Old River at Highway 4, Upstream	OR4U	B3a	38	16	18	72
Old River at Highway 4, Downstream	OR4D	B3b	38	15	18	71
Old River at Highway 4, SJR Route	OR4	B3	33	15	17	65
Old River at Highway 4, OR Route	OR4	B3	5	1	0	6
Old River at Highway 4 (Pooled)	OR4	B3	38	16	18	72
Old River near Empire Cut, Upstream	OLDU	B4a	29	16	10	55
Old River near Empire Cut, Downstream	OLDD	B4b	0	0	0	0
Old River near Empire Cut, SJR Route	OLD	B4	29	16	9	54
Old River near Empire Cut, OR Route	OLD	B4	0	0	1	1
Old River near Empire Cut (Pooled)	OLD	B4	29	16	10	55
Middle River Head	MRH	C1	1	0	2	3
Middle River at Highway 4, Upstream	MR4U	C2a	11	19	11	41
Middle River at Highway 4, Downstream	MR4D	C2b	13	21	11	45

Table 5. (Continued)

Detection Site	Site Code	Survival Model Code	Release Group 1	2	3	Total
Middle River at Highway 4, SJR Route	MR4	C2	12	21	9	42
Middle River at Highway 4, OR Route	MR4	C2	1	0	1	2
Middle River at Highway 4 (Pooled)	MR4	C2	13	21	11	45
Middle River near Empire Cut, Upstream	MREU	C3a	71	60	46	177
Middle River near Empire Cut, Downstream	MRED	C3b	1	59	41	101
Middle River near Empire Cut, SJR Route	MRE	C3	71	60	44	175
Middle River near Empire Cut, OR Route	MRE	C3	0	0	1	1
Middle River near Empire Cut (Pooled)	MRE	C3	71	60	46	177
Radial Gates Upstream: SJR Route	RGU	D1	7	8	11	26
Radial Gates Upstream: OR Route	RGU	D1	7	4	1	12
Radial Gates Upstream	RGU	D1	14	12	13	39
Radial Gates Downstream #1	RGD1	D2a	8	8	11	27
Radial Gates Downstream #2	RGD2	D2b	7	7	11	25
Radial Gates Downstream: SJR Route	RGD	D2	5	4	10	19
Radial Gates Downstream: OR Route	RGD	D2	3	4	1	8
Radial Gates Downstream (Pooled)	RGD	D2	8	8	11	27
CVP Trashrack: SJR Route	CVP	E1	21	19	13	53
CVP Trashrack: OR Route	CVP	E1	14	4	4	22
Central Valley Project Trashrack	CVP	E1	35	23	18	76
CVP tank: SJR Route	CVPtank	E2	4	9	2	15
CVP tank: OR Route	CVPtank	E2	2	0	1	3
Central Valley Project Holding Tank	CVPtank	E2	6	9	3	18
Threemile Slough South	TMS	T1a	20	24	6	50
Threemile Slough North	TMN	T1b	18	25	3	46
Threemile Slough (Pooled)	TMS/TMN	T1	21	25	6	52
Jersey Point East	JPE	G1a	101	121	57	279
Jersey Point West	JPW	G1b	96	112	57	265
Jersey Point: SJR Route	JPE/JPW	G1	103	125	62	290
Jersey Point: OR Route	JPE/JPW	G1	0	0	0	0
Jersey Point (Pooled)	JPE/JPW	G1	103	125	62	290
False River West	FRW	H1a	37	46	23	106
False River East	FRE	H1b	36	39	19	94
False River: SJR Route	FRE/FRW	H1	40	49	23	112
False River: OR Route	FRE/FRW	H1	0	0	0	0
False River (Pooled)	FRE/FRW	H1	40	49	23	112

Table 5. (Continued)

Detection Site	Site Code	Survival Model Code	Release Group			Total
			1	2	3	
Chipps Island East	MAE	G2a	86	105	47	238
Chipps Island West	MAW	G2b	89	103	51	243
Chipps Island: SJR Route	MAE/MAW	G2	88	109	55	252
Chipps Island: OR Route	MAE/MAW	G2	3	1	0	4
Chipps Island (Pooled)	MAE/MAW	G2	91	110	55	256

Table 6. Number of tags observed from each release group at each detection site in 2012 and used in the survival analysis, including predator-type detections. Pooled counts are summed over all receivers in array. Route could not be identified for some tags.

Detection Site	Site Code	Survival Model Code	Release Group			Total
			1	2	3	
Release site at Durham Ferry			477	478	480	1,435
Durham Ferry Upstream	DFU	A0	21	27	92	140
Durham Ferry Downstream	DFD	A2	281	77	107	465
Banta Carbona	BCA	A3	71	51	157	279
Mossdale	MOS	A4	329	315	173	817
Lathrop	SJL	A5	304	297	150	751
Garwood Bridge	SJG	A6	288	284	144	716
Navy Drive Bridge	SJNB	A7	273	271	134	678
MacDonald Island Upstream	MACU	A8a	185	176	82	443
MacDonald Island Downstream	MACD	A8b	186	176	79	441
MacDonald Island	MAC	A8	194	181	84	459
Medford Island East	MFE	A9a	116	126	65	307
Medford Island West	MFW	A9b	113	126	66	305
Medford Island (Pooled)	MFE/MFW	A9	118	127	66	311
Turner Cut East	TCE	F1a	24	58	48	130
Turner Cut West	TCW	F1b	13	57	50	120
Turner Cut (Pooled)	TCE/TCW	F1	30	58	50	138
Old River East	ORE	B1	20	11	17	48
Old River South Upstream	ORSU	B2a	20	9	13	42
Old River South Downstream	ORSD	B2b	20	2	0	22
Old River South (Pooled)	ORS	B2	20	9	13	42
Old River at Highway 4, Upstream	OR4U	B3a	33	13	16	62
Old River at Highway 4, Downstream	OR4D	B3b	33	12	16	61
Old River at Highway 4, SJR Route	OR4	B3	31	13	16	60
Old River at Highway 4, OR Route	OR4	B3	2	0	0	2
Old River at Highway 4 (Pooled)	OR4	B3	33	13	16	62
Middle River Head	MRH	C1	0	0	2	2
Middle River at Highway 4, Upstream	MR4U	C2a	6	17	8	31
Middle River at Highway 4, Downstream	MR4D	C2b	7	18	7	31
Middle River at Highway 4, SJR Route	MR4	C2	7	18	8	33
Middle River at Highway 4, OR Route	MR4	C2	1	0	1	2
Middle River at Highway 4 (Pooled)	MR4	C2	7	18	8	33
Radial Gates Upstream: SJR Route	RGU	D1	6	4	10	20

Table 6. (Continued)

Detection Site	Site Code	Survival Model Code	Release Group			Total
			1	2	3	
Radial Gates Upstream: OR Route	RGU	D1	6	4	1	11
Radial Gates Upstream	RGU	D1	12	8	11	31
Radial Gates Downstream #1	RGD1	D2a	8	8	11	27
Radial Gates Downstream #2	RGD2	D2b	7	7	11	25
Radial Gates Downstream: SJR Route	RGD	D2	5	4	10	19
Radial Gates Downstream: OR Route	RGD	D2	3	4	1	8
Radial Gates Downstream (Pooled)	RGD	D2	8	8	11	27
CVP Trashrack: SJR Route	CVP	E1	14	17	9	40
CVP Trashrack: OR Route	CVP	E1	9	2	4	15
Central Valley Project Trashrack	CVP	E1	23	19	13	55
CVP tank: SJR Route	CVPtank	E2	4	9	2	15
CVP tank: OR Route	CVPtank	E2	2	0	1	3
Central Valley Project Holding Tank	CVPtank	E2	6	9	3	18
Jersey Point East	JPE	G1a	90	112	55	257
Jersey Point West	JPW	G1b	87	102	56	245
Jersey Point: SJR Route	JPE/JPW	G1	94	116	61	271
Jersey Point: OR Route	JPE/JPW	G1	0	0	0	0
Jersey Point (Pooled)	JPE/JPW	G1	94	116	61	271
False River West	FRW	H1a	2	6	1	9
False River East	FRE	H1b	0	3	1	4
False River: SJR Route	FRE/FRW	H1	2	7	1	10
False River: OR Route	FRE/FRW	H1	0	0	0	0
False River (Pooled)	FRE/FRW	H1	2	7	1	10
Chipps Island East	MAE	G2a	85	104	46	234
Chipps Island West	MAW	G2b	89	101	51	241
Chipps Island: SJR Route	MAE/MAW	G2	88	108	55	251
Chipps Island: OR Route	MAE/MAW	G2	3	1	0	4
Chipps Island (Pooled)	MAE/MAW	G2	91	109	55	255

Table 7. Number of tags from each release group in 2012 first classified as in a predator at each detection site, based on the predator filter.

Detection Site and Code			Durham Ferry Release Groups							
			Classified as Predator on Arrival at Site				Classified as Predator on Departure from Site			
Detection Site	Site Code	Survival Model Code	1	2	3	Total	1	2	3	Total
Durham Ferry Upstream	DFU	A0	4	12	46	62	0	0	6	6
Durham Ferry Downstream	DFD	A2	7	10	39	56	0	0	0	0
Banta Carbona	BCA	A3	2	9	22	33	0	1	4	5
Mossdale	MOS	A4	2	2	1	5	0	0	0	0
Head of Old River	HOR	B0	2	2	4	8	1	0	0	1
Lathrop	SJL	A5	2	1	0	3	3	0	1	4
Garwood Bridge	SJG	A6	2	4	2	8	1	3	2	6
Navy Drive Bridge	SJNB	A7	0	4	2	6	4	0	1	5
MacDonald Island	MAC	A8	1	0	0	1	3	1	0	4
Medford Island	MFE/MFW	A9	1	0	1	2	0	0	0	0
Old River East	ORE	B1	0	0	3	3	0	0	0	0
Old River South	ORS	B2	1	0	1	2	0	0	0	0
Old River at Highway 4	OR4	B3	5	1	0	6	1	0	0	1
Old River near Empire Cut	OLD	B4	3	1	0	4	0	0	0	0
Middle River Head	MRH	C1	1	0	0	1	0	0	0	0
Middle River at Highway 4	MR4	C2	1	1	2	4	0	0	0	0
Middle River near Empire Cut	MRE	C3	0	0	0	0	1	1	1	3
Radial Gates Upstream	RGU	D1	0	0	1	1	3	4	0	7
Radial Gates Downstream	RGD	D2	0	0	0	0	0	0	0	0
Central Valley Project Trashrack	CVP	E1	4	1	2	7	0	2	1	3
Central Valley Project Holding Tank	CVPtank	E2	0	1	0	1	0	0	0	0
Turner Cut	TCE/TCW	F1	0	0	2	2	0	0	0	0
Jersey Point	JPE/JPW	G1	1	1	0	2	1	0	0	1
Chipps Island	MAE/MAW	G2	0	1	0	1	0	0	0	0
False River	FRE/FRW	H1	0	1	0	1	0	0	0	0
Threemile Slough	TMS/TMN	T1	0	0	0	0	0	0	0	0
Total Tags			39	52	128	219	18	12	16	46

Table 8. Number of tags from each release group that were detected after release in 2012, excluding predator-type detections, and including detections omitted from the survival analysis.

Release Group	1	2	3	Total
Number Released	477	478	480	1,435
Total Number Detected	422	380	337	1,139
Total Number Detected Downstream	405	360	280	1,045
Total Number Detected Upstream of Study Area	319	133	278	730
Total Number Detected in Study Area	333	312	176	821
Number Detected in San Joaquin River Route	306	301	161	768
Number Detected in Old River Route	21	8	13	42
Number Assigned to San Joaquin River Route	306	300	153	759
Number Assigned to Old River Route	21	8	13	42

Table 9. Number of tags observed from each release group at each detection site in 2012, excluding predator-type detections. Routes (SJR = San Joaquin River, OR = Old River) represent route assignment at the head of Old River. Pooled counts are summed over all receivers in array and all routes. Route could not be identified for some tags.

Detection Site	Site Code	Survival Model Code	Release Group			Total
			1	2	3	
Release site at Durham Ferry			477	478	480	1,435
Durham Ferry Upstream	DFU	A0	30	27	118	175
Durham Ferry Downstream	DFD	A2	285	78	109	472
Banta Carbona	BCA	A3	67	44	144	255
Mossdale	MOS	A4	333	312	176	921
Head of Old River	HOR	B0	332	308	167	807
Lathrop	SJL	A5	306	301	161	768
Garwood Bridge	SJG	A6	283	285	150	718
Navy Drive Bridge	SJNB	A7	269	275	139	683
MacDonald Island Upstream	MACU	A8a	191	196	92	479
MacDonald Island Downstream	MACD	A8b	188	187	87	462
MacDonald Island	MAC	A8	195	197	94	486
Medford Island East	MFE	A9a	121	130	66	317
Medford Island West	MFW	A9b	117	131	67	315
Medford Island (Pooled)	MFE/MFW	A9	122	132	67	321
Turner Cut East	TCE	F1a	25	63	53	141
Turner Cut West	TCW	F1b	14	60	55	129
Turner Cut (Pooled)	TCE/TCW	F1	32	63	55	150
Old River East	ORE	B1	21	8	13	42
Old River South Upstream	ORSU	B2a	20	8	10	38
Old River South Downstream	ORSD	B2b	20	3	0	23
Old River South (Pooled)	ORS	B2	20	8	10	38
Old River at Highway 4, Upstream	OR4U	B3a	34	15	18	67
Old River at Highway 4, Downstream	OR4D	B3b	34	14	18	66
Old River at Highway 4, SJR Route	OR4	B3	29	14	18	61
Old River at Highway 4, OR Route	OR4	B3	5	1	0	6
Old River at Highway 4 (Pooled)	OR4	B3	34	15	18	67
Old River near Empire Cut, Upstream	OLDU	B4a	26	15	9	50
Old River near Empire Cut, Downstream	OLDD	B4b	0	0	0	0
Old River near Empire Cut, SJR Route	OLD	B4	26	15	9	50
Old River near Empire Cut, OR Route	OLD	B4	0	0	0	0
Old River near Empire Cut (Pooled)	OLD	B4	26	15	9	50
Middle River Head	MRH	C1	1	0	0	1
Middle River at Highway 4, Upstream	MR4U	C2a	11	18	8	37
Middle River at Highway 4, Downstream	MR4D	C2b	12	20	8	40

Table 9. (Continued)

Detection Site	Site Code	Survival Model Code	Release Group 1	2	3	Total
Middle River at Highway 4, SJR Route	MR4	C2	11	20	8	39
Middle River at Highway 4, OR Route	MR4	C2	1	0	0	1
Middle River at Highway 4 (Pooled)	MR4	C2	12	20	8	40
Middle River near Empire Cut, Upstream	MREU	C3a	71	59	45	175
Middle River near Empire Cut, Downstream	MRED	C3b	1	58	40	99
Middle River near Empire Cut, SJR Route	MRE	C3	71	59	45	175
Middle River near Empire Cut, OR Route	MRE	C3	0	0	0	0
Middle River near Empire Cut (Pooled)	MRE	C3	71	59	45	175
Radial Gates Upstream: SJR Route	RGU	D1	7	7	10	24
Radial Gates Upstream: OR Route	RGU	D1	7	4	1	12
Radial Gates Upstream	RGU	D1	14	11	11	36
Radial Gates Downstream #1	RGD1	D2a	6	7	10	23
Radial Gates Downstream #2	RGD2	D2b	6	6	10	22
Radial Gates Downstream: SJR Route	RGD	D2	3	3	9	15
Radial Gates Downstream: OR Route	RGD	D2	3	4	1	8
Radial Gates Downstream (Pooled)	RGD	D2	6	7	10	23
CVP Trashrack: SJR Route	CVP	E1	19	19	13	51
CVP Trashrack: OR Route	CVP	E1	13	3	2	18
Central Valley Project Trashrack	CVP	E1	32	22	15	69
CVP tank: SJR Route	CVPtank	E2	3	8	2	13
CVP tank: OR Route	CVPtank	E2	2	0	1	3
Central Valley Project Holding Tank	CVPtank	E2	5	8	3	16
Threemile Slough South	TMS	T1a	18	23	6	47
Threemile Slough North	TMN	T1b	16	24	3	43
Threemile Slough (Pooled)	TMS/TMN	T1	19	24	6	49
Jersey Point East	JPE	G1a	95	120	57	272
Jersey Point West	JPW	G1b	91	111	57	259
Jersey Point: SJR Route	JPE/JPW	G1	97	124	62	283
Jersey Point: OR Route	JPE/JPW	G1	0	0	0	0
Jersey Point (Pooled)	JPE/JPW	G1	97	124	62	283
False River West	FRW	H1a	34	46	23	103
False River East	FRE	H1b	33	39	19	91
False River: SJR Route	FRE/FRW	H1	37	49	23	109
False River: OR Route	FRE/FRW	H1	0	0	0	0
False River (Pooled)	FRE/FRW	H1	37	49	23	109

Table 9. (Continued)

Detection Site	Site Code	Survival Model Code	Release Group			Total
			1	2	3	
Chipps Island East	MAE	G2a	83	104	47	234
Chipps Island West	MAW	G2b	86	102	51	239
Chipps Island: SJR Route	MAE/MAW	G2	86	108	55	249
Chipps Island: OR Route	MAE/MAW	G2	2	1	0	3
Chipps Island (Pooled)	MAE/MAW	G2	88	109	55	252

Table 10. Number of tags observed from each release group at each detection site in 2012 and used in the survival analysis, excluding predator-type detections. Pooled counts are summed over all receivers in array. Route could not be identified for some tags.

Detection Site	Site Code	Survival Model Code	Release Group			Total
			1	2	3	
Release site at Durham Ferry			477	478	480	1,435
Durham Ferry Upstream	DFU	A0	18	22	83	123
Durham Ferry Downstream	DFD	A2	280	75	82	437
Banta Carbona	BCA	A3	67	44	130	241
Mossdale	MOS	A4	333	311	170	814
Lathrop	SJL	A5	306	300	153	759
Garwood Bridge	SJG	A6	283	285	150	718
Navy Drive Bridge	SJNB	A7	269	273	137	679
MacDonald Island Upstream	MACU	A8a	178	179	85	442
MacDonald Island Downstream	MACD	A8b	181	179	81	441
MacDonald Island	MAC	A8	187	184	87	458
Medford Island East	MFE	A9a	114	126	65	305
Medford Island West	MFW	A9b	110	126	66	302
Medford Island (Pooled)	MFE/MFW	A9	115	127	66	308
Turner Cut East	TCE	F1a	24	58	50	132
Turner Cut West	TCW	F1b	14	57	52	123
Turner Cut (Pooled)	TCE/TCW	F1	31	58	52	141
Old River East	ORE	B1	21	8	13	42
Old River South Upstream	ORSU	B2a	20	7	10	37
Old River South Downstream	ORSD	B2b	20	2	0	22
Old River South (Pooled)	ORS	B2	20	7	10	37
Old River at Highway 4, Upstream	OR4U	B3a	31	14	18	63
Old River at Highway 4, Downstream	OR4D	B3b	31	13	18	62
Old River at Highway 4, SJR Route	OR4	B3	29	14	18	61
Old River at Highway 4, OR Route	OR4	B3	2	0	0	2
Old River at Highway 4 (Pooled)	OR4	B3	61	14	18	63
Middle River Head	MRH	C1	1	0	0	1
Middle River at Highway 4, Upstream	MR4U	C2a	6	16	7	29
Middle River at Highway 4, Downstream	MR4D	C2b	7	17	7	31
Middle River at Highway 4, SJR Route	MR4	C2	6	17	7	30
Middle River at Highway 4, OR Route	MR4	C2	1	0	0	1
Middle River at Highway 4 (Pooled)	MR4	C2	7	17	7	31
Radial Gates Upstream: SJR Route	RGU	D1	6	3	10	19
Radial Gates Upstream: OR Route	RGU	D1	6	4	1	11
Radial Gates Upstream	RGU	D1	12	7	11	30
Radial Gates Downstream #1	RGD1	D2a	6	7	10	23

Table 10. (Continued)

Detection Site	Site Code	Survival Model Code	Release Group 1	2	3	Total
Radial Gates Downstream #2	RGD2	D2b	6	6	10	22
Radial Gates Downstream: SJR Route	RGD	D2	3	3	9	15
Radial Gates Downstream: OR Route	RGD	D2	3	3	9	15
Radial Gates Downstream (Pooled)	RGD	D2	3	4	1	8
CVP Trashrack: SJR Route	CVP	E1	18	18	10	46
CVP Trashrack: OR Route	CVP	E1	8	1	2	11
Central Valley Project Trashrack	CVP	E1	26	19	12	57
CVP tank: SJR Route	CVPtank	E2	3	8	2	13
CVP tank: OR Route	CVPtank	E2	2	0	1	3
Central Valley Project Holding Tank	CVPtank	E2	5	8	3	16
Jersey Point East	JPE	G1a	88	113	55	256
Jersey Point West	JPW	G1b	85	103	56	244
Jersey Point: SJR Route	JPE/JPW	G1	92	117	61	270
Jersey Point: OR Route	JPE/JPW	G1	0	0	0	0
Jersey Point (Pooled)	JPE/JPW	G1	92	117	61	270
False River West	FRW	H1a	2	6	1	9
False River East	FRE	H1b	0	3	1	4
False River: SJR Route	FRE/FRW	H1	2	7	1	10
False River: OR Route	FRE/FRW	H1	0	0	0	0
False River (Pooled)	FRE/FRW	H1	2	7	1	10
Chipps Island East	MAE	G2a	82	104	46	232
Chipps Island West	MAW	G2b	86	101	51	238
Chipps Island: SJR Route	MAE/MAW	G2	86	108	55	249
Chipps Island: OR Route	MAE/MAW	G2	2	1	0	3
Chipps Island (Pooled)	MAE/MAW	G2	88	109	55	252

Table 11. Number of juvenile steelhead tagged by each tagger in each release group during the 2012 tagging study.

	Release Group			
Tagger	1	2	3	Total Tags
A	116	115	117	348
B	117	117	117	351
C	122	123	123	368
D	122	123	123	368
Total Tags	477	478	480	1,435

Table 12. Release size and counts of tag detections at key detection sites by tagger in 2012, excluding predator-type detections. * = omitted from chi-square test of independence because of low counts.

	Tagger			
Detection Site	A	B	C	D
Release at Durham Ferry	348	351	368	368
Mossdale (MOS)	203	191	219	201
Lathrop (SJL)	182	184	208	185
MacDonald Island (MAC)	107	113	129	109
Turner Cut (TCE/TCW)	31	34	38	38
Medford Island (MFE/MFW)	75	78	88	67
Old River East (ORE)	17	7	4	14
Old River South (ORS)	15	6	4	12
Old River at Highway 4 (OR4)	15	14	14	20
Middle River at Highway 4 (MR4)	6	6	11	8
Clifton Court Forebay Interior (RGD)*	7	4	4	8
Central Valley Project Holding Tank (CVPtank)*	6	3	4	3
Jersey Point (JPE/JPW)	72	71	73	54
Chipps Island (MAE/MAW)	66	67	68	51

Table 13. Performance metric estimates (standard error in parentheses) for tagged juvenile steelhead released in the 2012 tagging study, excluding predator-type detections. South Delta ("SD") survival extended to MacDonald Island and Turner Cut in Route A, and the Central Valley Project trash rack, exterior radial gate receiver at Clifton Court Forebay, and Old River and Middle River receivers at Highway 4 in Route B. (Population-level estimates were weighted averages over the release-specific estimates, using weights proportional to release size.)

Parameter	Release Occasion 1	2	3	Population Estimate
ψ_{AA}	0.72 (0.04)	0.75 (0.03)	0.58 (0.04)	0.68 (0.02)
ψ_{AF}	0.21 (0.04)	0.23(0.03)	0.34 (0.04)	0.26 (0.02)
ψ_{BB}[a]	0.06 (0.01)	0.03 (0.01)	0.08 (0.02)	0.06 (0.01)
ψ_{BC}[a]	0.00	0.00	0.00	0.00
S_{AA}	0.33 (0.03)	0.43 (0.03)	0.45 (0.05)	0.40 (0.02)
S_{AF}	0.10 (0.04)	0.14 (0.04)	0.21 (0.05)	0.15 (0.03)
S_{BB}[a]	0.07 (0.04)	0.10 (0.07)	0.05 (0.03)	0.07 (0.03)
S_{BC}[a]	NA	NA	NA	NA
ψ_{A}[b]	0.94 (0.01)	0.97 (0.01)	0.92 (0.02)	0.94 (0.01)
ψ_{B}[b]	0.06 (0.01)	0.03 (0.01)	0.08 (0.02)	0.06 (0.01)
S_{A}[c]	0.28 (0.03)	0.33 (0.03)	0.36 (0.04)	0.33 (0.02)
S_{B}[c]	0.07 (0.04)	0.10 (0.07)	0.05 (0.03)	0.07 (0.03)
S_{Total}	0.26 (0.02)	0.35 (0.03)	0.33 (0.04)	0.32 (0.02)
$S_{A(MD)}$	0.32 (0.03)	0.46 (0.03)	0.45 (0.04)	0.41 (0.02)
$S_{B(MD)}$[d]	0.00	0.00	0.00	0.00
$S_{Total(MD)}$	0.30 (0.03)	0.45 (0.03)	0.41 (0.04)	0.39 (0.02)
$S_{A(SD)}$	0.78 (0.04)	0.82 (0.02)	0.89 (0.03)	0.83 (0.02)
$S_{B(SD)}$	0.80 (0.08)	0.62 (0.17)	0.23 (0.11)	0.55 (0.07)
$S_{Total(SD)}$	0.78 (0.04)	0.81 (0.02)	0.84 (0.03)	0.81 (0.02)
ϕ_{A1A4}	0.70 (0.02)	0.65 (0.02)	0.36 (0.02)	0.57 (0.01)

a = No tags were detected in subroute C or insufficient tags were detected to subroute C for use in analysis, so assumed $\psi_{B2} = 1$, $\psi_{C2} = 0$, and $S_{B1} = \phi_{B1B2}$. No estimate of survival in subroute C was available.

b = Significant preference for route A (San Joaquin Route) ($\alpha = 0.05$) for all release occasions

c = Estimated survival is significantly higher in route A (San Joaquin River) than in route B (Old River) ($\alpha = 0.05$) for all release occasions (tested only for Delta survival)

d = No tags from fish that entered Old River at its head were later detected at Jersey Point or False River, although some were detected farther downstream at Chipps Island (presumably transported)

Table 14. Performance metric estimates (standard error in parentheses) for tagged juvenile steelhead released in the 2012 tagging study, including predator-type detections. South Delta ("SD") survival extended to MacDonald Island and Turner Cut in Route A, and the Central Valley Project trash rack, exterior radial gate receiver at Clifton Court Forebay, and Old River and Middle River receivers at Highway 4 in Route B. (Population-level estimates were weighted averages over the release-specific estimates, using weights proportional to release size.)

	Release Occasion			Population
Parameter	1	2	3	Estimate
ψ_{AA}	0.77 (0.04)	0.74 (0.03)	0.56 (0.04)	0.69 (0.02)
ψ_{AF}	0.17 (0.04)	0.23 (0.03)	0.33 (0.04)	0.25 (0.02)
ψ_{BB}[a]	0.06 (0.01)	0.04 (0.01)	0.10 (0.02)	0.07 (0.01)
ψ_{BC}[a]	0.00	0.00	0.00	0.00
S_{AA}	0.33 (0.03)	0.43 (0.03)	0.45 (0.05)	0.40 (0.02)
S_{AF}	0.11 (0.05)	0.14 (0.04)	0.2116 (0.05)	0.15 (0.03)
S_{BB}[a]	0.14 (0.05)	0.08 (0.05)	0.05 (0.03)	0.09 (0.03)
S_{BC}[a]	NA	NA	NA	NA[a]
ψ_{A}[b]	0.94 (0.01)	0.96 (0.01)	0.90 (0.02)	0.93 (0.01)
ψ_{B}[b]	0.06 (0.01)	0.04 (0.01)	0.10 (0.02)	0.07 (0.01)
S_{A}[ac]	0.29 (0.03)	0.36 (0.03)	0.36 (0.04)	0.34 (0.02)
S_{B}[c]	0.14 (0.05)	0.08 (0.05)	0.05 (0.03)	0.09 (0.03)
S_{Total}	0.28 (0.02)	0.35 (0.03)	0.33 (0.04)	0.32 (0.02)
$S_{A(MD)}$	0.33 (0.03)	0.46 (0.03)	0.45 (0.04)	0.41 (0.02)
$S_{B(MD)}$[d]	0.00	0.00	0.00	0.00
$S_{Total(MD)}$	0.31 (0.03)	0.44 (0.03)	0.31 (0.04)	0.39 (0.02)
$S_{A(SD)}$	0.79 (0.03)	0.81 (0.02)	0.86 (0.03)	0.82 (0.02)
$S_{B(SD)}$	0.89 (0.07)	0.53 (0.15)	0.34 (0.11)	0.59 (0.07)
$S_{Total(SD)}$	0.80 (0.03)	0.80 (0.02)	0.81 (0.03)	0.80 (0.02)
ϕ_{A1A4}	0.69 (0.02)	0.66 (0.02)	0.36 (0.02)	0.57 (0.01)

a = No tags were detected in subroute C or insufficient tags were detected to subroute C for use in analysis, so assumed $\psi_{B2} = 1$, $\psi_{C2} = 0$, and $S_{B1} = \phi_{B1B2}$. No estimate of survival in subroute C was available

b = Significant preference for route A (San Joaquin Route) ($\alpha = 0.05$) for all release occasions

c = Estimated survival is significantly higher in route A (San Joaquin River) than in route B (Old River) ($\alpha = 0.05$) for all release occasions (tested only for Delta survival)

d = No tags from fish that entered Old River at its head were later detected at Jersey Point or False River, although some were detected farther downstream at Chipps Island (presumably transported)

RECIRC2566.

Table 15a. Average travel time in days (harmonic mean) of acoustic-tagged juvenile steelhead from release at Durham Ferry during the 2012 tagging study, without predator-type detections. Standard errors are in parentheses. See Table 15b for travel time from release with predator-type detections.

	Without Predator-Type Detections							
	All Releases		Release 1		Release 2		Release 3	
Detection Site and Route	N	Travel Time	N	Travel Time	N	Travel Time	N	Travel Time
Durham Ferry Upstream (DFU)	13	1.74 (0.53)	18	0.35 (0.12)	22	3.37 (1.87)	83	6.72 (2.18)
Durham Ferry Downstream (DFD)	437	0.07 (<0.01)	280	0.05 (<0.01)	75	0.11 (0.02)	82	0.25 (0.06)
Banta Carbona (BCA)	241	0.89 (0.07)	67	0.56 (0.06)	44	0.78 (0.14)	130	1.37 (0.16)
Mossdale (MOS)	814	2.09 (0.07)	333	2.71 (0.15)	311	1.67 (0.08)	170	2.14 (0.15)
Lathrop (SJL)	759	2.57 (0.08)	306	3.55 (0.18)	300	2.09 (0.09)	153	2.35 (0.13)
Garwood Bridge (SJG)	718	3.95 (0.10)	283	5.27 (0.23)	285	3.35 (0.13)	150	3.46 (0.16)
Navy Drive Bridge (SJNB)	679	4.17 (0.11)	269	5.62 (0.24)	273	3.51 (0.13)	137	3.70 (0.17)
MacDonald Island (MAC)	458	5.64 (0.16)	187	7.95 (0.39)	184	4.64 (0.18)	87	4.83 (0.265)
Turner Cut (TCE/TCW)	141	5.79 (0.25)	31	7.08 (0.81)	58	6.24 (0.42)	52	4.886 (0.29)
Medford Island (MFE/MFW)	308	5.98 (0.21)	115	8.86 (0.63)	127	5.03 (0.22)	66	4.99 (0.29)
Old River East (ORE)	42	3.54 (0.54)	21	2.68 (0.45)	8	2.59 (0.65)	13	13.53 (6.35)
Old River South (ORS)	37	4.70 (0.69)	20	3.83 (0.65)	7	3.41 (0.80)	10	16.56 (7.18)
Old River at Highway 4 (OR4), SJR Route	61	9.51 (0.54)	29	12.73 (0.89)	14	8.38 (0.75)	18	7.30 (0.63)
Old River at Highway 4 (OR4), OR Route	2	15.39 (4.36)	2	15.39 (4.36)	0	NA	0	NA
Middle River Head (MRH)	1	12.98 (NA)	1	12.98 (NA)	0	NA	0	NA
Middle River at Highway 4 (MR4), SJR Route	30	9.70 (0.82)	6	12.94 (1.34)	17	9.26 (1.20)	7	8.82 (0.82)
Middle River at Highway 4 (MR4), OR Route	1	15.23 (NA)	1	15.23 (NA)	0	NA	0	NA
Radial Gates Upstream (DFU), SJR Route	19	9.97 (1.03)	6	15.99 (1.89)	3	10.49 (0.60)	10	8.04 (0.97)
Radial Gates Upstream (DFU), OR Route	11	9.66 (1.45)	6	10.57 (2.53)	4	7.50 (0.83)	1	26.70 (NA)
Radial Gates Downstream (DFD), SJR Route	15	8.82 (0.81)	3	14.00 (2.30)	3	10.69 (0.65)	9	7.47 (0.71)
Radial Gates Downstream (DFD), OR Route	8	9.56 (1.49)	3	10.85 (3.04)	4	7.65 (0.94)	1	26.70 (NA)
Central Valley Project Trashrack (CVP), SJR Route	46	11.24 (0.78)	18	14.55 (1.33)	18	10.05 (1.19)	10	9.40 (0.98)
Central Valley Project Trashrack (CVP), OR Route	11	9.18 (1.77)	8	7.65 (1.43)	1	13.25 (NA)	2	26.16 (7.66)
Central Valley Project Holding Tank (CVPtank), SJR Route	13	11.03 (0.97)	3	12.17 (1.83)	8	10.66 (1.31)	2	11.04 (2.90)
Central Valley Project Holding Tank (CVPtank), OR Route	3	9.03 (4.20)	2	7.00 (3.43)	0	NA	1	21.47 (NA)

Table 15a. (Continued)

Detection Site and Route	Without Predator-Type Detections							
	All Releases		Release 1		Release 2		Release 3	
	N	Travel Time	N	Travel Time	N	Travel Time	N	Travel Time
Jersey Point (JPE/JPW), SJR Route	270	7.66 (0.23)	92	11.94 (0.49)	117	6.58 (0.26)	61	6.25 (0.27)
Jersey Point (JPE/JPW), OR Route	0	NA	0	NA	0	NA	0	NA
False River (FRE/FRW), SJR Route	10	7.97 (0.86)	2	12.04 (1.55)	7	7.67 (0.91)	1	5.69 (NA)
False River (FRE/FRW), OR Route	0	NA	0	NA	0	NA	0	NA
Chipps Island (MAE/MAW), SJR Route	249	9.38 (0.25)	86	13.59 (0.51)	108	8.13 (0.27)	55	7.93 (0.37)
Chipps Island (MAE/MAW), OR Route	3	13.00 (2.57)	2	16.19 (0.66)	1	9.33 (NA)	0	NA
Chipps Island (MAE/MAW)	252	9.41 (0.25)	88	13.64 (0.51)	109	8.14 (0.27)	55	7.93 (0.37)

Table 15b. Average travel time in days (harmonic mean) of acoustic-tagged juvenile steelhead from release at Durham Ferry during the 2012 tagging study, with predator-type detections. Standard errors are in parentheses. See Table 15a for travel time from release without predator-type detections.

	With Predator-Type Detections							
	All Releases		Release 1		Release 2		Release 3	
Detection Site and Route	N	Travel Time	N	Travel Time	N	Travel Time	N	Travel Time
Durham Ferry Upstream (DFU)	140	2.25 (0.77)	21	0.42 (0.16)	27	5.24 (3.55)	92	13.76 (4.11)
Durham Ferry Downstream (DFD)	465	0.07 (<0.01)	281	0.05 (<0.01)	77	0.11 (0.02)	107	0.33 (0.08)
Banta Carbona (BCA)	279	1.04 (0.08)	71	0.60 (0.07)	51	0.90 (0.17)	157	1.68 (0.21)
Mossdale (MOS)	817	2.13 (0.07)	329	2.73 (0.15)	315	1.70 (0.08)	173	2.20 (0.15)
Lathrop (SJL)	751	2.59 (0.08)	304	3.57 (0.18)	297	2.11 (0.09)	150	2.34 (0.13)
Garwood Bridge (SJG)	716	3.98 (0.10)	288	5.36 (0.24)	284	3.38 (0.13)	144	3.39 (0.16)
Navy Drive Bridge (SJNB)	678	4.20 (0.11)	273	5.72 (0.25)	271	3.51 (0.13)	134	3.68 (0.17)
MacDonald Island (MAC)	459	5.70 (0.17)	194	8.14 (0.40)	181	4.63 (0.18)	84	4.77 (0.26)
Turner Cut (TCE/TCW)	138	5.73 (0.25)	30	7.12 (0.84)	58	6.20 (0.42)	50	4.75 (0.28)
Medford Island (MFE/MFW)	311	6.07 (0.21)	118	9.00 (0.64)	127	5.09 (0.23)	66	4.99 (0.29)
Old River East (ORE)	48	4.07 (0.67)	20	2.60 (0.44)	11	3.48 (1.05)	17	18.03 (8.80)
Old River South (ORS)	42	5.30 (0.83)	20	3.87 (0.67)	9	4.29 (1.22)	13	19.55 (7.82)
Old River at Highway 4 (OR4), SJR Route	60	9.78 (0.61)	31	14.24 (1.11)	13	8.07 (0.67)	16	6.81 (0.51)
Old River at Highway 4 (OR4), OR Route	2	15.39 (4.36)	2	15.39 (4.36)	0	NA	0	NA
Middle River Head (MRH)	2	45.00 (2.22)	0	NA	0	NA	2	45.00 (2.22)
Middle River at Highway 4 (MR4), SJR Route	31	9.74 (0.80)	6	13.27 (1.51)	18	9.30 (1.14)	7	8.82 (0.82)
Middle River at Highway 4 (MR4), OR Route	2	23.00 (11.74)	1	15.23 (NA)	0	NA	1	46.96 (NA)
Radial Gates Upstream (DFU), SJR Route	20	9.98 (0.98)	6	17.71 (2.96)	4	10.79 (0.54)	10	7.73 (0.74)
Radial Gates Upstream (DFU), OR Route	11	9.66 (1.45)	6	10.57 (2.53)	4	7.50 (0.83)	1	26.70 (NA)
Radial Gates Downstream (DFD), SJR Route	19	9.82 (0.97)	5	17.88 (3.71)	4	10.95 (0.55)	10	7.75 (0.74)
Radial Gates Downstream (DFD), OR Route	8	9.56 (1.49)	3	10.85 (3.04)	4	7.65 (0.94)	1	26.70 (NA)
Central Valley Project Trashrack (CVP), SJR Route	40	12.19 (1.13)	14	16.26 (2.22)	17	10.58 (1.46)	9	11.05 (2.11)
Central Valley Project Trashrack (CVP), OR Route	15	11.82 (2.59)	9	8.54 (1.84)	2	20.83 (11.93)	4	33.49 (7.59)
Central Valley Project Holding Tank (CVPtank), SJR Route	15	12.23 (1.36)	4	14.87 (3.81)	9	11.59 (1.70)	2	11.04 (2.90)
Central Valley Project Holding Tank (CVPtank), OR Route	3	9.03 (4.20)	2	7.00 (3.43)	0	NA	1	21.47 (NA)

Table 15b. (Continued)

Detection Site and Route	With Predator-Type Detections							
	All Releases		Release 1		Release 2		Release 3	
	N	Travel Time	N	Travel Time	N	Travel Time	N	Travel Time
Jersey Point (JPE/JPW), SJR Route	271	7.69 (0.23)	94	12.04 (0.49)	116	6.56 (0.26)	61	6.25 (0.27)
Jersey Point (JPE/JPW), OR Route	0	NA	0	NA	0	NA	0	NA
False River (FRE/FRW), SJR Route	10	8.47 (1.20)	2	12.04 (1.55)	7	8.35 (1.49)	1	5.698 (NA)
False River (FRE/FRW), OR Route	0	NA	0	NA	0	NA	0	NA
Chipps Island (MAE/MAW), SJR Route	251	9.46 (0.26)	88	13.75 (0.53)	108	8.18 (0.28)	55	7.93 (0.37)
Chipps Island (MAE/MAW), OR Route	4	15.41 (3.82)	3	19.68 (4.28)	1	9.33 (NA)	0	NA
Chipps Island (MAE/MAW)	255	9.52 (0.26)	91	13.89 (0.53)	109	8.19 (0.28)	55	7.93 (0.37)

Table 16a. Average travel time in days (harmonic mean) of acoustic-tagged juvenile steelhead through the San Joaquin River Delta river reaches during the 2012 tagging study, without predator-type detections. Standard errors are in parentheses. See Table 16b for travel time through reaches with predator-type detections.

Reach		Without Predator-Type Detections							
		All Releases		Release 1		Release 2		Release 3	
Upstream Boundary	Downstream Boundary	N	Travel Time	N	Travel Time	N	Travel Time	N	Travel Time
Durham Ferry (Release)	BCA	241	0.89 (0.07)	67	0.56 (0.06)	44	0.78 ().14)	130	1.37 (0.16)
BCA	MOS	198	0.60 (0.03)	59	0.76 (0.10)	34	0.46 (0.06)	105	0.59 (0.04)
MOS	SJL	759	0.19 (<0.01)	306	0.22 (0.01)	300	0.18 (0.01)	153	0.19 (0.01)
	ORE	42	0.29 (0.03)	21	0.27 (0.03)	8	0.26 (0.06)	13	0.35 (0.08)
SJL	SJG	718	0.76 (0.01)	283	0.77 (0.02)	285	0.71 (0.02)	150	0.83 (0.03)
SJG	SJNB	679	0.08 (<0.01)	269	0.08 (<0.01)	273	0.08 (<0.01)	137	0.08 (<0.01)
SJNB	MAC	444	1.02 (0.03)	182	1.18 (0.06)	181	0.96 (0.04)	81	0.87 (0.05)
	TCE/TCW	139	1.01 (0.06)	31	1.42 (0.17)	58	1.04 (0.09)	50	0.83 (0.08)
MAC	MFE/MFW	304	0.18 (0.01)	114	0.24 (0.02)	125	0.18 (0.01)	65	0.13 (0.01)
	JPE/JPW/FRE/FRW	253	1.61 (0.05)	88	2.05 (0.10)	111	1.58 (0.07)	54	1.23 (0.08)
	OR4	21	3.73 (0.36)	12	5.03 (0.46)	7	2.74 (0.35)	2	2.91 (0.76)
	MR4	10	2.57 (0.29)	3	2.01 (0.34)	4	2.60 (0.42)	3	3.51 (0.47)
MFE/MFW	JPE/JPW/FRE/FRW	211	1.19 (0.05)	77	1.52 (0.08)	89	1.20 (0.07)	45	0.87 (0.09)
	OR4	10	3.84 (0.52)	6	5.32 (0.68)	2	2.83 (0.47)	2	2.61 (0.49)
	MR4	2	1.90 (0.83)	0	NA	1	3.36 (NA)	1	1.33 (NA)
TCE/TCW	JPE/JPW/FRE/FRW	17	2.04 (0.31)	2	2.06 (1.16)	7	1.70 (0.49)	8	2.45 (0.17)
	OR4	34	2.33 (0.27)	11	3.77 (0.33)	7	2.68 (0.35)	16	1.76 (0.28)
	MR4	16	1.72 (0.24)	1	4.12 (NA)	11	1.86 (0.25)	4	1.27 (0.39)
ORE	ORS	35	0.47 (0.05)	20	0.49 (0.07)	7	0.44 (0.09)	10	0.46 (0.13)
	MRH	1	5.41 (NA)	1	5.41 (NA)	0	NA	0	NA
ORS	OR4	2	5.20 (1.53)	2	5.20 (1.53)	0	NA	0	NA
	MR4	1	2.07 (NA)	1	2.07 (NA)	0	NA	0	NA
	RGU	11	3.13 (0.57)	6	4.50 (0.80)	4	2.72 (0.72)	1	1.41 (NA)
	CVP	11	2.93 (0.69)	8	3.63 (0.99)	1	9.03 (NA)	2	1.39 (0.23)

Table 16a. (Continued)

Reach		Without Predator-Type Detections							
		All Releases		Release 1		Release 2		Release 3	
Upstream Boundary	Downstream Boundary	N	Travel Time	N	Travel Time	N	Travel Time	N	Travel Time
OR4 via OR	JPE/JPW/FRE/FRW	0	NA	0	NA	0	NA	0	NA
OR4 via SJR	JPE/JPW/FRE/FRW	3	2.48 (1.74)	1	11.87 (NA)	2	1.77 (1.28)	0	NA
	RGU	12	0.40 (0.09)	5	0.80 (0.22)	0	NA	7	0.29 (0.07)
	CVP	30	0.54 (0.11)	16	0.76 (0.15)	7	0.48 (0.17)	7	0.35 (0.16)
MRH	anywhere downstream[a]	0	NA	0	NA	0	NA	0	NA
MR4 via OR	JPE/JPW/FRE/FRW	0	NA	0	NA	0	NA	0	NA
MR4 via SJR	JPE/JPW/FRE/FRW	0	NA	0	NA	0	NA	0	NA
	RGU	7	1.03 (0.11)	1	1.23 (NA)	3	1.21 (0.21)	3	0.86 (0.12)
	CVP	16	0.79 (0.12)	2	0.91 (0.61)	11	0.70 (0.12)	3	1.28 (0.42)
RGU via OR	RGD	8	0.01 (<0.01)	3	0.01 (<0.01)	4	0.05 (0.03)	1	<0.01 (NA)
RGU via SJR	RGD	15	0.01 (<0.01)	3	0.01 (0.01)	3	0.09 (0.04)	9	0.01 (<0.01)
CVP via OR	CVPtank	3	0.23 (0.12)	2	0.16 (0.06)	0	NA	1	1.23 (NA)
CVP via SJR	CVPtank	13	0.18 (0.06)	3	0.15 (0.12)	8	0.20 (0.10)	2	0.16 (0.09)
JPE/JPW	MAE/MAW (Chipps Island)	209	0.89(0.04)	76	0.94 (0.10)	92	0.88 (0.05)	41	0.84 (0.08)
MAC		217	2.87 (0.07)	79	3.53 (0.13)	95	2.77 (0.08)	43	2.28 (0.14)
MFE/MFW		180	2.42 (0.07)	66	2.89 (0.11)	76	2.32 (0.08)	38	2.03 (0.14)
TCE/TCW		25	4.04 (0.41)	3	3.22 (1.98)	10	3.87 (0.49)	12	4.49 (0.35)
OR4		2	2.40 (1.48)	0	NA	1	1.49 (NA)	1	6.24(NA)
MR4		0	NA	0	NA	0	NA	0	NA
RGD		4	1.91 (0.22)	0	NA	1	2.43 (NA)	3	1.79 (0.22)
CVPtank		9	1.26 (0.14)	3	1.45 (0.18)	4	1.27 (0.23)	2	1.04 (0.33)

a = all detections at Middle River Head (MRH) used in the survival model were final detections for the tag, so no travel time is reported for reaches starting at MRH

Table 16b. Average travel time in days (harmonic mean) of acoustic-tagged juvenile steelhead through the San Joaquin River Delta river reaches during the 2012 tagging study, with predator-type detections. Standard errors are in parentheses. See Table 16a for travel time through reaches without predator-type detections.

Reach		With Predator-Type Detections							
		All Releases		Release 1		Release 2		Release 3	
Upstream Boundary	Downstream Boundary	N	Travel Time	N	Travel Time	N	Travel Time	N	Travel Time
Durham Ferry (Release)	BCA	279	1.04 (0.08)	71	0.60 (0.07)	51	0.90 (0.17)	157	1.68 (0.21)
BCA	MOS	208	0.63 (0.04)	60	0.76 (0.10)	37	0.853 (0.07)	111	0.62 (0.04)
MOS	SJL	751	0.20 (<0.01)	304	0.21 (0.01)	297	0.18 (0.01)	150	0.20 (0.01)
	ORE	48	0.26 (0.03)	20	0.26 (0.03)	11	0.27 (0.06)	17	0.27 (0.05)
SJL	SJG	716	0.77 (0.01)	288	0.79 (0.02)	284	0.72 (0.02)	144	0.82 (0.03)
SJG	SJNB	678	0.08 (<0.01)	273	0.08 (<0.01)	271	0.08 (<0.01)	134	0.08 (<0.01)
SJNB	MAC	445	1.02 (0.03)	189	1.17 (0.06)	178	0.96 (0.04)	78	0.89 (0.05)
	TCE/TCW	136	1.02 (0.06)	30	1.43 (0.18)	58	1.04 (0.09)	48	0.85 (0.08)
MAC	MFE/MFW	307	0.18 (0.01)	117	0.24 (0.02)	125	0.18 (0.01)	65	0.13 (0.01)
	JPE/JPW/FRE/FRW	253	1.61 (0.05)	89	2.05 (0.10)	110	1.58 (0.07)	54	1.23 (0.08)
	OR4	23	3.99 (0.44)	15	5.38 (0.67)	6	2.61 (0.34)	2	2.91 (0.76)
	MR4	10	2.65 (0.32)	2	1.71 (0.02)	5	2.84 (0.48)	3	3.51 (0.47)
MFE/MFW	JPE/JPW/FRE/FRW	209	1.19 (0.05)	76	1.51 (0.08)	88	1.19 (0.07)	45	0.87 (0.09)
	OR4	11	4.33 (0.68)	7	6.54 (0.65)	2	2.83 (0.47)	2	2.61 (0.49)
	MR4	2	1.90 (0.83)	0	NA	1	3.36 (NA)	1	1.33 (NA)
TCE/TCW	JPE/JPW/FRE/FRW	17	2.04 (0.31)	2	2.06 (1.16)	7	1.70 (0.49)	8	2.45 (0.17)
	OR4	30	2.18 (0.27)	9	3.97 (0.61)	7	2.31 (0.31)	14	1.65 (0.27)
	MR4	17	1.81 (0.26)	2	5.72 (2.22)	11	1.86 (0.25)	4	1.27 (0.39)
ORE	ORS	42	0.40 (0.04)	20	0.49 (0.07)	9	0.45 (0.09)	13	0.35 (0.05)
	MRH	2	0.53 (0.26)	0	NA	0	NA	2	0.53 (0.26)
ORS	OR4	2	5.20 (1.53)	2	5.20 (1.53)	0	NA	0	NA
	MR4	2	2.46 (0.47)	1	2.07 (NA)	0	NA	1	3.04 (NA)
	RGU	11	3.13 (0.57)	6	4.50 (0.80)	4	2.72 (0.72)	1	1.41 (NA)
	CVP	15	3.19 (0.65)	9	3.42 (0.82)	2	4.53 (2.26)	4	2.46 (1.13)

Table 16b. (Continued)

Reach		With Predator-Type Detections							
		All Releases		Release 1		Release 2		Release 3	
Upstream Boundary	Downstream Boundary	N	Travel Time	N	Travel Time	N	Travel Time	N	Travel Time
OR4 via OR	JPE/JPW/FRE/FRW	0	NA	0	NA	0	NA	0	NA
OR4 via SJR	JPE/JPW/FRE/FRW	4	2.33 (1.10)	2	3.42 (2.43)	2	1.77 (1.28)	0	NA
	RGU	14	0.46 (0.11)	6	0.86 (0.21)	1	1.66 (NA)	7	0.30 (0.08)
	CVP	24	0.46 (0.09)	12	0.65 (0.13)	6	0.43 (0.15)	6	0.31 (0.14)
MRH	anywhere downstream[a]	0	NA	0	NA	0	NA	0	NA
MR4 via OR	JPE/JPW/FRE/FRW	0	NA	0	NA	0	NA	0	NA
MR4 via SJR	JPE/JPW/FRE/FRW	0	NA	0	NA	0	NA	0	NA
	RGU	6	1.01 (0.12)	0	NA	3	1.21 (0.21)	3	0.86 (0.12)
	CVP	16	1.09 (0.27)	2	0.91 (0.61)	11	0.89 (0.23)	3	14.00 (7.40)
RGU via OR	RGD	8	0.01 (<0.01)	3	0.01 (<0.01)	4	0.05 (0.03)	1	<0.01 (NA)
RGU via SJR	RGD	19	0.01 (<0.01)	5	0.01 (0.01)	4	0.03 (0.02)	10	0.01 (<0.01)
CVP via OR	CVPtank	3	0.23 (0.12)	2	0.16 (0.06)	0	NA	1	1.23 (NA)
CVP via SJR	CVPtank	15	0.19 (0.06)	4	0.17 (0.11)	9	0.22 (0.11)	2	0.16 (0.09)
JPE/JPW	MAE/MAW (Chipps Island)	210	0.88(0.04)	77	0.92 (0.09)	92	0.88 (0.05)	41	0.84 (0.08)
MAC		218	2.88 (0.07)	80	3.51 (0.13)	95	2.78 (0.08)	43	2.28 (0.14)
MFE/MFW		180	2.43 (0.07)	66	2.89 (0.11)	76	2.34 (0.09)	38	2.03 (0.14)
TCE/TCW		26	4.19 (0.45)	4	4.18 (2.66)	10	3.87 (0.49)	12	4.49 (0.45)
OR4		2	2.40 (1.48)	0	NA	1	1.49 (NA)	1	6.24 (NA)
MR4		0	NA	0	NA	0	NA	0	NA
RGD		4	1.91 (0.22)	0	NA	1	2.43 (NA)	3	1.79 (0.22)
CVPtank		10	1.16 (0.14)	4	1.12 (0.26)	4	1.27 (0.23)	2	1.04 (0.33)

a = all detections at Middle River Head (MRH) used in the survival model were final detections for the tag, so no travel time is reported for reaches starting at MRH

Table 17. Results of single-variate analyses of route entrainment at the Turner Cut Junction (all release groups). The values df1, df2 are degrees of freedom for the F-test.

	F-test			
Covariate	*F*	df1	df2	*P*
Stage at TRN[a]	34.4221	1	503	<0.0001
Change in stage at TRN[a]	19.7119	1	500	<0.0001
Change in flow at TRN[a]	21.5089	1	500	<0.0001
Change in velocity at TRN[a]	21.2500	1	500	<0.0001
Release Group[a]	11.0050	2	502	<0.0001
Exports at CVP[a]	7.9417	1	503	0.0050
Fork Length[a]	5.5480	1	503	0.0189
Negative flow at TRN[a]	5.1778	1	503	0.0233
Exports at SWP	3.3004	1	503	0.0699
Flow at TRN	2.8136	1	503	0.0941
Velocity at TRN	2.7981	1	503	0.0950
Arrive at TCJ during day	0.5041	1	503	0.4780
Flow during transition from SJG	0.1434	1	503	0.7051
Velocity during transition from SJG	0.0286	1	503	0.8657

a = Significant at 5% level

Table 18. Results of single-variate analyses of route entrainment at the Turner Cut Junction (omit first release group). The values df1, df2 are degrees of freedom for the F-test.

	F-test			
Covariate	*F*	df1	df2	*P*
Change in flow at TRN[a]	20.8085	1	329	<0.0001
Change in velocity at TRN[a]	20.4498	1	329	<0.0001
Change in stage at TRN[a]	20.1618	1	329	<0.0001
Stage at TRN[a]	19.3936	1	332	<0.0001
Release Group[a]	6.9637	1	332	0.0087
Exports at CVP[a]	6.8495	1	332	0.0093
Fork Length	2.9545	1	332	0.0093
Flow during transition from SJG	0.9424	1	332	0.3324
Negative flow at TRN	0.8134	1	332	0.3678
Exports at SWP	0.7434	1	332	0.3892
Velocity during transition from SJG	0.4612	1	332	0.4975
Arrive at TCJ during day	0.0888	1	332	0.7659
Flow at TRN	0.0424	1	332	0.8370
Velocity at TRN	0.0337	1	332	0.8544

a = Significant at 5% level

Table 19. Results of multivariate analyses of route entrainment at the Turner Cut junction in 2012 (without first release group).

				t-test		
Model Type	Covariate[a]	Estimate	S.E.	*t*	df	*P*
Flow	Intercept	1.5564	0.1925	8.084	327	<0.0001
	ΔQ_{TRN}	0.6253	0.1335	4.684	327	<0.0001
	CVP	-0.3466	0.1028	-3.371	327	0.0008
	Release Group 3	-0.9689	0.2748	-3.527	327	0.0005
	Goodness-of-fit: χ^2=3.9664, df=13, P=0.9917; AIC = 347.63					
Velocity	Intercept	1.5539	0.1923	8.081	327	<0.0001
	ΔV_{TRN}	0.6215	0.1332	4.666	327	<0.0001
	CVP	-0.3491	0.1031	-3.387	327	0.0008
	Release Group 3	-0.9719	0.2747	-3.5375	327	0.0005
	Goodness-of-fit: χ^2=3.4164, df=13, P=0.9960; AIC = 347.83					
Stage	Intercept	1.4796	0.1892	7.820	327	<0.0001
	C_{TRN}	0.5690	0.1337	4.254	327	<0.0001
	ΔC_{TRN}	-0.5637	0.1381	-4.082	326	0.0001
	Release Group 3	-0.7960	0.2734	-2.911	327	0.0038
	Goodness-of-fit: χ^2=3.0594, df=13, P=0.9977; AIC = 342.43					

a = continuous covariates (ΔQ_{TRN}, CVP, ΔV_{TRN}, C_{TRN}, ΔC_{TRN}) are standardized

Table 20. Estimates of survival from downstream receivers at water export facilities (CVP holding tank or interior of Clifton Court Forebay at radial gates) through salvage to receivers after release from truck, excluding predator-type detections (95% profile likelihood interval in parentheses). Population estimate is based on data pooled from all release groups.

Facility	Upstream Model Site Code	Release Occasion			Population Estimate
		1	2	3	
CVP	E2	0.60 (0.20, 0.92)	0.50 (0.19, 0.81)	0.67 (0.16, 0.99)	0.57 (0.33, 0.79)
SWP	D2	0 (*n* = 6)	0.14 (0.01, 0.50)	0.30 (0.09, 0.62)	0.17 (0.06, 0.36)

Appendix A. Survival Model Parameters

Table A1. Definitions of parameters used in the release-recapture survival model. Parameters used only in particular submodels are noted.

Parameter	Definition
S_{A2}	Probability of survival from Durham Ferry Downstream (DFD) to Banta Carbona (BCA)
S_{A3}	Probability of survival from Banta Carbona (BCA) to Mossdale (MOS)
S_{A4}	Probability of survival from Mossdale (MOS) to Lathrop (SJL) or Old River East (ORE)
S_{A5}	Probability of survival from Lathrop (SJL) to Garwood Bridge (SJG)
S_{A6}	Probability of survival from Garwood Bridge (SJG) to Navy Drive Bridge (SJNB)
S_{A7}	Probability of survival from Navy Drive Bridge (SJNB) to MacDonald Island (MAC) or Turner Cut (TCE/TCW)
$S_{A7,G2}$	Overall survival from Navy Drive Bridge (SJNB) to Chipps Island (MAE/MAW) (derived from Submodel I)
$S_{A8,G2}$	Overall survival from MacDonald Island (MAC) to Chipps Island (MAE/MAW) (Submodel I)
S_{B1}	Probability of survival from Old River East (ORE) to Old River South (ORS)
$S_{B2,G2}$	Overall survival from Old River South (ORS) to Chipps Island (MAE/MAW) (derived from Submodel I)
$S_{B2(SD)}$	Overall survival from Old River South (ORS) to the exit points of the Route B Southern Delta Region: OR4, MR4, RGU, CVP (derived from Submodel I)
$S_{C1,G2}$	Overall survival from head of Middle River (MRH) to Chipps Island (MAE/MAW) (derived from Submodel I)
$S_{C1(SD)}$	Overall survival from head of Middle River (MRH) to the exit points of the Route B Southern Delta Region: OR4, MR4, RGU, CVP (derived from Submodel I)
$S_{F1,G2}$	Overall survival from Turner Cut (TCE/TCW) to Chipps Island (MAE/MAW) (Submodel I)
$\phi_{A1,A0}$	Joint probability of moving from Durham Ferry release site upstream toward DFU, and surviving to DFU
$\phi_{A1,A2}$	Joint probability of moving from Durham Ferry release site downstream toward DFD, and surviving to DFD
$\phi_{A1,A3}$	Joint probability of moving from Durham Ferry release site downstream toward BCA, and surviving to BCA; = $\phi_{A1,A2}$ s_{A2}
$\phi_{A8,A9}$	Joint probability of moving from MAC toward MFE/MFW, and surviving from MAC to MFE/MFW (Submodel II)
$\phi_{A8,B3}$	Joint probability of moving from MAC toward OR4, and surviving from MAC to OR4 (Submodel II)
$\phi_{A8,C2}$	Joint probability of moving from MAC toward MR4, and surviving from MAC to MR4 (Submodel II)
$\phi_{A8,GH}$	Joint probability of moving from MAC directly toward Jersey Point (JPE/JPW) or False River (FRE/FRW), and surviving JPE/JPW or FRE/FRW (Submodel II)
$\phi_{A8,G1}$	Joint probability of moving from MAC directly toward Jersey Point (JPE/JPW) and surviving to JPE/JPW (Submodel II); = $\phi_{A8,GH}\psi_{G1(A)}$
$\phi_{A9,B3}$	Joint probability of moving from MFE/MFW toward OR4, and surviving from MFE/MFW to OR4 (Submodel II)
$\phi_{A9,C2}$	Joint probability of moving from MFE/MFW toward MR4, and surviving from MFE/MFW to MR4 (Submodel II)
$\phi_{A9,GH}$	Joint probability of moving from MFE/MFW directly toward Jersey Point (JPE/JPW) or False River (FRE/FRW), and surviving to JPE/JPW or FRE/FRW (Submodel II)
$\phi_{A9,G1}$	Joint probability of moving from MFE/MFW directly toward Jersey Point (JPE/JPW) and surviving to JPE/JPW (Submodel II); = $\phi_{A9,GH}\psi_{G1(A)}$
$\phi_{B1,B2}$	Joint probability of moving from ORE toward ORS, and surviving from ORE to ORS; = $S_{B1}\psi_{B2}$
$\phi_{B2,B3}$	Joint probability of moving from ORS toward OR4, and surviving from ORS to OR4
$\phi_{B2,C2}$	Joint probability of moving from ORS toward MR4, and surviving from ORS to MR4
$\phi_{B2,D1}$	Joint probability of moving from ORS toward RGU, and surviving from ORS to RGU
$\phi_{B2,E1}$	Joint probability of moving from ORS toward CVP, and surviving from ORS to CVP
$\phi_{B3,D1}$	Joint probability of moving from OR4 toward RGU and surviving from OR4 to RGU conditional on coming from lower San Joaquin River (Submodel II)
$\phi_{B3,E1}$	Joint probability of moving from OR4 toward CVP, and surviving from OR4 to CVP, conditional on coming from lower San Joaquin River (Submodel II)
$\phi_{B3,GH(A)}$	Joint probability of moving from OR4 toward Jersey Point (JPE/JPW) or False River (FRE/FRW), and surviving from OR4 to JPE/JPW or FRE/FRW (Submodel II [route A])

Table A1. (Continued)

Parameter	Definition
$\phi_{B3,GH(B)}$	Joint probability of moving from OR4 toward Jersey Point (JPE/JPW) or False River (FRE/FRW), and surviving from OR4 to JPE/JPW or FRE/FRW (Submodel I [route B])
$\phi_{B3,G1(A)}$	Joint probability of moving from OR4 toward Jersey Point (JPE/JPW) and surviving from OR4 to JPE/JPW (Submodel II [route A]); = $\phi_{B3,GH(A)}\psi_{G1(A)}$
$\phi_{B3,G1(B)}$	Joint probability of moving from OR4 toward Jersey Point (JPE/JPW) and surviving from OR4 to JPE/JPW (Submodel I [route B]); = $\phi_{B3,GH(B)}\psi_{G1(B)}$
$\phi_{C1,B3}$	Joint probability of moving from MRH toward OR4, and surviving from MRH to OR4
$\phi_{C1,C2}$	Joint probability of moving from MRH toward MR4, and surviving from MRH to MR4
$\phi_{C1,D1}$	Joint probability of moving from MRH toward RGU, and surviving from MRH to RGU
$\phi_{C1,E1}$	Joint probability of moving from MRH toward CVP, and surviving from MRH to CVP
$\phi_{C2,D1}$	Joint probability of moving from MR4 toward RGU and surviving from MR4 to RGU conditional on coming from lower San Joaquin River (Submodel II)
$\phi_{C2,E1}$	Joint probability of moving from MR4 toward CVP, and surviving from MR4 to CVP, conditional on coming from lower San Joaquin River (Submodel II)
$\phi_{C2,GH(A)}$	Joint probability of moving from MR4 toward Jersey Point (JPE/JPW) or False River (FRE/FRW), and surviving from MR4 to JPE/JPW or FRE/FRW (Submodel II [route A])
$\phi_{C2,GH(B)}$	Joint probability of moving from MR4 toward Jersey Point (JPE/JPW) or False River (FRE/FRW), and surviving from MR4 to JPE/JPW or FRE/FRW (Submodel I [route B])
$\phi_{C2,G1(A)}$	Joint probability of moving from MR4 toward Jersey Point (JPE/JPW) and surviving from MR4 to JPE/JPW (Submodel II [route A]); = $\phi_{B3,GH(A)}\psi_{G1(A)}$
$\phi_{C2,G1(B)}$	Joint probability of moving from MR4 toward Jersey Point (JPE/JPW) and surviving from MR4 to JPE/JPW (Submodel I [route B]); = $\phi_{B3,GH(B)}\psi_{G1(B)}$
$\phi_{D1,D2}$	Joint probability of moving from RGU toward RGD, and surviving from RGU to RGD (equated between submodels I and II)
$\phi_{D2,G2}$	Joint probability of moving from RGD toward Chipps Island (MAE/MAW) and surviving from RGU to MAE/MAW (equated between submodels I and II)
$\phi_{D1,G2}$	Joint probability of moving from RGU toward Chipps Island (MAE/MAW) via CCFB and surviving to MAE/MAW (equated between submodels I and II); = $\phi_{D1,D2}\phi_{D2,G2}$
$\phi_{E1,E2}$	Joint probability of moving from CVP toward CVPtank, and surviving from CVP to CVPtank (equated between submodels I and II)
$\phi_{E2,G2}$	Joint probability of moving from CVPtank toward Chipps Island (MAE/MAW) and surviving from CVPtank to MAE/MAW (equated between submodels I and II)
$\phi_{F1,B3}$	Joint probability of moving from TCE/TCW toward OR4, and surviving from TCE/TCW to OR4 (Submodel II)
$\phi_{F1,C2}$	Joint probability of moving from TCE/TCW toward MR4, and surviving from TCE/TCW to MR4 (Submodel II)
$\phi_{F1,GH}$	Joint probability of moving from TCE/TCW directly toward Jersey Point (JPE/JPW) or False River (FRE/FRW), and surviving to JPE/JPW or FRE/FRW (Submodel II)
$\phi_{F1,G1}$	Joint probability of moving from TCE/TCW directly toward Jersey Point (JPE/JPW) and surviving to JPE/JPW (Submodel II); = $\phi_{F1,GH}\psi_{G1(A)}$
$\phi_{G1,G2(A)}$	Joint probability of moving from JPE/JPW toward Chipps Island (MAE/MAW), and surviving to MAE/MAW (Submodel II [route A])
$\phi_{G1,G2(B)}$	Joint probability of moving from JPE/JPW toward Chipps Island (MAE/MAW), and surviving to MAE/MAW (Submodel I [route B])
ψ_{A1}	Probability of remaining in the San Joaquin River at the head of Old River; = 1 - ψ_{B1}
ψ_{A2}	Probability of remaining in the San Joaquin River at the junction with Turner Cut; = 1 - ψ_{F2}
ψ_{B1}	Probability of entering Old River at the head of Old River; = 1 - ψ_{A1}
ψ_{B2}	Probability of remaining in Old River at the head of Middle River; = 1 - ψ_{C2}
ψ_{C2}	Probability of entering Middle River at the head of Middle River; = 1 - ψ_{B2}
ψ_{F2}	Probability of entering Turner Cut at the junction with the San Joaquin River; = 1 - ψ_{A2}

Table A1. (Continued)

Parameter	Definition
$\psi_{G1(A)}$	Probability of moving downriver in the San Joaquin River at the Jersey Point/False River junction (Submodel II [route A]); = 1 - $\psi_{H1(A)}$
$\psi_{G1(B)}$	Probability of moving downriver in the San Joaquin River at the Jersey Point/False River junction (Submodel I [route B]); = 1 - $\psi_{H1(B)}$
$\psi_{H1(A)}$	Probability of entering False River at the Jersey Point/False River junction (Submodel II [route A]); = 1 - $\psi_{G1(A)}$
$\psi_{H1(B)}$	Probability of entering False River at the Jersey Point/False River junction (Submodel I [route B]); = 1 - $\psi_{G1(B)}$
P_{A0a}	Conditional probability of detection at DFU1
P_{A0b}	Conditional probability of detection at DFU2
P_{A2a}	Conditional probability of detection at DFD1
P_{A2b}	Conditional probability of detection at DFD2
P_{A2}	Conditional probability of detection at DFD (either DFD1 or DFD2)
P_{A3}	Conditional probability of detection at BCA
P_{A4}	Conditional probability of detection at MOS
P_{A5}	Conditional probability of detection at SJL
P_{A6}	Conditional probability of detection at SJG
P_{A7}	Conditional probability of detection at SJNB
P_{A8a}	Conditional probability of detection at MACU
P_{A8b}	Conditional probability of detection at MACD
P_{A8}	Conditional probability of detection at MAC (either MACU or MACD)
P_{A9a}	Conditional probability of detection at MFE
P_{A9b}	Conditional probability of detection at MFW
P_{B1}	Conditional probability of detection at ORE
P_{B2a}	Conditional probability of detection at ORSU
P_{B2b}	Conditional probability of detection at ORSD
P_{B2}	Conditional probability of detection at ORS (either ORSU or ORSD)
P_{B3a}	Conditional probability of detection at OR4U
P_{B3b}	Conditional probability of detection at OR4D
P_{C1a}	Conditional probability of detection at MRHU
P_{C1b}	Conditional probability of detection at MRHD
P_{C1}	Conditional probability of detection at MRH
P_{C2a}	Conditional probability of detection at MR4U
P_{C2b}	Conditional probability of detection at MR4D
P_{D1}	Conditional probability of detection at RGU (either RGU1 or RGU2)
P_{D2a}	Conditional probability of detection at RGD1
P_{D2b}	Conditional probability of detection at RGD2
P_{D2}	Conditional probability of detection at RGD (either RGD1 or RGD2)
P_{E1}	Conditional probability of detection at CVP
P_{E2}	Conditional probability of detection at CVPtank
P_{F1a}	Conditional probability of detection at TCE
P_{F1b}	Conditional probability of detection at TCW

Table A1. (Continued)

Parameter	Definition
P_{F1}	Conditional probability of detection at TCE/TCW
P_{G1a}	Conditional probability of detection at JPE
P_{G1b}	Conditional probability of detection at JPW
P_{G1}	Conditional probability of detection at JPE/JPW
P_{G2a}	Conditional probability of detection at MAE
P_{G2b}	Conditional probability of detection at MAW
P_{G2}	Conditional probability of detection at MAE/MAW
P_{H1a}	Conditional probability of detection at FRW
P_{H1b}	Conditional probability of detection at FRE
P_{H1}	Conditional probability of detection at FRE/FRW

Table A2. Parameter estimates (standard errors in parentheses) for tagged juvenile steelhead released in 2012, excluding predator-type detections. Parameters without standard errors were estimated at fixed values in the model. Population-level estimates are weighted averages of the release-specific estimates. Some parameters were not estimable because of sparse data.

	Release Occasion			
Parameter	1	2	3	Population Estimate
S_{A2}	0.86 (0.04)			
S_{A3}	0.88 (0.04)	0.77 (0.06)	0.81 (0.03)	0.82 (0.03)
S_{A4}	0.98 (0.01)	0.99 (0.01)	0.98 (0.01)	0.98 (< 0.01)
S_{A5}	0.93 (0.02)	0.95 (0.01)	0.98 (0.01)	0.95 (0.01)
S_{A6}	0.97 (0.01)	0.97 (0.01)	0.97 (0.01)	0.97 (0.01)
S_{A7}	0.88 (0.05)	0.90 (0.02)	0.96 (0.02)	0.91 (0.02)
$S_{A7,G2}$	0.31 (0.03)	0.39 (0.03)	0.39 (0.04)	0.36 (0.02)
$S_{A8,G2}$	0.42 (0.04)	0.52 (0.04)	0.50 (0.05)	0.48 (0.03)
S_{B1}				
$S_{B2,G2}$	0.08 (0.04)	0.11 (0.08)	0.06 (0.04)	0.08 (0.03)
$S_{B2(SD)}$	0.85 (0.08)	0.72 (0.17)	0.30 (0.14)	0.62 (0.08)
$S_{C1,G2}$				
$S_{C1(SD)}$				
$S_{F1,G2}$	0.12 (0.05)	0.17 (0.05)	0.24 (0.06)	0.18 (0.03)
$\phi_{A1,A0}$	0.10 (0.08)	0.06 (0.01)	0.22 (0.03)	0.12 (0.03)
$\phi_{A1,A2}$	0.92 (0.02)			
$\phi_{A1,A3}$	0.79 (0.04)	0.85 (0.07)	0.44 (0.03)	0.69 (0.03)
$\phi_{A8,A9}$	0.61 (0.04)	0.66 (0.03)	0.75 (0.05)	0.67 (0.02)
$\phi_{A8,B3}$	0.03 (0.01)	0.03 (0.01)	0	0.02 (0.01)
$\phi_{A8,C2}$	0.02 (0.01)	0.03 (0.01)	0.02 (0.02)	0.02 (0.01)
$\phi_{A8,GH}$		0.16 (0.03)		
$\phi_{A8,G1}$	0.07 (0.02)	0.15 (0.13)	0.10 (0.03)	0.11 (0.02)
$\phi_{A9,B3}$	0.05 (0.02)	0.02 (0.01)	0.03 (0.02)	0.03 (0.01)
$\phi_{A9,C2}$	0	0.01 (0.01)	0.02 (0.02)	0.01 (0.01)
$\phi_{A9,GH}$		0.79 (0.04)		
$\phi_{A9,G1}$	0.69 (0.04)	0.74 (0.04)	0.80 (0.05)	0.74 (0.03)
$\phi_{B1,B2}$	0.95 (0.05)	0.88 (0.12)	0.77 (0.12)	0.87 (0.06)
$\phi_{B2,B3}$	0.10 (0.07)	0	0	0.03 (0.02)
$\phi_{B2,C2}$	0.05 (0.05)	0	0	0.02 (0.02)
$\phi_{B2,D1}$	0.30 (0.10)	0.57 (0.19)	0.10 (0.09)	0.32 (0.08)
$\phi_{B2,E1}$	0.40 (0.11)	0.14 (0.13)	0.20 (0.13)	0.25 (0.07)
$\phi_{B3,D1}$	0.17 (0.07)	0	0.39 (0.12)	0.19 (0.05)
$\phi_{B3,E1}$	0.55 (0.09)	0.50 (0.13)	0.39 (0.11)	0.48 (0.07)
$\phi_{B3,GH(A)}$		0.15 (0.10)		
$\phi_{B3,GH(B)}$				
$\phi_{B3,G1(A)}$	0.03 (0.03)	0.14 (0.09)	0.06 (0.05)	0.08 (0.04)
$\phi_{B3,G1(B)}$	0			

Table A2. (Continued)

Parameter	Release Occasion 1	2	3	Population Estimate
$\phi_{C1,B3}$				
$\phi_{C1,C2}$				
$\phi_{C1,D1}$				
$\phi_{C1,E1}$				
$\phi_{C2,D1}$	0.17 (0.15)	0.18 (0.09)	0.43 (0.19)	0.26 (0.09)
$\phi_{C2,E1}$	0.33 (0.19)	0.65 (0.12)	0.43 (0.19)	0.47 (0.10)
$\phi_{C2,GH(A)}$		0		
$\phi_{C2,GH(B)}$				
$\phi_{C2,G1(A)}$	0	0	0	0
$\phi_{C2,G1(B)}$	0			
$\phi_{D1,D2}$	0.50 (0.14)	1	0.91 (0.09)	0.80 (0.05)
$\phi_{D2,G2}$	0.00	0.14 (0.13)	0.31 (0.15)	0.15 (0.07)
$\phi_{D1,G2}$	0.00	0.14 (0.13)	0.28 (0.14)	0.14 (0.06)
$\phi_{E1,E2}$	0.32 (0.12)	0.42 (0.11)	0.25 (0.13)	0.33 (0.07)
$\phi_{E2,G2}$	0.60 (0.22)	0.50 (0.18)	0.68 (0.28)	0.59 (0.13)
$\phi_{F1,B3}$	0.32 (0.07)	0.12 (0.04)	0.31 (0.06)	0.25 (0.04)
$\phi_{F1,C2}$	0.06 (0.03)	0.19 (0.05)	0.08 (0.04)	0.11 (0.02)
$\phi_{F1,GH}$		0.13 (0.04)		
$\phi_{F1,G1}$	0.11 (0.05)	0.12 (0.04)	0.16 (0.05)	0.13 (0.03)
$\phi_{G1,G2(A)}$	0.84 (0.04)	0.79 (0.04)	0.72 (0.06)	0.78 (0.03)
$\phi_{G1,G2(B)}$				
ψ_{A1}	0.94 (0.01)	0.97 (0.01)	0.92 (0.02)	0.94 (0.01)
ψ_{A2}	0.77 (0.04)	0.77 (0.03)	0.63 (0.04)	0.72 (0.02)
ψ_{B1}	0.06 (0.01)	0.03 (0.01)	0.08 (0.02)	0.06 (0.01)
ψ_{B2}				
ψ_{C2}				
ψ_{F2}	0.23 (0.04)	0.23 (0.03)	0.37 (0.04)	0.28 (0.02)
$\psi_{G1(A)}$		0.94 (0.03)		
$\psi_{G1(B)}$				
$\psi_{H1(A)}$		0.06 (0.03)		
$\psi_{H1(B)}$				
P_{A0a}	0.06 (0.06)	0.56 (0.12)	0.65 (0.07)	0.42 (0.05)
P_{A0b}	0.33 (0.27)	0.60 (0.13)	0.47 (0.06)	0.47 (0.10)
P_{A2a}	[pooled]			
P_{A2b}	[pooled]			
P_{A2}	0.64 (0.03)			
P_{A3}	0.18 (0.02)	0.11 (0.02)	0.62 (0.04)	0.30 (0.02)
P_{A4}	1	1	1	1
P_{A5}	1	1	1	1
P_{A6}	1	1	1	1

Table A2. (Continued)

Parameter	Release Occasion 1	2	3	Population Estimate
P_{A7}	0.98 (0.01)	0.99 (0.01)	0.94 (0.02)	0.97 (0.01)
P_{A8a}	0.95 (0.02)	[pooled]	0.98 (0.02)	
P_{A8b}	0.97 (0.01)	[pooled]	0.93 (0.03)	
P_{A8}	1.00 (< 0.01)	0.97 (0.02)	1.00 (< 0.01)	0.99 (0.01)
P_{A9a}	0.99 (0.01)	0.99 (0.01)	0.98 (0.02)	0.99 (0.01)
P_{A9b}	0.96 (0.02)	0.99 (0.01)	1	0.98 (0.01)
P_{B1}	1	1	1	1
P_{B2a}	1	1	[pooled]	
P_{B2b}	1	0.29 (0.17)	[pooled]	
P_{B2}	1	1	1	1
P_{B3a}	1	1	1	1
P_{B3b}	1	0.93 (0.07)	1	0.98 (0.02)
P_{C1a}				
P_{C1b}				
P_{C1}				
P_{C2a}	0.86 (0.13)	0.94 (0.06)	1	0.93 (0.05)
P_{C2b}	1	1	1	1
P_{D1}	1	1	1	1
P_{D2a}	1	1	1	1
P_{D2b}	1	0.86 (0.13)	1	0.95 (0.04)
P_{D2}	1	1	1	1
P_{E1}	1	1	1	1
P_{E2}	0.60 (0.22)	1	1	0.87 (0.07)
P_{F1a}	0.43 (0.11)	1	0.96 (0.03)	0.80 (0.04)
P_{F1b}	0.25 (0.08)	0.98 (0.02)	1	0.75 (0.03)
P_{F1}	0.58 (0.11)	1	1	0.86 (0.04)
P_{G1a}	0.89 (0.03)	[pooled]	0.77 (0.05)	
P_{G1b}	0.86 (0.04)	[pooled]	0.79 (0.05)	
P_{G1}	0.98 (0.01)	0.88 (0.03)	0.95 (0.02)	0.94 (0.01)
P_{G2a}	0.93 (0.03)	0.95 (0.02)	0.82 (0.05)	0.90 (0.02)
P_{G2b}	0.98 (0.02)	0.92 (0.03)	0.91 (0.04)	0.94 (0.02)
P_{G2}	1.00 (< 0.01)	1.00 (< 0.01)0.99 (< 0.01)	0.98 (0.01)	0.99 (< 0.01)
P_{H1a}		0.67 (0.27)		
P_{H1b}		0.33 (0.19)		
P_{H1}		0.78 (0.22)		

Table A3. Parameter estimates (standard errors in parentheses) for tagged juvenile steelhead released in 2012, including predator-type detections. Parameters without standard errors were estimated at fixed values in the model. Population-level estimates are weighted averages of the release-specific estimates. Some parameters were not estimable because of sparse data.

Parameter	Release Occasion			Population Estimate
	1	2	3	
S_{A2}	0.89 (0.05)			
S_{A3}	0.84 (0.04)	0.72 (0.06)	0.70 (0.04)	0.75 (0.03)
S_{A4}	0.99 (0.01)	0.98 (0.01)	0.97 (0.01)	0.98 (0.01)
S_{A5}	0.95 (0.01)	0.96 (0.01)	0.96 (0.02)	0.96 (0.01)
S_{A6}	0.97 (0.01)	0.97 (0.01)	0.99 (0.01)	0.98 (0.01)
S_{A7}	0.87 (0.04)	0.89 (0.02)	0.94 (0.02)	0.90 (0.02)
$S_{A7,G2}$	0.32 (0.03)	0.40 (0.03)	0.39 (0.04)	0.37 (0.02)
$S_{A8,G2}$	0.41 (0.04)	0.53 (0.04)	0.52 (0.06)	0.49 (0.03)
S_{B1}				
$S_{B2,G2}$	0.14 (0.06)	0.10 (0.06)	0.07 (0.04)	0.10 (0.03)
$S_{B2(SD)}$	0.90 (0.07)	0.67 (0.16)	0.46 (0.14)	0.68 (0.07)
$S_{C1,G2}$				
$S_{C1(SD)}$				
$S_{F1,G2}$	0.13 (0.06)	0.17 (0.05)	0.24 (0.06)	0.18 (0.03)
$\phi_{A1,A0}$	0.07 (0.03)	0.07 (0.01)	0.21 (0.02)	0.12 (0.01)
$\phi_{A1,A2}$	0.93 (0.02)			
$\phi_{A1,A3}$	0.82 (0.04)	0.92 (0.08)	0.52 (0.03)	0.75 (0.03)
$\phi_{A8,A9}$	0.60 (0.04)	0.67 (0.03)	0.78 (0.05)	0.68 (0.02)
$\phi_{A8,B3}$	0.04 (0.01)	0.02 (0.01)	0	0.02 (0.01)
$\phi_{A8,C2}$	0.01 (0.01)	0.03 (0.01)	0.02 (0.02)	0.02 (0.01)
$\phi_{A8,GH}$		0.17 (0.03)		
$\phi_{A8,G1}$	0.08 (0.02)	0.15 (0.03)	0.11 (0.03)	0.11 (0.02)
$\phi_{A9,B3}$	0.06 (0.02)	0.02 (0.01)	0.03 (0.02)	0.04 (0.01)
$\phi_{A9,C2}$	0	0.01 (0.01)	0.02 (0.02)	0.01 (0.01)
$\phi_{A9,GH}$		0.79 (0.04)		
$\phi_{A9,G1}$	0.66 (0.04)	0.73 (0.04)	0.80 (0.05)	0.73 (0.03)
$\phi_{B1,B2}$	1	0.82 (0.12)	0.76 (0.10)	0.86 (0.05)
$\phi_{B2,B3}$	0.10 (0.07)	0	0	0.03 (0.02)
$\phi_{B2,C2}$	0.05 (0.05)	0	0.08 (0.07)	0.04 (0.03)
$\phi_{B2,D1}$	0.30 (0.10)	0.44 (0.16)	0.08 (0.07)	0.27 (0.07)
$\phi_{B2,E1}$	0.45 (0.11)	0.22 (0.14)	0.31 (0.13)	0.33 (0.07)
$\phi_{B3,D1}$	0.19 (0.07)	0.08 (0.07)	0.44 (0.12)	0.24 (0.05)
$\phi_{B3,E1}$	0.39 (0.09)	0.46 (0.14)	0.38 (0.12)	0.41 (0.07)
$\phi_{B3,GH(A)}$		0.16 (0.10)		
$\phi_{B3,GH(B)}$				
$\phi_{B3,G1(A)}$	0.06 (0.04)	0.15 (0.10)	0.06 (0.06)	0.09 (0.04)
$\phi_{B3,G1(B)}$	0			
$\phi_{C1,B3}$				

Table A3. (Continued)

Parameter	Release Occasion 1	2	3	Population Estimate
$\phi_{C1,C2}$				
$\phi_{C1,D1}$				
$\phi_{C1,E1}$				
$\phi_{C2,D1}$	0	0.17 (0.09)	0.43 (0.19)	0.20 (0.07)
$\phi_{C2,E1}$	0.33 (0.19)	0.61 (0.12)	0.44 (0.19)	0.46 (0.10)
$\phi_{C2,GH(A)}$		0		
$\phi_{C2,GH(B)}$				
$\phi_{C2,G1(A)}$	0	0	0	0
$\phi_{C2,G1(B)}$	0		0	
$\phi_{D1,D2}$	0.67 (0.14)	1	1	0.89 (0.05)
$\phi_{D2,G2}$	0.00	0.13 (0.12)	0.28 (0.14)	0.13 (0.06)
$\phi_{D1,G2}$	0.00	0.13 (0.12)	0.28 (0.14)	0.13 (0.06)
$\phi_{E1,E2}$	0.46 (0.13)	0.47 (0.11)	0.23 (0.12)	0.39 (0.07)
$\phi_{E2,G2}$	0.67 (0.19)	0.44 (0.17)	0.68 (0.28)	0.60 (0.13)
$\phi_{F1,B3}$	0.30 (0.07)	0.12 (0.04)	0.28 (0.06)	0.23 (0.03)
$\phi_{F1,C2}$	0.08 (0.04)	0.19 (0.05)	0.08 (0.04)	0.12 (0.02)
$\phi_{F1,GH}$		0.13 (0.04)		
$\phi_{F1,G1}$	0.11 (0.05)	0.12 (0.04)	0.16 (0.05)	0.13 (0.03)
$\phi_{G1,G2(A)}$	0.83 (0.04)	0.80 (0.04)	0.72 (0.06)	0.78 (0.03)
$\phi_{G1,G2(B)}$				
ψ_{A1}	0.94 (0.01)	0.96 (0.01)	0.90 (0.02)	0.93 (0.01)
ψ_{A2}	0.82 (0.04)	0.76 (0.03)	0.63 (0.04)	0.74 (0.02)
ψ_{B1}	0.06 (0.01)	0.04 (0.01)	0.10 (0.02)	0.07 (0.01)
ψ_{B2}				
ψ_{C2}				
ψ_{F2}	0.18 (0.04)	0.24 (0.03)	0.37 (0.04)	0.26 (0.02)
$\psi_{G1(A)}$		0.94 (0.03)		
$\psi_{G1(B)}$				
$\psi_{H1(A)}$		0.06 (0.03)		
$\psi_{H1(B)}$				
P_{A0a}	0.24 (0.10)	0.63 (0.11)	0.79 (0.05)	0.55 (0.05)
P_{A0b}	0.50 (0.18)	0.60 (0.11)	0.71 (0.05)	0.60 (0.07)
P_{A2a}	[pooled]			
P_{A2b}	[pooled]			
P_{A2}	0.64 (0.03)			
P_{A3}	0.18 (0.02)	0.12 (0.02)	0.64 (0.04)	0.31 (0.02)
P_{A4}	1	1	1	1
P_{A5}	1	1	1	1

P_{A6}	1	1	1	1
P_{A7}	0.98 (0.01)	0.99 (0.01)	0.94 (0.02)	0.97 (0.01)

Table A3. (Continued)

Parameter	Release Occasion			Population Estimate
	1	2	3	
P_{A8a}	0.92 (0.02)	[pooled]	0.95 (0.02)	
P_{A8b}	[pooled]	[pooled]	0.98 (0.02)	
P_{A8}	[pooled]	[pooled]	0.94 (0.03)	
P_{A9a}	0.97 (0.03)	0.97 (0.02)	1.00 (< 0.01)	0.98 (0.01)
P_{A9b}	0.98 (0.01)	0.99 (0.01)	0.98 (0.02)	0.99 (0.01)
P_{B1}	1	1	1	1
P_{B2a}	1	1	[pooled]	
P_{B2b}	1	0.22 (0.14)	[pooled]	
P_{B2}	1	1	1	1
P_{B3a}	1	1	1	1
P_{B3b}	1	0.92 (0.07)	1	0.97 (0.02)
P_{C1a}				
P_{C1b}				
P_{C1}				
P_{C2a}	0.86 (0.13)	0.94 (0.05)	1	0.93 (0.05)
P_{C2b}	1	1	1	1
P_{D1}	1	1	1	1
P_{D2a}	1	1	1	1
P_{D2b}	0.87 (0.12)	0.87 (0.12)	1	0.92 (0.06)
P_{D2}	1	1	1	1
P_{E1}	1	1	1	1
P_{E2}	0.57 (0.19)	1	1	0.86 (0.06)
P_{F1a}	0.54 (0.14)	1	0.96 (0.03)	0.83 (0.05)
P_{F1b}	0.29 (0.09)	0.98 (0.02)	1	0.76 (0.03)
P_{F1}	0.67 (0.13)	1	1	0.89 (0.04)
P_{G1a}	0.89 (0.03)0.81 (0.04)	[pooled]	0.77 (0.05)	
P_{G1b}	0.86 (0.03)	[pooled]	0.79 (0.05)	
P_{G1}	0.98 (0.01)	0.88 (0.03)	0.95 (0.02)	0.94 (0.01)
P_{G2a}	0.93 (0.03)	0.95 (0.02)	0.82 (0.05)0.90 (0.05)	0.90 (0.02)
P_{G2b}	0.98 (0.02)	0.92 (0.03)0.89 (0.03)	0.91 (0.04)	0.94 (0.02)
P_{G2}	1.00 (< 0.01)	1.00 (< 0.01)	0.98 (0.01)	0.99 (<0.01)
P_{H1a}		0.67 (0.27)		
P_{H1b}		0.33 (0.19)		
P_{H1}		0.78 (0.22)		

Appendix B. Update on 2011 Survival through Facilities

Survival through the water export facilities was estimated for the 2011 steelhead tagging study (Buchanan 2013). However, results presented in the 2011 OCAP report represented only those tagged steelhead that arrived at the interior receivers in or closest to the facilities via the Old River route, excluding those that arrived via the San Joaquin River route. In 2011, the majority of the steelhead detected at the radial gates at the Clifton Court Forebay (194 of 233) and at the CVP trashracks (66 of 80) came via the Old River route, but some steelhead arrived via the San Joaquin River route. Average estimated survival from the CVP holding tank to release from transport on the San Joaquin or Sacramento rivers was 0.94 ($\widehat{SE} = 0.03$) for Old River route fish alone, and 0.92 ($\widehat{SE} = 0.03$) for both the Old River route and the San Joaquin River route combined (Table B1). Average survival from the interior receivers at the radial gates at the Clifton Court Forebay to release from transport was 0.73 ($\widehat{SE} = 0.03$) for fish from the Old River route alone, and 0.70 ($\widehat{SE} = 0.03$) for both routes combined (Table B1). In each case, the difference observed by including the San Joaquin River route was not significant at the 5% level ($P \geq 0.4205$).

Table B1. Estimates of survival in 2011 from the CVP holding tank or interior radial gates receiver to Chipps Island, Jersey Point, and False River for tagged steelhead that arrived at CVP or radial gates via only the Old River route, or via either the Old River route or the San Joaquin River route. Standard errors are in parentheses.

Release Group	From CVP holding tank		From Radial Gates (Interior)	
	OR Route	OR and SJR Route	OR Route	OR and SJR Route
1[a]	0.88 (0.16)	0.88 (0.16)	0.72 (0.08)	0.72 (0.88)
2	0.90 (0.07)	0.88 (0.07)	0.74 (0.06)	0.70 (0.06)
3	0.91 (0.09)	0.87 (0.09)	0.73 (0.06)	0.71 (0.06)
4	1 (0) (n=22)	0.98 (0.05)	0.79 (0.08)	0.76 (0.06)
5	0.93 (0.07)	0.93 (0.07)	0.38 (0.17)	0.31 (0.13)
2-5	0.95 (0.03)	0.92 (0.03)	0.73 (0.04)	0.69 (0.03)
3-4	0.98 (0.04)	0.93 (0.05)	0.76 (0.05)	0.73 (0.04)
Pooled	0.94 (0.03)	0.92 (0.03)	0.73 (0.03)	0.70 (0.03)

a = No tagged steelhead from this release group were detected at the CVP holding tank or the radial gates coming from the San Joaquin River route.

Appendix C. Errata from 2011 Report

In Table A1 of the 2011 6-year study report (Buchanan 2013), the definition for parameter $S_{A8,G2}$ should read “Overall survival from STN to Chipps Island (CHPE/CHPW).”

North American Journal of Fisheries Management
Publication details, including instructions for authors and subscription information:
http://www.tandfonline.com/loi/ujfm20

Route Use and Survival of Juvenile Chinook Salmon through the San Joaquin River Delta

Rebecca A. Buchanan [a] , John R. Skalski [a] , Patricia L. Brandes [b] & Andrea Fuller [c]
[a] Columbia Basin Research, School of Aquatic and Fishery Sciences , University of Washington , 1325 4th Avenue, Suite 1820, Seattle , Washington , 98101-2509 , USA
[b] U.S. Fish and Wildlife Service , 850 Guild Avenue, Suite 105, Lodi , California , 96240 , USA
[c] FISHBIO Environmental, LLC, 1617 South Yosemite Avenue , Oakdale , California , 95361 , USA
Published online: 01 Feb 2013.

To cite this article: Rebecca A. Buchanan , John R. Skalski , Patricia L. Brandes & Andrea Fuller (2013) Route Use and Survival of Juvenile Chinook Salmon through the San Joaquin River Delta, North American Journal of Fisheries Management, 33:1, 216-229, DOI: 10.1080/02755947.2012.728178

To link to this article: http://dx.doi.org/10.1080/02755947.2012.728178

North American Journal of Fisheries Management 33:216–229, 2013

ISSN: 0275-5947 print / 1548-8675 online
DOI: 10.1080/02755947.2012.728178

ARTICLE

Route Use and Survival of Juvenile Chinook Salmon through the San Joaquin River Delta

Rebecca A. Buchanan* and John R. Skalski
Columbia Basin Research, School of Aquatic and Fishery Sciences, University of Washington, 1325 4th Avenue, Suite 1820, Seattle, Washington 98101-2509, USA

Patricia L. Brandes
U.S. Fish and Wildlife Service, 850 Guild Avenue, Suite 105, Lodi, California 96240, USA

Andrea Fuller
FISHBIO Environmental, LLC, 1617 South Yosemite Avenue, Oakdale, California 95361, USA

Abstract

The survival of juvenile Chinook Salmon through the lower San Joaquin River and Sacramento–San Joaquin River Delta in California was estimated using acoustic tags in the spring of 2009 and 2010. The focus was on route use and survival within two major routes through the Delta: the San Joaquin River, which skirts most of the interior Delta to the east, and the Old River, a distributary of the San Joaquin River leading to federal and state water export facilities that pump water out of the Delta. The estimated probability of using the Old River route was 0.47 in both 2009 and 2010. Survival through the southern (i.e., upstream) portion of the Delta was very low in 2009, estimated at 0.06, and there was no significant difference between the Old River and San Joaquin River routes. Estimated survival through the Southern Delta was considerably higher in 2010 (0.56), being higher in the Old River route than in the San Joaquin route. Total estimated survival through the entire Delta (estimated only in 2010) was low (0.05); again, survival was higher through the Old River. Most fish in the Old River that survived to the end of the Delta had been salvaged from the federal water export facility on the Old River and trucked around the remainder of the Delta. The very low survival estimates reported here are considerably lower than observed salmon survival through comparable reaches of other large West Coast river systems and are unlikely to be sustainable for this salmon population. More research into mortality factors in the Delta and new management actions will be necessary to recover this population.

The Central Valley of California marks the southern limit of Chinook Salmon *Oncorhynchus tshawytscha* in North America (Healey 1991). Chinook Salmon population abundances in this region have been much reduced from the 19th century in response to a number of factors, including habitat loss, hatcheries, and water development (e.g., pumping water out of the basin; Healey 1991; Fisher 1994). Today, the Sacramento–San Joaquin River Delta is a highly modified environment with levees and drained fields replacing tidal wetlands, and riprap replacing natural shoreline. Demand for Delta waters is high. State and federal water export facilities extract water from the southern portion of the Delta (Figure 1) for agricultural, industrial, and municipal use throughout California. The Delta provides drinking water for approximately 27 million Californians and irrigation water for more than 1,800 agricultural users, and 4.6–6.3 million acre-feet of water are exported from the Delta annually (DSC 2011). This intense exporting combined with tidal fluctuations can sometimes cause net flows in the Delta to be directed upstream rather than downstream (Brandes and McLain 2001). Pollution from industry, agricultural and urban runoff, and erosion are also concerns (DSC 2011). Both native and nonnative species of

*Corresponding author: rabuchan@u.washington.edu
Received March 28, 2012; accepted September 5, 2012
Published online February 1, 2013

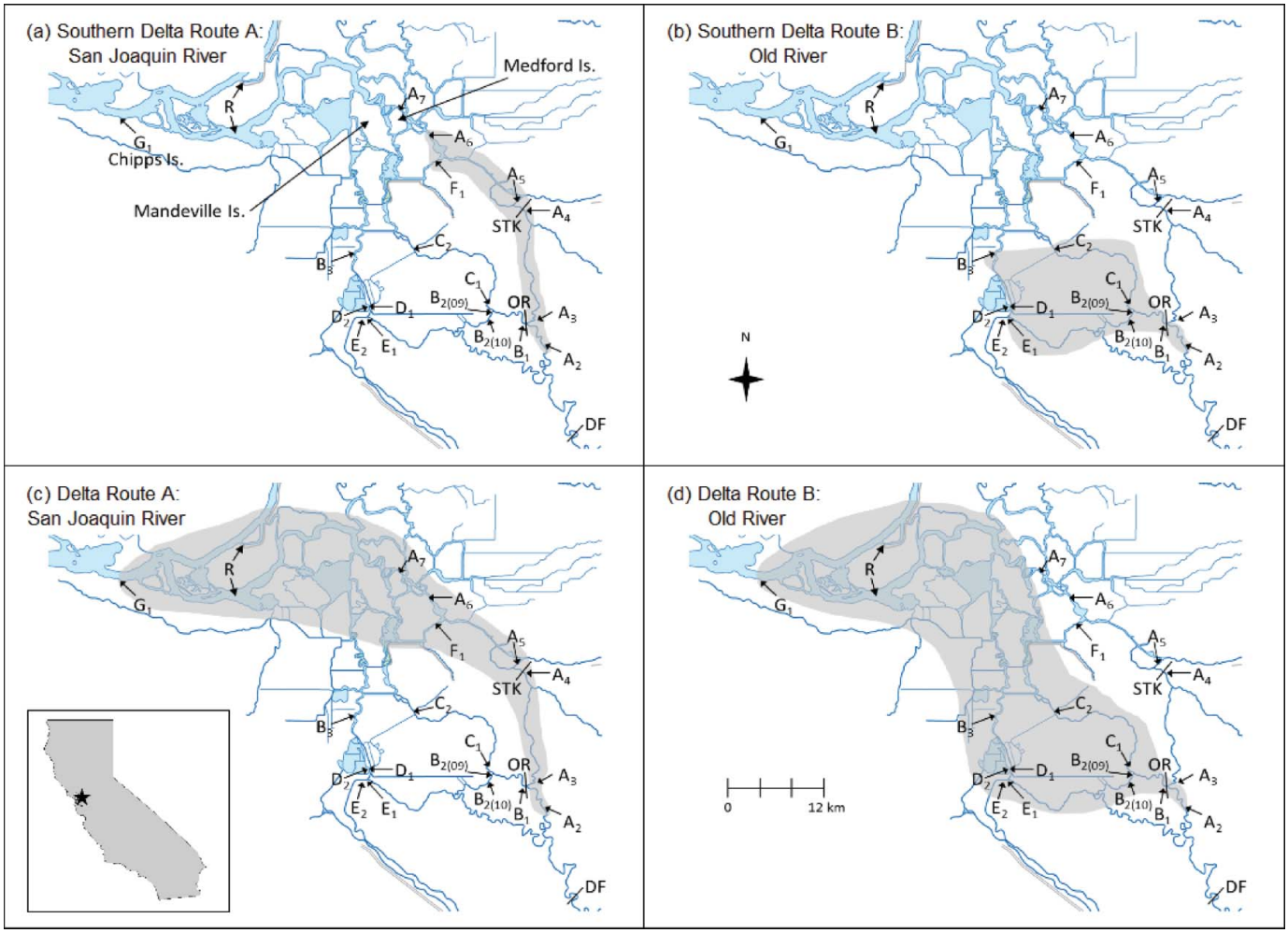

FIGURE 1. Acoustic telemetry receiver sites throughout the San Joaquin River Delta for the juvenile Chinook Salmon tagging studies in 2009 and 2010. The region included in each major route through the study area is shaded for the Southern Delta for the **(a)** San Joaquin River and **(b)** Old River routes and through the entire Delta for the **(c)** San Joaquin River and **(d)** Old River routes. Sites in the San Joaquin, Old, and Middle rivers are labeled A, B, and C, respectively. The label for site B2 includes the study years 2009 (09) and 2010 (10). Sites A7, C1, and G1 were used only in 2010. Mossdale is denoted by A2, Chipps Island at river kilometer 0 by G1, the federal water export facilities by E1 and E2, and state water export facilities by D1 and D2. The city of Stockton is near sites A5 and A6. Sites B3 and C2 are located near California Highway 4. Release sites are designated as follows: DF = Durham Ferry (2009, 2010), OR = Old River (2010), STK = Stockton (2010), and R = release after salvage and trucking. Route-specific survival and route entrainment probability were estimated for the Southern Delta in 2009 and 2010 and for the entire Delta in 2010. [Figure available in color online.]

predatory fish (e.g., Striped Bass *Morone saxatilis*, Largemouth Bass *Micropterus salmoides*, White Catfish *Ameiurus catus*) inhabit these areas and feed on migrating smolts, as do avian predators including double-crested cormorants *Phalacrocorax auritus* and white pelicans *Pelecanus erythrorhynchos*. All of these factors lower survival of migrating salmon smolts relative to historical conditions.

The Vernalis Adaptive Management Plan (VAMP) is a large-scale, long-term (12-year) experimental management program begun in 2000 that was designed to protect juvenile Chinook Salmon as they migrate from the San Joaquin River through the Sacramento–San Joaquin River Delta (Figure 1; SJRGA 2005, 2007, 2010, 2011). Part of the VAMP is a multiyear tagging study to monitor juvenile salmon survival through the Delta; the long-term goal is to relate Delta survival to changes in river flow (discharge) and water export levels in the presence of a temporary barrier at the head of the Old River, which was designed to prevent salmon from entering the Old River (Figure 1). Prior to 2006, VAMP tagging studies relied on coded wire tags (CWTs), which provided information on salmon survival on a large spatial scale using 100,000–300,000 study fish each year (Newman 2008). Starting in 2006, the tagging studies began using micro-acoustic tags, which provide more precise survival information on a smaller spatial scale with much smaller releases groups (e.g., about 1,000 fish). Coded wire tags were discontinued in 2007. Study years 2006 and 2007 were pilot studies providing feedback on design and implementation of the acoustic tag studies. The 2008 study deployed an extensive array of acoustic

hydrophones throughout the Delta but suffered from a high degree of premature tag failure (Holbrook et al. 2013). Thus, 2009 and 2010 were the first years that provided sufficient information to estimate salmon survival through portions of the Delta on a relatively detailed spatial scale, yielding the first estimates of how fish distribute across various migration routes. Further, these 2 years represent different hydrologic conditions—very low flows in 2009 and above normal flows in 2010—thus providing preliminary information needed to identify a relationship between survival and flow. Survival through the southern portion of the Delta was estimated in both 2009 and 2010, and survival through the entire Delta was estimated in 2010 (described below; Figure 1). In both years, survival estimates were compared through two major migration routes: the San Joaquin River route and the Old River route. We present here the first spatially detailed estimates of survival and route use by juvenile Chinook Salmon through the lower San Joaquin River into the Delta.

STUDY AREA

Historically, focus has been on the survival of fish through the Delta to Chipps Island, located in Suisan Bay at the confluence of the San Joaquin and Sacramento rivers near Pittsburg, California, at river kilometer (rkm) 0 (Figure 1). Fish moving through the Delta toward Chipps Island may use any of several routes. The simplest route follows the San Joaquin River until it joins the Sacramento River near Chipps Island (Figure 1a, c; route A). An alternative route uses the Old River from its head on the San Joaquin River to Chipps Island, either via its confluence with the San Joaquin River just west of Mandeville Island, or through Middle River or the state and federal water export facilities (Figure 1b, d; route B). Additional subroutes were monitored for fish use but were contained within either route A or route B. Subroute C consists of the Middle River from the Old River to the San Joaquin downstream of Medford Island. Two other subroutes were the water export facilities off the Old River: fish entering either the State Water Project (subroute D) or the Central Valley Project (subroute E) had the possibility of being trucked from those sites and released upstream of Chipps Island. Subroutes C, D, and E were all contained in route B (Old River). Finally, fish that remained in the San Joaquin River past Stockton may have entered Turner Cut and maneuvered to Chipps Island through the interior of the Delta (subroute F). Fish in routes B, C, and F all had multiple unmonitored pathways available for passing through the Delta toward Chipps Island.

Survival through the study area was estimated on two spatial scales: (1) the southern portion of the Delta, which is bounded downstream by the federal and state water export facilities, California Highway 4, and the Turner Cut junction with the San Joaquin River (the "Southern Delta"; Figure 1a, b) and (2) the entire Delta, which is bounded downstream by Chipps Island (the "Delta"; Figure 1c, d). Both the Southern Delta and Delta regions were bounded upstream by the acoustic receiver (site A2) located near Mossdale Bridge, upstream of the Old River junction with the San Joaquin River. The Southern Delta region was entirely contained within the Delta region (Figure 1). In 2009, no acoustic receivers were deployed at Chipps Island, so the study area was limited to the Southern Delta. In 2010, a more extensive detection field was installed, including dual receivers at Chipps Island (G1) (Figure 1). Thus, in 2010, the study area included the entire migration path through the Delta region. Two migration routes were monitored through both the Southern Delta and Delta regions: the San Joaquin Route (route A in Figure 1a, c) and the Old River route (route B in Figure 1b, d).

Since the 1990s, a temporary physical or nonphysical barrier (sound, strobe lights, and a bubble curtain) has often been installed at the head of the Old River with the aim of preventing migrating smolts from entering that river. In 2009 and 2010, a nonphysical barrier was installed there, and its smolt-guidance effectiveness was evaluated in studies concurrent with the VAMP studies (Bowen et al. 2009; Bowen and Bark 2012). The nonphysical barrier was operated during passage of approximately half of each VAMP release group in 2009 or 2010. No physical barrier was installed.

METHODS

Tagging and release methods.—Both study years used the Hydroacoustic Technology, Inc. (HTI) Model 795 microacoustic tag (diameter = 6.7 mm, length = 16.3–16.4 mm, average weight in air = 0.65 g). In 2009 a total of 933 juvenile Chinook Salmon (fall–spring-run hybrids) originating from the Feather River Fish Hatchery were tagged and released between 22 April and 13 May (fork length = 85.0–110.0 mm, mean = 94.8 mm; Table 1). Difficulties in rearing fish to size resulted in an average tag burden (i.e., the ratio of tag weight to body weight) of 7.1% (range = 4.4–10.2%), which was higher than desired ($\leq$5.5%; Brown et al. 2006). Six fish died in 2009 between tagging and release. In 2010, a total of 993 juvenile fall-run Chinook Salmon originating from the Merced River Fish Hatchery were tagged and released between 27 April and 20 May (fork length = 99.0–121.0 mm, mean = 110.5 mm). Tag burden in 2010 was 2.8–5.8% (mean = 4.2%; Table 1). Four fish died in 2010 between tagging and release.

In both years, tagging was performed at the Tracy Fish Facility located in the Delta approximately 30–45 km from the release site(s). Tagging procedures followed those outlined in Adams et al. (1998) and Martinelli et al. (1998). Fish were anesthetized in a 70-mg/L tricaine methanesulfonate solution, buffered with an equal concentration of sodium bicarbonate, and surgically implanted with programmed acoustic transmitters. Typical surgery times were less than 3 min. Nonfunctioning tags were removed from the study. After surgery, fish were placed in 19-L containers with high dissolved oxygen (DO) concentrations (110–130%) for recovery. Each holding container was perforated to allow partial water transfer and held no more than three tagged fish. After initial recovery from surgery, tagged fish were transported in buckets to the release site in transport

TABLE 1. Release data for groups of Chinook salmon smolts used in the 2009 and 2010 Vernalis Adaptive Management Plan studies, where DF = Durham Ferry, STK = Stockton, and OR = Old River. In 2009, releases were pooled into strata for analysis; in 2010, releases from separate locations were jointly analyzed for a single release occasion.

Release location	Release date	Release number	Mean (range) fork length (mm)	Tag burden (%)	Release stratum/occasion
			Study year 2009		
DF	Apr 22	133	96.1 (86–108)	6.9 (5.2–9.0)	1
	Apr 25	134	93.4 (88–105)	7.3 (5.2–9.6)	1
	Apr 29	134	97.1 (87–110)	6.8 (4.5–3.6)	2
	May 2	134	96.6 (87–108)	6.6 (4.4–9.3)	2
	May 6	132	92.6 (85–102)	7.7 (5.5–10.2)	2
	May 9	133	93.9 (88–100)	7.3 (5.4–9.1)	2
	May 13	133	93.8 (90–104)	7.2 (5.3–8.8)	3
			Study year 2010		
DF	Apr 27–28	74	108.0 (102–110)	4.4 (3.5–5.7)	1
	Apr 30–May 1	74	109.1 (103–115)	4.3 (3.1–5.4)	2
	May 4–5	73	109.4 (102–118)	4.3 (3.4–5.6)	3
	May 7–8	70	111.1 (101–119)	4.1 (3.1–5.4)	4
	May 11–12	70	112.0 (99–121)	4.1 (3.1–5.4)	5
	May 14–15	73	112.6 (101–119)	4.0 (3.1–5.3)	6
	May 18–19	70	112.1 (103–119)	3.9 (2.8–5.3)	7
STK	Apr 28–29	35	107.5 (100–115)	4.5 (3.5–5.6)	1
	May 1–2	36	108.5 (100–115)	4.4 (3.4–5.4)	2
	May 5–6	35	110.3 (104–118)	4.2 (3.4–5.0)	3
	May 8–9	36	109.6 (102–117)	4.3 (3.5–5.6)	4
	May 12–13	35	111.2 (105–119)	4.2 (3.3–5.4)	5
	May 15–16	34	112.9 (102–119)	4.0 (3.0–5.2)	6
	May 19–20	31	113.4 (108–119)	3.9 (3.1–5.0)	7
OR	Apr 28–29	36	108.2 (102–117)	4.5 (3.6–5.3)	1
	May 1–2	36	108.5 (102–115)	4.5 (3.5–5.6)	2
	May 5–6	36	108.6 (100–118)	4.5 (3.4–5.6)	3
	May 8–9	36	110.4 (104–118)	4.2 (3.5–5.1)	4
	May 12–13	36	111.8 (104–120)	4.2 (2.9–5.8)	5
	May 15–16	35	113.3 (105–119)	4.0 (3.0–5.2)	6
	May 19–20	32	112.3 (101–119)	3.9 (3.2–5.3)	7

tanks designed to guard against fluctuations in water temperature and DO. Transport to the release site took approximately 45–60 min. At the release site, tagged fish were held in either 1-m^3 net pens (3-mm mesh; first release in 2009) or in perforated 121.1-L plastic garbage cans (2010) for a minimum of 24 h before release.

In 2009, all fish were released on the San Joaquin River at Durham Ferry, located at approximately rkm 110 (measured from the river mouth at Chipps Island) approximately 20 km upstream of the boundary of the study area (Mossdale Bridge; Figure 1). The release site was located upstream of the study area to allow fish to recover from handling and distribute naturally in the river channel before entering the study area. In 2010, each of seven release occasions consisted of an initial release at Durham Ferry and two supplemental releases, one located in the Old River near the junction with the San Joaquin River and the other located in the San Joaquin River near the city of Stockton (Figure 1). The supplemental releases were designed to provide enough tagged fish in the lower reaches of the study area to estimate survival all the way to Chipps Island, even if survival was low from Durham Ferry.

For each study year, an in-tank tag life study was performed to measure the rate of tag failure under the tag operating parameters (i.e., encoding, range, and pulse width) used in the study. Stratified random sampling of tags across manufacturing lots and tag codes was used to ensure that tags in the tag-life study represented the population of tags released in study fish.

In both study years, tag effects on short-term (48-h) survival were assessed using dummy (i.e., inactive)-tagged and untagged fish that were handled using the same procedures as fish with active transmitters. No significant difference in survival was observed between dummy-tagged and untagged fish over the

48-h period (SRJGA 2010, 2011). Tag effects on longer-term (≤21 d) survival and predator avoidance were expected to be small based on existing studies on effects of acoustic tags on juvenile Chinook Salmon with comparable tag burden (e.g., Anglea et al. 2004).

Water temperatures at the release locations were <20°C during most releases, ranging from 16.1°C to 21.1°C in 2009 and from 14.2°C to 18.8°C in 2010. Temperature increased as a function of distance downstream from Durham Ferry in both the San Joaquin River main stem and the Delta and increased throughout the season. Temperatures in the study area exceeded 20°C starting in mid-May in 2009 and in early June in 2010.

Hydrophone placement.—An extensive array of acoustic hydrophones and receivers was deployed throughout the Delta in each study year, with 19 receivers and hydrophones being deployed in 2009 and 32 receivers (35 hydrophones) in 2010 (Figure 1). Acoustic receivers were named according to migration route (A–G). Chipps Island, the final destination of all routes in 2010, was assigned its own route name (G). At each location, one to four hydrophones were deployed to achieve full cross-sectional coverage of the channel.

Acoustic receivers were located at the Delta entrance (Mossdale, site A2) in both 2009 and 2010, at the Delta exit (Chipps Island, G1) in 2010, and at key points in between in both years (Figure 1). The Mossdale site was moved 1.4 km downstream in 2010 to an acoustically quieter site. All available migration routes were monitored at the Old River (sites A3 and B1) and Turner Cut (A6 and F1) diversions from the San Joaquin River (Figure 1). Receivers were located on the San Joaquin River in Stockton near the Stockton Waste Water Treatment Facility (A4) and near the Navy Drive Bridge just upstream of the Stockton Deep Water Ship Channel (A5) because of concern about salmon survival past the water treatment plant. Receivers were also located at the entrance to the state and federal water export facilities on the Old River (Figure 1). At the federal facility (Central Valley Project, CVP), receivers were placed just upstream and downstream of the trash racks (E1) and in the holding tank (E2), where salvaged fish were held before transportation by truck to release sites in the lower Delta on the San Joaquin and Sacramento rivers (R). At the state facility, receivers were placed both outside (D1) and inside (D2) the radial entrance gates to the Clifton Court Forebay (CCF), the reservoir from which the State Water Project draws water. Both the CVP trash racks and the CCF radial gates are known feeding areas for piscine predators (Vogel 2010, 2011). Receivers were also located downstream in the Old (B3) and Middle (C2) rivers near the Highway 4 bridge. Dual receiver arrays were placed at some sites to provide data to estimate detection probabilities, typically at the downstream boundary of the study area and at sites just downstream of river junctions. Both acoustic lines within each dual array (average 0.3 km apart) were designed for full coverage of the channel. The nonphysical barrier located at the head of the Old River was evaluated via a separate network of hydrophones that were not used in the VAMP study (Bowen et al. 2009; Bowen and Bark 2012).

The locations of the hydrophones were dictated by the possible migration routes (San Joaquin [A], and Old River [B]) and subroutes, and by the two spatial scales on which inference was to be made (Southern Delta and Delta). The acoustic receivers located in Turner Cut (F1) and at the channel markers in the San Joaquin River near the Turner Cut junction (A6) monitored the exit of the San Joaquin route through the Southern Delta region in both 2009 and 2010 (Figure 1a). Likewise, the exit of the Old River route through the Southern Delta region was monitored by receivers at the state and federal water facilities and near Highway 4 in both 2009 and 2010 (Figure 1b). In 2010, the exit of both the San Joaquin route (Figure 1c) and the Old River route (Figure 1d) through the entire Delta region was monitored by dual receivers at Chipps Island.

Signal processing.—The raw tag detection data generated by the acoustic telemetry receivers were processed by identifying the date and time of each tag detection. Unique tags were identified by the period (1/frequency) of the acoustic signal. The 2009 data were processed manually using the HTI proprietary software *MarkTags*. The 2010 data were processed using a combination of automatic and manual processing, manual processing being limited to key detection sites (SJRGA 2011).

The San Joaquin River Delta is home to several populations of predatory fish that are large enough to feed on juvenile salmonids, including Striped Bass, Largemouth Bass, and White Catfish. A predatory fish that has eaten an acoustic-tagged juvenile salmon and then moves past a hydrophone may introduce misleading tag detections into the data. Thus, it was necessary to identify and remove those detections that came from predators. Likely predator detections were identified in a decision process that used up to three levels of spatial–temporal analysis, based on the methods of Vogel (2010, 2011): near-field, mid-field, and far-field. Near-field analysis required manual processing of the raw acoustic telemetry data, and interpreted the pattern of the acoustic signal during detection as an indicator of fish movement near the receiver. Mid-field analysis focused on residence time within the detection field of each receiver, and transitions between neighboring receivers. Far-field analysis examined transitions on the scale of the study area. All available detection data were considered in identifying likely predator detections, as well as environmental data such as river flow and tidal stage, measured at several gaging stations throughout the Delta (downloaded from the California Data Exchange Center Web site: http://cdec.water.ca.gov). The predator decision process was based on the assumptions that Chinook Salmon smolts were emigrating and so were directed downstream, and that they were unlikely to move between acoustic receivers (≥2 km) against river flow. Movements directed upstream against the flow were considered evidence of predation, although short-term upstream movements under reverse flow or slack tide conditions were deemed consistent with a salmon smolt. Unusually fast or slow transitions between detection sites or particularly long residence time at a detection site were also considered evidence of predation. In 2009, the near-field analysis comprised the majority of the predation decision process. In 2010, more emphasis

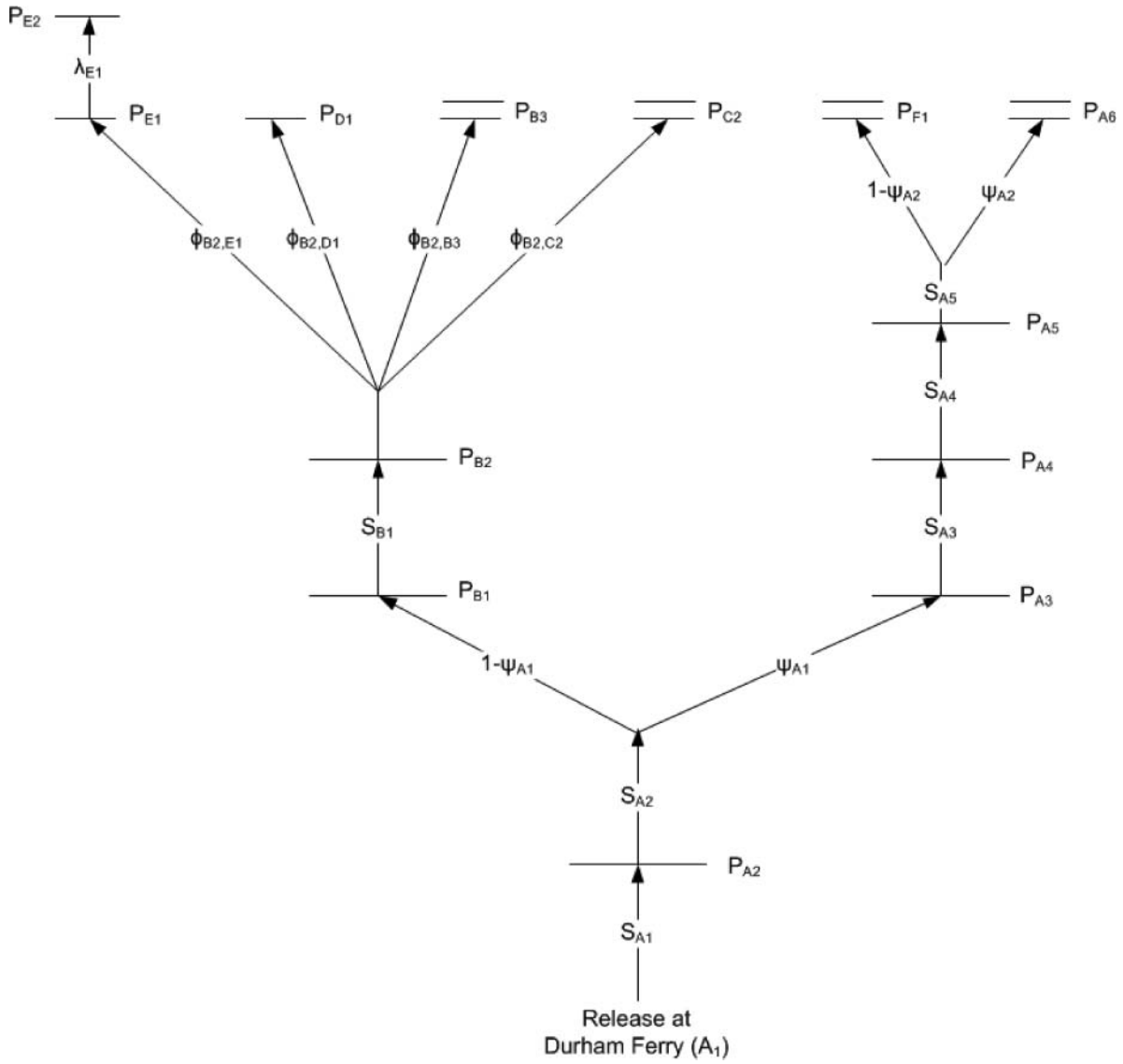

FIGURE 2. Model schematic for the 2009 Chinook Salmon smolt tagging study. Horizontal lines indicate acoustic receivers; parallel lines indicate dual receiver arrays. Model parameters are salmon reach survival (S), detection probabilities (P), route entrainment probabilities (ψ), transition probabilities ($\phi = \psi S$), and "last reach" parameters ($\lambda = \phi P$).

was placed on travel time, residence time, and movements in relation to river flow (mid-field and far-field analysis).

After removing the suspected predator detections, the processed data were converted to individual detection histories for each tagged fish. The detection history identified the chronological sequence of sites where the tag was detected. In the event that a tag was detected at a site or river junction multiple times, the last path past the site or river junction was used in the detection history as the best depiction of the final fate of the fish in the region.

Statistical survival and migration model.—A multistate statistical release–recapture model (Buchanan and Skalski 2010) was developed and used to estimate salmon smolt survival, detection probabilities, and route-use ("entrainment") probabilities (Figures 2, 3). The release–recapture model was similar to the model developed by Perry et al. (2010), with states representing the various routes through the Delta. Detection sites (acoustic receivers) were named according to route.

The release–recapture models used for both study years used parameters that denoted the probability of detection (P_{hi}), route entrainment probability (ψ_{hl}), salmon reach survival (S_{hi}), and transition probabilities ($\phi_{kj,hi}$) equivalent to the joint probability of movement and survival, where h and k represent route, i and j represent detection sites within a route, and l represents junctions within a route (Figures 2, 3). The transition probability $\phi_{kj,hi}$ from site j in route k to site i in route h included all

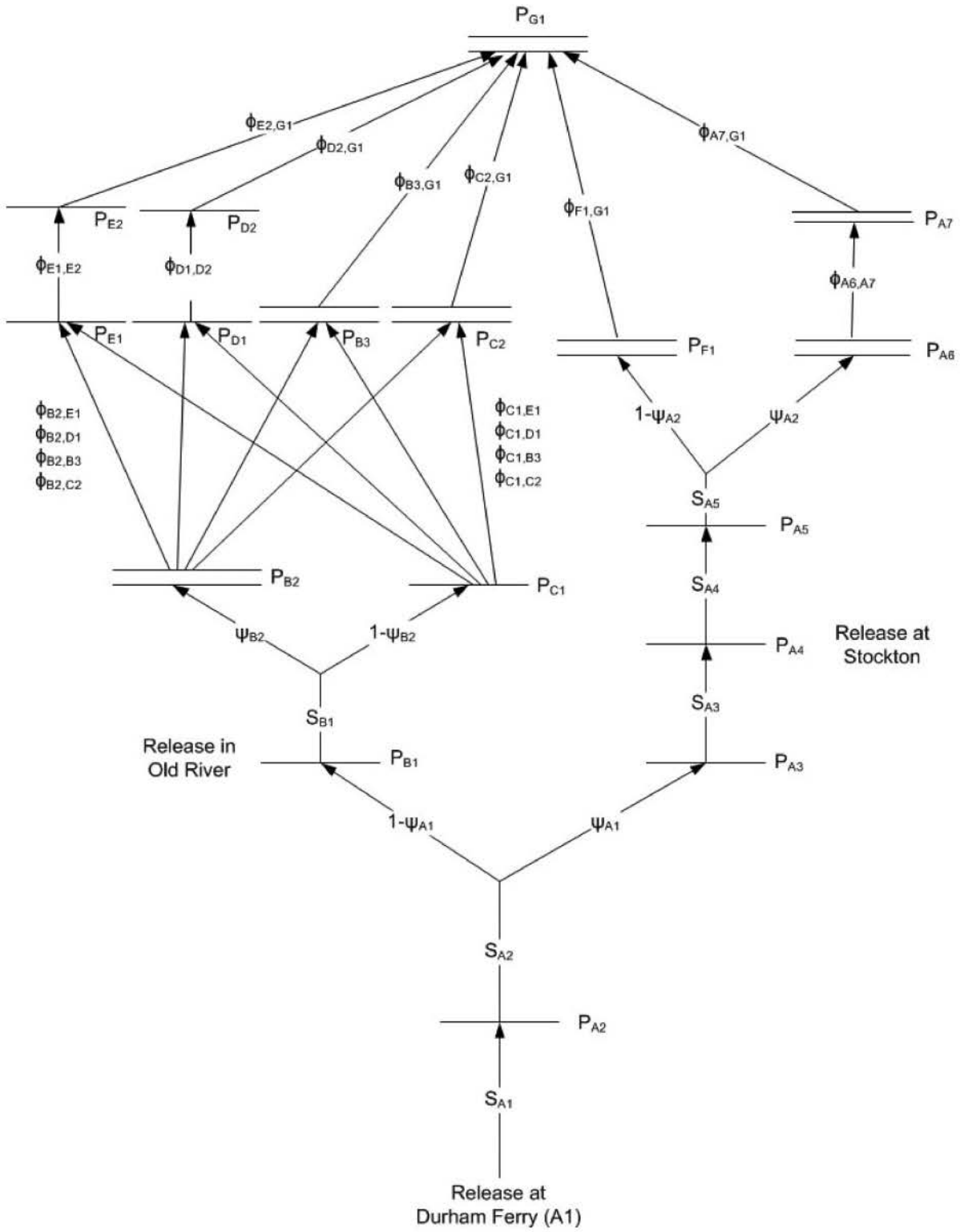

FIGURE 3. Model schematic for the 2010 Chinook Salmon smolt tagging study. See Figure 2 for additional information.

possible routes between the two sites and was used when it was not possible to separately estimate the route entrainment and survival probabilities. Unique transition parameters were estimated at receiver D1 located outside the radial gates of the Clifton Court Forebay depending on gate status at the time of fish arrival (open or closed) in the 2010 study. Gate status data were unavailable for the 2009 study.

In some cases, it was not possible to separately estimate the transition probability to a site and the detection probability at the site. This occurred primarily at the entrances to the water export facilities (E1 = CVP trash racks, and D1 = first CCF receiver) due to sparse data. In these cases, the joint probability of survival from the previous receiver to receiver i in route h was estimated as $\lambda_{hi} = \phi_{kj,hi} P_{hi}$. We assumed that the detection probability was 100% at the radial gate receivers inside Clifton Court Forebay and in the holding tank at the Central Valley Project. These assumptions, necessary in the absence of receivers located downstream of those detection sites and unique to those routes, were reasonable as long as the receivers were operating.

A multinomial likelihood model was constructed based on possible capture histories under the assumptions of common survival, route entrainment, and detection probabilities and independent detections among the tagged fish in each release group. The likelihood model was fit using maximum likelihood in the software Program USER (Lady and Skalski 2008), providing point estimates and standard errors of model parameters and derived performance measures.

In addition to the model parameters, performance at the migration route level was estimated as functions of the model parameters. The probability of a smolt taking the San Joaquin River route (route A) was ψ_{A1}, while the probability of using the Old River route (route B) was $1 - \psi_{A1}$. Regional passage survival (S_R for region R) was estimated on two spatial scales: the southern Delta (R = SD; 2009 and 2010) and the entire San Joaquin River delta (R = D) from Mossdale Bridge to Chipps Island (2010) (Figure 1). Regional passage survival for region R (R = SD or D) was defined in terms of both the route entrainment probability (ψ_{A1}) and the route-specific survival probabilities:

$$S_R = \psi_{A1} S_{A(R)} + (1 - \psi_{A1}) S_{B(R)}.$$

The route-specific survival probabilities through region R (i.e., $S_{A(R)}$ and $S_{B(R)}$ for R = SD or D) were defined as

$$S_{A(R)} = S_{A2} S_{A3} S_{A4} S_{A5(R)}$$

and

$$S_{B(R)} = S_{A2} S_{B1} S_{B2(R)}.$$

The survival probabilities through the final reaches of each route (i.e., $S_{A5(R)}$ and $S_{B2(R)}$) were defined as

$$S_{A5(R)} = \begin{cases} S_{A5}, & \text{for } R = SD \\ S_{A5}(\psi_{A2}\phi_{A6,A7}\phi_{A7,G1} + [1-\psi_{A2}]\phi_{F1,G1}), & \text{for } R = D \end{cases}$$

and

$$S_{B2(R)} = \begin{cases} \phi_{B2,B3} + \phi_{B2,C2} + \phi_{B2,D1} + \phi_{B2,E1}, & \text{for } R = SD \\ \phi_{B2,B3}\phi_{B3,G1} + \phi_{B2,C2}\phi_{C2,G1} \\ \quad + \phi_{B2,D1}\phi_{D1,D2}\phi_{D2,G1} \\ \quad + \phi_{B2,E1}\phi_{E1,E2}\phi_{E2,G1}, & \text{for } R = D. \end{cases}$$

For fish that reached the interior receivers at the Clifton Court Forebay or CVP in 2010, the parameters $\phi_{D2,G1}$ and $\phi_{E2,G1}$ included survival during and after collection and transport. Although a subroute of the Old River route to Chipps Island, through Middle River from the junction with the Old River (subroute C) was monitored in 2010, no salmon were observed leaving the Old River at that junction (site C1). Thus, the probability of a smolt taking the Middle River route to Chipps Island was estimated to be zero.

In 2009, release groups were pooled into three strata based on release timing, common environmental conditions, and monitoring equipment status: stratum 1 = releases 1–2, stratum 2 = releases 3–6, and stratum 3 = release 7 (Table 1). Malfunctioning acoustic receivers meant that some parameters could not be estimated for some strata. Model selection was used to assess the effect of stratum on model parameters common to multiple strata. In 2010, data from each of the seven release occasions (initial release at Durham Ferry combined with supplemental releases) were analyzed separately. For each release occasion, several alternative survival models were fit, differing in whether the initial (Durham Ferry) and supplemental release groups shared common detection, route entrainment, and survival parameters over common reaches. Model selection was used to find the most parsimonious model that fit all the data, following the general approach described in Burnham et al. (1987) for comparing treatment groups. Detection probabilities were parameterized first, with survival, transition, and route entrainment probabilities parameterized next. Backwards selection was used to identify the farthest reach upstream for which parameters from the initial and supplemental releases could be equated without reducing model fit. The most general models were considered first, with unique parameters for each release group for all reaches, and tested against simpler models with common parameters across the initial and supplemental release groups for the downstream reaches. All models used unique survival and transition probabilities in the first reach downstream of the supplemental release sites. Model selection was performed using the Akaike Information Criterion (AIC) as described in Burnham and Anderson (2002). Final parameter estimates were weighted averages of the release-specific estimates from the selected model, with weights equal to the

number of fish from the release group present at the supplemental release site (estimated for the initial release group). Goodness of fit was assessed using Anscombe residuals (McCullagh and Nelder 1989: p. 38).

RESULTS

2009 Results

None of the 50 tags in the 2009 tag-life study failed before day 21. Because all detections of tagged salmon smolts occurred well before day 21 after tag activation, no adjustment for tag failure was made to the survival estimates from the release–recapture model.

Initial survival after release was low in 2009, with estimates of survival from Durham Ferry to the Mossdale Bridge (site A2, approximately 20 rkm) averaging 0.47 ($SE = 0.02$). The majority of the acoustic-tag detections downstream of Durham Ferry were at the upstream sites in the San Joaquin (A2, A3) and in the Old River (B1). Very few tagged salmon smolts were detected at the exit points of the Southern Delta region in either the San Joaquin River route or the Old River route. No tagged salmon were detected at the Turner Cut receivers (F1), the Middle River receivers at Highway 4 (C2), or the interior receivers at Clifton Court Forebay (D2).

Total salmon survival through the Southern Delta region (S_{SD}) was estimable only for stratum 2 (releases 3–6) because the failure of certain acoustic receivers resulted in missing data from the three other release groups. Estimated route-specific survival through the Southern Delta was $\hat{S}_{A(SD)} = 0.05$ ($SE = 0.02$) in the San Joaquin route and $\hat{S}_{B(SD)} = 0.08$ ($SE = 0.02$) in the Old River route (Table 2). Survival estimates through the Southern Delta in the two routes were not significantly different (Z-test, $P = 0.4788$). The route entrainment probabilities at the junction of the Old River with the San Joaquin River were estimated at $\hat{\psi}_{A1} = 0.47$ ($SE = 0.03$) for the San Joaquin River, and $1-\hat{\psi}_{A1} = 0.53$ ($SE = 0.03$) for the Old River. Consequently, overall survival through the Southern Delta in 2009 was estimated as $\hat{S}_{SD} = 0.06$ ($SE = 0.01$; Table 2).

The first two release groups in 2009 (stratum 1) showed a higher probability of entering the Old River ($1 - \hat{\psi}_{A1} = 0.64$; $SE = 0.04$) than remaining in the San Joaquin (P = 0.0002). Release groups 3–6 (stratum 2) showed no preference for either route ($P > 0.05$), with $1 - \hat{\psi}_{A1} = 0.48$ ($SE = 0.04$) for the Old River route entrainment probability. No estimates of the route entrainment probabilities were available for group 7 (stratum 3) because of equipment malfunction.

Median travel time through the Southern Delta reaches ranged from 0.2 d ($SE = 0.2$) from the Stockton USGS gauge (A4) to the Navy Drive Bridge in Stockton (A5; approximately 3 km), to 2.1 d ($SE = 0.3$) from Lathrop (A3) to the Stockton USGS gauge (A4; approximately 15 km).

2010 Results

Failure times of the 48 tags in the tag-life study ranged from 10 to 36 d. The early failure of several tags in the tag-life study made it necessary to incorporate tag-life adjustments into survival estimates (Townsend et al. 2006). The estimated probability of tag survival to the time of arrival at each detection site ranged from 0.987 to Chipps Island (G1) to 0.995 to Mossdale (A2). Tag survival estimates for the supplemental releases at the Old River and Stockton were generally higher than for the initial releases at Durham Ferry.

TABLE 2. Estimates of route-specific survival (S; standard errors in parentheses) of Chinook Salmon smolts through the Southern Delta (SD) and the entire Delta to Chipps Island (D) in the San Joaquin River (A) and Old River (B) and route entrainment probability into the San Joaquin River (A) at the head of the Old River for study years 2009 and 2010. Estimates of survival through the entire Delta are not available for 2009.

		Southern Delta survival			Entire Delta survival		
Release date	Route entrainment $\hat{\psi}_{A1}$	$\hat{S}_{A(SD)}$	$\hat{S}_{B(SD)}$	$\hat{S}_{SD}$	$\hat{S}_{A(D)}$	$\hat{S}_{B(D)}$	$\hat{S}_{D}$
Study year 2009							
Apr 22–25	0.36 (0.04)						
Apr 29–May 9	0.52 (0.04)	0.05 (0.02)	0.08 (0.02)	0.06 (0.02)			
May 13				0.05 (0.03)			
Average	0.47 (0.03)	0.05 (0.02)	0.08 (0.02)	0.06 (0.01)			
Study year 2010							
Apr 27–29	0.48 (0.06)	0.47 (0.07)	0.78 (0.06)	0.63 (0.05)	0.07 (0.03)	0.00 (0.00)	0.03 (0.02)
Apr 30–May 2	0.44 (0.06)	0.40 (0.06)	0.90 (0.04)	0.68 (0.05)	0.01 (0.01)	0.03 (0.02)	0.02 (0.01)
May 4–6	0.39 (0.06)	0.16 (0.04)	0.75 (0.06)	0.52 (0.06)	0.01 (0.01)	0.01 (0.01)	0.01 (0.01)
May 7–9	0.52 (0.07)	0.24 (0.05)	0.56 (0.09)	0.39 (0.06)	0.04 (0.02)	0.10 (0.03)	0.06 (0.02)
May 11–13	0.45 (0.06)	0.49 (0.06)	0.88 (0.08)	0.71 (0.06)	0.06 (0.03)	0.13 (0.04)	0.10 (0.03)
May 14–16	0.43 (0.06)	0.11 (0.04)	0.68 (0.29)	0.43 (0.17)	0.01 (0.01)	0.07 (0.02)	0.05 (0.02)
May 18–20	0.59 (0.07)	0.35 (0.06)	0.83 (0.21)	0.55 (0.10)	0.07 (0.03)	0.15 (0.05)	0.10 (0.03)
Average	0.47 (0.02)	0.32 (0.02)	0.77 (0.06)	0.56 (0.03)	0.04 (0.01)	0.07 (0.01)	0.05 (0.01)

All releases in the 2010 study had high initial survival, with estimates of survival from Durham Ferry to the Mossdale Bridge receiver (site A2; approximately 21 km) averaging 0.94 (range = 0.86–1.00). The Old River supplemental release groups had an average estimated survival to the head of Middle River (sites B2, C1) of 0.89 (range = 0.84–0.97). The Stockton supplemental release groups had an average estimated survival to the Navy Bridge in Stockton (site A5) of 0.82–1.07 (average = 0.95). Only a single tag released at either Durham Ferry or the Old River was detected in Middle River, so Middle River was omitted from the survival model. None of the 14 tags detected at Turner Cut were subsequently detected at Chipps Island.

Estimates of the probability of fish remaining in the San Joaquin River at the head of the Old River in 2010 ranged from 0.39 to 0.59 across the seven release groups (average = 0.47; $SE = 0.02$; Table 2). Only for release 3 did fish show a statistically significant ($\alpha = 0.05$) preference for the Old River over the San Joaquin River ($P = 0.0443$; one-sided Z-test).

Route-specific survival through the Southern Delta region in 2010 had an average estimate of $\hat{\tilde{S}}_{A(SD)} = 0.32$ ($SE = 0.02$) in the San Joaquin route and $\hat{\tilde{S}}_{B(SD)} = 0.77$ ($SE = 0.05$) in the Old River route. For each release occasion, survival through the Southern Delta was significantly higher in the Old River route ($P \leq 0.003$; one-sided Z-test on the lognormal scale), which ended at the water export facilities and Highway 4. Combined salmon survival through the Southern Delta region in 2010 was estimated at $\hat{\tilde{S}}_{SD} = 0.56$ ($SE = 0.03$), averaged over all seven release groups (Table 2).

Survival through the entire San Joaquin River Delta region (from Mossdale to Chipps Island, approximately 89 km) was considerably lower than through only the Southern Delta region in 2010, the average overall estimate being $\hat{\tilde{S}}_D = 0.05$ ($SE = 0.01$; Table 2). Estimated survival from Mossdale to Chipps Island averaged $\hat{\tilde{S}}_{A(D)} = 0.04$ ($SE = 0.01$) in the San Joaquin route, and $\hat{\tilde{S}}_{B(D)} = 0.07$ ($SE = 0.01$) in the Old River route. Only the first release group showed a significant difference in survival to Chipps Island between the two routes, survival through the San Joaquin route ($\hat{S}_{A(D)} = 0.07$, $SE = 0.31$) being higher than through the Old River route ($\hat{S}_{B(D)} = 0.00$, $SE = 0$; $P = 0.0100$; Table 2). Lack of significance for other release groups may have been a result of low statistical power. Pooled over release groups, however, estimated survival to Chipps Island was significantly higher through the Old River route than through the San Joaquin River route ($P = 0.0133$).

For tags released at Durham Ferry, the median travel time through the reaches ranged from 0.1 d ($SE = 0.01$) between the two Stockton receivers (A4 to A5; approximately 3 km) to 3.2 d ($SE = 0.5$) from Medford Island (A7) to Chipps Island (G1); of the multiple paths between A7 and G1, the path that used only the San Joaquin River was approximately 46 km long. No tags were observed to move from Turner Cut to Chipps Island, and the median transition from Old River South (B2) to the CVP trash racks (E1) was 0.9 d ($SE = 0.1$).

Among the 29 salmon released at Durham Ferry in 2010 that were subsequently detected at Chipps Island, 31% (9 fish) used the San Joaquin route and 69% used the Old River route. The median travel time from the head of the Old River to Chipps Island was 5.7 d (migration rate = 14.0 km/d) through the San Joaquin route, compared with 7.2 d (7 km/d) for the single fish in the Old River route that migrated in-river past Highway 4, and 2.6 d for the 19 fish in the Old River route that passed through the Central Valley Project. Travel time for the CVP fish included time spent in holding tanks and truck transport to release sites just upstream of Chipps Island, as part of the salvage operation at the facility. It appears that the fastest route through the San Joaquin River Delta to Chipps Island in 2010 was through the Old River and the CVP.

DISCUSSION

The results of 2 years of acoustic-tagging studies reported here shed light on the survival of juvenile fall Chinook Salmon in the San Joaquin River Delta. Although estimated survival was considerably higher in 2010 than in 2009, overall survival was low in both years, and survival and migration rates tended to be higher upstream and lower downstream. This pattern was observed throughout the Southern Delta in both 2009 and 2010 and throughout the entire Delta in 2010. Some reduction in migration rate is expected as fish move downstream because the cyclic tidal environment may reverse the direction of river flow and temporarily push smolts upstream. Slower migration rates, in turn, may lead to lower survival in downstream reaches, with slower-moving smolts being less able to evade predators (Anderson et al. 2005).

When survival estimates were adjusted for reach length (i.e., survival rate = $\hat{S}^{(km^{-1})}$), two regions displayed consistently low survival rates. The San Joaquin River reach from the receiver near the Navy Drive Bridge in Stockton to the Turner Cut junction had an estimated survival rate of 0.85 in 2009 and 0.94 in 2010. The reaches in the southwestern portion of the Old River route (i.e., from the head of Middle River to the entrances of the CVP and Clifton Court Forebay and to the Old River at Highway 4) had comparable survival rate estimates in both years, ranging from 0.83 to 0.90 in 2009 and 0.94–0.95 in 2010. All other Southern Delta reaches had higher estimated survival rates, while the only reach in the full Delta study area with lower survival rate was the San Joaquin River reach from the Turner Cut junction to Medford Island (0.86 in 2010). The San Joaquin River reaches from Stockton to the Turner Cut junction and Medford Island and the western portions of the Old River route warrant further investigation into mortality factors.

The estimated probability of survival throughout the Southern Delta region was generally higher in 2010 than in 2009 in both the San Joaquin River route and the Old River route. In particular, survival in the Old River from the junction with Middle River to the entrance of the water export facilities and Highway 4 appeared considerably higher in 2010 (average estimate = 0.92)

than in 2009 (average = 0.16). Overall, the survival estimates through the Southern Delta region in 2009 (average = 0.06) were comparable to the survival estimates through the entire Delta region in 2010 (average = 0.05). Although no direct estimates of survival through the entire Delta were available in 2009, we can conclude that total survival was <0.06. The drop in survival in 2010 from the Southern Delta (0.56) to the entire Delta (0.05) suggests that total survival through the entire Delta in 2009 may have been as low as 0.005. Even considering the uncertainty inherent in the predator decision process, we can conclude that survival through the Delta was very low in 2009. If the survival probability estimated in 2009 was similar to survival in other low-flow years, current recovery efforts for San Joaquin River Chinook Salmon may be inadequate during dry years.

Despite interannual survival differences, the average estimated probability of fish entering the Old River from the San Joaquin (0.53) did not differ between 2009 and 2010. This route's entrainment probability was estimated in the presence of the nonphysical barrier operated at the head of the Old River. The barrier was found to be effective at deterring smolts from entering the Old River in 2010, but not in 2009 (Bowen et al. 2009; Bowen and Bark 2012, "protection efficiency"). Nevertheless, the effect of the barrier on the overall VAMP study results was limited because the barrier was operated only for approximately half of each release group, and estimates of the Old River route entrainment probability probably decreased by <0.1 because of the barrier study.

The 2009 and 2010 survival estimates reported here depend partly on the decision process used to identify and remove possible predator detections. Without removing any suspect detections, overall survival through the Southern Delta region would be estimated at 0.34 in 2009 and 0.79 in 2010 and at 0.11 through the entire Delta region in 2010. Thus, estimated survival would be higher in both years, but the comparisons between 2009 and 2010 and between the Southern Delta and the entire Delta would remain. However, many of the detections producing these higher survival estimates came from tags with considerably longer residence times (e.g., up to 810 h) or longer travel times than expected for emigrating juvenile salmonids (e.g., average residence time of approximately 0.5 h at most detection sites). Additionally, the fit of the statistical survival model declined when the presumed predator detections were included, suggesting that they were unlikely to have come from emigrating salmonids. The results presented here are based on our current understanding of behavior differences between juvenile salmon and predators such as striped bass. Nevertheless, more work needs to be done to develop methods for distinguishing between detections of salmon and detections of predators, especially for acoustic tagging studies in highly complex environments such as the Delta.

There are several possible explanations for the differences in Southern Delta survival observed between 2009 and 2010. River flows in 2009 were very low, whereas 2010 had considerably higher flows (Figure 4). Water exports from the federal and state export facilities occurred at a slightly higher and more variable rate in 2009, the combined average export level being 56.4 m^3/s (range = 38.2–73.3 m^3/s; SJRGA 2010). In 2010, the combined average export level was 43.0 m^3/s (range = 37.4–44.2 m^3/s) (SJRGA 2011). Both lower flows and higher exports may have contributed to the lower survival observed in 2009, although the difference in average export level between 2009 and 2010 is small compared with possible daily variation in export levels (42.5–322.8 m^3/s). Differences in the source and condition of the study fish may also have contributed to performance differences between the 2 years. The 2009 study fish were hybrids of spring and fall-run Chinook Salmon from the Feather River Fish Hatchery (FRH), located in the Sacramento River basin. These hybrid fish tended to be smaller than the 2010 study fish, which were fall-run Chinook Salmon from the Merced River Fish Hatchery (MRH; located in the San Joaquin River basin). Historically, experiments in the San Joaquin Delta have used MRH fish. In 2009, however, low numbers of MRH fish prompted the switch to the FRH for that year's tagging study, despite concern that FRH fish (genetically from the Sacramento River) may not adequately represent survival of San Joaquin fall-run Chinook Salmon (Brandes and McLain 2001). In 2010, rebounding numbers at the MRH allowed us to return to MRH fish for that year's tagging study.

The smaller size of the 2009 fish resulted in an average tag burden that was higher than in 2010, and also higher than desired (≤5.5%; Brown et al. 2006). The higher tag burden in 2009 may have contributed to the high mortality in the first reach after release (Durham Ferry to Mossdale Bridge), where an estimated 53% of study fish died in 2009. However, differences in river conditions and predator distribution may also have contributed to differences in estimated mortality in this reach between the 2 years. Dry conditions and low flows in 2009 may have concentrated predators and prey (smolts) in a smaller volume of water. Higher water temperatures in 2009 may have kept the predators more active (e.g., Niimi and Beamish 1974), and also more likely to reside in the San Joaquin River between Durham Ferry and Mossdale Bridge, where water temperatures tend to be cooler than in the Delta.

Despite the differences in survival between the 2009 and 2010 study years, both studies found that juvenile fall run Chinook Salmon have very low survival through the San Joaquin River Delta, well under 0.10. Our 2010 estimates were similar to the lower range of previous survival estimates of San Joaquin smolts based on CWT data (Brandes and McLain 2001). However, the extremely low survival potentially experienced through the Delta in 2009 would have been lower than the lowest CWT estimates. Even the higher survival observed in 2010 was considerably lower than survival estimates of juvenile late fall-run Chinook Salmon from the Sacramento River through the Delta, which ranged from 0.35 to 0.54 in the winter of 2007 (Perry et al. 2010). The Perry study used comparable methods, with similar study design, tagging, and analysis. However, the late fall run Chinook Salmon used in

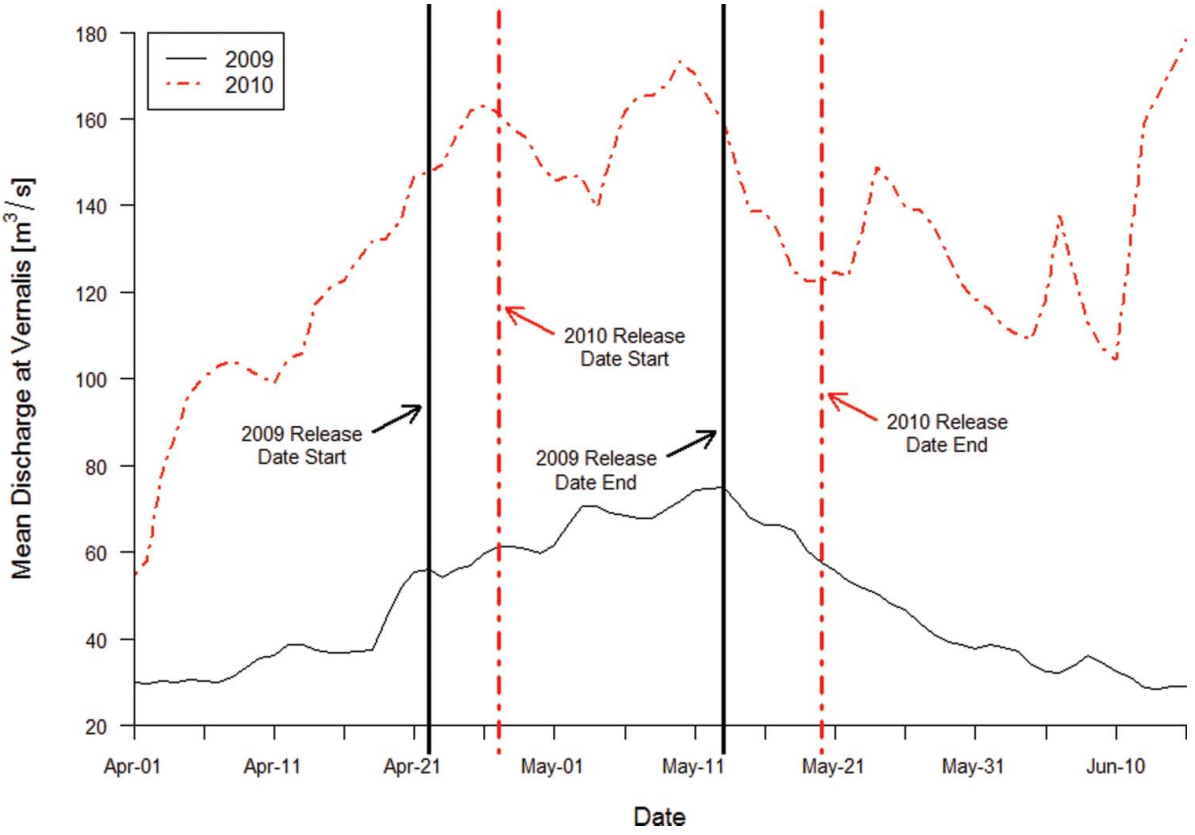

FIGURE 4. Mean daily discharge of the San Joaquin River at the U.S. Geological Survey gauge near Vernalis, California (rkm 113 from Chipps Island), during Chinook Salmon tagging studies in 2009 and 2010. [Figure available in color online.]

the Perry study migrate in winter, whereas the fall-run Chinook Salmon used in the VAMP study migrate months earlier in spring. Thus, not only were the VAMP fish smaller than the Perry study fish, they also migrated when higher predator activity is expected because of warmer temperatures and the striped bass spring spawning migration (Radtke 1966). Thus, there are several possible explanations why the VAMP study may be expected to estimate lower survival than the Perry study.

Estimates of juvenile Chinook Salmon survival through comparable environments in other basins tend to be higher than those observed in the 2009 and 2010 VAMP studies. McMichael et al. (2010) used acoustic tags to estimate survival of Chinook salmon smolts through the lower 192 rkm of the Columbia River to the river mouth; scaled by distance, the survival rate estimates ($\hat{S}^{(km^{-1})}$) were 0.999 for yearlings and 0.998 for subyearlings. Acoustic-tagged spring Chinook Salmon from the Thompson–Fraser river system had estimated survival rates of 0.989–0.997 (average = 0.995) through more than 330 rkm to the Fraser River mouth in 2004–2006 (Welch et al. 2008). These survival rates are considerably higher than both the VAMP-estimated Southern Delta survival rate of 0.92 in 2009 and the estimated entire Delta survival rate of 0.97 in 2010. Even the lowest survival rate estimate reported by Welch et al. (2008) for the Fraser River (0.989 in 2004) corresponds to much higher total survival over a distance comparable to the VAMP study area (approximately 89 rkm). Over this distance, a population with a survival rate of 0.989/km would have an overall survival probability of 0.37, as opposed to the 2010 estimate of 0.05. Although direct comparison with other basins is difficult, it appears that the salmon smolts used in the 2009 and 2010 VAMP studies are not surviving as well on their seaward migration as other salmon population on the western coast of North America.

Part of the VAMP is a management plan based on the assumption that salmon survival to Chipps Island is higher through the San Joaquin River route than through the Old River route. This assumption is based on CWT studies between 1985 and 1990 that consistently found higher (but not statistically significant) point estimates of survival for smolts released in the San Joaquin River downstream of the Old River than for those released in the Old River (Brandes and McLain, 2001). Modeling of these data and other CWT data indicated that keeping salmon out of the Old River improved their survival (Newman 2008). The 2008 VAMP acoustic tag study results, although hampered by a high degree of premature tag failure, suggest that survival to Chipps Island was also higher through the San Joaquin River than through the Old River route in 2008 (Holbrook et al. 2009). Furthermore, there is evidence that salmon from the Sacramento River have a higher probability of reaching Chipps Island if they

remain in the Sacramento River rather than entering the central Delta (Newman and Brandes 2010, Perry et al. 2010). Since the 1990s, management has experimented with efforts to keep fish in the San Joaquin River and out of the Old River by installing a barrier (physical or nonphysical) at the head of the Old River. Our results suggest that prevailing ideas about relative survival in the two routes may be too simple, given that we found no conclusive evidence that survival was higher in the San Joaquin River route than in the Old River route. One difference between the 2009 and 2010 study years and previous years was the switch from a physical barrier to testing a nonphysical barrier at the head of the Old River in 2009 and 2010. Historically, the physical barrier at the Old River routed both fish and river flow into the San Joaquin River (SJRGA 2005). In contrast, the nonphysical barrier used in 2009 and 2010 routed fish but not flow into the San Joaquin (Bowen et al. 2009; Bowen and Bark 2012). With salmon smolt survival in the San Joaquin River thought to increase with flow (SJRGA 2007), it is possible that the nonphysical barrier deprived smolts routed to the San Joaquin River of the increased flows necessary for improved survival (Perry et al. 2013). There is also a concern that the larger in-water structure associated with the nonphysical barrier may create habitat for increased predation at the site. More study is needed.

The San Joaquin River Delta represents just a small portion of the entire juvenile out-migration of San Joaquin Chinook Salmon and in recent years has typically been traversed in <2 weeks (SJRGA 2011; Holbrook et al. 2013). With survival through only a portion of the juvenile migration estimated at <0.10, management efforts in the lower San Joaquin River and Delta must be more protective if salmon populations are to persist in this region. However, effective management must be based on a better understanding of the factors influencing mortality than is currently available. More research into salmon use of and survival in the Delta is needed, especially in dry years that may represent future conditions under climate change. In light of increasing human demands for Central Valley water, it is unlikely that salmon survival will improve on its own. If the survival estimates observed in these two studies are representative of the future, only extreme measures have a chance of saving San Joaquin River Chinook Salmon.

ACKNOWLEDGMENTS

Many people and groups were involved in designing and implementing the VAMP study. We thank Natural Resource Scientists, Inc., California Department of Fish and Game, California Department of Water Resources, the U.S. Fish and Wildlife Service (Stockton office), the U.S. Bureau of Reclamation, Normandeau and Associates (Stevenson, Washington), and the U.S. Geological Survey (Columbia River Research Lab and Sacramento office) for their contributions to the study. We also thank Mark Bowen from the U.S. Bureau of Reclamation for access to detection data from the nonphysical barrier study at the head of the Old River, and three anonymous reviewers for their helpful suggestions. Funding for the VAMP study was provided by the signatories to the San Joaquin River Agreement, and funding for analysis and manuscript preparation was provided by the San Joaquin River Group Authority.

REFERENCES

Adams, N. S., D. W. Rondorf, S. D. Evans, and J. E. Kelly. 1998. Effects of surgically and gastrically implanted radio transmitters on growth and feeding behavior of juvenile Chinook Salmon. Transactions of the American Fisheries Society 127:128–136.

Anderson, J. J., E. Gurarie, and R. W. Zabel. 2005. Mean free-path length theory of predator–prey interactions: application to juvenile salmon migration. Ecological Modelling 186:196–211.

Anglea, S. M., D. R. Geist, R. S. Brown, K. A. Deters, and R. D. McDonald. 2004. Effects of acoustic transmitters on swimming performance and predator avoidance of juvenile Chinook Salmon. North American Journal of Fisheries Management 24:162–170.

Bowen, M. D., and R. Bark. 2012. 2010 effectiveness of a non-physical fish barrier at the divergence of the Old and San Joaquin rivers (CA). U.S. Department of the Interior, Bureau of Reclamation, Technical Memorandum 86-68290-10-07, Denver.

Bowen, M. D., S. Hiebert, C. Hueth, and V. Maisonneuve. 2009. 2009 effectiveness of a non-physical fish barrier at the divergence of the Old and San Joaquin rivers (CA). U.S. Department of the Interior, Bureau of Reclamation, Technical Memorandum 86-68290-09-05, Denver.

Brandes, P. L., and J. S. McLain. 2001. Juvenile Chinook Salmon abundance, distribution, and survival in the Sacramento–San Joaquin Estuary. Pages 39–138 *in* R. L. Brown, editor. Contributions to the biology of Central Valley salmonids, volume 2. California Department of Fish and Game, Fish Bulletin 179, Sacramento.

Brown, R. S., D. R. Geist, K. A. Deters, and A. Grassell. 2006. Effects of surgically implanted acoustic transmitters >2% of body mass on the swimming performance, survival and growth of juvenile Sockeye and Chinook Salmon. Journal of Fish Biology 69:1626–1638.

Buchanan, R. A., and J. R. Skalski. 2010. Using multistate mark–recapture methods to model adult salmonid migration in an industrialized river. Ecological Modelling 221:582–589.

Burnham, K. P., and D. R. Anderson. 2002. Model selection and multimodel inference: a practical information-theoretic approach, 2nd edition. Springer, New York.

Burnham, K. P., D. R. Anderson, G. C. White, C. Brownie, and K. H. Pollock. 1987. Design and analysis methods for fish survival experiments based on release-recapture. American Fisheries Society, Monograph 5, Bethesda, Maryland.

DSC (Delta Stewardship Council). 2011. Available: http://www.deltacouncil.ca.gov/. (13 December 2011).

Fisher, F. W. 1994. Past and present status of Central Valley Chinook Salmon. Conservation Biology 8:870–873.

Healey, M. C. 1991. Life history of Chinook Salmon (*Oncorhynchus tshawytscha*). Pages 311–393 *in* C. Groot and L. Margolis, editors. Pacific salmon life histories. University of British Columbia Press, Vancouver.

Holbrook, C. M., R. W. Perry, and N. S. Adams. 2009. Distribution and joint fish-tag survival of juvenile Chinook Salmon migrating through the Sacramento–San Joaquin River Delta, California, 2008. U.S. Geological Survey, Open-File Report 2009-1204, Reston, Virginia. Available: pubs.usgs.gov/. (November 2011).

Holbrook, C. M., R. W. Perry, P. L. Brandes, and N. S. Adams. 2013. Adjusting survival estimates for premature transmitter failure: a case study from the Sacramento–San Joaquin Delta. Environmental Biology of Fishes 96:165–173.

Lady, J. M., and J. R. Skalski. 2008. USER 4: user-specified estimation routine. School of Aquatic and Fishery Sciences, University of Washington, Seattle. Available: www.cbr.washington.edu/paramest. (July 2012).

Martinelli, T. L., H. C. Hansel, and R. S. Shively. 1998. Growth and physiological responses to surgical and gastric radio transmitter implantation techniques in subyearling Chinook Salmon (*Oncorhynchus tshawytscha*). Hydrobiologia 371/372:79–87.

McCullagh, P., and J. A. Nelder. 1989. Generalized linear models, 2nd edition. Chapman and Hall/CRC Press, Boca Raton, Florida.

McMichael, G. A., R. A. Harnish, B. J. Bellgraph, J. A. Carter, K. D. Ham, P. S. Titzler, and M. S. Hughes. 2010. Migratory behavior and survival of juvenile salmonids in the lower Columbia River and estuary in 2009. Pacific Northwest National Laboratory, PNNL-19545, Richland, Washington.

Newman, K. B. 2008. An evaluation of four Sacramento–San Joaquin River Delta juvenile salmon survival studies. CALFED Bay-Delta Program, Project SCI-06-G06-299, Sacramento, California. Available: www.science.calwater.ca.gov./ (November 2011).

Newman, K. B., and P. L. Brandes. 2010. Hierarchical modeling of juvenile Chinook Salmon survival as a function of Sacramento–San Joaquin Delta water exports. North American Journal of Fisheries Management 30:157–169.

Niimi, A. J., and F. W. H. Beamish. 1974. Bioenergetics and growth of Largemouth Bass (*Micropterus salmoides*) in relation to body weight and temperature. Canadian Journal of Zoology 52:447–456.

Perry, R. W., P. L. Brandes, J. R. Burau, A. P. Klimley, B. MacFarlane, C. Michel, and J. R. Skalski. 2013. Sensitivity of survival to migration routes used by juvenile Chinook Salmon to negotiate the Sacramento–San Joaquin River Delta. Environmental Biology of Fishes 96:381–392.

Perry, R. W., J. R. Skalski, P. L. Brandes, P. T. Sandstrom, A. P. Klimley, A. Ammann, and B. MacFarlane. 2010. Estimating survival and migration route probabilities of juvenile Chinook Salmon in the Sacramento–San Joaquin River Delta. North American Journal of Fisheries Management 30: 142–156.

Radtke, L. D. 1966. Distribution of adult and subadult Striped Bass, *Roccus saxatilis*, in the Sacramento–San Joaquin Delta. Pages 15–27 *in* J. L. Turner and D. W. Kelley, editors. Ecological studies of the Sacramento–San Joaquin Delta, part II: fishes of the Delta. California Department of Fish and Game, Fish Bulletin 136, Sacramento.

SJRGA (San Joaquin River Group Authority). 2005. 2004 annual technical report: on implementation and monitoring of the San Joaquin River agreement and the Vernalis Adaptive Management Plan. SJRGA, Report to the California Water Resources Control Board, Davis, California. Available: www.sjrg.org/technicalreport. (February 2012).

SJRGA (San Joaquin River Group Authority). 2007. 2006 annual technical report: on implementation and monitoring of the San Joaquin River agreement and the Vernalis Adaptive Management Plan. SJRGA, Report to the California Water Resources Control Board, Davis, California. Available: www.sjrg.org/technicalreport. (February 2012).

SJRGA (San Joaquin River Group Authority). 2010. 2009 annual technical report: on implementation and monitoring of the San Joaquin River agreement and the Vernalis Adaptive Management Plan. SJRGA, Report to the California Water Resources Control Board, Davis, California. Available: www.sjrg.org/technicalreport. (February 2012).

SJRGA (San Joaquin River Group Authority). 2011. 2010 annual technical report: on implementation and monitoring of the San Joaquin River agreement and the Vernalis Adaptive Management Plan. SJRGA, Report to the California Water Resources Control Board, Davis, California. Available: www.sjrg.org/technicalreport. (February 2012).

Townsend, R. L., J. R. Skalski, P. Dillingham, and T. W. Steig. 2006. Correcting bias in survival estimation resulting from tag failure in acoustic and radiotelemetry studies. Journal of Agricultural, Biological, and Environmental Statistics 11:183–196.

Vogel, D. A. 2010. Evaluation of acoustic-tagged juvenile Chinook Salmon movements in the Sacramento–San Joaquin Delta during the 2009 Vernalis Adaptive Management Program. San Joaquin River Group Authority, Technical Report to the California Water Resources Control Board, Davis, California. Available: www.sjrg.org/technicalreport/. (July 2012).

Vogel, D. A. 2011. Evaluation of acoustic-tagged juvenile Chinook Salmon and predatory fish movements in the Sacramento–San Joaquin Delta during the 2010 Vernalis Adaptive Management Program. San Joaquin River Group Authority, Technical Report to the California Water Resources Control Board, Davis, California. Available: www.sjrg.org/technicalreport./ (July 2012).

Welch, D. W., E. L. Rechisky, M. C. Melnychuk, A. D. Porter, C. J. Walters, S. Clements, B. J. Clemens, R. S. McKinley, and C. Schreck. 2008. Survival of migrating salmon smolts in large rivers with and without dams. PLoS (Public Library of Science) Biologyy [online serial] 6(10):e265. DOI: 10.1371/journal.pbio.0060265.

2012 South Delta Chinook Salmon Survival Study

Rebecca Buchanan, University of Washington;
Pat Brandes, Mike Marshall, J. Scott Foott, Jack Ingram and David LaPlante,
U.S. Fish and Wildlife Service;
Josh Israel, U.S. Bureau of Reclamation;
Compiled and edited by Pat Brandes, U.S. Fish and Wildlife Service

Introduction

The Vernalis Adaptive Management Plan (VAMP) as part of the San Joaquin River Agreement has been measuring juvenile salmon survival through the Delta since 2000 (SJRGA 2013). Prior to 2000, similar south Delta coded-wire-tag (CWT) studies were funded by the Interagency Ecological Program and others (Brandes and McLain 2001). Since 2008, survival of juvenile Chinook Salmon through, or in, the Delta has been measured using acoustic tags. The main objective of the VAMP was to better understand the relationship between Chinook Salmon smolt survival through the Delta and San Joaquin River flows and combined CVP and SWP exports in the presence of the physical head of Old River barrier (HORB). The San Joaquin River Agreement and the VAMP study ended in 2011.

In 2012, the main objective of the Chinook Salmon survival study was to estimate survival through the Delta during the San Joaquin River Flow Modification Project (USBR 2012), during which the Merced River flows were augmented between April 15 and May 15, and compare it to survival, without the flow augmentation (after May 15), in the presence of the HORB. As part of the National Marine Fisheries Service and California Department of Water Resources Joint Stipulation Regarding South Delta Operations during April and May of 2012 (http://www.westcoast.fisheries.noaa.gov/central_valley/water_operations/ocapstip.html; accessed 8/27/15), the physical HORB was installed in 2012. The barrier had eight culverts in 2012, compared to between two and six culverts as in past years. Funding for this study was provided by the restoration fund of the Central Valley Project Improvement Act, the California Department of Water Resources (CDWR) and the U.S. Bureau of Reclamation (USBR).

These salmon studies also estimated route selection at some channel junctions in the south Delta along the main stem San Joaquin River and provided information on how route selection into some reaches influences overall survival through the Delta to Chipps Island. Recent advances in acoustic technology have allowed investigators to evaluate the influence of route selection and reach-specific survival of salmon to overall survival through the Sacramento-San Joaquin Delta (Perry et al. 2010). In this study, the hypothesis focused on the impact of changes in hydrology with the HORB, as the primary factor relative to juvenile salmon survival however we are aware that many other factors also influence survival through the Delta.

Goals and Objectives

The goal of this study was to determine if there were differences in survival resulting from changes in hydrology (i.e. increased flow) with the HORB installed.

Objectives:

1. Determine survival of emigrating salmon smolts from Mossdale to Chipps Island during two time periods (prior to May 15 and after May 15) in the presence of the HORB to determine if there was a benefit from the flow augmentation from the Merced River in the spring of 2012.
2. Assess whether the higher flows resulted in a reduction in travel time; a potential mechanism for why survival may be higher with higher flows.
3. Identify route selection at HOR and Turner Cut under the two periods with varied flows to determine its effect on survival to Chipps Island in 2012.
4. Assess the influence of flow on survival between Mossdale and Jersey Point with the HOR barrier installed in 2012 and compare it to past years to further evaluate if the increased flow from the Merced River flow augmentation likely resulted in higher smolt survival through the Delta.

Background

Survival during the smolt life-stage was assumed to be the link associated with two statistically significant relationships between San Joaquin basin escapement and 1) San Joaquin River flow at Vernalis and 2) the ratio of San Joaquin River flow to Central Valley Project and State Water Project exports, 2 ½ years earlier (Figures 5-20 and 5-21 in SJRGA 2007). It is these relationships between flow and flow/exports and escapement that are the basis for the hypothesis that increasing flow and decreasing exports during the smolt outmigration would increase adult escapement and production in the San Joaquin basin.

The early, pre-VAMP studies compared survival of CWT Feather River Hatchery (FRH) smolts released into upper Old River to those released on the main stem San Joaquin River at Dos Reis. Dos Reis is located on the San Joaquin River downstream of the head of Old River. These studies were conducted between 1985 and 1990 and suggested that survival was higher for salmon smolts released on the main stem San Joaquin River at Dos Reis than for fish released into Old River (Brandes and McLain 2001). The results of these studies were the basis for recommending a rock barrier at the head of Old River (HORB) to prevent juvenile salmon from migrating down Old River where survival appeared to be less.

CWT releases made at Dos Reis were also used to assess the survival of salmon smolts on the San Joaquin River downstream of Old River. Although it is assumed that fish released at Dos Reis migrated downstream via the main stem San Joaquin River, there is the potential for fish released at Dos Reis to have moved upstream into Old River on flood tides, especially during periods of low San Joaquin River flows and high exports or into the interior Delta via Turner or Columbia Cuts or other downstream connections to the interior Delta. Data from 1989 to 1999 indicated that as San Joaquin River flows increased downstream of Old River, survival increased from Dos Reis to Jersey Point (Figure 5-14 in SJRGA 2007). These data provided the basis for the hypothesis that increased flow in the San Joaquin

River would increase salmon smolt survival. However, with the addition of more recent data (2005 and 2006) from recoveries in the trawls (as there were no or limited recovery data from the ocean fishery due to fishery closures in 2008 and 2009), the strength of this relationship appeared to lessen (Figure 5-13 in SJRGA 2007).

With the HORB in place, the majority of the fish migrating downstream would stay on the main stem San Joaquin River at the junction between the San Joaquin River and the head of Old River. With the HORB, a statistically significant relationship between CWT survival in the reach between Mossdale or Durham Ferry and Jersey Point and San Joaquin River flow at Vernalis has been observed ($r^2 = 0.73$, $p<0.01$; Figure 5-11 in SJRGA 2007), further supporting our hypothesis that increased flow in the San Joaquin River would increase juvenile salmon survival in the Delta.

In 2010, as part of the VAMP peer review, a statistical model was used to model survival through the Delta as a function of flow and exports, based on the CWT releases in the south Delta (Appendix 1). The results of this modeling also suggested survival was generally higher on the San Joaquin River than in Old River and flow tended to improve survival in the San Joaquin River route, but there was a lot of environmental noise (low signal to noise ratio). This modeling also supported our hypothesis that a HORB would improve survival, because it would reduce the number of smolts migrating through Old River.

Conceptual Model

Our hypothesis in 2012 was that survival would increase with increased flow from the Merced River flow augmentation in the presence of the HORB. Flows were an average of 3,543 cfs during the flow augmentation period and 2,327 cfs afterwards. A potential mechanism for increased survival with increased flow is that increased flow results in shorter travel times (i.e. increased migration rates) through the riverine parts of the Delta, and thus reduces the period of exposure to mortality factors such as high water temperature, predation and toxics (Figure 1). Increased flow is also expected to reduce the effect of the mortality factors by 1) decreasing water temperatures to less stressful levels for juvenile salmon, 2) decreasing the impacts of predation due to lower metabolic rates of predators at lower water temperatures and 3) reducing toxicity concentrations through dilution (Figure 1). Survival through the entire Delta (i.e. to Chipps Island) was expected to increase with the higher flows in 2012 as a consequence of higher survival through the riverine portion of the Delta because of these hypothesized relationships.

The higher flows provided by the Merced flow augmentation in 2012 may also have resulted in the tidal prism moving further downstream, because most of the increased flow would have stayed in the San Joaquin River at the head of Old River (HOR) junction with the HORB, in contrast to when there is no HORB and a large majority of the flow moves into Old River at that junction. The shift in the tidal prism's position serves to increase the portion of the Delta that is riverine and the portion of the migration pathway that potentially responds to decreases in travel time in response to increased flow (Figure 1). It is unclear how far the tidal prism would be moved downstream from the increase in flow of approximately 1200 cubic feet per second (cfs) from the Merced flow augmentation in 2012. Additionally, the shifted position of the tidal prism further downstream, which is dependent on the magnitude of the increased flow, could also potentially reduce the proportion of flow and tagged fish

that enter Turner Cut (Figure 1). In summary, survival through the entire Delta was expected to increase as the riverine component of the Delta increased and the proportion of water and fish that were diverted into Turner Cut was reduced from a positional shift of the tidal prism downstream from higher flows.

Once fish enter the interior Delta or into the strongly tidally influenced San Joaquin River, residence times are hypothesized to increase and survival is hypothesized to decrease compared to the river reaches. The increased residence times are anticipated to increase the exposure time of juvenile salmonids to predation or other mortality factors. The incremental increase in flow from the Merced River flow augmentation was not anticipated to decrease water temperatures or dilute toxics in the tidally dominant areas of the Delta as much as the riverine reaches because inflow is a much lower proportion of overall flow in these tidally dominated regions. Lastly, the change to the flow patterns at the HOR from the installation and operation of the HORB was expected to result in fewer tagged fish being salvaged or entrained at the CVP and SWP in 2012 because a low proportion of the San Joaquin flow (~ 5%) and tagged fish enter Old River when the HORB is in place.

Study Design and Methods

This study was conducted in conjunction with a separate, but coordinated study assessing the HORB in 2012 (CDWR, 2015). As part of this HORB assessment, other groups of juvenile salmon were tagged with Hydroacoustic Technology Incorporated (HTI) tags prior to, during, and after the salmon tagging as part of this study (with VEMCO V5 tags). While the methods and results of the HTI study will not be discussed in this report, we have listed when the HTI fish were released with our study fish (Table 1).

Sample Size Analyses

A unique sample size analyses was not conducted for the 2012 study, instead we used information derived from the 2011 VAMP sample size analyses to guide release numbers for the 2012 study (SJRGA 2013). For a single release at Durham Ferry it was determined that a sample size of 475 fish would allow estimation of parameters for low route specific survival (0.05), with high detection probability (90-97%) at Chipps Island. To estimate a relative effect of 100%, between two routes (San Joaquin and Old River), 790 fish would need to be tagged with low survival and 410 for medium survival (SJRGA 2013). To estimate a relative effect between the two routes of 50%, 3,510 would need to be released in years with low survival and 1,800 would need to be released in years with medium survival (SJRGA 2013). We did not have the resources to purchase enough tags to provide the power to estimate the relative effects between routes at either of these levels for the two groups released in 2012.

Study Fish

Study fish were obtained from the Merced River Hatchery (MRH) and transported to the Tracy Fish Collection Facility (TFCF) of the CVP on April 20 and May 7 for tagging. Fish were kept in chilled, ozonized, Delta water (14-15 ° C) until 3-4 days before tagging to minimize the progression of

proliferative kidney disease (PKD). Low water temperatures inhibit the development of PKD (Ferguson 1981): PKD is progressive at temperatures greater than 15° C (Ferguson 1981). Thus 3-4 days before tagging, tanks holding the fish were slowly switched to ambient Delta water so that they could acclimate to Delta water temperatures prior to tagging and transport to the release site. Fish were sorted such that they were greater than 13 grams (~105 mm forklength [FL]) prior to tagging. Tagged study fish averaged 18.0 grams (SD = 3.7), and 112.8 mm FL (SD = 7.2). Fish were taken off feed 24 hours prior to moving them from MRH to the TFCF and 24 hours prior to surgery.

Tags

Juvenile salmon were tagged with VEMCO V5 180 kHz transmitters that weighed 0.66 grams (g) in air on average (SD = 0.012). Tags were 12.7 millimeters (mm) long, 4.3 mm in height, and 5.6 mm wide (http://vemco.com/products/v4-v5-180khz/; accessed 6/15/15). The percentage of tag weight to body weight averaged 3.8% (SD = 0.7%) for the 960 fish tagged, well below the recommended 5%. Only 3% (34 of the 960 fish) had a tag weight to body weight ratio slightly greater than 5%, with all less than 5.4%.

Tags were custom programmed with two separate codes; a traditional Pulse Position Modulation (PPM) style coding along with a new hybrid PPM/High Residence (HR) coding. The HR component of the coding allows for detection at high residence receivers. High residence receivers were placed where tag signal collisions (i.e. many tags emitting signals at the same time to the same receiver) were anticipated (CVP, CCF). The transmission of the PPM identification code was followed by a 25-35 second delay, followed by the PPM/HR code, followed by a 25-35 second delay, and then back to the PPM code, etc. The PPM code consisted of 8 pings approximately every 1.2 to 1.5 seconds. The PPM/HR code consisted of 1 PPM code and 8 HR codes (all the same for each individual fish) with 8 pings approximately every 1.2-1.5 seconds.

Tags were soaked in saline water for at least 24 hours prior to tag activation. Tags were activated using a VEMCO tag activator approximately 24 hours prior to tag implantation. For the first week of releases, time of activation was estimated to the nearest hour, whereas tag activation was identified to the nearest minute for the second group of releases.

Photo credit: Jake Osborne

Tagging training

Training those who conducted the tagging occurred between April 9 and April 13 at the TFCF using Chinook Salmon from MRH. Three hundred fish were used for training, and were brought to the TFCF on April 4. The training was conducted by staff from the U.S. Geological Survey (USGS)'s Columbia River Research Laboratory (CRRL). During training, the CRRL refined standard operating procedures, (SOP), and trained personnel to surgically implant acoustic tags (Liedtke 2012). Returning taggers received a refresher course on training during which they were required to tag a minimum of 35 fish. New taggers received a more thorough training on surgical techniques and were required to tag a minimum of 75 fish during training. Training included sessions on knot tying, tagging bananas, tagging dead fish and finally tagging live fish, holding them overnight and necropsying them to evaluate techniques and provide feed-back. Lastly, a mock tagging session was held on April 13 to practice logistic procedures and to identify potential problems and discuss solutions.

Tagging

In 2012, two groups of 480 Chinook Salmon were tagged with VEMCO V5 tags over two weekly periods: May 1-5 and May 16-20. Each group of salmon was tagged in 3 days, over a 6 day period; Chinook Salmon were tagged every other day, to facilitate survival comparisons between Chinook Salmon and steelhead (the comparison between salmon and steelhead will not be discussed in this report). Two sessions of tagging were conducted for salmon: one in the morning and one in the afternoon. Morning and afternoon tagging sessions were further divided into shifts with each shift incorporating groups of salmon tagged with either VEMCO or HTI tags. The salmon tagged as part of this study were tagged on May 1, May 3, May 5 and May 16, May 18 and May 20 (Table 1). Tagging was conducted at the TFCF as was done since 2009. Four surgeons were used to tag the fish and each surgeon had an assistant. Three additional individuals (runners) helped to move fish into and out of the tagging operation.

Tags were inserted into the fish body cavity after the fish had been anesthetized with between 6.0 and 6.5 millileters (ml) of tricane methanesulfonate (MS-222) buffered with sodium bicarbonate,

until they lost equilibrium. Fish were weighed (to the nearest 0.1 g) and measured to the nearest mm (FL). Surgeries took between 1 minute 20 seconds and 6 minutes 57 seconds, but most were within 2 to 3 minutes. Tagging was done using standard operating procedures (SOP) developed by the CRRL and refined during the training week. The SOP (Appendix 2) directed all aspects of the tagging operation and was based on Adams et al. (1998) and Martinelli et al (1998) and modified as needed.

Photo credits: Pat Brandes

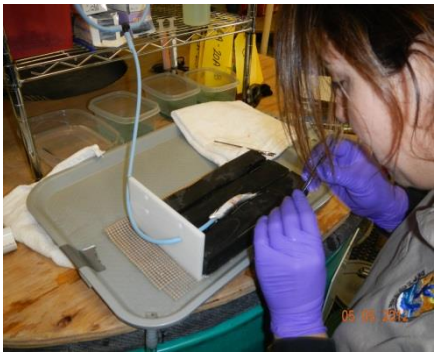

Photo credit: Pat Brandes

Photo credit: Jake Osborne

Photo credit: Pat Brandes

Photo credit: Jake Osborne

Transmitter Validation

After the surgical implantation of tags, one or two fish were placed into 19 liter (L) (5 gal) perforated buckets with high dissolved oxygen concentrations (110-130%) and allowed to recover from anesthesia for 10 minutes. During this time, tag codes were verified using a 180 khz hydrophone connected to a VR100. Tags that would not verify using the VR100 were replaced with a new tag in a new fish. After validation, a pair of buckets containing either one or two fish was combined to create a bucket of 3 fish. The bucket was then moved into a holding flume of circulating water to await loading to the transport truck once the tagging session was completed.

Photo credits: Pat Brandes

Transport to Release Site

After tagging, the 19L perforated buckets, which usually contained three tagged Chinook Salmon each, were held in a flume at the TFCF until they were loaded into transport tanks at the end of each tagging session (morning or afternoon). Immediately prior to loading, all fish were visually inspected for mortality or signs of poor recovery from tagging (e.g. erratic swimming behavior). Fish that died or were not recovering from surgery were replaced with a new tagged fish.

In order to minimize the stress associated with moving fish and for tracking smaller groups of individually tagged fish, two specially designed transport tanks were used to move Chinook Salmon from the TFCF, where the tagging occurred, to the release site at Durham Ferry. The transport tanks for Chinook Salmon were designed to securely hold a series of 19 L perforated buckets filled with fish. Tanks had an internal frame that held 21 or 30 buckets in individual compartments to minimize contact between containers and to prevent tipping. Buckets were covered in the transport tanks with stretched cargo nets to assure buckets did not tip over and lids did not come off. Both transport tanks were mounted on the bed of a 26 foot flatbed truck that was equipped with an oxygen tank and hosing to deliver oxygen to each of the tanks during transport. Two trips to the release site were made each tagging day, with the morning and afternoon sessions of tagged fish being transported separately (Table 1).

Photo credits: Jake Osborne

Photo credits: Jake Osborne

Photo credit: Pat Brandes

After loading buckets into the transport tank, de-chlorinated ice was usually added to the transport tanks to either 1) reduce water temperatures during transport such that they would be closer to the river temperature at the release site, or 2) to prevent water temperatures from increasing during transport. Water temperature and dissolved oxygen (DO) in the transport tanks were recorded after loading buckets and ice (if added) into transport tanks; before leaving the TFCF and at the release site after transport, prior to unloading buckets. The temperature and DO were also measured in the river at the holding/release site.

Transfer to Holding Containers

Once at the release site, the perforated buckets, which typically contained three Chinook Salmon each, were removed from the transport tanks and moved to the river. For all releases, perforated buckets were placed into "sleeves" in a pick-up truck and driven a short distance to the river's edge. A "sleeve" is a similar-sized, non-perforated bucket that allows more water to stay in the perforated bucket than would be the case without placing it in a "sleeve". Perforated buckets in sleeves were unloaded from the pick-up truck and carried to the river. Perforated buckets were then separated from the sleeves at the shoreline and submerged in-river to be transported to the holding containers which were anchored one to two meters from shore. Water temperature and dissolved oxygen levels were measured in the river prior to placing the salmon into the holding containers in the river.

Once at the river's edge, the tagged Chinook Salmon were transferred from the perforated buckets to the holding containers; 120 L (32 gal) perforated plastic garbage cans held in the river. These holding containers were perforated with hole sizes of 0.64 cm in diameter. Five buckets containing fish were emptied into each perforated garbage can. Only four of the five buckets emptied into the garbage cans contained VEMCO tagged fish while the fifth bucket of each group held 3 to 4 HTI fish. Each bucket and garbage can was labeled to track the specific tag codes and assure fish were transferred to the correct holding can for later release at the correct time. Tagged salmon were held in the perforated garbage cans for approximately 24 hours prior to release. Steelhead for the 6 Year Study were held at the same location and released either the day before or the day after the releases of Chinook Salmon; steelhead were released May 1-2, May 3-4, and May 5-6, and May 18-19, May 20-21, and May 22-23.

Photo credit: Pat Brandes

Fish Releases

The Chinook Salmon, held in perforated garbage cans, were transported downstream by boat to the release location which was in the middle of the channel downstream of the holding location. The fish were released downstream of the holding site to potentially reduce initial predation of tagged fish immediately after release, under the assumption that predators may congregate near the holding location. Releases were made every 4 hours after the 24 hour holding period, at approximately 1500, 1900, 2300 hours (the day after tagging), and 0300, 0700, and 1100 hours (2 days after tagging)(Table 1). Fish releases were made at these four-hour increments through-out the 24-hour period to spread the fish out and to better represent naturally spawned fish that may migrate downstream through-out the 24 hour period. The Chinook Salmon releases were made on May 2-3, May 4-5, May 6-7 and May 17-18, May 19-20, May 21-22 (Table 1).

Immediately prior to release, each holding container was checked for any dead or impaired fish. At the release time, the lid was removed and the holding container was rotated to look for mortalities. The container was then inverted to allow the fish to be released into the river. After the holding container was inverted, the time was recorded. As the holding containers were flipped back over, they were inspected to make sure that none of the released fish swam back into the container. Some exceptions to this procedure occurred as one group was released from shore due to high winds and waves, and three groups were released from shore due to a dead battery in the boat (Table 1).

Once the release was completed, the information on any dead fish was recorded and the tags removed. The tags were bagged and labeled and returned to the tagging location or office for tag code identification.

Photo credit: Pat Brandes

Dummy-tagged fish

In order to evaluate the effects of tagging and transport on the survival of the tagged fish, several groups of Chinook Salmon were implanted with inactive ("dummy") transmitters. Dummy tags in 2012 were systematically interspersed into the tagging order for each release group. For each day of tagging and transport, 15 fish were implanted with dummy transmitters and included in the tagging process (Table 1). Procedures for tagging these fish, transporting them to the release site, and holding them at the release site were the same as for fish with active transmitters. Dummy-tagged fish were evaluated for condition and mortality after being held at the release site for approximately 48 hours. After being held, dummy tagged fish were assessed qualitatively for percent scale loss, body color, fin hemorrhaging, eye quality, and gill coloration (Table 2). In addition, two additional groups of 15 dummy-tagged fish (tagged on the same day) were held for approximately 48 hours and assessed for pathogens and other diseases (discussed below).

Fish Health Assessment

As a part of the 2012 South Delta Chinook Salmon Survival Study, the U.S. Fish and Wildlife Service's CA-NV Fish Health Center (CNFHC) conducted a general pathogen screening and smolt physiological assessment on dummy-tagged fish held at the release site for 48 hours. The health and physiological condition of the study fish can help explain their performance and survival during the studies. Pathogen screenings during past VAMP studies using MRH Chinook Salmon have regularly found infection with the myxozoan parasite *Tetracapsuloides bryosalmonae*, the causative agent of Proliferative Kidney Disease (PKD). This parasite has been shown to cause mortality in Chinook Salmon with increased mortality and faster disease progression in fish at higher water temperatures (Ferguson 1981; Foott et al. 2007). The objectives of this element of the project were to evaluate the juvenile Chinook Salmon used for the studies for specific fish pathogens including *Tetracapsuloides bryosalmonae* and assess smolt development from gill Na^+ - K^+- ATPase activity to determine potential differences in health between groups. For a complete description of methods see Appendix 4.

Tag life tests

Two tag life tests were conducted in conjunction with this study. The first tag-life study began on May 16, with 43 tags. The second tag-life study began on May 24, with 40 tags. Tags were activated and then put into mesh bags and held in holding tanks at the TFCF containing ambient Delta water. A VEMCO VR2W was installed in each tank for recording detections of each individual tag. Files of detections were reviewed to identify the tag failure of each individual tag used in the tag life study. These results were then compared to observed tag travel times of the tags used in the study to estimate their tag life and make any necessary corrections to fish survival estimates.

Tag retention test

On May 25, 2012, each of the 4 surgeons tagged 9 to 10 fish with dummy tags to assess tag retention and longer-term mortality of tagged fish. Thirteen of these fish were held in each of 3 separate tanks for 30 days to determine if there was any longer-term mortality of the tagged fish and whether any tags were expelled. Fish were held in tanks at the TFCF for the duration of the 30 days.

Receiver deployment, retrieval, and receiver database

The 2012 Chinook Salmon Survival Study, in conjunction with the 6-Year Steelhead Study used receivers at 26 locations in the lower San Joaquin River and South Delta to Chipps Island (i.e. Mallard Slough) for detecting juvenile salmon and steelhead as they migrated through the Delta (Figure 2). These receivers were placed at key locations throughout the south Delta and similar to those used in VAMP in 2010 and 2011 (Figure 2). Although locations of receivers are similar, the VAMP study used an HTI receiver array, whereas the 2012 study used a VEMCO receiver array. The USBR funded the USGS to deploy, maintain and remove all of the receivers in the array, including receivers at both Jersey Point and Chipps Island in 2012. The detections of tagged salmon on these receivers allowed survival of juvenile salmon to be estimated from Durham Ferry to Chipps Island.

Data processing and survival model

This study used the tag detection data recorded on the receiver array to populate a release-recapture model similar to that used in the 2010 and 2011 VAMP studies (SJGRA 2011, 2013). The release-recapture model used the pattern of detections among all tags to estimate the probabilities of route selection, survival, and transition in various reaches and detection probability at receivers. Parameter estimates were then combined to calculate estimates of reach-specific survival, route-specific survival, and total survival through the Delta to Chipps Island. The release-recapture model (described in more detail below) is a multi-state model based on the models of Cormack (1964), Jolly (1965), and Seber (1965), in combination with the route-specific survival model of Skalski et al. (2002). Tags that appeared to be in predators were identified, and the model was fit first to the complete data set that included all detections, including those from predators, and then to the reduced data set that omitted detections that appeared to come from predators. This allowed comparison of estimates of survival and route selection probabilities with and without tags that appeared to come from predators in order to assess the potential bias associated with predator detections; this approach was similar to that used in the 2010 and 2011 VAMP studies (SJRGA 2011, 2013). More details on all statistical methods follow.

Statistical Methods

Data Processing for Survival Analysis

The University of Washington (UW) received the database of tagging and release data from the US Fish and Wildlife Service (USFWS). The tagging database included the date and time of tagging surgery for each tagged Chinook Salmon released in 2012, as well as the name of the surgeon (i.e., tagger), and the date and time of release of the tagged fish to the river. Fish size (length and weight), tag size, and any notes about fish condition were included, as well as the survival status of the fish at the time of release. Tag serial number and three unique tagging codes were provided for each tag, representing codes for various types of signal coding. Tagging data were summarized according to release group and tagger, and were cross-checked with Pat Brandes (USFWS) for quality control.

Acoustic tag detection data collected at individual monitoring sites (Table 3) were transferred to the USGS in Sacramento, California. A multiple-step process was used to identify and verify detections of fish in the data files, and produce summaries of detection data suitable for converting to tag detection histories. Detections were classified as valid if two or more pings were recorded within a 30 minute time frame on the hydrophones comprising a detection site from any of the three tag codes associated with the tag. The UW received the primary database of autoprocessed detection data from the USGS. These data included the date, time, location, and tag codes and serial number of each valid detection of the acoustic Chinook Salmon tags on the fixed site receivers. The tag serial number was linked to the acoustic tag ID, and was used to identify tag activation time, tag release time, and release group from the tagging database.

The autoprocessed database was cleaned to remove obviously invalid detections. The UW identified potentially invalid detections based on unreasonable travel times or unlikely transitions between detections, and queried the USGS processor about any discrepancies. All corrections were noted and made to the database. All subsequent analysis was based on this cleaned database.

The information for each tag in the database included the date and time of the beginning and end of each detection event when a tag was detected. Unique detection events were distinguished by detection on a separate hydrophone or by a time delay of 30 minutes between repeated hits on the same receiver. Separate events were also distinguished by unique tag encoding schemes (e.g., PPM vs. hybrid PPM/HR). The cleaned detection event data were converted to detections denoting the beginning and end of receiver “visits,” with consecutive visits to a receiver separated either by a gap of 12 hours or more between detections on the receiver, or by detection on a different receiver. Detections from receivers in dual or redundant arrays were pooled for this purpose, as were detections using different tag coding schemes.

Distinguishing between Detections of Salmon and Predators

The possibility of predatory fish eating tagged study fish and then moving past one or more fixed site receivers complicated analysis of the detection data. The Chinook Salmon survival model depended on the assumption that all detections of the acoustic tags represented live juvenile Chinook Salmon, rather than a mix of live salmon and predators that temporarily had a salmon tag in their gut. Without removing the detections that came from predators, the survival model would produce potentially biased

survival estimates of actively migrating juvenile Chinook Salmon through the Delta. The size and type (positive or negative) of the bias would depend on the amount of predation by predatory fish and the spatial distribution of the predatory fish after eating the tagged salmon. In order to minimize bias, the detection data were filtered for predator detections, and detections assumed to come from predators were identified.

The predator filter used for analysis of the 2012 data was based on the predator filter designed and used in the analysis of the 2011 data (SJRGA 2013). That predator filter in turn was based on predator analyses presented by Vogel (2010, 2011), as well as conversations with fisheries biologists familiar with the San Joaquin River and Delta regions and the predator decision processes used in previous years (SJRGA 2010, 2011). The filter was applied to all detections of all tags. Two data sets were then constructed: the full data set including all detections, including those classified as coming from predators (i.e., "predator-type"), and the reduced data set, restricted to those detections classified as coming from live Chinook Salmon smolts (i.e., "smolt-type"). The survival model was fit to both data sets separately. The results from the analysis of the reduced "smolt-type" data set are presented as the final results of the 2012 Chinook Salmon tagging study. Results from analysis of the full data set including "predator-type" detections were used to indicate the degree of uncertainty in survival estimates arising from the predator decision process.

The predator filter was based on assumed behavioral differences between salmon smolts and predators such as striped bass and white catfish. All detections were considered when implementing the filter, including detections from acoustic receivers that were not otherwise used in the survival model. As part of the decision process, environmental data including river flow, river stage, and water velocity were examined from several points throughout the Delta (Table 4), as available. Hydrologic data were downloaded from the California Data Exchange Center website (http://cdec.water.ca.gov/selectQuery.html) and the California Water Data Library (www.water.ca.gov/waterdatalibrary/) on 27 September 2013. Environmental data were reviewed for quality, and obvious errors were omitted.

For each tag detection, several steps were performed to determine if it should be classified as predator or salmon. Initially, all detections were assumed to be of live smolts. A tag was classified as a predator upon the first exhibition of predator-type behavior, with the acknowledged uncertainty that the salmon smolt may actually have been eaten sometime before the first obvious predator-type detection. Once a detection was classified as coming from a predator, all subsequent detections of that tag were likewise classified as predator detections. The assignment of predator status to a detection was made conservatively, with doubtful detections classified as coming from live salmon. In general, the decision process was based on the assumptions that (1) salmon smolts were unlikely to move against the flow, and (2) salmon smolts were actively migrating and thus wanted to move downriver, although they may have temporarily moved upstream with reverse flow.

A tag could be given a predator classification at a detection site on either arrival or departure from the site. A tag classified as being in a predator because of long travel time or movement against the flow was typically given a predator classification upon arrival at the detection site. On the other hand, a tag classified as being in a predator because of long residence time was given a predator classification upon departure from the detection site. Because the survival analysis estimated survival

within reaches between sites, rather than survival during detection at a site, the predator classifications on departure from a site did not result in removal of the detection at that site from the reduced data set. However, all subsequent detections were removed from the reduced data set.

The predator filter used various criteria on several spatial and temporal scales, as described in detail in previous reports (e.g., SJRGA 2013). Criteria fit under various categories, described in more detail in SJRGA (2013): fish speed, residence time, upstream transitions, other unexpected transitions, travel time since release, and movements against flow. The criteria used in the 2011 study were updated to reflect river conditions and observed tag detection patterns in 2012 (Table 5a and 5b). Differences between the 2011 filter and the filter used for the 2012 study (in addition to those identified in Table 5a and 5b) were:

1. Minimum migration rates on upstream-directed transitions were set to 0.1-0.2 km/hr for most upstream transitions. Upstream transitions in Old River from the Highway 4 area to the CVP trashracks and in the Sacramento or San Joaquin River from Threemile Slough to Chipps Island were limited to migration rates no less than 0.5 km/hr.
2. Maximum regional residence times allowed for smolts were set at 60 hours for the San Joaquin River upstream of the head of Old River, and 360 hours in all other regions. In most cases, the maximum regional residence time allowed for smolts making a downstream-directed transition was set at 3 – 5 times the maximum allowable near-field residence time.
3. A maximum of 3 upstream forays and 15 upstream river kilometers was imposed.
4. Maximum allowable travel time since release at Durham Ferry was set at 15 days (360 hours).

The predator scoring and classification method used for the 2011 study was used again for the 2012 study, resulting in tags being classified as in either a predator or a smolt upon arrival at and departure from a given receiver site and visit; for more details, see SJRGA (2013). All detections of a tag subsequent to its first predator designation were classified as coming from a predator, as well.

The criteria used in the predator filter were spatially explicit, with different limits defined for different receivers and transitions (Table 5a and 5b). General components of the approach to various regions are described below. Only regions with observed detections are described; regions that follow the general guidelines described in SJRGA (2013) are not highlighted here.

DFU, DFD = Durham Ferry Upstream (A0) and Durham Ferry Downstream (A2): ignore flow and velocity measures, allow long travel time to accommodate initial disorientation after release, and allow few if any repeat visits.

SJL = San Joaquin River near Lathrop (A5): upstream transitions from Stockton sites are not allowed.

ORE = Old River East (B1): repeat visits are not allowed.

SJG = San Joaquin River at Garwood Bridge (A6): transitions from upstream require arrival on flood tide

SJNB = San Joaquin River at Navy Bridge Drive (A7): allow longer residence time if arrive at slack tide; repeated visits require arriving with opposite flow and velocity conditions to departure conditions.

MAC, MFE/MFW = MacDonald Island (A8), Medford Island (A9): repeated visits require arriving with opposite flow and velocity conditions to departure conditions.

TCE/TCW = Turner Cut (F1): should not move against flow; repeated visits require arriving with opposite flow and velocity conditions to departure conditions.

ORS = Old River South (B2): repeated visits require arriving with opposite flow and velocity conditions to departure conditions.

CVP = Central Valley Project (E1): allow multiple visits; transitions from downstream Old River should not have departed Old River site against flow; no repeat visits or arrivals from downstream if not pumping.

JPE/JPW, FRE/FRW = Jersey Point (G1), False River (H1): no flow/velocity restrictions; allowed for transition from Threemile Slough (TMS/TMN)

Constructing Detection Histories

For each tag, the detection data summarized on the "visit" scale was converted to a detection history (i.e., capture history) that indicated the chronological sequence of detections on the fixed site receivers throughout the study area. In cases in which a tag was observed passing a particular receiver or river junction multiple times, the detection history represented the final route of the tagged fish past the receiver or river junction. Detections from the receivers comprising certain dual arrays were pooled, thereby converting the dual arrays to redundant arrays: the San Joaquin River near Mossdale Bridge (MOS, site A4), Lathrop (SJL, A5), and Garwood Bridge (SJG, A6); and Old River East near the head of Old River (ORE, B1). For some release groups, the receivers comprising the dual array just downstream of the initial release site (DFD, A2) were also pooled in order to achieve a better model fit; in other cases, very low detection probabilities at this site required omitting this site from analysis. Likewise, in some cases the dual arrays at either MacDonald Island (MAC, A8) or Old River South (B2) were pooled in order to improve model fit.

Survival Model

A two-part multi-state statistical release-recapture model was developed to estimate salmon smolt survival and migration route parameters throughout the study area. The full two-part model incorporates all receivers, with the exception of the San Joaquin River receiver just upstream of the head of Old River (HOR = B0), the northern-most receivers in Old and Middle rivers (OLD =B4 and MRE = C3) and the Threemile Slough receivers (TMS/TMN = T1) (Table 3, Figure 2). Because many acoustic receivers in the interior delta had no or few detections, a reduced model was developed by simplifying

the full model and limiting it to receivers with sufficient detections for analysis. The full model is described in detail first, and then the reduced model is presented.

Full Model

The full release-recapture model is a slightly simplified version of the model used to analyze 2011 steelhead data (Buchanan 2013), and similar to the model developed by Perry et al. (2010) and the model developed for the 2009 – 2011 VAMP studies (SJRGA 2010, 2011, 2013). Figure 2 shows the layout of the receivers using both descriptive labels for site names and the code names used in the survival model (Table 3). The survival model represents movement and perceived survival throughout the study area to the primary exit point at Chipps Island (i.e., Mallard Island) (Figure 3, Figure 4). Individual receivers comprising dual arrays were identified separately, using "a" and "b" to represent the upstream and downstream receivers, respectively. Not all sites were used in the survival model, although all were used in the predator filter.

Fish moving through the Delta toward Chipps Island may have used any of several routes. The two primary routes modeled were the San Joaquin River route (Route A) and the Old River route (Route B). Route A followed the San Joaquin River past the distributary point with Old River near the town of Lathrop and past the city of Stockton. Downstream of Stockton, fish in the San Joaquin River route (Route A) may have remained in the San Joaquin River past its confluence with the Sacramento River and on to Chipps Island. Alternatively, fish in Route A may have exited the San Joaquin River for the interior Delta at any of several places downstream of Stockton, including Turner Cut, Columbia Cut (just upstream of Medford Island), and the confluence of the San Joaquin River with either Old River or Middle River, at Mandeville Island. Of these four exit points from the San Joaquin River between Stockton and Jersey Point, only Turner Cut was monitored and assigned a route name (F, a subroute of route A). Fish that entered the interior Delta from any of these exit points may have either moved north through the interior Delta and reached Chipps Island by returning to the San Joaquin River and passing Jersey Point and the junction with False River, or they may have moved south through the interior Delta to the state or federal water export facilities, where they may have been salvaged and trucked to release points on the San Joaquin or Sacramento rivers just upstream of Chipps Island. All of these possibilities were included in both subroute F and route A.

For fish that entered Old River at its distributary point on the San Joaquin River just upstream of Lathrop (route B), there were several pathways available to Chipps Island. These fish may have migrated to Chipps Island either by moving northward in either the Old or Middle rivers through the interior Delta, or they may have moved to the state or federal water export facilities to be salvaged and trucked. The Middle River route (subroute C) was monitored and contained within Route B. Passage through the State Water Project via Clifton Court Forebay was monitored at the entrance to the forebay and assigned a route (subroute D). Likewise, passage through the federal Central Valley Project was monitored at the entrance trashracks and in the facility holding tank and assigned a route (subroute E). Subroutes D and E were both contained in subroutes C (Middle River) and F (Turner Cut), as well as in primary routes A (San Joaquin River) and B (Old River). All routes and subroutes included multiple unmonitored pathways for passing through the Delta to Chipps Island.

Several exit points from the San Joaquin River were monitored and given route names for convenience, although they did not determine unique routes to Chipps Island. The first exit point encountered was False River, located off the San Joaquin River just upstream of Jersey Point. Fish entering False River from the San Joaquin River entered the interior Delta at that point, and would not be expected to reach Chipps Island without subsequent detection in another route. Thus, False River was considered an exit point of the study area, rather than a waypoint on the route to Chipps Island. It was given a route name (H) for convenience. Likewise, Jersey Point and Chipps Island were not included in unique routes. Jersey Point was included in many of the previously named routes (in particular, routes A and B, and subroutes C and F), whereas Chipps Island (the final exit point) was included in all previously named routes and subroutes except route H. Thus, Jersey Point and Chipps Island were given their own route name (G). Three additional sets of receivers located in Old River (Route B) and Middle River (Subroute C) north of Highway 4 and in Threemile Slough (Route T) were not used in the survival model. The routes, subroutes, and study area exit points are summarized as follows:

A = San Joaquin River: survival
B = Old River: survival
C = Middle River: survival
D = State Water Project: survival
E = Central Valley Project: survival
F = Turner Cut: survival
G = Jersey Point, Chipps Island: survival, exit point
H = False River: exit point
T = Threemile Slough: not used in survival model

The release-recapture model used parameters that denote the probability of detection (P_{hi}), route entrainment (ψ_{hl}), Chinook Salmon survival (S_{hi}), and transition probabilities equivalent to the joint probability of movement and survival ($\phi_{kj,hi}$) (Figure 3, Figure 4, Table A5-1). Unique detection probabilities were estimated for the individual receivers in a dual array: P_{hia} represented the detection probability of the upstream array at station i in route h, and P_{hib} represented the detection probability of the downstream array.

The model parameters are:

P_{hi} = detection probability: probability of detection at telemetry station i within route h, conditional on surviving to station i, where $i = ia, ib$ for the upstream, downstream receivers in a dual array, respectively.

S_{hi} = perceived survival probability: joint probability of migration and survival from telemetry station i to station i+1 within route h, conditional on surviving to station i.

ψ_{hl} = route entrainment probability: probability of a fish entering route h at junction l (l =1, 2), conditional on fish surviving to junction l.

$\phi_{kj,hi}$ = transition probability: joint probability of route entrainment, and survival; the probability of migrating, surviving, and moving from station j in route k to station i in route h, conditional on survival to station j in route k.

A variation on the parameter naming convention was used for parameters representing the transition probability to the junction of False River with the San Joaquin River, just upstream of Jersey Point (Figure 2). This river junction marks the distinction between routes G and H, so transition probabilities to this junction are named $\phi_{kj,GH}$ for the joint probability of surviving and moving from station j in route k to the False River junction. Fish may arrive at the junction either from the San Joaquin River or from the interior Delta. The complex tidal forces present in this region prevent distinguishing between smolts using False River as an exit from the San Joaquin and smolts using False River as an entrance to the San Joaquin from Frank's Tract. Regardless of which approach the fish used to reach this junction, the $\phi_{kj,GH}$ parameter (e.g. $\phi_{A9,GH}$) is the transition probability from station j in route k to the junction of False River with the San Joaquin River via any route; ψ_{G1} is the probability of moving downstream toward Jersey Point from the junction; and $\psi_{H1} = 1 - \psi_{G1}$ is the probability of exiting (or re-exiting) the San Joaquin River to False River from the junction (Figure 3).

Because of the complexity of routing in the vicinity of MacDonald Island (referred to as "Channel Markers" in reports from previous years, e.g., SJRGA 2013) on the San Joaquin River, Turner Cut, and Medford Island, and the possibility of reaching the interior Delta via either route A or route B, the full survival model that represented all routes was decomposed into two submodels for analysis. Submodel I modeled the overall migration from release at Durham Ferry to arrival at Chipps Island without modeling the specific routing from the lower San Joaquin River (i.e., from the Turner Cut Junction) through the interior Delta to Chipps Island, although it included detailed subroutes in route B for fish that entered Old River at its upstream junction with the San Joaquin River (Figure 3). In Submodel I, transitions from MacDonald Island (A8) and Turner Cut (F1) to Chipps Island were interpreted as survival probabilities ($S_{A8,G2}$ and $S_{F1,G2}$) because they represented all possible pathways from these sites to Chipps Island. Submodel II, on the other hand, focused entirely on Route A, and used a virtual release of tagged fish detected at the San Joaquin River receiver array near Lathrop, (SJL) to model the detailed routing from the lower San Joaquin River near MacDonald Island and Turner Cut through or around the interior Delta to Jersey Point and Chipps Island (Figure 4). Submodel II included the Medford Island detection site (A9), which was omitted from Submodel I because of complex routing in that region.

Reduced Model

Detection data of tagged Chinook Salmon in the interior Delta in 2012 were very sparse. There were very few detections at the downstream Old and Middle river sites (OR4 [model code B3] and MR4

[C2]) and Central Valley Project (model codes E1 and E2) receivers, and no detections in Middle River at its head (C1) or radial gates (D1 and D2) receivers. There were also no detections at False River (H1) used in the survival analysis because all False River detections were followed by detections either at Jersey Point (G1) or Chipps Island (G2). With so few detections in the Old River route and the interior Delta portions of the San Joaquin River route, it was not possible to fit the full release-recapture model to the 2012 Chinook Salmon data set. Instead, it was necessary to omit all detection sites in the Old River route other than the first two sites in that route: ORE (B1) and ORS (B2). The simplified submodel I (Figure 5) includes the overall probability of surviving from the Old River receivers near the head of Middle River (ORS) to Chipps Island, $S_{B2,G2}$. This parameter includes all ways of getting from ORS (site B2) to Chipps Island (site G2), and is interpreted as the sum of products of the $\phi_{kj,hi}$ parameters from the full Submodel I:

$$S_{B2,G2} = \phi_{B2,D1}\phi_{D1,D2}\phi_{D2,G2} + \phi_{B2,E1}\phi_{E1,E2}\phi_{E2,G2} + \left(\phi_{B2,B3}\phi_{B3,GH} + \phi_{B2,C2}\phi_{C2,GH}\right)\psi_{G1}\phi_{G1,G2}.$$

The reduced Submodel I does not decompose $S_{B2,G2}$ into its route-specific components because of sparse data.

The reduced Submodel II focuses on transitions in and from the lower portions of the San Joaquin River, and omits transitions from this region to the interior Delta or water export facilities (Figure 6). While the full Submodel II included transitions from MacDonald Island, Medford Island, and Turner Cut to the interior Delta and water export facilities, insufficient observations of tags making these transitions made it necessary to omit these pathways from the reduced model. Thus, the reduced Submodel II models transitions only to the Jersey Point/False River junction from the MacDonald Island/Medford Island/Turner Cut region. In fact, because no tags were observed exiting the system at False River, it was not possible to separate the probability of getting to the Jersey Point/False River junction $\left(\phi_{hi,GH}\right)$ from the probability of turning toward Jersey Point $\left(\psi_{G1}\right)$; instead, only the product was estimable: $\phi_{hi,G1} = \phi_{hi,GH}\psi_{G1}$, for transitions from site i in route h. Thus, the reduced Submodel II used parameters $\phi_{A8,G1}$, $\phi_{A9,G1}$, and $\phi_{F1,G1}$, which jointly include all routes from the lower San Joaquin River receivers to Jersey Point, including those past the interior Delta receivers in northern Old and Middle rivers (B3 and C2). Likewise, without detections at the head of Middle River receiver (MRH, code C1), it was not possible to separately estimate the probability of surviving from the head of Old River to the head of Middle River $\left(S_{B1}\right)$ from the probability of remaining in Old River at the head of Middle River $\left(\psi_{B2}\right)$. Only the product was estimate: $\phi_{B1,B2} = S_{B1}\psi_{B2}$. Finally, there were insufficient detections at the receivers upstream of the Durham Ferry release site (DFU, code A0), so the A0 site was removed from the simplified submodel I (Figure 5).

The two simplified submodels I and II were fit concurrently using unique detection and transitions probabilities at shared receivers: SJG (A6), SJNB (A7), MAC (A8), TCE/TCW (F1), and MAE/MAW (G2). Parameters at these sites were estimated separately for the two submodels to avoid "double-counting" tags used in both submodels.

In addition to the model parameters, derived performance metrics measuring migration route probabilities and survival were estimated as functions of the model parameters. Both route entrainment and route-specific survival were estimated for the two primary routes determined by routing at the head of Old River (routes A and B). Route entrainment and route-specific survival were also estimated for the major subroutes of route A; subroutes were not distinguishable for route B. These subroutes were identified by a two-letter code, where the first letter indicates routing used at the head of Old River (i.e., A), and the second letter indicates routing used at the Turner Cut junction: A or F. Thus, the route entrainment probabilities for the route A subroutes were:

$\psi_{AA} = \psi_{A1}\psi_{A2}$: probability of remaining in the San Joaquin River past both the head of Old River and the Turner Cut Junction, and

$\psi_{AF} = \psi_{A1}\psi_{F2}$: probability of remaining in the San Joaquin River past the head of Old River, and exiting to the interior Delta at Turner Cut, where $\psi_{F2} = 1 - \psi_{A2}$.

Route entrainment probabilities were estimated on the large routing scale, as well, focusing on routing only at the head of Old River. The route entrainment parameters were defined as:

$\psi_A = \psi_{A1}$: probability of remaining in the San Joaquin River at the head of Old River

$\psi_B = \psi_{B1}$: probability of entering Old River at the head of Old River.

The probability of surviving from the entrance of the Delta near Mossdale Bridge (site A4, MOS) through an entire migration pathway to Chipps Island was estimated as the product of survival probabilities that trace that pathway:

$S_{AA} = S_{A4}S_{A5}S_{A6}S_{A7}S_{A8,G2}$: Delta survival for fish that remained in the San Joaquin River past the head of Old River and Turner Cut,

$S_{AF} = S_{A4}S_{A5}S_{A6}S_{A7}S_{F1,G2}$: Delta survival for fish that entered Turner Cut from the San Joaquin River, and

$S_B = S_{A4}\phi_{B1,B2}S_{B2,G2}$: Delta survival for fish that entered Old River at its head.

The overall probability of surviving through the Delta in the San Joaquin River route was defined using the subroute-specific survival probabilities and the probabilities of taking each subroute:

$S_A = \psi_{A2}S_{AA} + \psi_{F2}S_{AF}$: Delta survival (from Mossdale to Chipps Island) for fish that remained in the San Joaquin River at the head of Old River.

The parameters $S_{A8,G2}$ and $S_{F1,G2}$ used in S_{AA} and S_{AF} represent the probability of getting to Chipps Island (i.e., Mallard Island, site MAE/MAW) from A8 and F1, respectively. Both parameters represent multiple pathways around or through the Delta to Chipps Island (Figure 2). Fish that were detected at the A8 receivers (MacDonald Island) may have remained in the San Joaquin River all the way to Chipps Island, or they may have entered the interior Delta downstream of Turner Cut. Fish that entered the interior Delta either at Turner Cut or farther downstream may have migrated through the interior Delta to Chipps Island via Frank's Tract or Fisherman's Cut, False River, and Jersey Point; returned to the San Joaquin River via its downstream confluence with either Old or Middle River at Mandeville Island; or gone through salvage and trucking from the water export facilities. All such routes are represented in the $S_{A8,G2}$ and $S_{F1,G2}$ parameters, which were estimated directly using Submodel I.

The route-specific survival probability for the Old River route, S_B, includes a transition probability, $\phi_{B1,B2}$, as a factor. As indicated above, $\phi_{B1,B2}$ is the product of a survival probability and a route entrainment probability: $\phi_{B1,B2} = S_{B1}\psi_{B2}$. No tags were detected on the Middle River receivers near the head of Middle River (site C1). However, if some tags actually had entered Middle River at its head without detection, then $\psi_{B2} < 1$ and $\phi_{B1,B2} < S_{B1}$, resulting in S_B being a minimum estimate of true Delta survival in the Old River route.

Using the estimated migration route probabilities and route-specific survival for these two primary routes (A and B), survival of the population from A4 (Mossdale) to Chipps Island was estimated as:

$$S_{Total} = \psi_A S_A + \psi_B S_B .$$

Survival was also estimated from Mossdale to Jersey Point, although this was estimable only for fish in the San Joaquin River route. Survival through this region ("Mid-Delta" or MD) was defined as follows:

$S_{A(MD)} = \psi_{A2} S_{AA(MD)} + \psi_{F2} S_{AF(MD)}$: Mid-Delta survival for fish that remained in the San Joaquin River past the head of Old River,

where

$$S_{AA(MD)} = S_{A4}S_{A5}S_{A6}S_{A7}\left(\phi_{A8,G1} + \phi_{A8,A9}\phi_{A9,G1}\right), \text{ and}$$
$$S_{AF(MD)} = S_{A4}S_{A5}S_{A6}S_{A7}\phi_{F1,G1} .$$

Survival was also estimated through the southern portions of the Delta ("Southern Delta" or SD), although once again this was estimable only for fish in the San Joaquin River route:

$$S_{A(SD)} = S_{A4}S_{A5}S_{A6}S_{A7} .$$

The probability of reaching Mossdale from the release point at Durham Ferry, ϕ_{A1A4}, was defined as the product of the intervening reach survival probabilities:

$$\phi_{A1,A4} = \phi_{A1,A2} S_{A2} S_{A3}.$$

This measure reflects a combination of mortality and possible residualization upstream of Old River, although the Chinook Salmon in this study were assumed to be migrating (i.e., no residualization). In cases where the first detection site A2 (DFD) had to be removed from analysis, the alternative model parameter $\phi_{A1,A3} = \phi_{A1,A2} S_{A2}$ was used:

$$\phi_{A1,A4} = \phi_{A1,A3} S_{A3}.$$

Individual detection histories (i.e., capture histories) were constructed for each tag as described above. Each detection history consisted of one or more fields representing initial release (field 1) and the sites where the tag was detected, in chronological order. Detection on both receivers in a dual array was denoted by the code "ab", detection on only the upstream receiver was denoted "a0", and detection on only the downstream receiver was denoted "b0". For example, the detection history DF A2a0 A5 A7 A8ab A9b0 G1a0 G2ab represented a tag that was released at Durham Ferry and detected at the first (but not the second) receiver just downstream of the release site (A2a0), at one or both of the receivers near Lathrop (A5), at the single receiver in the San Joaquin River near the Navy Drive Bridge (A7), both receivers at MacDonald Island (A8ab), the downstream receiver at Medford Island (A9b0), the upstream receiver at Jersey Point (G1a0), and both receivers at Chipps Island (G2ab). A tag with this detection history can be assumed to have passed by certain receivers without detection: A2b, A3, A4, A6, A9a, and G1b. In Submodel I, the detections at A9 and G1 were not modeled, yielding Submodel I parameterization:

$$\phi_{A1,A2} P_{A2a} \left(1 - P_{A2b}\right) S_{A2} \left(1 - P_{A3}\right) S_{A3} \left(1 - P_{A4}\right) S_{A4} \psi_{A1} P_{A5} S_{A5} \left(1 - P_{A6}\right) S_{A6} P_{A7} S_{A7} \psi_{A2} P_{A8a} P_{A8b} S_{A8,G2} P_{G2a} P_{G2b}.$$

In Submodel II, this detection history was parameterized starting at the virtual release at site A5 and included detections at A8, A9, and G1:

$$S_{A5} \left(1 - P_{A6}\right) S_{A6} P_{A7} S_{A7} \psi_{A2} P_{A8a} P_{A8b} \phi_{A8,A9} \left(1 - P_{A9a}\right) P_{A9b} \phi_{A9,G1} P_{G1a} \left(1 - P_{G1b}\right) \phi_{G1,G2} P_{G2a} P_{G2b}.$$

Another example is the detection history DF A2ab A4 A5 A6 A7 G2b0. A fish with this detection history was released at Durham Ferry, migrated downstream in the San Joaquin River past the head of Old River with detections at the receivers just downstream of the release site (A2ab), as well as at the Mossdale Bridge (A4), Lathrop (A5), Garwood Bridge (A6), and Navy Drive Bridge (A7) before being detected on the second Chipps Island receiver (G2b0). This fish passed the Turner Cut junction but we have no information on which route it took there, so both routes must be parameterized in both submodels. This fish presumably passed Jersey Point without being detected on either receiver there.

This detection history is modeled partially in Submodel I and partially in Submodel II. In Submodel I, the probability of this detection history is

$$\phi_{A1,A2}P_{A2a}P_{A2b}S_{A2}\left(1-P_{A3}\right)S_{A3}P_{A4}S_{A4}\psi_{A1}P_{A5}S_{A5}P_{A6}S_{A6}P_{A7}S_{A7}\theta P_{G2a}P_{G2b},$$

where $\theta=\psi_{A2}\left(1-P_{A8}\right)S_{A8,G2}+\psi_{F2}\left(1-P_{F1}\right)S_{F1,G2}$, $1-P_{A8}=\left(1-P_{A8a}\right)\left(1-P_{A8b}\right)$, and $1-P_{F1}=\left(1-P_{F1a}\right)\left(1-P_{F1b}\right)$.

In Submodel II, this detection history is parameterized

$$S_{A5}P_{A6}S_{A6}P_{A7}S_{A7}\left\lfloor\psi_{A2}\left(1-P_{A8}\right)\left(\phi_{A8,G1}+\phi_{A8,A9}\phi_{A9,G1}\right)+\psi_{F2}\left(1-P_{F1}\right)\phi_{F1,G1}\right\rfloor\left(1-P_{G1}\right)\phi_{G1,G2}\left(1-P_{G2a}\right)P_{G2b},$$

where $1-P_{G1}=\left(1-P_{G1a}\right)\left(1-P_{G1b}\right)$.

A final example is the detection history DF A3 A4 B1 B2a0. A fish with this detection history was released at Durham Ferry, passed the first receivers without detection, passed the receivers at Banta Carbona (A3) and Mossdale Bridge (A4) with detection, entered Old River through the barrier and was detected on at least one receiver at the first Old River site (B1) and on the upstream receiver at the Old River South site (B2a0). The fish was not detected again after passing the Old River South site. It may have died between that site and Chipps Island (the next site modeled), or it may have reached Chipps Island but evaded detection there. Both possibilities must be included in the model parameterization. This detection history is parameterized only in Submodel I:

$$\phi_{A1,A2}\left(1-P_{A2}\right)S_{A2}P_{A3}S_{A3}P_{A4}S_{A4}\left(1-\psi_{A1}\right)P_{B1}\phi_{B1,B2}P_{B2a}\left(1-P_{B2b}\right)\left\lfloor 1-S_{B2,G2}P_{G2}\right\rfloor,$$

where $1-P_{A2}=\left(1-P_{A2a}\right)\left(1-P_{A2b}\right)$ and $P_{G2}=1-\left(1-P_{G2a}\right)\left(1-P_{G2b}\right)$.

Under the assumptions of common survival, route entrainment, and detection probabilities and independent detections among the tagged fish in each release group, the likelihood function for the survival model for each release group is a multinomial likelihood with individual cells denoting each possible capture history.

Parameter Estimation

The multinomial likelihood model described above was fit numerically to the observed set of detection histories according to the principle of maximum likelihood using Program USER software, developed at the UW (Lady et al. 2009). Point estimates and standard errors were computed for each parameter. Standard errors of derived performance measures were estimated using the delta method (Seber 2002: 7-9). Sparse data prevented some parameters from being freely estimated for some release groups. Transition, survival, and detection probabilities were fixed to 1.0 or 0.0 in the USER model as appropriate, based on the observed detections. The model was fit separately for each release.

For each release, the complete data set that included possible detections from predatory fish was analyzed separately from the reduced data set restricted to detections classified as Chinook Salmon smolt detections. Population-level estimates of parameters and performance measures, representing both release groups, were estimated by fitting the model to the pooled detection data from both release groups. For each model fit, goodness-of-fit was assessed visually using Anscombe residuals (McCullagh and Nelder 1989). The sensitivity of parameter and performance metric estimates to inclusion of detection histories with large absolute values of Anscombe residuals was examined for each release group individually.

For each release group and for the pooled data set, the effect of primary route (San Joaquin River or Old River) on estimates of survival to Chipps Island was tested with a two-sided *Z*-test on the log scale:

$$Z = \frac{\ln\left(\hat{S}_A\right) - \ln\left(\hat{S}_B\right)}{\sqrt{\hat{V}}},$$

where

$$V = \frac{Var\left(\hat{S}_A\right)}{\hat{S}_A} + \frac{Var\left(\hat{S}_B\right)}{\hat{S}_B} - \frac{2Cov\left(\hat{S}_A, \hat{S}_B\right)}{\hat{S}_A \hat{S}_B}.$$

The parameter *V* was estimated using Program USER. Also tested was whether tagged Chinook Salmon smolts showed a preference for the San Joaquin River route using a one-sided *Z*-test with the test statistic:

$$Z = \frac{\hat{\psi}_A - 0.5}{SE\left(\hat{\psi}_A\right)}.$$

Statistical significance was tested at the 5% level (α=0.05).

Analysis of Tag Failure

The first of two tag-life studies began on May 16 with 43 tags; the last tag failure was recorded on July 6. The second tag-life study began on May 24 with 40 tags, and the last tag failure was recorded on July 12. Observed tag survival was modeled using the 4-parameter vitality curve (Li and Anderson 2009). Stratifying by tag-life study (mid-May or late May) versus pooling across studies was assessed using the Akaike Information Criterion (AIC; Burnham and Anderson 2002).

The fitted tag survival model was used to adjust estimated fish survival and transition probabilities for premature tag failure using methods adapted from Townsend et al. (2006). In Townsend et al. (2006), the probability of tag survival through a reach is estimated based on the average observed travel time of tagged fish through that reach. For this study, travel time and the probability of tag survival to Chipps Island were estimated separately for the different routes (e.g., San Joaquin route

vs. Old River route). Standard errors of the tag-adjusted fish survival and transition probabilities were estimated using the inverse Hessian matrix of the fitted joint fish-tag survival model. The additional uncertainty introduced by variability in tag survival parameters was not estimated, with the result that standard errors may have been slightly low. In previous studies, however, variability in tag-survival parameters has been observed to contribute little to the uncertainty in the fish survival estimates when compared with other, modeled sources of variability (Townsend et al. 2006); thus, the resulting bias in the standard errors was expected to be small.

Analysis of Tagger Effects

Tagger effects were analyzed in several ways. The simplest method used contingency tests of independence on the number of tag detections at key detection sites throughout the study area. Specifically, a lack of independence (i.e., heterogeneity) between the detections distribution and tagger was tested using a chi-squared test (α=0.05; Sokal and Rohlf 1995). Detections from downstream sites were pooled for this test in order to achieve adequate cell counts, and the chi-squared test was performed via Monte Carlo simulations to accommodate remaining low cell counts.

Lack of independence may be caused by differences in survival, route entrainment, or detection probabilities. A second method visually compared estimates of cumulative survival throughout the study area among taggers. Sparse detection data in the Old River route for individual taggers prevented estimating reach survival within the Old River route by tagger, so only the overall survival to Chipps Island was estimated for route B for this analysis. A third method used Analysis of Variance to test for a tagger effect on individual reach survival estimates, and an F-test to test for a tagger effect on cumulative survival throughout each major route (routes A and B). Tagger effects on estimates of individual parameters were also assessed using an F-test. Finally, the nonparametric Kruskal-Wallis rank sum test (Sokal and Rohlf 1995, ch. 13) was used to test for whether one or more taggers performed consistently poorer than others, based on individual reach survival or transition probabilities through key reaches. In the event that survival was different for a particular tagger, the model was refit to the pooled release groups without tags from the tagger in question, and the difference in survival estimates due to the tagger was tested using a two-sided Z-test on the lognormal scale. The reduced data set (without predator-type detections), pooled over release groups, was used for these analyses.

Testing Effect of Release Group on Parameter Estimates

The effect of release group on the values of the model survival and transition probability parameters was examined by testing for a statistically significant decrease in parameter estimates for the second release group. For each model survival and transition probability parameter θ, where $\theta = \phi_{kj,hi}$ or $\theta = S_{hi}$, the difference in parameter values between the first and second release groups was defined as

$$\Delta_\theta = \theta_1 - \theta_2 \ ,$$

for model parameter θ_R for release group R ($R = 1, 2$). The difference was estimated by $\hat{\Delta}_\theta = \theta_1 - \theta_2$. The null hypothesis of no difference was tested against the alternative of a positive difference (i.e., higher parameter value for the first release group):

$$H_{0\theta} : \Delta_\theta = 0$$

vs

$$H_{A\theta} : \Delta_\theta > 0 .$$

A family-wise significance level of α=0.10 was selected, and the Bonferroni multiple comparison correction was used, resulting in a test-wise significance level of 0.0071 for 14 tests (Sokal and Rohlf 1995).

Analysis of Travel Time

Travel time was measured from release at Durham Ferry to each detection site. Travel time was also measured through each reach for tags detected at the beginning and end of the reach, and summarized across all tags with observations. Travel time between two sites was defined as the time delay between the last detection at the first site and the first detection at the second site. In cases where the tagged fish was observed to make multiple visits to a site, the final visit was used for travel time calculations. When possible, travel times were measured separately for different routes through the study area. The harmonic mean was used to summarize travel times.

To evaluate our hypotheses that reduced travel times increased survival, we compared average travel time and survival for the different reaches to see if they were different ($p<0.05$) for the two release groups. Given that the lengths of the reaches were different we also standardized the length of each reach and survival in the reach by the distance of each reach (in km) prior to comparing average travel time per km to survival per km (S^(1/km)) across reaches.

Route Entrainment Analysis

A physical barrier was installed at the head of Old River in 2012. The barrier was designed to keep fish from entering Old River, but included culverts that allowed limited fish passage. Only 11 of the 959 (1%) tags released in juvenile Chinook Salmon in 2012 were detected entering the Old River route in 2012, while 449 (47% of 959) were detected in the San Joaquin River route. Because of the barrier and the low number of tags detected in the Old River route, no effort was made to relate route entrainment at the head of Old River to hydrologic conditions in 2012. A route entrainment analysis was performed for the Turner Cut junction instead.

The effects of variability in hydrologic conditions on route entrainment at the junction of Turner Cut with the San Joaquin River were explored using statistical generalized linear models (GLMs) with a binomial error structure and logit link (McCullagh and Nelder 1989). The acoustic tags used in this analysis were restricted to those detected at either of the acoustic receiver dual arrays located just downstream of the Turner Cut junction: site MAC (model code A8) or site TCE/TCW (code F1). Tags

were further restricted to those whose final pass of the Turner Cut junction came from either upstream sites or from the opposite leg of the junction; tags whose final pass of the junction came either from downstream sites (e.g., MFE/MFW) or from a previous visit to the same receivers (e.g., multiple visits to the MAC receivers) were excluded from this analysis. Tags were restricted in this way in order to limit the delay between initial arrival at the junction, when hydrologic covariates were measured, and the tagged fish's final route selection at the junction. No Chinook Salmon tags were observed moving from one junction leg to the other, so in fact only tags that came from upstream were used in this analysis. Predator-type detections were also excluded. Detections from a total of 89 tags were used in this analysis: 79 from release group 1, and 10 from release group 2.

Hydrologic conditions were represented in several ways, primarily total river flow (discharge), water velocity, and river stage. These measures were available at 15-minute intervals from the TRN gaging station in Turner Cut, maintained by the USGS (Table 4). The Turner Cut acoustic receivers (TCE and TCW) were located 0.15 – 0.30 km past the TRN station in Turner Cut. No gaging station was available in the San Joaquin River close to the MAC receivers. The closest stations were PRI (13 km downstream from the junction), and SJG (18 km upstream from the junction) (Table 4). These stations were considered too far distant from the MAC receivers to provide measures of flow, velocity, and river stage sufficiently accurate for describing localized conditions at the Turner Cut junction for the route entrainment analysis. Thus, while measures of hydrologic conditions were available in Turner Cut, measures of flow proportion into Turner Cut were not available.

Additionally, there was no measure of river conditions available just upstream of the junction that might inform about the environment as the fish approached the junction. Instead, gaging data from the SJG gaging station (18 km upstream of the junction) were used as a surrogate for conditions upstream of the junction. Because of the distance between the SJG station and the Turner Cut junction, and the fact that the San Joaquin River becomes considerably wider between the SJG station and the junction, conditions at SJG were used only as an index of average conditions during the time when the fish was in this reach. In particular, no measure of tidal stage or flow direction was used at SJG. Instead, the analysis used the average magnitude (measured as the root mean square, RMS) of flow and velocity at SJG during the tag transition from the time of tag departure from the SJG acoustic receiver (model code A6) to the time of estimated arrival at the Turner Cut junction.

Conditions at the TRN gaging station were measured at the estimated time of arrival at the Turner Cut junction. The location (named TCJ for Turner Cut Junction) used to indicate arrival at the junction was located in the San Joaquin River 1.23 km from the TCE receiver and 2.89 km upstream of the MACU receiver. Time of arrival at TCJ $\left(t_i\right)$ was estimated for tag i by a linear interpolation from the observed travel time from the SJNB or SJG acoustic receivers upstream to detection on either the MAC or TCE/TCW receivers just downstream of the junction. Linear interpolation is based on the first-order assumption of constant movement during the transition from the previous site. In a tidal area, it is likely that movement was not actually constant during the transition, but in the absence of more precise spatiotemporal tag detection data, the linear interpolation may nevertheless provide the best estimate of arrival time.

The TRN gaging station typically recorded flow, velocity, and river stage measurements every 15 minutes. Linear interpolation was used to estimate the flow, velocity, and river stage conditions at the estimated time of tag arrival at TCJ:

$$x_i = w_i x_{t_{1(i)}} + (1 - w_i) x_{t_{2(i)}}$$

where $x_{t_{1(i)}}$ and $x_{t_{2(i)}}$ are the two observations of metric x (x = Q [flow], V [velocity], or C [stage]) at the TRN gaging station nearest in time to the time t_i of tag i arrival such that $t_{1(i)} \le t_i \le t_{2(i)}$. The weights w_i were defined as

$$w_i = \frac{t_{2(i)} - t_i}{t_{2(i)} - t_{1(i)}},$$

and resulted in weighting x_i toward the closest flow, velocity, or stage observation.

In cases with a short time delay between consecutive flow and velocity observations (i.e., $t_{2(i)} - t_{1(i)} \le 60$ minutes), the change in conditions between the two time points was used to represent the tidal stage (Perry 2010):

$$\Delta x_i = x_{t_{2(i)}} - x_{t_{1(i)}}$$

for $x = Q, V,$ or C, and tag i.

Negative flow measured at the TRN gaging station was interpreted as river flow being directed into the interior Delta, away from the San Joaquin River (Cavallo et al. 2013). Flow reversal (i.e., negative flow at TRN) was represented by the indicator variable U (Perry 2010):

$$U_i = \begin{cases} 1, & for\ Q_i < 0 \\ 0, & for\ Q_i \ge 0 \end{cases}$$

Prevailing flow and velocity conditions in the reach from the SJG acoustic receiver to arrival at the Turner Cut junction were represented by the root mean square (RMS) of the time series of observed conditions measured at the SJG gaging station during the estimated duration of the transition:

$$x_{RMS(i)} = \sqrt{\frac{1}{n_i} \sum_{j=T_{1(i)}}^{T_{2(i)}} x_j^2}$$

where x_j = observed covariate x at time j at the SJG gaging station $(x = Q \text{ or } V)$, $T_{1(i)}$ = closest observation time of covariate x to the final detection of tag i on the SJG acoustic receivers, and $T_{2(i)}$ =

closest observation time of covariate x to the estimated time of arrival of tag i at TCJ. If the time delay between either $T_{1(i)}$ and final detection of tag i on the SJG acoustic receivers, or $T_{2(i)}$ and estimated time of arrival of tag i at TCJ, was greater than 1 hour, then no measure of covariate x from the SJG gaging station was used for tag i.

Daily export rate for day of arrival of tag i at TCJ was measured at the Central Valley Project $\left(E_{iCVP}\right)$ and State Water Project $\left(E_{iSWP}\right)$ (data downloaded from DayFlow on November 5, 2013). Fork length at tagging L_i and release group RG_i were also considered. Finally, arrival time (day vs. night) at the Turner Cut Junction site (TCJ) was measured based on whether the tagged Chinook Salmon first arrived at TCJ between sunrise and sunset $\left(day_i\right)$.

All continuous covariates were standardized, i.e.,

$$\tilde{x}_{ij} = \frac{x_{ij} - \overline{x}_j}{s(x_j)}$$

for the observation x of covariate j from tag i. The indicator variables U, RG, and day were not standardized.

The form of the generalized linear model was

$$\ln\left(\frac{\psi_{iA}}{\psi_{iF}}\right) = \beta_0 + \beta_1\left(\tilde{x}_{i1}\right) + \beta_2\left(\tilde{x}_{i2}\right) + \cdots + \beta_p\left(\tilde{x}_{ip}\right)$$

where $\tilde{x}_{i1}, \tilde{x}_{i2}, \ldots, \tilde{x}_{ip}$ are the observed values of standardized covariates for tag i (covariates 1, 2, …, p, see below), ψ_{iA} is the predicted probability that the fish with tag i selected route A (San Joaquin River route), and $\psi_{iF} = 1 - \psi_{iA}$ (F = Turner Cut route). Route choice for tag i was determined based on detection of tag i at either site A8 (route A) or site F1 (route F). Estimated detection probabilities for the two release groups were 0.97 – 1.00 for site A8 and 1.00 for site F1 (Appendix 5, Table 5A-2), so no groups were omitted because of low detection probability.

Single-variate regression was performed first, and covariates were ranked by P-values from the appropriate F-test (if the model was overdispersed) or x^2 test (McCullagh and Nelder 1989). Covariates found to be significant alone (α=0.05) were then analyzed together in a series of multivariate regression models. Because of high correlation between flow and velocity measured from the same site, and to a lesser extent, correlation between flow or velocity and river stage, the covariates flow, velocity, and river stage were analyzed in separate models. The exception was that the flow index in the reach from SJG to TCJ $\left(Q_{SJG}\right)$ was included in the river stage model. Exports at CVP and SWP had low correlation over the time period in question, so CVP and SWP exports were considered in the same models. The general forms of the three multivariate models were:

Flow model: $Q_{TRN} + Q_{SJG} + \Delta Q_{TRN} + U + day + E_{CVP} + E_{SWP} + L + RG$

Velocity model: $V_{TRN} + V_{SJG} + \Delta V_{TRN} + U + day + E_{CVP} + E_{SWP} + L + RG$

Stage model: $C_{TRN} + Q_{SJG} + \Delta C_{TRN} + U + day + E_{CVP} + E_{SWP} + L + RG.$

In general, only terms that were significant in the single-variate models were included as candidates in the flow, velocity, and stage models. However, the flow, velocity, and stage metrics from the TRN gaging station were included as candidates in their respective models, regardless of their significance in the single-variate models. Backwards selection with F-tests was used to find the most parsimonious model in each category (flow, velocity, and stage) that explained the most variation in the data (McCullagh and Nelder 1989). Main effects and two-way interaction effects were considered. The model that resulted from the backwards selection process in each category (flow, velocity, or stage) was compared using an F-test to the full model from that category to ensure that all significant main effects were included. AIC was used to select among the flow, velocity, and stage models. Model fit was assessed by grouping data into discrete classes according to the independent covariate, and comparing predicted and observed frequencies of route entrainment into the San Joaquin using the Pearson chi-squared test (Sokal and Rohlf 1995).

Comparison of survival between Mossdale and Jersey Point in 2012 compared to past years.

A multiple regression was run on the combined data set of survival estimates from Mossdale to Jersey Point with the HORB using CWT's in 1994, 1997, 2000-2004 (SJRGA 2013) and using acoustic tags for the two releases in 2012 to determine if tag type (acoustic tag or coded wire tag) was a significant factor in addition to flow for predicting survival. We also compared the results observed in 2012 to those predicted from the CWT relationship with flow at the same flow levels as those experienced by tagged fish in the two 2012 releases. The data were also plotted and the two regression lines were compared; CWT data only and the CWT data combined with the 2012 acoustic tag data.

Results

Transport to Release Site

No mortalities were observed after transport to the release site. Water temperatures ranged from 16.8°C to 20.3° C after loading, prior to transport. Water temperatures ranged from 16.5°C to 20.5°C after transport and before unloading at the release site. Water temperature in the river at the release site ranged from 17.5°C to 20.7°C, with the average during the first week being lower (18.3°C) than for the second week (19.7°C) (Table 6). By adding ice, water temperatures did not change substantially during transport (Table 6 and Appendix 3) and water temperatures in the transport tanks when arriving at the release site were usually within a degree C of the water temperature in the river (Table 6). During transport water temperatures did not rise or lower more than 0.5°C, and transport

tank temperatures were similar between tanks within about 0.5 °C (Appendix 3). Dissolved oxygen levels ranged between 8.73 and 11.89 mg/l for all measurements in the transport tanks or in the river (Table 6).

Fish Releases

No mortalities occurred after holding and prior to release in the 2012 Chinook Salmon study (Table 6).

Dummy Tagged fish

None of the 60 dummy-tagged Chinook Salmon were found dead when evaluated after being held for 48 hours (Table 7). Three fish from the May 20 group had abnormal gill coloration. All remaining fish were found swimming vigorously, had normal gill coloration, normal eye quality, normal body coloration and no fin hemorrhaging. Mean scale loss for all fish assessed ranged from 2.3 to 5.5%. Eight of the 60 examined fish were found to have stitched organs. Mean FL of the four groups of dummy tagged fish ranged from 108.2 to 112.0 mm. These data indicate that the fish used for the Chinook Salmon study in 2012 appeared to be in generally good condition (Table 7).

Fish Health

Pathogen testing conducted on dummy-tag cohorts of acoustic tagged MRH juvenile Chinook Salmon used in studies corresponding to May 7 and May 23 releases showed no virus or *Renibacterium salmoninarum* infection detected in the fish. The May 23 group had 37% prevalence of both suture abnormalities and A*eromonas – Pseudomonas* sp. infection however there was little correlation between the two findings. As in the past, *Tetracapsuloides bryosalmonae* infection was highly prevalent ($\geq$ 97%) and the associated Proliferative Kidney Disease became more pronounced in the May 23 sample. No mortality occurred to these fish prior to assessment after they had been held for 48 hours for either sample date. Gill Na-K-ATPase data was not reported due to a problem with a key assay reagent. The combination of kidney impairment and poor suture condition of the May 23 salmon indicates that health of the two release groups was not equivalent. See Appendix 4 for more detail on the results of the fish health evaluations.

Tag retention test

Of the 39 dummy tagged fish held for 30 days, 3 died within the first 5 days after tagging. No other mortality was observed during the 30 day period. This suggests that the tagging process alone may have caused some (less than 10%) of the mortality observed during the study. None expelled their tag.

Detections of Acoustic-Tagged Fish

There were 960 acoustic tags released in juvenile Chinook Salmon at Durham Ferry in 2012, but one was removed from the analyses due to the tag “looking odd” resulting in data from only 959 being analyzed. Of these, 713 (74%) were detected on one or more receivers either upstream or downstream of the release site (Table 8), including any predator detections. A total of 707 tags (74%) were detected at least once downstream of the release site, and 482 (50%) were detected in the study area from

Mossdale to Chipps Island (Table 8). Although more tags from the second release group were detected between the release site and the upstream boundary of the study area (Mossdale), considerably more tags from the first release group were detected in the study area than from the second release group (301 vs. 181) (Table 8).

The large majority of the tags detected in the study area were detected in the San Joaquin River route (449 of 482), while only 11 tags were detected in the Old River route (Table 8). Additionally, some tags were detected in the study area near Mossdale Bridge but not downstream of the head of Old River. In general, tag detection counts in the San Joaquin River route decreased as distance from the release point increased. Of the 449 tags observed in the San Joaquin River route, 449 were detected on the receivers near Lathrop; 310 were detected on one or both of the receivers near Stockton (SJG or SJNB); 111 were detected on the receivers in the San Joaquin River near MacDonald Island or in Turner Cut; and 47 were detected at Medford Island (Table 9).

Some of the 449 tags detected in the San Joaquin River downstream of the head of Old River were not assigned to that route for survival analysis because they were subsequently observed upstream of Old River and had no later downstream detections (Table 8). Overall, 446 of the 449 tags observed in the San Joaquin River downstream of Old River were assigned to that route for survival analysis. Of these, 13 tags were observed exiting the San Joaquin River at Turner Cut, three were observed at the Old or Middle River receivers near of Empire Cut, one was observed at the Old and Middle River receivers near Highway 4, one was observed at the CVP trashrack, and none were observed at the radial gates at the entrance to the Clifton Court Forebay (Table 9). A total of 28 San Joaquin River route tags were detected at the Jersey Point/False River receivers, including seven detections on the False River receivers (Table 9). However, all of the tags detected at False River were later detected either at Jersey Point or at Chipps Island, and so no San Joaquin River route tags were used in the survival model at False River (Table10). A total of 14 San Joaquin River route tags were eventually detected at Chipps Island, including predator-type detections (Table 9).

Only 11 tags were detected in the Old River route, and all but one, were assigned to that route for survival analysis (Table 8). Nine (9) tags were detected both at the Old River East receivers near the head of Old River (ORE) and the Old River receivers near the head of Middle River (ORS). Four tags were detected at the CVP trashracks, and none at the radial gates at the entrance to the Clifton Court Forebay (Table 9). One tag from the Old River route was detected at both the Old River sites near Highway 4 and near Empire Cut; it was last detected at Empire Cut. No tags from the Old River route were detected at any of the Middle River sites (Table 9). One of the 11 tags in the Old River route was observed at Chipps Island, and it passed through the holding tank at the Central Valley Project (Tables 9 and 10).

In addition to the Old and Middle receivers located near Empire Cut, the Threemile Slough receivers recorded detections of tags but were purposely omitted from the full survival model. Six tags were detected on the Threemile Slough receivers: four came directly from the San Joaquin River receivers at Medford Island and MacDonald Island, and two were last detected at Jersey Point before being detected at Threemile Slough (Table 9). Those that had come from Medford Island and MacDonald Island continued on to either Jersey Point or Chipps Island, while those that came upriver to Threemile Slough from Jersey Point had no subsequent detections.

The predator filter used to distinguish between detections of juvenile Chinook Salmon and detections of predatory fish that had eaten tagged smolts classified 130 of the 959 tags released (14%) as being detected in a predator at some point during the study (Table 11). Of the 482 tags detected in the study area (i.e., at Mossdale or points downstream), 95 tags (20% of 482) were classified as being in a predator, and the majority (94 of 95) were first classified as being in a predator within the study area. The remaining tag was classified as a predator at Banta Carbona (upstream of the study area) but was later detected in the San Joaquin River at the Lathrop receiver (SJL). Approximately 7% (36 of 535) of the tags detected upstream of Mossdale were classified as being in a predator in that region (Table 11). Two of the tags that were first classified as predators in the study area were subsequently detected upstream of Mossdale. Two of the nine tags detected at upstream Old River sites (ORE and ORS) were classified as in a predator (Table 11).

Within the study area, the detection sites with the largest number of first-time predator-type detections were Lathrop (14 of 449, 3%), Garwood Bridge (18 of 310, 6%), Navy Drive Bridge (23 of 241, 10%), and MacDonald Island (18 of 100, 18%) (Tables 9 and 11). The majority of predator classifications at these four sites were assigned on tag departure from the detection site in question because of long residence times and movements against the flow. Because those detections that are assigned the predator classification only on departure are not removed from analysis in the survival model, only a few detections were actually removed from these sites.

When the predator-type detections were removed, slightly fewer detections were available for the survival analysis (Tables 12-14). With the predator-type detections removed, 697 of the 959 (73%) tags released were detected downstream of the release site, and 480 (50% of those released) were detected in the study area from Mossdale to Chipps Island (Table 12). A similar percentage of the tags from each release group were detected anywhere as a smolt (73% and 72% for the two release groups). Considerably more tags from the first release group were detected in the study area than from the second release group (63% vs. 37%) (Table 12).

Removing predator-type detections did not appreciably change the spatial patterns in the detection counts. The large majority of the tags detected in the study area were detected in the San Joaquin River route (444 of 480, 93%) and assigned to that route for the survival analysis. Only 11 tags were observed in the Old River route (Table 12). Another 25 tags were detected at the Mossdale receivers, but not downstream of the head of Old River (Table 12). Most of the changes to detection counts introduced by removing predator-type detections occurred at receivers in the San Joaquin River, both upstream and downstream of the head of Old River (Tables 9 and 13). There was no change in tag counts at Jersey Point, False River, and Chipps Island. There were very few detections at receivers throughout the western and northern regions of the interior Delta (Table 13), and somewhat fewer once detections were formatted for survival analysis (Table 14). Whether predator-type detections were included or not, detections from those sites had to be omitted from the survival model (Tables 10 and 14) (See *Statistical Methods: Survival Model – Reduced Model*).

Tag-Survival Model and Tag-Life Adjustments

The Akaike Information Criterion (AIC) indicated that pooling data from both tag-life studies (AIC = 18.1) was preferable to stratifying by study month (AIC = 33.4). Thus, a single tag survival model was

fitted and used to adjust fish survival estimates for premature tag failure. The estimated mean time to failure from the pooled data was 41.7 days ($SE = 7.5$ days) (Figure 7).

The complete set of detection data, including predator-type detections, contained some detections that occurred after the tags began dying (Figures 8 and 9). The sites with the latest detections were Banta Carbona and the San Joaquin River receivers near the Lathrop, Garwood Bridge, Navy Bridge and MacDonald Island. Some of these late-arriving detections may have come from predators. Tag-life corrections were made to survival estimates to account for the premature tag failure observed in the tag-life studies. All estimates of reach survival for the acoustic tags were greater than 0.99 (out of a possible range of 0 – 1). Thus, there was very little effect of either premature tag failure or corrections for tag failure on the estimates of salmon reach survival in 2012.

Tagger Effects

Fish in the release groups were evenly distributed across tagger (Table 15). For each tagger, the number tagged was distributed evenly across the two release groups. A chi-squared test found no evidence of lack of independence of tagger across the release groups (χ^2 =0.0279, df=3, P=0.9988). The distribution of tags detected at various key detection sites or regions of the study area was well-distributed across taggers, showing no evidence of a tagger effect on survival, route entrainment, or detection probabilities at these sites (χ^2 =16.8759, simulated P-value = 0.5372; Table 16).

Estimates of cumulative survival throughout the San Joaquin River route to Chipps Island showed generally small, non-significant effects of tagger through the system (Figure10). Tagger C had consistently higher point estimates of cumulative survival through the receiver at Navy Drive Bridge, after which cumulative survival from this tagger were no greater than from the other taggers. Despite the higher point estimates of survival observed for Tagger C, the differences were not statistically significant (ANOVA, P = 0.1944). Furthermore, rank tests found no evidence of consistent differences in reach survival across fish from different taggers either upstream of the head of Old River (P=0.9217) or in the San Joaquin River route (P=0.9704). Fish tagged by Tagger B had significantly lower survival estimates through the San Joaquin River reach from the Navy Bridge to the Turner Cut junction (i.e., MacDonald Island and Turner Cut) (F-test: P = 0.0078); however, fish from Tagger B showed no difference in survival estimates in other reaches or to Chipps Island overall compared to the other taggers (Figure 10).

In particular, there was no difference in overall survival to Chipps Island among taggers through the San Joaquin River route (P=0.4655). Only one fish was observed to arrive at Chipps Island via the Old River route, so no tagger effects could be explored for that route. The survival model was fit to the data pooled from all taggers without Tagger B, and estimates of four key performance measures were compared to results found with Tagger B: S_{Total}, S_A, S_B, and $\phi_{A1,A4}$. Statistical Z-tests on the log-scale found no significant difference between estimates of these parameters with and without data from fish tagged by Tagger B (P≥ 0.5835).

Survival and Route Entrainment Probabilities

As described above, detections from the receivers at the entrances to the water export facilities and in the holding tank at the Central Valley Project were removed from the survival model because of sparse data, as were detections from the Old and Middle River receivers near Highway 4. In some cases, there were too few detections at the dual array just downstream of Durham Ferry (DFD, site A2) to include this site in the model. In these cases, the model used the composite parameter $\phi_{A1,A3} = \phi_{A1,A2} S_{A2}$ in place of $\phi_{A1,A2}$ and S_{A2}. Also, in several cases analysis of model residuals showed that incorporating the full dual receiver array at some detection sites reduced the quality of the model fit to the data. In such cases when it was possible to simplify the data structure and still attain useful and valid parameter estimates, detections from the dual array in question were pooled to create a redundant array for better model fit. This occurred at the downstream Durham Ferry site (A2), MacDonald Island (A8), Old River South (near the head of Middle River, B2), and Jersey Point (G1).

No tags from the second release group (released in mid-May) were detected at Chipps Island in 2012, yielding a total Delta survival estimate of 0 ($SE = 0$) for that group whether or not predator-type detections were included. The first release group (released in early May) had positive survival ($S_{total} =$ 0.05; $SE = 0.01$), yielding a population estimate for all fish in the tagging study of 0.03 ($SE = 0.01$) (Table 17). Using only those detections classified as coming from juvenile Chinook Salmon and excluding the predator-type detections, the estimated probability of remaining in the San Joaquin River at the junction with Old River $\left(\psi_A = \psi_{A1}\right)$ was 0.98 ($SE = 0.01$) for both release groups (Table 17), and both release groups demonstrated a significant preference for the San Joaquin River route (P<0.0001 for each group). The estimated survival from Mossdale to Chipps Island via the San Joaquin River route $\left(S_A\right)$ was 0.05 ($SE = 0.01$) for the first release group, and 0 ($SE = 0$) for the second group; the overall population estimate was 0.03 ($SE = 0.01$)(Table 17). Very few fish took the Old River route (11 overall). Although the point estimate of survival to Chipps Island via this route ($S_B = 0.16$) was relatively high compared to the estimated survival via the San Joaquin River route ($S_A = 0.05$), the small number of fish observed taking the Old River route resulted in very high uncertainty in the Old River route survival estimate ($SE = 0.15$ for S_B); thus no significant difference in route-specific survival was detected for the first release group (P=0.1977). The estimated route-specific survival to Chipps Island via the Old River route was 0 for the second release group, yielding a population estimate of $S_B = 0.11$ ($SE = 0.10$); again, there was no significant difference in population survival estimates between the two routes (P=0.1999) (Table 17).

Survival in the Old River route used the parameter $\phi_{B1,B2}$ in place of S_{B1} because there were no detections at site C1 (MRH) (see *Statistical Methods*). The transition parameter $\phi_{B1,B2} = S_{B1}\psi_{B2}$, so if $\psi_{B2} < 1$, then S_B is underestimated using this formulation. For the first release group, $\phi_{B1,B2}$ = 1 ($SE =$

0), so both $S_{B1}=1$ and $\psi_{B2}=1$, and S_B is not underestimated (Table A5-2). For the second release group, $\phi_{B1,B2}$=0.67 ($SE=0.27$), implying that either $S_{B1}<1$ or $\psi_{B2}<1$, or both (Table A5-2). However, there was only a single tag detected at site B1 (ORE) that was not later detected as a smolt at site B2 (ORS), and this tag was actually detected at B2 with a predator classification at that site. Thus, there is no evidence that $\psi_{B2}<1$ for either release group, and so it reasonable to interpret estimates of S_B as unbiased rather than as minima. Furthermore, the lack of detections of tags from the second release group at Chipps Island would yield $S_B=0$ for that release group in any event. Thus, there is no reason to assume that survival to Chipps Island via the Old River route is underestimated.

Survival was estimated to Jersey Point for fish that used the San Joaquin River route. This survival measure $\left(S_{A(MD)}\right)$ was estimated at 0. 09 (SE =0.02) for the first release group, 0.01 (SE =0.01) for the second release group, and 0.06 (SE =0.01) overall (Table 17). No estimates were available for the Old River route. Survival $\left(S_{A(SD)}\right)$ to the receivers just downstream of the Turner Cut junction on the San Joaquin River (i.e., MacDonald Island and Turner Cut receivers) was estimated at 0.33 ($SE=0.03$) for the first release group, 0.07 ($SE=0.02$) for the second release group, and 0.23 ($SE=0.02$) overall (Table 17). Thus it is apparent that survival was low both to the Turner Cut junction and from that junction to Jersey Point, especially for fish from the second release group.

Survival was lower for the second release group than for the first group throughout the San Joaquin River. Estimated survival from the release site to Mossdale ($\phi_{A1,A4}$) was considerably lower ($p<0.0001$) for the second release group (0.37 for the second group vs. 0.63 for the first group), as was survival through the Southern Delta (0.07 vs. 0.33; $p<0.0001$), Middle Delta to Jersey Point (0.01 vs. 0.09; $p<0.0001$), and the entire Delta to Chipps Island (0 vs. 0.05; $p<0.0001$)(Table 17). Estimated survival was also lower through the modeled portions of the Old River route, i.e., from the head of Old River to the head of Middle River for the second release group. For the first release group, estimated survival through this reach was 1.0; for the second release group, it was 0.67 ($SE=0.27$); however, the difference was not statistically significant (p= 0.1106) (Table A5-2). Although the estimate for this reach for the second release group had high uncertainty, the point estimate fits the pattern observed in the San Joaquin River of lower survival for the second release group relative to the first release group.

Including predator-type detections in the analysis produced very similar results on all spatial scales, including survival to Chipps Island, Jersey Point, and the Turner Cut junction (Table 18). The largest difference was in estimates of San Joaquin River survival through the Southern Delta to the Turner Cut junction $\left(S_{A(SD)}\right)$, which increased by 0.01 for both release groups and overall (overall estimate = 0.24, $SE=0.02$) (Table 18). Including predator detections did not alter the comparisons between release groups; estimated survival was lower for the second release group throughout the various San Joaquin River regions (Table 18; $P<0.0001$).

Parameter estimates were significantly (family-wise α=0.10) higher for the first release group compared to the second release group for parameters S_{A2}, S_{A3}, S_{A4}, S_{A5}, S_{A7}, $\phi_{A8,G1}$, and $\phi_{G1,G2}$ (Table 19).

Travel Time

Average travel time through the system from release at Durham Ferry to Chipps Island was 5.75 days based on 11 detections ($SE = 0.41$ days) (Table 20a). Travel time to Chipps Island ranged from 4.1 days to 10.4 days, all from the first release group. The large majority of tags that reached Chipps Island came via the San Joaquin River route; the single tag that arrived at Chipps Island via the Old River route had a total travel time of 4.12 days, which was faster than any of the 14 tags that arrived via the San Joaquin River route. All tags observed at Jersey Point arrived via the San Joaquin River route in 3 – 9 days, with an average of approximately 6 days (Table 20a).

Travel time from release to the Mossdale Bridge receivers ranged from 0.3 to 3.9 days, and averaged 0.53 days (harmonic mean; $SE = 0.01$ days) (Table 20a). Fish with the longer travel times to Mossdale tended to come from the second release group, although both release groups included fish that arrived in under 8 hours. Travel time from release to the Turner Cut junction receivers (i.e., to Turner Cut or MacDonald Island) ranged from 1.5 days to 8.2 days, and averaged between 2 and 4 days (Table 20a). Fish with the longer travel times to Mossdale tended to come from the second release group, although both release groups included fish that arrived in under 8 hours. Travel time from release to the Turner Cut junction receivers (i.e., to Turner Cut or MacDonald Island) ranged from 1.5 days to 8.2 days, and averaged between 2 and 4 days (Table 20a).

Only 2 tags were detected at the Old River receivers near Highway 4 (OR4). One of these tags came via the Old River route and arrived 4.3 days after release, while the other tag arrived via Turner Cut from the San Joaquin River route 5.1 days after release. For the few tags that were detected at the entrance to the Central Valley Project, tags that came via the Old River route tended to have shorter travel times than tags that arrived via the San Joaquin River route (Table 20a). Sample sizes were too small to draw definitive conclusions, but these observations may have been expected because of the longer route to the interior and western receivers via the San Joaquin River route.

Including predator-type detections had only a small effect on average travel times through the system (Table 20b). Travel times to the San Joaquin River receivers at MacDonald Island and Turner Cut were generally slightly longer when predator-type detections were included. This was because travel times were measured to the beginning of the tag's final visit to each site, and many tags classified as being in predators at those sites were observed making multiple visits to those sites. The longer travel times observed for the data set that includes the predator-type detections reflect the assumption used in the predator filter that predators are more likely than smolts to exhibit long travel times.

Average travel time through reaches for tags classified as being in smolts ranged from 0.01 days (approximately 20 minutes) for the single tag observed moving from the Central Valley Project trashracks to the holding tank, to over 2 days for tags moving from MacDonald Island to Jersey Point, and over 3 days for tags moving from MacDonald Island and Medford Island to Chipps Island (Table 21a). While there were several tags that moved from MacDonald Island to Jersey Point in under 2 days, there

were also several tags that took over 5 days to make the journey. Similar travel times were observed from the Medford Island receivers to the Jersey Point receivers, although the average travel time was somewhat lower from Medford Island (approximately 1.54 days over both release groups) (Table 21a). The reach from MacDonald Island to Jersey Point was one of the longer reaches in the study area (approximately 26 rkm), so it not surprising that it had some of the longer observed travel times. However, the reach from Jersey Point to Chipps Island was also approximately 26 rkm in length, and travel time through this reached tended to be shorter, ranging from 16 hours to 2.1 days and averaging 1.21 days ($SE = 0.14$ days) (Table 21a). The region between Jersey Point and Chipps Island is strongly affected by tides, which may delay migrating fish, but it is nevertheless channelized. The region between MacDonald Island and Jersey Point, on the other hand, includes Frank's Tract, and it is possible that migrating Chinook Salmon smolts are delayed there for a considerable time. In general, there were too few detections in the interior Delta to make comparisons of travel time through reaches in that region with travel time through reaches contained within the San Joaquin River route. Including predator-type detections did not greatly affect the pattern of observed travel times through the various reaches (Table 21b).

There was a significant negative relationship ($p<0.05$) between travel time per km and survival per km in river reaches upstream of the Lathrop/Old River junction for the second release group, suggesting as travel time per km increased, survival per km decreased (Figure 11, Table 22). Survival also decreased as travel time increased in reaches between Durham Ferry and Lathrop/Old River junction for the first release group, but the regression line was not significant at the $p<0.05$ level. Survival was higher for the first release group, than for the second release group in these three reaches of the river (Figure 11, Table 19). Also there appeared to be a slight increase in travel time (slower migration rate) between Mossdale and Lathrop/Old River junction and between Banta Carbona and Mossdale for the second release group relative to the first release group (Figure 11, Table 22).

In contrast, there did not appear to be a relationship between travel time per km and survival per km for reaches between the Lathrop/Old River junction and Jersey Point (tidal reaches) for either of the release groups in 2012 (Figure 12). While survival through the reach (or joint probability of moving to and surviving to the downstream location) was significantly higher (Table 19) for the first release group for three of these reaches in the San Joaquin River downstream of Lathrop (Lathrop to Garwood Bridge, S_{A5} ; Navy Drive Bridge to MacDonald Island or Turner Cut, S_{A7} ; and the reach between MacDonald Island to Jersey Point, $\phi_{A8,G1}$ [not shown on Figure 12]0, others were not significantly higher (e.g. Garwood Bridge to Navy Bridge Drive [S_{A6}], MacDonald Island to Medford Island [$\phi_{A8,A9}$], and Medford Island to Jersey Point [$\phi_{,A9,G1}$]) (Table 19). Travel times in these reaches were similar for the two release groups (Figure 12).

Route Entrainment Analysis

River flow (discharge) at the TRN gaging station in Turner Cut ranged from -4,402 cfs to 3,361 cfs (average = -1070 cfs) during the estimated arrival time of the tagged Chinook Salmon at the Turner Cut junction location (TCJ) in 2012. Water velocity in Turner Cut was highly correlated with river flow ($r=0.999$), and velocity values ranged from -0.8 ft/s to 0.6 ft/s (average = -0.1 ft/s). The flow in Turner

Cut was negative (i.e., directed to the interior Delta) upon arrival at TCJ of approximately 61% (54 of 89) tags in this analysis. River stage measured in Turner Cut was moderately correlated with both river flow and velocity (r=-0.70), and ranged from 6.7 ft to 10.9 ft (average = 9.1 ft). Changes in river stage in the 15-minute observation period containing the arrival of the tagged Chinook Salmon to the TCJ ranged from -0.2 ft to 0.2 ft (average = 0 ft). Changes in river stage were not correlated with stage (r=-0.13). The index of river flow in the reach from Stockton to Turner Cut was uncorrelated with flow and velocity in Turner Cut upon arrival at TCJ (r= 0.01), and only moderately correlated with river stage at Turner Cut (r= -0.29). The flow index in the Stockton-Turner Cut reach ranged from 2,324 cfs to 3,400 cfs (average = 2,785 cfs).

The daily export rate at CVP ranged from 821 cfs to 1,016 cfs (average = 960 cfs); exports at CVP were generally low in both early and late May, and was greatest in mid-May. The daily export rate at the State Water Project (SWP) ranged from 507 cfs to 3,698 cfs (average = 1,908 cfs). SWP exports were more variable than CVP exports but also peaked in the third week of May. Exports from CVP and SWP were uncorrelated (r= -0.01). Neither CVP nor SWP exports was correlated with either flow (r=0.09 for CVP, r=-0.03 for SWP) or river stage (r=0.00 for CVP, r=-0.14 for SWP) in Turner Cut. The majority of tags (66 of 89, 74%) arrived at the Turner Cut junction during daylight hours.

The single-variate analyses found no significant effects (α=0.05) of any of the covariates considered (P>0.40 for all covariates; Table 23). This negative result may reflect the true lack of a relationship between environmental variables and route selection at Turner Cut, or it may be an artifact of the low degrees of freedom available and the resulting low statistical power; because only 11 fish were observed entering Turner Cut (out of 89), there were only 11 degrees of freedom total. A study with a larger sample size and more fish observed using Turner Cut may provide evidence of a relationship between one or more of the covariates and route selection at this junction in future.

Comparison of Delta Survival to Past Years

In a multiple regression, tag type (acoustic or CWT) did not come out as an important variable affecting survival, whereas flow did (Table 24). Using the relationship developed from the CWT data (Figure 13), we calculated what survival from Mossdale to Jersey Point was expected to be at the two flow levels in 2012: predicted survival was 0.12 at flows of 3543 cfs and 0 at flows of 2327cfs, very close to what we observed (0.09, $SE = 0.02$, at the higher flow and 0.01, $SE = 0.01$, at the lower flow). The relationships between flow at Vernalis and survival from Mossdale to Jersey Point with the HORB, developed from the historical CWT data and from all of the data (historic CWT data and acoustic tag data added from 2012), were similar (Figure 13). The slopes of the two linear regression lines were the same (0.0001), and the intercepts were similar (-0.2345 for the CWT data only and -0.2295 for the combined data (Figure 13)) . Both relationships were statistically significant (p <0.01).

Discussion

The similarity between parameter estimates with and without predator-type detections raises questions about the predator filter. One possible explanation for the similar estimates is that the

majority of the mortality was not directly caused by the predatory fish used to build the predator filter, or that many of the predatory fish feeding on the tagged salmon merely evaded detection. Chinook Salmon smolts may have been eaten by sedentary predators, birds, or mammals (e.g., otters), or by predatory fish that moved about the Delta but evaded the acoustic receivers. Alternatively, Chinook Salmon smolts may have died due to disease or habitat quality. In either case, the tags of the deceased salmon smolts may have settled on the river bottom away from the acoustic receivers; in these cases, the predator filter would correctly identify existing detections of these tags as in smolts rather than predators, and the survival model estimates would be unbiased.

Another possibility is that the filter missed detections of predators, and thus the resulting filtered data set (which supposedly has no detections from predators) is only artificially similar to the unfiltered data set (which includes detections from predators). If this is the case, then survival estimates for the (presumed) smolt-only data set would be biased because they would be based partially on predator detections. The type of bias depends on where the predator filter failed. For example, none of the tags detected at Chipps Island were classified as being in predators by the existing filter. A filter that recategorizes some of those detections as predator detections may yield survival estimates to Chipps Island that are lower than that estimated in this study (0.03). This would happen as long as the revised filter agreed with the original filter in upstream regions. On the other hand, if the predator filter was inefficient (i.e., wrong) upriver of Mossdale such that detections passed by the filter as smolts were actually detections of predators, then it is possible that true survival to Chipps Island was actually higher than estimated (0.03); this may happen if there were fewer actual smolts starting at Mossdale than appeared from the original filter. Of the 959 tags released at Durham Ferry, only 480 (50%) were detected at Mossdale, and 478 of them were classified as in smolts upon arrival at Mossdale (Tables 9 and 13). Only 15 of these tags were detected at Chipps Island. Adjusting the predator filter cannot add more detections at Chipps Island, but it may remove detections at Mossdale. A revised filter that used more stringent criteria upstream of Mossdale was constructed and implemented on the detection data. The revisions to the filter were:

- no upstream-directed transitions allowed upstream of Mossdale
- no repeat visits to sites upstream of Mossdale
- maximum residence time of 2 hours at any site upstream of Mossdale
- maximum regional residence time of 15 hours upstream of Mossdale
- minimum migration rate of 0.2 km/hr for all transitions upstream of Mossdale

This stricter filter resulted in 477 of the 480 detections at Mossdale being classified as in smolts, compared to 478 classified as in smolts using the original predator filter. The Delta survival estimate from the stricter predator filter was 0.03 for the population (i.e., both release groups pooled), unchanged from the estimate using the original filter. Thus, it is unlikely that errors in the predator filter resulted in the similar results with and without the predator-type detections.

Our first objective of the 2012 study was to determine survival of emigrating salmon smolts from Mossdale to Chipps Island during two time periods (prior to May 15 and after May 15) in the presence of the HORB to determine if there was a benefit from the flow augmentation from the Merced

River in 2012. Average river flow measured at the Vernalis gaging station when fish from the first release group were traveling through the Delta to Chipps Island (from release through approximately 10 days after the end of release period) was 3,543 cfs, while for the period of comparable length for the second release group was 2,327 cfs (Figure 14). Survival was higher ($p < 0.0001$) through the Delta (S_{Total}) for the first release group (0.05) relative to the second release group (0.00) (Table 17). Thus these findings appear to support our hypothesis that the increased flow from the Merced River flow augmentation increased survival through the Delta.

Our second objective was to assess whether the higher flows from the Merced River flow augmentation resulted in a reduction in travel time and higher survival, specifically in the riverine reaches of the Delta, and resulted in higher through-Delta survival. Shorter travel times would reduce the time tagged fish were exposed to mortality factors such as predation, high water temperatures, and toxics. Travel times in reaches of the Delta between Durham Ferry and a series of downstream locations (Mossdale, Lathrop, Garwood Bridge, Navy Drive Bridge, and MacDonald Island) were all significantly less (i.e. faster migration) for the first release group than the second release group (Table 20a; $p < 0.05$). The travel times in these reaches appeared to be strongly influenced by the travel time for the reach between Lathrop (SJL) and Garwood Bridge (SJG). Travel time between SJL and SJG was significantly less ($p < 0.05$) for the first release group (0.60; $SE = 0.02$) which experienced the higher flows, than for the second release group (0.86; $SE = 0.05$) which experienced the lower flows (Table 21a). Survival through this reach was also higher for the first release group (0.81; $SE = 0.02$) relative to the second release group (0.48; $SE = 0.04$)($p < 0.0001$) (S_{A5}; Table A5-2). Thus, the data in this specific, partly riverine, reach of the Delta are consistent with our hypothesis that an increase in flow would reduce travel time and be associated with higher survival.

To further evaluate the possible relationship between travel time and survival in the remaining reaches, travel time and survival were standardized to a per-km basis. With this standardization, we found that as travel time per km increased, survival decreased for both release groups in the three riverine reaches between Durham Ferry and the Lathrop/Old River junction (Figure 11). Travel time per km was greater for the second group relative to the first group for two of the three reaches; (Banta Carbona to Mossdale and Mossdale to Lathrop/Old River, but not Durham Ferry to Banta Carbona) whereas survival was always lower for the second release group (lower flows) relative to the first group (higher flows) for these three reaches (Figure 11, Table 22). Thus the difference in travel time per km for the first group relative to the second did not always support our hypotheses that the higher survival per km resulted from a decrease in travel time per km from the higher flows in these riverine reaches.

Travel time per km was somewhat less and survival greater for the first release group relative to the second release group in two reaches: 1) between Lathrop and Garwood Bridge (discussed above) and 2) between Garwood Bridge and Navy Bridge Drive (Figure 12, Table 22); the shorter travel time from the increased flow may partially explain the higher point estimate of survival for release 1 compared to release 2 between Garwood Bridge and Navy Bridge, although the increase in survival is not statistically significant at the 5% level (Table 19); however, it is not possible to determine causation from this study.

Once fish enter the interior Delta or into the strongly tidally influenced San Joaquin River, travel times were expected to increase and survival was expected to decrease. While we did generally see longer travel times per km in the tidal reaches (reaches downstream of Navy Bridge Drive), it was not always greater (Table 22; e.g. travel time per km was shorter from MacDonald Island to Medford Island than it was from Lathrop to Garwood Bridge). Travel time per km was also less for the second release group than for the first, even though survival was generally higher for the first group relative to the second in all reaches downstream of Navy Bridge Drive, except between MacDonald Island and Medford Island, when survival per km was higher for the second group (Table 22). Since the increased flow probably was not enough to change velocities significantly in the downstream tidal reaches, the increased survival of the first group relative to the second in most of these tidal reaches suggests there are other mechanisms either associated with flow or other factors that resulted in the increases in survival in these tidal reaches of the Delta.

Once fish move into the interior Delta, they are exposed to flows moving toward the export facilities, which may increase their travel time and reduce their survival to Jersey Point or Chipps Island. While many of the tagged fish may have been diverted from the San Joaquin River into the interior Delta downstream of Turner Cut, we were only able to identify those entering the interior Delta through Turner Cut. We had hypothesized that tagged fish moving into the interior Delta (e.g. Turner Cut) would have increased travel times over those not being diverted into Turner Cut. Since none of the tagged fish that entered Turner Cut survived to Chipps Island for either the first or second release group, we could not compare travel times between release groups or for the Turner Cut route relative to the other routes. One fish that entered Turner Cut from the first release group was observed in the CVP holding tank, but did not survive to reach Chipps Island. We were also not able to assess the impact on survival of tagged fish being routed to the SWP and CVP as detections from the receivers at the entrances to the water export facilities and in the holding tank at the Central Valley Project were removed from the survival model because of sparse data due to the presence of the HORB.

The results of comparing travel time to survival suggests that the increased flow during the first release did not always result in decreased travel times, although it did coincide with an increase in survival in more of the riverine reaches. It was the higher survival in the majority of the reaches (both riverine and tidal) during the first release that resulted in a higher overall survival through the Delta for the first release group relative to the second release group.

However, there are other possible hypotheses for the lower survival in the second release group compared to the first release group, including differences in fish condition, tagging and release procedures, and other environmental conditions. The same tagging and release procedures were used for both release groups, including the same taggers, presumably with the same skill set, so that does not appear to be responsible for the differences in survival we observed. Fish from the second release group were slightly larger on average than fish from the first release group (mean FL = 109.9 mm and 115.7 mm for the first and second release groups, respectively), so it was reasonable to expect higher survival for the second release group rather than lower survival, but we did not observe this. Although the two release groups were released only two weeks apart, they experienced different environmental conditions other than flow. During the same two time periods, combined exports at CVP and SWP varied from 1,513 cfs to 5,054 (mean = 3,200 cfs), with similar means in the two periods. However,

exports tended to be high toward the end of the first period, when relatively few fish from the first release were still migrating, and also high near the beginning of the second period, when the majority of fish from the second release group were migrating (Figure 15).

It is also possible that the difference in flow conditions may have resulted in the different survival rates via a mechanism other than travel time, such as temperature, increased predation or toxicity. We had hypothesized that the higher inflow from the Merced flow augmentation would potentially reduce the effects of these mortality factors by reducing temperature stress, diluting toxics or reducing predator metabolic demands from the lower water temperatures. Water temperature measured at the San Joaquin River gage near Lathrop was almost 2 degrees higher on average for the second release group (67.5 °F [19.7°C]) than for the first group (65.6 °F [18.7°C]), which may have negatively affected the survival of the second release group, and been a consequence of the lower flows experienced by the second release group (Figure 16). We were unable to assess the hypothesis that increased metabolic demands from predators due to the warmer water temperatures was the cause for the increased mortality for the second release group relative to the first release group.

To assess the hypothesis that the increased flow from the Merced River flow augmentation may have diluted toxicity in the Delta, we observed that survival was significantly higher for the first group relative to the second group in the reach between SJL and SJG (Table 19). This reach from SJL to the SJG is one of the longer reaches of the Delta at 18 km (Table 22), and it includes a variety of habitats. It is not entirely riverine, but includes the transition to tidal habitat, depending on inflow. The reach is more riverine at higher inflows, and more tidal at lower inflows. The Stockton Wastewater treatment plant releases its effluent in the lower part of this reach which may have an effect on survival, especially during periods of low flow. During periods of low flow the movement of the tidal prism upstream may result in concentration of the effluent in this reach and dilution from flow would be less. There is also the possibility that increased temperatures exacerbate the toxicity effects of the effluent on juvenile salmon survival. Further evaluation of water quality in this reach may be warranted, building on studies conducted near there in 2008 (SJRGA 2009) after a significant die-off of acoustic tags near this location in 2007 – a low flow year (SJRGA 2008).

In addition, it is possible that the higher incidence of PKD infection for the second release group reduced their survival to Chipps Island relative to the first release group. Infection does not necessarily lead to death but would reduce fitness from anemia, kidney dysfunction, and immune suppression even if the fish survived the disease (Angelidis et al 1987, Hedrick and Aronstien 1987 as cited in Nichols et al 2012). The increase in water temperature may have contributed to the higher incidence of PKD infection for the second release group relative to the first as PKD is a progressive disease at water temperatures greater than 15°C (Okamura and Wood 2002 as cited in SJRGA 2013).

Unfortunately, PKD infection is not just a problem for the experimental fish we used in 2012, but was noted as a problem in monitoring on the Merced River. Smolts caught in the Hopeton rotary screw trap on the Merced River (presumably wild stock) also had high levels of PKD infection in 2012 (Nichols et al. 2012). This is also not new, as 90-100% of naturally produced fish in a 2001 survey of Merced outmigrant salmonid health were observed to be infected with PKD (Nichols and Foott 2002 as cited in Nichols et al. 2012). Even some of salmon transferred from MRH to the lab at the Fish Health Center soon after ponding in February of 2012, developed light infections of PKD (Nichols et al 2012).

However, the worst infections identified in the 2012 study were later in the season, with gross clinical signs of PKD (anemia and swollen kidney) observed for naturally produced fish on May 9 (2 out of 24), and high numbers of parasites observed for both naturally produced (May 9 and May 15) and hatchery fish (May 15) (Nichols et al. 2012).

PKD is caused by infection by the endoparasitic myxozoan, *Tetracapsuloides bryosalmonae*. Reducing byrozoan habitat directly upstream of the hatchery and in the Merced River could be a viable disease management strategy (Foott et al. 2007). Increasing flows, if they result in decreasing water temperatures, would serve to reduce the severity of PKD for both experimental and wild fish emigrating from the San Joaquin basin. Higher water temperatures in the river and at the hatchery may have increased the severity of the PKD infection for the second group of tagged fish in 2012, relative to the first group; this may account for some of the increased mortality observed in the second group. Higher water temperatures are affected by both flow and air temperature upstream of the Delta. Cold water releases from the upstream reservoir on the Merced River may have reduced the water temperatures for the first release group over what they would have been without the water release.

Our third objective of the 2012 study was to identify route selection at HOR and at Turner Cut under the two different periods with varying flows and exports. Since the physical HORB was in place in 2012, route selection into the San Joaquin River was high for both groups (0.98; $SE = 0.02$) and did not vary between release groups (Table 17) or when predator type detections were included (Table 18). Route selection at Turner Cut was 0.11 ($SE = 0.03$) for the first release group, and 0.16 ($SE = 0.11$) for the second release group (Table 17) when predator-type detections were removed and similar when predator-type detections were included (0.12; $SE = 0.03$ for the first release group and 0.14; $SE = 0.04$ for the second release group) (Table 18). Differences in the proportion diverted into Turner Cut at the TCJ between release groups were not statistically different: with 11 to 16% of the tagged fish diverted into Turner Cut, none of which survived to Chipps Island ($S_{F1,G2}$; Tables A5-2 and A5-3). Zero probability of survival to Chipps Island for the tagged fish that entered Turner Cut negatively affected total through-Delta survival for both release groups. A study with a larger sample size and more fish observed using Turner Cut may provide evidence of a relationship between one or more covariates (e.g. flow, and tides) and route selection at this junction in future.

It is possible that the lower flows, higher water temperatures, higher toxicity, higher incident of disease (PKD) and possibly higher export rates during the time of peak migration may have combined to negatively affect salmon survival from the second release. Diversion into Turner Cut decreased survival of both groups. With only two release groups and observational data, however, it is not possible to conclude more. Combining these results with those from additional years may shed light on possible causes of mortality in the Delta. The Interagency Ecological Program has funded a multi-year analysis of the data from 2010, 2011, 2012 and 2013 and results will be forthcoming.

Based on the results of this study in 2012, naturally spawned or hatchery juvenile salmonids from the San Joaquin tributaries likely experienced variable survival within the migration period through the Delta, with greater survival during the Merced River flow augmentation period and lower survival during the later remainder period of migration. Higher flows appeared to benefit survival through

multiple intertwined mechanisms including shorter travel times, lower water temperatures, and reduced disease impacts.

The comparison of estimates of survival from Mossdale to Jersey Point for the two release groups in 2012, to estimates generated using CWT's with the HORB, suggests that survival observed in 2012 was within that expected based on the past CWT relationship, and that differences in flow between the two releases in 2012 likely increased survival over what it would have been without the flow pulse. However, without direct manipulation and further replication, cause and effect cannot be determined. While this comparison supports our hypothesis that the increased flow from the flow augmentation in the Merced River during the first release group increased survival, it also shows that survival for both groups in 2012 was relatively low, compared to that measured in other years with the HORB (Figure 13). These data suggest a higher flows of approximately 6,000 cfs with the HORB, are needed to achieve survival through the Delta of approximately 0.40. Additional studies, especially during higher flow periods, with the HORB in place, are needed to confirm these results.

List of References

Adams, N.S., D.W. Rondorf, S.D. Evans, and J.E. Kelly (1998). Effects of surgically and gastrically implanted radio tags on growth and feeding behavior of juvenile Chinook Salmon: Transactions of the American Fisheries Society, v.127, p. 128-136.

Brandes, P.L. and J.S. McLain (2001). Juvenile Chinook Salmon abundance, distribution, and survival in the Sacramento-San Joaquin Estuary. Contributions to the Biology of the Central Valley Salmonids, Fish Bulletin 179: Volume 2.

Buchanan, R. (2013). OCAP 2011 Steelhead Tagging Study: Statistical Methods and Results. Prepared for Bureau of Reclamation, Bay Delta Office, Sacramento CA. August 9, 2013. 110 p.

Burnham, K. P., and D. R. Anderson (2002). Model selection and multimodel inference: A practical information-theoretic approach. 2nd edition. Springer. New York, NY. 488 pp.

California Department of Water Resources (2015). Final: An Evaluation of Juvenile Salmonid Routing and Barrier Effectiveness, Predation, and Predatory Fishes at the Head of Old River, 2009-2012. Prepared by AECOM, ICF International and Turnpenny Horsfield Associates. http://baydeltaoffice.water.ca.gov/sdb/tbp/web_pg/tempbar/horbereport.cfm

Cavallo, B., P. Gaskill, and J. Melgo (2013). Investigating the influence of tides, inflows, and exports on sub-daily flow in the Sacramento-San Joaquin Delta. Cramer Fish Sciences Report. 64 pp. Available online at: http://www.fishsciences.net/reports/2013/Cavallo_et_al_Delta_Flow_Report.pdf.

Cormack, R.M. (1964) Estimates of survival from the sighting of marked animals. Biometrika 51, 429-438.

Ferguson, HW. (1981). The effects of water temperature on the development of Proliferative Kidney Disease in rainbow trout, *Salmo gairdneri* Richardson. Journal of Fish Disease 4: 175-177

Foott JS, R Stone and K Nichols (2007). Proliferative Kidney Disease (Tetracapsuloides bryosalmonae) in Merced River Hatchery juvenile Chinook Salmon: mortality and performance impairment in 2005 smolts. California Fish and Game 93: 57-76.

Jolly, G.M. (1965) Explicit estimates from capture-recapture data with both death and immigration - Stochastic model. Biometrika 52: 225-247.

Lady, J. M., and J. R. Skalski (2009). USER 4: User-Specified Estimation Routine. School of Aquatic and Fishery Sciences. University of Washington. Available from http://www.cbr.washington.edu/paramest/user/.

Li, T., and J. J. Anderson (2009). The Vitality model: A Way to understand population survival and demographic heterogeneity. Theoretical Population Biology 76: 118-131.

Liedtke, T. (2012). 2012 South Delta Study Tagger Training and QA/QC Summary. Prepared by Theresa Liedtke, U.S. Geological Survey, Western Fishereis Research Center, Columbia River Research Laboratory 5501A Cook-Underwood Road, Cook, WA 98605, for J. Israel, USBR Bay-Delta Office, 801 I Street, Suite 140, Sacramento, CA 95814. 97pgs.

Martinelli, T.L., H.C. Hansel, and R.S. Shively (1998). Growth and physiological responses to surgical and gastric radio tag implantation techniques in subyearling Chinook Salmon: Hydrobiologia, v. 371/372, p. 79-87.

McCullagh, P., and J. Nelder (1989). Generalized linear models. 2nd edition. Chapman and Hall, London.

Nichols, K., A. Bolick and J.Scott Foott (2012). FY2012 Technical Report: Merced River juvenile Chinook Salmon health and physiology assessment, March-May 2012. December 2012. US Fish and Wildlife Service, California-Nevada Fish Health Center, 24411 Coleman Hatchery Road, Anderson CA 96007.

Perry, R. W. (2010). Survival and Migration Dynamics of Juvenile Chinook Salmon (*Oncorhynchus tshawytscha*) in the Sacramento-San Joaquin River Delta. University of Washington, Ph.D. dissertation. 2010. 223 p.

Perry, R. W., J. R. Skalski, P. L. Brandes, P. T. Sandstrom, A. P. Klimley, A. Ammann, and B. MacFarlane (2010). Estimating survival and migration route probabilities of juvenile Chinook Salmon in the Sacramento-San Joaquin River Delta. North American Journal of Fisheries Management 30: 142-156.

San Joaquin River Group Authority (2007). 2006 Annual Technical Report: On Implementation and Monitoring of the San Joaquin River Agreement and the Vernalis Adaptive Management Plan (VAMP). Prepared for the California Water Resources Control Board. Available at www.sjrg.org.

San Joaquin River Group Authority (2008). 2007 Annual Technical Report: On Implementation and Monitoring of the San Joaquin River Agreement and the Vernalis Adaptive Management Plan (VAMP). Prepared for the California Water Resources Control Board. Available at www.sjrg.org.

San Joaquin River Group Authority (2010). 2009 Annual Technical Report: On Implementation and Monitoring of the San Joaquin River Agreement and the Vernalis Adaptive Management Plan (VAMP). Prepared for the California Water Resources Control Board. Available at www.sjrg.org.

San Joaquin River Group Authority (2011). 2010 Annual Technical Report: On Implementation and Monitoring of the San Joaquin River Agreement and the Vernalis Adaptive Management Plan (VAMP). Prepared for the California Water Resources Control Board. Available at www.sjrg.org.

San Joaquin River Group Authority (2013). 2011 Annual Technical Report: On Implementation and Monitoring of the San Joaquin River Agreement and the Vernalis Adaptive Management Plan (VAMP). Prepared for the California Water Resources Control Board. Available at www.sjrg.org.

Seber, G. A. F. (2002). The estimation of animal abundance. Second edition. Blackburn Press, Caldwell, New Jersey.

Seber, G.A. F. (1965) A note on the multiple recapture census. Biometrika 52, 249-259.

Skalski, J. R., R. Townsend, J. Lady, A. E. Giorgi, J. R. Stevenson, and R. D. McDonald (2002). Estimating route-specific passage and survival probabilities at a hydroelectric project from smolt radiotelemetry studies. Canadian Journal of Fisheries and Aquatic Sciences 59: 1385 - 1393

Sokal, R. R., and Rohlf, F. J. (1995). Biometry, 3rd ed. W.H. Freeman and Co., New York, NY, USA.

Townsend, R. L., J. R. Skalski, P. Dillingham, and T. W. Steig (2006). Correcting Bias in Survival Estimation Resulting from Tag Failure in Acoustic and Radiotelemetry Studies. Journal of Agricultural, Biological, and Environmental Statistics 11: 183-196.

US Bureau of Reclamation (2012). San Joaquin River Flow Modification Study. Finding of No Significant Impact. Division of Planning, Mid Pacific Region, Sacramento CA. 3 p.

Vogel, D. A. (2010). Evaluation of acoustic-tagged juvenile Chinook Salmon movements in the Sacramento-San Joaquin delta during the 2009 Vernalis Adaptive Management Program. Technical Report for San Joaquin River Group Authority. 72 p. Available http://www.sjrg.org/technicalreport/ (accessed 13 December 2011).

Vogel, D. A. (2011). Evaluation of acoustic-tagged juvenile Chinook Salmon and predatory fish movements in the Sacramento-San Joaquin Delta during the 2010 Vernalis Adaptive Management Program. Technical report for San Joaquin River Group Authority. Available http://www.sjrg.org/technicalreport/ (accessed 13 December 2011).

Acknowledgements:

Funding for the project came from the restoration funds of the Central Valley Project Improvement Act, the U.S. Bureau of Reclamation, and the Department of Water Resources. Several individuals from a variety of agencies made this project possible. Those agencies and individuals who participated in the tagging and release components of the project were; USFWS: Amber Aguilera, Denise Barnard, Crystal Castle, Dustin Dinh, David Dominguez, Kyle Fronte, Garrett Giannetta, Jack Ingram, Carlie Jackson, Joseph Kirsch, David LaPlante, Jerrica Lewis, Mike Marshall, Louanne McMartin, Greg Nelson, Jacob Osborne, Lori Smith, Brent Trim, and Rob Wilson; California Department of Water Resources: Roxanne Kesler, Bryce Kozak , and Matt Silva; AECOM: Curtis Yip; and USBR: Raymond Bark and Josh Israel. USGS provided training for the surgeons (Theresa [Marty] Liedtke) and was responsible for the deployment, maintenance and retrieval of the receiver array (Jon Burau, Chris Vallee, Jim George and Norbert VandenBranden). Mike Simpson, retired from USGS, processed the data prior to giving it to Rebecca Buchanan of University of Washington for analyses.

Figures

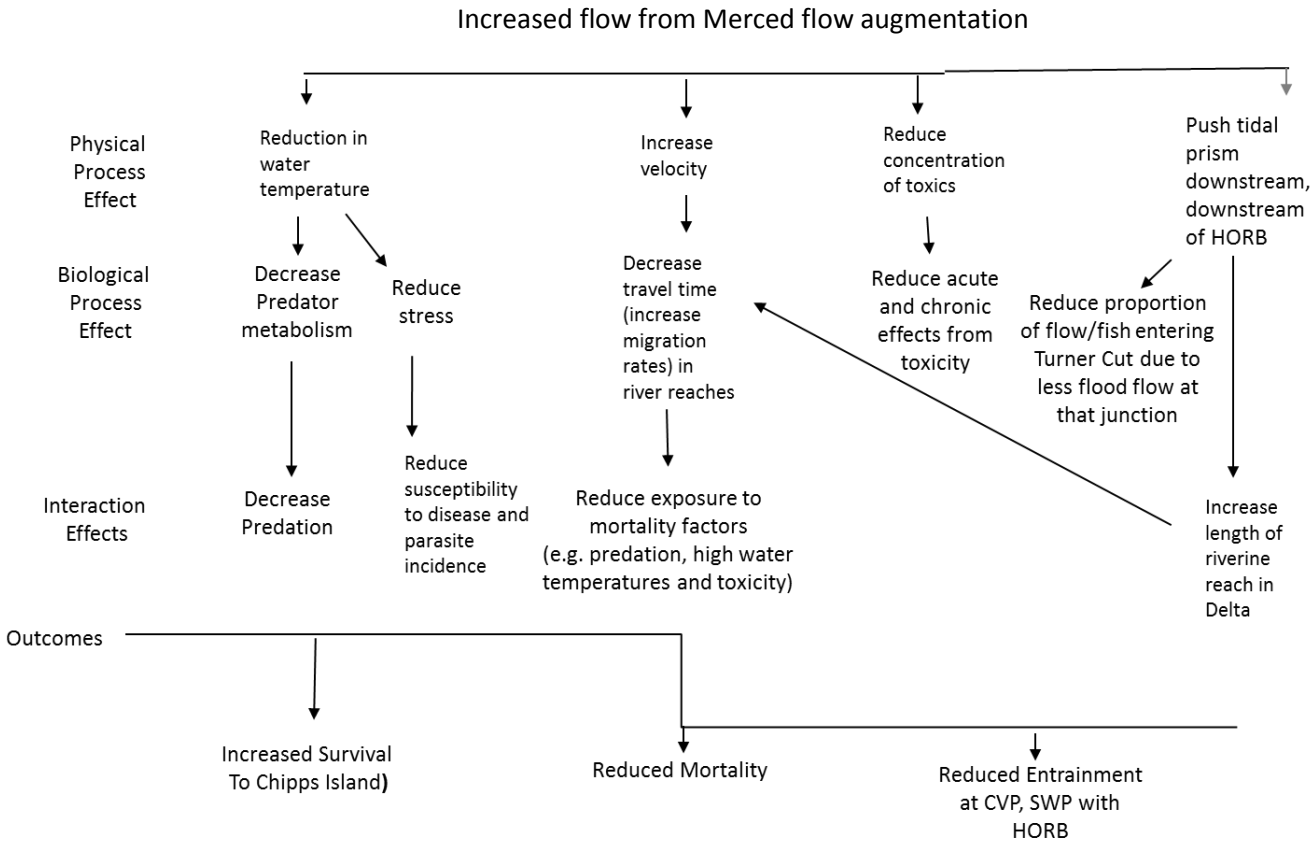

Figure 1: Conceptual model of mechanisms for increased survival from increasing Vernalis Flow with the head of Old River barrier in place.

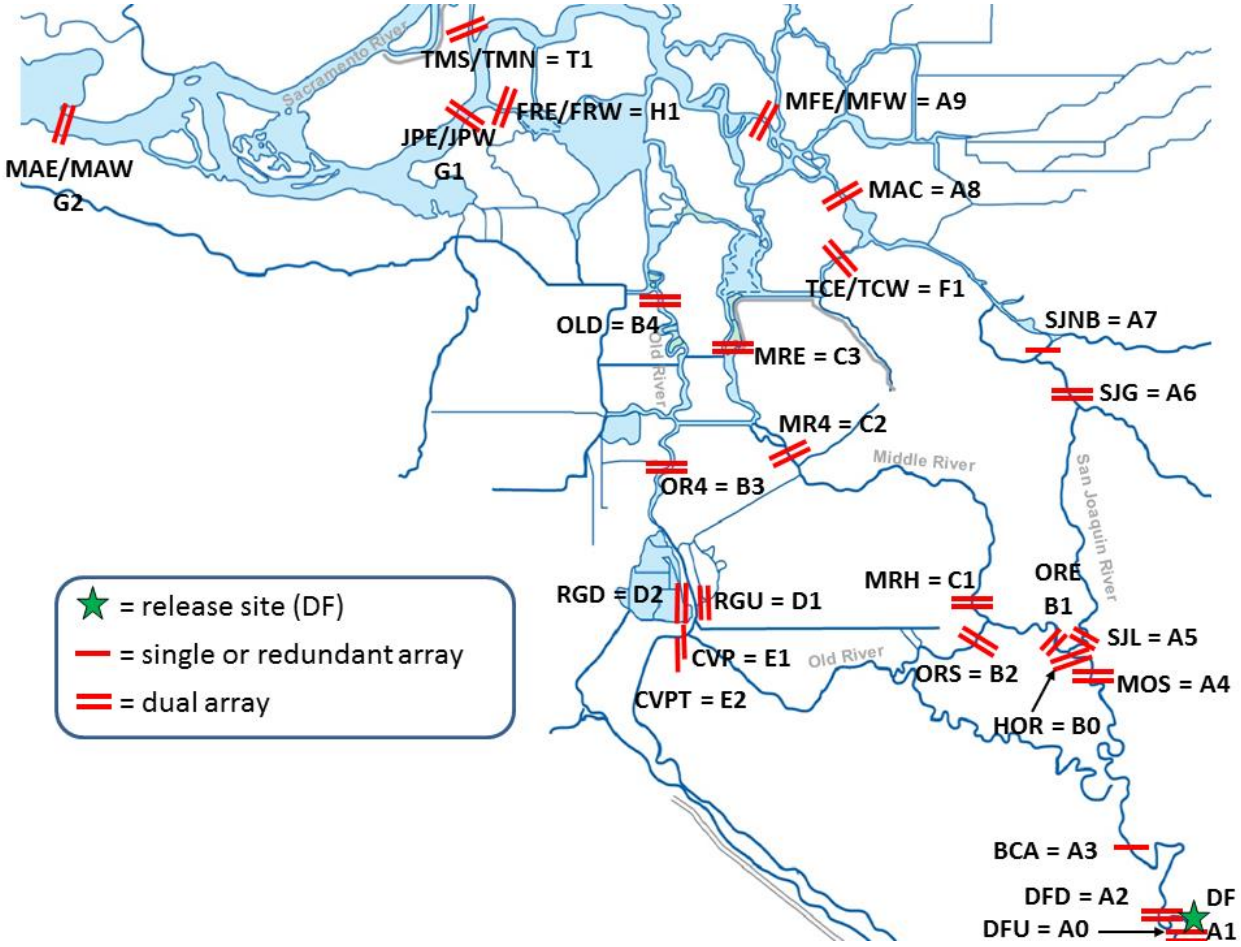

Figure 2. Locations of acoustic receivers and release site used in the 2012 Chinook Salmon study, with site code names (3- or 4-letter code) and model code (letter and number string). Site A1 is the release site at Durham Ferry. Sites B0, B4, C3, and T1 were excluded from the survival model.

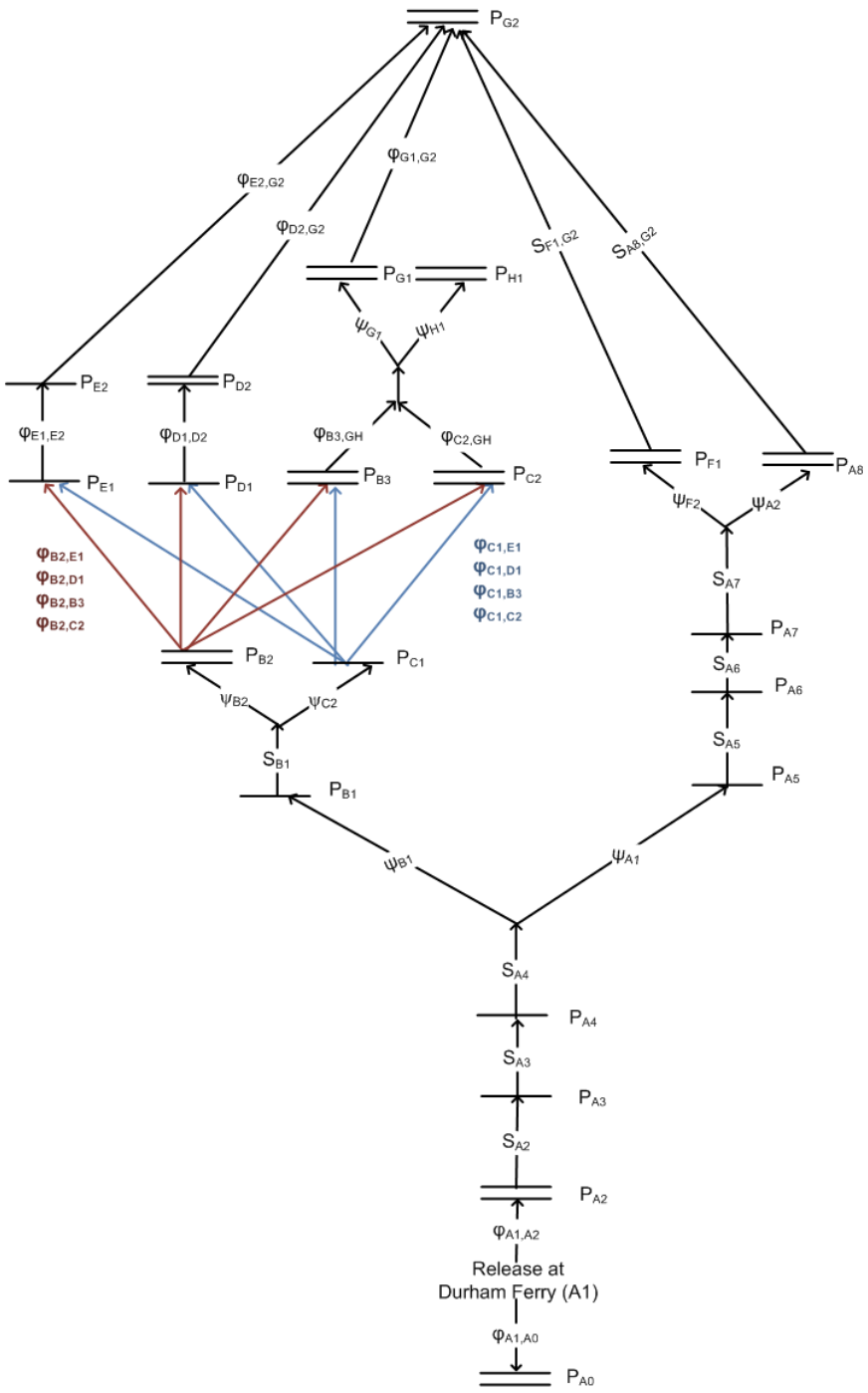

Figure 3. Schematic of 2012 mark-recapture Submodel I. Single lines denote single-array or redundant double-line telemetry stations, and double lines denote dual-array telemetry stations. Names of telemetry stations correspond to site labels in Figure 2. Migration pathways to sites B3 (OR4), C2 (MR4), D1 (RGU), and E1 (CVP) are color-coded by departure site.

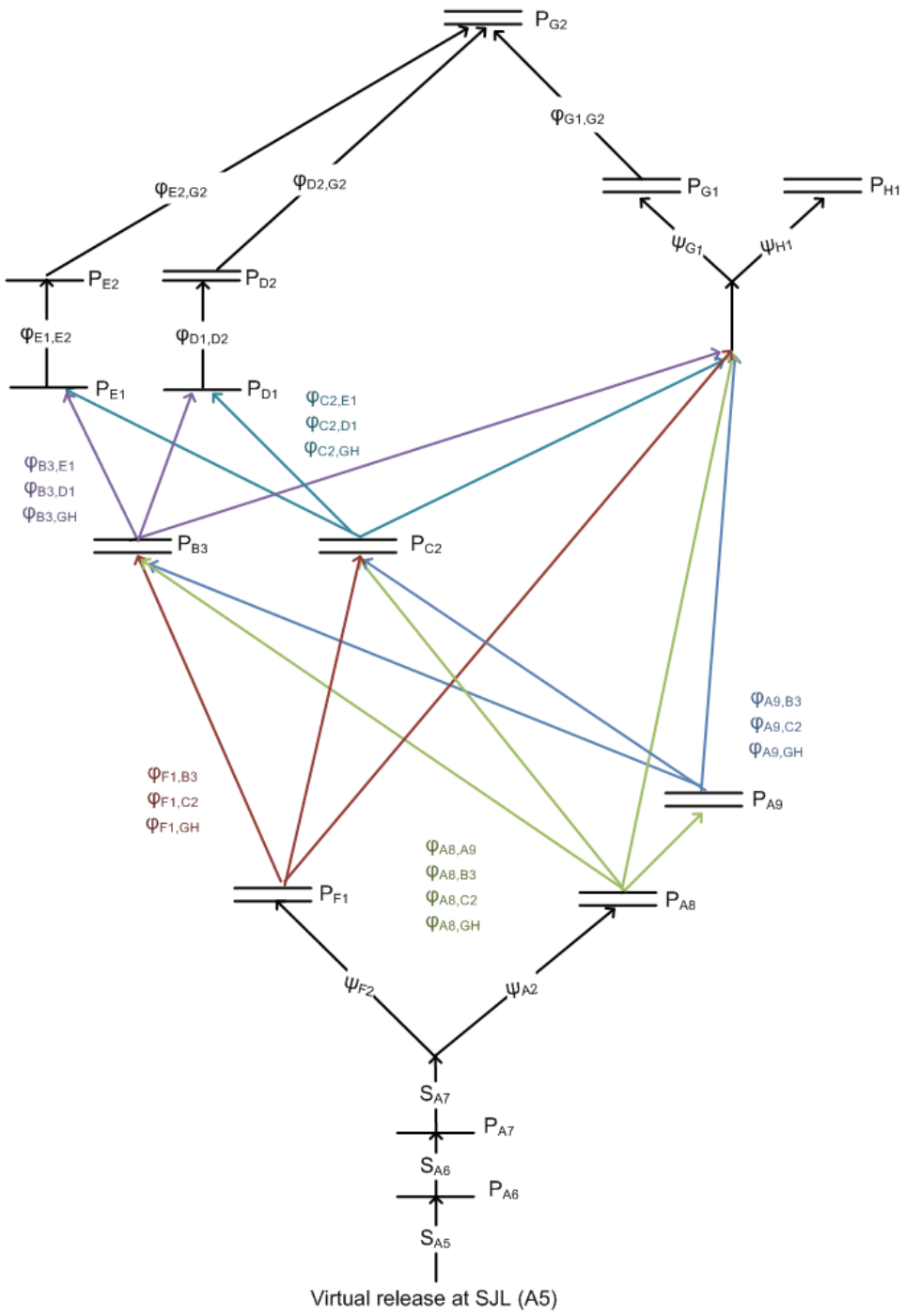

Figure 4. Schematic of 2012 mark-recapture Submodel II with estimable parameters. Single lines denote single-array or redundant double-line telemetry stations, and double lines denote dual-array telemetry stations. Names of telemetry stations correspond to site labels in Figure 2. Migration pathways to sites B3 (OR4), C2 (MR4), D1 (RGU), and E1 (CVP) are color-coded by departure site.

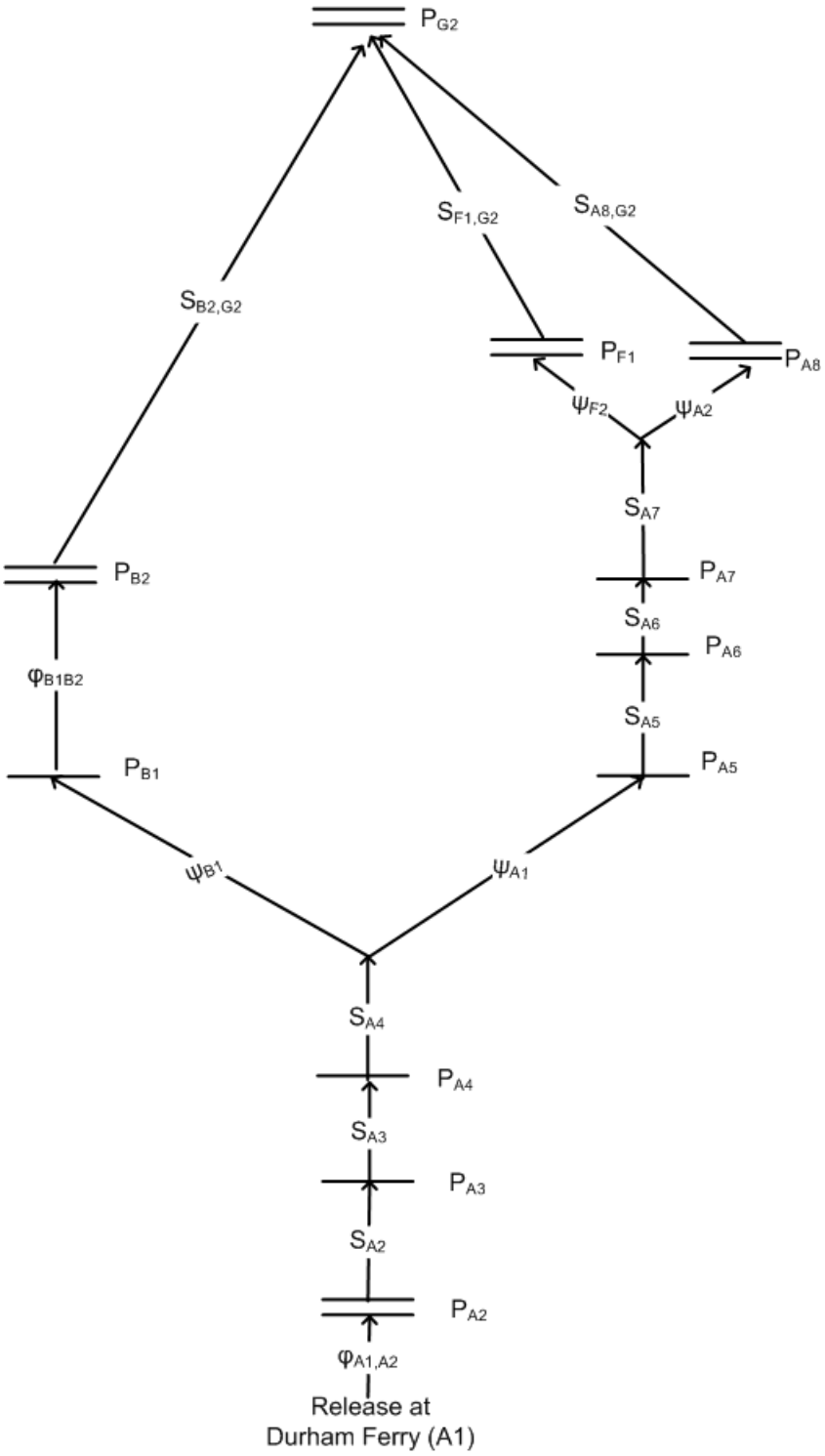

Figure 5. Schematic of reduced 2012 mark-recapture Submodel I with estimable parameters. Single lines denote single-array or redundant double-line telemetry stations, and double lines denote dual-array telemetry stations. Names of telemetry stations correspond to site labels in Figure 2.

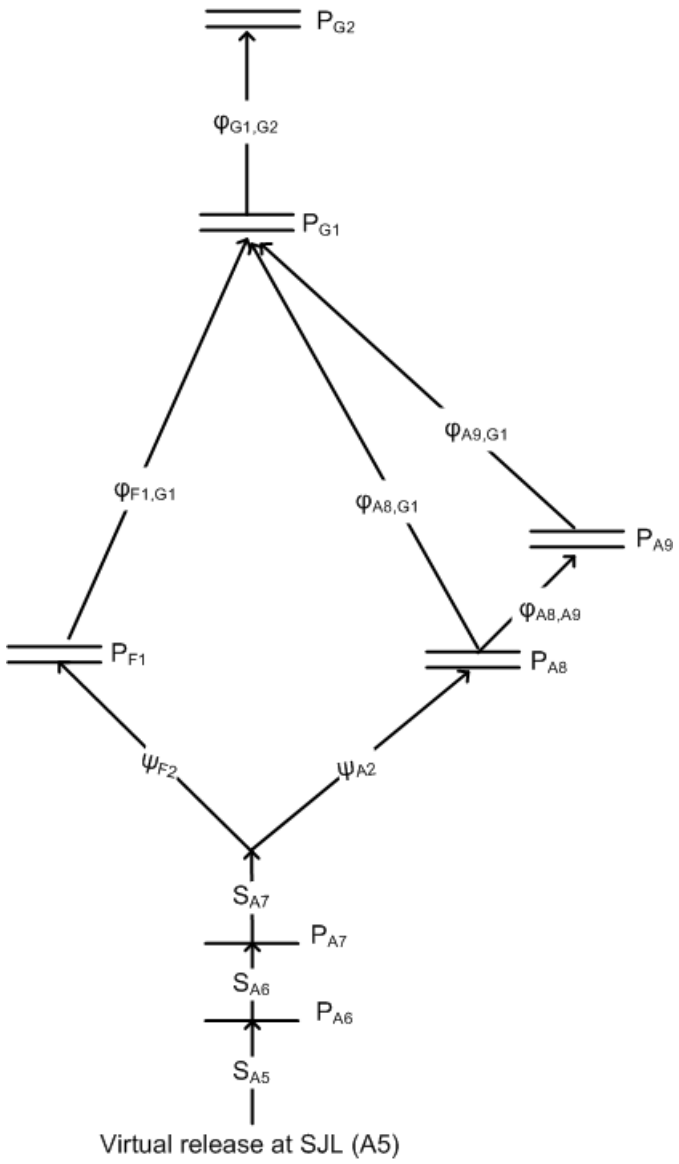

Figure 6. Schematic of reduced 2012 mark-recapture Submodel II with estimable parameters. Single lines denote single-array or redundant double-line telemetry stations, and double lines denote dual-array telemetry stations. Names of telemetry stations correspond to site labels in Figure 2.

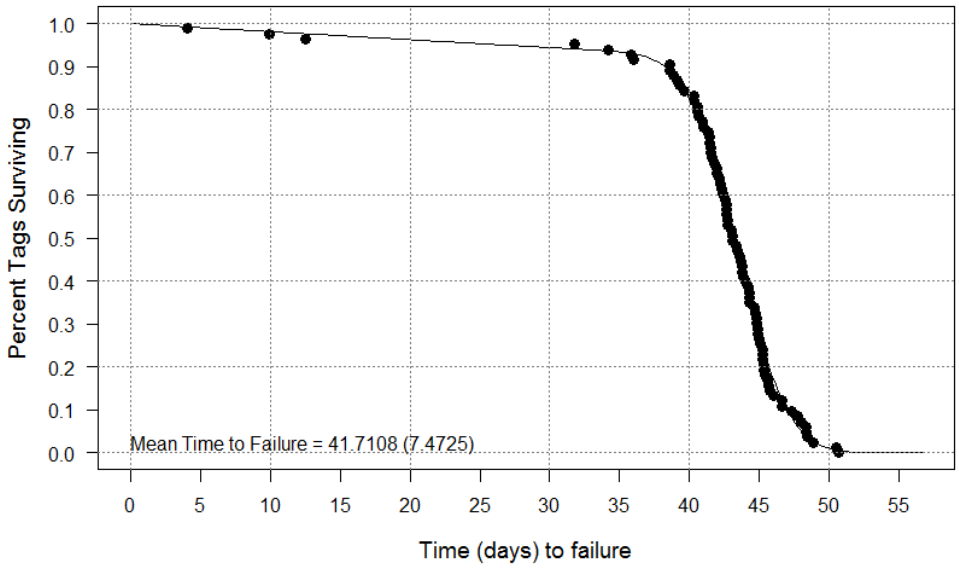

Figure 7. Observed tag failure times from the 2012 tag-life studies, pooled over the two studies, and fitted four-parameter vitality curve.

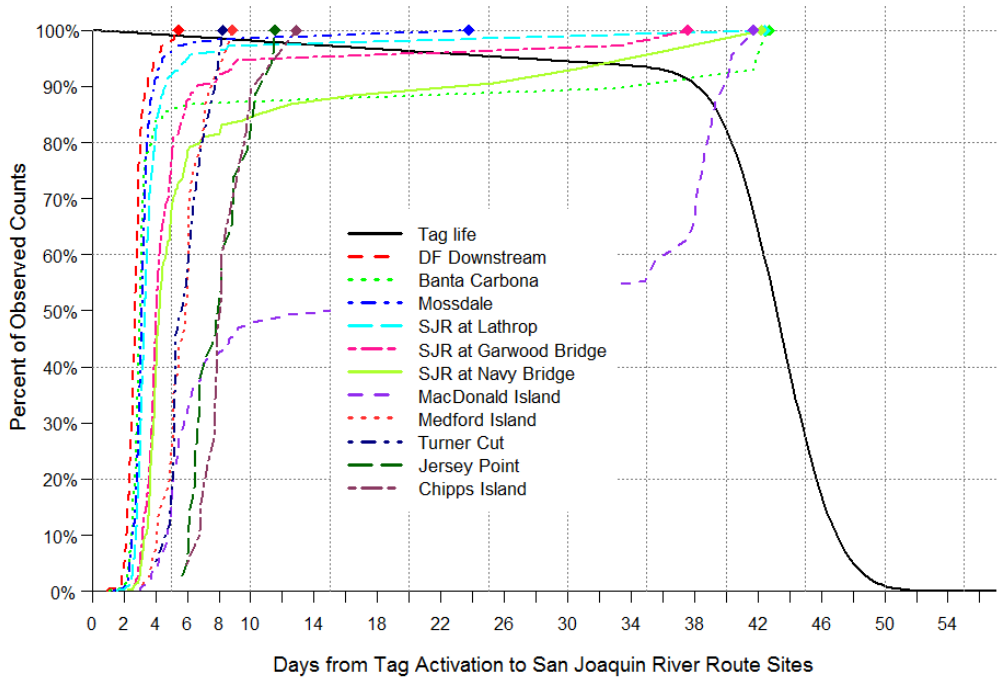

Figure 8. Four-parameter vitality survival curve for tag life, and the cumulative arrival timing of acoustic-tagged juvenile Chinook Salmon at receivers in the San Joaquin River route to Chipps Island in 2012, including detections that may have come from predators.

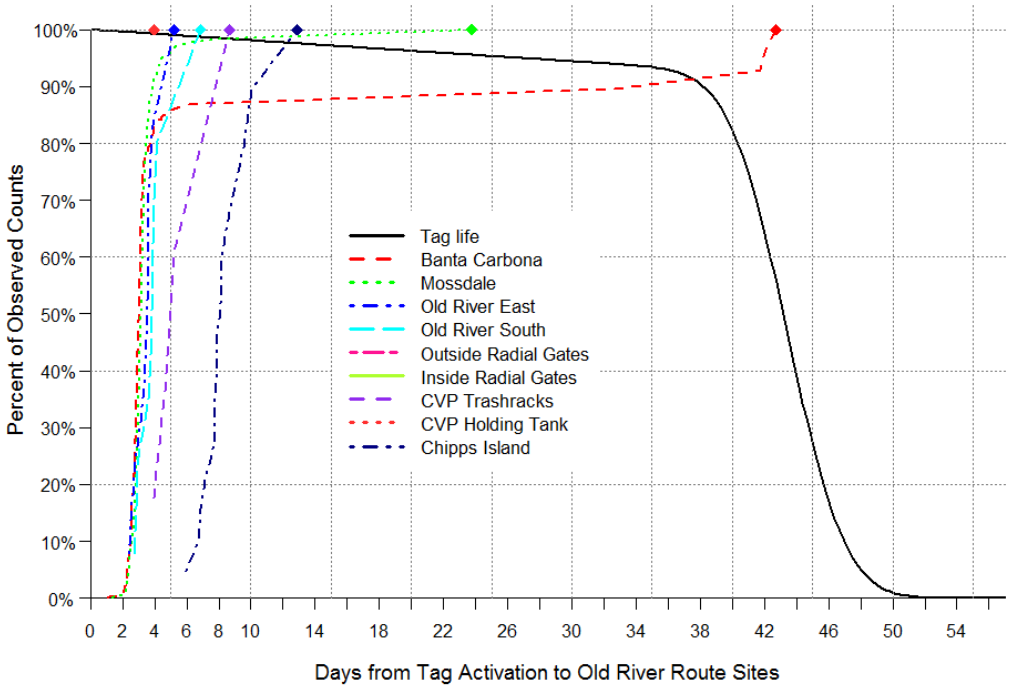

Figure 9. Four-parameter vitality survival curve for tag life, and the cumulative arrival timing of acoustic-tagged juvenile Chinook Salmon at receivers in the Old River route to Chipps Island in 2012, including detections that may have come from predators.

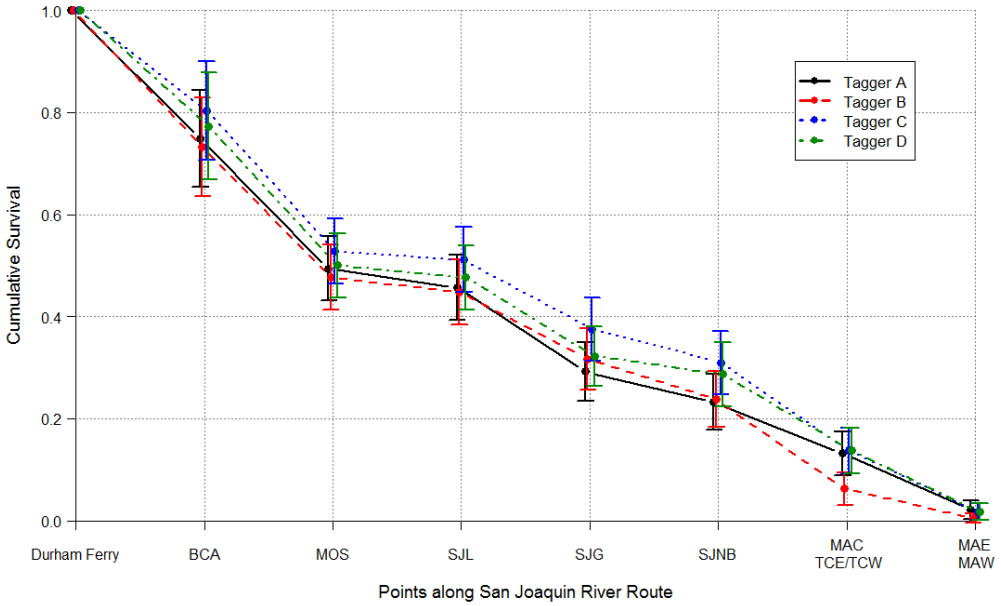

Figure 10. Cumulative survival from release at Durham Ferry to various points along the San Joaquin River route to Chipps Island, by tagger. Error bars are 95% confidence intervals.

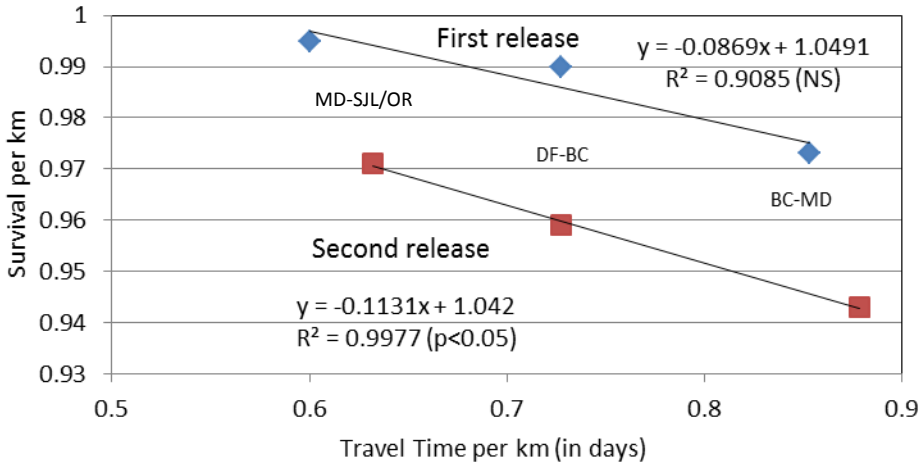

Figure 11: Travel time per km (in days) versus survival per km for river reaches, upstream of Mossdale in release group 1 and release group 2. Survival and travel time were without predator-type detections. Refer to Table 22 for data used.

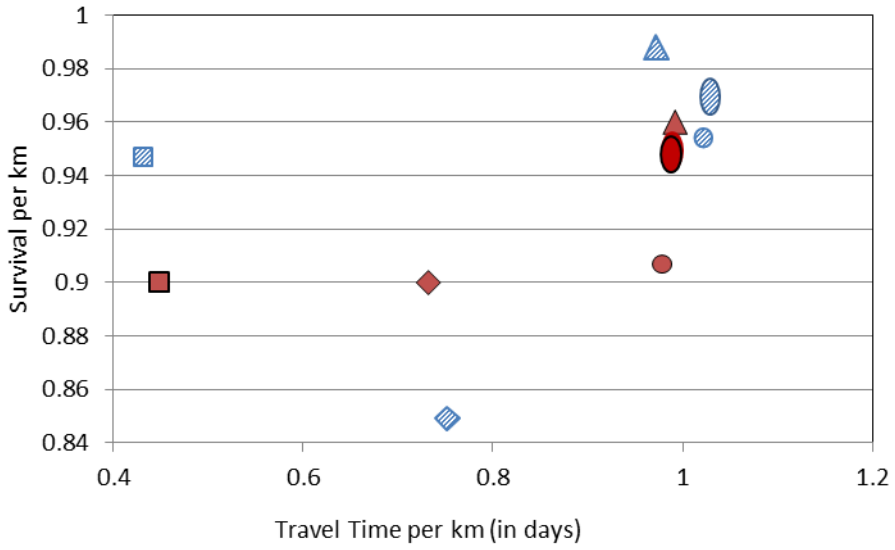

Figure 12: Travel time per km (in days) versus survival per km for reaches in the San Joaquin Delta for release group 1 (blue diagonal) and release group 2 (red solid). From Upstream to Downstream, reaches in order are: Lathrop to Garwood Bridge (triangles), Garwood Bridge to Navy Bridge Drive (squares), Navy Bridge to Turner Cut Junction (circles), MacDonald Island to Medford Island (diamonds) and Medford Island to Jersey Point (ovals). No recoveries were made at Chipps Island for the second release group to estimate travel time from Jersey Point to Chipps Island.

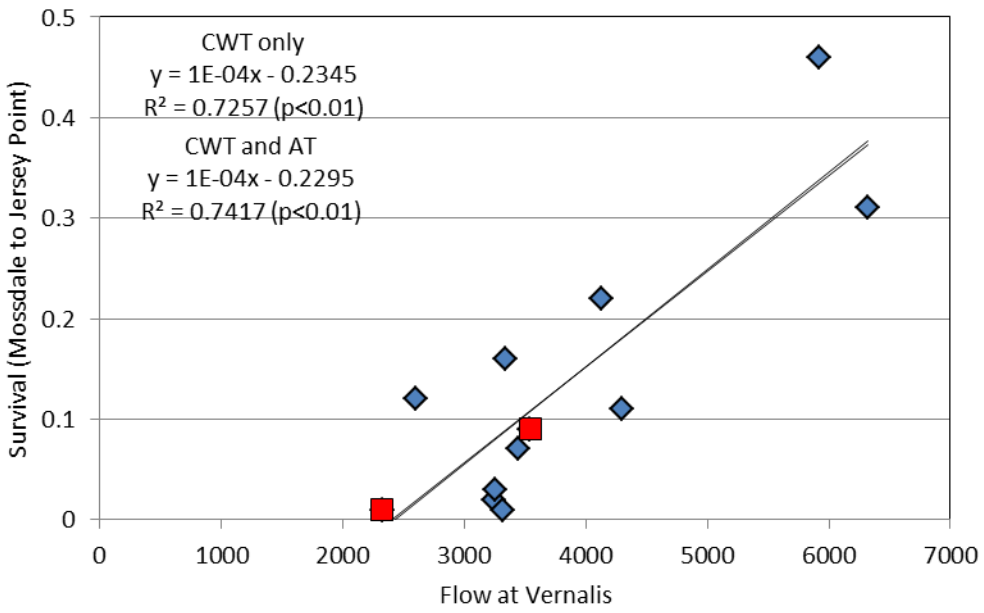

Figure 13: Estimates of survival between Mossdale and Jersey Point for CWT salmon (blue diamonds) and acoustic tag fish in 2012 (red squares) with the physical head of Old River barrier installed. Linear regression lines are plotted for both sets of data but overlap.

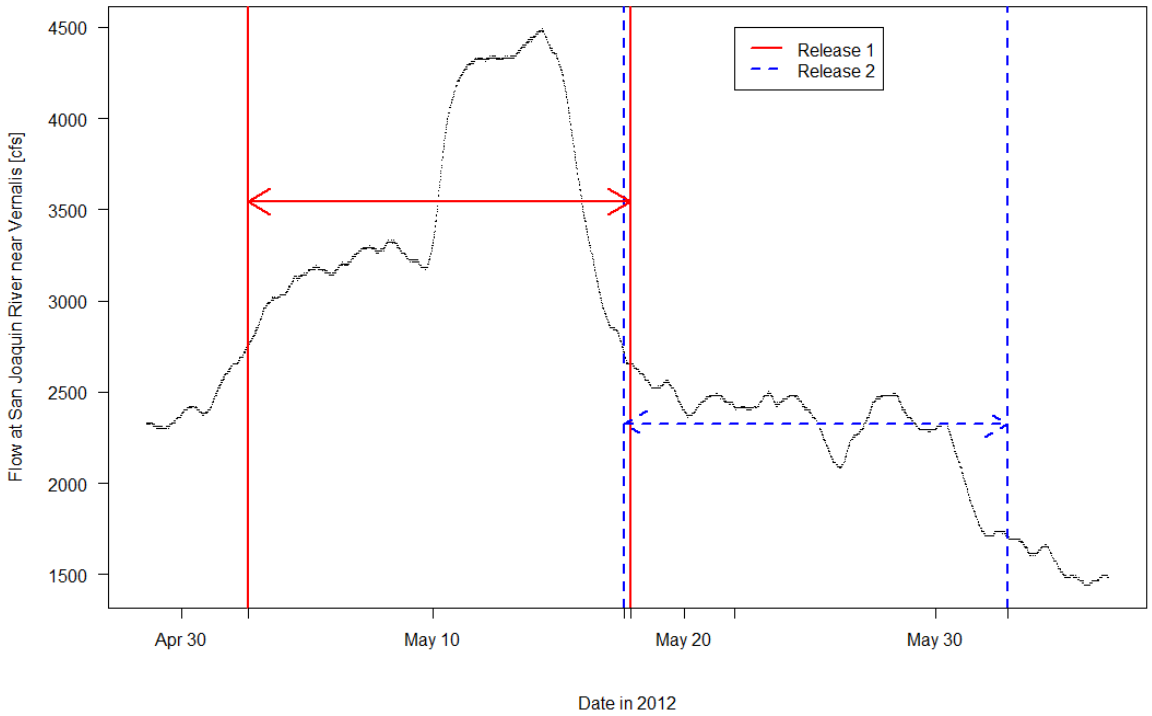

Figure 14. River discharge (flow) at Vernalis during 2012 study. Vertical lines represent expected period of travel from initial release at Durham Ferry to Chipps Island, based on release dates and maximum observed travel time over both releases. Arrow heights indicates mean flow during travel period.

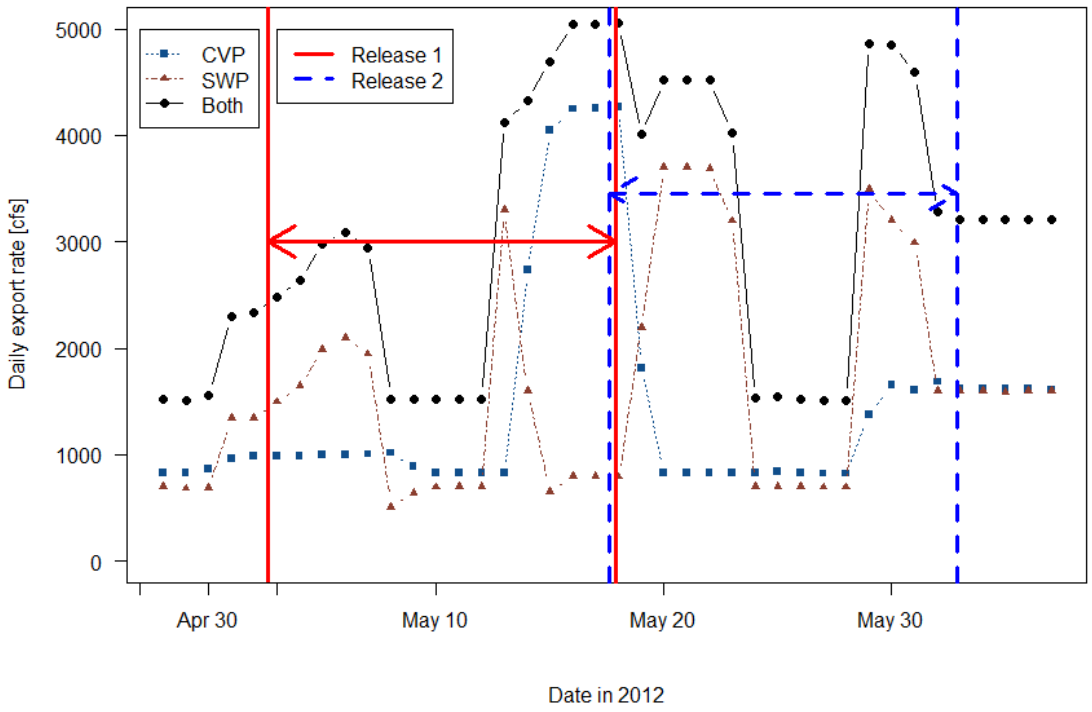

Figure 15. Daily export rate (cfs) at CVP and SWP during 2012 study. Vertical lines represent expected period of travel from initial release at Durham Ferry to Chipps Island, based on release dates and maximum observed travel time over both releases. Arrow height indicates mean combined export rate during travel period.

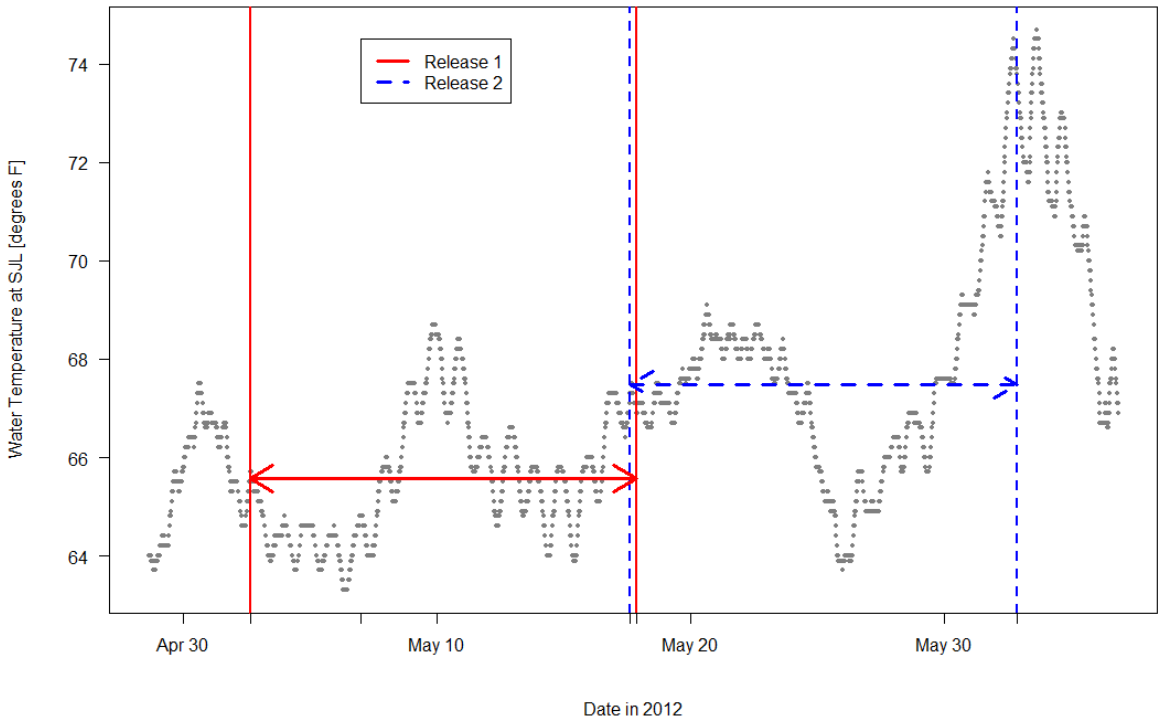

Figure 16. Temperature (°F) at the San Joaquin River gaging station near Lathrop during 2012 study. Vertical lines represent expected period of travel from initial release at Durham Ferry to Chipps Island, based on release dates and maximum observed travel time over both releases. Arrow height indicates mean temperature during travel period.

Tables

Table 1. Tagging, transport and holding date and times, and the number released (N) for Chinook Salmon as part of 2012 Chinook Salmon Study. Numbers of tagged fish use the format: [Number of Vemco-tagged fish]: [Number of HTI-tagged fish].

				Release A		Release B		Release C		Release D		Release E		Release F				
Tagging Date	Transport Date/ Time	Number trans-ported	Trans-port Tank #	Date; Time	N	Date; Time	N	Date; Time	N	Date; Time	N	Date; time	N	Date; Time	N	Dummy tagged	Start Holding Date; Time	Total released (A – F)
5/1/12	5/1/12; 1352-1435	60: 15	1	5/2; 1505, 1506	24: 6	5/2; 1900, 1901	24: 6	5/2; 2256	12: 3							6	5/1; 1538	160: 42
		20: 6	2					5/2; 2257, 2306	20: 6							1		
	5/1/12; 1850-1930	60:15	1							5/3; 0300, 0301	24: 6	5/3; 0703, 0704	36: 9			0	5/1; 2020	
		20: 6	2											5/3; 1100,	20: 6	8		
5/3/12	5/3/12; 1237-1322	60: 15	1	5/4; 1500, 1503	24: 6	5/4; 1855, 1856	24: 6	5/4; 2256	12: 3							3	5/3; 1415	160: 42
		20: 6	2					5/4; 2256, 2304	20: 6							5		
	5/3/12; 1640-1725	60: 15	1							5/5; 0300	24: 6	5/5; 0702, 0703	24: 6	5/5; 1102	12: 3	3	5/3; 1808	
		20: 6	2											5/5; 1101, 1103	20: 6	4		
5/5/12	5/5/12; 1235 - 1320	60: 15	1	5/6; 1502, 1503	24: 6	5/6; 1856; 1857	24: 6	5/6; 2255	12: 3							9	5/5; 1356	160: 42
		20: 6	2					5/6; 2254, 2255	20: 6							6		
	5/5/12; 1717 - 1756	60: 15	1							5/7; 0300,	24: 6	5/7; 0700, 0701, 0702	36: 9			5	5/5; 1839	
		20: 6	2											5/7; 1100,	20: 6	9		

Table 1: (Continued)

				Release A		Release B		Release C		Release D		Release E		Release F				
Tagging Date	Transport Date/ Time	Number trans-ported	Trans-port Tank #	Date; Time	N	Date; Time	N	Date; Time	N	Date; Time	N	Date; time	N	Date; Time	N	Dummy tagged	Start Holding Date; Time	Total released (A – F)
5/16/12	5/16; 1238 - 1323	60: 15	1	5/17; 1455, 1500	24[1]: 6	5/17; 1858, 1859[2]	24: 6	5/17; 2302	12: 3							1	5/16; 1449	160[1]: 45
		20: 8	2					5/17; 2301	20: 8							6		
	5/16; 1640 - 1731	60: 16	1							5/18; 0300	24: 6	5/18; 0700, 0701	36: 10			2	5/16; 1810	
		20: 6	2											5/18; 1100	20: 6	6		
5/18/12	5/18; 1246 - 1330	60: 16	1	5/19; 1458, 1459	24: 6	5/19; 1904, 1906	24: 6	5/19; 2259	12: 4							2	5/18; 1400	160: 46
		20: 8	2					5/19; 2258, 2259	20: 8							6		
	5/18; 1619 - 1709	60:16	1							5/19; 0303, 0305[2]	24: 6	5/19; 0700[2]	36: 10			1	5/18; 1736	
		20: 6	2											5/19; 1100[2]	20: 6	6		
5/20/12	5/20; 1206 - 1249	59: 15	1	5/21; 1505, 1506	23: 6	5/21; 1902, 1903	24: 6	5/21; 2259	12: 3							6	5/20; 1324	160: 44
		21: 8	2	5/21; 1506	1: 0			5/21; 2258, 2259	20: 8							9		
	5/20; 1557 - 1638	60: 15	1							5/22; 0300	24: 6	5/22; 0701, 0702	24: 6	5/22; 1100	12: 3	6	5/20; 1712	
		20: 6	2												20: 6	9		

[1] one tag not used in analyses; tag looked odd, [2] released from shore due to high winds or dead battery in boat.

Table 2. Characteristics assessed for Chinook Salmon smolt condition and short-term survival

Characteristic	Normal	Abnormal
Percent Scale Loss	Lower relative numbers based on 0-100%	Higher relative numbers based on 0-100%
Body Color	High contrast dark dorsal surfaces and light sides	Low contrast dorsal surfaces and coppery colored sides
Fin Hemorrhaging	No bleeding at base of fins	Blood present at base of fins
Eyes	Normally shaped	Bulging or with hemorrhaging
Gill Color	Dark beet red to cherry red colored gill filaments	Grey to light red colored gill filaments
Vigor	Active swimming (prior to anesthesia)	Lethargic or motionless (prior to anesthesia)

Table 3. Names and descriptions of receivers and hydrophones used in the 2012 Chinook Salmon tagging study, with receiver codes used in Figure 2, the survival model (Figures 2 – 5), and in data processing by the United States Geological Survey (USGS). The release site was located at Durham Ferry.

Individual Receiver Name and Description	Hydrophone Location		Receiver Code	Survival Model Code	Data Processing Code
	Latitude (°N)	Longitude (°W)			
San Joaquin River near Durham Ferry upstream of the release site, upstream node	37.685806	121.256500	DFU1	A0a	300856
San Joaquin River near Durham Ferry upstream of the release site, downstream node	37.686444	121.256806	DFU2	A0b	300857
San Joaquin River near Durham Ferry; release site (no acoustic hydrophone located here)	37.687011	121.263448	DF	A1	
San Joaquin River near Durham Ferry downstream of the release site, upstream node	37.688222	121.276139	DFD1	A2a	300858
San Joaquin River near Durham Ferry downstream of the release site, downstream node	37.688333	121.276139	DFD2	A2b	300859
San Joaquin River near Banta Carbona	37.727722	121.298917	BCA	A3	300860
San Joaquin River near Mossdale Bridge, upstream node	37.792194	121.307278	MOSU	A4a	300861
San Joaquin River near Mossdale Bridge, downstream node	37.792356	121.307369	MOSD	A4b	300862
San Joaquin River upstream of Head of Old River, upstream node (not used in survival model)	37.805528	121.320000	HORU	B0a	300863
San Joaquin River upstream of Head of Old River, downstream node (not used in survival model)	37.805000	121.321306	HORD	B0b	300864
San Joaquin River near Lathrop, upstream	37.810875[a]	121.322500[a]	SJLU	A5a	300869/300870
San Joaquin River near Lathrop, downstream	37.810807[a]	121.321269[a]	SJLD	A5b	300871/300872
San Joaquin River near Garwood Bridge, upstream	37.934972	121.329333	SJGU	A6a	300877
San Joaquin River near Garwood Bridge, downstream	37.935194	121.329833	SJGD	A6b	300878
San Joaquin River at Stockton Navy Drive Bridge	37.946806	121.339583	SJNB	A7	300879
San Joaquin River at MacDonald Island, upstream	38.018022[a]	121.462758[a]	MACU	A8a	300899/300901
San Joaquin River at MacDonald Island, downstream	38.023877[a]	121.465916[a]	MACD	A8b	300900/300902
San Joaquin River near Medford Island, east	38.053134[a]	121.510815[a]	MFE	A9a	300903/300904
San Joaquin River near Medford Island, west	38.053773[a]	121.513315[a]	MFW	A9b	300905/300906
Old River East, near junction with San Joaquin, upstream	37.811653[a]	121.335486[a]	OREU	B1a	300865/300866

a = Average latitude and longitude given for sites with multiple hydrophones or for sites with multiple locations throughout the study

Table 3. (Continued)

Individual Receiver Name and Description	Hydrophone Location		Receiver Code	Survival Model Code	Data Processing Code
	Latitude (°N)	Longitude (°W)			
Old River East, near junction with San Joaquin, downstream	37.812284[a]	121.335558[a]	ORED	B1b	300867/300868
Old River South, upstream	37.819583	121.378111	ORSU	B2a	300873
Old River South, downstream	37.820028	121.378889	ORSD	B2b	300874
Old River at Highway 4, upstream	37.893864[a]	121.567083[a]	OR4U	B3a	300882/300883
Old River at Highway 4, downstream	37.895125[a]	121.566403[a]	OR4D	B3b	300884/300885
Old River North of Empire Cut, upstream receiver (not used in survival model)	37.967125[a]	121.574514[a]	OLDU	B4a	450022
Old River North of Empire Cut, downstream receiver (not used in survival model)	37.967375[a]	121.574389[a]	OLDD	B4b	450023
Middle River Head, upstream	37.824744	121.380056	MRHU	C1a	300875
Middle River Head, downstream	37.824889	121.380417	MRHD	C1b	300876
Middle River at Highway 4, upstream	37.895750	121.493861	MR4U	C2a	300881
Middle River at Highway 4, downstream	37.896222	121.492417	MR4D	C2b	300880
Middle River at Empire Cut, upstream receiver (not used in survival model)	37.941685[a]	121.533250[a]	MREU	C3a	300898/450021
Middle River at Empire Cut, downstream receiver (not used in survival model)	37.942861[a]	121.532370[a]	MRED	C3b	300897/450030
Radial Gate at Clifton Court Forebay, upstream (in entrance channel to forebay), array 1	37.830086	121.556594	RGU1	D1a	300888
Radial Gate at Clifton Court Forebay, upstream, array 2	37.829606	121.556989	RGU2	D1b	300889
Radial Gate at Clifton Court Forebay, downstream (inside forebay), array 1 in dual array	37.830147[a]	121.557528[a]	RGD1	D2a	300890/300892/ 460009/460011
Radial Gate at Clifton Court Forebay, downstream, array 2 in dual array	37.829822[a]	121.557900[a]	RGD2	D2b	300891/460010
Central Valley Project trashracks, upstream	37.816900[a]	121.558459[a]	CVPU	E1a	300894/460012
Central Valley Project trashracks, downstream	37.816647	121.558981	CVPD	E1b	300895
Central Valley Project holding tank (all holding tanks pooled)	37.815844	121.559128	CVPtank	E2	300896
Turner Cut, east (closer to San Joaquin)	37.991694	121.455389	TCE	F1a	300887
Turner Cut, west (farther from San Joaquin)	37.990472	121.456278	TCW	F1b	300886
San Joaquin River at Jersey Point, east (upstream)	38.056351[a]	121.686535[a]	JPE	G1a	300915 - 300922
San Joaquin River at Jersey Point, west (downstream)	38.055167[a]	121.688070[a]	JPW	G1b	300923 - 300930

a = Average latitude and longitude given for sites with multiple hydrophones or for sites with multiple locations throughout the study

Table 3. (Continued)

Individual Receiver Name and Description	Hydrophone Location		Receiver Code	Survival Model Code	Data Processing Code
	Latitude (°N)	Longitude (°W)			
False River, west (closer to San Joaquin)	38.056834[a]	121.671403[a]	FRW	H1a	300913/300914
False River, east (farther from San Joaquin)	38.057118[a]	121.669673[a]	FRE	H1b	300911/300912
Chipps Island (aka Mallard Island), east (upstream)	38.048772[a]	121.931198[a]	MAE	G2a	300931 - 300942
Chipps Island (aka Mallard Island), west (downstream)	38.049275[a]	121.933839[a]	MAW	G2b	300943, 300979 - 300983, 300985 - 300990
Threemile Slough, south (not used in survival model)	38.107771[a]	121.684042[a]	TMS	T1a	300909/300910
Threemile Slough, north (not used in survival model)	38.111556[a]	121.682826[a]	TMN	T1b	300907/300908

a = Average latitude and longitude given for sites with multiple hydrophones or for sites with multiple locations throughout the study

Table 4. Environmental monitoring sites used in predator decision rule and route entrainment analysis. Database = CDEC (http://cdec.water.ca.gov/) or Water Library (http://www.water.ca.gov/waterdatalibrary/).

Environmental Monitoring Site			Detection Site	Data Available					Database
Site Name	Latitude (°N)	Longitude (°W)		River Flow	Water Velocity	River Stage	Pumping	Reservoir Inflow	
CLC	37.8298	121.5574	RGU, RGD	No	No	No	No	Yes	CDEC
FAL	38.0555	121.6672	FRE/FRW	Yes	Yes	Yes	No	No	CDEC
GLC	37.8201	121.4497	ORS	Yes	Yes	Yes	No	No	CDEC
MAL	38.0428	121.9201	MAE/MAW	No	No	Yes	No	No	CDEC
MDM	37.9425	121.534	MR4, MRE	Yes	Yes	Yes	No	No	CDEC[a]
MSD	37.7860	121.3060	HOR, MOS	Yes	Yes	Yes	No	No	Water Library
ODM	37.8101	121.5419	CVP	Yes	Yes	Yes	No	No	CDEC
OH1	37.8080	121.3290	ORE	Yes	Yes	Yes	No	No	CDEC
OH4	37.8900	121.5697	OR4	Yes	Yes	Yes	No	No	CDEC
ORI	37.8280	121.5526	RGU, RGD	Yes	Yes	No	No	No	Water Library
PRI	38.0593	121.5575	MAC, MFE/MFW	Yes	Yes	Yes	No	No	CDEC
RMID040	37.8350	121.3838	MRH	No	No	Yes	No	No	Water Library
ROLD040	37.8286	121.5531	RGU, RGD	No	No	Yes	No	No	Water Library
SJG	37.9351	121.3295	SJG, SJNB	Yes	Yes	Yes	No	No	CDEC
SJJ	38.0520	121.6891	JPE/JPW	Yes	Yes	Yes	No	No	CDEC
SJL	37.8100	121.3230	SJL	Yes	Yes	Yes	No	No	Water Library
TRN	37.9927	121.4541	TCE/TCW	Yes	Yes	Yes	No	No	CDEC
TRP	37.8165	121.5596	CVP	No	No	No	Yes	No	CDEC
TSL	38.1004	121.6866	TMS/TMN	Yes	Yes	Yes	No	No	CDEC
VNS	37.6670	121.2670	DFU, DFD, BCA	Yes	No	Yes	No	No	CDEC
WCI	37.8316	121.5541	RGU, RGD	Yes	Yes	No	No	No	Water Library

a = California Water Library was used for river stage

Table 5a. Cutoff values used in predator filter in 2012. Observed values past cutoff or unmet conditions indicate a predator. Only transitions observed in 2012 are represented here. No detections were observed at MRH, RGU, or RGD in 2012. See Table 5b for Flow, Water Velocity, Extra Conditions, and Comment. Footnotes refer to both this table and Table 5b.

Detection Site	Previous Site	Residence Time[a] (hr)		Migration Rate[b, c] (km/hr)		BLPS (Absolute value)	No. of Visits	No. of Cumulative Upstream Forays
		Near Field	Mid-field					
		Maximum	Maximum	Minimum	Maximum	Maximum	Maximum	Maximum
DFU	DF, DFD	0.5	1	0.2 (0.6[f])	4		1	1
	DFU	0.5	1				2	0
DFD	DF, DFU	4	8	0.05	4		1	0
	DFD	2	49				2	0
	BCA	2	4	0.1	4		0	0
BCA	DF, DFU	5	10	0.1	4		1	0
	BCA	0.1	168				2	0
	MOS	0.1	0.2	0.1	4		0	0
MOS	DF, DFD, BCA	10	20	0.2	5.5	8	1	0
	MOS	2	261				2	1
	HOR	1	2	0.2	5.5	8	2	1
SJL	MOS, HOR	5	15	0.2	5.5	8	2	0
	SJL	1	293				3	1
SJG	HOR, SJL	12	24	0.2	5.5	8	1	0
	SJG	6	360				1	1
	SJNB	3	6	0.2	4	8	2	2
SJNB	SJG	15 (6[f])	30 (12[f])	0.2	5.5	8	2	0
	SJNB	4	360				2	3
MAC	SJG, SJNB	30	60	0.2	5.5	8	1	0
	MAC	30	360				2	3
	MFE/MFW	15	30	0.2	4	8	2	3

a = Near-field residence time includes up to 12 hours missing between detections, while mid-field residence time includes entire time lag between first and last detections without intervening detections elsewhere

b = Approximate migration rate calculated on most direct pathway

c = Missing values for transitions to and from same site: travel times must be 12 to 24 hours, unless otherwise specified under "Extra conditions"

f = See comments for alternate criteria

Table 5a. (Continued)

Detection Site	Previous Site	Residence Time[a] (hr)		Migration Rate[b, c] (km/hr)		BLPS (Absolute value)	No. of Visits	No. of Cumulative Upstream Forays
		Near Field	Mid-field					
		Maximum	Maximum	Minimum	Maximum	Maximum	Maximum	Maximum
MFE/MFW	MAC	30	60	0.2	5.5	8	2	0
	MFE/MFW	15	360				3	3
HOR	DF, MOS	10	20	0.2	5.5	8	1 (2[f])	0
	HOR	3	288				2	1
	SJL	3 (4[f])	6 (8[f])	0.2 (0.1[f])	5.5 (6[f])	8	2	1
ORE	HOR	5	15	0.2	5.5	8	1	0
	ORE	1	287				1	0
ORS	ORE	12	24	0.2	5.5	8	1	0
	ORS	4	360				2	1
OR4	ORS	40	80	0.2	5.5	8	1	0
	MR4	40	80	0.1	5.5		2	3
	OR4	25	129				2	2
OLD	OR4	40	80	0.2	5.5	8	2	0
	MRE	40	80	0.1	5.5		1	0
MR4	MRE	10	20	0.2	5.5	8	1	2
MRE	SJNB, MAC	20	40	0.1	5.5		1	0
	TCE/TCW	20	40	0.1	5.5		1	0
CVP	DF, ORS	10	20	0.2	5.5	8	1	1
	CVP	10	390				3	3
	OR4	10	20	0.5	5.5	8	2	3
CVPtank	CVP	20	360				2	3

a = Near-field residence time includes up to 12 hours missing between detections, while mid-field residence time includes entire time lag between first and last detections without intervening detections elsewhere

b = Approximate migration rate calculated on most direct pathway

c = Missing values for transitions to and from same site: travel times must be 12 to 24 hours, unless otherwise specified under "Extra conditions"

f = See comments for alternate criteria

Table 5a. (Continued)

Detection Site	Previous Site	Residence Time[a] (hr)		Migration Rate[b, c] (km/hr)		BLPS (Absolute value)	No. of Visits	No. of Cumulative Upstream Forays
		Near Field	Mid-field					
		Maximum	Maximum	Minimum	Maximum	Maximum	Maximum	Maximum
TCE/TCW	SJG, SJNB	12	24	0.2	5.5	8	1	0
	MAC	12	24	0.2	5.5	8	2	3
	TCE/TCW	3	360				1	3
JPE/JPW	MAC, MFE/MFW, TMN/TMS	40	80	0.1	5.5	8	1	0
	FRE/FRW	30	360	0.1	5.5		3	3
	JPE/JPW	30	360				3	0
MAE/MAW	MFE/MFW, CVPtank	40	80	0.1	5.5	8	1	0
	TMN/TMS, JPE/JPW, FRE/FRW	40	80	0.1	5.5	8	2	0
FRE/FRW	MAC, MFE/MFW, OLD	40	80	0.1	5.5	8	1	0
	JPE/JPW	30	360	0.1			3	3
TMN/TMS	MAC, MFE/MFW	10	20	0.2	3	8	1	0
	JPE/JPW	10	20	0.5	3	8	1	3

a = Near-field residence time includes up to 12 hours missing between detections, while mid-field residence time includes entire time lag between first and last detections without intervening detections elsewhere

b = Approximate migration rate calculated on most direct pathway

c = Missing values for transitions to and from same site: travel times must be 12 to 24 hours, unless otherwise specified under "Extra conditions"

Table 5b. Cutoff values used in predator filter in 2012. Observed values past cutoff or unmet conditions indicate a predator. Only transitions observed in 2012 are represented here. No detections were observed at MRH, RGU, or RGD in 2012. Footnotes, Extra Conditions and Comment refer to both this table and Table 5a.

Detection Site	Previous Site	Flow[d] (cfs)		Water Velocity[d] (ft/sec)			Extra Conditions	Comment
		At arrival	At departure[e]	At arrival	At departure[e]	Average during transition		
DFU	DF, DFD							Alternate value if coming from DFD
	DFU						Not allowed	
DFD	DF, DFU							
	DFD						Not allowed	
	BCA						Not allowed	
BCA	DF, DFU							
	BCA						Travel time < 25	
	MOS						Not allowed	
MOS	DF, DFD, BCA							
	MOS						Travel time < 20	
	HOR					< 0.1		
SJL	MOS, HOR							
	SJL						Travel time < 20	
SJG	HOR, SJL							
	SJG							
	SJNB	< 1700	< 4000	< 0.5	< 1	< 0.5	Change in river stage at arrival: -0.1 to 0.1	
SJNB	SJG			< 2 (> 2[f])				Alternate values for change in river stage at arrival: < -0.1 or > 0.1
	SJNB	< 600 (> -250)[g]	> -250 (< 600)[g]	< 0.2 (> -0.1)[g]	> -0.1 (< 0.2)[g]	< 1.5		
MAC	SJG, SJNB							
	MAC			< 0.2 (> -0.1)[g]	> -0.1 (< 0.2)[g]			

d = Classified as predator if flow or velocity condition, if any, is violated
e = Condition at departure from previous site
f = See comments for alternate criteria
g = High flow/velocity on departure requires low values on arrival (and vice versa)

Table 5b. (Continued)

Detection Site	Previous Site	Flow[d] (cfs)		Water Velocity[d] (ft/sec)			Extra Conditions	Comment
		At arrival	At departure[e]	At arrival	At departure[e]	Average during transition		
MAC	MFE/MFW			< -0.4	< 0.2	< 0.2		
MFE/MFW	MAC							
	MFE/MFW			< 0.2 (> -0.1)[g]	> -0.1 (< 0.2)[g]			
	SJG	<100 (>-300)[g]	>-300 (<100)[g]	<0.1 (>-0.5)[g]	>-0.5 (<0.1)[g]	<0.5		
HOR	DF, MOS							Alternate value if coming from MOS
	HOR						Travel time < 20	
	SJL			< 1.5	< 0.15 (0.25[f])	< 1 (1.1[f])		Alternate value if next transition is downstream
ORE	HOR							
	ORE						Not allowed	
ORS	ORE	> -2500		> -0.5				
	ORS	< 2500 (> -2500)[g]	> -2500 (< 2500)[g]	< 0.5 (> -0.5)[g]	> -0.5 (< 0.5)[g]			
OR4	ORS	> -700		> -0.3				
	MR4							
	OR4	< 700 (> -700)[g]	> -700 (< 700)[g]	< 0.3 (> -0.3)[g]	> -0.3 (< 0.3)[g]			
OLD	OR4	> -2000	> -1000	> -0.1	> -0.05			
	MRE							
MR4	MRE	< 2500	< 1000	< 0.25	< 0.1	< 0.1		
MRE	SJNB, MAC	< 1000		< 0.1				
	TCE/TCW	< 1000	< 200	< 0.1	< 0.05			

d = Classified as predator if flow or velocity condition, if any, is violated

e = Condition at departure from previous site

f = See comments for alternate criteria

g = High flow/velocity on departure requires low values on arrival (and vice versa)

Table 5b. (Continued)

Detection Site	Previous Site	Flow[d] (cfs) At arrival	Flow[d] (cfs) At departure[e]	Water Velocity[d] (ft/sec) At arrival	Water Velocity[d] (ft/sec) At departure[e]	Water Velocity[d] (ft/sec) Average during transition	Extra Conditions	Comment
CVP	DF, ORS							
	CVP						CVP pumping > 1500 cfs on arrival, < 1500 cfs on departure	
	OR4	< 3000	< 2000	< 1.5	< 0.8	< 0.1	CVP pumping > 1500 cfs on arrival	
CVPtank	CVP						Travel time < 100	
TCE/TCW	SJG, SJNB	< 1200		< 0.2				
	MAC	< 1200		< 0.2	< 0.2	< 0.2		
	TCE/TCW	< 500 (> 500)[g]	> 500 (< 500)[g]	< 0.1 (> 0.1)[g]	> 0.1 (< 0.1)[g]	-0.2 to 0.2	Travel time < 13	
JPE/JPW	MAC, MFE/MFW, TMN/TMS FRE/FRW							
	JPE/JPW						Travel time < 50	
MAE/MAW	MFE/MFW, CVPtank			> -2.5				
	TMN/TMS, JPE/JPW, FRE/FRW			> -2.5				
FRE/FRW	MAC, MFE/MFW, OLD							
FRE/FRW	MAC, MFE/MFW, OLD JPE/JPW							
TMN/TMS	MAC, MFE/MFW JPE/JPW				> -0.4			

d = Classified as predator if flow or velocity condition, if any, is violated

e = Condition at departure from previous site

g = High flow/velocity on departure requires low values on arrival (and vice versa)

Table 6: Water temperature and dissolved oxygen in the transport tank after loading prior to transport, after transport, and in the river at Durham Ferry release site, just prior to placing fish in holding containers; the number of mortalities after transport and prior to release.

		Tank #1						Tank #2								
Transport			After loading		After transport				After loading		After transport			River		
Date	Loading time	Ice Added	Temp (˚C)	DO (mg/L)	Temp (˚C)	DO (mg/L)	# morts after transport	Ice Added	Temp (˚C)	DO (mg/L)	Temp (˚C)	DO (mg/L)	# morts after transport	Temp (˚C)	DO (mg/L)	Mortalities just prior to release
5/1/2012	1331	Yes	18.4	8.73	18.5	11.7	0	Yes	18.6	8.22	18.5	9.94	0	19.3	10.54	0
5/1/2012	1810	No	16.8	9.68	16.5	9.83	0	No	17.1	8.57	16.7	9.12	0	18.8	10.91	0
5/3/2012	1219	No	18.8	9.64	19.1	9.76	0	No	18.5	9.07	18.7	9.41	0	18.0	9.22	0
5/3/2012	1616	Yes	18.2	10.04	18.1	10.67	0	Yes	18.1	10.01	17.8	10.22	0	18.4	9.55	0
5/5/2012	1208	Yes	18.9	10.44	19.1	11.76	0	Yes	18.9	10.23	18.8	10.57	0	17.5	9.66	0
5/5/2012	1652	Yes	18.4	10.36	18.5	11.89	0	Yes	18.3	10.47	18.1	10.63	0	18.0	10.14	0
													Average	18.3		
5/16/2012	1222	Yes	19.3	9.37	19.7	9.38	0	Yes	19.4	9.46	19.7	9.42	0	19.1	11.45	0
5/16/2012	1617	Yes	19.4	9.35	19.7	10.25	0	Yes	19.5	9.38	19.5	9.51	0	19.9	9.59	0
5/18/2012	1228	Yes	19.0	9.71	19.8	10.86	0	Yes	18.9	9.64	19.3	9.74	0	19.0	8.4	0
5/18/2012	1556	Yes	19.5	9.66	19.6	10.74	0	Yes	19.6	9.67	19.8	9.73	0	19.8	8.56	0
5/20/2012	1143	Yes	19.4	10.05	19.6	10.97	0	Yes	19.0	9.67	19.3	9.81	0	19.6	9.40	0
5/20/2012	1537	Yes	20.0	10.16	20.3	11.38	0	Yes	20.3	9.61	20.5	9.84	0	20.7	10.38	0
													Average	19.7		

Table 7. Results of dummy tagged Chinook Salmon evaluated after being held for 48 hours at the release sites as part of the 2012 Chinook Salmon Study.

Holding Site	Examination Date, Time	Mean (sd) Fork Length (mm)	Mortality	Mean (sd) Scale Loss %	Normal Body Color	No Fin Hemorrhaging	Normal Eye Quality	Normal Gill Color
Durham Ferry	5/3/12, 1100	108.2 (5.6)	0/15	5.5 (2.9)	15/15	15/15	15/15	15/15
Durham Ferry	5/5/12, 1100	108.3 (3.7)	0/15	3.3 (1.0)	15/15	15/15	15/15	15/15
Durham Ferry	5/18/12, 1100	111.3 (5.4)	0/15	2.3 (1.0)	15/15	15/15	15/15	15/15
Durham Ferry	5/20/12, 1100	112.0 (4.8)	0/15	2.7 (1.5)	15/15	15/15	15/15	12/15

Table 8. Number of tags from each release group that were detected after release in 2012, including predator-type detections and detections omitted from the survival analysis.

Release Group	1	2	Total
Number Released	480	479	959
Number Detected	355	358	713
Number Detected Downstream	354	353	707
Number Detected Upstream of Study Area	196	339	535
Number Detected in Study Area	301	181	482
Number Detected in San Joaquin River Route	288	161	449
Number Detected in Old River Route	8	3	11
Number Assigned to San Joaquin River Route	286	160	446
Number Assigned to Old River Route	7	3	10

Table 9. Number of tags observed from each release group at each detection site in 2012, including predator-type detections. Routes (SJR = San Joaquin River, OR = Old River) represent route assignment at the head of Old River. Pooled counts are summed over all receivers in array and all routes. Route could not be identified for some tags.

Detection Site	Site Code	Survival Model Code	Release Group		Total
			1	2	
Release site at Durham Ferry			480	479	959
Durham Ferry Upstream	DFU	A0	1	10	11
Durham Ferry Downstream	DFD	A2	101	168	269
Banta Carbona	BCA	A3	120	244	364
Mossdale	MOS	A4	299	181	480
Head of Old River	HOR	B0	297	172	469
Lathrop	SJL	A5	288	161	449
Garwood Bridge	SJG	A6	232	78	310
Navy Drive Bridge	SJNB	A7	187	54	241
MacDonald Island Upstream	MACU	A8a	88	12	100
MacDonald Island Downstream	MACD	A8b	84	9	93
MacDonald Island (Pooled)	MAC	A8	88	12	100
Medford Island East	MFE	A9a	41	6	47
Medford Island West	MFW	A9b	41	6	47
Medford Island (Pooled)	MFE/MFW	A9	41	6	47
Turner Cut East	TCE	F1a	10	2	12
Turner Cut West	TCW	F1b	8	2	10
Turner Cut (Pooled)	TCE/TCW	F1	11	2	13
Old River East	ORE	B1	6	3	9
Old River South Upstream	ORSU	B2a	6	3	9
Old River South Downstream	ORSD	B2b	5	0	5
Old River South (Pooled)	ORS	B2	6	3	9
Old River at Highway 4, Upstream	OR4U	B3a	2	0	2
Old River at Highway 4, Downstream	OR4D	B3b	2	0	2
Old River at Highway 4, SJR Route	OR4	B3	1	0	1
Old River at Highway 4, OR Route	OR4	B3	1	0	1
Old River at Highway 4 (Pooled)	OR4	B3	2	0	2
Old River near Empire Cut, Upstream	OLDU	B4a	2	0	2
Old River near Empire Cut, Downstream	OLDD	B4b	0	0	0
Old River near Empire Cut, SJR Route	OLD	B4	1	0	1
Old River near Empire Cut, OR Route	OLD	B4	1	0	1
Old River near Empire Cut (Pooled)	OLD	B4	2	0	2
Middle River Head	MRH	C1	0	0	0
Middle River at Highway 4, Upstream	MR4U	C2a	1	0	1
Middle River at Highway 4, Downstream	MR4D	C2b	1	0	1
Middle River at Highway 4, SJR Route	MR4	C2	1	0	1
Middle River at Highway 4, OR Route	MR4	C2	0	0	0
Middle River at Highway 4 (Pooled)	MR4	C2	1	0	1

Table 9. (Continued)

Detection Site	Site Code	Survival Model Code	Release Group 1	Release Group 2	Total
Middle River near Empire Cut, Upstream	MREU	C3a	3	0	3
Middle River near Empire Cut, Downstream	MRED	C3b	3	0	3
Middle River near Empire Cut, SJR Route	MRE	C3	3	0	3
Middle River near Empire Cut, OR Route	MRE	C3	0	0	0
Middle River near Empire Cut (Pooled)	MRE	C3	3	0	3
Radial Gates Upstream (Pooled)	RGU	D1	0	0	0
Radial Gates Downstream (Pooled)	RGD	D2	0	0	0
Central Valley Project Trashrack	CVP	E1	4	1	5
CVP Trashrack: SJR Route	CVP	E1	1	0	1
CVP Trashrack: OR Route	CVP	E1	3	1	4
Central Valley Project Holding Tank	CVPtank	E2	1	0	1
CVP tank: SJR Route	CVPtank	E2	0	0	0
CVP tank: OR Route	CVPtank	E2	1	0	1
Threemile Slough South	TMS	T1a	6	0	6
Threemile Slough North	TMN	T1b	4	0	4
Threemile Slough (Pooled)	TMS/TMN	T1	6	0	6
Jersey Point East	JPE	G1a	26	2	28
Jersey Point West	JPW	G1b	25	2	27
Jersey Point: SJR Route	JPE/JPW	G1	26	2	28
Jersey Point: OR Route	JPE/JPW	G1	0	0	0
Jersey Point (Pooled)	JPE/JPW	G1	26	2	28
False River West	FRW	H1a	7	0	7
False River East	FRE	H1b	6	0	6
False River: SJR Route	FRE/FRW	H1	7	0	7
False River: OR Route	FRE/FRW	H1	0	0	0
False River (Pooled)	FRE/FRW	H1	7	0	7
Chipps Island East	MAE	G2a	15	0	15
Chipps Island West	MAW	G2b	15	0	15
Chipps Island: SJR Route	MAE/MAW	G2	14	0	14
Chipps Island: OR Route	MAE/MAW	G2	1	0	1
Chipps Island (Pooled)	MAE/MAW	G2	15	0	15

Table 10. Number of tags observed from each release group at each detection site in 2012 and used in the survival analysis, including predator-type detections. Pooled counts are summed over all receivers in array. Route could not be identified for some tags. * = site was included in full survival model but omitted from reduced model used for analysis.

Detection Site	Site Code	Survival Model Code	Release Group		Total
			1	2	
Release site at Durham Ferry			480	479	959
Durham Ferry Upstream*	DFU	A0	1	7	8
Durham Ferry Downstream	DFD	A2	101	166	267
Banta Carbona	BCA	A3	120	243	363
Mossdale	MOS	A4	297	181	478
Lathrop	SJL	A5	286	160	446
Garwood Bridge	SJG	A6	232	78	310
Navy Drive Bridge	SJNB	A7	186	53	239
MacDonald Island Upstream	MACU	A8a	80	11	91
MacDonald Island Downstream	MACD	A8b	74	8	82
MacDonald Island (Pooled)	MAC	A8	86	12	98
Medford Island East	MFE	A9a	38	6	44
Medford Island West	MFW	A9b	38	6	44
Medford Island (Pooled)	MFE/MFW	A9	38	6	44
Turner Cut East	TCE	F1a	10	2	12
Turner Cut West	TCW	F1b	7	2	9
Turner Cut (Pooled)	TCE/TCW	F1	11	2	13
Old River East	ORE	B1	6	3	9
Old River South Upstream	ORSU	B2a	6	3	9
Old River South Downstream	ORSD	B2b	5	0	5
Old River South (Pooled)	ORS	B2	6	3	9
Old River at Highway 4, Upstream*	OR4U	B3a	2	0	2
Old River at Highway 4, Downstream*	OR4D	B3b	2	0	2
Old River at Highway 4, SJR Route*	OR4	B3	1	0	1
Old River at Highway 4, OR Route*	OR4	B3	1	0	1
Old River at Highway 4 (Pooled)*	OR4	B3	2	0	2
Middle River Head*	MRH	C1	0	0	0
Middle River at Highway 4, Upstream*	MR4U	C2a	0	0	0
Middle River at Highway 4, Downstream*	MR4D	C2b	0	0	0
Middle River at Highway 4, SJR Route*	MR4	C2	0	0	0
Middle River at Highway 4, OR Route*	MR4	C2	0	0	0
Middle River at Highway 4 (Pooled)*	MR4	C2	0	0	0
Radial Gates Upstream (Pooled)*	RGU	D1	0	0	0
Radial Gates Downstream (Pooled)*	RGD	D2	0	0	0
Central Valley Project Trashrack*	CVP	E1	4	1	5
CVP Trashrack: SJR Route*	CVP	E1	1	0	1
CVP Trashrack: OR Route*	CVP	E1	3	1	4

Table 10. (Continued)

Detection Site	Site Code	Survival Model Code	Release Group 1	Release Group 2	Total
Central Valley Project Holding Tank*	CVPtank	E2	1	0	1
CVP tank: SJR Route*	CVPtank	E2	0	0	0
CVP tank: OR Route*	CVPtank	E2	1	0	1
Jersey Point East	JPE	G1a	24	2	26
Jersey Point West	JPW	G1b	23	2	25
Jersey Point: SJR Route	JPE/JPW	G1	24	2	26
Jersey Point: OR Route	JPE/JPW	G1	0	0	0
Jersey Point (Pooled)	JPE/JPW	G1	24	2	26
False River West	FRW	H1a	0	0	0
False River East	FRE	H1b	0	0	0
False River: SJR Route	FRE/FRW	H1	0	0	0
False River: OR Route	FRE/FRW	H1	0	0	0
False River (Pooled)	FRE/FRW	H1	0	0	0
Chipps Island East	MAE	G2a	15	0	15
Chipps Island West	MAW	G2b	15	0	15
Chipps Island: SJR Route	MAE/MAW	G2	14	0	14
Chipps Island: OR Route	MAE/MAW	G2	1	0	1
Chipps Island (Pooled)	MAE/MAW	G2	15	0	15

Table 11. Number of tags from each release group in 2012 first classified as in a predator at each detection site, based on the predator filter.

Detection Site and Code			Durham Ferry Release Groups					
			Classified as Predator on Arrival at Site			Classified as Predator on Departure from Site		
Detection Site	Site Code	Survival Model Code	1	2	Total	1	2	Total
Durham Ferry Upstream	DFU	A0	0	8	8	0	0	0
Durham Ferry Downstream	DFD	A2	4	7	11	0	10	10
Banta Carbona	BCA	A3	0	2	2	1	4	5
Mossdale	MOS	A4	1	2	3	0	3	3
Head of Old River	HOR	B0	1	4	5	0	1	1
Lathrop	SJL	A5	1	1	2	6	6	12
Garwood Bridge	SJG	A6	3	1	4	9	5	14
Navy Drive Bridge	SJNB	A7	1	2	3	11	9	20
MacDonald Island	MAC	A8	2	1	3	15	0	15
Medford Island	MFE/MFW	A9	0	0	0	0	0	0
Old River East	ORE	B1	0	1	1	0	0	0
Old River South	ORS	B2	0	0	0	0	1	1
Old River at Highway 4	OR4	B3	0	0	0	0	0	0
Old River near Empire Cut	OLD	B4	1	0	1	0	0	0
Middle River Head	MRH	C1	0	0	0	0	0	0
Middle River at Highway 4	MR4	C2	0	0	0	0	0	0
Middle River near Empire Cut	MRE	C3	0	0	0	0	0	0
Radial Gates Upstream	RGU	D1	0	0	0	0	0	0
Radial Gates Downstream	RGD	D2	0	0	0	0	0	0
Central Valley Project Trashrack	CVP	E1	0	0	0	0	1	1
Central Valley Project Holding Tank	CVPtank	E2	0	0	0	0	0	0
Turner Cut	TCE/TCW	F1	3	0	3	2	0	2
Jersey Point	JPE/JPW	G1	0	0	0	0	0	0
Chipps Island	MAE/MAW	G2	0	0	0	0	0	0
False River	FRE/FRW	H1	0	0	0	0	0	0
Threemile Slough	TMS/TMN	T1	0	0	0	0	0	0
Total Tags			17	29	46	44	40	84

Table 12. Number of tags from each release group that were detected after release in 2012, excluding predator-type detections, and including detections omitted from the survival analysis.

Release Group	1	2	Total
Number Released	480	479	959
Total Number Detected	351	346	697
Total Number Detected Downstream	350	345	695
Total Number Detected Upstream of Study Area	191	327	518
Total Number Detected in Study Area	301	179	480
Number Detected in San Joaquin River Route	287	157	444
Number Detected in Old River Route	8	3	11
Number Assigned to San Joaquin River Route	287	157	444
Number Assigned to Old River Route	7	3	10

Table 13. Number of tags observed from each release group at each detection site in 2012, excluding predator-type detections. Routes (SJR = San Joaquin River, OR = Old River) represent route assignment at the head of Old River. Pooled counts are summed over all receivers in array and all routes. Route could not be identified for some tags.

Detection Site	Site Code	Survival Model Code	Release Group		Total
			1	2	
Release site at Durham Ferry			480	479	959
Durham Ferry Upstream	DFU	A0	1	1	2
Durham Ferry Downstream	DFD	A2	97	159	256
Banta Carbona	BCA	A3	119	242	361
Mossdale	MOS	A4	299	179	478
Head of Old River	HOR	B0	297	169	466
Lathrop	SJL	A5	287	157	444
Garwood Bridge	SJG	A6	231	75	306
Navy Drive Bridge	SJNB	A7	186	51	237
MacDonald Island Upstream	MACU	A8a	88	10	98
MacDonald Island Downstream	MACD	A8b	84	8	92
MacDonald Island (Pooled)	MAC	A8	88	10	98
Medford Island East	MFE	A9a	41	6	47
Medford Island West	MFW	A9b	41	6	47
Medford Island (Pooled)	MFE/MFW	A9	41	6	47
Turner Cut East	TCE	F1a	9	2	11
Turner Cut West	TCW	F1b	8	2	10
Turner Cut (Pooled)	TCE/TCW	F1	10	2	12
Old River East	ORE	B1	6	3	9
Old River South Upstream	ORSU	B2a	6	2	8
Old River South Downstream	ORSD	B2b	5	0	5
Old River South (Pooled)	ORS	B2	6	2	8
Old River at Highway 4, Upstream	OR4U	B3a	2	0	2
Old River at Highway 4, Downstream	OR4D	B3b	2	0	2
Old River at Highway 4, SJR Route	OR4	B3	1	0	1
Old River at Highway 4, OR Route	OR4	B3	1	0	1
Old River at Highway 4 (Pooled)	OR4	B3	2	0	2
Old River near Empire Cut, Upstream	OLDU	B4a	1	0	1
Old River near Empire Cut, Downstream	OLDD	B4b	0	0	0
Old River near Empire Cut, SJR Route	OLD	B4	1	0	1
Old River near Empire Cut, OR Route	OLD	B4	0	0	0
Old River near Empire Cut (Pooled)	OLD	B4	1	0	1
Middle River Head	MRH	C1	0	0	0
Middle River at Highway 4, Upstream	MR4U	C2a	1	0	1
Middle River at Highway 4, Downstream	MR4D	C2b	1	0	1
Middle River at Highway 4, SJR Route	MR4	C2	1	0	1
Middle River at Highway 4, OR Route	MR4	C2	0	0	0
Middle River at Highway 4 (Pooled)	MR4	C2	1	0	1

Table 13. (Continued)

Detection Site	Site Code	Survival Model Code	Release Group 1	Release Group 2	Total
Middle River near Empire Cut, Upstream	MREU	C3a	3	0	3
Middle River near Empire Cut, Downstream	MRED	C3b	3	0	3
Middle River near Empire Cut, SJR Route	MRE	C3	3	0	3
Middle River near Empire Cut, OR Route	MRE	C3	0	0	0
Middle River near Empire Cut (Pooled)	MRE	C3	3	0	3
Radial Gates Upstream (Pooled)	RGU	D1	0	0	0
Radial Gates Downstream (Pooled)	RGD	D2	0	0	0
Central Valley Project Trashrack	CVP	E1	4	1	5
CVP Trashrack: SJR Route	CVP	E1	1	0	1
CVP Trashrack: OR Route	CVP	E1	3	1	4
Central Valley Project Holding Tank	CVPtank	E2	1	0	1
CVP tank: SJR Route	CVPtank	E2	0	0	0
CVP tank: OR Route	CVPtank	E2	1	0	1
Threemile Slough South	TMS	T1a	6	0	6
Threemile Slough North	TMN	T1b	4	0	4
Threemile Slough (Pooled)	TMS/TMN	T1	6	0	6
Jersey Point East	JPE	G1a	26	2	28
Jersey Point West	JPW	G1b	25	2	27
Jersey Point: SJR Route	JPE/JPW	G1	26	2	28
Jersey Point: OR Route	JPE/JPW	G1	0	0	0
Jersey Point (Pooled)	JPE/JPW	G1	26	2	28
False River West	FRW	H1a	7	0	7
False River East	FRE	H1b	6	0	6
False River: SJR Route	FRE/FRW	H1	7	0	7
False River: OR Route	FRE/FRW	H1	0	0	0
False River (Pooled)	FRE/FRW	H1	7	0	7
Chipps Island East	MAE	G2a	15	0	15
Chipps Island West	MAW	G2b	15	0	15
Chipps Island: SJR Route	MAE/MAW	G2	14	0	14
Chipps Island: OR Route	MAE/MAW	G2	1	0	1
Chipps Island (Pooled)	MAE/MAW	G2	15	0	15

Table 14. Number of tags observed from each release group at each detection site in 2012 and used in the survival analysis, excluding predator-type detections. Pooled counts are summed over all receivers in array. Route could not be identified for some tags. * = site was included in full survival model but omitted from reduced model used for analysis.

Detection Site	Site Code	Survival Model Code	Release Group		Total
			1	2	
Release site at Durham Ferry			480	479	959
Durham Ferry Upstream*	DFU	A0	1	1	2
Durham Ferry Downstream	DFD	A2	97	159	256
Banta Carbona	BCA	A3	119	242	361
Mossdale	MOS	A4	299	179	478
Lathrop	SJL	A5	287	157	444
Garwood Bridge	SJG	A6	231	75	306
Navy Drive Bridge	SJNB	A7	185	50	235
MacDonald Island Upstream	MACU	A8a	83	9	92
MacDonald Island Downstream	MACD	A8b	80	8	88
MacDonald Island (Pooled)	MAC	A8	87	10	97
Medford Island East	MFE	A9a	38	6	44
Medford Island West	MFW	A9b	38	6	44
Medford Island (Pooled)	MFE/MFW	A9	38	6	44
Turner Cut East	TCE	F1a	9	2	11
Turner Cut West	TCW	F1b	8	2	10
Turner Cut (Pooled)	TCE/TCW	F1	10	2	12
Old River East	ORE	B1	6	3	9
Old River South Upstream	ORSU	B2a	6	2	8
Old River South Downstream	ORSD	B2b	5	0	5
Old River South (Pooled)	ORS	B2	6	2	8
Old River at Highway 4, Upstream*	OR4U	B3a	2	0	2
Old River at Highway 4, Downstream*	OR4D	B3b	2	0	2
Old River at Highway 4, SJR Route*	OR4	B3	1	0	1
Old River at Highway 4, OR Route*	OR4	B3	1	0	1
Old River at Highway 4 (Pooled)*	OR4	B3	2	0	2
Middle River Head*	MRH	C1	0	0	0
Middle River at Highway 4, Upstream*	MR4U	C2a	0	0	0
Middle River at Highway 4, Downstream*	MR4D	C2b	0	0	0
Middle River at Highway 4, SJR Route*	MR4	C2	0	0	0
Middle River at Highway 4, OR Route*	MR4	C2	0	0	0
Middle River at Highway 4 (Pooled)*	MR4	C2	0	0	0
Radial Gates Upstream (Pooled)*	RGU	D1	0	0	0
Radial Gates Downstream (Pooled)*	RGD	D2	0	0	0
Central Valley Project Trashrack*	CVP	E1	4	1	5
CVP Trashrack: SJR Route*	CVP	E1	1	0	1
CVP Trashrack: OR Route*	CVP	E1	3	1	4

Table 14. (Continued)

Detection Site	Site Code	Survival Model Code	Release Group		Total
			1	2	
Central Valley Project Holding Tank*	CVPtank	E2	1	0	1
CVP tank: SJR Route*	CVPtank	E2	0	0	0
CVP tank: OR Route*	CVPtank	E2	1	0	1
Jersey Point East	JPE	G1a	24	2	26
Jersey Point West	JPW	G1b	23	2	25
Jersey Point: SJR Route	JPE/JPW	G1	24	2	26
Jersey Point: OR Route	JPE/JPW	G1	0	0	0
Jersey Point (Pooled)	JPE/JPW	G1	24	2	26
False River West	FRW	H1a	0	0	0
False River East	FRE	H1b	0	0	0
False River: SJR Route	FRE/FRW	H1	0	0	0
False River: OR Route	FRE/FRW	H1	0	0	0
False River (Pooled)	FRE/FRW	H1	0	0	0
Chipps Island East	MAE	G2a	15	0	15
Chipps Island West	MAW	G2b	15	0	15
Chipps Island: SJR Route	MAE/MAW	G2	14	0	14
Chipps Island: OR Route	MAE/MAW	G2	1	0	1
Chipps Island (Pooled)	MAE/MAW	G2	15	0	15

Table 15. Number of juvenile Chinook Salmon tagged by each tagger in each release group during the 2012 tagging study. OK with updated numbers

	Release Group		
Tagger	1	2	Total Tags
A	119	120	239
B	118	119	237
C	120	119	239
D	123	121	244
Total Tags	480	479	959

Table 16. Release size and counts of tag detections at key detection sites by tagger in 2012, excluding predator-type detections. * = used in chi-square test of independence.

	Tagger			
Detection Site	A	B	C	D
Release at Durham Ferry*	239	237	239	244
Mossdale (MOS)*	118	112	126	122
Lathrop (SJL)*	108	102	120	114
MacDonald Island (MAC)	27	13	29	28
Turner Cut (TCE/TCW)	4	1	3	4
Medford Island (MFE/MFW)	13	8	9	14
MacDonald Island, Medford Island, or Turner Cut (pooled)*	31	14	32	32
Old River East (ORE)*	1	4	2	2
Old River South (ORS)	1	3	2	2
Old River at Highway 4 (OR4)	1	0	0	1
Middle River at Highway 4 (MR4)	0	0	0	0
Clifton Court Forebay Interior (RGD)	0	0	0	0
Central Valley Project Holding Tank (CVPtank)	0	0	0	1
Jersey Point (JPE/JPW)*	10	3	6	7
Chipps Island (MAE/MAW)*	5	1	4	5

Table 17. Performance metric estimates (standard error in parentheses) for tagged juvenile Chinook Salmon released in the 2012 tagging study, excluding predator-type detections. South Delta ("SD") survival extended to MacDonald Island and Turner Cut in Route A. Population-level estimates were from pooled release groups.

	Release Occasion		
Parameter	1	2	Population Estimate
ψ_{AA}	0.88 (0.03)	0.82 (0.10)	0.87 (0.03)
ψ_{AF}	0.10 (0.03)	0.16 (0.10)	0.11 (0.03)
S_{AA}	0.05[d] (0.01)	0[d] (0)	0.03 (0.01)
S_{AF}	0 (0)	0 (0)	0 (0)
ψ_{A}[a]	0.98 (0.01)	0.98 (0.01)	0.98 (0.01)
ψ_{B}[a]	0.02 (0.01)	0.02 (0.01)	0.02 (0.01)
ψ_{F2}	0.11 (0.03)	0.16 (0.11)	0.11 (0.03)
S_{A}	0.05[cd] (0.01)	0[d] (0)	0.03[c] (0.01)
S_{B}[b]	0.16[c] (0.15)	0 (0)	0.11[c] (0.10)
S_{Total}	0.05[d] (0.01)	0[d] (0)	0.03 (0.01)
$S_{A(MD)}$	0.09[d] (0.02)	0.01[d] (0.01)	0.06 (0.01)
$S_{A(SD)}$	0.33[d] (0.03)	0.07[d] (0.02)	0.23 (0.02)
ϕ_{A1A4}	0.63[d] (0.02)	0.37[d] (0.02)	0.50 (0.02)

a = Significant preference for route A (San Joaquin Route) (α = 0.05) for all release occasions and for population estimate.

b = No tags were detected in subroute C; survival estimate used $\phi_{B1,B2} = S_{B1} * \psi_{B2}$ under assumption $\psi_{B2} = 1$.

c = No significant difference between route A and route B estimate ($P \geq 0.19$).

d = Release group 1 had significantly higher survival than release group 2 ($P < 0.0001$).

Table 18. Performance metric estimates (standard error in parentheses) for tagged juvenile Chinook Salmon released in the 2012 tagging study, including predator-type detections. South Delta ("SD") survival extended to MacDonald Island and Turner Cut in Route A. Population-level estimates were from pooled release groups.

	Release Occasion		
Parameter	1	2	Population Estimate
ψ_{AA}	0.86 (0.03)	0.85 (0.09)	0.86 (0.03)
ψ_{AF}	0.12 (0.03)	0.13 (0.09)	0.12 (0.03)
S_{AA}	0.05[d] (0.01)	0[d] (0)	0.03 (0.01)
S_{AF}	0 (0)	0 (0)	0 (0)
ψ_A[a]	0.98 (0.01)	0.98 (0.01)	0.98 (0.01)
ψ_B[a]	0.02 (0.01)	0.02 (0.01)	0.02 (0.01)
ψ_{F2}	0.12 (0.03)	0.14 (0.09)	0.12 (0.03)
S_A	0.05[cd] (0.01)	0[d] (0)	0.03[c] (0.01)
S_B[b]	0.16[c] (0.15)	0 (0)	0.11[c] (0.10)
S_{Total}	0.05[d] (0.01)	0[d] (0)	0.03 (0.01)
$S_{A(MD)}$	0.09[d] (0.02)	0.01[d] (0.01)	0.06 (0.01)
$S_{A(SD)}$	0.34[d] (0.03)	0.08[d] (0.02)	0.24 (0.02)
ϕ_{A1A4}	0.62[d] (0.02)	0.38[d] (0.02)	0.50 (0.02)

a = Significant preference for route A (San Joaquin Route) (α = 0.05) for all release occasions and for population estimate.

b = No tags were detected in subroute C; survival estimate used $\phi_{B1,B2} = S_{B1} * \psi_{B2}$ under assumption $\psi_{B2} = 1$.

c = No significant difference between route A and route B estimate ($P \geq 0.19$).

d = Release group 1 had significantly higher survival than release group 2 ($P < 0.0001$).

Table 19. Estimates (standard errors in parentheses) of model survival and transition parameters by release group, and of the difference (Δ) between release group estimates: Δ = Release group 1 - Release group 2. P = P-value from one-sized z-test of Δ>1. Estimates were based on data that excluded predator-type detections. * = significant (positive) difference between release groups for family-wise α=0.10.

Parameter	Release 1	Release 2	Δ	P
S_{A2}	0.90 (0.06)	0.63 (0.04)	0.27 (0.07)	0.0001*
S_{A3}	0.78 (0.04)	0.59 (0.03)	0.19 (0.05)	0.0001*
S_{A4}	0.98 (0.01)	0.89 (0.02)	0.08 (0.02)	0.0004*
S_{A5}	0.81 (0.02)	0.48 (0.04)	0.33 (0.05)	<0.0001*
S_{A6}	0.85 (0.03)	0.73 (0.08)	0.13 (0.08)	0.0594
S_{A7}	0.49 (0.04)	0.23 (0.06)	0.27 (0.07)	0.0001*
$S_{B2,G2}$[a]	0.17 (0.15)	0	0.17 (0.15)	0.1367
$\phi_{A1,A2}$	0.89 (0.05)	1.00 (0.06)	-0.11 (0.07)	0.9407
$\phi_{A8,A9}$	0.44 (0.05)	0.59 (0.16)	-0.16 (0.16)	0.8309
$\phi_{A8,G1}$	0.08 (0.03)	0	0.08 (0.03)	0.0030*
$\phi_{A9,G1}$	0.49 (0.09)	0.33 (0.19)	0.16 (0.21)	0.2265
$\phi_{B1,B2}$[a]	1	0.67 (0.27)	0.33 (0.27)	0.1106
$\phi_{F1,G1}$	0	0	0	NA
$\phi_{G1,G2(A)}$	0.54 (0.10)	0	0.54 (0.10)	<0.0001*

[a]These reaches are in the Old River route

Table 20a. Average travel time in days (harmonic mean) of acoustic-tagged juvenile Chinook Salmon from release at Durham Ferry during the 2012 tagging study, without predator-type detections (see Table 20b for travel time from release with predator-type detections). Standard errors are in parentheses. There were no detections at the MRH, RGU, or RGD sites; all tags detected at FRE/FRW or MR4 were later detected at competing receivers, so those sites are omitted here.

	Without Predator-Type Detections					
	All Releases		Release 1		Release 2	
Detection Site and Route	N	Travel Time	N	Travel Time	N	Travel Time
Durham Ferry Upstream (DFU)	2	0.06 (0.02)	1	0.10 (NA)	1	0.04 (NA)
Durham Ferry Downstream (DFD)	251	0.03 (<0.01)	92	0.03 (<0.01)	159	0.03 (<0.01)
Banta Carbona (BCA)	353	0.27 (0.01)	111	0.25 (0.01)	242	0.29 (0.01)
Mossdale (MOS)	464	0.53 (0.01)	285	0.48 (0.01)	179	0.61 (0.02)
Lathrop (SJL)	430	0.71 (0.01)	273	0.65 (0.01)	157	0.85 (0.03)
Garwood Bridge (SJG)	293	1.41 (0.03)	218	1.31 (0.02)	75	1.85 (0.08)
Navy Drive Bridge (SJNB)	226	1.48 (0.03)	176	1.39 (0.02)	50	1.96 (0.10)
MacDonald Island (MAC)	89	2.83 (0.10)	79	2.74 (0.10)	10	3.88 (0.44)
Turner Cut (TCE/TCW)	12	2.84 (0.16)	10	2.91 (0.19)	2	2.57 (0.19)
Medford Island (MFE/MFW)	44	3.39 (0.25)	38	3.32 (0.27)	6	3.88 (0.55)
Old River East (ORE)	9	0.70 (0.06)	6	0.66 (0.04)	3	0.80 (0.19)
Old River South (ORS)	8	1.01 (0.07)	6	0.97 (0.04)	2	1.16 (0.43)
Old River at Highway 4 (OR4), SJR Route	1	5.08 (NA)	1	5.08 (NA)	0	NA
Old River at Highway 4 (OR4), OR Route	1	4.29 (NA)	1	4.29 (NA)	0	NA
Central Valley Project Trashrack (CVP), SJR Route	1	5.62 (NA)	1	5.62 (NA)	0	NA
Central Valley Project Trashrack (CVP), OR Route	4	2.52 (0.57)	3	2.41 (0.72)	1	2.92 (NA)
Central Valley Project Holding Tank (CVPtank), SJR Route	0	NA	0	NA	0	NA
Central Valley Project Holding Tank (CVPtank), OR Route	1	2.15 (NA)	1	2.15 (NA)	0	NA
Jersey Point (JPE/JPW), SJR Route	26	5.98 (0.63)	24	6.91 (0.69)	2	4.26 (1.26)
Jersey Point (JPE/JPW), OR Route	0	NA	0	NA	0	NA
Chipps Island (MAE/MAW), SJR Route	10	5.99 (0.41)	10	5.99 (0.41)	0	NA
Chipps Island (MAE/MAW), OR Route	1	4.12 (NA)	1	4.12 (NA)	0	NA
Chipps Island (MAE/MAW)	11	5.75 (0.41)	11	5.75 (0.41)	0	NA

Table 20b. Average travel time in days (harmonic mean) of acoustic-tagged juvenile Chinook Salmon from release at Durham Ferry during the 2012 tagging study, with predator-type detections (see Table 20a for travel time from release without predator-type detections). Standard errors are in parentheses. There were no detections at the MRH, RGU, or RGD sites; all tags detected at FRE/FRW or MR4 were later detected at competing receivers, so those sites are omitted here.

	With Predator-Type Detections					
	All Releases		Release 1		Release 2	
Detection Site and Route	N	Travel Time	N	Travel Time	N	Travel Time
Durham Ferry Upstream (DFU)	8	0.20 (0.11)	1	0.10 (NA)	7	0.23 (0.16)
Durham Ferry Downstream (DFD)	262	0.03 (<0.01)	96	0.03 (<0.01)	166	0.04 (<0.01)
Banta Carbona (BCA)	355	0.28 (0.01)	112	0.25 (0.01)	243	0.29 (0.01)
Mossdale (MOS)	464	0.53 (0.01)	283	0.48 (0.01)	181	0.63 (0.02)
Lathrop (SJL)	432	0.72 (0.01)	272	0.65 (0.01)	160	0.89 (0.03)
Garwood Bridge (SJG)	297	1.44 (0.03)	219	1.33 (0.02)	78	1.93 (0.09)
Navy Drive Bridge (SJNB)	230	1.56 (0.04)	177	1.44 (0.03)	53	2.19 (0.13)
MacDonald Island (MAC)	90	3.21 (0.17)	78	3.07 (0.17)	12	4.55 (0.72)
Turner Cut (TCE/TCW)	13	3.11 (0.26)	11	3.23 (0.31)	2	2.57 (0.19)
Medford Island (MFE/MFW)	44	3.39 (0.25)	38	3.32 (0.27)	6	3.88 (0.55)
Old River East (ORE)	9	0.77 (0.09)	6	0.66 (0.04)	3	1.18 (0.46)
Old River South (ORS)	9	1.11 (0.13)	6	0.97 (0.04)	3	1.52 (0.64)
Old River at Highway 4 (OR4), SJR Route	1	5.08 (NA)	1	5.08 (NA)	0	NA
Old River at Highway 4 (OR4), OR Route	1	4.29 (NA)	1	4.29 (NA)	0	NA
Central Valley Project Trashrack (CVP), SJR Route	1	5.62 (NA)	1	5.62 (NA)	0	NA
Central Valley Project Trashrack (CVP), OR Route	4	2.52 (0.57)	3	2.41 (0.72)	1	2.92 (NA)
Central Valley Project Holding Tank (CVPtank), SJR Route	0	NA	0	NA	0	NA
Central Valley Project Holding Tank (CVPtank), OR Route	1	2.15 (NA)	1	2.15 (NA)	0	NA
Jersey Point (JPE/JPW), SJR Route	26	5.98 (0.63)	24	6.19 (0.69)	2	4.26 (1.26)
Jersey Point (JPE/JPW), OR Route	0	NA	0	NA	0	NA
Chipps Island (MAE/MAW), SJR Route	10	5.99 (0.41)	10	5.99 (0.41)	0	NA
Chipps Island (MAE/MAW), OR Route	1	4.12 (NA)	1	4.12 (NA)	0	NA
Chipps Island (MAE/MAW)	11	5.75 (0.41)	11	5.75 (0.41)	0	NA

Table 21a. Average travel time in days (harmonic mean) of acoustic-tagged juvenile Chinook Salmon through the San Joaquin River Delta river reaches during the 2012 tagging study, without predator-type detections (see Table 21b for travel time through reaches with predator-type detections). Standard errors are in parentheses. Reaches beginning at sites with no detections are not shown (i.e., reaches that start at MRH, MR4, RGU, RGD, and FRE/FRW).

Reach		Without Predator-Type Detections					
		All Releases		Release 1		Release 2	
Upstream Boundary	Downstream Boundary	N	Travel Time	N	Travel Time	N	Travel Time
Durham Ferry (Release)	BCA	251	0.03 (<0.01)	92	0.03 (<0.01)	159	0.03 (<0.01)
BCA	MOS	230	0.28 (0.01)	87	0.24 (0.01)	143	0.31 (0.01)
MOS	SJL	429	0.14 (<0.01)	272	0.13 (<0.01)	157	0.16 (0.01)
	ORE	9	0.25 (0.04)	6	0.23 (0.04)	3	0.32 (0.09)
SJL	SJG	293	0.65 (0.02)	218	0.60 (0.02)	75	0.86 (0.05)
SJG	SJNB	226	0.08 (<0.01)	176	0.08 (<0.01)	50	0.09 (0.01)
SJNB	MAC	84	1.25 (0.07)	75	1.21 (0.07)	9	1.72 (0.37)
	TCE/TCW	12	1.19 (0.18)	10	1.37 (0.15)	2	0.72 (0.31)
MAC	MFE/MFW	39	0.23 (0.03)	33	0.24 (0.03)	6	0.21 (0.07)
	JPE/JPW/FRE/FRW	22	2.20 (0.26)	20	2.47 (0.27)	2	1.05 (0.13)
	OR4	0	NA	0	NA	0	NA
	MR4	0	NA	0	NA	0	NA
MFE/MFW	JPE/JPW/FRE/FRW	17	1.54 (0.21)	15	1.80 (0.19)	2	0.74 (0.20)
	OR4	0	NA	0	NA	0	NA
	MR4	0	NA	0	NA	0	NA
TCE/TCW	JPE/JPW/FRE/FRW	0	NA	0	NA	0	NA
	OR4	1	2.25 (NA)	1	2.25 (NA)	0	NA
	MR4	0	NA	0	NA	0	NA
ORE	ORS	8	0.27 (0.03)	6	0.29 (0.03)	2	0.22 (0.05)
	MRH	0	NA	0	NA	0	NA
ORS	OR4	1	3.25 (NA)	1	3.25 (NA)	0	NA
	MR4	0	NA	0	NA	0	NA
	RGU	0	NA	0	NA	0	NA
	CVP	3	0.95 (0.12)	2	0.90 (0.16)	1	1.09 (NA)

Table 21a. (Continued)

Reach		Without Predator-Type Detections					
		All Releases		Release 1		Release 2	
Upstream Boundary	Downstream Boundary	N	Travel Time	N	Travel Time	N	Travel Time
OR4 via OR	JPE/JPW/FRE/FRW	0	NA	0	NA	0	NA
OR4 via SJR	JPE/JPW/FRE/FRW	0	NA	0	NA	0	NA
	RGU	0	NA	0	NA	0	NA
	CVP	1	0.55 (NA)	1	0.55 (NA)	0	NA
CVP via OR	CVPtank	1	0.01 (NA)	1	0.01 (NA)	0	NA
CVP via SJR	CVPtank	0	NA	0	NA	0	NA
JPE/JPW	MAE/MAW (Chipps Island)	9	1.21 (0.14)	9	1.21 (0.14)	0	NA
MAC		10	3.54 (0.34)	10	3.54 (0.34)	0	NA
MFE/MFW		8	3.04 (0.25)	8	3.04 (0.259)	0	NA
TCE/TCW		0	NA	0	NA	0	NA
OR4		0	NA	0	NA	0	NA
CVPtank		1	1.97 (NA)	1	1.97 (NA)	0	NA

Table 21b. Average travel time in days (harmonic mean) of acoustic-tagged juvenile Chinook Salmon through the San Joaquin River Delta river reaches during the 2012 tagging study, with predator-type detections (see Table 21a for travel time through reaches without predator-type detections). Standard errors are in parentheses. Reaches beginning at sites with no detections are not shown (i.e., reaches that start at MRH, MR4, RGU, RGD, and FRE/FRW).

Reach		With Predator-Type Detections					
		All Releases		Release 1		Release 2	
Upstream Boundary	Downstream Boundary	N	Travel Time	N	Travel Time	N	Travel Time
Durham Ferry (Release)	BCA	262	0.03 (<0.01)	96	0.03 (<0.01)	166	0.04 (<0.01)
BCA	MOS	231	0.28 (0.01)	86	0.24 (0.01)	145	0.31 (0.01)
MOS	SJL	431	0.14 (<0.01)	271	0.13 (<0.01)	160	0.17 (0.01)
	ORE	9	0.28 (0.06)	6	0.23 (0.04)	3	0.52 (0.27)
SJL	SJG	297	0.67 (0.02)	219	0.62 (0.02)	78	0.90 (0.05)
SJG	SJNB	230	0.08 (<0.01)	177	0.08 (<0.01)	53	0.09 (0.01)
SJNB	MAC	85	1.38 (0.10)	74	1.32 (0.10)	11	2.04 (0.49)
	TCE/TCW	13	1.33 (0.23)	11	1.57 (0.24)	2	0.72 (0.31)
MAC	MFE/MFW	39	0.23 (0.03)	33	0.24 (0.03)	6	0.21 (0.07)
	JPE/JPW/FRE/FRW	22	2.20 (0.26)	20	2.47 (0.27)	2	1.05 (0.13)
	OR4	0	NA	0	NA	0	NA
	MR4	0	NA	0	NA	0	NA
MFE/MFW	JPE/JPW/FRE/FRW	17	1.54 (0.21)	15	1.80 (0.19)	2	0.74 (0.20)
	OR4	0	NA	0	NA	0	NA
	MR4	0	NA	0	NA	0	NA
TCE/TCW	JPE/JPW/FRE/FRW	0	NA	0	NA	0	NA
	OR4	1	2.25 (NA)	1	2.25 (NA)	0	NA
	MR4	0	NA	0	NA	0	NA
ORE	ORS	9	0.29 (0.04)	6	0.29 (0.03)	3	0.31 (0.14)
	MRH	0	NA	0	NA	0	NA
ORS	OR4	1	3.25 (NA)	1	3.25 (NA)	0	NA
	MR4	0	NA	0	NA	0	NA
	RGU	0	NA	0	NA	0	NA
	CVP	3	0.95 (0.12)	2	0.90 (0.16)	1	1.09 (NA)

Table 21b. (Continued)

Reach		With Predator-Type Detections					
		All Releases		Release 1		Release 2	
Upstream Boundary	Downstream Boundary	N	Travel Time	N	Travel Time	N	Travel Time
OR4 via OR	JPE/JPW/FRE/FRW	0	NA	0	NA	0	NA
OR4 via SJR	JPE/JPW/FRE/FRW	0	NA	0	NA	0	NA
	RGU	0	NA	0	NA	0	NA
	CVP	1	0.55 (NA)	1	0.55 (NA)	0	NA
CVP via OR	CVPtank	1	0.01 (NA)	1	0.01 (NA)	0	NA
CVP via SJR	CVPtank	0	NA	0	NA	0	NA
JPE/JPW	MAE/MAW (Chipps Island)	9	1.21 (0.14)	9	1.21 (0.14)	0	NA
MAC		10	3.54 (0.34)	10	3.54 (0.34)	0	NA
MFE/MFW		8	3.04 (0.225)	8	3.04 (0.25)	0	NA
TCE/TCW		0	NA	0	NA	0	NA
OR4		0	NA	0	NA	0	NA
CVPtank		1	1.97 (NA)	1	1.97 (NA)	0	NA

Table 22: Distance in km, estimated survival and survival rate per km (S^(1/km)), travel time in days, and travel time in days per km (TT^(1/km)), for the first (1st) and second (2nd) release groups of Chinook Salmon in 2012. Survival and travel time data were obtained from tables Table A5-2, and Table 21a. Distance was estimated using the shortest distance between the two points calculated from Google Earth. Data were used to generate Figure 12.

Reach	Distance in km	Survival		Survival per km		Travel time		Travel time per km	
		1st	**2nd**	**1st**	**2nd**	**1st**	**2nd**	**1st**	**2nd**
Durham Ferry (Release) to Banta Carbona	11	0.90	0.63	0.990	0.959	0.03	0.03	0.727	0.727
Banta Carbona to Mossdale	9	0.78	0.59	0.973	0.943	0.24	0.31	0.853	0.878
Mossdale to Lathrop/Old River	4	0.98	0.89	0.995	0.971	0.13	0.16	0.600	0.632
Lathrop to Stockton South (Garwood Bridge)	18	0.81	0.48	0.988	0.960	0.60	0.86	0.972	0.992
Stockton South to Stockton Navy Bridge	3	0.85	0.73	0.947	0.900	0.08	0.09	0.431	0.448
Navy Bridge to Turner Cut Junction	15	0.49	0.23	0.954	0.907	1.37	0.72	1.021	0.978
MacDonald Island to Medford Island	5	0.44	0.59	0.849	0.900	0.24	0.21	0.752	0.732
Medford Island to Jersey Point	21	0.49	0.33	0.967	0.949	1.80	0.74	1.028	0.986
Jersey Point to Chipps Island	22	0.54	0.00	0.972	0.000	1.21		1.009	

Table 23. Results of single-variate analyses of route entrainment at the Turner Cut Junction (all release groups). The values df1, df2 are degrees of freedom for the F-test.

	F-test			
Covariate[a]	*F*	df1	df2	*P*
Change in flow at TRN	0.6896	1	8	0.4304
Change in velocity at TRN	0.6470	1	8	0.4444
Exports at CVP	0.3355	1	9	0.5766
Change in stage at TRN	0.2824	1	8	0.6095
Flow during transition from SJG	0.1864	1	9	0.6761
Stage at TRN	0.1696	1	9	0.6901
Velocity during transition from SJG	0.1311	1	9	0.7256
Release Group	0.0730	1	9	0.7931
Arrive during day at junction	0.0558	1	9	0.8185
Fork Length	0.0331	1	9	0.8597
Exports at SWP	0.0286	1	9	0.8694
Negative flow at TRN	0.0063	1	9	0.9385
Flow at TRN	0.0031	1	9	0.9568
Velocity at TRN	0.0024	1	9	0.9623

a = No covariate was significant at 5% level

Table 24. Summary statistics from multiple regression of flow at Vernalis and tag type to explain survival from Mossdale to Jersey Point with the physical head of Old River barrier. Tag type (CWT or Acoustic) was not significant (p value = 0.992775).

SUMMARY OUTPUT			Mossdale data only					
Regression Statistics								
Multiple R	0.86119676							
R Square	0.74165986							
Adjusted R Square	0.69468892							
Standard Error	0.07221227							
Observations	14							
ANOVA								
	df	*SS*	*MS*	*F*	*Significance F*			
Regression	2	0.164674977	0.082337	15.78976	0.000584865			
Residual	11	0.057360738	0.005215					
Total	13	0.222035714						
	Coefficients	*Standard Error*	*t Stat*	*P-value*	*Lower 95%*	*Upper 95%*	*Lower 95.0%*	*Upper 95.0%*
Intercept	-0.2287319	0.10572806	-2.1634	0.053388	-0.461437753	0.00397403	-0.46143775	0.003974031
X Variable 1 (tag)	-0.0005306	0.057279985	-0.00926	0.992775	-0.126603014	0.12554178	-0.12660301	0.125541781
X Variable 2 (flow)	9.533E-05	1.76263E-05	5.408389	0.000214	5.65346E-05	0.00013413	5.6535E-05	0.000134125

Appendices 1-5:

Appendix 1. Analyses of CWT salmon released in the south Delta by Ken Newman as part of the VAMP peer review in 2010.

Analyses of Salmon CWT Releases into the San Joaquin System

Ken B. Newman, USFWS

2 March 2010

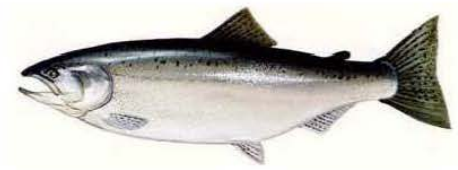

1. Overview
   - Objectives: to understand how different factors (flows, exports, barrier at head of Old River, HORB) affect survival of juvenile salmon outmigrating from San Joaquin system
   - Data Generation: CWT Release-Recovery "sets", 4-5 release locations and 2-3 recovery locations
   - Data Analysis: (Bayesian) Hierarchical Models
   - Key Results: Usually higher survival if stay in San Joaquin River than if go down Old River BUT lots of Environmental Variation, i.e., low Signal:Noise Ratio!
2. Data Generation
   (a) Between 1985 and 2006, 35 Release-Recovery sets.
   (b) Within a set, at most 3 release locations (e.g., Mossdale, Dos Reis, and Jersey Point).
   (c) At most 3 recovery locations: Chipps Island, Ocean fisheries, and since 2000, Antioch
   (d) $\Rightarrow$ 212 observations
3. Data Analysis
   (a) BHMs (Bayesian Hierarchical Models)
   (b) Key idea: 2 or more levels of modeling
   (c) Separate modeling of Observation (Sampling) noise from Survival (and capture) variation
   (d) Level 1: Observation Models y's $\sim$ Probability Distribution(R, S_t and p_t)
   (e) Level 2, Random effects: S_t, p_t $\sim$ Probability Distribution(η, Covariates)
   (f) Level 3, Hyperparameters: $\eta \sim$ Prior Probability Distribution
   (g)
   (h) Focus on Models for Survival down San Joaquin and Survival down Old River

$$E[logit(S_{DR \rightarrow JP})] = \xi_0 + \xi_1 \text{Flow}_{Dos.Reis} + \xi_2 \text{Exports}_{Dos.Reis}$$
$$E[logit(S_{OR \rightarrow JP})] = \zeta_0 + \zeta_1 \text{Flow}_{OldRiver} + \zeta_2 \text{Exports}_{Mossdale}$$

   (i) Fitting Details: WinBUGS with Reversible Jump model selection

4. Results

   (a) Posterior Probabilities

Models	$S_{MD \to JP}$	$S_{OR \to JP}$
Constant	0.38	0.45
Flow	0.29	0.23
Exports	0.17	0.21
Both	0.16	0.11

   (b) Coefficients

Covariate	Average	SD	2.5%	median	97.5%
SJ-flow	0.16	0.25	-0.09	0.0	0.77
SJ-exports	0.07	0.19	-0.17	0.0	0.61
OR-flow	0.04	0.22	-0.42	0.0	0.62
OR-exports	0.04	0.20	-0.32	0.0	0.60

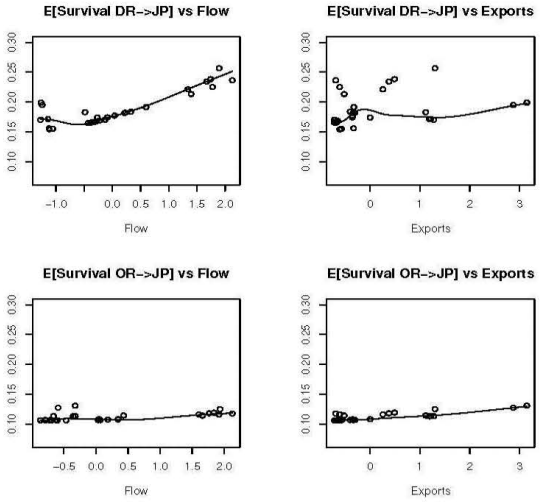

5. Caveats and Comments

   (a) Priors *do* matter, especially with Hierarchical Models

   (b) More to wring out of CWTs? Using time of capture? Add arrival time/travel time model?

   (c) Acoustic tags far preferable?

   (d) Value in probing extreme values for flows and exports

Some references:

- Clark, J.S. 2005. "Why environmental scientists are becoming Bayesians." *Ecology Letters*, **8**: 2–14.
- Clark, J.S., and Gelfand, A.E. 2006. "A future for models and data in environmental science." *Trends in Ecology and Evolution*, **21:** 375–380.
- Newman, K.B., and Brandes, P.L. 2010. Hierarchical modeling of juvenile Chinook salmon survival as a function of Sacramento-San Joaquin Delta water exports. *North American Journal of Fisheries Management*, **30:** 157–169.

Appendix 2: Standard Operating Procedure
Acoustic Tagging for Salmon 2012 South Delta Studies 4/10/12 (file dated 4/23/12)

Equipment Set Up:

- Fill surgical instrument disinfection trays with chlorhexidine (brand name Nolvasan)
    - Autoclave instruments such that each tagging event begins with sterile instruments
- Activate transmitters and confirm operational status
    - Position the transmitter in an isolated compartment to enable tracking of the transmitter ID through the implantation process
- Disinfect transmitters in chlorhexidine
    - Ensure at least 20 minutes of contact time with chlorhexidine
    - Following disinfection, thoroughly rinse transmitters in distilled or de-ionized water prior to implantation
    - Following disinfection, transmitters should only be handled by gloved hands or clean surgical instruments such as forceps
- Fill rinse tray with de-ionized or distilled water
- Set up scale, measuring board, and surgical platform or foam
    - Apply stress coat to weigh boat, measuring board, and platform to reduce damage to fish skin or mucus layer
- Fill gravity feed carboys. Add 2 ml of the MS-222 stock solution and 2 ml of the sodium bicarbonate stock solution to the 10 L of water in the MS-222 carboy. Concentration may be increased upon group consensus and in consultation with coordinator.
- Fill anesthesia container to indicated volume line. Set the initial concentration in collaboration with the tagging coordinator. Suggested starting concentration is 70 mg/ L. Concentration may be adjusted upon group consensus and in consultation with coordinator. Concentration changes should be executed for all taggers simultaneously and recorded on the tagging datasheet.
- Prepare recovery containers by filling with water, adding stress coat, and supersaturating with oxygen
    - Immediately following surgery fish will be held in recovery containers that provide 130% to 150% DO for a minimum of 10 minutes
    - Holding time in recovery containers begins when the last fish is added to the container and will be monitored using a timer
- Prepare a reject container for fish that cannot be tagged by filling with water and equipping with a bubbler . These fish will be returned to a separate holding tank.
- Start tagging data sheets. Note the time the tagging session was started and complete all appropriate data fields. Start a Daily Fish Reject Tally datasheet to account for fish that are handled but not tagged.
- The tagger should wear medical-grade exam gloves during all fish handling and tagging procedures
- Prepare the transport truck to accept containers of tagged fish.
- Prepare transport containers and lids to receive tagged fish

Surgery

- Food should be withheld from fish for ~24 h prior to surgical implantation of the transmitter.
- Anesthetize fish
    - Net one fish from source tank/raceway and place directly into an anesthesia container. Immediately start a timer to monitor anesthesia exposure time and place a lid on the container.
    - Remove the lid after about 1 minute to observe the fish for loss of equilibrium. Keep the fish in the water for an additional 30-60 seconds after it has lost equilibrium. Time to sedation should normally be 2-4 minutes, with an average of about 3 minutes. If loss of equilibrium takes less than 1 minute or if a fish is exposed to anesthesia for more than 5 minutes, reject that fish. If after anesthetizing a few fish they are consistently losing equilibrium in more or less time than typical, the anesthesia concentration may need to

be adjusted. Anesthesia concentration should only be adjusted in coordination with all study taggers and the tagging coordinator.
    - Changes to anesthesia concentration should be done at 5 mg/L increments. For example, if the initial dosage was 70 mg/L, an adjusted dose should be 65 mg/L or 75 mg/L.
    - When an anesthesia change is agreed upon, all taggers should drain their anesthesia containers, refill with 10 L of water, and re-mix to the new anesthesia concentration
  - If a fish is unacceptable for tagging due to issues with anesthesia, place the fish in the "Reject" container and log it on the reject tally datasheet.
  - The anesthesia container should be emptied and remixed at regular intervals throughout the tagging operation to ensure the appropriate concentration and to avoid warming
  - The gravity feed containers should be monitored for volume and temperature and changed as needed to avoid inadequate volume to complete a surgery and significant warming

- Recording fish length, weight, and condition
  - Start a timer when a fish is removed from the anesthesia container to record the time the fish is out of water (recorded as "air time").
  - Transfer the fish to the scale and record the weigh to the nearest 0.1g
    - Scales should be calibrated regularly to ensure accuracy
    - Fish must weigh at least 13 g to be selected for tagging so that tag burden does not exceed 5% of the weight of the fish. Transmitters used for this study are Vemco brand V5 models, weighing 0.65 g in air.
  - Transfer the fish to the measuring board and determine forklength to the nearest mm.
  - Check for any abnormalities and descaling. If the fish is abnormal or grossly descaled, note this on the datasheet and place the fish in the reject container.
    - Scale condition is noted as Normal (N), Partial (P), or Descaled (D) and is assessed on the most compromised side of each fish. The normal scale condition is defined as loss of less than 5% of scales on one side of the fish. Partial descaling is defined as loss of 6-19% of scales on one side of the fish. Fish are classified as descaled if they have lost 20% or more of the scales on one side of the fish, and should not be tagged due to compromised osmoregulatory ability.
  - Data must be vocally relayed to the recorder, and the recorder should repeat the information back to the tagger to avoid miscommunication.
  - Any fish dropped on the floor should be rejected.

- Transmitter Implantation
  - Anesthesia should be administered through the gravity feed irrigation system as soon as the fish is on the surgical platform. Use the flow control valves to adjust the flow rate as needed so that the opercular rate of the fish is steady.
    - Note that low-flow or inconsistent irrigation can mimic shallow anesthesia
  - Using a scalpel, make an incision approximately 3-5 mm in length beginning a few mm in front of the pelvic girdle. The incision should be about 3 mm away from and parallel to the mid-ventral line, and just deep enough to penetrate the peritoneum, avoiding the internal organs. The spleen is generally near the incision point so the depth and placement of the incision are critical.
    - There is no exact specification for the selection of a micro scalpel for steelhead. A general recommendation is to use a 5 mm blade for fish larger than about 50 g.
    - The incision should only be long enough to allow entry of the tag.
  - Forceps may be used to open the incision to check for potential organ damage. If you observe damage or note excessive bleeding, reject the fish.
  - Scalpel blades can be used on several fish, but if the scalpel is pulling roughly or making jagged incisions, it should be changed prior to tagging the next fish.

- Gently insert the tag into the body cavity and position it so that it lies directly beneath the incision and the ceramic head is facing forward. This positioning will provide a barrier between the suture needle and internal organs.
- Close the incision with two simple interrupted stitches.
  - Vicryl Plus sutures are recommended
  - 5-0 suture size is appropriate for juvenile Chinook Salmon or similar fish with weights less than~ 50 g
  - If the incision cannot effectively be closed with two stitches, a third stitch may be added. The presence of a third suture should be noted on the datasheet.
- Ideally the gravity feed irrigation system should be switched to fresh water or a combination of sedation and freshwater during the final stages of surgery to begin recovery from anesthesia. Typically a good time to switch to freshwater is when the second suture is initiated.
- Transfer the fish from the surgical platform to a recovery container and stop the timer recording air time
  - Avoid excessive handling of fish during transfer. Ideally the fish will be moved to the recovery container on the surgical platform to reduce handling.
- Once a recovery container has been fully stocked, start a timer to monitor the 10 min of exposure to high DO concentrations for recovery.
- Between surgeries the tagger should place surgical instruments and any partially consumed suture material into the chlorhexidine bath. Multiple sets of surgical instruments should be rotated to ensure 10 min of contact time with chlorhexidine. Once disinfected, instruments should be rinsed in distilled or de-ionized water. Organic debris in the disinfectant bath reduces effectiveness, so be sure to change the bath regularly.

Tag Validation

- Filled recovery containers will be moved to the tag validation station.
  - Recovery containers may be moved from the tagging location to the tag validation station during the 10 min recovery time, but they must not be established on flow-through water exchange. The flow-through exchange will immediately reduce the DO saturation.
- Use the appropriate receiving system to confirm the identity and function of the transmitters in the recovery container. Record validation on the datasheet.
- Following tag validation, recovery containers are held in a flow-through tank until the tagging session is complete, at which time they are loaded onto a truck for transport to the holding and release location.

Cleanup

- Both the tagger and assistant must review the full complement of tagging datasheets and initial each sheet to confirm that the set of transmitters they were assigned to implant have been implanted. Use the list of transmitters provided by the tag coordinator to ensure that all transmitters supplied to you were implanted and recorded. Both the tagger and the assistant must initial the header of each of the datasheets. This review step is completed for each tagging session (that is, for each transport truck that is loaded).
- Return tag tray and datasheets to coordinator at end of each tagging session.
- Complete the reject fish tally datasheet and return to the tag coordinator.
- Use a spray disinfectant to disinfect tagging surfaces and supplies, and position them to dry.
- Return any rejected fish to the appropriate raceway where they cannot be selected for future tagging efforts.
- At the completion of the tagging effort each day, package surgical instruments for the autoclave so they can be sterilized prior to the next tagging session.

Important things to remember:

- Water containers used for tagging should be filled just prior to tagging to avoid temperature changes and should be changed frequently.
- Fish cannot be transferred between water sources until the difference between the water temperatures of the two sources is less than two degrees Celsius.
- No water sources used in the tagging operation should be more than two degrees different in water temperature from the source water temperature.
- All containers holding fish should have lids in place.
- If a tag is dropped bring it to the tagging coordinator to confirm that it is still functioning before it is implanted. The transmitter may also require disinfection if it fell onto a dirty surface.
- Carefully handle all fish containers to minimize disturbances to fish.
- Containers used to transport fish to the release site cannot be used for tagging operations until they have been held in the freezer for 24 h.

Appendix 3: Water temperature (every 15 minutes) in transport tanks during transport of tagged fish from the Tracy Fish Collection Facility to the release site (Durham Ferry)

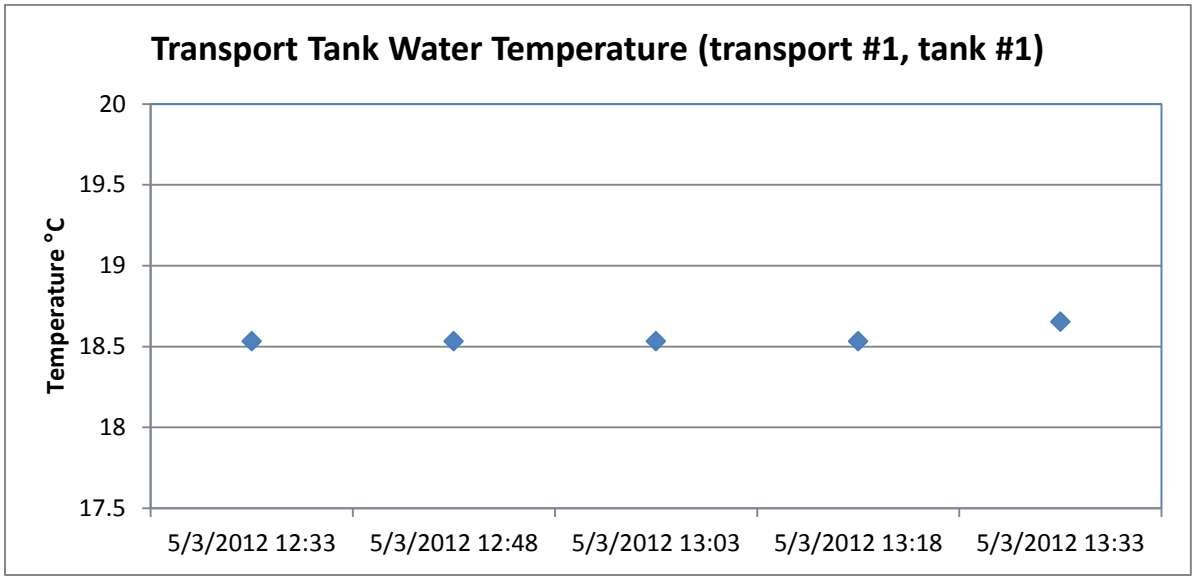

Figure A3-1. Transport tank water temperature during transport #1, tank #1 on May 3, 2012.

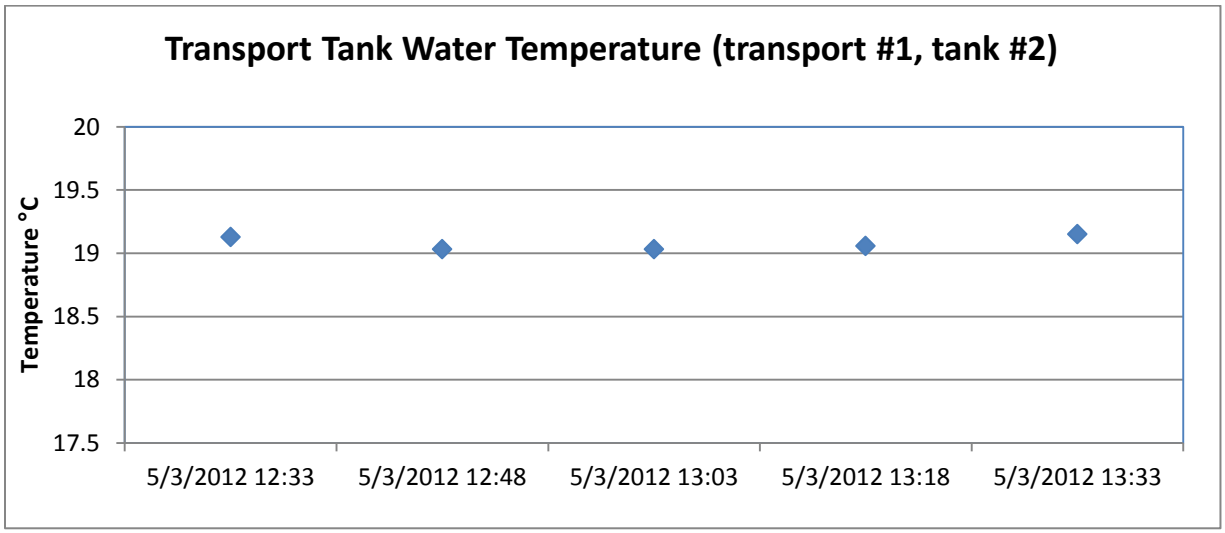

Figure A3-2. Transport tank water temperature during transport #1, tank #2 on May 3, 2012.

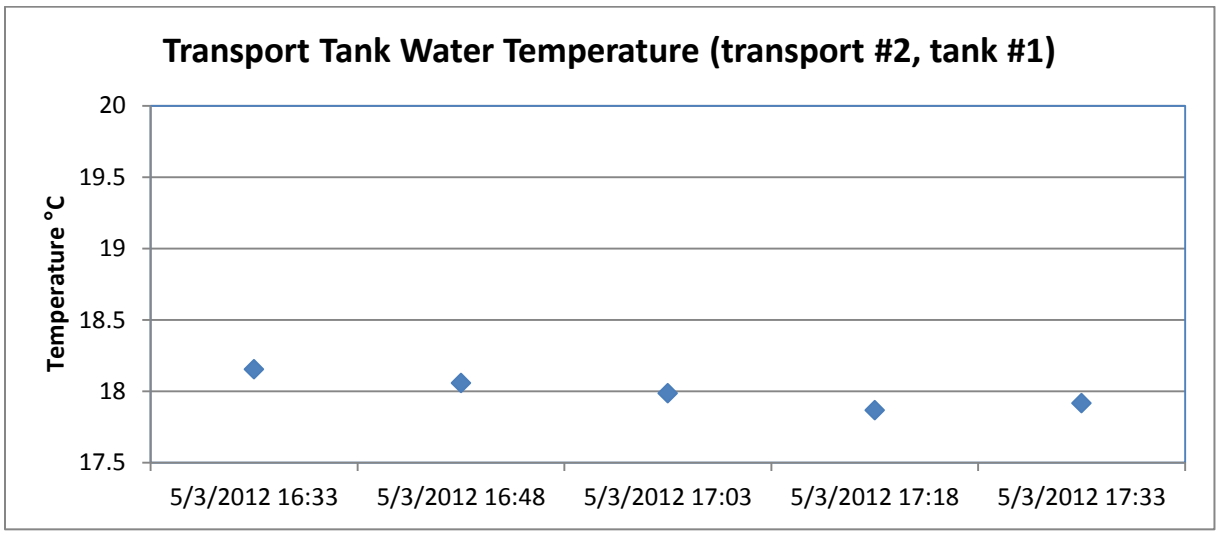

Figure A3-3. Transport tank water temperature during transport #2, tank #1 on May 3, 2012.

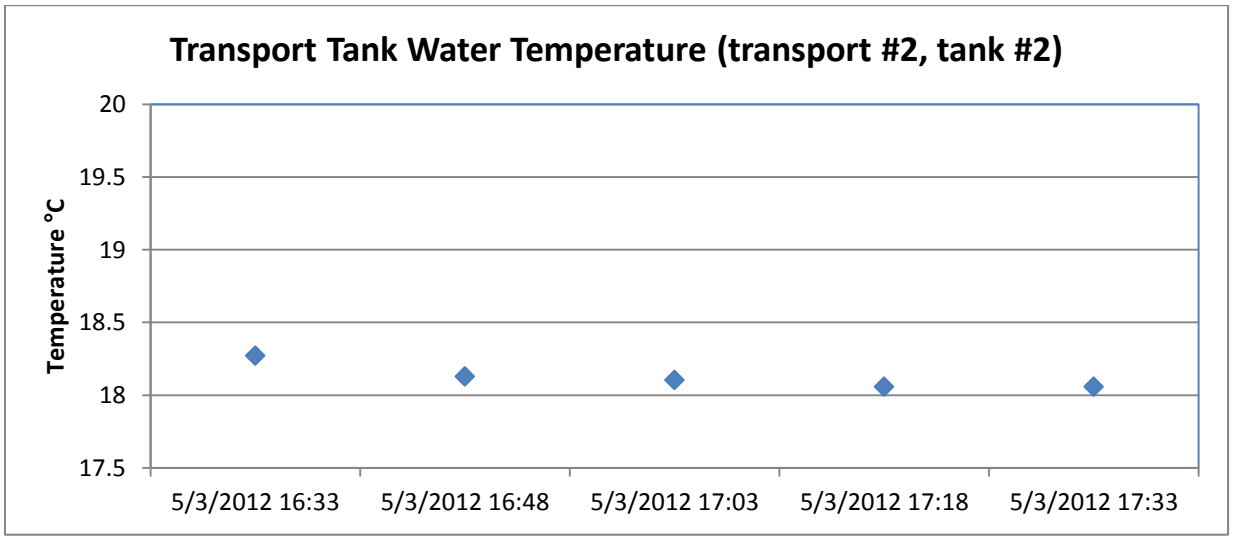

Figure A3-4. Transport tank water temperature during transport #2, tank #2 on May 3, 2012.

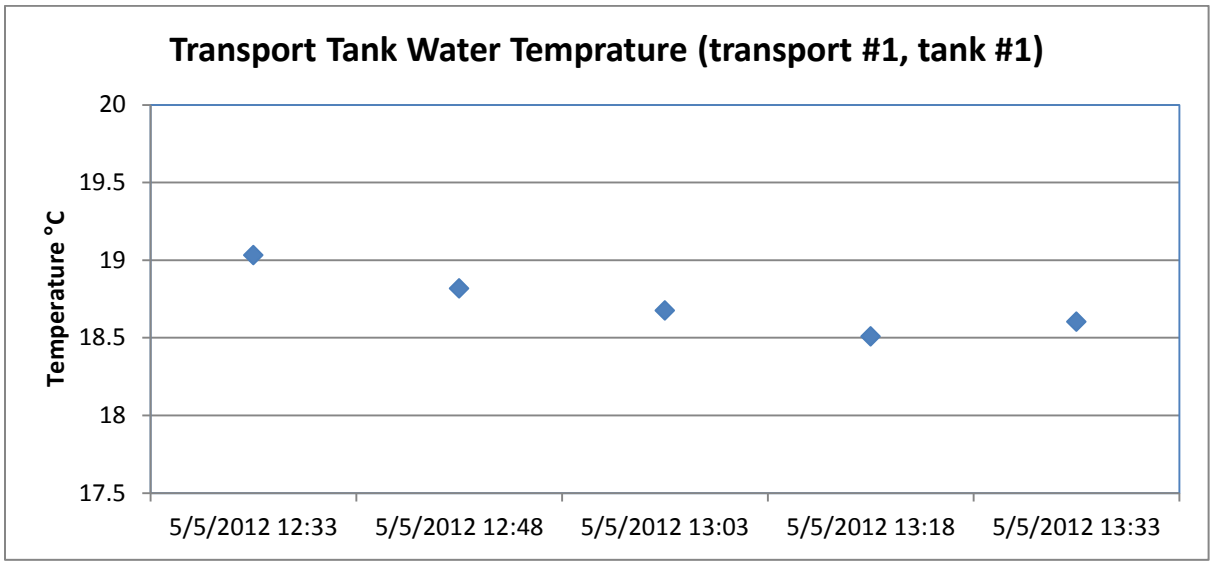

Figure A3-5. Transport tank water temperature during transport #1, tank #1 on May 5, 2012.

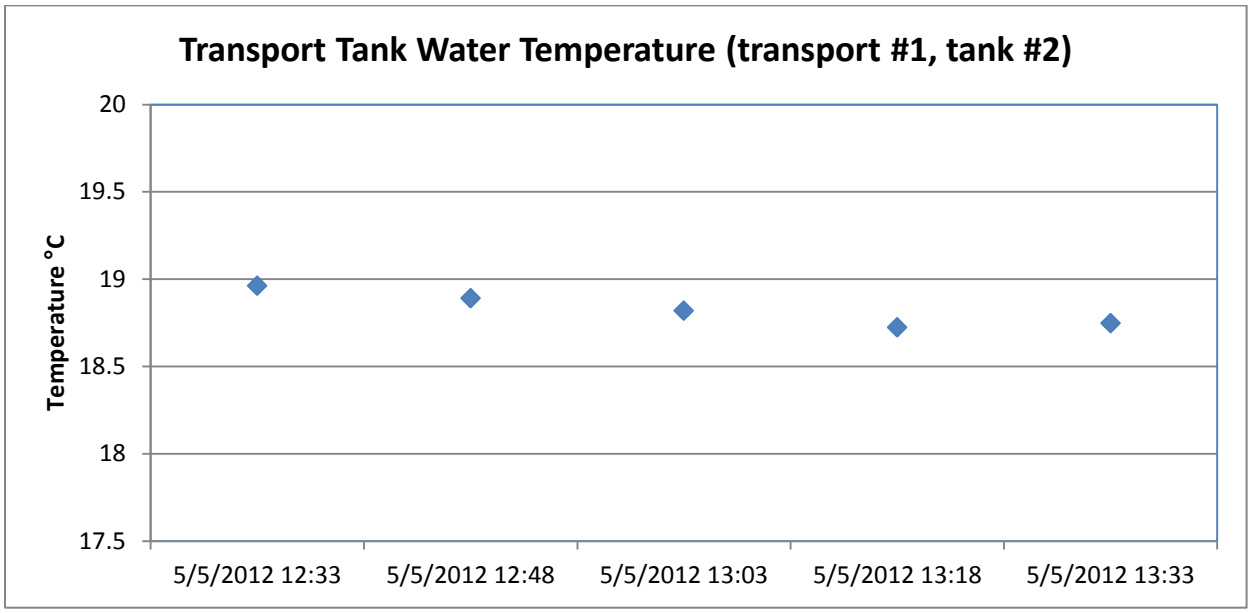

Figure A3-6. Transport tank water temperature during transport #1, tank #2 on May 5, 2012.

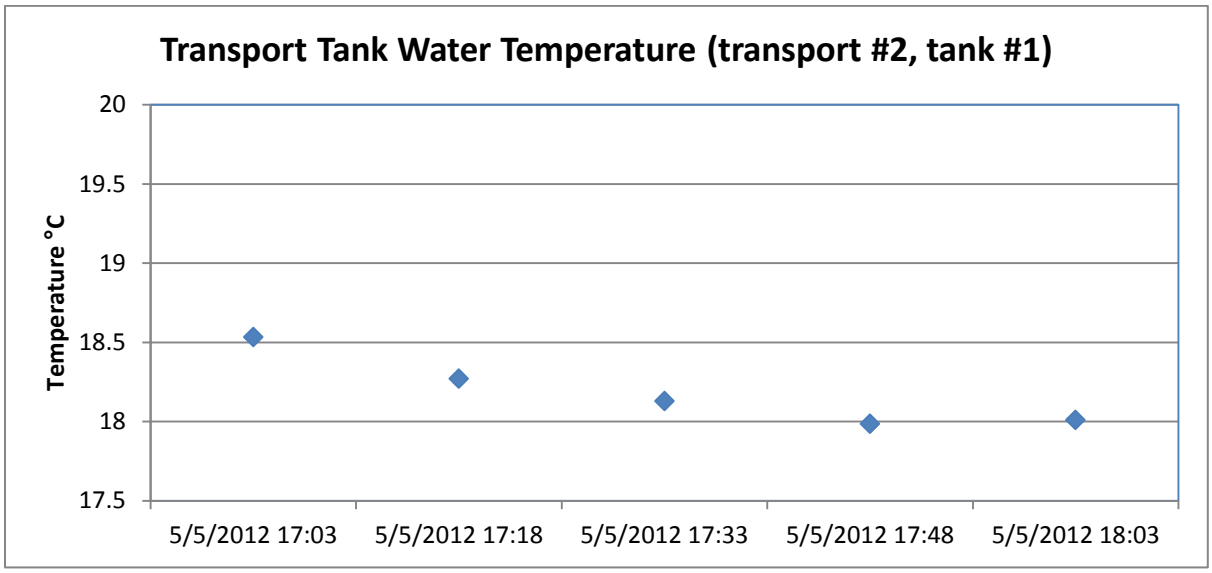

Figure A3-7. Transport tank water temperature during transport #2, tank #1 on May 5, 2012.

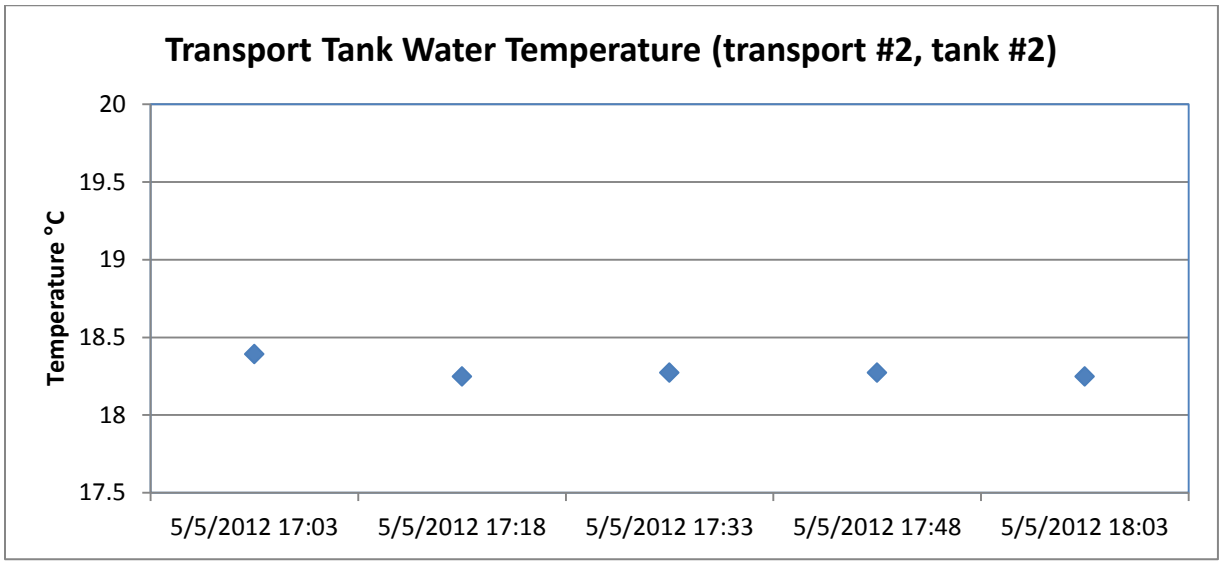

Figure A3-8. Transport tank water temperature during transport #2, tank #2 on May 5, 2012.

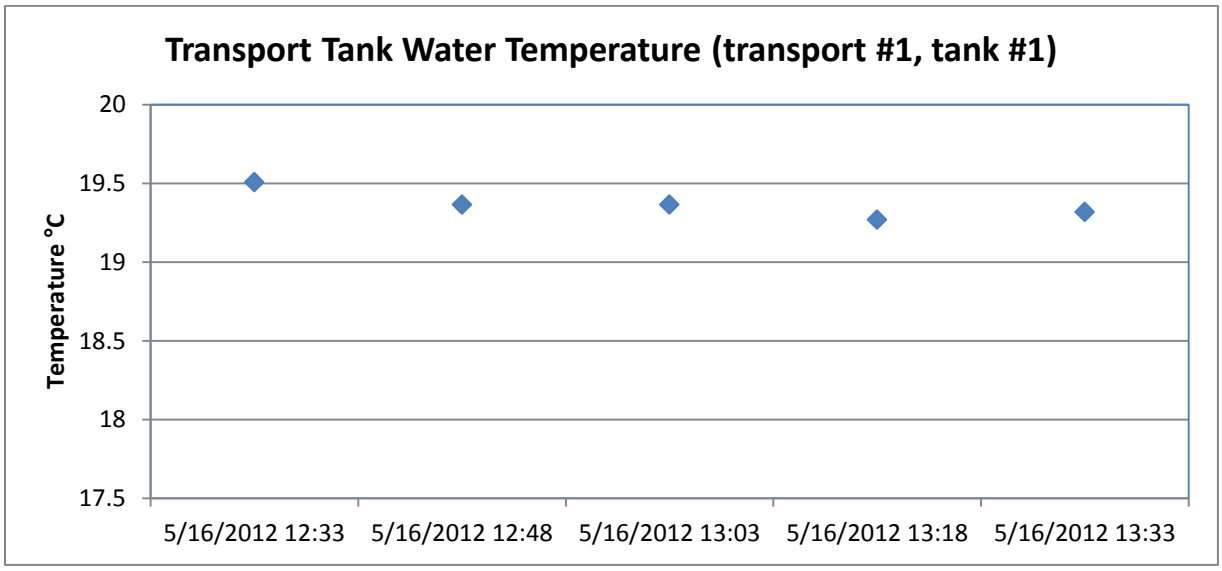

Figure A3-9. Transport tank water temperature during transport #1, tank #1 on May 16, 2012.

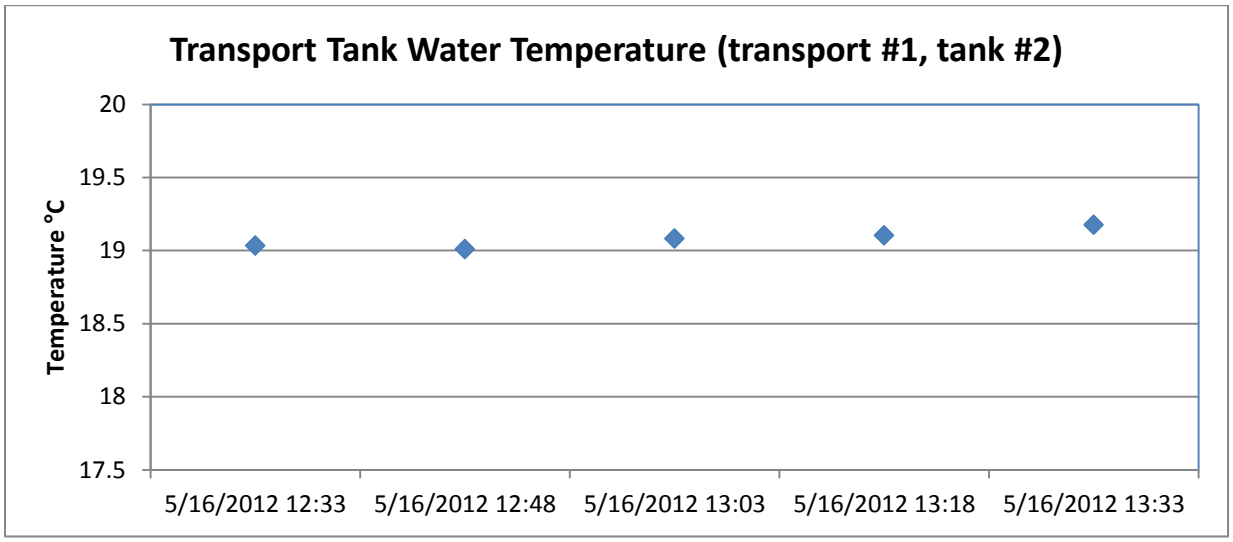

Figure A3-10. Transport tank water temperature during transport #1, tank #2 on May 16, 2012.

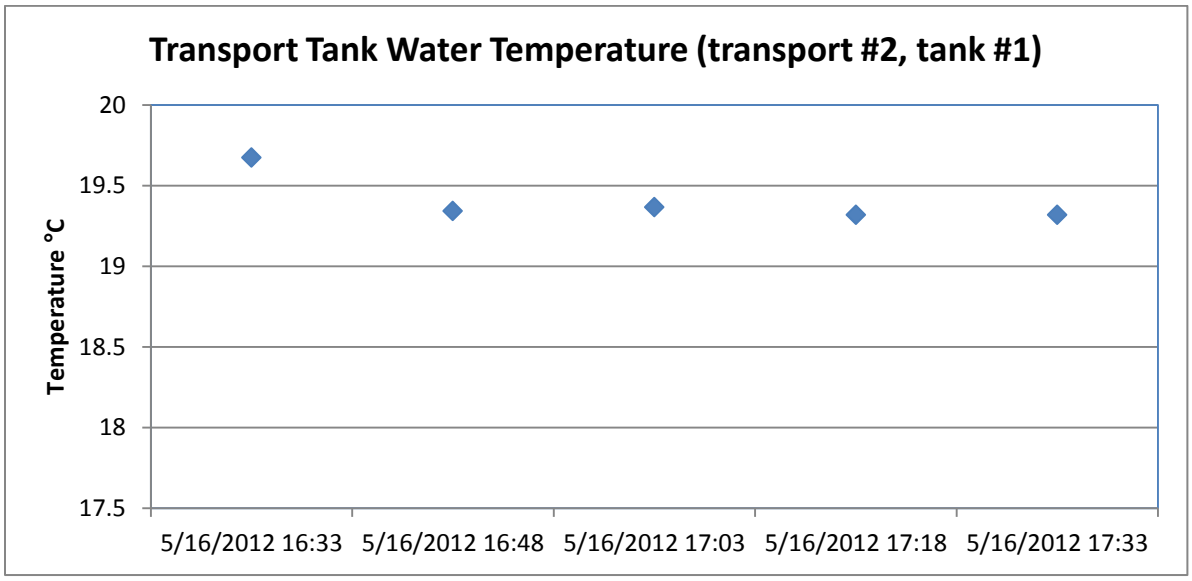

Figure A3-11. Transport tank water temperature during transport #2, tank #1 on May 16, 2012.

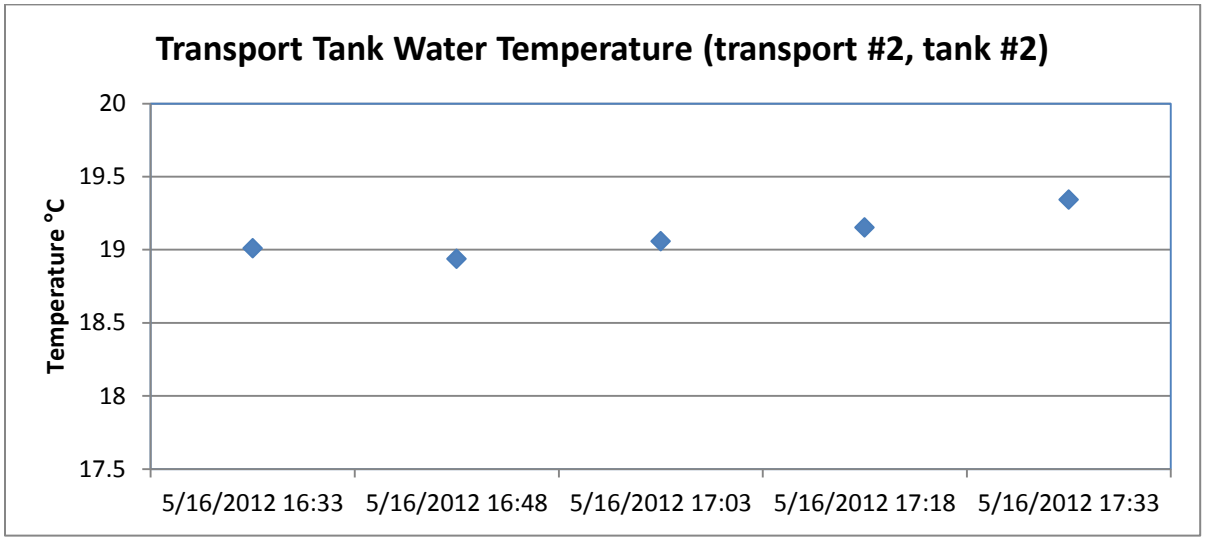

Figure A3-12. Transport tank water temperature during transport #2, tank#2 on May 16, 2012.

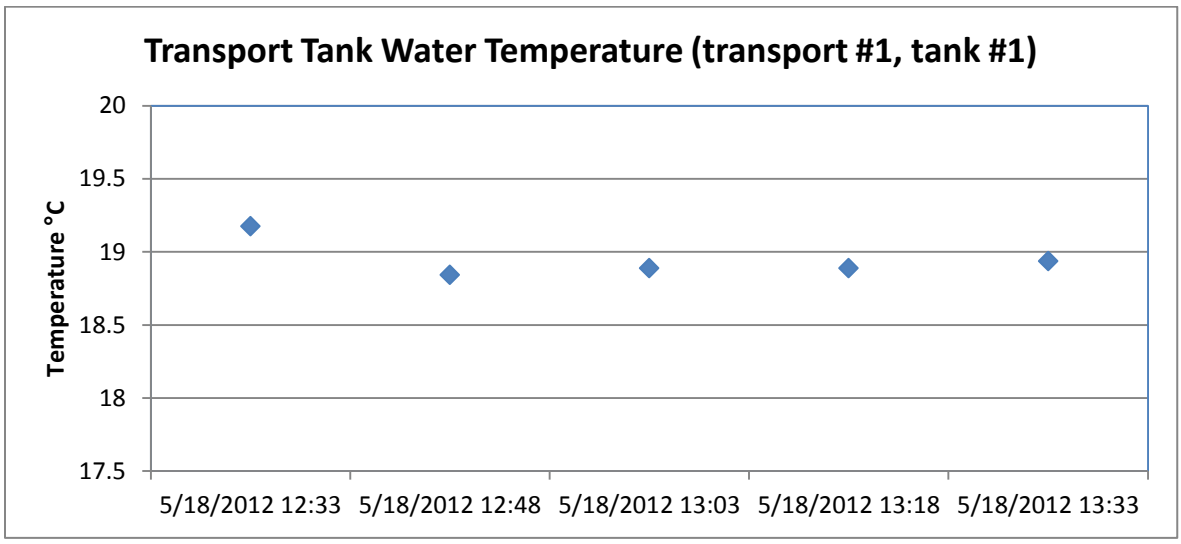

Figure A3-13. Transport tank water temperature during transport #1, tank #1 on May 18, 2012.

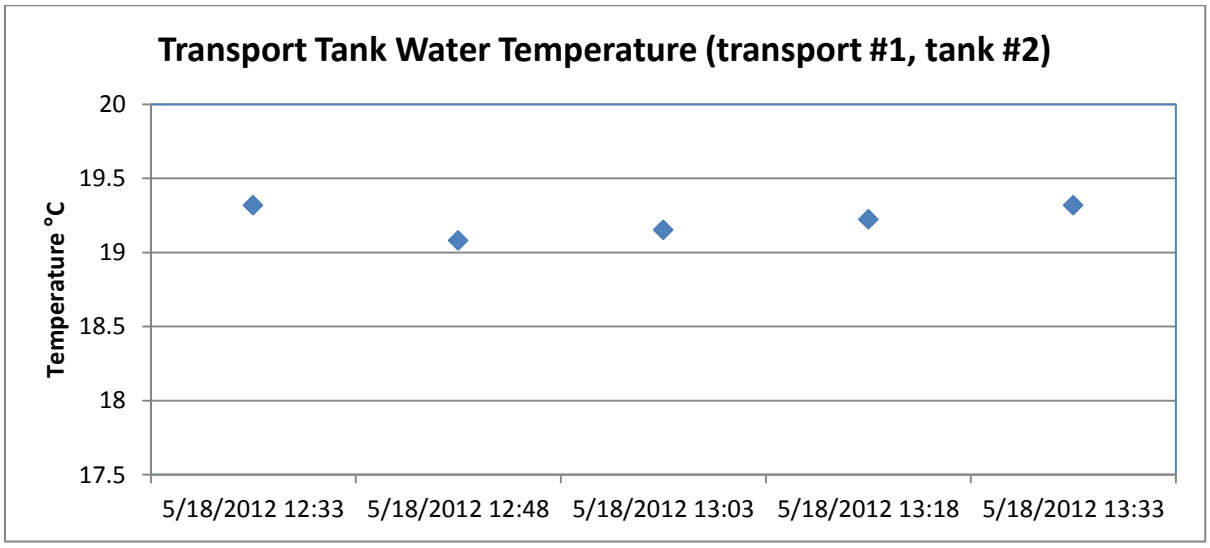

Figure A3-14. Transport tank water temperature during transport #1, tank #2 on May 18, 2012.

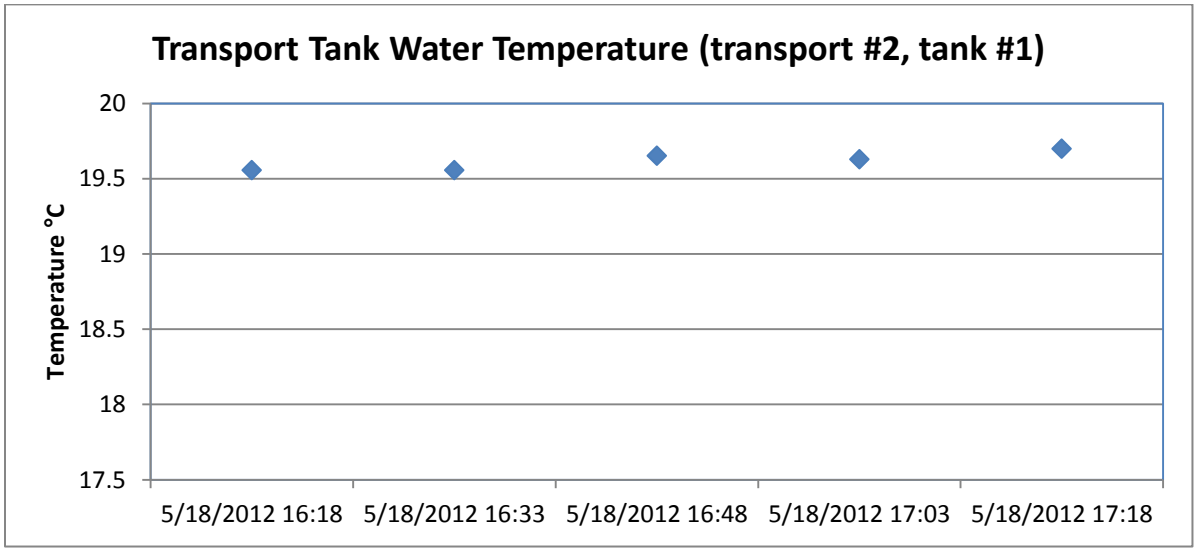

Figure A3-15. Transport tank water temperature during transport #1, tank #1 on May 18, 2012.

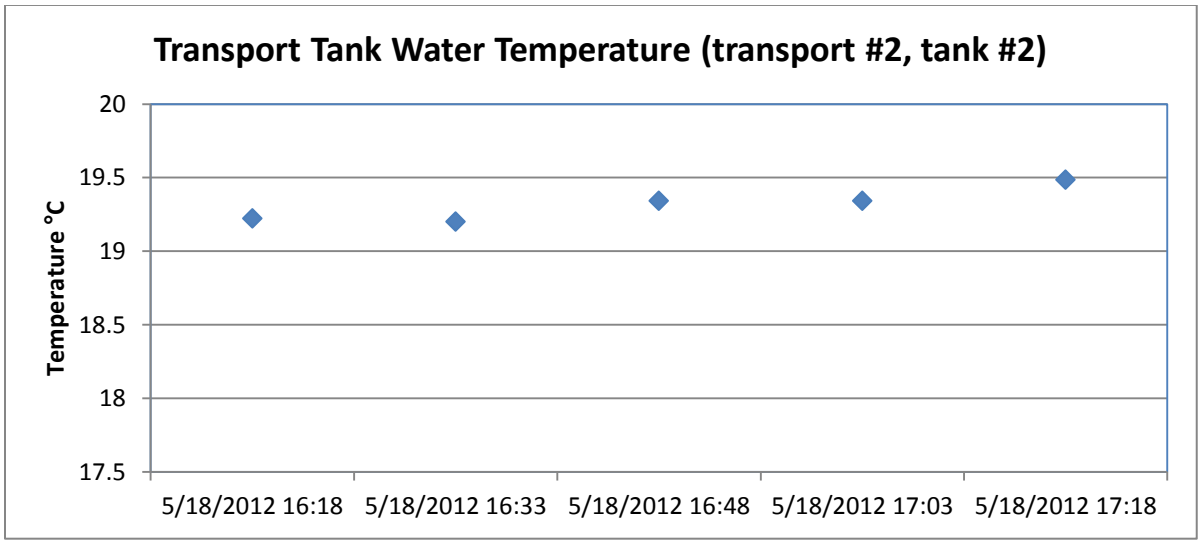

Figure A3-16. Transport tank water temperature during transport #2, tank #2 on May 18, 2012.

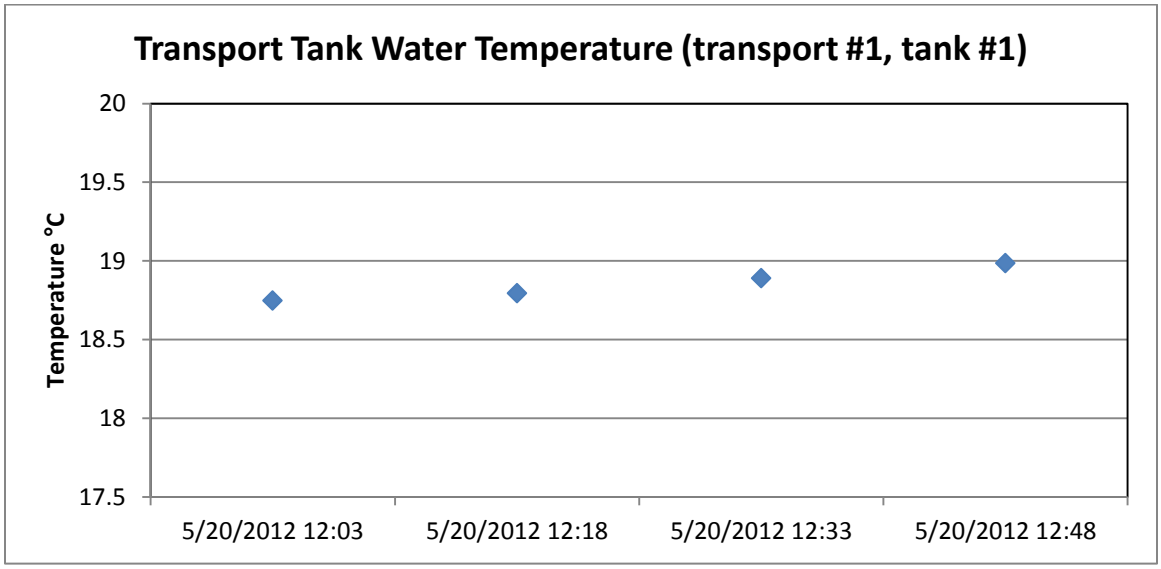

Figure A3-17. Transport tank water temperature during transport #1, tank #1 on May 20, 2012.

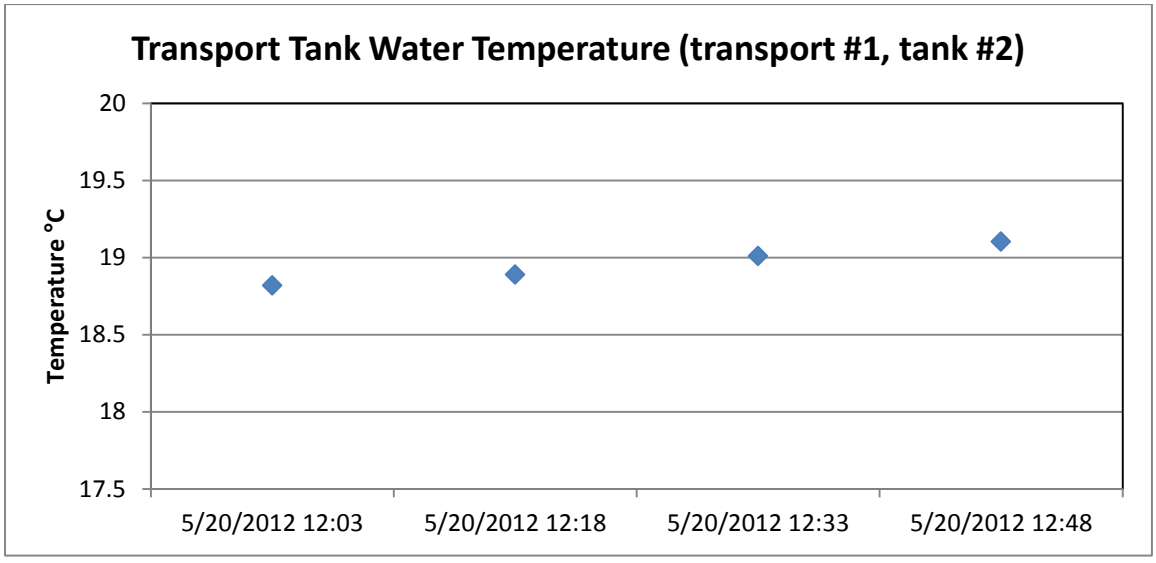

Figure A3-18. Transport tank water temperature during transport #1, tank #2 on May 20, 2012.

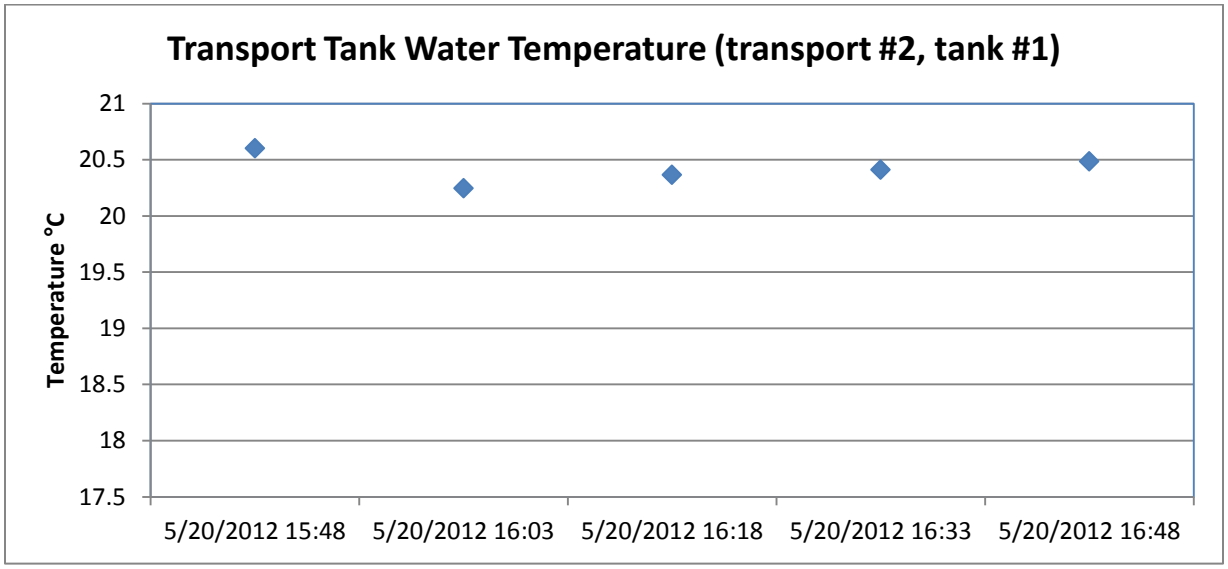

Figure A3-19. Transport tank water temperature during transport #2, tank #1 on May 20, 2012.

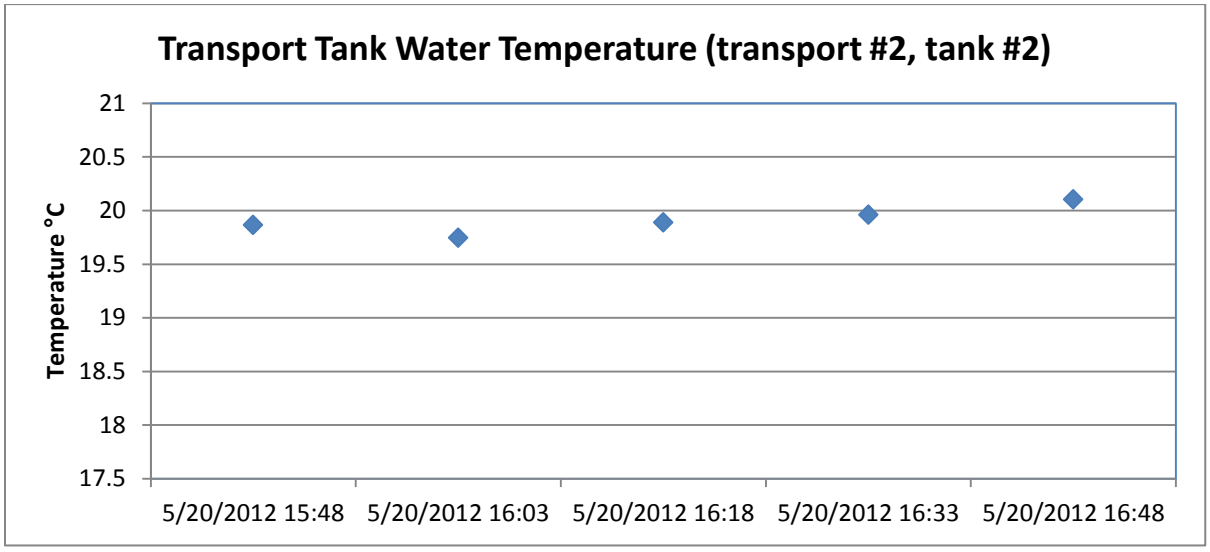

Figure A3-20. Transport tank water temperature during transport #2, tank #2 on May 20, 2012.

Appendix 4:

U.S. Fish & Wildlife Service

FY2012 Technical Report:
Pathogen screening and gill Na-K-ATPase assessment of juvenile Chinook salmon used in south delta acoustic tag studies.

J. Scott Foott

September 2012

US Fish and Wildlife Service

California-Nevada Fish Health Center

24411 Coleman Fish Hatchery Rd

Anderson, CA 96007

SUMMARY:
Pathogen testing was conducted on dummy-tag cohorts of acoustic tagged Merced River Hatchery juvenile Chinook salmon used in studies corresponding to 7 May and 23 May releases. No virus or *Renibacterium salmoninarum* infection was detected in the fish. The 23 May group had 37% prevalence of both suture abnormalities and A*eromonas – Pseudomonas* sp. infection however there was little correlation between the 2 findings. As in the past, *Tetracapsuloides bryosalmonae* infection was highly prevalent (≥ 97%) and the associated Proliferative Kidney Disease became more pronounced in the 23 May sample. No mortality occurred in the live cage populations at either sample date. Gill Na-K-ATPase data is not reported due to a problem with a key assay reagent. The combination of kidney impairment and poor suture condition of the 23 May salmon indicates that health of the two release groups was not equivalent.

Recommended citation for this report is:
Foott JS. 2012. FY2012 Technical Report: Pathogen screening and gill Na-K-ATPase assessment of juvenile Chinook salmon used in south delta acoustic tag studies. U.S. Fish & Wildlife Service California-Nevada Fish Health Center, Anderson, CA. Available: http://www.fws.gov/canvfhc/reports.asp.

INTRODUCTION

As a component of the 2012 Chinook salmon survival studies on reach-specific survival and distribution of migrating Chinook salmon in the San Joaquin River and delta, the CA-NV Fish Health Center conducted a general pathogen screening and smolt physiological assessment. The health and physiological condition of the study fish can help explain their performance and survival during the studies. Pathogen screenings during past VAMP studies using Merced River Hatchery (MRH) Chinook have regularly found infection with the myxozoan parasite *Tetracapsuloides bryosalmonae*, the causative agent of Proliferative Kidney Disease (PKD). This parasite has been shown to cause mortality in Chinook salmon with increased mortality and faster disease progression in fish at higher water temperatures (Ferguson 1981; Foott et al. 2007). The objectives of this project were to survey the juvenile Chinook salmon used for the studies for specific fish pathogens including *Tetracapsuloides bryosalmonae* and assess smolt development from gill Na^+ - K^+- ATPase activity.

METHODS

Prior to the 7 May and 23 May sample, 30 juvenile salmon were held within live cages for approximately 48h in the San Joaquin River at Durham Ferry. These fish were surgically-implanted with a dummy tag similar in size to the acoustic tag of release cohorts. Fish were evaluated for gill and skin condition (including suture) and tissues collected for assays. A grading scale ranging 0-3 was used to score inflammation or ulceration of tissue at the suture location and openness of the surgical incision (based on training session by Cramer Fish Sciences attended by J. Day).

> 0: Clean, completely closed and healed incision with taut suture. No external indication of pulling of tissue or inflammation.
>
> 1: Mostly closed, but not healed incision. Minor petechial hemorrhage.
>
> 2: Incision more than half open, and not healed. Inflammation present over more than half the suture area.
>
> 3: Incision completely open. Severely inflamed tissue surrounding and/or pushing out from incision site. Severe hemorrhaging extending equal to or greater than the length of the incision site. Suture may be lost entirely or embedded within inflamed tissue. Necrotic tissue visible.

Gill lamellae were collected first into SEI buffer and frozen on dry ice. Gill Na^+/K^+-Adenosine Triphosphatase (ATPase) activity was assayed by the method of McCormick (1993). Kidney was collected aseptically and inoculated onto brain-heart infusion agar. Bacterial isolates were screened by standard microscopic and biochemical tests (USFWS and AFS-FHS 2010). *Renibacterium salmoninarum* (bacteria that causes bacterial kidney disease) was screened by fluorescent antibody test (FAT) of kidney imprints. Three fish pooled samples of kidney and spleen were inoculated onto EPC and CHSE-214 cell lines held at 15°C for 21 d (USFWS and AFS-FHS 2010). The gill, liver, intestine and posterior kidney were rapidly removed from the fish and immediately fixed in Davidson's fixative, processed for 5 µm paraffin sections and stained with

hematoxylin and eosin (Humason 1979). Infections of the myxozoan parasite, *T. bryosalmonae,* were rated for intensity of parasite infection and associated tissue inflammation (Proliferative Kidney Disease). Intensity of infection was rated as none (zero), low (<10), moderate (11-30) or high (>30) based on number of *T. bryosalmonae* trophozoites observed in the kidney section. Severity of kidney inflammation (PKD) was rated as normal, focal, multifocal or diffuse.

RESULTS AND DISCUSSION

All salmon were alive at the time of sample collection for both dates. Suture condition of 23 May fish was judged to be poor (11 of 30 fish with #2 or 3 ratings). Several sutures were observed on the pelvic girdle. All sutures in the 7 May group were intact and showed no hemorrhage.

The prevalence of systemic bacterial infection (A*eromonas – Pseudomonas* sp. (aquatic bacteria clade) was also 37% in the 23 May group however there was little association with suture hemorrhage (only 4 of 11 fish with hemorrhaged sutures had bacterial infections). No virus or *Renibacterium salmoninarum* infection was detected in the fish (Table 1). *Tetracapsuloides bryosalmonae* was seen in ≥ 97% of the kidney sections from both sample groups (Table 1).

Table A4-1. Prevalence of infection (number positive / total sample) for systemic bacteria (AP= *Aeromonas* or *Pseudomonas sp.)*, *R. salmoninarum* by direct fluorescent antibody test (Rsal-DFAT), virus, and *T. bryosalmonae* observed in kidney sections.

Sample date	Bacteria	Rsal - DFAT	Virus	*T.byrosalmonae*
7 May	1 / 30 (3) AP	0 / 29	0 / 10 (3p)	29 / 30 (97)
23 May	11 / 30 (37) AP	0 / 30	0 / 10 (3p)	30 / 30 (100)

The *T. bryosalmonae* infection was judged to be at an early state in the 7 May sample fish. High numbers of the parasites were seen in both groups however kidney inflammation was markedly worse in the 23 May fish (Fig. 1 and 2). Swollen kidneys and spleens were also observed in the 23 May group. Overt anemia (pale gills) was not seen in any salmon on either collection date. The systemic nature of the infection was reflected in the occurrence of the parasite in multiple tissues (spleen, visceral adipose capillaries, liver sinuses, and kidney) including blood vessels within the gill (Fig. 3). One 7 May gill section contained two *Ichthyophthirius multifilii* trophozoites however there was little tissue response. Liver hepatocytes showed little glycogen or fat content in both sample groups possibly reflective of low feed rate. No gill Na-K-ATPase data is reported due to abnormal kinetic profiles. The ADP standard curve was normal which indicates that the majority of enzymes and co-factors were functional. The pH and magnesium conditions were also normal for the assay. We suspect that the recently purchased Sigma Chemical Adenosine TriPhosphate was faulty as this nucleotide is the substrate for the ouabain-sensitive gill Na-K-ATPase enzyme.

The advanced proliferative kidney disease, increased prevalence of systemic bacteria, and hemorrhaged sutures observed in the 23 May salmon suggests that the two release groups were not equivalent in health condition. The impact on immediate (1-3 days) post-release survival of these impairments on 23 May salmon is likely to be limited however longer term survival and swimming performance could be reduced. Past work on PKD effects on smolt performance have shown that severe kidney inflammation and anemia are associated with impaired swimming and saltwater adaptation (Foott et al. 2007 and 2008).

Figure A4-1. Prevalence of *T. byrosalmonae* intensity ratings for Chinook salmon sampled on 7 and 23 May. Intensity of *T. byrosalmonae* infection observed in kidney section rated as none (0), low (<10), moderate (11-30), and high (>30). Numbers over ratings are prevalence data. Majority of parasites observed in the 7 May kidneys were found in the sinuses indicating an early stage of infection.

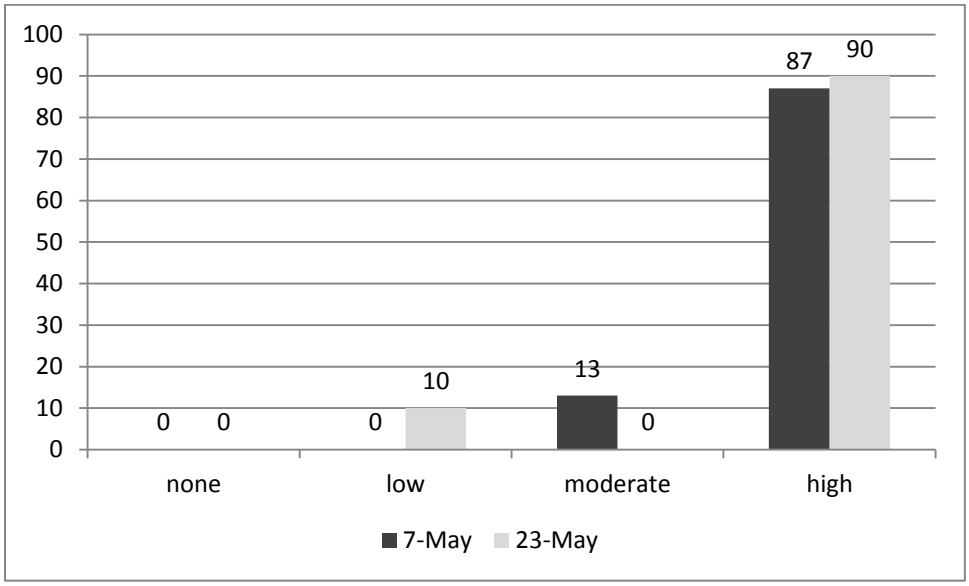

Figure A4-2. Prevalence of proliferative kidney disease ratings for Chinook salmon sampled on 7 and 23 May. Severity of kidney inflammation rated as normal, focal, multifocal, or diffuse. Numbers over ratings are prevalence data.

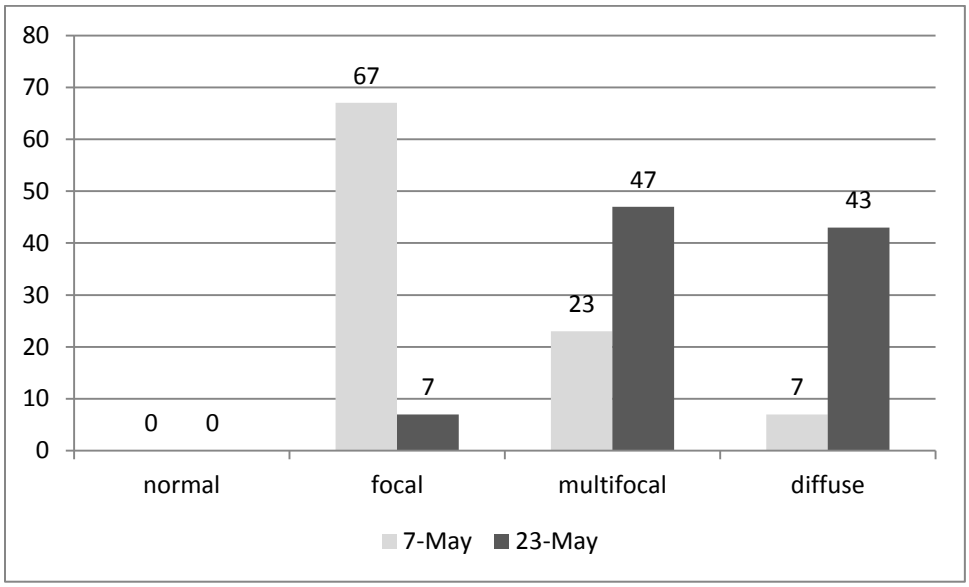

Figure A4-3. Micrograph of *T. byrosalmonae* (arrow) within gill blood vessel.

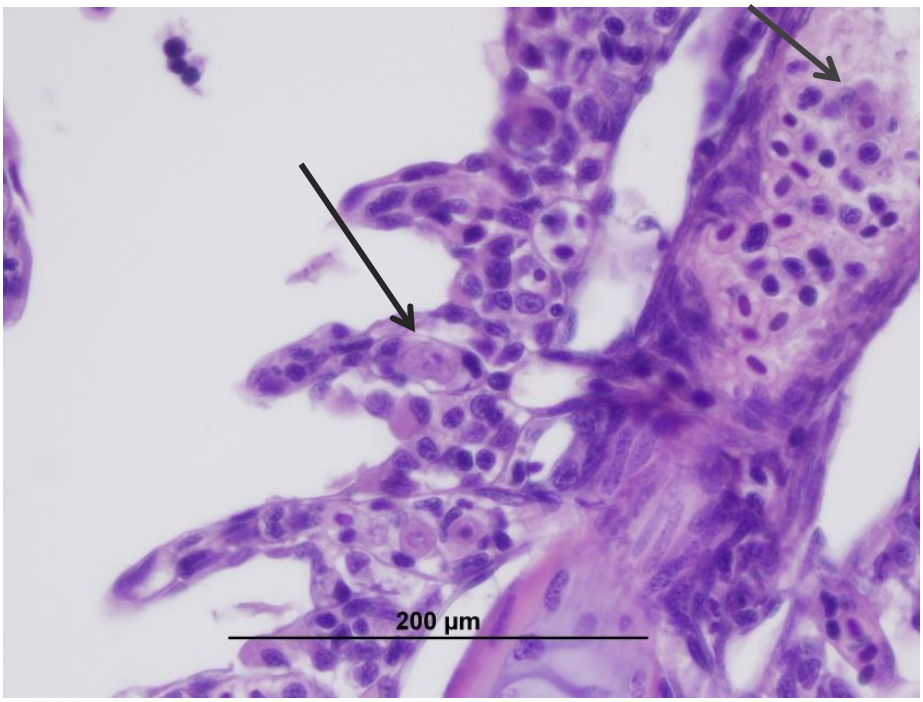

Figure A4-4. Suture condition rating 2 (exposed edge with hemorrhage) in 23 May salmon.

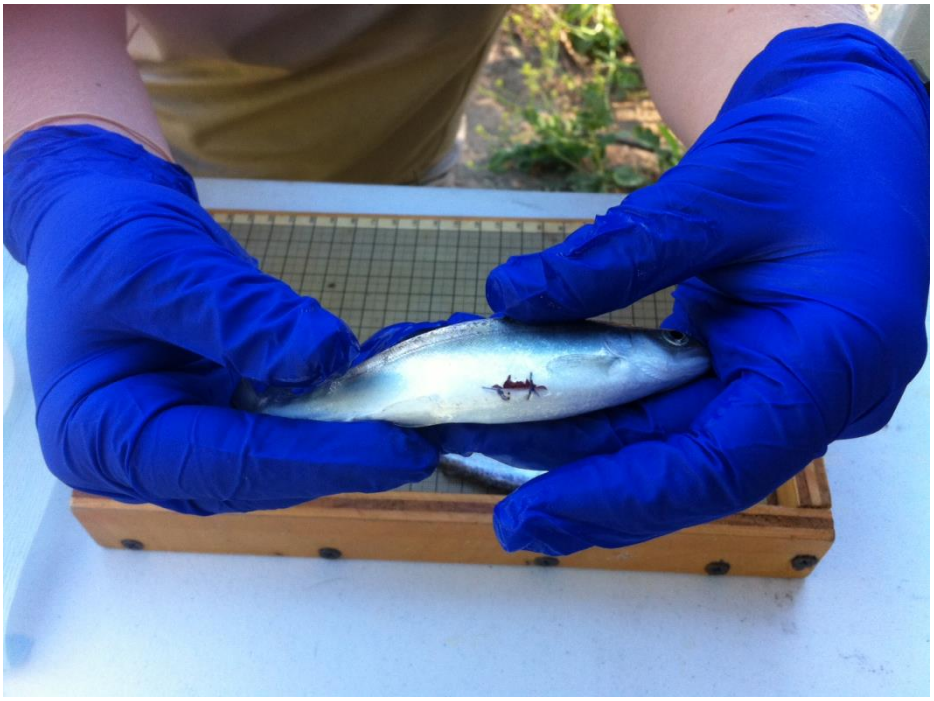

ACKNOWLEDGEMENTS
Ken Nichols, Anne Bolick, Kim True, and Julie Day with the FHC performed both field and laboratory work on this project and biologists with the USFWS Stockton FWO provided access to the live cages at Durham Ferry.

REFERENCES

Foott JS and R Stone. 2008. FY 2008 Investigational report: Evaluation of sonic tagged Chinook juveniles used in the 2008 VAMP study for delayed mortality and saltwater survival – effects of Proliferative Kidney Disease. US Fish and Wildlife Service, California-Nevada Fish Health Center, Anderson, CA. Available: http://www.fws.gov/canvfhc/reports.asp (September 2010).

Foott JS, R Stone and K Nichols. 2007. Proliferative Kidney Disease (*Tetracapsuloides bryosalmonae*) in Merced River Hatchery juvenile Chinook salmon: mortality and performance impairment in 2005 smolts. California Fish and Game 93: 57-76.

Ferguson, HW. 1981. The effects of water temperature on the development of Proliferative Kidney Disease in rainbow trout, *Salmo gairdneri* Richardson. Journal of Fish Disease 4: 175-177.

Humason GL. 1979. Animal Tissue Techniques, 4th edition. W H Freeman and Co., San Francisco.

McCormick SD. 1993. Methods for Nonlethal Gill Biopsy and Measurement of Na^+, K^+-ATPase Activity. Canadian Journal of Fisheries and Aquatic Sciences. 50: 656-658.

USFWS and AFS-FHS (U.S. Fish and Wildlife Service and American Fisheries Society-Fish Health Section). 2010. Standard procedures for aquatic animal health inspections. *In* AFS-FHS. FHS blue book: suggested procedures for the detection and identification of certain finfish and shellfish pathogens, 2010 edition. AFS-FHS, Bethesda, Maryland.

Appendix 5. Survival Model Parameters

Table A5-1. Definitions of parameters used in the release-recapture survival model; full or reduced model, or both, is specified. Parameters used only in particular submodels are noted.

Parameter	Model	Definition
S_{A2}	Both	Probability of survival from Durham Ferry Downstream (DFD) to Banta Carbona (BCA)
S_{A3}	Both	Probability of survival from Banta Carbona (BCA) to Mossdale (MOS)
S_{A4}	Both	Probability of survival from Mossdale (MOS) to Lathrop (SJL) or Old River East (ORE)
S_{A5}	Both	Probability of survival from Lathrop (SJL) to Garwood Bridge (SJG)
S_{A6}	Both	Probability of survival from Garwood Bridge (SJG) to Navy Drive Bridge (SJNB)
S_{A7}	Both	Probability of survival from Navy Drive Bridge (SJNB) to MacDonald Island (MAC) or Turner Cut (TCE/TCW)
$S_{A7,G2}$	Both	Overall survival from Navy Drive Bridge (SJNB) to Chipps Island (MAE/MAW) (derived from Submodel I)
$S_{A8,G2}$	Both	Overall survival from MacDonald Island (MAC) to Chipps Island (MAE/MAW) (Submodel I)
S_{B1}	Full	Probability of survival from Old River East (ORE) to Old River South (ORS)
$S_{B2,G2}$	Reduced	Overall survival from Old River South (ORS) to Chipps Island (MAE/MAW) (derived from Submodel I)
$S_{F1,G2}$	Both	Overall survival from Turner Cut (TCE/TCW) to Chipps Island (MAE/MAW) (Submodel I)
$\phi_{A1,A0}$	Full	Joint probability of moving from Durham Ferry release site upstream toward DFU, and surviving to DFU
$\phi_{A1,A2}$	Both	Joint probability of moving from Durham Ferry release site downstream toward DFD, and surviving to DFD
$\phi_{A1,A3}$	Both	Joint probability of moving from Durham Ferry release site downstream toward BCA, and surviving to BCA; = $\phi_{A1,A2}\, s_{A2}$
$\phi_{A8,A9}$	Both	Joint probability of moving from MAC toward MFE/MFW, and surviving from MAC to MFE/MFW (Submodel II)
$\phi_{A8,B3}$	Full	Joint probability of moving from MAC toward OR4, and surviving from MAC to OR4 (Submodel II)
$\phi_{A8,C2}$	Full	Joint probability of moving from MAC toward MR4, and surviving from MAC to MR4 (Submodel II)
$\phi_{A8,GH}$	Full	Joint probability of moving from MAC directly toward Jersey Point (JPE/JPW) or False River (FRE/FRW) without passing Highway 4 sites, and surviving JPE/JPW or FRE/FRW (Submodel II)
$\phi_{A8,G1}$	Reduced	Joint probability of moving from MAC toward Jersey Point (JPE/JPW) and surviving to JPE/JPW (Submodel II); = $\phi_{A8,GH}\psi_{G1(A)}$
$\phi_{A9,B3}$	Full	Joint probability of moving from MFE/MFW toward OR4, and surviving from MFE/MFW to OR4 (Submodel II)
$\phi_{A9,C2}$	Full	Joint probability of moving from MFE/MFW toward MR4, and surviving from MFE/MFW to MR4 (Submodel II)
$\phi_{A9,GH}$	Full	Joint probability of moving from MFE/MFW directly toward Jersey Point (JPE/JPW) or False River (FRE/FRW) without passing Highway 4 sites, and surviving to JPE/JPW or FRE/FRW (Submodel II)
$\phi_{A9,G1}$	Reduced	Joint probability of moving from MFE/MFW toward Jersey Point (JPE/JPW) and surviving to JPE/JPW (Submodel II); = $\phi_{A9,GH}\psi_{G1(A)}$
$\phi_{B1,B2}$	Reduced	Joint probability of moving from ORE toward ORS, and surviving from ORE to ORS; = $S_{B1}\psi_{B2}$
$\phi_{B2,B3}$	Full	Joint probability of moving from ORS toward OR4, and surviving from ORS to OR4
$\phi_{B2,C2}$	Full	Joint probability of moving from ORS toward MR4, and surviving from ORS to MR4
$\phi_{B2,D1}$	Full	Joint probability of moving from ORS toward RGU, and surviving from ORS to RGU
$\phi_{B2,E1}$	Full	Joint probability of moving from ORS toward CVP, and surviving from ORS to CVP
$\phi_{B3,D1}$	Full	Joint probability of moving from OR4 toward RGU and surviving from OR4 to RGU conditional on coming from lower San Joaquin River (Submodel II)

Table A5-1. (Continued)

Parameter	Model	Definition
$\phi_{B3,E1}$	Full	Joint probability of moving from OR4 toward CVP, and surviving from OR4 to CVP, conditional on coming from lower San Joaquin River (Submodel II)
$\phi_{B3,GH(A)}$	Full	Joint probability of moving from OR4 toward Jersey Point (JPE/JPW) or False River (FRE/FRW), and surviving from OR4 to JPE/JPW or FRE/FRW (Submodel II [route A])
$\phi_{B3,GH(B)}$	Full	Joint probability of moving from OR4 toward Jersey Point (JPE/JPW) or False River (FRE/FRW), and surviving from OR4 to JPE/JPW or FRE/FRW (Submodel I [route B])
$\phi_{C1,B3}$	Full	Joint probability of moving from MRH toward OR4, and surviving from MRH to OR4
$\phi_{C1,C2}$	Full	Joint probability of moving from MRH toward MR4, and surviving from MRH to MR4
$\phi_{C1,D1}$	Full	Joint probability of moving from MRH toward RGU, and surviving from MRH to RGU
$\phi_{C1,E1}$	Full	Joint probability of moving from MRH toward CVP, and surviving from MRH to CVP
$\phi_{C2,D1}$	Full	Joint probability of moving from MR4 toward RGU and surviving from MR4 to RGU conditional on coming from lower San Joaquin River (Submodel II)
$\phi_{C2,E1}$	Full	Joint probability of moving from MR4 toward CVP, and surviving from MR4 to CVP, conditional on coming from lower San Joaquin River (Submodel II)
$\phi_{C2,GH(A)}$	Full	Joint probability of moving from MR4 toward Jersey Point (JPE/JPW) or False River (FRE/FRW), and surviving from MR4 to JPE/JPW or FRE/FRW (Submodel II [route A])
$\phi_{C2,GH(B)}$	Full	Joint probability of moving from MR4 toward Jersey Point (JPE/JPW) or False River (FRE/FRW), and surviving from MR4 to JPE/JPW or FRE/FRW (Submodel I [route B])
$\phi_{D1,D2}$	Full	Joint probability of moving from RGU toward RGD, and surviving from RGU to RGD (equated between submodels I and II)
$\phi_{D2,G2}$	Full	Joint probability of moving from RGD toward Chipps Island (MAE/MAW) and surviving from RGU to MAE/MAW (equated between submodels I and II)
$\phi_{E1,E2}$	Full	Joint probability of moving from CVP toward CVPtank, and surviving from CVP to CVPtank (equated between submodels I and II)
$\phi_{E2,G2}$	Full	Joint probability of moving from CVPtank toward Chipps Island (MAE/MAW) and surviving from CVPtank to MAE/MAW (equated between submodels I and II)
$\phi_{F1,B3}$	Full	Joint probability of moving from TCE/TCW toward OR4, and surviving from TCE/TCW to OR4 (Submodel II)
$\phi_{F1,C2}$	Full	Joint probability of moving from TCE/TCW toward MR4, and surviving from TCE/TCW to MR4 (Submodel II)
$\phi_{F1,GH}$	Full	Joint probability of moving from TCE/TCW directly toward Jersey Point (JPE/JPW) or False River (FRE/FRW) without passing Highway 4 sites, and surviving to JPE/JPW or FRE/FRW (Submodel II)
$\phi_{F1,G1}$	Reduced	Joint probability of moving from TCE/TCW toward Jersey Point (JPE/JPW) and surviving to JPE/JPW (Submodel II); = $\phi_{F1,GH}\psi_{G1(A)}$
$\phi_{G1,G2(A)}$	Both	Joint probability of moving from JPE/JPW toward Chipps Island (MAE/MAW), and surviving to MAE/MAW (Submodel II [route A])
$\phi_{G1,G2(B)}$	Full	Joint probability of moving from JPE/JPW toward Chipps Island (MAE/MAW), and surviving to MAE/MAW (Submodel I [route B])
ψ_{A1}	Both	Probability of remaining in the San Joaquin River at the head of Old River; = 1 - ψ_{B1}
ψ_{A2}	Both	Probability of remaining in the San Joaquin River at the junction with Turner Cut; = 1 - ψ_{F2}
ψ_{B1}	Both	Probability of entering Old River at the head of Old River; = 1 - ψ_{A1}
ψ_{B2}	Full	Probability of remaining in Old River at the head of Middle River; = 1 - ψ_{C2}
ψ_{C2}	Full	Probability of entering Middle River at the head of Middle River; = 1 - ψ_{B2}
ψ_{F2}	Both	Probability of entering Turner Cut at the junction with the San Joaquin River; = 1 - ψ_{A2}
$\psi_{G1(A)}$	Full	Probability of moving downriver in the San Joaquin River at the Jersey Point/False River junction (Submodel II [route A]); = 1 - $\psi_{H1(A)}$
$\psi_{G1(B)}$	Full	Probability of moving downriver in the San Joaquin River at the Jersey Point/False River junction (Submodel I [route B]); = 1 - $\psi_{H1(B)}$

Table A5-1. (Continued)

Parameter	Model	Definition
$\psi_{H1(A)}$	Full	Probability of entering False River at the Jersey Point/False River junction (Submodel II [route A]); = 1 - $\psi_{G1(A)}$
$\psi_{H1(B)}$	Full	Probability of entering False River at the Jersey Point/False River junction (Submodel I [route B]); = 1 - $\psi_{G1(B)}$
P_{A0a}	Full	Conditional probability of detection at DFU1
P_{A0b}	Full	Conditional probability of detection at DFU2
P_{A2a}	Both	Conditional probability of detection at DFD1
P_{A2b}	Both	Conditional probability of detection at DFD2
P_{A2}	Both	Conditional probability of detection at DFD (either DFD1 or DFD2)
P_{A3}	Both	Conditional probability of detection at BCA
P_{A4}	Both	Conditional probability of detection at MOS
P_{A5}	Both	Conditional probability of detection at SJL
P_{A6}	Both	Conditional probability of detection at SJG
P_{A7}	Both	Conditional probability of detection at SJNB
P_{A8a}	Both	Conditional probability of detection at MACU
P_{A8b}	Both	Conditional probability of detection at MACD
P_{A8}	Both	Conditional probability of detection at MAC (either MACU or MACD)
P_{A9a}	Both	Conditional probability of detection at MFE
P_{A9b}	Both	Conditional probability of detection at MFW
P_{A9}	Both	Conditional probability of detection at MFE or MFW
P_{B1}	Both	Conditional probability of detection at ORE
P_{B2a}	Both	Conditional probability of detection at ORSU
P_{B2b}	Both	Conditional probability of detection at ORSD
P_{B2}	Both	Conditional probability of detection at ORS (either ORSU or ORSD)
P_{B3a}	Full	Conditional probability of detection at OR4U
P_{B3b}	Full	Conditional probability of detection at OR4D
P_{C1}	Full	Conditional probability of detection at MRH
P_{C2a}	Full	Conditional probability of detection at MR4U
P_{C2b}	Full	Conditional probability of detection at MR4D
P_{D1}	Full	Conditional probability of detection at RGU (either RGU1 or RGU2)
P_{D2a}	Full	Conditional probability of detection at RGD1
P_{D2b}	Full	Conditional probability of detection at RGD2
P_{E1}	Full	Conditional probability of detection at CVP
P_{E2}	Full	Conditional probability of detection at CVPtank
P_{F1a}	Both	Conditional probability of detection at TCE
P_{F1b}	Both	Conditional probability of detection at TCW
P_{F1}	Both	Conditional probability of detection at TCE/TCW
P_{G1a}	Both	Conditional probability of detection at JPE
P_{G1b}	Both	Conditional probability of detection at JPW

Table A5-1. (Continued)

Parameter	Model	Definition
P_{G1}	Both	Conditional probability of detection at JPE/JPW
P_{G2a}	Both	Conditional probability of detection at MAE
P_{G2b}	Both	Conditional probability of detection at MAW
P_{G2}	Both	Conditional probability of detection at MAE/MAW
P_{H1a}	Full	Conditional probability of detection at FRW
P_{H1b}	Full	Conditional probability of detection at FRE

Table A5-2. Parameter estimates (standard errors in parentheses) from reduced survival model for tagged juvenile Chinook Salmon released in 2012, excluding predator-type detections. Parameters without standard errors were estimated at fixed values in the model. Population-level estimates are from pooled release groups. Some parameters were not estimable because of sparse data.

	Release Occasion		
Parameter	1	2	Population Estimate
S_{A2}	0.90 (0.06)	0.63 (0.04)	0.79 (0.04)
S_{A3}	0.78 (0.04)	0.59 (0.03)	0.65 (0.03)
S_{A4}	0.98 (0.01)	0.89 (0.02)	0.95 (0.01)
S_{A5}	0.81 (0.02)	0.48 (0.04)	0.69 (0.02)
S_{A6}	0.85 (0.03)	0.73 (0.08)	0.82 (0.03)
S_{A7}	0.49 (0.04)	0.23 (0.06)	0.44 (0.03)
$S_{A7,G2}$	0.07 (0.02)	0	0.06 (0.01)
$S_{A8,G2}$	0.16 (0.04)	0	0.14 (0.04)
$S_{B2,G2}$	0.17 (0.15)	0	0.13 (0.12)
$S_{F1,G2}$	0	0	0
$\phi_{A1,A2}$	0.89 (0.05)	1.00 (0.06)	0.97 (0.04)
$\phi_{A1,A3}$	0.80 (0.04)	0.63 (0.03)	0.76 (0.02)
$\phi_{A8,A9}$	0.44 (0.05)	0.59 (0.16)	0.45 (0.05)
$\phi_{A8,G1}$	0.08 (0.03)	0	0.07 (0.03)
$\phi_{A9,G1}$	0.49 (0.09)	0.33 (0.19)	0.46 (0.08)
$\phi_{B1,B2}$	1	0.67 (0.27)	0.89 (0.10)
$\phi_{F1,G1}$	0	0	0
$\phi_{G1,G2(A)}$	0.54 (0.10)	0	0.52 (0.01)
ψ_{A1}	0.98 (0.01)	0.98 (0.01)	0.98 (0.01)
ψ_{A2}	0.89 (0.03)	0.84 (0.11)	0.89 (0.03)
ψ_{B1}	0.02 (0.01)	0.02 (0.01)	0.02 (0.01)
ψ_{F2}	0.11 (0.03)	0.16 (0.11)	0.11 (0.03)
P_{A2a}	[pooled]	[pooled]	[pooled]
P_{A2b}	[pooled]	[pooled]	[pooled]
P_{A2}	0.23 (0.02)	0.33 (0.03)	0.27 (0.02)
P_{A3}	0.31 (0.03)	0.80 (0.03)	0.49 (0.02)
P_{A4}	1.00 (< 0.01)	1	1.00 (< 0.01)
P_{A5}	1	1	1
P_{A6}	1	1	1
P_{A7}	0.94 (0.02)	0.92 (0.08)	0.94 (0.02)
P_{A8a}	[pooled]	0.88 (0.12)	0.94 (0.02)
P_{A8b}	[pooled]	0.78 (0.14)	0.90 (0.03)
P_{A8}	1	0.97 (0.03)	0.99 (< 0.01)
P_{A9a}	1	1	1
P_{A9b}	1	1	1
P_{A9}	1	1	1
P_{B1}	1	1	1

Table A5-2. (Continued)

Parameter	Release Occasion 1	Release Occasion 2	Population Estimate
P_{B2a}	1	[pooled]	1
P_{B2b}	0.83 (0.15)	[pooled]	1.00 (< 0.01)
P_{B2}	1	1	1
P_{F1a}	0.88 (0.12)	1	0.90 (0.09)
P_{F1b}	0.78 (0.14)	1	0.82 (0.12)
P_{F1}	0.97 (0.03)	1	0.98 (0.02)
P_{G1a}	[pooled]	1	0.96 (0.04)
P_{G1b}	[pooled]	1	0.92 (0.05)
P_{G1}	0.93 (0.07)	1	1.00 (< 0.01)
P_{G2a}	1		1
P_{G2b}	1		1
P_{G2}	1		1

Table A5-3. Parameter estimates (standard errors in parentheses) from reduced survival model for tagged juvenile Chinook Salmon released in 2012, including predator-type detections. Parameters without standard errors were estimated at fixed values in the model. Population-level estimates are from pooled release groups. Some parameters were not estimable because of sparse data.

	Release Occasion		
Parameter	1	2	Population Estimate
S_{A2}	0.87 (0.06)	0.62 (0.04)	0.77 (0.04)
S_{A3}	0.77 (0.04)	0.59 (0.03)	0.65 (0.02)
S_{A4}	0.98 (0.01)	0.90 (0.02)	0.95 (0.01)
S_{A5}	0.81 (0.02)	0.49 (0.04)	0.70 (0.02)
S_{A6}	0.86 (0.03)	0.73 (0.07)	0.82 (0.03)
S_{A7}	0.50 (0.04)	0.26 (0.06)	0.44 (0.03)
$S_{A7,G2}$	0.07 (0.02)	0	0.06 (0.01)
$S_{A8,G2}$	0.16 (0.04)	0	0.14 (0.03)
$S_{B2,G2}$	0.17 (0.15)	0	0.11 (0.11)
$S_{F1,G2}$	0	0	0
$\phi_{A1,A2}$	0.93 (0.05)	1.03 (0.06)	1.00 (0.04)
$\phi_{A1,A3}$	0.81 (0.04)	0.64 (0.03)	0.77 (0.03)
$\phi_{A8,A9}$	0.43 (0.05)	0.49 (0.14)	0.44 (0.05)
$\phi_{A8,G1}$	0.08 (0.03)	0	0.07 (0.03)
$\phi_{A9,G1}$	0.49 (0.09)	0.33 (0.19)	0.46 (0.08)
$\phi_{B1,B2}$	1	1	1
$\phi_{F1,G1}$	0	0	0
$\phi_{G1,G2(A)}$	0.54 (0.10)	0	0.52 (0.10)
ψ_{A1}	0.98 (0.01)	0.98 (0.01)	0.98 (0.01)
ψ_{A2}	0.88 (0.03)	0.86 (0.09)	0.88 (0.03)
ψ_{B1}	0.02 (0.01)	0.02 (0.01)	0.02 (0.01)
ψ_{F2}	0.12 (0.03)	0.14 (0.09)	0.12 (0.03)
P_{A2a}	[pooled]	[pooled]	[pooled]
P_{A2b}	[pooled]	[pooled]	[pooled]
P_{A2}	0.23 (0.02)	0.34 (0.03)	0.28 (0.02)
P_{A3}	0.31 (0.03)	0.80 (0.03)	0.49 (0.02)
P_{A4}	1.00 (< 0.01)	1	1.00 (< 0.01)
P_{A5}	1	1	1
P_{A6}	1	1	1
P_{A7}	0.94 (0.02)	0.93 (0.07)	0.94 (0.02)
P_{A8a}	[pooled]	0.87 (0.12)	[pooled]
P_{A8b}	[pooled]	0.64 (0.15)	[pooled]
P_{A8}	1	0.95 (0.05)	1
P_{A9a}	1	1	1
P_{A9b}	1	1	1
P_{A9}	1	1	1
P_{B1}	1	1	1

Table A5-3. (Continued)

Parameter	Release Occasion		Population Estimate
	1	2	
P_{B2a}	1	[pooled]	1
P_{B2b}	0.83 (0.15)	[pooled]	0.56 (0.17)
P_{B2}	1	1	1
P_{F1a}	0.86 (0.13)	1	0.89 (0.10)
P_{F1b}	0.60 (0.15)	1	0.67 (0.14)
P_{F1}	0.94 (0.06)	1	0.96 (0.04)
P_{G1a}	[pooled]	1	0.96 (0.04)
P_{G1b}	[pooled]	1	0.92 (0.05)
P_{G1}	0.93 (0.07)	1	1.00 (< 0.01)
P_{G2a}	1		1
P_{G2b}	1		1
P_{G2}	1		1

Appendix B. Errata from 2011 VAMP Report

In Table H-2 (page 283) of the 2011 VAMP report (SJRGA 2013), the definition for parameter $\phi_{A8,G2}$ should read “Overall survival from STN to Chipps Island (CHPE/CHPW).”

Final

An Evaluation of Juvenile Salmonid Routing and Barrier Effectiveness, Predation, and Predatory Fishes at the Head of Old River, 2009–2012

Prepared by:

California Department of Water Resources

April 2015

Final

An Evaluation of Juvenile Salmonid Routing and Barrier Effectiveness, Predation, and Predatory Fishes at the Head of Old River, 2009–2012

Prepared by:

California Department of Water Resources
1416 9th Street
Sacramento, CA 94236-001
Contact: Jacob McQuirk, P.E.
916.653.9883

April 2015

State of California
Edmund G. Brown Jr., Governor

Natural Resources Agency
John Laird, Secretary for Resources

Department of Water Resources
Mark W. Cowin, Director

Laura King Moon
Chief Deputy Director

Kasey Schimke
Asst. Director Legislative Affairs

Nancy Vogel
Asst. Director of Public Affairs

Cathy Crothers
Chief Counsel

Gary Bardini
Deputy Director

Kathie Kishaba
Deputy Director

John Pacheco
Deputy Director

Carl Torgersen
Deputy Director

Bay-Delta Office

Paul A. Marshall.....Chief

South Delta Branch

Mark A. Holderman.....Branch Chief, South Delta Branch

This report was prepared under the supervision of

Jacob McQuirk .....Chief, Temporary Barriers and Lower San Joaquin

Simon Kwan .....Senior Water Resources Engineer

Michael Cane..... Environmental Scientist

Prepared by AECOM, ICF International, and Turnpenny Horsfield Associates

ACKNOWLEDGMENTS

The report preparers wish to thank the following individuals: Sam Johnston and co-workers (Hydroacoustic Technology, Inc.) for work related to tracking acoustically tagged fishes and authorship of methods related to tracking; Mike Horn and Erwin van Nieuwenhuyse (U.S. Bureau of Reclamation) for funding and undertaking mobile hydroacoustic surveys; Trevor Kennedy and coworkers (Fishery Foundation of California) for capture and acoustic tagging of predatory fishes; Mike Dempsey, Mike Baldwin, and Mike Burns (California Department of Water Resources) for provision and collation of physical data from the California Data Exchange Center; Dennis Rondorf (U.S. Geological Survey), Cynthia LeDoux-Bloom (AECOM), Brad Cavallo and Steve Zeug (Cramer Fish Sciences), Chuck Hanson (Hanson Environmental, Inc.), Sean Hayes (National Marine Fisheries Service), and Pat Brandes (U.S. Fish and Wildlife Service) for document review; Javier Miranda, Kevin Clark, and Cynthia LeDoux-Bloom (California Department of Water Resources) and Marty Gingras (California Department of Fish and Wildlife) for input during study design and planning; Jonathan Speegle (U.S. Fish and Wildlife Service) for provision of seine and trawl survey data; Louise Conrad (California Department of Water Resources) for provision of electrofishing data; and Dennis Westcot (San Joaquin River Group Authority) for permission to reproduce materials included in Appendix I.

In addition to these individuals the report preparers thank the following agencies for providing the permits and approvals necessary to implement the multi-year studies reported in this report: California Department of Fish and Wildlife; State Water Resources Control Board; U.S. Army Corps of Engineers; U.S. Fish and Wildlife Service; and National Marine Fisheries Service.

TABLE OF CONTENTS

TABLE OF CONTENTS

continued **Page**

TABLE OF CONTENTS

continued **Page**

Appendices

TABLE OF CONTENTS

continued **Page**

Figures

TABLE OF CONTENTS

continued **Page**

TABLE OF CONTENTS

continued **Page**

TABLE OF CONTENTS

continued **Page**

TABLE OF CONTENTS

continued **Page**

TABLE OF CONTENTS

continued **Page**

TABLE OF CONTENTS

continued **Page**

Tables

TABLE OF CONTENTS

continued **Page**

TABLE OF CONTENTS

continued **Page**

TABLE OF CONTENTS

continued **Page**

ACRONYMS AND OTHER ABBREVIATIONS

.RAT	raw acoustic tag file
.TAT	track acoustic tag file
°C	degrees Celsius
2D	two-dimensional
3D	three-dimensional
6YSS	Six-Year Steelhead Study
ACV	average channel velocity
AIC	Akaike's Information Criterion
AIC_c	Akaike's Information Criterion corrected for small sample sizes
ANOVA	analysis of variance
ATR	acoustic tag receiver
ATTS	Acoustic Tag Tracking System
BAFF	bio-acoustic fish fence
BDCP	Bay Delta Conservation Plan
BL/s	body lengths per second
$\hat{c}$	variance inflation factor
CCW	counter-clockwise
CDEC	California Data Exchange Center
CFR	Code of Federal Regulations
cfs	cubic feet per second
CIMIS	California Irrigation Management Information System
cm	centimeters
cm/s	centimeters per second
CV	Central Valley
CVP	Central Valley Project
dB	decibels
D_E	deterrence efficiency
Delta	Sacramento–San Joaquin Delta
DGPS	Differential Global Positioning System
DL2D	two-dimensional velocity fields from DL-ADCP data
DL-ADCP	downward-looking acoustic Doppler current profiler
DPS	distinct population segment
DWR	California Department of Water Resources
ESA	federal Endangered Species Act

ACRONYMS AND OTHER ABBREVIATIONS

ESU	evolutionarily significant unit
FL	fork length
FR	*Federal Register*
GIS	geographic information system
GLM	generalized linear model
GPS	global positioning system
HD	Hydrophone
HOR	Head of Old River
HOR study site	Head of Old River, at the divergence of the San Joaquin and Old Rivers
HORB	Head of Old River Barrier
HR	High Residency
HTI	Hydroacoustic Technology Inc.
Hz	Hertz (cycles per second)
ID	identification
IML	Intense Modulated Light
IPLW	inverse path length weighting
J/g	Joules per gram
kg	kilogram
km	kilometer
kHz	kilohertz
LSZ	Low Salinity Zone
m	meter
m/s	meters per second
m^3/s	cubic meters per second
mm	millimeter
MSD	San Joaquin River at Mossdale
n	number of samples
NAVD	North American Vertical Datum of 1988
NFH	National Fish Hatchery
NMFS	National Marine Fisheries Service
NOAA	National Oceanic and Atmospheric Association
NTU	nephelometric turbidity units
OCAP	*Long-Term Central Valley Project and State Water Project Operations Criteria and Plan*
O_E	overall efficiency

ACRONYMS AND OTHER ABBREVIATIONS

OH1	Old River at Head
PAR	photosynthetically active radiation
PCC	percent correctly classified
P_E	protection efficiency
$QAIC_c$	the quasi-likelihood equivalent of Akaike's Information Criterion, corrected for small sample sizes
RBDD	Red Bluff Diversion Dam
Reclamation	U.S. Bureau of Reclamation
ROC	receiver operating characteristic
RPA	Reasonable and Prudent Alternative
SD	standard deviation
SE	standard error
SFPF	Skinner Delta Fish Protective Facility
SJL	San Joaquin River at Lathrop
SJR	San Joaquin River
SJRRP	San Joaquin River Restoration Program
SL2D	two-dimensional velocity fields from SL-ADCP data
SL-ADCP	side-looking acoustic Doppler current profiler
SWP	State Water Project
TFCF	Tracy Fish Collection Facility
TL	total length
Ua	main channel velocity
U-crit	critical swimming speed
Ue	fish escape velocity
Us	sweeping velocity
USFWS	U.S. Fish and Wildlife Service
UTC	Universal Coordinated Time
UTM	Universal Transverse Mercator
VAMP	Vernalis Adaptive Management Program

EXECUTIVE SUMMARY

ES.1 INTRODUCTION

ES.1.1 BACKGROUND AND PURPOSE

The California Department of Water Resources (DWR) and the U.S. Bureau of Reclamation (Reclamation) manage the State Water Project (SWP) and Central Valley Project (CVP), respectively, and are charged to do so in a manner that maintains the survival of anadromous salmonids subject to the terms of the National Marine Fisheries Service's (NMFS) 2009 Biological Opinion (BO) and 2011 amendments regarding the *Long-Term Central Valley Project and State Water Project Operations Criteria and Plan* (OCAP). Action IV.1.3 of the NMFS's 2009 BO instructs these agencies to "consider engineering solutions to further reduce diversion of emigrating juvenile salmonids to the interior and southern Delta, and reduce exposure to CVP and SWP export facilities." Specifically, one objective of Action IV.1.3 is to "prevent emigrating salmonids from entering channels in the south Delta (e.g., Old River, Turner Cut) that increase entrainment risk to Central Valley steelhead migrating from the San Joaquin River through the Delta."

Returning adult fish of the Distinct Population Segment (DPS) of California Central Valley steelhead (*Oncorhynchus mykiss*) and Central Valley fall-run Chinook salmon (*O. tshawytscha*) utilize the San Joaquin River and its connecting interior and south Sacramento-San Joaquin Delta (Delta) tributaries during their upstream spawning migration, while juveniles use these waterways to move downstream during their emigration to the Pacific Ocean. Increased susceptibility to entrainment and predation at DWR's and Reclamation's water export facilities has been associated with juvenile salmonids moving into Old River in comparison to those juveniles remaining in the mainstem of the San Joaquin River (Holbrook et al. 2009; SJRGA 2011). In an effort to reduce the movement of juvenile salmonids into Old River, engineering solutions (e.g., barriers) have been tested at the Head of Old River (HOR) pursuant to Action IV.1.3 of the NMFS BO. While a seasonal barrier in the fall has been part of California's protective fish management measures since 1968 (Hallock et al. 1970), deployment of a springtime barrier is more recent at this location (beginning in 1992) and uncertainties remain about its performance and effectiveness.

The purpose of this report is to contribute to the required BO Action IV.1.3 by evaluating and summarizing the effects of the non-physical barrier (2009, 2010), no barrier (2011), and physical barrier (2012) treatments and assess their effectiveness at retaining juvenile salmonids in the mainstem San Joaquin River. In addition to supporting Action IV.1.3, this report also provides critical information that improves understanding of how juvenile salmonids and predatory fish behave in the vicinity of the HOR and how effectively the tested barriers protect juvenile salmonids. This information can be used to improve barrier performance. The analyses included in the report focus on the barrier treatment effectiveness for juvenile salmonid route fate as influenced by the abiotic factors of ambient light level, water temperature, discharge, water velocity and turbidity. Additionally, predatory fish densities and predator fish interactions with the barrier treatments and juvenile salmonids were evaluated. Recommendations for future analyses and studies are identified.

ES.1.2 PHYSICAL PARAMETERS AND BARRIERS EVALUATION

The studies presented in this report were conducted during the spring (late April to May/June) of 2009–2012. San Joaquin River discharge (i.e., flow) varied among years. Discharge was lowest in 2009 and highest in 2011, and in

the intermediate years, 2012 was less than in 2010 (Figure ES-1). The official water year classifications based on May 1 runoff forecasts were described as dry in 2009 and 2012, above normal in 2010, and wet in 2011 (State of California 2013).

In 2009 and 2010, a non-physical barrier (Bio-Acoustic Fish Fence [BAFF], Fish Guidance Systems Limited, Southampton, United Kingdom) was installed at the HOR. The BAFF comprised an acoustic deterrent stimulus enclosed within a bubble curtain and illuminated by strobe lights. In 2011, high-flow conditions precluded installing a barrier treatment. In 2012, an eight-culvert physical rock barrier was installed.

Discharge and barrier treatment influenced the proportion of San Joaquin River flow that entered Old River. In 2009, low discharge coupled with the resultant relatively strong tidal influence, including many flow reversals in the San Joaquin River and the non-physical barrier treatment caused a high proportion of discharge to enter Old River (0.6 to 0.8 [i.e., 60-80%] of total San Joaquin River flow at the Old River divergence). By contrast, the proportion of discharge entering Old River was lower, about 0.45 to 0.55 in 2010 (non-physical barrier) and 2011 (no barrier). In 2012, discharge proportion was recorded at 0.2 or less, demonstrating the effect of the presence of the rock barrier treatment (Figure ES-1).

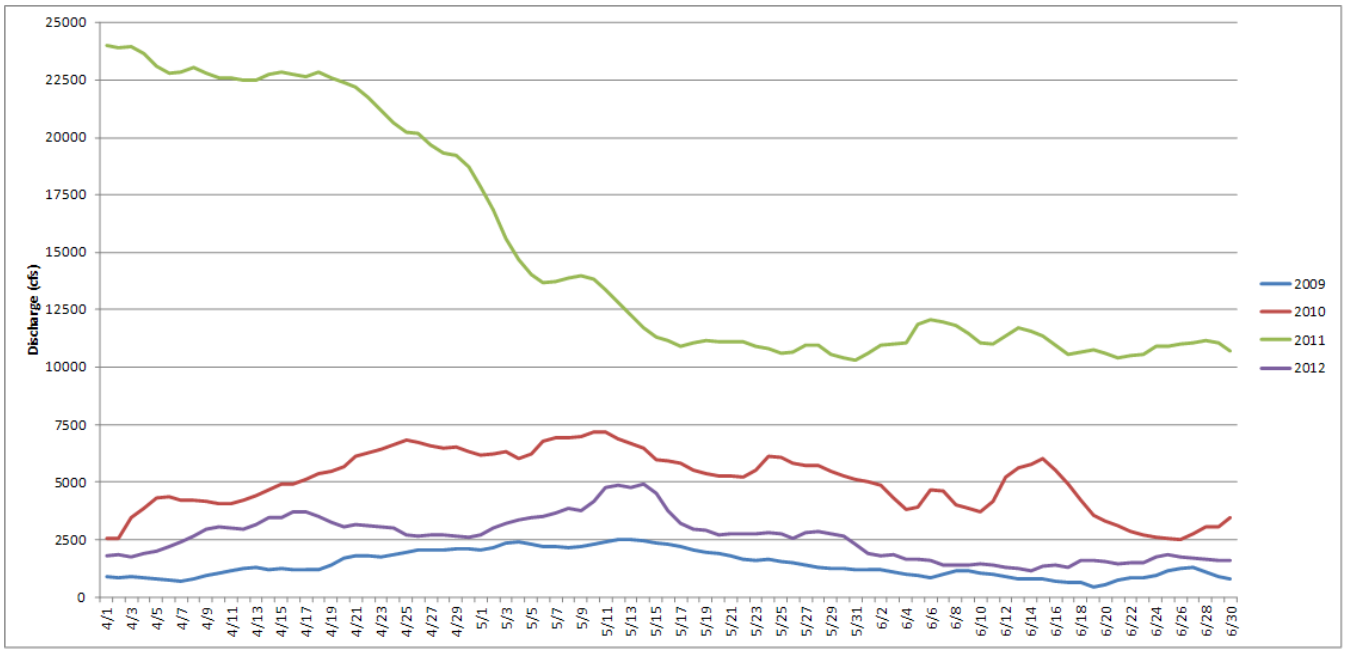

Figure ES-1 Mean Daily River Discharge (cubic feet per second) of the San Joaquin River at Mossdale (MSD), during the study period - April 1 to June 30, 2009–2012

ES.2 OBJECTIVES, METHODS, RESULTS, AND DISCUSSION

The present study included three main objectives, namely to conduct an evaluation at the Head of Old River of:

JUVENILE SALMONID ROUTING INCLUDING BARRIER EFFECTS

- Evaluate the effectiveness of different barrier treatments to influence the retention of acoustically tagged (tagged) juvenile Chinook salmon and steelhead in the San Joaquin River, under variable ambient light levels, water temperature, discharge, water velocity, and turbidity conditions.

PREDATION ON JUVENILE SALMONIDS INCLUDING BARRIER EFFECTS

- Evaluate predation on juvenile salmonids in response to a range of environmental conditions including barrier treatment effects.

BEHAVIOR AND DENSITY CHANGES IN PREDATORY FISHES

- Investigate behavior and density changes in predatory fishes in response to environmental conditions including residence time and assessment of areas occupied.

The following sections briefly summarize the methods used to evaluate the study objectives, the results, and their interpretation.

ES.2.1 EVALUATION OF JUVENILE SALMONID ROUTING INCLUDING BARRIER EFFECTS

STUDY FISH

Study fish were obtained from three hatcheries operated by the California Department of Fish and Wildlife. Chinook salmon juveniles were acquired from the Feather and Merced River hatcheries while the steelhead juveniles were acquired from the Mokelumne River Hatchery.

The number of juvenile Chinook salmon surgically implanted with Hydroacoustic Technology, Inc. (HTI; Seattle, Washington) tags was 933 in 2009, 504 in 2010, 1,915 in 2011, and 424 fish in 2012. The size of juvenile Chinook varied by year, but ranged from 80 millimeters (mm) to 140 mm in fork length. Steelhead juveniles implanted with HTI tags were released primarily in 2011 with a total of 2,208 fish which ranged from 149–396 mm fork length. Only 16 steelhead were released in 2012 and these fish ranged in size from 167–269 mm fork length. Juvenile salmonids implanted with VEMCO (Bedford, Nova Scotia, Canada) tags were released in 2012. These fish included 961 juvenile Chinook salmon (100–199 mm total length) and 1,435 juvenile steelhead (115–316 mm total length). Analyses presented in this report focus primarily on juvenile salmonids implanted with HTI tags, unless otherwise specified.

ROUTING AND FATE

The barrier evaluations described in this report were conducted as part of a coordinated suite of studies in the south Delta, which included the Vernalis Adaptive Management Program (VAMP) (SJRGA 1999) and the Six-Year Steelhead Study (6YSS) (NMFS 2009; SJRGA 2013). This coordinated suite of studies relied on one team (VAMP/6YSS) to conduct the surgical implantation, transport the fish to the release site (i.e., Durham Ferry on

the San Joaquin River for all years), handle the fish to minimize effects on behavior, and release the telemetered juveniles according to the schedule.

Each juvenile salmonid entering the HOR study area was categorized based on its apparent fate from observations of two-dimensional tracks detected with a hydrophone array: (1) Released, but never arrived; (2) Remained in San Joaquin River; (3) Entered Old River; (4) Predation; or (5) Unknown. Only fish with fates 2-4 were included in the analyses. Fate was determined qualitatively based on a directed downstream movement for juvenile salmonids. Steelhead did not always move in a downstream direction which made subsequent analyses problematic. In contrast, predatory fish behavior typically included slower movements, looping patterns, and holding the same position.

Each fish was assigned to a sample based on its arrival time into the HOR study area. Samples were created by pooling fish that had arrived at a similar barrier state (BAFF on, BAFF off, no barrier, or rock barrier), ambient light level (< 5.4 lux or ≥ 5.4 lux), and average channel velocity (< 0.61 meter per second [m/s] or ≥ 0.61 m/s).

When barrier treatment status (off/on), ambient light level, or velocity changed, a new sample was created. For testing of BAFF effectiveness in 2009 and 2010, the BAFF was alternated between the "off" and "on" settings so that the BAFF was operational about 50% of the time. This time split in off/on operation allowed about 50% of the tagged juvenile Chinook salmon to experience the BAFF when in operation.

Table ES-1 provides an overview of the fate of tagged juvenile Chinook salmon that entered the HOR study area by year, barrier treatment, and ambient light level. The proportions shown are population proportions (note that population proportions differ from the sample proportions used in hypothesis testing; see Table ES-2). Across all years, the proportion of juveniles that remained in the San Joaquin River (nearly 0.41, i.e., 41%) was similar to the proportion that went down Old River; the remaining 0.19 (19%) were preyed upon. The proportion of juvenile Chinook salmon remaining in the San Joaquin River ranged from 0.09 (BAFF on in the dark, 2009) to 0.84 (rock barrier in the dark, 2012). The proportion of juvenile Chinook salmon entering Old River ranged from 0 (rock barrier, 2012) to 0.78 (BAFF off in the dark, 2009). The proportion of juvenile Chinook salmon that were preyed upon at the HOR study area ranged from 0.03 (no barrier in the dark, 2011) to 0.45 (rock barrier in the light, 2012). The fates of 525 tagged juvenile steelhead were determined in 2011–2012, although only five of these fish entered the study area in 2012. Of the 520 juvenile steelhead entering the study area in 2011, the grand overall efficiency was 38.3%, 199 remained in the San Joaquin River, 196 (37.7%) entered Old River, and 125 (24.0%) were preyed upon. There was little difference in routing or predation between light and dark conditions for juvenile steelhead.

Several primary objectives and hypotheses were associated with the evaluation of juvenile salmonid routing and barrier effectiveness (Table ES-2). The evaluation judged efficiency, defining "more efficient" as greater use by juveniles of the San Joaquin River route (over that of Old River) to leave the HOR study area. This definition reflects the general view that survival is lower down the Old River route (see review by Hankin et al. 2010 but see also SJRGA 2013). For each sample, three main metrics were calculated:

- *Overall efficiency* (O_E), the number of tags, surgically implanted in salmonid juveniles, exiting downstream from the study area via the San Joaquin River, divided by the number of tags entering the study area from upstream. This metric provided the most comprehensive measure of barrier effectiveness, as it integrated both routing and loss from predation.

Table ES-1
Fate of Acoustically Tagged Juvenile Chinook Salmon at the Head of Old River Study Area during 2009–2012

Year/Barrier/Light*	Total No. of Juveniles	San Joaquin River			Old River			Predation		
		Total	Proportion	SE	Total	Proportion	SE	Total	Proportion	SE
2009 BAFF	525	127	0.242	0.019	278	0.530	0.022	120	0.229	0.018
a. Off	292	68	0.233	0.025	176	0.603	0.029	48	0.164	0.022
i. dark	59	10	0.169	0.049	46	0.780	0.054	3	0.051	0.029
ii. light	233	58	0.249	0.028	130	0.558	0.033	45	0.193	0.026
b. On	233	59	0.253	0.028	102	0.438	0.033	72	0.309	0.030
i. dark	45	4	0.089	0.042	35	0.778	0.062	6	0.133	0.051
ii. light	188	55	0.293	0.033	67	0.356	0.035	66	0.351	0.035
2010 BAFF	451	114	0.253	0.020	220	0.488	0.024	117	0.259	0.021
a. Off	219	45	0.205	0.027	129	0.589	0.033	45	0.205	0.027
i. dark	77	25	0.325	0.053	41	0.532	0.057	11	0.143	0.040
ii. light	142	20	0.141	0.029	88	0.620	0.041	34	0.239	0.036
b. On	232	69	0.297	0.030	91	0.392	0.032	72	0.310	0.030
i. dark	60	28	0.467	0.064	28	0.467	0.064	4	0.067	0.032
ii. light	172	41	0.238	0.032	63	0.366	0.037	68	0.395	0.037
2011 No barrier	1,075	551	0.513	0.015	415	0.386	0.015	109	0.101	0.009
a. dark	306	162	0.529	0.029	135	0.441	0.028	9	0.029	0.010
b. light	769	389	0.506	0.018	280	0.364	0.017	100	0.130	0.012
2012 Rock barrier	193	117	0.606	0.035	0	0.000	0.000	76	0.394	0.035
a. dark	38	32	0.842	0.059	0	0.000	0.000	6	0.158	0.059
b. light	155	85	0.548	0.040	0	0.000	0.000	70	0.452	0.040
Total	**2,244**	**909**	**0.405**	**0.010**	**913**	**0.407**	**0.010**	**422**	**0.188**	**0.008**

Notes: BAFF = Bio-Acoustic Fish Fence (Fish Guidance Systems Ltd., Southampton, UK) (non-physical barrier); SE = Standard Error

* Dark < 5.4 lux, light ≥ 5.4 lux

Source: Present study

Table ES-2
Objectives, Hypotheses, and Results Related to Juvenile Salmonid Routing Including Barrier Effects

Year and Treatment	Objective	Hypothesis Number	Hypotheses	Results*
2009 BAFF	Determine whether barrier efficiency (O_E, P_E, and D_E) for juvenile Chinook salmon was improved by BAFF operation	$H1_0$	For juvenile Chinook salmon, barrier efficiency (O_E, P_E, and D_E) with the BAFF on was equal to barrier efficiency with the BAFF off.	O_E: Accept hypothesis (BAFF on [0.209] = BAFF off [0.184]) P_E: Accept hypothesis (BAFF on [0.338] = BAFF off [0.234]) D_E: Reject hypothesis (BAFF on [0.732] > BAFF off [0.311])
2010 BAFF	Determine whether barrier efficiency (O_E, P_E, and D_E) for juvenile Chinook salmon was improved by BAFF operation	$H2_0$	For juvenile Chinook salmon, barrier efficiency (O_E, P_E, and D_E) with the BAFF on was equal to barrier efficiency with the BAFF off.	O_E: Accept hypothesis (BAFF on [0.355] = BAFF off [0.245]) P_E: Reject hypothesis (BAFF on [0.441] > BAFF off [0.286]) D_E: Reject hypothesis (BAFF on [0.150] > BAFF off [0.012])
	Determine whether BAFF barrier efficiency with the BAFF on changed significantly between years	$H3_0$	For juvenile Chinook salmon with BAFF on, barrier efficiency (O_E, P_E, and D_E) in 2009 was equal to barrier efficiency in 2010.	O_E: Accept hypothesis (2009 [0.209] = 2010 [0.355]) P_E: Accept hypothesis (2009 [0.338] = 2010 [0.441]) D_E: Reject hypothesis (2009 [0.732] > 2010 [0.150])
	Determine whether with the BAFF off, barrier efficiency changed significantly between years	$H4_0$	For juvenile Chinook salmon with BAFF off, barrier efficiency (O_E, P_E, and D_E) in 2009 was equal to barrier efficiency in 2010.	O_E: Accept hypothesis (2009 [0.184] = 2010 [0.245]) P_E: Accept hypothesis (2009 [0.234] = 2010 [0.286]) D_E: Reject hypothesis (2009 [0.312] > 2010 [0.012])
2011 No Barrier	Determine whether and to what extent the BAFF infrastructure affected O_E and P_E when the BAFF was turned off	$H5_0$	For juvenile Chinook salmon, O_E and P_E were equal for 2009 BAFF off, 2010 BAFF off, and 2011 no barrier conditions.	O_E: Reject hypothesis (2011 [0.519] > 2010 [0.245] = 2009 [0.184]) P_E: Reject hypothesis (2011 [0.574] > 2010 [0.286] = 2009 [0.234])
	Determine whether juvenile Chinook salmon and steelhead had the same O_E and P_E through the HOR study area	$H6_0$	O_E and P_E were the same for juvenile Chinook salmon and steelhead.	O_E: Reject hypothesis (Chinook salmon [0.519] > steelhead [0.368]) P_E: Accept hypothesis (Chinook salmon [0.574] = steelhead [0.490])
2012 Rock Barrier	Compare O_E and P_E across treatments to determine whether any barrier was more effective than no barrier and which produced the highest efficiency at retaining juvenile Chinook salmon in the San Joaquin River	$H7_0$	For juvenile Chinook salmon, O_E and P_E were equal for 2009 BAFF on, 2010 BAFF on, 2011 no barrier, and 2012 rock barrier treatments.	O_E: Reject hypothesis (2012 [0.618] = 2011 [0.519] > 2010 [0.355] = 2009 [0.209]) P_E: Reject hypothesis (2012 [1.000] > 2011 [0.574] > 2010 [0.441] = 2009 [0.338])

Table ES-2
Objectives, Hypotheses, and Results Related to Juvenile Salmonid Routing Including Barrier Effects

Year and Treatment	Objective	Hypothesis Number	Hypotheses	Results*

Notes: BAFF = Bio-Acoustic Fish Fence (Fish Guidance Systems Ltd., Southampton, UK) (non-physical barrier); D_E = deterrence efficiency; O_E = overall efficiency; P_E = protection efficiency

* Numbers in brackets indicate sample-based mean efficiency estimates, with statistically significant differences indicated by "<" or ">" and no significant difference indicated by "=."

Source: Present study

- *Protection efficiency* (P_E), the number of juveniles exiting downstream from the study area via the San Joaquin River, divided by the number of juveniles exiting via the San Joaquin River plus the number of individuals exiting via Old River, but considering only those juveniles that were not eaten at the HOR study area. This metric provided a measure of salmonid juvenile routing through the study area, excluding salmonid juveniles that were eaten.

- *Deterrence efficiency* (D_E), the number of juveniles approaching the BAFF that were deterred from continuing their approach or were guided along past the end of the BAFF, divided by the total number of juveniles approaching the BAFF. This metric was specific to the BAFF and evaluated its efficacy in producing stimuli noxious to the juvenile salmonids approaching it, as shown by their lack of desire to cross the BAFF.

The analyses of barrier effectiveness found that the BAFF effectively deterred juvenile Chinook salmon from approaching the BAFF in both 2009 and 2010 - that is, D_E was significantly higher with BAFF on than with BAFF off (Table ES-2; Hypotheses $H1_0$ and $H2_0$). D_E was significantly higher in 2009 than 2010 (Table ES-2; Hypothesis $H3_0$), possibly because in 2010 the discharge was higher, a lower proportion of the water column was occupied by the BAFF, and the barrier alignment was different. D_E was also higher in 2009 than 2010 with the BAFF off (Table ES-2; Hypothesis $H4_0$).

Although the BAFF's noxious stimuli were successful in deterring fish from approaching, the BAFF was not efficient in terms of allowing more juvenile Chinook salmon to leave the HOR study area via the San Joaquin River route. There was no significant difference in O_E between BAFF-on and BAFF-off treatments in either 2009 or 2010, and only in 2010 was P_E significantly higher with the BAFF on. These results reflected rates of predation that occurred during BAFF operations (discussed further in Section ES.2.2). There was no significant difference in O_E and P_E between 2009 and 2010, although O_E was close ($P = 0.0563$) to being significantly greater in 2010 (0.36) than in 2009 (0.21). With the BAFF off, O_E and P_E also were not significantly different between 2009 and 2010 (Table ES-2; Hypotheses $H3_0$ and $H4_0$).

The influence of the BAFF's infrastructure alone on survival through the HOR study area was assessed by comparing efficiency (O_E and P_E) with the BAFF off in 2009 and 2010 to efficiency in 2011 (Table ES-2; Hypothesis $H5_0$). Although both O_E and P_E were significantly lower in 2009 and 2010 than in 2011, this comparison was confounded by the very high discharge in 2011, which may have affected the comparison regardless of the presence of a BAFF.

The availability of tracking data for tagged juvenile steelhead moving through the HOR study area in 2011 allowed a comparison of juvenile Chinook salmon and steelhead efficiencies in that year (note that this was not a test of barrier efficiency, but of routing and survival [Table ES-2; Hypothesis $H6_0$]). The routing of juvenile Chinook and steelhead was similar (i.e., no significant difference in P_E), providing evidence of proportional movement that was similar to the proportional split in discharge between the San Joaquin and Old rivers. Juvenile steelhead had significantly lower O_E than the juvenile Chinook salmon, suggesting higher rates of predation. However, this may have been an artifact of juvenile steelhead behavior being similar to predator behavior at times (discussed further in Section ES.2.2).

The analysis of primary importance for addressing management at the HOR study area was the comparison of the efficiencies of different barrier treatments in retaining the juvenile Chinook salmon in the San Joaquin River

(Table ES-2; Hypothesis $H7_0$). This analysis revealed no significant difference in O_E between the no barrier and rock barrier treatments in 2011 and 2012, respectively, and that O_E was significantly greater in both of these years than in 2009 and 2010. The fact that all surviving Chinook salmon juveniles remained in the San Joaquin River with the 2012 rock barrier caused the P_E to be significantly higher in 2012 than in all other years, whereas greater discharge in 2011 resulted in significantly greater P_E in that year than in 2009 and 2010.

The primary hypotheses (Table ES-2) were supplemented with supporting hypotheses that evaluated BAFF efficiencies at different levels of light and channel velocity. The light levels considered were dark (< 5.4 lux), and light (≥ 5.4 lux), reflecting the threshold above which light might have affected juvenile Chinook salmon reactions to the BAFF's strobe lights. The channel velocity levels considered were low (≤ 0.61 m/s average channel velocity), and high (> 0.61 m/s average channel velocity), reflecting the sustained swimming speed of small juvenile Chinook salmon, corrected for BAFF angle. The analysis considered these different light levels and channel velocities to account for potential differences in barrier effectiveness because of the visibility of the BAFF and the ability of juvenile salmonids to exhibit swimming avoidance behavior.

Of the three measures of efficiency examined (O_E, P_E, and D_E), only D_E showed a difference between light levels or velocities, and it was significantly higher with the BAFF on in high light conditions (in both 2009 and 2010). This result may reflect a greater ability of juvenile Chinook salmon to orient away from the BAFF's main noxious stimulus (the acoustic deterrent) in high light because of the increased visibility of the BAFF. However, predation increases with higher light level, thus reducing much of the benefit of the BAFF in providing deterrence (as noted in Section ES.2.2).

ES.2.2 Evaluation of Predation on Juvenile Salmonids Including Barrier Effects

The data on tagged juvenile salmonids described previously were used to address several objectives related to predation in the HOR study area. Those objectives were evaluated by testing univariate sample–based hypotheses in relation to the proportion of salmonids in each sample that were eaten in the study area (Table ES-3; Hypotheses $H8_0$, $H9_0$, and $H10_0$). These analyses generated the following findings:

- The proportion of juvenile Chinook salmon eaten was significantly greater with the BAFF on than with the BAFF off in 2009, but not in 2010 (Table ES-3; Hypothesis $H8_0$);
- In 2011, a significantly greater proportion of juvenile steelhead was eaten than Chinook salmon (Table ES-3; Hypothesis $H9_0$). However, some of the tagged juvenile steelhead categorized as "eaten" may not have been eaten because steelhead sometimes exhibited looping behavior or swam against the flow - behaviors that were used as criteria for determining predation. This would have resulted in an overestimate of the proportion of steelhead eaten; and
- A significantly lower proportion of juvenile Chinook salmon was eaten in 2011 (a high-flow year) than in 2012 (a low-flow year, with the rock barrier in place), whereas the proportion eaten in 2009 and 2010 with the BAFF on was intermediate to, but not statistically different from, the other two years (Table ES-3; Hypothesis $H10_0$).

Table ES-3
Objectives, Hypotheses, and Results Related to Predation on Juvenile Salmonids Including Barrier Effects

Year(s)	Objectives	Hypothesis Number	Hypotheses	Results*
2009	Provide a direct test that the BAFF operation had some influence on proportion eaten.	$H8_0$	The proportion of juvenile Chinook salmon entering the HOR study area that were eaten with the BAFF was on was equal to the proportion eaten when the BAFF was off.	Reject hypothesis: Significantly greater proportion eaten with BAFF on (0.290) than with BAFF off (0.138).
2010	Provide a direct test that the BAFF operation had some influence on proportion eaten.	$H8_0$	The proportion of juvenile Chinook salmon entering the HOR study area that were eaten with the BAFF was on was equal to the proportion eaten when the BAFF was off.	Accept hypothesis: No difference in proportion eaten between BAFF on (0.217) and BAFF off (0.212).
2011	Evaluate the proportion eaten for Chinook salmon and steelhead juveniles in 2011.	$H9_0$	The proportions of juvenile Chinook salmon and steelhead entering the HOR study area that were eaten were equal.	Reject hypothesis: Significantly greater proportion of juvenile steelhead eaten (0.243) than Chinook salmon (0.087).
2009–2012	Show whether there were differences in proportion eaten between treatments.	$H10_0$	The proportions of juvenile Chinook salmon entering the HOR study area that were eaten were equal for 2009-BAFF on, 2010-BAFF on, 2011-no barrier, and 2012- rock barrier.	Reject hypothesis: Significantly greater proportion eaten in 2012 (0.354) than in 2011 (0.087), with 2009 (0.290) and 2010 (0.217) intermediate and not significantly different from other years.
2009, 2010, 2012	Evaluate the influence of abiotic and biotic factors, including barrier type/status, on probability of predation of juvenile Chinook salmon.	H11	Probability of predation of juvenile Chinook salmon is negatively related to discharge (shorter travel time/distance at higher discharge), turbidity (lower visual range of predators with greater turbidity), size (larger juveniles less susceptible to predators), and small-fish density (availability of alternative prey for predators). Probability of predation is positively related to water temperature (higher bioenergetic demands of predators with higher temperature) and ambient light level (greater visual range of predators with more light). Probability of predation is unrelated to barrier treatment/status (BAFF on/off, rock barrier).	Hypothesis supported only for ambient light: greater predation probability at higher light level. No support for other hypotheses. Significantly greater probability of predation with BAFF on or rock barrier than with BAFF off. Probability of predation positively related to small-fish density.

Table ES-3
Objectives, Hypotheses, and Results Related to Predation on Juvenile Salmonids Including Barrier Effects

Year(s)	Objectives	Hypothesis Number	Hypotheses	Results*
2011, 2012	Evaluate the influence of abiotic and biotic factors on probability of predation of juvenile Chinook salmon.	H12	Probability of predation of juvenile Chinook salmon is negatively related to discharge, turbidity, juvenile size, and small-fish density. Probability of predation is positively related to water temperature, ambient light level, and density of predatory fish (greater predation pressure with more large fish).	Hypothesis supported only for ambient light and turbidity: greater predation probability at higher light levels and lower turbidity.
2011	Evaluate the influence of abiotic and biotic factors on probability of predation of juvenile steelhead.	H13	Probability of predation of juvenile steelhead is negatively related to discharge, turbidity, size, and small-fish density. Probability of predation is positively related to water temperature, ambient light level, and density of predatory fish (greater predation pressure with more large fish).	Model was a poor fit to the data; results inconclusive.

Notes: BAFF Bio-Acoustic Fish Fence (Fish Guidance Systems Ltd., Southampton, UK) (non-physical barrier); HOR = Head of Old River

* Numbers in parentheses indicate sample-based mean proportion eaten estimates.

Source: Present study

In addition to the univariate sample-based method, generalized linear modeling (GLM) was undertaken. This modeling assessed the potential influence of several environmental variables on the probability of predation of juvenile salmonids in the HOR study area. It also tested the null hypothesis of no difference in predation probability of juvenile Chinook salmon between barrier treatments (BAFF on/BAFF off/rock barrier) for data from 2009, 2010, and 2012 (Table ES-3; Hypothesis H11). The GLM suggested that the probability of predation was significantly greater for the BAFF-on and rock barrier treatments than for the BAFF-off treatment, and that the probability of predation was greater under higher light conditions (presumably because predators could see the juvenile Chinook salmon more easily). This may be the case because juveniles have longer travel distances through the HOR study area as they avoid the noxious stimulus of the BAFF (and may be disoriented by the stimulus) or they are entrained into the eddies created by the rock barrier.

Further analysis was conducted of the data from GLM of juvenile Chinook salmon predation in 2011 and 2012 (Table ES-3; Hypothesis H12) so that the density of large fish from hydroacoustic surveys could be included as a measure of the density of potential predatory fish. This analysis found that the probability of predation was greater at higher light levels and lower turbidities, again suggesting the importance of visibility to predators.

Discharge was not found to be an important predictor of predation probability. To some extent, this may reflect the difficulty in accurately assigning a discharge measurement when conditions are changing rapidly; the higher probability of predation with lower turbidities partly reflects differences in discharge. Relatively low predation at the HOR study area in 2011 may have reflected a downstream shifting of predatory fish (as observed by LeDoux-Bloom [2012] in the broader San Francisco estuary), and predation pressure in response to discharge, because the VAMP study did not find overall through-Delta survival to be greater in 2011 than in other years (SJRGA 2013).

Bioenergetics modeling was conducted to assess potential striped bass predation on juvenile Chinook salmon at the HOR study area. This modeling illustrated that in 2012, the relatively high density of predatory fish (with large fish assumed to be striped bass based on side-looking mobile hydroacoustics), coupled with relatively high water temperature, may have resulted in predation rates similar to those estimated by observing the tagged juvenile Chinook salmon tracks. Lower predatory fish densities and water temperature estimates in 2011 led to considerably lower estimated predation rates for that year from bioenergetics modeling, which agrees with the considerably lower observed predation rate for that year (Tables ES-1 and ES-3).

GLM of the probability of predation on juvenile steelhead in 2011 did not yield informative results. To some extent, this may reflect difficulties in assigning steelhead fate, because steelhead movement patterns are less directed than those of Chinook salmon, and steelhead movement patterns may be confused with movement patterns of predatory fishes (Table ES-3; Hypothesis H13).

ES.2.3 Evaluation of Behavior and Density Changes in Predatory Fishes

The behavior of predatory fishes at the HOR study area was studied with more than 80 striped bass (*Morone saxatilis*), largemouth bass (*Micropterus salmoides*), channel catfish (*Ictalurus punctatus*), and white catfish (*Ameiurus catus*) that were captured by hook and line angling and externally fitted with acoustic tags, primarily in 2011 and 2012. The acoustic detection data from these fish allowed objectives related to residence time and areas occupied by predatory fishes at the HOR study area to be addressed (Table ES-4). In addition, information from mobile hydroacoustic surveys conducted in 2011–2012 and the locations of stationary juvenile salmonids' acoustic tags were used to provide information about the areas occupied by predatory fishes. It was assumed that the density of fish estimated by hydroacoustic surveys to be at least 30 centimeters (cm) in total length would indicate the density of predatory fishes (recognizing that not all large fish detected would be predatory fishes).

Table ES-4
Objectives Related to Behavior of Predatory Fishes

Years	Objective	Means of Study	Utility to Management
2009–2012	Describe residence time of predatory fishes at the HOR study area.	Tagged predatory fish	Indicates turnover of predatory fish, and therefore allows inference regarding the level of effort required for relocation of predatory fish, for example.
2009–2012	Describe areas (spatial and velocity) occupied by predatory fishes at the HOR study area.	Tagged predatory fish, mobile hydroacoustic surveys, tags from stationary juvenile salmonids (presumably eaten and defecated by predatory fishes)	Indicates where at the HOR study area to focus predator capture efforts for any contemplated relocation efforts, as well as indicating habitat areas that could be manipulated to reduce predator density and predation risk.

Note: HOR = Head of Old River
Source: Present study

The time spent at the HOR study area by tagged predatory fishes varied. Generally, however, channel catfish, white catfish, and largemouth bass spent appreciably longer amounts of time than striped bass (i.e., days or weeks, rather than hours). Most striped bass left the study area in a downstream direction. The significance of the present results for management is that turnover of striped bass generally is appreciable, with most fish spending a limited amount of time at the HOR study area. Thus, efforts to control fish numbers by removal/relocation would require a sustained effort (e.g., daily removal).

The scour hole at the HOR study area was confirmed as an important area for occupancy by predatory fishes. Tagged predatory fishes were found occupying portions of the HOR study area in the San Joaquin River downstream of the Old River divergence, both at the scour hole and in the immediately adjacent areas. Some differences existed in the areas occupied by the different species of tagged predatory fish. For example, striped bass generally were found more often in areas away from shore (although they also occurred near shore), whereas largemouth bass tended to occur more in the nearshore zones.

An analysis of velocities occupied by tagged predatory fishes confirmed the main patterns shown by the spatial analysis of areas occupied. Catfishes and largemouth bass occupied areas with estimated near-surface velocities that were very low compared to all velocities available in the HOR study area. Striped bass differed from the other predatory fishes in occupying a range of velocities, with some individuals having median occupation velocities greater than the median velocities available at the HOR study area; this reflects the species' pelagic nature and occupation of a variety of habitats.

Down-looking mobile hydroacoustic surveys showed an extremely high concentration of large fish (presumably including many predatory fishes, but possibly also including large-bodied nonpredatory fish such as common carp [*Cyprinus carpio*]) in the scour hole; side-looking hydroacoustic surveys similarly showed many large fish in the scour hole, but also showed appreciable numbers in other nearby locations within the study area.

Stationary tags originally inserted into juvenile salmonids, provided a third source of information about areas occupied by predators. The tags also indicated the considerable importance of the scour hole and vicinity because most stationary tags were found there, with very few stationary tags found elsewhere (one tag was also found closely associated with the 2012 rock barrier).

With respect to the occurrence of predatory fish near the installed barriers, tagged largemouth bass that were released downstream of the rock barrier tended to remain at or close to the barrier much of the time, and therefore could have posed a predation threat to any fish passing through the barrier's culverts. A single largemouth bass tagged in 2009 spent an appreciable amount of time (nearly 50% of all detections) within 5 meters of the BAFF (at the upstream end, closest to shore). Little evidence existed of striped bass spending much time close to the BAFF in 2009/2010, although the number of tagged striped bass during these years was very low (n = 4). These findings have important implications for limiting predator abundance at the HOR study area, whether directly (through capture/relocation) or indirectly (through habitat manipulation, such as scour hole filling).

Data from mobile hydroacoustic surveys also were used to address several objectives related to changes in predatory fish density at the HOR study area caused by changes in environmental variables, and to compare density to several reference sites in the San Joaquin River (Table ES-5). GLM suggested that based on both down-looking and side-looking mobile hydroacoustic surveys, the main environmental predictors associated with changes in the density of large fish (greater than 30 cm total length) were same-day discharge and water temperature (Table ES-5; Hypothesis $H14_0$). Density increased as discharge decreased and water temperature increased.

To some extent, the correlation between density of large fish and discharge and water temperature reflected both differences between years and differences within years. The density of large fish was considerably less in 2011 than in 2012; discharge was considerably higher in 2011 than in 2012. The lower density of large fish, presumably including many predatory fish, in 2011 may reflect lower habitat suitability associated with higher water velocities. The 2012 surveys provided a contrast between very low abundance during March, which had low water temperatures (approximately 12–15°C), and higher abundance in May (18–22°C). This suggests seasonal migration to and through the HOR study area by large fish, such as striped bass that spawn in the river during the spring. Although density estimates were quite variable at all the sites, positive correlations in large-fish density existed between the HOR study area and the reference sites in approximately half of the comparisons (Table ES-5; Hypothesis $H15_0$). Large-fish density at the HOR study area was either greater than or not significantly different from large-fish density at the three reference sites (Table ES-5; Hypothesis $H16_0$).

Taken together, these results suggest that wide-ranging factors (e.g., discharge and water temperature) affect fish density over much of the San Joaquin River, and that the HOR study area has a relatively high density of large fishes compared to reference sites. These findings have management implications when prioritizing predator management efforts at the HOR study area and elsewhere in the interior and south Delta, both temporally (within and between years; e.g., there may be more need to capture/relocate predators in warmer years with lower discharge) and spatially (e.g., if the location of large concentrations of predatory fishes changes based on discharge).

Table ES-5
Objectives, Hypotheses, and Results Related to Density of Predatory Fishes

Year	Objectives	Hypothesis Number	Hypotheses	Results
2011–2012	Determine whether environmental variables are associated with changes in large-fish densities at the HOR study area.	$H14_0$	The density of large fish (> 30 cm in total length, i.e., potential predators) at the HOR site is not correlated with environmental variables (discharge, water temperature, turbidity, ambient light level, and small-fish density [representing availability of potential prey]).	Down-looking and side-looking hydroacoustics: Null hypothesis not supported for discharge (negative relationship with large-fish density) and water temperature (positive relationship with large-fish density). Null hypothesis accepted for other variables.
2011–2012	Determine whether there are broad-scale environmental influences on predatory fish densities at the HOR study area that result in similar changes in density to reference sites.	$H15_0$	Changes in the density of large fish (> 30 cm in total length, i.e., potential predators) at the HOR study area during the spring are not correlated with changes in density at three reference sites.	Down-looking hydroacoustics: Accept null hypothesis for two of three comparisons; reject null hypothesis for the remaining comparison (positive correlation in density between the HOR study area and the reference sites). Side-looking hydroacoustics: Reject null hypothesis for two of three comparisons (positive correlations in density between HOR study area and reference sites); accept null hypothesis for the remaining comparison.
2011–2012	Determine whether predatory fish density at the HOR study area is greater than at similar reference sites.	$H16_0$	The density of large fish (> 30 cm in total length, i.e., potential predators) at the HOR study area during the spring is not significantly different from density at three reference sites.	Down-looking hydroacoustics: Accept null hypothesis for two of three comparisons; reject null hypothesis for the remaining comparison (significantly greater density at the HOR study area than at one reference site). Side-looking hydroacoustics: Reject null hypothesis for two of three comparisons (significantly greater density at the HOR study area than at two reference sites); accept null hypothesis for the remaining comparison.

Notes: cm = centimeters; HOR = Head of Old River
Source: Present study

ES.3 RECOMMENDATIONS

Several recommendations for future study are provided to advance the findings of the present study (Table ES-6). With respect to juvenile salmonid routing and barrier effects, it is recommended that the cost and benefit of barriers at the HOR study area be studied relative to the cost and benefits of alternative management strategies, particularly non-engineering solutions such as habitat restoration (e.g., floodplain restoration and other actions proposed under the Bay Delta Conservation Plan [BDCP]). This recommendation is made for the following reasons:

- None of the barriers that were studied provided overall efficiency (O_E) greater than 62% and simultaneously - less than 22% proportion eaten (see Table ES-1 for the proportion of fish remaining in the San Joaquin River and Table ES-3 for the results of sample proportion eaten in 2009-2012); the only barrier (rock) that produced an O_E greater than 62% also showed a sample proportion eaten of 35.4% and the only barrier (BAFF on, 2010) that produced a proportion eaten of 21.7% yielded an O_E of only 29.4%; in other words, with respect to the barriers studied in the report, it is possible to have high overall efficiency (rock barrier) or relatively low predation (BAFF on), but both of these desirable qualities are not available from the same barrier.
- Recent studies concluded that the San Joaquin River may not necessarily be the best migration route for juvenile salmonid survival (SJRGA 2011, 2013; Buchanan et al. 2013); and
- Survival through the south Delta generally is low by any route, suggesting that habitat improvements and restoration are desirable regardless of any routing influenced by a barrier at the HOR.

Table ES-6
Recommendations for Future Study

Juvenile Salmonid Routing Including Barrier Effects
► Study the costs and benefits of barriers in relation to alternative (non-engineering) management strategies. ► Conduct additional integrated analysis of existing data using supplementary techniques. ► Investigate new physical barrier alternatives to the rock barrier and BAFF.
Predation on Juvenile Salmonids Including Barrier Effects
► Further examine predation classification. ► Study the feasibility of physical habitat reconfiguration. ► Conduct a pilot predatory fish relocation study. ► Study the effects of physical barriers on predation hotspots. ► Study potential effects of changing recreational fishing regulations.
Behavior and Density Changes in Predatory Fishes
► Assess movement patterns of predatory fish as part of a pilot predatory fish relocation study. ► Assess predatory fish density in relation to predation hotspots.
Notes: BAFF = Bio-Acoustic Fish Fence (Fish Guidance Systems Ltd., Southampton, UK) (non-physical barrier). Source: Present study

The generally limited effectiveness of the BAFF (Tables ES-1 and ES-2), coupled with what appeared to be relatively high predation with installation of the 2012 rock barrier, leads to the recommendation to study alternative barriers. In this regard, it is recommended to consider the suggestions made by the VAMP's review

panel (Hankin et al. 2010) about the features of such a barrier, particularly because of the BDCP's proposal to construct an operable gate at the HOR. As part of such studies of physical barriers, it is recommended that juvenile Chinook salmon survival through the Delta by the San Joaquin and Old river routes be studied further. Historically, the San Joaquin River was the safer route (reviewed by Hankin et al. 2010) but survival by the Old River route has been similar to or higher than the San Joaquin River route since 2010 (SJRGA 2011, 2013; Buchanan et al. 2013).

Additionally, it is recommended that the existing juvenile salmonid routing data undergo additional analysis, using techniques supplementary to the univariate approach used in the present study (e.g., GLM). The purpose of such additional analysis would be to elucidate further barrier effectiveness across ranges of environmental variables and provide outputs that may support present analyses or provide a different interpretation than the current approach. It is also recommended that additional analyses be undertaken of data collected in 2013 (i.e., from the study similar to the VAMP's release of tagged juvenile Chinook salmon and from tagged steelhead released as part of the 6YSS mandated by the NMFS [2009] OCAP BO). Such analyses would allow comparison of juvenile salmonid routing and survival with a low-discharge, no-barrier treatment (i.e., 2013) with the other years (2009–2012) included in the present evaluation.

With respect to predation on juvenile salmonids, a key uncertainty warranting further research is the actual fate of fish that have been classified as having been preyed upon or having survived passage through the HOR study area. Therefore, it is recommended that the 2009–2012 data from the HOR study area be examined for the correspondence between qualitative fate classification (as used in the present investigations) and classifications based on mixture models that use data from tagged predatory fishes (e.g., from Georgiana Slough or, preferably, from the HOR study area). It is also recommended that predation classification in future studies (by mixture models, qualitative fate classification, or other means) at the HOR study area incorporate the use of the new predation tag technology (e.g., HTI's Predation Tag) that is currently being tested by DWR and its partners.

The preponderance of stationary juvenile salmonid acoustic tags in the scour hole and the association of predatory fishes with the scour hole and adjacent areas at the HOR study area leads to the recommendation that a study be undertaken of the feasibility of reconfiguring the physical habitat (e.g., modifying the scour hole's bathymetry by filling). Regardless of the presence or absence of a barrier at the HOR study area, predation was high in all years—bioenergetics modeling completed as part of this evaluation suggested that the estimated predation rates were reasonable—and a pilot predatory fish relocation study may be warranted. Such a study is already proposed for 2014–2017 and, together with any such future studies, will serve to inform management at the HOR study area and other predation hotspots.

At the broader scale, it is also recommended that changes to fishing regulations be studied to assess their potential for improving juvenile salmonid survival from the San Joaquin River region through the south Delta area, including the HOR study area. Associated with the pilot predator-relocation studies, it is recommended that broad-scale movement patterns of relocated predatory fishes also be studied. It is recommended that, at the broader scale of the south Delta, the study of the physical barriers recommended above be coupled with both the study of the locations of predation hotspots and the density of predatory fishes at hotspots, to assess the extent to which these vary under differing discharge conditions and the location of the tidal transition zone.

1 INTRODUCTION

1.1 BACKGROUND

The California Department of Water Resources (DWR) and the U.S. Bureau of Reclamation (Reclamation) manage the State Water Project (SWP) and Central Valley Project (CVP), respectively, with the goal of improving abundance, productivity, and diversity of anadromous salmonids subject to the terms of the National Marine Fisheries Service's (NMFS) 2009 Biological Opinion (BO) and 2011 amendments regarding the Long-Term Central Valley Project and State Water Project Operations Criteria and Plan (OCAP). Action IV.1.3 of the NMFS's 2009 BO instructs these agencies to "consider engineering solutions to further reduce diversion of emigrating juvenile salmonids to the interior and southern Delta,[1] and reduce exposure to CVP and SWP export facilities." Specifically, one objective of Action IV.1.3 is to "prevent emigrating salmonids from entering channels in the south Delta (e.g., Old River, Turner Cut) that increase entrainment risk to Central Valley steelhead migrating from the San Joaquin River through the Delta."

Returning adult fish of the Distinct Population Segment (DPS) of California Central Valley steelhead (*Oncorhynchus mykiss*) and Central Valley fall-run Chinook salmon (*O. tshawytscha*) utilize the San Joaquin River and its connecting interior and south Sacramento-San Joaquin Delta (Delta) tributaries during their upstream spawning migration, while juveniles use these waterways to move downstream during their emigration to the Pacific Ocean. Increased susceptibility to entrainment and predation at DWR's and Reclamation's water export facilities has been associated with juvenile salmonids moving into Old River in comparison to those juveniles remaining in the mainstem of the San Joaquin River (Holbrook et al. 2009; SJRGA 2011). In an effort to reduce the movement of juvenile salmonids into Old River, engineering solutions (e.g., barriers) have been tested at the Head of Old River (HOR) pursuant to Action IV.1.3 of the NMFS BO. While a seasonal barrier in the fall has been part of California' protective fish management measures since 1968 (Hallock et al. 1970), deployment of a springtime barrier is more recent at this location (1992) and uncertainties remain about its performance and effectiveness.

The purpose of this report is to contribute to the required BO Action IV.1.3 by evaluating and summarizing the effects of non-physical barrier (2009, 2010), no barrier (2011), and physical barrier (2012) treatments and assess their effectiveness at retaining juvenile salmonids in the mainstem San Joaquin River. Analyses include the effectiveness of the barrier treatments on juvenile salmonid route fate as influenced by the abiotic factors of light level, water temperature, discharge, and turbidity. These studies were augmented by investigations into the predation rates, predatory fish density, and predatory fish behavior that occurred in the vicinity of the HOR study area. Recommendations for future analyses and studies are identified.

1.1.1 SALMONID SPECIES MIGRATING PAST HEAD OF OLD RIVER

The two salmonid species of primary concern for the HOR studies were California Central Valley steelhead and Central Valley fall-run Chinook salmon (herein steelhead and Chinook salmon). For both species, the outmigrating juvenile life stage was most at risk at the study area. As the outmigrating juvenile salmonids pass the study area, they could remain in the San Joaquin River, shown by previous studies to be the safer route. Brandes

[1] Further detail of the study area is provided in Chapter 2, "Study Area and Focal Fish Species." Additional detail is provided in Appendix A, "Additional Background on the Study Area and Nearby Areas."

and McLain (2001) showed that recovery rates of tagged juvenile Chinook salmon at Chipps Island (Suisun Bay, Solano County, California) between 1985 and 1990 were higher if they were released in the mainstem San Joaquin River compared to being released in Old River. Additionally, they found that recovery rates from the Pacific Ocean were higher for these same fish released between 1986 and 1990 at Dos Reis (mainstem San Joaquin River downstream from the HOR study area) compared to those released in Old River (downstream from the HOR study area). Therefore, two sets of independent estimates appeared to indicate that migration down the San Joaquin River resulted in higher survival rates for juvenile Chinook salmon compared to those that migrated down Old River. Newman (2008) also found increased survival in the San Joaquin River over the Old River route.

Although juvenile salmonids taking the San Joaquin River route were documented to remain in the San Joaquin River at the HOR study area, they could also move into the interior Delta and to the Harvey O. Banks Pumping Plant (SWP) and C.W. "Bill" Jones Pumping Plant (CVP) through other downstream junctions (i.e., Turner and Columbia cuts, Old and Middle rivers). While referred to as the San Joaquin River route, it is acknowledged that fish can move from that route into Old River farther downstream. Alternatively, the juvenile salmonids could pass into Old River and traverse a route that would bring them closer to potential entrainment at the SWP and CVP pumping plants, both substantial water diversions. A third possible fate was that the juvenile salmonids could be subject to mortality (likely predation) near the HOR study area.

CHINOOK SALMON

The only Chinook salmon run in the San Joaquin River during the 2009–2012 study was the fall-run (see Section B.1.2, "Chinook Salmon—Fall-Run," in Appendix B, "Focal Fish Species Information"). Fall-run Chinook salmon are not listed under the federal Endangered Species Act (ESA). Fall-run spawn in Central Valley water courses primarily during October through December, and most of the juvenile Chinook salmon migrate to the Pacific Ocean in spring (NMFS 2013:Figure 1; Vogel and Marine 1991).

The San Joaquin River Restoration Program (SJRRP) conducted the first release of juveniles of an experimental spring-run juvenile Chinook salmon population in spring 2014 (NMFS 2013; Reclamation 2014; SJRRP 2012). Central Valley spring-run Chinook salmon were listed in 1999 as threatened under the ESA (Federal Register 64: 50394–50415; Federal Register 70: 37160-37204). A non-physical or physical barrier at the HOR could deter these spring-run juveniles from entering Old River. With the release of juveniles in 2014, spring-run adults may ascend the San Joaquin River passing through the HOR study area as early as 2016. The spawning migration of spring-run adult Chinook salmon may be affected by the operation of a barrier present at the HOR from April through June, the period during which barrier(s) would be installed.

CENTRAL VALLEY STEELHEAD

Steelhead were listed as threatened in 1998 (Federal Register 63: 13347–13371) (see Section B.1.4, "Steelhead," in Appendix B). Steelhead spawning peaks from December through April (McEwan 2001). Juveniles aged 1+ to 3+ move through the Delta (McEwan and Jackson 1996) toward the Pacific Ocean from November through June (Reclamation 2004b:Table 4-1). A barrier at HOR operated from April through June could affect juvenile steelhead migrating to the ocean during this period.

Because of its threatened status, interest in protecting juvenile steelhead has risen in recent years. Thus, the evaluation of the barriers installed at the HOR was extended to include steelhead in 2011. Two years (2011, 2012)

of data collection and analyses included juvenile steelhead. These data allowed determination of the proportion of juvenile steelhead that remained in the San Joaquin River at the HOR study area when no barrier was present in 2011, and the proportion that remained in the San Joaquin River with a physical rock barrier installed in 2012.

1.1.2 TYPES OF BARRIERS

Barriers that deter fish movement fall in two primary categories: non-physical and physical.

Non-physical barriers do not rely on physically obstructing fish from entering waterways, instead, these barriers take advantage of behavioral patterns of avoidance or attraction. Non-physical barriers offer the advantage of deterring fish from undesirable locations without physically blocking waterways (Noatch and Suski 2012) which can be important hydraulically, from a water quality perspective, and to navigation. Some types of behavioral barriers include electric (Savino et al. 2001), louvers (Kynard and Buerkett 1997), strobe lights (Anderson et al. 1998), bubble curtains (Sager et al. 1987), noise (Knudsen et al. 1992), or combinations of some of these stimuli (e.g., Perry et al. 2012).

Physical barriers do not rely on fish behavior, but exclude entry by obstructing passage. Physical barriers are the most commonly used type of fish barrier (Katapodis et al. 2004). Some physical barriers (e.g., wedgewire screens) have been important in demonstrating that fish protection can be provided at a screening location (State of Wisconsin 2003).

NON-PHYSICAL BARRIERS

Perry et al. (2012) found that the OVIVO™ Bio-Acoustic Fish Fence (BAFF) (Fish Guidance Systems, Southampton, United Kingdom) comprising an acoustic deterrent stimulus enclosed within a bubble curtain and illuminated by strobe lights, decreased the entrainment of juvenile Chinook salmon into Georgiana Slough (Sacramento County, California). Entrainment was 22.3% with the BAFF turned off, but decreased to 7.7% with the BAFF on. The mainstem Sacramento River route previously was shown to be a safer route to the Pacific Ocean than emigrating via Georgiana Slough (Perry et al. 2010). Perry et al. (2012) also found that the effectiveness of the BAFF decreased with increasing river discharge, suggesting the concomitant increase in discharge velocity was more likely to force fish through the barrier compared to lower discharge/velocity conditions.

Elsewhere, Welton et al. (2002) found a large proportion of juvenile Atlantic salmon (*Salmo salar*) were deterred by a BAFF in the River Frome, United Kingdom. Furthermore, the BAFF diverted a higher proportion of juvenile Atlantic salmon at night than during the day.

Flammang et al. (2013) reported that a BAFF deterred walleye (*Sander vitreus*) and also suggested that the strobe light was not an important part of the deterrent. The sensitivity of walleye to a strobe light may be substantially different from other fish species. Chinook salmon deterrence may be enhanced by a strobe light (Bowen et al. 2010:Table 5).

Ruebush et al. (2012) concluded that a sound/strobe/bubble barrier (similar to the BAFF described herein) could be used as a deterrent for two Asian carp species: bighead carp (*Hypophthalmichthys nobilis*) and silver carp

(*H. molitrix*). However, those authors suggested the sound/strobe/bubble barrier should not be used as an "absolute" barrier to keep these carp species from extending their range.

PHYSICAL BARRIERS

The San Joaquin River Group Authority (SJRGA 2006) found that a physical barrier constructed of rock installed at the HOR appeared to increase juvenile Chinook salmon survival from Mossdale or Durham Ferry to Jersey Point, San Joaquin River, Contra Costa County, California (SJRGA 2006:Figure 5-19) using recapture recoveries of fish collected at Chipps Island and Antioch. However, it is difficult to determine conclusively whether the rock barrier improved survival using the Pacific Ocean recapture recovery information alone (SJRGA 2006).

The SJRGA (2006) evaluated survival data for south Delta releases to Jersey Point between 1989 and 2005, including three estimates with the rock barrier installed at the HOR in 1997. The recovery rate estimates for groups released upstream of the HOR study area (Mossdale) and downstream of the study area (Dos Reis) were similar. These results supported previous conclusions that survival was increased with the rock barrier installed. In addition, the SJRGA (2007) showed that an increase in juvenile Chinook salmon survival occurred with higher discharge of the San Joaquin River.

However, if management actions were implemented to increase the discharge of the San Joaquin River with a rock barrier installed, there might be unintended consequences on ESA-listed fishes. For example, there is evidence that positive Old River flows in April and May could benefit delta smelt (*Hypomesus transpacificus*) by reducing entrainment at south Delta diversions (Lichatowich et al. 2005). One compromise between these competing demands for discharge could be to increase the number or size of the culverts placed in the rock barrier installed at the HOR.

The physical rock barrier studied in 2012 that was included in the present study was similar to those investigated by Brandes and McLain (2001) and the SJRGA (2003, 2006, 2007). All of these physical barriers were temporary obstructions installed across the entire channel width of Old River in March or April and removed in June (see Chapter 4, "Barrier Descriptions").

1.2 STUDY DESIGN, OBJECTIVES, AND HYPOTHESES

1.2.1 STUDY DESIGN

BACKGROUND

The present study used a partially controlled experimental design with uncontrollable exogenous factors influencing the treatment conditions. The principal focus of the study was the effects of barriers to influence juvenile salmonid routing (see Section 1.2.2, "Juvenile Salmonid Routing Including Barrier Effects"). The controlled portion of the design was the selection of treatments for the March through June period in each of the years studied (2009 through 2012): a non-physical barrier (BAFF) in 2009 and 2010; no barrier in 2011; and a physical barrier (rock) in 2012. The "no barrier" condition provided information about the proportion of juvenile salmonids entering Old River in the absence of a barrier. Because no barrier was present, 2011 provided a reference condition, but it was not a control condition for 2009, 2010, or 2012 because of major differences in exogenous factors between those years, in particular, discharge.

A number of physical factors were identified as parameters that may have influenced salmonid behavior in the various treatments. These parameters were discharge, water velocity, water temperature, light level, and turbidity. Variability in discharge, water velocity, water temperature, and turbidity from 2009 through 2012 is discussed in Chapter 3, "Physical Parameters."

The effectiveness of retaining juvenile salmonids in the San Joaquin River between barrier treatments was evaluated through acoustic telemetry. In each year, acoustic transmitters (tags), either Hydroacoustic Technology, Inc. (HTI) (Seattle, Washington) or VEMCO (Bedford, Nova Scotia, Canada) were implanted into juvenile Chinook salmon and/or steelhead. Movement patterns of the tagged juvenile salmonids were tracked by hydrophone arrays deployed in or near the HOR study area.

For the HTI equipment, the hydrophone array was deployed within the HOR study area from April through June during all the study years (2009-2012). The tagged juvenile Chinook and steelhead were released 24.4 kilometers (km) upstream from the HOR study area at Durham Ferry State Recreation Area. As the tagged juvenile salmonids moved through the area of the divergence, the HTI hydrophones recorded two-dimensional (2D) tracks, and these tracks were used to derive measures of juvenile salmonid routing, including barrier effects and predation rates on juvenile salmonids.

Previous publications (Bowen et al. 2012; Bowen and Bark 2012) reported results of BAFF deterrence and efficiency at the HOR study area during 2009 and 2010. The present study provides reanalysis of these same data, but reclassifies all juvenile Chinook salmon fates into samples based upon the barrier status (i.e., BAFF on/off no barrier, rock barrier) and environmental conditions (i.e., light level and velocity). Earlier publications relied on analysis of experimental groups based on the release time of the tagged juvenile salmonids from Durham Ferry without respect to the abiotic environmental conditions encountered when the tagged salmonids arrived at the HOR study area. A reanalysis approach was applied to all data (2009-2012) evaluated in this report. All tagged juvenile salmonids were grouped into samples based on the conditions when the fish arrived at the HOR study area. This approach was applied to both HTI and VEMCO tag detection data sets.[2]

In association with the main studies of juvenile salmonid routing and predation, investigation of predatory fishes was also undertaken in 2011 and 2012, using acoustic tagging and mobile hydroacoustic surveys (see Section 1.2.4, "Behavior and Density Changes in Predatory Fishes").

METRICS OF EFFICIENCY

HTI equipment (i.e., transmitters, hydrophones, and receivers) was deployed from 2009-2012, and measures of barrier efficiency and salmonid behavior were derived from the time-stamped tag detections arriving at different hydrophones.

The first measure of barrier efficiency determined using HTI equipment for 2009-2012 was Overall Efficiency (O_E) (see equation in Chapter 5, "Methods"). O_E was defined as the total number of tags implanted into juvenile Chinook salmon determined to have passed by the HOR study area and continued down the San Joaquin River divided by the total number of tags that arrived at the HOR study area. O_E was calculated in the same manner for steelhead.

[2] Comparisons between HTI and VEMCO data are provided in Appendix C.

A second measure of barrier efficiency was developed for 2009-2012 because the 2D tracks made behavioral analysis possible, and was defined as Protection Efficiency (P_E). A set of rules was developed that defined when a 2D tag track exhibited very strong evidence that the juvenile salmon implanted with that tag had been eaten (Appendix E, "Fish Fate Determination Guidelines"). When a tagged juvenile salmonid was classified as having been eaten, it was removed from analysis of P_E. Only surviving "tags-in-salmonids" remained in the data sets. The P_E was calculated as the number of surviving tagged juvenile salmonids determined to have passed by the HOR study area and continued down the San Joaquin River, divided by the sum of surviving tags-in-salmonids that passed out of the HOR study area through either the San Joaquin or Old rivers.

A third measure of BAFF efficiency was developed using the 2D tracks for 2009-2010 and was termed Deterrence Efficiency (D_E). As each tagged juvenile Chinook salmon approached the BAFF line, its path was determined to have been either deterred or undeterred by the BAFF. The determination of deterrence was made with the status of the BAFF on and off. With the BAFF off, the physical infrastructure of the BAFF remained in the water but the BAFF was not in operation.

For the 2009 through 2012 data sets, a measure of predation was developed using the 2D tracks, termed proportion eaten. The fate of each tagged juvenile Chinook salmon was assessed according to the rules described in Appendix E, "Fish Fate Determination Guidelines." The determination of predation was made by the judgment of two experts. Uncertainties associated with the expert assessments are explored in Chapter 7, "Discussion." After the predation fate had been assessed, the population proportion eaten was determined and defined as the quotient of the number of juveniles eaten divided by the total number passing through the HOR study area. Next, the proportion eaten in each sample group (see "Grouping Juvenile Salmonid into Samples" in Section 5.2.1) was used for hypothesis testing.

In addition to the sample-based metrics of proportion eaten that was investigated with univariate hypothesis testing, analyses based on the fates of individual juvenile salmonids evaluated as the probability of predation also were conducted (see Section 1.2.3, "Predation on Juvenile Salmonids Including Barrier Effects").

1.2.2 JUVENILE SALMONID ROUTING INCLUDING BARRIER EFFECTS

PRIMARY OBJECTIVES AND HYPOTHESES RELATED TO JUVENILE SALMONID ROUTING INCLUDING BARRIER EFFECTS

The objectives in this section relate to the effectiveness of the barriers as management tools to keep juvenile salmonids from entering Old River, in compliance with NMFS (2009, 2011) Action IV.1.3. The objectives are enunciated as hypotheses and they are listed in Table 1-1.

Non-physical Barrier - BAFF (2009 and 2010)

In 2009, a BAFF was operated from April 20 to May 26, and tagged juvenile Chinook salmon passed through the HOR study area from April 23 to May 18. The status of the BAFF alternated between off and on so that, approximately 50% of the time, it was operational. Exact BAFF operation times may be found in Bowen et al. (2012:Table 1). This time split between off/on operation also allowed approximately 50% of the tagged juvenile Chinook salmon to experience the BAFF when in operation.

In 2010, a BAFF was operated from April 15 to June 15, and tagged juvenile Chinook salmon passed through the HOR study area from April 27 to May 20. Similar to 2009, the status of the BAFF alternated between on and off so that it was operational approximately 50% of the time. Exact operation times may be found in Bowen and Bark (2012:Table 2). This time split between on/off operation allowed approximately 50% of the tagged juvenile Chinook salmon to experience the BAFF when in operation. In 2009 and 2010, no steelhead were surgically implanted or released.

The goal of the analysis was to determine if the BAFF was effective in retaining a significant proportion of the juvenile Chinook salmon in the San Joaquin River. If the BAFF retained a significant proportion, then it could be an effective deterrent. Hypotheses numbered $H1_0$, $H2_0$, $H3_0$, and $H4_0$ were tested to measure O_E, P_E, and D_E to determine BAFF efficiency (Table 1-1).

Table 1-1
Objectives and Hypotheses Related to Juvenile Salmonid Routing Including Barrier Effects

Year and Treatment	Objective	Hypothesis Number	Hypotheses
2009 BAFF	Determine whether barrier efficiency (O_E, P_E, and D_E) for juvenile Chinook salmon was improved by BAFF operation.	$H1_0$	For juvenile Chinook salmon, barrier efficiency (O_E, P_E, and D_E) with the BAFF on was equal to barrier efficiency with the BAFF off.
2010 BAFF	Determine whether barrier efficiency (O_E, P_E, and D_E) for juvenile Chinook salmon was improved by BAFF operation.	$H2_0$	For juvenile Chinook salmon, barrier efficiency (O_E, P_E, and D_E) with the BAFF on was equal to barrier efficiency with the BAFF off.
	Determine whether BAFF barrier efficiency with the BAFF on changed significantly between years.	$H3_0$	For juvenile Chinook salmon with BAFF on, barrier efficiency (O_E, P_E, and D_E) barrier efficiency in 2009 was equal to barrier efficiency in 2010.
	Determine whether with the BAFF off, barrier efficiency changed significantly between years.	$H4_0$	For juvenile Chinook salmon with BAFF off, barrier efficiency (O_E, P_E, and D_E) in 2009 was equal to barrier efficiency in 2010.
2011 No Barrier	Determine whether and to what extent the BAFF infrastructure affected O_E and P_E when the BAFF was turned off.	$H5_0$	For juvenile Chinook salmon, O_E and P_E were equal for 2009 BAFF off, 2010 BAFF off, and 2011 no barrier conditions.
	Determine whether juvenile Chinook salmon and steelhead had the same O_E and P_E through the HOR study area.	$H6_0$	O_E and P_E were the same for juvenile Chinook salmon and steelhead.
2012 Rock Barrier	Compare OE and PE across treatments to determine whether any barrier was more effective than no barrier and which produced the highest efficiency at retaining juvenile Chinook salmon in the San Joaquin River.	$H7_0$	For juvenile Chinook salmon, O_E and P_E were equal for 2009 and 2010 BAFF on, 2011 no barrier, and 2012 rock barrier treatments.

Notes: BAFF = Bio-Acoustic Fish Fence (Fish Guidance Systems Ltd., Southampton, UK); D_E = deterrence efficiency; HOR = Head of Old River; O_E = overall efficiency; P_E = protection efficiency; Barrier Efficiency = O_E, P_E, and D_E

Source: Present study

No Barrier (2011)

In 2011, no barrier was operated although both tagged juvenile Chinook salmon and steelhead passed through the HOR study area from May 4 to June 22. Using information collected by the hydrophone array, two measures of efficiency were obtained from the 2011 data. O_E and P_E were determined with exactly the same method mathematically (see Chapter 5, "Methods") as the barrier efficiency in years with barriers present.

Determining whether the BAFF infrastructure alone affected the routing of juvenile Chinook salmon is most appropriate when compared with the no barrier treatment (2011). Therefore, one hypothesis tested (Table 1-1: $H5_0$) if O_E and P_E varied between the status when the BAFF was installed but not in operation and when there was no barrier.

It also needed to be determined whether the routing of tagged juvenile Chinook salmon and steelhead were the same in a year in which no barrier was installed. Hence, hypothesis $H6_0$ tested if there was a difference between tagged juvenile Chinook salmon and steelhead for O_E and P_E (Table 1-1).

Physical Barrier - Rock (2012)

In 2012, a physical barrier made of rock was installed and operated from April 1 through May 31, and tagged juvenile Chinook salmon and steelhead passed through the HOR study area from April 28 through May 29. In contrast to BAFF operations, the physical barrier located at the HOR was always operational (on) because it could not be turned off or uninstalled.

It needed to be determined how the barrier treatments performed relative to each other and relative to no barrier. For example, if the physical rock barrier retained a significant proportion of the juvenile Chinook salmon in the San Joaquin River, then it might be an effective deterrent. Hence, one hypothesis tested measures O_E and P_E to determine the routing proportions with different treatments and discharge regime (Table 1-1:$H7_0$).

Supporting Hypotheses Related to Juvenile Salmonid Routing Including Barrier Effects

DWR (2012) studied the effect of a BAFF under variable velocity conditions. A substantial proportion of the juvenile Chinook salmon were deterred by the BAFF under both low (<0.25 meters per second [m/s] "fish escape" velocity (Figure 4-2) and high (<0.25 m/s "fish escape" velocity) velocity (DWR 2012:Table 3-12). In addition, for the BAFF on status, O_E, P_E, and D_E were all greater under low-velocity compared to high-velocity conditions. These results suggest that the BAFF's effectiveness at the HOR study area might also be affected by discharge/velocity. As previously noted, Perry et al. (2012) also found that the effectiveness of the BAFF was inversely related to discharge. Perry et al. (2012) suggested that higher discharges and correspondingly higher velocities were more likely to force fish through the barrier compared to lower discharge/velocity conditions.

DWR (2012) described studies of a BAFF at Georgiana Slough (Sacramento County, California). This was the same BAFF studied by Perry et al. (2012). A significant proportion of juvenile Chinook salmon were deterred by the BAFF under both low (< 5.4 lux) and high (≥ 5.4 lux) light conditions (DWR 2012:Table 3-11). However, for the BAFF "on" status, D_E under high-light conditions was 13.7% greater than the D_E under low-light conditions. The results from the Georgiana Slough study suggest that the BAFF's performance at the HOR study area may be affected by ambient light level similar to the findings of Welton et al. (2002).

Because of these findings, the effects of light level and water velocity on O_E, P_E, and D_E were studied and are reported herein. For each hypothesis, where possible, analyses were conducted at various light and discharge/velocity levels. These analyses showed whether or not the O_E, P_E, and D_E were affected by these abiotic environmental variables and if so, to what extent.

1.2.3 PREDATION ON JUVENILE SALMONIDS, INCLUDING BARRIER EFFECTS

Several major objectives of the present study are related to predatory fish ecology and predation at the HOR study area. The HOR area and the scour hole downstream of the divergence of San Joaquin and Old rivers were previously noted as regional "hotspots" of high predation, although recent studies do not concur (e.g., SJRGA 2010, 2011, and 2013, and references therein). In the 2009 study of BAFF deterrence, Bowen et al. (2012) noted that predation was intense in the HOR area and appeared associated with the scour hole just downstream of the divergence of Old River from the San Joaquin River. They concluded the following (Bowen et al. 2012:20–21):

> The data suggest that much of the gains accomplished by the BAFF's determent of juvenile Chinook salmon are offset by the predatory fishes inhabiting the scour hole. We recommend that if the BAFF is installed in the future that predator relocation be employed near the Old River barrier area. For example, striped bass and largemouth bass could be moved from the HOR study area to San Luis Reservoir. Failure to do so could lead to a high predation rate situation and the highly efficient BAFF's deterrence may be offset by the heavy predation in the scour hole.
>
> It is possible that the high 2009 predation rates observed were a function of the low discharge (dry year) in the San Joaquin River. Juvenile Chinook salmon and predators might have been concentrated into a smaller habitat area due to the reduced volume of water than during average or wet years. Such a concentration could result in higher encounter rates between predators and juvenile Chinook salmon leading to an increased predation rate.

The predation rate on tagged juvenile Chinook salmon in the HOR was also high in 2010, despite greater river discharge (Bowen and Bark 2012).

In the present study, predation was examined using a sample-based, univariate approach (proportion eaten) and a generalized linear modeling (GLM) approach (probability of predation). Perspective on rates of predation suggested by tagged juvenile salmonids was provided with bioenergetics modeling of potential predatory fish consumption of prey fish (see Appendix H, "Illustrative Example of Striped Bass Predation Using Bioenergetics Modeling").

OBJECTIVES AND HYPOTHESES RELATED TO PROPORTION OF JUVENILE SALMONIDS EATEN

Because of the importance of predation in affecting the usefulness of a fish barrier, various hypotheses were tested regarding the proportion of juvenile salmonids entering the HOR study area that were determined to have been eaten based on the aforementioned "predation rules" (see Appendix E, "Fate Determination Guidelines"). In addition to this hypothesis testing approach based on proportions of juvenile salmonids entering the HOR study area that were eaten (grouping juvenile salmonids into samples, and using univariate statistics; see Section 5.2, "Evaluation of Juvenile Salmonid Routing Including Barrier Effects"), an approach based on the probability of

predation of individual fish entering the HOR study area from GLM also was used (see "Objectives and Hypotheses Related to Probability of Predation" in the following section).

For 2009 and 2010 data analyses, it needed to be determined if the BAFF increased the proportion eaten when it was operating compared to when it was not operating. The outcome would be important in determining the effectiveness of the BAFF as a management tool. Thus, the proportion of those juvenile Chinook salmon eaten was tested as determined by expert opinion for 2009 and 2010 data separately, with the status of the BAFF on compared to BAFF off (Table 1-2: $H8_0$).

For 2011 data, it was possible to compare juvenile Chinook salmon and steelhead estimates of the proportion determined to have been eaten (Table 1-2: $H9_0$). It needed to be determined if species differences may have led to differential susceptibility to predation in the HOR study area. Differences between the species (described in Section 5.1.1, "Fish Sources and Tag Specifications," and Section B.1, "Focal Salmonid Species for Protection at Head of Old River" [Appendix B, "Focal Fish Species Information"]) in migration timing, size when in the vicinity of the HOR study area, and presumably swimming ability might all influence differences in predation probabilities.

For 2012 data analyses, the physical rock barrier was installed and all juvenile Chinook salmon that were determined to have been eaten were used to estimate the proportion eaten in each sample. It needed to be determined if the proportion eaten in each year was different, and what proportion might be eaten. For 2009 and 2010, BAFF-on observations of juvenile Chinook salmon determined to have been eaten were used. No BAFF-off observations were included. This approach simulated what would be expected if the BAFF were operated continuously. This hypothesis would identify if one of the barrier types caused a substantially higher proportion to be eaten (Table 1-2: $H10_0$).

OBJECTIVES AND HYPOTHESES RELATED TO PROBABILITY OF PREDATION

In addition to hypotheses related to proportion eaten that were tested with a univariate, sample-based approach (see "Objectives and Hypotheses Related to Proportion Eaten" previously presented), a GLM approach was used to address objectives and hypotheses related to probability of predation (Table 1-2: H11, H12, and H13). This approach allowed the probability of predation to be framed in terms of abiotic factors (light level, water temperature, turbidity, and discharge/velocity), biotic factors (juvenile size, density of large fish [assumed to be representative of predatory fish], density of small fish [assumed to be representative of alternative prey for predators]), and the presence/operational status of non-physical (BAFF) or physical barriers (rock) at the HOR study area. More detailed discussion of the underlying hypotheses is provided in Section 5.3.2 "Probability of Predation (Generalized Linear Modeling)."

Table 1-2
Objectives and Hypotheses Related to Predation on Juvenile Salmonids Including Barrier Effects

Year	Objectives	Hypothesis Number	Hypotheses
2009	Provide a direct test that the BAFF operation had some influence on proportion eaten.	$H8_0$	The proportion of juvenile Chinook salmon entering the HOR study area that were eaten with the BAFF on was equal to the proportion eaten when off.
2010	Provide a direct test that the BAFF operation had some influence on proportion eaten.	$H8_0$	The proportion of juvenile Chinook salmon entering the HOR study area that were eaten with the BAFF on was equal to the proportion eaten when off.
2011	Evaluate the proportion eaten for juvenile Chinook salmon and steelhead.	$H9_0$	The proportions of juvenile Chinook salmon and steelhead entering the HOR study area that were eaten were equal.
2009–2012	Show whether there were differences in proportion eaten between treatments.	$H10_0$	The proportions of juvenile Chinook salmon entering the HOR study area that were eaten were equal for 2009 and 2010 BAFF on, 2011 no barrier, and 2012 rock barrier.
2009, 2010, 2012	Evaluate the influence of abiotic and biotic factors, including barrier treatment/status, on probability of predation of juvenile Chinook salmon.	H11	Probability of predation of juvenile Chinook salmon is negatively related to discharge (shorter travel time/distance at higher discharge), turbidity (lower visual range of predators with greater turbidity), size (larger juveniles less susceptible to predation), and small-fish density (availability of alternative prey for predators). Probability of predation is positively related to water temperature (higher bioenergetic demands of predators with higher temperature) and ambient light level (greater visual range of predators with more light). Probability of predation is unrelated to barrier treatment/ status (BAFF on/off, rock barrier).
2011, 2012	Evaluate the influence of abiotic and biotic factors on probability of predation of juvenile Chinook salmon.	H12	Probability of predation of juvenile Chinook salmon is negatively related to discharge, turbidity, juvenile size, and small-fish density. Probability of predation is positively related to water temperature, ambient light level, and density of predatory fish (greater predation pressure with more large fish).
2011	Evaluate the influence of abiotic and biotic factors on probability of predation of juvenile steelhead.	H13	Probability of predation of juvenile steelhead is negatively related to discharge, turbidity, juvenile size, and small-fish density. Probability of predation is positively related to water temperature, ambient light level, and density of predatory fish (greater predation pressure with more large fish).

Notes: BAFF = Bio-Acoustic Fish Fence (Fish Guidance Systems Ltd., Southampton, UK); HOR = Head of Old River
Source: Present study

1.2.4 BEHAVIOR AND DENSITY CHANGES IN PREDATORY FISHES

OBJECTIVES RELATED TO BEHAVIOR OF PREDATORY FISHES

Objectives related to predatory fish behavior at the HOR study area consisted of analyses based on acoustically tagged predatory fish and mobile hydroacoustics. These analyses generally did not test specific hypotheses (although see the following section on "Objectives and Hypotheses Related to Changes in Density of Predatory Fishes") and were more exploratory and descriptive. The objectives and their utility to management are summarized in Table 1-3.

Table 1-3
Objectives Related to Behavior of Predatory Fishes at the HOR Study Area

Year	Objective	Means of Study	Utility to Management
2009–2012	Describe residence time of predatory fish.	Acoustically tagged predatory fish	May indicate turnover of predatory fish, and therefore allows inference regarding the level of effort required for relocation of predatory fish.
2009–2012	Describe areas (spatial and velocity) occupied by predatory fish.	Acoustically tagged predatory fish, mobile hydroacoustic surveys, stationary tags from juvenile salmonid (presumably eaten and defecated by predatory fish)	May indicate location within the study area to focus predator capture efforts for any contemplated relocation efforts, as well as indicates habitat areas that could be manipulated to reduce predator density and predation risk.

Note: HOR = Head of Old River
Source: Present study

OBJECTIVES AND HYPOTHESES RELATED TO CHANGES IN DENSITY OF PREDATORY FISH

Mobile hydroacoustic survey data from 2011 and 2012 were used to determine if there was evidence of changes in environmental variables associated with changes in density of large fish (>30 centimeters [cm] total length (TL), of which many are assumed to be predatory fish), by testing $H14_0$ (Table 1-4). Knowledge of the potential influence of these variables on density has the potential to guide management action (e.g., by allowing efforts such as predator relocation or reduction to be focused at times of potentially high density). In addition, two objectives related to $H15_0$ and $H16_0$ were intended to determine whether changes in density at the study area were similar to changes in the broader south Delta area, and whether the density at the study area was greater than at other areas. These objectives/hypotheses were examined by comparing density at the study area to three reference sites in the San Joaquin River (Table 1-4).

Table 1-4
Objectives and Hypotheses Related to Density of Predatory Fishes at the HOR Study Area

Year	Objectives	Hypothesis Number	Hypotheses
2011–2012	Determine if environmental variables are associated with changes in large-fish density at the HOR study area.	$H14_0$	Density of large fish (>30 cm TL) (i.e., potential predators) at the HOR site is not correlated with environmental variables (discharge, water temperature, turbidity, light level, and small-fish density [representing availability of potential prey]).
2011–2012	Determine if there are broad-scale environmental influences on predatory fish density at the HOR site that result in similar changes in density to reference sites.	$H15_0$	Changes in density of large fish (>30 cm TL) (i.e., potential predators) at the HOR site during the spring are not correlated with changes in density at three reference sites.
2011–2012	Determine if predatory fish density at the HOR site is greater than at reference sites.	$H16_0$	The density of large fish (>30 cm TL) (i.e., potential predators) at the HOR site during the spring is not significantly different from density at three reference sites.

Notes: cm = centimeters; HOR = Head of Old River; TL = total length
Source: Present study

2 STUDY AREA AND FOCAL FISH SPECIES

2.1 STUDY AREA

2.1.1 THE SACRAMENTO–SAN JOAQUIN DELTA

The Delta is a complex of reclaimed islands[1] and tidally influenced freshwater sloughs and channels at the confluence of the Sacramento and San Joaquin rivers. It is part of a larger estuary system to the west that includes Suisun, San Pablo, and San Francisco bays. The Delta watershed includes more than one-third of California's land surface area, and stretches from the eastern slopes of the Coast Range to the western slopes of the Sierra Nevada (Lund et al. 2007). The Delta is approximately 39 km wide and 77 km long. The Delta is located in an area roughly delimited by the cities of Sacramento, Stockton, Tracy, and Antioch (Thompson 1957) and includes portions of Sacramento, San Joaquin, Contra Costa, Solano, and Yolo counties. Before settlement and reclamation activities, the tidal basin included approximately 129,499 hectares, and another 82,961 hectares was subject to seasonal flooding (Thompson 1957).

Historically, the Delta was a natural wetland complex, fed by discharge from the Sacramento and San Joaquin rivers. The vast wetland complex consisted of tidal channels, sloughs, islands with tule (*Schoenoplectus* spp.) marsh plains, complex water channels characterized by dendritic branching, and natural levees colonized by riparian forests (Bay Institute 1998). A slow rise in sea level and gradual regional tectonic subsidence created an "accommodation space" that allowed for the continuous accumulation of large volumes of sediment within the Delta (Atwater et al. 1979; Orr et al. 2003). The Delta essentially was formed by a combination of upstream sediment deposition and the decay of large quantities of marsh vegetation (Lund et al. 2007). The formation of thick deposits of peat, capped by tidal marshes, kept up with a slow rise in sea level. Approximately 60% of the Delta land mass was flooded by daily tides, and spring tides could submerge it completely (Lund et al. 2007; Thompson 1957). Large areas frequently flooded during heavy winter rains. The interior waterways were primarily freshwater, although saltwater intrusion from the west occurred during summer months (Jackson and Paterson 1977).

Today, the Delta is a highly modified system when compared to conditions that existed before European settlement and reclamation activities. Many waterways are channelized and contained within riprap-stabilized levees. Floodplains, backwaters, and riparian vegetation are absent from many areas. The reduction of riparian vegetation and shaded riverine habitat through levee construction and protection activities has contributed to increased annual water temperatures (NMFS 2011). These changes have contributed to the decline of many native fish species while benefitting non-native fish species that are more adaptable to the highly altered environment (Lund et al. 2007; Moyle 2002). In addition, the simplified environment and loss of habitat complexity may have contributed to the success of non-native fish species and the decline of native fish populations (Moyle 2002).

Supplemental information is provided in Appendix A, "Additional Background on the Study Area and Nearby Areas," which includes information on the upstream tributaries leading to the HOR study area (Figures 2-1 and A-1).

[1] These "islands" are actually polders.

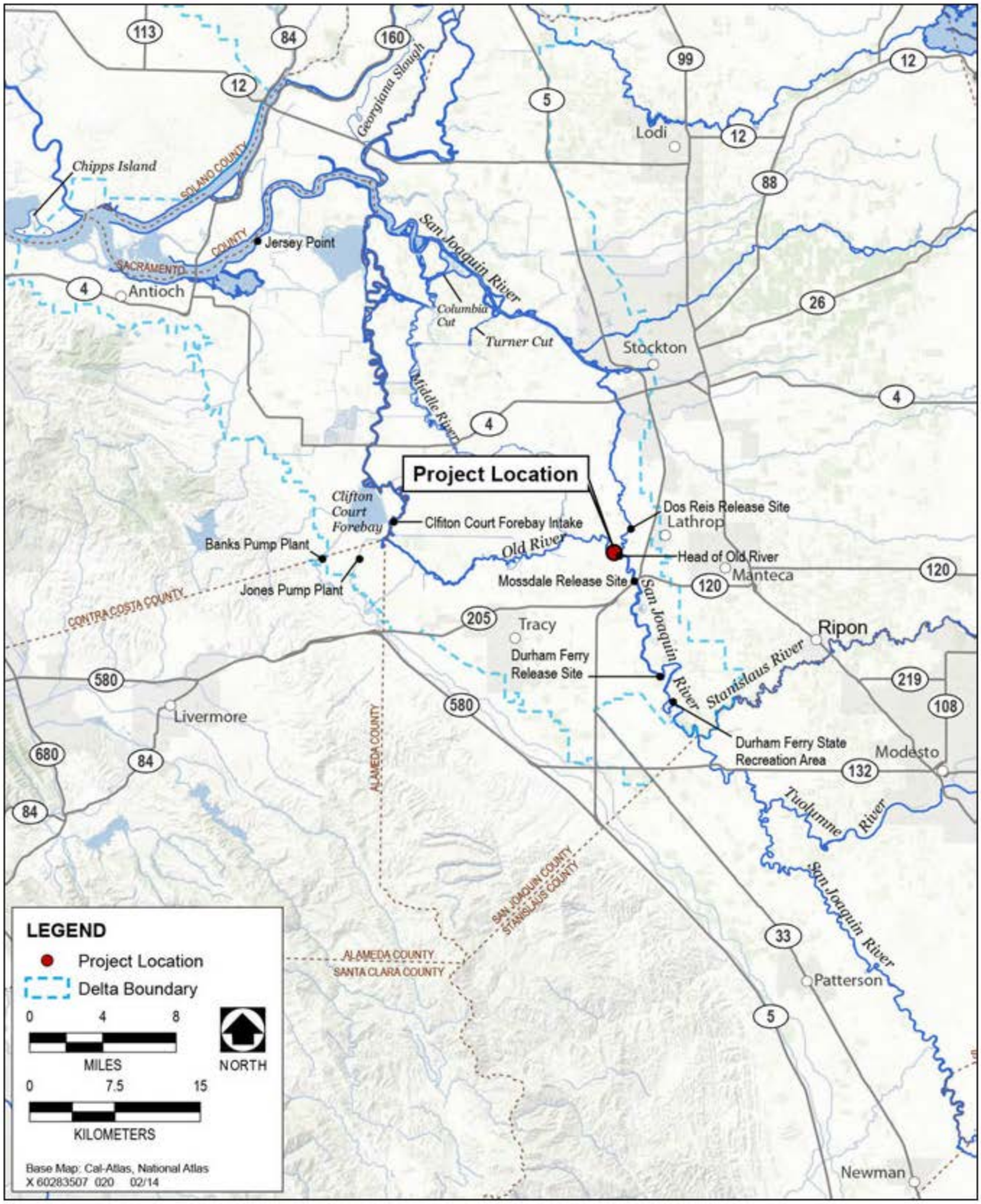

Source: Data compiled by AECOM in 2013

Figure 2-1 Location and Study Area Indicating Major Tributaries of the San Joaquin River

2.1.2 RESEARCH PROJECT STUDY AREA

The field data collection activities of the research described in this report were conducted between April 1, 2009 and June 30, 2012, within a study area located in the southeast corner of the Delta at the divergence of the San Joaquin and Old rivers. The HOR study area boundary was delineated by the location of the most upstream and downstream hydrophones (discussed in further detail in Chapter 5, "Methods").

The primary land use is agricultural, including row crops, nut trees, dairies, and hay production. The banks of the San Joaquin River within the study area are heavily fortified with riprap with steep slopes that drop quickly to the river thalweg. Overstory riparian vegetation is absent. The river channel generally is featureless with an average depth of approximately 3 meters (m) and a maximum depth of 9 m, and the benthic substrate is composed primarily of fine sediments. Maximum depth occurs in a large scour hole, located just downstream from the divergence with Old River.

The Old River represents the first watercourse downstream of the convergences of the three main tributaries and the San Joaquin River (Figure 2-1). This divergence is the first potential migration fork for emigrating juvenile salmonids. If the Old River route is selected, it leads the juvenile salmonids into the interior Delta where susceptibility to predation and entrainment by the SWP and CVP intake pumps are increased. All emigrating juvenile salmonids produced in the San Joaquin River must pass by the HOR. Predation rates in this area may be comparatively high because:

- predatory fish densities can be particularly high in this location;
- the area is narrow and highly channelized;
- the area lacks littoral vegetation, instream structure and floodplain habitat;
- the river margins quickly become steep dropping into the river thalweg; and
- discharge patterns have created the fairly large, deep scour hole in the San Joaquin River just downstream of the divergence, which may attract predatory fish and increase their foraging opportunities (Figure 2-2).

These characteristics may create a predatory gauntlet, especially in the spring, when annual predictable high densities of juvenile salmonids are migrating downstream (Tables B-2 and B-4 in Appendix B, "Focal Fish Species Information"). Previous studies suggest that predation rates on juvenile Chinook salmon can be 12% to 40% at the HOR study area (Bowen et al. 2012; Bowen and Bark 2012). Appendix A, "Additional Background on the Study Area and Nearby Areas," briefly describes the three main tributaries of the San Joaquin River, including the current status of their steelhead and Chinook salmon populations.

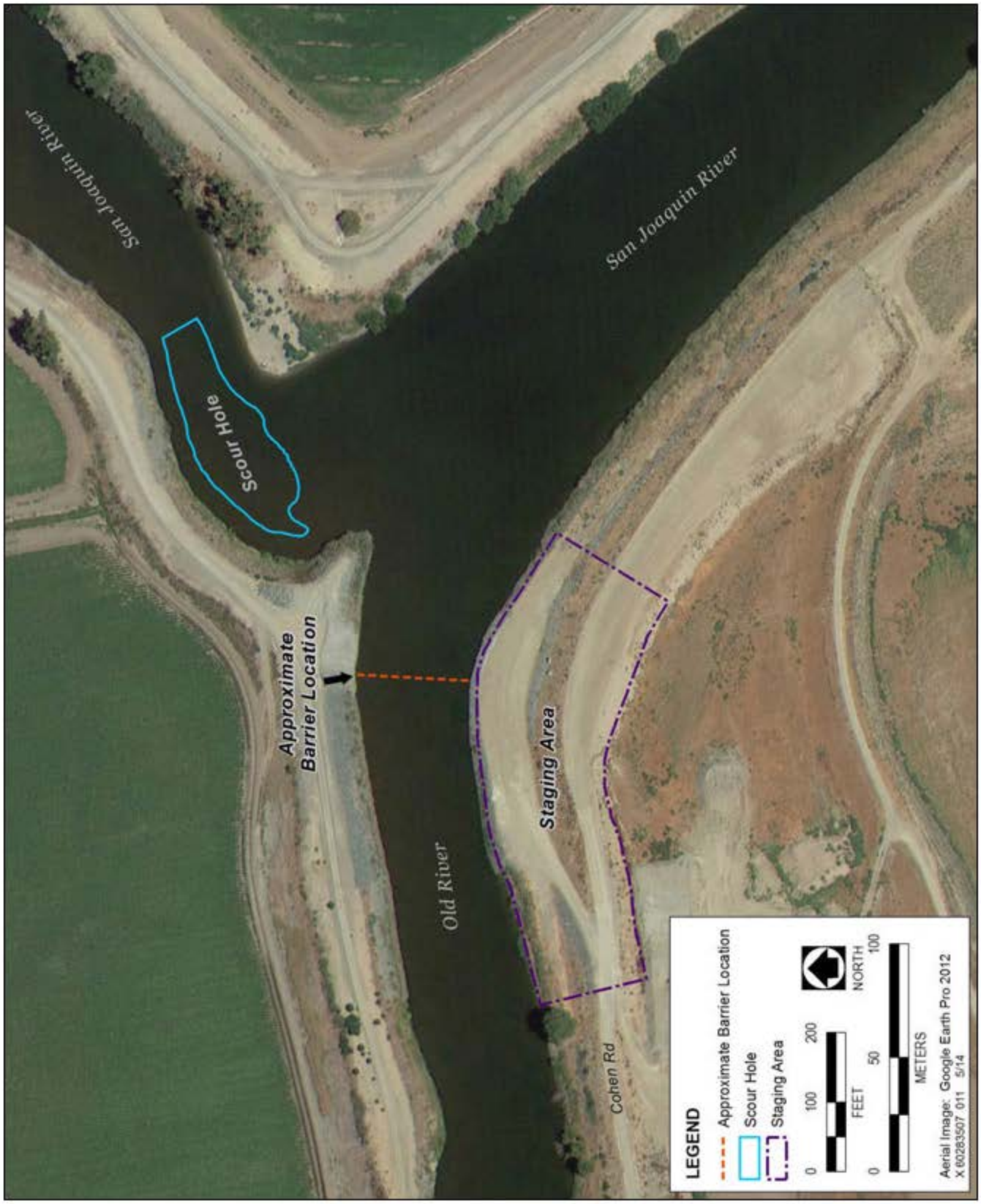

Source: Data compiled by AECOM in 2013

Figure 2-2 **San Joaquin River–Old River Divergence, Scour Hole Location, Approximate Rock Barrier Line and Staging Area**

2.1.3 HEAD OF OLD RIVER

In 2009, DWR began assessing the deterrence capabilities of alternative barrier types to facilitate the retention of juvenile salmonids in the mainstem San Joaquin River during the downstream migration toward the Pacific Ocean. A non-physical BAFF barrier was installed in 2009 and 2010 at the divergence of Old and the San Joaquin rivers, approximately 5 km west of the City of Lathrop and 11 km northeast of the City of Tracy (Figure 2-3). No barrier was installed in 2011 because of very high discharge, and a physical rock barrier was installed in 2012 (Figure 2-4). Barriers were designed to improve migration conditions for juvenile salmonids that originated in the San Joaquin River watershed by blocking and/or deterring passage into Old River and directing movements to the mainstem San Joaquin River. Barrier descriptions, objectives, installation dates, and operations are summarized in Chapter 4, "Barrier Descriptions."

2.2 FOCAL FISH SPECIES

2.2.1 FOCAL FISH SPECIES FOR PROTECTION

The primary focal fish species that management intends to protect using barriers at the HOR are Chinook salmon and steelhead, both of which originate in tributaries of the San Joaquin River upstream of the HOR. Both Chinook salmon and steelhead are in long-term decline in California. Historically, the San Joaquin River supported three runs of Chinook salmon: fall, late fall, and spring (Fisher 1994). The late fall and spring-runs were extirpated in the 1940s (Fisher 1994). At present, the only Chinook salmon in the San Joaquin River region are fall-run, although spring-run are proposed for reintroduction under the San Joaquin River Restoration Program (SJRRP). Historically, steelhead were widely distributed throughout the Sacramento and San Joaquin river basins, and were composed of summer and winter-runs. Presently, only the winter-run steelhead persist in the Central Valley (Williams 2006) due to dam construction that prevents summer steelhead from reaching higher elevation stream reaches where they previously over-summered in deep, cool pools. An important period of interest for fish species protection is spring, when juvenile Chinook salmon and steelhead migrate downstream through the Delta. More detailed information on the status and life history of Chinook salmon and steelhead is presented in Section B.1, "Focal Salmonid Species for Protection at Head of Old River," in Appendix B, "Focal Fish Species Information."

In addition to the salmonid fish species for protection at the HOR, two other listed species are relevant for consideration of barrier operations: delta smelt (*Hypomesus transpacificus*) and green sturgeon (*Acipenser medirostris*). More detailed information on these two species is presented in Section B.2, "Other Species for Protection at Head of Old River," in Appendix B.

2.2.2 FOCAL PREDATORY FISH SPECIES

Several predatory fish species occur at the HOR study area and may influence barrier effectiveness if they are attracted to structures or capitalize on changed hydrodynamics or juvenile salmonid behavior that results from barrier deployment (see Bowen et al. 2012; Bowen and Bark 2012). The main predatory fish species that have been observed at the HOR study area during the studies from 2009 through 2012 are striped bass (*Morone saxatilis*), largemouth bass (*Micropterus salmoides*), channel catfish (*Ictalurus punctatus*), and white catfish (*Ameiurus catus*). A more detailed overview of the biology of the predatory fish species is provided in Section B.3, "Focal Predatory Fish Species at Head of Old River," in Appendix B.

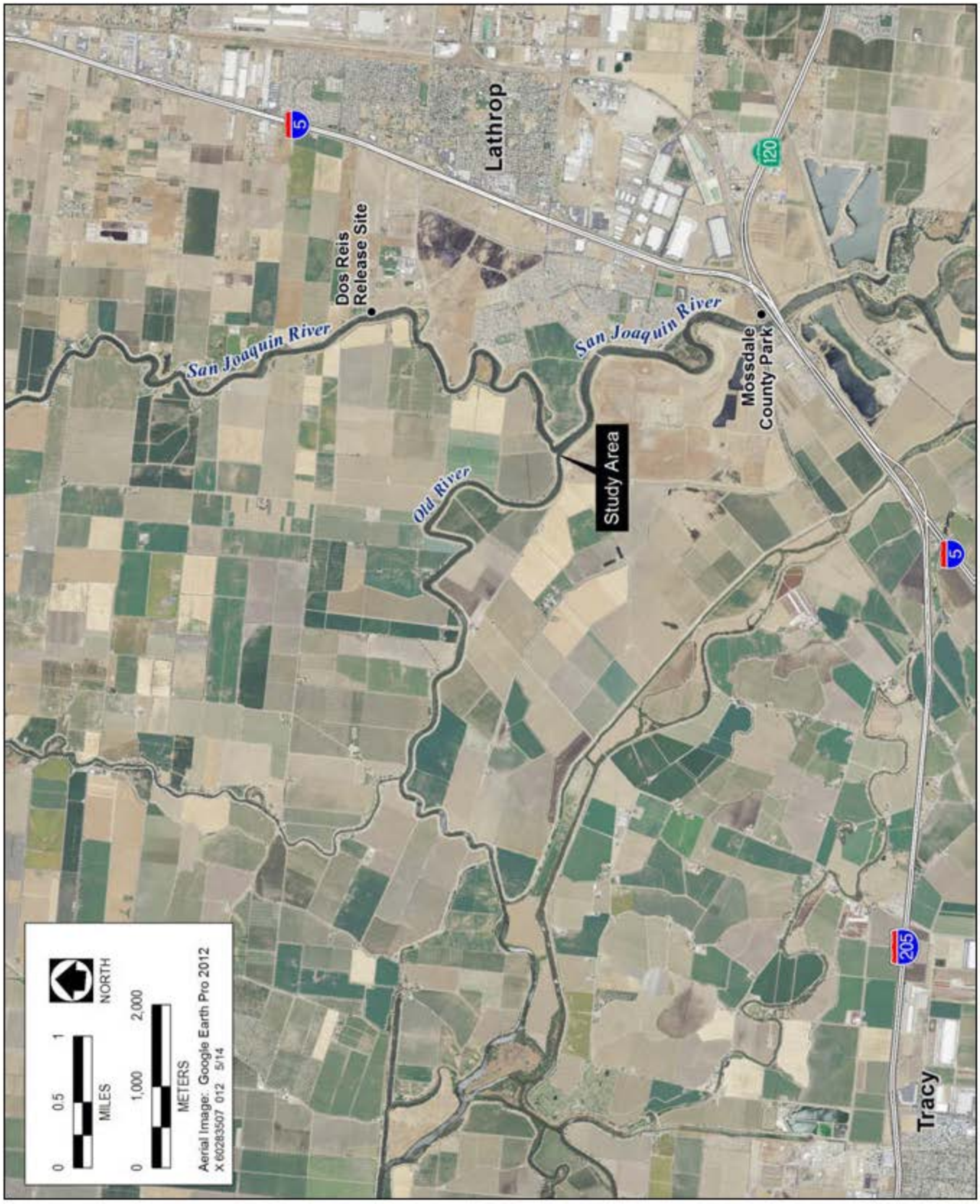

Source: Data compiled by AECOM in 2013

Figure 2-3 Vicinity of the Head of Old River Study Area Depicting Salmonid Release Points

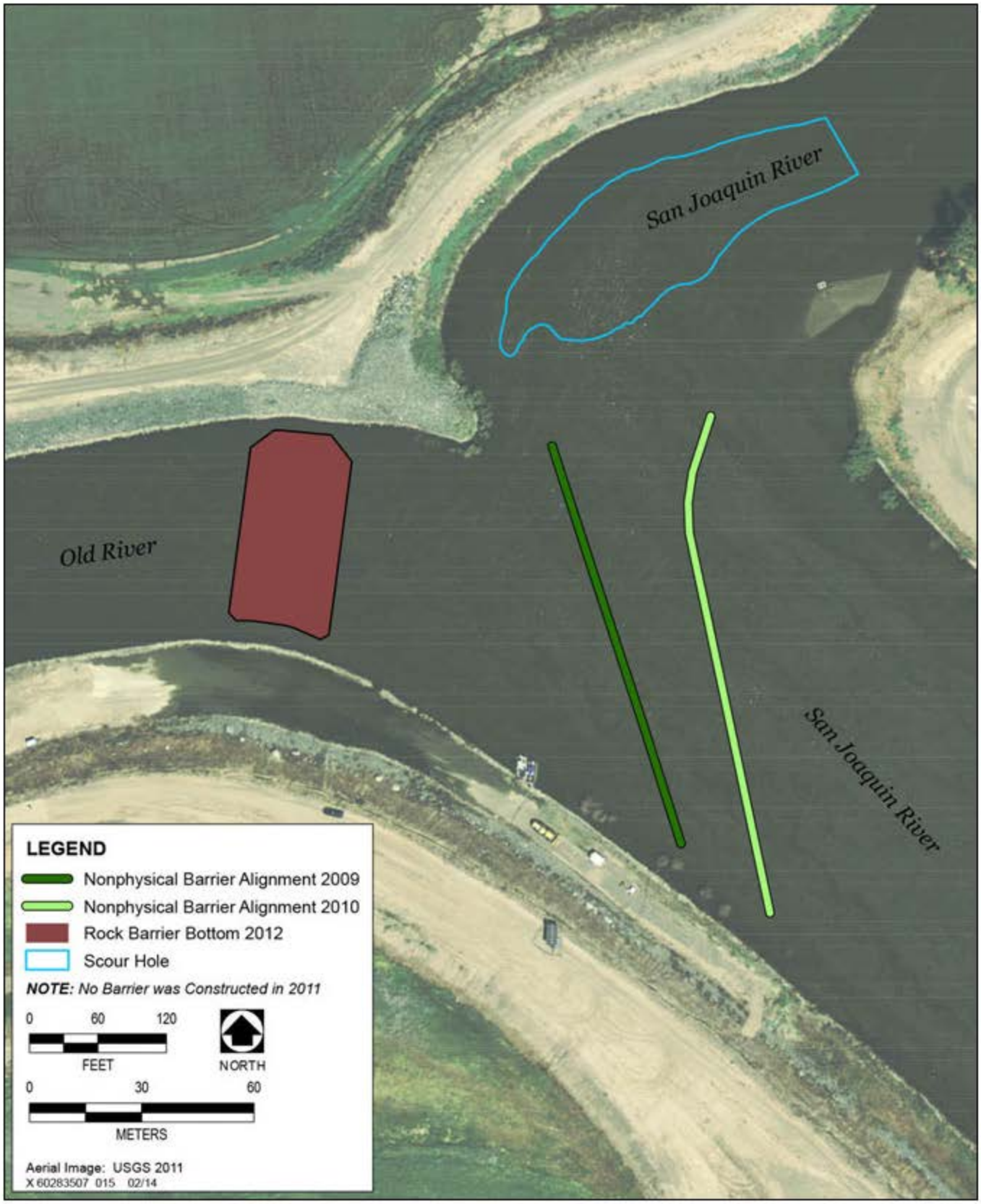

Sources: DWR 2012; Bianchini and Cane pers. comm. 2013; data compiled by AECOM in 2013

Figure 2-4 **Barrier Alignments near the Head of Old River, 2009–2012**

2.2.3 FOCAL FISH ASSEMBLAGE

A basic description of the spring (March through June) fish assemblage in the vicinity of the HOR study area is provided herein from three surveys: (1) trawling in the San Joaquin River at Mossdale which provides an indication of small fish relative abundance in the river channel (Dekar et al. 2013); (2) seining at three sites in the San Joaquin River which provides information on small fish in the nearshore, shallow water environment (Dekar et al. 2013); and (3) electrofishing in the San Joaquin River downstream from the HOR study area which samples small and large fish in the nearshore environment (Conrad, pers. comm., 2013). Of these surveys, Mossdale trawling occurs most frequently (near daily) at the highest intensity (generally 10 trawls per day) and is efficient at collecting the main salmonid species for protection at the HOR study area (i.e., juvenile Chinook salmon). For the summary presented next, trawl and seine data were limited to small fish (i.e., less than 150 millimeters [mm] fork length [FL]), because the trawling gear used was most suited for smaller fish. In addition, the Mossdale trawl estimates for small fish density were used in subsequent analyses of large fish abundance and salmonid juvenile predation probability, discussed in Chapter 5, "Methods." More information regarding the methods for trawling and seining is provided by Dekar et al. (2013). Electrofishing consisted of 300-meter-long transects from a survey vessel at 50 sites bimonthly from October 2008 through October 2010 (Conrad, pers. comm., 2013). Of this total effort, the spring (April and June, 2009 and 2010) data from the site (SAN_1) closest to the HOR study area are summarized herein.

RIVER CHANNEL (MOSSDALE TRAWL)

Thirty-five fish taxa were collected with trawling at Mossdale from March through June in 2009 through 2012, of which 12 were native species (Table 2-1). Daily abundance indices of small fish (less than 150 mm FL) from March through June 2009 were calculated as the geometric mean abundance per 10,000 cubic meters trawled at Mossdale. The mean abundance indices varied considerably among years. Sacramento splittail (*Pogonichthys macrolepidotus*) and juvenile Chinook salmon were the most abundant species collected. A very high abundance of Sacramento splittail in 2011 coincided with very high discharge in the San Joaquin River that probably provided a greater extent of spawning habitat; the species responds positively to increased availability of ephemeral habitats with inundated vegetation, such as floodplains (Sommer et al. 1997). Juvenile Chinook salmon mean abundance indices in 2011 and 2012 were appreciably greater than in 2009 and 2010. Threadfin shad (*Dorosoma petenense*) and inland silverside (*Menidia beryllina*) were the third and fourth most abundant small fish collected in the Mossdale trawl, and their mean abundance indices were greatest in 2009. Marked (i.e., adipose-fin-clipped or dyed for gear efficiency studies) juvenile Chinook salmon and striped bass were the only other taxa with mean daily abundance indices greater than 0.1 (Table 2-1).

In 2009, high occasional catches of inland silverside occurred from April through June, and a relatively high abundance of threadfin shad and striped bass occurred in June (Figure 2-5). Juvenile Chinook salmon capture occurred from late March to late May, with greatest abundance generally in mid-May. In 2010, peaks in abundance of all fish combined were driven by a number of high catches of splittail from early May to mid-June (Figure 2-6). Catches of juvenile Chinook salmon in 2010 were sporadic, and they were low from early April to early June, but a large peak of marked fish occurred in early June. In 2011, very few fish were collected before late April (Figure 2-7). Subsequently, extremely high catches of splittail occurred in mid- to late May and mid-June, as well as appreciably high catches of juvenile Chinook salmon over the same period. In contrast, very few splittail were collected in 2012, whereas Chinook salmon (marked and unmarked) abundance was by far the highest of all fish, and occurred from early April to early June (Figure 2-8).

Table 2-1
Mean Daily Abundance Index of Fish Species Caught by Mossdale Trawling, Site SAN_1, March–June, 2009–2012

Species	2009	2010	2011	2012	All Years
Sacramento splittail	0.16	2.46	34.52	0.10	10.10
Chinook salmon	0.52	0.23	1.53	1.98	1.10
Threadfin shad	1.22	0.20	0.03	0.03	0.35
Inland silverside	1.09	0.04	0.18	0.10	0.34
Chinook salmon (marked)	0.00	0.25	0.34	0.71	0.33
Striped bass	0.49	0.00	0.00	0.01	0.12
Common carp	0.00	0.00	0.20	0.00	0.06
Goldfish	0.00	0.03	0.10	0.00	0.03
Red shiner	0.04	0.00	0.01	0.07	0.03
Bluegill	0.07	0.01	0.00	0.01	0.02
Largemouth bass	0.00	0.04	0.00	0.01	0.01
Channel catfish	0.01	0.00	0.00	0.03	0.01
Golden shiner	0.02	0.00	0.00	0.01	0.01
White catfish	0.00	0.01	0.00	0.02	0.01
Hardhead	0.00	0.00	0.00	0.03	0.01
Sacramento sucker	0.00	0.00	0.01	0.01	0.01
Pacific lamprey	0.01	0.01	0.00	0.00	0.00
American shad	0.00	0.00	0.00	0.01	0.00
Bass unknown	0.01	0.00	0.00	0.00	0.00
Spotted bass	0.00	0.00	0.00	0.01	0.00
Smallmouth bass	0.00	0.00	0.00	0.00	0.00
Redear sunfish	0.00	0.00	0.00	0.00	0.00
White crappie	0.00	0.00	0.00	0.00	0.00
Black crappie	0.00	0.00	0.00	0.00	0.00
Hitch	0.00	0.00	0.00	0.00	0.00
Tule perch	0.00	0.00	0.00	0.00	0.00
Sacramento pikeminnow	0.00	0.00	0.00	0.00	0.00
Longfin smelt	0.00	0.00	0.00	0.00	0.00
Bigscale logperch	0.00	0.00	0.00	0.00	0.00
Delta smelt	0.00	0.00	0.00	0.00	0.00
Green sunfish	0.00	0.00	0.00	0.00	0.00
Prickly sculpin	0.00	0.00	0.00	0.00	0.00
Wakasagi	0.00	0.00	0.00	0.00	0.00
Lamprey unknown	0.00	0.00	0.00	0.00	0.00
Shimofuri goby	0.00	0.00	0.00	0.00	0.00
Sacramento blackfish	0.00	0.00	0.00	0.00	0.00

Note: Abundance index = geometric mean number of fish per 10,000 cubic meters trawled each day (typical sampling effort = 10 trawls per day).

Source: Compiled from data provided by Speegle, pers. comm., 2011–2012

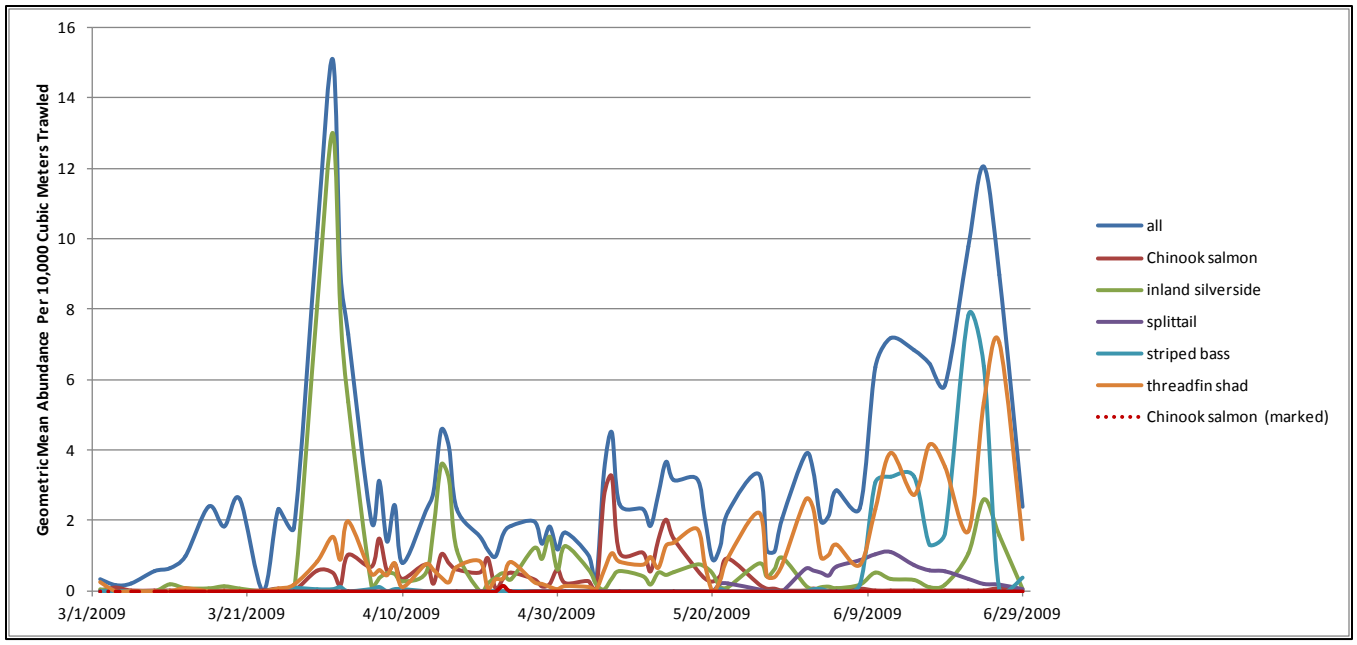

Source: Compiled from data provided by Speegle, pers. comm., 2011–2012

Figure 2-5 **Common Fish Species Geometric Mean Abundance per 10,000 Cubic Meters from Mossdale Trawling, Site SAN_1, March–June 2009**

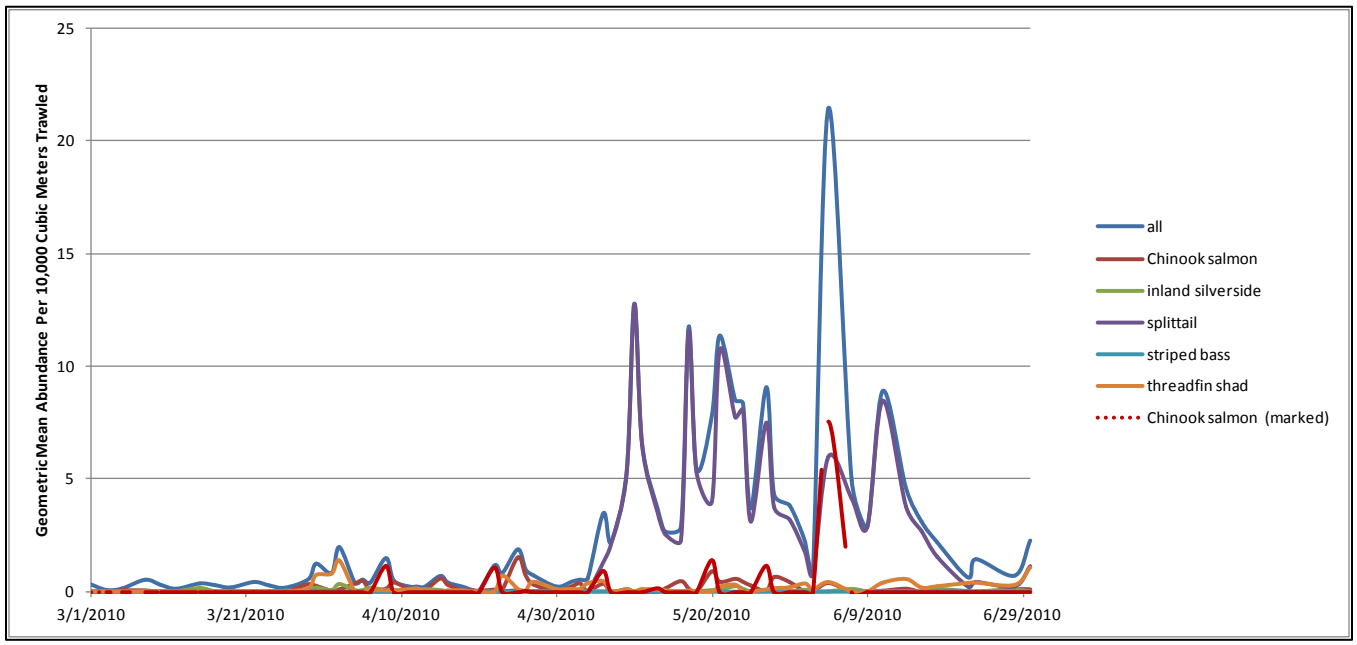

Source: Compiled from data provided by Speegle, pers. comm., 2011–2012

Figure 2-6 **Common Fish Species Geometric Mean Abundance per 10,000 Cubic Meters from Mossdale Trawling, Site SAN_1, March–June 2010**

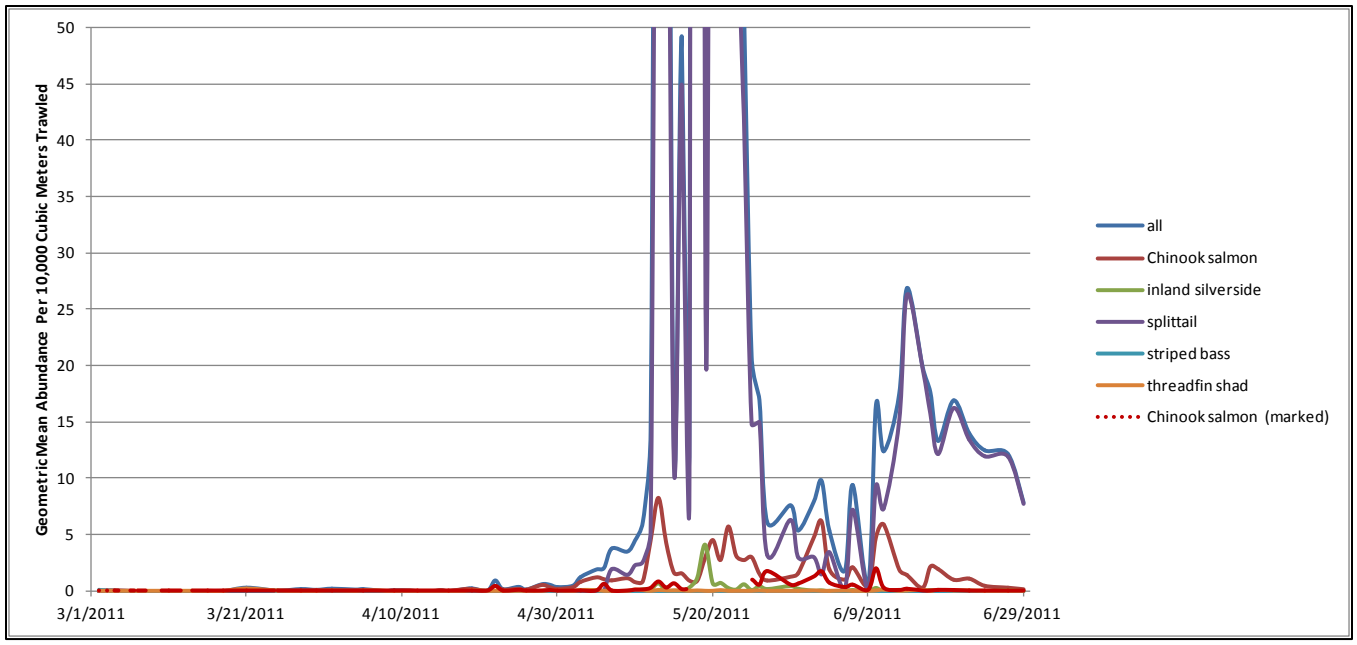

Note: Y-axis is truncated; maximum abundance was greater than 600.

Source: Compiled from data provided by Speegle, pers. comm., 2011–2012

Figure 2-7 **Common Fish Species Geometric Mean Abundance per 10,000 Cubic Meters from Mossdale Trawling, Site SAN_1, March–June 2011**

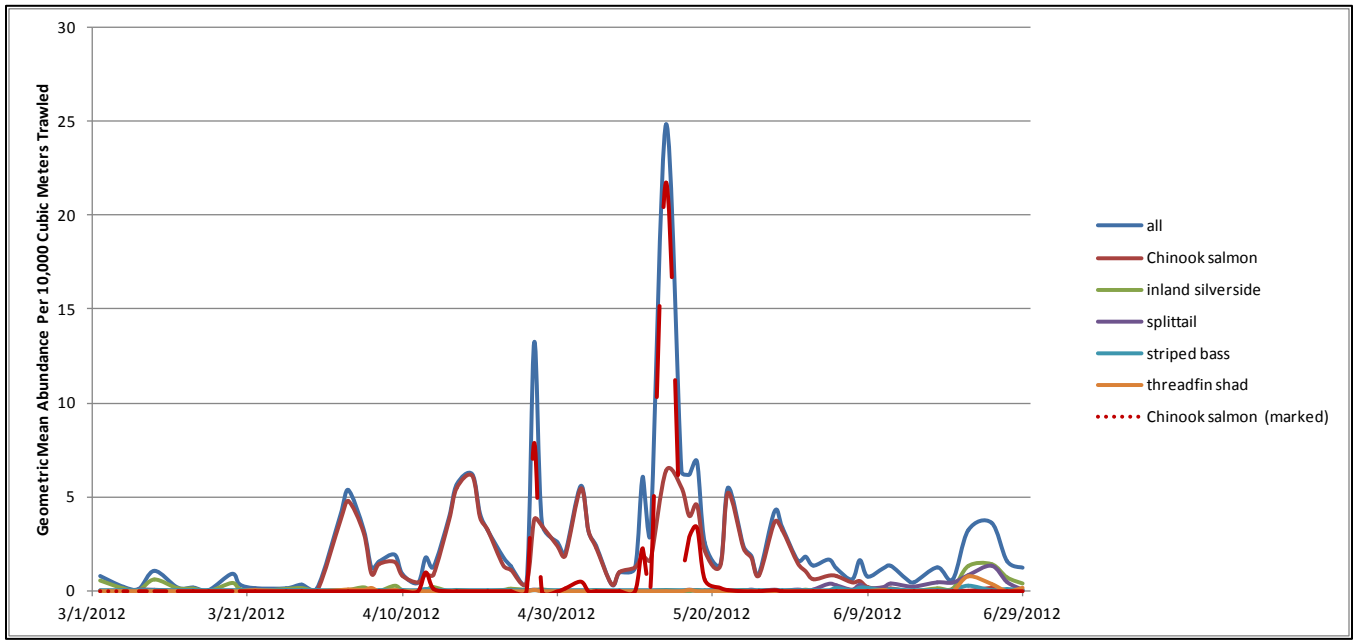

Source: Compiled from data provided by Speegle, pers. comm., 2011–2012

Figure 2-8 **Common Fish Species Geometric Mean Abundance per 10,000 Cubic Meters from Mossdale Trawling, Site SAN_01, March–June 2011**

NEARSHORE (SEINING AND ELECTROFISHING)

Seining at three stations in the general vicinity of the HOR study area from March through June, 2009 through 2012, collected 25 fish taxa of less than 150 mm FL, of which nine were native (Table 2-2). The introduced species inland silverside and red shiner (*Cyprinella lutrensis*) dominated the catch (approximately 70% of all fish collected), with two native species (Sacramento sucker [*Catostomus occidentalis*] and splittail) constituting nearly 18% of all fish collected.

Table 2-2
Number of Fish Collected at San Joaquin River Beach Seining Stations SJ051E, SJ056E, SJ058W, March–June, 2009–2012

Species	2009	2010	2011	2012	All Years
Inland silverside	746	708	365	336	2155
Red shiner	442	750	301	273	1766
Sacramento sucker	54	194	74	232	554
Sacramento splittail	6	206	230	2	444
Largemouth bass	18	20	17	57	112
Bluegill	26	37	6	41	110
Threadfin shad	58	8	0	6	72
Prickly sculpin	0	1	6	52	59
Common carp	0	2	52	2	56
Western mosquitofish	15	19	7	3	44
Black crappie	1	0	0	36	37
Golden shiner	5	6	8	14	33
Chinook salmon	0	7	14	10	31
Redear sunfish	6	3	0	10	19
Sacramento pikeminnow	0	13	3	0	16
Striped bass	7	2	0	6	15
Tule perch	2	1	0	11	14
Chinook salmon (marked)	0	0	9	2	11
Bigscale logperch	0	2	0	7	9
Yellowfin goby	8	0	0	0	8
Spotted bass	0	1	1	4	6
Fathead minnow	1	0	4	0	5
Pacific staghorn sculpin	0	0	0	3	3
American shad	0	0	0	2	2
Hardhead	0	0	1	0	1
Sacramento blackfish	0	0	0	1	1

Source: Speegle, pers. comm., 2011–2012

Thirteen fish species were collected during four electrofishing samples in the San Joaquin River downstream from the HOR study area in April and June 2009 and 2010 (Table 2-3). The most abundant fish collected were bluegill (*Lepomis macrochirus*) (35% of total catch), white catfish (18%), threadfin shad (9%), and striped bass (8%). Native fish (Sacramento sucker and prickly sculpin [*Cottus asper*]) made up only 3% of the total catch. Of the four focal predatory fish species from the present study, white catfish (68–301 mm FL) were most abundant, followed by striped bass (115–459 mm FL), largemouth bass (160–385 mm FL; 7% of total catch), and channel catfish (199–447 mm FL; 5% of total catch). Other potential predatory fish collected during electrofishing (smallmouth bass [*Micropterus dolomieu*] and prickly sculpin) were a very minor part of the catch (Table 2-3).

Table 2-3
Number and Size of Fish Collected By Electrofishing in the San Joaquin River Downstream from the HOR Study Area, April and June, 2009–2010

Species	Number					Fork Length (mm)		
	4/21/2009	6/17/2009	4/15/2010	6/23/2010	Total	Min.	Mean	Max.
Bluegill	9	48	8	27	92	52	133.0	231
White catfish	20	6	6	15	47	68	246.0	301
Threadfin shad	0	20	1	4	25	84	100.1	126
Striped bass	9	6	2	3	20	115	190.8	459
Largemouth bass	3	3	8	4	18	160	262.5	385
Redear sunfish	4	9	1	4	18	44	178.8	293
Channel catfish	7	3	0	3	13	199	334.3	447
Common carp	4	0	2	4	10	NA	NA	NA
Green sunfish	3	1	1	1	6	119	146.8	171
Inland silverside	3	2	1	0	6	71	80.3	95
Sacramento sucker	1	0	4	1	6	428	466.8	510
Spotted bass	1	1	0	0	2	190	195.5	201
Prickly sculpin	1	0	0	0	1	128	128.0	128

Notes: HOR = Head of Old River; mm = millimeters
Data are for site SAN_1 (UTM Zone 10 N, Northing: 4187551.004; Easting: 648320.84).
Source: Conrad, pers. comm., 2013

3 PHYSICAL PARAMETERS

Data summarized in this chapter for physical parameters during the 2009 through 2012 study years were from local monitoring stations and generally consisted of 15-minute observations (discharge, water temperature, and turbidity). These data were from the California Data Exchange Center (CDEC) (Baldwin, pers. comm., 2013; Dempsey, pers. comm., 2013). In addition, water velocity data were modeled, as described herein.

3.1 DISCHARGE AND TIDAL REGIME

3.1.1 2009 DISCHARGE

Within the study area, discharge from April through June 2009 was the lowest during the 4-year study period (Figure 3-1). The official water year classifications based on May 1 runoff forecasts were dry in 2009 and 2012, above normal in 2010, and wet in 2011 (State of California 2013). In 2009, low discharge in the San Joaquin River at Mossdale (MSD) led to frequent flow reversals at that location, and the San Joaquin River at Lathrop (SJL), just downstream of the HOR study area, was close to fully tidal much of the time (Figure 3-2). Ebb tide discharge rarely exceeded 2,000 cubic feet per second (cfs) at SJL, and flood tide discharge was nearly as low at -2,000 cfs. SJL flows during the period in which tagged juvenile Chinook salmon arrived into the HOR study area generally were within the range of -1,000 to 2,000 cfs (Figure 3-2).

The division of discharge at the HOR between Old and San Joaquin rivers is of considerable relevance to the analyses of barrier effectiveness described later in this chapter. Estimates of the proportion of discharge entering Old River tend to be extremely variable when made at the 15-minute scale, so summaries were created by calculating daily sums of 15-minute readings of discharge at the Old River at Head (OH1) and dividing by the corresponding daily sums of 15-minute San Joaquin River at Mossdale (MSD) discharge. From April through June 2009, daily discharge at OH1 averaged 0.81 (81%) of daily discharge at Mossdale (range: 0.60 to 1.18), suggesting that the great majority of discharge had entered Old River during this time (Figure 3-3). During the period from April 23 through May 18 in which tagged juvenile Chinook salmon arrived at the HOR study area, daily discharge at OH1 averaged 0.65 of the daily discharge at MSD (range 0.60 to 0.73) (Table 3-1).

3.1.2 2010 DISCHARGE

The April through June discharge in 2010 was appreciably higher than in 2009 (Figure 3-1), with the MSD discharge varying between a low of approximately 650 cfs in early April and a high of nearly 7,900 cfs during the period of tagged juvenile Chinook salmon entry in May (Figure 3-4). The SJL discharge exhibited tidal reversals in April, late May, and June, but during the period of juvenile entry, discharge was higher and generally ranged from 1,000 cfs to 3,000 cfs.

From April through June 2010, daily discharge at OH1 averaged 0.54 (54%) of daily discharge at MSD (range: 0.43 to 0.80), suggesting that just more than one-half of discharge had entered Old River during this time (Figure 3-3). During the period from April 27 through May 20, in which tagged juvenile Chinook salmon entered the area, daily discharge at OH1 averaged 0.44 of the daily discharge at MSD (range 0.43 to 0.45) (Table 3-1).

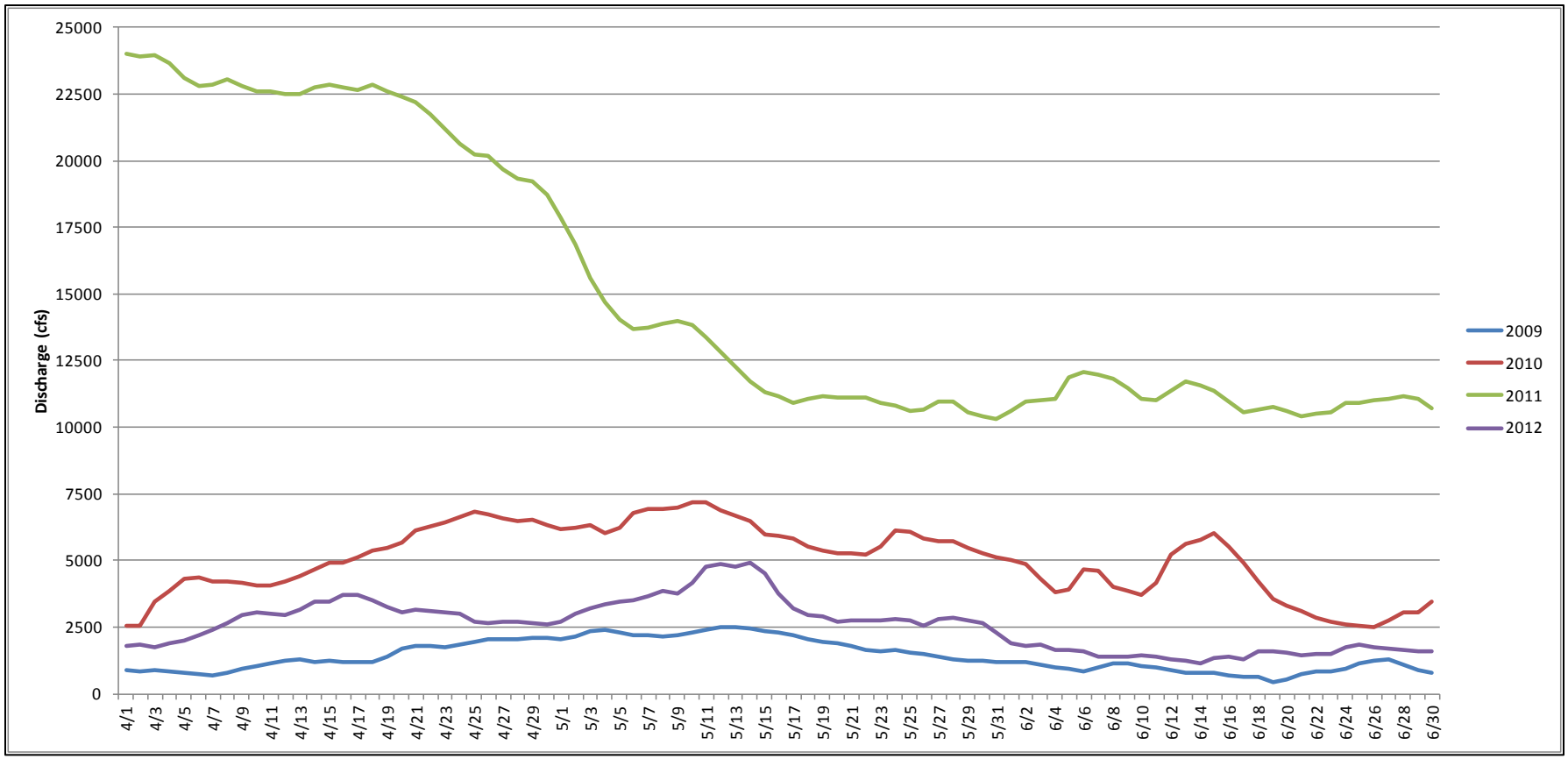

Sources: Baldwin, pers. comm., 2013; Dempsey, pers. comm., 2013

Figure 3-1 **Daily Mean River Discharge in the San Joaquin River at Mossdale (MSD), 4/1 through 6/30, 2009–2012**

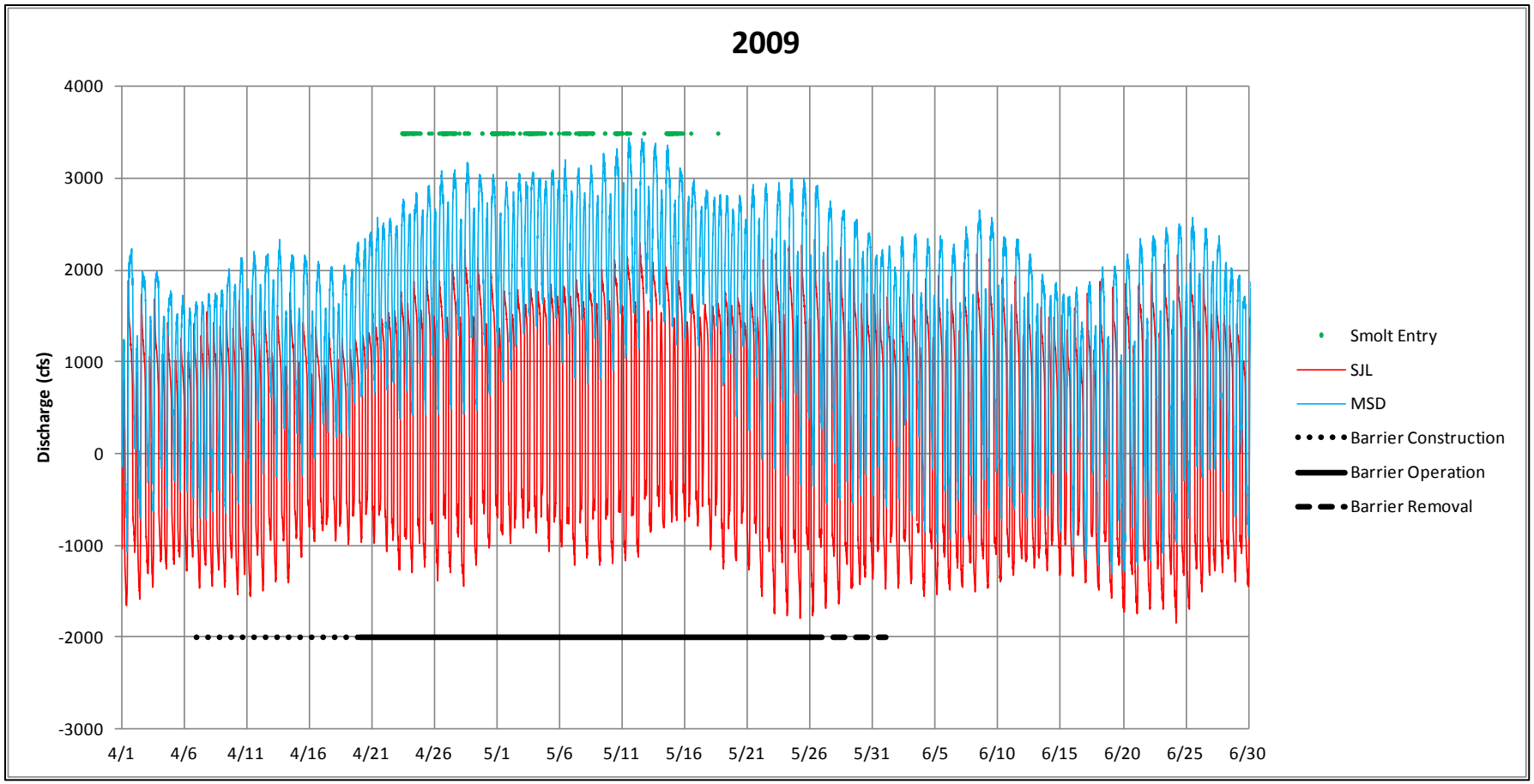

Sources: Baldwin, pers. comm., 2013; Dempsey, pers. comm., 2013

Note: The barrier referred to in the legend was a non-physical fish barrier called a BAFF (Fish Guidance Systems Ltd., Southampton, UK). Barrier operation was not continuous, with the BAFF off approximately 50% of the time during the period of BAFF operation.

Figure 3-2 **15-Minute River Discharge in the San Joaquin River at Mossdale (MSD) and Lathrop (SJL), 4/1/09 through 6/30/09, in Relation to Acoustically Tagged Juvenile Chinook Salmon Arrival into the Head of Old River Study Area (Green Dots)and Non-physical Barrier Construction/Operation/Removal (Black Lines)**

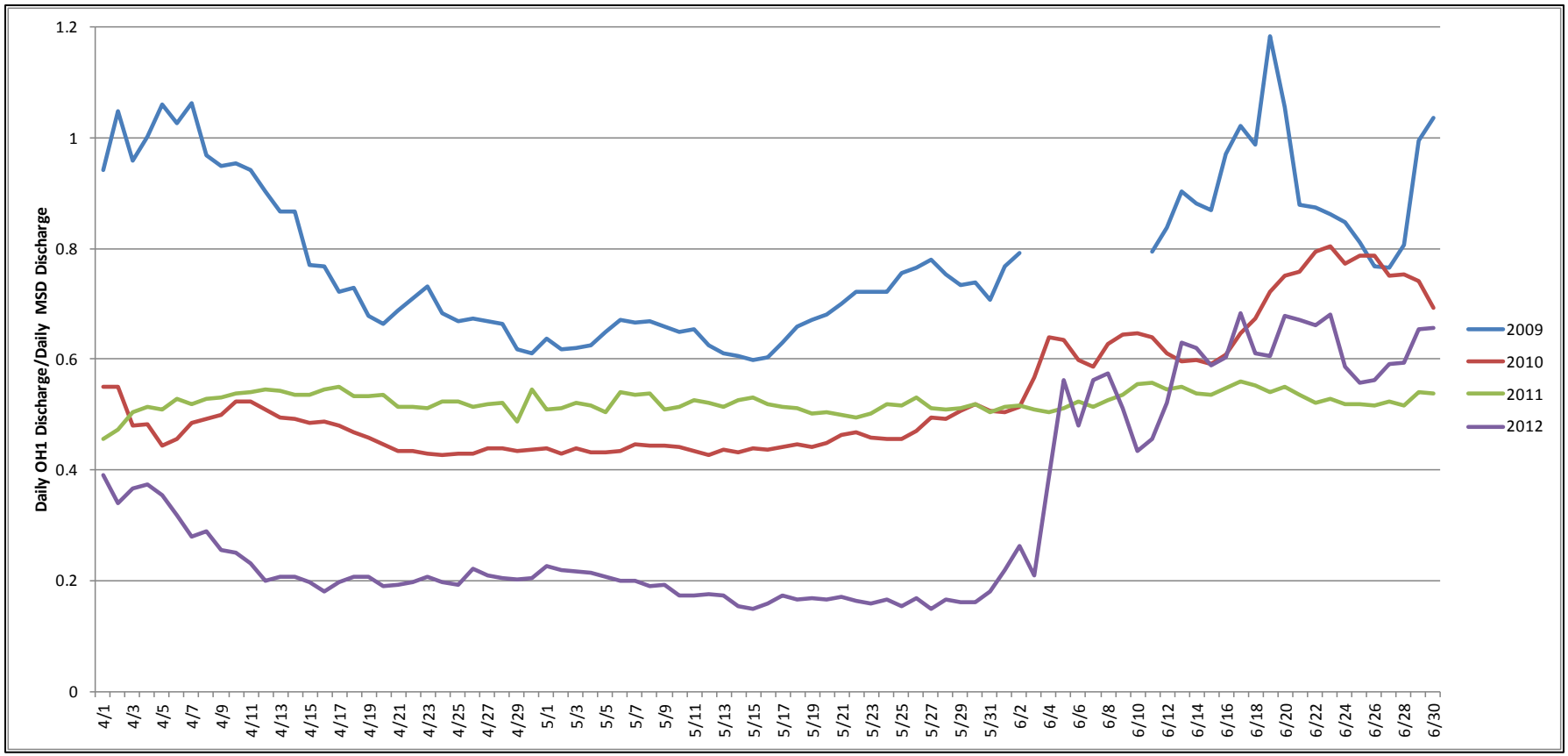

Sources: Baldwin, pers. comm., 2013; Dempsey, pers. comm., 2013

Figure 3-3 **Old River Head (OH1) Daily Discharge as a Proportion of San Joaquin River at Mossdale, Daily Discharge, April-June, 2009-2013**

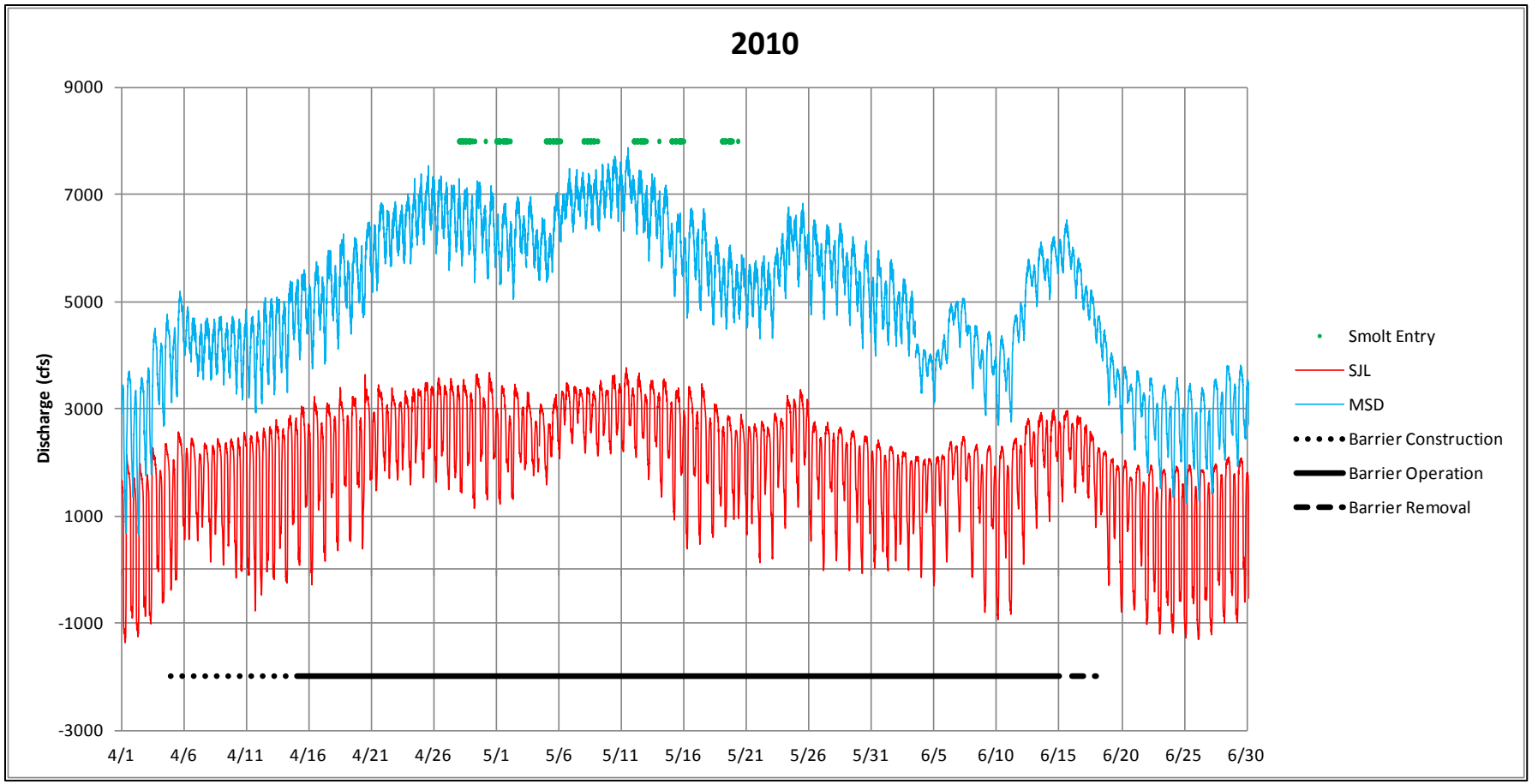

Sources: Baldwin, pers. comm., 2013; Dempsey, pers. comm., 2013

Note: The barrier referred to in the legend was a non-physical fish barrier called a BAFF (Fish Guidance Systems Ltd., Southampton, UK). Barrier operation was not continuous with the BAFF off approximately 50% of the time during the period of BAFF operation.

Figure 3-4 **15-Minute River Discharge in the San Joaquin River at Mossdale (MSD) and Lathrop (SJL), 4/1/10 through 6/30/10, in Relation to Acoustically Tagged Juvenile Chinook Salmon Entry into the Head of Old River Study Area (Green Dots)and Non-physical Barrier Status (Black Lines)**

Table 3-1
Descriptive Statistics for 2009–2012 HOR Average Daily Discharge as Proportion of San Joaquin River at Mossdale Average Daily Discharge during Periods when Tagged Juvenile Chinook Salmon Arrived at the HOR Study Area

			Daily OH1 Discharge/Daily MSD Discharge				
Year	First Fish[1]	Last Fish[2]	Mean	Standard Deviation	Minimum	Maximum	Count
2009	4/23/09; 8:24	5/18/09; 13:48	0.65	0.03	0.60	0.73	26
2010	4/27/10; 22:25	5/20/10; 5:54	0.44	0.01	0.43	0.45	24
2011	5/4/11; 2:51	6/22/11; 4:24	0.52	0.02	0.49	0.56	50
2012	4/28/12; 4:13	5/29/12; 16:35	0.18	0.02	0.15	0.23	32

Notes: HOR = Head of River; OH1 = Old River at Head; MSD = San Joaquin River at Mossdale
The OH1 gauge is 0.25 km downstream of the HOR site; the MSD gauge is ~4.5 km upstream of the HOR site. The periods reported here are based on values observed during the period between first and last detections of fish.

[1] Date/time when the first tagged salmonids was nearest the BAFF line.

[2] Date/time the last tagged salmonids was nearest the BAFF line.

[3] SJR Flow Proportion = 1 - (Mean of (Daily OH1 Discharge/Daily MSD Discharge)); therefore SJR Flow Proportion = 0.35 (2009), 0.56 (2010), 0.48 (2011), and 0.82 (2012).

Source: Baldwin, pers. comm., 2013; Dempsey, pers. comm., 2013

3.1.3 2011 DISCHARGE

Discharge from April through June 2011 was exceptionally high as a result of unseasonably high precipitation (Figure 3-1). Discharge at MSD exceeded 24,000 cfs in early April and remained higher than 10,000 cfs for most the entire 3-month period (Figure 3-5). The discharge at the SJL gauge was higher than 10,000 cfs during much of April, and was approximately 7,500 cfs at the beginning of tagged juvenile salmonid entry into the HOR study area in early May, before decreasing to approximately 5,000 cfs from approximately mid-May thru the end of June. The tidal signal was appreciably muted in 2011 because of the high river discharge.

From April through June 2011, daily discharge at OH1 averaged 0.51 (51%) of daily discharge at MSD (range: 0.44 to 0.90), suggesting that approximately one-half of the discharge had entered Old River during this time (Figure 3-3). During the period from May 5 through June 22, in which tagged juvenile salmonids entered the area, daily discharge at OH1 averaged 0.52 of the daily discharge at MSD (range 0.49 to 0.56) (Table 3-1).

3.1.4 2012 DISCHARGE

Discharge in 2012 from April through June was greater than in 2009, but less than 2010 (Figure 3-1). Tidal flow reversals occurred at SJL in April and June, with a handful of reversals at MSD in June (Figure 3-6). The SJL discharge during the period of tagged juvenile salmonid entry to the HOR study area generally varied from more than 1,000 to 2,500 cfs in late April/early May, and from less than 1,000 cfs to just more than 2,000 cfs from mid- to late June. No juveniles entered the area during elevated discharge of approximately 4,500 to 5,000 cfs at MSD from May 10 through 15 (Figure 3-6).

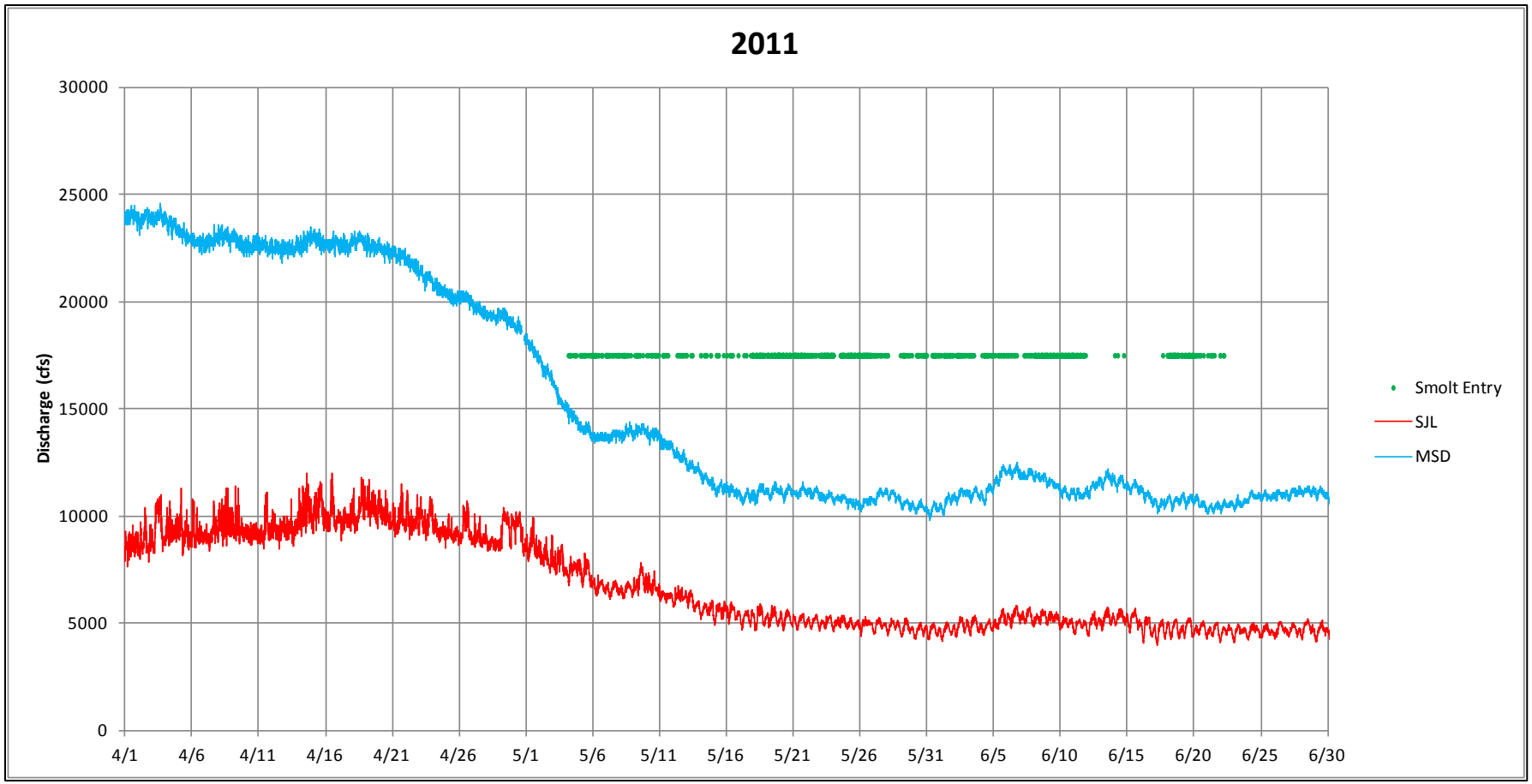

Sources: Baldwin, pers. comm., 2013; Dempsey, pers. comm., 2013

Figure 3-5 **15-Minute River Discharge in the San Joaquin River at Mossdale (MSD) and Lathrop (SJL), 4/1/11 through 6/30/11, in Relation to Acoustically Tagged Juvenile Chinook Salmon and Steelhead Arrival into the Head of Old River Study Area (Green Dots)**

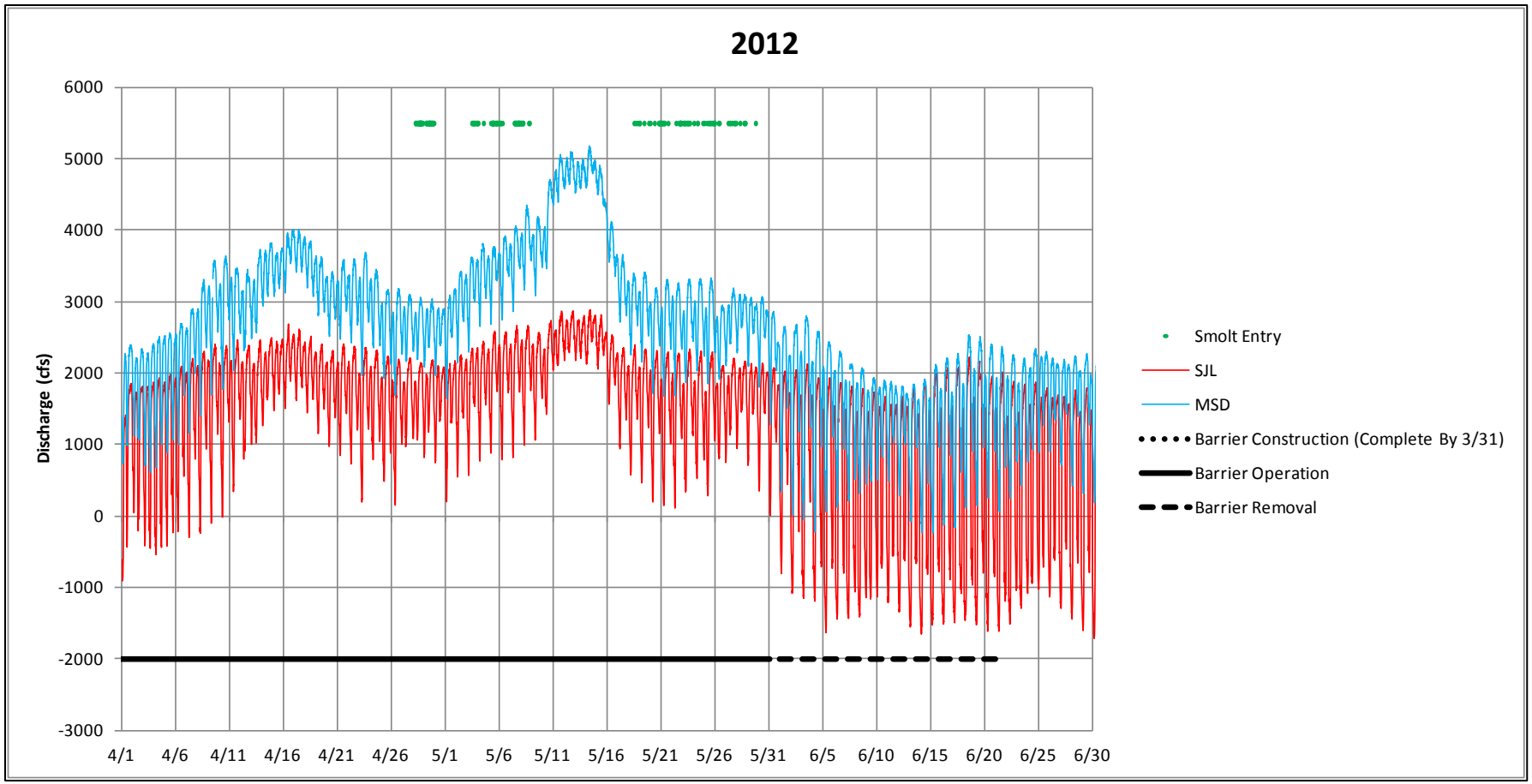

Sources: Baldwin, pers. comm., 2013; Dempsey, pers. comm., 2013

Note: The barrier referred to in the legend was a rock barrier with eight culverts.

Figure 3-6 **15-Minute River Discharge in the San Joaquin River at Mossdale (MSD) and Lathrop (SJL), 4/1/12 through 6/30/12, in Relation to Acoustically Tagged Juvenile Chinook Salmon Entry into the Head of Old River Study Area (Green Dots) and Rock Barrier Status (Black Lines)**

From April through June 2012, daily discharge at OH1 averaged 0.44 (44%) of daily discharge at MSD (range: 0.15 to 1.05), suggesting that just less than one-half of the discharge had entered Old River during this time interval (Figure 3-3). During the period from April 28 through May 29, in which tagged juvenile salmonids entered the area, daily discharge at OH1 averaged 0.18 of the daily discharge at MSD (range 0.15 to 0.23) (Table 3-1). This relatively low proportion of discharge reflected the installation of the rock barrier that occurred from April 1 through May 31 (Figure 3-6), and represents the discharge either passing through the barrier's culverts or between the rocks that made up the barrier.

3.2 VELOCITY FIELD

Hydrodynamic data were collected in 2009, 2011, and 2012 to provide information on the velocity field at the HOR study area. These data sets provide a three-dimensional (3D) water velocity field at discrete time periods.

3.2.1 METHODS

In 2009 and 2011, hydrodynamic data were collected using a downward-looking acoustic Doppler current profiler (DL-ADCP) from a moving boat. Measurements were taken on February 2, March 3 and 13, May 29, and June 5, 2009, and on April 12, 2011. In 2012, near-surface hydrodynamic data were collected using side-looking (SL) ADCPs, deployed near the bank and profiling across the river at four locations for the duration of the study period, April 23 through May 30. The SL-ADCP data were interpolated to generate a near-surface 2D velocity field. On May 8 and 30, 2012, DL-ADCP measurements were taken to validate the 2D velocity interpolation.

DL-ADCP DATA PROCESSING AND INTERPOLATION

The DL-ADCP measurements were made synoptically during the same time intervals for 8 days in each year (i.e., 2009, 2011, and 2012). The processing methods included correcting Differential Global Positioning System (DGPS) tracks, objectively filtering out suspect data, spatially smoothing based on a 3-point weighted average, and extrapolating velocity vectors to the bed (bottom substrate) (Dinehart and Burau 2005). The processed DL-ADCP measurements were interpolated to produce a 3D velocity field for each time interval in 2009, 2011, and 2012. The 3D interpolated velocity fields were generated using an algorithm that releases particles into the initial velocity field and interpolates velocities along the particle pathlines, using an inverse path length weighting (IPLW) function. This algorithm iterates until the changes in the velocity field are minimal.

SL-ADCP DATA PROCESSING AND INTERPOLATION

The SL-ADCP measurements were made continuously at 15-minute intervals from April 23 through May 30, 2012, except for an 18-hour period from April 29 through April 30 and a 27-hour period from May 5 through May 7 due to a technical malfunction that resulted in recording erroneous data. The data processing included merging the SL-ADCP data into a single file, geo-referencing the measurement locations, conducting visual quality assurance/quality control checks, and estimating (when possible) data gaps. The 2D interpolated velocity fields were generated for a 5-meter by 5-meter set of grid points every 15 minutes using an algorithm that releases particles into the processed velocity field and interpolates velocities along the particle pathlines using an IPLW function. This algorithm iterates until the changes in the mean velocity field are minimal.

3.2.2 RESULTS

Near-surface 2D velocity fields from the DL-ADCP and SL-ADCP data (hereafter referred to as DL2D and SL2D) were used to examine velocity fields and hydrodynamic features over a range of river discharges (Table 3-2). The discharge values (SJL) were chosen to represent reverse and typical flows from 2009; very high flows from 2011; and the 5th, 25th, 50th, 75th, and 95th percentile flows from 2012.

Table 3-2
Summary of Velocity Fields Generated from DL-ADCP Data in 2009 and 2011, and SL-ADCP Data from 2012

Discharge at San Joaquin near Lathrop (cfs)	-1,360	780	1,450	1,500	1,970	2,000	2,250	2,660	9,535
Timestamp (PST)	5/29/2009 09:25	2012[1]	6/05/2009 10:00	2012[1]	2012[1]	2012[1]	2012[1]	2012[1]	04/12/2011 10:10
Rationale	Negative-flow condition (common occurrence in 2009)	5th percentile of 2012 flows	Common low-flow condition in 2009 (and 2010)	25th percentile of 2012 flows	50th percentile of 2012 flows	Intermediate discharge of interest	75th percentile of 2012 flows	95th percentile of 2012 flows	High-flow condition observed only in 2011

Notes: cfs = cubic feet per second; DL-ADCP = downward-looking acoustic Doppler current profiler; PST = Pacific Standard Time; SL-ADCP = side-looking acoustic Doppler current profiler

[1] Multiple instances for specified discharge value.

Source: Present study

VELOCITY MODELING OF 2009 AND 2011 (NO ROCK BARRIER)

Data from 2009 and 2011 provided information on the HOR velocity field in the absence of a physical barrier. At a SJL discharge of approximately 1,450 cfs, a commonly observed discharge in 2009, near-surface velocity was primarily in a downstream direction and was greatest in the mid-channel San Joaquin River, close to the divergence with Old River (Figure 3-7).

An eddy formed near a sand spit on the right bank of the San Joaquin River east of the deepest part of the scour hole (Figure 3-8). Vertical velocity primarily was downward at around 0 to 2 centimeters per second (cm/s). With reverse flows of approximately -1,360 cfs in 2009, a large eddy and related irregular velocities occurred on the right side of the San Joaquin River upstream of the divergence with Old River (Figures 3-9 and 3-10). Upstream velocity was of relatively high magnitude (approximately 0.33 m/s at discharge of approximately -1,300 to -1,450 cfs) (see Figure 3-9) on the left side of the San Joaquin River closest to the divergence with Old River. A low-velocity eddy also was apparent at the scour hole. Vertical velocity was primarily upward near the scour hole and mostly downward elsewhere.

Very high discharge in 2011 resulted in a downstream velocity of appreciable magnitude (e.g., $\geq\geq$1 m/s) (Figure 3-11). Vertical velocity during this time was primarily downward, at more than 6 cm/s in many areas (Figures 3-7 through 3-12).

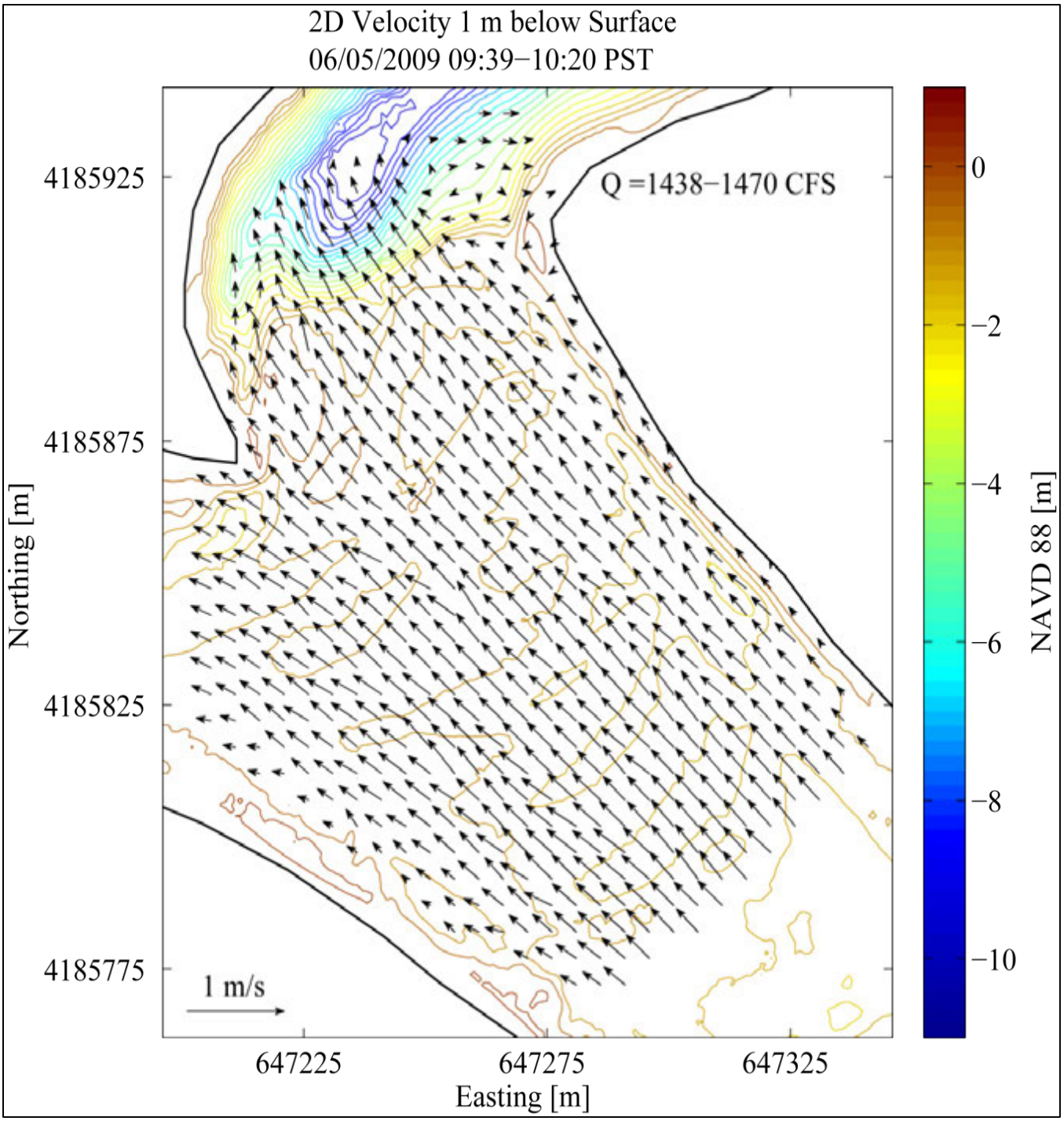

Source: Present study

Figure 3-7 **Two-Dimensional Near-Surface Velocity Vectors (m/s) Estimated from Data Collected with a DL-ADCP at the Head of Old River, 6/5/2009, 0939–1020 PST, with River Discharge in the San Joaquin River near Lathrop (Q) of 1,438 to 1,470 cfs**

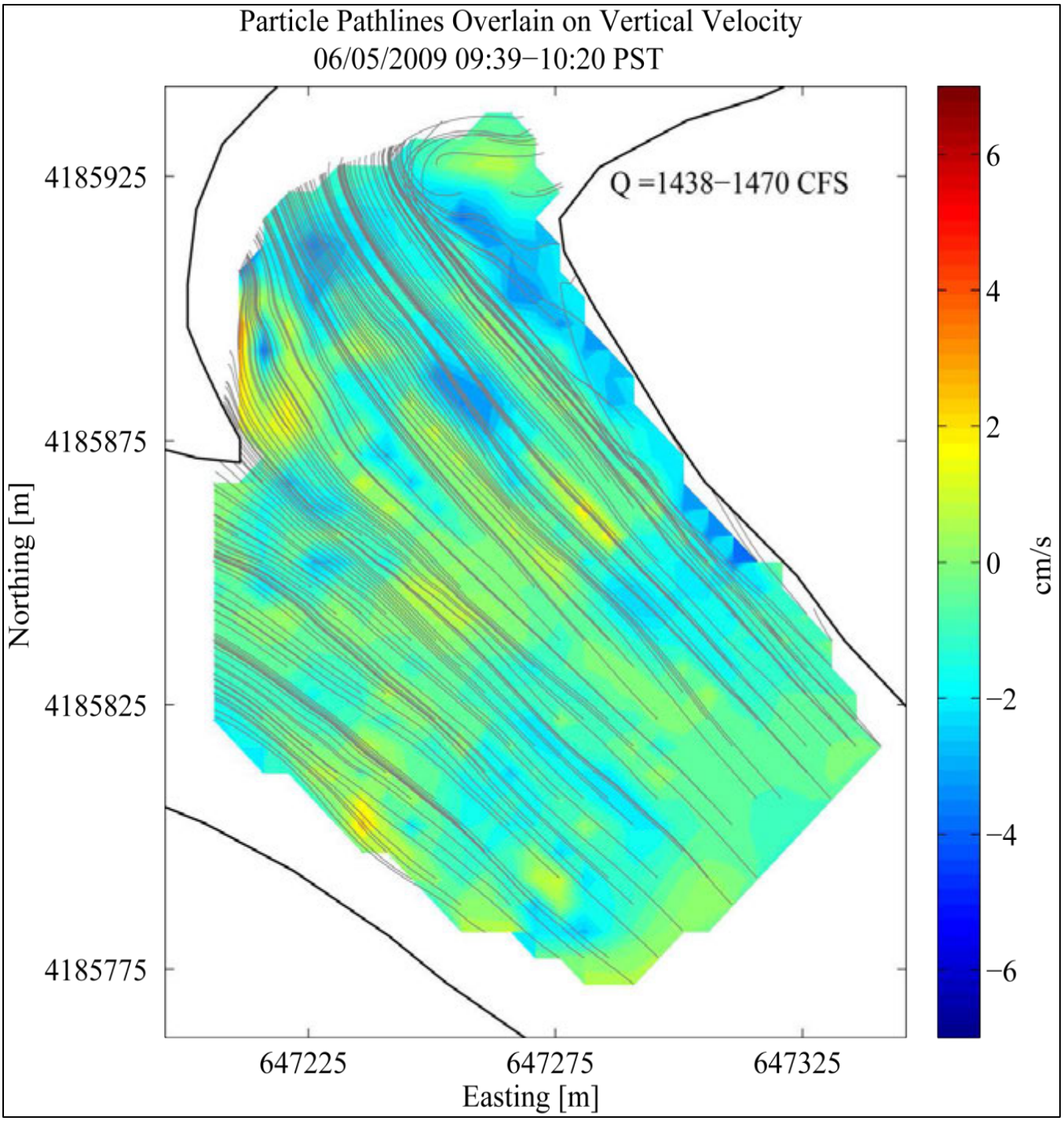

Source: Present study

Figure 3-8 **Vertical Velocity (cm/s) and Particle Pathlines Estimated from Data Collected with a DL-ADCP at the Head of Old River, 6/5/2009, 0939–1020 PST, with River Discharge in the San Joaquin River near Lathrop (Q) of 1,438 to 1,470 cfs**

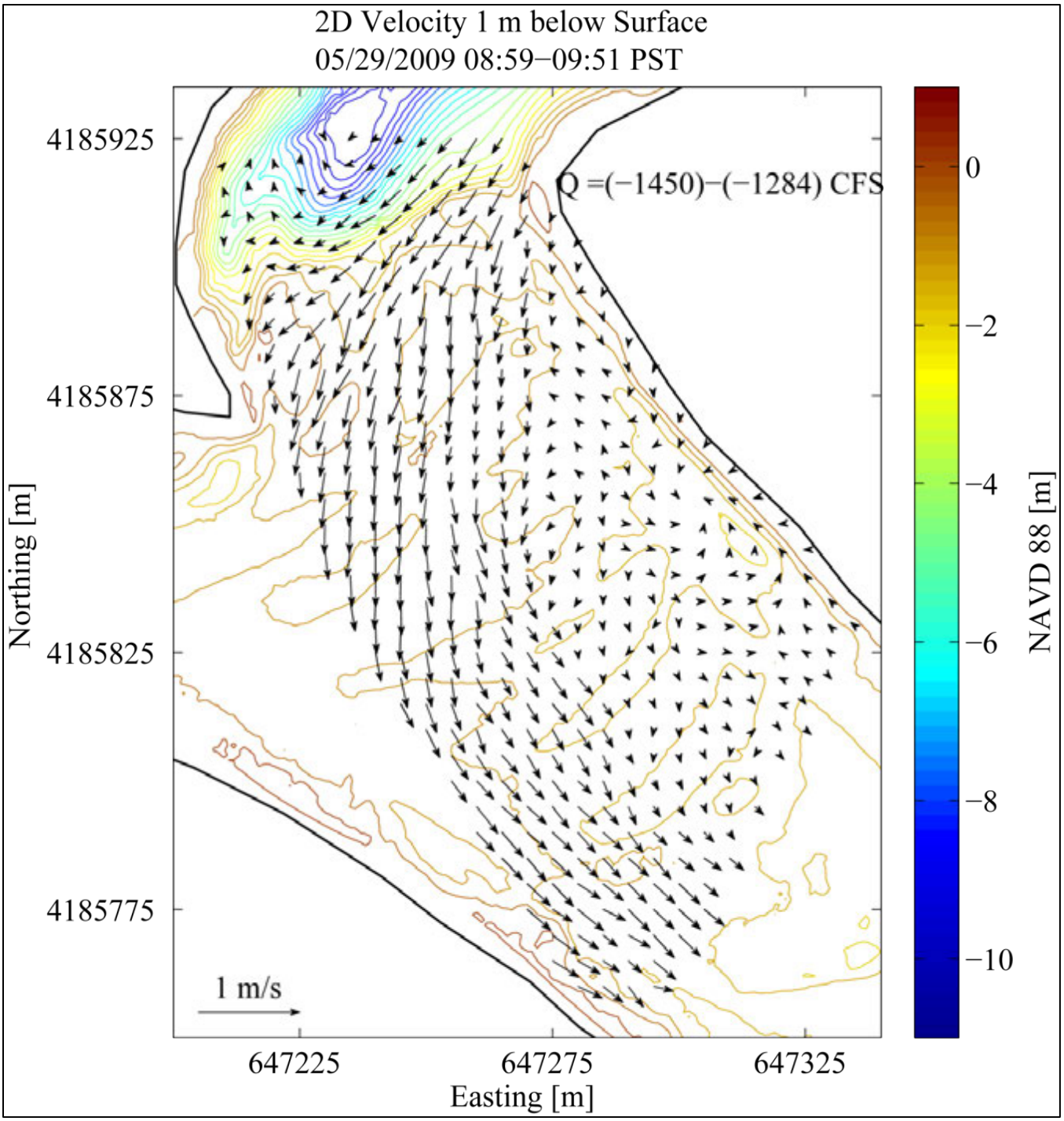

Source: Present study

Figure 3-9 **Two-Dimensional Near-Surface Velocity Vectors (m/s) Estimated from Data Collected with a DL-ADCP at the Head of Old River, 5/29/2009, 0859–0951 PST, with River Discharge in the San Joaquin River near Lathrop (Q) of -1,450 to -1,284 cfs**

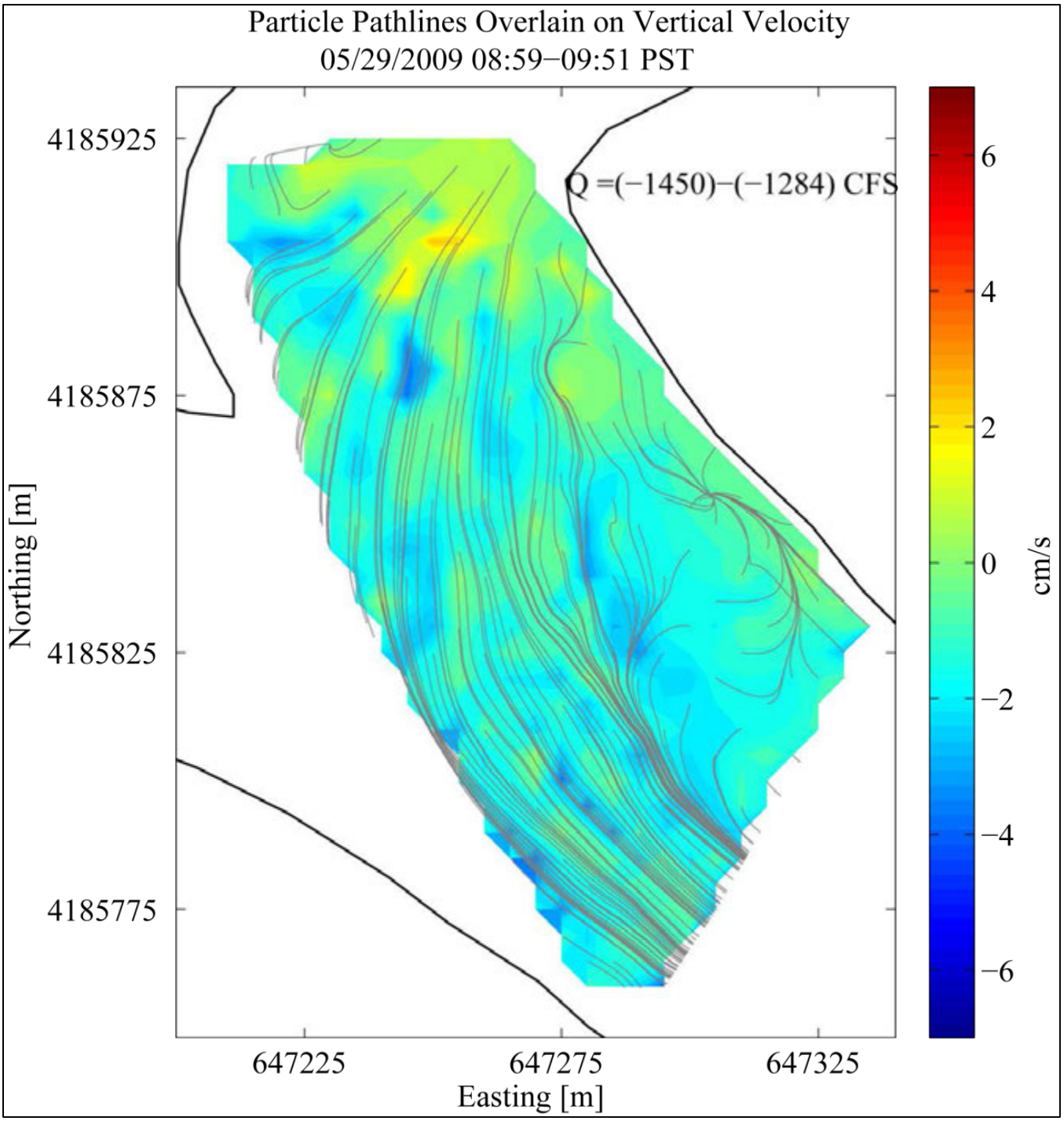

Source: Present study

Figure 3-10 **Vertical Velocity (cm/s) and Particle Pathlines Estimated from Data Collected with a DL-ADCP at the Head of Old River, 5/29/2009, 0859–0951 PST, with River Discharge in the San Joaquin River near Lathrop (Q) of -1,450 to -1,284 cfs**

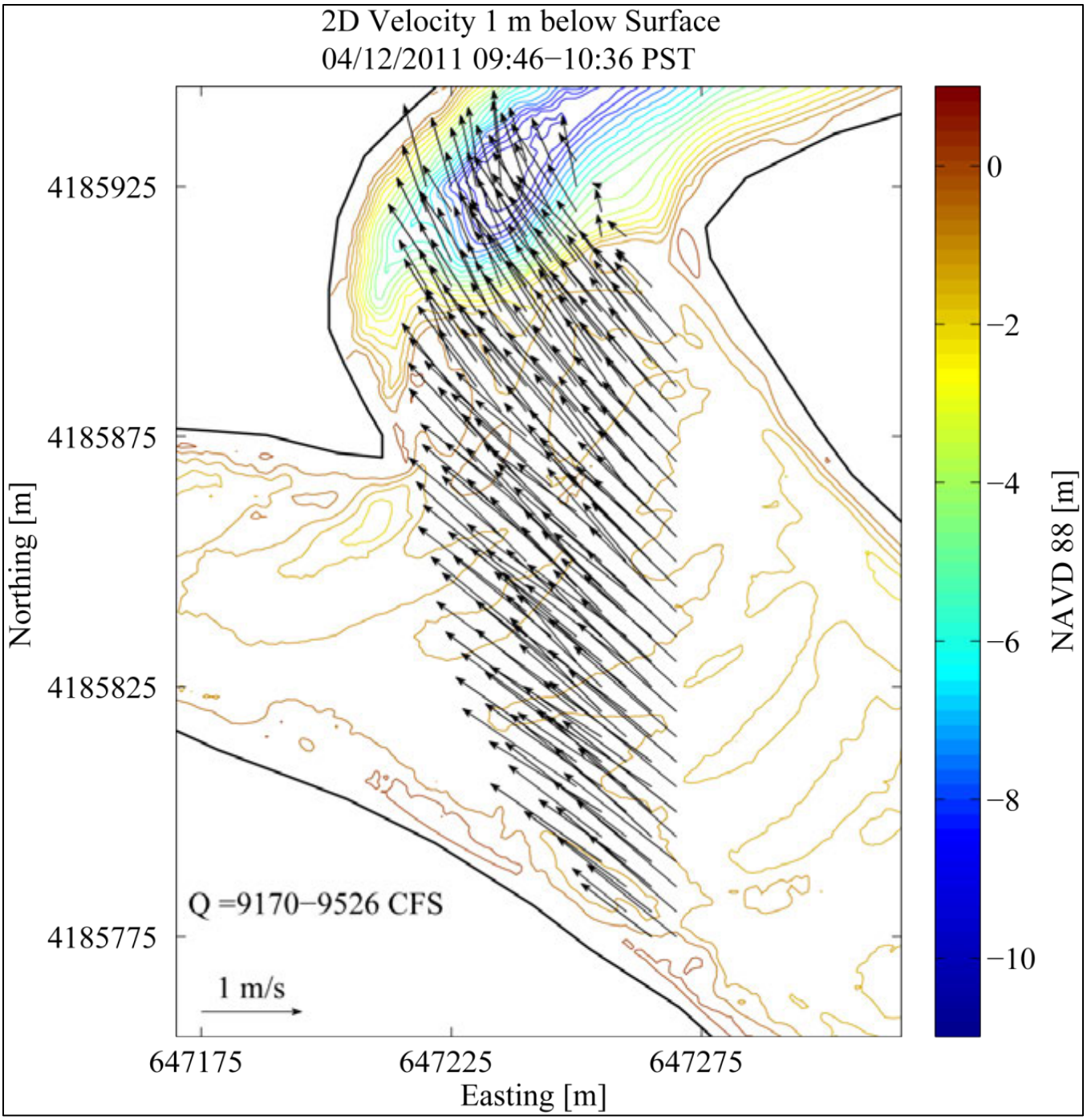

Source: Present study

Figure 3-11 **Two-Dimensional Near-Surface Velocity Vectors (m/s) Estimated from Data Collected with a DL-ADCP at the Head of Old River, 4/12/2011, 0946–1036 PST, with River Discharge in the San Joaquin River near Lathrop (Q) of 9,170 to 9,526 cfs**

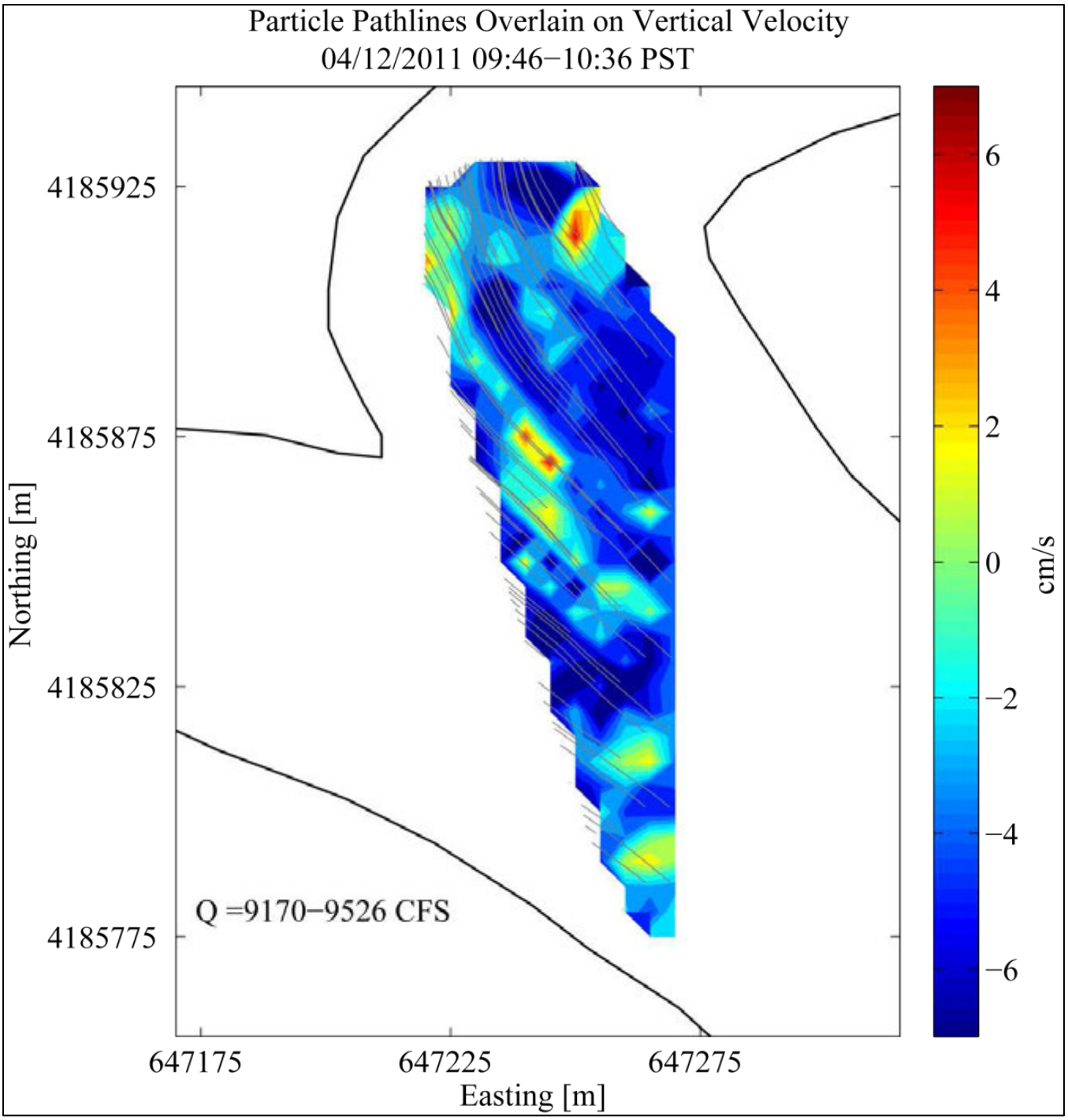

Source: Present study

Figure 3-12 **Vertical Velocity (cm/s) and Particle Pathlines Estimated from Data Collected with a DL-ADCP at the Head of Old River, 4/12/2011, 0946–1036 PST, with River Discharge in the San Joaquin River near Lathrop (Q) of 9,170 to 9,526 cfs**

VELOCITY MODELING OF 2012 (PHYSICAL ROCK BARRIER)

The set of observations from the 2012 SL2D velocity fields are the most extensive available over a range of discharge values. The most notable observations are described herein. At low discharge (approximately 780 cfs; the 5th percentile discharge in 2012), the flow field does not exhibit much variability, and the velocity vectors near the barrier are low (Figures 3-13 and 3-14).

At moderate discharge values (1,500 to 1,970 cfs; the 25th to 50th percentile discharge in 2012), more variability occurred in the flow field, with higher velocities mid-channel and near the scour hole downstream of the divergence, and low velocities near the barrier (Figures 3-15, 3-16, 3-17, and 3-18). Two large-scale eddies appear at these discharge levels: one eddy forms near the barrier with a counter-clockwise (CCW) rotation, and a smaller eddy forms near the left bank adjacent to the scour hole, also with a CCW rotation.

At higher discharge values (2,250 to 2,660 cfs; the 75th to 95th percentile discharge in 2012), the flow field remains consistent, with higher velocity magnitudes (Figures 3-19, 3-20, 3-21, and 3-22). The eddy near the barrier becomes larger during moderate discharges. The eddy near the scour hole is not consistently present throughout the set of observations. As noted in the following section ("Comparison of DL2D and SL2D"), the SL2D velocity fields do not represent the eddy near the scour hole consistently in comparison to the DL2D.

COMPARISON OF DL2D AND SL2D

A comparison was made of the DL2D and SL2D velocity fields. The DL-ADCP data collected on May 8 and 30, 2012 were from a range of discharge values (1,840 to 2,660 cfs). These data were collected near the physical rock barrier and near the scour hole. The DL2D velocity field is considered more accurate because the interpolation was based on larger data density, but fewer observations exist over a smaller range of discharge. The most important observations from these comparisons are as follows:

- The SL2D velocity field accurately represented the velocity variability throughout the domain, except near the barrier, where the magnitude of the velocity vectors from the SL2D velocity field are smaller than those from the DL2D velocity field.
- The SL2D velocity field failed to capture or fully represent the eddy that was present near the scour hole for all observations, but this eddy was seen in nearly all of the observations of the DL2D velocity field.
- The eddy near the barrier appears to be accurately captured by the SL2D velocity field and was present in the DL2D velocity field.

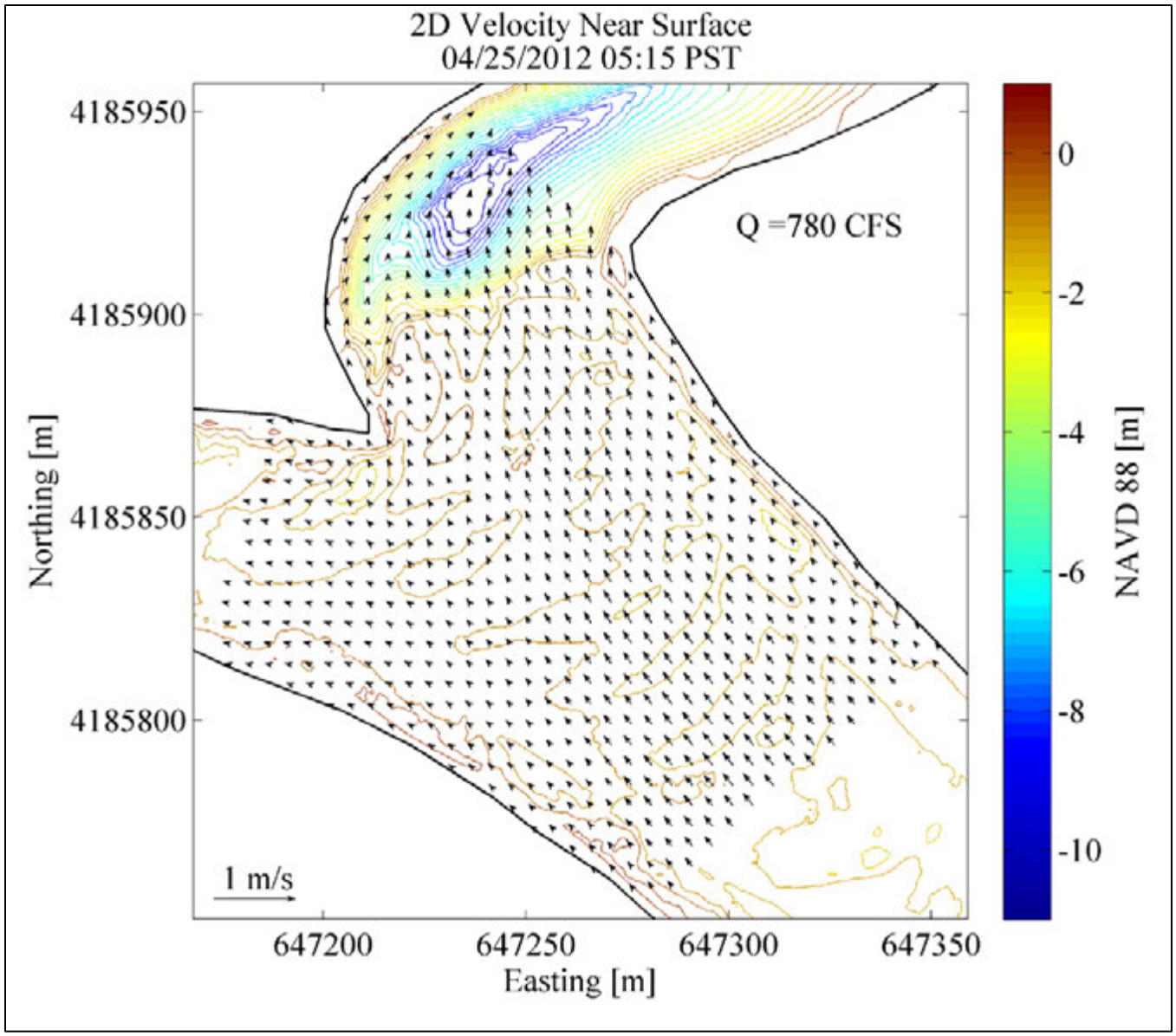

Source: Present study

Figure 3-13 **Two-Dimensional Near-Surface Velocity Vectors (m/s) Estimated from Data Collected with a SL-ADCP at the Head of Old River, 4/25/2012, 0515 PST, with River Discharge in the San Joaquin River near Lathrop (Q) of 780 cfs**

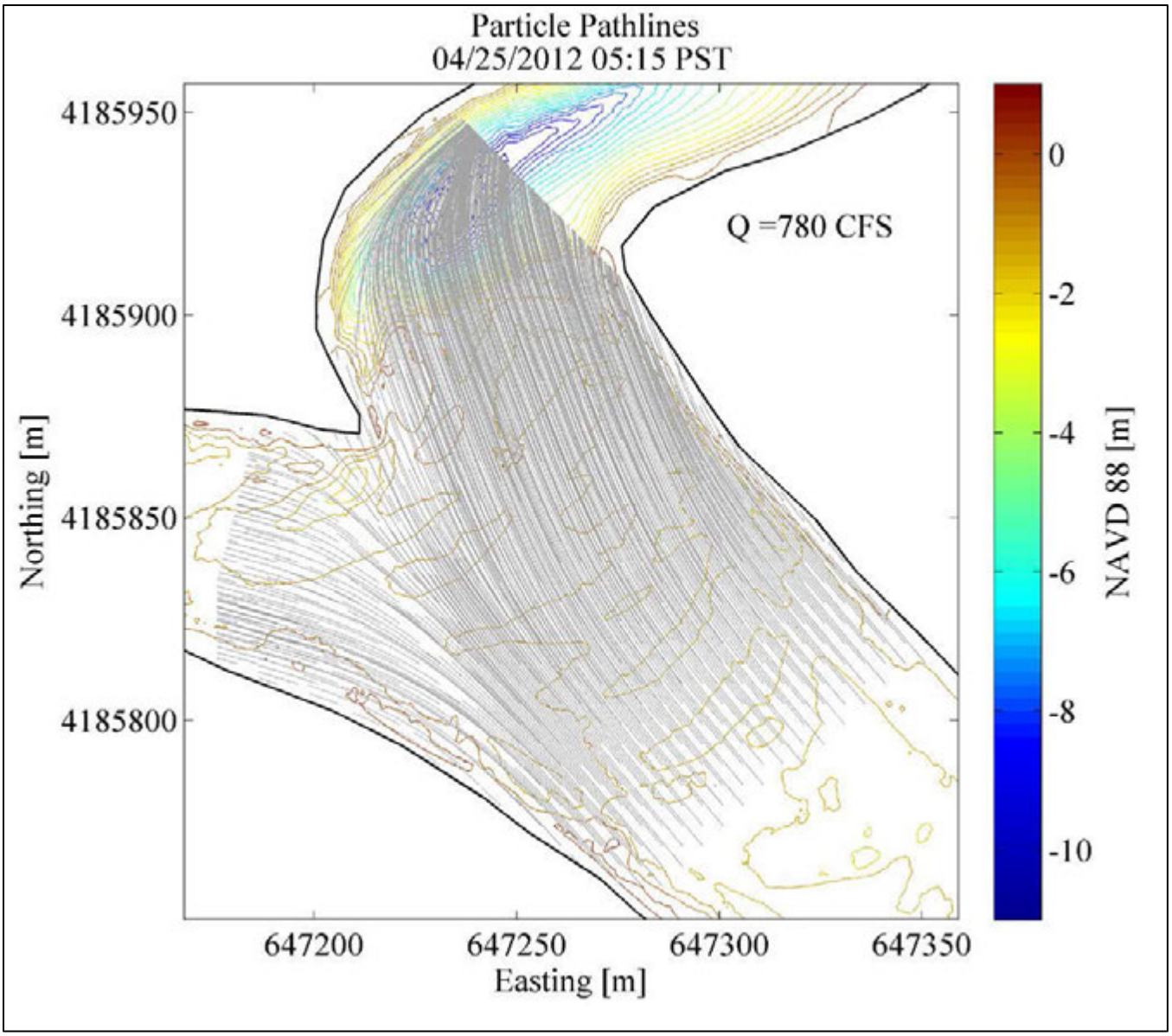

Source: Present study

Figure 3-14 Two-Dimensional Near-Surface Particle Pathlines (m/s) Estimated from Data Collected with a SL-ADCP at the Head of Old River, 4/25/2012, 0515 PST, with River Discharge in the San Joaquin River near Lathrop (Q) of 780 cfs

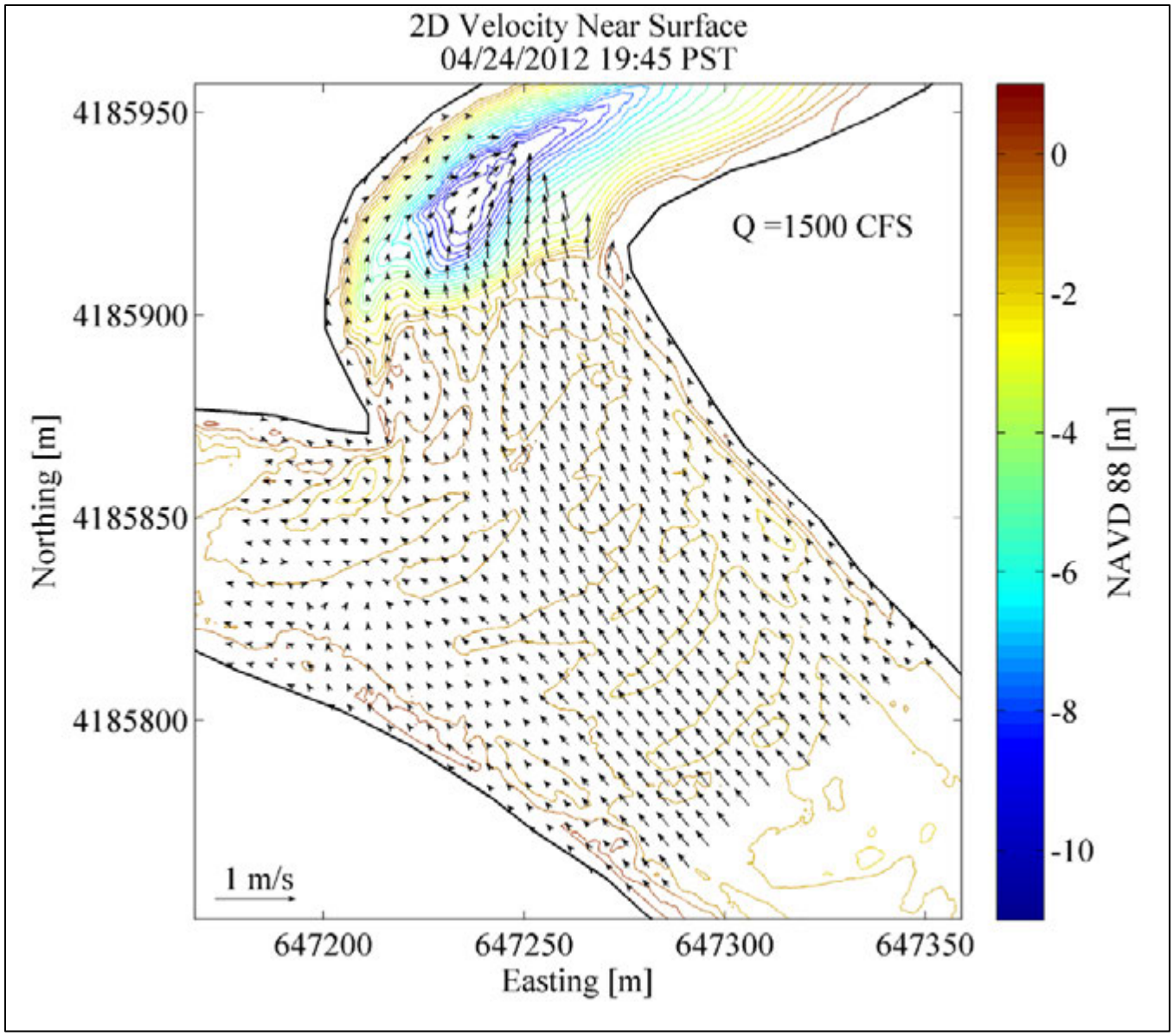

Source: Present study

Figure 3-15 **Two-Dimensional Near-Surface Velocity Vectors (m/s) Estimated from Data Collected with a SL-ADCP at the Head of Old River, 4/24/2012, 1945 PST, with River Discharge in the San Joaquin River near Lathrop (Q) of 1,500 cfs**

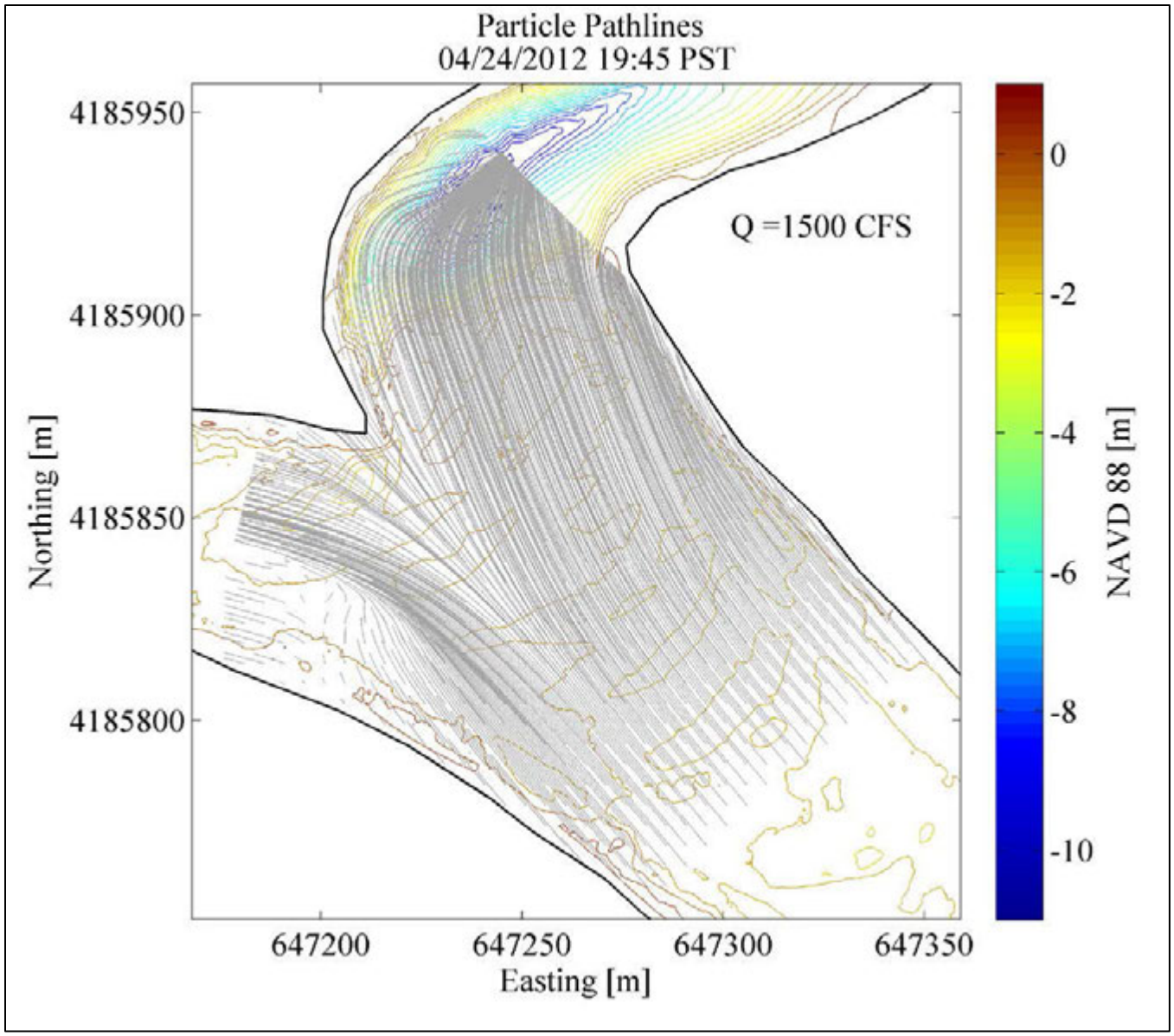

Source: Present study

Figure 3-16 Two-Dimensional Near-Surface Particle Pathlines (m/s) Estimated from Data Collected with a SL-ADCP at the Head of Old River, 4/24/2012, 1945 PST, with River Discharge in the San Joaquin River near Lathrop (Q) of 1,500 cfs

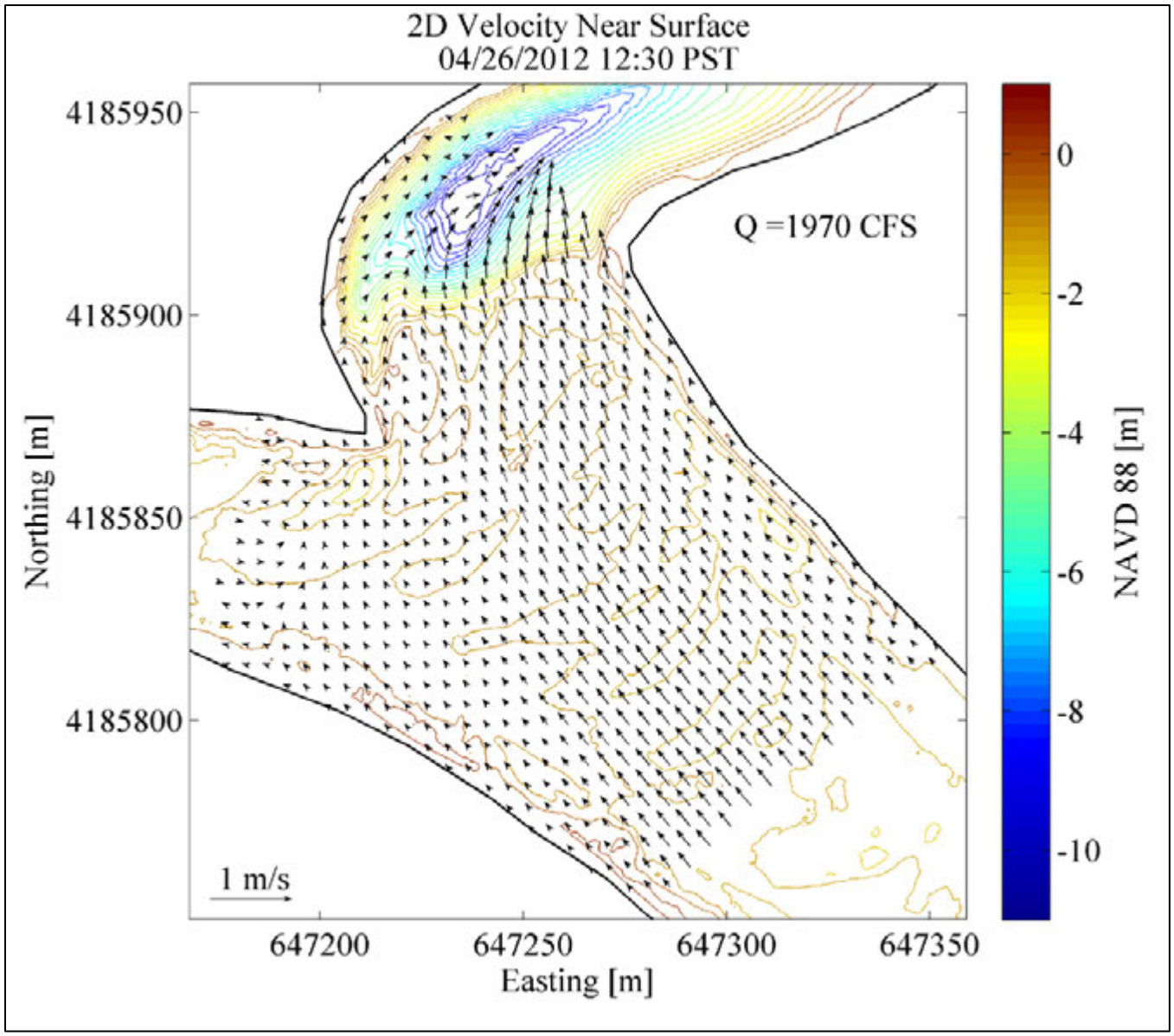

Source: Present study

Figure 3-17 **Two-Dimensional Near-Surface Velocity Vectors (m/s) Estimated from Data Collected with a SL-ADCP at the Head of Old River, 4/26/2012, 1230 PST, with River Discharge in the San Joaquin River near Lathrop (Q) of 1,970 cfs**

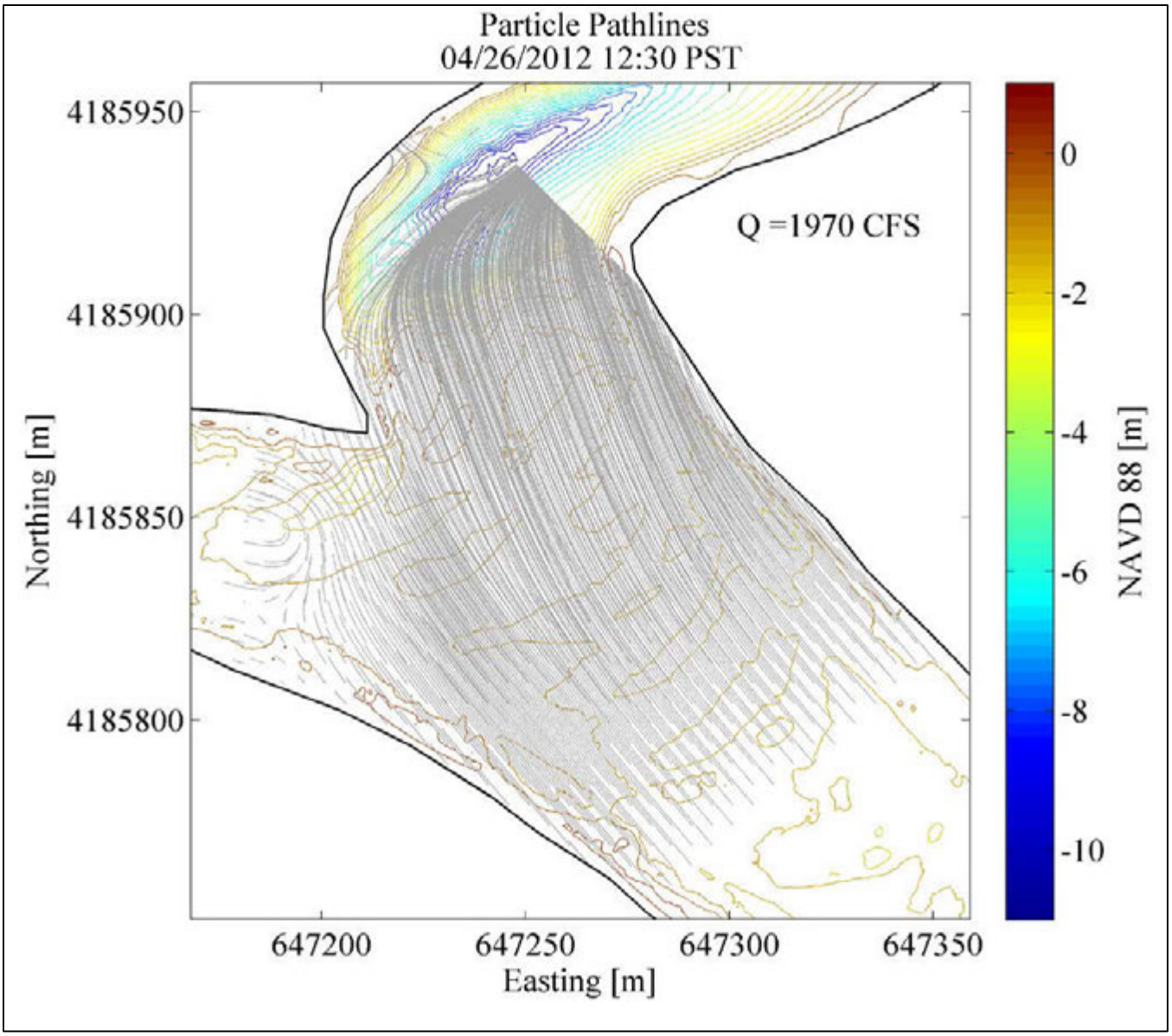

Source: Present study

Figure 3-18 Two-Dimensional Near-Surface Particle Pathlines (m/s) Estimated from Data Collected with a SL-ADCP at the Head of Old River, 4/26/2012, 1230 PST, with River Discharge in the San Joaquin River near Lathrop (Q) of 1,970 cfs

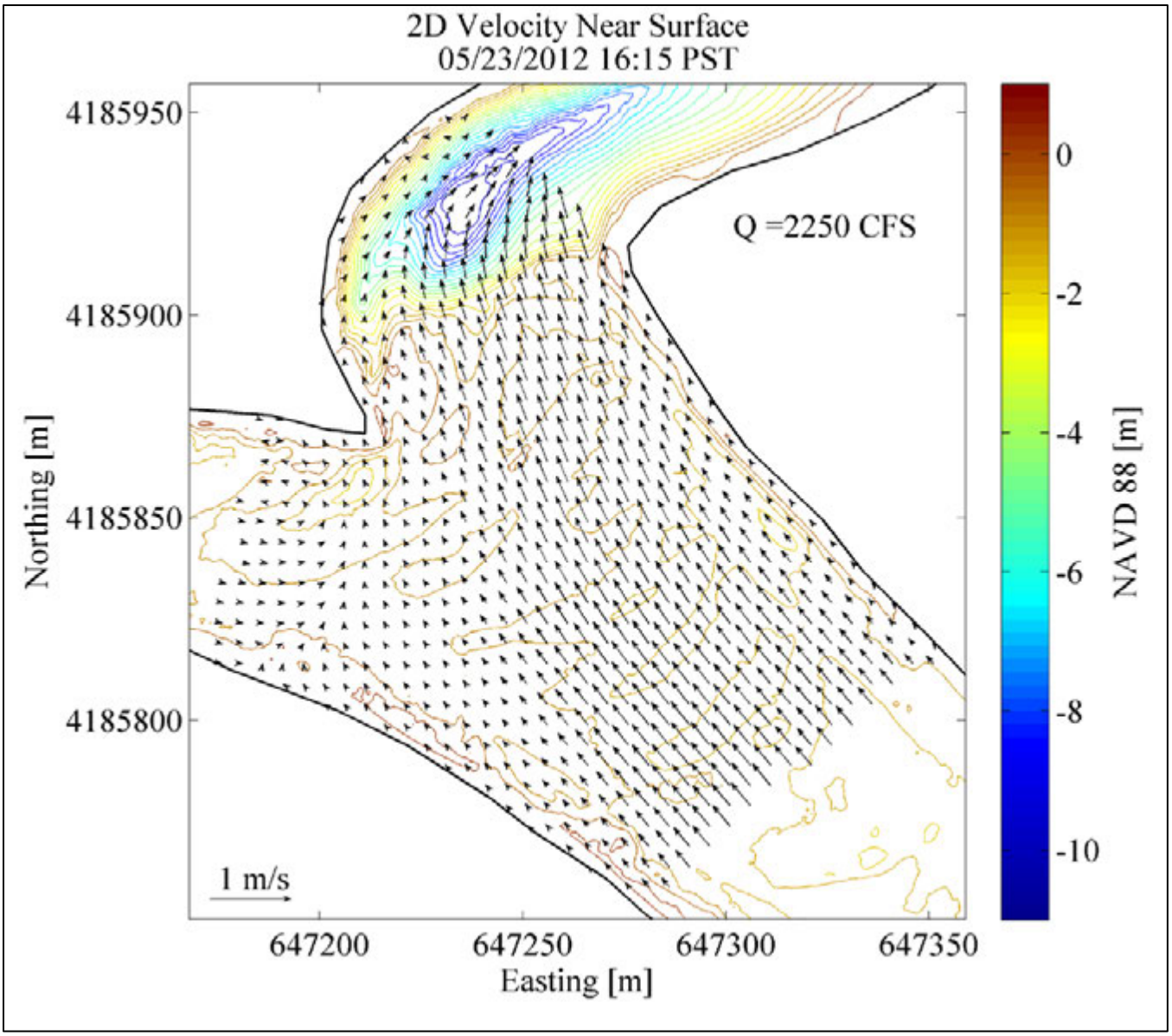

Source: Present study

Figure 3-19 **Two-Dimensional Near-Surface Velocity Vectors (m/s) Estimated from Data Collected with a SL-ADCP at the Head of Old River, 5/23/2012, 1615 PST, with River Discharge in the San Joaquin River near Lathrop (Q) of 2,250 cfs**

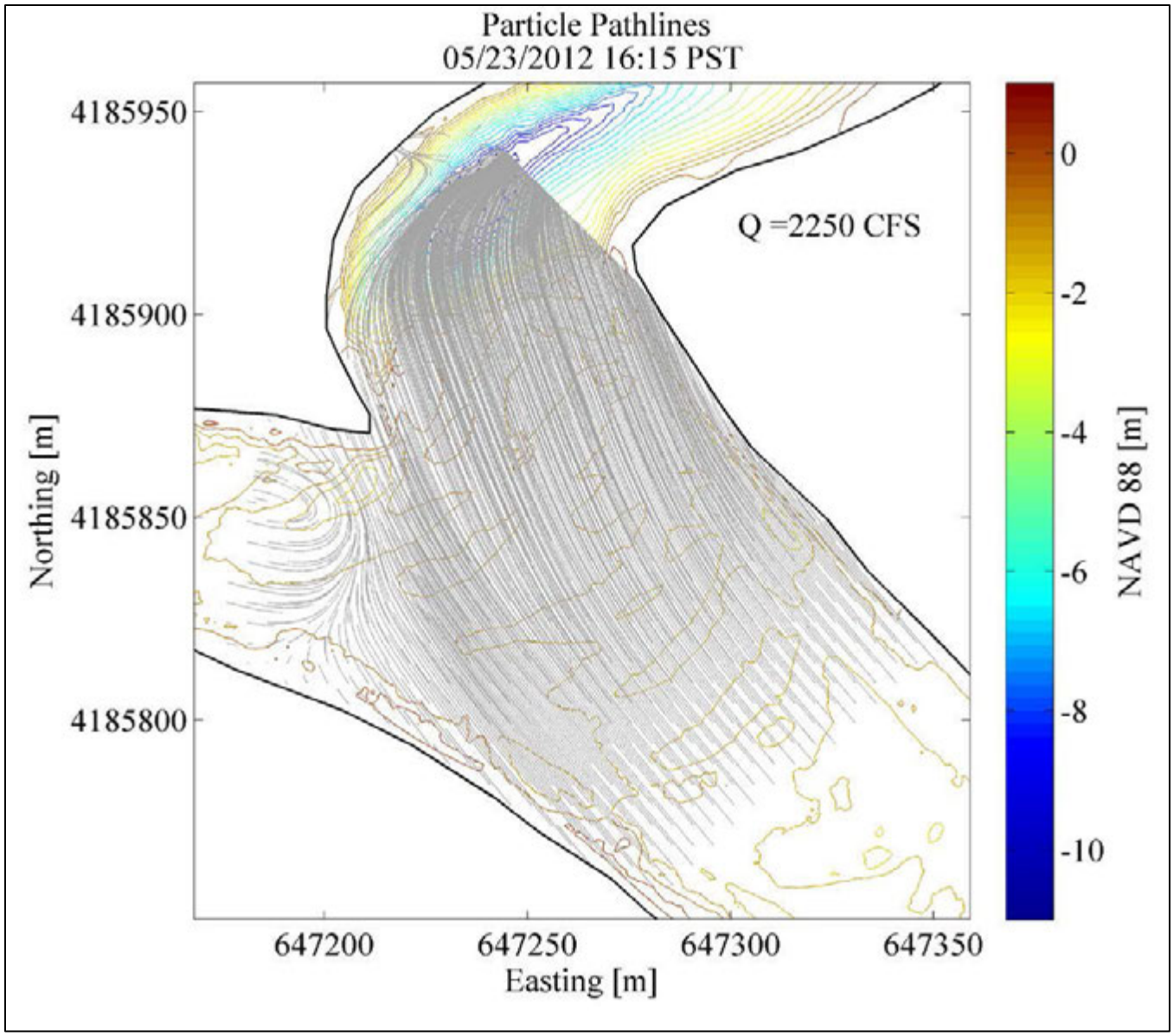

Source: Present study

Figure 3-20 Two-Dimensional Near-Surface Particle Pathlines (m/s) Estimated from Data Collected with a SL-ADCP at the Head of Old River, 5/23/2012, 1615 PST, with River Discharge in the San Joaquin River near Lathrop (Q) of 2,250 cfs

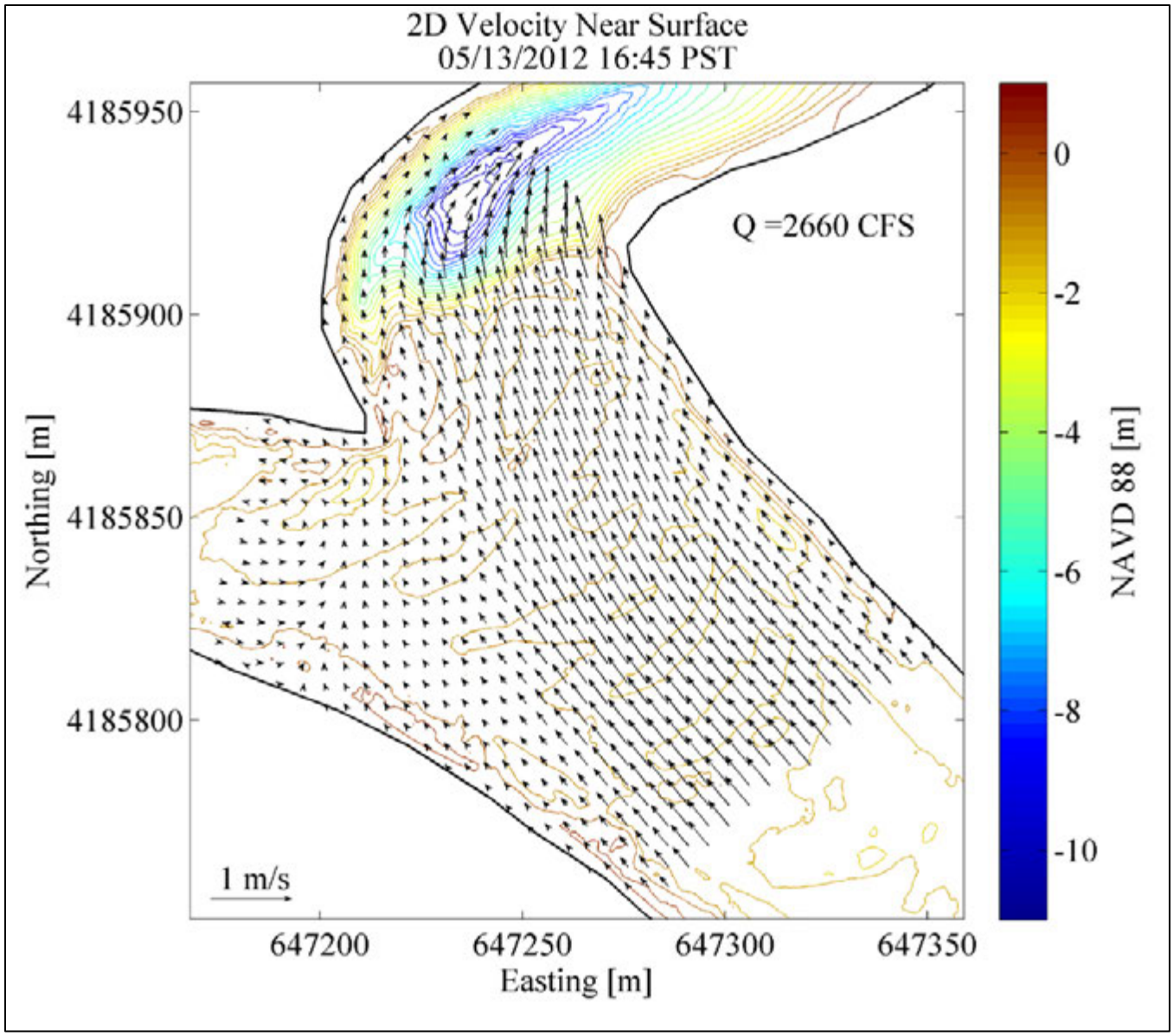

Source: Present study

Figure 3-21 **Two-Dimensional Near-Surface Velocity Vectors (m/s) Estimated from Data Collected with a SL-ADCP at the Head of Old River, 5/13/2012, 1645 PST, with River Discharge in the San Joaquin River near Lathrop (Q) of 2,660 cfs**

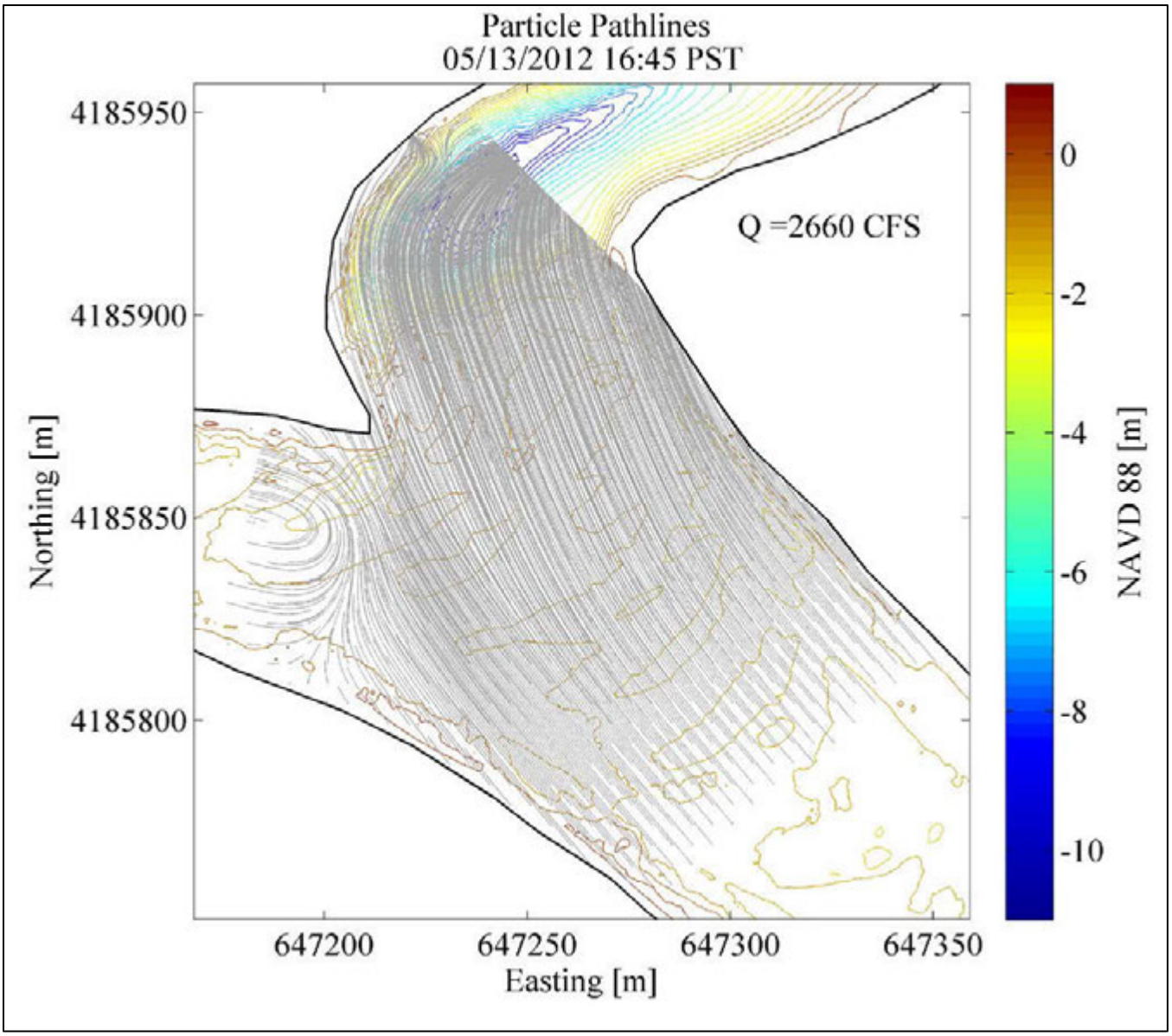

Source: Present study

Figure 3-22 Two-Dimensional Near-Surface Particle Pathlines (m/s) Estimated from Data Collected with a SL-ADCP at the Head of Old River, 5/13/2012, 1645 PST, with River Discharge in the San Joaquin River near Lathrop (Q) of cfs

3.3 WATER TEMPERATURE

3.3.1 2009 TEMPERATURE

Mean daily water temperature between April 1 and June 30 was higher in 2009 compared to 2010 and 2011, but more similar to 2012 (Figure 3-23). Between April 1 and June 30, 2009, the water temperature in the San Joaquin River at the closest gauge in physical proximity (SJL) to the HOR study area ranged from 13.9 to 26.9 °C (Figure 3-24). When tagged juvenile Chinook salmon were in the water, the mean temperature in 2009 generally was warmer than in 2010 and 2011, but was similar to the mean temperature in 2012 (Table 3-3; Figures 3-24, 3-25, 3-26, and 3-27).

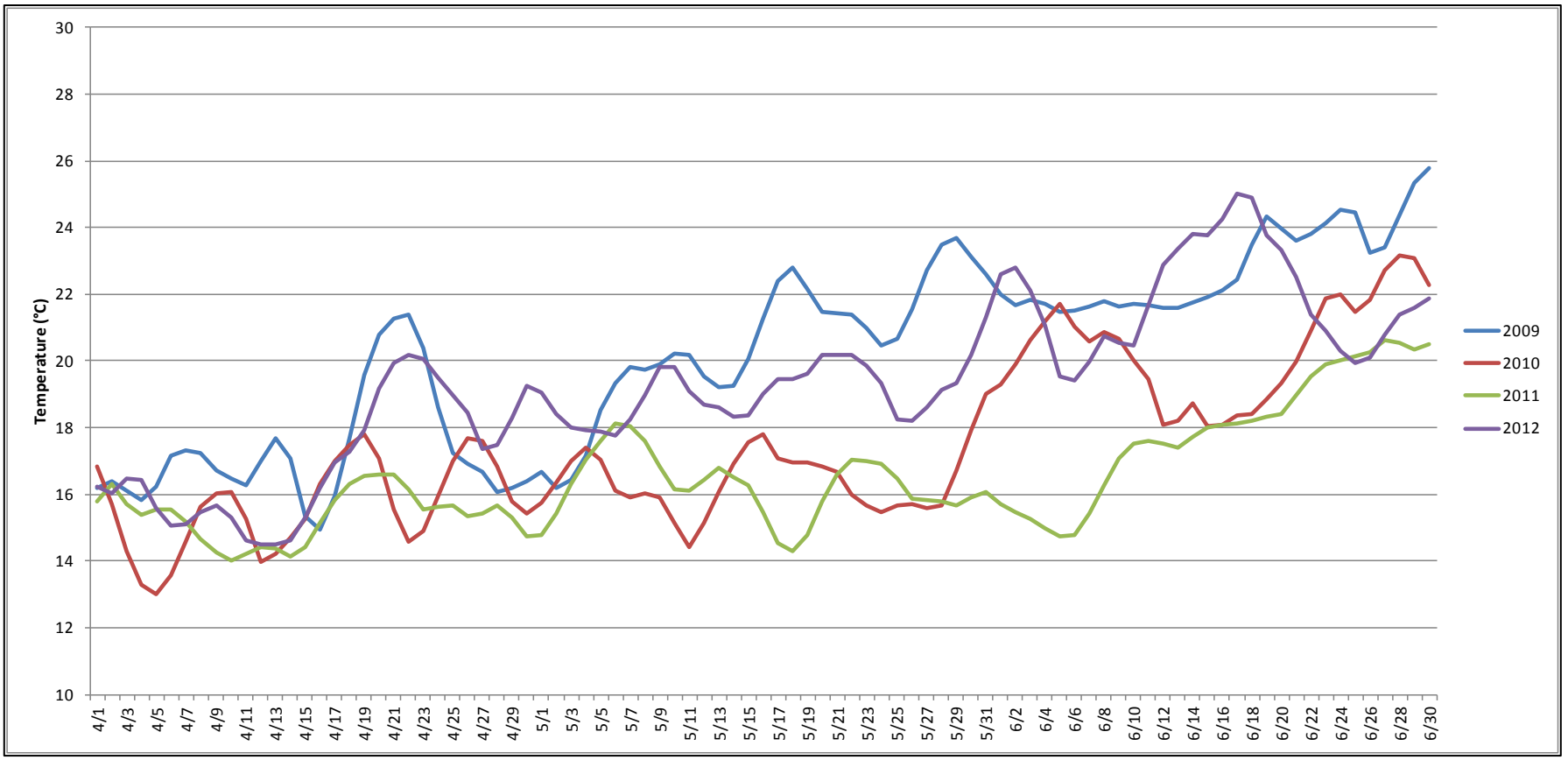

Sources: Baldwin, pers. comm., 2013; Dempsey, pers. comm., 2013

Figure 3-23 **Daily Mean Water Temperature (°C) in the San Joaquin River at Lathrop (SJL), 4/1–6/30, 2009–2012**

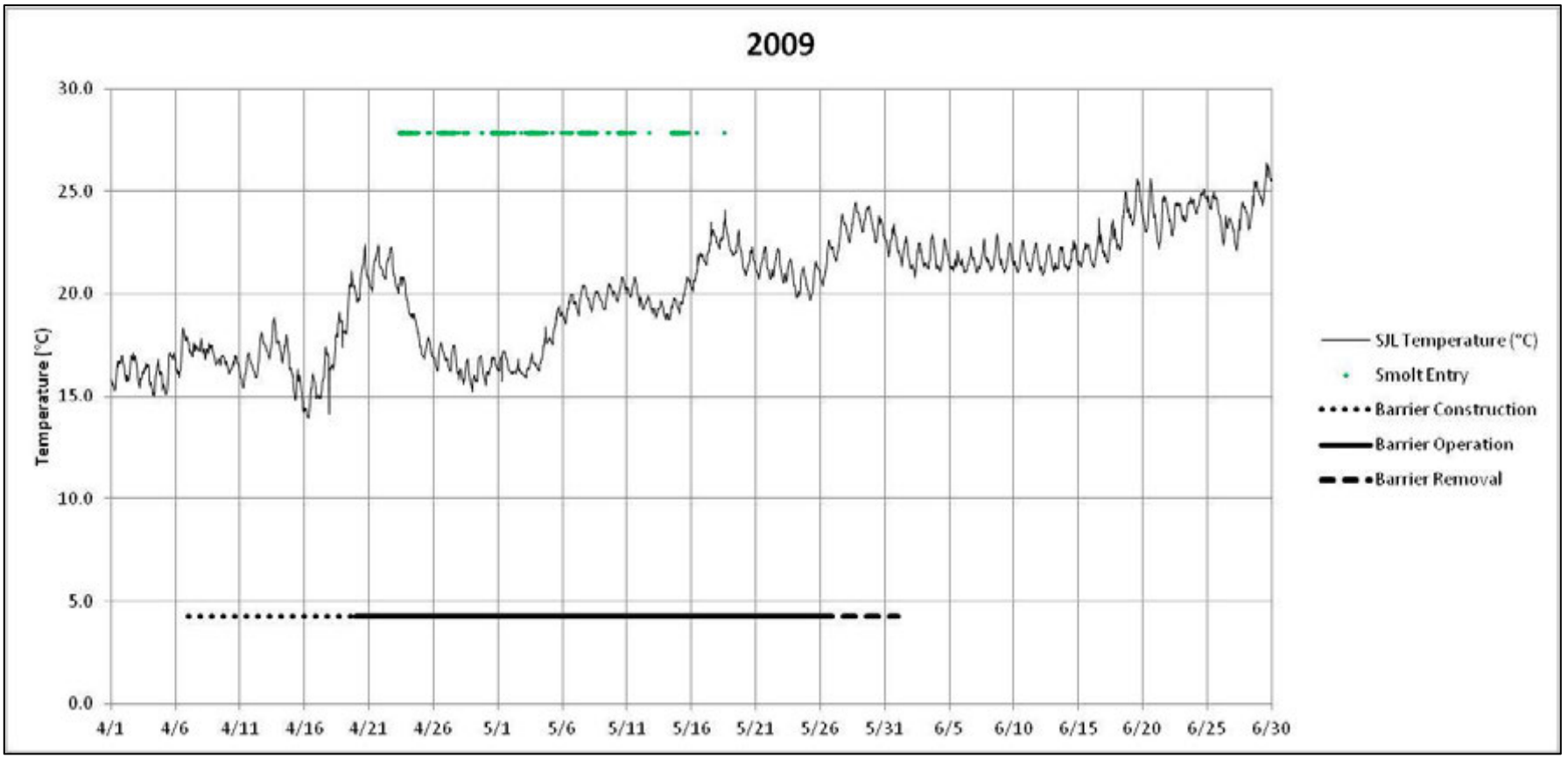

Sources: Baldwin, pers. comm.; 2013; Dempsey, pers. comm., 2013

Note: The barrier referred to in the legend was a non-physical fish barrier called a BAFF (Fish Guidance Systems Ltd, Southampton, UK). Barrier operation was not continuous, with the BAFF off approximately 50% of the time during the period of BAFF operation.

Figure 3-24 **Water Temperature (°C), Juvenile Chinook Salmon Releases and Barrier Status in the San Joaquin River at Lathrop Gauge from 4/1/09 through 6/30/09**

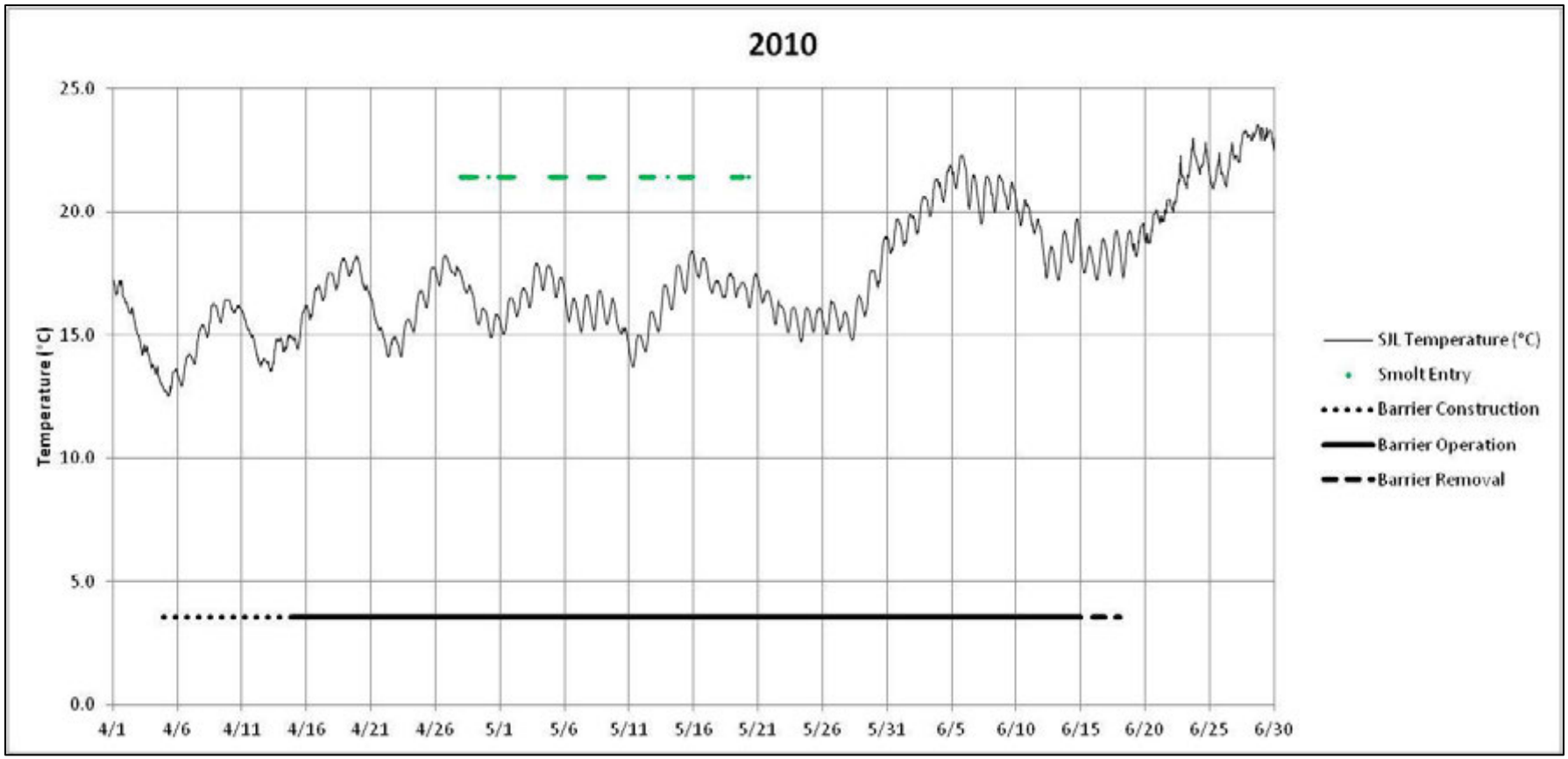

Sources: Baldwin, pers. comm., 2013; Dempsey, pers. comm., 2013

Note: The barrier referred to in the legend was a non-physical fish barrier called a BAFF (Fish Guidance Systems Ltd, Southampton, UK). Barrier operation was not continuous, with the BAFF off approximately 50% of the time during the period of BAFF operation.

Figure 3-25 **Water Temperature (°C), Juvenile Chinook Salmon Releases and Barrier Status in the San Joaquin River at Lathrop Gauge from 4/1/10 through 6/30/10**

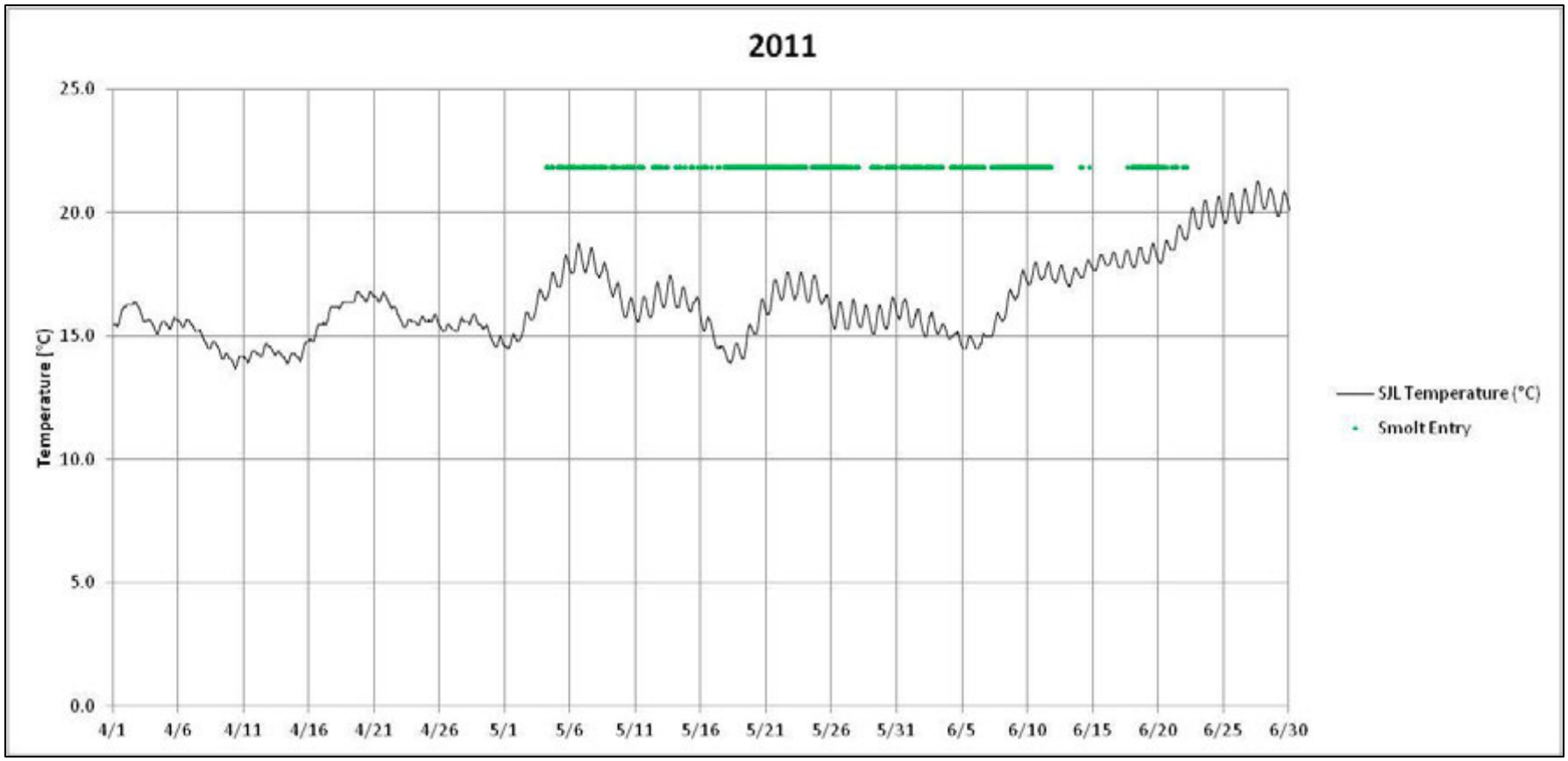

Sources: Baldwin, pers. comm., 2013; Dempsey, pers. comm., 2013
Note: No barrier was installed or operated during this period.

Figure 3-26 **Water Temperature (°C) and Juvenile Chinook Salmon Releases in the San Joaquin River at Lathrop Gauge from 4/1/11 through 6/30/11**

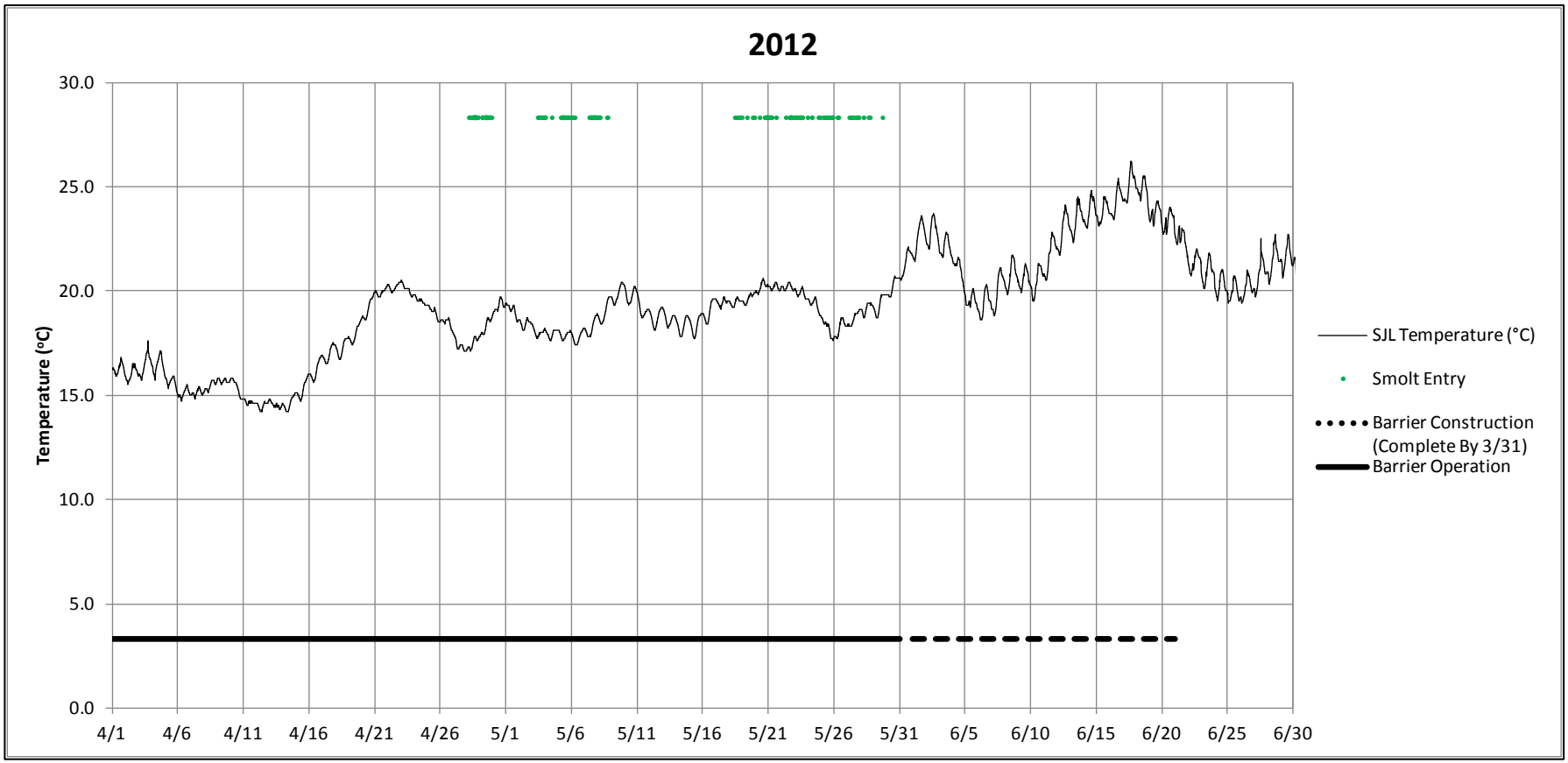

Sources: Baldwin, pers. comm., 2013; Dempsey, pers. comm., 2013

Note: The barrier installed during this period was a rock barrier with eight culverts.

Figure 3-27 **Water Temperature (°C), Juvenile Chinook Salmon Releases and Barrier Status in the San Joaquin River at Lathrop Gauge from 4/1/12 through 6/30/12**

Table 3-3
Descriptive Statistics for 2009–2012 Water Temperature in the San Joaquin River at the SJL Gauge when Tagged Juvenile Salmonids were at the HOR Study Area

			SJL Temperature (°C)				
Year	First Fish[1]	Last Fish[2]	Mean	Standard Deviation	Minimum	Maximum	Count
2009	4/23/09 8:24	5/18/09 13:48	18.6	1.9	15.2	23.6	2422
2010	4/27/10 22:25	5/20/10 5:54	16.4	1.0	13.7	18.4	2143
2011	5/4/11 2:51	6/22/11 4:24	16.6	1.2	13.9	19.5	4712
2012	4/28/12 4:13	5/29/12 16:35	18.9	0.8	17.1	20.6	3026

Notes: HOR = Head of River; SJL = San Joaquin River at Lathrop
The SJL gauge is the closest gauge in physical proximity to the HOR study area, and was 0.5 km of the HOR site. The periods reported here are those when experimentally released fish were nearest the 2009 BAFF line (in 2009, 2011, and 2012) and nearest the 2010 BAFF line (in 2010).
[1] Date/time when the first tagged salmonids was nearest the BAFF line.
[2] Date/time the last tagged salmonids was nearest the BAFF line.
Sources: Baldwin, pers. comm., 2013; Dempsey, pers. comm., 2013

Although 2009 and 2012 were similar in mean water temperature, differences existed. During the tagged juvenile Chinook salmon release period, the water temperature in 2009 increased to 22 °C, a critical temperature that can cause major mortality in wild populations of Chinook salmon (Moyle 2002), for 30 hours during one interval; this never occurred in 2012 (see temperature maxima in Table 3-3). Furthermore, the standard deviation (SD) of water temperature was considerably higher in 2009 than in 2012 (Table 3-3).

Although juvenile steelhead were not released, by June 12, temperatures at the SJL gauge had risen to a point where the respiratory efficiency of steelhead would be affected (21 °C) (Hooper 1973). This date was earlier than in any other year studied (Table 3-4). Wild, non-hatchery steelhead could have been passing through the HOR study area (Table B-2 in Appendix B, "Focal Fish Species Information"). Experimental releases constrain the study juvenile fish to migrate at prescribed periods, whereas wild, non-hatchery fish may respond more strongly to environmental cues, such as water temperature.

Table 3-4
Day of the Year at which the Water Temperature in the San Joaquin River at SJL Gauge Reached and Remained at Least 15 Days at Two Critical Temperatures for Juvenile Salmonids

Year	Temperature > 21.0 °C[1]	Temperature > 23.9 °C[2]
2009	June 12	July 14
2010	July 5	July 10
2011	July 27	Not Exceeded
2012	June 29	July 7

Notes: SJL = San Joaquin River at Lathrop
For Chinook salmon, major mortality occurred at 22–23 °C in wild populations, and very few individuals survived temperatures greater than 24 °C (Moyle 2002).
[1] Temperature at which steelhead juveniles had difficulty absorbing oxygen from the water, 21.0 °C (Hooper 1973)
[2] Steelhead upper lethal thermal limit, 23.9 °C (Bell 1986)
Sources: Baldwin, pers. comm., 2013; Dempsey, pers. comm., 2013

3.3.2 2010 TEMPERATURE

From April 1, 2010, through June 30, 2010, the water temperature at the SJL gauge ranged from 12.5 to 23.5 °C (Figure 3-25). When tagged juvenile Chinook salmon were present in the study area, the mean water temperature in 2010 was lower than in any other year, but was very similar to 2011 (Table 3-3; Figures 3-23, 3.24, 3-25, and 3-26). Furthermore, in 2010, it took longer to reach 21 °C and remain there for 15 days or more, longer than any year except 2011 (Table 3-4).

3.3.3 2011 TEMPERATURE

From April 1 through June 30, 2011, the water temperature at the SJL gauge ranged from 13.7 to 21.3 °C (Figure 3-26). The water temperature in 2011 was consistently cooler than in 2009 and throughout spring and summer of 2012 (Figure 3-23). Although 2011 did not have the lowest mean water temperature (Table 3-3), the temperature never increased to 23.9 °C, the upper lethal limit for steelhead (Bell 1986). Among the 4 years included in this study, the only year that the water temperature never exceeded 23.9 °C was 2011 (Table 3-4).

3.3.4 2012 TEMPERATURE

From April 1 through June 30, 2012, the water temperature in the San Joaquin River at Lathrop ranged from 14.2 to 26.2 °C (Figure 3-27). When tagged juvenile Chinook salmon and steelhead were present in the study area, the mean water temperature in 2012 was higher than in any other year. Furthermore, the mean 2012 water temperatures generally were warmer than 2010 and 2011, but similar to 2009 temperatures (Table 3-3; Figures 3-23 to 3-27). Also, by June 29, 2012, water temperatures at the SJL gauge had risen to a point where steelhead respiratory efficiency was affected (21 °C) (Hooper 1973).

3.4 WATER CLARITY (TURBIDITY)

3.4.1 2009 TURBIDITY

Turbidity varied between years (Figure 3-28). From April 1 through June 30, 2009, the turbidity at MSD, the closest gauge in physical proximity to the HOR study area (4.6 km), ranged from 9.1 to 48.3 Nephelometric Turbidity Units (NTU) (Figure 3-29). When tagged juvenile Chinook salmon were recorded by the receivers, the mean turbidity in 2009 generally was lower than in 2010, but was similar to 2011 and 2012 turbidity (Table 3-5; Figures 3-28, 3-29, 3-30, 3-31, and 3-32). The turbidity also was more variable in 2009 than in any other year (Table 3-5).

3.4.2 2010 TURBIDITY

From April 1 through June 30, 2010, the turbidity at the MSD gauge ranged from 12.1 to 42.9 NTU (Figure 3-30). When tagged juvenile Chinook salmon were recorded by the receivers, the mean turbidity in 2010 was higher than in any other year (Table 3-5; Figures 3-29, 3-30, 3-31, and 3-32). The turbidity also was the least variable in 2010 (Table 3-5; Figure 3-28).

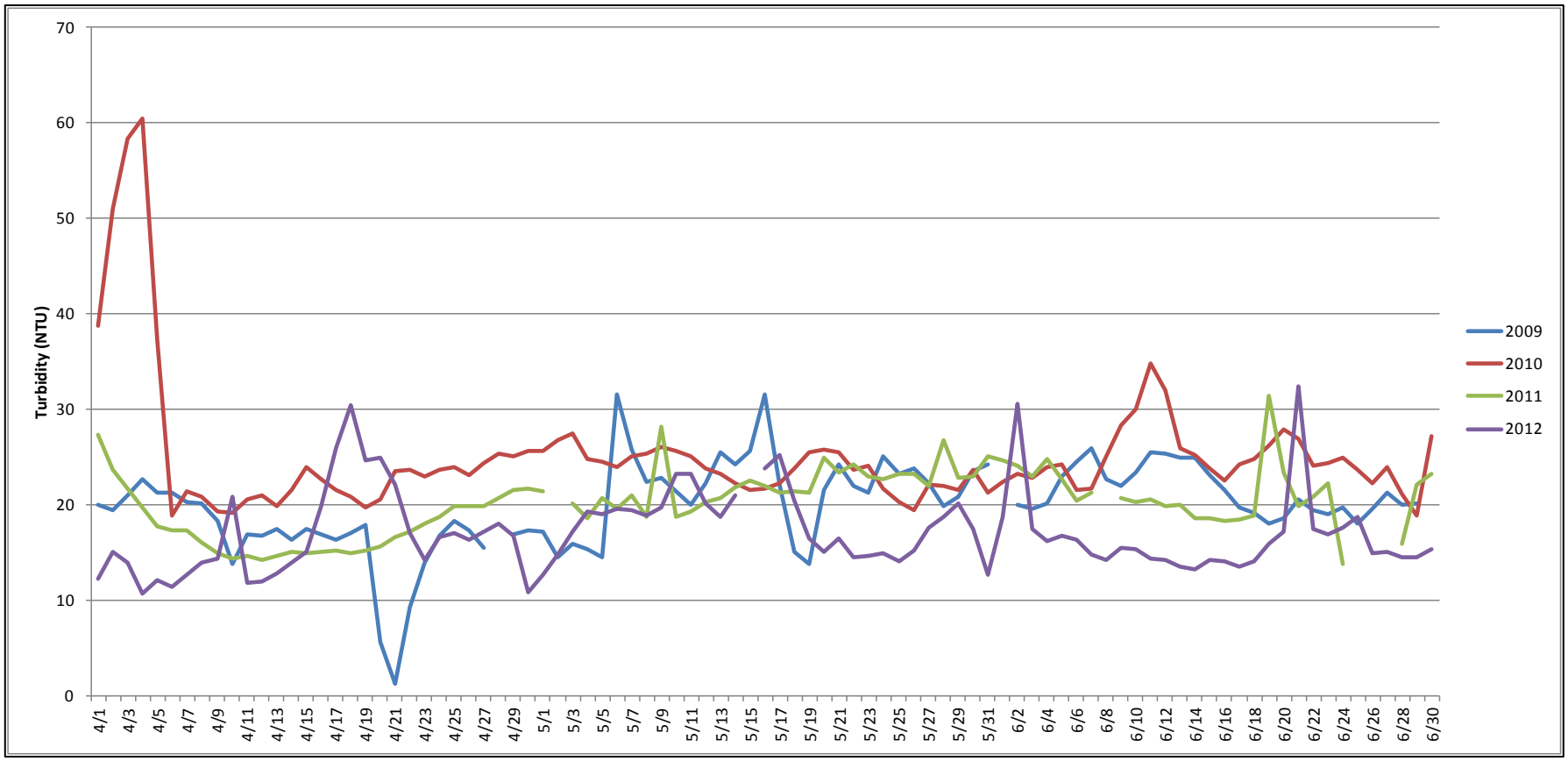

Sources: Baldwin, pers. comm., 2013; Dempsey, pers. comm., 2013

Figure 3-28 **Daily Mean Turbidity in the San Joaquin River at Mossdale (MSD), 4/1 to 6/30, 2009–2012**

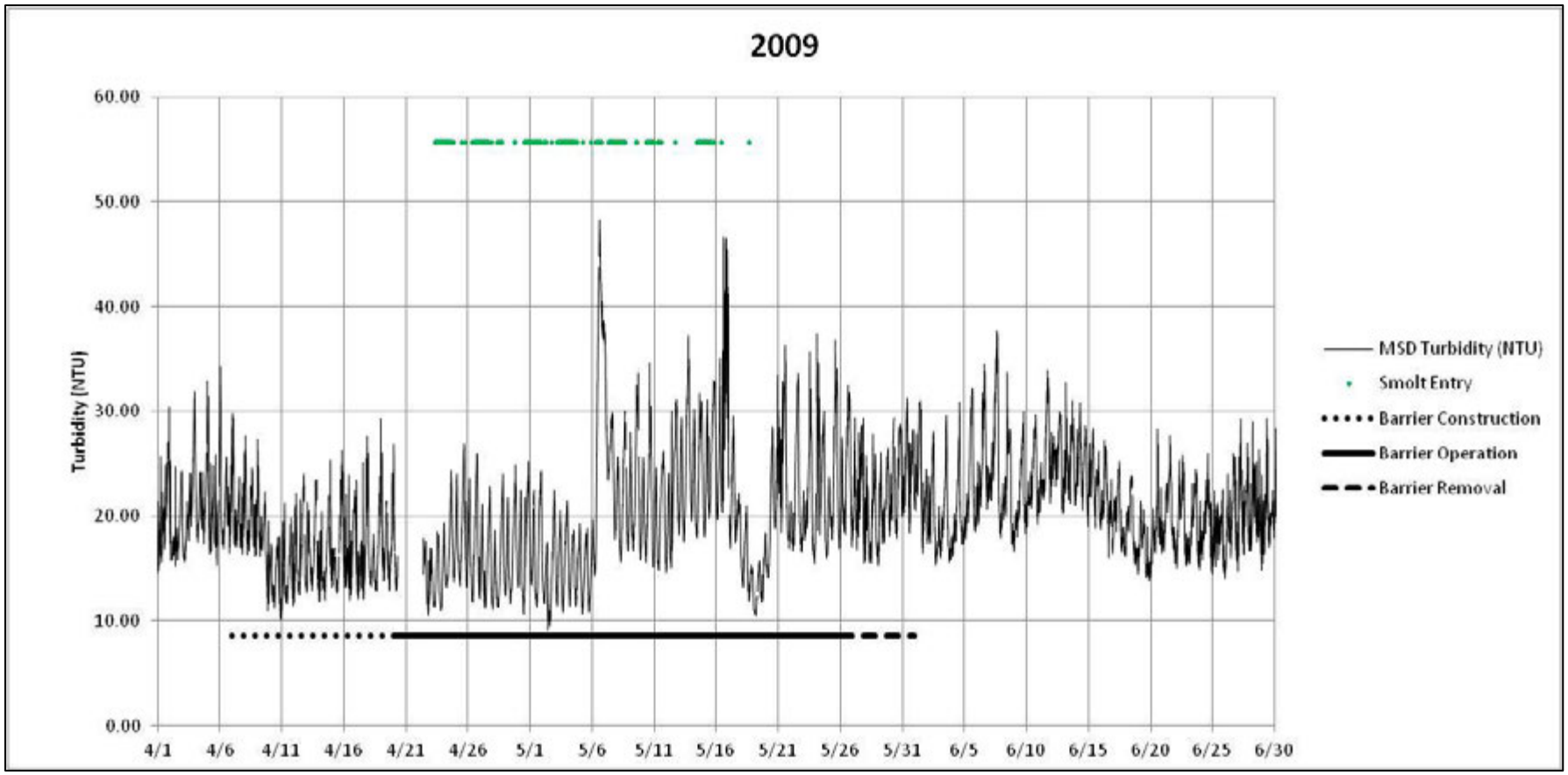

Sources: Baldwin, pers. comm., 2013; Dempsey, pers. comm., 2013

Note: The barrier referred to in the legend was a non-physical fish barrier called a BAFF (Fish Guidance Systems Ltd, Southampton, UK). Barrier operation was not continuous, with the BAFF off approximately 50% of the time during the period of BAFF operation.

Figure 3-29 **Turbidity of the San Joaquin River at the Mossdale Gauge from 4/1/09 through 6/30/09 and Tagged Juvenile Chinook Salmon Presence**

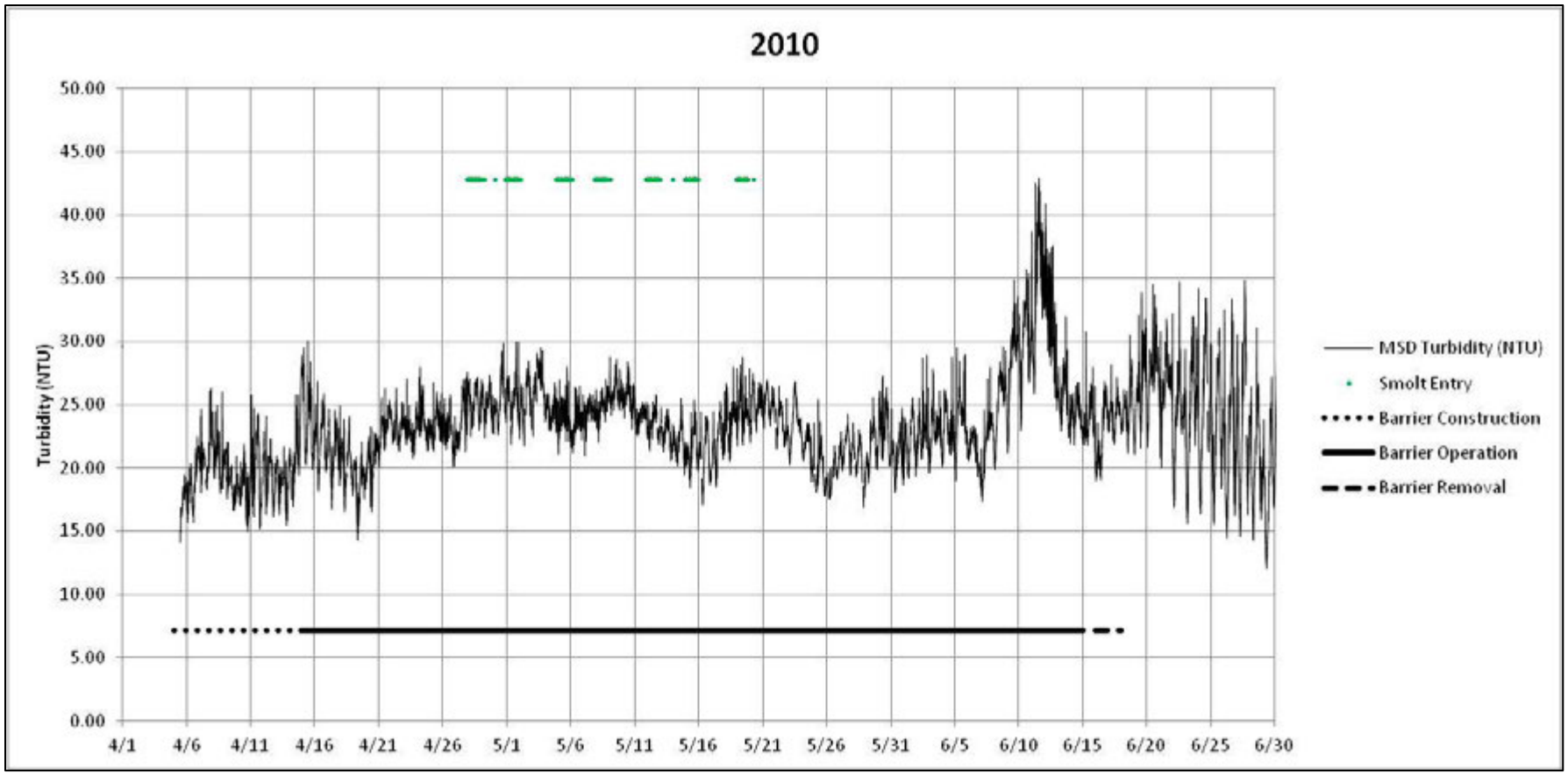

Sources: Baldwin, pers. comm., 2013; Dempsey, pers. comm., 2013

Note: The barrier referred to in the legend was a non-physical fish barrier called a BAFF (Fish Guidance Systems Ltd, Southampton, UK). Barrier operation was not continuous, with the BAFF off approximately 50% of the time during the period of BAFF operation.

Figure 3-30 **Turbidity of the San Joaquin River at the Mossdale Gauge from 4/1/10 through 6/30/10 and Tagged Juvenile Chinook Salmon Presence**

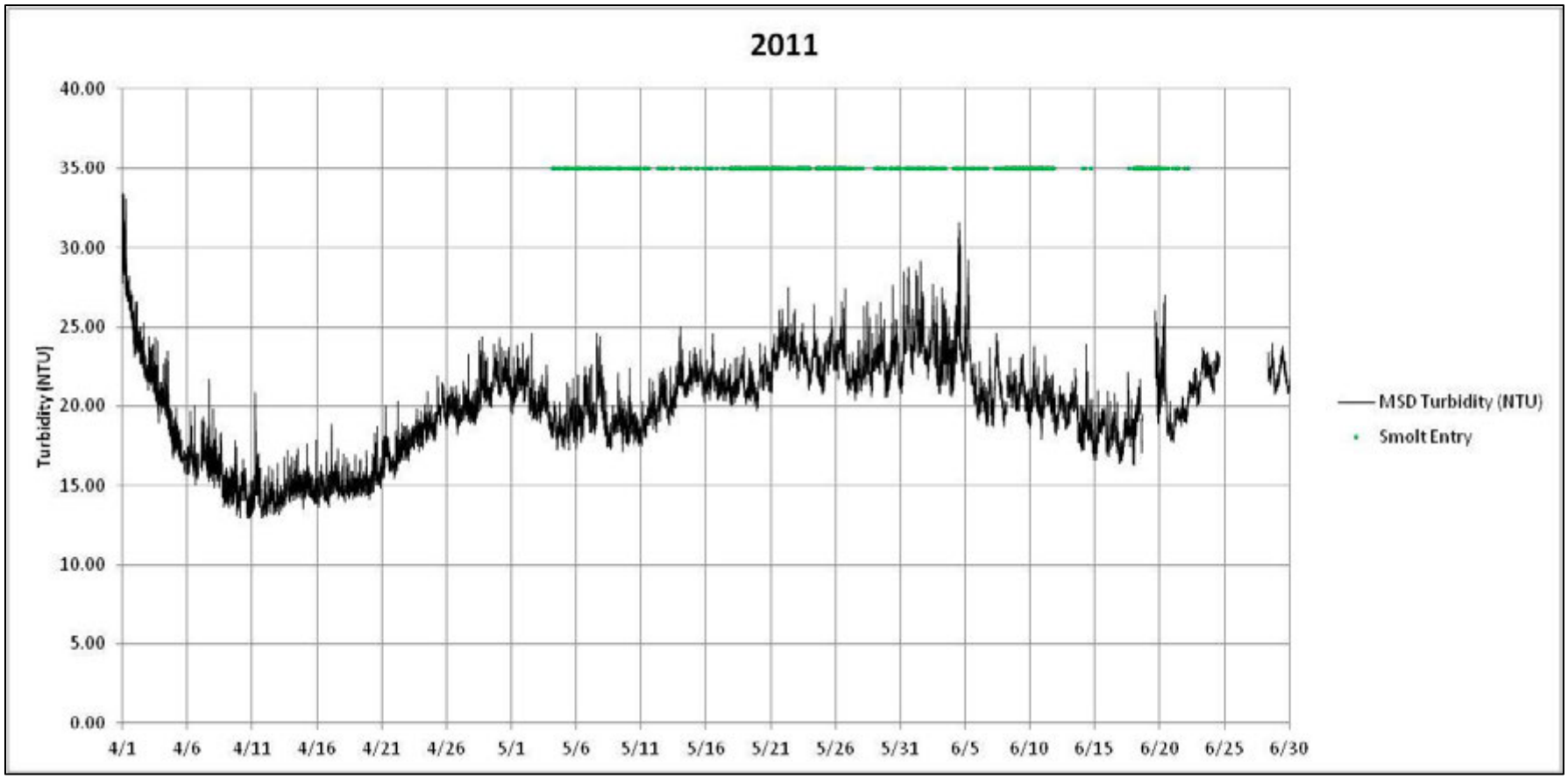

Sources: Baldwin, pers. comm., 2013; Dempsey, pers. comm., 2013

Note: No barrier was installed or operated during this period.

Figure 3-31 **Turbidity of the San Joaquin River at the Mossdale Gauge from 4/1/11 through 6/30/11 and Tagged Juvenile Chinook Salmon and Steelhead Presence**

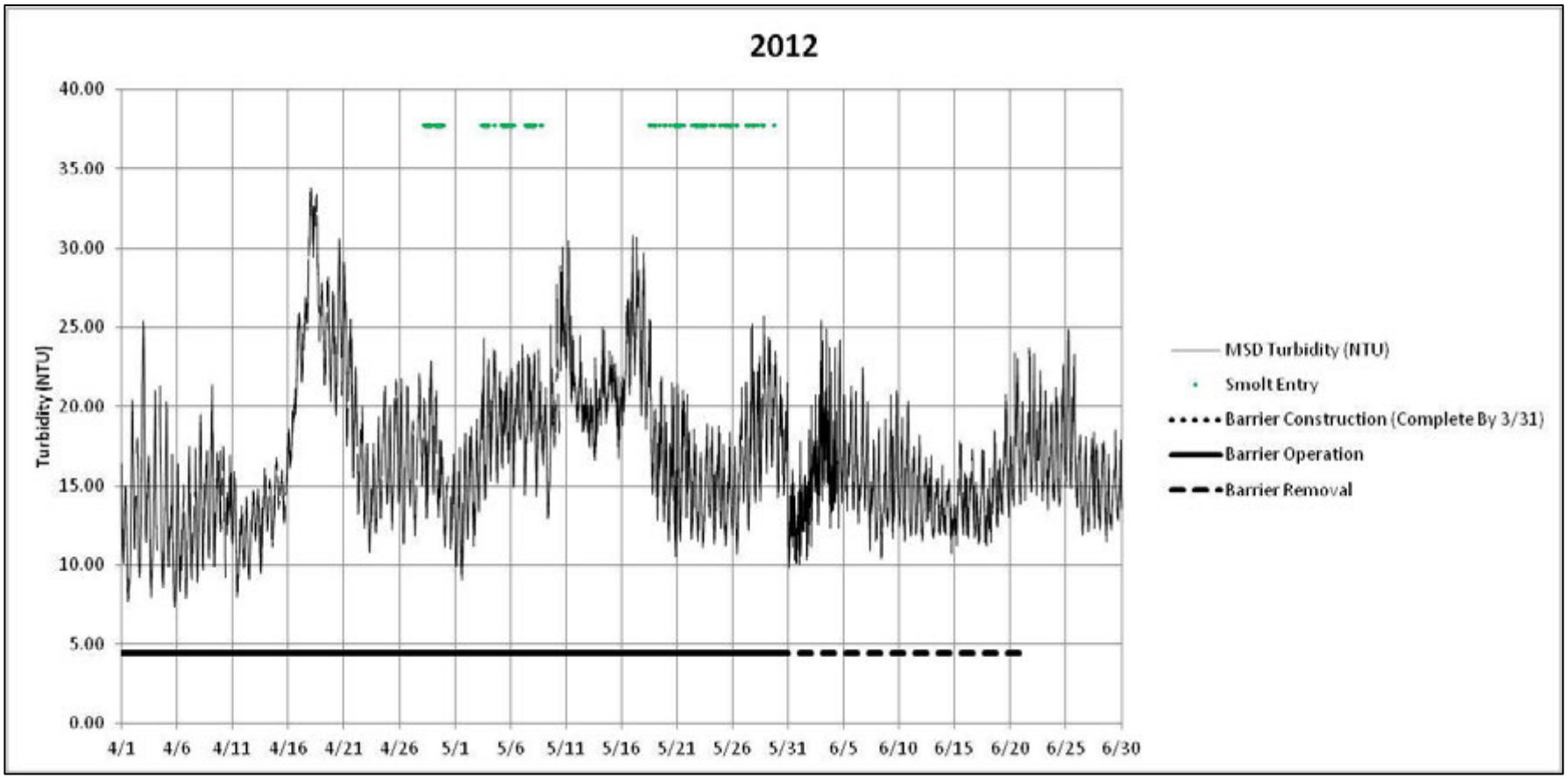

Sources: Baldwin, pers. comm., 2013; Dempsey, pers. comm., 2013

Note: The barrier installed was a rock barrier with eight culverts.

Figure 3-32 **Turbidity of the San Joaquin River at the Mossdale Gauge from 4/1/12 through 6/30/12 and Tagged Juvenile Chinook Salmon and Steelhead Presence**

Table 3-5
Descriptive Statistics for 2009–2012 Turbidity at the MSD Gauge

Year	First Fish[1]	Last Fish[2]	MSD Turbidity (NTU)				
			Mean	Standard Deviation	Minimum	Maximum	Count
2009	4/23/09 8:24	5/18/09 13:48	19.9	6.6	9.1	48.3	2405
2010	4/27/10 22:25	5/20/10 5:54	24.1	1.9	17.1	30.0	2073
2011	5/4/11 2:51	6/22/11 4:24	21.1	2.1	16.3	31.6	4523
2012	4/28/12 4:13	5/29/12 16:35	18.0	3.8	9.1	30.8	2945

Notes: MSD = San Joaquin River at Mossdale; NTU = Nephelometric Turbidity Units
[1] Date/time when the first tagged salmonids was nearest the BAFF line.
[2] Date/time the last tagged salmonids was nearest the BAFF line.
Source: Baldwin, pers. comm., 2013; Dempsey, pers. comm., 2013

3.4.3 2011 TURBIDITY

From April 1 through June 30, 2011, the turbidity at the MSD gauge ranged from 12.9 to 33.4 NTU (Figure 3-31). When tagged juvenile Chinook salmon and steelhead were present, the mean turbidity in 2011 generally was lower than in 2010, but was similar to 2009 turbidity (Table 3-5; Figures 3-28, 3-29, 3-30, and 3-31). The standard deviation in turbidity was similar in 2010 and 2011, and both of these years exhibited lower standard deviation than in other years (Table 3-5).

3.4.4 2012 TURBIDITY

From April 1 through June 30, 2012, the turbidity at the MSD gauge ranged from 7.3 to 33.8 NTU (Figure 3-32). Furthermore, in this same period, the mean turbidity was 16.6 NTU, the lowest recorded mean for the 4 years studied (Figure 3-28). The turbidities from April 1, 2012, until fish were released on April 28, 2012, represented the lowest turbidity of any 4-week period in the 4 years studied. In addition, when tagged juvenile Chinook salmon and steelhead were present, the mean turbidity in 2012 was lower than in than any other year (Table 3-5; Figures 3-29, 3-30, 3-31, and 3-32). Only 2009 exhibited a higher standard deviation in turbidity than 2012 while tagged juvenile Chinook salmon and steelhead were released (Table 3-5).

4 BARRIER TREATMENTS

4.1 NON-PHYSICAL BARRIER: THE BIO-ACOUSTIC FISH FENCE (BAFF)

Installation of the spring rock barrier has been controversial because of the area of habitat impacted and its potential effects on the risk of entrainment into the SWP and CVP export facilities for delta smelt, a species that is listed under the federal and California endangered species acts (see Section B.2.1 in Appendix B, "Focal Fish Species Information"). In 2008, a court order designed to protect delta smelt prohibited the installation of the spring rock barrier pending fishery agency actions or further order of the court. Subsequently, the U.S. Fish and Wildlife Service (USFWS) issued a BO for delta smelt and its critical habitat for the OCAP (USFWS 2008). USFWS determined that, as a result of its influence on the hydrodynamics of the Delta, the rock barrier potentially increases the vulnerability of delta smelt, particularly larvae and juveniles, to entrainment at CVP and SWP south Delta export facilities.

When the rock barrier is in place, a proportion of the water that would ordinarily flow down Old River is forced to flow down the San Joaquin River which benefits outmigrating juvenile salmonids. However, the rock barrier can also cause or augment net flow reversal in Old River. In addition, the barrier increases flows in Turner and Columbia cuts, two major central Delta channels that flow toward the south Delta. The result of these hydrodynamic changes is an increase in reverse flow in several channels, which has been noted to have coincided with increases in salvage of delta smelt (e.g., in 1996) (Nobriga et al. 2000). Therefore, DWR proposed use of a BAFF as an option at the HOR to meet the objective of excluding outmigrating salmonid juveniles from Old River while also minimizing the potential effects to delta smelt and Delta hydrodynamics. The BAFF allowed unobstructed flows into Old River, thus helping to lessen reverse flows in Old River as a result of SWP/CVP exports.

The BAFF is a multi-stimulus fish barrier that combines strobe lights, an air bubble curtain, and sound at frequencies and levels repellent to fish. The BAFF is intended to form a behavioral deterrent for juvenile salmonids in the San Joaquin River, rather than a physical barrier (e.g., rock barrier), to prevent entry into Old River. The sound system and strobe light flash rate can be tuned to known sensitivities of various fish species. Studies with Chinook salmon and delta smelt have shown that when the sound and strobe light flash rate are tuned according to these species' sensitivities, the barrier was effective as a deterrent for juvenile Chinook salmon (Bowen et al. 2009) and delta smelt (Bowen et al. 2010). The sound frequency range used was 50 to 600 Hertz (Hz). Audiogram studies (Oxman et al. 2007) have shown maximum hearing sensitivity at around 250 Hz for juvenile Chinook salmon. The BAFF's strobe lights flashed at 360 flashes per minute. Nemeth and Anderson's (1992) data showed a strong reaction to strobe lights at this flash rate.

Although future minor design adjustments may occur based on the 2010 design, the BAFF is 138 m long and made up of 17 separate 7.9-m sections. The barrier frame includes 64 Fish Guidance Systems Model 15-100 sound projectors, spaced approximately 2.0 m apart; 136 strobe lights (Fish Guidance Systems 100-centimeter-linear intense modulated lights [IMLs]), and perforated pipe. The sound projectors are driven by a signal generator (Fish Guidance Systems Model 1-08) and eight Fish Guidance Systems Model 400 power amplifier/control units, located in an onshore building. The strobe lights are powered from a "power supply accumulator," a unit that accumulates energy until it is discharged to the IML, positioned every 12 strobe lights; the flash rate is triggered from the Model 1-08 signal generator. The exact power rating for the IMLs and the

wavelength of the light are proprietary (Fish Guidance Systems Ltd, Southampton, UK). However, on visual inspection at the barrier study area under low-light conditions, the IMLs could be detected, flashing in the water at a maximum of 10 m distance from the BAFF. This led to the 10-m line, developed under low-light conditions; it was assumed that if a human eye could perceive the IML at 10 m, then a juvenile Chinook salmon would definitely experience the IML at less than or equal to 10 m from the BAFF.

The barrier is positioned diagonally across the main river channel, upstream of the divergence, and is aligned to guide outmigrating juvenile Chinook salmon to the San Joaquin River (Figure 2-4, "Barrier Alignments near the Head of Old River, 2009–2012," in Chapter 2, "Study Area and Focal Fish Species"). In designing the barrier, the flow was assumed to split 50/50 at the divergence, and the streamlines were assumed to divide midway across the river. Therefore, the angled barrier was designed so that fish present in streamlines that were entering Old River would be guided into streamlines entering the San Joaquin River. Thus, the barrier was planned to extend from the left bank (Old River side) to beyond the mid-channel position upstream of the divergence (Figure 2-4 in Chapter 2).

The diagonal fish screen/barrier concept is well known (Turnpenny and O'Keeffe 2005). The velocity perpendicular to the barrier line must be kept at or below the maximum sustainable swimming speed of the fish. In 2009, during BAFF design, the critical swimming speed (U-crit) was estimated from swimming performance data given by Muir et al. (1993:Figure 3), who give a U-crit range of 3.4 to 3.9 body lengths per second (BL/s). For design purposes, a value of 3.4 BL/s was assumed. The smallest size of fish desirable to protect was assumed to be 58 mm FL based on the minimum of length range for juvenile Chinook salmon (58 to 100 mm FL) expected in the south Delta, reflecting salvage data at the Tracy Fish Collection Facility and the Skinner Fish Protection Facility (NMFS 2013). This gave a conservative design figure for escape velocity (*Ue*) of 0.2 m/s (Figure 4-1).

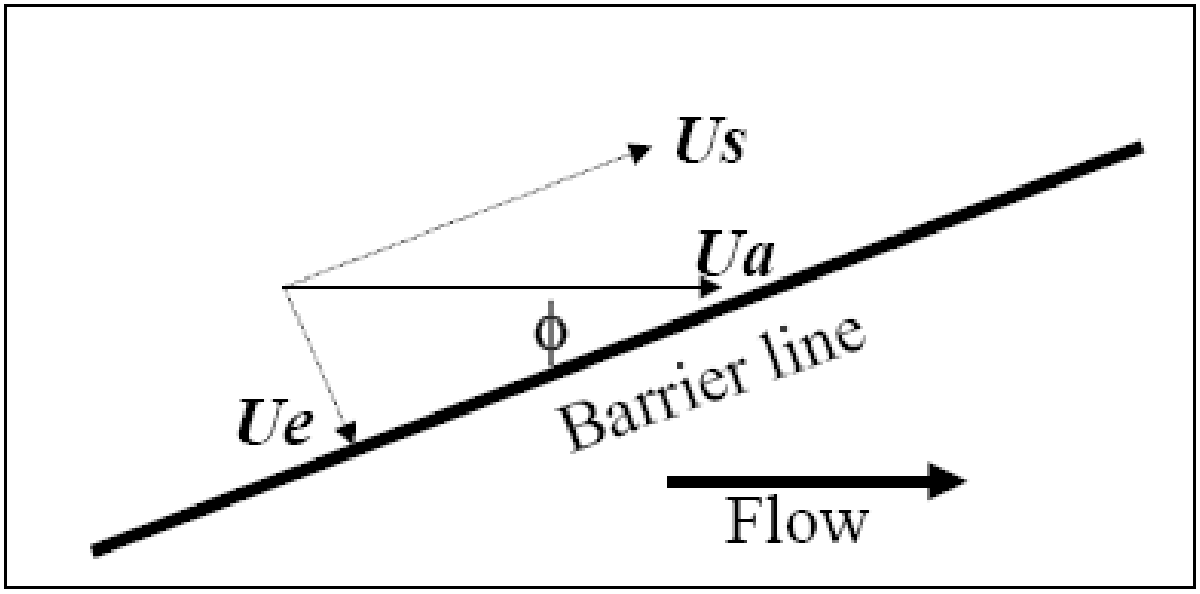

Note: Ua = main channel velocity; Ue = fish escape velocity; Us = sweeping velocity component along the face of the screen
Source: Turnpenny and O'Keeffe 2005

Figure 4-1 **Flow Velocity Components in Front of an Angled Fish Barrier**

Figure 4-1 shows the relevant velocity components for an angled fish barrier. The main channel velocity is denoted *Ua*. The velocity perpendicular to the screen face is the fish escape velocity, *Ue*. For a barrier angle φ, this is calculated as Equation 4-1:

$$Ue = Ua \sin \varphi$$

The sweeping velocity, *Us*, is the component parallel to the screen face. This can be used to calculate the time taken for the fish to traverse the screen from any given point when swimming at velocity *Ue*. It is calculated as Equation 4-2:

$$Us = Ua \cos \varphi$$

The BAFF design for the barrier study area was based on the following values:

- River width at barrier line equaled 91 m;
- Average velocity (data from the MSD gauge, approximately 4.5 km upstream of HOR junction) was 0.41 m/s. Therefore, the average velocity used for the design was 0.5 m/s. This value was slightly larger than the observed mean to provide a safety margin; and
- River depth along barrier line exhibited a maximum of 4.5 m, and averaged approximately 2.5 m.

To achieve *Ue* = 0.20 m/s perpendicular to the barrier, the barrier angle φ was arcsin (0.2/0.5) equals 24°. This is the angle relative to the centerline of the river flow at the upstream point of the barrier. This was the angle, 24°, of the BAFF as deployed in 2009 (Figure 4-2).

In 2010, the barrier length was increased from 114 m to 138 m to reduce the risk of diverting fish into the deep scour hole in the concave bend of the San Joaquin River limb at the HOR study area. Also, the angle of the BAFF incident to the left (west) bank was increased to 27° to allow more distance between a deterred juvenile Chinook salmon and the scour hole. Additionally, a "hockey-stick" bend was shaped toward the tip of the barrier, made up of the last four barrier units; this was angled at 30° to the main barrier angle. This bend was intended to deter juvenile Chinook salmon away from the deep scour hole, where predation events were observed in 2009. The alignment of the 2010 BAFF barrier is shown in Figure 4-2.

Consideration was given to two methods of barrier deployment: either suspending the barrier from the surface or mounting it rigidly on the riverbed. Surface mounting is simpler for a temporary barrier but less robust. Owing to the risk of high flows and debris, bed mounting was selected. The San Joaquin River could provide habitat for the protected green sturgeon (see Chapter 2, "Study Area and Focal Fish Species"), and a condition of permitting the installation was that a gap of 0.46 m should be left below the barrier infrastructure to allow sturgeon to pass. This was achieved by supporting the BAFF chassis with piles inserted for this purpose. This also facilitated free bedload movement and reduced the risk of equipment becoming inundated by fine sediments. The resulting gap below the BAFF meant that approximately 18% of the cross-sectional area of the barrier channel was not "screened" by the BAFF.

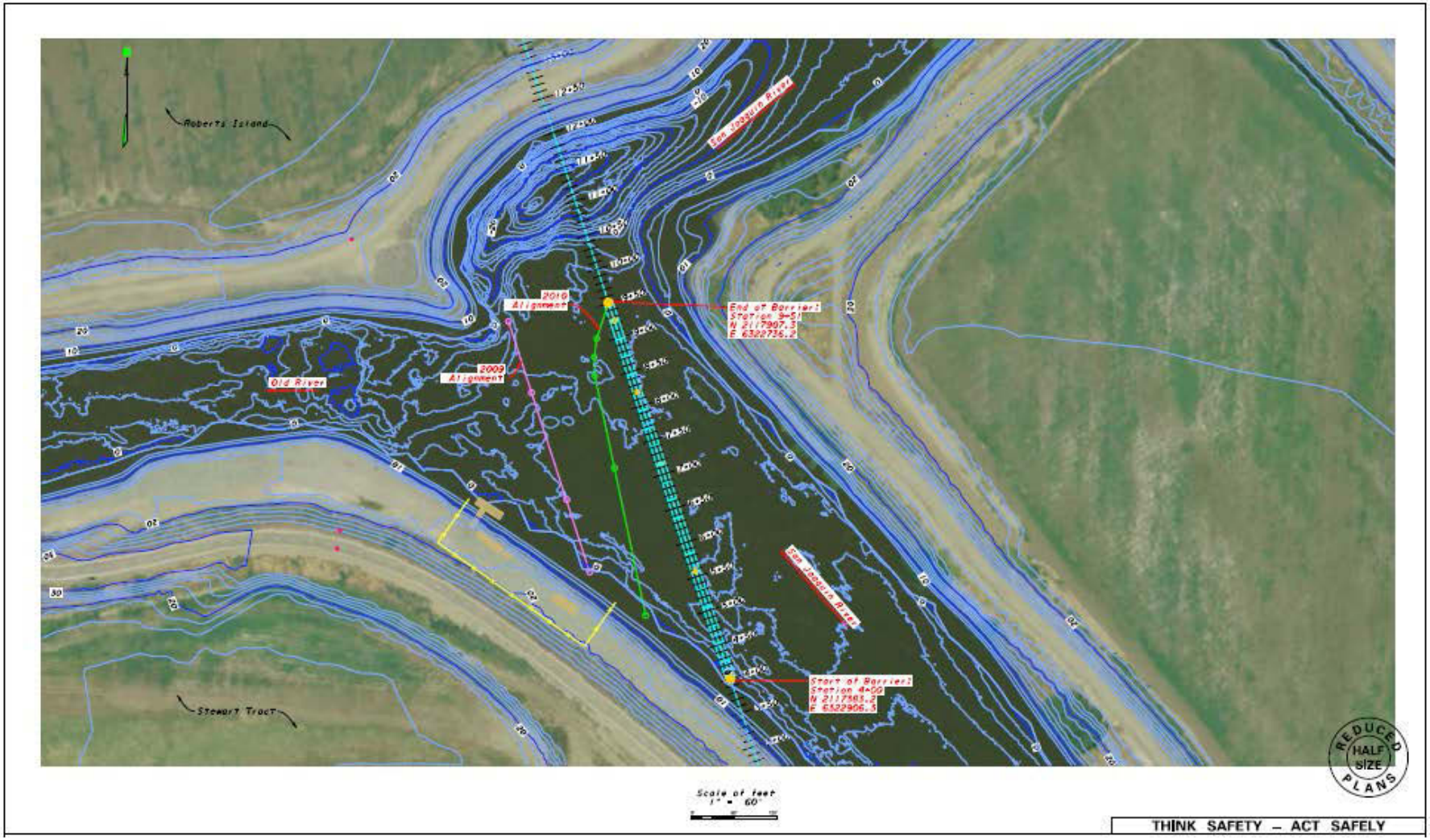

Source: DWR 2013

Figure 4-2 **Plan View of the Head of Old River Divergence (BAFF line in 2009 shown by pink line and in 2010 by green line)**

Each of the 7.9-m sections had adjustable height pivots to provide flexibility in lowering or raising each section to follow the riverbed contour. The barrier frame was supported by up to four piles in the river channel. Additionally, concrete piers were placed to support the frame above the riverbed in several locations so that the system would not move out of alignment and would allow for vertical adjustment of the barrier relative to the riverbed or water surface (Figure 4-3).

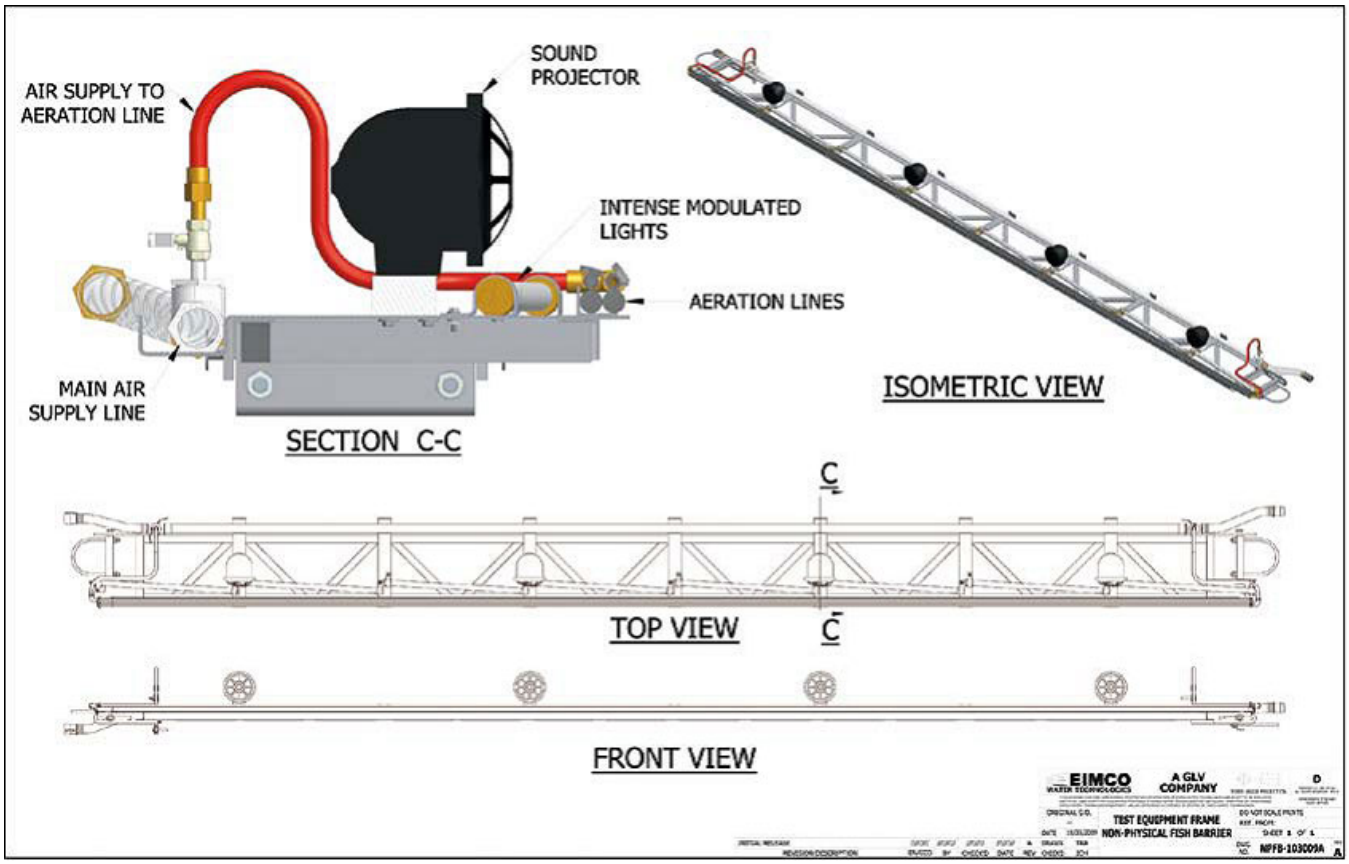

Source: Data provided by EIMCO

Figure 4-3 **Schematic of the Lattice Construction of the Barrier Support Frames (with sound projectors, strobes, and aeration lines)**

The air bubble curtain was generated by passing air (approximately 16.4 cubic meters per minute) through a uniformly perforated pipe attached to the barrier frame. The air was supplied by a trailer-mounted air compressor capable of an operating pressure up to 7 bar, although the actual operating pressure was lower, typically 2 to 3 bar. The air pipe was a rubberized construction, allowing the pores to open under pressure and self-seal when the air flow stopped. The primary function of the bubble curtain was to contain the sound that was generated by the sound projectors. The air bubble/water mixture acted as a pseudo-medium in which sound would travel at a velocity intermediate between that of air and water alone. Essentially, the sound was refracted and became encapsulated within the bubble curtain, which allowed a precise linear wall of sound to be developed (Bowen et al. 2009). Sound levels decayed very rapidly in the water outside of the bubble curtain, dropping to a few percent of the sound projector level within 3 m (Bowen et al. 2012:Appendix A). This led to the development of the 3-m line; a juvenile Chinook salmon would definitely experience the sound deterrent when it passed within 3 m of the BAFF. Therefore, during the day, a 3-m line was established, and at night a 10-m line was established (see

Section 5.2.2, "Calculation of Barrier Deterrence Efficiency"). These lines were used to determine if a tagged salmonid "experienced" the BAFF; if the tagged individual passed within 3 m of the BAFF during the day, or within 10 m at night, it was determined to have "experienced" the BAFF.

Up to 120 amps (115 volts, alternating current) of an inductively rated power supply was required to run the complete light and sound generating system. A small trailer housed the control units, signal generators, and amplifiers, because these units had to be kept dry.

4.2 HEAD OF OLD RIVER PHYSICAL ROCK BARRIER

The rock barrier is installed biannually, in spring and fall. The spring rock barrier is intended to prevent downstream-migrating juvenile salmonids in the San Joaquin River from entering Old River and, thereby, avoiding their exposure to SWP and CVP diversion operations and unscreened agricultural diversions. The spring rock barrier is constructed with approximately 9,560 cubic meters of rock to form a 68.5-meter-long by 25.9-meter-wide (at the base) berm. The spring rock barrier has a crest elevation of +3.8 m North American Vertical Datum of 1988 (NAVD) (Figure 4-4). The south end of this barrier has eight 1.2-meter-diameter culverts with slide-gates built into the barrier abutment, and a 22.9-m clay weir at an elevation of +2.5 m NAVD. Unlike the Old River at Tracy and Grant Line Canal barriers, no boat portage facility exists at this barrier.

The fall rock barrier is similar in design to the spring rock barrier, but smaller. The fall rock barrier is intended to benefit migrating adult salmon in the San Joaquin River by improving flow and dissolved oxygen conditions. The fall rock barrier has six 1.2-m culverts with slide-gates and a 6.1-m weir section at an elevation of +0.7 m NAVD. It is approximately 68.5 m long by 16.8 m wide at the base, and has a crest elevation of +2.5 m NAVD. The fall rock barrier is composed of approximately 5,730 cubic meters of rock.

Source: DWR 2013 and AECOM 2013

Figure 4-4 **Physical Rock Barrier at the Head of Old River with Eight Culverts in 2012**

5 METHODS

5.1 ANALYSIS OF TAGGED JUVENILE SALMONIDS

5.1.1 FATE OF TAGGED JUVENILE SALMONIDS

The analysis of tagged juvenile Chinook salmon and steelhead followed the methodology used for the 2011 analysis of the effects of a non-physical barrier at Georgiana Slough (DWR 2012). Acoustic transmitters were originally inserted in juvenile salmonids in accordance with the Vernalis Adaptive Management Program (VAMP) (SJRGA 1999, 2010, 2011, and 2013) and the Six-Year Steelhead Study (6YSS) (NMFS 2009; SJRGA 2013) by the VAMP/6YSS team. The fates of the tagged fish were classified as follows:

1. Released but never arrived;
2. San Joaquin River;
3. Old River;
4. Predation; or
5. Unknown.

These fates were used to estimate O_E, P_E, and D_E. These three metrics (O_E, P_E, and D_E) were evaluated through samples of tagged juvenile salmonid as they arrived at the HOR study area. If a tagged juvenile salmonid was determined to have been eaten, then that tag was evaluated in an analysis of proportion eaten. The possible errors that could have been made in determining the fate of being eaten are assessed for implications with respect to the proposed recommendations (Section 8.2.1, "Further Examine Predation Classification").

From 2009 through 2012, there were two types of acoustic telemetry gear used for evaluations of movement and behavior of acoustic tags: HTI and VEMCO. HTI gear provided sub-meter positioning and was used to evaluate behavior in the vicinity of the barrier location; this was the primary gear used in the analyses presented in this report. VEMCO gear provided one-dimensional information and collected route selection information and overall barrier effectiveness measures in 2012. Analyses related to VEMCO gear are presented in Appendix C, "Comparisons of HTI and VEMCO Data."

5.1.2 STUDY FISH SOURCES AND TAG SPECIFICATIONS

HTI EQUIPMENT

Three hatchery sources were used to provide juvenile Chinook salmon and steelhead for the study during the four study years, as shown in Table 5-1. For Chinook salmon, the Feather River Fish Hatchery and the Merced River Fish Hatchery supplied fish. All steelhead were from the Mokelumne River Fish Hatchery.

Table 5-1
Juvenile Salmonids Used for Head of Old River Barrier Evaluations Using HTI Gear

Study Year	Species	Fish Hatchery	Run	Total Number Released	Minimum Size (mm FL)	Maximum Size (mm FL)
2009	Chinook Salmon	Feather River	Fall-Spring Hybrid	933	80	110
2010	Chinook Salmon	Merced River	Fall	504	99	121
2011	Chinook Salmon	Merced River	Fall	1,915	94	140
2011	Steelhead	Mokelumne River	Winter	2,208	149	396
2012	Chinook Salmon	Merced River	Fall	424	95	135
2012	Steelhead	Mokelumne River	Winter	16	167	269

Notes: FL = fork length; mm = millimeter
Sources: SJRGA 2010, 2011, 2013

The Chinook pre-smolts and smolts (referred to as "juveniles" in this report) from the Feather River and Merced River fish hatcheries for this study mimicked the ocean-type life history pattern (described in Appendix B, "Focal Fish Species Information"). These two hatcheries take ocean-type adults, spawn them between September and January, house the fry (30 to 55 mm TL) in raceways, where they are maintained for several months. At the Feather River Fish Hatchery, the target size is 96 mm TL by April (Kastner, pers. comm., 2013). At the Merced River Fish Hatchery, the target is to maximize growth by feeding approximately 3.5% of body weight per day (Kollenborn, pers. comm., 2013). The fry become parr in a few months and eventually begin to undergo the physiological and behavioral changes of smoltification. The ocean-type parr begin to smoltify in March or April. The largest individuals, a minimum of 102 mm TL, were selected in April for use in the study. These juveniles may be considered pre-smolt or smolt, depending on the state of smoltification in each individual. These juveniles were produced in the hatchery and used as surrogates for naturally produced (wild) juveniles. Chinook juveniles were surgically implanted with acoustic transmitters and released in the San Joaquin River 24.4 km upstream of the HOR study area.

In 2009, the HTI Model 795 *Lm* acoustic transmitter ranged in mass from 0.62 to 0.69 grams (in air) and were surgically inserted into the coelomic cavity of the juvenile Chinook salmon (Table 5-2). The target tag burden (i.e., tag:body mass ratio) of 5% (as recommended by Liedtke et al. 2012) was exceeded in 98% of cases (Table 5-3). The high number of exceptions existed because the spring/fall hybrids from the Feather River Fish Hatchery grew more slowly than expected once they were transferred to the Merced River Fish Hatchery (SJRGA 2010). From 2010 through 2012, juvenile Chinook salmon supplied for tagging were larger (Table 5-1) and the target tag burden was reduced and exceeded in 5.3 to 11% of the juvenile Chinook salmon tagged (Table 5-3).

Table 5-2
Acoustic Tag Models and Specifications Used in the Head of Old River Studies from 2009–2012

Study Year	Tag Model Number	Quantity Used	Diameter (millimeters)	Length (millimeters)	Mass in Air Mean (grams)	Used for Sampling
2009	795*Lm*	950	6.8	16.5	0.65	Juvenile Chinook Salmon
2010	795*Lm*	508	6.8	16.5	0.65	Juvenile Chinook Salmon
2011	795*Lm*	1,089	6.8	16.5	0.65	Juvenile Chinook Salmon
	795*LD*	540	6.8	21.0	1.0	Juvenile Steelhead
	795*LX*	36	16	45.0	13.0	Predator Species
	795*LG*	13	11	25.0	4.5	Predator Species
2012	M800	76	6.7	16.4	0.50	Juvenile Chinook Salmon
	795*Lm*	348	6.8	16.5	0.65	Juvenile Chinook Salmon
	795*LD*	16	6.8	21.0	1.0	Juvenile Steelhead
	795*LX*	3	16.0	45.0	13.0	Predator Species
	795*LG*	45	11.0	25.0	4.5	Predator Species

Source: Data compiled by AECOM and Turnpenny Horsfield Associates in 2013.

Table 5-3
Range of HTI Tag Burdens Experienced by Salmonid Juveniles in 2009–2012

Study Year	Tag Model Number	Minimum Tag Burden	Mean Tag Burden	Maximum Tag Burden	Percentage of Tags Exceeding 5% of Body Mass	Species
2009	795*Lm*	0.044	0.071	0.102	98.0	Chinook Salmon
2010	795*Lm*	0.028	0.042	0.058	6.8	Chinook Salmon
2011	795*Lm*	0.020	0.041	0.065	11.0	Chinook Salmon
2012	M800	0.022	0.039	0.054	5.3	Chinook Salmon
2012	795*Lm*	0.020	0.039	0.124	6.6	Chinook Salmon
2012	795*LD*	0.004	0.006	0.008	0.0	Steelhead

Source: Data compiled by AECOM and Turnpenny Horsfield Associates in 2013.

5.1.3 SURGICAL, HANDLING, AND RELEASE METHODS

The barrier effectiveness evaluations described in this report were conducted as part of a coordinated suite of studies in the south Delta, which included the VAMP (SJRGA 1999) and the 6YSS (NMFS 2009; SJRGA 2013). The coordinated studies relied on one husbandry team (VAMP/6YSS) to conduct the surgical implantation, transport of the fish to the release site (i.e., Durham Ferry for all years, 2009 through 2012), handling of the fish to minimize effects on behavior and health, and release of the tagged juveniles according to the agreed schedule.

Concept guidelines important to the tag implantation procedures for HTI and VEMCO tags are described by Adams et al. (1998) and Martinelli et al. (1998). These guidelines were used to develop the methodologies

employed in these coordinated studies (this study, VAMP [SJRGA 1999; SJRGA 2010, 2011, and 2013], and 6YSS [NMFS 2009; SJRGA 2013]); the south Delta applications for surgery, handling, and release were described in general by Liedtke et al. (2012) and specifically for each year: 2009 (SJRGA 2010), 2010 (SJRGA 2011), 2011 (SJRGA 2013), and 2012 (J. Israel, pers. comm., 2013). For 2011, the methodology describing the specifics of surgical implantation, handling, and release can be evaluated in SJRGA (2013). For the 2012 methodology, Israel (pers. comm., 2013) reported that methods varied in only minor details from SJRGA (2013).

For tagged juvenile Chinook salmon, the 2009 releases were executed earlier than any other year, with an initial release of April 22, 2009, and initial arrival at the HOR study area on April 23, 2009 (an arrival onset 4 to 11 days earlier than other years) (Table 5-4). In contrast, the 2011 tagged juvenile releases were executed later than any other year, with the initial release of May 17, 2011, later by 22 to 26 days.

Table 5-4
Release and Detection Dates for Tagged Juvenile Salmonid Releases Used in the Studies

Year	Species	First Release[1]	First Fish[2]	Last Release[3]	Last Fish[4]
2009	Chinook Salmon	4/22/2009, 17:05	4/23/2009, 8:24	5/13/2009, 21:38	5/18/2009, 13:48
2010	Chinook Salmon	4/27/2010, 14:02	4/27/2010, 22:25	5/19/2010, 08:00	5/20/10, 5:54
2011	Chinook Salmon	5/17/2011, 15:00	5/17/2011, 21:24:47	6/19/2011, 12:00	6/22/2011, 4:24
2011	Steelhead	3/22/2011, 15:00[5]	5/4/2011, 02:51:51	6/18/2011, 0:00	6/22/2011, 04:24:00
2012	Chinook Salmon	4/26/2012, 13:00	4/28/2012, 4:13	5/27/2012, 05:00	5/29/2012, 16:35
2012	Steelhead	5/22/2012, 23:00	5/23/2012, 23:38:44	5/22/2012, 23:00	5/28/2012, 15:56:39

Notes: BAFF = bio-acoustic fish fence.
1 First Release is the date/time the first fish went in the water at Durham Ferry.
2 First Fish is the date/time when the first tagged fish was nearest the 2009 (2009 data) or 2010 (2010–2012 data) BAFF line and detected by the HOR study area hydrophone array.
3 Last Release is the date/time the last fish went in the water at Durham Ferry.
4 Last Fish is the date/time the last tagged fish was nearest the 2009 (2009 data) or 2010 (2010–2012 data) BAFF line.
5 The hydrophone array at the HOR study area was not operational between 3/22/11 and 4/5/11.
Sources: Johnston, pers. comm., 2013; SJRGA 2010, 2011, and 2013

5.1.4 ACOUSTIC TELEMETRY ASSESSMENTS

HTI HYDROPHONE DEPLOYMENT

Hydrophone arrays allowing 2D tracking of tagged fish were installed at the HOR study area from 2009 through 2012. A hand-held global positioning system (GPS) (precision level 2 to 3 m) was used to deploy each hydrophone at the appropriate location and to measure the Universal Transverse Mercator (UTM) coordinates for each hydrophone in the array. Once all hydrophones were in place, a procedure was performed to fine-tune the measured locations. This procedure used the transmitting capability of each hydrophone to produce a signal that all other hydrophones received. By measuring the time delay between the signal of the transmitting hydrophone and the signal arriving at each receiving hydrophone, the location of each hydrophone could be adjusted to fit all other time delays from all other hydrophones. In addition, the water temperature at each hydrophone was measured at the time of signal transmission to calculate the speed of sound during the procedure. For stationary hydrophones, this process results in hydrophone position estimates that allow sub-meter accuracy for acoustic tags

located within the bounds of the array. During 2009, this procedure was performed once at the start of the monitoring period. During 2010, 2011, and 2012, the procedure was performed seven, four, and three times throughout the monitoring period, respectively.

In 2009, four hydrophones were installed around the BAFF (Figure 5-1). In 2010, eight hydrophones were installed: four located upstream and four downstream of the BAFF (Figure 5-2). In 2011, nine hydrophones were installed in approximately the same configuration as 2010, with the addition of one hydrophone deployed deep in the scour hole (Figure 5-3). For 2012, 13 hydrophones were installed around the rock barrier. Four hydrophones were located in the San Joaquin River upstream of the Old River divergence, three downstream of the divergence in the San Joaquin River, two upstream of the rock barrier in the Old River, and four downstream of the rock barrier in the Old River (Figure 5-4).

Source: Hydroacoustic Technology, Inc. 2013

Figure 5-1 **HOR Study Area—2009 Hydrophone Array with BAFF (red line)**

Source: Hydroacoustic Technology, Inc. 2013

Figure 5-2 **HOR Study Area—2010 Hydrophone Array with BAFF (red line)**

Source: Hydroacoustic Technology, Inc. 2013

Figure 5-3 **HOR Study Area—2011 Hydrophone Array, No Barrier Treatment**

Source: Hydroacoustic Technology, Inc. 2013

Figure 5-4 **HOR Study Area—2012 Hydrophone Array with Rock Barrier**

All hydrophones near the San Joaquin-Old River divergence were deployed using bottom mounts fabricated from a section of railroad tie as an anchor. The hydrophones were installed using tensioned aircraft cable or rope lines extending to subsurface floats (Figure 5-5).

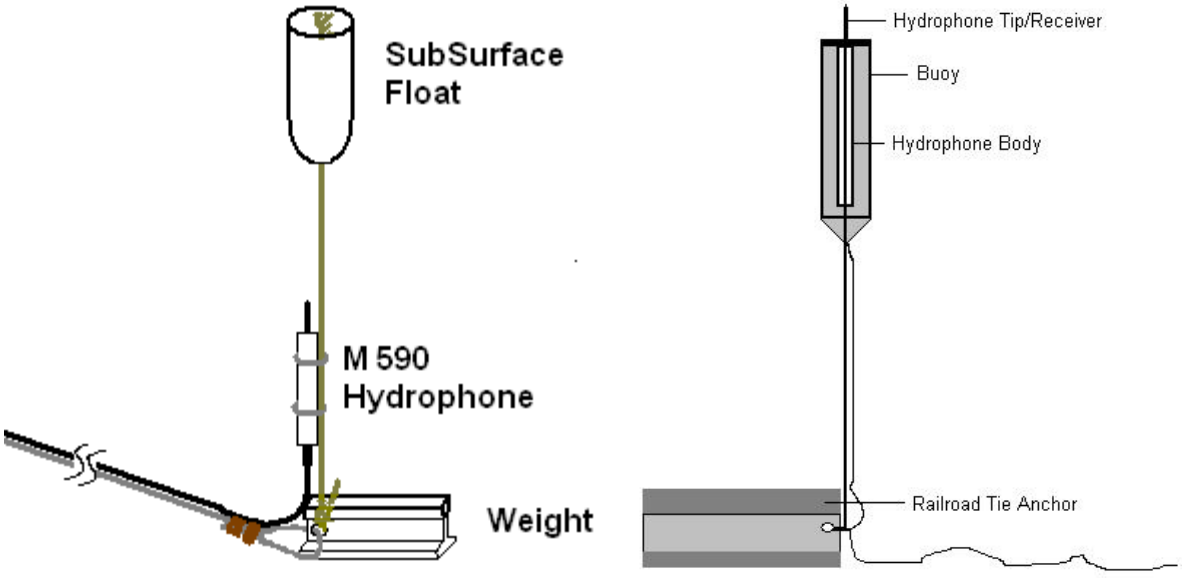

Source: Hydroacoustic Technology, Inc. 2013

Figure 5-5 **Conceptual Depiction of the Two Types of Hydrophone Bottom Mounts with Tensioned Lines**

HTI Acoustic Tag Specifications

HTI Model 795 and 800 acoustic tags were used for the telemetry studies conducted 2009 through 2012 at the HOR study area (Table 5-2). The tags operate at a frequency of 307 kilohertz (kHz), and were encapsulated with a nonreactive, inert, low-toxicity resin compound.

During the 2009 through 2012 study period, three different sizes of acoustic tags were used to tag juvenile Chinook salmon and steelhead, and two different sizes were used for the predator fish. Table 5-2 lists the quantity of each tag type used, with basic tag specifications, for each year of the study period.

Two-Dimensional Track Development

Data Collection

The acoustic tag tracking system consisted of acoustic tags implanted in fish, hydrophones deployed underwater, and an on-shore receiver and data storage computer. Each acoustic tag transmitted an underwater sound signal or acoustic "ping" that sent identification information about the tagged fish to the hydrophones. The hydrophones were deployed at known locations within the array to maximize spacing of the hydrophones in a 2D or 3D format. For 3D tracking, tags must be received on at least four hydrophones; for 2D tracking, tags must be received on at least three hydrophones. By comparing the time of arrival of the sound signal at multiple hydrophones, the 2D (or if the hydrophones are arranged appropriately, the 3D) position of the tagged fish can be calculated.

2D acoustic tag tracking was conducted using an HTI Model 290 Acoustic Tag Tracking System (ATTS). The primary components of the ATTS included the acoustic tag receiver, hydrophones, and a user interface/data storage computer (Figure 5-6). The system used a fixed array of underwater hydrophones to track movements of fish implanted with HTI acoustic tags.

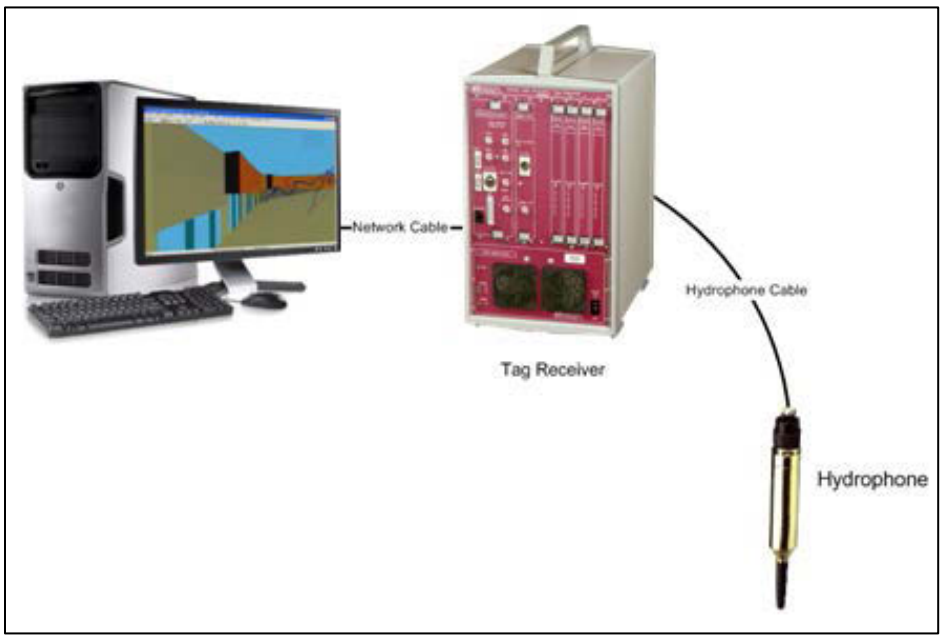

Source: Hydroacoustic Technology, Inc. 2013

Figure 5-6 **Basic Components of the HTI Model 290 Acoustic Tag Tracking System Used to Track Movements of Fish Implanted with HTI Acoustic Tags**

As tagged fish approached the study area, the ping or signal was detected and the arrival time recorded at several hydrophones. The differences in tag signal arrival time at each hydrophone were used to calculate the 2D position of each tagged fish. The ATTS includes the following hardware and software components:

- A tag programmer that activates and programs the tag;
- Acoustic tags each transmitting a pulse of sound at regular intervals;
- Hydrophones that function like underwater microphones, listening within a defined volume of water;
- Cables connecting hydrophones to tag receivers; and
- Tag receiver that receives the tag signal from the hydrophones; conditions the signal; and, using specialized software, outputs the data into a format that is stored in computer data files.

Acoustic Tags

The HTI Model 795 acoustic tags use "pulse-rate encoding," which provides increased detection range, improves the signal-to-noise ratio and pulse-arrival resolution, and decreases position variability when compared to other types of acoustic tags (Ehrenberg and Steig 2003). Pulse-rate encoding used the interval between each transmission to detect and identify the tag (Figure 5-7). Each tag was programmed with a unique pulse-rate encoding to detect and track the behavior of individual tagged fish moving within the array.

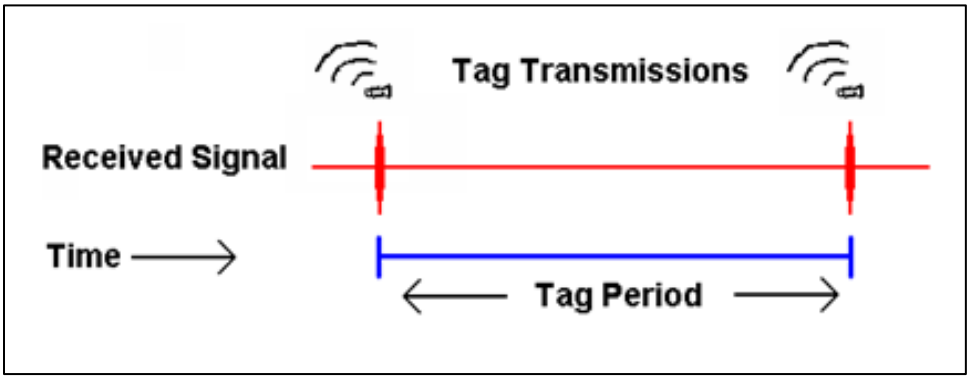

Source: Hydroacoustic Technology, Inc. 2013

Figure 5-7 **Pulse-Rate Interval Describing the Amount of Elapsed Time Between Each Primary Tag Transmission**

The pulse rate was measured from the leading edge of one pulse to the leading edge of the next pulse in sequence. By using slightly different pulse rates, tags can be uniquely identified. The timing of the start of each transmission was precisely controlled by a microprocessor within the tag. Each tag was programmed to have its own tag period to uniquely identify each tag.

In addition to the tag period, the HTI tag double-pulse mode or "subcode" option was used to increase the number of unique tag identification (ID) codes available. Using this tag coding option, each tag was programmed with a defined primary tag period and with a defined secondary transmit signal, called the subcode. This subcode defined a precise elapsed time period between the primary and secondary tag transmissions (Figure 5-8). There were 31 different subcodes possible for each tag period, resulting in more than 100,000 total unique tag ID codes.

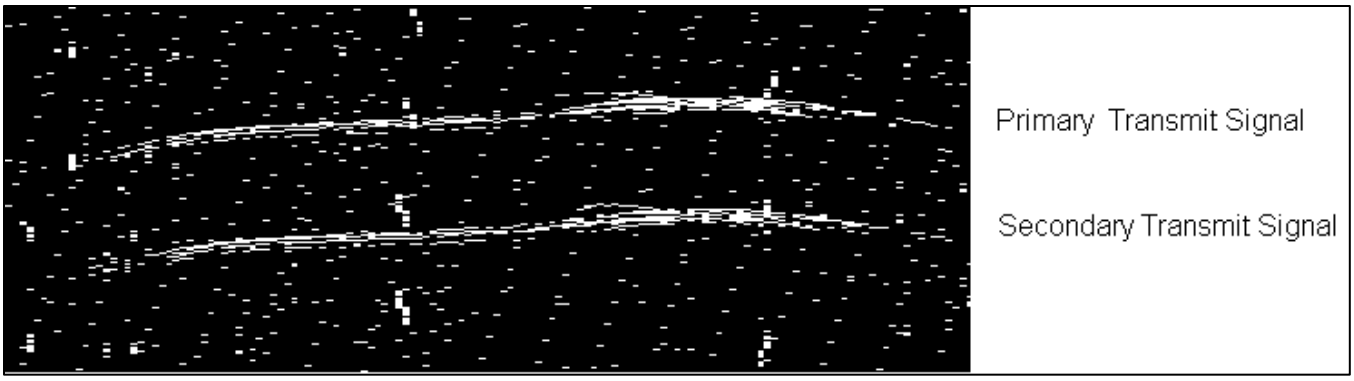

Source: Hydroacoustic Technology, Inc. 2013

Figure 5-8 Example Graphic from the Data Collection Program Showing the Primary (tag period) and Secondary (subcode) Transmit Signal Returns from a Model 795 Acoustic Tag

Hydrophones

The Model 590 hydrophones operate at 307 kHz and include a low-noise preamplifier and temperature sensor. Hydrophone directional coverage is approximately 330°, with equivalent sensitivity in all directions, except for a 30° limited-sensitivity cone directly behind the hydrophone where the cable is attached. The hydrophone sensor element tip is encapsulated in specially treated rubber with acoustic impedance close to that of water to ensure maximum sensitivity. The hydrophone and connector housing are made of a corrosion-resistant aluminum/bronze alloy. Specially designed cables incorporating twisted pair wire and double shields for noise reduction were used to connect each deployed hydrophone to the acoustic tag receiver.

The hydrophone preamplifier circuit provides signal conditioning and background noise filtering for transmission over long cable lengths and in acoustically noisy environments. A calibration circuit in the preamplifier provides a method for field testing hydrophone operation and was used to measure the signal time delays between hydrophones in the array. Measurement of the signal delays was used to verify the absolute position of each hydrophone within the sampling array, which is a critical part of monitoring equipment deployment. This process of measuring the hydrophone positions via the signal travel times between each hydrophone is typically referred to as the "ping-around." The Model 590 hydrophones include temperature sensors to measure water temperature at each location within the array, which was used to precisely estimate the sound velocity in water and referenced during the "ping-around" procedure.

Acoustic Tag Receiver

An HTI Model 290 acoustic tag receiver (ATR) can receive acoustic tag information simultaneously on up to 16 separate channels. Each ATR channel was assigned to a single hydrophone. The ATR was connected to the data collection computer, which analyzed and stored the acoustic data. An individual raw data file was automatically created for each sample hour and contained the complete set of information describing detection of each tag for all hydrophones. Data acquisition filters in the ATR were configured to identify the acoustic tag sound pulse and discriminate tag transmissions from background noise that may have been present.

The ATR pulse measurements were automatically reported for each tag signal from each hydrophone and were written to Raw Acoustic Tag (*.RAT suffix) files by the HTI acoustic tag data collection software program. Each

*.RAT file contains header information describing all data acquisition parameters, followed by the raw tag signal data. Each raw tag signal data file contains all acoustic signals detected during the time period, including signals from tagged fish and some amount of unfiltered acoustic noise, which is removed during the data analysis processes.

Mathematical Derivation of Position Calculations

Detection of a tagged fish by a single hydrophone is sufficient to confirm the presence and identity of the target, but a tag must be simultaneously detected by at least four hydrophones to be positioned in three dimensions (Figure 5-9). To be accurately positioned in two dimensions, a tag must be simultaneously detected on at least three hydrophones. 2D and 3D acoustic tag coordinates with sub-meter accuracy require accurate knowledge of the individual hydrophone positions. In addition, the hydrophones detecting the tag signal must have a direct "line of sight" path to the tag, and must be located in different vertical planes (for 3D only). As an acoustic tag is detected by three or four hydrophones that are all cabled to a single receiver, the difference in the arrival time of the transmission to each sensor was used to triangulate the exact location of the tag. HTI receivers have a built-in GPS receiver that updates to Universal Coordinated Time (UTC), so there is no clock drift. HTI receiver clock times are within 20 to 50 nanoseconds of UTC. Typically, many sequential tag positions are derived for each fish, providing a time series of locations. These positions are tracked and associated to define a swimming path for each tagged fish, which is mapped and presented in a 2D or 3D display. The underlying data are all stored for additional analyses.

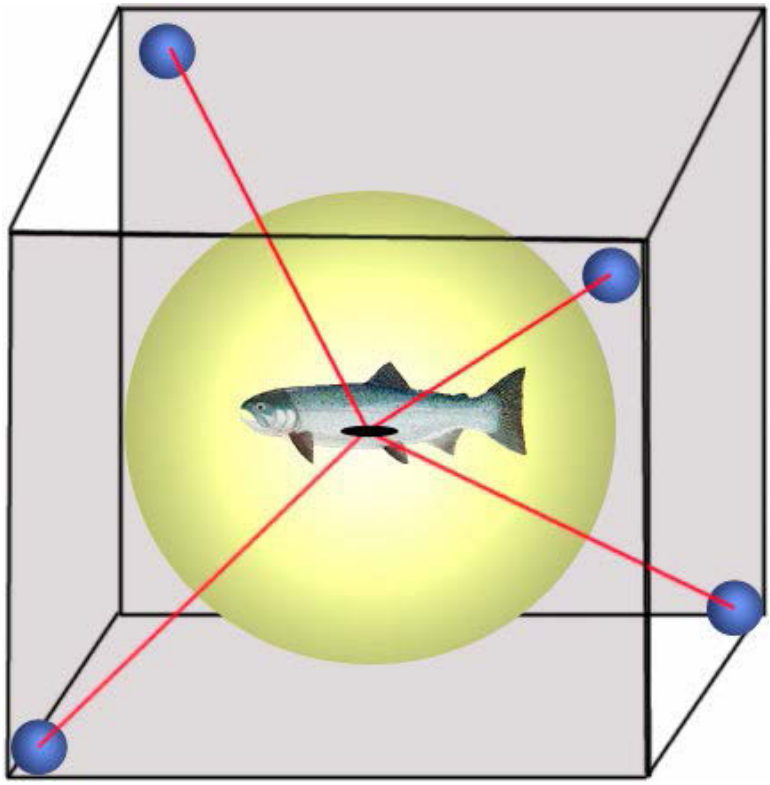

Source: Hydroacoustic Technology, Inc. 2013

Figure 5-9 Positioning of an Acoustic Tag in Three Dimensions with a Four-Hydrophone Array

The method that is used to determine acoustic tag positions by the HTI systems follows the same basic principles employed by GPS technology. The acoustic tag transmits a signal that is received by at least four hydrophones. By knowing the positions of the four hydrophones and measuring the relative signal arrival times at the hydrophones, the locations of the tagged fish can be estimated.

This process is described mathematically in the following equation. Assuming that h_{ix}, h_{iy}, h_{iz} define the x, y, z coordinate locations of the i[th] hydrophone, and F_x, F_y, F_z represent the unknown x, y, z locations of the tagged fish, the signal travel time from the tagged fish to the i[th] hydrophone, t_i, is given by:

$$t_i = \frac{1}{c}\sqrt{(h_{ix} - F_x)^2 + (h_{iy} - F_y)^2 + (h_{iz} - F_z)^2}$$

The constant "c" in the above equation defines the underwater sound velocity. This equation cannot be solved for a single hydrophone detection; however, given the three unknown fish coordinates, a solution can be determined based on the convergence of multiple hydrophone measurements. The differences between the arrival times of the signal at the multiple hydrophones ($t_i - t_j$) is described as follows:

$$t_i - t_j = \frac{1}{c}\left[\sqrt{(h_{ix} - F_x)^2 + (h_{iy} - F_y)^2 + (h_{iz} - F_z)^2} - \sqrt{(h_{jx} - F_x)^2 + (h_{jy} - F_y)^2 + (h_{jz} - F_z)^2}\right]$$

For four hydrophones, there are three such distinct signal arrival-time difference equations. The system of nonlinear equations is determined by solving the tagged fish coordinates, such that the mean squared difference between the measured (left side of the equation above) and calculated time differences (right side of the equation above) are minimized.

Individual tag positions were then assembled in chronological order to form a 2D trace representing the movement of the fish as it passed through the array. This process was done from stored arrival time data (from *.RAT files) and in real time through the acoustic tracking system.

The relatively shallow water depths present in the vicinity of the HOR study area dictated the use of a 2D tracking approach. The 2D HTI tracking algorithm requires time delays from just three hydrophones, modifying the above equation to address only the x and y dimensions. Although 3D tracking is possible in shallow water, it requires close hydrophone spacing and a large increase in the total number of hydrophones to accurately derive the depth component. 2D tracking provided the necessary fish passage and behavioral information required for the HOR study area evaluation at a lower cost than a 3D array. The HTI data collection and analysis software programs incorporated both 2D and 3D tag tracking algorithms and automatically selected the best available solutions from multiple hydrophone detections.

Data Analysis

Two separate programs were used to process acoustic tag data: AcousticTag (Version 5.00.04) and MarkTags software (HTI, Seattle, Washington). AcousticTag was used initially to acquire data from the ATR and store it in raw acoustic echoes files. MarkTags was used to read the raw acoustic echo files, identify tag signals, and create

acoustic tag files. These processed acoustic tag files were used again in AcousticTag to position the tags in 2D space.

As described previously, AcousticTag acquires data and stores it in *.RAT files. These raw echoes are not associated with any specific tag ID or spatial positioning. Depending on the project site and environmental conditions, many echoes found within these files are not tag data, but originate from secondary sources such as ambient noise or reflections from the surface or nearby structure (called multipath). Thus, the first phase of post-processing was to identify and select the acoustic echoes that were received directly from tags, and to assign the unique tag ID to these echoes.

The echo selection process was completed in the MarkTags program. The procedure for isolating the signals from a given tag follows from the method used for displaying the signals themselves. Each vertical scan in the time-scaled window shows the detected arrivals that are equal to the pulse-rate encoding of a particular tag (Ehrenberg and Steig 2003). Only signals from the tag programmed with the same period will fall along the straight line. The results of the tag selection process completed in MarkTags was written to track acoustic tag files (*.TAT file). These files contain the individual raw acoustic echoes with assigned tag ID codes, but without spatial positioning assignments.

AcousticTag was used for the triangulation calculations and to output a database of 2D coordinate locations for each fish. This program provided information describing date and time; the x, y, and z coordinates; and hydrophones used in creating the 2D track. It then recorded this information to a Microsoft® Access database file.

DETERRENCE AND FATE DETERMINATION GUIDELINES

Deterrence Determination from Two-Dimensional Track

For all years of the study, a hydrophone array was deployed that allowed tracks of individual fish to be developed from tag transmission data. Each individual position calculated from a single tag transmission was developed in a geo-referenced UTM coordinate system, so it could be overlaid onto a geo-referenced map of the HOR study area. The time-stamped positions for each tagged fish were assembled into a time-ordered track which could be viewed in the context of the HOR study area and the barrier treatment, barrier status (Off/On), or no barrier, present for that time period.

Each tagged fish track was evaluated to determine if the tagged fish encountered the barrier (if present), if the tagged fish was deterred by the barrier (if BAFF was present and status was On), if the tagged fish exhibited predator-like behavior, and finally the ultimate fate of the tagged fish.

The guidelines for categorizing each tagged fish track into deterred (BAFF years 2009 and 2010), non-deterred (BAFF years 2009 and 2010), predation, route selected (San Joaquin River or Old River), or unknown, are listed in Appendix E. There were small differences in the guidelines for each study year based on the presence of a BAFF, the presence of a physical rock barrier (which caused large scale hydraulic effects unlike a non-physical barrier), or the absence of any barrier. Example tracks for tagged fish that were categorized as deterred, non-deterred, and predation are shown in Figures 5-10, 5-11, and 5-12, respectively. More examples of tracks for each deterrence category for each year are presented in Appendix E.

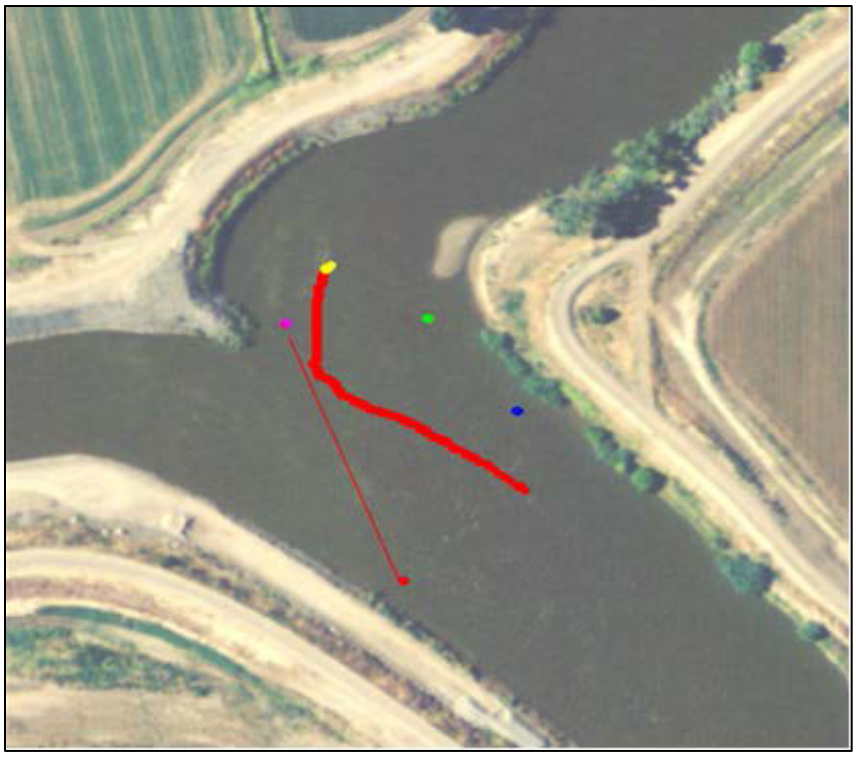

Source: Hydroacoustic Technology, Inc. 2013

Figure 5-10 **Tagged Chinook Number 5674.21 Deterred by the BAFF (On) at 03:38 PDT on May 15, 2009 and Exiting the Array down the San Joaquin River**

Source: Hydroacoustic Technology, Inc. 2013

Figure 5-11 **Tagged Chinook Number 5437.14 Passing through the BAFF (On) at 0:27 PDT on April 28, 2010 and Exiting the Array down the Old River**

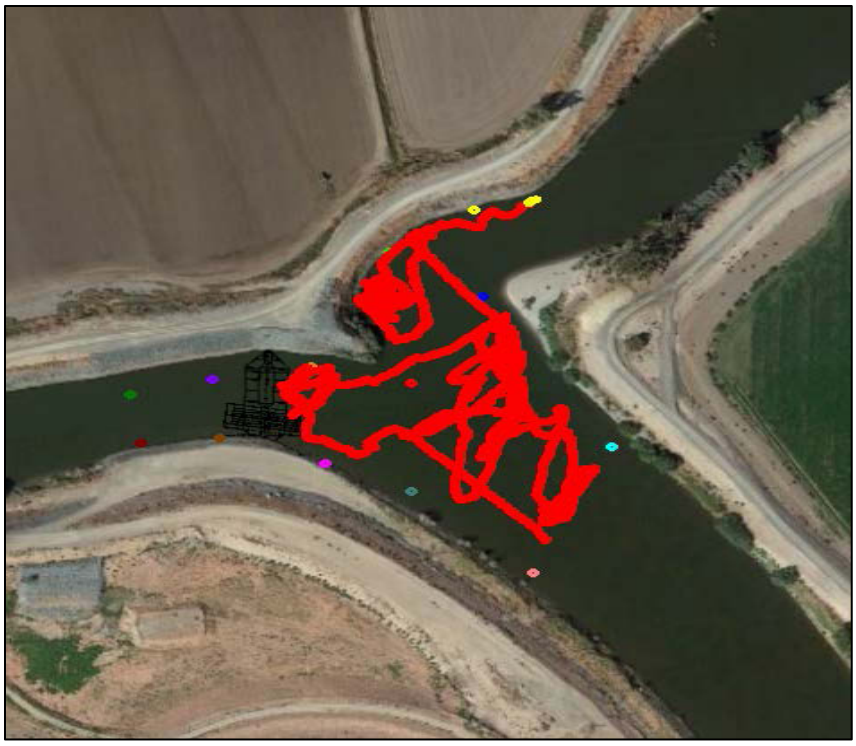

Source: Hydroacoustic Technology, Inc. 2013

Figure 5-12 **Tagged Chinook Number 2203.03 (designated as having been eaten by a predator) Showing Directed Movement Downstream at the Beginning of the Track, then Becoming "Predator-Like," Exhibiting Both Upstream and Looping Movement between 19:16 and 21:24 PDT on May 20, 2012 at the HOR Study Area**

Tag Drags and Ping-Arounds

In each year, after the hydrophones were set up, several tag drags were conducted. The tag drags ensured that a tag could be heard by three or more hydrophones at all locations within the hydrophone array.

The tagged fish-release periods are defined in Table 5-4. During the periods when the tagged fish were in the water, ping-arounds were done periodically using AcousticTag software. The ping-around information was used to improve the precision of the tag positions. These tag positions were used to build the 2D tracks. Tag positioning precision was estimated by HTI personnel at ≤1 m (Johnston, pers. comm., 2009).

5.2 EVALUATION OF JUVENILE SALMONID ROUTING INCLUDING BARRIER EFFECTS

5.2.1 GROUPING JUVENILE SALMONIDS INTO SAMPLES

The data analyses described were reanalyses of the data published in Bowen et al. (2012) and Bowen and Bark (2012), combined with analyses of new data collected in 2011 and 2012. An essential element of this reanalysis was assigning tags to samples depending on the time they were at the HOR study area, rather than the date and time at which they were released.

The first sample was assigned when the first fish arrived at the HOR study area. As long as the barrier state did not change, ambient light did not cross a critical threshold, and average water velocity did not cross a critical threshold, each fish that arrived was placed in this sample. When barrier state, or light, or velocity changed, a new sample was assigned. In this manner, all tagged fish were placed in samples. Samples with only one fish were removed from the analysis.

Barrier state was defined by the type and its status. For example, in 2009 and 2010, the barrier was a BAFF and the status was determined by whether the BAFF was turned on or off. In 2011, no barrier was installed. Thus, this treatment was referred to as "No Barrier" and the barrier status was always off. In 2012, a physical rock barrier was installed, thus the barrier was always on.

The critical threshold used for determining low- and high-light conditions was 5.4 lux. This critical threshold was chosen with regard to the operation of the BAFF. Based on the work of Anderson et al. (1988) on juvenile Chinook salmon strobe-light avoidance reactions, it was assumed that if the ambient light was ≥ 5.4 lux, then ambient light may influence the ability of the high-intensity modulated lights to produce a reaction in juvenile Chinook salmon encountering the BAFF. This critical light threshold (5.4 lux) was also used in analysis of the effects of a non-physical barrier at Georgiana Slough (DWR 2012).

The critical velocity threshold used to determine low- and high-velocity conditions was 0.61 m/s average channel velocity. This critical velocity threshold was selected based on a conservative estimate of the sustained swimming speed of juvenile Chinook salmon of 4.37 body lengths per second (BL/s) (Appendix B: Table B-1). This threshold was designed to protect juvenile Chinook salmon measuring 57 mm FL, which was the minimum size observed for a fall-run individual at the Tracy Fish Collection Facility and Skinner Delta Fish Protective Facility from August 1, 2011, through July 31, 2012 (NMFS 2013). Therefore, at a sustained swimming speed of 4.37 BL/s, a 57-mm FL juvenile Chinook salmon could swim 0.25 m/s. Thus, it was assumed that a fall-run juvenile had the capacity to swim away from the BAFF when the approach velocity was ≤ 0.25 m/s. An approach velocity of 0.25 m/s occurred when the average channel velocity was 0.61 m/s for the angle incident to the flow for the 2009 BAFF (24°) (Figure 5-1).

5.2.2 CALCULATION OF OVERALL EFFICIENCY

Overall efficiency (O_E) for the BAFF and the rock barrier were determined for each sample using Equation 5-1, in relation to start and finish lines similar to those depicted in Figure 5-13 (exact locations differed depending on hydrophone coverage in each year).

Equation 5-1:

$$O_E = S_A/L_A$$

Where:

O_E = overall efficiency,
S_A = the number of tags that left the HOR study area downstream via the San Joaquin River, passing the San Joaquin River finish line, and
L_A = the number of tags that entered the HOR study area from the upstream San Joaquin River, passing the San Joaquin River start line.

Source: Data compiled by AECOM in 2013

Figure 5-13 **Head of Old River Study Area: Start and Finish Lines and 2012 VEMCO Hydrophone Placements**

The calculation of O_E for 2011 (the "No Barrier" year) was the same mathematically as the calculation of O_E in Equation 5-1; therefore, it was possible to compare this parameter statistically across years. The hypotheses used for these comparisons are discussed under "Primary Objectives and Hypotheses Related to Juvenile Salmonid Routing, Including Barrier Effects" in Section 1.2.2, "Juvenile Salmonid Routing Including Barrier Effects," in Chapter 1.

5.2.3 CALCULATION OF PROTECTION EFFICIENCY

Protection efficiency (P_E) for the BAFF and the rock barrier were determined for each sample using Equation 5-2, in relation to start and finish lines similar to those depicted in Figure 5-13 (exact locations differed depending on hydrophone coverage in each year).

Equation 5-2:

$$P_E = S_N/(S_N+L_N)$$

Where:

P_E = protection efficiency,
S_N = the number of juvenile salmonids that left the HOR study area via the downstream San Joaquin River, passing the San Joaquin River finish line that were not eaten, and
L_N = the number of juvenile salmonids that left the HOR study area via Old River, passing the Old River finish line that were not eaten.

This calculation for P_E in relation to the BAFF and rock barriers (Equation 5-2) was also used to calculate P_E for 2011 (the "No Barrier" year), noting that there was no actual "protection" afforded by the lack of a barrier. Because the same equation was used for all years, it was possible to compare these two parameters statistically across years. The hypotheses used for these comparisons are discussed under "Primary Objectives and Hypotheses Related to Juvenile Salmonid Routing Including Barrier Effects" in Section 1.2.2, "Juvenile Salmonid Routing Including Barrier Effects," in Chapter 1.

5.2.4 CALCULATION OF BARRIER DETERRENCE EFFICIENCY

Deterrence efficiency (D_E) for the BAFF when it was on and off was evaluated using 2009 and 2010 data. A juvenile salmonid was determined to have experienced the BAFF if it came within 10 m of the BAFF in low-light conditions and if it came within 3 m of the BAFF in high-light conditions. D_E was determined for each sample according to Equation 5-3.

Equation 5-3:

$$D_E = R/E$$

Where:

D_E = barrier deterrence efficiency,
R = the number of tags that were deterred, and
E = the number of tags that experienced the BAFF.

D_E was calculated only for the years in which the BAFF was used: 2009 and 2010. The hypotheses used for these comparisons are discussed under "Primary Objectives and Hypotheses Related to Juvenile Salmonid Routing Including Barrier Effects," in Section 1.2.2, "Juvenile Salmonid Routing Including Barrier Effects," of Chapter 1.

5.2.5 CALCULATION OF BAFF EFFECT

It was possible to calculate the BAFF's effect when two samples occurred immediately adjacent in time, and therefore had the same light and velocity conditions, but where the BAFF was changed as part of an tagged manipulation. Thus, there was a directly comparable BAFF "on" to "off" condition. The BAFF effect was calculated according to a simple calculation (Equation 5-4).

Equation 5-4:

$$F = E_N - E_O$$

Where:

F = BAFF effect,
E_N = efficiency with the BAFF on, and
E_O = efficiency with the BAFF off.

The results for BAFF effect are reported in Chapter 6, "Results." The results are uncommon because it was unusual for the conditions to occur to acquire a BAFF effect sample.

5.2.6 STATISTICAL COMPARISONS

Using the samples assigned as described in Section 5.2.1, each of the null hypotheses described in Section 1.2, "Study Design, Objectives, and Hypotheses," was tested statistically. Additionally, when appropriate, the null hypotheses were also tested at each combination of light and velocity.

Four dependent variables of interest were compared. The first dependent variable was O_E, which provided an estimate of the proportion of tags that left the HOR study area via the San Joaquin River. The second dependent variable was P_E, which provided an estimate of the proportion of juvenile salmonids that left the HOR study area via the San Joaquin River that were not eaten. The third variable of interest was D_E, which provided an estimate of the proportion of juvenile salmonids that turned away from or were guided by the BAFF. The fourth variable of interest was BAFF effect, calculated when possible, which was the difference in an efficiency metric (O_E, P_E, or D_E) between the BAFF on and off.

An independent variable of interest was BAFF status, specific to the years when the BAFF was operated. In 2009 and 2010, it was possible to obtain a set of samples with the BAFF on and off for comparison. The comparison between BAFF on and off showed whether or not operation of the BAFF deterred juvenile Chinook salmon from entering Old River. If BAFF operation could not be shown to be better with the BAFF on compared to off, then the BAFF would have no utility as a fish deterrent.

The independent variable of primary interest was treatment, which had four states: (1) BAFF-2009; (2) BAFF-2010; (3) No Barrier-2011; and (4) Rock Barrier-2012. Each of these treatments occurred in a particular year

because it was not logistically feasible to change the barriers during a single study season. Thus, each treatment was also a function of a particular combination of physical attributes described in Chapter 3, "Physical Parameters." Because the physical attributes might have significant impact on barrier function, the treatment/year was depicted as the independent variable.

The independent variables of secondary interest were light intensity and water velocity. These were developed because of published literature accounts (Perry et al. 2012; Welton et al. 2002) of their effects on the operation of a BAFF. Thus, when appropriate, O_E, P_E, and D_E were evaluated at two light and velocity levels. The critical light and velocity thresholds are described in Section 5.2.1.

For each comparison, a one-way analysis of variance (ANOVA) was conducted for an independent variable and a dependent variable. For example, the first comparison was made in 2009: O_E was evaluated for the BAFF on versus off. Then, after the ANOVA was completed, the data were evaluated to determine whether they met the assumptions of the ANOVA procedure (Sokal and Rohlf 1995). With only one exception in the entire study, the data did not meet the assumptions of the ANOVA, and it was necessary to rely on a nonparametric equivalent: the Kruskal-Wallis Test (Hollander and Wolfe 1973).

The test statistic and P-value were reported. If the null hypothesis was rejected and there were more than two sets of samples, the sets of samples were then subjected to pair-wise comparisons to determine which populations were different. When more than one two-sample comparison was made, a Bonferroni adjustment in the critical alpha was made to control the experiment-wise error rate (Sokal and Rohlf 1995).

5.3 EVALUATION OF PREDATION ON JUVENILE SALMONIDS INCLUDING BARRIER EFFECTS

5.3.1 PROPORTION EATEN (UNIVARIATE ANALYSES)

The proportion of tagged fish in a sample that were eaten was determined for each sample according to Equation 5-5.

Equation 5-5:

$$C = C_P/L_A$$

Where:

C = sample proportion eaten;
C_P = the number of tags that were identified as having been eaten; and
L_A = the number of tags that entered the HOR study area from the upstream San Joaquin River, passing the San Joaquin River start line.

The procedure for grouping juvenile salmonids into samples is described in Section 5.2.1, "Grouping Juvenile Salmonids into Samples." The sample proportion eaten was used for testing hypotheses $H8_0$, $H9_0$, and $H10_0$, which were described under "Objectives and Hypotheses Related to Proportion Eaten" in Section 1.2.3, "Predation on Juvenile Salmonids, Including Barrier Effects." The sample proportion eaten is reported with the results of the statistical comparisons used for the hypothesis testing. In addition, when mean sample proportion

eaten was reported, population proportion eaten was also reported. The population proportion eaten for a given year is the grand proportion eaten determined by the total number of tagged juveniles eaten divided by the total number of tagged juveniles passing by the HOR study area in that year. The population proportion eaten summarizes the proportion eaten across all barrier states and light and velocity levels, and is comparable to the probability of predation described in Section 5.3.2, "Probability of Predation (Generalized Linear Modeling)," and in San Joaquin River Group Authority reports (SJRGA 2010, 2011, and 2013).

Statistical comparisons to test hypotheses $H8_0$, $H9_0$, and $H10_0$ were made with univariate tests in an analogous manner to that described for O_E, P_E, and D_E in Section 5.2.6, "Statistical Comparisons." In addition, interpretation was conducted in the same way using a comparison of the P-value and critical alpha (0.05), to determine if the null hypothesis should be rejected.

5.3.2 PROBABILITY OF PREDATION (GENERALIZED LINEAR MODELING)

The probability of tagged juvenile salmonids being preyed upon at the HOR study area was assessed in relation to several predictor variables that were hypothesized *a priori* to have potential influence on predation (see "Objectives and Hypotheses Related to Proportion Eaten" in Section 1.2.3, "Predation on Juvenile Salmonids Including Barrier Effects)": discharge, water temperature, turbidity, light level, juvenile size, small-fish density, and large-fish density. Discharge is highly correlated with velocity, and thus chosen for inclusion in modeling, as it is the more commonly used variable for planning and operations purposes. Discharge has been positively associated with salmonid survival probability through the Delta in several studies (Cavallo et al. 2013; Newman 2003; Perry 2010; but see also Zeug and Cavallo 2013). This may be because greater discharge results in shorter travel time or more direct migration routing, and therefore, less exposure to predators (Anderson et al. 2005). It was hypothesized that this predictor would be negatively related to predation probability at the HOR study area. Salmonid survival in the Delta has been demonstrated to be negatively associated with water temperature (Newman 2003; Zeug and Cavallo 2013), perhaps because predatory fish energy requirements increase at higher temperatures, and so food requirements are greater (Hanson et al. 1997). It was hypothesized that water temperature would be positively related to predation probability at the HOR study area.

Studies have found a positive relationship between turbidity and survival of Delta native fishes, both in the field (Chinook salmon: Newman 2003) and in the laboratory (delta smelt: Ferrari et al. 2013), presumably because the visual range of predators is less under more turbid conditions (Aksnes and Giske 1993). Similarly, light level affects the visual range of predators (Aksnes and Giske 1993), and some predatory species, such as largemouth bass, predominantly feed during the day (Moyle 2002). Accordingly, it was hypothesized that predation probability in the HOR study area would be negatively related to turbidity and positively related to light level.

The size of juvenile Chinook salmon migrating through the Delta was found to be positively associated with subsequent ocean recovery rate by Zeug and Cavallo (2013), possibly because of greater escape ability and reduced probability of being eaten by gape-limited predators. Predation probability at the HOR study area, therefore, was hypothesized to be negatively related to juvenile size. Small-fish density at the HOR study area (see predictor definition and description that follows; Table 5-5) was hypothesized to be negatively related to predation probability, reflecting the potential that greater density of alternative prey would reduce the predation risk to any individual juvenile. Large-fish density at the HOR study area was hypothesized to be positively related to predation probability because there is evidence that predator abundance is negatively related to juvenile Chinook salmon survival in the Delta (Cavallo et al. 2013). Barrier status also was included as a predictor (see

further discussion that follows), with the null hypothesis that there was no difference between barrier states in predation probability at the HOR study area. Survival in relation to barrier status at the HOR study area previously had been evaluated at a broader scale. For example, recent analysis by Zeug and Cavallo (2013) found no well-supported effect on ocean recovery rate of Chinook salmon in relation to installation of the physical rock barrier during the juvenile migration period through the Delta, whereas previous analysis by Newman (2008) suggested that survival was higher in the San Joaquin River than in Old River, and therefore, effective installation of the rock barrier would increase survival through the Delta.

Table 5-5
Summary of Predictor Variables Used in Generalized Linear Modeling of Juvenile Salmonid Probability of Predation at the Head of Old River Study Area

Variable (Unit)	Location	Source	Transformation	Notes
Water temperature (°C)	SJL	CDEC (Baldwin, pers. comm., 2013)	None	15-minute average data
Discharge (m^3/s)	SJL	CDEC (Baldwin, pers. comm., 2013)	None	15-minute average data
Turbidity (NTU)	MSD	CDEC (Dempsey, pers. comm., 2013)	None	15-minute average data
Ambient light (lux)	Manteca (CIMIS site #70)	CIMIS (State of California 2009)	Natural logarithm + 1	Original CIMIS data (Langley/day) were first converted into PAR per Clark et al. (2009: PAR, $\mu mol/m^2/s$ = 1.1076*Langley/day), and subsequently PAR was converted into lux per Apogee Instruments, Inc. (2013:Lux = 54*PAR). Original hourly data were linearly interpolated to 15-minute increments for consistency with water quality data.
Small fish density (<15 cm FL/10,000 m^3)	Mossdale (trawling)	USFWS survey data (Speegle, pers. comm., 2011 and 2013)	Natural logarithm + 1	
Large fish density (> 30 cm TL/10,000 m^3)	HOR study area	Mobile hydroacoustic data (this study)	Natural logarithm + 1	

Notes: °C = degrees Celsius; CDEC = California Data Exchange Center; CIMIS = California Irrigation Management Information System; cm = centimeters; m^3 = cubic meters; m^3/s = cubic meters per second; MSD = San Joaquin River at Mossdale; NTU = nephelometric turbidity units; PAR = photosynthetically active radiation; SJL = San Joaquin River at Lathrop; USFWS = U.S. Fish and Wildlife Service
Source: Present study

Each tagged juvenile entering the HOR study area was assigned a fate according to Bowen et al. (2012) and Bowen and Bark (2012) (i.e., visual examination of juvenile tracks using Eonfusion software (Myriax Software, Hobart, Tasmania, Australia); see Appendix E, "Fish Fate Determination Guidelines"). Tracks that initially entered the HOR study area with well-directed downstream movement but subsequently displayed evidence of predation (e.g., looping movements through the study area without clear downstream movement) were assigned the fate of "predation." It was not possible to assign a fate to every fish that entered the HOR study area, because it was not always clear when fish may have been preyed upon or may have survived; only fish that were

successfully classified as preyed upon or survived were included in the analysis. Complex hydrodynamics within the HOR study area caused by the physical rock barrier during 2012 made fate assignment particularly challenging for data from this year, and hydrodynamic modeling (see Section 3.2, "Velocity Field") was used to aid these classifications. The qualitative procedure used to assign fates is being compared to quantitative mixture model analyses for data generated at Georgiana Slough in 2012 (DWR in review; Romine et al. 2014).

The predictor variables included in the predation-probability analyses generally were the same as those used for analyses of greater than 30-cm fish abundance from mobile hydroacoustics (Table 5-5) (see also "Statistical Methods" in Section 5.4.2, "Hydroacoustic Surveys"). Abiotic variables (discharge, water temperature, turbidity, and ambient light) were based on the closest 15-minute observation to the time that the juveniles were at their minimum distance from common reference points: the 2009 or 2010 non-physical barrier alignments. Two estimates of the density of large fish (> 30 cm TL), taken to be indicators of potential predatory fish abundance at the HOR study area, were included in the analysis based on side-looking and down-looking mobile surveys conducted in 2011 and 2012 (see Section 5.4.2, "Hydroacoustic Surveys"). Consistent with small-fish density estimates, the large-fish density estimates associated with each juvenile's fate were averaged over the 3-day period, ending the day a juvenile entered the HOR study area. A 3-day period was used to increase the number of juveniles that could be retained in the analysis by avoiding missing values for this predictor variable. In addition, juvenile length was included per the hypothesis that larger fish may have a greater probability of survival.

Three analyses of predation probability were conducted based on species, barrier/discharge conditions, and the availability of > 30-cm fish density data from mobile hydroacoustic surveys. The first analysis tested hypothesis H11 (see Table 1-2 in Section 1.2.3, "Predation on Juvenile Salmonids Including Barrier Effects") and was based on tagged juvenile Chinook salmon predation data from 2009, 2010, and 2012 (n = 1,169); it included all previously mentioned predictor variables except large fish density from mobile hydroacoustics, which was not undertaken in 2009 and 2010. Barrier status was included as a predictor variable with three levels: BAFF on, BAFF off, and physical rock barrier. Data from 2011 were not included in this analysis because it would have been difficult to ascertain whether any differences in predation probability resulted from the absence of the barrier or from the very high discharge; these variables were confounded. The second analysis tested hypothesis H12 and was based on Chinook salmon predation data from 2011 and 2012 (n = 876); it included all predictor variables except barrier status. The third analysis tested hypothesis H13 and was based on steelhead predation data from 2011 (n = 163); it included all predictor variables except barrier status. There were insufficient data (n = 5) from 2012 for inclusion in the steelhead predation probability analysis.

The probability-of-predation analyses were undertaken using a GLM within a model averaging/information theoretic framework (Burnham and Anderson 2002) based on the R software (Version 3.0.0; R Core Team 2013) package "glmulti" (Calcagno and de Mazancourt 2010). This modeling technique has been applied on a number of recent occasions for fish research in the San Francisco Bay–Delta and Central Valley (e.g., Beakes et al. 2012; Perry et al. 2012; Zeug and Cavallo 2013). In addition to the standard reference text (Burnham and Anderson 2002) for this modeling technique, a useful summary is provided by Mazerolle (2006).

The glmulti package was used to provide all possible first-order GLMs for probability of predation (response = 1) versus survival (response = 0), with the response modeled with a binomial distribution and logit link function. The relative level of support for each possible model was estimated in glmulti with Akaike's Information Criterion (AIC), corrected for small sample sizes (AIC_c) (Mazerolle 2006). The difference in AIC_c, Δ_i, between each model

and the best model (i.e., the model with the lowest AIC_c) was calculated, and Akaike weights (w_i) were calculated based on the Δ_i. Model averaging of the predictor variable coefficients was undertaken based on the Akaike weights for each model, and unconditional confidence intervals were calculated for each coefficient (Mazarolle 2006). The importance of each predictor variable was assessed by summing the w_i of all models in which the variable appeared; following Calcagno and de Mazancourt (2010), importance of 0.8 or greater was used to infer support for a variable's potential influence on predation probability, in addition to unconditional 95% confidence intervals for variable coefficients not overlapping zero (per Zeug and Cavallo 2013).

GLMs including predictors were assessed to provide a better fit to the data than intercept-only models if the AIC_c of the full model (with all predictors included) was three or more units greater than the AIC_c of the intercept-only model (Zeug and Cavallo 2013). Model fit to observed data was assessed using similar methods to those of Beakes et al. (2012) and Perry et al. (2012). Model-fit assessment was conducted with the PresenceAbsence package of the R software (Freeman and Moisen 2008). As described by Beakes et al. (2012), an optimized threshold based on Kappa was calculated for each GLM. The threshold value was set where Kappa was maximized for each GLM, and this threshold value was used to estimate Kappa and several additional threshold-dependent model performance statistics: Cohen's Kappa statistic, percent correctly classified (PCC), sensitivity, and specificity. Each statistic is a measure of the capacity to accurately discriminate the correct outcome of predation of tagged juvenile salmonids observed in the data, where probabilities that exceed the threshold were classified as predation (positive) and probabilities below the threshold were classified as survival (negative). Beakes et al. (2012) described these statistics as follows:

> The Kappa statistic is a measure of all possible outcomes of presence or absence that are predicted correctly, after accounting for chance predictions; it is generally accepted as a conservative and standardized metric for comparing the predictive accuracy of binary models regardless of their statistical algorithm (Manel et al. 2001). PCC compares the proportion of outcomes correctly classified. In this application, sensitivity represents the proportion of true positives correctly identified, and specificity is the proportion of true negatives correctly identified, where 1-specificity is the proportion of false positives.

In addition to the threshold-dependent model performance statistics, a threshold-independent measure of model performance was also used: the area under the receiver operating characteristic (ROC). This measure indicates the probability of detecting a true signal (sensitivity) versus a false signal (1–specificity) (Hosmer and Lemeshow 2000). The area under the ROC is interpreted based on the following general rule (Hosmer and Lemeshow 2000: 162):

- If ROC = 0.5, this suggests no discrimination (i.e., the net result is the same).
- If 0.7 ≤ ROC less than 0.8, this is considered acceptable discrimination.
- If 0.8 ≤ ROC less than 0.9, this is considered excellent discrimination.
- If ROC ≥ 0.9, this is considered outstanding discrimination.

Similar to Perry et al. (2012), the fit of the GLM of juvenile Chinook salmon predation in 2009/2010/2012 was assessed by plotting the observed response in relation to model predictions. This involved plotting predation proportions in light (≥ 5.4 lux) and dark (< 5.4 lux) conditions across all three levels of the barrier status predictor (non-physical barrier on, non-physical barrier off, and physical rock barrier) versus the predicted predation probabilities, using the average continuous covariate values for each of these levels.

5.4 EVALUATION OF BEHAVIOR AND DENSITY CHANGES IN PREDATORY FISHES

5.4.1 PREDATORY FISH ACOUSTIC TAGGING

FIELD METHODS

Predatory fish (striped bass, largemouth bass, channel catfish, and white catfish) at the HOR study area were captured by hook-and-line fishing using bait and artificial lures, primarily in 2011 and 2012. Three additional fish were captured and tagged in 2009 and 2010; two fish (both striped bass) tagged outside the study area that moved into the HOR study area were also included in the analysis. Barbed circle hooks were used during bait fishing to minimize hooking injuries. Captured predatory fish having hooking or other injuries and/or displaying obvious abnormal behavior were released immediately and not included in the study. Predatory fish capture occurred primarily from fishing boats, but also from shoreline locations such as the sandy point on the right bank of the San Joaquin River across from the divergence with Old River. Hooks were removed carefully immediately after capture, and fish were placed in aerated live wells (1,500 gallons per hour pumping capacity) filled with water of temperature nearly identical to river temperature. To increase tagging efficiency, tagging generally was undertaken after several fish had been captured (holding duration generally was no more than 1 to 2 hours, and sometimes less than 1 hour). Tagging took place either on board the fishing boat or on the sandy point mentioned previously.

Predatory fish retained for tagging were identified to species and had length (FL in 2011, TL in 2012) and weight (2012) recorded. Tagged predatory fish generally were 30 cm or longer to allow a focus on the individuals most likely to prey on primarily juvenile Chinook salmon. Predatory fish typically consume prey that is 20% to 30% of their length (Uphoff 2003), and thus, would have greater potential to consume juvenile Chinook salmon of approximately 80 to 100 mm when 30 cm or larger. It is acknowledged that predatory fish occur at smaller sizes than 30 cm. Fish were fitted with HTI 795*LX* or 795*LG* tags (see Table 5-2) that were attached externally in the same manner described by Vogel (2011). External tag attachment consisted of two plastic-coated stainless steel wires attached to the transmitter, inserted through the musculature under the dorsal fin using hypodermic needles, and held in place with two plastic plates crimped on the opposite side of the fish.

Each tag had a unique four-digit identifier that was used to cross-reference detections with the identity and characteristics of tagged fish as recorded in field datasheets. The life span of the tags used in this study is several hundred days, depending on pulse width and pulse rate interval.

Fish generally were released where they were tagged. In 2011, fish releases typically occurred near capture locations. In 2012, fish were released near capture locations (which included the San Joaquin River upstream of the HOR study area and Old River downstream of the HOR study area, to allow an examination of how predatory fish behaved in relation to each of the barriers), from the sandy point referenced previously, or from other locations chosen to ensure that the fish remained within the range of the acoustic array. Fish tagging lasted from May 6 through June 15 in 2011 and from April 22 through May 24 in 2012.

DATA ANALYSIS

A total of 102 predatory fish were captured and tagged (including two individuals captured and tagged elsewhere in the south Delta), but only 84 were detected within the acoustic array at the HOR study area and were included in this analysis. The acoustic tags used for predatory fish in this study emitted double pulses every few seconds. Only the first of the double pulses was used in the present analysis.

Residence Time

Residence time at the HOR study area is an important factor because it has implications for the feasibility of predatory fish control (Gingras and McGee 1997). The length of time that each tagged predatory fish spent at the HOR study area was estimated based on detections by the HTI array and summarized as the number of days detected. Examination of the data indicated that several fish were not detected continuously for long periods, but were frequently detected over many days, suggesting that they occupied areas on the periphery of the array's detection ability. In addition, the potential length of time that each tagged fish could spend at the HOR study area depended on when each fish was tagged relative to the deactivation and removal of the acoustic array at the end of the study period. Deactivation/removal dates were May 20, 2009, May 25, 2010, June 22, 2011, and May 31, 2012.

To account for these factors, the percentage of possible dates that a tagged predator spent at the HOR study area between tagging/release and array deactivation/removal was calculated. For example, largemouth bass tag code 3324 was captured, tagged, and released on May 24, 2011, and subsequently detected from June 9 through 11, June 13, June 15 through June 18, and June 20 through June 22, 2011, for a total of 11 dates detected out of 29 dates between the day of tagging and the day of array deactivation/removal (i.e., 38%). Data calculated in this manner for all individual fish were then summarized for several groups defined by species, year, and—for 2012 data only—location of release (referred to as "San Joaquin River" for fish released upstream of the physical rock barrier and "Old River" for fish released downstream of the rock barrier).

Few fish (one largemouth bass and four striped bass, including two individuals captured outside the HOR study area) were tagged in 2009 and 2010. The striped bass were grouped together for analysis because BAFF was installed in both years. A resampling method ("bootstrapping") (Brown et al. 2012) was used to produce statistical summaries of the data to account for the small sample sizes (i.e., relatively few [generally less than 10] fish in each species/year/release location group). For each species/year/release location group, the percentage-of-dates-detected data for fish within the group were resampled with replacement until each resample contained the same number of observations (fish) as the original sample. This procedure was repeated 10,000 times, and the arithmetic mean was calculated for each of the 10,000 resamples. The 10,000 resamples were then used to generate statistical summaries for the percentage of dates detected within each species/year/release location group. The quantities estimated included the mean (50th percentile of the 10,000 resamples), interquartile range (25th and 75th percentiles of the 10,000 resamples), and 95% confidence interval (2.5th and 97.5th percentiles of the 10,000 resamples).

Spatial Analysis

A GIS map of the HOR study area was divided into zones to facilitate spatial analysis (Figure 5-14). A total of 83 zones were delineated on the basis of bathymetric features such as the scour hole, proximity to shoreline, and the locations of the 2012 rock barrier and the 2009/2010 BAFF alignments. Three major groupings of zones encompassed the San Joaquin River upstream of the divergence with Old River (zones 1–33), San Joaquin River downstream of the divergence with the Old River (zones 34–59), and the HOR (zones 60–83). Within each of these major zonal groupings, nearshore ("buffer") zones were within 5 m of shore, and offshore zones were greater than 5 m from shore. The scour hole in the San Joaquin River downstream of the Old River divergence was divided longitudinally (upstream/downstream) approximately in two, and several depth zones were defined on the basis of four major elevation ranges from 2012 bathymetric data:

- -12 to -17 feet [-3.66 to -5.18 m] NAVD of 1988 (zones 44, 45, 52, and 59)
- -17 to -27 feet [-5.18 to -8.23 m] (zones 46, 47, 53, 58)
- -27 to -32 feet [-8.23 to -9.75 m] (zones 48, 49, 54, and 57)
- deeper than -32 feet [-9.75 m] (zones 50, 51, 55, 56)

The 2012 rock barrier was represented by several zones encompassing the base of the barrier (zones 70–73) and the culverts (zones 67 and 75), in addition to near-field areas within 5 m of the barrier and its culverts (zones 65, 66, 68, and 69 upstream; zones 74, 76, 77, and 78 downstream). The extent of the barrier base that was accessible by fish in 2012 was variable based on water level; the trapezoidal shape of the barrier (relatively narrow top tapering to a wider base) is evident in the aerial image underlying Figure 5-14 (the top of the barrier is the white area in zones 70–73). The immediate (within 5 m) vicinity of the BAFFs was delineated for the 2009 (zones 27–33) and 2010 (zones 20–26) alignments.

Geo-referenced datasets (easting and northings, UTM Zone 10 N) of confirmed positive detections (i.e., "positive echoes") were output for each tagged predatory fish. To facilitate manipulation of the very large datasets generated during the study for spatial analysis, eastings and northings were rounded to the nearest meter for each detection. A grid of 1-m by 1-m points was generated that included the area of the HOR study area spatial zones (Figure 5-14), so that each grid point was assigned to a single spatial zone. Each predatory fish detection was merged with the database of grid points and spatial zones. The number and percentage of detections occurring within each spatial zone was calculated for each predatory fish. Similar to the analysis of residence time (described previously), the percentage of detections was summarized statistically for each species/year/release location group using 10,000 resamples of grouped spatial zones. Only predatory fish with at least 1,000 detections were included in the analysis to exclude information on fish that rapidly left the study area. The threshold of 1,000 detections was chosen on the basis of this value generally representing at least several hours of continuous detections, as opposed to rapid exit from the study area. In addition, only species, year, and release location groups with at least three tagged fish were included in the analysis.[1] A total of 14 spatial zone groupings were used for the analysis:

- San Joaquin River upstream of the Old River divergence, offshore (zones 2–4, 6–8, 12–18)
- San Joaquin River upstream of the Old River divergence, nearshore (zones 1, 5, 9–11, 19)

[1] Two striped bass (tag codes 2024 and 2472) that were tagged and released in 2010 met the criterion of 1,000 detections, but no other striped bass met this criterion in 2010. The results of these fish are discussed separately because their association with the 2010 BAFF is of management interest. For the same reason, the results for largemouth bass tag code 4306 are discussed in relation to the 2009 BAFF.

- Less than 5 m from the 2010 non-physical barrier (zones 20–26)
- Less than 5 m from the 2009 non-physical barrier (zones 27–33)
- San Joaquin River downstream of the Old River divergence, offshore (zones 35–37, 39, 41–42)
- San Joaquin River downstream of the Old River divergence, nearshore (zones 34, 38, 40, 43)
- Scour hole (zones 44–59)
- Head of Old River upstream of the 2012 rock barrier, offshore (zones 61–63)
- Head of Old River upstream of the 2012 rock barrier, nearshore (zones 60, 64)
- Near-field (less than 5 m) upstream of the 2012 rock barrier (zones 65–69)
- 2012 rock barrier (zones 70–73)
- Near-field (less than 5 m) downstream of the 2012 rock barrier (zones 74–78)
- Head of Old River downstream of the 2012 rock barrier, offshore (zones 80–82)
- Head of Old River downstream of the 2012 rock barrier, nearshore (zones 79, 83)

The spatial zones differ in size, and therefore, also differ in the number of 1-m by 1-m grid points that they possessed. To provide an indication of the extent of use of each zone relative to its size, a simple index was calculated for each group of spatial zones: percentage of detections within the grouped zone divided by percentage of grid points within the grouped zone. Values greater than 1 for this index indicated that the zone was used more frequently than would be expected based on its relative size. Predatory fish tagged in 2012 were released into either Old River downstream of the 2012 rock barrier or the San Joaquin River upstream of the 2012 rock barrier; therefore, the number of grid points used as the denominator in the calculation was adjusted to exclude the zones to which the fish would not have had access. This included the apparently unwetted portions of the 2012 rock barrier (i.e., zones 70–73 in Figure 5-14) that formed the bottom of the barrier. This adjustment removed approximately 79% of the area of zones 70–73 from consideration for fish released into the Old River downstream of the rock barrier in 2012, and approximately 71% of the area of zones 70–73 for fish released upstream of the rock barrier in 2012. In addition, the 2011 acoustic array was not able to detect fish beyond the zones downstream of the 2012 rock barrier bottom, so these zones were excluded from the calculations for fish released in 2011.

Near-surface water velocity within the areas occupied by tagged predatory fish in 2012 was estimated using velocity fields estimated from data collected with the SL-ADCP (see Section 3.2, “Velocity Field”). Tag detection data for each tagged predatory fish released upstream of the 2012 rock barrier that had more than 1,000 detections was merged with the 15-minute estimated velocity data. This was done by assigning each tag detection to the nearest 5-m by 5-m velocity grid point for the same 15-minute period in which the tag detection had occurred. Only tag detections within the grid of velocity estimates were included. The velocities at which each tagged fish had occurred were compared to all of the velocities that had occurred within the HOR study area at the time the fish had been detected. This was accomplished by comparing medians and by examining graphically the percentage of observations in velocity increments rounded to the nearest 0.05 m/s. Only velocity magnitude was considered (i.e., direction was not included in the analysis). Similar to the index of spatial use described above, an index of velocity occupied in relation to available velocity was calculated for each individual of each species; values greater than 1 suggested that fish occupied a particular velocity in greater proportion than its availability. As with the residence time and spatial analyses, statistical summaries of the data for each species were generated from 10,000 resamples of the velocity index results. Higher velocities that occurred only for some individuals within a given species were excluded from the analysis.

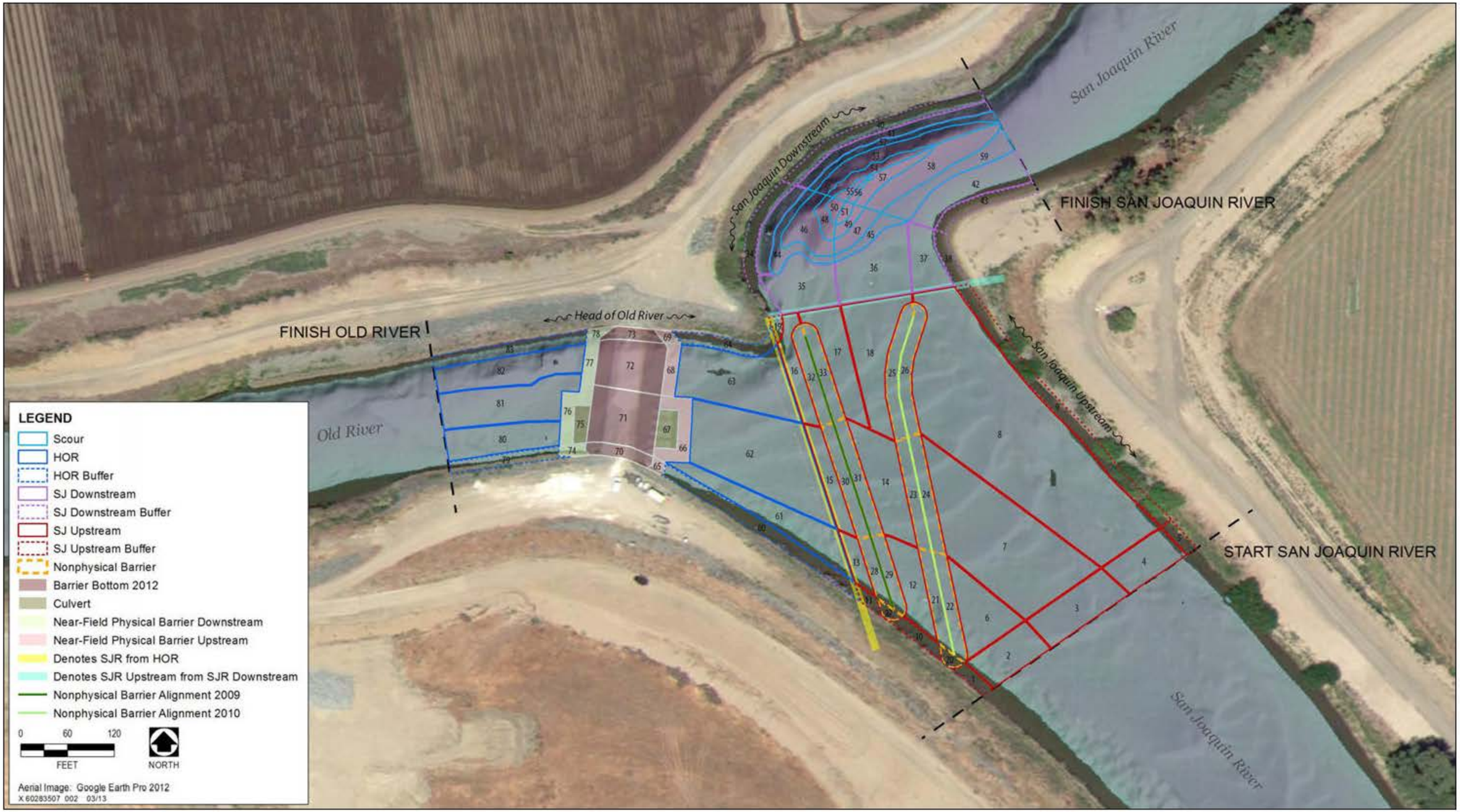

Sources: DWR 2012; Bianchini and Cane pers. comms., 2013; Present study; Data compiled by Turnpenny Horsfield Associates and AECOM in 2013

Figure 5-14

Spatial Zones Used in the Analysis of Predatory Fish and Predation at the Head of Old River

Emigration from the area of the HOR study area was determined for fish that left the study area before the deactivation of the acoustic array. Each fish was classified as having emigrated upstream (in the San Joaquin River) or downstream (into Old River or San Joaquin River) based on the final zone of detection. In addition to fish evaluated from 2009 through 2011, only the fish tagged and released to the upstream side of the 2012 rock barrier were included in this analysis.

Stationary Tag Locations

Information on spatial distribution of predatory fish at the HOR study area was provided by acoustic tagging (as described previously) and hydroacoustic surveys (as described under "Data Analysis" in Section 5.4.2, "Hydroacoustic Surveys"). Additional information on predator locations was obtained by examining the locations of stationary tags from juvenile salmonids. Stationary tags may represent juveniles that were preyed upon and subsequently defecated by predatory fish (or other predators) (Vogel 2011). Areas of high predation—or at least areas of high tag defecation—have been inferred from relatively high numbers of stationary tags, and include locations such as the trash racks leading to the Tracy Fish Facilities, Grant Line Canal, San Joaquin River near Stockton, and in some years, the HOR (SJRGA 2013).

The locations of stationary salmonid tags at the HOR study area from 2009 through 2012 were plotted with GIS and enumerated by spatial zone, separating tags by salmonid species (Chinook salmon or steelhead) and year.

5.4.2 HYDROACOUSTIC SURVEYS

SURVEY METHODS

Mobile hydroacoustic surveys were conducted at the HOR study area to provide information on fish distribution and fluxes in fish density; surveys also were conducted at three reference sites. Mobile survey methods were similar to those used by Miranda et al. (2010) during the fish salvage facilities' Release Site Predation Study. Much of their description of the methods they used is provided herein. The acoustics unit employed for the mobile hydroacoustics survey was a BioSonics DT6000 split-beam system (BioSonics, Seattle, Washington). The unit employed two 201-kHz transducers, with one transducer mounted to point vertically down into the water column and the other mounted to point laterally off to the port side of the survey vessel (Figure 5-15). The acoustics unit used a -70-decibel (dB) threshold. A Wide Area Augmentation System-enabled E-Trex Vista (Garmin International, Olathe, Kansas) GPS unit was connected to the surface unit, and a location was recorded for each target detected.

Mobile hydroacoustic surveys consisted of driving the boat through the area of the HOR study area at a speed of approximately 7.2 km per hour (4.5 miles per hour). Surveys at the HOR study area typically lasted 30 to 40 minutes, and each individual survey covering all four sites generally lasted approximately 2 hours (Table 5-6). Nearly all surveys included sampling at all four sites. In 2011, sampling that yielded usable data was undertaken at the HOR study area during all 23 surveys (compared to 21 surveys for site 1 and 22 surveys for sites 2 and 4). In 2012, sampling that yielded usable data was undertaken on 26 of 29 surveys at the HOR study area (compared to 29 surveys for site 2, 27 surveys for site 1, and 28 surveys for site 4). Example survey paths from March and May 2012 are illustrated in Figure 5-16, with the physical rock barrier out and in, respectively.

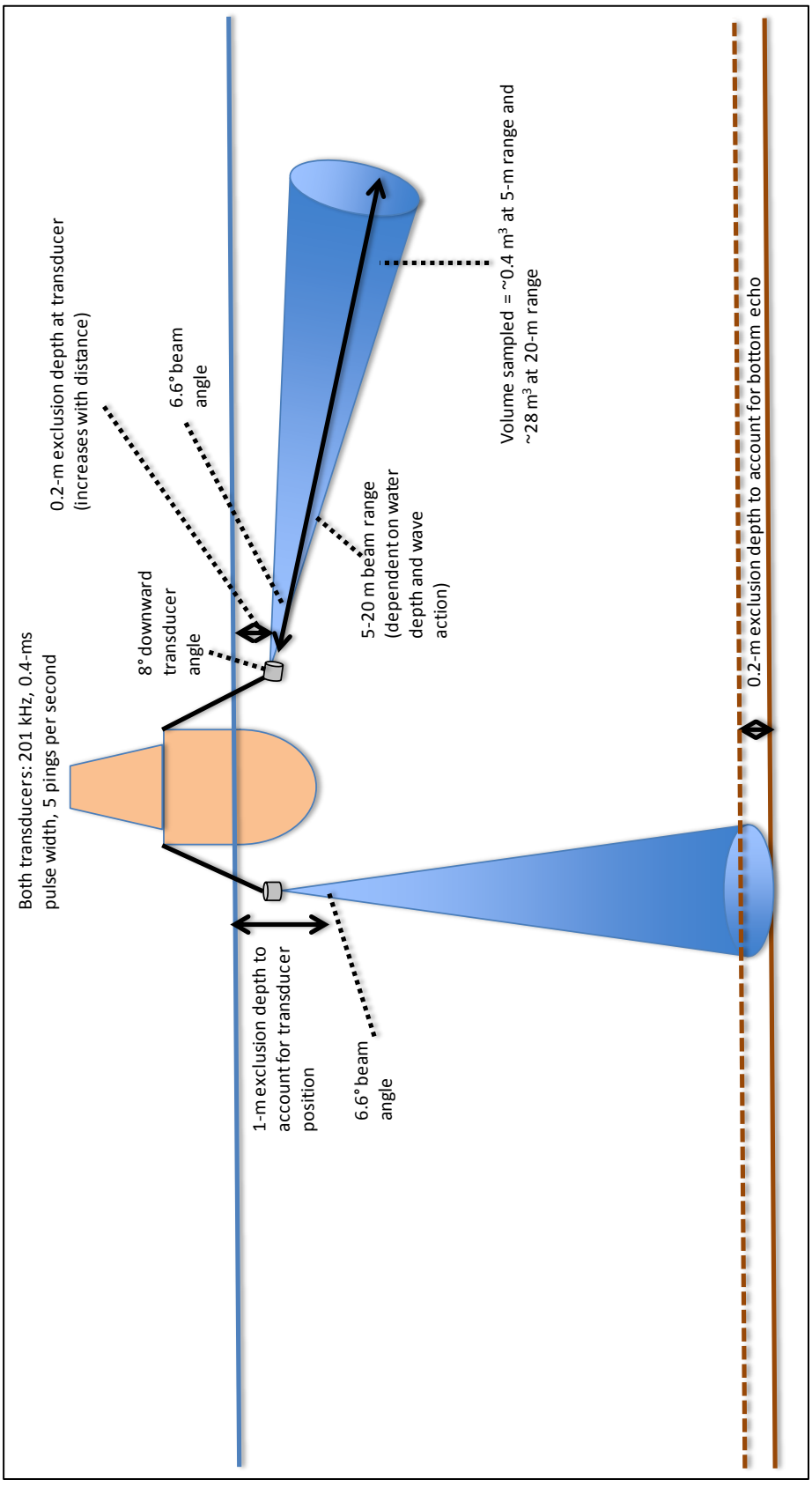

Source: Present study.

Figure 5-15 **Schematic Diagram of Mobile Hydroacoustic Survey Equipment**

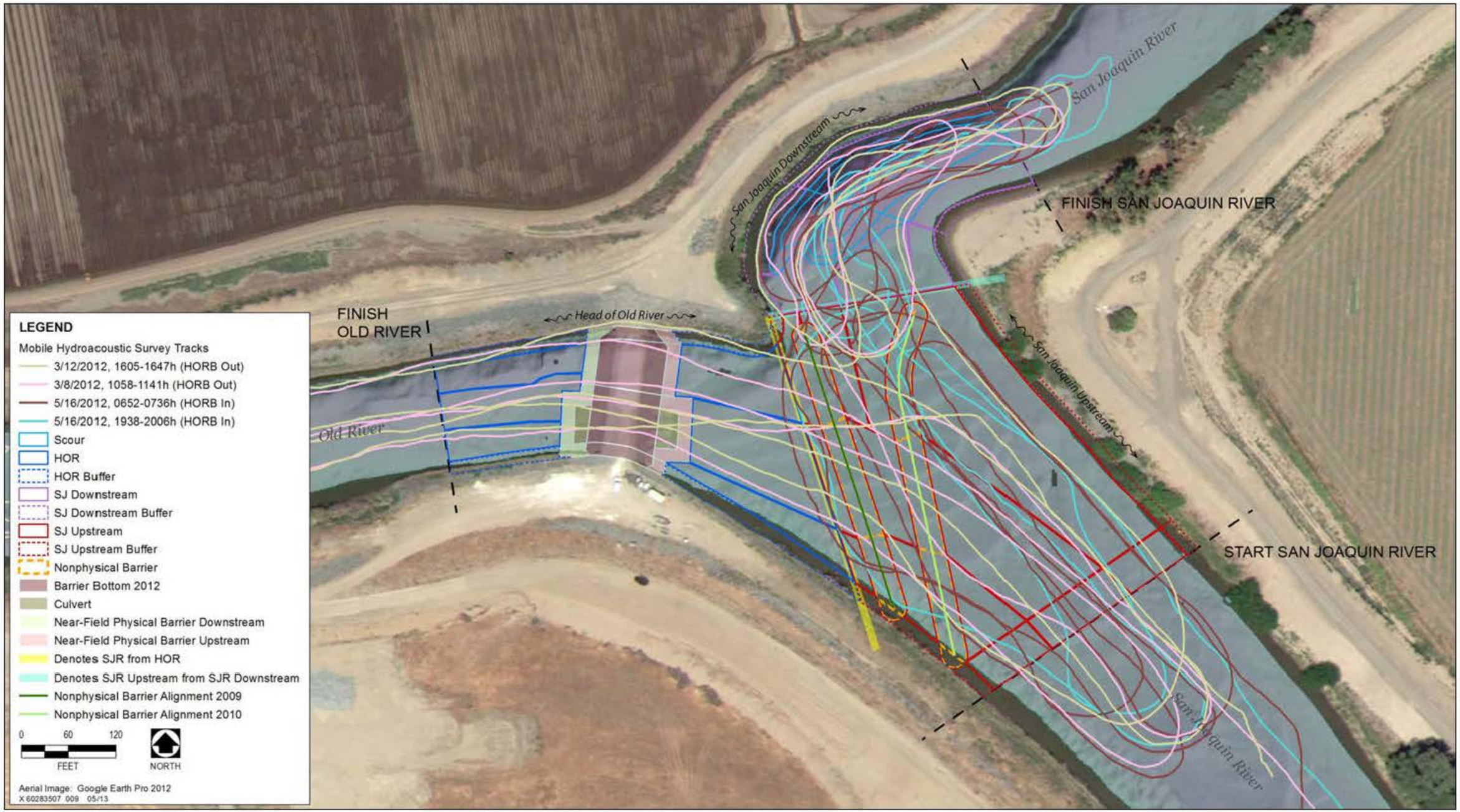

Sources: DWR 2012; ICF International 2013; AECOM 2013

Figure 5-16

Examples of Mobile Hydroacoustic Survey Tracks with Head of Old River Barrier In and Out

Table 5-6
Start and End Times of Mobile Hydroacoustics Surveys, 2011 and 2012

Survey Number	2011		2012	
	Start	End	Start	End
1	5/16/11, 16:30	5/16/11, 19:02	3/8/12, 9:14	3/8/12, 12:19
2	5/16/11, 20:03	5/16/11, 22:36	3/12/12, 13:40	3/12/12, 16:14
3	5/16/11, 23:25	5/17/11, 1:00	3/14/12, 13:56	3/14/12, 16:25
4	5/18/11, 7:46	5/18/11, 10:47	3/15/12, 6:44	3/15/12, 9:33
5	5/18/11, 11:52	5/18/11, 14:42	5/2/12, 6:48	5/2/12, 9:04
6	5/18/11, 17:36	5/18/11, 20:25	5/2/12, 9:18	5/2/12, 11:29
7	5/18/11, 21:16	5/18/11, 23:55	5/3/12, 8:55	5/3/12, 11:18
8	5/23/11, 7:56	5/23/11, 10:50	5/3/12, 12:17	5/3/12, 14:10
9	5/23/11, 11:49	5/23/11, 14:40	5/15/12, 6:43	5/15/12, 8:57
10	5/23/11, 18:34	5/23/11, 21:13	5/15/12, 10:22	5/15/12, 12:29
11	5/23/11, 21:57	5/24/11, 0:30	5/15/12, 16:50	5/15/12, 18:56
12	5/25/11, 7:49	5/25/11, 10:20	5/16/12, 4:41	5/16/12, 7:01
13	5/25/11, 11:09	5/25/11, 13:49	5/16/12, 9:55	5/16/12, 11:50
14	5/25/11, 18:30	5/25/11, 21:07	5/16/12, 17:35	5/16/12, 19:28
15	5/25/11, 21:56	5/26/11, 0:37	5/17/12, 4:42	5/17/12, 6:37
16	6/6/11, 14:26	6/6/11, 17:43	5/17/12, 10:28	5/17/12, 11:11
17	6/6/11, 18:28	6/6/11, 21:17	5/22/12, 4:55	5/22/12, 7:03
18	6/6/11, 21:53	6/7/11, 0:37	5/22/12, 8:36	5/22/12, 11:03
19	6/7/11, 9:02	6/7/11, 12:01	5/23/12, 4:28	5/23/12, 6:24
20	6/8/11, 9:19	6/8/11, 12:05	5/23/12, 6:41	5/23/12, 8:07
21	6/8/11, 12:23	6/8/11, 15:11	5/23/12, 17:42	5/23/12, 19:19
22	6/8/11, 18:59	6/8/11, 21:14	5/24/12, 4:42	5/24/12, 6:34
23	6/8/11, 21:35	6/9/11, 0:13	5/24/12, 6:49	5/24/12, 8:50
24			5/24/12, 11:28	5/24/12, 13:11
25			5/29/12, 15:34	5/29/12, 17:11
26			5/30/12, 4:18	5/30/12, 6:03
27			5/30/12, 13:30	5/30/12, 15:39
28			5/31/12, 4:41	5/31/12, 5:56
29			5/31/12, 6:50	5/31/12, 8:28

Source: Present study

Mobile hydroacoustic surveys also were conducted at three reference sites to provide comparisons to fish density at the HOR study area. The reference sites were on river bends and possessed deep holes somewhat similar to the HOR study area (Figure 5-17). A summary of water depths encountered by down-looking mobile hydroacoustic surveys in 2012 is provided in Table 5-7.

Table 5-7
Summary of Water Depths during Mobile Hydroacoustic Surveys in 2012

Statistic	Site 1		Site 2		HOR		Site 4	
	Meters	Feet	Meters	Feet	Meters	Feet	Meters	Feet
Minimum	0.7	2.4	0.9	2.8	0.9	3.0	0.8	2.7
5th Percentile	1.6	5.3	2.5	8.1	1.5	5.0	1.6	5.3
25th Percentile	2.5	8.1	4.1	13.3	2.3	7.4	2.3	7.5
Median	3.4	11.1	5.5	17.9	2.8	9.3	3.3	10.8
75th Percentile	5.6	18.5	6.7	21.9	4.3	14.0	4.5	14.9
95th Percentile	8.3	27.3	8.2	27.0	9.1	29.9	7.4	24.3
Maximum	10.0	32.7	10.5	34.5	11.6	38.2	8.2	26.8

Note: HOR = Head of Old River
Source: Present study

DATA ANALYSIS

Echo Counting/Processing

Echo counting methods following those described by Miranda et al. (2010) were used to measure acoustic target strength (fish size). The account herein was adapted from that of Miranda et al. (2010), and a useful introduction to fisheries acoustics is provided by Rudstam et al. (2012). Target strengths were measured using split-beam techniques for all sample locations. The target strength of a fish generally is related to the size of the fish, and is a measure of the capacity of a fish to reflect sound energy. Target strength, measured in units of decibels, is calculated from the energy reflected from the target, and is a function of the cross-sectional area of the target and the density difference between water and the component parts of the target (e.g., bones, scales, flesh, gas bladder).

Fish orientation, and to an extent species, can play a significant role in estimation of target size. The dB scale used to measure fish size is logarithmic and referenced in negative numbers (i.e., where the larger the negative number, the smaller the fish). Fish size was estimated from echo target strength using the following equation (Horn, pers. comm., 2013):

$$\text{Fish TL (cm)} = 1{,}529 * e^{(-0.1142 * |\text{Target Strength (dB)}|)}$$

Thus, for example, an echo intensity of -30 dB is estimated to be a fish of nearly 50 cm, whereas an echo intensity of -40 dB is estimated to be a fish just less than 16 cm. These sizes assume a transducer is looking down on a perfectly oriented fish from above. This is typically the case when looking down on a fish. When looking from the side, however, fish may not be perfectly oriented parallel to the transducer. When this occurs, a fish target will appear smaller than it actually is due to the reduced cross-sectional area of the target. Little can be done to rectify this problem.

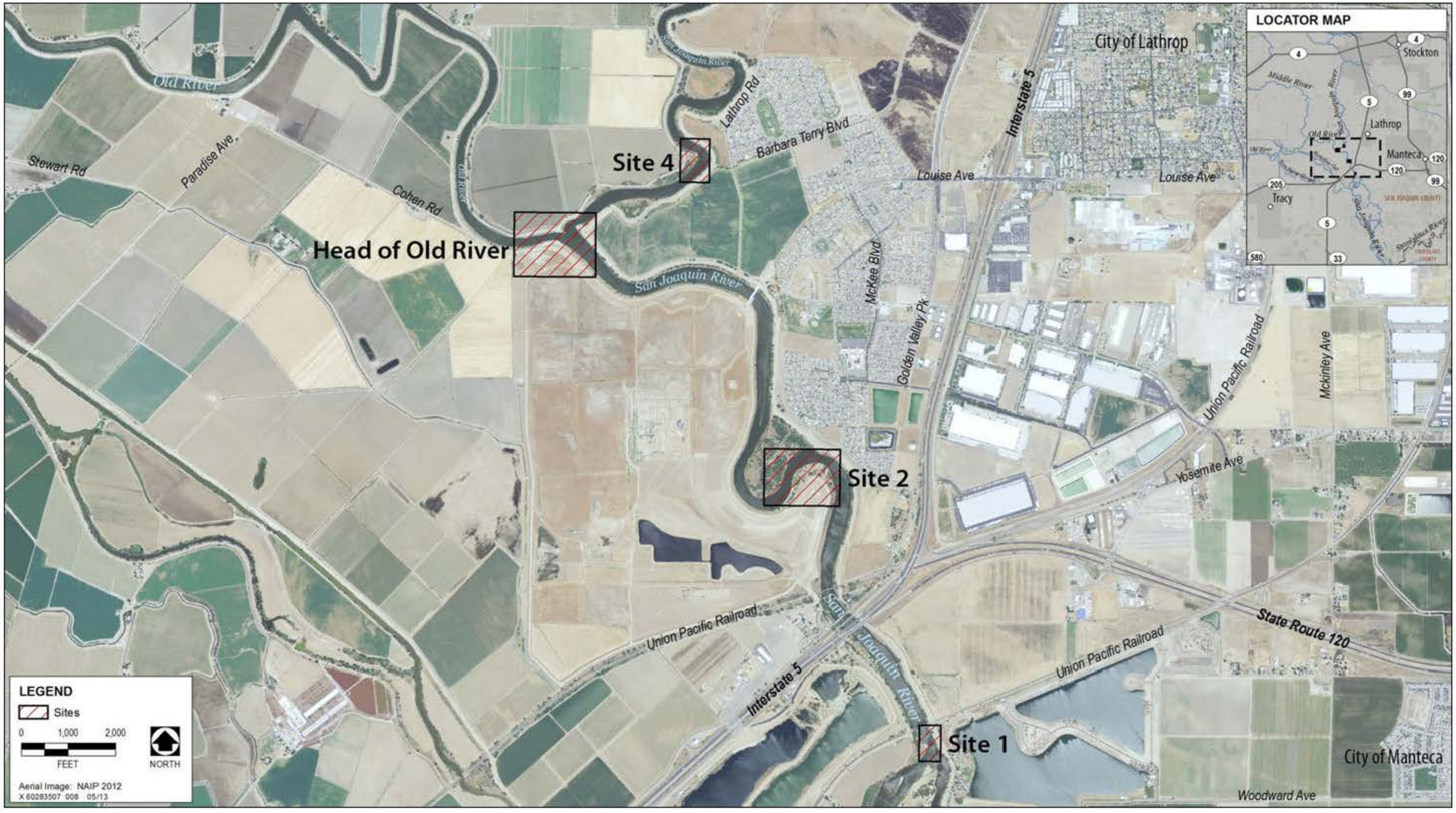

Source: Present study

Figure 5-17

Locations of Head of Old River and Reference Mobile Hydroacoustic Survey Sites

The SonarData software package, Echoview v4.x (Myriax Software, Hobart, Tasmania, Australia) was used to analyze all data. The echogram was reviewed to locate individual fish targets, which were acquired and logged to data files. An amplitude threshold was used to reject echoes smaller than a predetermined voltage, and areas of high acoustic noise were manually removed from the raw echogram data prior to analysis by defining a line or region below which any data are ignored during the analysis phase (see Figure 38 in Miranda et al. 2010:87). Analyses of acoustic data consisted of a series of post-processing steps that are described in Appendix J of Miranda et al. (2010): observation, calibration and thresholding, regions for exclusion (noise), echo extraction, and output formatting/quality assurance. Considerable debris and acoustic noise within the system, as well as the study's emphasis on larger, potential predatory fish, led to the use of a target strength threshold of approximately 15 cm TL (i.e., approximately -40 dB), with fish less than this size being excluded from the data outputs.

The number of targets (assumed to be fish) detected, mean target strength, and beam volume sum were output into a number of "bins" of information from each survey at each site. Data from 2011 were output into bins of 200 pings, whereas data from 2012 were output into bins of 100 pings. Potential predator-sized targets were assessed to be those estimated to be greater than 30 cm TL for consistency with sizes of predatory fish studied with acoustic tagging (see "Field Methods" in Section 5.4.1, "Predatory Fish Acoustic Tagging"). Analyses focused on the targets that measured greater than 30 cm TL, with other fish being binned into a 15- to 30-cm TL size class. In addition to binned outputs, data on each individual target were output, and included target strength (fish size), location (latitude/longitude), target water depth, and total water column depth (for down-looking hydroacoustic data).

Statistical Methods

Areas Occupied

Data derived from mobile hydroacoustic surveys in 2011 and 2012 were used to address several of the study objectives. GIS plots of individual targets (estimated to be greater than 30 cm TL) were made to illustrate fish distribution within the study area, particularly with respect to habitat features such as the scour hole. The number of targets from down- and side-looking transducers were summed for each spatial zone.

Density Changes

Changes of greater than 30 cm TL fish density (abundance per unit volume) at the HOR study area in 2011 and 2012 were examined in relation to several environmental variables that could influence density and that were included in the analysis of probability of predation of juvenile salmonids: water temperature, discharge, turbidity, light level, and small fish density. Features of the environmental data are summarized in Table 5-8. Abiotic habitat variables such as water temperature have been shown to correlate with movements and behavior of predatory fish such as striped bass (e.g., upstream movement in spring for spawning purposes; Moyle 2002). Biotic variables such as prey fish density have also been hypothesized to influence striped bass distribution (e.g., predators moving to areas where prey are relatively abundant; LeDoux-Bloom 2012). For some predatory fish species such as largemouth bass, habitat suitability may be inversely related to river discharge and channel velocity (Stuber et al. 1982).

Table 5-8
Summary of Predictor Variables Used in GLM of Abundance of Fish Greater than 30 cm TL at the Head of Old River Study Area

Variable (Unit)	Location	Source	Transformation	Notes
Water Temperature (°C)	SJL	CDEC (Baldwin, pers. comm., 2013)	None	15-minute average data
River Discharge (m^3/s)	SJL	CDEC (Baldwin, pers. comm., 2013)	None	15-minute average data
Turbidity (NTU)	MSD	CDEC (Dempsey, pers. comm., 2013)	None	15-minute average data
Ambient light (lux)	Manteca (CIMIS site #70)	CIMIS (State of California 2009)	Natural logarithm + 1	Original CIMIS data (Langley/day) were first converted into PAR per Clark et al. (2009: PAR, $\mu mol/m^2/s$ = 1.1076*Langley/day), and subsequently PAR was converted into lux per Apogee Instruments, Inc. (2013: Lux = 54*PAR). Original hourly data were linearly interpolated to 15-minute increments for consistency with water quality data.
Small-fish density (fish < 15 cm FL/10,000 m^3)	Mossdale (trawling)	USFWS survey data (Speegle, pers. comm., 2011 and 2013)	Natural logarithm + 1	

Notes: °C = degrees Celsius; CDEC = California Data Exchange Center; CIMIS = California Irrigation Management Information System; cm = centimeters; m^3 = cubic meters; m^3/s = cubic meters per second; MSD = San Joaquin River at Mossdale; NTU = nephelometric turbidity units; PAR = photosynthetically active radiation; SJL = San Joaquin River at Lathrop; USFWS = U.S. Fish and Wildlife Service
Source: Present study

In contrast to the analysis of predation probability, however, the analysis of changes in predatory fish density (as represented by density of echoes greater than 30 cm TL) in relation to environmental variables was more of an exploratory analysis that relied on a model-averaging approach to examine support for the influence of the different variables on predatory fish density. Accordingly, the analysis was conducted to test the null hypothesis $H14_0$ (see "Objectives and Hypotheses Related to Changes in Density of Predatory Fishes" in Section 1.2.4, "Behavior and Density Changes in Predatory Fishes").

The analysis of changes in density in relation to environmental variables was conducted with GLM within a model averaging/information theoretic framework similar to that used for modeling predation probability of juvenile salmonids (see Section 5.3.2, "Probability of Predation [Generalized Linear Modeling]"). The number of fish targets greater than 30 cm TL in each survey at the HOR study area was modeled in the GLM as a count response variable with a negative binomial error structure and logarithmic link function, incorporating the beam volume sum as an offset to account for differences in the volume of water ensonified with the acoustic equipment during each survey.

The glmulti package was used to provide all possible first-order GLMs for fish targets greater than 30 cm TL as a function of water temperature, discharge, turbidity, light, and small-fish density (i.e., a measure of potential prey for predatory fish). The relative level of support for each possible model was estimated in glmulti with the quasi-

likelihood equivalent of AIC corrected for small sample sizes ($QAIC_c$) (Mazerolle 2006). The variance inflation factor, $\hat{c}$, required to compute $QAIC_c$ was estimated by initially running a single GLM with all predictor variables included, and then providing $\hat{c}$ to the glmulti package for the automated model averaging procedure. The difference in $QAIC_c$, Δ_i, between each model and the best model (i.e., the model with the lowest $QAIC_c$) was calculated, and Akaike weights (w_i) were calculated based on the Δ_i. Model averaging of the predictor variable coefficients was undertaken based on the Akaike weights for each model, and unconditional confidence intervals were calculated for each coefficient (Mazarolle 2006). The importance of each predictor variable was assessed by summing the w_i of all models in which the variable appeared. Following Calcagno and de Mazancourt (2010), importance of 0.8 or greater was used to infer support for a variable's potential influence on greater than 30-cm fish density, in addition to unconditional 95% confidence intervals for variable coefficients not overlapping zero (per Zeug and Cavallo 2013). GLMs, including predictors, were assessed to provide a better fit to the data than intercept-only models if the $QAIC_c$ of the full models (with all predictors included) was 3 or more units greater than the $QAIC_c$ of the intercept-only models (Zeug and Cavallo 2013).

Four sets of GLM analyses were included, with two each for the down-looking and side-looking greater than 30-cm fish density data. "Same-day" GLM analyses used water quality and light variables that were averaged based on the time that the survey had occurred at the HOR study area (e.g., if a survey took place between 0500 and 0545 hours, the water quality data and light data were the average values for this time period).

The small-fish density data variable from Mossdale trawling was based on the mean daily densities from the day of the mobile hydroacoustic survey and the previous 2 days (see description of calculation of abundance index in Section 2.2.3, "River Channel Mossdale Trawl"), because trawling did not necessarily occur daily and it was desirable to retain all mobile hydroacoustic survey data points. (The 3-day-average small-fish density avoided censoring of mobile hydroacoustic data because of missing data.) It was felt that this was a reasonable approach to provide a general indication of small-fish (potential prey) density in the area at the time of the mobile hydroacoustic surveys, given that the Mossdale trawl site is upstream of the HOR study area, and there would be some delay in fish reaching the HOR study area, coupled with natural variability in these data.

The "7-day" GLM analyses used water-quality and small-fish-density data averaged over the time of the mobile hydroacoustic survey and the 6 days. These analyses were included to account for potential longer-term environmental influences on greater than 30-cm fish density at the HOR study area. Light data for the GLM analyses were identical to those for the "same-day" analyses because light level was hypothesized only to be a short-term potential influence on density.

Comparisons to Reference Sites

The HOR study area was compared to the three reference sites to assess whether changes in greater than 30-cm fish density were correlated and to assess the evidence for common environmental influences on fish density (e.g., migration). Density (number of targets per 10,000 cubic meters) of greater than 30-cm fish from each survey at the HOR study area were paired with corresponding densities from the same survey at each reference site. Density data were incremented by 1 to account for 0 values and natural-log-transformed to accommodate the assumptions of the parameter statistical tests. Pearson correlation analyses were used to test the null hypothesis $H15_0$ (see "Objectives and Hypotheses Related to Density of Predatory Fishes" in Section 1.2.4, "Behavior and Density Changes in Predatory Fishes") of no significant correlation between density at the HOR study area with density at each reference site. A Bonferroni-adjusted statistical significance of $P < 0.017$ was used to correct for

the three comparisons. The null hypothesis $H16_0$ of no significant difference in density between the HOR study area and the reference sites was tested using paired t-tests. Statistical analyses comparing the HOR study area to the reference sites were undertaken with SAS/STAT software, Version 9.3, of the SAS System for Windows.[2]

Diel Changes in Depth

Fish depth is of management interest because it influences capture methods that can be used for predatory fish. Fish are often found deeper in the water column by day (Hrabik et al. 2006; Miranda et al. 2010). In addition, large densities of common carp were visually observed in the vicinity of the physical rock barrier in 2012, suggesting that many large-fish targets detected with mobile hydroacoustics may not be predatory fish. Common carp are omnivorous bottom feeders (Moyle 2002) that would be expected to be associated with the bottom at all times of day. Depth of greater than 30-cm TL targets from down-looking mobile hydroacoustic surveys was examined in relation to total water column depth for evidence of changes in distribution with diel period. Following Hrabik et al. (2006), plots of individual target depth against distance from the bottom (based on water column depth) were made to assess differences between day, night, dawn, and dusk. Day was defined as greater than 1 hour after sunrise and before sunset, dawn was the 2-hour period centered around sunrise, dusk was the 2-hour period centered around sunset, and night was greater than 1 hour after sunset and before sunrise. Sunrise and sunset times were estimated for SJL using the National Oceanic and Atmospheric Administration's sunrise/sunset spreadsheet calculator (NOAA 2013).

[2] Copyright 2002–2010, SAS Institute (SAS). SAS and all other SAS Institute product or service names are registered trademarks or trademarks of SAS Institute Inc., Cary, North Carolina.

6 RESULTS

6.1 JUVENILE SALMONID ROUTING INCLUDING BARRIER EFFECTS

6.1.1 2009 RESULTS

SALMONID SIZE DISTRIBUTION

The juvenile Chinook salmon tagged and released in 2009 were smaller overall than those from any other year (Table 5-1). In addition, the tagged 2009 juvenile Chinook salmon were Feather River Fish Hatchery fall-spring–run hybrids; 2009 was the only year when this hatchery and these hybrids were used as a source of juvenile Chinook salmon.

OVERALL EFFICIENCY

Chinook Salmon

The data were evaluated to determine whether they satisfied the assumptions of ANOVA. In every case, except as noted in the following discussion, the data were not distributed normally and/or did not meet the assumption of homogeneity of variances. In general, the lack of normally distributed data stemmed from the common occurrence of 0.0 and 1.0 values in the samples. These categories tended to be among the most common values observed which resulted in many variables exhibiting a bimodal distribution.

The overall efficiency (O_E) was only 2.5 percentage points better with the BAFF on than off (Table 6-1). Only 20.9% of tags in juvenile Chinook salmon continued down the San Joaquin River with the BAFF on, compared with 18.4% with the BAFF off. These results suggested that the BAFF did not significantly change the proportion of fish remaining in the San Joaquin River in 2009 (i.e., hypothesis $H1_0$ was accepted).

Table 6-1
Statistics for Overall Efficiency during BAFF Operations in 2009

Statistic	BAFF On	BAFF Off	Percentage Point Change	Kruskal-Wallis X^2	P-value
Mean	0.209	0.184	2.5	0.030	0.8635
Standard Deviation	0.218	0.185			
Minimum	0.000	0.000			
Maximum	0.750	0.500			
Samples (n)	21	27			

Notes: BAFF = bio-acoustic fish fence; n = number of samples
Source: Data compiled by Turnpenny Horsfield Associates and AECOM

Effect of Ambient Light Level on Overall Efficiency

Tagged juvenile Chinook salmon approached the 2009 BAFF line at various light levels (Figure 6-1). When the 2009 fish were placed into samples, and the juvenile Chinook salmon O_E samples were partitioned by ambient light

level, eight to 17 samples were distributed throughout the experimental matrix (Table 6-2). For high-ambient-light conditions, it was noted that O_E with the BAFF on was 9.9 percentage points higher than with the BAFF off (Table 6-3). However, there was no significant improvement in O_E with the BAFF on compared to off at either ambient light level. In 2009, it appeared that there was insufficient statistical power to resolve any effect or ambient light did not influence the BAFF's O_E.

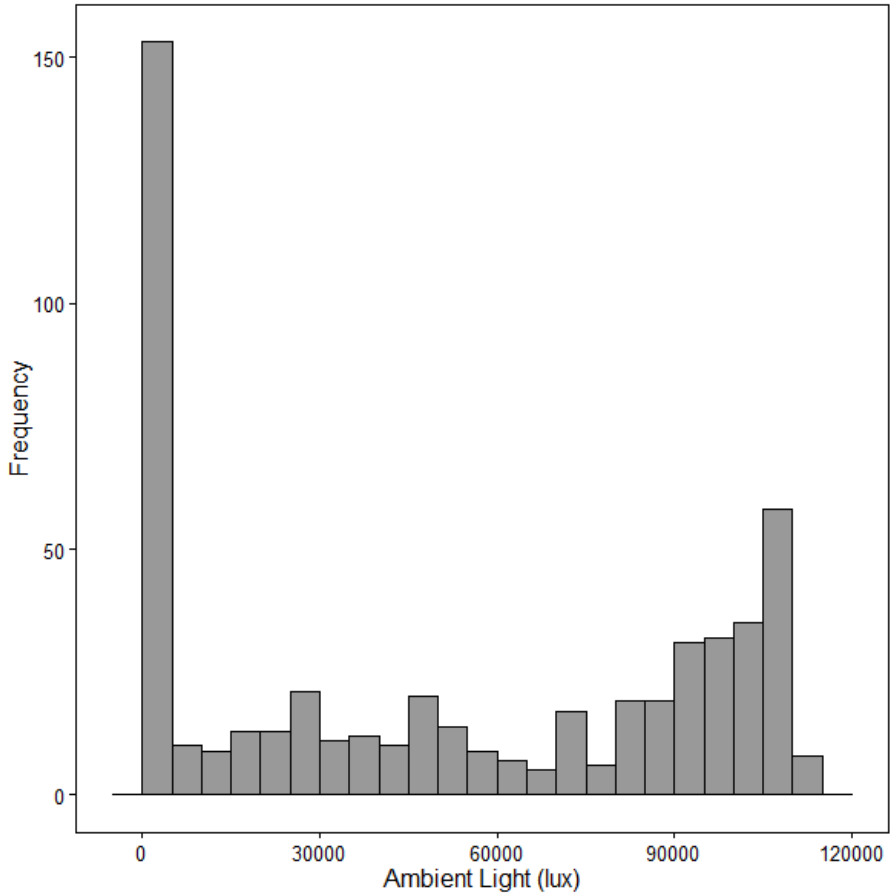

Source: Data compiled by AECOM and Turnpenny Horsfield Associates

Figure 6-1 Frequency Histogram of 2009 Light-Level Observations (collected at CIMIS, Station #70–Manteca, 37.834822, -121.223194) Obtained for Each Tagged Juvenile Chinook Salmon when the Individual was Nearest the 2009 BAFF Line

Table 6-2
Summary of Overall Efficiency Samples for Tagged Juvenile Chinook Salmon Encountering the BAFF during On/Off Operations at Low and High Ambient Light Levels in 2009

Ambient Light Level	BAFF On (n)	BAFF Off (n)
Low Light (<5.4 lux)	8	10
High Light (≥5.4 lux)	13	17
Total	21	27

Notes: BAFF = bio-acoustic fish fence; n = number of overall efficiency samples
Source: Data compiled by Turnpenny Horsfield Associates and AECOM

Table 6-3
Mean Overall Efficiency of the BAFF for Tagged Juvenile Chinook Salmon at Low and High Ambient Light Levels in 2009

Overall Efficiency—Ambient Light Level	BAFF On Mean	BAFF Off Mean	Percentage Point Change	Kruskal-Wallis X^2	P-value
Low Light (<5.4 lux)	0.068	0.159	-9.1	0.772	0.3797
High Light (≥5.4 lux)	0.297	0.198	9.9	1.131	0.2876

Notes: BAFF = bio-acoustic fish fence
Source: Data compiled by Turnpenny Horsfield Associates and AECOM

Effect of Average Channel Velocity on Overall Efficiency

Tagged juvenile Chinook salmon approached the 2009 BAFF line at various average channel velocities (ACV) (Figure 6-2). When the 2009 fish were placed into samples and the O_E samples for juvenile Chinook salmon were partitioned by ACV value (low = less than 0.61 m/s ACV; high = greater than or equal to 0.61 m/s ACV), no samples existed at high ACV values (Figure 6-2). This result was expected because in 2009 the water year had the lowest discharge range and mean among the years studied. The maximum ACV recorded during the tagged juvenile Chinook salmon release period was 0.48 m/s.

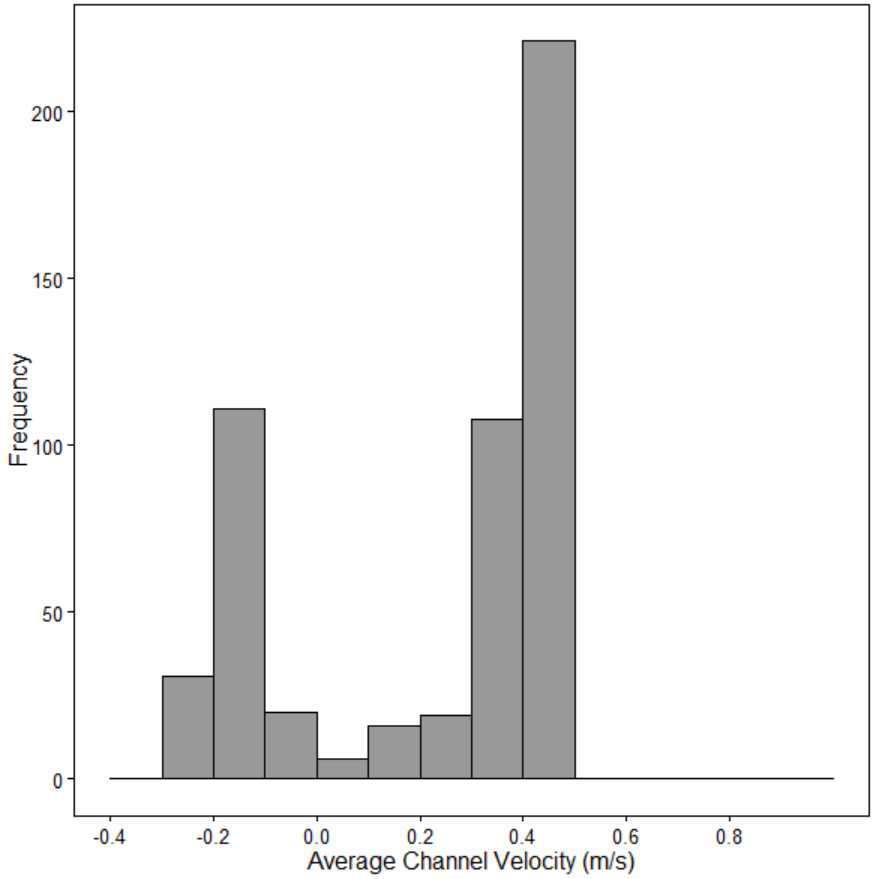

Source: Data compiled by AECOM and Turnpenny Horsfield Associates

Figure 6-2 **Frequency Histogram of 2009 Average Channel Velocity Observations (SJL Gauge) Obtained for Each Tagged Juvenile Chinook Salmon when the Individual was Nearest the 2009 BAFF Line**

PROTECTION EFFICIENCY

BAFF protection efficiency (P_E) (efficiency after the removal from the data set of juvenile Chinook salmon that were eaten) was 0.234 with the BAFF off. The proportion of flow into the San Joaquin River during the study period was 0.35 (Table 3-1). Thus, in the present study, without the BAFF in operation, the fraction of juvenile Chinook salmon was smaller than the fraction of water entering the San Joaquin River. In contrast, in Table I-1 in Appendix I, "Route Entrainment Analysis at Head of Old River, 2009 and 2010," the proportion of flow entering the San Joaquin River was correlated with the probability that an individual juvenile Chinook salmon would continue down the San Joaquin River route. The model that included flow at the San Joaquin River at Lathrop (SJL) gauge fit the data better than did the proportion of flow into the San Joaquin River (Table I-2 in Appendix I).

P_E was 10.4 percentage points better with the BAFF on than with the BAFF off, but this result was not significant (Table 6-4) (i.e., hypothesis $H1_0$ was accepted). However, a comparison of Tables 6-1 and 6-4 showed that with "tagged juvenile Chinook determined to have been eaten" removed, the BAFF-on performance improved from an O_E of 20.9% to a P_E of 33.8%. These results showed that the BAFF maintained juvenile Chinook salmon in the San Joaquin River at a proportion (0.338) similar to the fraction of water entering the San Joaquin River (0.35) at the HOR study area. The GLM presented in Appendix I showed that with the BAFF on, there was a greater probability (P = 0.0010) that a juvenile Chinook salmon would enter the San Joaquin River route (Table 7-1 in Appendix I).

Table 6-4
Statistics for Protection Efficiency during BAFF Operations in 2009

Statistic	BAFF On	BAFF Off	Percentage Point Change	Kruskal-Wallis X^2	P-Value
Mean	0.338	0.234	10.4	0.669	0.4133
Standard Deviation	0.330	0.220			
Minimum	0.000	0.000			
Maximum	1.000	0.667			
Samples (n)	18	25			

Notes: BAFF = bio-acoustic fish fence; n = number of protection efficiency samples
Source: Data compiled by Turnpenny Horsfield Associates and AECOM

Effect of Ambient Light Level on Protection Efficiency

When the samples for 2009 BAFF P_E were partitioned by ambient light level (Table 6-5), seven to 16 samples were found for various combinations of BAFF operations with ambient light levels. For high-ambient-light levels, it was noted that BAFF P_E with the BAFF on was 21.9 percentage points higher than with the BAFF off (Table 6-6); the statistical power of the test was only 0.435. In addition, there was no improvement in P_E with the BAFF on compared to the BAFF off at either ambient light level. In 2009, it appeared that there was insufficient power to resolve any effect, or ambient light did not influence BAFF P_E.

Table 6-5
Summary of Protection Efficiency Samples for Tagged Chinook Salmon Encountering BAFF during On/Off Operations at Low and High Light Levels in 2009

Ambient Light Level	BAFF On (n)	BAFF Off (n)
Low Light (<5.4 lux)	7	9
High Light (≥5.4 lux)	11	16
Total	18	25

Notes: BAFF = bio-acoustic fish fence; n = number of protection efficiency samples
Source: Data compiled by Turnpenny Horsfield Associates and AECOM

Table 6-6
2009 BAFF Operations—Mean Protection Efficiency for Chinook Salmon at Low and High Light Levels

Ambient Light Level	BAFF On Mean	BAFF Off Mean	Percentage Point Change	Kruskal-Wallis X^2	P-value
Low Light (<5.4 lux)	0.108	0.178	-7.0	0.720	0.3960
High Light (≥5.4 lux)	0.484	0.265	21.9	3.126	0.0771

Notes: BAFF = bio-acoustic fish fence
Source: Data compiled by Turnpenny Horsfield Associates and AECOM

Effect of Average Channel Velocity on Protection Efficiency

No samples were acquired under high-ACV conditions in 2009. Thus, sample sizes and means under low-velocity conditions were the same as those shown in Table 6-4.

DETERRENCE EFFICIENCY

For deterrence efficiency (D_E), some tags were removed for the calculation. If a tag was determined to have been eaten before it experienced the BAFF, then it was not included. D_E with the BAFF on showed a significant improvement (Kruskal-Wallis $X^2 = 11.398$, $P = 0.007$), 2.35 times greater, than D_E with the BAFF off (Table 6-7). Hypothesis $H1_0$ was rejected for D_E. It appeared that the BAFF was effective at deterring juvenile Chinook salmon when individuals approached the BAFF.

Table 6-7
Deterrence Efficiency Statistics for BAFF Operations in 2009

Statistic	BAFF On	BAFF Off	Percentage Point Change	Kruskal-Wallis X^2	P-Value
Mean	0.732	0.311	42.1	11.398	0.0007
Standard Deviation	0.335	0.322			
Minimum	0.000	0.000			
Maximum	1.000	1.000			
Samples (n)	18	23			

Notes: BAFF = bio-acoustic fish fence; n = number of deterrence efficiency samples
Source: Data compiled by Turnpenny Horsfield Associates and AECOM

The D_E with the BAFF off was 31.1%. This is the percentage of fish that exhibited movements that appeared to be movements away from the BAFF and toward the San Joaquin River, or movements of a fish guided along the line of, and past the end of, the BAFF. These movements may have occurred because the BAFF infrastructure took up some proportion of the water column, which may create turbulence or reflect ambient light. It is possible that a proportion of the fish would sense the turbulence created by the BAFF infrastructure or see ambient light reflected from barrier components and would move away from it or be guided along it.

The mean D_E with the BAFF on was 73.2% in the 2009 analysis reported. This is slightly less than the grand D_E reported in Bowen et al. (2012) of 81.4%. This difference arose from the reanalysis of the deterrence data in the present study because fish were placed into samples from the same time period with similar ambient light and ACV values when the fish arrived at the HOR study area (see definition of samples in Chapter 5, "Methods") instead of being placed in groups that were associated with the release date/time.

Effect of Ambient Light Level on BAFF Deterrence Efficiency

When the samples for 2009 BAFF D_E were partitioned by ambient light level (Table 6-8), seven to 15 samples were found for various combinations of BAFF operations and ambient light levels. For high-ambient-light conditions, it was noted that D_E with the BAFF on was 52.7 percentage points higher than with the BAFF off (Table 6-9), and this difference was significant. This result was consistent with the laboratory study of a BAFF by Bowen et al. (2009), which found the highest D_E for juvenile Chinook salmon occurred during the day and at the lower turbidity condition studied: 10 NTU. The lowest mean turbidity in the HOR study area of all the years studied, 19.9 NTU (Table 3-4), occurred in 2009.

Table 6-8
Summary of Deterrence Efficiency Samples for Tagged Juvenile Chinook Salmon Encountering BAFF during On/Off Operations at Low and High Light Levels in 2009

Ambient Light Level	BAFF On (n)	BAFF Off (n)
Low Light (<5.4 lux)	7	8
High Light (≥5.4 lux)	11	15
Total	18	23

Notes: BAFF = bio-acoustic fish fence; n = number of deterrence efficiency samples
Source: Data compiled by Turnpenny Horsfield Associates and AECOM

Table 6-9
2009 BAFF Operations—Mean Deterrence Efficiency for Tagged Juvenile Chinook Salmon at Low and High Light Levels

Ambient Light Level	BAFF On Mean	BAFF Off Mean	Percentage Point Change	Kruskal-Wallis X^2	P-value
Low Light (<5.4 lux)	0.474	0.202	27.2	2.330	0.1269
High Light (≥5.4 lux)	0.897	0.370	52.7	12.448	0.0004

Notes: BAFF = bio-acoustic fish fence
Source: Data compiled by Turnpenny Horsfield Associates and AECOM

There was an improvement of 27.2% in D_E with the BAFF on compared to operations with the BAFF off at low ambient light levels (Table 6-9). However, this result was not significant. In 2009, it was concluded that the BAFF delivered juvenile Chinook salmon deterrence (Table 6-9), and that the performance of the BAFF was the best at high ambient light magnitudes, in contrast to the findings of Welton et al. (2002), who found the highest proportion deflected at night.

Effect of Average Channel Velocity on Barrier Deterrence Efficiency

In 2009, all samples were categorized as "low velocity," where ACV is less than 0.61 m/s (= Approach Velocity <0.25 m/s). Thus, no comparisons of D_E at various ACV ranges were possible.

6.1.2 2010 RESULTS

SIZE AND SOURCE OF JUVENILE CHINOOK SALMON USED

The juvenile Chinook salmon tagged and released in 2010 were similar in size to those from 2011 and 2012, and larger than those from 2009 (Table 5-1). In 2010, and in all subsequent years of the research reported herein, the Merced River Hatchery was the source of juvenile Chinook salmon.

OVERALL EFFICIENCY

Chinook Salmon

The O_E for the BAFF was only 11.0 percentage points higher with the BAFF on than with the BAFF off, which was not statistically significant (Table 6-10); hypothesis $H2_0$ was accepted.

Table 6-10
Statistics for Overall Efficiency during BAFF Operations in 2010

Statistic	BAFF On	BAFF Off	Percentage Point Change	Kruskal-Wallis X^2	P-value
Mean	0.355	0.245	11.0	1.392	0.2380
Standard Deviation	0.243	0.183			
Minimum	0.000	0.000			
Maximum	1.000	0.500			
Samples (n)	19	22			

Notes: BAFF = bio-acoustic fish fence; n = number of overall efficiency samples
Source: Data compiled by Turnpenny Horsfield Associates and AECOM

Effect of Ambient Light Level on Overall Efficiency

Tagged juvenile Chinook salmon approached the 2010 BAFF line at various light levels (Figure 6-3). When the 2010 juvenile Chinook salmon were placed into samples, and the O_E samples were partitioned by light level, nine to 12 samples were acquired in the BAFF status and light level combinations (Table 6-11). For low-light levels, mean O_E with the BAFF on was 19.1 percentage points higher than with the BAFF off (Table 6-12), but there was no improvement in O_E with the BAFF on compared to off at either light level. In 2010, it appeared that there was insufficient statistical power to resolve any effect, or light level did not influence the BAFF's O_E.

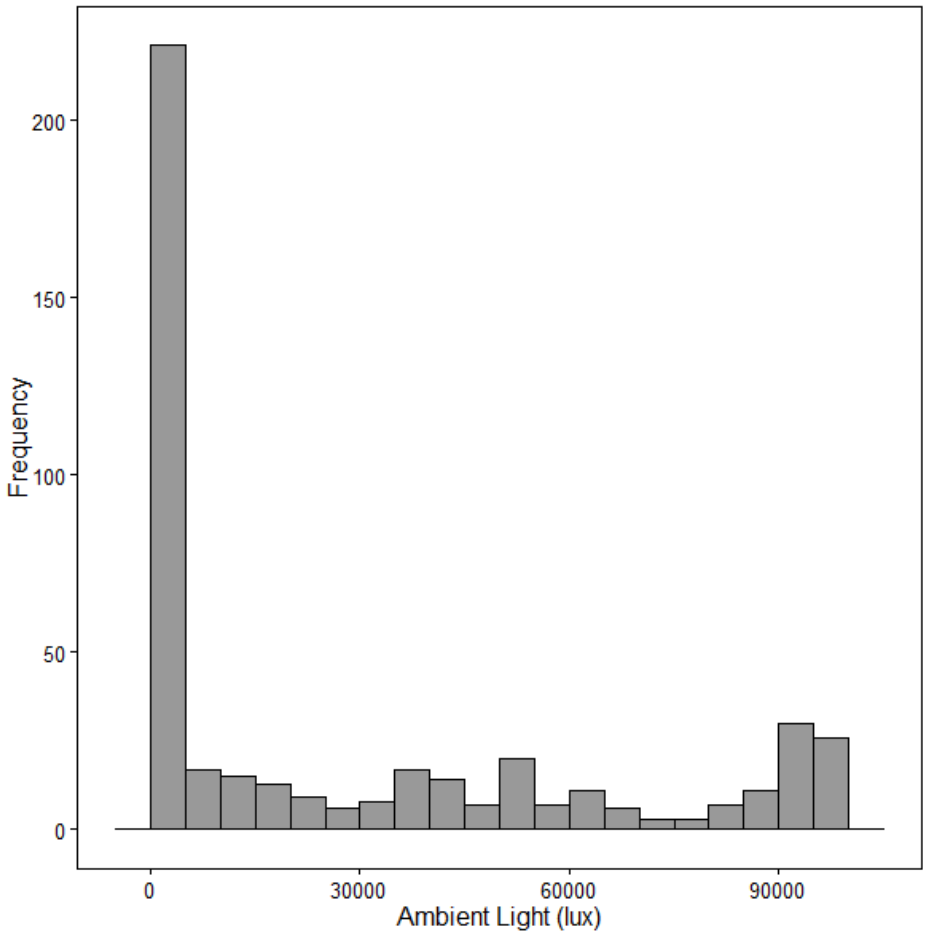

Source: Data compiled by Turnpenny Horsfield Associates and AECOM

Figure 6-3 Frequency Histogram of 2010 Light-Level Observations (collected at CIMIS, Station #70–Manteca, 37.834822, -121.223194) Obtained for Each Tagged Juvenile Chinook Salmon when the Individual was Nearest the 2010 BAFF Line

Table 6-11
Summary of Overall Efficiency Samples for Tagged Juvenile Chinook Salmon Encountering BAFF during On/Off Operations at Low and High Ambient Light Levels in 2010

Ambient Light Level	BAFF On (n)	BAFF Off (n)
Low Light (<5.4 lux)	9	12
High Light (≥5.4 lux)	10	10
Total	19	22

Notes: BAFF = bio-acoustic fish fence; n = number of overall efficiency samples
Source: Data compiled by Turnpenny Horsfield Associates and AECOM

Table 6-12
2010 BAFF Operations—Mean Overall Efficiency for Tagged Juvenile Chinook Salmon at Low and High Light Levels

Ambient Light Level	BAFF On Mean	BAFF Off Mean	Percentage Point Change	Kruskal-Wallis X^2	P-Value
Low Light (<5.4 lux)	0.506	0.315	19.1	2.155	0.1421
High Light (≥5.4 lux)	0.219	0.161	5.8	1.379	0.2403

Note: BAFF = bio-acoustic fish fence
Source: Data compiled by Turnpenny Horsfield Associates and AECOM

Effect of Average Channel Velocity on Overall Efficiency

Tagged juvenile Chinook salmon approached the 2010 BAFF line at various light levels (Figure 6-4). When the 2010 fish were placed into samples and the O_E samples for juvenile Chinook salmon were partitioned by ACV level, only four samples were acquired for high-velocity conditions for both the BAFF on and off (Table 6-13). For low-velocity conditions, mean O_E with the BAFF on was 11.9 percentage points higher than with the BAFF off (Table 6-14), but there was no significant improvement in O_E with the BAFF on compared to off at either ACV level. In 2010, it appeared that there was insufficient statistical power to resolve any effect or ACV did not influence the BAFF's O_E.

Table 6-13
Summary of Overall Efficiency Samples for Tagged Juvenile Chinook Salmon Encountering BAFF during On/Off Operations at Low and High Average Channel Velocity Levels in 2010

Average Channel Velocity Level	BAFF On (n)	BAFF Off (n)
Low Velocity (<0.61 m/s)	15	18
High Velocity (≥0.61 m/s)	4	4
Total	19	22

Notes: BAFF = bio-acoustic fish fence; n = number of overall efficiency samples; m/s = meters per second; n = number of samples
Source: Data compiled by Turnpenny Horsfield Associates and AECOM

Table 6-14
2010 BAFF Operations—Mean Overall Efficiency for Tagged Juvenile Chinook Salmon at Low and High Average Channel Velocity Levels

Average Channel Velocity Level	BAFF On Mean	BAFF Off Mean	Percentage Point Change	Kruskal-Wallis X^2	P-Value
Low Velocity (<0.61 m/s)	0.352	0.233	11.9	1.479	0.2240
High Velocity (≥0.61 m/s)	0.367	0.298	6.9	0.021	0.8845

Notes: BAFF = bio-acoustic fish fence; m/s = meters per second
Source: Data compiled by Turnpenny Horsfield Associates and AECOM

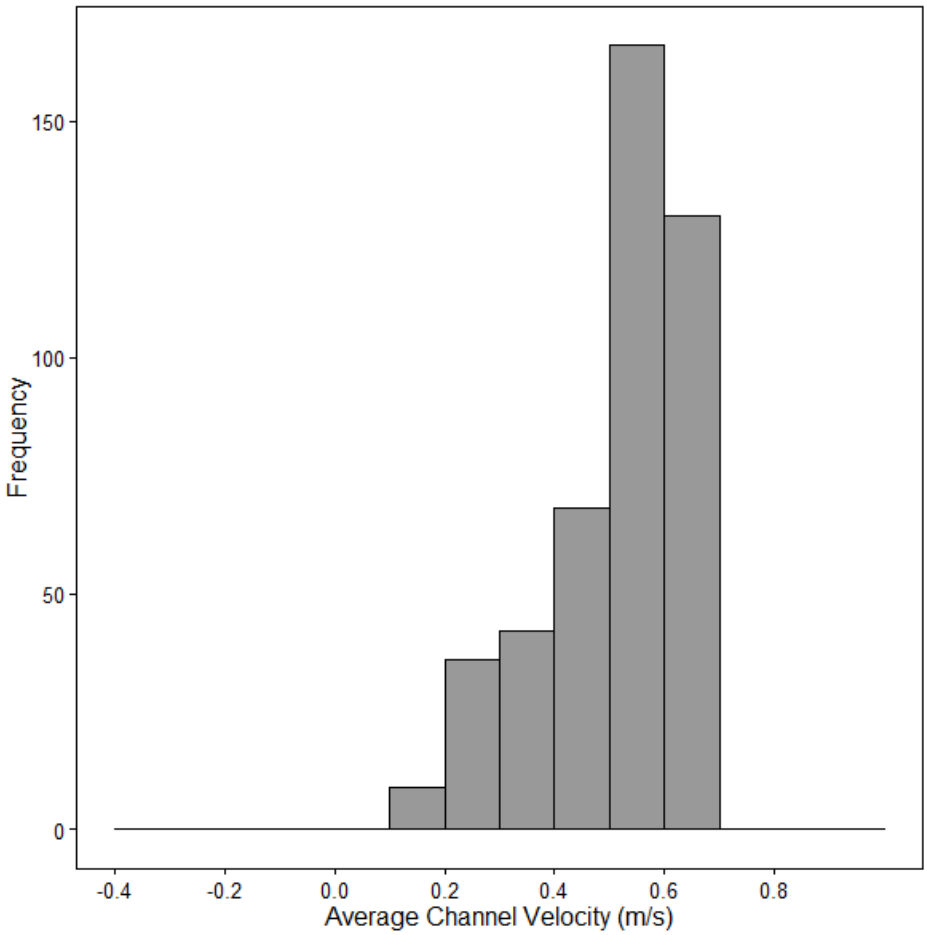

Source: Data compiled by Turnpenny Horsfield Associates and AECOM

Figure 6-4 Frequency Histogram of 2010 Average Channel Velocity Observations (SJL Gauge) Obtained for Each Tagged Juvenile Chinook Salmon when the Individual was Nearest the 2010 BAFF Line

PROTECTION EFFICIENCY

BAFF P_E was 0.286 with the BAFF off, and the proportion of flow into the San Joaquin River during the study period was 0.56 (Table 3-1). Similar to 2009, the proportion of juvenile Chinook salmon entering the San Joaquin River in 2010 was not the same as the proportion of flow. The fraction was lower. In contrast, in Table 7-3 in Appendix I, the proportion of flow entering the San Joaquin River was correlated (P = 0.0003) with the probability that an individual juvenile Chinook salmon would continue down the San Joaquin River route. The multivariate analysis showed that the proportion of flow into the San Joaquin River (SJL gauge), and ACV models fit the data equally well (Table 7-2 in Appendix I). All analyses showed correlation with the probability that a juvenile Chinook salmon would be entrained into the San Joaquin River route.

P_E was 15.5 percentage points higher with the BAFF on than with the BAFF off and, in contrast to 2009, this result was statistically significant (Table 6-15). Hypothesis $H2_0$ was rejected. It was found that 44.1% of tagged juvenile Chinook salmon continued down the San Joaquin River with the BAFF on. These results showed that the BAFF improved the proportion of juvenile Chinook salmon remaining in the San Joaquin River in 2010, but it is unknown whether this improvement was biologically significant at the population level. These results were

consistent with the GLM presented in Appendix I. It showed that with the BAFF on a greater probability (P = 0.0002) existed that a juvenile Chinook salmon would enter the San Joaquin River route (Table 7-3 in Appendix I).

Table 6-15
Statistics for Protection Efficiency during BAFF Operations in 2010

Statistic	BAFF On	BAFF Off	Percentage Point Change	Kruskal-Wallis X^2	P-Value
Mean	0.441	0.286	15.5	3.943	0.0471
Standard Deviation	0.239	0.206			
Minimum	0.000	0.000			
Maximum	1.000	0.667			
Samples (n)	19	20			

Notes: BAFF = bio-acoustic fish fence; n = number of protection efficiency samples
Source: Data compiled by Turnpenny Horsfield Associates and AECOM

Effect of Ambient Light Level on Protection Efficiency

When the samples for 2010 P_E were partitioned by ambient light level (Table 6-16), nine to 10 samples were found for various combinations of BAFF operations with ambient light levels. For low-ambient-light levels, mean P_E with the BAFF on was 16.7 percentage points higher than off (Table 6-17). For high-ambient-light levels, mean P_E with the BAFF on was 15.3 percentage points higher than with the BAFF off, the P_E test provided a P value of 0.0812 and a statistical power of just 0.417. It appeared that it may not have been possible to reject a false null hypothesis because of the low power of the test. As in 2009, at both low and high light levels, there was no statistically significant improvement in P_E with the BAFF on compared to off. In 2010, it appeared that there was insufficient power to resolve any effect, or light level did not influence the BAFF's P_E.

Table 6-16
Summary of Protection Efficiency Samples for Tagged Juvenile Chinook Salmon Encountering BAFF during On/Off Operations at Low and High Light Levels in 2010

Ambient Light Level	BAFF On (n)	BAFF Off (n)
Low Light (<5.4 lux)	9	10
High Light (≥5.4 lux)	10	10
Total	19	20

Notes: BAFF = bio-acoustic fish fence; n = number of protection efficiency samples
Source: Data compiled by Turnpenny Horsfield Associates and AECOM

Table 6-17
2010 BAFF Operations—Mean Protection Efficiency for Juvenile Chinook Salmon at Low and High Light Levels

Ambient Light Level	BAFF On Mean	BAFF Off Mean	Percentage Point Change	Kruskal-Wallis X^2	P-Value
Low Light (<5.4 lux)	0.526	0.359	16.7	1.513	0.2186
High Light (≥5.4 lux)	0.365	0.212	15.3	3.041	0.0812

Notes: BAFF = bio-acoustic fish fence
Source: Data compiled by Turnpenny Horsfield Associates and AECOM

Effect of Average Channel Velocity on Protection Efficiency

When the samples for 2010 P_E were partitioned by ACV level only, four samples were acquired for high-ACV conditions for both BAFF on and off (Table 6-18) status. For low-ACV conditions, P_E with the BAFF on was 16.9 percentage points higher than off (Table 6-19), but there was no statistically significant improvement in P_E with the BAFF on compared to off at either velocity level. These results suggested that there may have been insufficient power to resolve any effect, or ACV did not influence the BAFF's P_E. However, the P-value for low ACV was 0.0544 but the statistical power of this test was only 0.544. It appears that more research in this area would be useful.

Table 6-18
Summary of Protection Efficiency Samples for Tagged Juvenile Chinook Salmon Encountering BAFF during On/Off Operations at Low and High Average Channel Velocity Levels in 2010

Average Channel Velocity Level	BAFF On (n)	BAFF Off (n)
Low Velocity (<0.61 m/s)	15	16
High Velocity (≥0.61 m/s)	4	4
Total	19	20

Notes: BAFF = bio-acoustic fish fence; n = number of protection efficiency samples; m/s = meters per second
Source: Data compiled by Turnpenny Horsfield Associates and AECOM

Table 6-19
2010 BAFF Operations—Mean Protection Efficiency for Tagged Juvenile Chinook Salmon at Low and High Average Channel Velocity Levels

Average Channel Velocity Level	BAFF On Mean	BAFF Off Mean	Percentage Point Change	Kruskal-Wallis X^2	P-Value
Low Velocity (<0.61 meter per second)	0.435	0.266	16.9	3.699	0.0544
High Velocity (≥0.61 meter per second)	0.465	0.365	10.0	0.527	0.4678

Notes: BAFF = bio-acoustic fish fence
Source: Data compiled by Turnpenny Horsfield Associates and AECOM

DETERRENCE EFFICIENCY

The BAFF-on treatment showed an improvement (Kruskal-Wallis $X^2 = 13.095$, $P = 0.0003$) in D_E: 13.8 percentage points greater than with the BAFF off (Table 6-20). Thus, hypothesis $H2_0$ was rejected. The analysis showed that the BAFF provided a statistically significant deterrent for diverting juvenile Chinook salmon when an individual approached the BAFF. It is unknown whether this level of improved deterrence is biologically significant at the population level.

Table 6-20
Deterrence Efficiency Statistics for BAFF Operations in 2010

Statistic	BAFF On	BAFF Off	Percentage Point Change	Kruskal-Wallis X^2	P-Value
Mean	0.150	0.012	13.8	13.095	0.0003
Standard Deviation	0.193	0.044			
Minimum	0.000	0.000			
Maximum	0.680	0.200			
Samples (n)	19	22			

Notes: BAFF = bio-acoustic fish fence; n = number of deterrence efficiency samples
Source: Data compiled by Turnpenny Horsfield Associates and AECOM

The apparent D_E with the BAFF off was 1.2%. This is the percentage of juvenile Chinook salmon that exhibited movements that appeared to be movements away from the BAFF or guided along the line of the BAFF even though the BAFF was off.

The 2010 mean D_E with the BAFF on was 15.0% in the analysis reported in Table 6-20. This is slightly less than the grand D_E reported in Bowen et al. (2012), which was 23.0%. Similar to 2009, this difference arose from the reanalysis of the deterrence data in the present study, because fish were placed into samples from the same time period with similar values for ambient light and ACV when the fish arrived at the HOR study area (see definition of samples in Chapter 5, "Methods"), instead of being placed in groups that were associated with the release date/ time.

Effect of Ambient Light Level on BAFF Deterrence Efficiency

When the samples for 2010 BAFF D_E were partitioned by ambient light level (Table 6-21), 9 to 12 samples were found for various combinations of BAFF operations and light levels. For high-light levels, D_E with the BAFF on was 26.0 percentage points higher than with the BAFF off (Table 6-22), and this difference was statistically significant. However, there was no improvement in D_E with the BAFF on compared to off at low light levels. In 2010, similar to 2009, it appeared that light did influence the BAFF's D_E at light levels greater than or equal to 5.4 lux.

Table 6-21
Summary of Deterrence Efficiency Samples for Tagged Juvenile Chinook Salmon Encountering BAFF during On/Off Operations at Low and High Light Levels in 2010

Ambient Light Level	BAFF On (n)	BAFF Off (n)
Low Light (<5.4 lux)	9	12
High Light (≥5.4 lux)	10	10
Total	19	22

Notes: BAFF = bio-acoustic fish fence; n = number of deterrence efficiency samples
Source: Data compiled by Turnpenny Horsfield Associates and AECOM

Table 6-22
2010 BAFF Operations—Mean Deterrence Efficiency for Tagged Juvenile Chinook Salmon at Low and High Light Levels

Ambient Light Level	BAFF On Mean	BAFF Off Mean	Percentage Point Change	Kruskal-Wallis X^2	P-Value
Low Light (<5.4 lux)	0.019	0.017	0.2	0.575	0.4481
High Light (≥5.4 lux)	0.267	0.007	26.0	15.093	0.0001

Note: BAFF = bio-acoustic fish fence
Source: Data compiled by Turnpenny Horsfield Associates and AECOM

Effect of Average Channel Velocity on Barrier Deterrence Efficiency

When the samples for 2010 D_E were partitioned by ACV level, only four samples were acquired for high-ACV conditions for both the BAFF on and BAFF off (Table 6-23). For low-ACV conditions, D_E with the BAFF on was 11.1 percentage points higher than off (Table 6-24). In addition, D_E with the BAFF on was 23.6 percentage points higher than off for high-ACV conditions (Table 6-24). In 2010, the BAFF improved D_E under both low- and high-ACV conditions.

Table 6-23
Summary of Deterrence Efficiency Samples for Tagged Juvenile Salmon Encountering BAFF during On/Off Operations at Low and High Average Channel Velocity Levels in 2010

Average Channel Velocity Level	BAFF On (n)	BAFF Off (n)
Low Velocity (<0.61 m/s)	15	18
High Velocity (≥0.61 m/s)	4	4
Total	19	22

Notes: BAFF = bio-acoustic fish fence; n = number of deterrence efficiency samples; m/s = meters per second
Source: Data compiled by Turnpenny Horsfield Associates and AECOM

Table 6-24
2010 BAFF Operations—Mean Deterrence Efficiency for Tagged Juvenile Chinook Salmon at Low and High Average Channel Velocity Levels

Average Channel Velocity Level	BAFF On Mean	BAFF Off Mean	Percentage Point Change	Kruskal-Wallis X^2	P-Value
Low Velocity (<0.61 m/s)	0.122	0.011	11.1	8.562	0.0034
High Velocity (≥0.61 m/s)	0.254	0.018	23.6	5.600	0.0180

Note: BAFF = bio-acoustic fish fence; m/s = meters per second
Source: Data compiled by Turnpenny Horsfield Associates and AECOM

6.1.3 2009 COMPARED TO 2010

STUDY FISH

There were three important differences in the juvenile Chinook salmon used in 2009 and 2010. The juvenile Chinook salmon used in 2009 were from the Feather River Hatchery and were fall-spring–run hybrids. Juvenile Chinook salmon used in 2010 were from the Merced River Hatchery and were fall-run (Table 5-1). Also, the range of sizes was different between the two years. The Feather River Hatchery fall-spring hybrid individuals were 80 to 110 mm TL while the Merced River Hatchery fall-run individuals were 99 to 121 mm TL. Finally, the tag burden was higher than 5.4% for a large proportion of juvenile Chinook salmon in 2009 over 2010 (Table 5-3).

In addition to differences in the juvenile Chinook salmon, there were differences in the BAFF location, orientation, length, and shape (Figure 4-3). The principal objective in comparing 2009 and 2010 was to determine which of these two shapes seemed to best improve P_E. However, the analysis was confounded by the three important differences between the juvenile Chinook salmon between the two years.

OVERALL EFFICIENCY

The number of samples ranged from 19 to 27 for BAFF operations in 2009 and 2010 (Table 6-25). There was not a statistical difference between 2009 and 2010 in any measured variable (Table 6-26); hypotheses $H3_0$ and $H4_0$ were accepted. With the BAFF on, O_E was never higher than 35.5%. Thus, it appeared the BAFF was not effective at maintaining juvenile Chinook salmon in the San Joaquin River. The 2010 O_E with the BAFF on showed a 14.6-percentage-point improvement over 2009; the P-value was 0.0563, but the statistical power was only 0.489. These results suggested that there could be differences between 2009 and 2010 BAFF alignments, but low power meant it was not possible to reject a false null hypothesis (Table 1-1: $H3_0$).

Table 6-25
Overall Efficiency Samples with BAFF Operations—2009 vs. 2010

Treatment	2009 (n)	2010 (n)	Total
BAFF On	21	19	40
BAFF Off	27	22	49
BAFF Effect	15	11	26

Notes: BAFF = bio-acoustic fish fence; n = number of samples
Source: Data compiled by Turnpenny Horsfield Associates and AECOM

Table 6-26
Overall Efficiency Statistics with BAFF Operations—2009 vs. 2010

Treatment	2009 Mean	2010 Mean	Percentage Point Change	Kruskal-Wallis X^2	P-Value
BAFF On	0.209	0.355	-14.6	3.645	0.0563
BAFF Off	0.184	0.245	-6.1	1.958	0.1617
BAFF Effect	0.047	0.080	-3.3	0.017	0.8967

Note: BAFF = bio-acoustic fish fence
Source: Data compiled by Turnpenny Horsfield Associates and AECOM

PROTECTION EFFICIENCY

The number of P_E samples ranged from 18 to 25 in 2009 and 2010 (Table 6-27). There were fewer BAFF effect samples, 11 to 12. Calculation of BAFF effect required a switch in BAFF status while ACV and light level were consistent. That did not happen on every BAFF switch occasion. No statistical difference was observed between 2009 and 2010 in any measured variable (Table 6-28); P_E with the BAFF on was never higher than 44.1%. Hypotheses $H3_0$ and $H4_0$ were accepted. Thus, it appeared the BAFF was not effective under any conditions studied, thus it did not facilitate maintaining juvenile Chinook salmon in the San Joaquin River.

Table 6-27
Protection Efficiency Samples with BAFF Operations—2009 vs. 2010

Treatment	2009 (n)	2010 (n)	Total
BAFF On	18	25	43
BAFF Off	19	20	39
BAFF Effect	12	11	33

Notes: BAFF = bio-acoustic fish fence; n = number of samples
Source: Data compiled by Turnpenny Horsfield Associates and AECOM

Table 6-28
Protection Efficiency Statistics with BAFF Operations—2009 vs. 2010

Treatment	2009 Mean	2010 Mean	Percentage Point Change	Kruskal-Wallis X^2	P-Value
BAFF On	0.338	0.441	-10.4	1.567	0.2106
BAFF Off	0.234	0.286	-5.2	0.635	0.4256
BAFF Effect	0.108	0.145	-3.7	0.077	0.7817

Note: BAFF = bio-acoustic fish fence
Source: Data compiled by Turnpenny Horsfield Associates and AECOM

DETERRENCE EFFICIENCY

The number of D_E samples ranged from 18 to 23 in 2009 and 2010 (Table 6-29). In 2009, operation of the BAFF produced much greater D_E than in 2010 (a 58.2-percentage-point improvement). However, with the BAFF off, there was also a 29.9-percentage-point greater D_E in 2009 than in 2010 (Table 6-30). The percentage of juvenile Chinook salmon that appeared deterred with the BAFF off was 31.1% in 2009 and 1.2% in 2010, and were different (see Table 6-30). Hypotheses $H3_0$ and $H4_0$ were rejected.

Table 6-29
Deterrence Efficiency Samples with BAFF Operations—2009 vs. 2010

Treatment	2009 (n)	2010 (n)	Total
BAFF On	18	19	37
BAFF Off	23	22	45
BAFF Effect	10	11	21

Notes: BAFF = bio-acoustic fish fence; n = number of samples
Source: Data compiled by Turnpenny Horsfield Associates and AECOM

Table 6-30
Deterrence Efficiency Statistics with BAFF Operations—2009 vs. 2010

Treatment	2009 Mean	2010 Mean	Percentage Point Change	Kruskal-Wallis X^2	P-Value
BAFF On	0.732	0.150	58.2	16.997	<0.0001
BAFF Off	0.311	0.012	29.9	18.351	<0.0001
BAFF Effect	0.432	0.166	26.6	3.248	0.0715

Notes: BAFF = bio-acoustic fish fence
Source: Data compiled by Turnpenny Horsfield Associates and AECOM

In 2009, the calculated BAFF effect on D_E was 26.6 percentage points greater than in 2010. Thus, the difference in calculated D_E due to the BAFF effect from 2009 to 2010 accurately approximated the difference in D_E from 2009 to 2010, due only to BAFF operation rather than other factors. Although it appeared that BAFF operation resulted in much greater deterrence in 2009, the deterrence due to the BAFF effect was not different from 2009 to 2010, possibly due to sample sizes of 10 and 11 (Table 6-29), and relatively low statistical power (0.444).

6.1.4 2011 RESULTS

SIZE AND SOURCE OF JUVENILE CHINOOK SALMON AND STEELHEAD USED

The juvenile Chinook salmon tagged and released in 2011 were similar in size to those in 2010 and 2012 and larger than 2009 (Table 5-1).

The juvenile steelhead implanted with tags and released in 2011 were larger than the tagged juvenile Chinook salmon (Table 5-1). In 2011, the Mokelumne River Fish Hatchery provided the juvenile steelhead used in the studies; the production of the juvenile steelhead is described in Section B.1 of Appendix B.

CHINOOK SALMON OVERALL AND PROTECTION EFFICIENCY STATISTICS

In 2011, there were 53 samples of tagged juvenile Chinook salmon for which O_E and P_E could be calculated (Table 6-31). With no barrier installed, 51.9% of tags in juvenile Chinook salmon continued down the San Joaquin River. However, when the juvenile Chinook salmon that had been determined to be eaten were removed, the P_E improved. With no barrier installed, 57.4% of the juvenile Chinook salmon determined to have not been consumed went down the San Joaquin River. The mean proportion of flow into the San Joaquin River during the period of fish release was 48% (Table 3-1). In 2009 and 2010 the proportion of juvenile Chinook salmon entering the San Joaquin River was lower than the proportion of flow. In contrast in 2011, the proportion of juvenile Chinook salmon entering the San Joaquin River was similar to the proportion of flow.

Table 6-31
Chinook Salmon Statistics for the No-Barrier Treatment in 2011

	Mean	Standard Deviation	Minimum	Maximum	Number of Samples (n)
Overall Efficiency	0.519	0.160	0.000	1.000	53
Protection Efficiency	0.574	0.178	0.000	1.000	53

Notes: n = number of samples
Source: Data compiled by Turnpenny Horsfield Associates and AECOM

6.1.5 2009 BAFF OFF COMPARED TO 2010 BAFF OFF COMPARED TO 2011

OVERALL EFFICIENCY— JUVENILE CHINOOK SALMON

O_E was significantly different between treatments at the HOR study area with the BAFF off in 2009 and 2010, and with no barrier in 2011 (Kruskal-Wallis $X^2 = 49.008$, P-value <0.0001). Hypothesis $H5_0$ was rejected. There was no significant difference in O_E in 2009 with the BAFF off compared to 2010 with the BAFF off (Table 6-26). Thus, 2009 with the BAFF off was grouped with 2010 with the BAFF off (Table 6-32). Because the data did not meet the assumptions of ANOVA, one nonparametric two-sample comparison was made between treatments (i.e., 2010 vs. 2011). The O_E in 2011 was significantly greater than O_E in 2010 with the BAFF off (Kruskal-Wallis $X^2 = 26.577$, P-value <0.0001).

Table 6-32
Statistics for Overall Efficiency for 2009–2011

Treatment—Year	Mean	Standard Deviation	Number of Samples (n)	Statistical Grouping
BAFF Off—2009	0.184	0.185	27	a
BAFF Off—2010	0.245	0.183	22	a
No Barrier—2011	0.519	0.160	53	b

Note: BAFF = bio-acoustic fish fence; n = number of samples
Source: Data compiled by Turnpenny Horsfield Associates and AECOM

PROTECTION EFFICIENCY—JUVENILE CHINOOK SALMON

P_E was significantly different for the BAFF-off and "no barrier" years at the HOR study area (Kruskal-Wallis $X^2 = 39.650$, P-value <0.0001). Hypothesis $H5_0$ was rejected. There was no significant difference in P_E with the BAFF off in 2009 compared to 2010 (Table 6-28); so, the "BAFF Off—2009" statistics were grouped with the "BAFF Off—2010" statistics (Table 6-33). Because the data did not meet the assumptions of ANOVA, one nonparametric two-sample comparison was made between treatments (i.e., 2010 vs. 2011). The P_E in 2011 was greater than the P_E with the BAFF off for 2009 and 2010 (Kruskal-Wallis $X^2 = 21.378$, P-value <0.0001).

Table 6-33
Statistics for Protection Efficiency for 2009–2011

Treatment—Year	Mean	Standard Deviation	Number of Samples (n)	Statistical Grouping
BAFF Off—2009	0.234	0.220	25	a
BAFF Off—2010	0.286	0.206	20	a
No Barrier—2011	0.574	0.178	53	b

Note: BAFF = bio-acoustic fish fence; n = number of samples
Source: Data compiled by Turnpenny Horsfield Associates and AECOM.

6.1.6 2011 JUVENILE CHINOOK SALMON COMPARED TO JUVENILE STEELHEAD

OVERALL EFFICIENCY

The number of O_E samples ranged from 53 to 93 for juvenile Chinook salmon and juvenile steelhead (Table 6-34). The O_E for tagged juvenile Chinook salmon that passed the San Joaquin River finish line was 51.9% (Table 6-34).

Table 6-34
Statistics for Overall Efficiency for Tagged Juvenile Chinook Salmon and Steelhead in 2011

Statistic	Chinook Salmon	Steelhead	Percentage Point Change	Kruskal-Wallis X^2	P-value
Mean of Samples	0.519	0.368	15.1	12.717	0.0004
Standard Deviation	0.160	0.287			
Minimum	0.000	0.000			
Maximum	1.000	1.000			
Samples (n)	53	93			

Note: n = number of samples
Overall Efficiency reported in this table is the mean of samples. The grand overall efficiency (see text) was 38.3%.
Source: Data compiled by Turnpenny Horsfield Associates and AECOM

For juvenile steelhead, the O_E was significantly lower (Kruskal-Wallis $X^2 = 12.717$, P = 0.0004) than for juvenile Chinook salmon (Table 6-34). Hypothesis $H6_0$ was rejected. However, in 2011, 37.7% of steelhead selected the Old River route and this was similar to the usage of the Old River route by Chinook (38.6%). Recall that O_E includes all tags (even those originally in juvenile salmonids that were eaten and now in predators) that pass by

the finish lines. This largely appeared to reflect greater predation on juvenile steelhead (see section 6.2.1, "Proportion Eaten (Univariate Analyses)").

The mean of overall efficiency samples was 36.8% (Table 6-34). This mean was calculated as the mean of all the samples derived by the method described in Methods (Section 5.2.1 "Grouping Juvenile Salmonids Iinto Samples"). The grand overall efficiency was 38.3%. The grand mean overall efficiency was calculated as the total number of tags, originally inserted into steelhead, that remained in the San Joaquin River (199) divided by the total number tags (520) that moved past the Head of Old River study site. This difference between these values arose from how the tags were allocated into samples but the difference was very small between the two measures.

Tagged juvenile Chinook salmon and steelhead passed through the HOR study area at various light levels (Figure 6-5). When the 2011 juvenile salmonids were placed into samples, and the O_E samples were partitioned by light level, 25 to 61 samples were distributed throughout the experimental matrix (Table 6-35). Also, tagged juvenile Chinook salmon and steelhead passed through the HOR study area at various ACV levels (Figure 6-6). When the 2011 juvenile salmonids were placed into samples and the O_E samples were partitioned by ACV level, sample sizes ranged from 24 to 48 (Table 6-37). The relationships (discussed in Section 6.1.6, "Overall Efficiency") for juvenile Chinook salmon and steelhead O_E were similar for all light and ACV levels. That is, juvenile Chinook salmon had an approximate 15-percentage-point greater O_E than did steelhead for all light levels and ACV levels (Tables 6-34, 6-36, and 6-38), and this difference was significant. It was concluded that, at both light levels and at both ACV levels studied, tagged juvenile Chinook salmon had an approximately 15% greater chance of following the San Joaquin River route compared to tagged steelhead.

Table 6-35
Summary of Overall Efficiency Samples for Tagged Chinook Salmon and Steelhead at Low and High Ambient Light Levels in 2011

Ambient Light Level	Chinook Salmon (n)	Steelhead (n)	Total (n)
Low Light (<5.4 lux)	25	32	57
High Light (≥5.4 lux)	28	61	89

Note: n = number of samples
Source: Data compiled by Turnpenny Horsfield Associates and AECOM

Table 6-36
Mean Overall Efficiency for Tagged Juvenile Chinook Salmon and Steelhead at Low and High Light Levels in 2011

Ambient Light Level	Chinook Salmon	Steelhead	Percentage Point Change	Kruskal-Wallis X^2	P-Value
Low Light (<5.4 lux)	0.540	0.367	17.3	5.426	0.0198
High Light (≥5.4 lux)	0.501	0.368	13.3	6.854	0.0088

Source: Data compiled by Turnpenny Horsfield Associates and AECOM

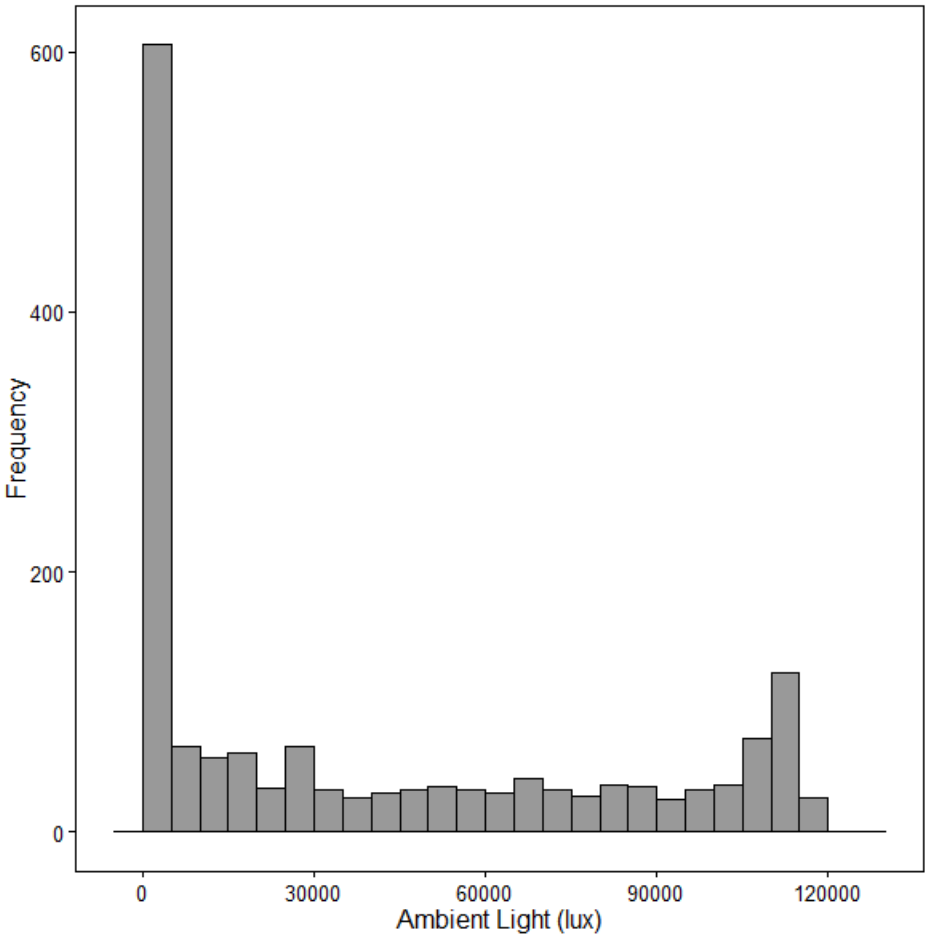

Source: Data compiled by Turnpenny Horsfield Associates and AECOM

Figure 6-5 Frequency Histogram of 2011 Light-Level Observations (collected at CIMIS, Station #70–Manteca, 37.834822, -121.223194) Obtained for Each Tagged Juvenile Salmonid when the Individual was Nearest the 2010 BAFF Line

Table 6-37
Summary of Overall Efficiency Samples for Tagged Juvenile Chinook Salmon and Steelhead at Low and High Average Channel Velocity Levels in 2011

Average Channel Velocity Level	Chinook Salmon (n)	Steelhead (n)	Total (n)
Low Velocity (<0.61 m/s)	29	48	77
High Velocity (≥0.61 m/s)	24	45	69
Total	53	93	146

Note: n = number of samples; m/s = meters per second
Source: Data compiled by Turnpenny Horsfield Associates and AECOM

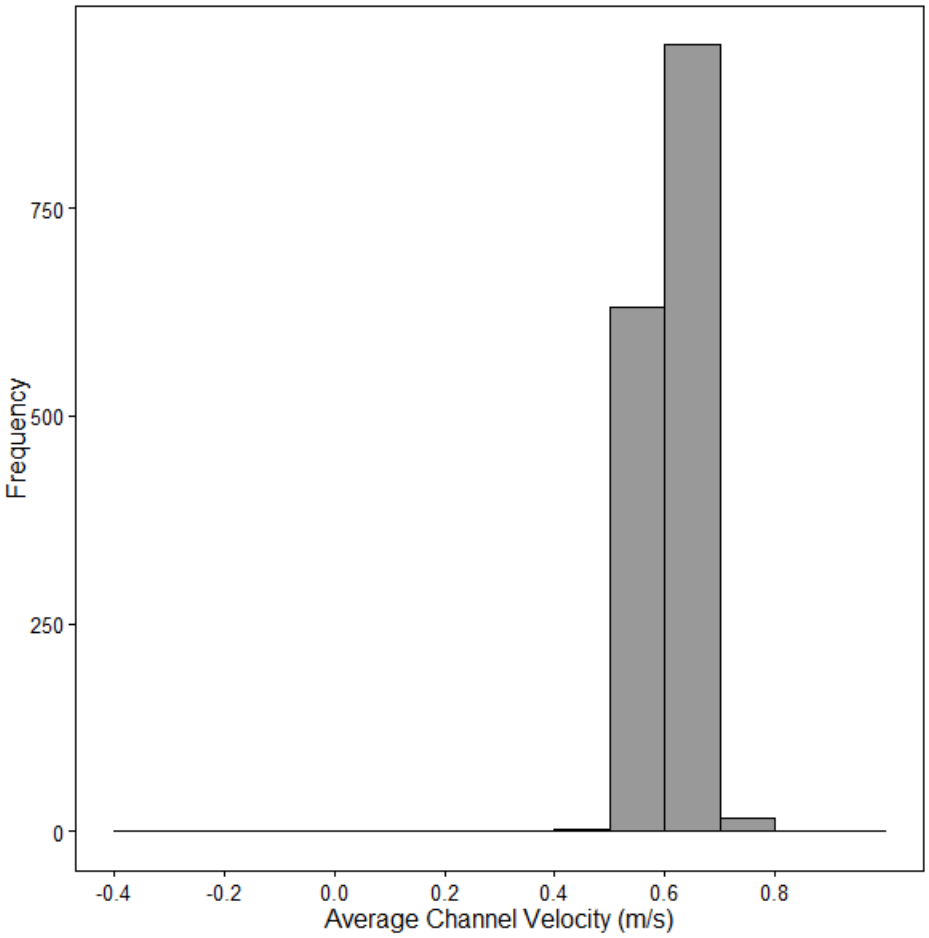

Source: Data compiled by Turnpenny Horsfield Associates and AECOM

Figure 6-6 **Frequency Histogram of 2011 Average Channel Velocity Observations (SJL Gauge) Obtained for Each Tagged Juvenile Salmonid when the Individual was Nearest the 2010 BAFF Line**

Table 6-38
Mean Overall Efficiency for Tagged Juvenile Chinook Salmon and Steelhead at Low and High Average Channel Velocity Levels in 2011

Average Channel Velocity Level	Chinook Salmon	Steelhead	Percentage Point Change	Kruskal-Wallis X^2	P-Value
Low Velocity (<0.61 m/s)	0.489	0.341	14.8	6.793	0.0092
High Velocity (≥0.61 m/s)	0.555	0.396	15.9	7.063	0.0079

Note: m/s = meters per second
Source: Data compiled by Turnpenny Horsfield Associates and AECOM

PROTECTION EFFICIENCY

The difference observed in O_E for juvenile Chinook salmon compared to steelhead was not observed in P_E (Table 6-39). It was notable that the P_E for steelhead, 49.0%, was consistent with the proportion of flow into the San Joaquin River, 48% (Table 3-1), but the P_E for juvenile Chinook salmon, 57.4%, was higher; the difference was not significant. Hypothesis $H6_0$ was accepted.

Table 6-39
Statistics for Protection Efficiency for Tagged Juvenile Chinook Salmon and Steelhead in 2011

Statistic	Chinook Salmon	Steelhead	Percentage Point Change	Kruskal-Wallis X^2	P-Value
Mean	0.574	0.490	8.4	2.511	0.1131
Standard Deviation	0.178	0.296			
Minimum	0.000	0.000			
Maximum	1.000	1.000			
Samples (n)	53	77			

Note: n = number of samples
Source: Data compiled by Turnpenny Horsfield Associates and AECOM

The sample-size tables for ambient light level and ACV (Tables 6-40 and 6-42) show greater than 20 samples for every combination of species, light level, and ACV. There were no differences in P_E between juvenile Chinook salmon and steelhead for any light level or ACV level (Tables 6-41 and 6-43).

Table 6-40
Summary of Protection Efficiency Samples for Tagged Juvenile Chinook Salmon and Steelhead at Low and High Ambient Light Levels in 2011

Ambient Light Level	Chinook Salmon (n)	Steelhead (n)	Total (n)
Low Light (<5.4 lux)	25	26	51
High Light (≥5.4 lux)	28	51	79

Note: n = number of samples
Source: Data compiled by Turnpenny Horsfield Associates and AECOM

Table 6-41
Mean Protection Efficiency for Tagged Juvenile Chinook Salmon and Steelhead at Low and High Ambient Light Levels in 2011

Ambient Light Level	Chinook Salmon	Steelhead	Percentage Point Change	Kruskal-Wallis X^2	P-Value
Low Light (<5.4 lux)	0.565	0.440	12.5	1.786	0.1814
High Light (≥5.4 lux)	0.581	0.516	6.5	1.112	0.2916

Source: Data compiled by Turnpenny Horsfield Associates and AECOM

Table 6-42
Summary of Protection Efficiency Samples for Tagged Juvenile Chinook Salmon and Steelhead at Low and High Average Channel Velocity Levels in 2011

Average Channel Velocity Level	Chinook Salmon (n)	Steelhead (n)	Total (n)
Low Velocity (<0.61 m/s)	29	38	67
High Velocity (≥0.61 m/s)	24	39	63

Note: n = number of samples; m/s = meters per second
Source: Data compiled by Turnpenny Horsfield Associates and AECOM

Table 6-43
Mean Protection Efficiency for Tagged Juvenile Chinook Salmon and Steelhead at Low and High Average Channel Velocity Levels in 2011

Average Channel Velocity Level	Chinook Salmon	Steelhead	Percentage Point Change	Kruskal-Wallis X^2	P-Value
Low Velocity (<0.61 meter per second)	0.545	0.473	7.2	1.384	0.2395
High Velocity (≥0.61 meter per second)	0.608	0.508	10.0	1.459	0.2271

Source: Data compiled by Turnpenny Horsfield Associates and AECOM

6.1.7 2012 RESULTS

SIZE AND SOURCE OF JUVENILE CHINOOK SALMON AND STEELHEAD USED

The juvenile Chinook salmon tagged and released in 2012 were similar in size to those released in 2010 and 2011 and came from the Merced River Hatchery (Table 5-1). Similar to 2011, the tagged juvenile steelhead released in 2012 were larger than the tagged juvenile Chinook salmon (Table 5-1). In 2012, the Mokelumne River Hatchery was the source of juvenile steelhead.

PHYSICAL BARRIER OVERALL AND PROTECTION EFFICIENCY—CHINOOK SALMON

In 2012, there were 21 to 27 samples of tagged juvenile Chinook salmon for which O_E and P_E could be calculated (Table 6-44).[1] The number of samples available for P_E was always less than or equal to the number of samples of O_E because, for some samples, enough juvenile Chinook salmon were eaten to remove the samples from P_E consideration due to insufficient sample size (n <2). With a physical rock barrier installed, 61.8% of tagged juvenile Chinook salmon continued down the San Joaquin River. In contrast, 100% of tagged juvenile Chinook salmon that were not eaten continued down the San Joaquin River. In addition, the mean proportion of flow into the San Joaquin River during the study period was 82% (Table 3-1). Thus, the proportion of juvenile Chinook salmon remaining in the San Joaquin River was higher than the proportion of flow.

[1] Note: The BAFF 2010 line was used in 2010, 2011, and 2012 for a consistent reference line across years.

Table 6-44
Physical Rock Barrier Statistics for Tagged Juvenile Chinook Salmon in 2012

Efficiency Type	Mean	Standard Deviation	Minimum	Maximum	Number of Samples (n)
O_E	0.618	0.321	0.000	1.000	27
P_E	1.000	0.000	1.000	1.000	21

Note: n = number of samples
Source: Data compiled by Turnpenny Horsfield Associates and AECOM

Tagged juvenile Chinook salmon passed through the HOR study area at various ambient light levels (Figure 6-7). When the 2012 juvenile Chinook salmon were placed into samples and the O_E samples were partitioned by light level, 11 to 16 samples were found (Table 6-45). Tagged juvenile Chinook salmon passed through the HOR study area at various ACV levels (Figure 6-8). When the 2012 juvenile Chinook salmon were placed into samples, no samples were obtained at ACVs greater than 0.61 m/s.

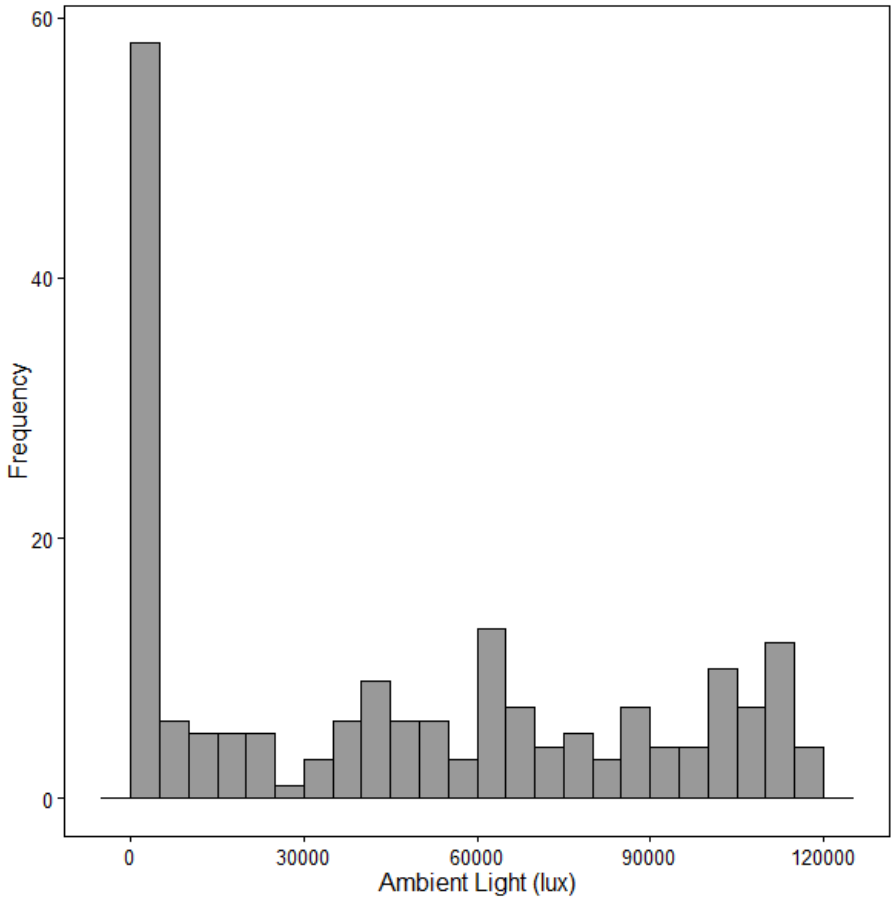

Source: Data compiled by Turnpenny Horsfield Associates and AECOM

Figure 6-7 Frequency Histogram of 2012 Light-Level Observations (collected at CIMIS, Station #70–Manteca, 37.834822, -121.223194) Obtained for Each Tagged Juvenile Chinook Salmon when the Individual was Nearest the 2010 BAFF Line

Table 6-45
Statistics for Overall Efficiency for Tagged Juvenile Chinook Salmon at Low and High Ambient Light Levels in 2012

Statistic	Low Ambient Light (<5.4 lux)	High Ambient Light (≥5.4 lux)	Percentage Point Change	Kruskal-Wallis X^2	P-Value
Mean	0.868	0.446	42.2	12.204	0.0005
Standard Deviation	0.203	0.271			
Minimum	0.500	0.000			
Maximum	1.000	0.842			
Samples (n)	11	16			

Note: n = number of samples
Source: Data compiled by Turnpenny Horsfield Associates and AECOM

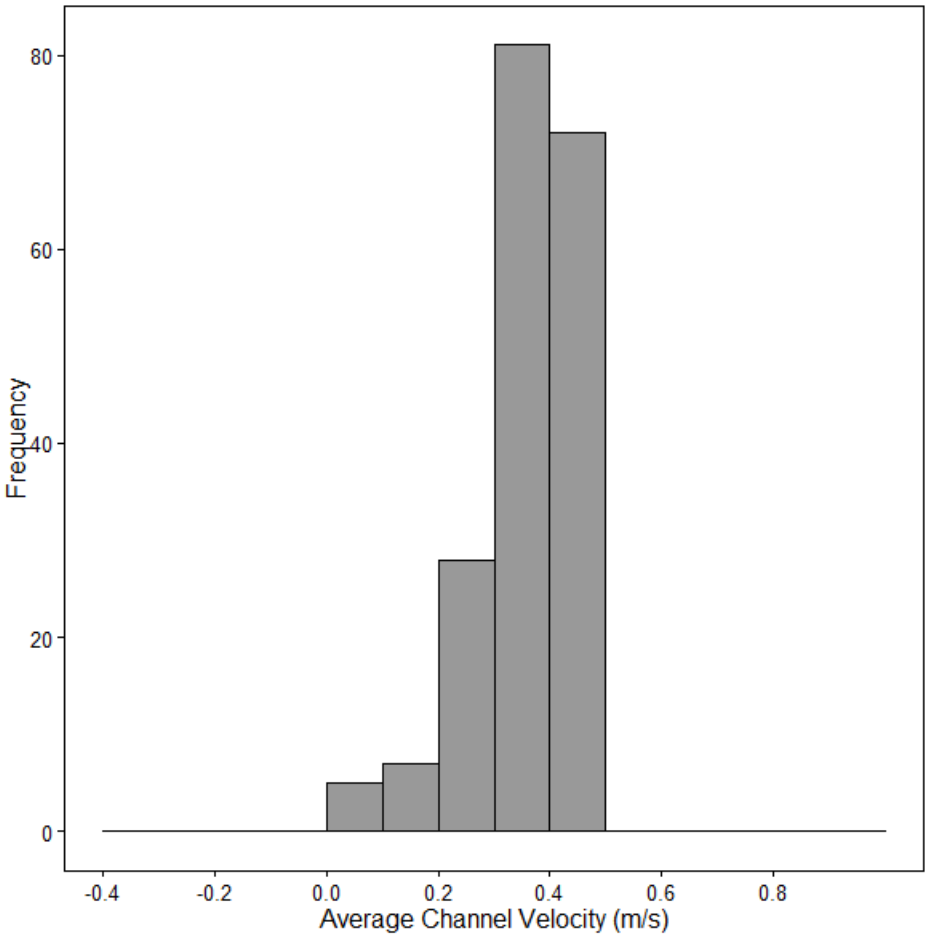

Source: Data compiled by Turnpenny Horsfield Associates and AECOM

Figure 6-8 **Frequency Histogram of 2012 Average Channel Velocity Observations (SJL Gauge) Obtained for Each Tagged Juvenile Chinook Salmon when the Individual was Nearest the 2010 BAFF Line**

In 2012, the mean O_E for tagged juvenile Chinook salmon was 42.2 percentage points greater for tagged juvenile Chinook salmon encountering the rock barrier in low-light levels than for tagged juvenile Chinook salmon encountering the barrier in high-light levels (Table 6-45). This difference was statistically significant, and may have been a result of higher predation rates at high-light levels, a feature that was apparent from GLM of juvenile Chinook salmon for 2009 through 2012 data (see Section 6.2.2). This is explored further under in Section 6.2.1, "Proportion Eaten (Univariate Analyses)."

When tags implanted in juvenile Chinook salmon and subsequently determined to have been eaten by predators were removed from consideration, the physical rock barrier's P_E was 100% efficient for both low- and high-light levels. In addition, P_E was not different for juvenile Chinook salmon that encountered the rock barrier at different light levels (Table 6-46). This result supports the hypothesis that the large difference in O_E under varying light levels (Table 6-45) was due to greater predation on juvenile Chinook salmon during the day. As noted previously, this topic is explored further under in Section 6.2.1, "Proportion Eaten (Univariate Analyses)."

Table 6-46
Statistics for Protection Efficiency for Tagged Juvenile Chinook Salmon at Low and High Ambient Light Levels in 2012

Statistic	Low Ambient Light (<5.4 lux)	High Ambient Light (≥5.4 lux)	Percentage Point Change	Kruskal-Wallis X^2	P-Value
Mean	1.000	1.000	0.0	NA	NA
Standard Deviation	0.000	0.000			
Minimum	1.000	1.000			
Maximum	1.000	1.000			
Samples (n)	10	11			

Note: n = number of samples
Source: Data compiled by Turnpenny Horsfield Associates and AECOM

OVERALL AND PROTECTION EFFICIENCY—STEELHEAD

Of the five tagged steelhead that arrived at the HOR study area in 2012, one was eaten in the study area and four went down the San Joaquin River. Thus, the grand O_E for steelhead in 2012 was 0.800, and the grand P_E was 1.000.

6.1.8 COMPARISON AMONG CONDITIONS FROM 2009 (BAFF ON), 2010 (BAFF ON), 2011 (NO BARRIER), AND 2012 (PHYSICAL ROCK BARRIER)

OVERALL EFFICIENCY—CHINOOK SALMON

O_E was significantly different between barrier treatments at the HOR study area (Kruskal-Wallis $X^2 = 34.311$, P-value <0.0001). Hypothesis $H7_0$ was rejected. The BAFF showed no difference in O_E in 2009 compared to 2010 (Table 6-26); therefore, the 2009 "BAFF On" statistics were grouped with the 2010 "BAFF On" statistics (Table 6-47). Because the data did not meet the assumptions of ANOVA, three nonparametric two-sample comparisons were made between treatments: 2010 compared to 2011; 2010 compared to 2012; and 2011 compared to 2012.

To make multiple two-sample comparisons, a Bonferroni-method reduction of the critical alpha was employed to control the experiment-wise error rate: 0.05/3 = 0.0167 (Sokal and Rohlf 1995). The only two-sample comparison that was not among these three tests was 2011 compared to 2012 (Kruskal-Wallis $X^2 = 2.759$, P-value = 0.0967). The statistical power of this last test was 0.885, which exceeds the conventional value of 0.80 (Cohen 1988). Thus, it was concluded that there is likely no true difference between O_E of 2011 compared to 2012.

It was concluded that the BAFF produced the lowest O_E among the three treatment types. There was no difference in "no barrier" O_E and "physical rock barrier" O_E.

Table 6-47
Statistics for Overall Efficiency from 2009–2012

Treatment—Year	Mean	Standard Deviation	Number of Samples (n)	Statistical Grouping
BAFF On—2009	0.209	0.218	21	a
BAFF On—2010	0.355	0.243	19	a
No Barrier—2011	0.519	0.160	53	b
Rock Barrier—2012	0.618	0.321	27	b

Note: BAFF = bio-acoustic fish fence; n = number of samples
Source: Data compiled by Turnpenny Horsfield Associates and AECOM

PROTECTION EFFICIENCY—CHINOOK SALMON

P_E was significantly different between barrier treatments at the HOR study area (Kruskal-Wallis $X^2 = 49.630$, P-value <0.0001). Hypothesis $H7_0$ was rejected. The BAFF showed no significant difference in P_E in 2009 compared to 2010 (Table 6-28); therefore, the 2009 "BAFF On" statistics were grouped with the 2010 "BAFF On" statistics (Table 6-48). Because the data did not meet the assumptions of ANOVA, three nonparametric two-sample comparisons were made between treatments (i.e., 2010 compared to 2011; 2010 compared to 2012; and 2011 compared to 2012). As noted above, the critical alpha for these comparisons was 0.0167. The 2010 and 2011 data met the assumptions of ANOVA, and the pairwise comparison used this traditional parametric statistical approach (F = 6.413, P-value = 0.0136).

Table 6-48
Statistics for Protection Efficiency from 2009–2012

Treatment—Year	Mean	Standard Deviation	Number of Samples (n)	Statistical Grouping
BAFF On—2009	0.338	0.330	18	a
BAFF On—2010	0.441	0.239	19	a
No Barrier—2011	0.574	0.178	53	b
Rock Barrier—2012	1.000	0.000	21	c

Note: BAFF = bio-acoustic fish fence; n = number of samples
Source: Data compiled by Turnpenny Horsfield Associates and AECOM

It was concluded that the BAFFs in 2009 and 2010 grouped together had the lowest P_E among the three treatment types (Table 6-48). However, once eaten tags were removed, leaving only surviving tags-in-Chinook-salmon, there was considerable improvement in P_E compared to O_E (compare Tables 6-47 and 6-48). In contrast to the O_E results, there was a difference in "no barrier" P_E and "physical rock barrier" P_E. The rock barrier P_E for surviving tags-in-Chinook-salmon was 100%. The mean proportion of flow passing through the culverts was 18% (Table 3-1), which was higher than the percentage of juvenile Chinook salmon passing down Old River. Note that two juvenile Chinook salmon were actually detected passing through the culverts, but these were subsequently preyed upon in the HOR study area downstream of the rock barrier, so their fate was not recorded as "Old River" but as "Predation."

6.2 PREDATION ON JUVENILE SALMONIDS INCLUDING BARRIER EFFECTS

6.2.1 PROPORTION EATEN (UNIVARIATE ANALYSES)

2009 RESULTS

In 2009, the proportion of juvenile Chinook salmon determined to have been eaten with the BAFF on and off combined was 22.9% in the HOR study area. Thus, the percentage uneaten was 77.1%; this value was similar to that reported for 2009 survival in the Mossdale-to-HOR reach, 83.0%, by SJRGA (2010). The proportion eaten was 15.2% higher with the BAFF on than with the BAFF off, and this difference was significant (Table 6-49). Hypothesis $H8_0$ was rejected. These results suggested that the BAFF caused an increase in predation when it was operated in 2009.

Table 6-49
Proportion of Juvenile Chinook Eaten Statistics for BAFF Operations in 2009

Statistic	BAFF On	BAFF Off	Percentage Point Change	Kruskal-Wallis X^{2a}	P-Value[a]
Mean Sample Proportion Eaten[a]	0.290	0.138	15.2	5.391	0.0202
Standard Deviation[a]	0.216	0.167			
Samples (n)[a]	21	27			
Population Proportion Eaten[b]	0.309	0.164	14.5		
Standard Error[b]	0.030	0.022			

Notes: BAFF = bio-acoustic fish fence; n = number of samples
[a] Sample proportion eaten parameters
[b] Population proportion eaten parameters
Source: Present study

2010 RESULTS

The proportion of juvenile Chinook salmon eaten with the BAFF on and off combined was 25.9% in the HOR study area. Because the proportion eaten reported in 2009 was 22.9%, it appeared that in both years the BAFF was studied (2009 and 2010), the predation rate was consistent. In contrast to 2009, in 2010, the proportion eaten was 0.5 percentage point higher with the BAFF on than off; this difference was not statistically significant (Table 6-50). Hypothesis $H8_0$ was accepted. It is not known why this difference occurred in 2009 but not in 2010.

Table 6-50
Proportion of Juvenile Chinook Eaten Statistics for BAFF Operations in 2010

Statistic	BAFF On	BAFF Off	Percentage Point Change	Kruskal-Wallis X^2[b]	P-Value[b]
Mean Sample Proportion Eaten[a]	0.217	0.212	0.5	0.051	0.8218
Standard Deviation[a]	0.217	0.167			
Samples (n)[a]	19	22			
Population Proportion Eaten[b]	0.310	0.205			
Standard Error[b]	0.030	0.027			

Notes: BAFF = bio-acoustic fish fence; n = number of samples
[a] Sample proportion eaten parameters
[b] Population proportion eaten parameters
Source: Present study

The major differences between the two years were the lower mean turbidities and lower discharge magnitudes in 2009. These results suggest an area of interesting future inquiry. It was notable that, for 2010, the sample proportion eaten with the BAFF on, 0.217, was lower than the population proportion eaten, 0.310. This difference was a result of how the tags were sorted into samples: Of the 19 samples in question, seven samples, each containing two to 11 tags, had a proportion eaten of zero. In contrast, the remaining 12 samples ranged in size from six to 28 tags, with an average proportion eaten of 0.344, which was consistent with the population proportion eaten.

2009 COMPARED TO 2010

The number of proportion eaten samples ranged from 19 to 27 in 2009 and 2010 (Table 6-51). In 2009, the ratio of proportion eaten with the BAFF on compared to the BAFF off was 1.88, and that was similar to the ratio in 2010 (1.51), suggesting similar predation pressure between years. In 2009, the proportion of tags eaten was not statistically different from the proportion eaten in 2010 (Table 6-52) for the BAFF on or off. However, the statistical power of the test for the BAFF off was only 0.426, and the P-value for the comparison between 2009 and 2010 with the BAFF off was 0.0749. Thus, it is possible that there was a difference in the "BAFF off" proportion eaten in 2009 compared to 2010, and low power made it difficult to resolve.

Table 6-51
Proportion of Juvenile Chinook Eaten Samples with BAFF Operations—2009 vs. 2010

Treatment	2009 (n)	2010 (n)	Total (n)
BAFF On	21	19	40
BAFF Off	27	22	49

Notes: BAFF = bio-acoustic fish fence; n = number of samples
Source: Present study

Table 6-52
Proportion of Juvenile Chinook Eaten Statistics with BAFF Operations—2009 vs. 2010

Sample Proportion Eaten					
Treatment	2009 Mean Proportion Eaten[a]	2010, Mean Proportion Eaten[a]	Percentage Point Change	Kruskal-Wallis X^2[a]	P-value[a]
BAFF On	0.290	0.217	7.3	1.530	0.2161
BAFF Off	0.138	0.212	-7.4	3.173	0.0749
Population Proportion Eaten					
Treatment	2009 Proportion Eaten[b]	2010 Proportion Eaten[b]	Percentage Point Change		
BAFF On	0.309	0.310	-0.1		
BAFF Off	0.164	0.205	-4.1		
Ratio On/Off	1.88	1.51			

Notes: BAFF = bio-acoustic fish fence

[a] Sample proportion eaten parameters are those derived from the proportion eaten of each group of fish that arrived at the HOR study area forming a single sample (see Section 5.2.1 in Chapter 5, "Methods," for the definition of a sample).

[b] Population proportion eaten parameters are those derived from the grand total eaten divided by the total number of tags in juvenile Chinook salmon (see definition in Section 5.3.1 in Chapter 5, "Methods").

Source: Present study

Another method to evaluate predation on juvenile Chinook salmon was to pool the proportion eaten with the BAFF on for 2009 and 2010. Then, the proportion eaten observations for the BAFF off were pooled for 2009 and 2010. There was no difference between the BAFF on proportion eaten (mean = 0.256) and the BAFF-off proportion eaten (mean = 0.171) when the years were pooled (Kruskal Wallis $X^2 = 3.043$, P = 0.0811); however, the statistical power of the test was low (0.427). It was concluded that it might not have been possible to resolve a true difference, given the sample size and power achieved.

COMPARISON OF 2009 BAFF OFF, 2010 BAFF OFF, AND 2011 CONDITIONS

In Table 6-53, the proportion of tags eaten was not significantly different between "BAFF Off—2009" and "No Barrier—2011" at the HOR study area (Kruskal-Wallis $X^2 = 0.523$, P-value = 0.4694). Additionally, the proportion of tags eaten was not significantly different between "BAFF Off—2009" and "BAFF Off—2010" (Table 6-52). The proportion of tags eaten was significantly different between "BAFF Off—2010" and "No Barrier—2011" at the HOR study area (Kruskal-Wallis $X^2 = 10.989$, P-value = 0.0009). The "No Barrier—2011" treatment produced the lowest predation level among all years studied at 0.101.

This may have been related to high discharge in 2011, resulting in several potential changes in the environment: (1) higher channel velocities that increased the salmonid juvenile transit rates (see Appendix D, "Transit Speed Analyses," Table D-13); (2) increased stage height that caused the predators to search a larger volume of water; (3) greater energetic cost for predators to swim in the thalweg than in other years, potentially reducing searched volume; (4) lower habitat suitability and fewer predators inhabiting the area; and/or (5) greater turbidity and, therefore, less ability for predators to see prey. Factors influencing predation rate are analyzed further in Section 6.2.2, "Probability of Predation (Generalized Linear Modeling)."

Table 6-53
Statistics for Proportion of Juvenile Chinook Eaten, 2009, 2010, and 2011

Sample Proportion Eaten				
Treatment—Year	Proportion Eaten[1]	Standard Deviation[1]	Number of Samples (n)[1]	Statistical Grouping[2]
BAFF Off—2009	0.138	0.167	27	ab
BAFF Off—2010	0.212	0.167	22	a
No Barrier—2011	0.087	0.091	53	b
Population Proportion Eaten				
Treatment—Year	Proportion Eaten[2]	Standard Error[2]		
BAFF Off—2009	0.164	0.022		
BAFF Off—2010	0.205	0.027		
No Barrier—2011	0.101	0.009		

Notes: BAFF = bio-acoustic fish fence

[1] Sample proportion eaten parameters are those derived from the proportion eaten of each group of fish that arrived at the HOR study area forming a single sample (see Section 5.2.1 in Chapter 5, "Methods," for the definition of a sample).

[2] Population proportion eaten parameters are those derived from the grand total eaten divided by the total number of tags in juvenile Chinook salmon (see definition in Section 5.3.1 in Chapter 5, "Methods").

Source: Present study

2011 Chinook Salmon Compared to Steelhead

For 2011, the proportion of juvenile Chinook salmon determined to have been eaten was 0.087, and the proportion of juvenile steelhead determined to have been eaten was 0.243; this difference was significant (Table 6-54). Hypothesis $H9_0$ was rejected. However, there were two important related concepts: (1) there was a greater likelihood of steelhead being incorrectly assigned a fate of "eaten" compared to juvenile Chinook salmon (see the subsection entitled "Chinook Salmon Compared to Steelhead" in Section 7.1.4, "2011 No Barrier", of Chapter 7, "Discussion"); and (2) the juvenile steelhead used in this study were much larger than juvenile Chinook salmon (see Table 5-1 in Chapter 5, "Methods") and, therefore, probably had better swimming capabilities.

There were major differences in the behavior pattern of juvenile Chinook salmon and steelhead determined to have not been eaten at the HOR study area. Juvenile Chinook salmon had a consistent downstream migratory pattern, but steelhead swam upstream on occasion and even had some looping patterns. The similarity between steelhead behavior and predator behavior was at times difficult to distinguish. Thus, many steelhead may have been inappropriately classified as eaten. It is hypothesized that the statistical difference between juvenile Chinook salmon and steelhead proportion eaten was not because of "real" differences between the species, but because of misclassification errors in assigning predation to steelhead two-dimensional tracks. This hypothesis was supported by the observation that, after "eaten" tags were removed, juvenile Chinook salmon and steelhead P_E was not different (Table 6-39).

Table 6-54
Statistics for Proportion Eaten for Chinook Salmon and Steelhead in 2011

Statistic	Chinook Salmon	Steelhead	Percentage Point Change	Kruskal-Wallis X^{2a}	P-Value[a]
Mean Sample Proportion Eaten[a]	0.087	0.243	-15.6	13.463	0.0002
Standard Deviation[a]	0.091	0.238			
Samples (n)[a]	53	93			
Proportion Eaten[b]	0.101	0.240			
Standard Error[b]	0.009	0.019			

Notes: n = number of samples.

[a] Sample proportion eaten parameters are those derived from the proportion eaten of each group of fish that arrived at the HOR study area forming a single sample (see Section 5.2.1 in Chapter 5, "Methods," for the definition of a sample).

[b] Population proportion eaten parameters are those derived from the grand total eaten divided by the total number of tags in juvenile Chinook salmon (see definition in Section 5.3.1 in Chapter 5, "Methods").

Source: Present study

2012 RESULTS

Chinook Salmon

In 2012, 39.3% of the tagged juvenile Chinook salmon were identified as having been eaten (Table 6-55). This was the highest proportion eaten observed in this study for any treatment/year combination, and was examined further in relation to the barrier treatments (see "Comparison of 2009 [BAFF On], 2010 [BAFF On], 2011[No Barrier], and 2012 [Rock Barrier] Conditions," below).

Table 6-55
Statistics for Proportion Eaten, 2009–2012

Sample Proportion Eaten				
Treatment—Year	Proportion Eaten[1]	Standard Deviation[1]	Number of Samples (n)[1]	Statistical Grouping[1]
BAFF On—2009	0.290	0.216	21	ab
BAFF On—2010	0.217	0.217	19	ab
No Barrier—2011	0.087	0.091	53	a
Rock Barrier—2012	0.382	0.321	27	b
Population Proportion Eaten				
Treatment—Year	Proportion Eaten[2]	Standard Error (SE)[2]		
BAFF On—2009	0.309	0.030		
BAFF On—2010	0.310	0.030		
No Barrier—2011	0.101	0.009		
Rock Barrier—2012	0.394	0.035		

Notes: BAFF = bio-acoustic fish fence; n = number of samples

[1] Sample proportion eaten parameters are those derived from the proportion eaten of each group of fish that arrived at the HOR study area forming a single sample (see Section 5.2.1 in Chapter 5, "Methods," for the definition of a sample).

[2] Population proportion eaten parameters are those derived from the grand total eaten divided by the total number of tags in juvenile Chinook salmon (see definition in Section 5.3.1 in Chapter 5, "Methods").

Source: Present study

The proportion of tagged juvenile Chinook salmon classified as having been eaten at the HOR study area under different ambient light levels supported the hypothesis that the large difference in O_E, between low-light and high-light conditions, was due to greater predation on juvenile Chinook salmon during the day (see Section 6.1.7). In high-light conditions, the mean proportion of tagged juvenile Chinook salmon that were determined to have been eaten at the HOR study area was 42.3 percentage points greater than the proportion determined to have been eaten in low light (Table 6-56). A large difference in predation rates between low and high light was expected because the predators were primarily visual, and was one of the main hypotheses examined with GLM analysis (see Section 6.2.2, "Probability of Predation [Generalized Linear Modeling]"). This also is discussed in Section 7.2, "Predation on Juvenile Salmonids Including Barrier Effects," in Section 7, "Discussion".

Table 6-56
Statistics for Sample Proportion of Chinook Salmon Tags Eaten at Low and High Ambient Light Levels in 2012

Statistic	Low Ambient Light (<5.4 lux)	High Ambient Light (≥5.4 lux)	Percentage Point Change	Kruskal-Wallis X^2	P-Value
Mean	0.131	0.554	-42.3	12.204	0.0005
Standard Deviation	0.203	0.271			
Minimum	0.000	0.158			
Maximum	0.500	1.000			
Samples (n)	11	16			

Note: n = number of samples
Source: Present study

Steelhead

Of the five tagged steelhead that arrived at the HOR study area in 2012, one was eaten in the study area, so the proportion eaten was 0.200.

WATER TEMPERATURE AND TURBIDITY EFFECTS ON PROPORTION EATEN

Samples from all years were considered together, and mean sample water temperature was positively correlated with proportion of juvenile Chinook salmon eaten (Spearman's $\rho = 0.264$, $P = 0.0005$, Figure 6-9). It was hypothesized that as water temperatures moved toward critically warmer temperatures for juvenile Chinook salmon (Table 3-4 in Section 3.3.1 of Section 3, "Physical Parameters"), predators gained an advantage over the juvenile salmonids in swimming performance and survival. It is also possible that increased water temperatures led to greater bioenergetic demands for prey consumption, thus increasing predation pressure at the warmer temperatures.

Similar to water temperature, turbidity samples from all years were considered together. In contrast to the effect of water temperature, turbidity was not correlated with proportion eaten for juvenile Chinook salmon (Spearman's $\rho = 0.098$, $P = 0.2034$, Figure 6-10). Further examination of water temperature and turbidity effects is provided with the GLM of predation probability (see Section 6.2.2, "Probability of Predation [Generalized Linear Modeling]").

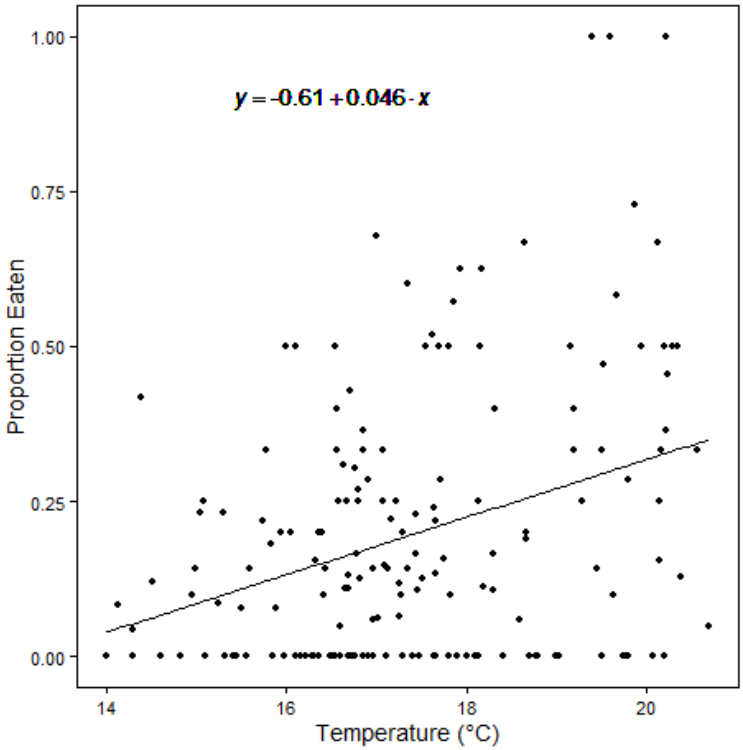

Source: Present study

Figure 6-9 Sample Mean Temperatures and Proportion of Tagged Juvenile Chinook Salmon Eaten During Fish Release Periods from 2009–2012 with Equation of Fitted Line Shown

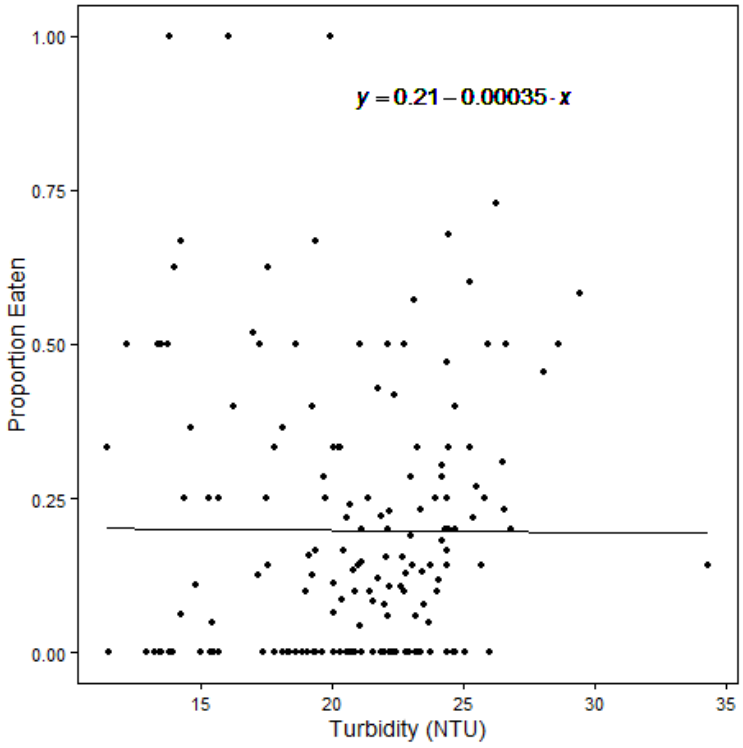

Source: Present study

Figure 6-10 Sample Mean Turbidities and Proportion of Tagged Juvenile Chinook Salmon Eaten During Fish Release Periods from 2009–2012 with Equation of Fitted Line Shown

COMPARISON OF 2009 (BAFF ON), 2010 (BAFF ON), 2011(NO BARRIER), AND 2012 (ROCK BARRIER) CONDITIONS

Proportion eaten was different between barrier treatments at the HOR study area (Kruskal-Wallis $X^2 = 20.505$, P-value = 0.0001). Hypothesis H_{10} was rejected. The BAFF showed no significant difference in proportion eaten in 2009 compared to 2010 (Table 6-52); therefore, the "BAFF On—2009" statistics were grouped with the "BAFF On—2010" statistics (Table 6-55). Because the data did not meet the assumptions of ANOVA, three nonparametric two-sample comparisons were made between treatments: 2010 compared to 2011; 2010 compared to 2012; and 2011 compared to 2012. As noted previously, the critical alpha for these comparisons was 0.0167. Only the two-sample comparison of 2011 vs. 2012 was significant (Kruskal-Wallis $X^2 = 77.938$, P-value <0.0001) (Table 6-55).

Among the three treatment/year types, "No Barrier—2011" produced a smaller proportion of tagged juveniles eaten (Table 6-55) compared to 2012. However, in 2011 the highest discharges were exhibited of all years studied (Appendix D, "Transit Speed Analyses," Table D-13). It was hypothesized that high discharges led to high ACVs, and these high ACVs reduced the proportion eaten by reducing predator/prey encounters. Other potential mechanisms are discussed in Section 7.1, "Predation on Juvenile Salmonids Including Barrier Effects," and Section 7.2, "Predation on Juvenile Salmonids Including Barrier Effects," in Section 7, "Discussion".

The proportion of tagged juvenile Chinook salmon that did not arrive at the HOR study area after release provided additional information about survival and predation for each year (Table 6-57). In 2009, 44.6% of the tagged juvenile Chinook salmon did not arrive at the study area, which indicated that the tags may have experienced a high predation rate prior to encountering the BAFF, and/or were more vulnerable to predation due to tag burden. In contrast, in 2010, just 11.2% of the tagged juvenile Chinook salmon did not arrive. In 2011, the high-discharge year, only a subset of tags was analyzed and so it is not possible to make inferences regarding the proportion of fish that never arrived at the HOR study area. The 2012 statistics included the highest proportion of tags eaten (39.3%), and also the highest percentage of tags released that never arrived (53.9%). Thus, it was hypothesized that the high rate of 2012 predation was not due solely to the presence of the physical rock barrier, but also was influenced by other factors contributing to greater predator numbers or better predator capture success in 2012 than in 2011 (see Sections 6.3.2, "Hydroacoustic Data," and 7.3.3, "Changes in Density of Predatory Fishes").

Table 6-57
Statistics for Chinook Salmon Tags Released and Arrived, 2009–2012

Treatment—Year	Released (n)	Arrived (n)	Never Arrived (n)	Proportion Never Arrived
BAFF—2009	960	532	428	0.446
BAFF—2010	508	451	57	0.112
No Barrier—20111	—	—	—	—
Rock Barrier—2012	419	193	226	0.539

Notes: BAFF = bio-acoustic fish fence; n = number of samples
[1] Only a subset of data were processed in 2011 and so the proportion not arriving in the study area is unknown.
Source: Present study

6.2.2 PROBABILITY OF PREDATION (GENERALIZED LINEAR MODELING)

CHINOOK SALMON

Of the 2,244 tagged juvenile Chinook salmon entering the HOR study area from 2009 through 2012, it was estimated that 422 were preyed upon (0.188, or approximately 19%) (Table 6-58). A lower proportion of juvenile Chinook salmon were preyed upon with the non-physical barrier (BAFF) turned off in 2009 and 2010 (0.182), compared to a noticeably higher proportion of juveniles that were preyed upon with the non-physical barrier turned on (0.310) and with the 2012 physical rock barrier (0.394). Approximately 0.10 of juveniles were preyed upon with no barrier (2011), which coincided with appreciably higher SJL discharge (mean of approximately 5,000 cfs) than in other years (mean of approximately 1,600 to 1,900 cfs). The proportion of juvenile Chinook salmon that were preyed upon was lower in the dark (<5.4 lux) than in the light (≥5.4 lux), and this pattern was consistent across all barrier treatments (Table 6-58). The magnitude of difference between predation proportion in the light and dark light levels ranged from double with the non-physical barrier turned off to approximately three times greater with the physical rock barrier.

GLM and modeling averaging of the 2009, 2010, and 2012 data for juvenile Chinook salmon found good support for the ambient light level, barrier status, and small-fish density predictors of predation probability, as indicated by coefficient 95% confidence intervals excluding zero and importance greater than 0.8 (Table 6-59).

The positive coefficient for the ambient light level predictor indicates a greater predation probability with increasing light level, which allowed acceptance of hypothesis H11 for this predictor (see "Objectives and Hypotheses Related to Probability of Predation" in Section 1.2.3, "Predation on Juvenile Salmonids Including Barrier Effects"). In contrast, the positive coefficient for the small-fish density predictor was contrary to the hypothesis that predation probability would be lower with greater density of small fish (i.e., greater safety in numbers for an individual juvenile entering the HOR study area).

The coefficients for the barrier status predictor indicated that there was greater predation probability with the physical rock barrier and with the non-physical barrier turned on (for which the 95% coefficient confidence intervals excluded zero) than with the non-physical barrier turned off (which was the baseline barrier treatment in the model [i.e., a value of zero]). This led to the rejection of the null hypothesis of no difference between barrier treatment included in H11. None of the other predictors of predation probability were well supported by the GLMs, and H11 was rejected for these predictors.

The GLMs with predictors included provided a better fit to the data than the intercept-only model. The full model with all predictors was the second-ranked model (out of 128 total models) and had AIC_c of 1,258.2, in comparison to AIC_c of 1,360.4 for the intercept-only model (rank 128) (Table F-1 in Appendix F, "Model Fit and Weight Tables from Results of Predation Probability Generalized Linear Modeling").

Table 6-58
Number and Proportion of Tagged Juvenile Chinook Salmon Preyed Upon at the Head of Old River in 2009, 2010, 2011, and 2012, with Means and Standard Deviations of Environmental Variables

Barrier/ Light Level	No. of Juveniles		Predation		Juvenile Length (mm)		Small-Fish Density (No./10,000 m^3)		Discharge (cfs)		Turbidity (NTU)		Temperature (°C)	
	Total	Predation	Proportion	SE	Mean	SD	Mean	SD	Mean	SD	Mean	SD	Mean	SD
1. Non-physical Barrier Off	511	93	0.182	0.017	101.8	8.6	2.7	2.6	1,642.5	1,240.7	21.1	5.1	17.6	1.8
a. Dark	136	14	0.103	0.026	103.3	8.8	2.6	2.3	1,723.5	1,283.9	21.0	4.4	17.1	1.4
b. Light	375	79	0.211	0.021	101.3	8.5	2.8	2.8	1,613.1	1,225.1	21.1	5.4	17.8	1.9
2.Non-physical Barrier On	465	144	0.310	0.021	102.6	8.9	2.7	2.4	1,740.4	1,270.4	23.0	4.6	17.5	1.6
a. Dark	105	10	0.095	0.029	103.6	8.4	2.6	2.6	1,342.2	1,547.9	21.4	4.2	17.1	1.5
b. Light	360	134	0.372	0.025	102.3	9.0	2.8	2.4	1,856.5	1,154.2	23.5	4.6	17.6	1.6
3.No Barrier	1,075	109	0.101	0.009	110.1	6.2	140.8	145.2	5,117.4	268.3	21.7	1.5	16.5	1.2
a. Dark	306	9	0.029	0.010	109.5	5.8	136.1	144.6	5,042.9	266.6	21.1	1.4	16.2	1.2
b. Light	769	100	0.130	0.012	110.4	6.3	142.6	145.5	5,147.1	263.3	22.0	1.4	16.7	1.2
4.Rock Barrier	193	76	0.394	0.035	110.0	7.4	4.1	2.3	1,855.4	465.1	17.2	3.1	18.6	0.9
a. Dark	38	6	0.158	0.059	106.4	6.2	3.2	1.9	1,880.2	382.7	18.0	3.5	19.0	0.9
b. Light	155	70	0.452	0.040	110.9	7.4	4.4	2.3	1,849.3	484.0	17.0	2.9	18.5	0.9
Total	2,244	422	0.188	0.008	106.7	8.4	69.0	121.8	3,345.8	1,904.6	21.5	3.8	17.2	1.6

Notes: Shaded rows indicate data used in GLM of predation probability for juvenile Chinook salmon in 2009, 2010, and 2012.
°C = degrees Celsius; cfs = cubic feet per second; m^3 = cubic meters; mm = millimeters; No. = number; NTU = nephelometric turbidity units; SD = standard deviation; SE = standard error; Dark <5.4 lux; Light ≥5.4 lux
Source: Present study

Table 6-59
Model-Averaged Coefficients, 95% Confidence Limits, and Variable Importance for Generalized Linear Modeling of Predation Probability of Tagged Juvenile Chinook Salmon at Head of Old River in 2009, 2010, and 2012

Variable	Estimate	95% Confidence Limits		Importance
		Lower	Upper	
Ambient Light	0.108	0.072	0.144	1.00
Barrier (Non-physical Barrier On)	0.605	0.285	0.924	1.00
Barrier (Physical Rock)	0.853	0.310	1.396	1.00
Small-Fish Density	0.222	0.049	0.394	0.96
Turbidity	0.035	-0.005	0.076	0.86
Juvenile Length	0.015	-0.011	0.041	0.72
Water Temperature	0.078	-0.059	0.215	0.71
Discharge	0.002	-0.003	0.007	0.44

Note: Barrier status coefficients are in relation to baseline estimates with the non-physical barrier turned off (Non-physical Barrier Off).
Source: Present study

The optimum threshold for the model-averaged predictor coefficients was 0.36 based on the maximum Kappa method. The Kappa statistic indicated that approximately 33% of all possible predation and survival fates were correctly predicted by the model-averaged coefficients, adjusting for correct predictions by chance. The percent of outcomes correctly classified was 73.5%. The model-averaged coefficients correctly predicted 51.4% of true positives (juveniles that had been preyed upon [i.e., sensitivity]) and 81.5% of true negatives (juveniles that had survived [i.e., specificity]), indicating a false positive classification of 19.5%. The area under ROC was 0.70, indicating that the model-averaged coefficients were at the lower end of the "acceptable discrimination" range (Hosmer and Lemeshow 2000: 162). Overall, the model-averaged predictors provided a reasonable representation of the predation probability in relation to the observed predation proportion, although the model somewhat underestimated the higher predation proportion that occurred in light conditions (Figure 6-11).

A second set of GLMs was used to assess the probability of predation on juvenile Chinook salmon for 2011 and 2012. As described in Section 5.3.2, "Probability of Predation (Generalized Linear Modeling)," this analysis included estimates of the density of large fish (greater than 30 cm TL) from mobile hydroacoustics as a potential indicator of predatory fish abundance at the HOR study area. Such estimates were not available for 2009 and 2010. These GLMs did not include barrier status as a predictor because discharge was considerably different between 2011 and 2012 and so confounded the barrier predictor. Table 6-60 summarizes the data used in this analysis. These data are a subset of the data from Table 6-58 because many juveniles had missing values for the large-fish density predictor (i.e., their entry into the study area did not coincide suitably with mobile hydroacoustic surveys).

Table 6-60
Number and Proportion of Tagged Juvenile Chinook Salmon Preyed Upon at the Head of Old River in 2011 and 2012, with Means and Standard Deviations of Environmental Variables

Barrier/ Light Level	No. of Juveniles		Predation		Juvenile Length (mm)		Large-Fish Density, Down (No./10,000 m^3)		Large-Fish Density, Side (No./10,000 m^3)		Small-Fish Density (No./10,000 m^3)		Discharge (cfs)		Turbidity (NTU)		Temperature (°C)	
	Total	Predation	Proportion	SE	Mean	SD	Mean	SD	Mean	SD	Mean	SD	Mean	SD	Mean	SD	Mean	SD
1.No Barrier	797	80	0.100	0.011	109.1	5.3	4.3	2.0	1.6	0.4	157.7	151.5	5,165.5	248.2	21.7	1.3	16.1	1.1
a. Dark	240	8	0.033	0.012	108.9	5.2	3.9	2.2	1.6	0.5	142.2	150.3	5,071.5	259.1	21.0	1.2	15.9	1.1
b. Light	557	72	0.129	0.014	109.2	5.3	4.4	1.9	1.6	0.4	164.4	151.7	5,206.0	232.1	22.0	1.3	16.2	1.1
2.Rock Barrier	79	30	0.380	0.055	110.5	7.6	144.3	143.7	6.1	2.1	3.7	1.1	1,850.0	478.1	16.7	2.9	18.7	1.0
a. Dark	15	3	0.200	0.103	105.5	5.2	136.2	149.4	6.0	2.1	4.1	1.4	1,976.0	328.7	17.4	2.6	18.8	1.0
b. Light	64	27	0.422	0.062	111.7	7.6	146.2	143.4	6.1	2.1	3.6	0.9	1,820.4	504.3	16.5	3.0	18.7	1.1
Total	876	110	0.126	0.011	109.3	5.5	16.9	58.8	2.0	1.5	143.8	151.1	4,866.5	989.7	21.2	2.1	16.4	1.3

Notes: °C = degrees Celsius; cfs = cubic feet per second; m^3 = cubic meters; mm = millimeters; No. = number; NTU = nephelometric turbidity units; SD = standard deviation; SE = standard error; Dark <5.4 lux; Light ≥5.4 lux.

Shaded rows indicate data used in GLM of predation probability for juvenile Chinook salmon in 2011 and 2012.

Source: Present study

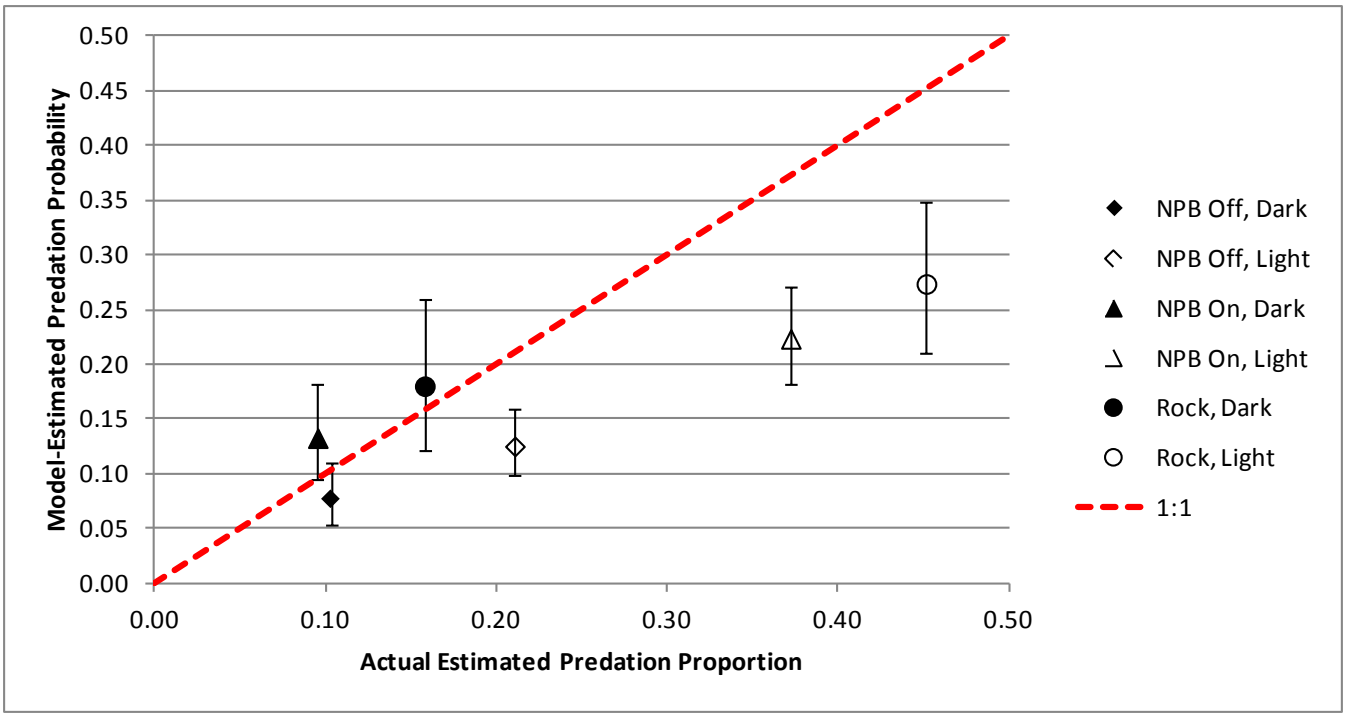

Note: NPB = non-physical barrier
Source: Present study

Figure 6-11 **Probability of Predation (with 95% Confidence Interval) of Tagged Juvenile Chinook Salmon at Head of Old River, Estimated from GLM in Relation to Observed Predation Proportion, for Various Combinations of Barrier Status and Light/Dark Conditions in 2009, 2010, and 2012**

Model-averaging indicated that only ambient light level and turbidity were well-supported predictors of the probability of predation on juvenile Chinook salmon in 2011 and 2012 (Table 6-61). The signs of the coefficients indicated support for hypothesis H12 that predation probability would be greater under higher visibility conditions (lower turbidity, higher light levels). None of the other predictors were well-supported from model-averaging (coefficient 95% confidence intervals included zero and importances were less than 0.8); hypothesis H12 was rejected for these predictors.

The GLMs including predictors provided a better fit to the data than the intercept-only model, with the full model having AIC_c = 593.3 (model rank = 17 out of 256 models) and the intercept-only model having AIC_c = 664.0 (ranked last out of all models) (Table F-2 in Appendix F, "Model Fit and Weight Tables from Results of Predation Probability Generalized Linear Modeling"). The optimum threshold for the model-averaged predictor coefficients was 0.18 based on the maximum Kappa method. The Kappa statistic indicated that approximately 29% of all possible predation and survival fates were correctly predicted by the model-averaged coefficients, adjusting for correct predictions by chance. The percent correctly classified was 82.8%. The model-averaged coefficients correctly predicted 43.6% of true positives (i.e., sensitivity) and 88.4% of true negatives (i.e., specificity), for a false positive classification of 11.6%. The area under the ROC was 0.73, which was slightly greater than the GLMs of predation probability in 2009, 2010, and 2012, and indicated that the model-averaged coefficients were within the "acceptable discrimination" range (Hosmer and Lemeshow 2000:162).

Table 6-61
Model-Averaged Coefficients, 95% Confidence Limits, and Variable Importance for the Generalized Linear Modeling of Predation Probability of Tagged Juvenile Chinook Salmon at the Head of Old River in 2011 and 2012

Variable	Estimate	95% Confidence Limits		Importance
		Lower	Upper	
Ambient Light	0.127	0.071	0.182	1.00
Turbidity	-0.270	-0.412	-0.129	1.00
Water Temperature	0.171	-0.105	0.448	0.74
Large-Fish Density (Down)	-0.126	-0.467	0.215	0.49
Juvenile Length	0.012	-0.024	0.047	0.44
Small-Fish Density	0.038	-0.109	0.184	0.39
Large-Fish Density (Side)	0.164	-0.580	0.908	0.35
Discharge	0.000	-0.005	0.005	0.31

Source: Present study

STEELHEAD

A total of 525 tagged juvenile steelhead entered the HOR study area in 2011 and 2012, and 126 (0.24, or 24%) were estimated to have been preyed upon (Table 6-62). Only five juveniles entered the area in 2012 when the physical rock barrier was present, and one was preyed upon. For 2011 (no barrier), the predation proportion was higher in light (0.261) than dark (0.182) conditions.

Only 2011 data were included in the GLM analysis for steelhead predation probability at the HOR study area. The desire to include large-fish density data from mobile hydroacoustics as an indication of predator abundance reduced sample size because steelhead entry did not always coincide with mobile hydroacoustics. Table 6-63 summarizes the data included in the steelhead GLM of predation probability for 163 steelhead entering the study area in 2011. GLMs with predictors included did not produce a better fit to the data than the intercept-only model. The full model with all predictors included ranked 250 out of 256 models, with an AIC_c of 199.0, which was higher than the intercept-only model (AIC_c = 192.1, rank = 16) (Table F-3 in Appendix F, "Model Fit and Weight Tables from Results of Predation Probability Generalized Linear Modeling"). The lack of support for all predictors of steelhead predation probability included in the GLM was also evident from model-averaged coefficients, for which all 95% confidence intervals included zero and importances were all less than 0.8.

Table 6-62
Number and Proportion of Tagged Juvenile Steelhead Preyed Upon at the Head of Old River in 2011 and 2012, with Means and Standard Deviations of Environmental Variables

	No. of Juveniles		Predation		Juvenile Length (mm)		Small-Fish Density (No./10,000 m^3)		Discharge (cfs)		Turbidity (NTU)		Temperature (°C)	
Barrier/Light	Total	Predation	Proportion	SE	Mean	SD	Mean	SD	Mean	SD	Mean	SD	Mean	SD
2011 No Barrier	520	125	0.240	0.019	282.2	23.3	69.3	119.7	5,424.4	857.7	21.8	2.3	16.4	1.1
a. Dark	137	25	0.182	0.033	279.5	20.4	80.5	131.9	5,603.4	947.8	20.9	1.8	16.6	1.2
b. Light	383	100	0.261	0.022	283.1	24.2	65.3	115.0	5,360.4	814.9	22.2	2.4	16.3	1.0
2012 Rock Barrier	5	1	0.200	0.179	242.8	14.0	3.6	0.6	1,320.8	635.2	15.0	3.2	19.2	0.3
a. Dark	2	0	0.000	0.000	232.0	2.8	3.7	0.3	1,223.0	589.7	13.2	1.0	19.2	0.6
b. Light	3	1	0.333	0.272	250.0	14.0	3.5	0.8	1,386.0	785.6	16.2	3.9	19.3	0.2
Total	525	126	0.240	0.019	281.8	23.6	68.7	119.3	5,385.4	943.9	21.8	2.4	16.4	1.1

Notes: °C = degrees Celsius; cfs = cubic feet per second; m^3 = cubic meters; mm = millimeters; No. = number; NTU = nephelometric turbidity units; SD = standard deviation; SE = standard error; Dark <5.4 lux; Light ≥5.4 lux

Source: Present study

Table 6-63
Number and Proportion of Tagged Juvenile Steelhead Preyed Upon at the Head of Old River in 2011 and 2012, with Means and Standard Deviations of Environmental Variables

	No. of Juveniles		Predation		Juvenile Length (mm)		Large-Fish Density, Down (No./10,000 m^3)		Large-Fish Density, Side (No./10,000 m^3)		Small-Fish Density (No./10,000 m^3)		Discharge (cfs)		Turbidity (NTU)		Temperature (°C)	
Barrier/Light	Total	Predation	Proportion	SE	Mean	SD	Mean	SD	Mean	SD	Mean	SD	Mean	SD	Mean	SD	Mean	SD
2011 No Barrier	163	44	0.270	0.035	284.9	24.3	4.6	2.0	1.8	0.6	132.8	143.8	5,116.3	239.4	22.1	1.3	16.2	0.9
a. Dark	44	8	0.182	0.058	282.3	22.3	4.9	1.9	1.7	0.5	156.6	157.0	5,036.4	278.2	21.2	1.0	16.0	0.9
b. Light	119	36	0.303	0.042	285.9	25.0	4.6	2.1	1.8	0.6	124.0	138.3	5,145.8	217.4	22.4	1.3	16.2	0.9
2012 Rock Barrier	4	0	0.000	0.000	238.5	11.8	311.2	19.5	8.3	0.1	3.8	0.2	1,133.5	551.5	13.7	1.8	19.2	0.3
a. Dark	2	0	0.000	0.000	232.0	2.8	320.9	27.5	8.3	0.1	3.7	0.3	1,223.0	589.7	13.2	1.0	19.2	0.6
b. Light	2	0	0.000	0.000	245.0	15.6	301.4	0.0	8.3	0.0	3.9	0.0	1,044.0	729.7	14.3	2.8	19.2	0.1
Total	167	44	0.263	0.034	283.8	25.1	12.0	47.1	1.9	1.2	129.7	143.5	5,020.9	659.2	21.9	1.8	16.2	1.0

Notes: °C = degrees Celsius; cfs = cubic feet per second; m^3 = cubic meters; mm = millimeters; No. = number; NTU = nephelometric turbidity units; SD = standard deviation; SE = standard error; Dark <5.4 lux; Light ≥5.4 lux

Shaded rows indicate data used in GLM of predation probability for juvenile steelhead in 2011.

Source: Present study

6.3 BEHAVIOR AND DENSITY CHANGES IN PREDATORY FISH

6.3.1 DATA FROM TAGGED PREDATORY FISH

OVERVIEW OF TAGGED PREDATORY FISH

One hundred predatory fish were captured, acoustically tagged, and released at the HOR study area from 2009 through 2012 (Table 6-64). However, only 82 were detected post-tagging within the acoustic arrays, which, when combined with an additional two fish tagged elsewhere in the system (both striped bass in 2010), provided an overall total of 84 fish for analysis. Only two fish were tagged in 2009 (largemouth bass tag code 4306 and striped bass tag code 4222), and only one fish was tagged in 2010 (striped bass tag code 2472). In 2011, 37 fish were tagged, of which three were largemouth bass (290 to 300 mm FL), 30 were striped bass (340 to 686 mm FL), and four were white catfish (255 to 375 mm FL). In 2012, 42 fish were tagged, of which six were channel catfish (305 to 625 mm TL; one released into Old River below the HOR physical rock barrier, the remainder San Joaquin River side of the physical rock barrier), 13 were largemouth bass (307 to 440 mm TL; six released into Old River below the physical rock barrier, the remainder into the San Joaquin River), 22 were striped bass (310 to 667 mm TL; 15 released into Old River below the physical rock barrier, the remainder upstream of the physical rock barrier), and one was a white catfish (320 mm TL, released into the San Joaquin River) (Table 6-64).

In the following sections describing the detailed results related to tagged predatory fish, fish tagged in 2012 are referred to either as being released into the HOR if they were released downstream of the physical rock barrier, or released into the San Joaquin River if they were released upstream of the physical rock barrier (either into the San Joaquin River or into Old River upstream).

RESIDENCE TIME

The approximate duration that tagged predatory fish spent within the detectable distance of the acoustic arrays at the HOR study area ranged from 0.01 hour (striped bass tag code 3366 in 2011) to 622 hours (white catfish tag code 3408 in 2011) (Table 6-64). There were considerable ranges in the length of time spent at the HOR study area by each species: channel catfish (0.08 to 71.5 hours), largemouth bass (0.11 to 242.6 hours), striped bass (0.01 to 282.6 hours), and white catfish (1.0 to 621.9 hours).

The percentage of dates between tagging/release and deactivation of the acoustic array was assessed to account for two factors: capture and tagging events occurring over a number of weeks (which affected the potential maximum duration that a fish could spend at the HOR study area), and the observation that some fish were detected on many dates but had relatively few positive detections by the array. Striped bass generally were detected on the smallest percentage of possible dates between tagging/release and acoustic array deactivation of the four predatory fish species. Striped bass had bootstrapped mean percentages of dates detected in all years of 10% to 20%, with bootstrapped 95% confidence intervals ranging from around 8% to 14% for 2011, and 2012 Old River releases from 4% to 38% for 2012 San Joaquin River releases (Figure 6-12).

The 95% confidence intervals of the percentage of dates when striped bass were detected in 2009 and 2010 (4.5 to 26%), 2011, and 2012 (Old River releases) did not overlap the 95% confidence intervals for largemouth bass in 2012 (San Joaquin River releases: 33 to 90%) or white catfish in 2011 (35 to 100%). They also had very little overlap with the 95% confidence interval for channel catfish released into Old River in 2012 (22 to 61%) (Figure 6-12).

Table 6-64
Tagged Predatory Fish at the Head of Old River, 2009-2012

Species	Length (mm FL unless noted in "Comments")	Tag Code	Tagging/ Release Date	Dates Detected in Study Area	Approx. Duration in Study Area (Hours)	Release Area	Comments
Channel Catfish	515	2511	4/22/2012	NA	Undetected	SJ River	Total Length
Channel Catfish	460	2847	5/9/2012	5/9/2012, 5/14/2012, 5/20/2012 to 5/24/2012, 5/26/2012, 5/27/2012	6.57	SJ River	Total Length
Channel Catfish	305	2490	5/20/2012	5/20/2012	4.76	SJ River	Total Length
Channel Catfish	625	2112	5/22/2012	5/22/2012	0.08	Old River	Total Length
Channel Catfish	473	2952	5/22/2012	5/22/2012, 5/23/2012, 5/27/2012, 5/29/2012	10.69	SJ River	Total Length
Channel Catfish	545	2763	5/23/2012	5/23/2012 to 5/28/2102	71.54	SJ River	Total Length
Channel Catfish	535	2994	5/23/2012	5/23/2012, 5/24/2012, 5/31/2012	3.54	SJ River	Total Length
Largemouth Bass	315	4306	5/6/2009	5/06/2009 to 5/16/2009	88.17		
Largemouth Bass	300	3324	5/24/2011	6/9/2011 to 6/11/2011, 6/13/2011, 6/15/2011 to 6/18/2011, 6/20/2011 to 6/22/2011	17.09		
Largemouth Bass	290	3436	5/24/2011	5/24/2011	0.11		
Largemouth Bass	320	3464	5/24/2011	NA	Undetected		
Largemouth Bass	290	3492	5/24/2011	5/25/2011 to 5/28/2011, 5/30/2011 to 6/1/2011, 6/7/2011, 6/9/2011, 6/13/2011, 6/15/2011, 6/16/2011, 6/21/2011, 6/22/2011	20.86		
Largemouth Bass	350	2049	4/22/2012	NA	Undetected	SJ River	Total Length
Largemouth Bass	440	2280	4/22/2012	4/23/2012, 4/27/2012, 5/17/2012, 5/18/2012	3.09	SJ River	Total Length
Largemouth Bass	440	2091	4/29/2012	4/29/2012, 5/10/2012, 5/12/2012 to 5/20/2012	96.61	Old River	Total Length
Largemouth Bass	360	2742	4/29/2012	4/29/2012, 5/5/2012	3.61	Old River	Total Length
Largemouth Bass	323	2322	5/6/2012	5/6/2012 to 5/9/2012, 5/11/2012 to 5/31/2012	242.57	Old River	Total Length
Largemouth Bass	350	2133	5/15/2012	5/15/2012	0.70	Old River	Total Length
Largemouth Bass	316	3078	5/18/2012	5/18/2012 to 5/27/2012	95.27	SJ River	Total Length
Largemouth Bass	420	2826	5/19/2012	NA	Undetected	Old River	Total Length
Largemouth Bass	335	3057	5/19/2012	5/19/2012	1.68	Old River	Total Length

Table 6-64
Tagged Predatory Fish at the Head of Old River, 2009-2012

Species	Length (mm FL unless noted in "Comments")	Tag Code	Tagging/ Release Date	Dates Detected in Study Area	Approx. Duration in Study Area (Hours)	Release Area	Comments
Largemouth Bass	323	2028	5/20/2012	5/20/2012 to 5/31/2012	182.51	SJ River	Total Length
Largemouth Bass	380	2196	5/20/2012	5/20/2012	0.45	Old River	Total Length
Largemouth Bass	395	2259	5/20/2012	5/20/2012 to 5/22/2012	39.13	SJ River	Total Length
Largemouth Bass	374	2070	5/22/2012	5/22/2012, 5/25/2012	3.07	SJ River	Total Length
Largemouth Bass	316	2301	5/22/2012	NA	Undetected	SJ River	Total Length
Largemouth Bass	307	2721	5/22/2012	5/22/2012 to 5/31/2012	192.89	SJ River	Total Length
Largemouth Bass	345	2532	5/23/2012	5/23/2012 to 5/31/2012	48.18	SJ River	Total Length
Largemouth Bass	332	3141	5/24/2012	NA	Undetected	SJ River	Total Length
Striped Bass	370	4222	5/12/2009	5/12/2009	0.26		
Striped Bass	406	2024	4/4/2010	4/28/2010, 5/7/2010	0.61		Tagged downstream of the HOR study area in San Joaquin River near Weston Ranch
Striped Bass	480	2976	5/5/2010	5/22/2010	0.54		Tagged downstream of the HOR study area at Tracy Fish Facility
Striped Bass	508	2472	5/16/2010	5/16/2010 to 5/18/2010	3.04		
Striped Bass	425	2136	5/14/2011	NA	Undetected		
Striped Bass	570	2234	5/14/2011	5/14/2011, 5/15/2011	7.14		
Striped Bass	405	2206	5/19/2011	5/19/2011	0.13		
Striped Bass	565	2262	5/19/2011	5/19/2011 to 5/28/2011	38.77		
Striped Bass	340	3422	5/19/2011	5/19/2011	0.20		
Striped Bass	405	2556	5/20/2011	5/20/2011, 5/28/2011	0.60		
Striped Bass	360	3338	5/20/2011	5/20/2011	0.07		
Striped Bass	330	3478	5/20/2011	NA	Undetected		
Striped Bass	415	2290	5/21/2011	5/21/2011, 5/23/2011 to 5/25/2011, 6/9/2011	5.90		

Table 6-64
Tagged Predatory Fish at the Head of Old River, 2009-2012

Species	Length (mm FL unless noted in "Comments")	Tag Code	Tagging/ Release Date	Dates Detected in Study Area	Approx. Duration in Study Area (Hours)	Release Area	Comments
Striped Bass	540	3060	5/21/2011	5/21/2011	0.66		
Striped Bass	405	3366	5/21/2011	5/21/2011	0.01		
Striped Bass	381	3380	5/22/2011	5/22/2011, 5/24/2011	0.19		
Striped Bass	390	3450	5/24/2011	5/24/2011, 5/27/2011, 6/22/2011	0.60		
Striped Bass	490	3074	5/26/2011	5/26/2011	0.07		
Striped Bass	350	2122	6/1/2011	6/1/2011	0.07		
Striped Bass	399	3172	6/2/2011	NA	Undetected		
Striped Bass	686	3382	6/2/2011	6/2/2011	0.09		
Striped Bass	360	3200	6/6/2011	NA	Undetected		
Striped Bass	385	3270	6/6/2011	6/6/2011	0.30		
Striped Bass	461	3298	6/6/2011	6/6/2011	7.40		
Striped Bass	544	2094	6/7/2011	NA	Undetected		
Striped Bass	445	2486	6/7/2011	6/7/2011, 6/8/2011	6.35		
Striped Bass	440	3340	6/7/2011	6/7/2011	12.99		
Striped Bass	374	3088	6/8/2011	6/8/2011, 6/9/2011	24.50		
Striped Bass	433	3144	6/8/2011	6/8/2011	0.06		
Striped Bass	455	3186	6/8/2011	6/8/2011	0.03		
Striped Bass	400	3242	6/8/2011	6/8/2011	0.05		
Striped Bass	410	3158	6/9/2011	6/9/2011	0.04		
Striped Bass	370	3284	6/9/2011	6/9/2011, 6/10/2011	0.81		
Striped Bass	395	2178	6/13/2011	6/13/2011	0.09		
Striped Bass	430	2248	6/13/2011	6/13/2011, 6/14/2011	2.44		
Striped Bass	420	2332	6/13/2011	NA	Undetected		
Striped Bass	390	3102	6/13/2011	NA	Undetected		

Table 6-64
Tagged Predatory Fish at the Head of Old River, 2009-2012

Species	Length (mm FL unless noted in "Comments")	Tag Code	Tagging/ Release Date	Dates Detected in Study Area	Approx. Duration in Study Area (Hours)	Release Area	Comments
Striped Bass	385	3130	6/13/2011	NA	Undetected		
Striped Bass	390	3312	6/13/2011	6/13/2011	0.07		
Striped Bass	580	3354	6/13/2011	6/13/2011	0.03		
Striped Bass	410	3368	6/13/2011	NA	Undetected		
Striped Bass	450	3228	6/14/2011	6/14/2011, 6/16/2011	7.57		
Striped Bass	620	3256	6/15/2011	6/15/2011, 6/16/2011, 6/18/2011	11.95		
Striped Bass	400	2007	4/24/2012	4/24/2012, 4/25/2012	0.66	SJ River	Total Length
Striped Bass	450	2238	4/24/2012	NA	Undetected	SJ River	Total Length
Striped Bass	405	2469	4/24/2012	4/24/2012	0.04	SJ River	Total Length
Striped Bass	411	2700	4/27/2012	4/27/2012	0.99	SJ River	Total Length
Striped Bass	398	2973	4/29/2012	4/29/2012, 5/1/2012, 5/2/2012, 5/25/2012	12.39	Old River	Total Length
Striped Bass	504	2154	5/6/2012	5/6/2012, 5/15/2012 to 5/26/2012, 5/29/2012 to 5/31/2012	282.60	SJ River	Total Length
Striped Bass	405	2385	5/6/2012	5/6/2012	0.05	SJ River	Total Length
Striped Bass	415	2553	5/6/2012	5/6/2012, 5/7/2012	8.53	Old River	Total Length
Striped Bass	420	2616	5/6/2012	5/6/2012	0.02	SJ River	Total Length
Striped Bass	450	2784	5/15/2012	5/15/2012	0.13	Old River	Total Length
Striped Bass	425	3015	5/15/2012	5/15/2012	8.73	Old River	Total Length
Striped Bass	433	2364	5/16/2012	5/16/2012	0.42	Old River	Total Length
Striped Bass	410	2595	5/16/2012	5/16/2012, 5/17/2012	12.14	Old River	Total Length
Striped Bass	310	2427	5/20/2012	5/20/2012, 5/21/2012	20.09	Old River	Total Length
Striped Bass	400	2658	5/21/2012	5/21/2012	1.61	Old River	Total Length
Striped Bass	355	2217	5/22/2012	5/22/2012	0.18	Old River	Total Length
Striped Bass	667	2343	5/22/2012	5/22/2012 to 5/25/2012	43.02	SJ River	Total Length

Table 6-64
Tagged Predatory Fish at the Head of Old River, 2009-2012

Species	Length (mm FL unless noted in "Comments")	Tag Code	Tagging/ Release Date	Dates Detected in Study Area	Approx. Duration in Study Area (Hours)	Release Area	Comments
Striped Bass	409	2889	5/22/2012	5/22/2012	0.23	Old River	Total Length
Striped Bass	401	3120	5/22/2012	5/22/2012	0.35	Old River	Total Length
Striped Bass	330	2448	5/24/2012	5/24/2012	0.20	Old River	Total Length
Striped Bass	440	2574	5/24/2012	5/24/2012	7.40	Old River	Total Length
Striped Bass	330	2679	5/24/2012	5/24/2012	0.11	Old River	Total Length
Striped Bass	325	2910	5/24/2012	5/24/2012	0.23	Old River	Total Length
White Catfish	255	3352	5/25/2011	5/25/2011 to 6/22/2011	572.04		
White Catfish	286	3394	5/25/2011	5/25/2011, 5/26/2011, 6/1/2011 to 6/22/2011	412.51		
White Catfish	280	3408	5/25/2011	5/25/2011 to 6/22/2011	621.88		
White Catfish	325	2598	6/6/2011	NA	Undetected		
White Catfish	375	2346	6/7/2011	6/7/2011, 6/9/2011	1.04		
White Catfish	405	3116	6/8/2011	NA	Undetected		
White Catfish	320	2931	4/27/2012	4/27/2012	1.54	SJ River	Total Length

Notes: HOR = Head of Old River; mm = millimeters; SJ = San Joaquin
Source: Present study

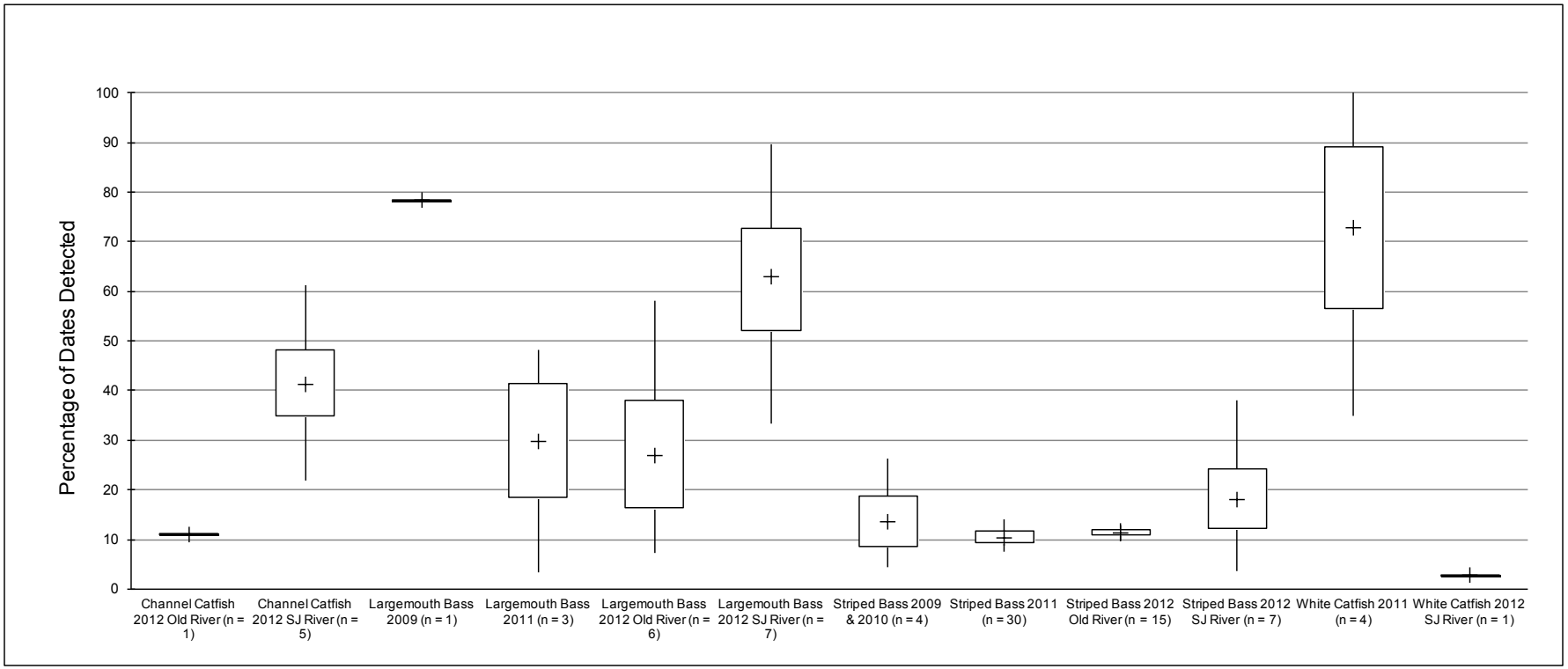

Source: Present study

Figure 6-12 **Percentage of Dates when Tagged Predatory Fish Were Detected within the HOR Study Area: Bootstrapped Mean (+), Interquartile Range (Box), and 95% Confidence Interval (Whiskers)**

The 95% confidence intervals of the percentage of dates detected generally overlapped for the other species/year/release location groups, probably as a result of relatively small sample size (i.e., few fish per group). Individual channel catfish (San Joaquin River release) and white catfish (Old River release) in 2012 were detected on a much lower percentage of dates than the 95% confidence intervals of dates detected for the other species/year/release location group of each of these species. The single largemouth bass tagged in 2009 was detected on nearly 80% of dates; this was within the 95% confidence interval for the 2012 San Joaquin River releases and greater than the 95% confidence intervals for 2011 (3.4 to 48%) and 2012 Old River (7 to 58%) releases of this species (Figure 6-12).

AREAS OCCUPIED AND EMIGRATION

Areas Occupied

A full summary of the percentage of total detections by zone for each of the 84 individual tagged predatory fish at the HOR study area is provided in Table 6-65. Zone location was presented in Figure 5-14 in the "Spatial Analysis" subsection of the "Data Analysis" subsection of Section 5.4.1, "Predatory Fish Acoustic Tagging." More detailed analyses were conducted only for fish with at least 1,000 detections in the study area. The following seven species/year/release location groups with more than one fish per group were evaluated:

- Channel catfish released in the San Joaquin River in 2012
- Largemouth bass released into the San Joaquin River in 2012 (i.e., upstream of the physical rock barrier)
- Largemouth bass released into the HOR in 2012 (i.e., downstream of the physical rock barrier)
- Striped bass released in 2011
- Striped bass released into the San Joaquin River in 2012 (i.e., upstream of the physical rock barrier)
- Striped bass released into the HOR in 2012 (i.e., downstream of the physical rock barrier)
- White catfish released in 2011

In addition, a summary of detections from a single largemouth bass tagged and released in 2009, as well as observations from several striped bass tagged and released in 2009 and 2010, were made in relation to the non-physical barrier (BAFF) installed in those years.

Channel Catfish

Channel catfish released on the San Joaquin River side of the physical rock barrier in 2012 (n = 5 fish) were detected most frequently at two locations (Figure 6-13):

- In the San Joaquin River downstream of the Old River divergence (San Joaquin River downstream offshore: bootstrapped mean = 29%, 95% confidence interval = 13–52%; the scour hole: bootstrapped mean = 23%, 95% confidence interval = 5–48%)
- At the HOR upstream (HOR study area upstream offshore: bootstrapped mean = 22%, 95% confidence interval = 7–38%)

Table 6-65
Percentage of Tag Detections by Zone for Predatory Fish at the Head of Old River, 2009–2012

Species/Year/Release Site	Tag Code	Total Detections	Dates in Area		Zones		San Joaquin River Upstream																																	San Joaquin River Downstream																										Head of Old River																							
							N				N				N	N	N								N	< 5 m 2010 NPB							< 5 m 2009 NPB							N				N		N			N	Scour Hole																N				N	< 5 m HORB ustr.					2012 HORB				< 5 m HORB dstr.					N				N
			First	Last	First	Last	1	2	3	4	5	6	7	8	9	10	11	12	13	14	15	16	17	18	19	20	21	22	23	24	25	26	27	28	29	30	31	32	33	34	35	36	37	38	39	40	41	42	43	44	45	46	47	48	49	50	51	52	53	54	55	56	57	58	59	60	61	62	63	64	65	66	67	68	69	70	71	72	73	74	75	76	77	78	79	80	81	82	83
Channel Catfish 2012 Old River	2112	153	22 May	22 May	71	81																																																																						1				2	10				10	41	21	16
Channel Catfish 2012 SJ River	2490	9,732	20 May	20 May	43	58																																		10	9				60	0	3	1	0	8		4		1		0		1	1	0	0	0	0	0	0																								
Channel Catfish 2012 SJ River	2763	102,050	23 May	28 May	67	2		0	0	0		0	0					0	0	0	0	1	0	0	0		0	0	0					0	0	0	0	1	0	1	2	0			3	0	1	0		6	2	6	3	1	0	0	0	4	4	0	0	0	0	0	0	0	0	1	40	0		1	0	3	0		0	16	0				0						
Channel Catfish 2012 SJ River	2847	6,347	9 May	22 May	42	2		1		1				4										1							0	0								1	2	1	0		6	0	11	1		6	0	5	0	6	0	3	0	10	20	12	3	0	1	2	1																								
Channel Catfish 2012 SJ River	2952	17,274	22 May	29 May	33	4		0	0	1		0	1	4				2	1	1	1	3	3	0	0		1	0	0	0	0	0		3	1	0	1	4	0	1	30				1					0																	2	36	0																			
Channel Catfish 2012 SJ River	2994	5,907	23 May	31 May	58	52		0	0			1	1					1	0	0	0	6	9	0	1		0	0	0	0				0	0			8	7	3	8	0			0	5	6			0		0						2	1				0	1			1	3	29			0		1	0			1											
Largemouth Bass 2009	4306	80,179	6 May	16 May	21	62											39	0	11								0						8	37	1																															1	4	0																						
Largemouth Bass 2011	3324	834	9 Jun	18 Jun	52	9				15	4			5	75																																											0																																
Largemouth Bass 2011	3436	32	24 May	24 May	36	59																																				31									34														34																								
Largemouth Bass 2011	3492	1,284	27 May	21 Jun	9	5				1	1			1	97																																																																									
Largemouth Bass 2012 Old River	2091	63,523	29 Apr	20 May	77	71																																																																					6	48	16	2	1	4	4	2	1	1	0	0	8	8
Largemouth Bass 2012 Old River	2133	219	15 May	15 May	71	82																																																																							1				3	3					26	42	25
Largemouth Bass 2012 Old River	2196	747	20 May	20 May	76	82																																																																					0	40	2			3	13	2			0	33	6
Largemouth Bass 2012 Old River	2322	150,067	6 May	31 May	72	71																																																													0	0			1	13	0		16	9	33	0	0	13	12	2	1	0
Largemouth Bass 2012 Old River	2742	4,341	29 Apr	5 May	80	82																																																																					0	9	1	0	0	1	8	1	0	1	0	0	47	31
Largemouth Bass 2012 Old River	3057	811	19 May	19 May	75	82																																																																						11	15			10	7	5			0	0	19	32
Largemouth Bass 2012 SJ River	2028	137,170	20 May	31 May	69	63																0			1												0	0	23	17				32	5	1			3		0																0	11	5		0	0	1	0	0	0	0	0										
Largemouth Bass 2012 SJ River	2070	4,849	22 May	25 May	60	6		2				2				1		4	2			2	0		1	1	1	1					0	1	1			0	0	8	2				8	16	9											5	0							0	14	2	4	3	0	2	3	0	0		0	1											
Largemouth Bass 2012 SJ River	2259	77,211	20 May	22 May	68	41		0				2	0			0		32	0		0	3	0	0	0	0	1	1		0	0	0		1	11			0	0	17	1	0			1	0	0			0																0	3	1	3	22		0		0	0		0	0	0										
Largemouth Bass 2012 SJ River	2280	5,401	23 Apr	18 May	4	52				0	1			5	7																											0	2	0		17	51	1	1		0							14	1	0				0	0																								
Largemouth Bass 2012 SJ River	2532	74,498	23 May	31 May	66	66	0	2				1				13	0	2	4		0	1	0	0	1	0	0	0					9	1	5	0		0	0	1	0	0			0	2	0				0		0		0		0	0	0	0		0				14	37	1	0	0	2	1	0	0	0	0	1	1	0										
Largemouth Bass 2012 SJ River	2721	310,489	22 May	31 May	33	9	0	0		1	3			54	42	0	0	0	0			0	0	0	0	0	0				0	0	0	0	0			0	0	0	0				0																					0	0	0	0	0	0	0	0	0	0	0	0	0										
Largemouth Bass 2012 SJ River	3078	121,293	18 May	27 May	63	41																4			0												0	0	13	1		0		5	44	25	0											6	1	0			0	0	0				1	0				0															
Striped Bass 2009 & 2010	2024	1,153	28 Apr	7 May	37	37				3	1			30	1								3	7							0	0							4		1	10	5	3				5	17		5		2											0	2																								
Striped Bass 2009 & 2010	2472	4,883	16 May	18 May	62	67		10	3	1		8	8	16	1							0	1	2							0	1						0	1		3	18	1	0			0	1	0	0	1	0	3		1	1	1	0	2	1	1	1	2	3	1		0	2	2			0	0															
Striped Bass 2009 & 2010	2976	688	22 May	22 May	62	2		3				5	2							12	3						2	4	3	12				2	4	8	17																															24				1	0				1												
Striped Bass 2009 & 2010	4222	301	12 May	12 May	8	8								77																	4	19																																																									
Striped Bass 2011	2122	101	1 Jun	1 Jun	25	53																		3							8	12										36									3		3		2		5		9	14	2	2	2																										
Striped Bass 2011	2178	159	13 Jun	13 Jun	35	63																16	21															9	8		21																										6	19																				
Striped Bass 2011	2206	249	19 May	19 May	9	9							9	82	8																																																																										
Striped Bass 2011	2234	6,042	14 May	15 May	3	58			0				0	1									1	8							3	0							0		13				1	0	2			42		23		0				1	1		0	0	0	0																									
Striped Bass 2011	2248	4,983	13 Jun	14 Jun	36	18																0	18	44														0	12		15	1								2	1	4	0	1		0		0	1	1	0			0																								
Striped Bass 2011	2262	31,753	19 May	28 May	42	58	1	7	0	0		3	0	4	20	1	0	6	1	1	1	8	2	0	0	0	5	4	0	0	0	0	1	1	1	0	0	11	1	0	5	1	0	1	0	0	1	0	0	2	0	1	0	0	0	0	0	1	2	0	0	0	0	0	0	0	2	3	1	0				0														
Striped Bass 2011	2290	7,536	21 May	8 Jun	8	64	0	0	0			0	1	1	1	0		1	0		0	34	2	0	1	0	0	0	0	0	0			0	0			13	1	0	16	1	0	0	2	0	3	0	0	2	0	2	0	0	0	0	0	3	3	0	0	0	1	1	0		4	1	0	1																		
Striped Bass 2011	2486	10,357	7 Jun	8 Jun	16	61										0	0	0	1		0	1	1		0								0	1	1			1	1	0	17	0			1	0	1			10	0	50	0	5		0		0	3	1	0					0	4	1	0	0																		
Striped Bass 2011	2556	934	20 May	28 May	9	52								1	0																									0	27	3	4	1	1		0		2	15	1	22	2	5	2	4	1	1	3	3	0	2	0	0																								
Striped Bass 2011	3060	321	21 May	21 May	9	59								39	30																	1										6									3		3		2		2					4	7	1	4																								
Striped Bass 2011	3074	72	26 May	26 May	9	42								29	4									1																		17						6			3		3		3		1					3	14	11	6																								
Striped Bass 2011	3088	30,021	8 Jun	9 Jun	62	59										0	0	3	6		7	1	0										1	9	8	3	1	2	0		0									0		0		0		0			0	0	0	0		0	0	4	17	37	0																				
Striped Bass 2011	3144	80	8 Jun	8 Jun	45	58																																													4							3	8			28	54	5																								
Striped Bass 2011	3158	55	9 Jun	9 Jun	46	42																																		2					7			2		5		9							9	7		13	22	24																								
Striped Bass 2011	3186	38	8 Jun	8 Jun	46	59																																									16					18		16		5	5		13	3		13		8	3																								
Striped Bass 2011	3228	7,215	14 Jun	16 Jun	9	2	1	1						0	0	0		2	0			0	0			0	0	0					0	0	2			0	0		0	0	0							0	0	0	0	0					0	0	0	0	0	0		12	43	36	0																			
Striped Bass 2011	3242	30	8 Jun	8 Jun	48	42																																										7						13	3	3	10						10	30	23																								
Striped Bass 2011	3256	12,865	15 Jun	18 Jun	58	63		1	0			0	0					1	0	0	0	0	0		0	0	0	0	0					0	0	0	0	0		2	0				7	1	33			6		5		0		0		33	4	0				0			2	1	0																			
Striped Bass 2011	3270	111	6 Jun	6 Jun	9	40								1	2																											11	14	3		3	5	3	14		6		9		2			1	5	4	4	4	2		10																								
Striped Bass 2011	3284	607	9 Jun	10 Jun	46	53			1	2			2	29	36																												1	8				4	3			1	0	0	0	0	0		0					8	1																								
Striped Bass 2011	3298	7,072	6 Jun	6 Jun	64	62	4	12				5				3	2	5	2	0	0	11	0	0	1	3	5	11	0	0			5	2	3	0	0	3	0	1	10	0			0					1		0														1	5	1	0	0																		
Striped Bass 2011	3312	103	13 Jun	13 Jun	39	63																3	17															2	6		31				2					10		9																2	18																			
Striped Bass 2011	3338	84	20 May	20 May	9	71								25	8							4	6	11							5	8						4	4																													6	18			1					1												
Striped Bass 2011	3340	14,090	7 Jun	7 Jun	9	62	0	0						0	0	0	0	0	0		0	0	0	0		0	0	0			0	0	1	0	0	0		0	0																											29	47	21																					
Striped Bass 2011	3354	47	13 Jun	13 Jun	46	54																																			2									2		23		9		2	15		2			6	38																									
Striped Bass 2011	3366	13	21 May	21 May	57	57																																																								##																											
Striped Bass 2011	3380	221	22 May	24 May	9	64		2		5		5		40	29					4	1	1						2	1							2	1																															5	4																			
Striped Bass 2011	3382	114	2 Jun	2 Jun	7	40							6	37																												1	15	9		1	5											6	2	3	2		4	5	5																								
Striped Bass 2011	3422	75	19 May	19 May	2	66	9	8				13						1		7	5						4	9								4	4																															31				3	1																
Striped Bass 2011	3450	718	24 May	22 Jun	36	16								2							1	1	6	11							0	1						1	2		12	6	0							1	5	5	2	0					13	4			10	3	3			8	2																			
Striped Bass 2012 Old River	2217	360	22 May	22 May	75	82																																																																							0				3	2				11	26	34	23
Striped Bass 2012 Old River	2364	486	16 May	16 May	71	82																																																																						6	21				4	19				30	21	
Striped Bass 2012 Old River	2427	31,613	20 May	21 May	75	82																																																																							0			0	0	0				0	90	9
Striped Bass 2012 Old River	2448	128	24 May	24 May	75	80																																																																										15	2				63	20		
Striped Bass 2012 Old River	2553	252	6 May	6 May	76	81																																																																							1				5	2			0	73	19	
Striped Bass 2012 Old River	2574	12,424	24 May	24 May	76	82																																																																						0	16	7	0	0	36	20	4	0	0	0	8	7	0
Striped Bass 2012 Old River	2595	5,550	16 May	16 May	76	79																																																																							2	8				2	7		20	26	35	0	
Striped Bass 2012 Old River	2658	1,780	21 May	21 May	76	80																																																																									5	1	18			13	61	2		
Striped Bass 2012 Old River	2679	160	24 May	24 May	80	82																																																																									9	4				1	46	41	
Striped Bass 2012 Old River	2784	30	15 May	15 May	76	81																																																																										83					17		
Striped Bass 2012 Old River	2889	288	22 May	22 May	76	82																																																																							1	17	3			20	9	7			1	25	17
Striped Bass 2012 Old River	2910	270	24 May	24 May	76	82																																																																							4	17	1		2	5	24				0	33	12
Striped Bass 2012 Old River	2973	5,995	29 Apr	25 May	82	80																																																																															1	20	74	5	0
Striped Bass 2012 Old River	3015	338	15 May	15 May	81	82																																																																												7				2	88	3
Striped Bass 2012 Old River	3120	348	22 May	22 May	71	82																																																																							5	28	4			1	10	4				33	14
Striped Bass 2012 SJ River	2007	1,527	24 Apr	25 Apr	68	59		5		5	0	1		40	2			3	1					1			2	2				1		1	2							4				0	3				1		1		0	0	0	2	3	0	0			0	0		4	8	1			2		2				2											
Striped Bass 2012 SJ River	2154	666,469	6 May	31 May	43	37			0	0			0	0	0				0	0	1	1	0	0					0	0	0	0				0	0	0	0	0	23	4	17	5	0	0	0	2	0	5	2	11	6	7	6	3	3	0	0	0	0	0	0	0	0		0	0	0	0		0		0			0	0											
Striped Bass 2012 SJ River	2343	85,049	22 May	25 May	62	4		0		0		1	0	13	0	0		2	1		1	5	4	1	0	0	1	1			0	0		1	1	0	0	3	2	1	9	2	12	0	1	0	0	1	0	1	0	0	0		0		0	0	0				0	0	0	0	4	14	11	2	0	2	0	2	0		0	2	0										
Striped Bass 2012 SJ River	2385	7	6 May	6 May	43	42																																										71	29																																								
Striped Bass 2012 SJ River	2469	88	24 Apr	24 Apr	42	59																																										53																15	32																								
Striped Bass 2012 SJ River	2616	33	6 May	6 May	43	59																																										39	15																45																								
Striped Bass 2012 SJ River	2700	1,488	27 Apr	27 Apr	42	41																																				11	46	3		0	2	26	2		0							0	1					1	7																								
White Catfish 2011	2346	1,712	7 Jun	9 Jun	4	62		0		7		1		26	16			1			0						0	0						0	0	1	0					17	16	1				2	3		1		0											0	1			5																					
White Catfish 2011	3352	473,942	25 May	22 Jun	35	47							0	0	0				0				0						0	0									0	0	0	0	0		0	0	0			1	0	11	37	11	28	1	1	0	6	1	0	1	1	0	0																								
White Catfish 2011	3394	185,620	25 May	22 Jun	39	44																0	1	0							0							0	0	0	17	0	0		3	0	1			36	0	31	0	0	0	0	0	1	8	2	0	0	0	0	0			0	0																				
White Catfish 2011	3408	490,453	25 May	22 Jun	49	51								0	0									0							0	0								0	0	0	0		1	0	0			2	0	9	6	14	63	2	3	0	0	0	0	0	0	0	0																									
White Catfish 2012 SJ River	2931	2,504	27 Apr	27 Apr	47	40																																		83	1				6	6	1			0			0		0	0	0	0	1	1	1																										

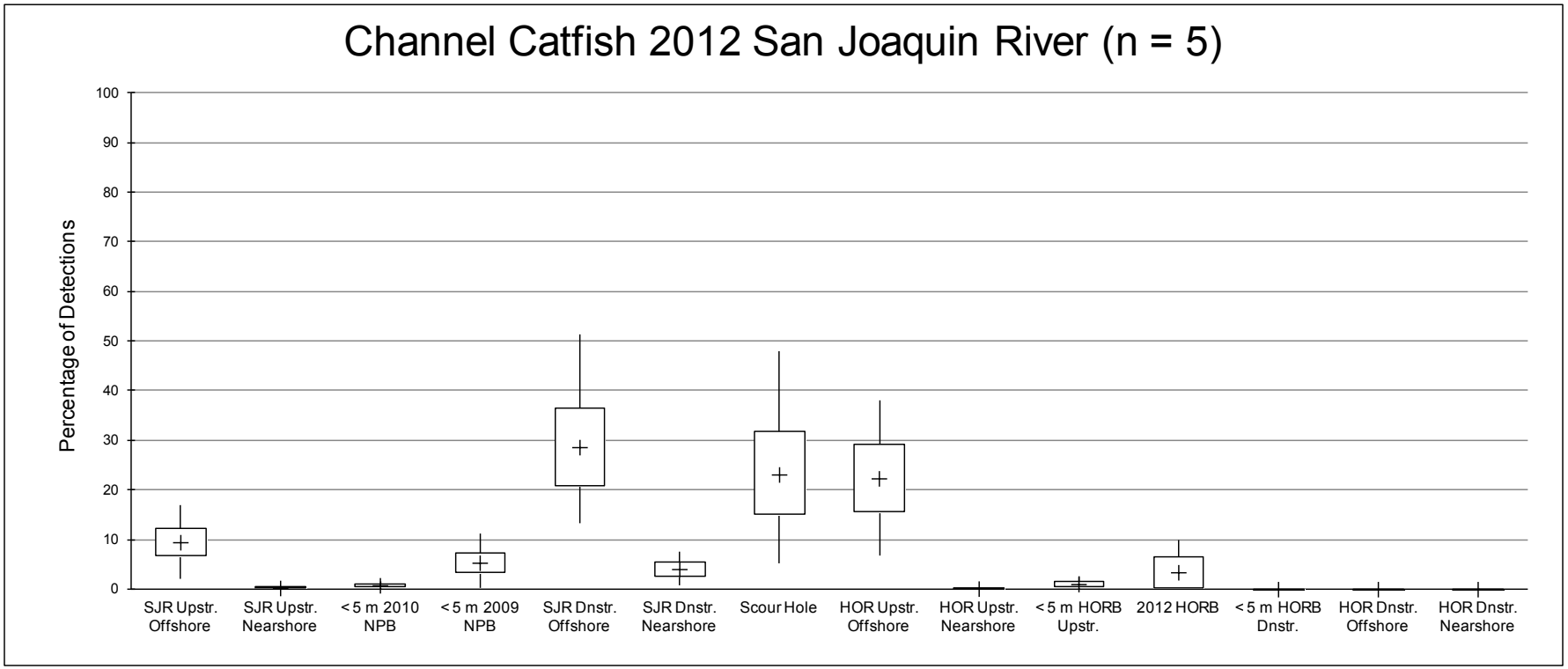

Notes: Dnstr. = downstream; HOR = Head of Old River; HORB = Head of Old River Physical Rock Barrier; NPB = non-physical barrier (BAFF); SJR = San Joaquin River; Upstr. = upstream
Source: Present study

Figure 6-13 **Percentage of Tag Detections for Channel Catfish within Different Zones of the HOR Study Area for 2012 San Joaquin River Releases: Bootstrapped Mean (+), Interquartile Range (Box), and 95% Confidence Interval (Whiskers)**

The index of zone use relative to zone size was computed as the percentage of detections divided by the percentage of grid points in each zone; values of 1 indicated that the use of the zone was exactly proportional to its size. This index indicated that use of the San Joaquin River's downstream offshore zone was proportionally greater than the zone's size (95% confidence interval = 1.4 to 5.3) (Figure 6-14). By contrast, several zones in the upstream San Joaquin River and the HOR's upstream nearshore zone were used considerably less than proportional to their size (95% confidence intervals <1).

Largemouth Bass

Largemouth bass released into the San Joaquin River in 2012 (n = 7 fish) were detected most frequently in the San Joaquin River downstream of the Old River divergence (San Joaquin River downstream offshore: bootstrapped mean = 22%, 95% confidence interval = 7 to 39%; San Joaquin River downstream nearshore: bootstrapped mean = 21%, 95% confidence interval = 9 to 35%) (Figure 6-15). This result was notable because five of these seven fish were released at the HOR just upstream of the physical rock barrier (Table 6-65).

Relative to zone size, the San Joaquin River downstream nearshore zone was used to a considerable extent by largemouth bass (95% confidence interval: 2.3 to 8.6) (Figure 6-16). Two other nearshore zones (San Joaquin River upstream nearshore and HOR upstream nearshore), as well as the San Joaquin River downstream offshore zone, also were used appreciably relative to their size.

Three largemouth bass released into HOR downstream of the 2012 physical rock barrier were detected most frequently within the footprint of the physical rock barrier bottom (bootstrapped mean: 32%, 95% confidence interval: 13 to 72%) or within 5 m of the barrier (bootstrapped mean: 27%, 95% confidence interval: 10 to 58%) (Figure 6-17). The small surface area of the wetted portion of the barrier bottom zone, coupled with the relatively large percentage of detections within this zone, led to a high use index (95% confidence interval: 1.2 to 8.0); the HOR study area downstream offshore zone was used infrequently relative to its size (95% confidence interval: 0.13 to 0.77) (Figure 6-18).

The largemouth bass with tag code 4306 was tagged and released in 2009. Approximately 40% of its detections were nearshore in a quite restricted area (zone 11), whereas 46% of its detections were within 5 m of the 2009 non-physical barrier (either nearshore in zone 8, or offshore in zones 28 and 29) (Table 6-65).

Striped Bass

Striped bass tagged and released in 2011 (n = 10) were detected most frequently in offshore areas (San Joaquin River upstream offshore and HOR upstream offshore), as well as the scour hole; there was a bootstrapped mean of approximately 20% of detections in these zones (Figure 6-19). Note that the acoustic array's detection ability was somewhat limited in the HOR study area zones in 2011. As a result, the HOR zones downstream of the 2012 physical rock barrier bottom zones would not have registered detections (and were excluded from the calculations of use relative to zone size).

There was considerable variability in the percentage of detections in each zone relative to zone size. Detections within 5 m of the 2009 non-physical barrier alignment were relatively frequent relative to the small size of this zone (95% confidence interval: 0.9 to 3.1); this was also the case for the scour hole (95% confidence interval: 0.7 to 4.1) (Figure 6-20). Relative to zone size, there was low use of the San Joaquin River upstream offshore and San Joaquin River downstream nearshore zones by striped bass in 2011.

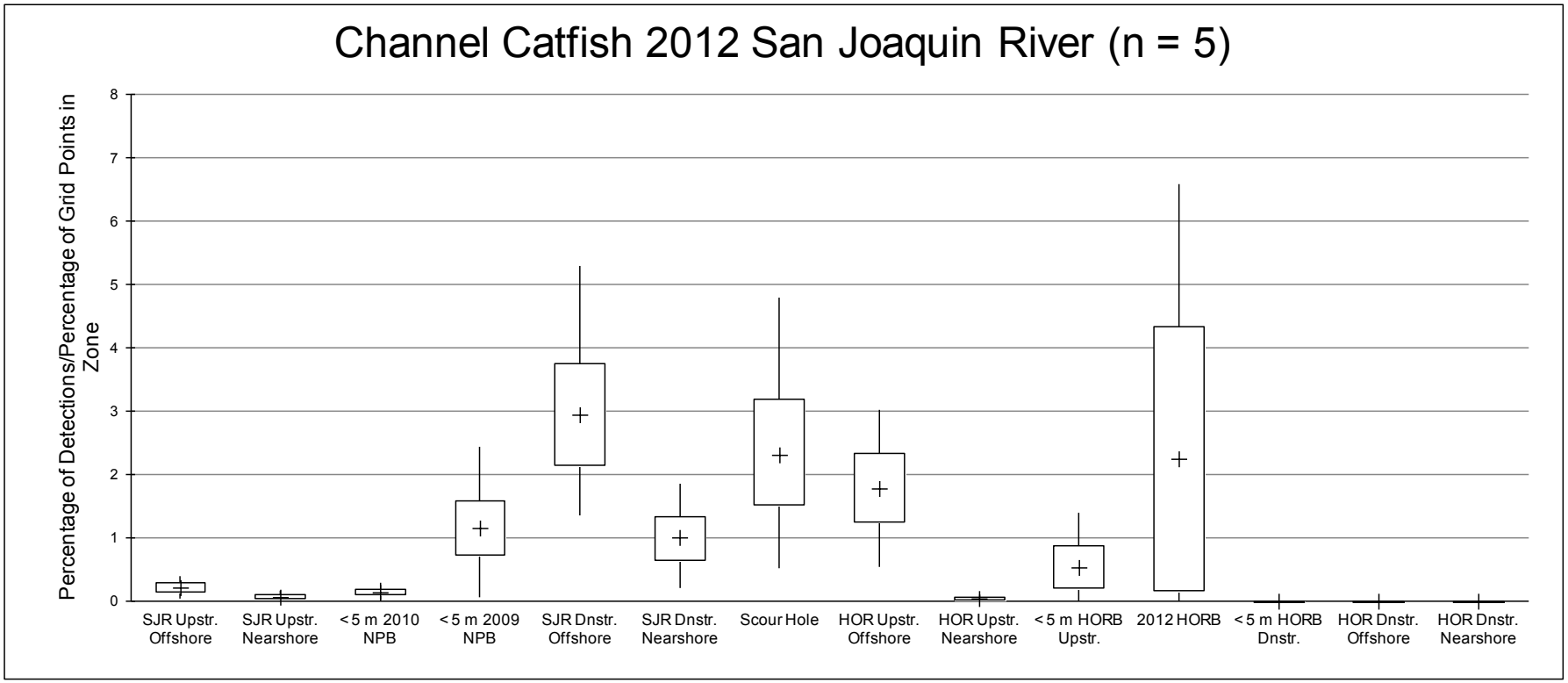

Notes: Dnstr. = downstream; HOR = Head of Old River; HORB = Head of Old River Physical Rock Barrier; NPB = non-physical barrier (BAFF); SJR = San Joaquin River; Upstr. = upstream
Source: Present study

Figure 6-14 **Percentage of Tag Detections for Channel Catfish within Different Zones of the HOR Study Area, Divided by Percentage of Grid Points in Each Zone for 2012 San Joaquin River Releases: Bootstrapped Mean (+), Interquartile Range (Box), and 95% Confidence Interval (Whiskers)**

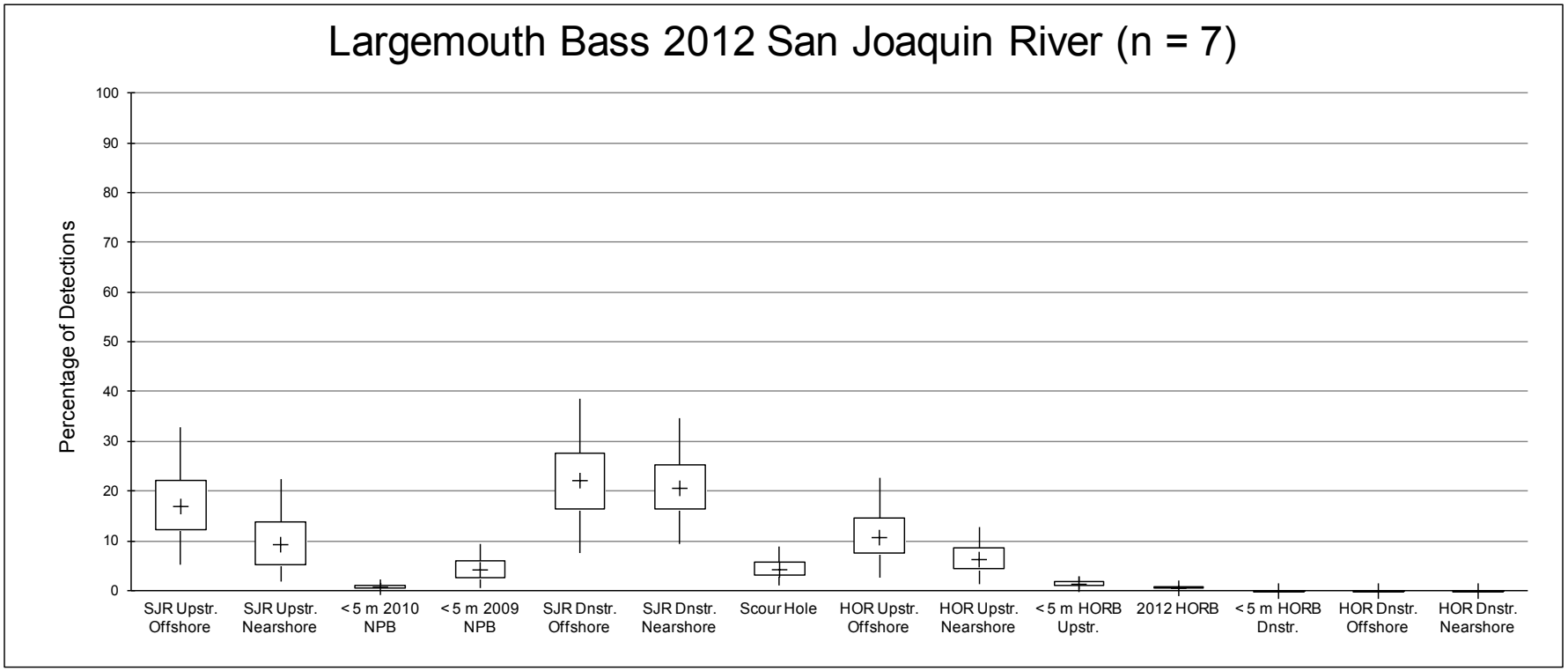

Notes: Dnstr. = downstream; HOR = Head of Old River; HORB = Head of Old River Physical Rock Barrier; NPB = non-physical barrier (BAFF); SJR = San Joaquin River; Upstr. = upstream

Source: Present study

Figure 6-15 **Percentage of Tag Detections for Largemouth Bass within Different Zones of the HOR Study Area for 2012 San Joaquin River Releases: Bootstrapped Mean (+), Interquartile Range (Box), and 95% Confidence Interval (Whiskers)**

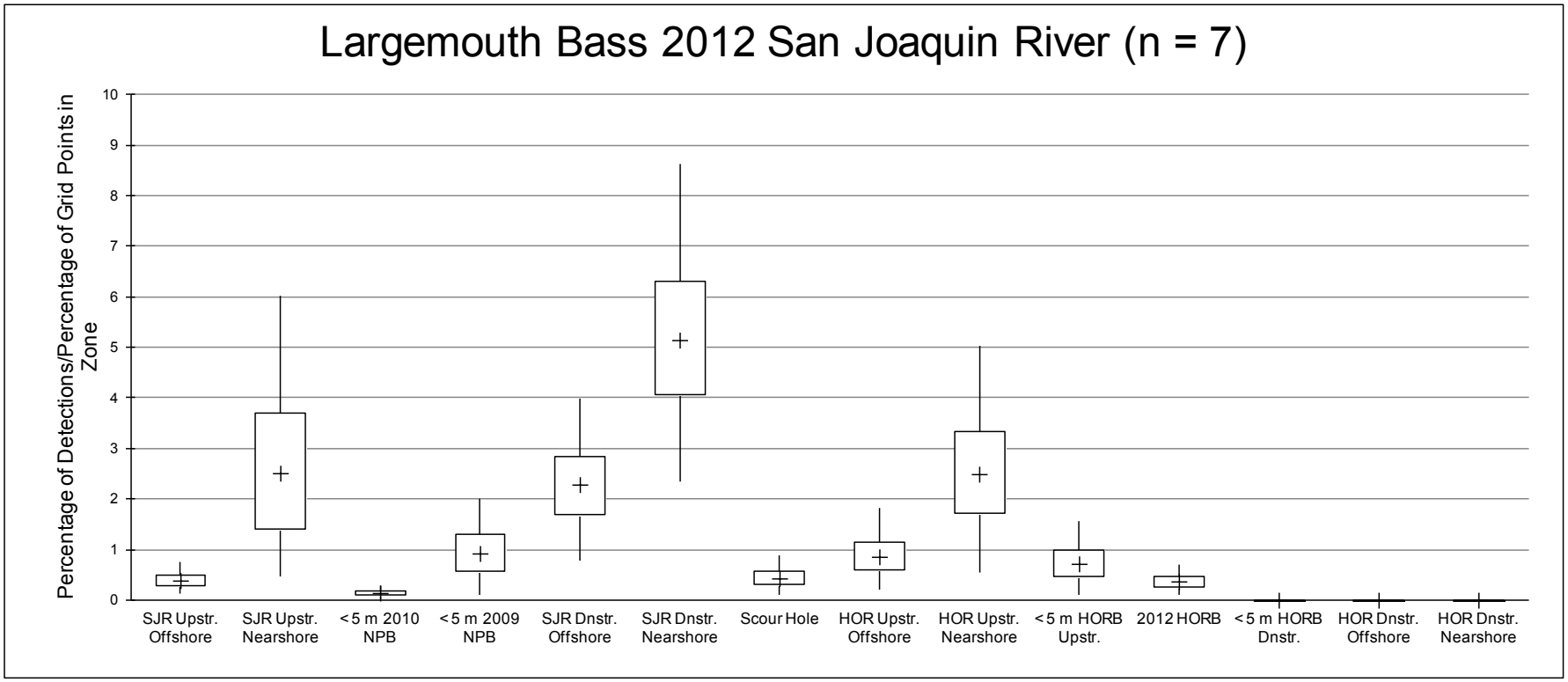

Notes: Dnstr. = downstream; HOR = Head of Old River; HORB = Head of Old River Physical Rock Barrier; NPB = non-physical barrier (BAFF); SJR = San Joaquin River; Upstr. = upstream
Source: Present study

Figure 6-16 **Percentage of Tag Detections for Largemouth Bass within Different Zones of the HOR Study Area, Divided by Percentage of Grid Points in Each Zone for 2012 San Joaquin River Releases: Bootstrapped Mean (+), Interquartile Range (Box), and 95% Confidence Interval (Whiskers)**

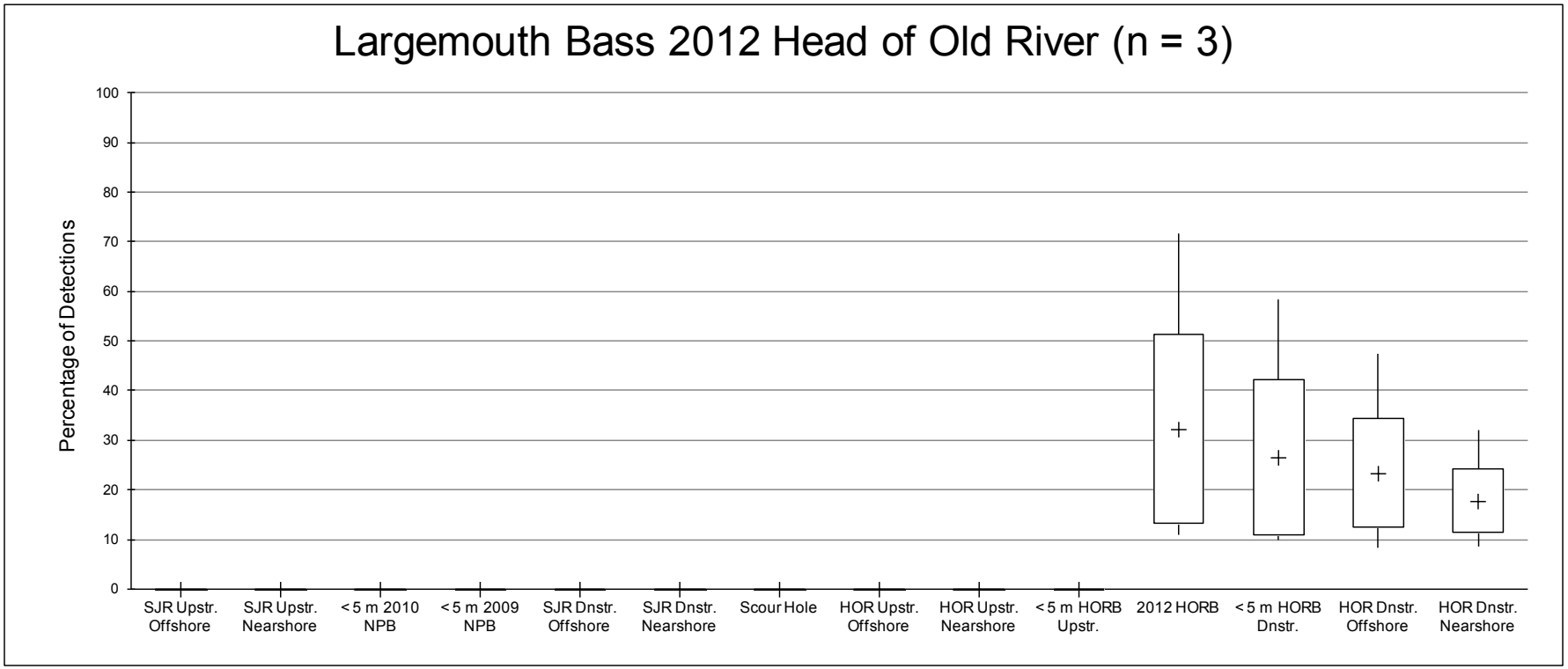

Notes: Dnstr. = downstream; HOR = Head of Old River; HORB = Head of Old River Physical Rock Barrier; NPB = non-physical barrier (BAFF); SJR = San Joaquin River; Upstr. = upstream
Source: Present study

Figure 6-17 **Percentage of Tag Detections for Largemouth Bass within Different Zones of the HOR Study Area for 2012 Head of Old River Releases: Bootstrapped Mean (+), Interquartile Range (Box), and 95% Confidence Interval (Whiskers)**

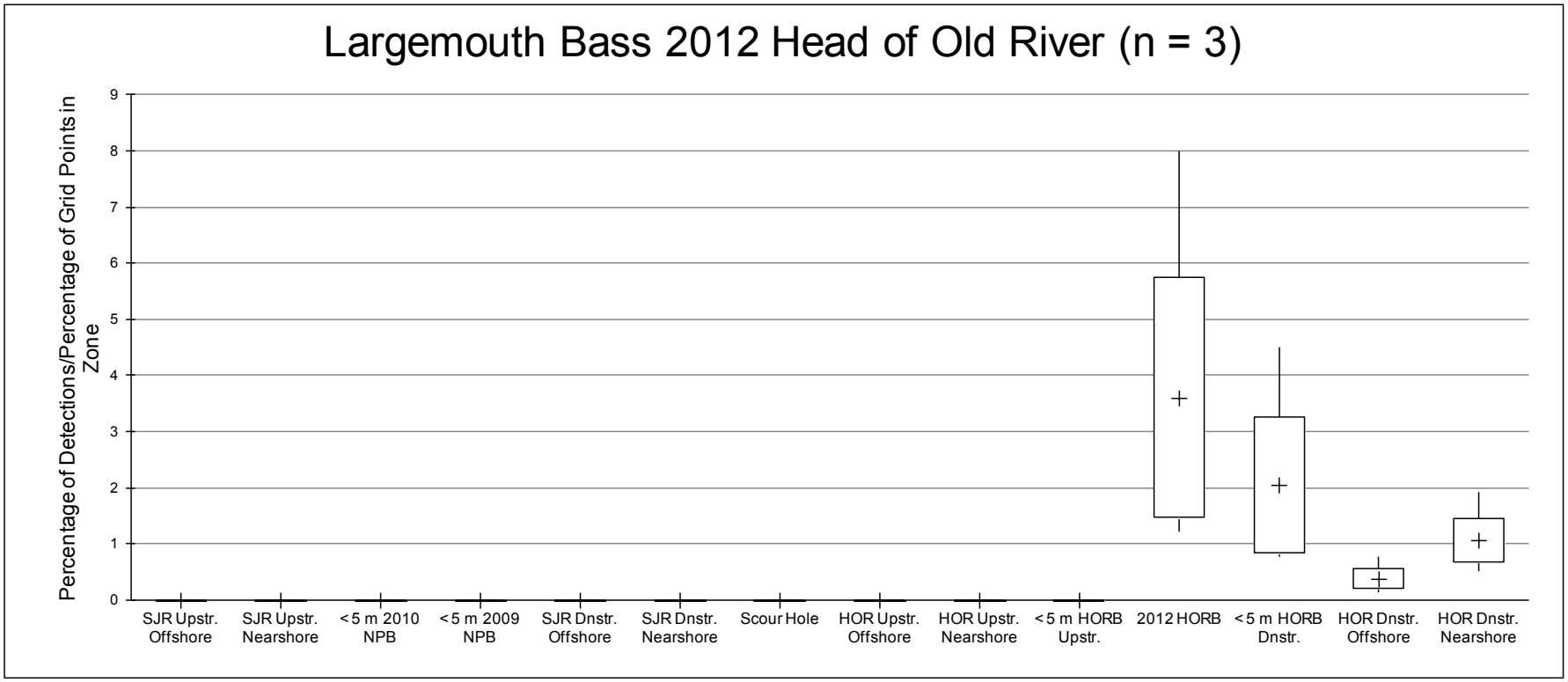

Notes: Dnstr. = downstream; HOR = Head of Old River; HORB = Head of Old River Physical Rock Barrier; NPB = non-physical barrier (BAFF); SJR = San Joaquin River; Upstr. = upstream
Source: Present study

Figure 6-18 **Percentage of Tag Detections for Largemouth Bass within Different Zones of the HOR Study Area, Divided by Percentage of Grid Points in Each Zone for 2012 Head of Old River Releases: Bootstrapped Mean (+), Interquartile Range (Box), and 95% Confidence Interval (Whiskers)**

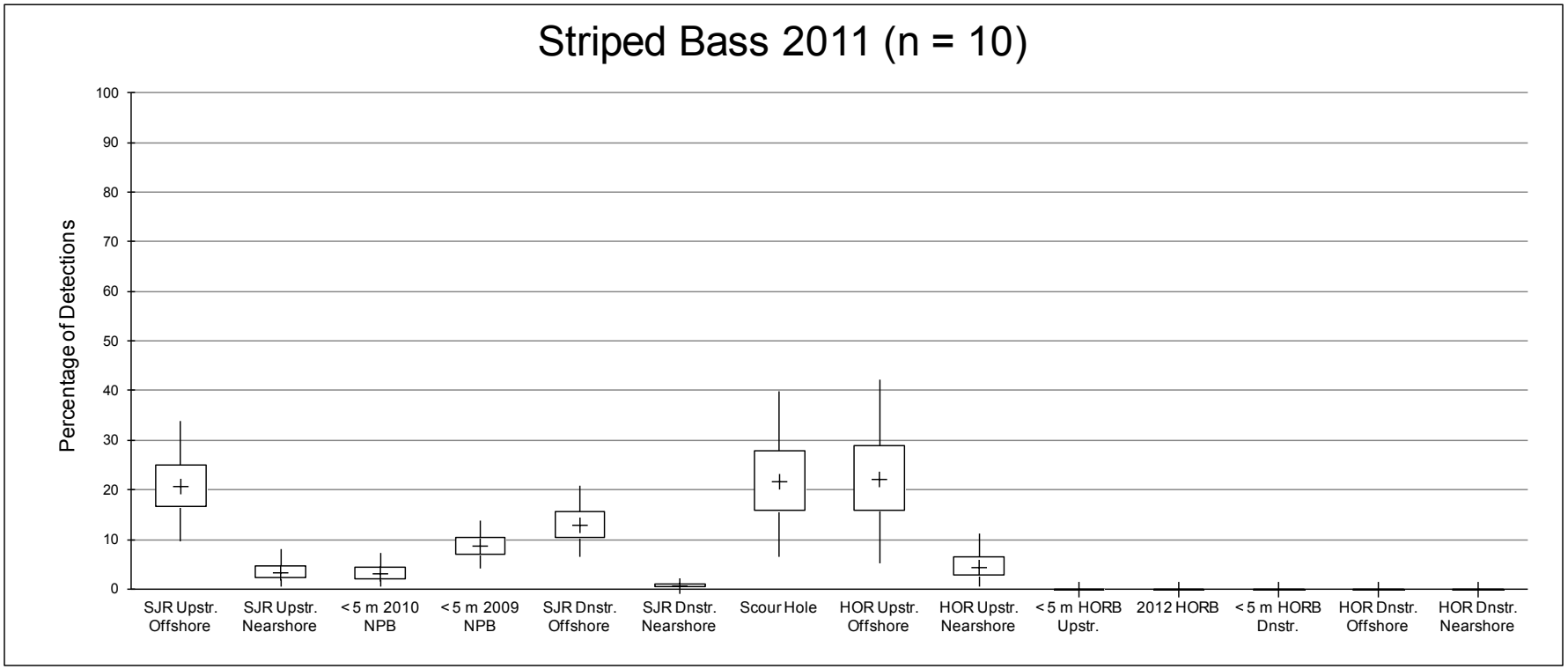

Notes: Dnstr. = downstream; HOR = Head of Old River; HORB = Head of Old River Physical Rock Barrier; NPB = non-physical barrier (BAFF); SJR = San Joaquin River; Upstr. = upstream
Source: Present study

Figure 6-19 **Percentage of Tag Detections for Striped Bass within Different Zones of the HOR Study Area for 2011 Releases: Bootstrapped Mean (+), Interquartile Range (Box), and 95% Confidence Interval (Whiskers)**

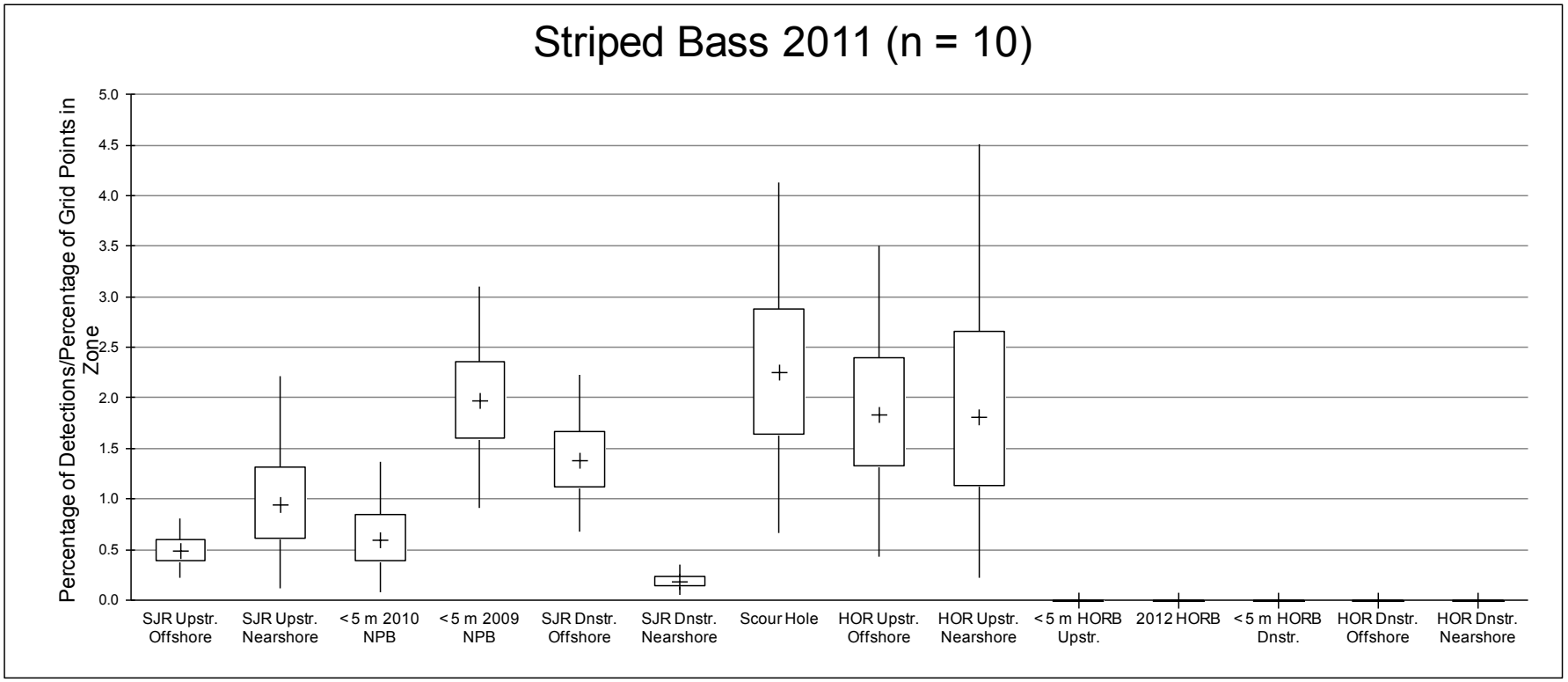

Notes: Dnstr. = downstream; HOR = Head of Old River; HORB = Head of Old River Physical Rock Barrier; NPB = non-physical barrier (BAFF); SJR = San Joaquin River; Upstr. = upstream
Source: Present study

Figure 6-20 Percentage of Acoustic Tag Detections for Striped Bass within Different Zones of the HOR Study Area, Divided by Percentage of Grid Points in Each Zone for 2011 Releases: Bootstrapped Mean (+), Interquartile Range (Box), and 95% Confidence Interval (Whiskers)

Striped bass released in the San Joaquin River in 2012 (n = 4) had the highest frequency of detection in the San Joaquin River downstream offshore zone (bootstrapped mean: 41%, 95% confidence interval: 16 to 70%) (Figure 6-21). The percentage of detections relative to zone size also was high for this zone (95% confidence interval: 4.2 to 7.2) (Figure 6-22). Most of the other zones upstream of the divergence and in the upstream HOR study area were used considerably less, both relative to their size and in absolute terms.

Five striped bass released into HOR downstream of the physical rock barrier in 2012 were most frequently detected offshore in the HOR study area downstream of the physical rock barrier (HOR study area downstream offshore; bootstrapped mean: 66%, 95% confidence interval: 40 to 90%) and less frequently near the physical rock barrier or nearshore (Figure 6-23). Relative to zone size, there was less difference in use of the zones than when comparing the percentage of detections alone (Figure 6-24).

In addition to the striped bass included in the foregoing analyses, two striped bass (tag codes 2024 and 2472) were tagged and released in 2010. These fish each had more than 1,000 detections (Table 6-65) and were detected at the HOR study area for 0.6 to 3 hours (Table 6-64). Of interest is the extent to which they were found near the 2010 non-physical barrier. The acoustic tag detection data suggest that they spent a small proportion (1% or less) of their time within 5 m of the non-physical barrier (Table 6-65). Other striped bass tagged and released in 2009 and 2010 (tag codes 2976 and 4222) were present in the study area for short durations (0.3 to 0.5 hours). Striped bass 2976 spent approximately 20% of its time within 5 m of the 2010 non-physical barrier, whereas striped bass 4222 was not detected within 5 m of the 2009 non-physical barrier (Table 6-65).

White Catfish

White catfish tagged and released in 2011 spent a considerable percentage of their time at the scour hole (bootstrapped mean: 69%, 95% confidence interval: 26–99%) (Figure 6-25). Three individuals (tag codes 3352, 3394, and 3408) that were captured, tagged, and released at the scour hole subsequently remained almost entirely within that area; one individual (tag code 2346) was caught and released in the San Joaquin River upstream of the divergence, and only 2% of its detections were at the scour hole, with the final detection suggesting emigration down Old River. The percentage of detections for white catfish at the scour hole was high relative to the size of this zone (Figure 6-26).

Velocity

The estimated near-surface velocities at the portions of the HOR study area occupied by tagged predatory fish generally were quite different from all of the available velocities at the overall HOR study area upstream of the physical rock barrier (Table 6-66). Channel catfish, largemouth bass, and white catfish all had median detection velocities that were considerably lower than the overall median velocities present in the study area. Striped bass detection velocity was variable in relation to all available velocities.

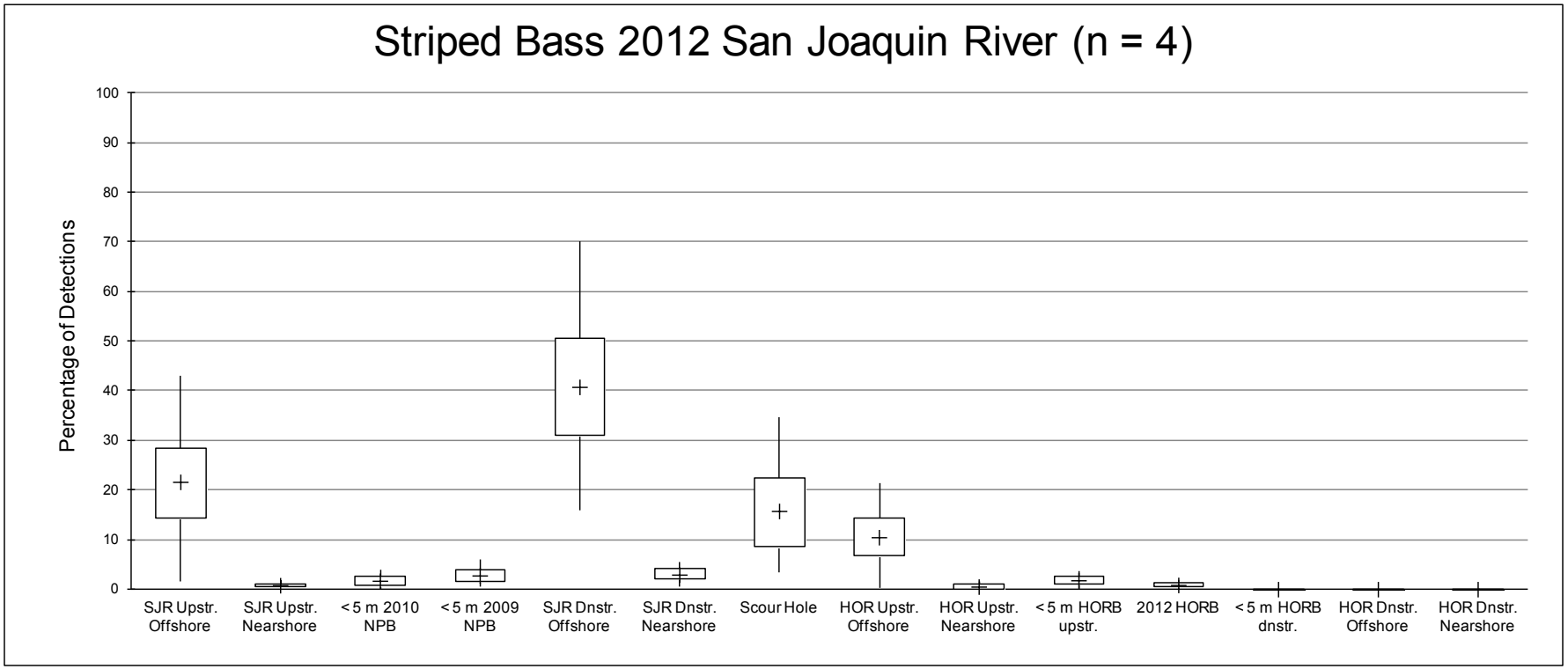

Notes: Dnstr. = downstream; HOR = Head of Old River; HORB = Head of Old River Physical Rock Barrier; NPB = non-physical barrier (BAFF); SJR = San Joaquin River; Upstr. = upstream
Source: Present study

Figure 6-21 **Percentage of Tag Detections for Striped Bass within Different Zones of the HOR Study Area, for 2012 San Joaquin River Releases: Bootstrapped Mean (+), Interquartile Range (Box), and 95% Confidence Interval (Whiskers)**

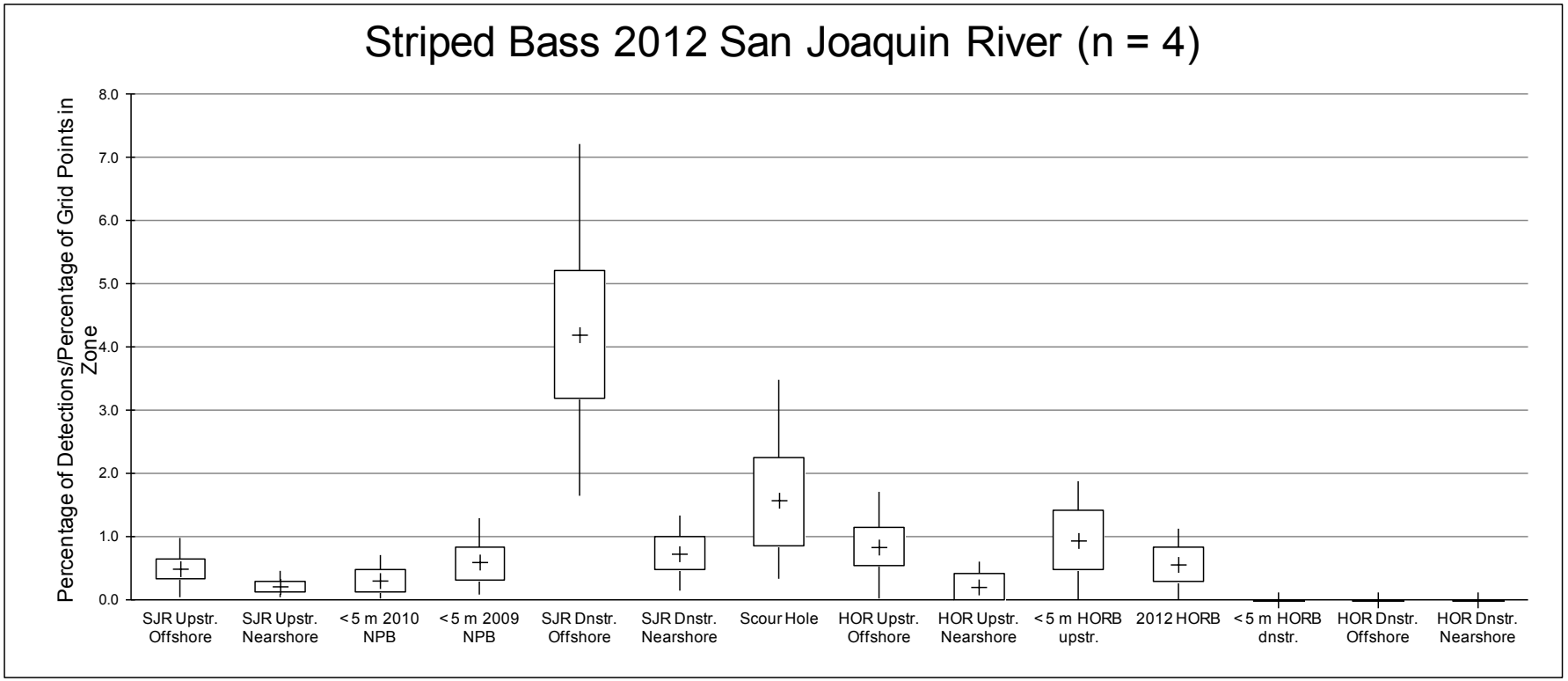

Notes: Dnstr. = downstream; HOR = Head of Old River; HORB = Head of Old River Physical Rock Barrier; NPB = non-physical barrier (BAFF); SJR = San Joaquin River; Upstr. = upstream
Source: Present study

Figure 6-22

Percentage of Tag Detections for Striped Bass within Different Zones of the HOR Study Area, Divided by Percentage of Grid Points in Each Zone for 2012 San Joaquin River Releases: Bootstrapped Mean (+), Interquartile Range (Box), and 95% Confidence Interval (Whiskers)

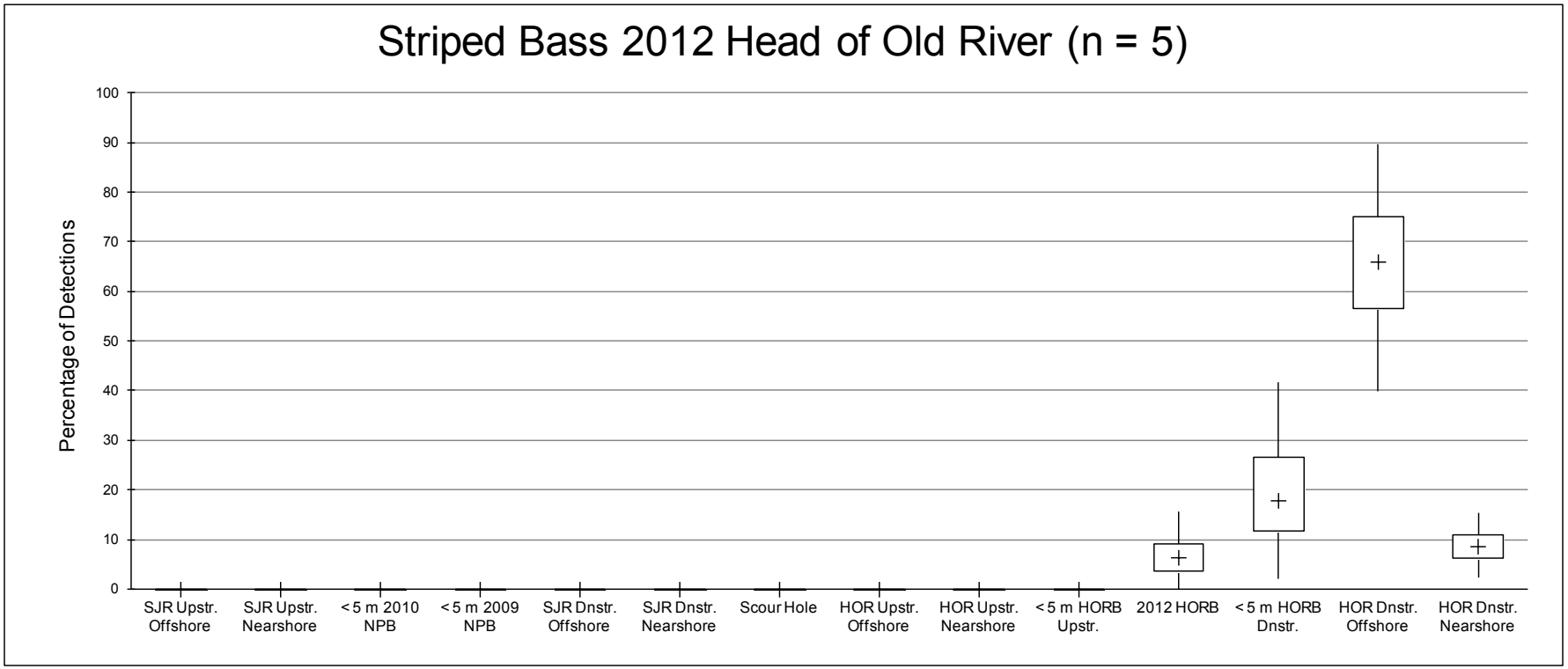

Notes: Dnstr. = downstream; HOR = Head of Old River; HORB = Head of Old River Physical Rock Barrier; NPB = non-physical barrier (BAFF); SJR = San Joaquin River; Upstr. = upstream
Source: Present study

Figure 6-23 **Percentage of Tag Detections for Striped Bass within Different Zones of the HOR Study Area for 2012 Head of Old River Releases: Bootstrapped Mean (+), Interquartile Range (Box), and 95% Confidence Interval (Whiskers)**

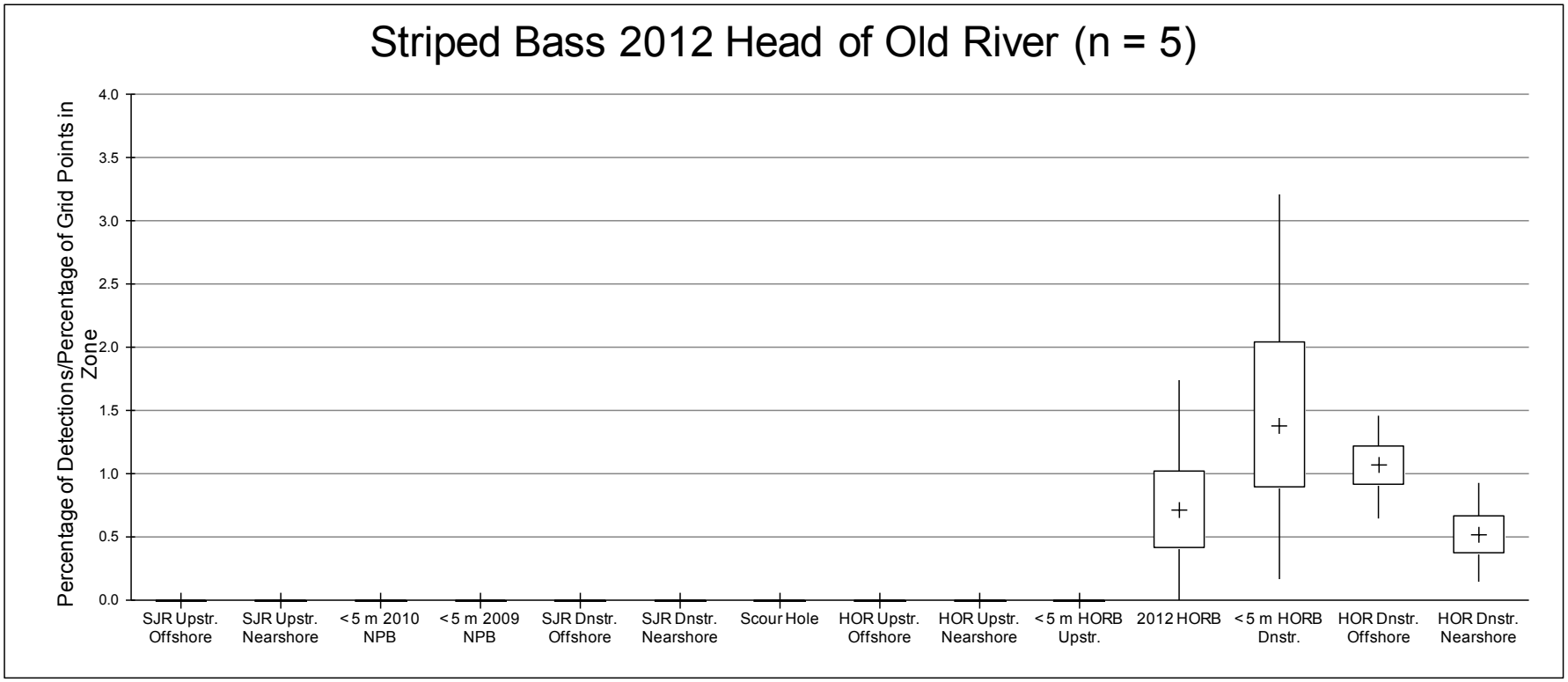

Notes: Dnstr. = downstream; HOR = Head of Old River; HORB = Head of Old River Physical Rock Barrier; NPB = non-physical barrier (BAFF); SJR = San Joaquin River; Upstr. = upstream

Source: Present study

Figure 6-24

Percentage of Tag Detections for Striped Bass within Different Zones of the HOR Study Area, Divided by Percentage of Grid Points in Each Zone for 2012 Head of Old River Releases: Bootstrapped Mean (+), Interquartile Range (Box), and 95% Confidence Interval (Whiskers)

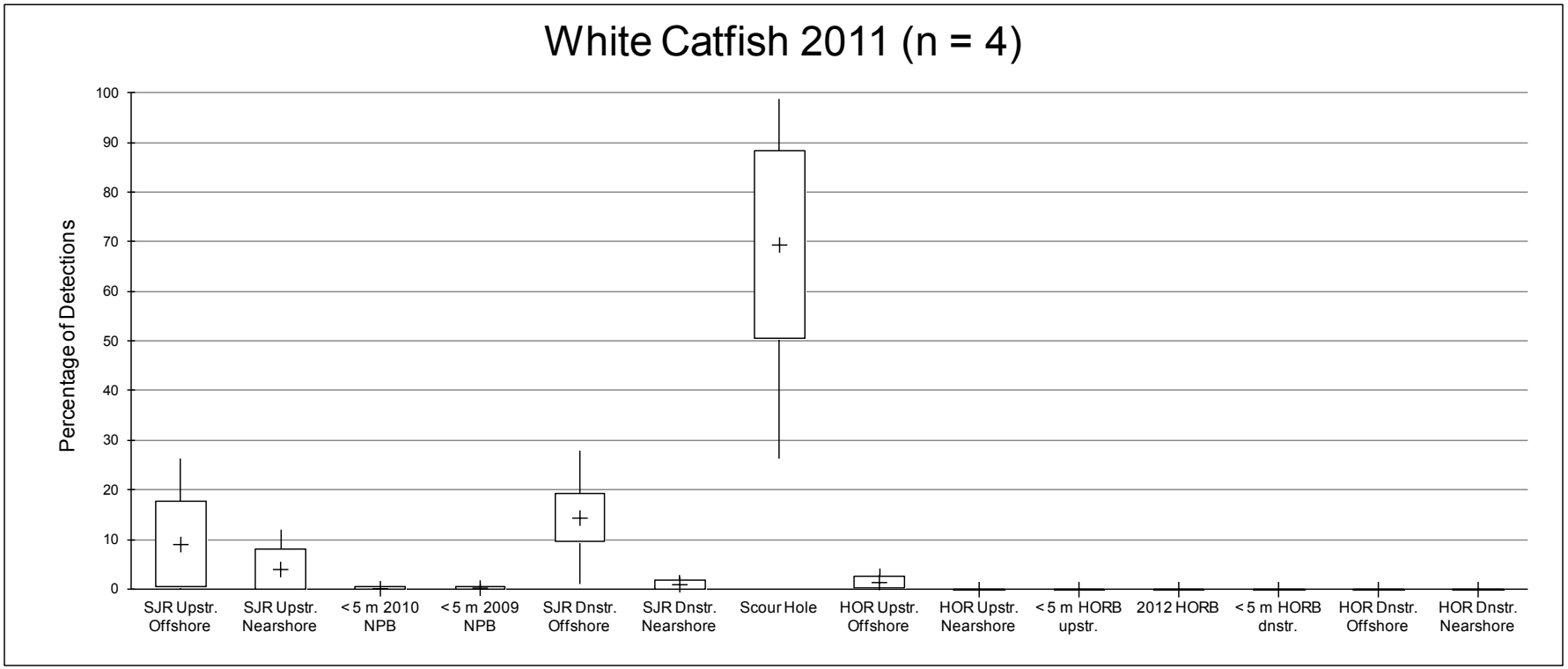

Notes: Dnstr. = downstream; HOR = Head of Old River; HORB = Head of Old River Physical Rock Barrier; NPB = non-physical barrier (BAFF); SJR = San Joaquin River; Upstr. = upstream
Source: Present study

Figure 6-25 **Percentage of Tag Detections for White Catfish within Different Zones of the HOR Study Area for 2011 Releases: Bootstrapped Mean (+), Interquartile Range (Box), and 95% Confidence Interval (Whiskers)**

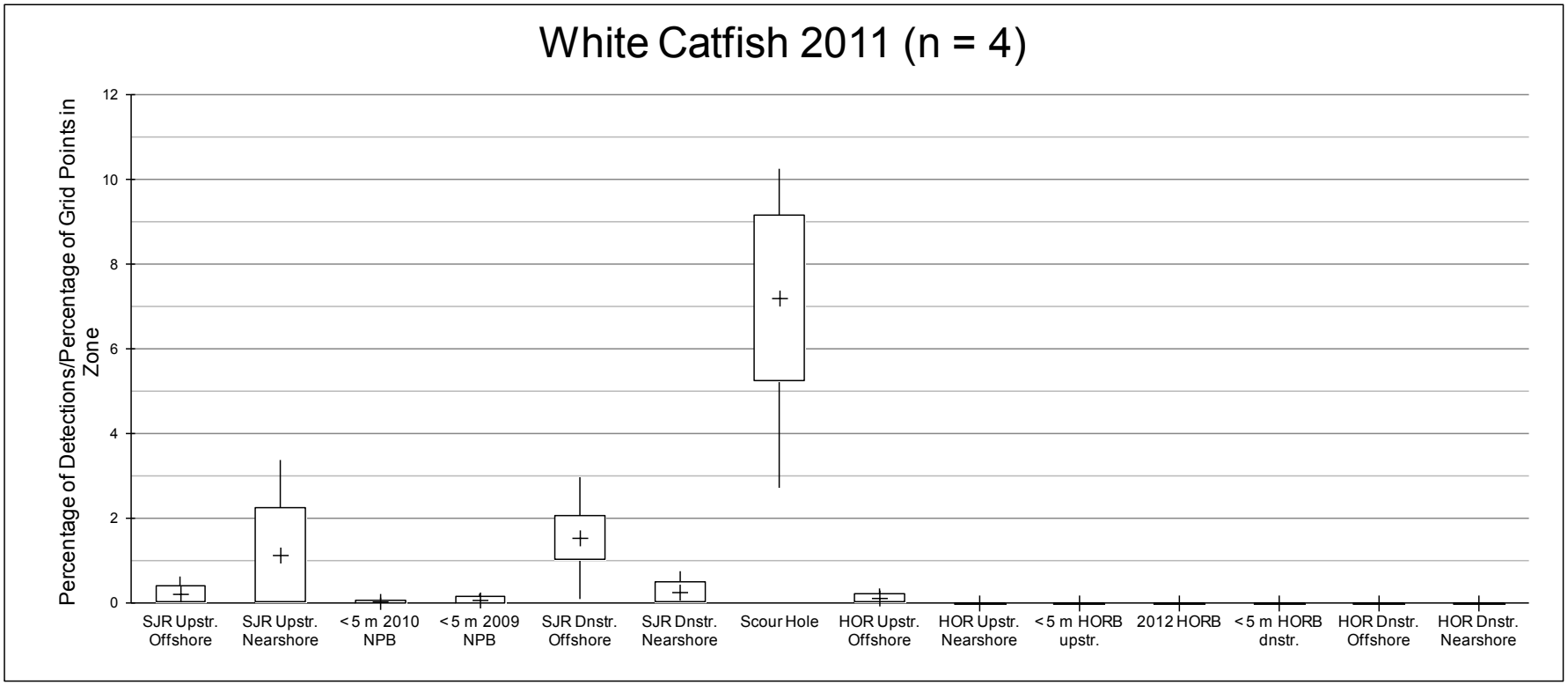

Notes: Dnstr. = downstream; HOR = Head of Old River; HORB = Head of Old River Physical Rock Barrier; NPB = non-physical barrier (BAFF); SJR = San Joaquin River; Upstr. = upstream

Source: Present study

Figure 6-26

Percentage of Tag Detections for White Catfish within Different Zones of the HOR Study Area, Divided by Percentage of Grid Points in Each Zone for 2011 Releases: Bootstrapped Mean (+), Interquartile Range (Box), and 95% Confidence Interval (Whiskers)

Table 6-66
Summary of Estimated Median Near-Surface Velocity and Percentage of Observations in Areas in which Tagged Predatory Fish Were Detected, Relative to All Available Velocities at the Head of Old River Study Area, Upstream of the 2012 Physical Rock Barrier

Species	Tag Code	Available Velocities (All) or at which Fish Detected	No. of Observations	Median Velocity (m/s)	Percentage of Observations by Velocity (roundest to nearest 0.05 m/s)												
					0	0.05	0.1	0.15	0.2	0.25	0.3	0.35	0.4	0.45	0.5	0.55	0.6
Channel Catfish	2490	All	7,425,516	0.15	16	19	9	10	14	15	9	7	0	0	0	0	0
	2490	Detected	9,120	0.03	31	61	5	2	1	0	0	0	0	0	0	0	0
Channel Catfish	2763	All	77,864,150	0.11	18	22	15	15	13	11	5	2	0	0	0	0	0
	2763	Detected	66,018	0.05	35	42	16	7	1	0	0	0	0	0	0	0	0
Channel Catfish	2847	All	4,842,761	0.23	13	18	8	6	5	6	9	14	18	2	0	0	0
	2847	Detected	3,969	0.11	4	27	23	19	10	12	2	2	0	0	0	0	0
Channel Catfish	2952	All	13,180,062	0.11	17	21	15	18	15	8	4	1	0	0	0	0	0
	2952	Detected	16,417	0.03	28	57	5	4	5	1	0	0	0	0	0	0	0
Channel Catfish	2994	All	4,273,563	0.12	18	20	13	17	17	12	1	0	0	0	0	0	0
	2994	Detected	3,761	0.03	49	28	12	11	1	0	0	0	0	0	0	0	0
Largemouth Bass	2028	All	98,542,213	0.10	17	23	16	12	12	11	7	2	0	0	0	0	0
	2028	Detected	114,293	0.02	61	39	0	0	0	0	0	0	0	0	0	0	0
Largemouth Bass	2070	All	3,699,787	0.09	18	25	18	7	8	12	10	2	0	0	0	0	0
	2070	Detected	2,997	0.01	72	25	3	0	0	0	0	0	0	0	0	0	0
Largemouth Bass	2259	All	58,911,993	0.11	17	23	15	12	12	11	8	3	0	0	0	0	0
	2259	Detected	68,472	0.03	47	51	1	0	0	0	0	0	0	0	0	0	0
Largemouth Bass	2280	All	3,782,191	0.15	16	19	10	13	18	15	5	4	0	0	0	0	0
	2280	Detected	398	0.03	38	31	5	2	6	0	0	12	6	0	0	0	0
Largemouth Bass	2532	All	49,136,437	0.11	17	22	15	16	15	11	4	0	0	0	0	0	0
	2532	Detected	39,305	0.02	81	19	1	0	0	0	0	0	0	0	0	0	0
Largemouth Bass	2721	All	207,541,341	0.11	17	21	15	14	13	11	6	2	0	0	0	0	0
	2721	Detected	207,818	0.02	50	46	3	0	0	0	0	0	0	0	0	0	0
Largemouth Bass	3078	All	92,546,559	0.12	17	21	14	10	11	12	10	4	0	0	0	0	0
	3078	Detected	32,571	0.03	48	48	3	0	0	0	0	0	0	0	0	0	0

Table 6-66
Summary of Estimated Median Near-Surface Velocity and Percentage of Observations in Areas in which Tagged Predatory Fish Were Detected, Relative to All Available Velocities at the Head of Old River Study Area, Upstream of the 2012 Physical Rock Barrier

Species	Tag Code	Available Velocities (All) or at which Fish Detected	No. of Observations	Median Velocity (m/s)	Percentage of Observations by Velocity (roundest to nearest 0.05 m/s)												
					0	0.05	0.1	0.15	0.2	0.25	0.3	0.35	0.4	0.45	0.5	0.55	0.6
Striped Bass	2007	All	1,165,101	0.21	10	16	11	7	6	9	16	12	11	0	0	0	0
	2007	Detected	1,058	0.16	5	23	20	15	6	17	8	5	1	0	0	0	0
Striped Bass	2154	All	470,252,923	0.12	16	21	14	12	12	11	8	4	2	0	0	0	0
	2154	Detected	566,232	0.16	1	9	20	27	21	12	6	3	2	1	0	0	0
Striped Bass	2343	All	64,892,387	0.10	17	24	18	13	11	9	5	2	0	0	0	0	0
	2343	Detected	75,883	0.04	28	41	17	9	5	1	0	0	0	0	0	0	0
Striped Bass	2700	All	1,135,344	0.20	14	18	8	6	7	13	21	11	1	0	0	0	0
	2700	Detected	780	0.36	0	0	0	0	0	0	22	29	47	2	0	0	0
White Catfish	2931	All	1,910,552	0.20	11	17	10	7	7	11	16	19	2	0	0	0	0
	2931	Detected	2,192	0.00	85	13	1	0	1	0	0	0	0	0	0	0	0

Notes: m/s = meters per second; No. = number
Source: Present study

Channel Catfish

The median detection velocity for channel catfish ranged from 0.03 m/s (tag codes 2490, 2952, and 2994) to 0.11 m/s (tag code 2847), compared with median available velocities of 0.11 to 0.23 m/s (Table 6-66). A generally large percentage (approximately 75% or more) of tag detections was estimated to occur in areas with near-surface velocity less than 0.075 m/s (the exception was tag code 2847); by contrast, only 35 to 40% of available velocities were in this range. This was reflected in the index of detection velocity to available velocity, which generally was well above 1 (Figure 6-27), while the 95% confidence intervals for velocity of 0.075 to 0.275 m/s overlapped 1, indicating that this range of velocity was used more in proportion to its availability; higher velocity (>0.275 m/s) was rarely used (Table 6-66; Figure 6-27).

Largemouth Bass

The median detection velocity for largemouth bass ranged from 0.01 m/s (tag code 2070) to 0.03 m/s (tag codes 2259, 2280, and 3078), compared with median available velocities of 0.09 to 0.15 m/s (Table 6-66). For most tagged largemouth bass, nearly all (96% to 100%) of tag detections were estimated to be in areas with near-surface velocity less than 0.075 m/s. The exception was tag code 2280 (70% of detections in this range), and this individual was detected relatively rarely during the period for which velocity was modeled. By contrast, approximately 38–44% of all available velocities were less than 0.075 m/s.

Occupation of lower-velocity areas was reflected in the index of detection velocity to available velocity, for which the 95% confidence intervals were considerably above 1, indicating greater use than proportionally available (Figure 6-28). By contrast, the 95% confidence intervals for velocity indices over the range of 0.075 to 0.325 m/s were below 1, indicating that this range of velocity was used considerably less than its proportional availability. Overlap of the 95% confidence intervals of velocity from 0.325 to 0.425 m/s with a velocity use index of 1 reflects the single individual (tag code 2280) that was detected relatively rarely.

Striped Bass

Four acoustically tagged striped bass met the criterion for inclusion in the velocity analysis, 1,000 or more detections before merging with velocity modeling estimates. (Note that the number of detections remaining after the merge with velocity data was lower than 1,000 for some fish [e.g., striped bass tag code 2700] because not all detections were within the grid of velocity estimates or occurred outside the period of velocity data availability.)

The median detection velocity was appreciably greater for striped bass than for the other species (0.16 to 0.34 m/s) for three individuals (tag codes 2007, 2154, and 2700), and similar (0.04 m/s) for the other individual (tag code 2343) (Table 6-66). The median detection velocity for striped bass tag code 2007 (0.16 m/s) was similar to the median of all available velocities (0.21 m/s); the median detection velocities for striped bass tag codes 2154 and 2700 were greater than the median of all available velocities; and the median detection velocity of striped bass 2343 was considerably less than the median of all available velocities (0.04 vs. 0.20 m/s).

The approximate velocity ranges in which tag detections occurred most frequently differed by fish: 0.025 to 0.275 m/s (tag code 2007), 0.075 to 0.275 m/s (tag code 2154), 0 to 0.125 m/s (tag code 2343), and 0.275 to 0.425 m/s (tag code 2700). This led to little evidence of occupation by fish of any particular velocity in greater or less proportion than it was available in the study area, as judged by the 95% confidence intervals of the velocity index across most velocity increments overlapping an index value of 1 (Figure 6-29).

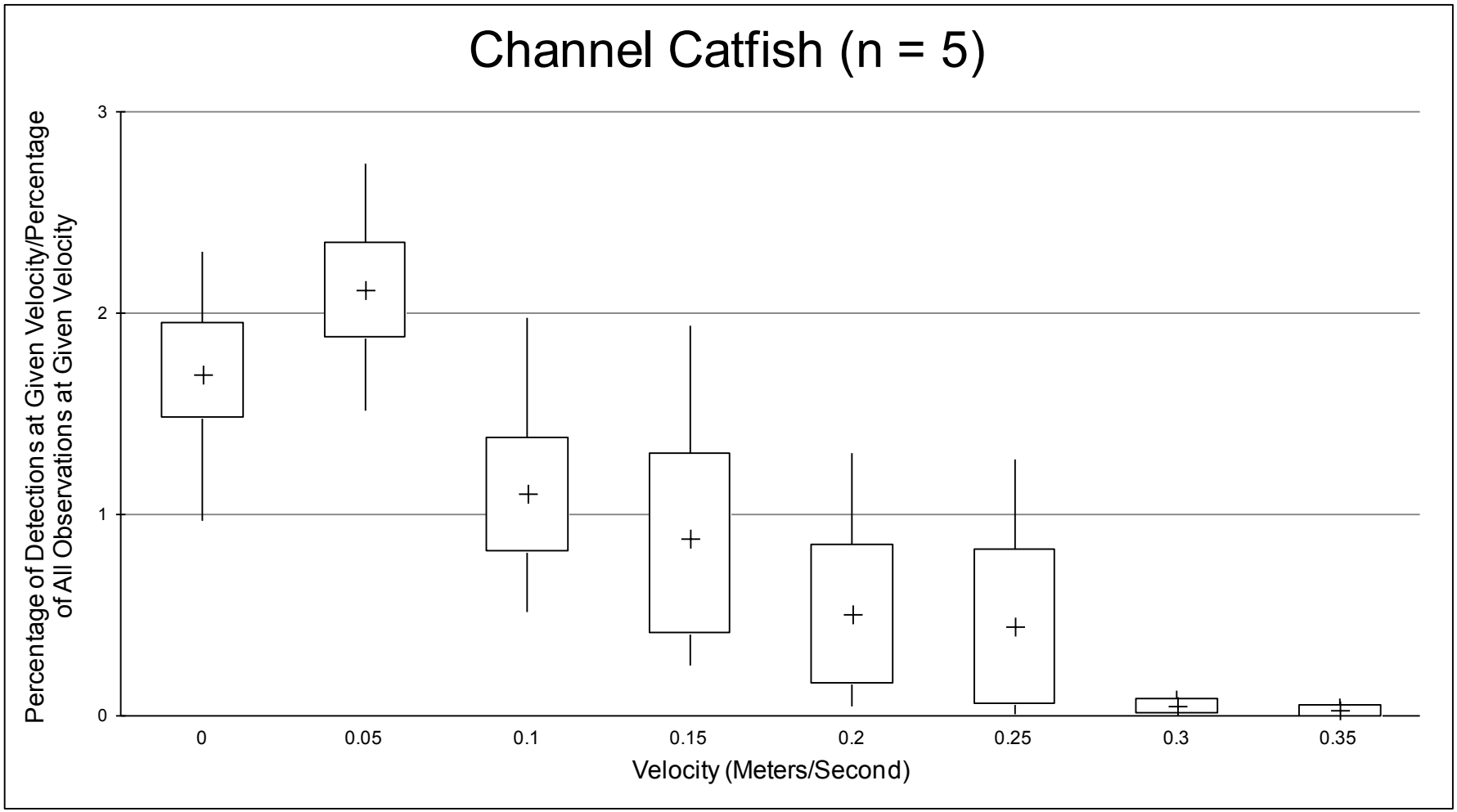

Note: Velocity is rounded to the nearest 0.05 meter per second.

Source: Present study

Figure 6-27 **Percentage of Tag Detections for Channel Catfish at Different Near-Surface Velocities at the HOR Study Area, Divided by Percentage of All Near-Surface Velocities in the HOR Study Area, Upstream of the 2012 Physical Rock Barrier: Bootstrapped Mean (+), Interquartile Range (Box), and 95% Confidence Interval (Whiskers)**

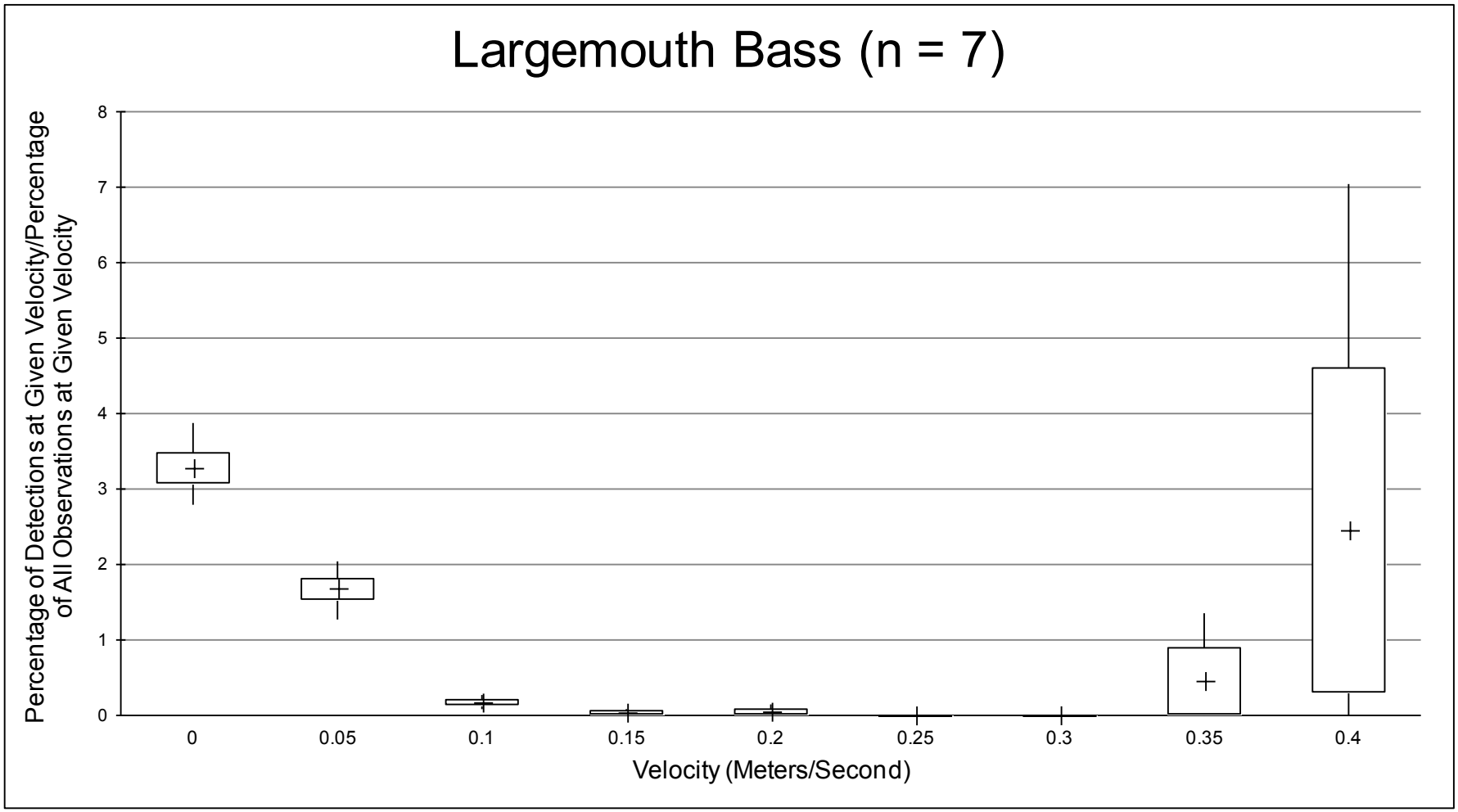

Note: Velocity is rounded to the nearest 0.05 meter per second.

Source: Present study

Figure 6-28 **Percentage of Tag Detections for Largemouth Bass at Different Near-Surface Velocities at the HOR Study Area, Divided by Percentage of All Near-Surface Velocities in the HOR Study Area, Upstream of the 2012 Physical Rock Barrier: Bootstrapped Mean (+), Interquartile Range (Box), and 95% Confidence Interval (Whiskers)**

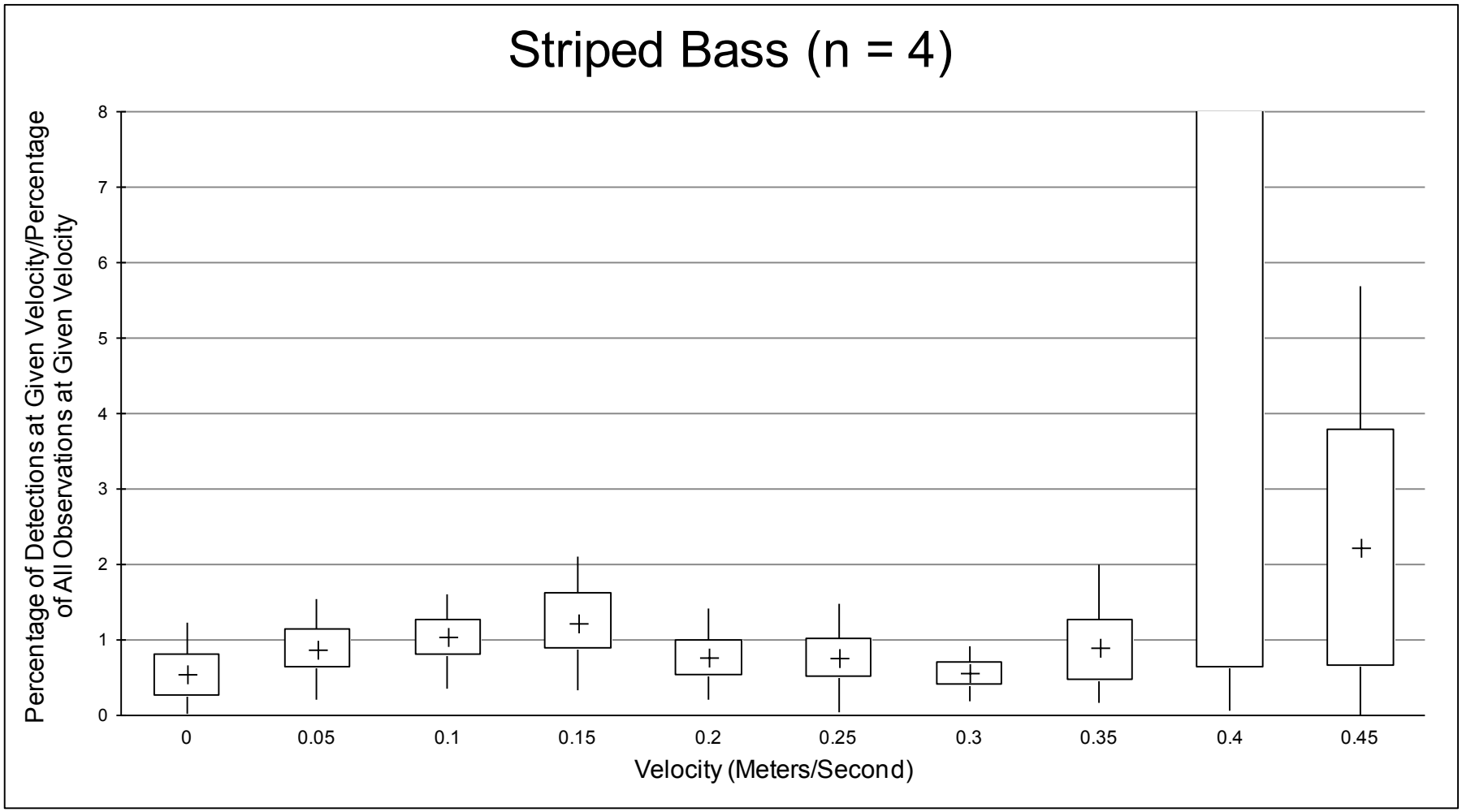

Notes: Velocity is rounded to the nearest 0.05 meter per second. The y-axis of plot is truncated at 8; 95th percentile at 0.4 meters per second was 46.5.
Source: Present study

Figure 6-29 **Percentage of Tag Detections for Striped Bass at Different Near-Surface Velocities at the HOR Study Area, Divided by Percentage of All Near-Surface Velocities in the HOR Study Area, Upstream of the 2012 Physical Rock Barrier: Bootstrapped Mean (+), Interquartile Range (Box), and 95% Confidence Interval (Whiskers)**

White Catfish

The single white catfish (tag code 2931) included in the velocity analysis had a median near-surface detection velocity of 0.00 m/s (Table 6-66), and 97% of its tag detections occurred in areas with velocity of 0.075 m/s or less. This was considerably less than the available velocities at the times of detection (median = 0.20 m/s, 28% of observations less than 0.075 m/s).

Emigration from Study Area

Four of five channel catfish tagged and released into the San Joaquin River in 2012 were last detected within the spatially defined zones of the study area before deactivation of the acoustic array; the last detections suggested that three of the four moved upstream and one moved downstream (Table 6-65). Five of six largemouth bass that were released into and moved out of the study area during the 2009 through 2012 physical rock barrier studies moved downstream. The single largemouth bass tagged and released in 2009 (tag code 4306) was last detected moving downstream into Old River; the single largemouth bass tagged and released in 2011 that appeared to leave the study area (tag code 3436) moved downstream in the San Joaquin River. Three of four largemouth bass tagged and released in the San Joaquin River that left the study area in 2012 moved downstream and one moved upstream.

Of the four striped bass detected in the study area in 2009 and 2010, two appeared to move upstream in the San Joaquin River, one moved downstream in the San Joaquin River, and one moved downstream in Old River, as indicated by the last zones of detections (Table 6-65). There were 29 tagged striped bass for which movement out of the study area could be deduced by the zone of last detection in 2011. Of these, 16 moved downstream in the San Joaquin River, 11 moved downstream in Old River, and two moved upstream in the San Joaquin River. One of six tagged striped bass released into the San Joaquin River in 2012 moved upstream out of the study area, and the remainder moved downstream.

The single white catfish tagged and released in 2011 (tag code 2346) that moved out of the range of detection of the acoustic array was last detected in Old River (i.e., downstream movement) (Table 6-65). The single white catfish tagged and released in the San Joaquin River in 2012 (tag code 2931) moved downstream out of the study area.

STATIONARY TAG LOCATIONS

A total of 24 stationary (i.e., no longer moving, as judged by consistent positions from signals received by hydrophones) salmonid tags were detected at the HOR study area from 2009 through 2012. This finding may indicate predation following these salmonids' entry into the study area as juveniles, and subsequent defecation. In both 2009 and 2010, only a single stationary tag was detected; 16 stationary tags were detected in 2011 (juvenile Chinook salmon, 10; steelhead, 6) and 6 in 2012 (all juvenile Chinook salmon).

The majority of stationary tags (20 of 24; 83%) was detected in the San Joaquin River downstream of the divergence with Old River; of these, a greater percentage was found at the scour hole (12 of 20; 60%) than offshore (8 of 20; 40%) (Figure 6-30). One stationary juvenile Chinook salmon tag was detected immediately adjacent to the downstream side of the physical rock barrier, with another tag approximately 91 m downstream in Old River. The stationary steelhead tag immediately adjacent to the upstream culvert zone of the physical rock barrier was detected in 2011, and therefore, was not associated with the physical rock barrier. No stationary tags were detected within 5 m of shore (Figure 6-30).

To some extent, the differences in the number of stationary tags detected in each year are related to hydrophone placement, as well as to the number of tagged juveniles entering the study area. In 2011, a hydrophone was placed deep within the scour hole, and therefore, allowed better detection of stationary tags in that year, even though tags classified as having been preyed upon were less frequent in that year than other years (see Section 6.2, "Predation on Juvenile Salmonids Including Barrier Effects"). However, the number of tagged juveniles entering the study area in 2011 (approximately 1,200) was considerably greater than in the other years (approximately 270 to 650 per year). These two factors combined resulted in relatively more stationary tags being detected in 2011 than other years.

6.3.2 HYDROACOUSTIC DATA

AREAS OCCUPIED AND DIEL CHANGES IN DEPTH

Areas Occupied

A total of 600 fish greater than 30 cm TL were detected within the spatially defined zones of the HOR study area during 49 mobile hydroacoustic surveys in 2011 and 2012. The number of fish detected by down-looking surveys was 20 in 2011 and 279 in 2012, which compared with 57 fish in 2011 and 244 fish in 2012 from side-looking surveys. The greatest proportions of fish detected by down-looking surveys were found in the San Joaquin River downstream of the divergence with Old River (75% of fish in 2011, 99% of fish in 2012) (Figure 6-31; Table 6-67). In particular, many fish were detected at the scour hole (35% of fish in 2011, 95% of fish in 2012). (Note that the ability of mobile hydroacoustic surveys to detect fish in the HOR study area zones was limited following installation of the physical rock barrier in 2012.)

Fish distribution as assessed by side-looking mobile hydroacoustic surveys was more equitable at the HOR study area than the distribution assessed by down-looking surveys, with approximately half of the fish detected in the San Joaquin River downstream of Old River in both 2011 and 2012 (Figure 6-32; Table 6-67). Approximately 23% of fish were detected at the scour hole in both years. An appreciable percentage of fish was detected in the offshore portion of the San Joaquin River upstream of the Old River divergence: 14% in 2011 and 32% in 2012.

Diel Changes in Depth

There was little evidence that the depth distribution of fish detected by down-looking mobile hydroacoustic surveys changed in relation to diel period. Figure 6-33 shows the vertical distance from the river bottom, where 23 individual fish were detected (12 during the day, 11 at night), in relation to the total water column (bottom) depth in 2011. Evidence of movement higher into the water column at night would be provided by the black symbols being relatively closer to the dashed water-surface line than the yellow circles for a given bottom depth. No such relationship was apparent. No nighttime were data available from the 2012 sampling, and there was no apparent relationship between diel period (day, dawn, or dusk) and position in the water column for 287 fish (Figure 6-34).

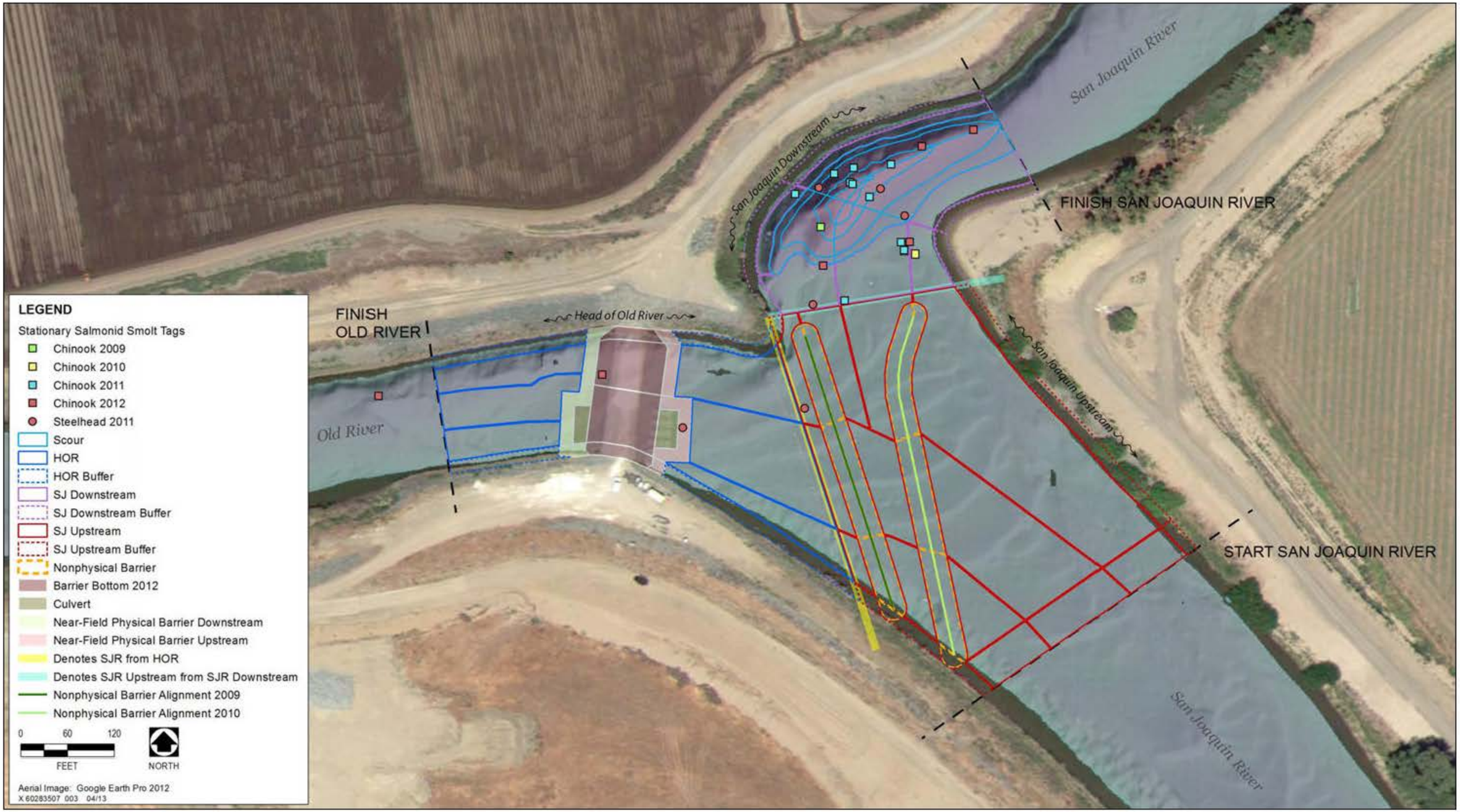

Sources: Google Earth Pro 2012; DWR 2012; Present study

Figure 6-30

Locations of Stationary Juvenile Salmonid Tags, 2009-2012

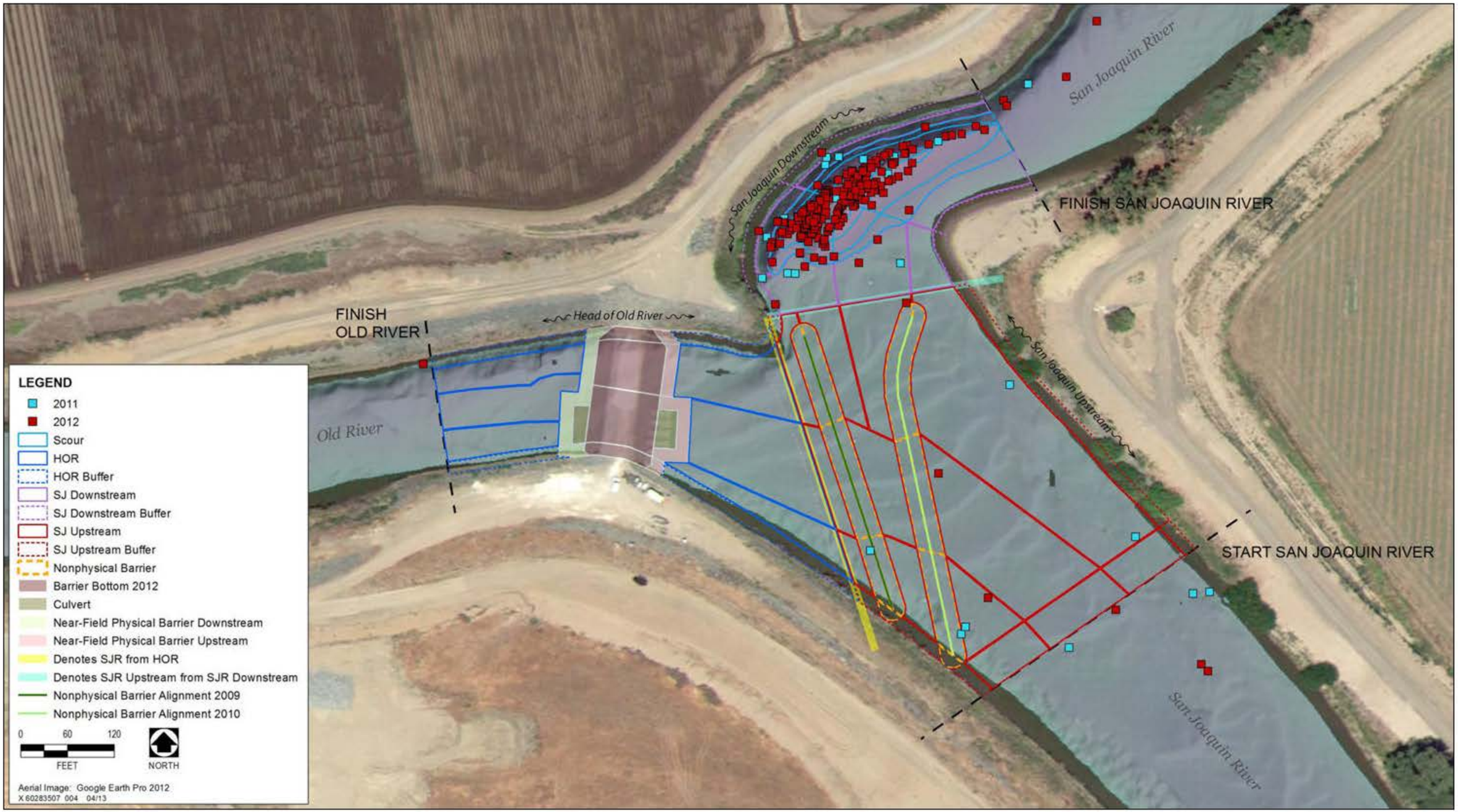

Sources: Google Earth Pro 2012; DWR 2012; Present study

Figure 6-31 **Locations of Fish Estimated to be >30 Centimeters Total Length from Down-Looking Mobile Hydroacoustic Surveys, 2011 and 2012**

Table 6-67
Number and Percentage of Large Fish >30 Centimeters Total Length Detected by Down- and Side-Looking Mobile Hydroacoustic Surveys in Different Zones at the Head of Old River, 2011 and 2012

Year/Survey Type	SJR Upstr. Offshore	SJR Upstr. Nearshore	<5 m 2010 Nonphysical Barrier	<5 m 2009 Nonphysical Barrier	SJR Dnstr. Offshore	SJR Dnstr. Nearshore	Scour Hole	HOR Upstr. Offshore	HOR Upstr. Nearshore	<5 m HORB Upstr.	2012 HORB	<5 m HORB Dnstr.	HOR Dnstr. Offshore	HOR Dnstr. Nearshore
2011/down	3 (15%)	0 (%)	1 (5%)	1 (5%)	8 (40%)	0 (%)	7 (35%)	0 (%)	0 (%)	0 (%)	0 (%)	0 (%)	0 (%)	0 (%)
2011/side	8 (14%)	0 (%)	2 (4%)	2 (4%)	18 (32%)	0 (%)	13 (23%)	8 (14%)	0 (%)	0 (%)	5 (9%)	0 (%)	1 (2%)	0 (%)
2012/down	3 (1%)	0 (%)	0 (%)	0 (%)	9 (3%)	3 (1%)	264 (95%)	0 (%)	0 (%)	0 (%)	0 (%)	0 (%)	0 (%)	0 (%)
2012/side	79 (32%)	0 (%)	8 (3%)	7 (3%)	69 (28%)	4 (2%)	57 (23%)	17 (7%)	0 (%)	1 (%)	0 (%)	0 (%)	2 (1%)	0 (%)

Notes: Dnstr. = downstream; HOR = Head of Old River; HORB = Head of Old River Barrier; m = meters; SJR = San Joaquin River; Upstr. = upstream
Source: Present study

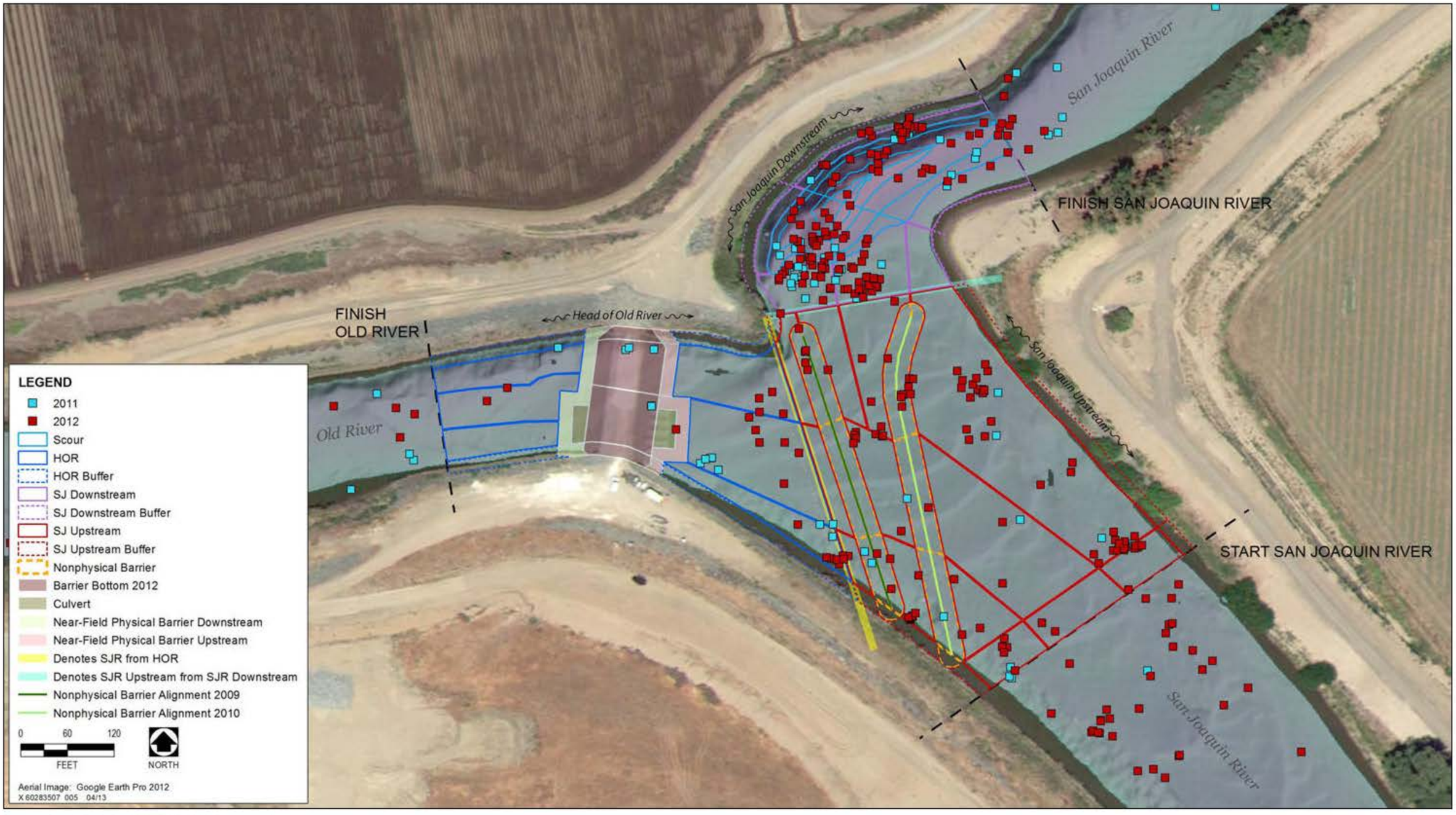

Sources: Google Earth Pro 2012; DWR 2012; Present study

Figure 6-32

Locations of Fish Estimated to be >30 Centimeters Total Length from Side-Looking Mobile Hydroacoustic Surveys, 2011 and 2012

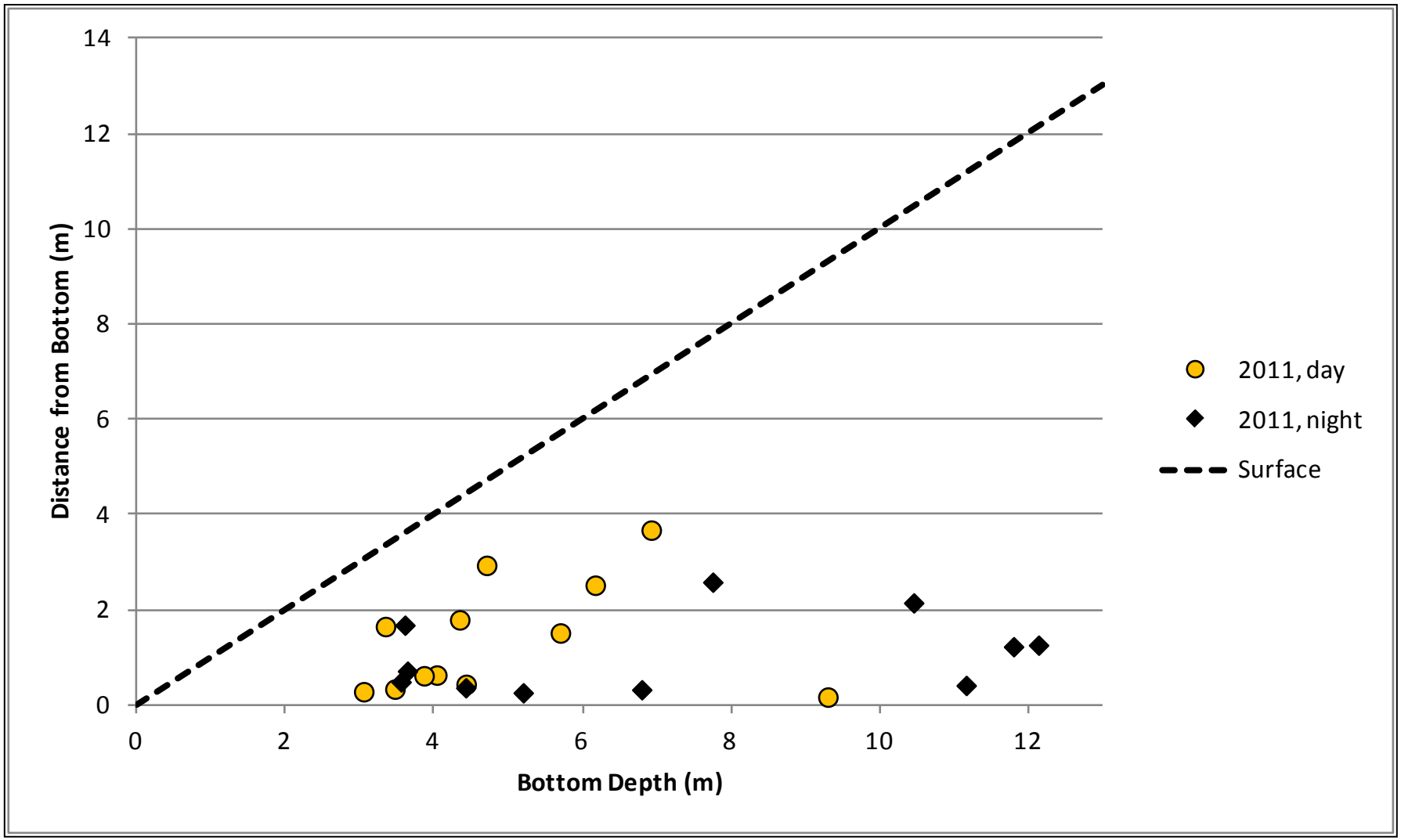

Source: Present study

Figure 6-33 **Distance from River Bottom of Individual Fish Echoes Estimated to be >30 Centimeters Total Length as a Function of Bottom Depth, as Detected during the Day and Night in Down-Looking Mobile Hydroacoustic Surveys in 2011**

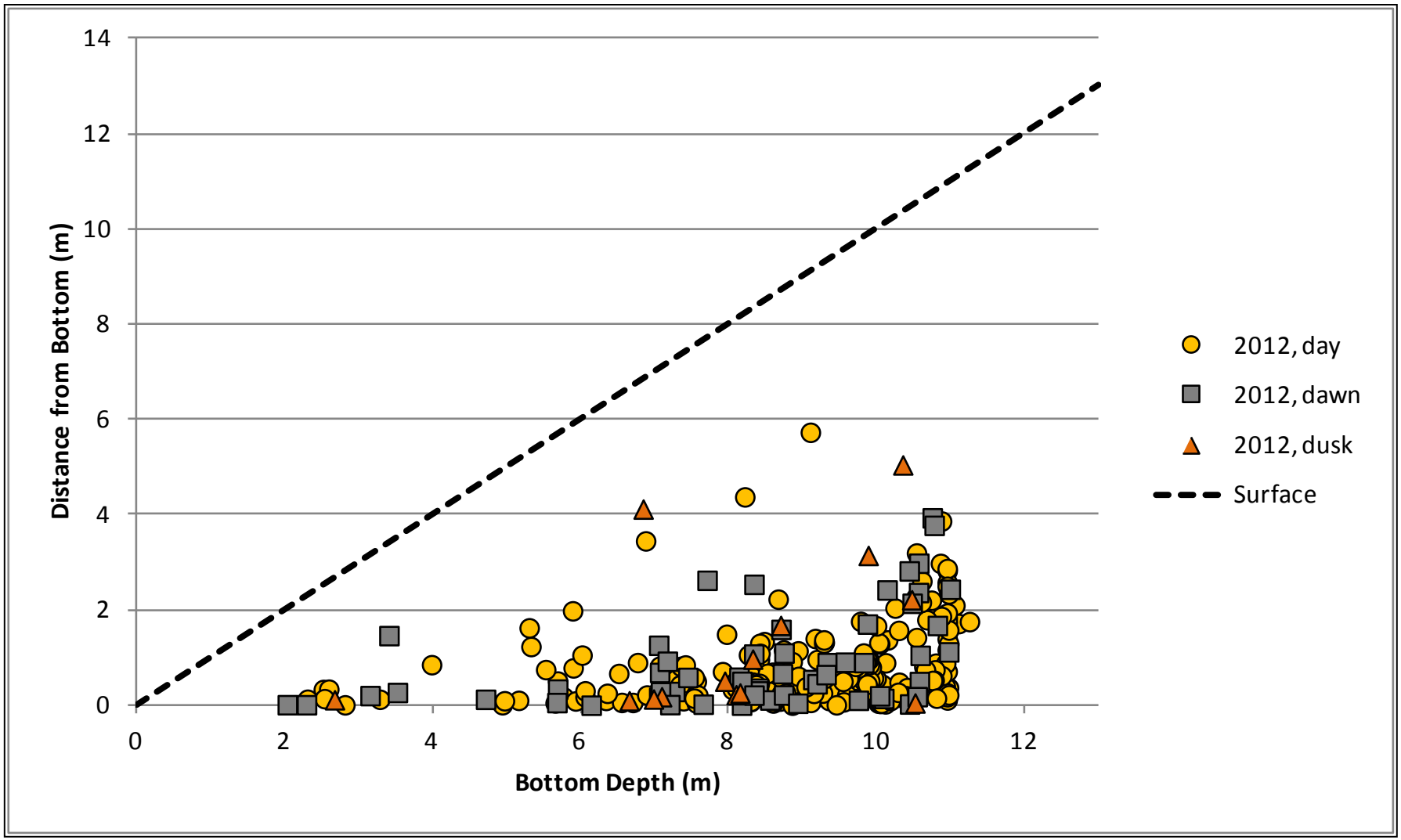

Source: Present study

Figure 6-34 **Distance from River Bottom of Individual Fish Echoes Estimated to be >30 Centimeters Total Length as a Function of Bottom Depth, as Detected during the Day, Dawn, and Dusk in Down-Looking Mobile Hydroacoustic Surveys in 2012**

DENSITY CHANGES AND COMPARISONS TO REFERENCE SITES

Density Changes

The density of large fish (greater than 30 cm TL) estimated from down-looking mobile hydroacoustic surveys generally was considerably greater in 2012 (mean = 146 fish per 10,000 m^3, median = 66.6 fish per 10,000 m^3) than 2011 (mean = 3.9 fish per 10,000 m^3, median = 1.4 fish per 10,000 m^3). Figures of down-looking density from each survey are presented in relation to environmental variables (discharge, water temperature, turbidity, and small-fish density) for 2011 (Figures G-1, G-2, G-3, and G-4 in Appendix G, "Plots of Environmental Variables and Large-Fish Density from Mobile Hydroacoustic Surveys") and 2012 (Figures G-5, G-6, G-7, and G-8 in Appendix G). The 2011 surveys occurred between May 16 and June 8, and density ranged from zero (10 of 23 surveys) to more than 20 fish per 10,000 m^3 on May 23 (night). In 2012, surveys occurred between March 8 and May 31 (no surveys occurred in April during rock barrier construction), with density ranging from zero (3 of 26 surveys) to more than 1,000 fish per 10,000 m^3 at dusk on May 23. Density in 2012 generally was greater after the physical rock barrier was installed, during higher water temperatures (Figure G-6 in Appendix G).

The density of large fish (greater than 30 cm TL) estimated from side-looking mobile hydroacoustic surveys generally was considerably greater in 2012 (mean = 8.0 fish per 10,000 m^3, median = 6.6 fish per 10,000 m^3) than in 2011 (mean = 1.7 fish per 10,000 m^3, median = 1.4 fish per 10,000 m^3). Figures of side-looking density from each survey are presented in relation to environmental variables in 2011 (Figures G-9, G-10, G-11, and G-12 in Appendix G) and 2012 (Figures G-13, G-14, G-15, and G-16 in Appendix G). Density in 2011 surveys ranged from zero (2 of 23 surveys) to more than 4.2 fish per 10,000 m^3 on May 25 (night). Density in 2012 surveys ranged from just more than 1.2 fish per 10,000 m^3 on March 8 (day) to nearly 35 fish per 10,000 m^3 at dawn on May 23. As with the down-looking data, density in 2012 generally was greater after the physical rock barrier was installed, during higher water temperatures (Figure G-14 in Appendix G).

Plots of the hydroacoustic data included in the GLM analyses (Figures 6-35, 6-36, 6-37, 6-38, and 6-39) showed evidence for greater density of large fish with higher water temperature and lower discharge.

GLM and model-averaging suggested support for same-day discharge and water temperature as predictors of large-fish density from down-looking surveys at the HOR study area, as indicated by predictor coefficients with 95% confidence intervals excluding zero and importance greater than 0.8 (Tables 6-68 and 6-69). Therefore, the null hypothesis $H14_0$ was rejected for these predictors (see "Objectives and Hypotheses Related to Changes in Density of Predatory Fishes" in Section 1.2.4, "Behavior and Density Changes in Predatory Fishes").

Consistent with the observations from the original data described previously, density was negatively related to discharge and positively related to water temperature. There was little support for any other predictors, so null hypothesis $H14_0$ was accepted for these predictors. The GLMs with predictors included provided a better fit to the data than the intercept-only model: the full model with all predictors was ranked eighth out of 32 total models and had the quasi-likelihood equivalent of AIC corrected for small sample sizes ($QAIC_c$) of 255.8, in comparison to $QAIC_c$ of 282.1 for the intercept-only model (ranked last of all models) (Table 6-70). The GLMs using 7-day-mean predictors also suggested support for water temperature as a predictor of large-fish density (Table 6-68). However, the full model had a higher $QAIC_c$ (266.1; 26th-ranked model) (Table 6-71) than the full model for same-day predictors (255.8), suggesting that the model-averaged coefficients based on same-day predictors provided a better fit to the data.

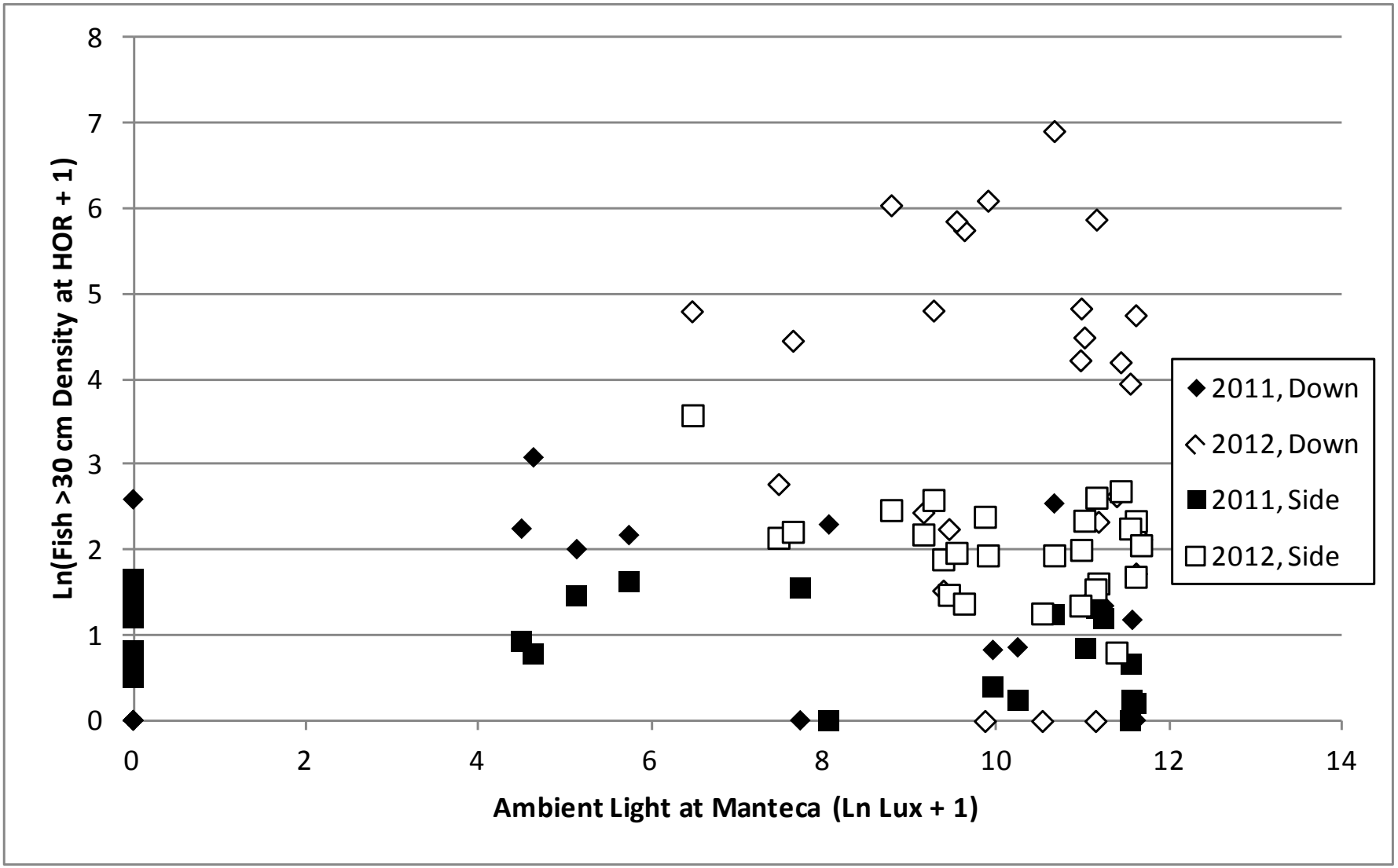

Source: Present study

Figure 6-35 **Estimated Density of Fish >30 Centimeters Total Length in Relation to Ambient Light for 2011 and 2012 Down- and Side-Looking Mobile Hydroacoustic Surveys**

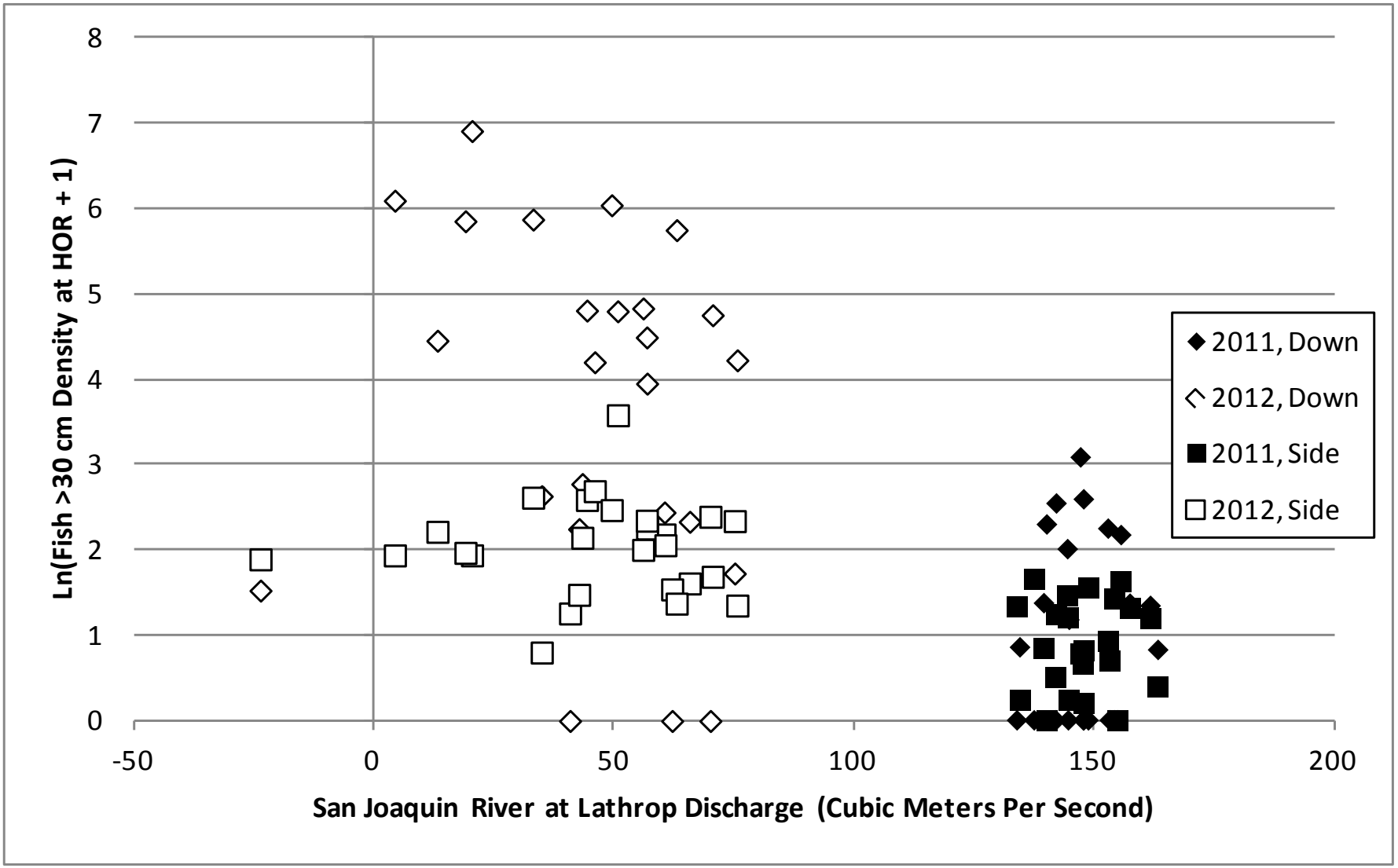

Source: Present study

Figure 6-36 **Estimated Density of Fish >30 Centimeters Total Length in Relation to River Discharge for 2011 and 2012 Down- and Side-Looking Mobile Hydroacoustic Surveys**

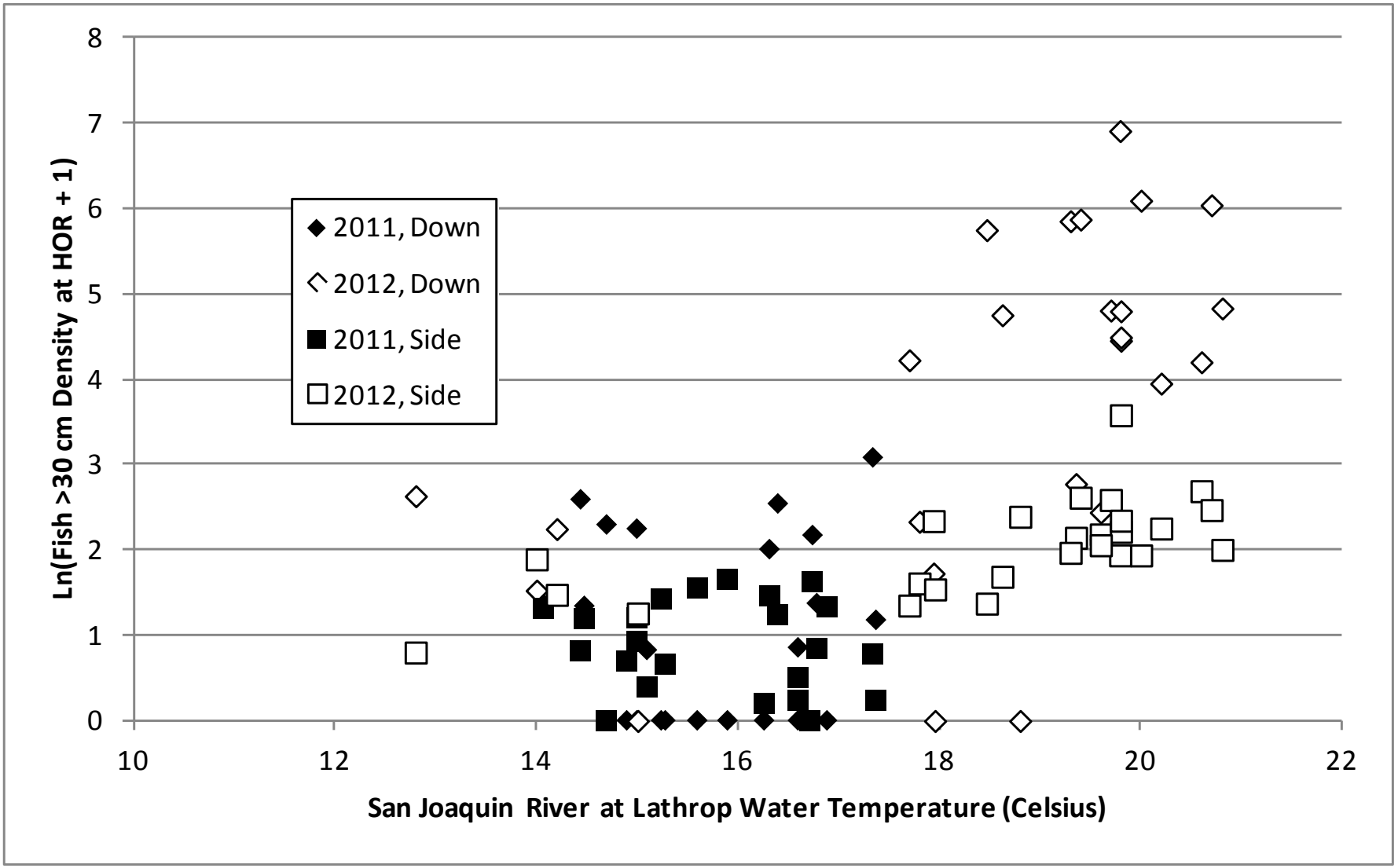

Source: Present study

Figure 6-37 **Estimated Density of Fish >30 Centimeters Total Length in Relation to Water Temperature for 2011 and 2012 Down- and Side-Looking Mobile Hydroacoustic Surveys**

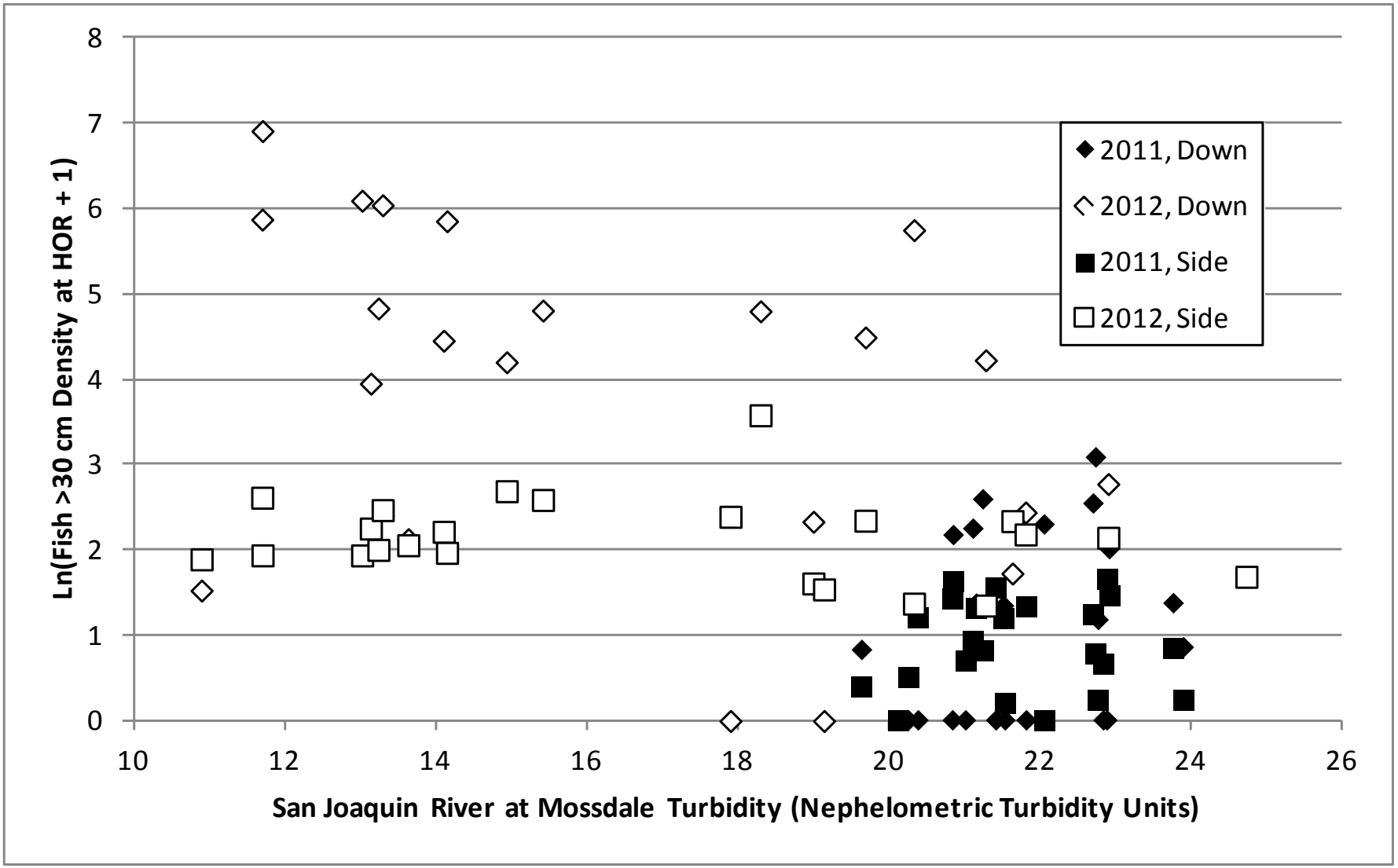

Source: Present study

Figure 6-38 **Estimated Density of Fish >30 Centimeters Total Length in Relation to Turbidity for 2011 and 2012 Down- and Side-Looking Mobile Hydroacoustic Surveys**

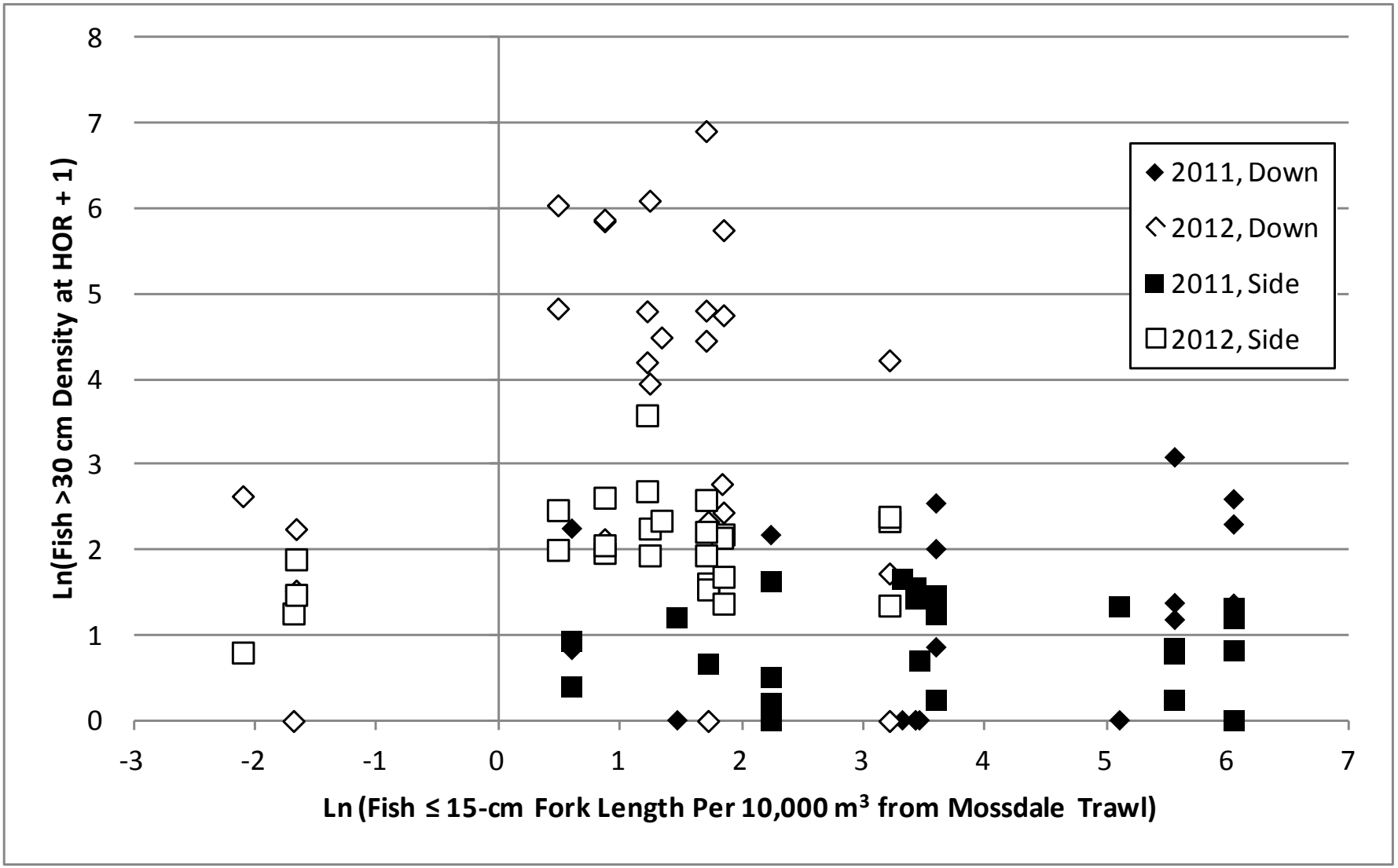

Source: Present study

Figure 6-39 **Estimated Density of Fish >30 Centimeters Total Length in Relation to Density of Fish ≤ 15 Centimeters Fork Length from Mossdale Trawling for 2011 and 2012 Down- and Side-Looking Mobile Hydroacoustic Surveys**

Table 6-68
Model-Averaged Coefficients, 95% Confidence Limits, and Variable Importance for the Generalized Linear Modeling of Changes in Density of Large Fish (>30 Centimeters Total Length) from Down-Looking Mobile Hydroacoustic Surveys as a Function of 7-Day Environmental Variables

Variable	Estimate	95% Confidence Limits		Importance
		Lower	Upper	
Water Temperature	0.693	0.354	1.032	0.97
Discharge	-0.013	-0.035	0.009	0.69
Small-Fish Density	0.064	-0.220	0.349	0.35
Turbidity	-0.031	-0.169	0.107	0.32
Ambient Light Level	-0.005	-0.042	0.032	0.22

Source: Present study

Table 6-69
Model-Averaged Coefficients, 95% Confidence Limits, and Variable Importance for the Generalized Linear Modeling of Changes in Density of Large Fish (>30 Centimeters Total Length) from Down-Looking Mobile Hydroacoustic Surveys as a Function of Same-Day Environmental Variables

Variable	Estimate	95% Confidence Limits		Importance
		Lower	Upper	
Discharge	-0.024	-0.040	-0.007	0.95
Water Temperature	0.357	0.022	0.692	0.86
Small-Fish Density	0.101	-0.179	0.381	0.51
Ambient Light Level	-0.004	-0.038	0.030	0.23
Turbidity	-0.003	-0.035	0.029	0.15

Source: Present study

Table 6-70
Model Fit and Weight for Generalized Linear Modeling of Changes in Density of Large Fish (>30 Centimeters Total Length) from Down-Looking Mobile Hydroacoustic Surveys as a Function of Same-Day Environmental Variables

Model Rank	Variables	$QAIC_c$	w_i
1	Intercept + Discharge + Temperature	252.760	0.218
2	Intercept + Small-Fish Density + Discharge + Temperature	253.237	0.172
3	Intercept + Small-Fish Density + Discharge + Temperature + Turbidity	253.237	0.172
4	Intercept + Ambient Light + Discharge + Temperature	255.138	0.066
5	Intercept + Discharge + Temperature + Turbidity	255.238	0.063
6	Intercept + Discharge	255.728	0.049
7	Intercept + Ambient Light + Small-Fish Density + Discharge + Temperature	255.774	0.048
8	Intercept + Ambient Light + Small-Fish Density + Discharge + Temperature + Turbidity	255.774	0.048
9	Intercept + Small-Fish Density + Discharge	256.476	0.034
10	Intercept + Temperature + Turbidity	257.222	0.023
11	Intercept + Ambient Light + Discharge + Temperature + Turbidity	257.724	0.018
12	Intercept + Discharge + Turbidity	257.932	0.016
13	Intercept + Ambient Light + Discharge	258.080	0.015
14	Intercept + Ambient Light + Small-Fish Density + Discharge	258.947	0.010
15	Intercept + Small-Fish Density + Discharge + Turbidity	258.953	0.010
16	Intercept + Small-Fish Density + Temperature + Turbidity	259.484	0.008
17	Intercept + Ambient Light + Temperature + Turbidity	259.500	0.007
18	Intercept + Temperature	260.013	0.006
19	Intercept + Ambient Light + Discharge + Turbidity	260.369	0.005
20	Intercept + Small-Fish Density + Temperature	261.245	0.003
21	Intercept + Ambient Light + Temperature	261.455	0.003
22	Intercept + Ambient Light + Small-Fish Density + Discharge + Turbidity	261.538	0.003
23	Intercept + Ambient Light + Small-Fish Density + Temperature	263.388	0.001
24	Intercept + Ambient Light + Small-Fish Density + Temperature + Turbidity	263.388	0.001
25	Intercept + Ambient Light + Turbidity	272.783	0.000
26	Intercept + Turbidity	274.698	0.000
27	Intercept + Ambient Light + Small-Fish Density + Turbidity	275.166	0.000
28	Intercept + Small-Fish Density + Turbidity	275.333	0.000
29	Intercept + Small-Fish Density	277.677	0.000
30	Intercept + Ambient Light	277.763	0.000
31	Intercept + Ambient Light + Small-Fish Density	278.070	0.000
32	*Intercept Only*	*282.148*	*0.000*

Notes: $QAIC_c$ = Akaike's Information Criterion adjusted for small sample sizes, accounting for overdispersion; w_i = weight
Source: Present study

Table 6-71
Model Fit and Weight for Generalized Linear Modeling of Changes in Density of Large Fish (>30 Centimeters Total Length) from Down-Looking Mobile Hydroacoustic Surveys as a Function of 7-Day Environmental Variables

Model Rank	Variables	$QAIC_c$	w_i
1	Intercept + Discharge + Temperature	255.029	0.219
2	Intercept + Temperature + Turbidity	255.832	0.147
3	Intercept + Small-Fish Density + Discharge + Temperature	256.241	0.120
4	Intercept + Small-Fish Density + Discharge + Temperature + Turbidity	256.241	0.120
5	Intercept + Ambient Light + Discharge + Temperature	257.309	0.070
6	Intercept + Ambient Light + Discharge + Temperature + Turbidity	257.309	0.070
7	Intercept + Discharge + Temperature + Turbidity	257.509	0.063
8	Intercept + Small-Fish Density + Temperature + Turbidity	258.254	0.044
9	Intercept + Ambient Light + Temperature + Turbidity	258.272	0.043
10	Intercept + Small-Fish Density + Temperature	259.008	0.030
11	Intercept + Temperature	259.714	0.021
12	Intercept + Small-Fish Density + Discharge + Turbidity	260.883	0.012
13	Intercept + Ambient Light + Temperature	261.349	0.009
14	Intercept + Ambient Light + Small-Fish Density + Temperature	261.440	0.009
15	Intercept + Ambient Light + Small-Fish Density + Temperature + Turbidity	261.440	0.009
16	Intercept + Discharge + Turbidity	262.761	0.005
17	Intercept + Small-Fish Density + Discharge	263.796	0.003
18	Intercept + Ambient Light + Discharge + Turbidity	265.089	0.001
19	Intercept + Discharge	265.627	0.001
20	Intercept + Ambient Light + Small-Fish Density + Discharge	266.056	0.001
21	Intercept + Ambient Light + Small-Fish Density + Discharge + Temperature	266.056	0.001
22	Intercept + Ambient Light + Small-Fish Density + Discharge + Turbidity	266.056	0.001
23	Intercept + Ambient Light + Small-Fish Density + Discharge + Temperature + Turbidity	266.056	0.001
24	Intercept + Ambient Light + Discharge	267.995	0.000
25	Intercept + Small-Fish Density	279.895	0.000
26	Intercept + Ambient Light + Small-Fish Density	280.513	0.000
27	Intercept + Ambient Light	281.994	0.000
28	Intercept + Small-Fish Density + Turbidity	282.225	0.000
29	Intercept + Ambient Light + Turbidity	282.508	0.000
30	Intercept + Ambient Light + Small-Fish Density + Turbidity	282.999	0.000
31	Intercept + Turbidity	284.671	0.000
32	*Intercept Only*	*286.484*	*0.000*

Notes: $QAIC_c$ = Akaike's Information Criterion adjusted for small sample sizes, accounting for overdispersion; w_i = weight
Source: Present study

Similar to the down-looking density results, GLM and model-averaging suggested support for same-day discharge (negative relationship) and water temperature (positive relationship) as predictors of the density of large fish from side-looking surveys at the HOR study area (Table 6-72). Null hypothesis $H14_0$ was therefore rejected for these predictors. Note that the upper 95% confidence interval for discharge is 0.000. No other predictors were supported through model-averaging; $H14_0$ was accepted for these predictors. Inclusion of predictors improved the fit of the model to the data (full model $QAIC_c = 300.5$, intercept-only model $QAIC_c = 320.5$) (Table 6-73). Water temperature was also supported as a predictor of side-looking density for 7-day-mean predictor data (Table 6-74), although the full model had a $QAIC_c$ (303.9) (Table 6-75) that was more than three units greater than the $QAIC_c$ for the full model based on same-day predictors (300.5). As with down-looking density data, this suggests that the model-averaged coefficients based on same-day predictors provided a better fit to the data.

Table 6-72
Model-Averaged Coefficients, 95% Confidence Limits, and Variable Importance for Generalized Linear Modeling of Density Changes of Large Fish (>30 Centimeters Total Length) from Side-Looking Mobile Hydroacoustic Surveys as a Function of Same-Day Environmental Variables

Variable	Estimate	95% Confidence Limits		Importance
		Lower	Upper	
Water Temperature	0.205	0.057	0.354	0.93
Discharge	-0.008	-0.016	0.000	0.87
Ambient Light Level	-0.025	-0.090	0.041	0.47
Small-Fish Density	0.009	-0.069	0.087	0.35
Turbidity	-0.001	-0.022	0.020	0.20

Source: Present study

Table 6-73
Model Fit and Weight for Generalized Linear Modeling of Density Changes of Large Fish (>30 Centimeters Total Length) from Side-Looking Mobile Hydroacoustic Surveys as a Function of Same-Day Environmental Variables

Model Rank	Variables	$QAIC_c$	w_i
1	Intercept + Discharge + Temperature	298.333	0.211
2	Intercept + Ambient Light + Discharge + Temperature	298.432	0.201
3	Intercept + Ambient Light + Small-Fish Density + Discharge + Temperature	300.508	0.071
4	Intercept + Ambient Light + Small-Fish Density + Discharge + Temperature + Turbidity	300.508	0.071
5	Intercept + Small-Fish Density + Discharge + Temperature	300.681	0.065
6	Intercept + Small-Fish Density + Discharge + Temperature + Turbidity	300.681	0.065
7	Intercept + Discharge + Temperature + Turbidity	300.730	0.064
8	Intercept + Ambient Light + Discharge + Temperature + Turbidity	300.966	0.057
9	Intercept + Temperature + Turbidity	301.971	0.034
10	Intercept + Small-Fish Density + Temperature	302.442	0.027
11	Intercept + Temperature	303.361	0.017
12	Intercept + Discharge	303.392	0.017
13	Intercept + Ambient Light + Temperature + Turbidity	303.445	0.016
14	Intercept + Ambient Light + Discharge	303.998	0.012
15	Intercept + Small-Fish Density + Temperature + Turbidity	304.167	0.011
16	Intercept + Ambient Light + Small-Fish Density + Temperature	304.480	0.010
17	Intercept + Ambient Light + Small-Fish Density + Temperature + Turbidity	304.480	0.010
18	Intercept + Discharge + Turbidity	304.543	0.009
19	Intercept + Small-Fish Density + Discharge	305.016	0.007
20	Intercept + Ambient Light + Small-Fish Density + Discharge	305.105	0.007
21	Intercept + Ambient Light + Discharge + Turbidity	305.304	0.006
22	Intercept + Ambient Light + Temperature	305.658	0.005
23	Intercept + Small-Fish Density + Discharge + Turbidity	306.807	0.003
24	Intercept + Ambient Light + Small-Fish Density + Discharge + Turbidity	307.255	0.002
25	Intercept + Small-Fish Density	317.184	0.000
26	Intercept + Turbidity	318.391	0.000
27	Intercept + Small-Fish Density + Turbidity	318.972	0.000
28	Intercept + Ambient Light + Small-Fish Density	319.461	0.000
29	*Intercept Only*	*320.544*	*0.000*
30	Intercept + Ambient Light + Turbidity	320.728	0.000
31	Intercept + Ambient Light + Small-Fish Density + Turbidity	321.437	0.000
32	Intercept + Ambient Light	322.063	0.000

Notes: $QAIC_c$ = Akaike's Information Criterion adjusted for small sample sizes, accounting for overdispersion; w_i = weight
Source: Present study

Table 6-74
Model-averaged Coefficients, 95% Confidence Limits, and Variable Importance for Generalized Linear Modeling of Density Changes for Large Fish (>30 Centimeters Total Length) from Side-Looking Mobile Hydroacoustic Surveys as a Function of 7-Day Environmental Variables

Variable	Estimate	95% Confidence Limits		Importance
		Lower	Upper	
Water Temperature	0.362	0.204	0.521	1.00
Ambient Light Level	-0.059	-0.136	0.019	0.77
Turbidity	-0.076	-0.196	0.044	0.65
Discharge	-0.003	-0.012	0.006	0.35
Small-Fish Density	-0.007	-0.044	0.030	0.09

Source: Present study

Table 6-75
Model Fit and Weight for Generalized Linear Modeling of Density Changes for Large Fish (>30 Centimeters Total Length) from Side-Looking Mobile Hydroacoustic Surveys as a Function of 7-Day Environmental Variables

Model Rank	Variables	$QAIC_c$	w_i
1	Intercept + Ambient Light + Temperature + Turbidity	289.010	0.485
2	Intercept + Ambient Light + Discharge + Temperature	291.663	0.129
3	Intercept + Ambient Light + Discharge + Temperature + Turbidity	291.663	0.129
4	Intercept + Temperature + Turbidity	292.120	0.102
5	Intercept + Discharge + Temperature	294.228	0.036
6	Intercept + Small-Fish Density + Temperature + Turbidity	294.589	0.030
7	Intercept + Discharge + Temperature + Turbidity	294.605	0.030
8	Intercept + Ambient Light + Small-Fish Density + Temperature	296.426	0.012
9	Intercept + Ambient Light + Small-Fish Density + Temperature + Turbidity	296.426	0.012
10	Intercept + Small-Fish Density + Temperature	296.487	0.012
11	Intercept + Small-Fish Density + Discharge + Temperature	296.707	0.010
12	Intercept + Small-Fish Density + Discharge + Temperature + Turbidity	296.707	0.010
13	Intercept + Temperature	301.578	0.001
14	Intercept + Ambient Light + Discharge	302.974	0.000
15	Intercept + Discharge	303.067	0.000
16	Intercept + Ambient Light + Discharge + Turbidity	303.818	0.000
17	Intercept + Ambient Light + Temperature	303.829	0.000
18	Intercept + Ambient Light + Small-Fish Density + Discharge	303.860	0.000
19	Intercept + Ambient Light + Small-Fish Density + Discharge + Temperature	303.860	0.000
20	Intercept + Ambient Light + Small-Fish Density + Discharge + Turbidity	303.860	0.000
21	Intercept + Ambient Light + Small-Fish Density + Discharge + Temperature + Turbidity	303.860	0.000
22	Intercept + Discharge + Turbidity	304.119	0.000
23	Intercept + Small-Fish Density + Discharge	304.531	0.000
24	Intercept + Small-Fish Density + Discharge + Turbidity	306.075	0.000
25	Intercept + Small-Fish Density	312.476	0.000
26	Intercept + Ambient Light + Small-Fish Density	314.740	0.000
27	Intercept + Small-Fish Density + Turbidity	314.755	0.000
28	Intercept + Turbidity	315.641	0.000
29	Intercept + Ambient Light + Small-Fish Density + Turbidity	317.117	0.000
30	Intercept + Ambient Light + Turbidity	318.010	0.000
31	*Intercept only*	*318.914*	*0.000*
32	Intercept + Ambient Light	320.436	0.000

Notes: $QAIC_c$ = Akaike's Information Criterion adjusted for small sample sizes, accounting for overdispersion; w_i = weight
Source: Present study

Comparisons to Reference Sites

There was considerable variability in the density of large fish (>30 cm TL) as estimated from down-looking mobile hydroacoustic surveys at the HOR study area and at the reference sites (Figures 6-40, 6-41, and 6-42). There was a statistically significant (P = 0.01) positive correlation between density at the HOR study area and density at Site 4 (San Joaquin River downstream of the HOR study area) (Figure 6-42), which led to rejection of null hypothesis $H15_0$ (See "Objectives and Hypotheses Related to Changes in Density of Predatory Fishes" in Section 1.2.4, "Behavior and Density Changes in Predatory Fishes,"). However, there was no significant correlation between density at the HOR study area and density at the other two sites (allowing acceptance of $H15_0$) (Table 6-76). The density of large fish from down-looking surveys at the HOR site was significantly greater than at Site 4 (P <0.0001), leading to rejection of hypothesis $H16_0$, and not significantly different from density at Sites 1 and 2 (hypothesis $H16_0$ was accepted for these comparisons).

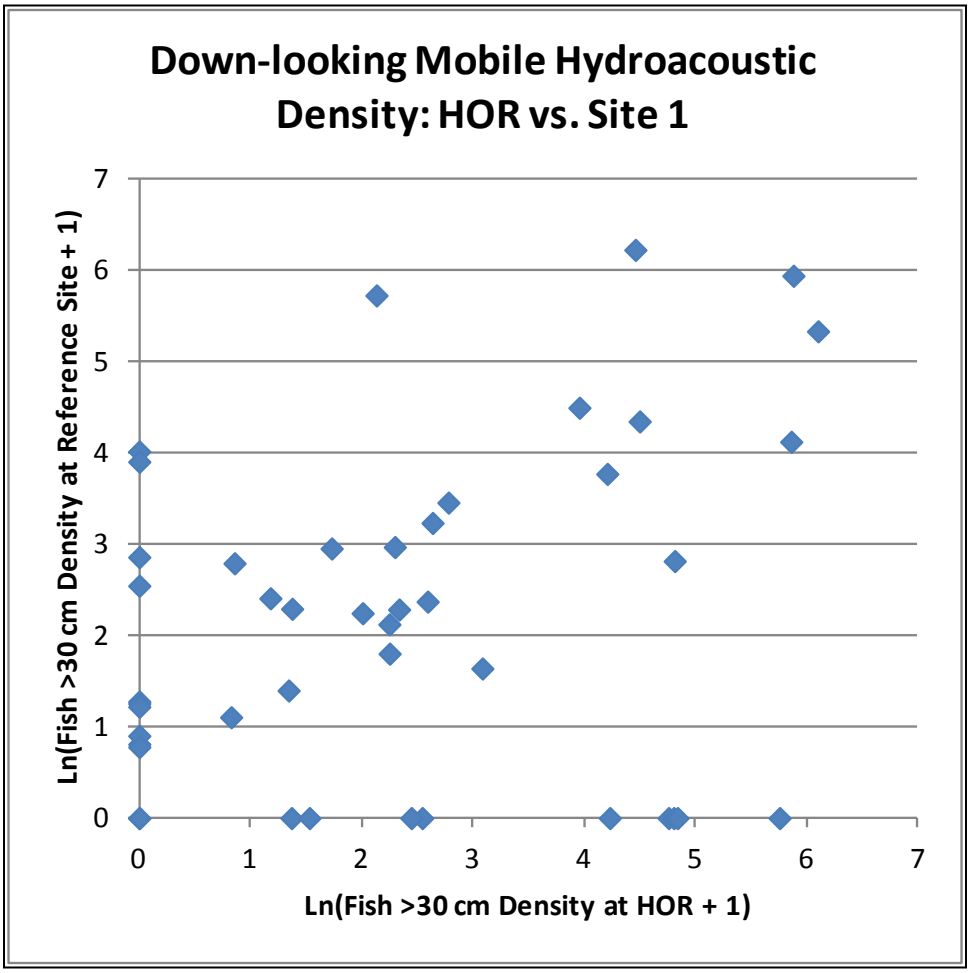

Source: Present study

Figure 6-40 **Estimated Density of Fish >30 Centimeters Total Length at the HOR Study Area in Relation to Density of Fish at Reference Site 1, 2011 and 2012 Down-Looking Mobile Hydroacoustic Surveys**

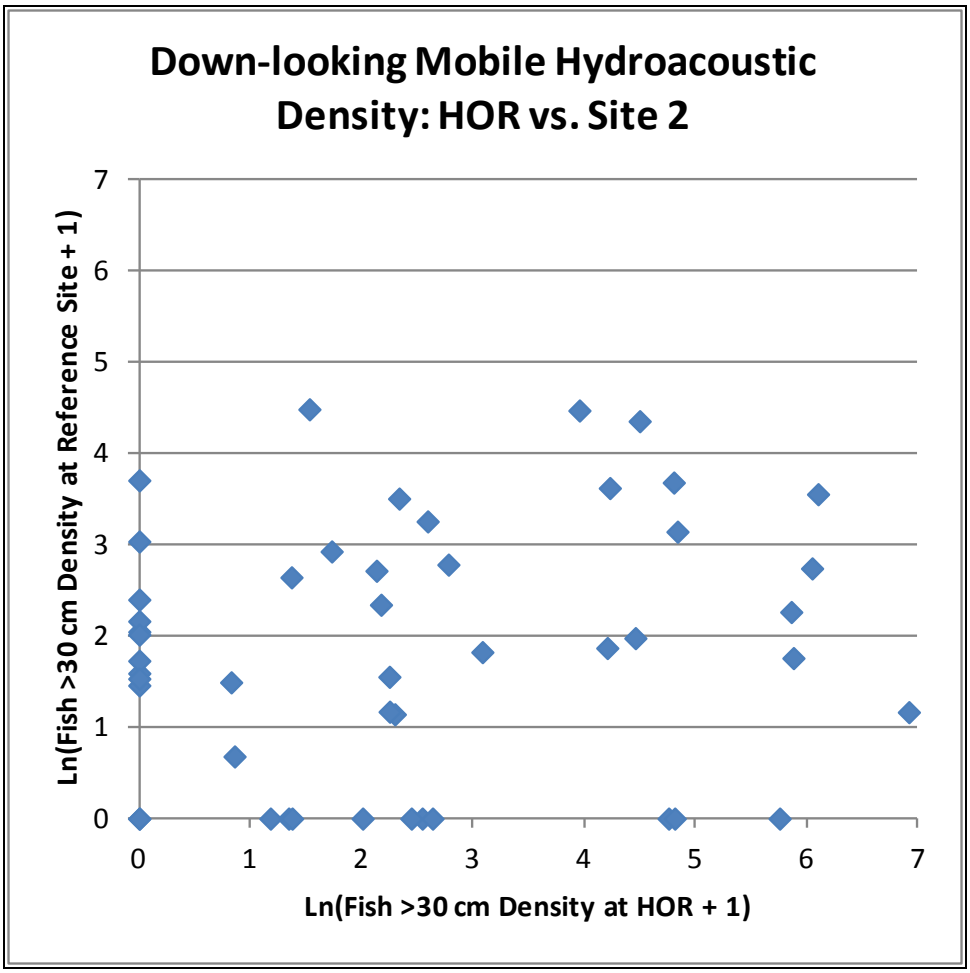

Source: Present study

Figure 6-41 **Estimated Density of Fish >30 Centimeters Total Length at the HOR Study Area in Relation to Density of Fish at Reference Site 2, 2011 and 2012 Down-Looking Mobile Hydroacoustic Surveys**

Table 6-76
Summary of Statistical Tests Comparing Density of Large Fish (>30 Centimeters Total Length) at the Head of Old River Study Area to Reference Sites in the San Joaquin River from Down-Looking Mobile Hydroacoustic Surveys in 2011 and 2012

Comparisons	Correlations		Paired Differences		
	Pearson R	*P* (no. of observations)	Mean Difference (HOR—Reference Site)	Paired T-test t (degrees of freedom)	*P*
HOR vs. Site 1	0.29	0.06 (n = 45)	0.14	0.41 (44 d.f.)	0.68
HOR vs. Site 2	0.14	0.34 (n = 48)	0.62	1.85 (47 d.f.)	0.07
HOR vs. Site 4	**0.37**	**0.01 (n = 48)**	**1.47**	**4.91 (47 d.f.)**	**<0.0001**

Notes: HOR = Head of Old River study area; n = number of observations; n = number; d.f. = degrees of freedom
Comparisons were based on natural-logarithm-transformed data.
Bold Indicates statistical significance at Bonferroni-adjusted $P < 0.017$.
Source: Present study

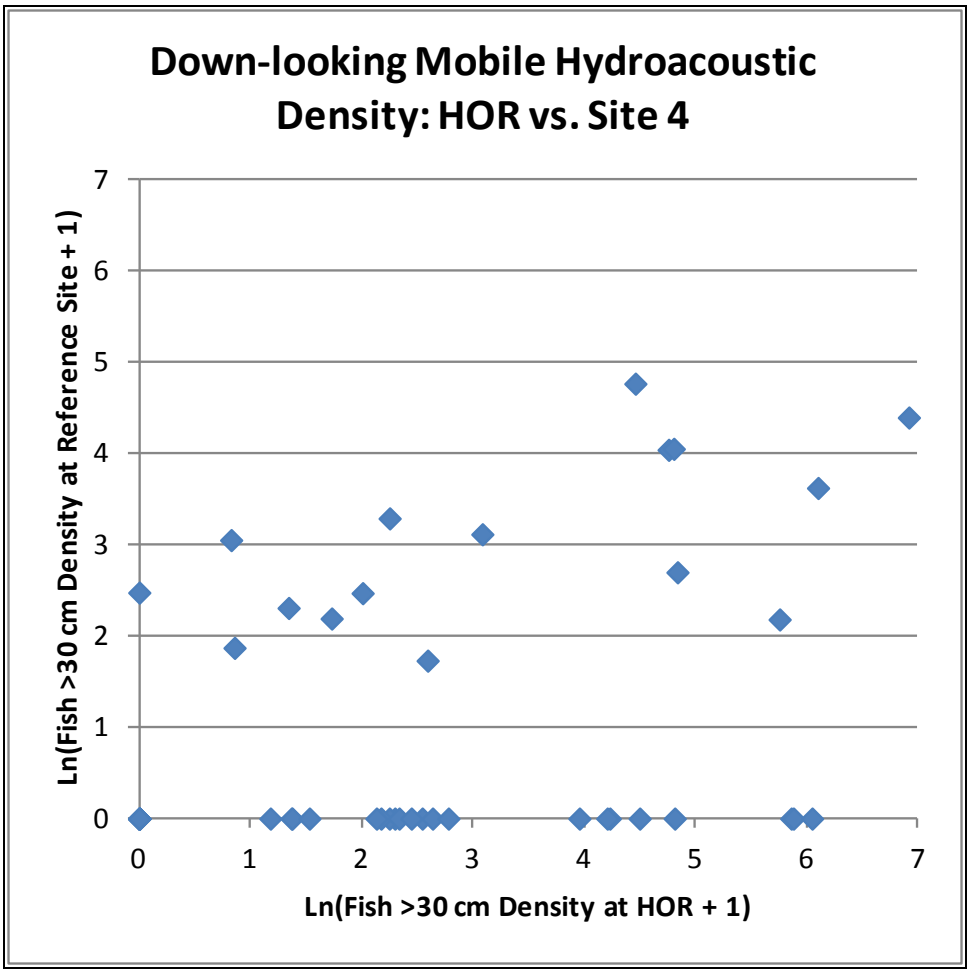

Source: Present study

Figure 6-42 **Estimated Density of Fish >30 Centimeters Total Length at the HOR Study Area in Relation to Density of Fish at Reference Site 4, 2011 and 2012 Down-Looking Mobile Hydroacoustic Surveys**

As noted for down-looking density data, appreciable variability in large-fish density was estimated from side-looking mobile hydroacoustic surveys at the HOR study area and at the reference sites (Figures 6-43, 6-44, and 6-45). Statistically significant positive correlations existed between density at the HOR study area and density at Sites 2 and 4 ($P \leq 0.01$) (Table 6-77), so that $H15_0$ was rejected for these comparisons. There was no correlation between density at the HOR study area and density at Site 1 ($H15_0$ was accepted). Density of large fish from side-looking surveys at the HOR study area was significantly greater than at Sites 1 ($P = 0.01$) and 4 ($P < 0.001$), leading to rejection of hypothesis $H16_0$, and not significantly different from density at Site 2 (hypothesis $H16_0$ was accepted) (Table 6-77).

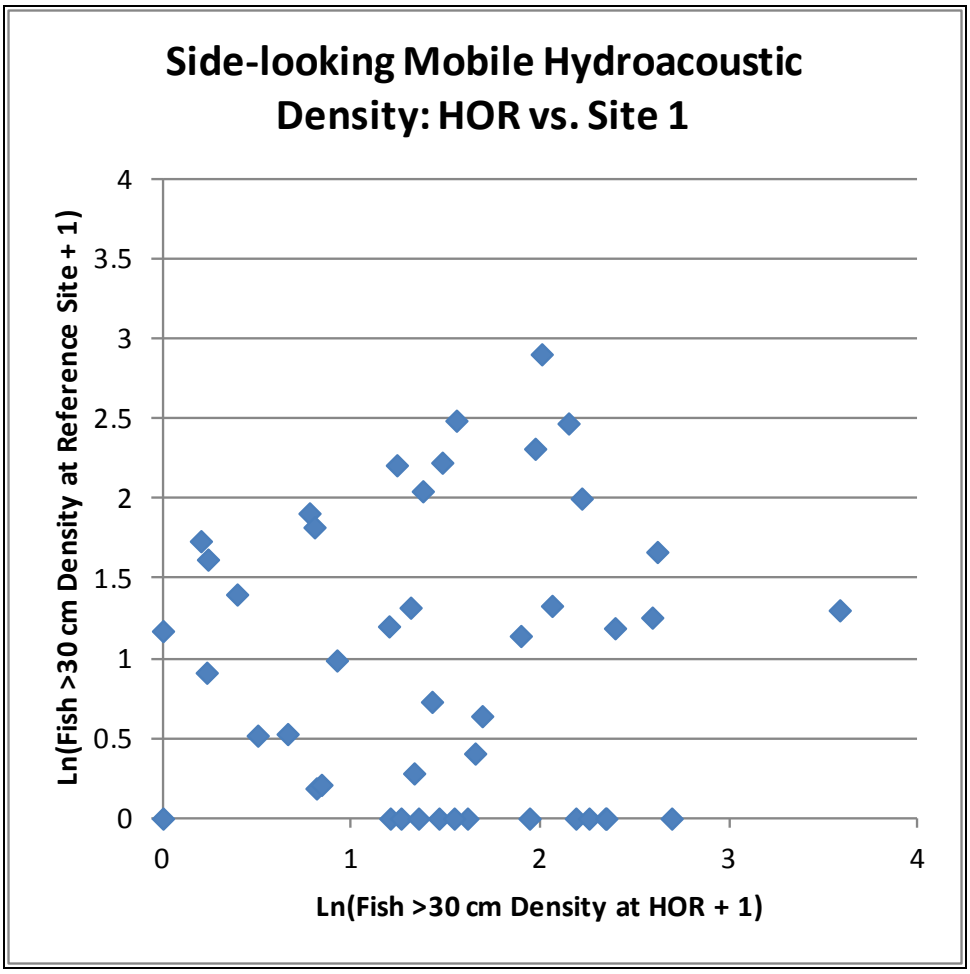

Source: Present study

Figure 6-43 **Estimated Density of Fish >30 Centimeters Total Length at the HOR Study Area in Relation to Density of Fish at Reference Site 1, 2011 and 2012 Side-Looking Mobile Hydroacoustic Surveys**

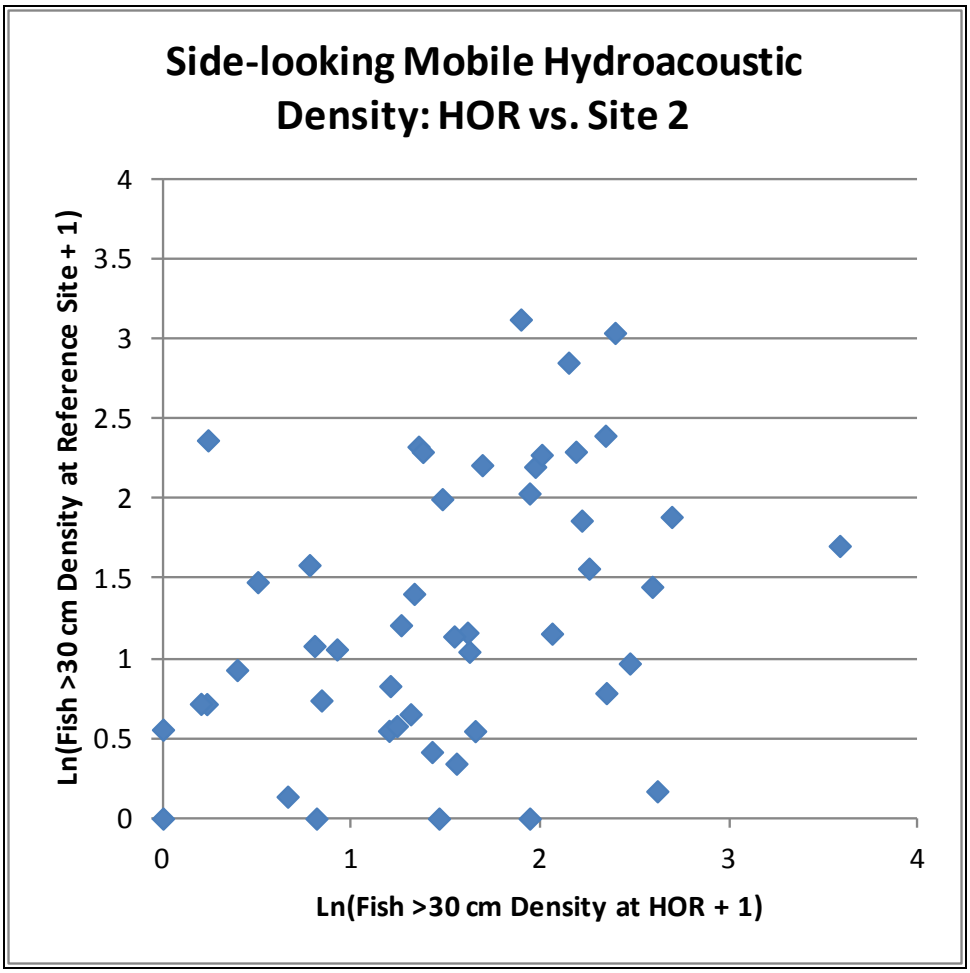

Source: Present study

Figure 6-44 **Estimated Density of Fish >30 Centimeters Total Length at the HOR Study Area in Relation to Density of Fish at Reference Site 2, 2011 and 2012 Side-Looking Mobile Hydroacoustic Surveys**

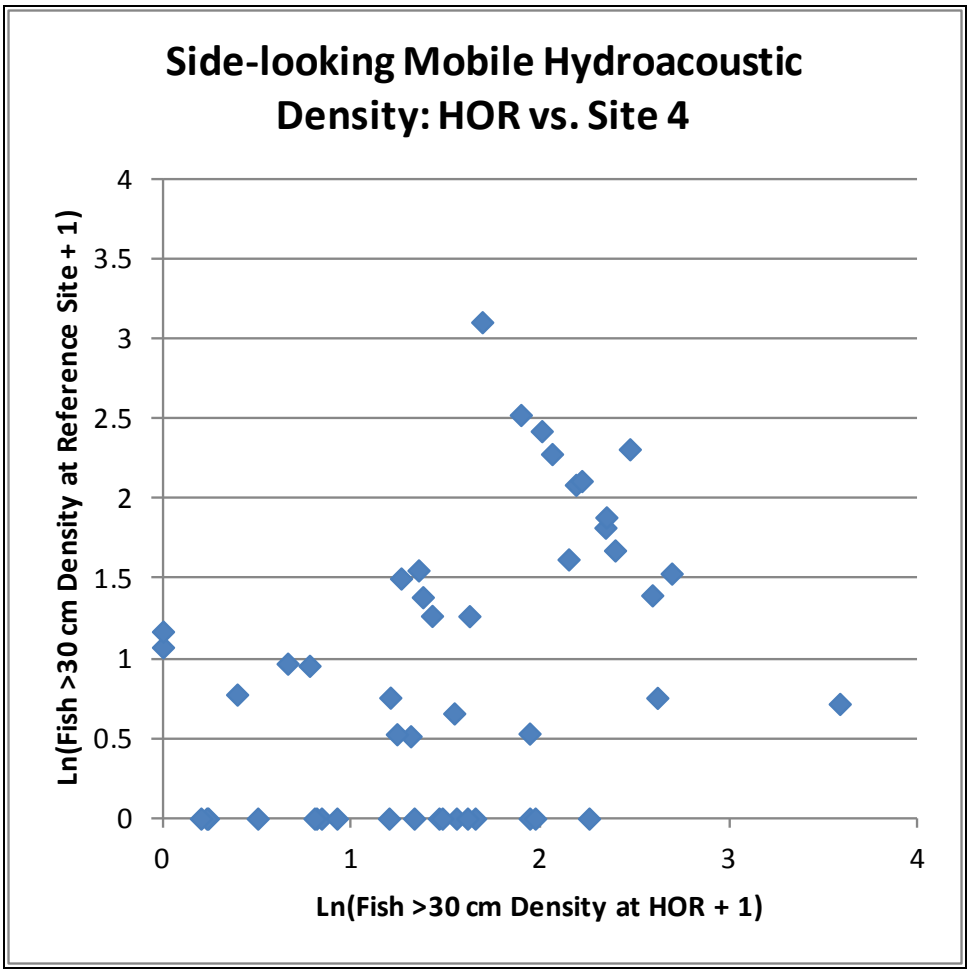

Source: Present study

Figure 6-45 **Estimated Density of Fish >30 Centimeters Total Length at the HOR Study Area in Relation to Density of Fish at Reference Site 4, 2011 and 2012 Side-Looking Mobile Hydroacoustic Surveys**

Table 6-77
Summary of Statistical Tests Comparing Density of Large Fish (>30 Centimeters Total Length) at the Head of Old River Study Area to Reference Sites in the San Joaquin River from Side-Looking Mobile Hydroacoustic Surveys in 2011 and 2012

Comparisons	Correlations		Paired Differences		
	Pearson R	*P* (no. of observations)	Mean difference (HOR—Reference Site)	Paired T-test t (degrees of freedom)	*P*
HOR vs. Site 1	0.01	0.92 (n = 45)	**0.49**	**2.78 (44 d.f.)**	**0.01**
HOR vs. Site 2	**0.37**	**0.01 (n = 48)**	0.22	1.63 (47 d.f.)	0.11
HOR vs. Site 4	**0.41**	**<0.01 (n = 48)**	**0.61**	**4.61 (47 d.f.)**	**<0.0001**

Notes: HOR = Head of Old River study area; No. = number; n = number of observations; d.f. = degrees of freedom
Comparisons were based on natural-logarithm-transformed data.
Bold Indicates statistical significance at Bonferroni-adjusted *P* < 0.017.
Source: Present study

7 DISCUSSION

7.1 JUVENILE SALMONID ROUTING INCLUDING BARRIER EFFECTS

Considerable differences existed between barrier treatments for all dependent variables measured: barrier efficiency, predation rates measured as proportion eaten, and transit speed. In this chapter, the differences between barrier treatments and years are described and compared in tandem, because the associations between barrier treatment and year cannot be separated due to study design. The results of the univariate analyses and proportion eaten are discussed in this chapter because they are closely related. Section 7.2, "Predation on Juvenile Salmonids Including Barrier Effects," focuses on explaining the results from the probability of predation as investigated with generalized linear modeling (GLM). Results related to transit speed are addressed in Appendix D, "Transit Speed Analyses."

7.1.1 2009 BAFF

In 2009, with the BAFF on, overall efficiency ($O_{E)}$ for tagged juvenile Chinook salmon was 20.9% and protection efficiency (P_E) was 33.8% (Tables 6-1 and 6-4). These results were difficult to reconcile with the observed BAFF deterrence efficiency (D_E) of 73.2% (Table 6-7). Two explanations were explored: predation and other factors.

The first explanation for the large gap between O_E and P_E was that a large proportion of the deterred tagged juvenile Chinook salmon subsequently were eaten which decreased O_E. When proportion eaten and the 2D tracks were evaluated for the 2009 data, many tagged juvenile Chinook salmon were determined to have been deterred and then eaten. Therefore, it seems that some of the benefit obtained by the BAFF's deterrence of tagged juvenile Chinook salmon could have been nullified by predation before they successfully migrated past the San Joaquin River finish line.

The difference between D_E and P_E for tagged juvenile Chinook salmon in 2009 was consistent with the striped bass tracking performed in 2011 and 2012. The tracking showed that the scour hole, the San Joaquin River's downstream and upstream offshore areas, and the HOR's upstream offshore areas were the most commonly used places at the HOR study area (Figures 6-19 and 6-21). The data from the mobile hydroacoustic survey also suggested that, in 2011 and 2012, the distribution of the majority of fish greater than 30 cm TL were downstream of the BAFF area (Figures 6-31 and 6-32). Although these data were collected in 2011 and 2012, they support the conclusion that the predator/prey encounter rates may be highest downstream of the 2009 BAFF line. Thus, the 2011 and 2012 data on predators support the conclusion that the difference in D_E and P_E in 2009 may have been caused by predation. Further discussion of areas occupied by predatory fish is provided in Section 7.3.2, "Areas Occupied by Predatory Fishes."

The predation explanation for the 2009 difference between D_E and P_E was consistent with other data collected from 2009 to 2012. Eighty-three percent of stationary/defecated tags were detected in the San Joaquin River downstream of the divergence and of these, 60% were found in the scour hole and 40% were found in the downstream San Joaquin River offshore areas (Figure 6-30). Although the number of stationary tags was small in 2009 and 2010, the pattern was similar through all years studied.

The ability to determine which tags were eaten was imperfect. In 2009, 532 tagged juvenile Chinook salmon released at Durham Ferry passed the San Joaquin River start line (Table 6-57). The total number of tags that passed the finish lines (San Joaquin River and Old River combined) was 410. Therefore, at least 122 perished at the HOR study area. In addition, the proportion of those that were eaten was not definitively determined. It was possible only to estimate the proportion eaten with the data that existed: the 2D tracks. The process by which this was done for tagged juvenile Chinook salmon was expert assessment without validation. No validation was possible because no tagged juvenile Chinook salmon were recaptured to determine the rate of incorrect "eaten" determinations. This error rate for tagged juvenile Chinook salmon therefore, must be estimated. If that error rate is high, many incorrect determinations were made, and the explanation for the discrepancy between 2009 O_E and D_E may not be acceptable. If it is accepted that the error rate is intermediate or small, then it may be concluded that the predation of tagged juvenile Chinook salmon explains some proportion of the difference between O_E and D_E.

The proportion of the difference between O_E and D_E that may be explained by predation was calculated. In 2009, the number of deterred tagged juvenile Chinook salmon was 103 and the number subsequently eaten, after they were deterred, was 36. If those 36 are added in, then the O_E in 2009 under "BAFF On" conditions increases to 36.5%, recall D_E was 73.2%. Thus, predation alone, even if it is accepted that the eaten determination error rate is not high, cannot explain the difference in O_E and D_E.

The second explanation for the large difference between O_E and D_E was the discharge regime in 2009 (Figure 3-2). Many tagged juvenile Chinook salmon were deterred by the BAFF, but may have ultimately exited the HOR study area via Old River because they were transported back on reverse flows. These fish passed between the BAFF and the north shore on reverse flows or passed through the BAFF.

Therefore, predation may account for some of the difference between BAFF deterrence and O_E in 2009. The calculations presented suggest that reverse flows may also have been responsible for some of this difference. Thus, it is concluded that predation on tagged juvenile Chinook salmon that were deterred but exited via Old River, contributed to the difference.

Other researchers working in the south Delta in 2009, including at the HOR study area, found a P_E of 47.4% (SJRGA 2013:155; reproduced in Appendix I, "Route Entrainment Analysis at Head of Old River, 2009 and 2010"). A total of 173 tagged juvenile salmonids passed the San Joaquin River finish line, compared to a total of 365 that passed the Old River or San Joaquin River finish line. This was much higher than the combined (BAFF on and off) P_E of 27.7% reported in this study. At least three reasons explain this difference: (1) the way in which predation was assigned by the two groups; (2) the distance between the San Joaquin River start and finish lines for the two studies; and (3) the fact that in 2009, the San Joaquin River Group Authority (SJRGA) (2013) used one-dimensional detection data (i.e., used one hydrophone's detections at a time), while 2D positions with track visualization were used for this study.

In 2009, the predator classification was based on the acoustic signal pattern through time within the detection of the tag at each individual hydrophone, using the method of Vogel (2010). This method used limited comparison to detections on other Vernalis Adaptive Management Program (VAMP) hydrophones. In this study, predation was assigned using behavior patterns that could be observed with the 2D track visualizations (see Appendix E, "Fish Fate Determination Guidelines"). The method used in the SJRGA (2010) study apparently was less likely to determine that a tag from a salmonid juvenile had been consumed by a predator compared to the method used in the present study.

The finish line used in this study (Figure 5-13) was approximately 303 m upstream of the finish line used by SJRGA (2010). Within this distance, an unknown amount of predation took place. Those salmonids eaten between the two finish lines would count as protected in this study, and SJRGA (2013) would have determined that those juveniles never arrived at the finish line.

The third difference between these two methodologies was that SJRGA (2013) used one-dimensional detection data. By contrast, in this study, 2D positions with track visualization were used for predation determinations. Which of these techniques is more conservative for predation determinations is unknown. Compared to this study, SJRGA (2013) apparently assigned fewer tags a fate of predation.

The effect of light level was evaluated relative to all three measures of barrier efficiency. The only measure that showed a significant influence from light level was D_E; when compared to the BAFF off, D_E was significantly higher when the BAFF was on (Table 6-9). D_E with the BAFF on during high light conditions was 89.7%. This may reflect a greater ability of tagged juvenile Chinook salmon to orient away from the BAFF's main noxious stimulus (the acoustic deterrent) in high light because of the increased visibility of the BAFF. An analogous situation occurs when fish are able to better avoid water intakes by day than by night in low-turbidity water (Helvey and Dorn 1981). However, a previous BAFF trial in England found greater efficiency by night than by day because the increased daytime visibility possibly allowed Atlantic salmon smolts to pass through gaps in the bubble curtain (Welton et al. 2002). However, in this study, the visual predators at the HOR study area were more likely to prey on juvenile Chinook salmon under daylight conditions. Thus, this exceptionally high deterrence delivered with the BAFF only provided a P_E of 48.4%. The benefit gained by BAFF deterrence appears reduced by predation.

No high-velocity samples were acquired in 2009 because of the low magnitude and negative discharges in the San Joaquin River (Figure 3-2). Thus, evaluating the effect of velocity on BAFF efficiency was not possible.

7.1.2 2010 BAFF

In 2010, "BAFF on" O_E was 35.5% (i.e., including tags preyed on at the HOR study area). When the tags that were determined to have been eaten were removed, the P_E improved substantially by operation of the BAFF (44.1%) (Table 6-15). The combined (BAFF on and BAFF off) P_E for 2010 was 36.1%. In 2010, SJRGA (2011) found that the P_E for "tags-in-juveniles" was 47.0%. As with 2009, the value reported in this study was lower than that of SJRGA (2013).

In Section 7.1.1 three reasons were given to explain this difference: (1) the way in which predation was assigned; (2) the distance between the San Joaquin River start and finish lines for the two studies; and (3) the fact that SJRGA (2011) used one-dimensional detection data, while 2D positions with track visualization were used in this study. The one major difference in methodology between 2009 and 2010 was that SJRGA (2011) used a different method for determining predation. In 2010, predation was assigned by SJRGA (2013:Table 5-8) to tag detections using residence time, migration rate, number of return visits to a hydrophone, discharge, and water velocity. In addition, some special conditions were applied to tag detection patterns regarding tide and pumping by the CVP or SWP. Also, the spatial/temporal pattern of detections throughout the VAMP hydrophone array was considered as a whole to determine predation, rather than limiting analysis to a single spatial area. Still, the result was the same: SJRGA (2011, 2013) was less likely to assign a fate of predation in 2010 than this study. These factors

probably played a role in the difference between the estimate reported in this study and the SJRGA estimate; the relative importance of each factor is unknown.

The difference in D_E with the BAFF on compared to the BAFF off was 13.8%. This was very similar in magnitude to the difference between P_E with the BAFF on and off (15.5%). These results suggest that the BAFF operation was deterring about 14% of the tagged juvenile Chinook salmon that approached the BAFF, and that translated to a similar improvement in P_E. In addition, in 2010, a very low percentage of tagged juvenile Chinook salmon exhibited deterrence with the BAFF off (1.2%).

No difference existed in sample proportion eaten between the BAFF on and off, suggesting that, in 2010, BAFF operation did not increase predation rate over the BAFF infrastructure's effect (Table 6-50). This was in contrast to 2009, when the BAFF on proportion eaten was significantly higher than the BAFF off proportion eaten (Table 6-49).

In 2010, light level was not shown to have a substantial effect on O_E (Table 6-12). As in 2009, it was possible that this lack of significance occurred because of small sample sizes and low statistical power. At high light levels, P_E with the BAFF on was higher than with the BAFF off (P-value = 0.0812; Table 6-17); however, the statistical power of this test was only 0.417. The lack of significance (using a critical α of 0.05) could have been a function of low power; thus, it appeared that at high light levels, there could have been significantly higher P_E with the BAFF on than off. This could have been driven by substantial improvement in D_E at high light levels with the BAFF on relative to off conditions (Table 6-22). These results were similar to those of Bowen et al. (2010), at low turbidities (10 NTU), the highest deterrence was observed at high light levels. These results suggest that for the 2010 juvenile Chinook salmon at the HOR study area, additional visual cues to avoid the BAFF were available to the tagged juvenile Chinook salmon during high light, as noted previously for 2009 data.

Velocity did not affect O_E. However, at low velocity, P_E was 16.9 percentage points higher with the BAFF on than off (Kruskal-Wallis $X^2 = 3.699$; P-value = 0.0544) (Table 6-19). This result may have been a consequence of the tagged juvenile Chinook salmon having had more time to evaluate the BAFF and move away before being swept through. The average channel velocity (ACV) did not affect deterrence; deterrence with the BAFF on was significantly better than BAFF off at both velocity levels evaluated (Table 6-24).

For 2010, D_E was significantly improved with the BAFF on, by about 14 percentage points (Table 6-20). This was reflected in an improvement in P_E with the BAFF on by approximately this same amount. These improvements in D_E and P_E were the largest during high-light conditions. Thus, the BAFF's operation did significantly improve the tagged juvenile Chinook salmon proportion selecting the San Joaquin River route (Table 6-15) (Table I-3 in Appendix I), but BAFF-on conditions also exhibited a population proportion eaten of 31.0% (Table 6-50).

7.1.3 BAFF OPERATIONS: 2009 VS. 2010

No significant difference in O_E occurred with the BAFF on in 2009 versus in 2010; however, the P-value (0.0563) (Table 6-26) and the low statistical power observed for the test, 0.489, suggest that a difference could exist between these years with different BAFF alignments. It was concluded that the low statistical power made it impossible to determine if O_E was higher in 2010 than in 2009.

The difference in O_E and P_E between BAFF on and off status was greater in 2010 than in 2009. At least three phenomena contributed to explaining these differences: (1) the discharge regimes differed; (2) tagged juvenile Chinook salmon differed between the two years; and (3) in 2010, the BAFF alignment was longer and curved more than in 2009 (Figure 4-3).

First, in 2009, BAFF efficiencies (Tables 6-1 and 6-4) and the discharge magnitudes (Figure 3-2; see also Appendix D, "Transit Speed Analyses") were the lowest, and the percentage of flow into the San Joaquin River during the study period was the lowest observed across all years (35%). In 2010, BAFF efficiencies were higher (Tables 6-10 and 6-15), discharge magnitude was intermediate (Figure 3-4), and the percentage of flow into the San Joaquin River was 56% (Table 3-1).

Second, the tagged juvenile Chinook salmon were smaller in 2009, and the tag burden was higher in 2009 than in 2010 (described in Tables 5-1 and 5-3 in Chapter 5, "Methods," and in Section 6.3 in Chapter 6, "Results").

Third, the longer-curved 2010 BAFF alignment could have improved O_E and P_E relative to the 2009 alignment without improving D_E. A number of tagged fish in 2010 were not deterred (by the strict definition of deterrence used in the study), but their route was changed from the Old River to the San Joaquin River (Figure 7-1). This would add to the O_E and P_E values, but not to the D_E value (see discussion by Bowen and Bark [2012]).

Like O_E, P_E was 10.4 percentage points higher in 2010 than 2009, but this difference was not significant. In addition, D_E was significantly higher with the BAFF on than off in both years. This study concluded that a statistically significant but small increase in D_E always occurred during BAFF operation (13.8% to 42.1%), and this deterrence increased P_E in both years. However, the increases in P_E were not significant.

A significantly higher proportion of tagged juvenile Chinook salmon were deterred when the BAFF was off in 2009 than in 2010 (Table 6-30). One possible explanation for this was the difference in discharge patterns between the two years, with negative discharges common in 2009 (Figure 3-2) and no negative discharges during the experimental fish releases occurring in 2010, only positive discharges (see Figure 3-4). A second possible explanation was that higher discharges and concomitant higher stage heights in 2010 meant that the BAFF infrastructure took up a smaller proportion of the water column than in 2009; perhaps a smaller proportion of the fish could sense the turbulence created by the BAFF infrastructure or its visual presence, and they did not move away from it or did not follow the alignment in as great a proportion. Alternatively, the higher deterrence rate with the BAFF off in 2009 compared to 2010 could have been due to the different BAFF alignments in the two years. In 2009, the BAFF alignment was straight, and in 2010 the alignment was curved at the end like a hockey stick (Figure 4-3). Thus, a tagged juvenile Chinook salmon turning once guiding along the BAFF would appear to be deterred in 2009. However, the same path in 2010 might cross the BAFF line, and it would be determined to have been undeterred.

In 2010, no substantial difference occurred between the proportions eaten with the BAFF on and off (Table 6-50). However, in 2009, the proportion eaten was significantly higher with the BAFF on than off (Table 6-49). There were no differences in the proportions eaten between 2009 and 2010 for both the BAFF on and off (Table 6-52), suggesting somewhat similar levels of predation in both years.

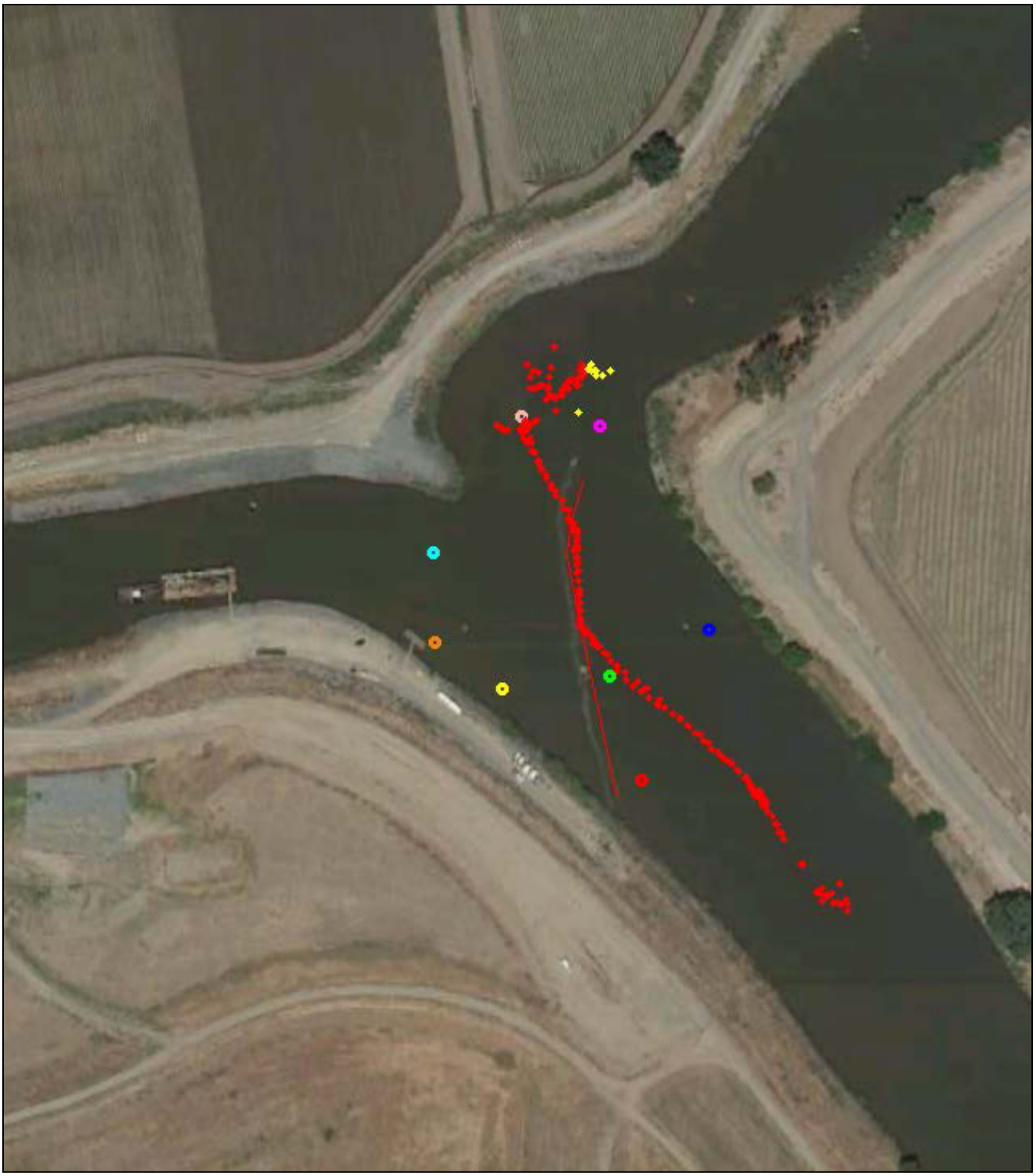

Note: This tagged juvenile Chinook salmon was determined to have been "not deterred," was guided along the BAFF, passed into the San Joaquin River where it was determined to have not been eaten, and successfully passed the San Joaquin River finish line.

Source: Data compiled by Hydroacoustic Technology Inc. this study

Figure 7-1 **Tagged Juvenile Chinook Salmon Number 5353.14 2D Track through the Head of Old River Study Area in 2010**

The 2011 and 2012 GLM modeling of changes in predator density from downward- and sideward-looking hydroacoustics suggests another possible mechanism besides tag burden and turbidity. The GLM modeling showed a negative relationship between same-day discharge and the density of large fish greater than 30 cm TL (Section 6.3.2, "Hydroacoustic Data"). The same-day discharges in 2009 (Figure 3-2) were smaller than those in 2010 (Figure 3-4).

The GLM modeling also found a positive relationship between large-fish density and water temperature. The temperature averaged 2°C warmer in 2009 than in 2010 (Table 3-3). Thus, it was hypothesized that 2009 also supported a greater predator density than 2010. In theory, when the BAFF was turned on in 2009, more predators were at the HOR study area to use the BAFF to improve prey encounter rate or capture probability. Furthermore, because it was, on average, 2°C warmer in 2009, there would have been increased energetic demand per predator and greater total energetic demand (see also Appendix H, "Illustrative Example of Striped Bass Predation Using Bioenergetics Modeling"). These results suggest an area of interesting future inquiry. In addition, tagged juvenile Chinook salmon were smaller in 2009 (Table 5-1); thus, the gape size of a predator needed to eat these fish would be smaller. This would tend to increase the size of the effective predator pool.

For both 2009 and 2010, a portion of the benefit from deterrence was removed by predation. With the BAFF on a range of 30.9 to 31.0% of the tagged juvenile Chinook salmon passing through the HOR study area was eaten. Most of this predation may have taken place after the fish had passed the BAFF in the scour hole and the San Joaquin River downstream offshore areas. However, in 2009, some of this predation could have been caused by BAFF operation itself; the proportion eaten was significantly greater with the BAFF on (0.290) than off (0.138).

7.1.4 2011 No Barrier

In 2011, the discharge magnitudes ranged from 5,000 to 7,500 cfs, far greater than in 2009 or 2010. The 2011 results were also very different, with a mean O_E for tagged juvenile Chinook salmon (0.519) that was similar to the proportion of flow remaining in the San Joaquin River (0.48: Table 3-1). It was concluded that, in a high-discharge year with no barrier, tagged juvenile Chinook salmon entered the San Joaquin River in approximately the same proportion as the fraction of flow.

2009 BAFF Off Compared To 2010 BAFF Off Compared To 2011 No Barrier

In 2009 with the BAFF off, many flow reversals in the San Joaquin River (Figure 3-2) led to flow lines routinely moving toward Old River (Figure 3-9), and the population proportion eaten at the HOR study area with the BAFF off was estimated to be 16.4% that year (Table 6-49). In 2010 with the BAFF off, positive discharges always occurred, but the ACVs were intermediate compared to 2011 ACVs, and the population proportion eaten was estimated to be 20.5% (Table 6-50). In contrast, in 2011, high discharges led to the highest ACVs measured during the entire study, with flow lines more toward the San Joaquin River (Figure 3-11); the measured population proportion eaten was 10.1% (Table 6-53).

These discharge and predation patterns resulted in the pattern of O_E (Table 6-32). It was concluded that the effect of the BAFF infrastructure during BAFF off conditions could not be discerned from these data because of the confounding effects of differing environmental conditions, principally discharge, between years.

CHINOOK SALMON COMPARED TO STEELHEAD

In 2011, tagged juvenile Chinook salmon seemed to enter the San Joaquin River in approximately the same proportion as the fraction of flow. By contrast, steelhead appeared to be less likely than juvenile Chinook salmon to enter the San Joaquin River. However, when tags that were determined to have been eaten were removed, the P_E was not different between tagged juvenile Chinook salmon and steelhead. This suggests that steelhead, like tagged juvenile Chinook salmon, remained in the San Joaquin River in a proportion that was approximately the same as the fraction of the flow.

In 2011, tagged juvenile steelhead appeared to be subject to predation at a higher rate than tagged juvenile Chinook salmon (Table 6-54). However, some of the tags originally inserted into steelhead that were deemed eaten possibly were not eaten. The possibility that steelhead were more likely to receive an incorrect eaten determination than were tagged juvenile Chinook salmon evolved from the steelhead released at Durham Ferry by the Six-Year Steelhead Study/VAMP team and detected at the CVP and SWP holding tanks (see Appendix E, "Fish Fate Determination Guidelines," for discussion). From these steelhead juveniles it was learned that steelhead at the HOR study area sometimes exhibited looping behavior or swam against the flow (Figure 7-2), behavior that also was used as a criterion for determining predation on tagged juvenile Chinook salmon.

For a more accurate understanding of the effects of predation on outmigrating juvenile steelhead in the HOR study area, further research may be required, and alternative methods may need to be developed to distinguish eaten tags. The issue of determining whether a juvenile salmonid has been eaten, for both tagged juvenile Chinook salmon and steelhead, is of prime importance, and is discussed further in Section 8.2.1, "Further Examine Predation Classification."

There did not appear to be any effect on tagged juvenile Chinook salmon or steelhead O_E at different light or velocity levels. However, small sample sizes and low statistical power could have caused an inability to detect any influence. O_E was always higher for tagged juvenile Chinook salmon (13.3 to 17.3 percentage points) than for steelhead, and it was hypothesized in Section 6.1.6, "2011 Chinook Salmon Compared to Steelhead," that steelhead might prefer the Old River route compared to tagged juvenile Chinook salmon.

When tags that had been eaten were removed, no statistical difference was shown between P_E for tagged juvenile Chinook salmon and for steelhead at any light or velocity levels. Thus, the pattern seen in P_E was consistent across all examined light and velocity conditions. However, small sample sizes and low statistical power could have made it impossible to resolve a true difference caused by light or velocity.

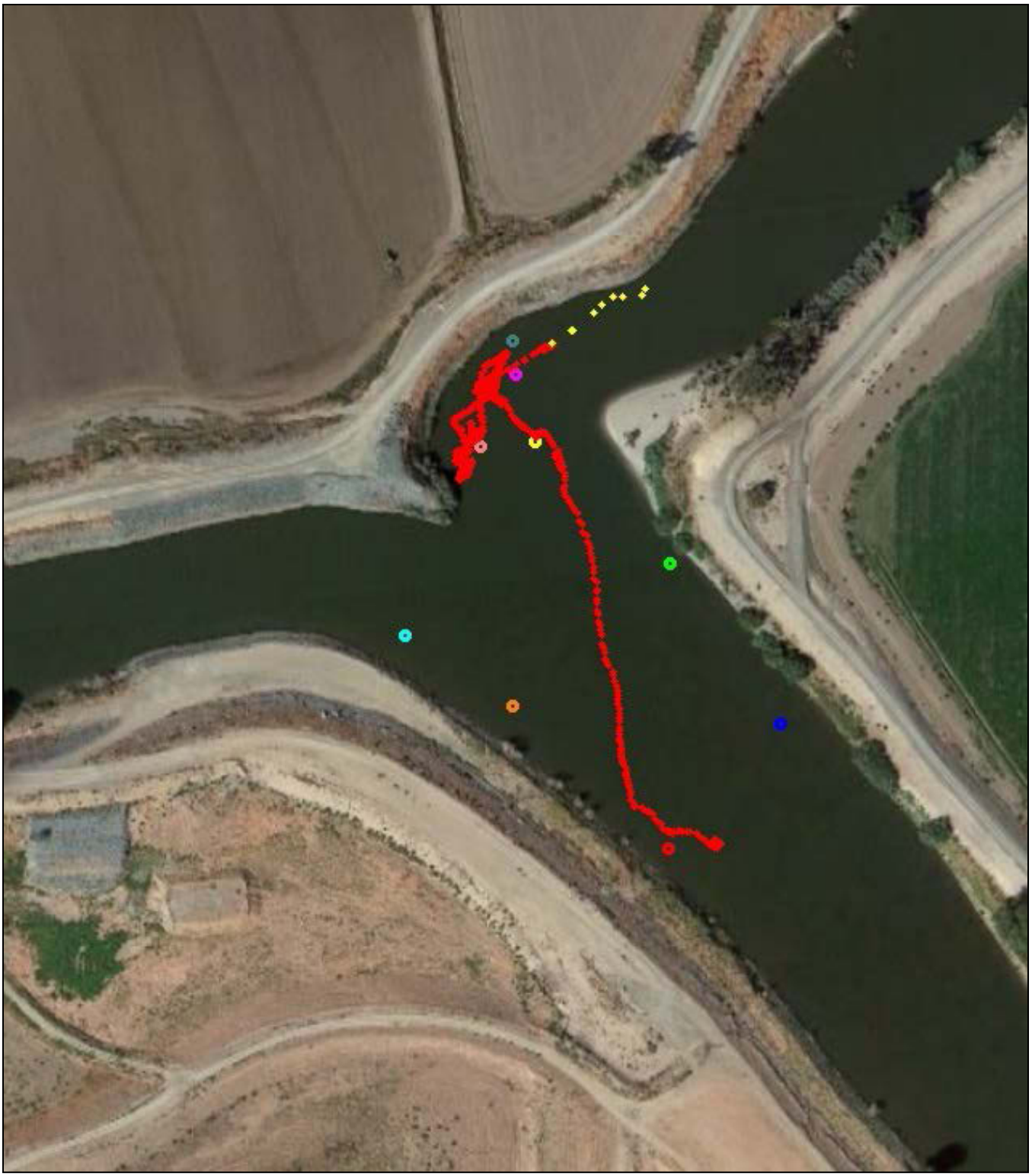

Note: Steelhead 5171.04 entered the HOR study area on June 1, 2011, at 11:17 a.m., departed the same day at 11:43 a.m., and was determined to have not been eaten; this determination was confirmed because 5171.04 was later detected at an export facility's holding tank.

Source: Data compiled by Hydroacoustic Technology Inc. this study.

Figure 7-2 **Tagged Juvenile Steelhead Number 5171.04 2D Track in the Vicinity of the Head of Old River Study Area**

7.1.5 2012 PHYSICAL ROCK BARRIER

For tagged juvenile Chinook salmon, the physical rock barrier's O_E was 61.8%. When tags eaten were removed, the rock barrier's P_E was 100%.

The proportion of flow that went down the San Joaquin River in 2012 was 0.82. Eight culverts were installed for the first time in a rock barrier at the HOR study area. Even with eight culverts, however, the proportion of flow entering Old River was relatively low because the rock barrier physically blocked much of the flow.

Of the tagged juvenile Chinook salmon in 2012, a mean of 38.2% were classified as having been eaten in the sample proportion eaten determination (Table 6-55). This was the highest proportion eaten in all four years of study, although no statistically significant difference existed between 2012 and 2009 and 2010 with the BAFF on (2009: 29.0%; 2010: 21.7%), whereas the 2012 proportion eaten was significantly higher than the 2011 proportion eaten (8.7%).

Tagged juvenile Chinook salmon may have been more vulnerable to predation in 2012 than in other years because of eddies that formed near the rock barrier (Figure 3-18). Additionally, a higher density of large fish (greater than 30 cm TL) occurred in 2012 than in 2011. Large-fish density in 2012 increased after the physical rock barrier was installed, during higher water temperatures (see Appendix G, "Plots of Environmental Variables and Large-Fish Density from Mobile Hydroacoustic Surveys," Figure G-6). Thus, the high density of large fish in 2012 may have been caused, in part, by the rock barrier's role in creating more favorable habitat for predation, coupled with more predatory fish moving into the area as water temperatures increased. Additional discussion is provided in Section 7.2, "Predation on Juvenile Salmonids Including Barrier Effects."

7.2 PREDATION ON JUVENILE SALMONIDS INCLUDING BARRIER EFFECTS

This section focuses on the results of the probability of predation analyses as investigated using GLM. The results of the univariate analyses related to proportion eaten are discussed in Section 7.1, "Juvenile Salmonid Routing Including Barrier Effects," because they are closely related to calculations and analysis of O_E and P_E.

Based on the GLM, the present study found the best support for light level, barrier status, and turbidity as predictors of predation probability on tagged juvenile Chinook salmon in the HOR study area. Light level was important in the GLM for 2009/2010/2012 and 2011/2012; because light level was positively related to predation probability, this supported the hypothesis that visual-feeding predators (such as striped bass and largemouth bass) would have lower predation rates in darkness. Examination of the raw data shows that the proportion of tagged juvenile Chinook salmon entering the HOR study area that were preyed upon by day was two to four times greater than the proportion preyed upon at night (Tables 6-58 and 7-1).

The negative relationship between turbidity and predation probability for the 2011/2012 GLM also agrees with greater predation rate with better visibility, as hypothesized based on observed relationships in the Delta (Ferrari et al. 2013). Turbidity is not as highly correlated with discharge (e.g., to the extent that velocity is). Nevertheless, turbidity is higher with greater discharge, and thus, it reflects to some degree the importance of discharge as a master variable that may influence predation.

Table 7-1
Number and Population Proportion Eaten of Tagged Juvenile Chinook Salmon Preyed Upon at the HOR Study Area, 2009–2012

Year/Barrier/Light	Number of Juveniles		Predation	
	Total	Predation	Proportion	Standard Error
2009	525	120	0.229	0.018
a. NPB Off	292	48	0.164	0.022
i. dark	59	3	0.051	0.029
ii. light	233	45	0.193	0.026
b. NPB On	233	72	0.309	0.030
i. dark	45	6	0.133	0.051
ii. light	188	66	0.351	0.035
2010	451	117	0.259	0.021
a. NPB Off	219	45	0.205	0.027
i. dark	77	11	0.143	0.040
ii. light	142	34	0.239	0.036
b. NPB On	232	72	0.310	0.030
i. dark	60	4	0.067	0.032
ii. light	172	68	0.395	0.037
No Barrier (2011)	1,075	109	0.101	0.009
a. dark	306	9	0.029	0.010
b. light	769	100	0.130	0.012
Rock Barrier (2012)	193	76	0.394	0.035
a. dark	38	6	0.158	0.059
b. light	155	70	0.452	0.040
Total	**2,244**	**422**	**0.188**	**0.008**

Notes: NPB = non-physical barrier (bio-acoustic fish fence); Dark <5.4 lux, light ≥5.4 lux
Source: Present study

Turbidity was not found to be a well-supported predictor of predation probability for the 2009/2010/2012 data, which was in agreement with the absence of a statistically important univariate relationship between proportion eaten and turbidity when using groups of juveniles combined across all years (See "Temperature and Turbidity Effects on Proportion Eaten" in Section 6.2.1, "Proportion Eaten [Univariate Analyses]."") The years 2011 and 2012 may have offered sufficient contrast in turbidity to detect the relationship of this variable to predation, and this may have been masked when including the other years.

Discharge alone was not supported as an important predictor of predation probability at the HOR study area. This finding is consistent with a recent study that related discharge to the survival of tagged juvenile Chinook salmon in the Delta (Zeug and Cavallo 2013), but not consistent with the results of other studies (Newman 2010; Perry 2010). To some extent, this may reflect difficulties in assigning a particular discharge to each juvenile for the GLM analysis; the present study used the nearest 15-minute discharge reading from the San Joaquin River at

Lathrop (SJL) gauge at the time when the juvenile track was nearest the 2009 or 2010 BAFF alignments. For variables such as discharge, which may change more rapidly in tidal situations, this means of assigning a discharge value to each juvenile's fate may cause the conditions relevant to predation to differ from those included in the analysis.

Other predictors that change less rapidly (e.g., light level, turbidity) may be more reflective of the conditions experienced by juveniles at the time of predation. However, although water temperature changes would be less rapid, this predictor was not found to be an important predictor of predation probability. The univariate analysis using data from all years did give a statistically significant positive correlation between water temperature and proportion of juveniles eaten. (See "Temperature and Turbidity Effects on Proportion Eaten" in Section 6.2.1, "Proportion Eaten [Univariate Analyses]."") This could be explained by the increased bioenergetics requirements of predators and possibly the greater ability of predatory fish to swim faster in warmer waters compared to tagged juvenile Chinook salmon.

At the broader, annual scale, the predation rate of tagged juvenile Chinook salmon at the HOR study area was appreciably less in 2011 (0.10) than in the other years (0.23 to 0.39). To some degree, this finding likely was related to discharge and its effect on other abiotic and biotic factors (e.g., density of predatory fishes). (See Section 7.3.3, "Changes in Density of Predatory Fishes." Also see the comments in "Comparison of 2009 BAFF Off, 2010 BAFF Off, and 2011 Conditions" in Section 6.2.1, "Proportion Eaten [Univariate Analyses]," about potential mechanisms for differences between years in the proportion of juveniles eaten.) However, despite considerably higher discharge in 2011 than 2010, the overall through-Delta survival of tagged juvenile Chinook salmon released in the San Joaquin River in 2011 (0.02, i.e., 2%) (SJRGA 2013) was not greater than survival in 2010 (0.05, i.e., 5%) (SJRGA 2011). This latter finding could suggest that in 2011, the relatively intense rates of predation observed in 2010 occurred in areas farther downstream where tidal influence was greater (Cavallo et al. 2013). This topic is revisited in Section 8.2.4, "Study Effects of Physical Barriers on Location of Predation Hotspots", in Section 8, "Recommendations."

Barrier status was found to be a well-supported predictor of predation probability for tagged juvenile Chinook salmon in the analysis comparing the non-physical BAFF on/off from 2009/2010 and the physical rock barrier in 2012. Predation probability was appreciably higher with the non-physical barrier turned on or with the rock barrier than with the non-physical barrier off. The analysis did not aim to differentiate between the 2009 and 2010 barrier configurations; still, a reexamination of the basic proportional predation data subdivided by year gives confidence to the conclusion that the results were reasonably consistent for both years of the BAFF deployment (Table 7-1).

In both 2009 and 2010, approximately 0.31 (i.e., 31%) of tagged juvenile Chinook salmon were preyed on with the non-physical BAFF barrier on, compared to 0.16 (2009) and 0.21 (2010) off. Pairwise, statistical comparisons of the proportion eaten using groups of juvenile Chinook salmon found differences between BAFF on and off conditions in 2009, but not in 2010; no substantial difference existed between years in the proportion eaten when the BAFF was on or off. (See "2009 Results," "2010 Results," and "2009 Compared to 2010" in Section 6.2.1, "Proportion Eaten [Univariate Analyses]."")

The higher proportion of predation in light conditions than in the dark also was consistent between years (Table 7-1). Operation of the BAFF has been shown to have some efficacy in deterring juveniles from entering Old River (see "Deterrence Efficiency" in Section 6.1.1, "2009 Results," and Section 6.1.2, "2010 Results"). The

results of the present study suggest, however, that a tagged juvenile Chinook salmon has as high a probability of being preyed upon when the BAFF is operational compared to when the physical rock barrier is installed. This may be the case because juveniles have longer travel distances through the HOR study area as they avoid the noxious stimuli of the BAFF and may be disoriented by the stimuli, or because they are entrained into the eddies that are created by the rock barrier (Johnston, pers. comm., 2013) (see Section 3.2, "Velocity Field"). The transit speed of tagged juvenile Chinook salmon through the HOR study area was greater with the BAFF on than off in 2009 (but not in 2010; see Appendix D, "Transit Speed Analyses," Tables D-4 and D-6). This finding would support the hypothesis that longer travel distance and speed influence predation rate. Anderson et al. (2005) concluded that survival of juvenile salmon in the Snake River depends more on travel distance than travel time or migration velocity. Deterrence away from Old River to the scour hole also may increase predation probability at the HOR study area with the BAFF turned on or with the physical rock barrier installed. The scour hole was one area where the density and occurrence of predatory fish were relatively high, based on the 2011/2012 mobile hydroacoustic surveys and the occurrence of tagged predatory fish (see discussion in Section 7.3.2, "Areas Occupied by Predatory Fishes").

The fit of the binomial GLMs of predation probability (area under receiver operating characteristic [ROC] = 0.70, 0.73) in the present study was within the range of acceptability based on the criteria of Hosmer and Lemeshow (2000). The fit was somewhat better than the fit from a study predicting the presence of Chinook salmon fry in the American River as a function of velocity, depth, substrate, and cover (Beakes et al. 2012); those authors described their model fit (area under ROC = 0.65) as fair predictive ability. By contrast, the GLMs from the present study fit the data considerably less well than the GLMs used to predict the probability of tagged juvenile Chinook salmon entering Georgiana Slough from the Sacramento River, as a function of the operation of the BAFF and other factors (area under ROC = 0.93, "excellent ability to predict fates" [Perry et al. 2012]). The response data (predation) from the present study include some uncertainty because it is not known whether predation actually occurred. Classifying predation was challenging in 2012. Discharge conditions and the physical rock barrier produced juvenile movement patterns that were unlike those seen in previous years (Johnston, pers. comm., 2013).

As noted previously, some difficulty existed in temporally matching the most relevant periods for abiotic predictor variables to juveniles entering the HOR study area. The closest 15-minute readings were used in the present study. Longer averaging periods also would be possible, which may reduce variability (e.g., averages of readings 30 to 60 minutes before and after). The biotic predictor variables representing the potential abundance of predators and abundance of alternative prey—large-fish density from mobile hydroacoustics and small-fish density from Mossdale trawling, respectively—had longer averaging periods than would have been ideal to avoid reducing the sample size of juvenile-response data because of missing values. A better situation would have been to include data specific to the HOR study area that co-occurred more directly in time and space with each juvenile's arrival.

Despite these shortcomings, the statistical analyses of predation probability for tagged juvenile Chinook salmon provided some insights that supported the initial hypotheses. This was not the case for the tagged juvenile steelhead, for which model fits were poor and no better than intercept-only models. Assigning fates to juvenile steelhead was very difficult because their movement patterns were quite different from those of juvenile Chinook salmon (e.g., steelhead holding behavior and upstream movement was reminiscent of movements by tagged

predatory fish [Johnston, pers. comm., 2013]). Further research into means of determining predation is warranted, and this topic is discussed further in Section 8.2.1, "Further Examine Predation Classification."

Bioenergetics modeling conducted as an ancillary part of this study illustrated the relative differences in prey-fish consumption rates between striped bass of different sizes at water temperatures observed at the HOR study area in 2011 and 2012 (Appendix H, "Illustrative Example of Striped Bass Predation Using Bioenergetics Modeling"). The illustrative example of potential consumption rate for prey fish entering the HOR study area produced estimates of predation that were of similar magnitude to the predation estimates for tagged juvenile Chinook salmon in 2012. However, the bioenergetics-derived estimates for 2011 were appreciably lower than the estimates for tagged fish. The relative difference between years (i.e., higher predation in 2012 than in 2011) from bioenergetics modeling was consistent with estimates from the studies of tagged juvenile salmonids, and reflected higher predator density, higher water temperature, and lower prey-fish biomass in 2012. Although illustrative and subject to appreciable uncertainty, the results of the bioenergetics modeling suggested that the rates of predation estimated at the HOR study area from the studies of juvenile salmonid survival may be plausible.

The findings of this study regarding barrier status and its association with predation have clear management implications, particularly when compared to recent studies of the relative survival of tagged juvenile Chinook salmon through the Old River and San Joaquin River routes (Buchanan et al. 2013). This topic is discussed further in Chapter 8, "Recommendations." (In particular, see Section 8.1.1, "Study the Cost-Benefit of Barriers in Relation to Alternative [Non-engineering] Management Strategies," and Section 8.1.3, "Investigate Physical Barrier Alternatives to the Rock Barrier and BAFF.")

7.3 BEHAVIOR AND DENSITY CHANGES IN PREDATORY FISHES

In the following discussion of the results of the evaluation of behavior and density changes in predatory fish at the HOR study area, the results from the study's main elements (tagged predators and mobile hydroacoustics) are considered together. This discussion emphasizes these elements' main findings with respect to several topics of management importance regarding predatory fish at the HOR study area: residence time, areas occupied, and changes in density.

7.3.1 RESIDENCE TIME OF PREDATORY FISHES

The time spent at the HOR study area by tagged predatory fish varied. Generally, however, channel catfish, white catfish, and largemouth bass spent appreciably longer amounts of time overall than striped bass. Variability existed both within and among species.

In other Delta studies, tagged white catfish mostly have been recaptured close to the original site of capture (Moyle 2002). Largemouth bass adults may remain or may wander more widely (Moyle 2002). Nearly all of the largemouth bass that left the HOR study area moved downstream. Studies of channel catfish in the lower Wisconsin River found that they occupied small home ranges in summer, migrated downstream in fall, and migrated upstream to spawn in spring (Pellett et al. 1998). Consistent with these studies, three of the four tagged channel catfish moving from the HOR study area moved upstream in the San Joaquin River.

The residence time of striped bass at discrete areas in the Delta has been the subject of several studies. One study for which the basic data can be summarized in a similar manner to the present study is the 2011 Georgiana Slough Non-

physical Barrier Study (DWR 2012). In that study, which also included spotted bass and Sacramento pikeminnow (not discussed here), 35 acoustically tagged striped bass were detected by the acoustic array near the divergence of Georgiana Slough from the Sacramento River on one to five dates after tagging. The mean percentage of dates when the fish were detected between tagging and deactivation of the acoustic array was 8% (in a range of 2% to 27%), which is comparable to the rates observed in the present study. Miranda et al. (2010) described little fidelity of six tagged adult striped bass within the State Water Project's Horseshoe Bend fish-salvage release site, as fish were detected on one to three dates after tagging. Gingras and McGee (1997) found that the flux of striped bass into or out of Clifton Court Forebay was appreciable; 0 to 100% (mean 17%) of weekly fish movements at the forebay were through the radial gates, as opposed to other parts of the forebay.

The length of time that striped bass spent at the HOR study area before capture and tagging is unknown, although the two striped bass (tag codes 2024 and 2976) that were captured and tagged outside of the study area in 2010 spent short durations (0.5 to 0.6 hour) at the site. These short durations were similar for many of the fish captured and tagged at the HOR study area.

Most movement of striped bass out of the HOR study area (indicated by zone of last detection) was downstream in the San Joaquin or Old rivers. Vogel (2011) described the movements of 24 striped bass tagged and released at the Tracy Fish Facility in spring 2010 that were detected elsewhere in the Delta. Of these, 13 moved downstream to Chipps Island, four moved into various south Delta locations and were last detected in Clifton Court Forebay, four moved north in Old River, two moved upstream to Mossdale via the HOR study area, and one moved to the San Joaquin Deep Water Ship Channel via Old River. This is consistent with a predominantly downstream migration from the south Delta.

Tagged sub-adult striped bass (n = 99) studied by LeDoux-Bloom (2012) showed three main migratory strategies: (1) bay residency; (2) residency in the low-salinity zone; and (3) riverine residency. The riverine resident fish spent summer in the Sacramento and American rivers before migrating downstream to the south Delta (Clifton Court Forebay) in fall, then returned back upstream to the Sacramento and American rivers in the spring to again spend the summer before the fall downstream migration. Adult striped bass generally migrate upstream in spring to spawn, with optimum water temperatures being 15 to 20°C, with no spawning occurring outside the range of 14° to 21°C (Moyle 2002). In 2011, the optimum water temperature range occurred during most of April, May, and June based on water temperatures recorded at the SJL gauge. Most striped bass spawning in the San Joaquin River are found downstream of the HOR study area because of water quality issues (Moyle 2002), but the range extends farther upstream in wetter years, and some striped bass migrating downstream in 2011 possibly had spawned upstream of the HOR study area.

The present study's results indicate that the turnover of striped bass generally is appreciable, with most fish spending a limited amount of time within the HOR study area. Although the residence time of the other predatory fish species is longer, turnover is apparently considerable. Cavallo et al. (2013) conducted a predator removal effort on a 1.6-km reach of the North Fork Mokelumne River on May 19, 2010, and collected an estimated 91% (i.e., 144 of 158) of predatory fish that were vulnerable to electrofishing; 6 days later, a similar effort yielded 83% (i.e., 497 of 601) of predatory fish. The most abundant of these fish were redear sunfish (*Lepomis microlphus*), largemouth bass, bluegill, redeye bass (*Micropterus coosae*), and spotted bass (*Micropterus punctulatus*), with only 10 striped bass collected on both dates. This shows that turnover may be substantial in species other than striped bass. Cavallo et al. (2013) noted:

> While mechanisms are unclear, removal of a stable predator community accomplished in the first treatment was apparently undone within one week by an influx of new predators. If site-specific predator removals are to benefit juvenile salmon survival, sustained effort over time (with daily rather than weekly removals) may be necessary.

The issue of the intensity of predator relocation efforts is discussed further in Section 8.2.3, "Conduct a Pilot Predatory Fish Relocation Study," in Section 8, "Recommendations."

7.3.2 AREAS OCCUPIED BY PREDATORY FISHES

The present study confirms the importance of the scour hole at the HOR study area as an important area for occupancy by predatory fish, as previously suggested on a regional scale from many detections of stationary tags at that location (Vogel 2007, 2010; as cited by SJRGA 2011). One of the reference sites used for comparison to the fish-salvage release sites at Horseshoe Bend (Sacramento River) included a deep hole that harbored high densities of fish (Miranda et al. 2010), as observed in the present study at the HOR study area.

Tagged predatory fish often were found occupying portions of the HOR study area in the San Joaquin River downstream of the Old River divergence, both at the scour hole and in the immediately adjacent areas. To some extent, the areas occupied by tagged predatory fish during the present study reflect the location of release. In this regard, the three white catfish that spent almost all of their time at the scour hole in 2011 were captured, tagged, and released at the scour hole. They remained very close to where they were released, which is not uncommon for the species (see previous comments; Moyle 2002). Capture and tagging crews often found the scour hole to be a profitable place for fishing, although standardized fishing was not undertaken to compare capture rates at the scour hole with other areas. Standardized hook-and-line fishing was conducted at the HOR study area in spring 2013 (Kennedy, pers. comm., 2013). The results, currently being evaluated, will provide data to compare capture rates of predatory fish at the scour hole and vicinity.

Some differences existed in the areas occupied by the different species of tagged predatory fish. For example, striped bass generally were found more often in areas away from shore, although they also occurred nearshore; by contrast, largemouth bass tended to occur more in the nearshore zones. (The index of zone use relative to zone size emphasized the relatively frequent use of nearshore zones.) Such findings reflect differences in the biology of the species, with largemouth bass tending to be more structure-oriented inhabitants of lower-velocity areas (Stuber et al. 1982), and striped bass being pelagic (Moyle 2002). Channel catfish were found more in offshore areas, which may indicate their movement into somewhat faster water to feed, although areas with cover also were important (Moyle 2002). The aforementioned occurrence of white catfish in the scour hole for much of the time was in keeping with aggregation in deeper parts of the channel for this species (Moyle 2002).

The analysis of velocities occupied by tagged predatory fish confirmed the main patterns shown by the spatial analysis of the areas occupied. Catfish and largemouth bass occupied areas with estimated near-surface velocities that were very low in comparison to all velocities available at the HOR study area. Largemouth bass is the only focal predatory fish species from the present study with a published habitat suitability index for velocity. That suitability index is expressed as average summer-current velocity at 0.6 of water depth and ranges from optimal (index = 1) at zero to 0.06 m/s, before a steep decline to zero at 0.2 m/s (Stuber et al. 1982). The results of the present study were in agreement with this index; largemouth bass rarely were found in waters with estimated near-surface velocity of 0.1 m/s or more. Near-surface velocity is not truly representative of velocity in the

demersal habitats occupied by catfishes or largemouth bass, but it may still provide an index of velocity differences at greater depths.

Striped bass was different from the other predatory fish in that it occupied a wide range of velocities. Some individuals had median occupation velocities greater than the median velocities available at the HOR study area. As noted previously, this reflects the species' pelagic nature and occupation of a variety of habitats.

Down-looking mobile hydroacoustic surveys showed an extremely high concentration of fish in the scour hole, whereas side-looking hydroacoustic surveys showed many fish at that location, but also appreciable numbers in other areas. This probably reflects a combination of fish distribution and sampling efficiency. The spread of the down-looking beam is less in shallow areas than in deeper areas, so a greater likelihood to detect fish in deeper areas such as the scour hole may be possible. By contrast, the side-looking beam does not have this issue, and generally samples over a greater range. It was nevertheless apparent from side-looking mobile hydroacoustics that the scour hole and the area just upstream were areas of high fish density.

This study assumed that mobile hydroacoustic surveys reasonably indicate changes in the abundance of large-bodied predatory fish at the HOR study area, although the proportion of predatory fish versus non-predatory fish was unknown. Considerable aggregations of common carp were observed visually near the 2012 HOR physical rock barrier. Many of the large-bodied fish observed with down-looking mobile hydroacoustics also may have been common carp; the analysis of fish depth relative to water column depth found that many fish remained close to the substrate at all times of the day. Such a pattern would be consistent with a primarily demersal, benthic-feeding fish such as common carp (Moyle 2002). Catfish, one of the focal predatory fish from the present study, also are primarily demersal (Moyle 2002).

Stationary tags (thought to be from juvenile salmonids that had been preyed upon) provided a third source of information about areas occupied by predators. These tags also indicated the considerable importance of the scour hole and vicinity, because most stationary tags were found there, with very few stationary tags found elsewhere. The acoustic arrays at the HOR in the present study allowed the locations of stationary tags to be determined more precisely than the mobile surveys undertaken as part of the VAMP studies (SJRGA 2010, 2011, 2013). In the present study, one stationary tag from a tagged juvenile Chinook salmon was found immediately adjacent to the downstream side of the 2012 physical rock barrier (another was found farther downstream in Old River), suggesting that the near-barrier area was occupied by predatory fish. These two stationary tags suggest that the only two juveniles entering Old River through the culverts of the 2012 physical rock barrier were preyed upon, based on the detection data. Previous studies have found stationary tags close to other barriers, as with those that were installed as part of the Temporary Barriers Project (Vogel 2010, as cited by SJRGA 2010).

In the present study, tagged largemouth bass that were released downstream of the 2012 physical rock barrier were detected at the barrier bottom or within 5 m of the barrier much of the time. Detection of these largemouth bass indicated a tendency by these fish to remain at or close to the barrier, and therefore, to potentially pose a predation threat to any fish passing through the barrier's culverts. The single largemouth bass tagged in 2009 spent an appreciable amount of time (nearly 50% of all detections) within 5 m of the 2009 BAFF at the upstream end, closest to shore. Little evidence existed of striped bass spending much time close to the 2009/2010 BAFF, although the number of tagged fish during these years was very low (n = 4).

The main importance of the present study's results is that the scour hole was confirmed as an area of high predator occupation. Areas adjacent to the scour hole also were found to be important for predatory fish, and species-specific differences existed in habitat use (e.g., nearshore/offshore). Also, the barrier treatments (particularly the 2012 physical rock barrier) were apparently somewhat important as a location for predatory fish. These findings have important implications for limiting predator abundance at the HOR study area, whether through direct means (capture/relocation) or through indirect means (habitat manipulation, such as scour hole filling). This is discussed further in Section 8.2.2, "Study Feasibility of Physical Habitat Reconfiguration," and Section 8.2.3, "Conduct a Pilot Predatory Fish Relocation Study," in Section 8, "Recommendations."

7.3.3 CHANGES IN DENSITY OF PREDATORY FISHES

The main environmental predictors associated with changes in the density of large fish (greater than 30 cm TL) from both down-looking and side-looking mobile hydroacoustic surveys were same-day discharge and water temperature. Large-fish density increased as discharge decreased and water temperature increased. To some extent, this reflected differences both between and within years. The density of large fish was considerably less in 2011 than in 2012; discharge was considerably higher in 2011 than in 2012. The lower density of large fish in 2011, presumably including many predatory fish, may reflect lower habitat suitability with higher velocity, as has been described for largemouth bass (Stuber et al. 1982). The 2012 surveys provided a contrast between very low abundance during March, which had low water temperatures (approximately 12° to 15°C), and higher abundance in May (18° to 22°C). This suggests seasonal migration to and through the HOR study area by large fish, such as striped bass that spawn during spring.

The results found little evidence for much importance of other predictors of large-fish density. However, in relation to the predictor of small-fish abundance (from Mossdale trawling), which was taken to be a measure of potential prey abundance in the general area, the extent to which upstream trawling would provide an indication of small-fish abundance at the HOR study area is unknown. Nevertheless, pulses of fish in Mossdale trawls generally were followed by pulses of fish at the south Delta's salvage facilities (Jones & Stokes 2007). Therefore, the issue may be more of a temporal mismatch (i.e., 3-day mean small-fish density is not necessarily representative of the density of small fish at the time of the mobile hydroacoustic surveys).

Considerable noise in the water column (e.g., from suspended, non-fish materials being washed downstream) precluded using the hydroacoustic surveys to estimate the density of small fish at the HOR study area. In addition, and as discussed briefly in Section 7.3.2, "Areas Occupied by Predatory Fishes," a difficulty in interpreting data from mobile hydroacoustic surveys existed because the proportion of large fish actually consisting of predatory fish was unknown.

The density of large fish at the HOR study area was either greater than or not substantially different from the density of large fish at the reference sites. In addition, although density estimates were quite variable at all sites, important correlations existed between the HOR study area and the reference sites in approximately half of the comparisons. Taken together, these results suggest that wide-ranging factors (e.g., discharge and water temperature) affect fish density over much of the San Joaquin River, and that the HOR study area has a relatively high density of large fish compared to other sites. As noted previously, the scour hole at the HOR study area was found to be a hotspot of predation in some years, based on stationary tag detections (Vogel 2007, 2010; as cited by SJRGA 2010).

In more recent years, other locations farther downstream in the San Joaquin River and Grant Line Canal have had greater concentrations of stationary tags (SJRGA 2011, 2013), suggesting that more intense predation occurs at those locations. Indeed, SJRGA (2011 2013) noted that "predation did not appear to be a problem near the Head of Old River" in 2010 and 2011 based on the relative density of stationary tags. As described in Section 7.2, "Predation on Juvenile Salmonids, Including Barrier Effects," predation at the HOR study area was lower in 2011 than in the other years, but predation in 2009 and 2010 during BAFF operations was comparable to predation in 2012 (and overall appeared somewhat high, with predation of more than 30% of juveniles entering the area). This study's findings of discharge- and water temperature-related differences in the density of large fish and relatively high large-fish density compared to other areas of the San Joaquin River have implications in terms of prioritizing predator management efforts at the HOR study area, both temporally (within and between years) and spatially (at which location). These implications are discussed further in Appendix J, "Recommended Aspects of a Pilot Predatory Fish Relocation Study," and Appendix K, "Relevant Aspects of the Proposed Bay Delta Conservation Plan" (see Section K.2, "Predation Reduction").

8 RECOMMENDATIONS

8.1 JUVENILE SALMONID ROUTING INCLUDING BARRIER EFFECTS

8.1.1 STUDY THE COST-BENEFIT OF BARRIERS IN RELATION TO ALTERNATIVE (NONENGINEERING) MANAGEMENT STRATEGIES

The present study showed that non-physical (BAFF) and physical (rock) barriers had varying levels of effectiveness in influencing juvenile salmonid routing at the HOR study area. No option that was studied provided overall efficiency (O_E) greater than 62% and a population proportion eaten less than 30 % (Table 8-1). The O_E result provided herein does not depend upon classification of salmonid juvenile fate from 2D tracks. (Note that there is some uncertainty about classification of salmonid juvenile fate, and this is recommended for further study; see Section 8.2.1, "Further Examine Predation Classification").

Table 8-1
Summary of Statistics for Tagged Juvenile Chinook Salmon Released, 2009–2012

Year/Treatment	Overall Efficiency	Protection Efficiency	Proportion Eaten at Study Area	Proportion Never Arrived at Study Area	Mean Water Temperature (°C)[1]	Mean Discharge (cfs)[1]
2009 BAFF on	0.209	0.338	0.309	0.446[2]	18.6	864
2010 BAFF on	0.355	0.441	0.310	0.112[2]	16.4	2,646
2011 no barrier	0.519	0.574	0.101	*	16.6	5,117
2012 rock barrier	0.618	1.000	0.393	0.539	18.9	1,855

Notes: °C = degrees Celsius; BAFF = bio-acoustic fish fence; cfs = cubic feet per second

[1] Water temperature and discharge mean values were calculated from measurements when fish were detected in the Head of Old River study area, and refer to the San Joaquin River at Lathrop gauge.

[2] Proportion Never Arrived was calculated with all tags, rather than only tags that later encountered the BAFF when it was on.

[*] Unknown because only a subset of tags were processed in this year, with the focus on the Head of Old River study area.

Sources: Present study; Baldwin, pers. comm., 2013; Dempsey, pers. comm., 2013

Since 2010, the rate of juvenile salmonid survival through the Delta along the San Joaquin River route has been similar to or lower than the survival rate along the Old River route (SJRGA 2011, 2013); previous studies showed that survival was higher along the San Joaquin River route than along the Old River route (see review by Hankin et al. 2010). Lower survival along the San Joaquin River route is contrary to the management goal that a HOR barrier is intending to achieve—less use of the Old River route. However, survival rates are very low along either route, generally less than 10% (SJRGA 2011, 2013; Buchanan et al. 2013). This suggests that conditions in the south Delta are generally poor, particularly compared to through-Delta survival rates for Sacramento River–origin salmonids, 35.1 to 54.3% (Perry et al. 2010). Perry et al. (2013:389) noted that:

> …while shifting the distribution of fish among routes influences overall survival, the magnitude of absolute change in [through-Delta survival] is constrained by the maximum survival observed in any given route. Further increases in [through-Delta survival] require management actions that affect not only migration routing, but also survival within migration routes.

In this light, it is recommended that the cost and benefit of barriers at the HOR study area be studied in relation to the costs and benefits of alternative management strategies, particularly nonengineering solutions such as habitat restoration.

Existing planning efforts are considering the potential for habitat restoration in the south Delta, which could improve the quality of different migration routes. The proposed BDCP contemplates a suite of conservation measures that would restore floodplain habitat, tidally influenced habitat, and channel margin habitat, while enhancing flood control benefits for surrounding areas (see Section K.3, "South Delta Habitat Restoration," in Appendix K, "Relevant Aspects of the Proposed Bay Delta Conservation Plan," of this report). It is recommended that the potential benefits of barrier installation at the HOR study area be considered in light of such efforts. Note that this recommendation is consistent with a recommendation to study physical barriers further (see Section 8.1.3, "Investigate Physical Barrier Alternatives to the Rock Barrier and BAFF"), because the potential benefits of a physical barrier involves both near-field effects (preventing fish from entering an undesirable route, e.g., Old River) and potential far-field effects (retaining flow in the San Joaquin River; see also Section 8.2.4, "Study Effects of Physical Barriers on Location of Predation Hotspots"). The far-field effects may contribute to a potential change in survival along a given route (Perry et al. 2013). The potential to change habitat and directly affect numbers of predatory fish is discussed in Section 8.2.2, "Study Feasibility of Physical Habitat Reconfiguration," and Section 8.2.3, "Conduct a Pilot Predatory Fish Relocation Study."

The potential synergy between nonengineering and engineering strategies therefore is recommended for further study. Barrier installation at the HOR study area may have more value if habitat is improved along the south Delta migration routes.

8.1.2 Conduct Additional Analysis of Existing Data Using Supplementary Techniques

The assessment of juvenile salmonid routing, including barrier effects, was based on a number of univariate analyses that generally tested null hypotheses specified *a priori*. This approach was adopted largely to maintain consistency with previous evaluations at the HOR study area (Bowen et al. 2012; Bowen and Bark 2012). It is recommended that additional analysis of these data be considered using supplementary techniques, such as GLM. The GLM approach was used in the present study's analysis of probability of predation (see Section 7.2, "Predation on Juvenile Salmonids Including Barrier Effects"). Recently this approach was applied to an analysis of the probability of route entrainment at the HOR study area (SJRGA 2013; reproduced in this report as Appendix I, "Route Entrainment Analysis at Head of Old River, 2009 and 2010").

The GLM approach supplements the univariate approach by allowing simultaneous consideration of many environmental variables. In addition, the GLM approach allows consideration of the continuous nature of environmental variables, as opposed to grouping variables (e.g., velocity) by predefined thresholds (as was undertaken with the univariate analyses in the present study). This allows consideration of barrier effects across the range of a given environmental variable. Thus, for example, SJRGA (2013) found that in 2009, below approximately 1,000 cfs (San Joaquin River at Lathrop discharge), there was little difference between BAFF-on and BAFF-off treatments in the probability that juvenile Chinook salmon would remain in the San Joaquin River. In contrast, above a discharge of 1,000 cfs, the probability was appreciably greater with the BAFF on (see Figure 7-1 in Appendix I, "Route Entrainment Analysis at Head of Old River, 2009 and 2010").

The analysis of route entrainment conducted by SJRGA (2013) is analogous to the univariate analysis of protection efficiency (P_E) (i.e., only surviving juvenile Chinook salmon are considered). It is recommended that a GLM analysis be undertaken that is more analogous to the univariate analysis of O_E, i.e., including juveniles that were preyed upon at the HOR study area. This could be done with a GLM based on a trinomial response distribution, for example, with three juvenile Chinook salmon fates ("remained in San Joaquin River," "entered Old River," or "preyed upon").

It is also recommended that additional analyses be undertaken of data collected in 2013 (i.e., from the study similar to the Vernalis Adaptive Management Program's release of tagged juvenile Chinook salmon and from tagged juvenile steelhead released as part of the Six Year Steelhead Study mandated by the NMFS [2009] OCAP BO). Such analyses would allow comparison of juvenile salmonid routing and survival with a low-discharge, no-barrier treatment (i.e., 2013) with the other years (2009–2012) included in the present study.

8.1.3 Investigate Physical Barrier Alternatives to the Rock Barrier and BAFF

Deploying a BAFF at the HOR study area is not recommended at this time, for two main reasons. First, estimated population proportion eaten of juvenile Chinook salmon during BAFF operation in 2009/2010 was very high, at 31%, and predation was not significantly different from predation when the physical rock barrier was installed in 2012, as discussed in Section 7.2, "Predation on Juvenile Salmonids Including Barrier Effects." Second, in 2009, predation was significantly greater with the BAFF on than off.

As described in Section 8.2.1, "Further Examine Predation Classification," there is a need to develop further the methods to classify the fate of tagged juvenile salmonids. Irrespective of this need, even if predation had been overestimated considerably with the BAFF on, the BAFF's influence on routing of juvenile salmonids produced only a modest gain in the proportion of juvenile salmonids remaining in the San Joaquin River (e.g., in 2010, mean P_E of 0.441 with BAFF on versus 0.286 with BAFF off; see also Figures 7-3 and 7-4 of Appendix I, "Route Entrainment Analysis at Head of Old River, 2009 and 2010"). Sample proportion eaten was relatively high with the physical rock barrier (and not significantly different than with the BAFF on); however, the rock barrier eliminated entry into Old River of tagged juvenile Chinook salmon determined to have not been eaten, the primary management goal of the barrier installation (see Protection Efficiency in Table 8-1).

The second reason for not recommending deployment of a BAFF is that recent studies have not found through-Delta survival to be lower for juvenile Chinook salmon entering Old River instead of remaining in the San Joaquin River, in contrast to the situation generally observed historically (Hankin et al. 2010). Indeed, survival along the Old River route has been comparable to or greater than survival along the San Joaquin River route in recent years (SJRGA 2010, 2013; Buchanan et al. 2013). The reasons for this recent change are unknown, although Buchanan et al. (2013: 228) have suggested that "it is possible that the non-physical barrier deprived smolts routed to the San Joaquin River of the increased flows necessary for improved survival." It is recommended that juvenile Chinook salmon survival through the Delta be studied further to assess if evidence persists into the future for the Old River route having higher survival than the San Joaquin River route. Because no long-term route survival data series exists for steelhead, juvenile Chinook salmon survival is the only metric currently available for assessment of the through-Delta success of the Old River route compared to the mainstem San Joaquin River route.

Hankin et al. (2010:27) considered the installation of a physical barrier at the HOR study area to be potentially beneficial because, in addition to the more desirable mainstem San Joaquin River fish routing, it would "ensure that essentially all San Joaquin flow proceeds down the main channel, thereby presumably enhancing (juvenile) smolt survival via a mainstem flow effect." Furthermore, they made the following recommendation (Hankin et al. 2010: 28):

> If an Obermeyer Gate is considered, it should be located near the edge of the hydraulic flow line of the main channel of the San Joaquin River. Data support that in-river structures such as a fill dam, but also bridge abutments, scour holes, piers and pump stations, provide habitat for predators in this reach of the river (Vogel, pers. comm., 2010). The position of the original HORB [Head of Old River Barrier] was set back into the entrance of the channel leading into Old River. This site was chosen most likely for ease and cost to construct and remove. Unfortunately, it also set up hydraulic conditions ideally suited for predators: slack water and cover. If a future barrier at the HOR is constructed, alignment along the San Joaquin embankment would create a higher sweeping velocity down the main channel, would move smolts more swiftly past this location, and should reduce predator habitat.

The results of the present study tend to support the foregoing recommendation of Hankin et al. (2010). Predation at the HOR study area with a physical rock barrier installed may have been relatively high. Population proportion eaten was 39% of tagged juveniles entering the study area, if the estimates of juvenile Chinook salmon eaten are reasonably accurate. This appeared to be at least partly attributable to unfavorable hydraulic conditions, such as eddies generated by the position of the rock barrier. Therefore, it is recommended that the feasibility of physical barrier alternatives be considered for the HOR study area, following the recommendations of Hankin et al. (2010).

Important considerations for the feasibility of a physical barrier include the need to consider water use in Old River (i.e., maintaining adequate water levels for agricultural diversions) and the Old and Middle River flows necessary to limit the potential for delta smelt (and other species of concern) to move toward the south Delta export facilities from the central or west Delta. In addition, locating a physical barrier closer to the San Joaquin River's hydraulic flow line would increase construction and operations/maintenance costs (J. McQuirk, pers. comm., 2013).

Further investigation of the feasibility of a physical barrier at the HOR site would inform the proposal to construct an HOR operable gate under the Bay Delta Conservation Plan (DWR 2013). This is discussed further in Section K.1, "Operable HOR Gate," in Appendix K, "Relevant Aspects of the Proposed Bay Delta Conservation Plan," of this report. Such a gate would obviate the need for a non-physical barrier and may facilitate the types of mainstem San Joaquin River discharge–related benefits suggested by Hankin et al. (2010).

Study of a physical barrier should consider any effects on the potential for changes in delta smelt entrainment at the south Delta export facilities because of changes in Old and Middle river discharges. This could be done at a planning level, for example, by modeling Old and Middle river discharges under different physical barrier configurations. The modeling then could be applied to established relationships between proportional entrainment of larval/juvenile delta smelt and spring (March–June) Old/Middle River discharge and the location of the low-salinity zone (see USFWS 2008:220).

Any study of physical barrier alternatives to the rock barrier and BAFF should consider the timing of barrier installation relative to juvenile salmonids' outmigration periods. Historic installation of the HOR barrier has been tailored to coincide with the spring (April–June) outmigration period of juvenile Chinook salmon in the San Joaquin River watershed, whereas juvenile steelhead outmigration may warrant earlier installation. (For example, the migration period noted for the Stanislaus River at Caswell is January to July, with a peak in March, and moderate abundance from February to June [NMFS 2009:Table 4-6].)

The recommendation to investigate physical barrier alternatives includes a recommendation to consider possible effects of the San Joaquin River Restoration Program (SJRRP). The SJRRP aims to implement the restoration goal of the San Joaquin River Restoration Settlement: "To restore and maintain fish populations in 'good condition' in the main stem of the San Joaquin River below Friant Dam to the confluence of the Merced River, including naturally reproducing and self-sustaining populations of salmon and other fish" (SJRRP 2011).

The SJRRP's actions occur well upstream of the HOR study area. The migration route of spring-run and fall-run Chinook salmon emigrating to or from the restoration area includes the HOR study area. Therefore, management actions at the HOR study area would affect these fish. The timing of fall-run Chinook salmon migration presumably would be similar to that observed elsewhere in the San Joaquin River basin (i.e., primarily juvenile spring outmigration and fall adult immigration). However, the timing of spring-run Chinook salmon may result in new considerations (e.g., with respect to adult spring upstream migration). In addition, depending on the juvenile phenotypes expressed, a broader variety of outmigration timing may exist, with differences between young-of-the-year, fry migrants, and older juveniles that may have reared in-river for over a year. These are considerations for the timing of any barrier operation at the HOR study area, as well as any other associated activities that may be planned (e.g., predator relocation; see Section 8.2.3, "Conduct a Pilot Predatory Fish Relocation Study").

Clearly, the potential exists for any future management activities at the HOR study area to affect migrating salmonids from a restored San Joaquin River above the Merced River confluence. Based on the SJRRP's use of tagging studies to assess juvenile Chinook salmon survival in the watershed above the Merced River confluence (SJRRP 2012), it is recommended that study efforts specific to the HOR study area and the SJRRP be coordinated, to track the same tagged study fish as they pass through the HOR study area. This would be of value because these study fish would have had considerably longer to acclimate to the natural environment by the time they reached the HOR study area, compared to fish released at more typical locations, such as Durham Ferry (e.g., Bowen et al. 2012). Sample sizes may be low, however, because of the losses that may occur between the release sites and the HOR study area. Coordinated efforts may have to significantly increase the number of study fish.

8.2 PREDATION ON JUVENILE SALMONIDS INCLUDING BARRIER EFFECTS

8.2.1 FURTHER EXAMINE PREDATION CLASSIFICATION

With respect to predation, a key uncertainty that warrants further research is the actual fate of tagged juvenile salmonids that have been classified as having been preyed upon or having survived at the HOR study area. The GLM statistical analysis of juvenile Chinook salmon at the HOR study area was successful in supporting some of the *a priori* hypotheses regarding factors affecting juvenile predation (i.e., light level and turbidity), as well as highlighting the fact that predation was greater with the physical rock barrier and BAFF operations than with the BAFF not operating.

However, the GLM analysis for steelhead provided no insight into mechanisms affecting predation. This may be attributable to the difficulty in assigning predation fate. Predation studies of both juvenile Chinook salmon and steelhead would benefit from some means of verifying predation fate, or of developing objective, quantitative criteria to classify predation. An example of this was provided in the 2012 Georgiana Slough Non-physical Barrier Study (DWR in review), which used mixture models to estimate the probability of a track being a predator based on the tortuosity of the track in the study area (Romine et al. 2014). It is recommended that the 2009–2012 data from the HOR study area be examined to determine how fate classification corresponds with classifications from mixture models based on data either from tagged predatory fishes at Georgiana Slough or, preferably, from the tagged predatory fishes from the HOR study area presented in this study.

It is also recommended that predation classification in future studies at the HOR study area (by mixture models, qualitative fate classification, or other means) incorporate the use of the new predation tag. Predation tags are proprietary technology that has been developed by Hydroacoustic Technology, Inc., and for which a patent application is in process. The acoustic signal emitted by predation tags changes sometime after a tagged juvenile salmonid has been preyed upon, thus indicating the fate of the juvenile salmonid. Classification by mixture models or other means can then be compared to the known fate of the predation tag. Therefore predation rules described in Appendix E could be tested as follows: (1) develop 2D tracks for juvenile Chinook salmon before and after known predation events from the predation tag; (2) experts apply human rules described in Appendix E to assign fate; and (3) statistically compare the groups of uneaten, eaten, and unknown from predation-tag known to those for expert human assessments.

The primary limitation to using predation tags is the lag time between the predation event and the change in signal from the predation tag, which may preclude assigning predation by predatory fishes at the HOR study area if these predatory fishes have a relatively short residence time (striped bass). Nevertheless, predation tags appear to hold promise for informing broader-scale survival estimates through the south Delta as a whole. Thus, they would tie in to studies that consider the broader circumstances along the migration route rather than just the HOR study area (see Section 8.1.1, “Study the Cost-Benefit of Barriers in Relation to Alternative [Nonengineering] Management Strategies”).

Transit speed was identified as a quantitative attribute that can assist in classifying predation on juvenile salmonids (see Appendix D, “Transit Speed Analyses”). It is recommended that this attribute be used to aid predation classification in future studies. Tagged juvenile Chinook salmon that were classified as having been preyed upon passed through the HOR study area at a much slower rate than tagged fish that were not eaten.

It is further recommended that the use of transit speed as one criterion for classifying predation also take into account the relationship between discharge, average channel velocity, and transit speed. Individual transit speed should be evaluated as an indicator of predation probability. The individual transit speed should be compared to the mean transit speed for all tags experiencing the same conditions in a specific year. However, because the behavior of steelhead juveniles can appear similar to the behavior of predators, it is recommended that transit speed evaluation be species-specific.

8.2.2 Study Feasibility of Physical Habitat Reconfiguration

The preponderance of stationary acoustic tags for juvenile salmonids in the scour hole and the association of predatory fish with the scour hole and adjacent areas at the HOR study area (see Section 7.3.2, “Areas Occupied

by Predatory Fishes") leads to the recommendation that a study be undertaken regarding modification of the scour hole's bathymetry. Modification could involve filling the scour hole with suitable substrate. Such actions are under consideration in other planning efforts for the Delta, e.g., the Bay Delta Conservation Plan (Section K.2, "Predation Reduction," in Appendix K, "Relevant Aspects of the Proposed Bay Delta Conservation Plan," of this report). Clearly, such action would require a detailed modeling effort to ascertain the potential effects on both the river near the HOR study area and upstream and downstream of the site. Particular consideration would be needed for effects on river banks and levees that could occur as a result of any modification to the scour hole.

8.2.3 Conduct a Pilot Predatory Fish Relocation Study

Regardless of the presence or absence of a barrier at the HOR, sufficient evidence is apparent to conclude that predation is considerable at the study area. The present study suggests that the population proportion eaten of juvenile Chinook salmon entering the site has been high in most years (0.23 in 2009, 0.26 in 2010, 0.10 in 2011, and 0.39 in 2012; see Table 7-1 of Section 7.2, "Predation on Juvenile Salmonids Including Barrier Effects", in Section 7, "Discussion"). As noted previously in Section 8.2.1, "Further Examine Predation Classification," there is the need to investigate further the uncertainty about the fates of juvenile salmonids.

Mobile surveys of stationary acoustic tags from dead salmonids have not always shown that the HOR study area and vicinity to be a regional hotspot of predation (SJRGA 2010, 2011, 2013); however, the foregoing rates of predation, assuming that they are reasonably accurate, are of concern. Consideration of relocating predators from the HOR study area and vicinity may be warranted; as described further in Section 8.2.4, "Study Effects of Physical Barriers on Location of Predation Hotspots," identifying the locations of predation hotspots and how they shift seasonally in relation to environmental conditions is valuable, so that efforts to relocate predatory fish could focus on problem areas. Given the scarcity of predator control studies in the Delta (see Grossman et al. 2013) and the proposed use of such actions in planning efforts (see Section K.2, "Predation Reduction," in Appendix K, "Relevant Aspects of the Proposed Bay Delta Conservation Plan"), it is recommended that a pilot predatory fish relocation study be undertaken at the HOR study area.

The feasibility of relocating predators is highly uncertain and problematic, particularly with respect to an open area such as the HOR study area. Gingras and McGee (1997:13) discussed the feasibility of predator control in Clifton Court Forebay, another open system in the Delta, and concluded:

> Because removal efforts at Clifton Court Forebay would not affect reproduction in the striped bass (predator) population or recruitment to Clifton Court Forebay, logic dictates that the level of exploitation to substantially reduce predation at Clifton Court Forebay would need to be very high.
>
> Notwithstanding the extraordinary effort that predator removal would pose as a means to improve prescreen survival of fish entrained at Clifton Court Forebay, a coordinated program to reduce predation should be expected to yield some degree of positive effect. In this respect, initiating a predator control program may seem attractive; however, in a review of 250 fish control projects, Meronek et al. (1996) classified most of them as failures. They documented many proximate causes for failure (e.g., insufficient reduction in numbers) but suggested that unreported "seminal reasons" were more often the cause. Suggested seminal causes of failure were insufficient pre- and post-treatment study and lack of criteria for success. Proposed predator removal activities at Clifton Court Forebay have been delayed in substantial part due to the inability to reach a

consensus on the criteria to quantify success. Because fundamental assumptions of mark/recapture methods for abundance estimation are not valid when Clifton Court Forebay is operated normally, predator control activities would need to be evaluated without accurate predator abundance estimates. Quantifying any improvement in prescreen survival attributable to predator removal efforts would be difficult.

In the only available published Delta study of predator control efforts, a study on the North Fork Mokelumne River, Cavallo et al. (2013) demonstrated that predator removal may be feasible[1]. Electrofishing was used to catch predatory fishes in a 1.6-km impact reach; the survival rates of tagged juvenile Chinook salmon were compared before and after the removal in the impact reach and in an upstream 2-km control reach. Survival was greater than 99% in the reach after the removal, compared to less than 80% before the removal. Survival in the control reach was variable and did not differ before and after the removal. However, survival in the impact reach declined to initial levels after a second predator removal effort, before increasing to very high levels (again greater than 99%) after a considerable increase in discharge caused by the opening of the Delta Cross Channel gates.

Although the results of Cavallo et al. (2013) show predator removal may be challenging, their study serves as a useful template for the type of study that could be considered as a pilot predator relocation effort at the HOR study area. Indeed, the National Marine Fisheries Service's Southwest Fisheries Science Center has commenced study to manipulate predatory fish density at the HOR study area in 2014-2016. This study and any other similar studies would have direct relevance for the proposed BDCP (see Section K.2, "Predation Reduction," in Appendix K, "Relevant Aspects of the Proposed Bay Delta Conservation Plan," of this report).

The results of the present study also have the potential to guide any pilot predator relocation efforts that may be considered, such as by illustrating the areas of greatest predatory fish density (see "Areas Occupied" in Section 6.3.2, "Hydroacoustic Data" of Section 6, "Results"). Features of a pilot predator relocation study are summarized in Appendix J, "Recommended Aspects of a Pilot Predatory Fish Relocation Study." That appendix, as well as Section K.2, "Predation Reduction", of Appendix K, "Relevant Aspects of the Proposed Bay Delta Conservation Plan," also discuss how the results of the present study have the power to inform future studies and planning efforts.

8.2.4 Study Effects of Physical Barriers on Location of Predation Hotspots

With respect to the influence of a physical barrier on flow, Cavallo et al. (2013) illustrated that river inflow to the Delta has an important effect on the extent of the channel under appreciable tidal influence (i.e., with bi-directional flows much of the time). They suggested, "If the tidal transition zone occurs where habitat conditions are poor, or where predator densities are high, juvenile salmon are likely to experience greater predation mortality, and perhaps impaired growth. This should be studied more fully."

In relation to the situation at the HOR study area, and to the broader San Joaquin River and south Delta, examining the locations where predation hotspots occur (SJRGA 2010, 2011, 2013) is recommended, to see how they relate to the tidal transition zone. Clearly, deploying a physical barrier would have the potential to influence

[1] Note that Sabal (2014), in her master's thesis work, found that juvenile Chinook salmon survival below Woodbridge Irrigation District Dam on the lower Mokelumne River increased by approximately 25-30% following removal of predatory fishes by electrofishing.

the position of the tidal transition zone and may guide future management efforts, such as predator relocation (see Section 8.2.3, "Conduct a Pilot Predatory Fish Relocation Study," and Section 8.3.2, "Assess Predatory Fish Density in Relation to Predation Hotspots") and the proposal for a physical barrier in the Bay Delta Conservation Plan (Section K.1, "Operable HOR Gate," in Appendix K, "Relevant Aspects of the Proposed Bay Delta Conservation Plan").

In addition, understanding the factors influencing predation hotspots would improve planning of complementary management strategies such as habitat restoration and habitat reconfiguration. (See Section K.2, "Predation Reduction," and Section K.3, "South Delta Restoration," in Appendix K, "Relevant Aspects of the Proposed Bay Delta Conservation Plan.") Therefore it is recommended that the influence of a physical barrier on the location of predation hotspots and the tidal transition zone be studied further to elucidate potential far-field effects of physical barrier installation.

8.2.5 Study Potential Effects of Changing Recreational Fishing Regulations

The results of the present study suggested that predation on juvenile salmonids is considerable at the HOR study area. In addition to studying localized effects of predatory fish manipulation (see Section 8.2.3, "Conduct a Pilot Predatory Fish Relocation Study"), it is recommended that additional study be pursued into the potential effects of changing recreational fishing regulations for striped bass and other predatory fish species. The goal of such study would be to assess the prospects for an increase in the survival of juvenile salmonids, including those emigrating from the San Joaquin River region through the HOR study area.

The California Department of Fish and Game (now California Department of Fish and Wildlife) recently proposed changes to fishing regulations for striped bass (DFG 2011). The changes included generally increased bag limits and decreased size limits, with very large bag limits and no size limit in a "South Delta Hot Spot" region (including Clifton Court Forebay and portions of nearby channels such as Old River and West Canal). The California Fish and Game Commission (2012) rejected this proposal amid concerns from the recreational fishing community about potential adverse effects on the fishery which is currently in decline. In addition, leading fish biologists have expressed concerns about potential adverse effects on the Delta ecosystem, such as compensatory increases in predation by other predatory fishes and increases in the abundance of fishes that may compete with threatened fishes (Moyle and Bennett 2010). Therefore, it is recommended that additional studies be conducted into the potential effects of changes in fishing regulations. It is important to note that DWR cannot implement any changes to fishing regulations; these are the purview of the California Fish and Game Commission.

Under this recommendation, DWR would facilitate studies that would inform future decision making, with the recognition that a broader California Resources Agency effort probably would be needed to engage stakeholders from the recreational fishing and other communities (e.g., scientific and environmental organizations) in order to explore fully all considerations related to the feasibility and utility of changes in fishing regulations. Any studies undertaken as part of this recommendation should adhere to the guidelines of Grossman et al. (2013) for studies of predation in the Delta, and should include consideration of:

- changes in survival of listed species (e.g., juvenile Central Valley steelhead, including those from the San Joaquin River basin, and delta smelt) and other species of concern (e.g., juvenile San Joaquin River fall-run Chinook salmon);

- age-specific changes in abundance of striped bass; and
- changes in fishing opportunities (e.g., catch rates of recreational fishers).

8.3 BEHAVIOR AND DENSITY CHANGES IN PREDATORY FISHES

8.3.1 ASSESS PREDATORY FISH MOVEMENTS AS PART OF A PILOT PREDATORY FISH RELOCATION STUDY

It is recommended that predatory fish movements be studied as part of a pilot predatory fish relocation study (see Section 8.2.3, "Conduct a Pilot Predatory Fish Relocation Study"), if the study includes relocation of predators to other parts of the Delta. As described in Appendix J, "Recommended Aspects of a Pilot Predatory Fish Relocation Study," it may be desirable to hold captured predatory fishes in net pens during assessments of changes in survival of tagged salmonids in reaches that have had predatory fishes removed; after completion of the study, the captured predatory fishes could be released (Cavallo et al. 2013). In this case, an assessment of predatory fish movement would not be required. If, on the other hand, predatory fish are relocated elsewhere in the system, then it is recommended that their movements be tracked with acoustic tagging to assess the locations to which they disperse and determine whether they return to the HOR study area (or to other areas from which they were relocated).

Important considerations for such a study include the locations to which releases of predatory fish should be made, particularly because of the potential to enhance predation on listed fishes in other parts of the Delta. Bowen and Bark (2012) suggested that relocating predatory fish from the HOR study area could involve moving captured fish to San Luis Reservoir; however, this may not be desirable because it would remove predatory fish from the Delta system and therefore could provide less opportunity for recreational fishing. Additionally, relocating fish raises concerns about spread of disease between populations. As noted in Section K.2, "Predation Reduction," of Appendix K, "Relevant Aspects of the Proposed Bay Delta Conservation Plan," the Bay Delta Conservation Plan proposes only localized reduction of predatory fishes to relieve predation pressure at hotspots, rather than achieving a system-wide reduction in predatory fishes.

8.3.2 ASSESS PREDATORY FISH DENSITY IN RELATION TO PREDATION HOTSPOTS

In association with a study of predation hotspots (see Section 8.2.4, "Study Effects of Physical Barriers on Location of Predation Hotspots"), it is recommended that predatory fish density be assessed by species and seasonally to determine whether there is evidence of a concentration of predatory fishes at predation hotspots compared to other areas where predation is not so intense. It is of interest to determine whether physical and environmental conditions as well as predatory fish density contribute to predation hotspots. For example, do hotspots have modest densities of predatory fishes that are not significantly different from densities in other areas, but these fishes are more efficient in feeding because of physical and/or environmental conditions? (Examples of such hotspots include areas of flow reversals at the intersection of riverine conditions with tidally influenced areas; see Section 8.2.4, "Study Effects of Physical Barriers on Location of Predation Hotspots.")

Predation hotspots are not solely attributable to predatory fishes; thus, the potential for predation by other piscivorous taxa (bullfrogs, birds, river otters, harbor seals, and sea lions) at hotspots is also recommended for investigation. Clark et al. (2009) and Miranda et al. (2010) examined the abundance of piscivorous birds at

Clifton Court Forebay and at the south Delta export facility's salvage release sites. Similar methods could be applied to evaluate the evidence of high densities of piscivorous birds relative to predation hotspots at the HOR study area and along the main migration routes through the south Delta. In addition, avian scat and river otter latrine sites could be sampled for Chinook salmon and steelhead otoliths/scales and scanned for acoustic tags.

9 REFERENCES

Adams, N. S., D.W. Rondorf, S. D. Evans, and J. E. Kelly. 1998. Effects of Surgically and Gastrically Implanted Radio Tags on Growth and Feeding Behavior of Juvenile Chinook Salmon. *Transactions of the American Fisheries Society* 127:128–136.

Aksnes, D. L., and J. Giske. 1993. A Theoretical Model of Aquatic Visual Feeding. *Ecological Modeling* 67(2):233–250.

Anderson, J. J., E. Gurarie, and R. W. Zabel. 2005. Mean Free-Path Length Theory of Predator–Prey Interactions: Application to Juvenile Salmon Migration. *Ecological Modelling* 186(2):196–211.

Anderson, J. J., K. J. Puckett, and R. S. Nemeth. 1988. *Studies on the Effect of Behavior on Fish Guidance Efficiency at the Rocky Reach Dam: Avoidance to Strobe Light and Other Stimuli*. Report UW-8801. Seattle: Fisheries Research Institute of the University of Washington.

Apogee Instruments. 2013. Conversion—PPF to Lux. Available: http://www.apogeeinstruments.com/conversion-ppf-to-lux/. Accessed May 8, 2013.

Atwater, B. F., S. G. Conard, J. N. Dowden, C. W. Hedel, R. L. Donald, and W. Savage. 1979. History, Landforms, and Vegetation of the Estuary's Tidal Marshes. In *San Francisco Bay: the Urbanized Estuary*, ed. T. J. Conomos, A. E. Leviton, and M. Berson. San Francisco: American Association for the Advancement of Science, Pacific Division.

Baldwin, Mike. Engineer. Flow Monitoring and Special Studies Section, Division of Integrated Regional Water Management, North Central Region Office, California Department of Water Resources, West Sacramento, CA. January 2013—Excel file with CDEC water quality data provided to Michael Burns, Bay-Delta Office, California Department of Water Resources, Sacramento, CA.

Bay Institute. 1998. *From the Sierra to the Sea: the Ecological History of the San Francisco Bay–Delta Watershed*. Novato, CA: The Bay Institute of San Francisco. Available: http://www.bay.org/publications/from-the-sierra-to-the-sea-the-ecological-history-of-the-san-francisco-bay-delta-waters. Accessed July 2013.

Beakes, M., J. Moore, N. Retford, R. Brown, J. Merz, and S. Sogard. 2012. Evaluating Statistical Approaches to Quantifying Juvenile Chinook Salmon Habitat in a Regulated California River. *River Research and Applications*. DOI: 10.1002/rra.2632.

Bell, M. C. 1986. *Fisheries Handbook of Engineering Requirements and Biological Criteria*. Fish Passage Development and Evaluation Program. Portland, OR: U.S. Army Corps of Engineers, North Pacific Division.

Bianchini, Kari. Senior Engineer, California Department of Water Resources, Division of Engineering, General Engineering Section, Sacramento, CA. May 26, 2011—e-mail containing coordinates of 2009 and 2010 bioacoustic fish fences, sent to Marin Greenwood, Aquatic Ecologist, ICF International, Sacramento, CA.

Bowen, M. D., L. Hanna, R. Bark, V. Maisonneuve, and S. Hiebert. 2009. *2008 Non-Physical Barrier Evaluation in a Laboratory Model, Physical Configuration I*. Draft Technical Memorandum 86-68290-10-01. Denver, CO: U.S. Bureau of Reclamation, Technical Service Center.

———. 2010. *2008 Non-Physical Barrier Evaluation in a Laboratory Model, Physical Configuration II*. Draft Technical Memorandum 86-68290-10-01. Denver, CO: U.S. Bureau of Reclamation, Technical Service Center.

Bowen, M. D. and R. Bark. 2012. *2010 Effectiveness of a Non-Physical Fish Barrier at the Divergence of the Old and San Joaquin Rivers (CA)*. Technical Memorandum 86-68290-10-07. Denver, CO: U.S. Bureau of Reclamation, Technical Service Center.

Bowen, M. D., S. Hiebert, C. Hueth, and V. Maisonneuve. 2012. *2009 Effectiveness of a Non-Physical Fish Barrier at the Divergence of the Old and San Joaquin Rivers (CA)*. Technical Memorandum 86-68290-09-05. Denver, CO: U.S. Bureau of Reclamation, Technical Service Center.

Brandes, P. L., and J. S. McLain. 2001. Juvenile Chinook Salmon Abundance, Distribution, and Survival in the Sacramento–San Joaquin Estuary. In *Contributions to the Biology of Salmonids*, ed. R. Brown. California Department of Fish and Game. Fishery Bulletin 179, Volume 2:39–138.

Brown, M. L., M. S. Allen, and T. D. Beard. 2012. Data Management and Statistical Techniques. In *Fisheries Techniques*, ed. A. V. Zale, D. L. Parrish, and T. M. Sutton, 15–77. Third edition. Bethesda, MD: American Fisheries Society.

Buchanan, R. A., J. R. Skalski, P. L. Brandes, and A. Fuller. 2013. Route Use and Survival of Juvenile Chinook Salmon through the San Joaquin River Delta. *North American Journal of Fisheries Management* 33(1):216–229.

Burnham, K. P., and D. R. Anderson. 2002. *Model Selection and Multi-Model Inference: A Practical Information-Theoretic Approach*. New York: Springer-Verlag Inc.

Calcagno, V., and C. de Mazancourt. 2010. GLMULTI: An R Package for Easy Automated Model Selection with (Generalized) Linear Models. *Journal of Statistical Software* 34(12):29.

California Department of Fish and Game. 2011. *Report and Recommendation to the Fish and Game Commission in Support of a Proposal to Revise Sportfishing Regulations for Striped Bass.* Sacramento, CA.

California Department of Water Resources. 2012 (September 5). *2011 Georgiana Slough Non-Physical Barrier Performance Evaluation Project Report*. State of California, Natural Resources Agency, Department of Water Resources, Bay-Delta Office, Sacramento, CA.

———. 2013. *Experimental Design and Study Plan for the 2014 Georgiana Slough Floating Fish Guidance Structure Performance Evaluation*. State of California, Natural Resources Agency, Department of Water Resources, Bay-Delta Office, Sacramento, CA.

———. 2013. (November). *Bay Delta Conservation Plan*. Public Draft. Prepared by ICF International (ICF 00343.12). Sacramento, CA. Available: http://baydeltaconservationplan.com/PublicReview/PublicReviewDraftBDCP.aspx. Accessed June 24, 2014.

———. In review. *2012 Georgiana Slough Non-Physical Barrier Performance Evaluation Project Report*. State of California, Natural Resources Agency, Department of Water Resources, Bay-Delta Office, Sacramento, CA.

Cane, Michael. Environmental Scientist. California Department of Water Resources, Delta Conveyance Branch, Bay-Delta Office, Sacramento, CA. January 4, 2013—e-mail messages containing as-built coordinates and aerial photograph of 2012 rock barrier, sent to Marin Greenwood, Aquatic Ecologist, ICF International, Sacramento, CA.

Cavallo, B., J. Merz, and J. Setka. 2013. Effects of Predator and Flow Manipulation on Chinook Salmon (*Oncorhynchus tshawytscha*) Survival in an Imperiled Estuary. *Environmental Biology of Fishes* 96(2–3):393–403.

Clark, K. W., M. D. Bowen, R. B. Mayfield, K. P. Zehfuss, J. D. Taplin, and C. H. Hanson. 2009. *Quantification of Pre-Screen Loss of Juvenile Steelhead in Clifton Court Forebay*. Sacramento, CA: California Department of Water Resources.

Cohen, J. 1988. *Statistical Power Analysis for the Behavioral Sciences*. Second edition. Hillsdale, NJ: Lawrence Erlbaum Associates, Publishers.

Conrad, Louise. Senior Environmental Scientist, California Department of Water Resources, Division of Environmental Services, Aquatic Ecology Section, West Sacramento, CA. March 12 and 20, 2013—Excel files containing University of California, Davis/California Department of Water Resources electrofishing data provided to Marin Greenwood, Aquatic Ecologist, ICF International, Sacramento, CA.

Dekar, M., P. Brandes, J. Kirsch, L. Smith, J. Speegle, P. Cadrett, and M. Marshall. 2013 (June). *USFWS Delta Juvenile Fish Monitoring Program Review.* Background report prepared for review by the IEP Science Advisory Group. Lodi, CA: U.S. Fish and Wildlife Service, Stockton Fish and Wildlife Office.

Dempsey, Mike. Environmental Services Control System Technician III. Division of Environmental Services, California Department of Water Resources, West Sacramento, CA. January 2013—Excel file with CDEC water quality data provided to Michael Burns, Bay-Delta Office, California Department of Water Resources, Sacramento, CA.

DFG. *See* California Department of Fish and Game.

Dinehart, R., and J. Burau. 2005. Repeated Surveys by Acoustic Doppler Current Profiler for Flow and Sediment Dynamics in a Tidal River. *Journal of Hydrology* 314(1):1–21.

DWR. *See* California Department of Water Resources.

Ehrenberg, J. E., and T. W. Steig. 2003. Improved Techniques for Studying the Temporal and Spatial Behavior of Fish in a Fixed Location. *ICES Journal of Marine Science* 60:700–706.

Ferrari, M. C. O., L. Ranåker, K. L. Weinersmith, M. J. Young, A. Sih, and J. L. Conrad. 2013. Effects of Turbidity and an Invasive Waterweed on Predation by Introduced Largemouth Bass. *Environmental Biology of Fishes*. DOI: 10.1007/s10641-013-0125-7.

Fisher, W. F. 1994. Past and Present Status of Central Valley Chinook Salmon. *Conservation Biology* 8(3):870–873.

Flammang, M., M. Thul, and B. Ellison. 2013. *Behavioral Response of Walleye to a Bioacoustic Bubble Strobe Light Barrier*. Des Moines: Iowa Department of Natural Resources. Available: http://www.fisheriessociety.org/iowa/statepdfs/Newsletters/2013_Volume_31_1.pdf. Accessed June 2013.

Ford, T., and S. Kirihara. 2010. *Tuolumne River* Oncorhynchus mykiss *Monitoring Report*. Submitted in compliance with ordering paragraph (C) (5) of the April 3, 2008, Federal Energy Regulatory Commission order on 10-year summary report under Article 58 for Project No. 2299.

Freeman, E. A., and G. Moisen. 2008. Presence-Absence: An R Package for Presence Absence Analysis. *Journal of Statistical Software* 23(11).

Gingras, M., and M. McGee. 1997 (January). *A Telemetry Study of Striped Bass Emigration from Clifton Court Forebay: Implications for Predator Enumeration and Control*. IEP Technical Report 54. Interagency Ecological Program for the San Francisco Bay/Delta Estuary.

Grossman, G. D., T. Essington, B. Johnson, J. Miller, N. Monsen, and T. N. Pearsons. 2013 (September 25). *Effects of Fish Predation on Salmonids in the Sacramento River–San Joaquin Delta and Associated Ecosystems*. Panel Report for State of the Science Workshop on Fish Predation on Central Valley Salmonids in the Bay-Delta Watershed.

Hankin, D., D. Dauble, J. Pizzimenti, and P. Smith. 2010 (May 11). *The Vernalis Adaptive Management Program (VAMP): Report of the 2010 Review Panel*. Prepared for the Delta Science Program. Available: http://www.sjrg.org/peerreview/review_vamp_panel_report_final_051110.pdf. Accessed May 23, 2013.

Hanson, P., T. Johnson, D. Schindler, and J. Kitchell. 1997. Fish Bioenergetics 3.0. Sea Grant Institute, Center for Limnology, University of Wisconsin, Madison.

Helvey, M., and P. B. Dorn. 1981. The Fish Population Associated with an Offshore Water Intake Structure. *Bulletin of the Southern California Academy of Sciences* 80:23–31.

Holbrook, C. M., R. W. Perry, and N. S. Adams. 2009. *Distribution and Joint Fish-Tag Survival of Juvenile Chinook Salmon Migrating through the Sacramento–San Joaquin River Delta, 2008*. Biological Resources discipline report to San Joaquin River Group Authority. Cook, WA: U.S. Geological Survey.

Hollander, M., and D. A. Wolfe. 1973. *Nonparametric Statistical Methods*. New York: John Wiley and Sons.

Hooper, D. R. 1973. Evaluation of the Effects of Flows on Trout Stream Ecology. Department of Engineering Resources, Pacific Gas and Electric, Emeryville, CA.

Horn, Michael. Research Scientist, GP Client Liaison. U.S. Bureau of Reclamation, Denver, CO. February 21, 2013—e-mail communication to Marin Greenwood, Aquatic Ecologist, ICF International, Sacramento, CA.

Hosmer, D. W., and S. Lemeshow. 2000. *Applied Logistic Regression*. New York: John Wiley and Sons.

Hrabik, T. R., O. P. Jensen, S. J. Martell, C. J. Walters, and J. F. Kitchell. 2006. Diel Vertical Migration in the Lake Superior Pelagic Community. I. Changes in Vertical Migration of Coregonids in Response to Varying Predation Risk. *Canadian Journal of Fisheries and Aquatic Sciences* 63(10):2286–2295.

Israel, Josh. Fishery Biologist. U.S. Bureau of Reclamation, Sacramento, CA. June 25, 2013—e-mail communication to Turnpenny Horsfield Associates personnel regarding Surgical and Handling Methods Standard Operating Procedure for the Six-Year Steelhead Study (2012).

Jackson, W. T., and A. M. Paterson. 1977. *The Sacramento–San Joaquin Delta and the Evolution and Implementation of Water Policy: An Historical Perspective*. California Water Resources Center, Contribution No. 163, University of California, Davis.

Johnston, Sam. Senior Fish Biologist. Hydroacoustic Technology Inc., Seattle, WA. April 2009—oral discussion and e-mail to Mark D. Bowen, Fishery Biologist. U.S. Bureau of Reclamation, Denver, CO.

———. April 11 and May 22, 2013—e-mail communications to Marin Greenwood, Aquatic Ecologist, ICF International, Sacramento, CA.

———. June 19, 2013 to Turnpenny Horsfield Associates personnel.

Jones & Stokes. 2007 (September). *Evaluation of Fish Protection from Installation of the Head of Old River Temporary Barrier*. J&S 06757.06. Sacramento, CA. Prepared for U.S. Bureau of Reclamation.

Kastner, Anna. Hatchery Manager, California Department of Fish and Wildlife, Oroville, CA – e-mails to THA personnel June 10, and 14, 2013.

Katapodis, C., D. Scruton, and K. Meade. 2004. Science Gaps for Fish Passage at Hydroelectric Projects. Appendix A: Discussion Papers. In *Canada Electricity Association/Fisheries and Oceans Canada Science Workshop Proceedings: Setting Research Priorities on Hydroelectricity and Fish or Fish Habitat,* ed. M. G. Stoneman. Ottawa, Canada: Fisheries and Oceans Canada. Available: http://publications.gc.ca/collections/collection_2007/dfo-mpo/Fs97-6-2614E.pdf. Accessed June 2013.

Kennedy, Trevor. Executive Director and Senior Fishery Biologist. The Fishery Foundation of California, Elk Grove, CA. August 27, 2013—e-mail communication with Marin Greenwood, Aquatic Ecologist, ICF International, Sacramento, CA.

Knudsen, F. R., P. S. Enger, and O. Sand. 1992. Awareness Reactions and Avoidance Responses to Sound in Juvenile Atlantic Salmon, *Salmo salar*. *Journal of Fish Biology* 40:523–534.

Kollenborn, Greg. Senior Hatchery Supervisor, California Department of Fish and Wildlife, Snelling, CA—e-mail to THA personnel June 12, 2013.

Kynard, B., and C. Buerkett. 1997. Passage and Behavior of Adult American Shad in an Experimental Louver Bypass System. *North American Journal of Fisheries Management* 17:734–742.

LeDoux-Bloom, C. M. 2012. Distribution, Habitat Use, and Movement Patterns of Sub-Adult Striped Bass *Morone saxatilis* in the San Francisco Estuary Watershed, California. Ph.D. dissertation. University of California, Davis.

Lichatowich, J.A., J. Anderson, M. Deas, A. Giorgi, K. Rose, and J. Williams. 2005 (December). *Review of the Biological Opinion of the Long-Term Central Valley Project and State Water Project Operations Criteria and Plan*. A Report of the Technical Review Panel. Prepared for California Bay-Delta Authority, Sacramento, CA.

Liedtke, T. L., J. W. Beeman, and L. P. Gee. 2012. *A Standard Operating Procedure for the Surgical Implantation of Transmitters in Juvenile Salmonids*. U.S. Geological Survey Open-File Report 2012–1267.

Lund, J., E. Hanak, W. Fleenor, R. Howitt, J. Mount, and P. Moyle. 2007. *Envisioning Futures for the Sacramento–San Joaquin Delta.* San Francisco: Public Policy Institute of California.

Manel, S., H. C. Williams, and S. J. Ormerod. 2001. Evaluating Presence-Absence Models in Ecology: The Need to Account for Prevalence. *Journal of Applied Ecology* 38:921–931.

Martinelli, T. L., H. C. Hansel, and R. S. Shively. 1998. Growth and Physiological Responses to Surgical and Gastric Radio Transmitter Implantation Techniques in Subyearling Chinook Salmon (*Oncorhynchus tshawytscha*). *Hydrobiologia* 371/372:79–87.

Mazerolle, M. J. 2006. Improving Data Analysis in Herpetology: Using Akaike's Information Criterion (AIC) to Assess the Strength of Biological Hypotheses. *Amphibia-Reptilia* 27(2):169–180.

McEwan, D. 2001. Central Valley Steelhead. In *Contributions to the Biology of Central Valley Salmonids*, Fish Bulletin 179. Sacramento: California Department of Fish and Game.

McEwan, D., and T. A. Jackson. 1996. *Steelhead Restoration and Management Plan for California*. Sacramento: California Department of Fish and Game, Inland Fisheries Division.

McQuirk, Jacob. Chief, Temporary Barriers and Lower San Joaquin. California Department of Water Resources, Sacramento, CA. October 28, 2013—e-mail concerning feasibility of gate at Head of Old River, sent to Marin Greenwood, Aquatic Ecologist, ICF International, Sacramento, CA.

Meronek, T. G., P. M. Bouchard, E. R. Buckner, T. M. Burri, K. K. Demmerly, D. C. Hatleli, R. A. Klumb, S. H. Schmidt, and D. W. Coble. 1996. A Review of Fish Control Projects. *North American Journal of Fisheries Management* 16(1):63–74.

Miranda, J., R. Padilla, J. Morinaka, J. DuBois, and M. Horn. 2010. *Release Site Predation Study*. Sacramento, CA: California Department of Water Resources.

Moyle, P. B. 2002. *Inland Fishes of California*. Second edition. Berkeley: University of California Press.

Moyle, P. B., and W. A. Bennett. 2010 (August 26). *Striped Bass Predation on Listed Fishes: Can a Control Program be Justified?* Letter to Mr. Jim Kellogg, President, California Fish and Game Commission. Davis: Center for Watershed Sciences, University of California, Davis.

Muir, W. D., A. E. Giorgi, and T. C. Coley. 1993. *Behavioral and Physiological Changes in Yearling Chinook Salmon during Hatchery Residence and Downstream Migration*. Seattle, WA: National Marine Fisheries Service. Available: http://www.nwfsc.noaa.gov/assets/26/8668_07232012_151230_Muir.et.al.1993b-rev.pdf. Accessed July 2013.

National Marine Fisheries Service. 2005. 2005. *5-Year Review: Summary and Evaluation of Central Valley Spring-Run Chinook Salmon ESU*. Long Beach, CA: Southwest Region. Available: http://www.nmfs.noaa.gov/pr/pdfs/species/centralvalley_springrunchinook_5yearreview.pdf. Accessed November 3, 2013.

———. 2009. *Biological Opinion on the Long-Term Central Valley Project and State Water Project Operations Criteria and Plan*. Long Beach, CA: Southwest Region. Available: http://swr.nmfs.noaa.gov/ocap/NMFS_Biological_and_Conference_Opinion_on_the_Long-Term_Operations_of_the_CVP_and_SWP.pdf. Accessed June 2013.

———. 2011. *2009 Reasonable and Prudent Alternative Revised to Include the 2011 Amendments*. Long Beach, CA: Southwest Region. Available: http://swr.nmfs.noaa.gov/ocap/040711_OCAP_opinion_2011_amendments.pdf. Accessed June 2013.

———. 2011. *Biological Opinion for the 2011 South Delta Temporary Barriers Project, Including Installation and Operation of a Non-physical Barrier at the Head of Old River*. Long Beach, CA: Southwest Region.

———. 2013 (February 23). *Considerations for Accounting of Incidental Take and Triggers at the Delta Federal and State Export Facilities of Reintroduced San Joaquin River Spring-Run Chinook Salmon*. Draft Technical Memorandum. Available: http://swr.nmfs.noaa.gov/sjrrestorationprogram/SJR%20Spring-run%20Tech%20Memo_2013-0223.pdf. Accessed July 2013.

———. 2013. *The Temporary Barriers Project Programmatic Biological Opinion for the Sacramento River Winter-Run Chinook Salmon, the Central Valley Spring-Run Chinook Salmon, the California Central Valley Steelhead, and the North American Green Sturgeon.* Long Beach, CA: Southwest Region.

National Oceanic and Atmospheric Administration. 2013. Solar Calculation Details. Earth System Research Laboratory. Available: http://www.esrl.noaa.gov/gmd/grad/solcalc/calcdetails.html. Accessed May 7, 2013.

Nemeth, R. S., and J. J. Anderson. 1992. Response of Juvenile Coho and Chinook Salmon to Strobe and Mercury Vapor Lights. *North American Journal of Fisheries Management* 12:684–692.

Newman, K. B. 2003. Modelling Paired Release-Recovery Data in the Presence of Survival and Capture Heterogeneity with Application to Marked Juvenile Salmon. *Statistical Modelling* 3:157–177.

———. 2008. *An Evaluation of Four Sacramento–San Joaquin River Delta Juvenile Salmon Survival Studies*. Stockton, CA: U.S. Fish and Wildlife Service.

———. 2010. Analyses of Salmon CWT Releases into the San Joaquin System. Handout to the VAMP review panel on March 2, 2010.

NMFS. *See* National Marine Fisheries Service.

NOAA. *See* National Oceanic and Atmospheric Administration.

Noatch, M. R., and C. D. Suski. 2012. Non-Physical Barriers to Deter Fish Movements. *Environmental Reviews* 20(1):71–82.

Nobriga, M., Z. Hymanson, and R. Oltmann. 2000. Environmental Factors Influencing the Distribution and Salvage of Young Delta Smelt: A Comparison of Factors Occurring in 1996 and 1999. *IEP Newsletter* 13(2):55–65.

Orr, M., S. Crooks, and P. B. Williams. 2003. Will Restored Tidal Marshes be Sustainable? In *Issues in San Francisco Estuary Tidal Wetlands Restoration, San Francisco Estuary and Watershed Science*, Vol. 1, Article 5L, ed. R. Brown. Available: http://repositories.cdlib.org/jmie/sfews/vol1/iss1/art5/. Accessed July 2013.

Oxman, D. S., R. Barnett-Johnson, M. E. Smith, A. Coffin, D. L. Miller, R. Josephson, and A. N. Popper. 2007. The Effect of Vaterite Deposition on Sound Reception, Otolith Morphology, and Inner Ear Sensory Epithelia in Hatchery-Reared Chinook Salmon (*Oncorhynchus tshawytscha*). *Canadian Journal of Fisheries and Aquatic Sciences* 64:1469–1478.

Pellett, T. D., G. J. Van Dyck, and J. V. Adams. 1998. Seasonal Migration and Homing of Channel Catfish in the Lower Wisconsin River, Wisconsin. *North American Journal of Fisheries Management* 18(1):85–95.

Perry, R. W. 2010. Survival and Migration Dynamics of Juvenile Chinook Salmon (*Oncorhynchus tshawytscha*) in the Sacramento–San Joaquin River Delta. Ph.D. dissertation. University of Washington, Seattle.

Perry, R. W., J. G. Romine, N. S. Adams, A. R. Blake, J. R. Burau, S. V. Johnston, and T. L. Liedtke. 2012. Using a Non-Physical Behavioural Barrier to Alter Migration Routing of Juvenile Chinook Salmon in the Sacramento–San Joaquin River Delta. *River Research and Applications*. DOI: 10.1002/rra.2628.

Perry, R. W., J. R. Skalski, P. L. Brandes, P. T. Sandstrom, A. P. Klimley, A. Ammann, and B. MacFarlane. 2010. Estimating Survival and Migration Route Probabilities of Juvenile Chinook Salmon in the Sacramento–San Joaquin River Delta. *North American Journal of Fisheries Management* 30:142–156.

Perry, R. W., P. L. Brandes, J. R. Burau, A. P. Klimley, B. MacFarlane, C. Michel, and J. R. Skalski. 2013. Sensitivity of Survival to Migration Routes Used by Juvenile Chinook Salmon to Negotiate the Sacramento–San Joaquin River Delta. *Environmental Biology of Fishes* 96(2–3):381–392.

R Core Team. 2013. R: A Language and Environment for Statistical Computing. R Foundation for Statistical Computing, Vienna, Austria. Available: http://www.R-project.org/. Accessed May 7, 2013.

Reclamation. *See* U.S. Bureau of Reclamation.

Romine, J. G., R. W. Perry, S. V. Johnston, C. Fitzer, S. Pagliughi, and A. R. Blake. 2014. Identifying When Tagged Fishes Have Been Consumed by Piscivorous Predators: Application of Multivariate Mixture Models to Movement Parameters of Telemetered Fishes. *Animal Biotelemetry* 2(1):3.

Rudstam, L. G., J. M. Jech, S. L. Parker-Stetter, J. K. Horne, P. J. Sullivan, and D. M. Mason. 2012. Fisheries Acoustics. In *Fisheries Techniques*, eds. A. V. Zale, D. L. Parrish, and T. M. Sutton, 597–636. Third edition. Bethesda, MD: American Fisheries Society.

Ruebush, B. C., G. G. Sas, J. H. Chick, and J. D. Stafford. 2012. In-situ Tests of Sound Bubble Strobe Light Barrier Technologies to Prevent Range Expansions of Asian Carp. *Aquatic Invasions* 7:37–48.

Sabal, M. 2014. Interactive effects of non-native predators and anthropogenic habitat alterations on native juvenile salmon. Master's Thesis. University of California, Santa Cruz, Santa Cruz, CA.

Sager, D. R., C. H. Hocutt, and J. R. Stauffer Jr. 1987. Estuarine Fish Responses to Strobe Light, Bubble Curtains and Strobe Light/Bubble-Curtain Combinations as Influenced by Water Flow Rate and Flash Frequencies. *Fisheries Research* 5:383–399.

San Joaquin River Group Authority. 1999. *Summary Report for Meeting the Flow Objectives for the San Joaquin River Agreement*. Davis, CA.

———. 2003 (January). *2002 Annual Technical Report on Implementation and Monitoring of the San Joaquin River Agreement and the Vernalis Adaptive Management Plan (VAMP)*. Davis, CA. Prepared for California Water Resources Control Board in compliance with D-1641.

———. 2006 (January). *2005 Annual Technical Report on Implementation and Monitoring of the San Joaquin River Agreement and the Vernalis Adaptive Management Plan (VAMP)*. Davis, CA. Prepared for California Water Resources Control Board in compliance with D-1641.

———. 2007 (January). *2006 Annual Technical Report on Implementation and Monitoring of the San Joaquin River Agreement and the Vernalis Adaptive Management Plan (VAMP)*. Davis, CA. Prepared for California Water Resources Control Board in compliance with D-1641.

———. 2010 (January). *2009 Annual Technical Report on Implementation and Monitoring of the San Joaquin River Agreement and the Vernalis Adaptive Management Plan (VAMP)*. Davis, CA. Prepared for California Water Resources Control Board in compliance with D-1641.

———. 2011 (September). *2010 Annual Technical Report on Implementation and Monitoring of the San Joaquin River Agreement and the Vernalis Adaptive Management Plan (VAMP)*. Davis, CA. Prepared for California Water Resources Control Board in compliance with D-1641.

———. 2013 (February). *2011 Annual Technical Report on Implementation and Monitoring of the San Joaquin River Agreement and the Vernalis Adaptive Management Plan (VAMP)*. Davis, CA. Prepared for California Water Resources Control Board in compliance with D-1641.

San Joaquin River Restoration Program. 2011 (November 28). Background and History. San Joaquin River Restoration Program Web site. Available: http://restoresjr.net/background.html. Accessed May 23, 2013.

———. 2012 (July 31). Planned Fall 2012 and Spring 2013 Fall-Run and Spring-Run Chinook Salmon Activities. Available: http://www.restoresjr.net/program_library/02-Program_Docs/2012-2013_Fish%20Actions_20120731_Final.pdf. Accessed May 23, 2013.

Savino, J., D. Jude, and M. Kostich. 2001. Use of Electrical Barriers to Deter Movement of Round Goby. *American Fisheries Society Symposium* 26:171–182.

SJRGA. *See* San Joaquin River Group Authority.

SJRRP. *See* San Joaquin River Restoration Program.

Sokal, R. R., and F. J. Rohlf. 1995. *Biometry*. Third edition. New York: W. H. Freeman and Company.

Sommer, T., R. Baxter, and B. Herbold. 1997. Resilience of Splittail in the Sacramento–San Joaquin Estuary. *Transactions of the American Fisheries Society* 126(6):961–976.

Speegle, Jonathan. Fish Biologist (Data Manager), U.S. Fish and Wildlife Service, Stockton Field Office, Stockton, CA. November 11, 2011, and January 4, 2013—Excel files containing USFWS seine and trawl sampling data provided to Marin Greenwood, Aquatic Ecologist, ICF International, Sacramento, CA.

State of California. 2009. California Irrigation Management Information System. Available: http://wwwcimis.water.ca.gov/cimis/welcome.jsp. Accessed May 7, 2013.

State of Wisconsin. 2003. *Decision in the Matter of the Waterway and Wetland Alterations Relating to the Wisconsin Electric Power Company Oak Creek Power Plant Expansion*. Case Numbers 3-SE-01-41-005-0019 & 1456MW. Madison: State of Wisconsin, Division of Hearings and Appeals.

Stuber, R. J., G. Gebhart, and O. E. Maughan. 1982. Habitat Suitability Index Models: Largemouth Bass. U.S. Fish and Wildlife Service. FWS/OBS-82/10.16.

Thompson, J. 1957. *Settlement Geography of the Sacramento–San Joaquin Delta, California.* Dissertation. Stanford, CA: Stanford University.

Turnpenny, A. W. H., and N. O'Keeffe. 2005. *Screening for Intakes and Outfalls; A Best Practice Guide*. Science Report SC030231. Bristol, UK: Environment Agency.

Uphoff, J. 2003. Predator–Prey Analysis of Striped Bass and Atlantic Menhaden in Upper Chesapeake Bay. *Fisheries Management and Ecology* 10(5):313–322.

U.S. Bureau of Reclamation. 2004a. *Long-Term Central Valley Project Operation Criteria and Plan (CVP-OCAP)*. Sacramento, CA: Mid-Pacific Regional Office. Available: http://www.usbr.gov/mp/cvo/OCAP/OCAP_6_30_04.pdf. Accessed June 2013.

———. 2004b. *Long-Term Central Valley Project and State Water Project Operations Criteria and Plan Biological Assessment*. Sacramento, CA: Mid-Pacific Regional Office.

———. 2014. *U.S. Fish and Wildlife Service and Reclamation Release Spring-run Chinook Salmon into the San Joaquin River for Study*. Sacramento, CA: Mid-Pacific Regional Office. Available: http://www.usbr.gov/newsroom/newsrelease/detail.cfm?RecordID=46544. Accessed: June 23 2014.

U.S. Fish and Wildlife Service. 2008. *Biological Opinion and Formal Endangered Species Act Consultation on the Proposed Coordinated Operations of the Central Valley Project (CV) and State Water Project (SWP)*. Sacramento, CA: Region 8. Available: http://www.fws.gov/sfbaydelta/cvp-swp/ocap_legal_archives.cfm. Accessed June 2013.

USFWS. *See* U.S. Fish and Wildlife Service.

Vogel, D. A. 2007 (May 20). *Technical Memorandum to Participating Agencies in the 2007 Adaptive Management Program Concerning High Fish Mortality near Stockton, California*. Red Bluff, CA: Natural Resource Scientists, Inc.

———. 2010 (March). *Evaluation of Acoustic-Tagged Juvenile Chinook Salmon Movements in the Sacramento–San Joaquin Delta during the 2009 Vernalis Adaptive Management Program*. Red Bluff, CA: Natural Resource Scientists, Inc.

———. 2011. *Evaluation of Acoustic-Tagged Juvenile Chinook Salmon Movements and Predatory Fish Movements in the Sacramento-San Joaquin Delta during the 2010 Vernalis Adaptive Management Program*. Red Bluff, CA: Natural Resource Scientists, Inc.,

Vogel, D. A., and K. R. Marine. 1991. *Guide to Upper Sacramento River Chinook Salmon Life History*. Prepared for the U.S. Bureau of Reclamation Central Valley Project, Sacramento, CA, by CH2M HILL, Sacramento, CA.

Vogel pers. comm. 2010. Cited in Hankin et al. 2010.

Welton, J. S., W. R. C. Beaumont, and R. T. Clarke. 2002. The Efficacy of Air, Sound and Acoustic Bubble Screens in Deflecting Atlantic Salmon, *Salmo salar* L., Smolts in the River Frome, UK. *Fisheries Management and Ecology* 9(1):11–18.

Williams, J. G. 2006. Central Valley Salmon. A Perspective on Chinook and Steelhead in the Central Valley of California. *San Francisco Estuary and Watershed Science* 4(3):Article 2.

Zeug, S. C., and B. J. Cavallo. 2013. Influence of Estuary Conditions on the Recovery Rate of Coded-Wire-Tagged Chinook Salmon (*Oncorhynchus tshawytscha*) in an Ocean Fishery. *Ecology of Freshwater Fish* 22(1):157–168.

State of California

The California Natural Resources Agency

Department of Water Resources

Stipulation Study: Steelhead Movement and Survival in the South Delta with Adaptive Management of Old and Middle River Flows

Prepared by

David Delaney, Paul Bergman, Brad Cavallo, and Jenny Melgo

Cramer Fish Sciences

13300 New Airport Road, Suite 102

Auburn, CA 95602

Under the direction of:

Kevin Clark

Bay-Delta Office

Biotelemetry and Special Investigations Unit

February 2014

State of California
Edmund G. Brown, Jr., Governor

California Natural Resources Agency
John Laird, Secretary for Natural Resources

Department of Water Resources
Mark W. Cowin, Director

Laura K. Moon
Chief Deputy Director

Kasey Schimke
Asst. Director Legislative Affairs

Nancy Vogel
Asst. Director Public Affairs

Cathy Crothers
Chief Counsel

Gary Bardini
Deputy Director
Integrated Water Management

Paul Helliker
Deputy Director
Delta/Statewide Water Management

Kathie Kishaba
Deputy Director
Business Operations

John Pacheco
Deputy Director
California Energy Resources Scheduling

Carl Torgersen
Deputy Director
State Water Project

Katherine Kelly

Chief, Bay-Delta Office

Victor Pacheco

Chief, Delta Conveyance Branch

Matthew Reeve

Chief, Delta Conveyance Fish Science Section

California Department of Water Resources

1416 9th Street, Sacramento, CA 95814, USA

EXECUTIVE SUMMARY

Juvenile steelhead (*Oncorhynchus mykiss*) migrating downstream in the San Joaquin River are vulnerable to mortality from a variety of stressors. Two of these stressors are entrainment and predation (entrainment at State Water Project [SWP] and federal Central Valley Project [CVP] facilities, and exposure to predation within the Sacramento-San Joaquin Delta [Delta] and predation near and associated with the two facilities). The SWP and CVP facilities are south of the confluence of the San Joaquin and Sacramento rivers. Export of water can change the flow dynamics in the central and south Delta (e.g., Old and Middle River [OMR] reverse flows, flows passing into Old River, etc.). All OMR flows referred to in this report are average daily values. The hydrodynamic changes have been hypothesized to result in altered migration pathways, migration delays, and other indirect effects that contribute to reduced survival of juvenile salmonids passing through the lower San Joaquin River and Delta. To protect fish, SWP and CVP export rates in the late winter and spring months have been regulated to reduce the magnitude of OMR reverse flows.

Current management actions are calendar and trigger based during the period when Endangered Species Act (ESA)-listed salmonids are present in the Delta. Triggers are based, in part, on rates of entrainment of fish at the SWP and CVP. If salmonid protection measures could be implemented based on fish presence farther from the export facilities, it is hypothesized that: (1) the direct and indirect risks to salmonids associated with the export facilities may be reduced, and measurement of take at SWP and CVP facilities can be replaced with other metrics for reducing impacts from the water projects; and (2) exposure of ESA-listed salmonids to predation in the south Delta channels can be reduced.

On January 12, 2012, Plaintiffs, Plaintiff-Intervener, and Federal Defendants to the Consolidated Salmonid Cases (Case 1: 09-cv-Ol 053-LJO-DLB) signed and filed a Joint Stipulation (Document 659-2; Attachment 1 in NMFS 2012) that specified a collaborative acoustic tag study for steelhead and CVP and SWP operations for April and May 2012 (NMFS 2012). The three objectives for the 2012 Stipulation Study were to:

(1) Evaluate potential effects of OMR flows during April and May on the survival, migration rate, and net migration direction of acoustically tagged juvenile steelhead in the Delta.

(2) Estimate the route entrainment of acoustically tagged juvenile steelhead in the Delta under different tidal conditions and OMR flows.

(3) Provide daily and weekly steelhead tag detection data that could be used to adaptively manage OMR flows within the adaptive range specified in the Joint Stipulation.

To address the Joint Stipulation objectives, in the spring of 2012, a mark-recapture experiment was implemented by the California Department of Water Resources (the Department) and its contractors, with collaboration from the United States Bureau of Reclamation (Reclamation), United States Fish and Wildlife Service (USFWS), and United States Geological Survey (USGS) to examine the survival and movement patterns of acoustically tagged juvenile steelhead emigrating through the central and southern Delta. This field experiment implemented different OMR flow levels for three, 2-week release periods when acoustically tagged steelhead were used to gather information about the responses of tagged fish to different hydrodynamic conditions. During the study, the Head of Old River Barrier (HORB) was in place, which prevented flow from entering the interior Delta through Old River and directed flow along the Mainstem San Joaquin River. Included in the study was an "exposure trigger" that, if reached or exceeded, shifted operations from the experimental OMR flow level to the least negative OMR flow level within the adaptive range. This was intended to protect naturally produced steelhead migrating through the Delta by shifting hydrodynamic conditions in a direction that may be less disruptive to outmigration routing while simultaneously allowing investigation of the response of steelhead tags to changes in OMR flow levels. This "Railroad Cut trigger" was calculated as 5% of the release group reaching the acoustic receiver arrays at Railroad Cut, under the assumption that 5% of fish arriving at Railroad Cut would be expected to result in a 2% loss of the release group at the fish collection facilities (NMFS 2012).

The original experimental design called for each 2-week experimental period to represent one of three OMR reverse flow magnitude targets (-1,250, -3,500, and -5,000 cubic feet per second [cfs]). Average observed OMR flows during the first 7 days following release were -2,446, -2,933, and -5,038 cfs for Release Groups 1, 2, and 3, respectively. Near-real-time monitoring (i.e., daily data collection) of detections of steelhead tags at Railroad Cut exceeded the trigger and caused OMR flow modifications during each experimental period.

Every 2 weeks, acoustically tagged juvenile steelhead were released at regular intervals over 24 hours at Buckley Cove in the lower San Joaquin River. In total, 166, 167, and 168 acoustic coded transmitters (VEMCO, model V6-4X) were functioning in live steelhead for release groups (Group 1, 2, or 3) when released on April 15-16, May 1-2, and May 15-16, 2012, respectively. Tag detection data were collected from 15 acoustic receiver arrays deployed for this study and nine acoustic receiver arrays deployed for the Six-Year Steelhead Study (Six-Year Study). The release groups acted as a surrogate for the average OMR flow conditions that occurred during the three study periods. The release groups experienced an "OMR treatment" measured as the average OMR flows during the first 7 days of each study period. Based on a recommendation in the 2012 Independent Review Panel (IRP) on the Long-term Operations Opinions (LOO) Annual Review, we also pooled the data from Release Groups 1 and 2 and hereafter referred to as the less negative OMR flow treatment because OMR flow levels were similar during these two time periods. We then compared this less negative OMR flow treatment group to the more negative OMR flow treatment level experienced by Release Group 3. The data were examined using both qualitative, descriptive analyses and quantitative, statistical hypothesis-testing analyses. The analyses were separated into three report sections based on the spatial level ranging from system, route, and junction-level discussion.

SYSTEM-WIDE LEVEL RESULTS

System-wide results are those that focus on the large-scale movement patterns across the Delta. The quantitative statistical analyses determined that a physically based model in the form of the Delta Simulation Model II (DSM2) Hydro Particle Tracking Model (PTM) was not able to predict the movement of steelhead tags. The model greatly underestimated the steelhead tag movement rate through the study area. Steelhead tags were traveling significantly greater distances than passive particles 3 days and 7 days after their release. Steelhead have a complex set of behaviors and respond to both biotic and abiotic factors that can affect where and how fast they migrate. Further investigation indicated that tags deployed in juvenile steelhead exhibited limited selective tidal-stream transport (STST) movement patterns, which could explain why steelhead tags moved far faster than passive particles. This was likely the result of steelhead tags being transported by ebbing tides while holding position on flood tides. This investigation revealed that overall, there seemed to be some evidence that steelhead tags were being transported more during the night in the Mainstem San Joaquin River, while more steelhead tags were being transported during the day at some interior Delta arrays.

ROUTE-LEVEL RESULTS

Route-level analysis refers to the specific travel pathways (routes) that fish can take from one point to another, and the survival rates, travel times, and other variables resulting from these different routes. We examined if the route-specific survival probabilities, transition probabilities (a measure of steelhead tags that went through a route and survived), and travel times for steelhead tags varied between the routes taken and, where possible, between release groups. Data from the release groups used in the model were pooled, but the individual release group data were used to estimate travel times and subsequent travel time analysis.

A multistate model was built to evaluate route-specific transition probabilities, survival probabilities, and detection probabilities of steelhead tags. This model allowed us to estimate route-specific transition probability for each of the six different routes (all routes started downstream of Buckley Cove and ended at Chipps Island):

- The route-specific probability via Turner Cut was 7.0% (standard error [SE]=1.6%).
- The route-specific probability without using Turner Cut was 24.8% (SE=2.0%).

- The route-specific probability via Turner Cut and the SWP was 0.5% (SE=0.5%).
- The route-specific probability via the SWP without using Turner Cut was 0.2% (SE=0.2%).
- The route-specific probability via Turner Cut and the CVP was 19.6% (SE=2.8%).
- The route-specific probability via CVP without using Turner Cut was 31.7% (SE=1.9%).

When combined, the model indicated that most steelhead tags remained in the Mainstem San Joaquin River (77.6%); however, approximately one quarter (22.4%) of them entered Turner Cut. The overall survival was 50.2% (SE=2.0%) for all routes combined. Route-specific survival probability for steelhead tags using the Turner Cut route was 27.0% (SE=3.0%). The survival probability for steelhead tags using the Mainstem route was 56.7% (SE=2.4%).

In an analysis outside of the model, we found that travel times for steelhead tags differed between these two routes. Steelhead tags that used the Mainstem route reached Chipps Island significantly sooner than those that used the Turner Cut route. This result remained valid for all three release groups and when Groups 1 and 2 were combined. Travel time was not significantly affected by the OMR flow treatments examined in this study.

JUNCTION-LEVEL RESULTS

The junction-level analysis specifically looked at three locations in the Delta to evaluate the influence of OMR flows on steelhead tag movement at these locations. There was no evidence that the routing of steelhead tags at the Columbia Cut, Middle River, and Turner Cut junctions along the San Joaquin River was affected by the OMR flow treatments examined in this study. When the data were examined using two release groups (less negative vs. more negative OMR flows), we found no significant differences in routing of the steelhead tags. While not significant, there was some evidence that fish movement toward each export facility could be influenced by relative flow entering the export facility.

One of the goals of this study was to determine whether steelhead tags at Railroad Cut were more likely to move away from the SWP and CVP intakes (north) after the adaptive management option triggered less negative OMR flows. This could not be completed in a statistically valid manner because of the small sample size (N=7) of steelhead tags passing through Railroad Cut after the effect of the management action was observed (OMR flows reached -1,250 cfs). However, there was marginally significant evidence that steelhead tags at Railroad Cut were more likely to move north under less negative (Groups 1 and 2) OMR flows than in more negative (Group 3) OMR flow conditions. We examined nine predictor variables in separate tests. Only the test that used average OMR flow on the day that the steelhead tag was first detected downstream of Railroad Cut was found to be significant.

CONCLUSIONS

The overarching objectives for this study were to evaluate the effects of OMR flows on survival, migration rate, and migration direction; estimate route selection under different OMR flow conditions; and provide steelhead tag detection data that could be used to adaptively manage OMR flows. The quantitative statistical analyses determined that the DSM2 Hydro PTM was not able to predict the movement of steelhead tags because the model greatly underestimated steelhead tag movement through the study area. We found that diurnal and nocturnal movement patterns of steelhead tags might be occurring, but these patterns were location-specific and worthy of future study.

Under the OMR flow treatments tested in this study, there appeared to be little influence of OMR flows tested on steelhead tag travel times on the route-level and steelhead tag movement at the junctions and routes examined in this study. There was limited evidence of an influence of OMR flows on steelhead tag routing at Railroad Cut to the south and the export facilities; sample size limited our ability to be more specific. More than 90% of steelhead tags passed the detection point at Railroad Cut before the less negative OMR flow conditions were triggered and observed to take effect.

Improvements to experimental design of future real-time monitoring studies could be made; however, this study indicated that tagged steelhead cannot effectively be used as "sentinels" to trigger export changes. There is little evidence that altering OMR flows within the range that we examined in this study would alter fish behavior in a meaningful way. The observed limited influence of OMR flows evaluated in this study on steelhead tag behavior does not support real-time monitoring as an effective tool to protect salmonids from entrainment.

This study was limited by the amount of time for its preparation and the ranges of OMR flows tested. Therefore, we recommend an additional more comprehensive study that examines a wider range of OMR flows in replicated treatments with larger samples sizes as one of the future studies.

ACKNOWLEDGEMENTS

We would like to acknowledge contributions (e.g., reviewing data analysis plans, draft of final report, and/or models) to this work from the following people in alphabetical order by last name:

Pat Brandes, United States Fish and Wildlife Service

Rebecca Buchanan, Columbia Basin Research, School of Aquatic and Fishery Sciences, University of Washington, Seattle, WA

Barbara Byrne, National Oceanic and Atmospheric Administration National Marine Fisheries Service

Chuck Hanson, Hanson Environmental

Josh Israel, United States Bureau of Reclamation

Javier Miranda, California Department of Water Resources

Victor Pacheco, California Department of Water Resources

Kevin Reece, California Department of Water Resources

We would like to thank Annie Brodsky and Jenny Melgo for querying and conducting quality assurance/quality control for the data that was the basis for the analyses. Also, we would like to thank Travis Hinkelman for creating the web-based tool. We would like to thank Josh Israel for providing data on the duration of battery lives, from the 2012 battery life studies. Further, we would like to thank Josh Israel for providing data from Six-Year Study tags and acoustic receiver arrays.

Finally, we would like to thank Peter Carr and Demian Ebert at AECOM for editing and formatting the document.

This page intentionally left blank.

TABLE OF CONTENTS

Appendices

TABLE OF CONTENTS

Continued **Page**

Figures

TABLE OF CONTENTS

Continued **Page**

TABLE OF CONTENTS

Continued **Page**

Tables

TABLE OF CONTENTS

Continued **Page**

ACRONYMS AND OTHER ABBREVIATIONS

ANOVA	analysis of variance
CDEC	California Data Exchange Center
CDFW	California Department of Fish and Wildlife
CFS	Cramer Fish Sciences
cfs	cubic feet per second
CHTR	Collection, Handling, Transport, and Release
cm	centimeter
CVP	Central Valley Project
Delta	Sacramento-San Joaquin Delta
Department	California Department of Water Resources
DSM2	Delta Simulation Model II
ESA	Endangered Species Act
GLM	generalized linear model
GPS	Global Positioning System
HORB	Head of Old River Barrier
HRR	high residence receiver
HTI	Hydroacoustic Technology Inc.
ID	identification
IRP	Independent Review Panel
JSATS	Juvenile Salmon Acoustic Telemetry System
kHz	kilohertz
km	kilometer
L	liter
LOO	Long-term Operations Opinions
m	meter
m/sec	meters per second
mg	milligram
mm	millimeter
MS	Microsoft
MS-222	tricane methanesolfonate
N/A	not applicable
NMFS	National Marine Fisheries Service
OMR	Old and Middle River
ppm	pulses per minute

ACRONYMS AND OTHER ABBREVIATIONS

PTM	Particle Tracking Model
PVC	polyvinyl chloride
QA/QC	quality assurance/quality control
Reclamation	United States Bureau of Reclamation
RMS	root-mean-square
RPA	Reasonable and Prudent Alternative
SE	standard error
SJR	San Joaquin River
SJRGA	San Joaquin River Group Authority
SOP	Standard Operating Procedure
STH	steelhead
STST	selective tidal-stream transport
SWP	State Water Project
TRN	Turner Cut
USER	User Specified Estimation Routine
USFWS	United States Fish and Wildlife Service
USGS	United States Geological Survey
VAMP	Vernalis Adaptive Management Program
VUE	VEMCO User Environment

This page intentionally left blank.

1 STUDY DESCRIPTION

CHAPTER SUMMARY:

On January 12, 2012, Plaintiffs, Plaintiff-Intervener, and Federal Defendants to the Consolidated Salmonid Cases (Case 1: 09-cv-Ol 053-LJO-DLB) signed and filed a Joint Stipulation (Document 659-2) that specified Central Valley Project (CVP) and State Water Project (SWP) operations for April and May 2012, installation of the Head of Old River Barrier (HORB), and broadened acoustic tagging and release program in 2012 to track juvenile steelhead (*Oncorhynchus mykiss*) migrations through the south Sacramento-San Joaquin Delta (Delta) for the purpose of generating better information by which to manage south Delta operations and other activities to improve fish survival. The three objectives for the 2012 Stipulation Study were to:

(1) Evaluate potential effects of Old and Middle River (OMR) flows during April and May on the survival, migration rate, and net migration direction of acoustically tagged juvenile steelhead in the Delta.

(2) Estimate route entrainment of acoustically tagged juvenile steelhead in the Delta under different tidal conditions and OMR flows.

(3) Provide daily and weekly steelhead tag detection data that could be used to adaptively manage OMR flows within the adaptive range specified in the Joint Stipulation.

The 2012 Stipulation Agreement called for the operation and maintenance of an acoustic receiver array in the Delta, fish tagging and releases, adaptive management of OMR reverse flow magnitude, and data analysis and report writing. The Stipulation Study was a collaborative project that involved the California Department of Water Resources (the Department), some of its contractors (AECOM, Cramer Fish Sciences, Hanson Environmental, Inc., and Bole and Associates), United States Bureau of Reclamation (Reclamation), United States Fish and Wildlife Service (USFWS), and United States Geological Survey (USGS).

1.1 STUDY OBJECTIVES

Objectives for the 2012 Stipulation Study were to:

- Evaluate potential effects of OMR flows during April and May on the survival, migration rate, and net migration direction of acoustically tagged juvenile steelhead in the Delta.
- Estimate route entrainment of acoustically tagged juvenile steelhead in the Delta under different tidal conditions and OMR flows.
- Provide daily and weekly steelhead tag detection data that could be used to adaptively manage OMR flows within the adaptive range specified in the Joint Stipulation.

1.2 BIOLOGICAL AND REGULATORY BACKGROUND

Juvenile steelhead and Chinook salmon (*Oncorhynchus tshawytscha*) migrating downstream in the San Joaquin River are vulnerable to entrainment at the SWP and the CVP export facilities and the associated exposure to pre-screen predation mortality within Clifton Court Forebay and near the trash racks at the CVP fish collection facility. These facilities are located south of the confluence of the San Joaquin and Sacramento rivers (Figure 1-1). Thus, by the time Endangered Species Act (ESA)-listed salmonids (Central Valley steelhead and Central Valley winter-run and spring-run Chinook salmon) are detected at the salvage facilities, OMR flow changes may be enacted too late to achieve fish protection. In addition, changes in the direction and/or magnitude

of flows in the central and south Delta channels (e.g., OMR reverse flows, flows passing into Old River, etc.) have been hypothesized to result in altered migration pathways, migration delays, and other indirect effects that contribute to reduced survival of juvenile salmonids passing through the lower San Joaquin River and Delta. In response to these concerns, the National Marine Fisheries Service (NMFS) included several Reasonable and Prudent Alternative (RPA) actions in the biological opinion that focused on Delta flow management during the winter and spring (NMFS 2009). SWP and CVP export rates in the late winter and spring months have been regulated to reduce the magnitude of OMR reverse flows. Action IV.2.1 of the biological opinion restricts south Delta exports in April and May to a fraction of the flow in the lower San Joaquin River.

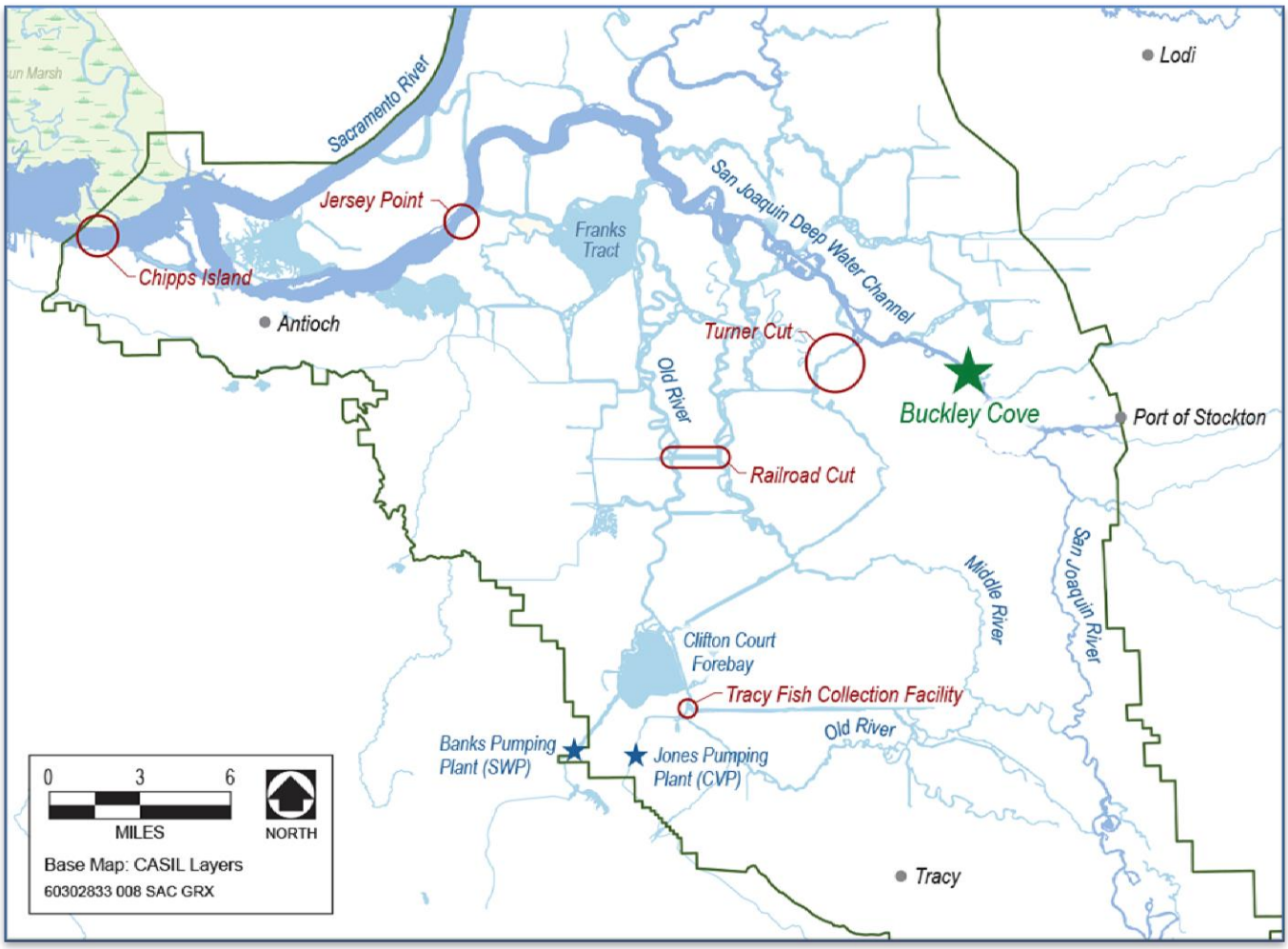

Figure 1-1 **Locations of Chipps Island, Jersey Point, Railroad Cut, Turner Cut, the SWP, and the state and federal export facilities in relation to the 2012 Stipulation Study's release location near Buckley Cove** (depicted by the green star).

Flow management during winter and spring has become the focus of management actions for fish protection along the OMR corridor. These management actions are calendar- and trigger-based during the period when ESA-covered salmonids are present in the Delta. If salmonid protection measures could be implemented based on fish presence farther from the export facilities, it is hypothesized that: (1) the duration of direct risks and indirect risks to salmonids associated with the export facilities may be reduced; and (2) exposure of ESA-covered salmonids to predation in south Delta channels can be reduced. The ultimate goal is to increase through-Delta survival and abundance of salmonids entering the ocean.

Under the Study Plan for the Stipulation Study (NMFS 2012), beginning in early to mid-April, when supplemental steelhead releases began, OMR flow targets shifted to a pilot "managed-risk experimental" approach. This approach implemented different OMR flow "treatment levels" for each Stipulation Study release of acoustically tagged steelhead to gather information about responses of tagged fish to different hydrodynamic conditions. The approach also included an "exposure trigger" (NMFS 2012) that, if reached or exceeded, shifted operations from the experimental OMR flow level to the less negative OMR flow level within the adaptive range (-1,250 cubic feet per second [cfs]). This trigger was intended to protect steelhead by shifting hydrodynamic conditions in a direction that may be less disruptive to outmigration routing or timing and improve survival through the Delta. The ordering of OMR flow management targets through April and May was intended to maximize the feasibility of implementing these targets while avoiding confounding OMR flow management targets with temperature.

NMFS measured the exposure trigger as the cumulative fraction of the supplemental release group that passed a pair of receiver arrays on Old River and Middle River near Railroad Cut and was designed to protect steelhead by shifting hydrodynamic conditions in a direction thought to be less disruptive to outmigration routing or timing. NMFS calculated the "Railroad Cut trigger" as 5% of the release group reaching the acoustic receiver arrays at Railroad Cut, under the assumption that 5% of fish arriving at Railroad Cut would be expected to result in a 2% loss of the release group at the fish collection facilities (NMFS 2012). We assumed that juvenile steelhead migrate fairly rapidly through the Delta and likely do not spend more than 14 days in the Delta. We found this to be true as 94% of the steelhead tags that were ever detected at Chipps Island were detected within 15 days after their release. Thus, for each Stipulation Study release, NMFS based the primary trigger on fish only from that release and not from prior releases.

The NMFS biological opinion included an RPA action that required the design and implementation of a Six-Year Acoustic Tag Study (Six-Year Study) of juvenile steelhead in the San Joaquin River. Studies of the survival and movement patterns of juvenile Chinook salmon in the Delta have also been conducted in the past as part of the Vernalis Adaptive Management Program (VAMP) and other programs (e.g., south Delta temporary barrier project, etc.). The experimental design implemented for the 2012 Stipulation Study represents an augmentation and expansion of the Six-Year Study.

In addition to providing information about the effects of OMR flows on route selection and survival in the south Delta, we also tested an alternative approach to managing water export risks to ESA-listed salmonids. The experimental approach relied on releases of "sentinel fish" and monitoring stations to detect patterns of movement of these fish within the south Delta. Sentinel fish were acoustically tagged fish assumed to represent wild fish in the system. Thus, rather than using modeling results to predict broad-scale, often subtle hydrodynamic changes hypothesized to cause indirect effects on fish survival through the Delta, the sentinel fish approach set a threshold based on the observed movement of tagged fish within the Delta. Protection measures were implemented when this threshold was exceeded.

In summary, we sought to evaluate the relationship between OMR flows and the migration and survival of juvenile salmonids, while at the same time conducting an adaptive management experiment intended to help refine decision-making for the protection of San Joaquin River steelhead.

1.3 STUDY HISTORY AND TIMELINE

The Department initiated the Stipulation Study in February 2012 and completed field operations by that summer. The preliminary results from this field study were reported in a status report issued October 15, 2012 (Cavallo et al. 2012). The Independent Review Panel (IRP) released its review of the project in the form of its Report of the *2012 Delta Science Program Independent Review Panel (IRP) on the Long-term Operations Opinions (LOO) Annual Review* (hereafter referred to as the "2012 IRP LOO Annual Review") on December 1, 2012 (Kneib et al. 2012). Funding for additional data analysis and final report production was finalized on February 21, 2013. A

Data Analysis Plan for Phase II of the project was submitted to representatives of various federal, state, and local agencies on March 29, 2013 (Cramer Fish Sciences 2013). A meeting was held on April 19, 2013 to assess the Data Analysis Plan and our response to the reviewers' feedback. Below, we document these events, the challenges, and changes made to the document through the process that have resulted in the analysis that is presented in this report.

The analysis for the Stipulation Study was conducted in two phases.

- **Phase I.** A preliminary analysis of the data completed in October 2012 focusing on routing of steelhead tags at key Delta junctions, and an initial examination of the effect of OMR flows and local hydrodynamics on steelhead tag movement.

- **Phase II.** A thorough analysis of data completed by February 2014, including the development of a multistate statistical release-recapture model built in the User Specified Estimation Routine (USER) program (Lady et al. 2008) to estimate survival, route entrainment, transition probabilities, and detection probabilities. Multiple secondary hypotheses to examine how OMR flows affected steelhead tag behavior were also tested. These results are reported in the results section of this report (Chapter 4).

Additional details regarding the process of developing the 2012 experimental design and analysis are summarized in Table 1-1, and described below.

Table 1-1 Major events and dates conducted for this project.

Project initiated and data for report were collected	February – June 2012
Phase I Report	October 15, 2012
Phase I animation and results presented at 7th Biennial Bay-Delta Science Conference 2012 held in Sacramento, California	October 16-18, 2012
Delta Science Program Independent Review Panel Report	December 1, 2012
Work Team Meeting	December 6, 2012
Phase II Data Analysis Plan submitted to agencies	March 29, 2013
Work Team meeting	April 19, 2013
Final Data Analysis Plan	June 28, 2013
Results Work Team meeting	August 28, 2013
Draft Technical Report distributed for review	November 19, 2013
Final Department Technical Report was released	February 2014

PROJECT INITIATION AND DATA COLLECTION (FEBRUARY – JUNE, 2012)

The Department initiated the project in February of 2012. In the spring of 2012, the mark-recapture experiment was conducted to examine the survival and movement patterns of acoustically tagged juvenile steelhead emigrating through the south Delta. Three groups of juvenile steelhead were released near Buckley Cove in the lower San Joaquin River downstream of Stockton and upstream of Turner Cut (Figure 1-1). Juvenile steelhead for the study were provided by the Mokelumne River Hatchery. Releases for Group 1 began on April 15 and finished on April 16. Group 2 releases began on May 1 and finished on May 2. Group 3 releases began on May 15 and finished on May 16. The tagging and releases for Release Group 1 were complicated by severe thunderstorms. Release Groups 2 and 3 did not have any of these complications.

On average, 167 acoustically tagged steelhead were released for each of the three release groups. Data collection was completed by the end of June 2012.

PHASE I REPORT (OCTOBER 15, 2012)

The Phase I Report was completed on October 15, 2012. The following objectives were addressed in the report:

- **Objective 1:** Identify the fraction of acoustically tagged steelhead that were observed moving south at Middle and Old rivers near Railroad Cut and used as an exposure risk trigger to manage OMR flows.
- **Objective 2**: Evaluate how hydrodynamic factors influenced the route entrainment into the interior Delta from Turner Cut, Colombia Cut, and Middle River.
- **Objective 3:** Evaluate how hydrodynamic conditions and OMR flows influenced migration behavior and survival in the interior Delta.

Fine-Scale Hydrodynamic Data Difficulties

Sub-daily (15-minute) hydrodynamic influences (proportional flow movement at junctions, average flow, percent positive flow) on fine-scale fish movement were expected to be analyzed to examine how tidal influences affect juvenile steelhead migration into the interior Delta, and patterns of migration behavior and survival once fish enter the interior Delta. However, as statistical analyses were being completed, we consistently observed fish moving opposite the direction of flow movement at the Turner Cut junction (the only junction analyzed in this way). These unexpected movement patterns were observed for both steelhead and Chinook smolts, suggesting these findings likely were not a true observation of fish behavior, but rather a spurious artifact of fish timing not being in-sync with available sub-daily Delta Simulation Model II (DSM2) flow data used to inform flow conditions.

To examine if the fish and flow timing were out of sync, we compared DSM2 output near Turner Cut with observed flow data at the gauging station. For an example 24-hour period, we examined how the 15-minute flow data for the DSM2 channel 172 (Figure 1-2) immediately downstream (toward pumping facilities) of Turner Cut varied from actual observed flow data from the gauging station at Turner Cut (TRN) near Holt (via the California Data Exchange Center [CDEC]). This gauging station is operated by the USGS.

Figure 1-2 The location of DSM2 channel 172 and the gauging station at Turner Cut.

Although the daily flow magnitude was similar between datasets, the tidal cycle appeared to be off-sync by approximately 2 hours (Figure 1-3). We were unable to determine whether DSM2 Hydro or CDEC data were correct, and most locations of interest for this analysis do not host a CDEC-reported monitoring station. If the CDEC data represent the true flow conditions, then by analyzing DSM2 Hydro data at Turner Cut and other locations, we may be relating fish behavior with incorrect flow conditions. Preliminarily, we believed our findings of fish (both Chinook and steelhead smolts) moving against flow movement were likely a result of fish timing being paired with flow conditions opposite of what they may have actually experienced. Rapid changes in tidal flow conditions mean that small discrepancies in timing between predicted and actual flow patterns can lead to results directly the opposite of expectations.

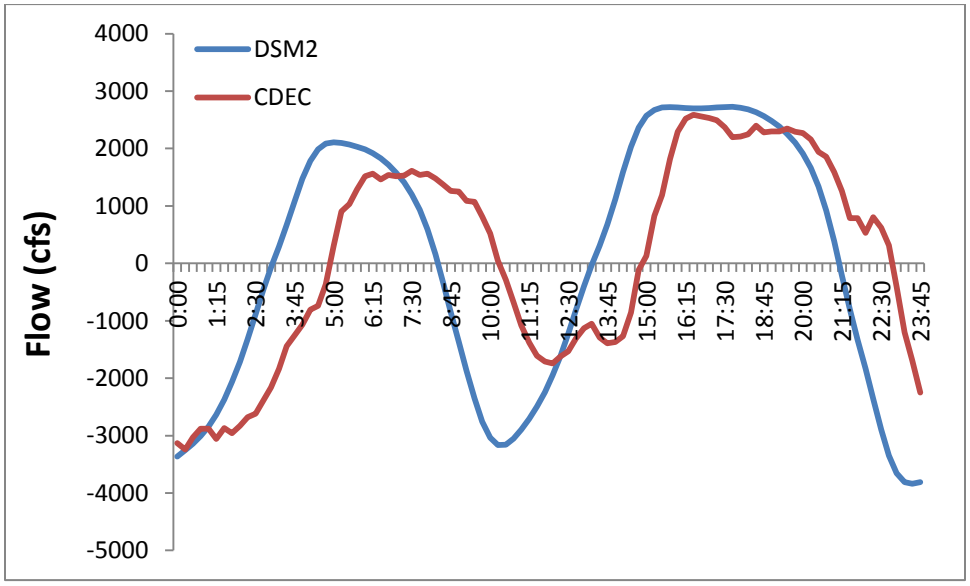

Figure 1-3 15-minute flow data over an example 24-hour period for DSM2 channel 172 and the gauging station at TRN, both indexing flow immediately downstream (toward pumping facilities) of the Turner Cut junction. Source: Cavallo et al. 2012.

This problem brought to our attention the extraordinary importance of having accurate times reported for steelhead detections. Minor discrepancies in clock settings for computers used to launch or download receiver data could lead to inaccurate time data. It is important to note that this analysis attempted to examine sub-daily fish behavior and flows in an unusually detailed way. As a consequence of these problems with how to use and reconcile DSM2 Hydro and CDEC data, findings in the Phase I Report were largely descriptive—examining broad-scale relationships between fish behavior and OMR flow conditions, or DSM2 data at a daily scale. Although this is only a single location, this further exemplified the difficulty of examining fine-scale flow and steelhead tag relationships using the existing hydrodynamic data available. Because of the strong tidal influence in the Delta, flow measurements and steelhead tag observations must be paired perfectly together to know exactly what the flow conditions a steelhead tag was experiencing when making a routing "decision." Therefore, all Phase II analyses used average 2-hour or daily periods to estimate the hydrodynamic conditions.

PHASE I ANIMATION AND RESULTS PRESENTED AT 7TH BIENNIAL BAY-DELTA SCIENCE CONFERENCE 2012 HELD IN SACRAMENTO, CALIFORNIA – OCTOBER 16–18, 2012

We presented an animation of the particle and steelhead data at the 7th Biennial Bay-Delta Science Conference 2012 held at the Sacramento Convention Center in Sacramento, California. The animation is located online and can be viewed the following website address: http://www.fishsciences.net/projects/media/Stip_Study_Animation.mp4.

We compared the relative movement patterns of simulated particles with steelhead tags to evaluate the efficacy of using simulated particles (DSM2 Particle Tracking Model [PTM]) to mimic steelhead tag behavior. We generated an animation of steelhead tags and simulated particles. The animation is based on raw data, and detection probabilities were not considered. Therefore, movement patterns of steelhead tags depict actual tag movement and the ability of each receiver array to detect each tag. However, it is important to note that detection probability was only found to vary across release groups for receiver 6. Therefore, differences in broad movement patterns between release groups should generally reflect actual differences in tag movement. Given the data observed, the following figures display screen shots from the animation, depicting days 3 and 7 after release for Release Group 1 (Figure 1-4 and Figure 1-5), Release Group 2 (Figure 1-6 and Figure 1-7), and Release Group 3 (Figure 1-8 and Figure 1-9).

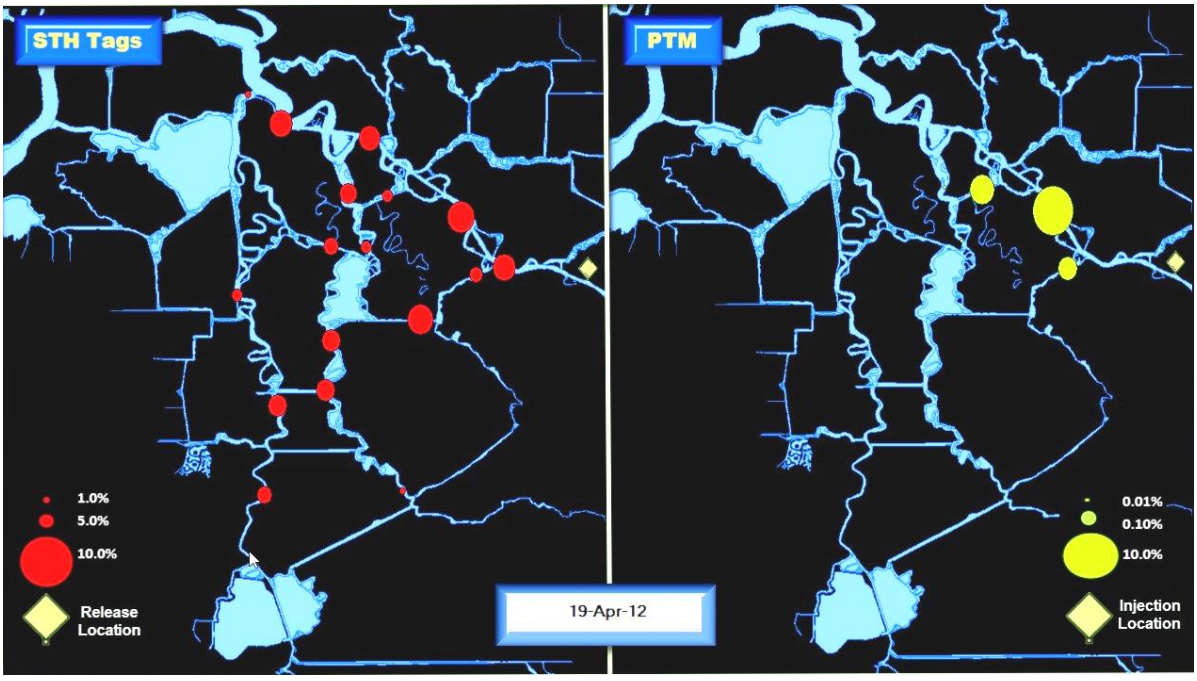

Figure 1-4 **The proportion of steelhead tags (STH tags) and simulated particles (PTM) located at each array for Release Group 1 on the third day after the fish releases were completed (April 19, 2012).**

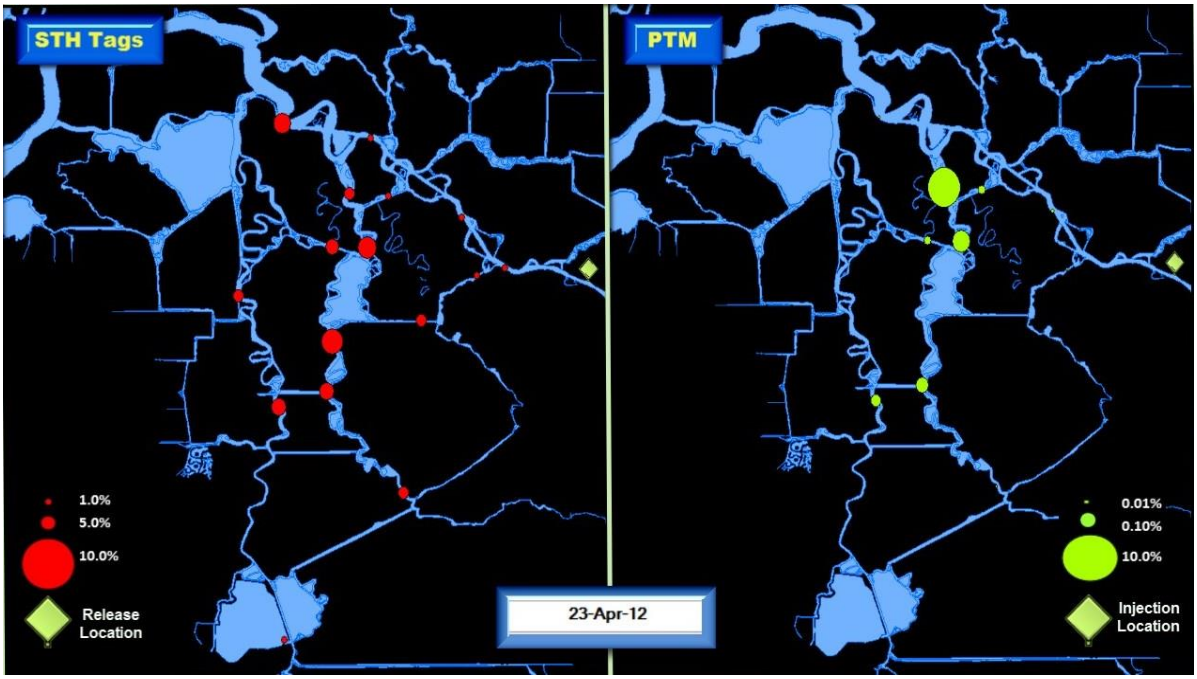

Figure 1-5 **The proportion of steelhead tags (STH tags) and simulated particles (PTM) located at each array for Release Group 1 on the seventh day after the fish releases were completed (April 23, 2012).**

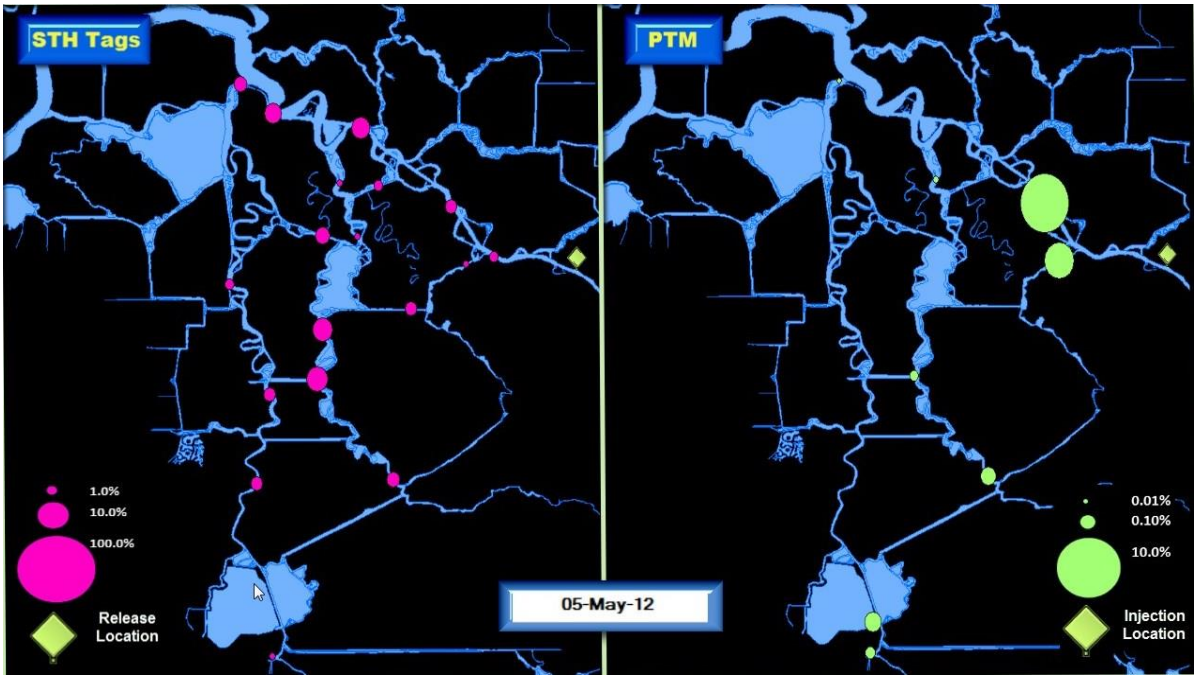

Figure 1-6 **The proportion of steelhead tags (STH tags) and simulated particles (PTM) located at each array for Release Group 2 on the third day after the fish releases were completed (May 5, 2012).**

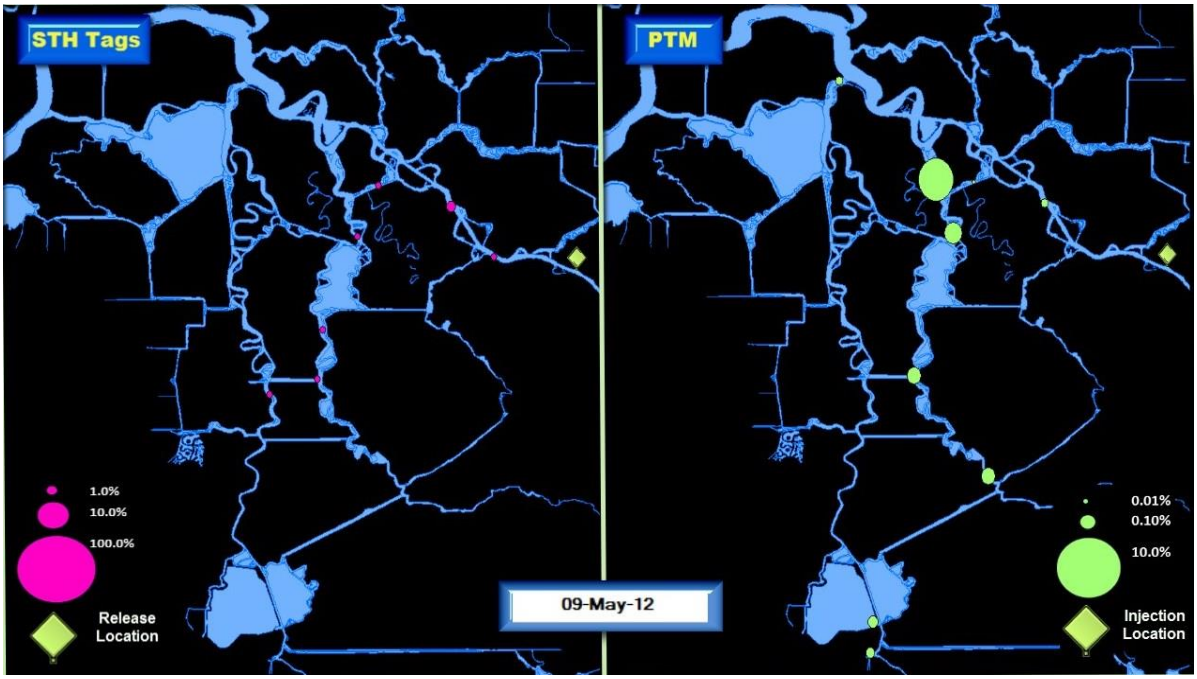

Figure 1-7 **The proportion of steelhead tags (STH tags) and simulated particles (PTM) located at each array for Release Group 2 on the seventh day after the fish releases were completed (May 9, 2012).**

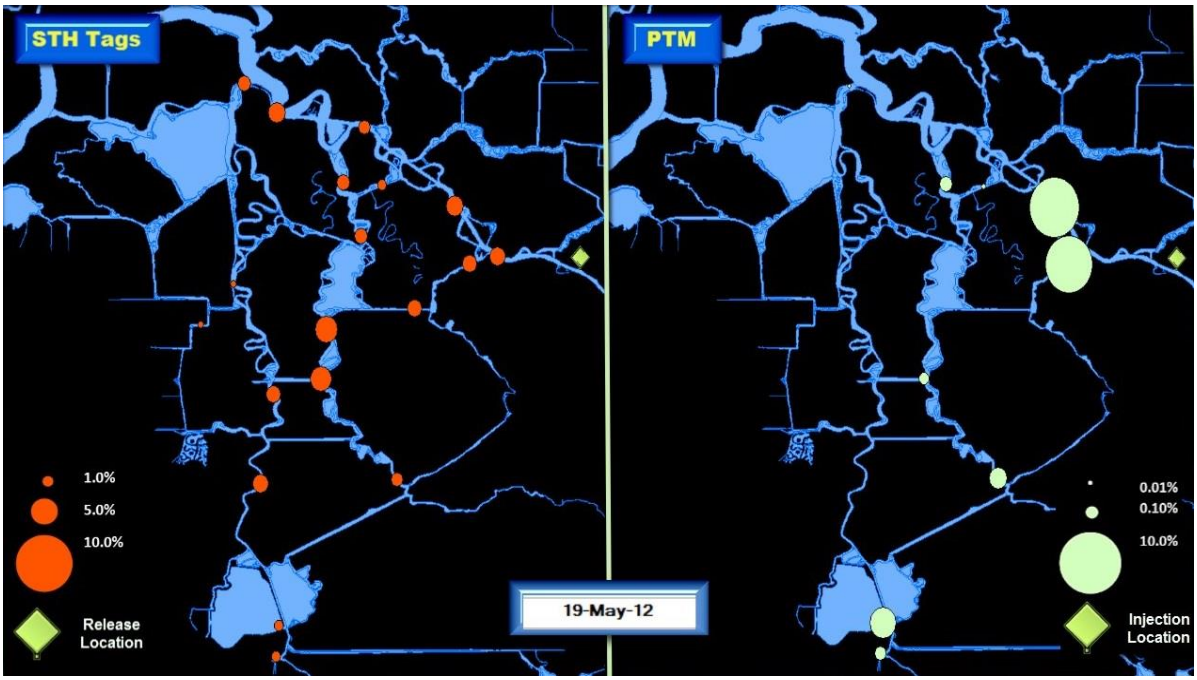

Figure 1-8 **The proportion of steelhead tags (STH tags) and simulated particles (PTM) located at each array for Release Group 3 on the third day after the fish releases were completed (May 19, 2012).**

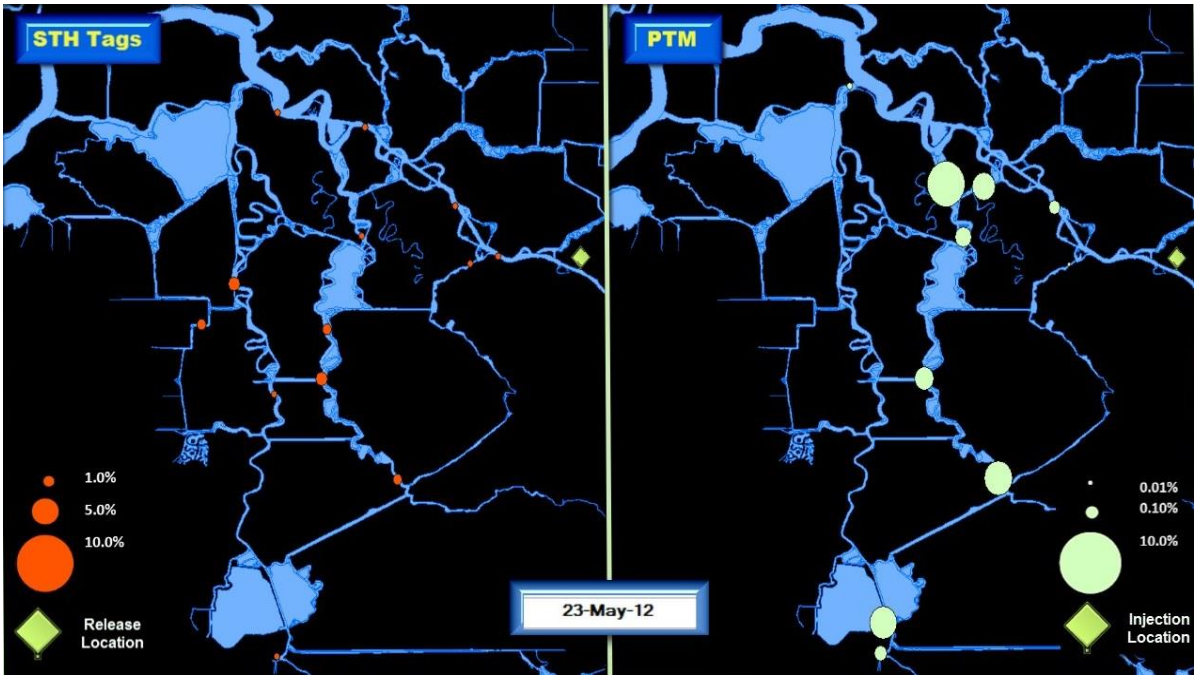

Figure 1-9 The proportion of steelhead tags (STH tags) and simulated particles (PTM) located at each array for Release Group 3 on the seventh day after the fish releases were completed (May 23, 2012).

DELTA SCIENCE PROGRAM INDEPENDENT REVIEW PANEL REPORT (DECEMBER 1, 2012)

An IRP was assembled by the Delta Science Program to inform NMFS and the USFWS as to the efficacy of the water operations and regulatory actions prescribed by their respective LOO RPAs as applied from October 1, 2011 through September, 30 2012 (Water Year 2012). The 2012 annual review focused in part on the implementation of NMFS's RPA for the Spring 2012 Delta Operations Joint Stipulation for water operations and fisheries that was required to be executed in water year 2012 in lieu of the NMFS RPA Action IV.2.1. The IRP released the 2012 IRP LOO Annual Review on December 1, 2012, which detailed their review of preliminary analysis of Stipulation Study acoustic data detailed in the Phase I Report. Their assessment of this report can be downloaded from:
http://deltacouncil.ca.gov/sites/default/files/documents/files/Report_2012_DSPIRP_LOOAR_120112_final.pdf.

The IRP presented three major criticisms of the Phase I analysis, summarized as follows:

- Tidal Influences: The effect of tidal hydrodynamics on the movement and survival of smolts though the Delta was not addressed in the Phase I analysis. The current paradigm for characterizing movement of smolts through the Delta reaches relies on mean flow to characterize the movement and routing of fish. The steelhead tagging studies in 2012 and earlier years clearly indicated that this characterization is inadequate. Therefore, the IRP suggested that the travel, routing, and survival of fish through the system needed to account for migrant behavior and the behaviors of the predators in response to the strong tidal influences in the Delta (Kneib et al. 2012).

- Inadequate Statistical Analysis: The IRP stated that many of the Phase I study's initial conclusions were not adequately supported by the analyses because they failed to make use of statistical testing or confidence intervals, and they suggested that the analyses be redone with greater statistical rigor, where possible.

- Re-coding Release Groups: The IRP suggested re-coding the release groups to test for evidence of an OMR flow effect on fish behavior within the range of flow levels examined using the available data. They suggested recoding Release Groups 1 and 2 as "intermediate" OMR flow, and Group 3 as "high" OMR flow. Groups 1 and 2 can be pooled as "intermediate" flow treatment level and compared to Group 3 as "high" flow treatment level. In this report, we refer to data from Groups 1 and 2 as less negative OMR flows and Group 3 as more negative OMR flows.

The IRP suggestions provided us with a direction moving forward with the Phase II analysis. As suggested by the IRP, we incorporated a hypothesis that examined the movement of steelhead tags in relation to tidal hydrodynamics in a small reach of the interior Delta. However, the large-scale mechanistic analysis suggested by the IRP was not possible with the data available, and would require fine-scale hydrodynamic data collected simultaneously with fish movement data, which are unavailable with the current dataset. Second, as many analyses as possible in Phase II were tested statistically. Likewise, a statistically rigorous multistate release-recapture model was applied to examine fish routing and survival. Lastly, release groups were re-coded as suggested by the IRP, with Groups 1 and 2 as less negative OMR flow, and Group 3 as more negative OMR flows, to better examine the effect of OMR flows on steelhead tag behavior.

WORK TEAM MEETING (DECEMBER 6, 2012)

A technical Work Team comprised of participants from the Department, Reclamation, USGS, NMFS, USFWS, and the consultant team working on the project was convened to help address issues and discuss data analysis topics as they arose. The Work Team met on December 6, 2012, to discuss the initial draft of the data analysis plan for Phase II analyses. The discussion primarily focused on three major topics:

- Hydrodynamics: As described earlier, the difficulties with trying to examine fine-scale (sub-daily) movements of steelhead tags in relation to flow were discussed. The general consensus was that only daily hydrodynamic data would be paired with tag data.

- Inclusion of Six-Year Study Tags: A discussion of whether or not to include Six-Year Study tags in the Phase II analyses was conducted. The general agreement was that the analysis of Stipulation Study tags was the primary goal of the Phase II analysis, and therefore the Six-Year Study tags would be left out of Phase II analyses, except if additional time and resources were available to examine them at the end.

- Particle Tracking Comparisons: In the Phase I analysis, comparisons between the movement of steelhead tags and simulated particles were conducted to examine the efficacy of using simulated particles to mimic fish behavior. The Work Team discussed the need for additional analyses in Phase II and agreed that one additional analysis examining the end location of tags and particles would be beneficial.

PHASE II DATA ANALYSIS PLAN SUBMITTED TO AGENCIES (MARCH 29, 2013)

Funding for Phase II of the project was finalized on February 21, 2013. Many of the action items from the December 6 meeting were completed and incorporated into a draft of the Data Analysis Plan completed on February 11, 2013. A Data Analysis Plan for Phase II was submitted to representatives of various federal, state, and local agencies on March 29, 2013. We received feedback and responded to the reviews by email on April 17, 2013.

DATA ANALYSIS PLAN PRESENTED TO THE WORK TEAM MEETING (APRIL 19, 2013)

A Work Team meeting was held on April 19, 2013, to discuss the Phase II Data Analysis Plan and the response to the reviews. Suggested revisions and comments were sent prior to the meeting, discussed during the meeting, and followed-up after the meeting.

FINAL DATA ANALYSIS PLAN (JUNE 28, 2013)

Following receipt of comments from the Work Team on the draft Data Analysis Plan for Phase II, a final plan was created and submitted to the Department for final review and approval. This document laid the groundwork for the analysis contained in this report.

PRELIMINARY RESULTS PRESENTED TO THE WORK TEAM MEETING (AUGUST 28, 2013)

The preliminary results of the Phase II analyses were presented to the Work Team during a meeting on August 28, 2013. Some of the major discussion points during the meeting were the following:

- New Qualitative Analyses: New qualitative analyses were presented for the first time, including a web-based data viewer tool of Stipulation Study steelhead tag data, and new descriptive figures of the final fate of steelhead tags.
- Release-specific Model Did Not Converge: The mark-recapture models that only used data from an individual release group did not converge for all release groups; therefore, we ran the model on all release group steelhead tag data as a single model. When the model was run using all the data, it converged. Therefore, the effect of release group on steelhead tag behavior and survival was examined exclusively in the Objective 2 hypotheses.
- Array 6 versus 7: The detection probabilities experienced across release groups at these dual receiver arrays were examined. The results showed that detection probabilities at array 6 varied greatly across release groups. Because receiver 7 showed consistently high detection probabilities across all release groups, the mark-recapture model was run with receiver 7 instead of receiver 6. Likewise, array 7 was used in all Objective 2 hypotheses where Turner Cut was examined. For more detail, see Section 4.2.1.
- Study History Table: The Work Team asked that a table be created detailing the changes in objectives and hypotheses since the first incarnation of the Data Analysis Plan (see Appendix A for the concordance table).
- Reorganization of Objectives and Hypotheses: A re-organization of study objectives was agreed upon for the final report that grouped all hypotheses into different spatial categories, including system, route, and junction.

This entire study process described above along with the collaboration with the interested parties led to the development of the study objectives and this final report. A detailed history of the Phase II analyses, including the evolution of study objectives and hypotheses, is presented in the concordance table in Appendix A.

DRAFT OF FINAL REPORT DISTRIBUTED TO THE WORK TEAM (NOVEMBER 18, 2013)

The preliminary results of the Phase II analyses, a draft of this report, were distributed to the Work Team by the Department.

FINAL REPORT PUBLISHED (FEBRUARY 7, 2014)

The final Technical Report was released following the review by the Work Team.

1.4 STUDY ANALYSES

The analysis was spatially divided into three sections: system-wide, route, and junction-level. The first set of analyses focused on large-scale movement patterns and whether a particle simulation model could predict the system-wide movement patterns of steelhead tags. In the second section, we examined how steelhead tags moved

through the system using different defined routes. We examined if their transition, detection, survival, route entrainment, and travel times were affected by different OMR flow conditions. In the last section, we examined how fish moved through key Delta junctions (Turner Cut, Columbia Cut, Middle River, and Railroad Cut). The following describes the areas of discussion and hypothesis-testing presented in the results section (Chapter 4). Areas of discussion are those where the data are discussed qualitatively, compared to the hypothesis where statistical tests can be applied.

4.1 System: Examine large-scale movement patterns of steelhead tags.

- Discussion 4.1.1: Relative steelhead tag detection at arrays
- Discussion 4.1.2: Last detection at arrays
- Discussion 4.1.3: Residence time at arrays
- Discussion 4.1.4: Final fate at arrays
- Discussion 4.1.5: Web-based detection history
- **Hypothesis 4.1.6**: The distance traveled by steelhead tags was not significantly different than the distance traveled by the passive particles.
- **Hypothesis 4.1.7:** Steelhead tags did not move using selective tidal-stream transport (STST).
- **Hypothesis 4.1.8:** The movement of steelhead tags in the San Joaquin River and interior Delta was not related to day/night.

4.2 Route: Examine how steelhead tags move through the system using different defined routes.

- **Hypothesis 4.2.1**: Route-specific transition probabilities of steelhead tags were not significantly related to the route taken and/or release group.
- **Hypothesis 4.2.2:** The estimated route-specific survival for the Turner Cut route was not significantly different from the Mainstem route.
- **Hypothesis 4.2.3**: The travel times of steelhead tags were not significantly different between routes or release groups.

4.3 Junction: Examine how steelhead tags move through junctions.

- **Hypothesis 4.3.1:** The probability of steelhead tags entering the interior Delta at Turner Cut, Columbia Cut, and Middle River was not related to OMR flows.
- **Hypothesis 4.3.2:** Steelhead tag arrival at each facility was not related to the proportion of total export flow entering SWP.
- **Hypothesis 4.3.3:** The movement patterns of steelhead tags after passing through Railroad Cut were not affected by OMR flows.

2 EXPERIMENTAL DESIGN AND FIELD METHODS

CHAPTER SUMMARY:

In the spring of 2012, we initiated a mark-recapture experiment to examine the survival and movement patterns of acoustically tagged juvenile steelhead emigrating through the south Delta. We released three groups of juvenile steelhead near Buckley Cove in the lower San Joaquin River downstream of Stockton, and upstream of Turner Cut (Figure 1-1). We began releases for Group 1 on April 15 and finished on April 16. We began Group 2 releases on May 1 and finished on May 2. We began Group 3 releases on May 15 and finished on May 16. All releases began at approximately 3:00 pm and ended within 24 hours. We released a minimum of 166 acoustically tagged steelhead for each of the three release groups. We obtained the juvenile steelhead from the Mokelumne River Fish Hatchery, and those steelhead were used in the 2012 Stipulation Study as surrogates for wild fish. We tagged the hatchery-produced steelhead with acoustic coded transmitters (VEMCO, model V6-4X) at the hatchery following the 2012 Stipulation Study Tagging Standard Operating Procedure (SOP). This SOP was identical to the 2012 Six-Year Study SOP. Tag burden was very low and battery life of the tags far exceeded the study period.

The study plan required the measurement of the fraction of acoustically tagged steelhead that reach and are observed to be moving southward near Railroad Cut toward the export facilities. Regulatory agencies used this fraction as an exposure risk trigger to manage OMR flows. During the study, near-real-time detections of Stipulation Study fish resulted in changes to OMR flows during each experimental period. Under the Stipulation Study Plan, beginning in early to mid-April (coincident with experimental steelhead releases), OMR flow targets shifted to a pilot "managed-risk experimental" approach. The experimental design was intended to gather information about responses of tagged fish to different hydrodynamic conditions. Different OMR flow "treatment levels" were implemented for each release of acoustically tagged steelhead. This approach included an "exposure trigger" that, if reached or exceeded, shifted operations from the experimental OMR flow level to the least negative OMR flow level within the adaptive range (-1,250 cfs). This action was intended to protect steelhead by shifting hydrodynamic conditions in a direction thought to be less disruptive to outmigration routing or timing. The exposure trigger was measured as the cumulative fraction of the supplemental release group that passed a pair of receiver arrays on Old River and Middle River near Railroad Cut. The trigger was calculated as 5% of the release group reaching the acoustic receiver arrays at Railroad Cut, under the assumption that 5% of fish arriving at Railroad Cut would be expected to result in a 2% loss of the release group at the fish collection facilities (NMFS 2012).

The original experimental design called for each 2-week experimental period to represent one of three OMR flow targets (-1,250, -3,500, and -5,000 cfs). Real-time evaluation of tag detections at Railroad Cut for each group resulted in exceedance of the trigger for each release group, which in turn altered experimental OMR flow levels and resulted in variable OMR flows during the study. Average observed OMR flows during the first 7 days following release were -2,446, -2,933, and -5,038 cfs for Release Groups 1, 2, and 3, respectively (Figure 2-1).

One of the major goals of this report was to determine if behavioral differences exist between any of these three release groups in relation to OMR flow. Also, based on a recommendation in the 2012 IRP LOO Annual Review (Kneib et al. 2012), the analysis pooled the data from Release Groups 1 and 2, which were considered a less negative OMR flow group and were compared to the data from the more negative flow treatment level data from the third release group.

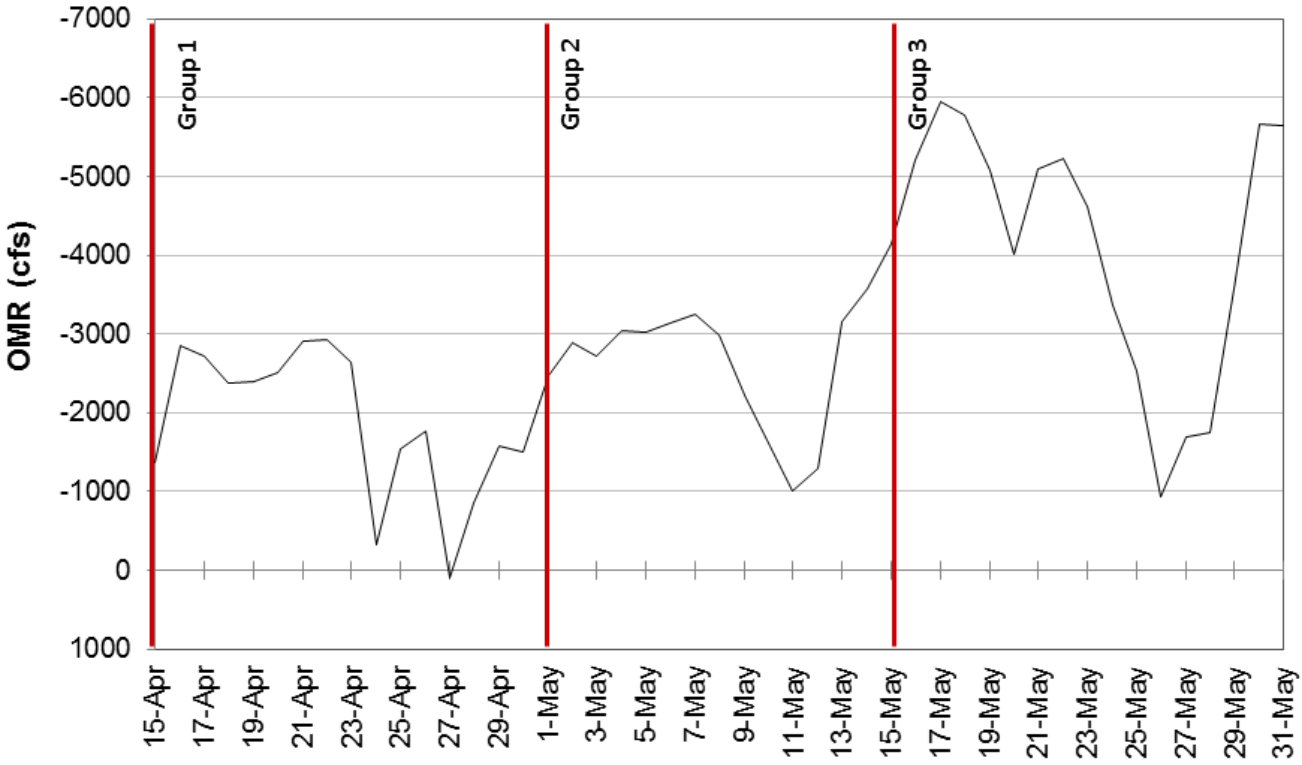

Figure 2-1 Daily OMR flow conditions and release dates for acoustically tagged steelhead smolts from the 2012 Stipulation Study.

2.1 HYDRODYNAMIC SETTING

In the spring of 2012, a mark-recapture experiment was performed to examine the survival and movement patterns of acoustically tagged juvenile steelhead emigrating through the south Delta. We released three groups of juvenile steelhead near Buckley Cove in the lower San Joaquin River downstream of Stockton, and upstream of Turner Cut (Figure 1-1). Releases for Group 1 began on April 15 and finished on April 16. Group 2 releases began on May 1 and finished on May 2. Group 3 releases began on May 15 and finished on May 16. The original experimental design called for each 2-week experimental period to represent one of three OMR flow targets (-1,250, -3,500, and -5,000 cfs). Real-time evaluation of steelhead tag detections at Railroad Cut for each group resulted in exceedance of the trigger for each release group, which in turn altered experimental OMR flow levels and resulted in variable OMR flows during the study. Average observed OMR flows during the first 7 days following release were -2,446, -2,933, and -5,038 cfs for Release Groups 1, 2, and 3, respectively (Figure 2-1). The triggered less negative OMR flow levels (-1,250 cfs) were observed to be achieved on April 24, May 11, and May 26 for Release Groups 1 through 3, respectively (Figure 2-1). Figure 2-2 shows the daily export rates entering Clifton Court Forebay and CVP, these two values combined, and flows of the San Joaquin River at Vernalis during the three release periods of the study.

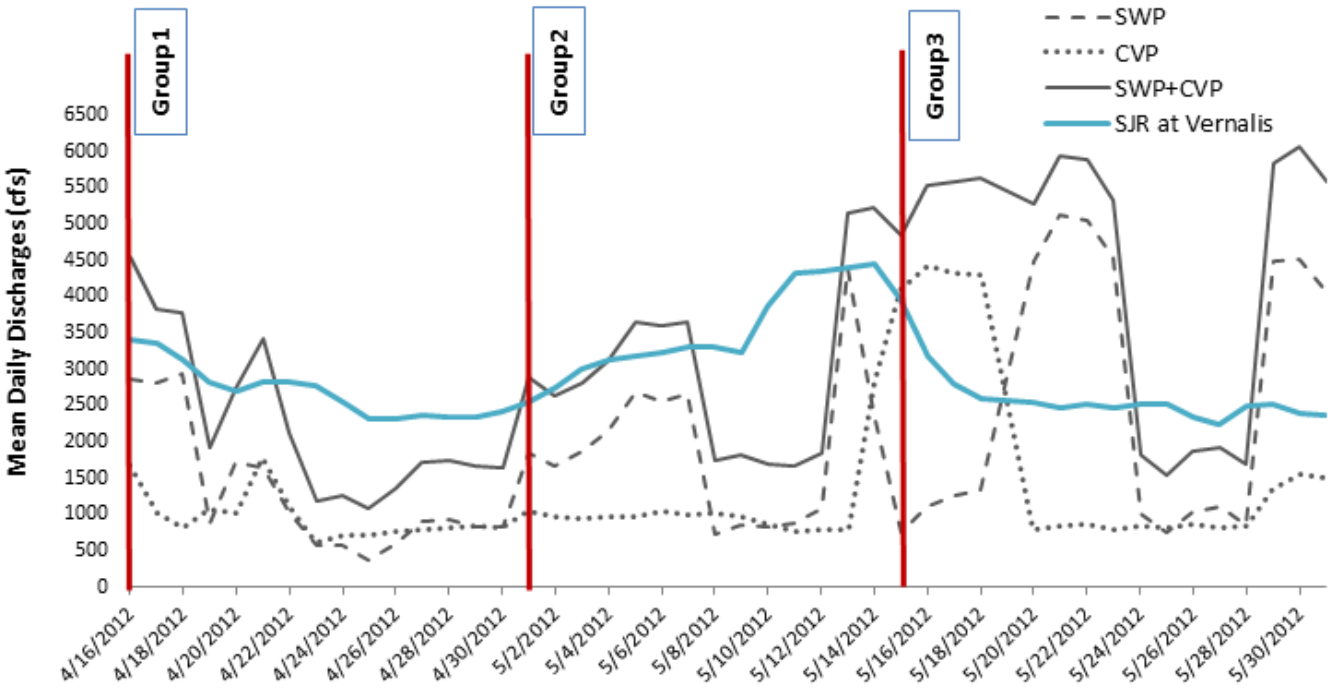

Figure 2-2 Mean daily export flows at the SWP and CVP, combined export flows, and flow discharge of San Joaquin River (SJR) at Vernalis in relation to steelhead release groups.

2.2 ACOUSTIC ARRAYS, RECEIVER DEPLOYMENT, AND REPORTING

2.2.1 ACOUSTIC RECEIVER ARRAYS

VEMCO VR2W-180 kilohertz (kHz) receivers were used to continuously monitor for the presence of acoustically tagged juvenile steelhead. A total of 33 receivers were deployed at 15 different sites within the south and central regions of the Delta (red squares in Figure 2-3). We placed at least one receiver on each side of the riverbank and two to four receivers at each site to attempt to provide full coverage of the channel cross-section. The VR2W-180 kHz receivers are omni-directional passive acoustic listening stations that record and store the presence of multiple acoustic transmitters. Each fixed-position hydrophone provided detailed date and time information regarding the presence of tagged steelhead at each specific site. We complemented these acoustic receiver arrays with nine acoustic receiver arrays from the Six-Year Study (blue squares in Figure 2-3) for a total of 24 arrays used for analysis (Table 2-1).

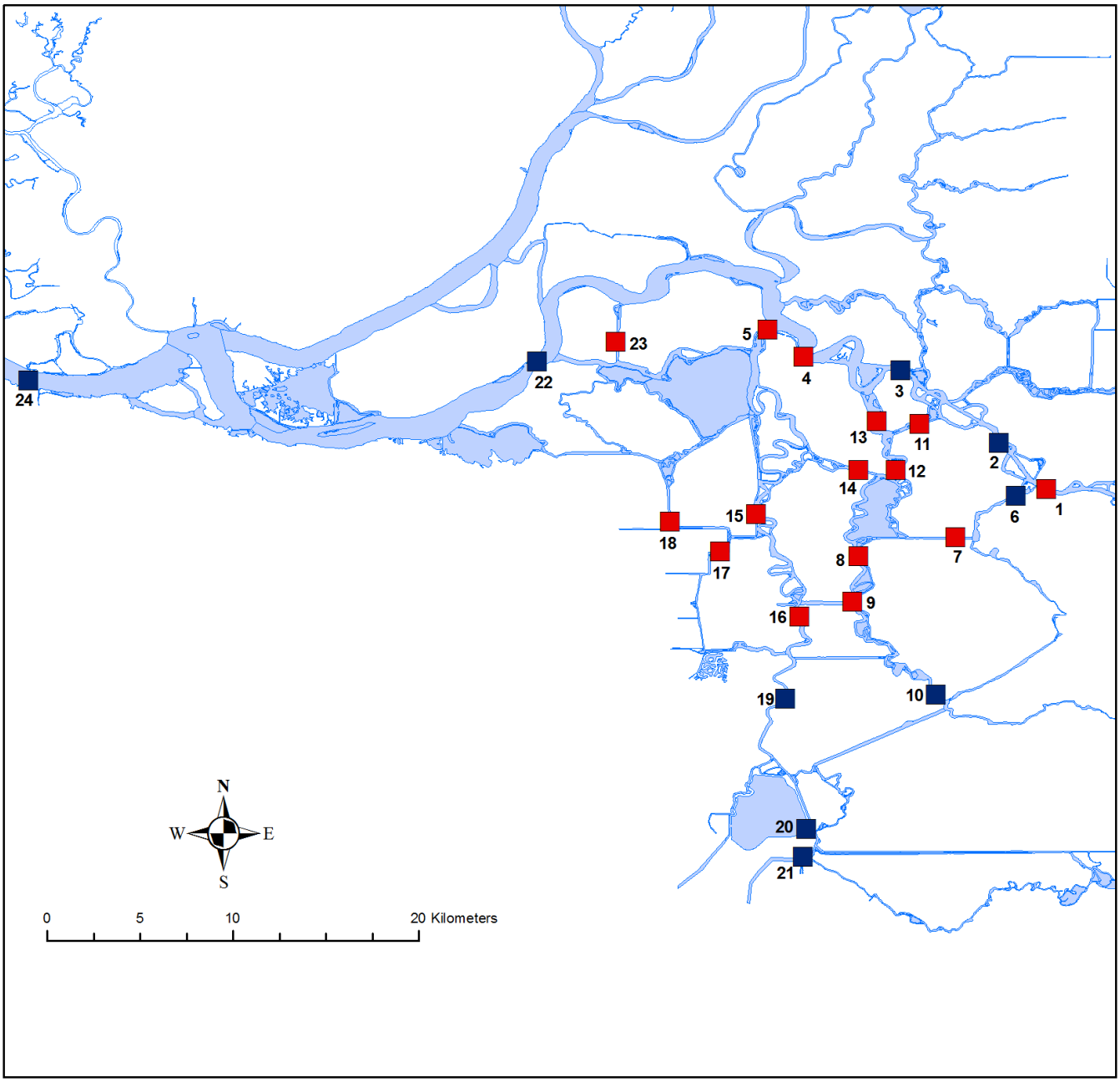

Figure 2-3 **The 24 acoustic receiver array sites in the south Sacramento-San Joaquin Delta.** The red squares are sites where arrays were deployed for the Stipulation Study. The blue squares are sites where arrays were deployed for the 2012 Six-Year Study.

Table 2-1 The array number, its latitude (decimal degrees), longitude (decimal degrees), what study the arrays were deployed for (Stipulation Study denoted as "Stip" or for the Six-Year Study denoted as "6yr"), and a description of the where the array was located.

Array	Study	Latitude	Longitude	Site Description
1	Stip	37.9949	-121.4404	An array along the San Joaquin River upstream of Turner Cut
2	6yr	38.0175	-121.4634	An array along the San Joaquin River downstream of Turner Cut
3	6yr	38.0524	-121.5111	An array along the San Joaquin River at the north point of Medford Island
4	Stip	38.0589	-121.5580	An array along the San Joaquin River at the southwest tip of Venice Island
5	Stip	38.0721	-121.5754	An array along the San Joaquin River at the southeastern tip of Webb Tract and northwest tip of Mandeville Island
6	6yr	37.9917	-121.4554	An array in Turner Cut
7	Stip	37.9719	-121.4846	An array in Empire Cut, downstream of Turner Cut
8	Stip	37.9626	-121.5316	An array in the northwest region of Jones Tract and just south of Mildred Island
9	Stip	37.9407	-121.5344	An array at the east end of Railroad Cut
10	6yr	37.8958	-121.4939	An array in Middle River just north of its intersection with Trapper Slough and Highway 4
11	Stip	38.0267	-121.5020	An array in Columbia Cut, southeast of Medford Island
12	Stip	38.0041	-121.5132	An array at the southeast tip of Mandeville Island
13	Stip	38.0279	-121.5227	An array in Middle River at the southwest tip of Medford Island
14	Stip	38.0043	-121.5315	An array at the northeast tip of Bacon Island
15	Stip	37.9828	-121.5810	An array at the southeast part of Holland Tract
16	Stip	37.9335	-121.5598	An array at the west end of Railroad Cut and northwest of Woodward Island
17	Stip	37.9647	-121.5984	An array northwest of Palm Tract
18	Stip	37.9794	-121.6225	An array southeast of Hotchkiss Tract and southwest of Holland Tract
19	6yr	37.8938	-121.5667	An array in Old River just west of Victoria Island and north of Highway 4
20	6yr	37.8306	-121.5566	An array with receivers located upstream and downstream of the radial gates of Clifton Court Forebay
21	6yr	37.8171	-121.5583	An array with receivers upstream and downstream of the trash racks as well as an array in the holding tank
22	6yr	38.0567	-121.6869	An array along the San Joaquin River at Jersey Point
23	Stip	38.0661	-121.6487	An array located east of Bradford Island and west of Webb Tract
24	6yr	38.0476	-121.9330	An array located near Chipps Island

2.2.2 RECEIVER SET UP AND DEPLOYMENT

When deploying the Stipulation Study receivers, we bolted each receiver using metal U-bolts to 4.5–7.6 meter (m) of 0.6-centimeter (cm) diameter stainless steel cable. We attached one end of the cable to a 13.6- to 27.2-kg anchor weight. We then positioned the receiver 1.8 m above the channel bottom using a buoy that was cable-tied to the stainless steel cable. This allowed the receiver to stay in an upright position within the water column at a fixed depth. We attached the other end of the cable to a permanent fixture (i.e., tree, buoy, pier piling, etc.) on the riverbank at each site (Figure 2-4). Because one cable end was permanently attached to the riverbank, retrieval of each receiver for inspection and data download was straightforward. Coordinates for each receiver were recorded using a Global Positioning System (GPS) device to allow for easy relocation.

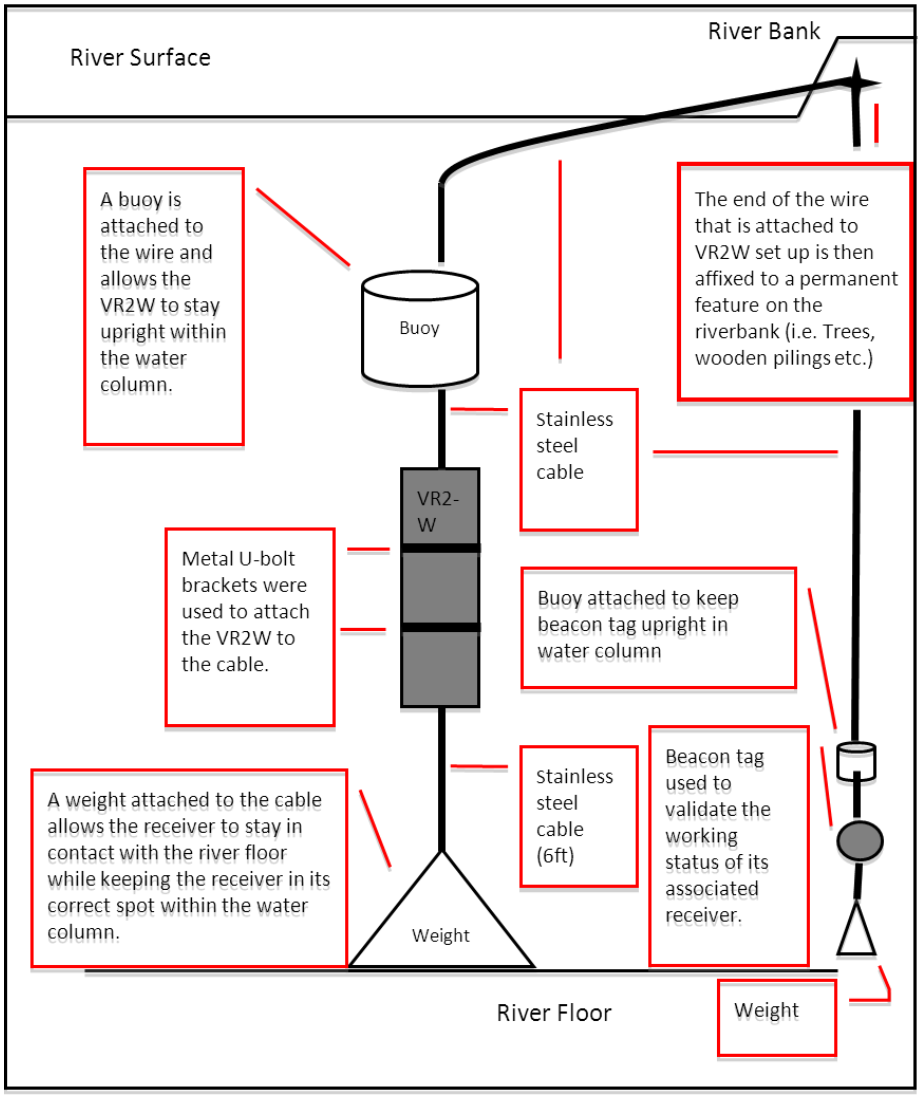

Figure 2-4 Schematic of typical receiver deployment.

We deployed a beacon tag or "sync" tag adjacent to each receiver to monitor and document the correct operation. The beacon tag was attached to a separate stainless steel cable connected to the receiver's cable at each site (Figure 2-4). We attached the beacon tag to the anchor system with a buoy to keep the beacon tag about 0.6 m from the river bottom. Each beacon tag was the same model of transmitter that was implanted into the juvenile steelhead. VEMCO programmed these tags to transmit the same signal as the implanted tags but over a longer time interval. Each receiver recorded the exact beacon tag identification (ID) number, date, and time it was recorded. During data analysis, we used beacon tag detections to validate that each individual receiver was functioning properly. Proper function of the receiver was documented when there were 102 detections and corresponding data records for the beacon tag within a 24-hour period.

2.2.3 Receiver Data Download Procedure

We generated a download schedule to create a manageable, daily workload and to prioritize sites by importance and proximity to the south Delta SWP/CVP export facilities. Sites were either downloaded daily or weekly. The sites most important for management discussions were the Railroad Cut sites near OMR (array sites 9 and 16 as seen in Figure 2-5). Data from these sites were downloaded, analyzed, summarized, and distributed daily. This

provided the near-real-time monitoring data necessary for the 2012 experimental design. Six-Year Study arrays were checked less frequently. The weekly downloading schedule was as follows (Figure 2-5):

- Tuesdays: arrays 4, 5, 17, 18, and 23.
- Wednesdays: arrays 1, 8, and 14.
- Thursdays: arrays 7, 11, 12, 13, and 15.

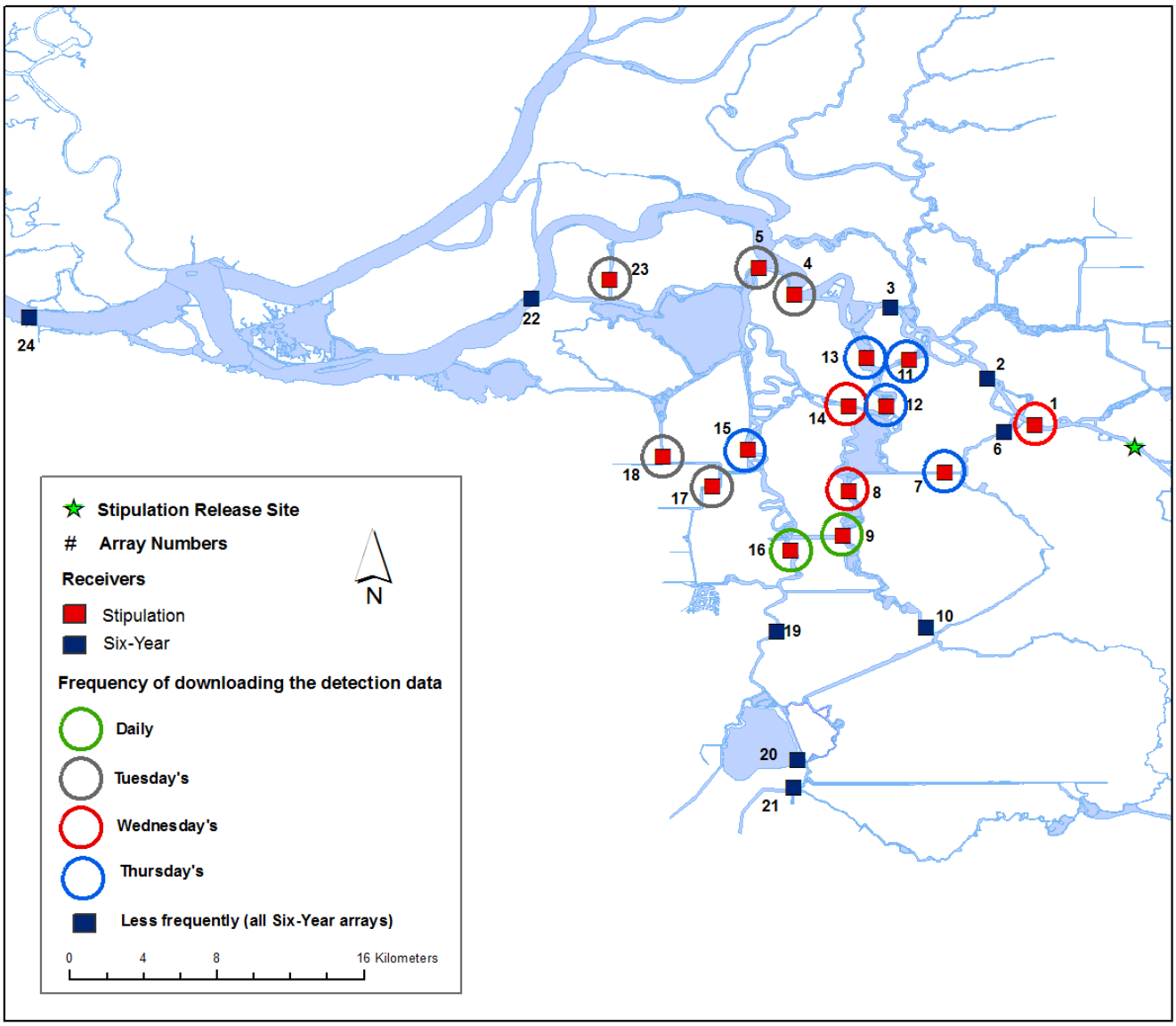

Figure 2-5 The 24 arrays color-coded by the frequency that the data were downloaded.

To retrieve the transmitter detection data from each receiver, a team of two staff used a boat to access each receiver. Using GPS coordinates, we retrieved the desired VR2W receivers from each site for that day. We inserted a Bluetooth key in the VR2W to initiate the download and a laptop aboard the boat equipped with VEMCO User Environment (VUE) software created a wireless interface with the receiver. Once we synchronized the receiver and software, we wirelessly downloaded the data from the Bluetooth enabled receiver. After each download, we erased the receiver memory of the prior days' data and immediately reset to start new detection recording. After the Bluetooth-interface with the VUE software was connected to a recorder, proper internal

equipment checks were also done to ensure the receiver was actively recording and ready to be placed back into the water column. This procedure was followed for each receiver at each site according to the download schedule and helped to avoid equipment malfunctions that could occur and negatively affect the receiver performance.

2.3 TAGGING METHODS, EVALUATION, RELEASE, TAG LIFE, AND BURDEN

2.3.1 TAGGING METHODS

We obtained juvenile steelhead from the Mokelumne River Fish Hatchery. We tagged the hatchery-produced steelhead with acoustic coded transmitters (VEMCO, model V6-4X) at the hatchery following the 2012 Stipulation Study Tagging SOP. This SOP was identical to the 2012 Six-Year Study SOP. The tags used in the Stipulation Study were compatible with the tags and receivers used with the 2012 Six-Year Study. Each V6-4X acoustic coded transmitters is 6 millimeters (mm) in diameter and 16.5 mm long (Figure 2-6).

Surgical implantation of the acoustic tags took place during three tagging events according to the detailed procedure in the tagging SOP, which is summarized here. To reduce the stress associated with chasing fish with a net, we netted juvenile steelhead from the raceway and placed them into perforated garbage cans within the raceway. We individually netted steelhead from the garbage cans and placed them into 18.9 liter (L) buckets containing 70 milligram (mg)/L of tricane methanesolfonate (MS-222). We left the juvenile steelhead in the bucket for 1–5 minutes until anesthetized. We removed the anesthetized fish from the bucket and recorded their length (mm) and weight (grams). Literature suggests that fish should not be tagged with transmitters that weigh more than 2% of the fish's body weight (e.g., Kneib et al. 2012). Because transmitters weighed 1 gram, we did not tag steelhead weighing less than 50 grams to maintain a maximum 2% tag to body weight ratio as per the literature recommendations. This was done even though the SOP would have allowed a 5% tag to body weight ratio (equaling a 20 gram fish).

We then checked each steelhead for any abnormalities. Abnormal fish were those that suffered from extremely eroded fins, abnormal body shape, or other structural deformities that could impair normal behavior. We placed abnormal fish in a reject bucket and did not tag them.

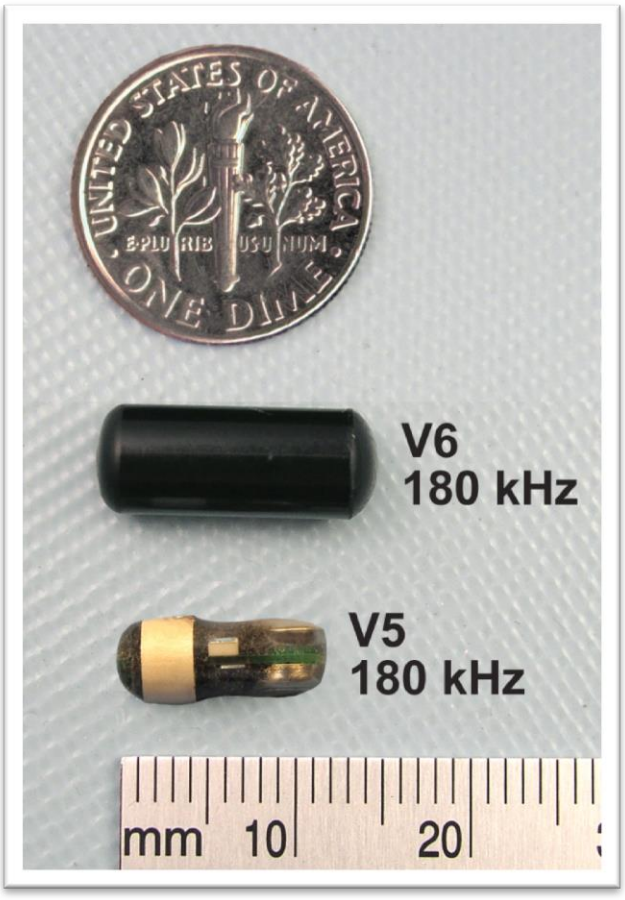

Source: VEMCO

Figure 2-6 Examples of VEMCO acoustic tags (e.g., V5), including the V6-4X tag used in the Stipulation Study.

After we checked for abnormalities, we placed the still-anesthetized steelhead into a holding cradle treated with a 25% solution of Stress Coat®. Handling fish causes damage to the fish's slime coat, and Stress Coat® replaces the fish's natural slime coat with a synthetic one, thereby reducing stress. We irrigated the fish's gills with water containing 20 mg/L of MS-222 through a soft rubber tube to maintain anesthesia during surgery.

We then assessed the scale condition of the steelhead on the most compromised side of the fish. We noted scale condition as Normal, Partial, or Descaled. We defined normal scale condition as the loss of less than 5% of scales on one side of the steelhead. We defined partial descaling as the loss of 6–19% of scales on one side of the steelhead. We classified steelhead as descaled if they had lost 20% or more of the scales on one side of the fish. Descaled fish likely suffer from compromised osmoregulatory ability. We placed descaled fish in a reject bucket and did not tag them.

Using a micro-scalpel equipped with a 5 mm blade, we made a 3–5 mm-long incision to one side of the mid-ventral line immediately anterior to the pelvic girdle. We inserted the acoustic tag into the body cavity through this incision. We then closed the incision with two or three simple interrupted sutures using Vicryl Plus 4-0 suture material to form the sutures (Figure 2-7). During the final stages of surgery, we switched the gill irrigation water supply from the MS-222 maintenance solution to supersaturated oxygen rich fresh water to begin the recovery process. Once the surgical procedure was completed, we moved the fish to a recovery bucket that provided 130% to 150% dissolved oxygen for a minimum of 10 minutes.

While fish were recovering, we used a VEMCO mobile tracking receiver (VR100) to verify that each transmitter was functioning properly. We recorded tag validation data for each fish. After the recovery period and tag validation were complete, we transferred the tagged steelhead to 68-L totes (Figure 2-8). We placed three steelhead in each labeled tote, and we subsequently loaded the tote into a fish transport tank that was attached to a flatbed truck. During loading and prior to transport, we maintained water temperature and oxygen levels inside the transport tank by pumping water into the tank from the hatchery raceway.

Figure 2-7 Tagging and suturing of a typical steelhead.

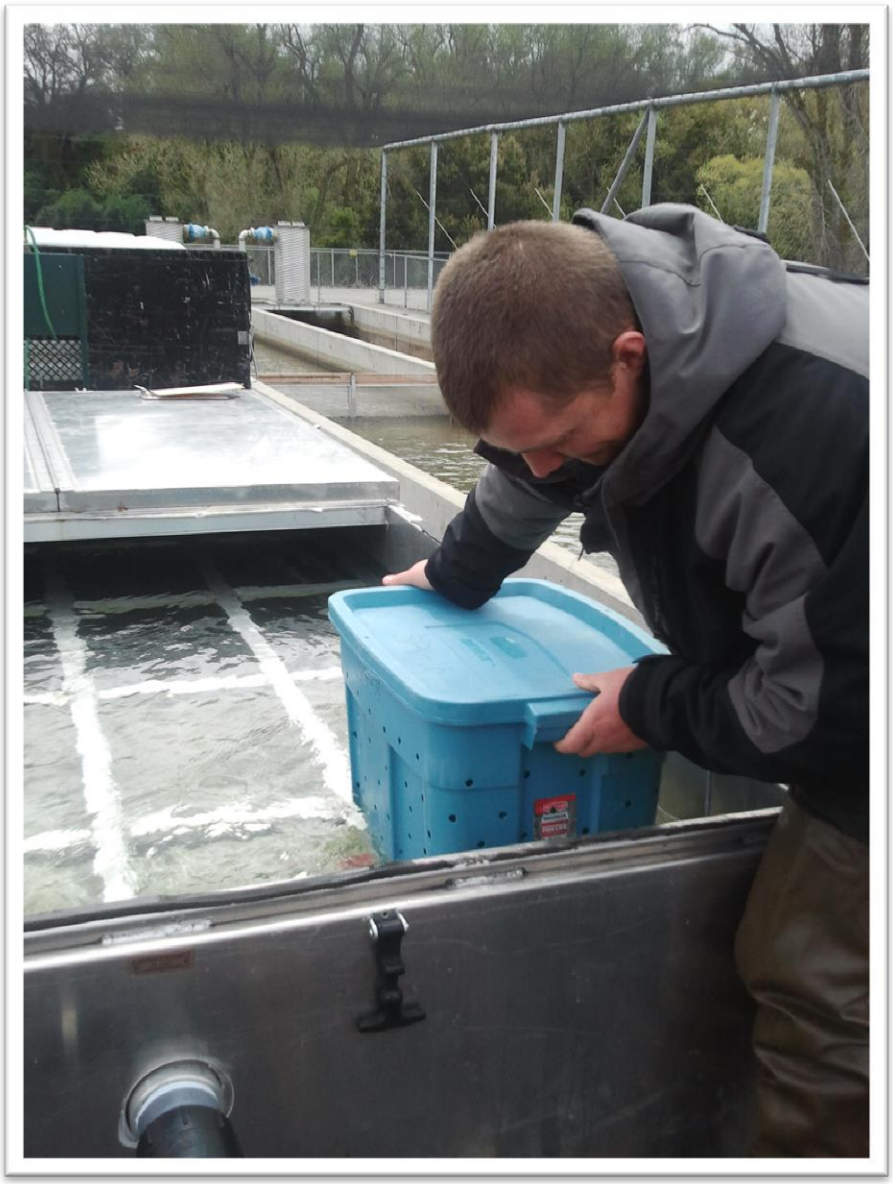

Figure 2-8 Loading tagged juvenile steelhead into the transport tank.

2.3.2 STEELHEAD TAGGING EVALUATION

Survival and delayed mortality of tagged fish are important factors to consider in any tagging study. To monitor the effects of surgical implantation of acoustic tags on fish mortality, we surgically implanted dummy tags into nine steelhead for each of the three tagging events. We transported the dummy-tagged steelhead to the Department's Collection, Handling, Transport, and Release (CHTR) facility for holding and observation. We surgically implanted dummy tags into these fish using the same methods (handling, data collection, tagging, recovery, transport, etc.) as for fish with active acoustic tags. We kept the three groups of dummy-tagged fish in three separate aerated holding tanks and fed them once daily. On June 5, 2012, we evaluated these fish for tag retention and healing. Because we evaluated all of the fish on the same day, each of the groups had been held for different lengths of time following tag implantation (Table 2-2). We euthanized each control group of steelhead and made external and internal observations to evaluate healing and recovery. We took photographs and recorded observations on a standardized data sheet.

Each of the three control groups began with nine steelhead (Table 2-2). There was one mortality from Release Group 1 within 24 hours after transfer to the CHTR facility. Release Groups 1 and 2 each had a single mortality later in the holding period when water temperature spiked upward due to an improperly functioning water chiller at the CHTR facility. Except for one fish in Group 1 that had fungus on the tail and fins, the tagged steelhead appeared healthy when evaluated. We observed no fungal infections on any other fish from any of the other control groups.

Table 2-2 Summary of control groups, holding period, and mortality.

Control Group	Holding Period (days)	Number of Fish		
		Tagged	Total Mortality	Evaluated
1	53	9	2[a]	7[b]
2	37	9	1[a]	8
3	23	9	0	9

Notes:
[a] One mortality from each of Group 1 and Group 2 was related to an improperly functioning water chiller and was not considered a tagging mortality.
[b] One fish had fungus infection on fins and tail at time of evaluation.

We examined suture sites and rated those sites on a scale from 0 (no irritation) to 4 (ulcerated). The group that had had tags implanted most recently, Group 3 at 23 days, showed ulcerated sites for 8 of 9 fish. After 37 days, Group 2 had 56% of the suture sites showing irritation ranging from slight redness (1) to ulcerated (4). Related to the irritation rates was the presence or absence of the sutures. After 53 days, Group 1 showed no irritation at any of the suture sites for fish without suture presence. In Group 1, the only steelhead to show ulceration at the suture site was the single fish of the group that still retained the sutures. The other six steelhead in that group did not have sutures remaining and did not show irritation. About half of the total sutures in Group 2 were missing after 37 days, and half of the fish in this group showed no irritation. Five steelhead from Group 2 had lost one suture and the second suture was still present. In this situation the site around the remaining suture showed signs of irritation and ulceration of the tissues. Group 3 only had one steelhead that showed no irritation, and this was the only fish whose sutures were not present. The remaining steelhead in the group had sutures in place, and these sites were ulcerated.

We reviewed and rated the incision sites on a scale of 0 to 4 for incision closure, where 0 was completely closed with no overlap and 4 was where the incision was completely open or overlapped. The results indicated that similar to irritation, the longer the time since tagging, the higher the rate of closure. All of Group 1 showed complete incision closure. Group 2 had 50% completely closed with 38% rated as partially closed (a 1 on the scale), and 12% were half open or overlapped (a 2 on the scale). Two-thirds of Group 3 were completely closed with the other third rated as partially closed (a 1 on the scale). Of the incisions that were less than completely closed, the musculature layer was fully apposed, but the dermal layer had not joined together.

We then dissected the dummy-tagged steelhead to observe the tags and how the tags interacted with tissues and organs. In 24 total tagged control group fish, 71% of the tags were located directly under the incision, 17% were located anterior to the incision, and 12.5% of the tags were located posterior to the incision. When looking for tag encapsulation, we observed that for tags in Group 1, 28.5% were not encapsulated, 57% were encapsulated in a transparent membrane, and 14% (1 tag) were encapsulated in an opaque membrane. Group 2 had 62.5% of the tags encapsulated in a transparent membrane and 37.5% encapsulated in a partially transparent membrane. Group 3 had only 33% of the tags encapsulated in a transparent membrane and the remaining 67% were not encapsulated.

A prime concern for proper internal healing is the apposition of the peritoneum. Twenty-three (23) of the 24 steelhead showed complete apposition of the peritoneum, and one steelhead had 75% of the incision that was apposed. This one fish had moderate inflammation in the section of the peritoneum that had not apposed. The rest of the steelhead, all with complete apposition, showed no internal incision irritation.

We evaluated each dummy-tagged fish for the presence of organ and internal tissue damage caused by either the suturing procedure or the tag itself. We observed no damage to internal tissues or organs in Groups 1 or 2, while Group 3 showed evidence of organ inclusion in the sutures, which was present in five of the nine fish. In addition, four of the nine fish in this group also showed some organ damage caused by the tag resting inside the pyloric caeca.

In conclusion, the suture material appeared to cause tissue irritation and ulceration around the incision site. The longer the time post-surgery, the more likely the suture was no longer present and the less likely there was irritation. While the sutures are considered absorbable, what appeared to be happening in the study fish was that the sutures were expelled. They became progressively looser and closer to the surface and were eventually completely expelled from the body. This process allowed the suture tag ends and knots to rub on the skin surface, causing the observed irritation. Based on the steelhead we observed, sutures were starting to be expelled somewhere between 23 and 37 days with most shed after 57 days.

2.3.3 TRANSPORT AND RELEASE OF ACOUSTIC TAGGED STEELHEAD

We transported totes containing three tagged steelhead each in a large aluminum tank from the Mokelumne River Fish Hatchery to Buckley Cove (near Stockton) where we offloaded the totes. We supplemented the water with bottled oxygen during transport.

After arriving at Buckley Cove, we tempered the water in each tote by gradually adding river water to allow steelhead to adjust to the warmer river water temperature. Once water temperatures had adjusted, we transported the totes on a small boat (Figure 2-9) from Buckley Cove to a houseboat moored in the San Joaquin River (Figure 2-10). At the houseboat, we emptied seven totes (for a total of 21 steelhead) into each of the eight net pens. The eight net pens were constructed of a polyvinyl chloride (PVC) conduit frame covered with netting and were approximately 1.2 x 1.2 x 1.2 m in dimension (Figure 2-11). We used pool noodles around the top of the net pen to float the net pen in the W-shaped dock. Each net pen encompassed an approximate volume of 1,800 L, and we specially designed each net pen to allow the natural flow-through of water. We designed the net pens for release of tagged fish in slow-moving water only. We held tagged steelhead in the net pens for a minimum of 48 hours prior to release to fully acclimate to the conditions in the river. Prior to release, we visually checked the fish in each net pen for mortalities. We removed one dead steelhead from net pen #2 on May 1, 2012 prior to release (Release Group 2). We observed no other mortalities. Following the minimum 48-hour acclimation period, we released one net pen of steelhead every 3 hours until all eight net pens of tagged steelhead had been released. We released the tagged steelhead by opening the net pen lid and tipping the net pen over. All releases occurred within 24 hours after they were started at approximately at 3:00 pm on the first day of the release period. A total of 501 healthy tagged steelhead were released with functional tags. Of the 501 tags, 166 were released in Group 1, 167 in Group 2, and 168 in Group 3. Average lengths (mm) and weights (grams) of the 501 steelhead are listed in Table 2-3.

Table 2-3 Lengths and weights of 501 tagged steelhead that were observed to be healthy prior to release and had functional tags.

Release Group	Release Dates	Number of Fish Tags	Fish Length (mm)		Fish Weight (g)	
			Mean	Standard Error	Mean	Standard Error
1	April 15-16, 2012	166	223.0	1.4	106.8	2.2
2	May 1-2, 2012	167	230.5	1.4	119.0	2.5
3	May 15-16, 2012	168	241.5	1.5	157.3	3.1

Figure 2-9 **Totes containing acoustically tagged steelhead on-board a boat that transported the totes to floating net pens on a houseboat.**

Figure 2-10 **The houseboat with the floating net pens.**

Figure 2-11 Floating net pens used to hold experimental release groups of steelhead prior to release.

2.3.4 TAG LIFE AND BURDEN

The V6-4X acoustic coded transmitters (tags) used in the Stipulation Study were compatible with the tags and receivers used with other study programs throughout the Delta, including the 2012 Six-Year Study.

Data on the duration of battery lives of this type of tags were from the currently unpublished 2012 battery life studies provided by Dr. Josh Israel (pers. comm.). For the tag-life study, more than 90 tags were activated and observed the length of time that tags functioned. This study had two replicates with one starting on April 6, 2012 (i.e., trial 1) and the other starting on May 25, 2012 (i.e., trial 2). In total, 48 and 45 tags were used in trials 1 and 2, respectively. One tag in trial 2 was not functioning properly. The tag worked correctly for >70 days at the pulses per minute (ppm) code (even), but not the high residence receiver (HRR)/ppm hybrid code, therefore this tag did work correctly for being detected on VR2Ws, but not correctly for being detected on HRR-cabled receivers (J. Israel, pers. comm.). This tag was removed from the tag life vitality study and was not considered in the calculation of the following numbers. For trial 1, the average tag life was 78.4 days (standard error [SE]=0.4 days). For trial 2, the average tag life was 76.6 days (SE=1.6 days). The minimum tag life was 58.5 and 19.5 days for trial 1 and 2, respectively. In both trials, 100.0% of the tags examined in the tag life vitality study lasted longer than the monitoring period for the Stipulation Study (15 days).

Each V6-4X acoustic coded transmitter weighed approximately 1 gram. To examine the tag burden for acoustically tagged steelhead in the study, tag weight (1 gram) was divided by steelhead weight and expressed as a percentage. The tag burden for Release Group 1, Release Group 2, and Release Group 3 was 1.0% (SE<0.1%), 0.9% (SE<0.1%), and 0.7% (SE<0.1%), respectively. The average tag burden for live steelhead released for this study was 0.9% (SE<0.1%).

2.4 STUDY ASSUMPTIONS

The assumptions used in the 2012 Stipulation Study are listed below.

1. Tagging did not affect survival.
2. There was little or no mortality from handling.
3. Tag expulsion was minimal.
4. The tag burden (weight of tag:weight of smolt) was appropriate.
5. Tags did not affect swimming performance or predator avoidance.
6. The tag burden was similar across release groups.
7. Tag detection probability at each location was high (>80%).
8. Detection probability at the acoustic receiver arrays did not vary between release groups.
9. The influence of predation on steelhead tags was minimal and did not bias results.
10. OMR flow differences between Group 3 and Groups 1 and 2 were sufficient to test hypotheses.
11. Treating Release Group 3 versus Groups 1 and 2 as different OMR flow treatments was appropriate despite OMR flow fluctuations during release groups.
12. Hatchery steelhead and wild steelhead smolts behaved similarly.
13. Hatchery steelhead were appropriately used as wild steelhead "sentinels."
14. Tag life was sufficient for the duration that data were collected.

As noted by the 2012 IRP LOO Annual Review (Kneib et al. 2012), the credibility and reliability of the findings in any analysis depend substantially on whether or not assumptions are reasonable. Therefore, we examined the validity of many of these assumptions.

Tagging did not affect survival.

Although it is unknown how steelhead tagging affected survival of fish once released, proper tagging procedures were followed during tagging and release, leading to very limited mortality prior to release. Of the 505 tagged steelhead, only one died prior to release. Of the 27 steelhead implanted with dummy tags and monitored in a controlled environment for tagging survival, only one steelhead died within 24 hours after tagging. Two other steelhead died after 24 hours as a result of an improperly functioning water chiller. Except for one control fish with a fungal infection, all other steelhead appeared healthy following tagging.

There was little or no mortality from handling.

Only one of the 505 tagged steelhead died prior to release, indicating that handling mortality was very low. Although an unknown amount of handling mortality could occur shortly after release, in the model, we only used data for tags that were detected at array 1 to minimize the impact.

The tag burden (weight of tag:weight of smolt) was appropriate.

The tag burden was less than 1%, which is far under the acceptable threshold level in similar studies. A maximum of 2% tag to body weight ratio is typically accepted as per the literature recommendations. The SOP for this study would have allowed a 5% tag to body weight ratio (equaling a 20 gram fish). The average weight of fish used in the study was 128 grams.

Tags did not affect swimming performance or predator avoidance.

We did not conduct an analysis to examine this and do not know if predator avoidance was affected. However, because the tag burden was far below the acceptable threshold level, we feel we met this assumption. Also, the speed at which steelhead tags moved in the system (Section 4.2.3) provided evidence that swimming performance was not hindered by tag burden.

The tag burden was similar across release groups.

The tag burden was different between groups, as the heaviest fish were observed in Release Group 3 (mean=157 grams), and lightest fish were observed in Release Group 1 (mean=107 grams). This was due to steelhead feeding and growing during the study, as fish released for Release Group 3 had the longest time to grow prior to being tagged and released. While the tag burden was different across release groups, the tag burden was far below the acceptable threshold for all release groups.

Tag detection probability at each location was high (>80%).

While the analyses conducted in the multistate mark-recapture model do not require high detection probabilities, it is important for analyses conducted without the model. As estimated by the multistate model (Sections 4.2.1 and 4.2.2), detection probability was high (>80%) for arrays 7, 20, 22, and 24. However, detection probability was much lower for arrays 2 and 21, with detection probabilities of 64% and 12% at the array-level for arrays 2 and 21, respectively (see Section 4.2.1). Although detection probability was low for these arrays, the model accounts for detection probabilities and the model was able to converge. In Sections 4.3.1 and 4.3.3, using Manly-Parr estimates (described in Section 4.2.1), detection probabilities for the dual arrays used in those analyses (arrays 3, 11, 15, and 19) were 100% at array-level for all release periods that we could estimate.

Detection probability at acoustic receiver arrays did not vary between release groups.

For all arrays used in the analyses and where detection probabilities could be estimated, detection probability did not vary between release groups. Detection probabilities did not vary across release groups for arrays 2 and 7 (Section 4.2.1) and arrays 3, 11, 15, and 19 (Sections 4.3.1 and 4.3.3). We did find that detection probability varied across release groups at array 6 (Section 4.2.1); however, array 6 was replaced with array 7 for all study analyses.

The influence of predation on steelhead tags was minimal and did not bias results.

As found in previous Delta acoustic studies (SJRGA 2011), some steelhead tags may have been present inside predators rather than tagged free-swimming steelhead smolts. When analyzing acoustic tagging data of Chinook salmon smolts for the 2010 VAMP study, attempts were made to distinguish between tagged salmon smolts and those tags that had been consumed by predators (SJRGA 2011). A filter was applied to all tag detections based on

assumed behavioral differences between Chinook salmon smolts and predators. For example, Chinook salmon smolts were expected to move with the flow while actively migrating downriver, while predators were not expected to show such unidirectional movement. Although the best available information was used to inform the predator filter, no validation was performed, and therefore its accuracy is unknown.

Utilizing the predator filter developed for Chinook salmon would likely produce biased results as juvenile steelhead may behave differently than Chinook salmon. We could have attempted to create our own predator filter for distinguishing between steelhead and predators, however, the inability to validate such a steelhead predator filter would have introduced an unknown amount of uncertainty to the study results. Given the larger size of juvenile steelhead, predation on steelhead tagged in this study may have been less frequent than in other mark-recapture studies that used smaller Chinook salmon. However, the true influence of predation on study findings is unknown.

OMR flow differences between Release Group 3 and Release Groups 1 and 2 were sufficient to test hypotheses.

Because the original goal of achieving three distinctly different OMR flow treatments was not met, we analyzed the data as two release groups, with Release Groups 1 and 2 pooled as a less negative OMR flow treatment, and Release Group 3 as a more negative OMR flow treatment, as recommended by the 2012 IRP LOO Annual Review (Kneib et al. 2012). Therefore, study results should reflect how the range of OMR flows during the study influenced fish behavior in each OMR flow treatment group. However, because OMR flows only spanned approximately 70% of the proposed range of flows, and historical flows have been much more negative than observed during the study, it is uncertain how well study results extrapolate to OMR flow conditions outside of the range observed. In addition, only two replicates of less negative OMR flows and a single replicate of more negative flows were examined. Therefore, additional replications of stable OMR flows across the examined range and beyond are recommended to corroborate study findings and understand how OMR flows affect fish behavior and survival.

Treating Release Group 3 versus Release Groups 1 and 2 as different OMR flow treatments was appropriate despite OMR flow fluctuations during release groups.

The average OMR flows following release for each release group was used to assign Release Groups 1 and 2 to a less negative OMR flow treatment and Release Group 3 to a more negative OMR flow treatment. However, OMR flows varied following each release, especially after a point in the second week when the trigger was activated and flows were brought to -1,250 cfs. This occurred on April 24, May 11, and May 26, 2012 for Release Groups 1, 2, and 3, respectively. We believe that the impact of these flow fluctuations was minimal because the majority of steelhead tags in all release groups moved through the Delta before these dates.

Hatchery steelhead and wild steelhead smolts behave similarly.

The assumption that tagged hatchery steelhead are a valid proxy for wild steelhead was likely violated because of behavioral differences between hatchery and wild fish, as observed in other Central Valley studies. Wild steelhead have been shown to behave differently than hatchery steelhead (e.g., Chittenden et al. 2008; and reviews by Melnychuk et al. 2010 and Drenner et al. 2012). An alternative would have been to use tagged wild steelhead instead of hatchery surrogates. However, using wild steelhead would be challenging. This species is threatened, and collecting large numbers of wild steelhead smolts would be difficult if not impossible.

Hatchery steelhead were appropriately used as wild steelhead "sentinels."

The arrival of steelhead tags implanted in hatchery steelhead in the interior Delta (Railroad Cut) was used as a trigger for altering export pumping levels and thereby protecting wild steelhead from entrainment to CVP and SWP. However, as described in the previous assumption, hatchery steelhead likely behave differently than their wild counterparts; the arrival timing of tagged steelhead was highly dependent on their release date, and likely

different than when wild steelhead arrived. Although this assumption was likely violated, it is unknown to what extent wild steelhead arrival timing differed from tagged hatchery steelhead. Future studies should be completed to understand how well tagged hatchery steelhead mimic the behavior of their wild counterparts.

Tag life was sufficient for the duration that data were collected.

A tag life study showed that failure occurred on average after 78.4 days (SE=0.4 days) in the first trial and 76.6 days (SE=1.6 days) in the second tag life study. One of the tags stopped functioning after 19.5 days but all the tags included in this study, which were all tags that were detected on both types of acoustic receivers from the beginning, were functioning for the entire 15-day period that steelhead tags were monitored during the study.

3 DATA MANAGEMENT

CHAPTER SUMMARY:

In the spring of 2012, we initiated a mark-recapture experiment to examine the survival and movement patterns of acoustically tagged juvenile steelhead emigrating through the Delta. The dataset was for the 501 live fish released with tags that were known to be functional. We also received detection data for Stipulation Study steelhead tags that were detected by receivers deployed for the Six-Year Study. We performed quality assurance/quality control (QA/QC) on the data and produced a Microsoft (MS) Access 2010 database file composed of four separate table objects:

1. Fish measurements, release, and transport.
2. Release dates, timing, and corresponding group number.
3. Filtered Stipulation Study fish detection data.
4. Receiver codes, identification, station names, and arrays.

We only examined steelhead tags that were detected within 15 days of release. We processed these data by filtering out detection records which were: (1) at a date/time prior to the release date, (2) beyond the 15 days of release date, and/or (3) detected at a receiver only once within the ± 30-minute time-frame.

3.1 DATABASE DESIGN AND IMPLEMENTATION

This section describes the Access database, which included data on acoustically tagged steelhead from the 2012 Stipulation Study. The database included detection data from acoustic receiver arrays as shown in Figure 2-3. Where possible, data descriptions described in this report are included within the Access database under data field definitions and table comments. We received a set of fish detection data from all receiver arrays shown in Figure 2-3 on August 24, 2012. We corrected all fish detection data for time drift using VUE software. We also received detection data for Stipulation Study tagged fish detected from the receivers deployed by the 2012 Six-Year Study (care of Josh Israel, Reclamation). By the end of February of 2013, we received all the data from receivers of the arrays.

We checked and verified the tagging, transport, release, and detection data in the database to ensure quality control. We checked for duplicated serial numbers and tag-IDs per release and bucket/tote IDs, checking for blank records for each field, the units used for fish measurements, and reviewing comments noted by the field biologist to ensure that they were properly represented in the data (e.g., failed tag, functioning tag number, dummy serial number, fish behavior prior to release). We flagged data found to be questionable or unmatched to field notes and sent those data to Kevin Clark (field implementation lead) to verify. Because of the limited file size available in the Access database, we excluded fish data for non-Stipulation Study tagged fish from this database.

Data were provided in the MS Access database in four separate table objects:

01_TagData&FishInfo contains data on fish measurements, release, and transport (Table 3-1).

02_ReleaseDates_GroupNum contains specific data on release dates, timing, and corresponding group number (Table 3-2).

03_All_FishDetection_within15dayofrelease contains all the detection data for all fish for the entire study (Table 3-3).

04_Receiver_Array contains receiver codes, ID numbers, station names, and arrays service details (Table 3-4).

We structurally organized and shaped the data in several table objects into a relational database. Table objects were connected via "one-to-many" relationships between tables (Figure 3-1). For example, the table 01_FishSerialNum and 02_FishSerialNum_TagCodes had a one-to-many relationship indicating that each fish serial number had two fish tag ID numbers, but each fish tag ID number had only one unique fish serial number. This approach maintained the integrity, quality, and accessibility of the large dataset. Our approach also prevented duplicates in fish tag serial numbers or tag ID numbers, and allowed efficient accessibility and flexibility of records necessary when creating data queries to conduct the analysis in the following chapter.

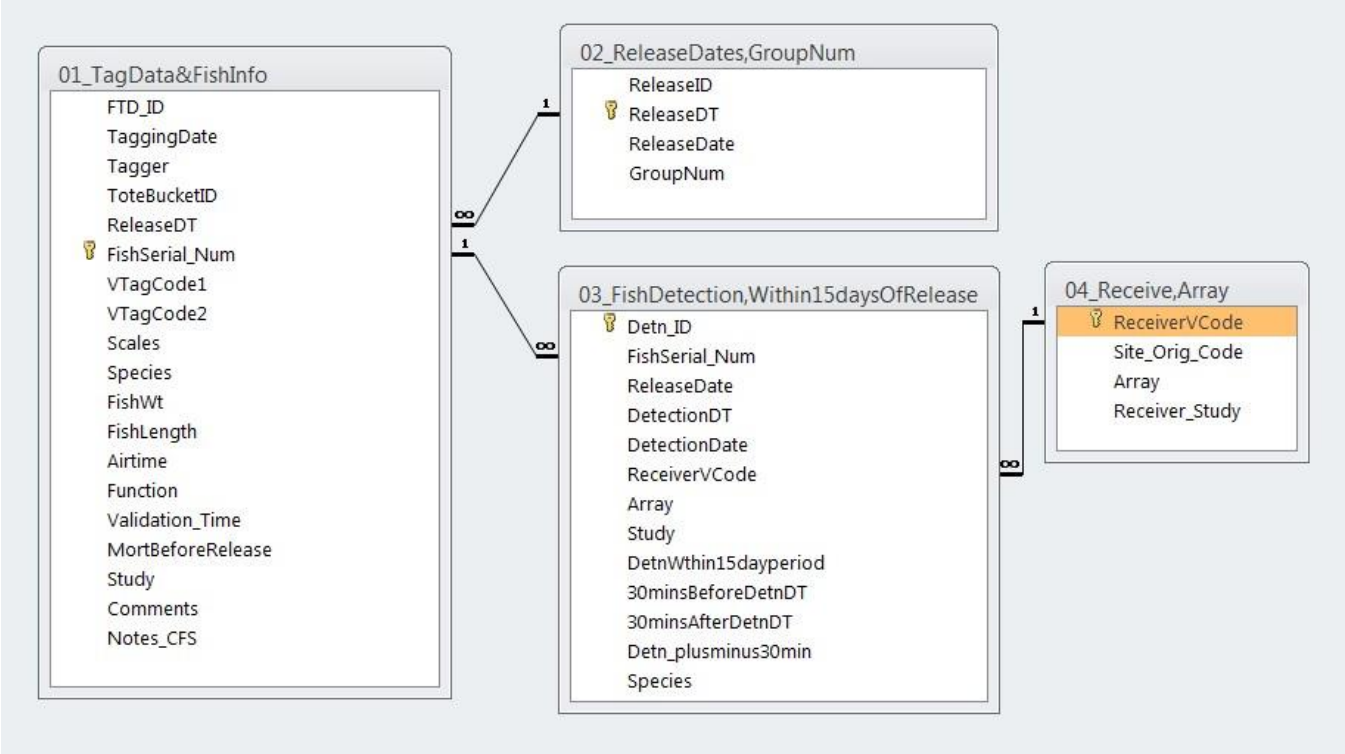

Figure 3-1 Tables and relationships used in the Stipulation Study database.

01_TAGDATA&FISHINFO

The Access table "01_TagData&FishInfo" included fish measurements, tagging, transport, and release date data. A total of 505 fish were acoustically tagged and of these, one steelhead died. All live acoustically tagged fish were released. Four steelhead were recorded to have non-functioning tags prior to release, although we subsequently detected one fish that was thought to have a non-functional tag. Therefore, the dataset consists of 501 fish with functioning tags, as included in Table 3-1.

Table 3-1 List of field names, data types, and descriptions in 01_TagData&FishInfo.

Field Name	Data Type	Description
FTD_ID	Text	Tagging data row ID assigned by Cramer Fish Sciences (CFS). FTD stands for **F**ish **T**agging **D**ata row ID.
TaggingDate	Date/Time	Tagging date.
Tagger	Text	Name of the field biologist who tagged fish.
ToteBucketID	Text	Tote and/or Bucket ID.
ReleaseDT	Date/Time	Release Date and Time.
FishSerial_Num	Number	VEMCO Fish tag serial number.
VTagCode1	Number	VEMCO tag code 1.
VTagCode2	Number	VEMCO tag code 2.
Scales	Text	Fish scales condition; N=Normal (loss of $\leq$5% scales on one side of the steelhead), P=Partial (loss of 6-19% of scales on one side of the steelhead), D=Descaled (lost $\geq$20% or more of the scales on one side of the fish, and were not being tagged due to compromised osmoregulatory ability).
Species	Text	Species code: STH=steelhead (in Stipulation Study, all were STH smolts).
FishWt	Number	Fish weight (grams).
FishLength	Number	Fish fork length (mm).
Airtime	Date/Time	Time when the fish was out of the water during tagging. Airtime started when the steelhead was removed from the bucket containing MS-222, and airtime stopped when the fish was placed into a recovery bucket.
Function	Text	Y: tag was verified to be functioning; N: tag was verified to be not functioning.
Validation_Time	Date/Time	Time at which the tag function was verified by a biologist.
MortBeforeRelease	Number	Number of fish mortality observed before fish release (all live fish herein since we excluded one dead fish).
Study	Text	Study name (all Stipulation Study).
Comments	Text	Field notes.
Notes_CFS	Text	Data notes by CFS.

02_RELEASEDATES_GROUPNUM

The Access table "02_ReleaseDates_GroupNum" included the list of release dates and times, and the associated group number. Acoustically tagged fish were released in three groups at Buckley Cove: April 15–16 (Group 1), May 1–2 (Group 2), and May15–16 (Group 3), 2012 (Table 3-2).

Table 3-2 List of field names, data types, and descriptions in 02_ReleaseDates_GroupNum.

Field Name	Data Type	Description
ReleasedID	Autonumber	Data row ID.
ReleasedDT	Date/Time	Release date and time.
ReleaseDate	Date/Time	Release date.
GroupNum	Number	Group number assigned to each release date.

03_ALL_FISHDETECTION_WITHIN15DAYOFRELEASE

The Access table "03_ALL_FISHDETECTION_WITHIN15DAYOFRELEASE" included Stipulation Study fish detection data within the 15 days of release (Table 3-3). These data were processed by filtering out detection records that were: (1) at a date/time prior to the release date, (2) beyond the 15 days of release date, and/or (3) detected at a receiver only once within the ± 30 minutes time-frame.

Table 3-3 List of field-names, data type, and description for table 03_All_FishDetection_within15dayofrelease.

Field Name	Data Type	Description
Detn_ID	Text	Data row ID from "raw detection data" (from the raw database, which is not described herein). These IDs were used as cross-reference ID between the filtered Stipulation Study detection data and the original "raw" detection data. Detn_IDs were assigned by CFS. In addition, Detn_IDs with labels "DtnStip_### (e.g., DtnStip_865247)" indicated detection data of tagged Stipulation Study fish downloaded from the Stipulation Study and "6yr_#### (e.g., 6yr_940896) and #### (e.g., 1003)" detection data for Six-Year Study receivers.
FishSerial_Num	Number	VEMCO fish tag serial number of an individual fish.
ReleaseDate	Date/Time	Release date and time.
DetectionDT	Date/Time	Detection date and time.
DetectionDate	Date/Time	Detection date.
ReceiverVCode	Number	VEMCO receiver serial code.
Array	Number	Array numbers assigned by CFS.
Study	Text	Study name (in the case herein, all Stipulation Study).
DetnWthin15dayperiod	Text	Yes: detection data within the 15 days of release (all yes herein since these are all filtered detection data).
30minBeforeDetnDT	Date/Time	30-mins before the detection date/time of an individual fish at a receiver.
30minAfterDetnDT	Date/Time	30-mins after the detection date/time of an individual fish at a receiver.
Detn_plusminus30min	Number	Count of detection hits within the ± 30 minutes time-frame from the recorded detection date/time of an individual fish at a receiver (only records with series of detection hits >1 at a receiver).
Species	Text	STH: steelhead smolt (Stipulation Study tagged fish are all steelhead smolts).

04_RECEIVER_ARRAY

The Access table "04_Receiver_Array" included the list of receiver codes (old and new), original station name, array, and the project that deployed the receivers. Geographic coordinates and visualizations of telemetry stations and a release site were plotted on a map and saved in KMZ file format.

Table 3-4 List of field names, data types and descriptions in 04_Receiver_Array.

Field Name	Data Type	Description
ReceiverVCode	Number	VEMCO receiver serial number/code.
Site_Orig_Code	Text	Site/station name assigned originally by Kevin Clark.
Array	Number	Arbitrary array number assigned by CFS.
Receiver_Study	Text	A project name that deployed the receiver.

TAG DATA USED IN EACH ANALYSIS AND FULL DETECTION HISTORIES

Appendix B (*Crosswalk Table of Tag and Dependent Analysis*) shows what tags were used in what analysis. This appendix presents the data used to produce the figures and results for the analyses in this report (Chapter 4).

This page intentionally left blank.

4 RESULTS

CHAPTER SUMMARY:

We performed the analyses at three spatial levels: system, route, and junction-level. For the system-level analysis, we displayed the data in a variety of tables, figures, and a web-based data viewing tool. We found that a physically based model (the DSM2 Hydro PTM) was unable to predict the movement of steelhead tags, because the model greatly underestimated steelhead tag movement rates through the study area. Using a t-test, we found that steelhead tags were traveling significantly greater distances 3 days and 7 days after their release than particles in the PTM. Steelhead tag movement patterns seemed to exhibit limited STST behaviors, which could explain why particles traveled less distance after both 3 and 7 days. Using binomial tests, we also found that diurnal and nocturnal movement patterns might be occurring, but these patterns were location-specific.

For the route-level analysis, we developed a multistate model to estimate route-specific transition probabilities (a measure of steelhead tags that went through a route and survived, so the complement of route-specific transition probability is not just mortality but the probability of mortality, using a different route, or not reaching Chipps Island in 15 days), route-specific survival probabilities (the complement of survival is the probability of mortality or not reaching Chipps Island in 15 days), and overall survival probability. Data were pooled for all release groups as the model using data from a single release group (e.g., Release Group 3) did not converge. This model with the pooled data allowed us to estimate route-specific transition probability for each of the six different routes (all routes started downstream of Buckley Cove and ended at Chipps Island):

- The route-specific probability via Turner Cut was 7.0% (SE=1.6%).
- The route-specific probability without using Turner Cut was 24.8% (SE=2.0%).
- The route-specific probability via Turner Cut and the SWP was 0.5% (SE=0.5%).
- The route-specific probability via the SWP without using Turner Cut was 0.2% (SE=0.2%).
- The route-specific probability via Turner Cut and the CVP was 19.6% (SE=2.8%).
- The route-specific probability via CVP without using Turner Cut was 31.7% (SE=1.9%).

Overall survival to Chipps Island was 50.2% (SE=2.0%). Route-specific survival probability for the Turner Cut route was 27.0% (SE=3.0%). Route-specific survival probability for the Mainstem route was 56.7% (SE=2.4%). The model estimated that the majority of steelhead tags (77.6%, SE=1.6%), continued along the San Joaquin River, and 22.4% (SE=1.6%) of the steelhead tags were entrained into the interior Delta at the Turner Cut junction. Using an analysis of variance (ANOVA), we found that travel times for steelhead tags differed between these two routes, with steelhead tags reaching Chipps Island more rapidly for the Mainstem route compared to the steelhead tags that successfully reached Chipps Island using the Turner Cut route (using these routes as defined in the model). The faster migration of steelhead tags using the Mainstem route was consistent with higher survival for this route.

We found no evidence that the routing of steelhead tags at the three junctions along the San Joaquin River (Columbia Cut, Middle River, and Turner Cut) was affected by the OMR flow treatment levels examined in this study. When the data were examined using two release groups (less negative vs. more negative OMR flows), we found no significant differences for the OMR levels tested in this study. In the analysis of steelhead tags arriving into Clifton Court Forebay or the CVP, we found that while not significant, on average the proportion of water arriving at an export facility was higher at the facility for the period of time when a steelhead tag was arriving at the facility that first detected it.

We wanted to determine whether steelhead tags at Railroad Cut were more likely to move north away from the SWP and CVP intakes after the adaptive management option was triggered and less negative OMR flows were observed. However, when we examined if adaptive management trigger was effective, we were unable to successfully complete the test due to the small sample size of steelhead tags passing through Railroad Cut after

the management option was observed to take effect (N=7). Yet, there was marginally significant (statistical test values over 0.05 but less than 0.1) evidence that steelhead tags at Railroad Cut were more likely to move north in less negative (Groups 1 and 2) OMR flows than in more negative (Group 3) OMR flow conditions. We examined nine predictor variables in separate tests. Only the test that used average OMR flow on the day that the steelhead tag was first detected downstream of Railroad Cut was found to be significant.

4.1 SYSTEM-LEVEL ANALYSES

In this section, we present the analysis of system-level movement patterns of steelhead tags both descriptively through spatial display of tag data, and statistically by examining key large-scale hypotheses. We begin with the descriptive results where tag data are displayed in a suite of figures, tables, and a web-based tool. We describe the percentage of steelhead tags detected at each array, where last detections occurred, the residence time at each array, the final fate of steelhead tags at each array, and provide a web-based tool displaying tag detection histories. In Sections 4.1.6, 4.1.7, and 4.1.8, we examine three statistical hypotheses to determine how well movement of simulated particles mimicked steelhead tag behavior, whether tags exhibited selective movement behavior in relation to tides, and how steelhead tag movement related to time of day.

Although we did not account for detection probability at arrays when calculating system-level results, we assume that detection probability did not vary between release groups, and therefore relative differences in spatial patterns of tags across release groups reflect the true movement of tags. In later results sections (Sections 4.2.1, 4.3.1, and 4.3.3), we examined if detection probability varied across release groups for arrays with dual receivers (2, 3, 6, 7, 11, 15, and 19) and found that detection probability only varied across release groups for array 6. Therefore, except for array 6, relative differences in the spatial pattern of tags can likely be attributed to release group differences and not to differences in detection probabilities. Also, most arrays had high detection probabilities (>80%) so system-wide biases in tag spatial patterns are very unlikely when examining system-level results.

4.1.1 RELATIVE TAG DETECTION AT ARRAYS

We examined the spatial pattern of steelhead tags detected by release group, by depicting the percentage of tags detected at each array (Figure 4-1 and Table 4-1). The results generally showed a decreasing number of individual steelhead tags detected the farther away tags moved from the release location of Buckley Cove, indicating a declining number of tags as they traveled downstream, most likely resulting from mortality. No consistent pattern between release groups was evident, indicating that the OMR flows tested likely had minimal effect on the general movement patterns of steelhead tags during the study.

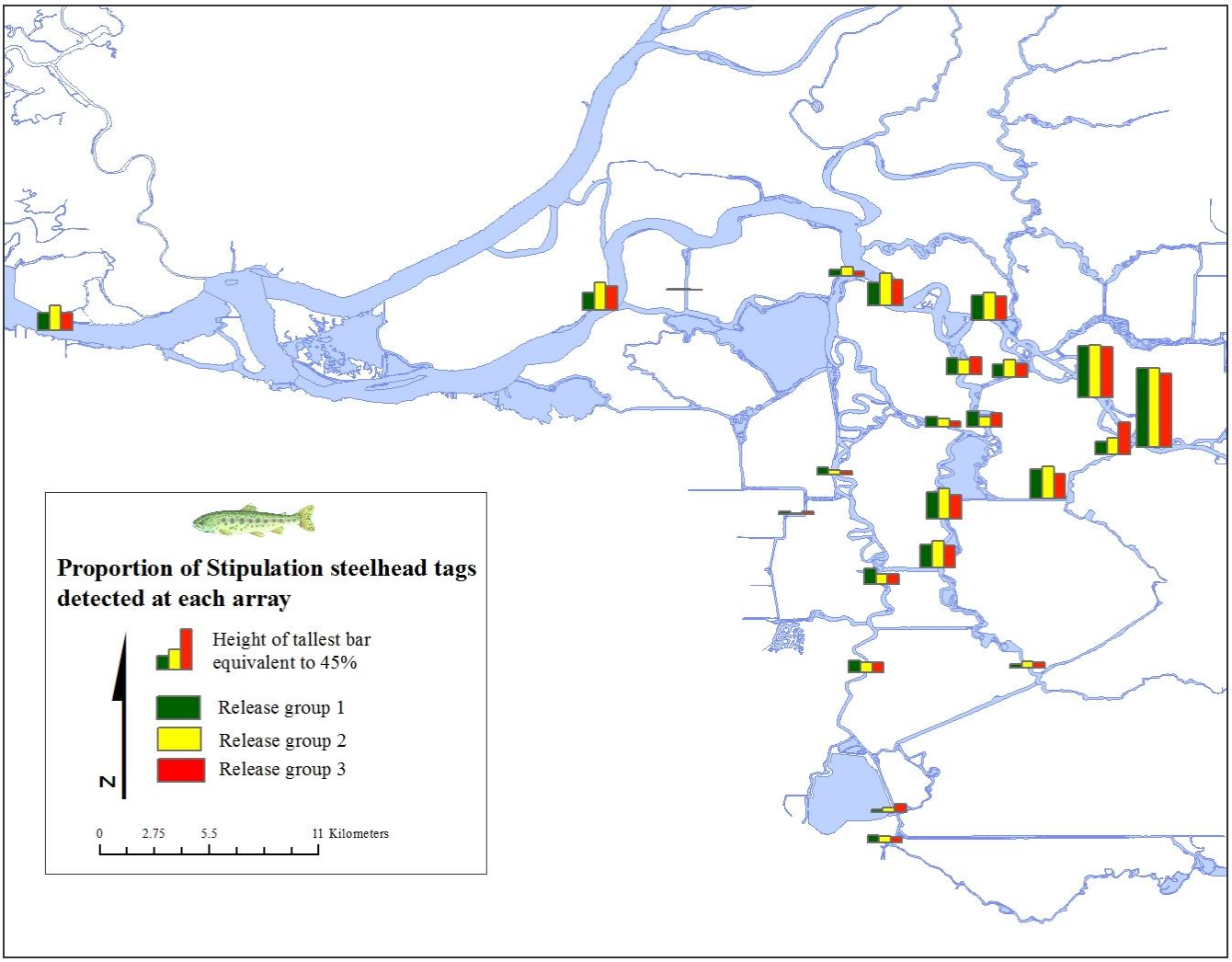

Figure 4-1 **Percentage of individual steelhead tags detected in each array by release group.** See Table 4-1 for the source data.

Table 4-1 Number and percentage of Stipulation Study steelhead tags detected in each array by release group. The percentage was calculated as the number of tags detected at that array from that release group divided by the total number of tags released for the release group. The total number of tags released was 166, 167, and 168 for Release Groups 1, 2, and 3, respectively.

Array	Number of Tags Detected			Percentage of Tags Detected (%)		
	Group 1	Group 2	Group 3	Group 1	Group 2	Group 3
1	147	149	139	88.6	89.2	82.7
2	95	98	96	57.2	58.7	57.1
3	45	51	44	27.1	30.5	26.2
4	42	60	48	25.3	35.9	28.6
5	13	17	9	7.8	10.2	5.4
6	24	31	61	14.5	18.6	36.3
7	55	61	47	33.1	36.5	28.0
8	50	58	46	30.1	34.7	27.4
9	44	51	42	26.5	30.5	25.0
10	6	12	11	3.6	7.2	6.5
11	23	33	26	13.9	19.8	15.5
12	29	20	27	17.5	12.0	16.1
13	30	27	32	18.1	16.2	19.0
14	18	16	10	10.8	9.6	6.0
15	14	8	6	8.4	4.8	3.6
16	29	18	18	17.5	10.8	10.7
17	6	2	5	3.6	1.2	3.0
18	0	0	0	0.0	0.0	0.0
19	22	18	18	13.3	10.8	10.7
20	6	9	15	3.6	5.4	8.9
21	13	11	10	7.8	6.6	6.0
22	33	52	45	19.9	31.1	26.8
23	1	1	0	0.6	0.6	0.0
24	33	47	33	19.9	28.1	19.6

4.1.2 LAST DETECTION AT ARRAYS

We examined the spatial pattern of where steelhead tags were last detected by release group, by depicting the percentage of tags last detected at each array (Figure 4-2 and Table 4-2). The largest number of final detections occurred at the Chipps Island array, providing evidence that a large proportion of steelhead tags migrated through the system successfully. The next highest percentage was at the first array. The large percentage of last detections at the first array may indicate high mortality, possibly due to high predation or handling mortality following release. No consistent pattern between release groups appeared evident, indicating that the OMR flows tested likely were not driving the general patterns seen in the final detection data.

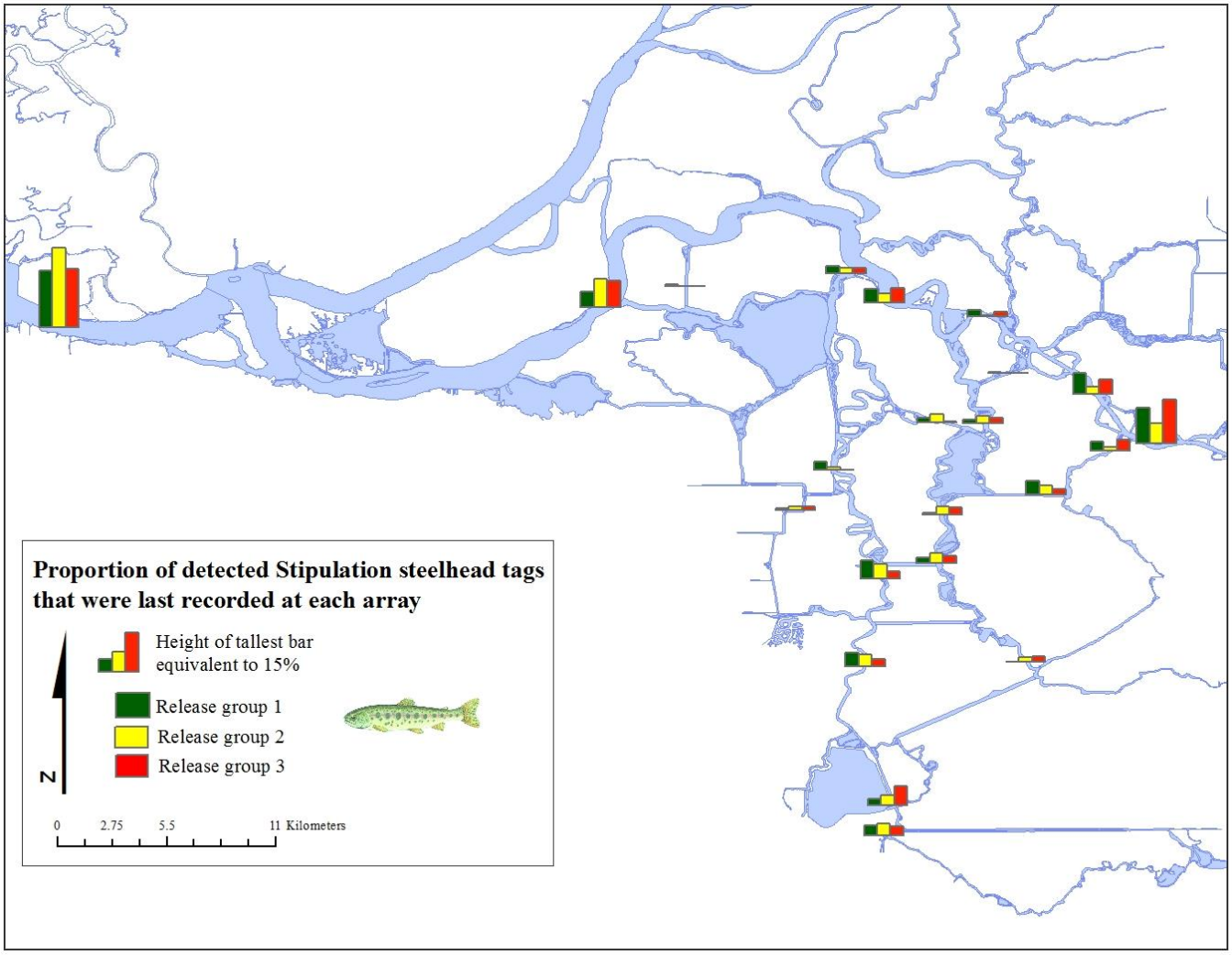

Figure 4-2 **Percentage of steelhead tags last detected at each array by release group.** The distribution of last detections indicates areas where fish mortality occurred or where tags left the area of receiver coverage. See Table 4-2 for the source data.

Table 4-2 Number and percentage of steelhead tags last detected at each array by release group. Each tag was only counted at the single array where the tag was last detected. The percentage was calculated as the number of tags last detected at that array divided by the total number of tags from that release group that were detected at any array. The total number of tags detected at any array was 150, 152, and 145 for Release Groups 1, 2, and 3, respectively.

Array	Number of Tags Detected			Percentage of Tags Detected (%)		
	Group 1	Group 2	Group 3	Group 1	Group 2	Group 3
1	21	12	25	14.0	7.9	17.2
2	12	4	8	8.0	2.6	5.5
3	4	1	3	2.7	0.7	2.1
4	8	5	8	5.3	3.3	5.5
5	4	3	3	2.7	2.0	2.1
6	5	2	6	3.3	1.3	4.1
7	8	5	3	5.3	3.3	2.1
8	1	5	4	0.7	3.3	2.8
9	3	6	4	2.0	3.9	2.8
10	0	3	3	0.0	2.0	2.1
11	1	0	0	0.7	0.0	0.0
12	2	4	3	1.3	2.6	2.1
13	0	0	0	0.0	0.0	0.0
14	3	5	1	2.0	3.3	0.7
15	5	2	0	3.3	1.3	0.0
16	11	9	4	7.3	5.9	2.8
17	1	2	2	0.7	1.3	1.4
18	0	0	0	0.0	0.0	0.0
19	8	7	4	5.3	4.6	2.8
20	4	6	11	2.7	3.9	7.6
21	6	7	5	4.0	4.6	3.4
22	9	17	15	6.0	11.2	10.3
23	1	0	0	0.7	0.0	0.0
24	33	47	33	22.0	30.9	22.8

4.1.3 RESIDENCE TIME AT ARRAYS

We examined the spatial pattern of residence time at each array by release group, by depicting the average time spent by steelhead tags at each array (Figure 4-3 and Table 4-3). The results indicated that the time between first and last detections at each array was generally consistent among arrays, except for the arrays located at the radial gates of Clifton Court Forebay (array 20) and CVP (array 21). On average, steelhead tags spent more time at arrays 20 and 21 than any other array in the study system, indicating that steelhead tags may have been consumed by a predator and defecated at these locations, trapped, or delayed from leaving the vicinity of those arrays. No consistent pattern between release groups was evident, indicating that OMR flows tested were not likely driving the general patterns seen in tag residence time. See Table 4-3 for the source data.

A potential bias influencing array residence time results was the 15-day filter applied to steelhead tag data. By cutting off detection data beyond 15 days, array residence time may be underestimated, especially at more downstream arrays that were not reached until later in the study period (i.e., arrays 20–24). However, since the majority of steelhead tags that successfully traveled through the system did so in less than 7 days (see Section 4.2.3), the proportion of tags being detected at Chipps Island eliminated by the 15-day filter was small (6%). Also, very large residence times observed at arrays 20 and 21 provided evidence that underestimation of residence time was likely not a problem.

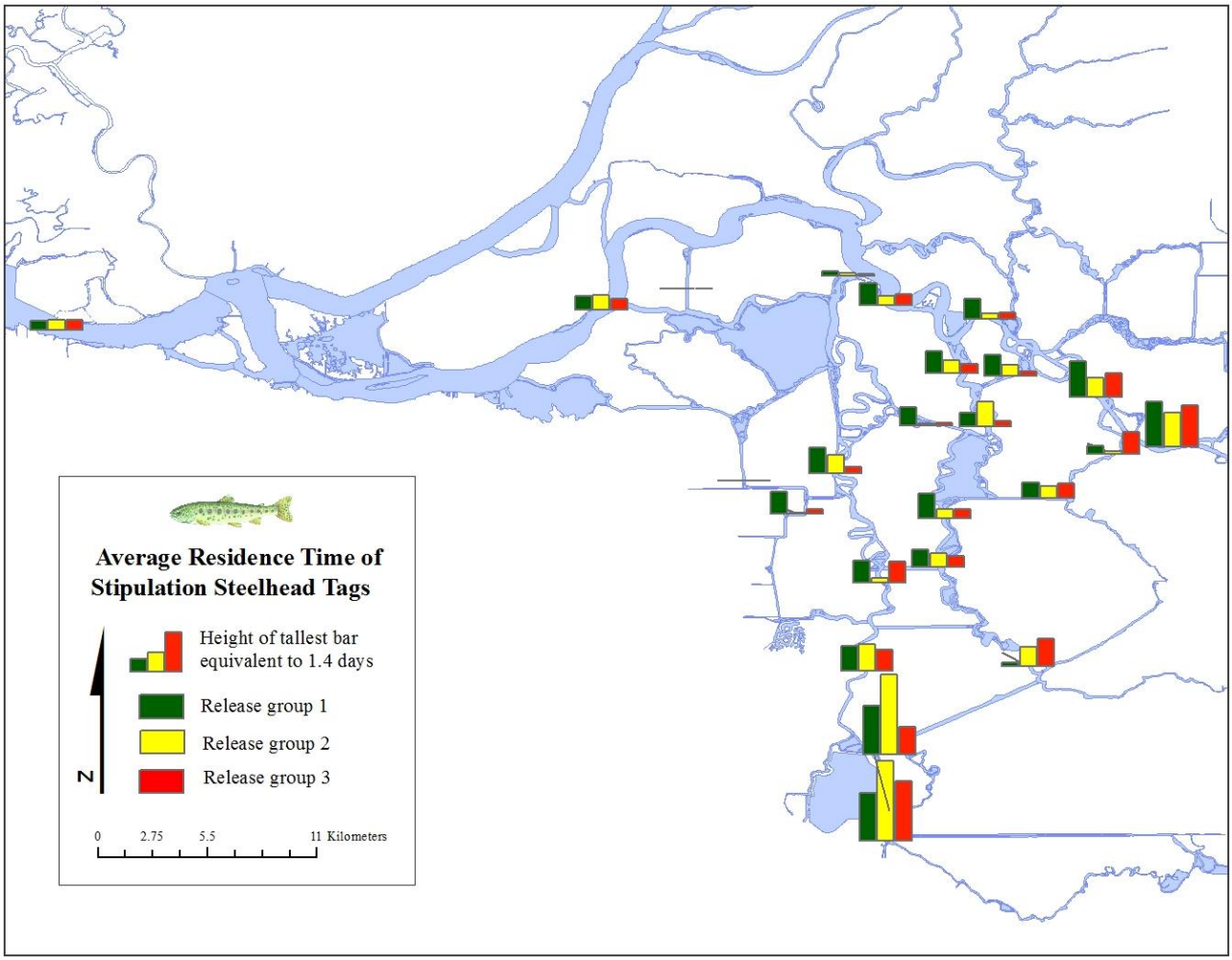

Figure 4-3 **Average residence time of steelhead tags at each array by release group.** Residence time is equal to the difference between the last and first detections of individual tags. See Table 4-3 for the source data.

Table 4-3 Sample sizes, average, minimum, and maximum values of residence time (days) of steelhead tags at each array by release group. Residence time of a tag is equal to the difference between the last and first detection at each array.

	Release Group 1				Release Group 2				Release Group 3			
Array	N	Average	Minimum	Maximum	N	Average	Minimum	Maximum	N	Average	Minimum	Maximum
1	147	1.5	<0.1	14.6	149	1.2	<0.1	14.3	139	1.4	<0.1	12.4
2	95	1.2	<0.1	13.3	98	0.7	<0.1	14.0	96	0.8	<0.1	11.3
3	45	0.7	<0.1	9.7	51	0.2	<0.1	2.5	44	0.2	<0.1	2.4
4	42	0.7	<0.1	10.2	60	0.3	<0.1	1.7	48	0.4	<0.1	1.8
5	13	0.2	<0.1	1.1	17	0.1	<0.1	0.7	9	0.1	<0.1	0.3
6	24	0.3	<0.1	2.7	31	0.1	<0.1	1.2	61	0.7	<0.1	13.4
7	55	0.5	<0.1	4.6	61	0.4	<0.1	4.5	47	0.5	<0.1	10.7
8	50	0.8	<0.1	8.4	58	0.3	<0.1	4.0	46	0.3	<0.1	1.6
9	44	0.6	<0.1	10.2	51	0.5	<0.1	10.2	42	0.4	<0.1	5.5
10	6	0.1	<0.1	0.3	12	0.7	<0.1	3.6	11	0.9	<0.1	5.8
11	23	0.7	<0.1	8.9	33	0.4	<0.1	7.3	26	0.2	<0.1	1.1
12	29	0.5	<0.1	2.9	20	0.8	<0.1	9.4	27	0.2	<0.1	3.1
13	30	0.8	<0.1	5.4	27	0.5	<0.1	7.6	32	0.3	<0.1	3.4
14	18	0.7	<0.1	6.8	16	0.1	<0.1	0.6	10	0.1	<0.1	0.7
15	14	0.9	<0.1	3.2	8	0.6	<0.1	1.8	6	0.2	<0.1	0.9
16	29	0.8	<0.1	3.8	18	0.2	<0.1	0.8	18	0.7	<0.1	7.4
17	6	0.8	<0.1	3.1	2	<0.1	<0.1	<0.1	5	0.1	<0.1	0.4
18	0	-	-	-	0	-	-	-	0	-	-	-
19	22	0.9	<0.1	5.5	18	0.9	<0.1	9.0	18	0.7	<0.1	6.2
20	6	1.7	<0.1	7.8	9	2.7	<0.1	10.5	15	1.0	<0.1	7.0
21	13	1.6	0.2	7.3	11	2.7	0.2	10.2	10	2.0	0.1	12.0
22	33	0.5	<0.1	1.9	52	0.5	<0.1	3.9	45	0.4	<0.1	1.8
23	1	<0.1	<0.1	<0.1	1	<0.1	<0.1	<0.1	0	-	-	-
24	33	0.3	<0.1	0.9	47	0.3	<0.1	1.4	33	0.3	<0.1	2.0

4.1.4 FINAL FATE AT ARRAYS

We examined the spatial pattern of the final fate of steelhead tags at each array by release group, by depicting the last location of tags at each array. The data from each array were categorized and displayed based on final fate (i.e., the location of last detection of a steelhead tag) at four final destinations (CVP, SWP, Chipps Island, or in-river) for each of the three release groups (Figure 4-4 to Figure 4-6 and Table 4-4). Successfully salvaged steelhead tags were recorded at Chipps Island (array 24). The steelhead tags recorded as having the SWP destination were last detected at array 20, which is the array upstream and downstream of the radial gates of Clifton Court Forebay. Array 21 was located at the CVP and was the last detection location for steelhead tags that entered the CVP. The steelhead tags recorded as in-river were not detected last at array 20, 21, or 24.

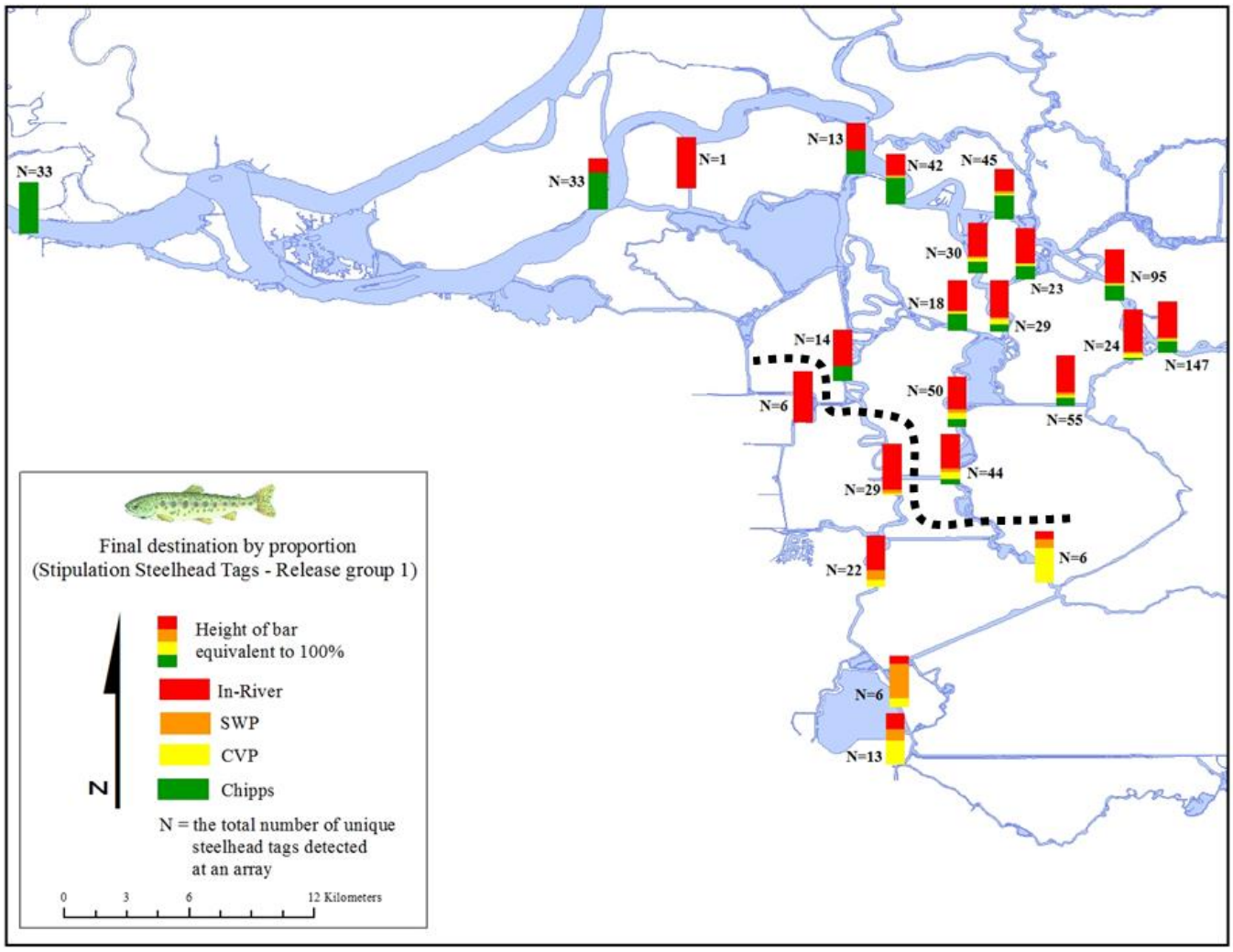

Figure 4-4 **For each array, the proportion of steelhead tags from Release Group 1 last detected at one of four destinations (CVP, SWP, Chipps Island, or in-river).** No tags were successfully salvaged for Release Group 1. The sample size (N) for each array is denoted next to each bar. See Table 4-4 for the source data. The dashed black line indicates the "point of no return," the southern-most locations where at least one steelhead tag successfully arrived at Chipps Island without assistance through salvage.

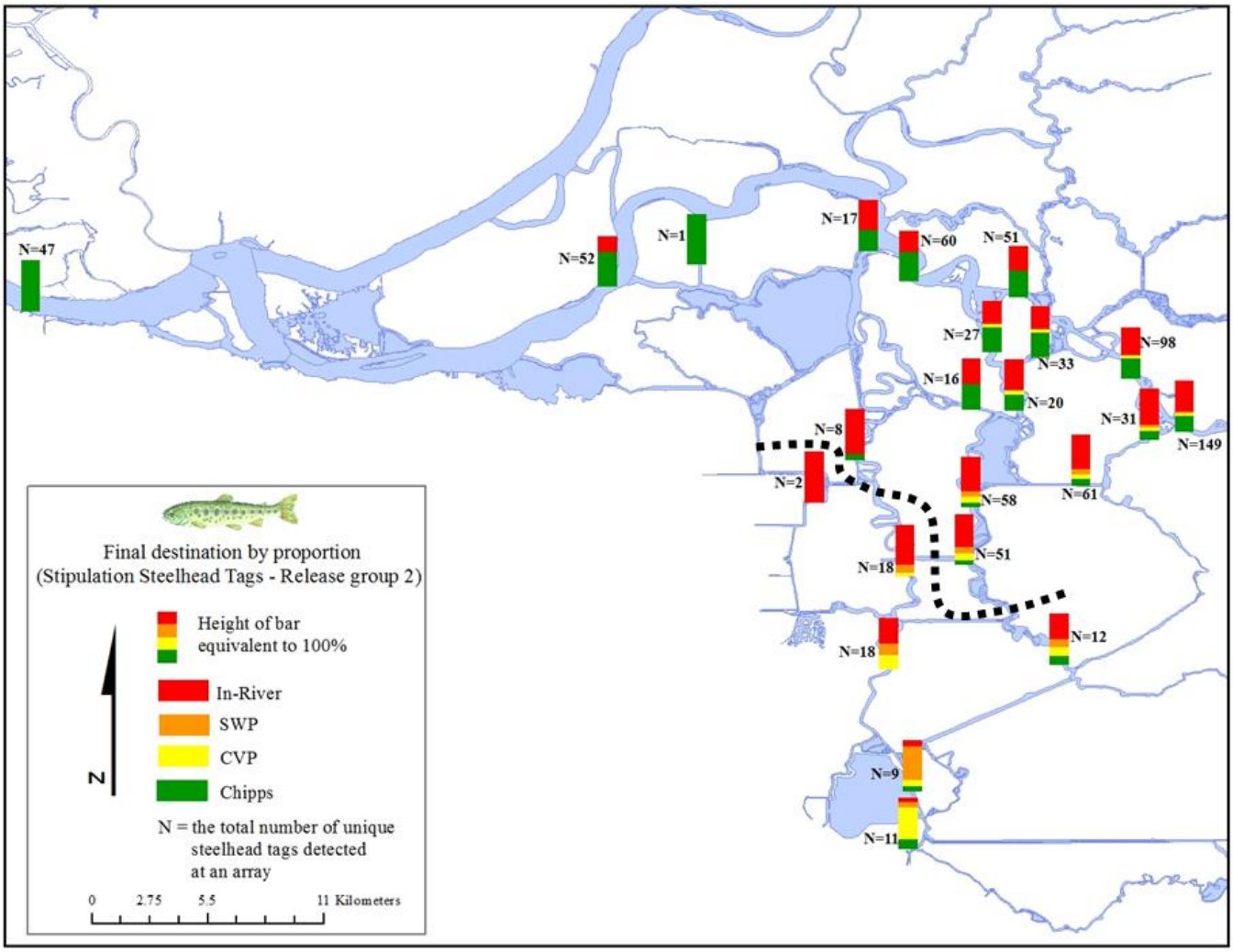

Figure 4-5 **For each array, the proportion of steelhead tags from Release Group 2 last detected at one of four destinations (CVP, SWP, Chipps Island, or in-river).** Successfully salvaged tags were recorded at Chipps Island. The sample size (N) for each array is denoted next to each bar. See Table 4-4 for the source data. The dashed black line indicates the "point of no return," the southern-most locations where at least one steelhead tag successfully arrived at Chipps Island without assistance through salvage.

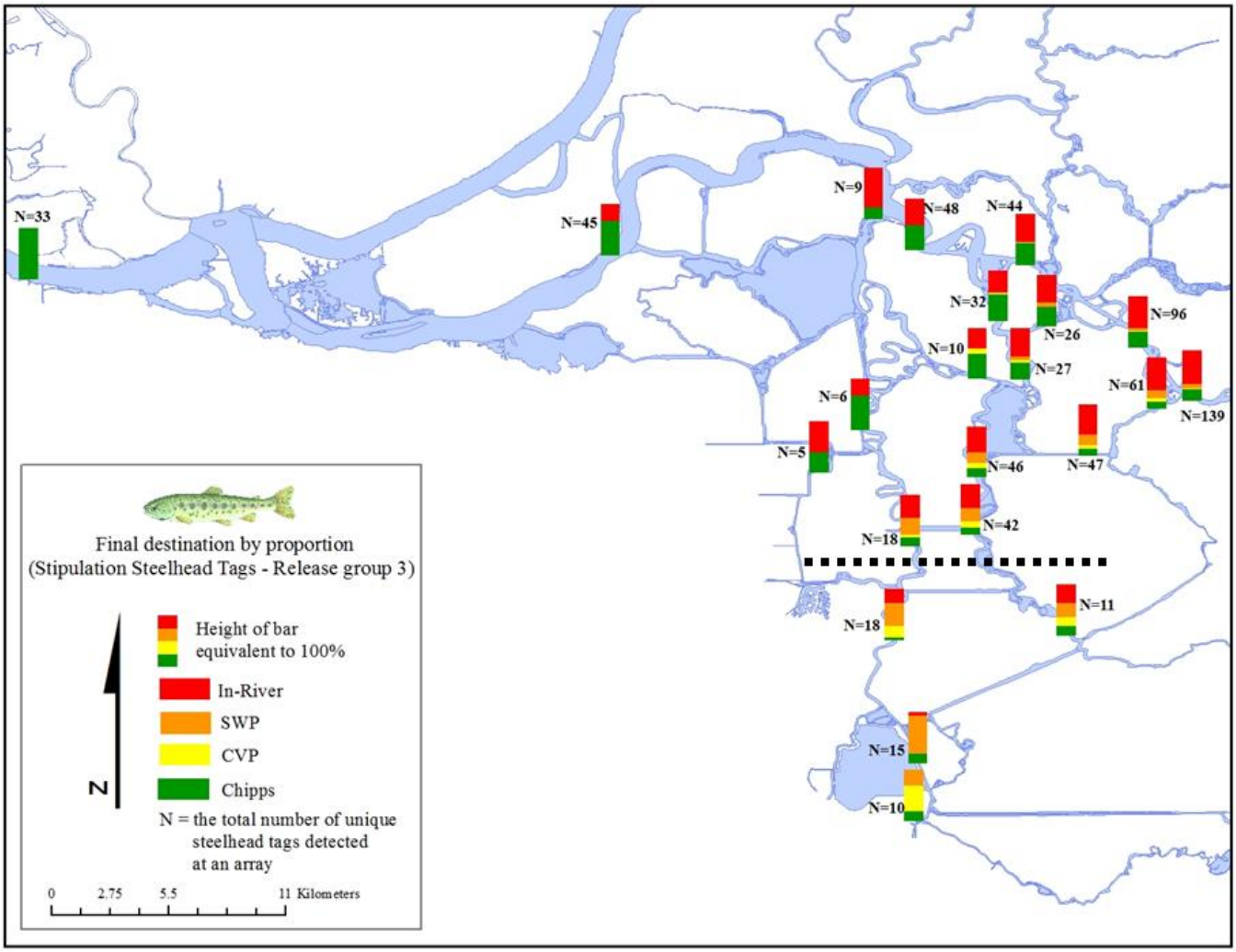

Figure 4-6 **For each array, the proportion of steelhead tags from Release Group 3 last detected at one of four destinations (CVP, SWP, Chipps Island, or in-river).** Successfully salvaged tags were recorded at Chipps Island. The sample size (N) for each array is denoted next to each bar. See Table 4-4 for the source data. The dashed black line indicates the "point of no return," the southern-most locations where at least one steelhead tag successfully arrived at Chipps Island without assistance through salvage.

Table 4-4 For each array, the percent of steelhead tags last detected at one of four destinations (CVP, SWP, Chipps Island, or in-river). Successfully salvaged tags were recorded at Chipps Island (array 24). The tags recorded as having the destination at SWP were last detected at array 20, which is the array upstream and downstream of the radial gates of Clifton Court Forebay. The tags last detected at CVP were last detected at array 21. The tags recorded as in-river were not detected last at array 20, 21, or 24.

Array	Chipps Island			In-River			CVP			SWP		
	Group 1	Group 2	Group 3	Group 1	Group 2	Group 3	Group 1	Group 2	Group 3	Group 1	Group 2	Group 3
1	22.4	30.9	22.3	70.7	60.4	66.9	4.1	4.7	2.9	2.7	4.0	7.9
2	28.4	40.8	32.3	65.3	53.1	61.5	4.2	4.1	1.0	2.1	2.0	5.2
3	46.7	51.0	43.2	44.4	49.0	54.5	4.4	0.0	2.3	4.4	0.0	0.0
4	52.4	58.3	47.9	42.9	41.7	52.1	2.4	0.0	0.0	2.4	0.0	0.0
5	46.2	41.2	22.2	53.8	58.8	77.8	0.0	0.0	0.0	0.0	0.0	0.0
6	4.2	16.1	13.1	83.3	71.0	63.9	8.3	6.5	8.2	4.2	6.5	14.8
7	16.4	14.8	12.8	72.7	67.2	59.6	5.5	8.2	8.5	5.5	9.8	19.1
8	16.0	10.3	17.4	64.0	67.2	50.0	12.0	12.1	10.9	8.0	10.3	21.7
9	11.4	9.8	14.3	68.2	64.7	47.6	13.6	13.7	11.9	6.8	11.8	26.2
10	0.0	16.7	18.2	16.7	50.0	36.4	66.7	16.7	18.2	16.7	16.7	27.3
11	26.1	48.5	38.5	69.6	45.5	53.8	4.3	6.1	0.0	0.0	0.0	7.7
12	13.8	30.0	33.3	72.4	60.0	55.6	10.3	10.0	3.7	3.4	0.0	7.4
13	23.3	48.1	53.1	66.7	44.4	43.8	6.7	7.4	3.1	3.3	0.0	0.0
14	33.3	50.0	50.0	61.1	50.0	40.0	5.6	0.0	10.0	0.0	0.0	0.0
15	28.6	12.5	66.7	71.4	87.5	33.3	0.0	0.0	0.0	0.0	0.0	0.0
16	0.0	0.0	16.7	89.7	77.8	44.4	3.4	5.6	5.6	6.9	16.7	33.3
17	0.0	0.0	40.0	100.0	100.0	60.0	0.0	0.0	0.0	0.0	0.0	0.0
18	0.0	0.0	0.0	0.0	0.0	0.0	0.0	0.0	0.0	0.0	0.0	0.0
19	0.0	0.0	5.6	68.2	50.0	27.8	13.6	27.8	22.2	18.2	22.2	44.4
20	0.0	11.1	20.0	16.7	11.1	6.7	16.7	11.1	0.0	66.7	66.7	73.3
21	0.0	18.2	20.0	30.8	9.1	0.0	46.2	63.6	50.0	23.1	9.1	30.0
22	72.7	67.3	66.7	27.3	32.7	33.3	0.0	0.0	0.0	0.0	0.0	0.0
23	0.0	100.0	0.0	100.0	0.0	0.0	0.0	0.0	0.0	0.0	0.0	0.0
24	100.0	100.0	100.0	0.0	0.0	0.0	0.0	0.0	0.0	0.0	0.0	0.0

As expected, the proportion of steelhead tags last detected at Chipps Island or at either export facility (arrays 20 and 21) increased as tags approached each of these final destinations across all release groups (Figure 4-4 to Figure 4-6 and Table 4-4). In other words, as steelhead tags approached their final destination, the arrays closer to that destination showed a higher relative proportion of tags with that final destination. The proportion of tags at the export facilites that were successfully salvaged and were ultimately recorded at Chipps Island (indicated by green bar) was zero for Release Group 1, while successfully salvaged tags that were detected at the export facilities ranged from 11 to 20% for Release Groups 2 and 3. If OMR flows tested were driving salvage success, we would have expected salvage success to be different for Release Group 3 versus 1 and 2. However, the observed differences appeared to be driven by factors other than OMR flows.

Additionally, we wanted to examine the "point of no return" for steelhead tags by identifying at what point steelhead tags in the interior Delta no longer arrived at Chipps Island without assistance (through salvage operations at export facilities). For each release group figure (Figure 4-4 to Figure 4-6), we demarcated a line indicating the southern-most locations where at least one steelhead tag succesfully arrived at Chipps Island without assistance through salvage. If OMR flows tested had a large influence on the "point of no return" for steelhead, we would expect this line to move north for Release Group 3 versus 1 and 2, indicating a larger influence of pumping facilities when OMR flows were more negative.

The "point of no return" for steelhead tags was identical between Release Groups 1 and 2, and slightly more to the south for Release Group 3. This result is the opposite of our expectation that the more negative OMR flows occuring during Release Group 3 would lead to a larger zone of infuence of export pumping, with the "point of no return" moving more north. This finding indicated that the different levels of OMR flows examined in this study likely did not influence the ability of steelhead tags in the interior Delta to return to the Mainstem San Joaquin River and reach Chipps Island without assistance.

A potential bias influencing the "point of no return" demarcation was the small sample sizes of steelhead tags at interior Delta arrays. As indicated in Figure 4-1 and Table 4-1, the proportion of overall tags that reached arrays near the export facilities was very low. Therefore, our ability to precisely identify the "point of no return" line for each release group was limited.

4.1.5 WEB-BASED DETECTION HISTORY

A web-based dissemination tool was created to spatially display the full detection history of individual steelhead tags. The application was built in Shiny (RStudio Inc. 2013), which is a statistical package from RStudio for the program R (R Project 2013). The base map type used (e.g., terrain, satellite) and the size of the map can be controlled by the user (Kahle and Wickham 2013). The data can be sorted in a variety of ways, such as by serial number, by release group, or final detection location (export facilities and/or Chipps Island). The speed at which data can be displayed is also controlled by the user. As the application runs, static information is displayed in the top-right panel that includes the fish serial number, release group, release date, and whether it was detected at the export facilities and/or at Chipps Island. Below that panel is dynamic information that changes as the application shows each array where the steelhead tag was detected. This information includes the array number, the arrival and departure date and time for that array, number of detections, and residence time spent at the current array. The bottom-right panel displays the number of days since the tag was last detected at that array after its release. This web-based tool can be viewed at: http://glimmer.rstudio.com/hinkelman/stip-study/.

4.1.6 MOVEMENT OF STEELHEAD TAGS VERSUS SIMULATED PARTICLES

The distance that steelhead travel through the Delta in a certain amount of time not only determines their speed but also probably their survival (Sections 4.2.2 and 4.2.3). Therefore, managers are very interested in being able to predict the distance and destination of migrating steelhead smolts, as well as for other species. The DSM2 PTM was used to predict this information and design this experiment (NMFS 2012). Therefore, we developed the following hypothesis to examine if the DSM2 Hydro PTM model could predict the distance travelled by steelhead tags:

Hypothesis 4.1.6: The distance traveled by steelhead tags was not significantly different than the distance traveled by the passive particles.

METHODS FOR TESTING HYPOTHESIS 4.1.6

The distances traveled by simulated particles and steelhead tags observed 3 and 7 days after their release date were compared to evaluate the efficacy of using neutrally bouyant simulated particles to mimic steelhead tag behavior. The final location of a tag or a particle was the array where the tag or particle was last known to be on

the day of interest (day 3 or 7) according to the acoustic telemetry data or the data generated from the DSM2 PTM for tags and particles, respectively. We used all arrays that were located where we had particle data. This led to excluding only a single tag that was detected at array 17 on the 3rd and 7th day (Table 4-5 and Table 4-6).

Particles were released in a similar fashion as were acoustically tagged steelhead. Simulated particles were injected at node 22 (Buckley Cove area) in the DSM2 PTM model at a rate of 1,250 every 3 hours for a total 10,000 particles over 24 hours starting at 3:00 pm on April 15, May 1, and May 15, 2012. The distance to an array that tags or particles were detected was estimated as the Euclidean distance from the array to the release site.

For particles, the DSM2 PTM model run data we were provided did not include the order of arrays that a particle went to nor the arrival and departures time of particles to individual receiver arrays. Thus, we were unable to calculate individual particle distances and had to rely on the relative particle flux across receiver arrays. The proportion of particles at each receiver array on the day of interest was scaled to the number of steelhead tags present on that day to have equal sample sizes of distances for particles and tags. Also, we assumed that all particles were released on the second day of a release group because we could not track individual particle histories.

A t-test was used to determine if significant differences existed between the distances traveled by the particles and steelhead tags. The datasets from the two days of interest (day 3 and 7) were analyzed separately.

Table 4-5 The Euclidean distance (km) of each array from the release site and the percentage of simulated particles and steelhead tags at that array on the third day after their release.

Array	Euclidean Distance from Release (km)	Particle Percentage	Tag Percentage
1	3.8	0.0	14.9
2	5.8	50.2	14.1
3	9.3	0.0	4.0
4	11.4	0.0	10.9
5	12.7	0.3	2.5
6	4.6	26.4	3.6
7	6.3	0.0	6.9
8	8.5	0.0	4.7
9	8.9	1.4	4.7
10	8.5	4.4	1.4
11	7.9	5.0	0.7
12	7.7	0.1	3.3
13	8.9	1.5	1.4
14	8.8	0.0	4.0
15	10.9	0.0	2.2
16	10.5	0.0	2.2
19	11.7	0.0	3.3
20	14.2	7.5	0.7
21	14.8	1.7	2.2
22	17.9	1.1	9.4
24	31.1	0.4	2.9

Table 4-6 The Euclidean distance (km) of each array from the release site and the percentage of simulated particles and steelhead tags at that array on the seventh day after their release.

Array	Euclidean Distance From Release (km)	Particle Percentage	Tag Percentage
1	3.8	0.0	11.8
2	5.8	2.3	6.9
3	9.3	0.0	0.7
4	11.4	0.1	5.6
5	12.7	1.0	0.0
6	4.6	0.2	2.1
7	6.3	0.0	4.9
8	8.5	0.0	4.2
9	8.9	8.4	2.8
10	8.5	11.7	2.1
11	7.9	6.9	2.8
12	7.7	10.7	4.2
13	8.9	43.1	0.7
14	8.8	0.7	2.8
15	10.9	0.0	5.6
16	10.5	1.0	3.5
19	11.7	0.0	2.8
20	14.2	10.1	6.3
21	14.8	2.7	4.2
22	17.9	0.1	9.0
24	31.1	1.0	17.4

RESULTS FOR THE HYPOTHESIS 4.1.6 TEST

As expected, steelhead tags and particles moved farther from the release site of Buckley Cove in relation to days from release (Figure 4-7 and Figure 4-8), as shown by the higher average distance traveled by particles and steelhead tags on day 7 compared to day 3. A t-test found that steelhead tags traveled significantly farther than the particles 3 and 7 days following release. After 3 days, steelhead tags traveled (9.5 km, SE=0.3 km, Table 4-5) significantly farther ($P<0.01$) compared to the particles (6.8 km, SE=0.2 km, Table 4-5). On average, particles only traveled 71.6% (6.8 km / 9.5 km) of the distance traveled by tags after 3 days (Figure 4-7). After 7 days, steelhead tags traveled (13.4 km, SE=0.8 km, Table 4-6) significantly farther ($P<0.01$) compared to the particles (9.5 km, SE=0.2 km, Table 4-6). On average, particles only traveled 70.9% (9.5 km / 13.4 km) of the distance traveled by steelhead tags after 7 days (Figure 4-8).

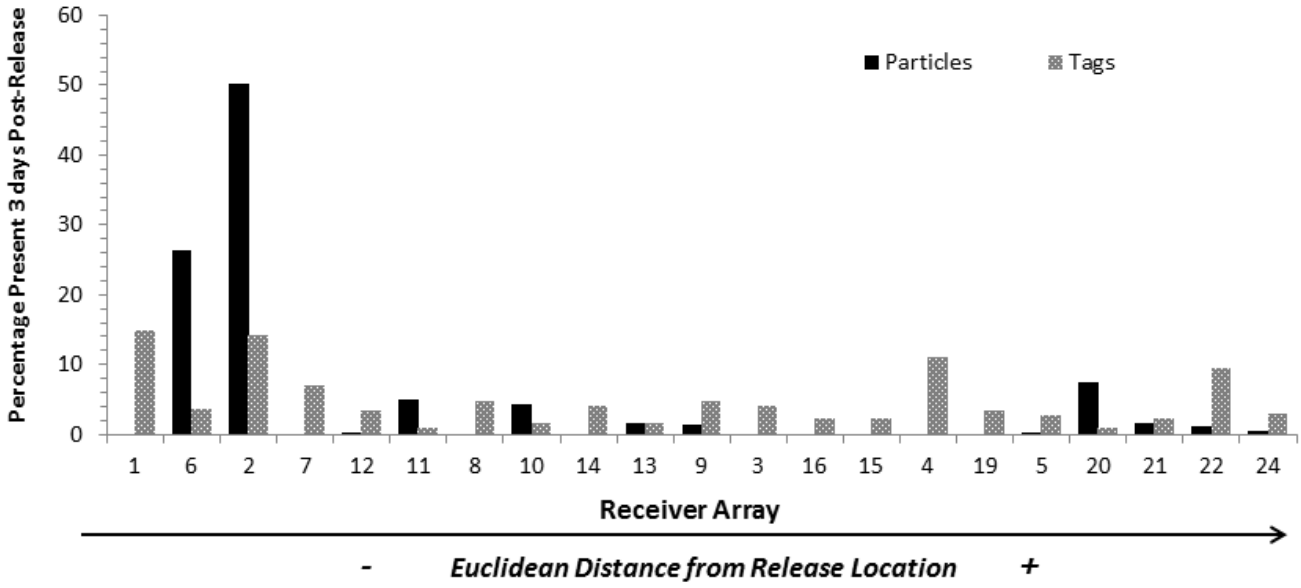

Figure 4-7 **The percentage of steelhead tags and simulated particles at the arrays on the third day after release.** Arrays are ordered from shortest Euclidean distance (left) to greatest (right) Euclidean distance (km) from the release site of Buckley Cove.

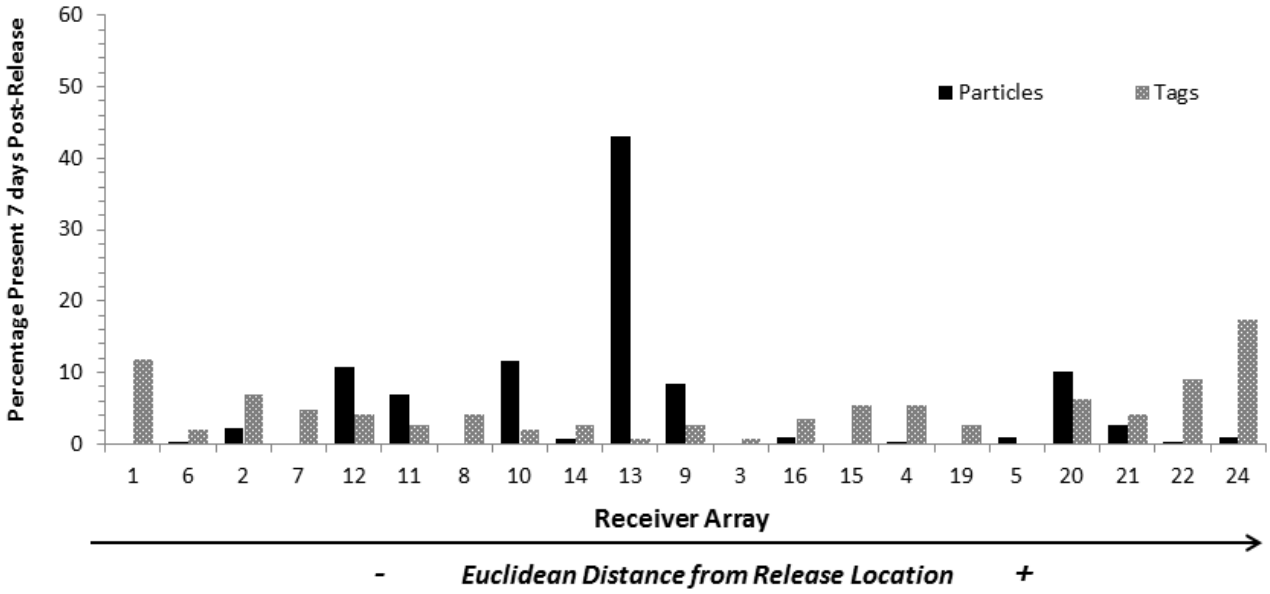

Figure 4-8 **The percentage of steelhead tags and simulated particles present at the arrays on the seventh day after release.** Arrays are ordered from shortest Euclidean distance (left) to greatest (right) Euclidean distance (km) from the release site of Buckley Cove.

Steelhead tags moved much faster than simulated neutrally bouyant particles. This appears to show evidence that steelhead tags either selectively moved with the tides or exhibited constant directed movement while moving

through the Delta to travel faster than the water. The next hypothesis (Section 4.1.7) specifically examined if steelhead tags exhibited STST behaviors.

Because we could not determine the exact release time of particles, we assumed that all particles were released on the second day of a release period. Therefore, distances traveled by particles were likely overestimated because particles released on the first day of a release group traveled for longer than 3 days before the distance measurement was calculated. However, because we found that steelhead tags traveled farther than particles, this bias did not affect the outcome of this analysis.

In additon to differences in speed between particles and steelhead tags, the final locations of particles and steelhead tags were very different 7 days following release. Nearly all particles (91%) ended up at one of six arrays in the interior Delta (arrays 12, 11, 10, 13, 9, 20) 7 days following release. Conversly, the final locations of steelhead tags after 7 days were spread out across 20 of 21 arrays, with single-digit percentages occuring at 19 of the 21 arrays. Also, a much higher percentage of steelhead tags (17.4%) were ultimately detected at Chipps Island versus particles (1%). These results show evidence that the PTM inaccurately predicts the final location of steelhead, as well as their speed.

4.1.7 SELECTIVE TIDAL-STREAM TRANSPORT

Whether the migration of juvenile salmonids is passive, partly active, or active has been debated for decades (Martin et al. 2009 and references therein). Because acoustically tagged steelhead tags moved significantly faster than passive particles (see Section 4.1.6), this could indicate that steelhead are undergoing active migration (i.e., swimming downstream irrespective of tidal conditions) or selectively moving with the tides. These fish may exhibit behaviors that allow them to move faster than they would if they were simply passive particles drifting with the water and the processes that control the flow of water, such as tides. Anadromous fish are known to use STST, including salmonids (Moore et al. 1995, Martin et al. 2009). STST behaviors are those where fish actively move into high and low/no flow conditions to facilitate movement up- or downstream. Clements et al. (2012) hypothesized that salmonid smolts move into low-velocity areas during flood tides and into the highest velocity areas during the ebb tides.

The interpretation of results from DSM2 Hydro PTM for management purpose commonly assumes that acoustically tagged salmonids move in a similar manner to passive particles driven purely by hydrodynamics. While this assumption is commonly used for modeling the movement of aquatic species, even in peer-reviewed literature (e.g., Kimmerer and Nobriga 2008), this assumption was probably not accurate for most species including juvenile steelhead (see Section 4.1.6). In particular, salmonids have a complex set of behaviors in response to both biotic (e.g., predators) and abiotic factors (e.g., temperature, salinity, tides). For example, juvenile steelhead that want to reach the ocean as quickly as possible could achieve this by moving into fast-flowing surface waters during ebb tides and moving to lower velocity flows on the flood tides by moving to the sides of the water body or moving to deeper waters (Clements et al. 2012). Moore et al. (1995) found that Atlantic salmon (*Salmo salar*) smolts exhibited a nocturnal, selective ebb tide transport pattern of migration. Therefore, in this analysis, we examined if acoustically tagged juvenile steelhead used STST, and in the next analysis we examined if they migrate more nocturnally or diurnally.

Hypothesis 4.1.7: Steelhead tags did not move using STST.

METHODS FOR TESTING HYPOTHESIS 4.1.7

Following the suggested methods in Appendix 2.2 of the 2012 IRP LOO Annual Review (Kneib et al. 2012), we attempted to estimate φ, which is the contribution of STST behavior to migration (Anderson et al. 2005). Whether a steelhead tag is exhibiting STST behavior or active directed swimming is determined by the value of φ. This value is generated by subtracting the mean particle velocity from the mean velocity of tags, and this product is divided by the root-mean-square (RMS) tidal velocity. If this value, φ, is greater than 0.5, then it is evidence of

active directed swimming in the seaward direction. If φ is 0.5, smolts are effectively hiding in zero-velocity areas during the entire flood tide and drift downstream during the ebb tide. If φ is less than 0.5, this indicates that tidal selective movement occurs during only part of the flood tide and/or that the smolts move into low velocity, but not zero-velocity, areas on the flood tide. A φ of 0 indicates passive drift of smolts.

We calculated the mean velocity of particles as predicted by the DSM2 PTM model and steelhead tags between arrays 1 and 7 (Figure 2-3) for the tags detected at both arrays in that order. We calculated φ with the following equation: (*U*-*V*) / (*RMS tidal velocity*). *U* is the mean velocity of steelhead tags estimated between arrays 1 and 7, and *V* is the mean velocity of particles that was estimated by conducting the following steps:

- In each of the three PTM runs, 10,000 particles were released from node 25 (array 1) at 1:30 am on the second day of the fish release periods (April 16, May 2, and May 16, 2012).
- We identified the particle flux at node 143 (array 7) at the end of each model run and identified how long before at least half of this value was predicted for node 143 (array 7) in each model run and then subtracted 15 minutes from this number to get an estimate of mean travel time for particles. Because it is unclear when during the time interval that half the particles passed node 143, we chose to err on the side of overestimating mean particle velocity by assuming that they arrived at the beginning of the last 15-minute interval (by subtracting 15 minutes).
- We calculated this value from each of the three new PTM runs that corresponded to the study periods of the three release groups and averaged these three values to estimate the mean travel time of particles. Then, to estimate the mean velocity of particles, we divided 5,660 m by the mean travel time.

To calculate the RMS tidal velocity, we gathered data from the Turner Cut CDEC station (CDEC 2013). The average RMS tidal velocity across the three release groups was calculated for the 5 days after the release of fish (3:00 pm on the day that releases began until 2:45 pm on the fifth day after).

RESULTS FOR HYPOTHESIS 4.1.7

Steelhead tags seemed to exhibit limited STST behavior (φ=0.39), as shown in Table 4-7. This suggests that at least in one reach of the Delta, steelhead were exhibiting STST behavior, with selective movement only occurring during part of the flood tide and/or that the steelhead tags move into low velocity, but not zero-velocity areas on the flood tide.

Table 4-7 The mean velocity of particles, mean velocity of steelhead tags, and root-mean-square tidal velocity, and φ, which is the contribution of STST behavior to migration.

	Estimates
Mean velocity of particles (m/sec):	0.02
Mean velocity of tags (m/sec):	0.07
RMS tidal velocity (m/sec):	0.13
φ:	0.39

This result further illustrates that steelhead tags should not be treated as passive particles when estimating their migration rate. By not accounting for these specific fish behaviors in the movement rules of simulated particles, physically based models cannot predict the movement of this species. There is growing support for no longer having models treat species as passive particles (Metaxas and Saunders 2009, Delaney et al. 2012). We recommend that models used for predicting smolt movement incorporate important behaviors in response to environmental conditions and be validated using biotelemetry data.

This analysis was conducted to address the concern raised in the 2012 IRP LOO Annual Review to include tidal information to better understand the movement patterns of steelhead tags. However, because this analysis required a confined reach of the Delta (to better ensure steelhead tag routing) paired with locally measured hydrodynamic data, we were limited to examining a single reach. Therefore, this analysis was exploratory in nature, and we suggest that future studies (including deployment of tidal velocity monitoring stations necessary to collect site-specific data) be conducted to quantify this behavior on a larger scale in various parts of the Delta.

4.1.8 DIURNAL MOVEMENT PATTERNS

Another behavior that could be important in understanding the migration, routing, and survival of steelhead is whether steelhead are migrating more during the day or night. Because migrating steelhead are vulnerable to visual ambush predators, such as striped bass (*Morone saxatilis)*, it may be beneficial for steelhead to migrate during the nighttime to reduce their chance of being preyed upon. However, the limited studies of activity patterns of steelhead show that they are more active during the day (Bégout Anras and Lagardère 2004, Chapman et al. 2013).

Hypothesis 4.1.8: The movement of steelhead tags in the San Joaquin River and interior Delta was not related to day/night.

METHODS FOR TESTING HYPOTHESIS 4.1.8

The timing of when steelhead tags are first detected at arrays 4 (San Joaquin River) and 9 (interior Delta) was examined for a day/night effect. Two-tail binomial tests were conducted to determine if significantly more steelhead tags were first detected during the day (i.e., 06:00:01–18:00:00) than during the night (i.e., 18:00:01–06:00:00). This exploratory analysis allowed us to examine if there was any evidence that tags were moving more during the day or night. We assumed that if steelhead tags were migrating more during the day, then a significantly greater proportion of tags would be first detected during the daytime. Similarly, we assumed that if steelhead tags were migrating more during the night, then a significantly greater of proportions of tags would be first detected during the nighttime.

RESULTS FOR HYPOTHESIS 4.1.8

We found that 46.7% and 62.8% of steelhead tags were first detected during the day (06:00:01–18:00:00) at arrays 4 and 9, respectively. Given the different results found between the two arrays, we analyzed all 23 arrays where Stipulation Study steelhead tags were detected and analyzed for this hypothesis (Table 4-8). Array 18 did not detect any steelhead tags deployed for the Stipulation Study and therefore was not examined in the analysis. When we examined all the arrays, only 34.8% of the arrays had more tags detected during the day than during the night (Table 4-8).

There seems to be a spatial pattern in significant results for steelhead tags released for the Stipulation Study (Figure 4-9). At many of the arrays (arrays 2, 3, 11, 22, and 24) along the San Joaquin River, significantly ($P<0.05$) more Stipulation Study steelhead tags were first detected during the night. Conversely, some arrays (arrays 8, 9, 10, and 12) in the southeast section of the study area had significantly ($P<0.05$) more tags first detected during the day. Arrays 7 and 20, also in the southeast section of the study area, had marginally significantly (i.e., $0.05 \geq P \leq 0.10$) more steelhead tags first detected during the day.

There is some evidence for a spatial pattern in diurnal steelhead tag movements. However, the mechanism for this pattern is unknown and should be further examined in future studies. A potential bias in diurnal timing data is the possible ingestion of steelhead tags by predators. The spatial pattern observed in diurnal movements may be due to spatial patterns in predation. For example, if more predation is occurring in the interior Delta versus the Mainstem, the diurnal patterns in movement may be the result of differences in predator versus steelhead

movement behavior. However, this relationship is purely speculative, and future studies specifically designed to examine diurnal movement behavior should be conducted to understand the underlying mechanism.

Table 4-8 For each array, the number of Stipulation Study steelhead tags that were first detected during the daytime and nighttime, the total number of tags detected, the proportion of tags first detected during the daytime and nighttime, and the two-tail P-value from the binomial test to see if more tags were detected during the day or night.

Array	Tags first detected between 06:01-18:00	Tags first detected between 18:01-06:00	Total number of tags	Percent first detected during the day	Percent first detected during the night	P-value
1	215	220	435	49.4	50.6	0.85
2	109	180	289	37.7	62.3	<0.01
3	51	89	140	36.4	63.6	<0.01
4	70	80	150	46.7	53.3	0.46
5	15	24	39	38.5	61.5	0.20
6	49	67	116	42.2	57.8	0.11
7	94	69	163	57.7	42.3	0.06
8	90	64	154	58.4	41.6	0.04
9	86	51	137	62.8	37.2	<0.01
10	25	4	29	86.2	13.8	<0.01
11	25	57	82	30.5	69.5	<0.01
12	49	27	76	64.5	35.5	0.02
13	39	50	89	43.8	56.2	0.29
14	24	20	44	54.5	45.5	0.65
15	12	16	28	42.9	57.1	0.57
16	32	33	65	49.2	50.8	1.00
17	4	9	13	30.8	69.2	0.27
19	32	26	58	55.2	44.8	0.51
20	20	10	30	66.7	33.3	0.10
21	13	21	34	38.2	61.8	0.23
22	49	81	130	37.7	62.3	0.01
23	0	2	2	0.0	100.0	0.50
24	30	83	113	26.5	73.5	<0.01

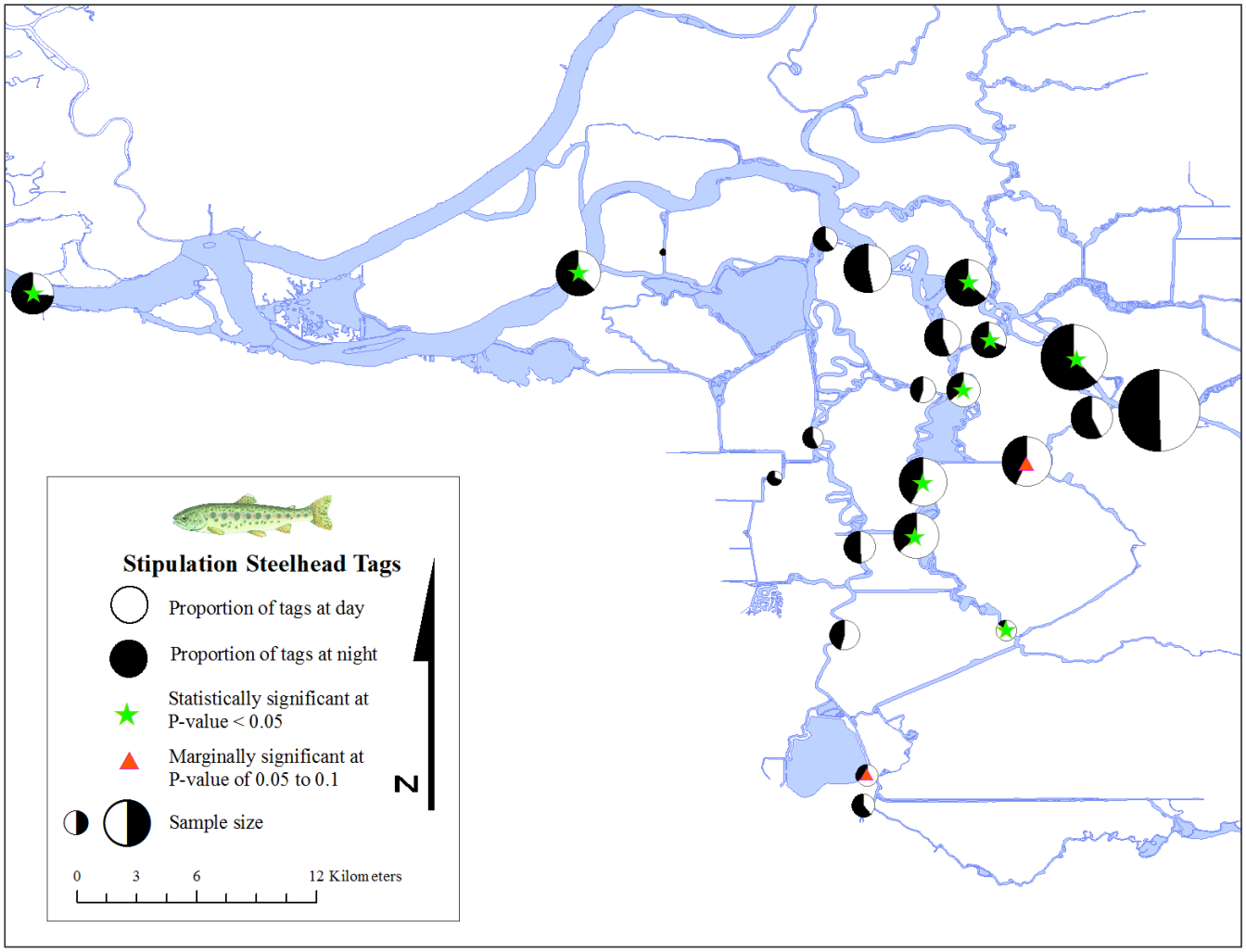

Figure 4-9 **The proportion of steelhead tags deployed for the 2012 Stipulation Study first detected during the day or night.** The size of the pie chart is scaled to the number of tags detected at each of the arrays. The white portion of the pie chart is the percent of tags detected during the day (i.e., 06:00:01–18:00:00), and the black portion is the percent of tags detected during the night (i.e., 18:00:01-06:00:00). The green star indicates the result for that array is significant as determined by the two-tail P-value from the binomial test. The red triangle indicates the result for that array is marginally significant as determined by the two-tail P-values from the binomial tests.

4.2 ROUTE-LEVEL ANALYSES

In this section, we examine how steelhead tags moved and survived through the Delta using different defined routes. We built a multistate statistical release-recapture model to estimate receiver detection probabilities, route entrainment probabilities, transition probabilities, and survival probabilities. In analyses not using the model we estimated if travel times of steelhead tags were affected by the different OMR flow conditions examined in this study.

4.2.1 ROUTE-SPECIFIC TRANSITION PROBABILITIES

To properly manage a species and promote its survival through the Delta, we hypothesize that we need to know if the survival of a species varies between different routes. Also, we hypothesize that certain OMR flows may foster more favorable conditions for the survival of the species. If the survival of steelhead varies between routes and/or release groups, we can try to re-create conditions or promote the use of specific routes through specific OMR flows that will result in increased steelhead survival.

Hypothesis 4.2.1: Route-specific transition probabilities of steelhead tags were not significantly related to the route taken and/or release group.

METHODS FOR TESTING HYPOTHESIS 4.2.1

To estimate detection probabilities, route entrainment, survival, and transition probabilities, we built a multistate statistical release-recapture model in the program USER (Lady et al. 2008), which is similar to those developed by Perry et al. (2010), SJRGA (2011, 2013), and Buchanan et al. (2013). For the Stipulation Study model, we used all steelhead tags that were detected at array 1 (Figure 2-3). Last detection data were used in the model, as was done in previous modeling efforts (e.g., Buchanan et al. 2013).

Originally, we intended to include release group as a covariate in the model to examine how survival and routing differed between release groups or OMR flow levels (Groups 1 and 2 versus Group 3). However, during the model fitting process, USER failed to converge on individual release group models and only converged and provided parameter estimates and standard errors for the pooled data from all release groups. Therefore, the following methods and results reflect a model that combined all data across release groups (i.e., release group were not included as a covariate).

Acoustic receiver coverage and detection data informed the delineation of fish routes from approximately Stockton to Chipps Island (including through the interior Delta and south Delta salvage facilities). In the analysis, we examined six primary fish routes to estimate route-specific transition probabilities. Route-specific transition probability is a measure of the number of steelhead tags that went through a route and survived. Therefore, the complement of route-specific transition probability is not just mortality but is mortality, using a different route, or not reaching Chipps Island in 15 days. However, 94% of the steelhead tags that reached Chipps Island did so in the 15 days after their release, therefore the complement of route-specific transition probability is mainly mortality and the probability of using a different route. The following are the six defined routes (for points of reference listed below, refer to Figure 1-1):

- Turner Cut to Chipps Island area (Figure 4-10).
- Route to Chipps Island area without using Turner Cut (Figure 4-11).
- Turner Cut to Chipps Island area via SWP (Figure 4-12).
- Route to Chipps Island area via SWP without using Turner Cut (Figure 4-13).
- Turner Cut to Chipps Island area via CVP (Figure 4-14).
- Route to Chipps Island area via CVP without using Turner Cut (Figure 4-15).

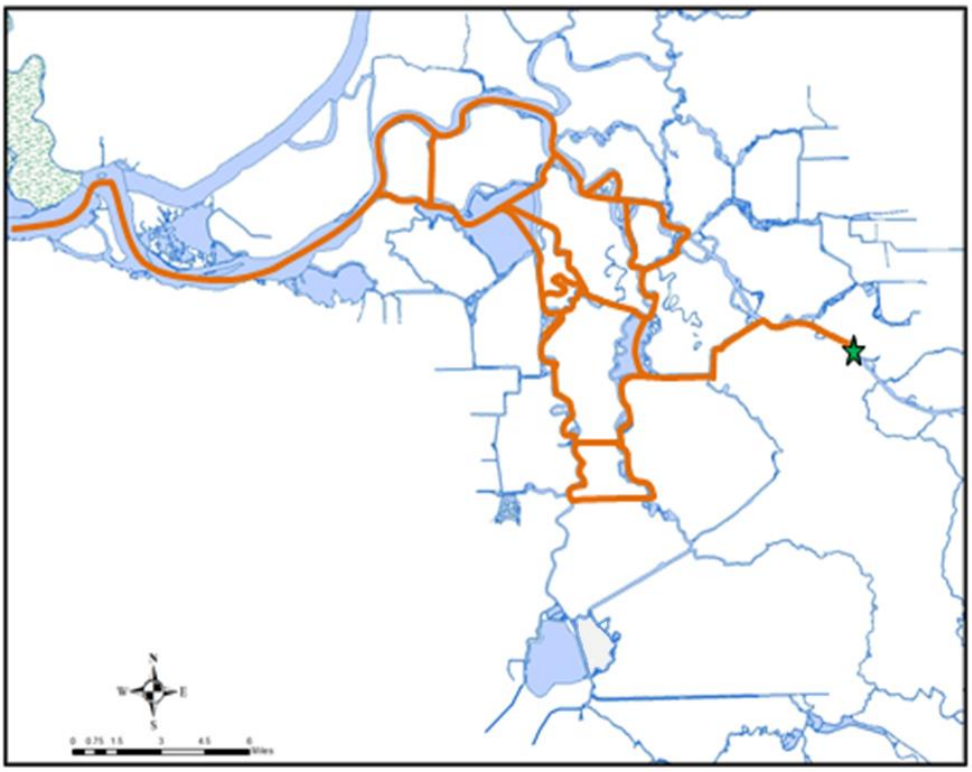

Figure 4-10 **Turner Cut to Chipps Island area route.**

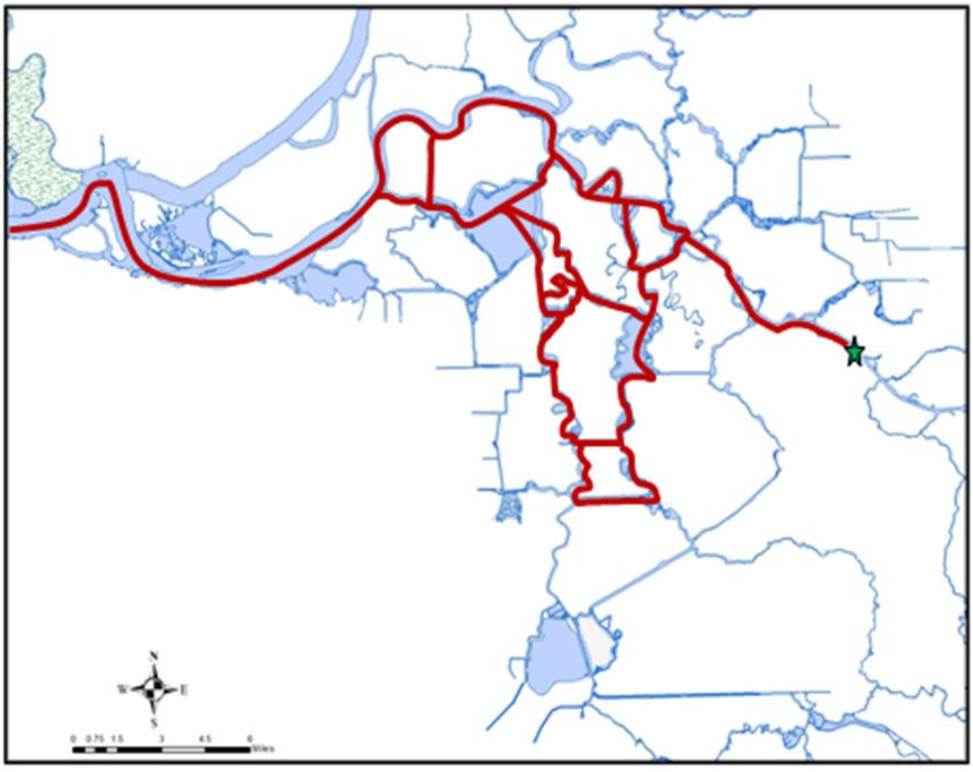

Figure 4-11 **Route to Chipps Island area without using Turner Cut.**

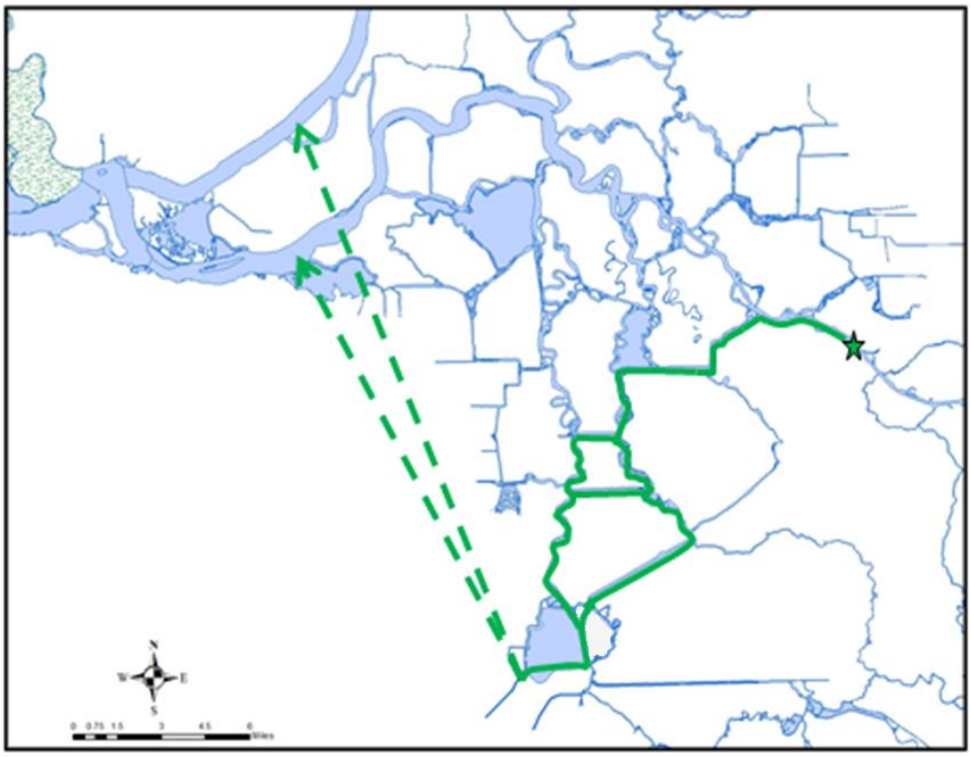

Figure 4-12 **Route using Turner Cut to Chipps Island area via SWP**. Dashed lines represent overland transport of steelhead tags in salvage trucks from an export facility to one of the release sites upstream of Chipps Island.

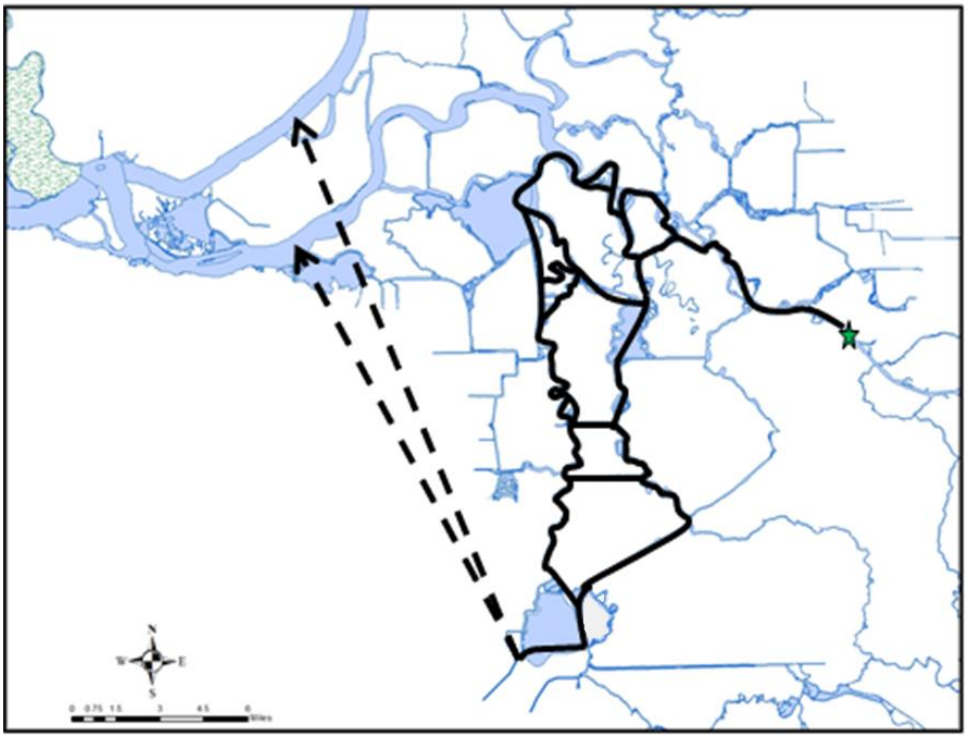

Figure 4-13 **Route to Chipps Island area via SWP without using Turner Cut**. Dashed lines represent overland transport of steelhead tags in salvage trucks from an export facility to one of the release sites upstream of Chipps Island.

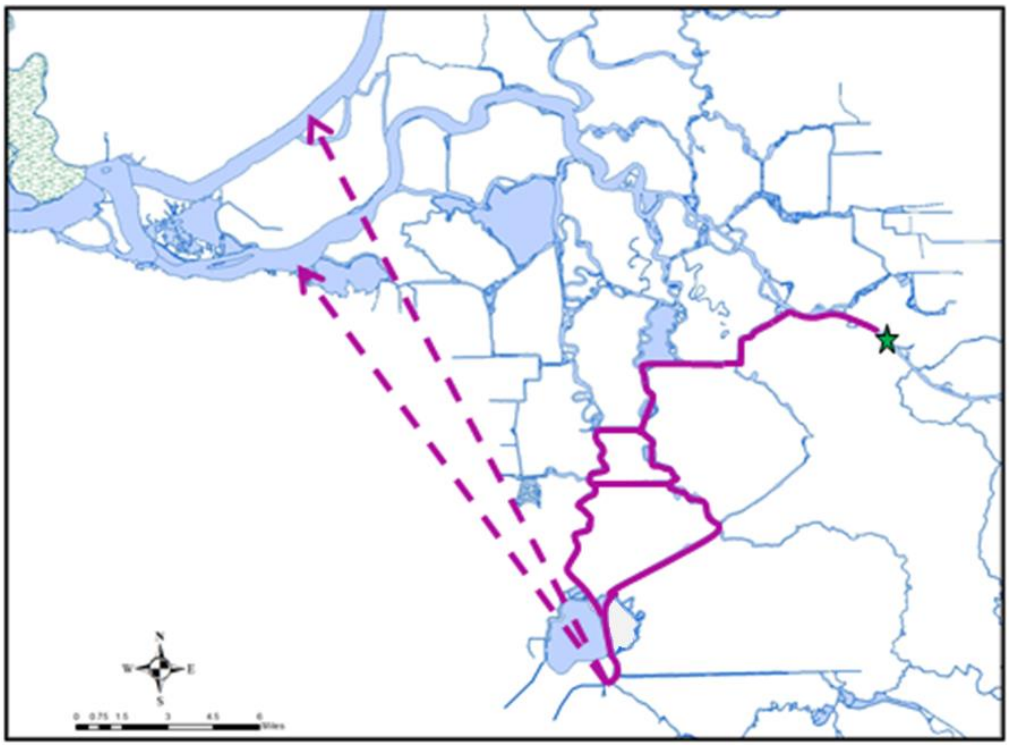

Figure 4-14 **Route using Turner Cut to Chipps Island area via CVP**. Dashed lines represent overland transport of steelhead tags in salvage trucks from an export facility to one of the release sites upstream of Chipps Island.

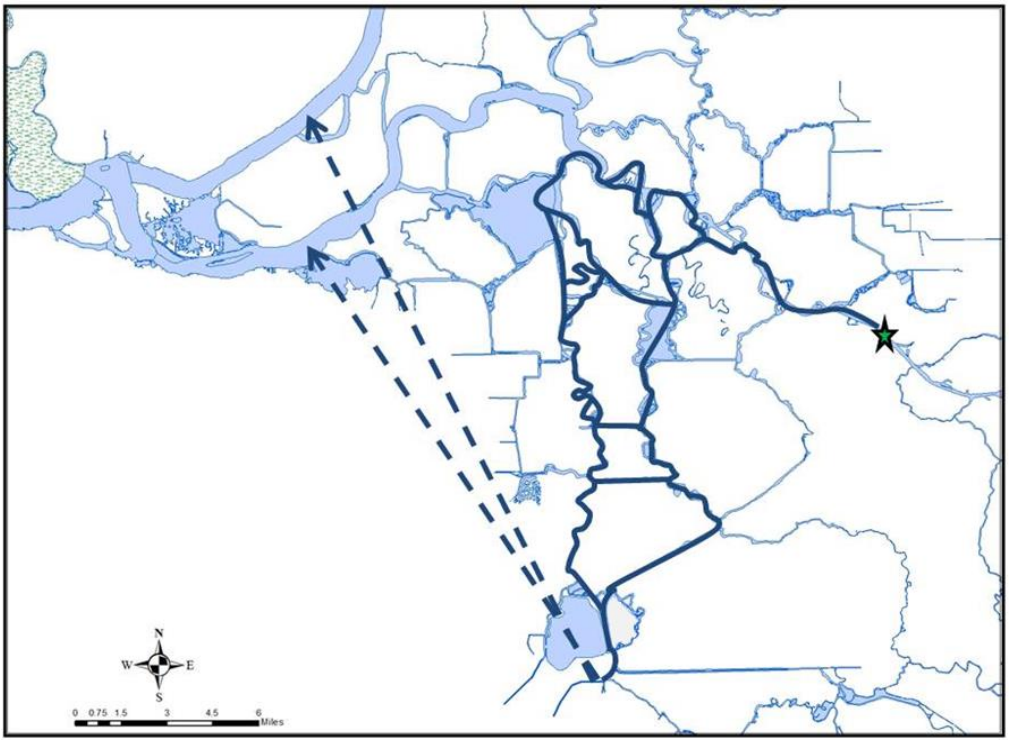

Figure 4-15 **Route to Chipps Island area via CVP without using Turner Cut**. Dashed lines represent overland transport of steelhead tags in salvage trucks from an export facility to one of the release sites upstream of Chipps Island.

These routes (Figure 4-10 to Figure 4-15) were the basis for selecting a subset of arrays from the arrays deployed for the Stipulation Study and Six-Year Study in the study area (Figure 2-3). Because of the complexity of Delta channels and the lack of a priori consideration of the placement of receiver arrays to test specific routing and survival hypotheses, we eliminated receiver arrays from the analysis that did not allow a calculation of unique route entrainment or reach survival probabilities. For example, incomplete receiver coverage at the San Joaquin River junctions downstream of Turner Cut and in the myriad of channel bifurcations in the interior Delta limited our ability to calculate route entrainment and survival probabilities in these areas. Based on these considerations, the locations of arrays that we used in the model are shown in Figure 4-16, and the locations of each array's individual receivers are described in Table 4-9. Using these arrays, we generated the model schematic shown in Figure 4-17. In the model, we only used steelhead tags that were initially detected at array 1 to remove the expression of handling mortality. This schematic (Figure 4-17) incorporates the six routes, but allowed us to derive a model that balances complexity with clarity.

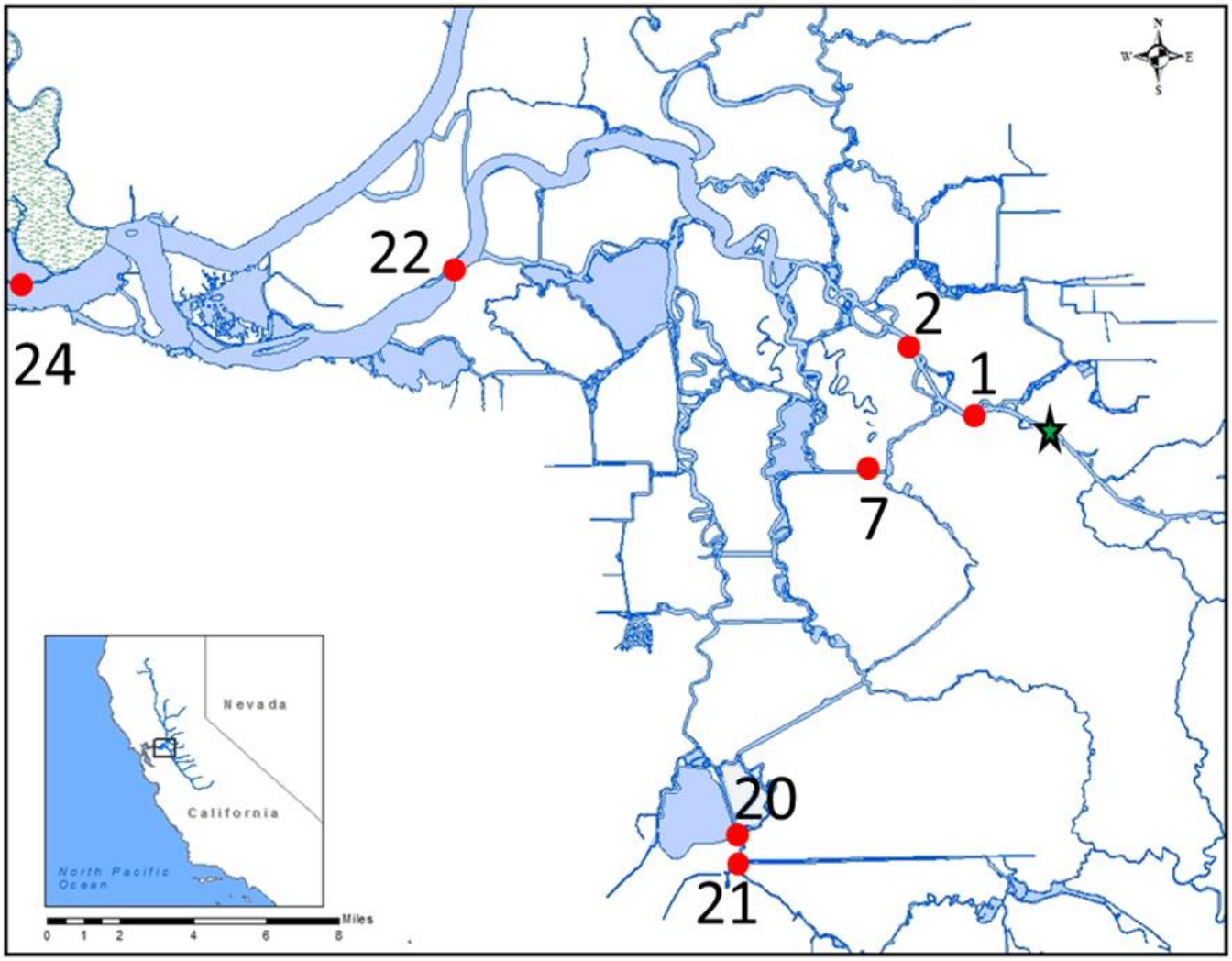

Figure 4-16 The location of acoustic telemetry arrays that were included in the schematic of the multistate statistical model described in Figure 4-17 to estimate route entrainment, survival, detection, and transition probabilities. The green star is where the acoustically tagged steelhead were released for the 2012 Stipulation Study.

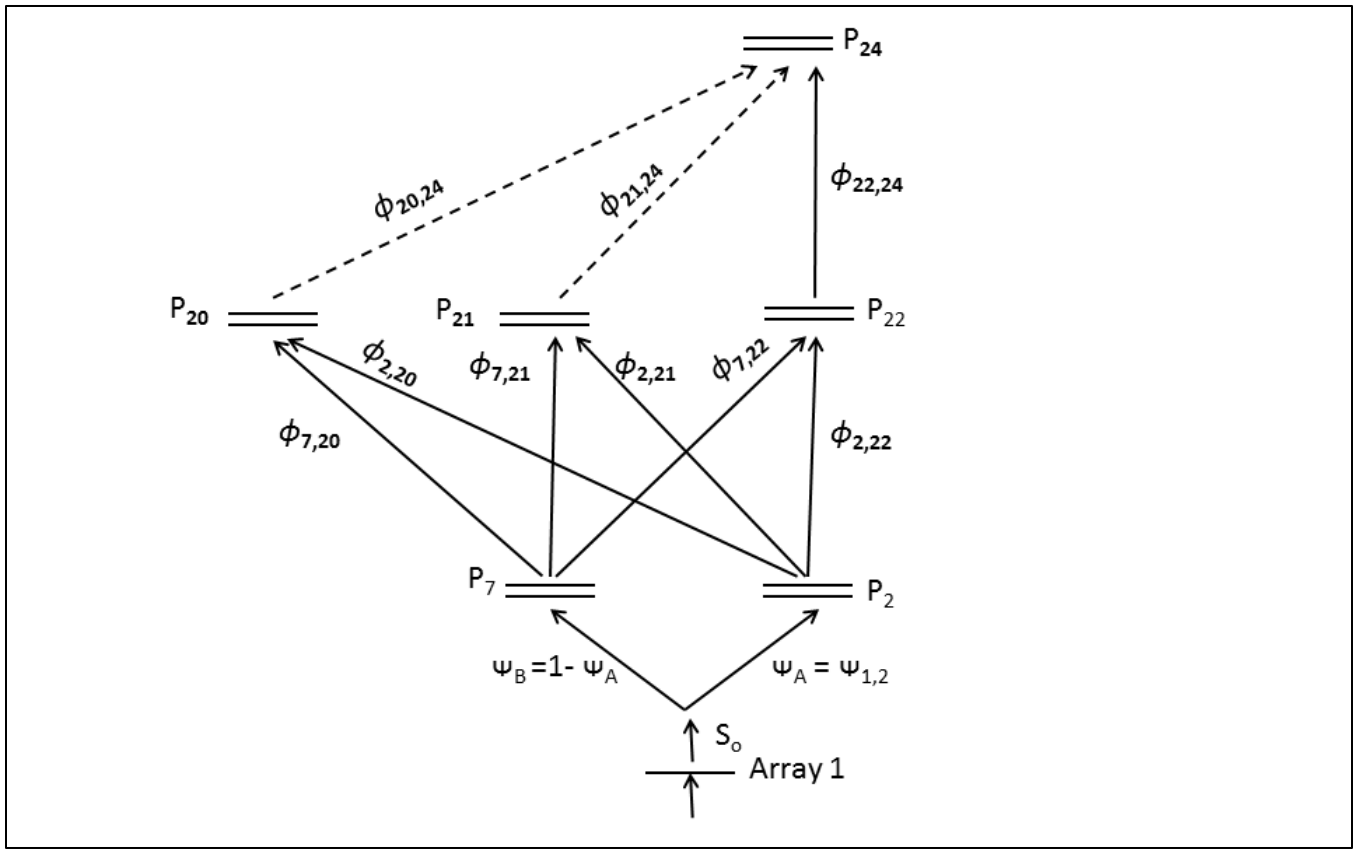

Figure 4-17 **Schematic of the multistate statistical model.** Estimated parameters are the probabilities of survival (S), route entrainment (ψ), transition (ϕ), and detection (P). Single arrays are denoted with a single line where dual rays are shown as double lines. Dashed lines represent overland transport of steelhead tags in salvage trucks from an export facility to one of the release sites upstream of Chipps Island.

Table 4-9 Array number, receiver location upstream or downstream, receiver code, station name, and latitude/longitude (decimal degrees). *Only has one location point available as receivers were deployed very close to each other in a station (e.g., station name "JPE.1a/b" for receivers 300915 and 300916). Data from KMZ (version 19) provided to us by Dr. Josh Israel.

Array	Upstream (A) or Downstream (B)	Receiver Code	Station Name	Latitude	Longitude
1	A	300995	9B	37.9950	-121.4381
1	A	300998	9A	37.9949	-121.4404
2	A	300899	MACU.1	38.0175	-121.4634
2	A	300900	MACD.1	38.0234	-121.4667
2	B	300901	MACU.2	38.0184	-121.4620
2	B	300902	MACD.2	38.0246	-121.4651
7	A	301004	5B	37.9719	-121.4846
7	B	300999	5A	37.9711	-121.4862
20	A	300888	RGU1	37.8301	-121.5566
20	A	300889	RGU2	37.8297	-121.5569
20	B	460009	RGD2-HRR	37.8304	-121.5572
20	B	460010	RGD2-HRR	37.8299	-121.5576
20	B	460011	RGD1-HRR	37.8299	-121.5576
21	A	460012	CVPU-HRR	37.8170	-121.5583
21	A	300895	CVPD	37.8167	-121.5589
21	B	300896	CVPT	37.8158	-121.5591
22	A	300915	JPE.1a*	38.0569*	-121.6850*
22	A	300916	JPE.1b*	38.0569*	-121.6850*
22	A	300917	JPE.2a*	38.0576*	-121.6861*
22	A	300918	JPE.2b*	38.0576*	-121.6861*
22	A	300919	JPE.3a*	38.0561*	-121.6842*
22	A	300920	JPE.3b*	38.0561*	-121.6842*
22	A	300921	JPE.4a*	38.0581*	-121.6873*
22	A	300922	JPE.4b*	38.0581*	-121.6873*
22	B	300923	JPW.1a*	38.0553*	-121.6876*
22	B	300924	JPW.1b*	38.0553*	-121.6876*
22	B	300925	JPW.2a*	38.0560*	-121.6885*
22	B	300926	JPW.2b*	38.0560*	-121.6885*
22	B	300927	JPW.3a*	38.0544*	-121.6870*
22	B	300928	JPW.3b*	38.0544*	-121.6870*
22	B	300929	JPW.4a*	38.0564*	-121.6896*
22	B	300930	JPW.4b*	38.0564*	-121.6896*

Table 4-9 Array number, receiver location upstream or downstream, receiver code, station name, and latitude/longitude (decimal degrees). *Only has one location point available as receivers were deployed very close to each other in a station (e.g., station name "JPE.1a/b" for receivers 300915 and 300916). Data from KMZ (version 19) provided to us by Dr. Josh Israel.

Array	Upstream (A) or Downstream (B)	Receiver Code	Station Name	Latitude	Longitude
24	A	300931	MAE.1a*	38.0474*	-121.9320*
24	A	300932	MAE.1b*	38.0474*	-121.9320*
24	A	300933	MAE.2a*	38.0489*	-121.9304*
24	A	300934	MAE.2b*	38.0489*	-121.9304*
24	A	300935	MAE.3a*	38.0468*	-121.9324*
24	A	300936	MAE.3b*	38.0468*	-121.9324*
24	A	300937	MAE.4a*	38.0507*	-121.9309*
24	A	300938	MAE.4b*	38.0507*	-121.9309*
24	A	300939	MAE.5a*	38.0458*	-121.9328*
24	A	300940	MAE.5b*	38.0458*	-121.9328*
24	A	300941	MAE.6a*	38.0513*	-121.9306*
24	A	300942	MAE.6b*	38.0513*	-121.9306*
24	B	300943	MAW.1a*	38.0480*	-121.9332*
24	B	300979	MAW.1b*	38.0480*	-121.9332*
24	B	300980	MAW.2a*	38.0499*	-121.9331*
24	B	300981	MAW.2b*	38.0499*	-121.9331*
24	B	300982	MAW.3a*	38.0474*	-121.9338*
24	B	300983	MAW.3b*	38.0474*	-121.9338*
24	B	300985	MAW.4a*	38.0518*	-121.9341*
24	B	300986	MAW.4b*	38.0518*	-121.9341*
24	B	300987	MAW.5a*	38.0467*	-121.9352*
24	B	300988	MAW.5b*	38.0467*	-121.9352*
24	B	300989	MAW.6a*	38.0523*	-121.9337*
24	B	300990	MAW.6b*	38.0523*	-121.9337*

In addition to estimating these six route-specific transition probabilities, we also estimated two route-specific survival probabilities (Mainstem and Turner Cut route), route entrainment probability at Turner Cut, and overall Delta survival (see Section 4.2.2 for entrainment and survival results). The equations for each of the transition probability, entrainment, and survival calculations are shown in Table 4-10.

To estimate parameters, we used seed values of 0.1 in a Fletch Quasi-Newton optimizer and an alpha level of 0.05. We used the default settings for the Fletch Quasi-Newton optimizer, which are a maximum of 200 iterations, with a precision of 1e-06, and a proportional step size of 1e-06. For a steelhead tag to be included in the analyses for the model, it needed to be detected at array 1 (Figure 4-17). If a steelhead tag were detected at more than one array on the same level of the schematic (e.g., arrays 7 and 2; Figure 4-17), the tag was considered

to have only been detected by the array on that level of the schematic that last detected the tag. The only exception to this rule was that if a steelhead tag were detected at an export facility and array 22 (Jersey Point), it was considered to be detected at the export facility where it was last detected. For example, if a tag was detected at array 21 then 22 then 24, in the model it would be considered to have been detected at array 21 and then next at array 24. We feel this assumption is valid because otherwise tags that went through salvage and were later detected at array 22 before reaching array 24 (Chipps Island) would not be identified as a "salvaged" steelhead tag because these arrays are on the same level in the model. This would be misleading.

Table 4-10 The codes and equations for route-specific transition probabilities, Turner Cut route entrainment (into the interior Delta), and survival probabilities. Turner Cut route entrainment was fit by model. Terms that start with "ϕ" denote a transition probability, terms that start with "s" denote a route-specific transition probability, terms that start with "S" denote a route-specific survival probability, s0 is the initial survival, terms that start with "Ψ" denote a route entrainment probability and is the parameter that is estimated by the model. The number and letter following one of these terms in the equation are from the array to the next array. For example, ϕ2,22 is the transition probability from 2 to 22 and ϕ2,21 is the transition probability from 2 to 21.

Description of the route	Code	Equation
Turner Cut to Chipps Island area (route-specific transition probability)	sA	ϕ7,22 * ϕ22,24
Route to Chipps Island area without using Turner Cut (route-specific transition probability)	sB	ϕ2,22 * ϕ22,24
Turner Cut to Chipps Island area via SWP (route-specific transition probability)	sC	ϕ7,20 * ϕ20,24
Route to Chipps Island area via SWP without using Turner Cut (route-specific transition probability)	sD	ϕ2,20 * ϕ20,24
Turner Cut to Chipps Island area via CVP (route-specific transition probability)	sE	ϕ7,21 * ϕ21,24
Route to Chipps Island area via CVP without using Turner Cut (route-specific transition probability)	sF	ϕ2,21 * ϕ21,24
Route to Chipps Island without using Turner Cut (route-specific survival probability)	S2C	ϕ2,22 * ϕ22,24 + ϕ2,20 * ϕ20,24 + ϕ2,21 * ϕ21,24
Route to Chipps Island using Turner Cut (route-specific survival probability)	S7C	ϕ7,22 * ϕ22,24 + ϕ7,20 * ϕ20,24 + ϕ7,21 * ϕ21,24
Turner Cut route entrainment	ΨB=1-ΨA	Fit by model
Overall survival	STotal	s0*(ΨA * sB + ΨA * sD + ΨA * sF + ΨB * sA + ΨB * sC + ΨB * sE)

Many assumptions are made when fitting a multistate statistical release-recapture model for estimating survival and routing in a branching system. The following are the modeling assumptions adapted from the presentation "*Survival Analysis of Tagging Data*" by Drs. R. Buchanan and R. Perry as part of a survival analysis workshop, June 28–29, 2011 (Buchanan and Perry 2011):

1. No tag failure or tag loss.
2. Every fish has equal and independent probability of success.
3. Every fish has equal and independent probability of detection, given it survives to the detection location.
4. Upstream detection history has no effect on downstream survival and detection.
5. Tagging has no effect on survival.
6. Detection is instantaneous.

7. Tags are read correctly.
8. Tagged sample is representative of the population.
9. All detections come from live study fish.
10. All mortality occurs first; then transition occurs.
11. Equal survival from the junction to each of the downstream arrays.

We assumed that these assumptions were met, but as occurs in any model, these assumptions could be violated. Also, given the complexity of the study system and the long list of stringent assumptions of the model, collecting data, and designing a model where all assumptions were met was challenging. Further, attempting to meet one assumption can sometimes cause a violation of another assumption of the model. For this reason, the effect of each modeling decision needed to be weighed upon all the assumptions to determine what form of the model was best. In the following paragraphs, we describe key modeling decisions that were made to best meet several key assumptions that were vital to our goal of estimating a route entrainment probability at Turner Cut.

In the model, we wanted to estimate route entrainment probabilities for steelhead tags that continued traveling along the Mainstem San Joaquin River and those entering Turner Cut. To estimate these routes without bias, all assumptions of the model should be met. We originally proposed to use arrays 2 and 6 (Figure 2-3) at the Turner Cut junction in the model since we wanted to use arrays immediately downstream of Turner Cut to avoid violating the assumption that all mortality occurs first and then transition occurs.

However, during exploration of the model input data, we estimated release group-specific detection probabilities for dual receiver arrays at this junction to examine if detection probabilities were constant across release groups, therefore meeting the assumption of equal and independent detection probability. The Manly and Parr (1968) method was applied to estimate detection probabilities at each dual array. The Manly and Parr method requires dual arrays and is based on the assumption that tags passing an array are detected by one or more of the receivers of the arrays. If this assumption is not met, then the detection probability for that array will be overestimated because tags not detected by any receiver are not counted in the estimation of the detection probability. All arrays that we considered using for the Turner Cut junction (arrays 2, 6, and 7) were dual arrays. Probability of detection was estimated at the array-level using these equations:

$$\hat{p}_1 = \frac{AB}{AB + B0},\ \hat{p}_2 = \frac{AB}{A0 + AB}, \text{ and } \hat{P} = 1 - (1 - \hat{p}_1)(1 - \hat{p}_2);$$

where $\hat{p}_1$ is the detection probability of the upstream receiver(s), *AB* is the number of fish detected at both upstream and downstream receiver(s), *B0* is the number of fish detected at the downstream receiver(s) only, *A0* is the number of fish detected at the upstream receiver(s) only, $\hat{p}_2$ is the detection probability of the downstream receiver(s), and $\hat{p}$ is the overall detection probability of the array.

Unlike at receiver arrays 2 and 7 (Table 4-11), the probability of detection varied with release group at array 6 (Table 4-12). For array 6, Release Group 3 had a high detection probability (100%), while the detection probabilities of Release Groups 1 and 2 were much lower, with estimates of 47% and 83%, respectively. These results justified the use of array 7 instead of array 6 in the multistate model, as the model that incorporated array 6 violated the assumption that every steelhead tag has an equal and independent probability of detection.

Table 4-11 The estimated detection probabilities p for arrays 2 and 7, for the model that included array 7 instead of 6, for Release Groups 1, 2, and 3. $\hat{p}1$ is the detection probability of the upstream receiver(s), $\hat{p}2$ is the detection probability of the downstream receiver(s), and $\hat{p}$ is the overall detection probability for the array. All detection probabilities are expressed as percentages.

Array 2			
Release Group	**1**	**2**	**3**
$\hat{p}_1$	100	99	100
$\hat{p}_2$	97	96	93
$\hat{p}$	100	100	100

Array 7			
Release Group	**1**	**2**	**3**
$\hat{p}_1$	100	98	100
$\hat{p}_2$	98	100	100
$\hat{p}$	100	100	100

Table 4-12 The estimated detection probabilities (p) for arrays 2 and 6, for the model that included array 6 instead of 7, for Release Groups 1, 2, and 3. $\hat{p}1$ is the detection probability of the upstream receiver(s), $\hat{p}2$ is the detection probability of the downstream receiver(s), and $\hat{p}$ is the overall detection probability for the array. All detection probabilities are expressed as percentages.

Array 2			
Release Group	**1**	**2**	**3**
$\hat{p}_1$	100	99	100
$\hat{p}_2$	93	93	93
$\hat{p}$	100	100	100

Array 6			
Release Group	**1**	**2**	**3**
$\hat{p}_1$	20	50	100
$\hat{p}_2$	33	67	96
$\hat{p}$	47	83	100

The detection probability for array 2 varies slightly (<5%) in the two different tables (Table 4-11 and Table 4-12) since the raw data for these tables and the model both use last detection data. Therefore, the exact number of tags last detected at array 2 depends on whether the interior array is array 6 or 7. The receivers making the upstream and downstream lines of the dual arrays 7 and 2 are reported in Table 4-9. The receivers and their locations that are part of array 6 are shown in Table 4-13.

Table 4-13 Receiver details for array 6 including receiver location (upstream or downstream), receiver code, station name, and longitude and latitude (decimal degrees).

Array	Upstream (A) or Downstream (B)	Receiver Code	Station Name	Latitude	Longitude
6	A	300886	TCE	37.9917	-121.4554
6	B	300887	TCW	37.9905	-121.4563

While including array 7 instead of array 6 avoided violation of the equal and independent detection probability assumption, the distances from array 1 (upstream of the junction) to arrays 2 and 7 were different, and therefore there was a risk of violating the assumption of equal survival from the junction to each of the downstream arrays. However, although absolute distance between arrays 1 and 2 might be slightly closer to the distance between arrays 1 and 6 versus 1 and 7, there is great inequality in the distance between array 1 and either pair of downstream receivers. If arrays 2 and 6 were used, the distance between arrays 1 and 2 was more than twice the distance between arrays 1 and 6. If arrays 2 and 7 were used, the distance between array 1 and 7 was almost twice as far as the distance between arrays 1 and 2. Therefore, arguably using either array 6 or 7 could violate the assumption of equal survival.

With array 7 being farther downstream from array 2 than array 6, we wanted to make sure that most steelhead tags arrived at array 7 from the Turner Cut junction and did not reach array 7 from the interior Delta side (possibly entering the interior Delta from Columbia Cut). We examined this assumption and found that less than 5% of steelhead tags did not reach array 7 from Turner Cut, thereby, providing further support for the use of array 7 in the model.

Another concern with using array 7 involves Whiskey Slough, a channel between arrays 6 and 7. If steelhead tags were lost in Whiskey Slough prior to reaching array 7, then route entrainment estimates at Turner Cut would be biased. However, Whiskey Slough is a dead-end and does not connect to the network of Delta channels. And since it is a dead-end and flow does not pass all the way through this slough, we assumed that there is low flow attraction for steelhead tags at the head of Whiskey Slough, thereby limiting movement into the slough.

In conclusion, we decided to run the model with array 7 instead of array 6 because only array 6 clearly violated a model assumption, with detection probability varying with release group. Also, these findings argued for use of array 7 in all additional analyses, which was the way we preceded with the analysis in this report.

RESULTS FOR HYPOTHESIS 4.2.1

The route-specific transition probabilities for the six defined routes are summarized in Table 4-14.

Table 4-14 Route-specific transition probabilities and standard error for the six transition probability routes.

Route to Chipps Island	Route-specific Transition (%)	Standard Error (%)
Via Turner Cut	7.0	1.6
Without using Turner Cut	24.8	2.0
Via Turner Cut and SWP	0.5	0.5
Via SWP without using Turner Cut	0.2	0.2
Via Turner Cut and CVP	19.6	2.8
Via CVP without using Turner Cut	31.7	1.9

The highest transition probability was for the route that did not use Turner Cut and traveled to Chipps Island though salvage operations of CVP. The second highest transition probability was the route that did not use Turner Cut and traveled to Chipps Island without being salvaged. The two lowest transition probabilities were for the two routes to Chipps Island that traveled through Clifton Court Forebay and salvage operations at SWP.

4.2.2 ROUTE-SPECIFIC AND OVERALL SURVIVAL PROBABILITIES

While route-specific transition probabilities were useful, they were harder to interpret than route-specific and overall survival probabilities. While the complement of route-specific transition probability was not just

mortality, but was mortality, using a different route or not reaching Chipps Island in 15 days, the complement of overall survival and route-specific survival estimates was mortality and not reaching Chipps Island in 15 days. However, 94% of the steelhead tags that were ever detected at Chipps Island were detected in the 15 days after their release, therefore the complement of survival is mainly mortality. Therefore, we also estimated the overall survival probabilities and route-specific survival probabilities where the data, study design, and the assumptions of the model allowed. These offered invaluable insights on what percent of the steelhead tags successfully migrated through the system and what routes had the greater proportion making it to the end point (i.e., at array 24, the array near Chipps Island [Figure 2-3]).

Hypothesis 4.2.2: The estimated route-specific survival for the Turner Cut route was not significantly different from the Mainstem route.

From the release-recapture model, we could not only estimate the six route-specific transition probabilities (see Section 4.2.1), but we could also estimate route entrainment at Turner Cut, overall Delta survival, and two route-specific survival probabilities:

- Turner Cut Route (Figure 4-18): steelhead tags that were last detected at array 7 if detected at array 2 and/or array 7.
- Mainstem Route (Figure 4-19): steelhead tags that were last detected at array 2 if detected at array 2 and/or array 7.

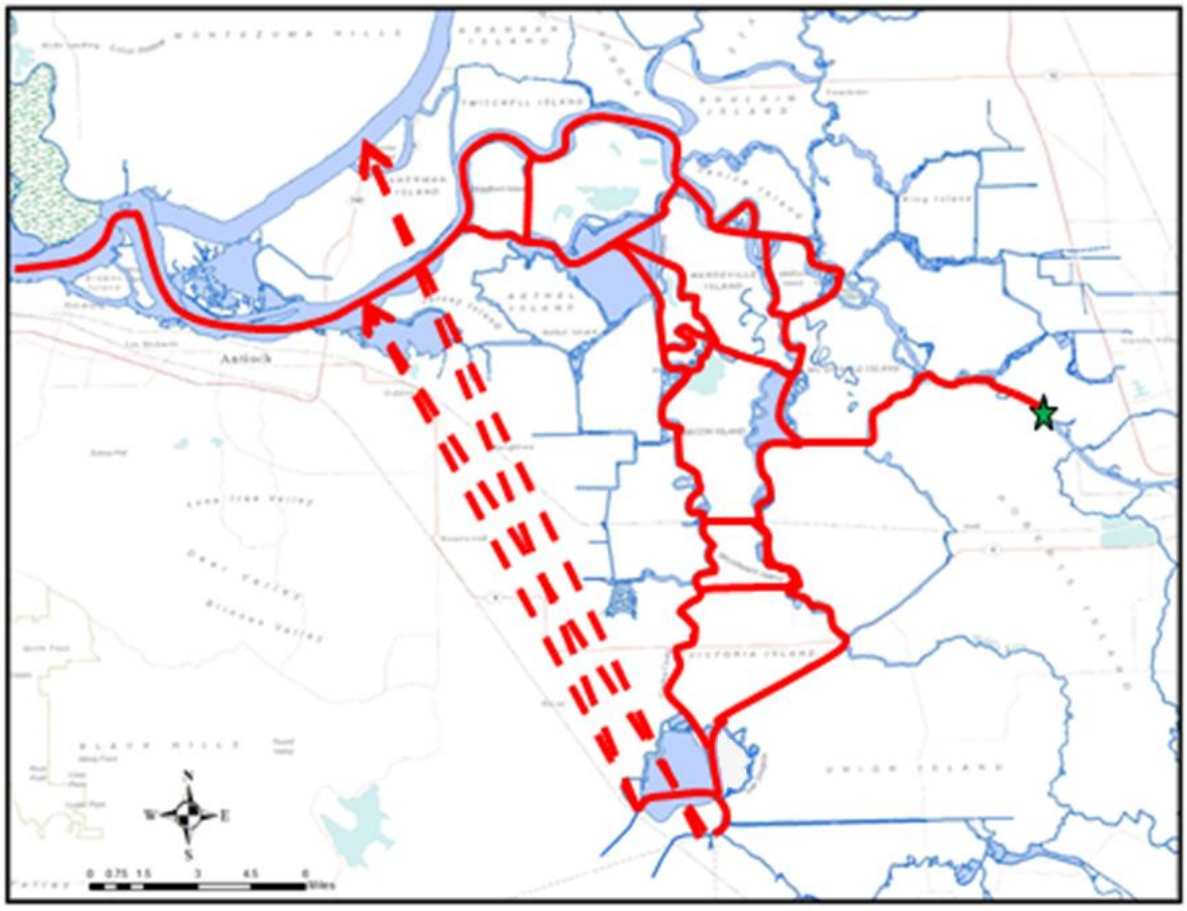

Figure 4-18 The Turner Cut route to Chipps Island for estimating overall and route-specific survival probability. Dashed lines represent overland transport of steelhead tags in salvage trucks from an export facility to one of the release sites upstream of Chipps Island.

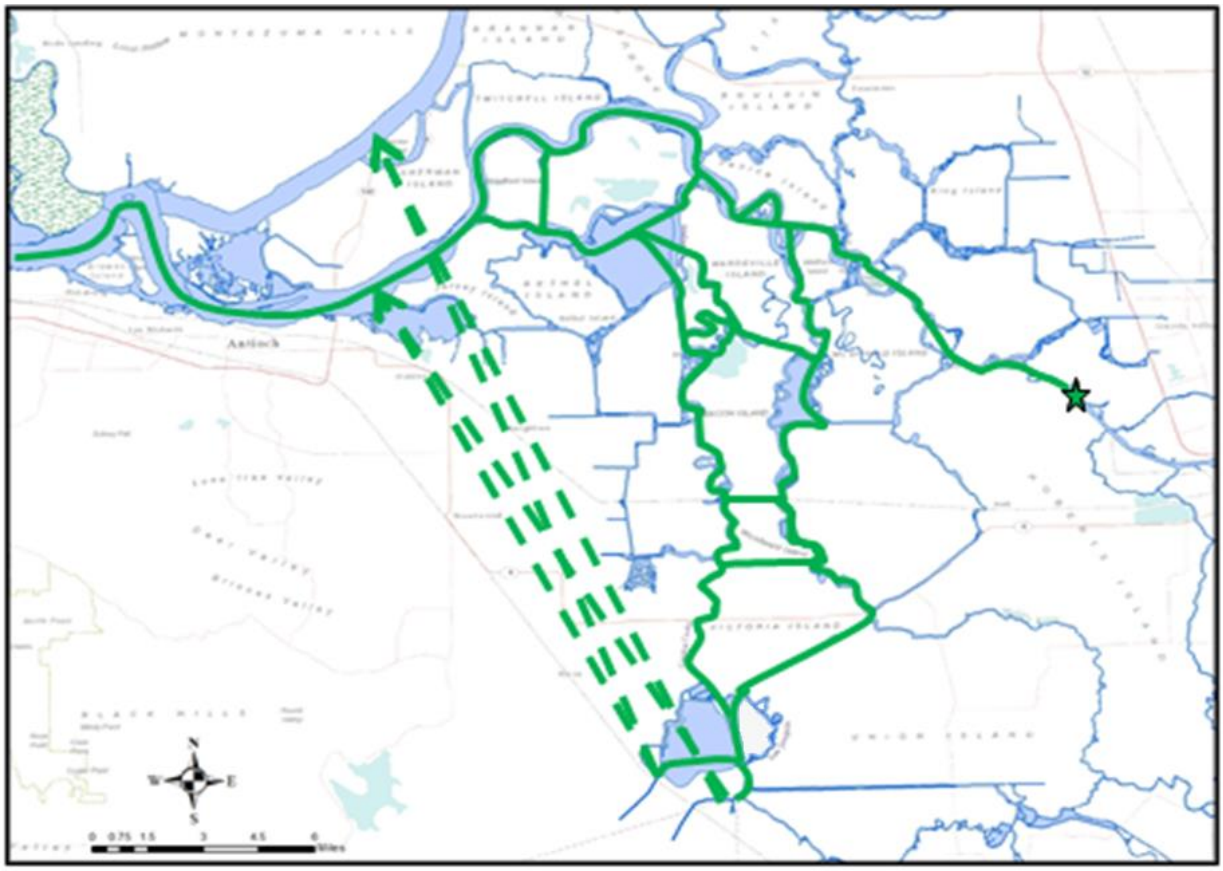

Figure 4-19 The Mainstem route to Chipps Island for estimating overall and route-specific survival probability. Dashed lines represent overland transport of steelhead tags in salvage trucks from an export facility to one of the release sites upstream of Chipps Island.

METHODS FOR TESTING HYPOTHESIS 4.2.2

The same methods used for Hypothesis 4.2.1 (multistate model) were employed for Hypothesis 4.2.2. As seen in Table 4-10, the route-specific survival probabilities are the sum of route-specific transition probabilities that encompass the routes. Overall survival probability incorporated the initial survival and the proportion of steelhead tags using each route. Route entrainment at Turner Cut was a parameter fit by the model (Table 4-10).

RESULTS FOR HYPOTHESIS 4.2.2 TEST

Overall survival to Chipps Island was 50.2% (SE=2.0%) (Table 4-15). Route-specific survival probability for the Turner Cut route was 27.0% (SE=3.0%) (Table 4-15). Route-specific survival probability for the Mainstem route was 56.7% (SE=2.4%) (Table 4-15). The model estimated that the majority of steelhead tags (77.6%, SE=1.6%), continued along the San Joaquin River and only 22.4% (SE=1.6%) of the steelhead tags were entrained into the interior Delta at the Turner Cut junction (Table 4-15). The model also generated detection probabilities, route entrainment probabilities, and transition probabilities (Table 4-16).

Table 4-15 Route-specific survival probabilities, Turner Cut route entrainment, overall survival, and standard errors for each estimate.

Description	Probability (%)	Standard Error (%)
Mainstem route survival	56.7	2.4
Turner Cut route survival	27.0	3.0
Turner Cut route entrainment	22.4	1.6
Overall survival	50.2	2.0

Table 4-16 Estimates and standard errors for parameters estimated in the model. s0 is the initial survival. Terms that start with "p" are detection probabilities for the upstream ("a") and downstream ("b") receivers. Terms that start with "Ψ" denote route entrainment probabilities. Terms that start with "ϕ" denote transition probabilities. Numbers following one of these terms in the left column are the arrays that the term is describing. For example, p2a is the detection probability of upstream receivers of array 2 and ϕ2,22 is the transition probability from array 2 to array 22.

	Estimate (%)	Standard Error (%)
s0	100.3	1.2
p2a	41.0	2.2
p2b	39.4	2.2
P7a	99.4	0.6
P7b	99.4	0.6
ΨA	77.6	1.6
ΨB	22.4	1.6
ϕ2,22	35.9	2.0
ϕ2,21	71.6	12.0
ϕ2,20	4.5	0.8
ϕ7,22	10.1	2.3
ϕ7,21	44.2	9.3
ϕ7,20	12.6	2.5
p22a	97.3	1.1
p22b	92.4	1.7
p21a	9.4	2.0
p21b	2.6	0.8
p20a	90.5	4.5
p20b	82.6	5.6
ϕ22,24	68.9	4.2
ϕ20,24	4.0	3.9
ϕ21,24	44.3	7.9
p24a	95.1	1.2
p24b	98.6	0.7

Survival estimated in the model was similar but lower than an estimate from another study using similar modeling approaches and data from steelhead but from another year. Survival of San Joaquin River (SJR) steelhead smolts in 2011 as estimated by a mark-recapture study for the Six-Year Study was 55% (SE=2%) (Buchanan 2013). In this study, we found the survival for this area in 2012 to be 50.2% (SE=2.0%). Acoustically tagged steelhead in

this study were released at Buckley Cove, which is much closer to Chipps Island than Durham Ferry, where Six-Year Study steelhead were released.

4.2.3 TRAVEL TIME

Next, we examined how travel times varied between routes and release groups. Because survival was higher for the Mainstem versus the Turner Cut route (Table 4-15), we hypothesized that steelhead tags using the Mainstem route would have shorter travel times than tags using the Turner Cut route. We assumed that shorter travel times would lead to less exposure time to predators, and therefore higher survival.

Hypothesis 4.2.3: The travel times of steelhead tags were not significantly different between routes or release groups.

METHODS FOR TESTING HYPOTHESIS 4.2.3

Travel times (i.e., time between first detection at array 24 and last detection at array 1) were calculated for each steelhead tag that successfully migrated through each route used in the model (six transition probability and two survival probability routes) and that was detected at array 1 and array 24 (Chipps Island). We used ANOVA to test for a significant difference in travel times between release groups and two survival probability routes. We were also able to examine how the OMR flow levels affected the amount of time it took steelhead tags to reach their destination by comparing travel times of Release Groups 1 and 2 combined versus Release Group 3. For a steelhead tag to be included in the analyses, it needed to be detected at arrays 1, 2 or 7; 20 or 21 or 22; and 24 (Figure 2-3). If a steelhead tag was detected at more than one array on the same level of the schematic (Figure 4-17), it was considered to use the array on that level that the steelhead tag was last detected. The only exception to this rule was that if a steelhead tag was detected at array 20 and/or 21 (radial gates of Clifton Court Forebay and/or CVP) and array 22 (Jersey Point), the steelhead tag was considered to be detected at the export facility where it was last detected. Therefore, for the few steelhead tags that were detected at an export facility and then at Jersey Point and then at Chipps Island, the steelhead tags were identified as steelhead tags that went through the salvage operations of the export facility that last detected the steelhead tag before next being detected at Chipps Island.

RESULTS FOR HYPOTHESIS 4.2.3

We first calculated the travel times for each of the six transition probability routes across all release groups (Table 4-17). Due to the limited sample sizes (N<4) for four of the six transition probability routes, we were unable to test for significant differences. The average travel time was longest for steelhead tags using the Turner Cut to Chipps Island area via CVP route (7.2 days), and shortest for steelhead tags using the route to Chipps Island area without using Turner Cut (4.5 days) (Table 4-17).

Table 4-17 The average travel time (days), standard error, and sample size of the six routes that the model estimated route-specific transition probabilities.

Route to Chipps Island	Avg. travel time (days)	Standard Error (%)	N
Via Turner Cut	6.0	0.9	13
Without using Turner Cut	4.5	0.2	71
Via Turner Cut and SWP	4.8	N/A	1
Via SWP without using Turner Cut	-	-	0
Via Turner Cut and CVP	7.2	2.7	3
Via CVP without using Turner Cut	6.8	N/A	1

We found that the average travel time was always longer for steelhead tags in the Turner Cut route versus the Mainstem route for each release group and combined Release Groups 1 and 2 (Table 4-18). As we expected, Mainstem route steelhead tags, which had double the survivorship, had shorter travel times than the Turner Cut route steelhead tags that did not go through salvage. Likely lower exposure times to predators in the Mainstem route lead to higher survival.

Table 4-18 The mean travel time for steelhead tags using each of the two survival probability routes, standard errors (in parentheses), and sample sizes for Release Groups 1, 2, and 3, and Release Groups 1 and 2 combined.

Route	Travel Time of RG #1		Travel Time of RG #2		Travel Time of RG #3		Travel Time of RG #1&2	
	Days	N	Days	N	Days	N	Days	N
Mainstem	5.5 (0.5)	18	4.1 (0.3)	30	4.2 (0.3)	24	4.6 (0.3)	48
Turner Cut	7.1 (1.5)	6	4.8 (1.1)	6	6.5 (1.6)	5	6.0 (1.0)	12

When not combining release groups, we found that travel times for release groups (P=0.02) and route taken were both significant (P=0.02). When the data were analyzed using two release groups (1 and 2 versus 3), we found that route taken was again significant (P=0.01), where release group was no longer significant (P=0.69). These results suggest that the OMR flows tested did not affect the travel times of steelhead tags, as we would have expected travel times to be significantly different for Release Group 3 versus 1 and 2 combined. Instead, we found that significant differences only occurred in travel times when Release Groups 1 and 2 were treated separately in the statistical analysis. Travel times were longer for Release Group 1 versus 2 or 3 for both routes (Table 4-18). Because OMR flows were similar between Release Groups 1 and 2, it is unlikely that OMR flows were driving these differences.

4.3 JUNCTION-LEVEL ANALYSES

In this section, we examine how steelhead tags moved through key Delta junctions. We examine if different OMR flow conditions affected the routing of steelhead tags at three junctions along the San Joaquin River (Turner Cut, Columbia Cut, and Middle River), at the state and federal export facilities, and in the interior Delta at Railroad Cut.

4.3.1 ROUTING AT DELTA JUNCTIONS

The routing of steelhead into the interior Delta along the San Joaquin River may be affected by the activities of the export facilities, given that they can create negative river flows (toward the facilities). Previously, we found that travel times were longer for steelhead tags taking the interior Delta route compared to those that remained in the San Joaquin River (Section 4.2.3), likely leading to the observed lower survival rates for steelhead tags in the interior Delta (Section 4.2.2) due to increased time for mortality to occur. Therefore, it is important to understand if more negative OMR flows increased the proportion of steelhead tags entering the interior Delta. In this section, we examine if the probability of migrating into the interior Delta at three junctions along the San Joaquin River (Turner Cut, Columbia Cut, and Middle River) was related to the OMR flow levels tested in this study.

Hypothesis 4.3.1: The probability of steelhead tags entering the interior Delta at Turner Cut, Columbia Cut, and Middle River was not related to OMR flows.

METHODS FOR TESTING HYPOTHESIS 4.3.1

As steelhead tags travel along the Mainstem route, they reach a junction and have two options: remain in the San Joaquin River, or turn into the interior Delta. We analyzed whether the proportion of steelhead tags entering the

interior Delta was related to release groups. Release group acted as a surrogate for OMR flow, with Release Group 3 representing more negative OMR flow, and Release Groups 1 and 2 representing less negative OMR flow. Junction analyses were conducted where Turner Cut, Columbia Cut, and the Middle River meet the San Joaquin River. Separate statistical tests were performed to test for differences in routing of steelhead tags at each of these three junctions. For each junction, we examined how routings differed across all three release groups, and across OMR flow levels (Release Groups 1 and 2 combined versus 3). If OMR flow affected the routing of steelhead tags, we would expect the highest proportion of tags entering into the interior Delta for Release Group 3 and more remaining on the Mainstem for Release Groups 1 and 2.

For a particular junction, a steelhead tag was included for analysis if the tag moved through the junction from upstream to downstream. The route that a tag took was defined as the last downstream array within the junction that it was detected at before leaving the junction area (i.e., the green circle in Figure 4-20 to Figure 4-22). A steelhead tag was deemed as "leaving" the junction area if it no longer was detected after being detected at a downstream junction array, or it was later detected at an array farther downstream outside of the junction area. For Turner Cut, we used data from steelhead tags that were detected at array 1 and then at arrays 2 or 7 (Figure 4-20). Array 6 was not used for this analysis because of unequal detection probabilities, as earlier described (see Section 4.2.1). For the junction at Columbia Cut, we considered steelhead tags that were detected at array 2 and then detected at array 11 or array 3 (Figure 4-21). For the junction at Middle River, we considered steelhead tags that were detected at array 3 and then at either array 4 or 13 (Figure 4-22).

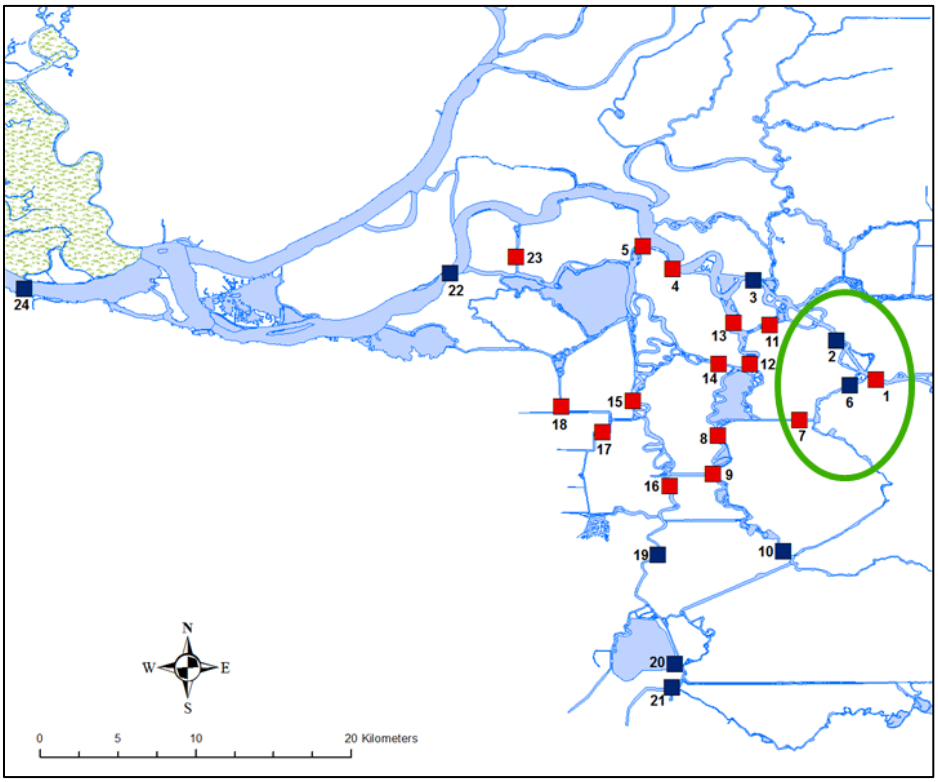

Figure 4-20 **The junction of Turner Cut as used in the junction analysis is shown in the green circle.** The red squares are sites where arrays were deployed for the Stipulation Study. The blue squares are sites where arrays were deployed for the 2012 Six-Year Study.

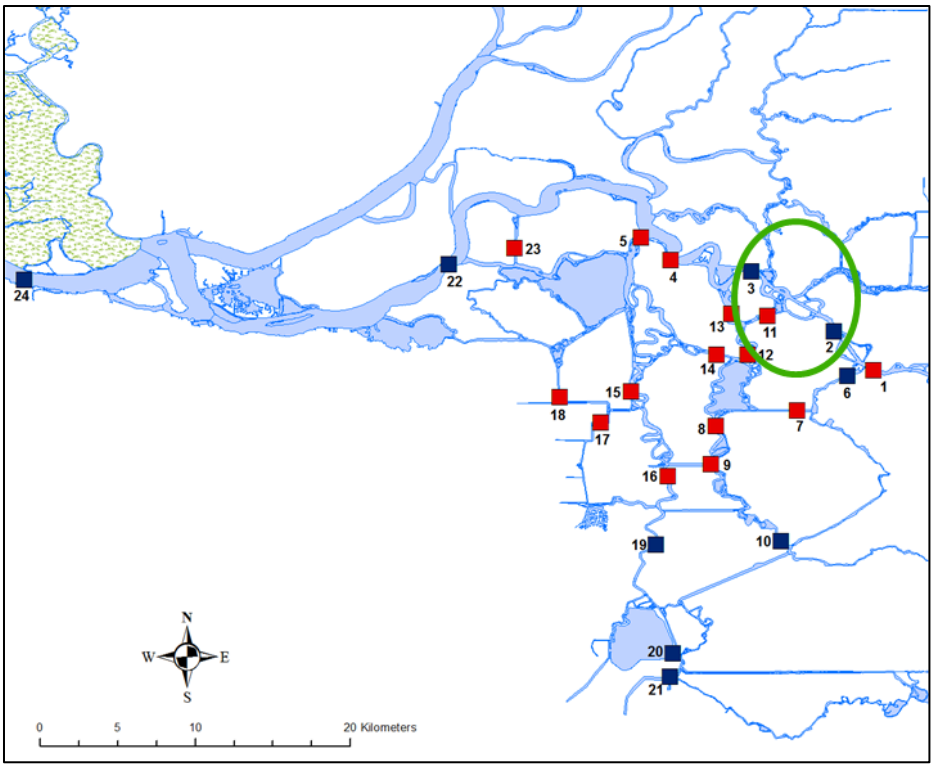

Figure 4-21 **The junction of Columbia Cut as used in the junction analysis is shown in the green circle.** The red squares are sites where arrays were deployed for the Stipulation Study. The blue squares are sites where arrays were deployed for the 2012 Six-Year Study.

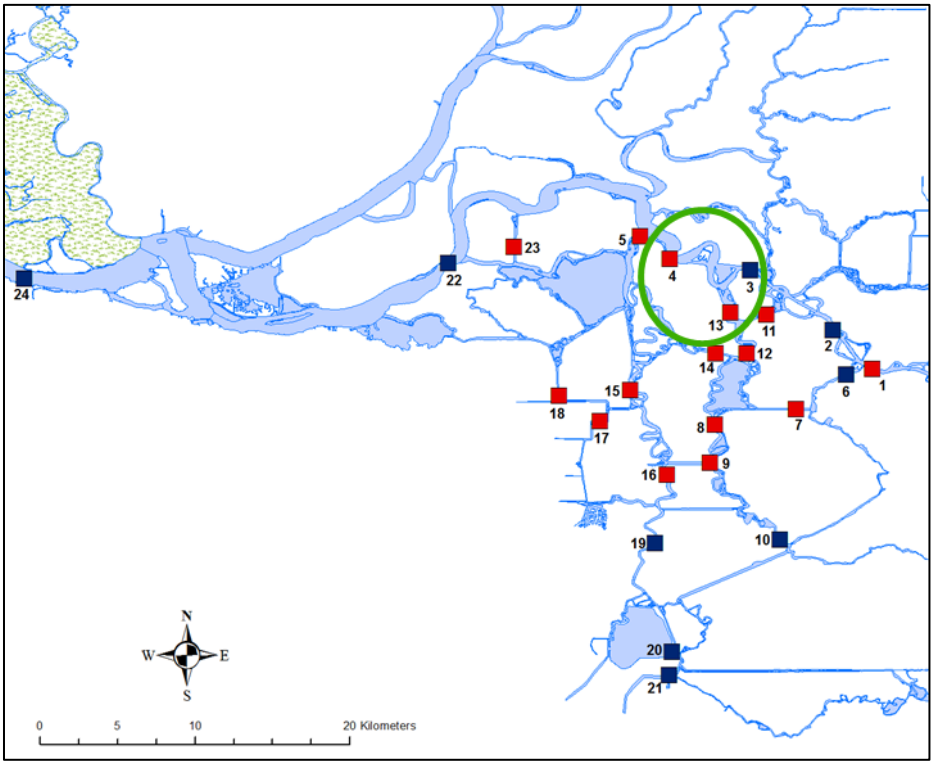

Figure 4-22 **The junction of Middle River as used in the junction analysis is shown in the green circle.** The red squares are sites where arrays were deployed for the Stipulation Study. The blue squares are sites where arrays were deployed for the 2012 Six-Year Study.

We examined if a significant difference in the proportion of steelhead tags migrating into the interior Delta existed between the different release groups by fitting a generalized linear model (GLM) with a binomial response variable using the R commander package (Fox 2005) of the software program R (R Project 2013). We fit the GLM with a binomial distribution of errors and a logit link function. We tested for overdispersion by comparing the residual deviance to the residual degrees of freedom using a Chi-square test. If the data were overdispersed, we re-fitted the GLM with a quasibinomial distribution of errors and a logit link function. To determine the overall effect of release group, we ran an analysis of deviance on the GLM based on either a Chi-square test or F-test depending on whether the model used a binomial or quasibinomial distribution, respectively. If we found significant differences between release groups, we then looked at how the proportion of the steelhead tags varied between release groups to identify if it occurred in a way that supported the alternative hypothesis that OMR flow affects the proportion of steelhead tags entering the interior Delta. For this to be supported, we expected a lower proportion of steelhead tags entering the interior Delta during less negative OMR flows experienced during Release Groups 1 and 2 than during the more negative OMR flows that occurred during Release Group 3.

RESULTS FOR HYPOTHESIS 4.3.1

At all three junctions, we did not find significant patterns of steelhead tag movement between release groups that would support the alternative hypothesis that release groups, a proxy for OMR flow levels tested, affected the routing of steelhead tags (Table 4-19 to Table 4-24). At Turner Cut, we found non-significant results for both the three ($P=0.60$) and two release ($P=0.32$) group analyses. At Columbia Cut, we found non-significant results for both the three ($P=0.62$) and two release ($P=0.70$) group analyses. At the Middle River, we found a significant result for the three ($P<0.01$) group analysis but a non-significant result for the two release group analyses ($P=0.88$).

For Middle River, the significant result found across three release groups was due to a lower proportion of steelhead tags migrating into the interior Delta for Release Group 2 (2.2%) versus Release Groups 1 and 3. We found that steelhead tags from Release Group 1, which experienced the less negative OMR flows, had the highest probability of migration into the Middle River (25.0%). Release Group 3, which was the most negative average OMR flow treatment, had an intermediate number of steelhead tags migrating at the Middle River (13.2%). If OMR flows were affecting movement at the Middle River, we would have expected tags from Release Groups 1 and 2 (less negative OMR flows) to have similar proportion, with tags from Release Group 3 (more negative OMR flows) having the highest proportion. However, when the data were analyzed using only two release groups, we found a similar proportion of steelhead tags entering the interior Delta between the less negative OMR flow treatment (12.2%) and the more negative OMR flow treatment (13.2%). Therefore, the differences in movement observed at the Middle River were unrelated to OMR flows observed during this study.

Table 4-19 Number of steelhead tags detected for each release group at the downstream SJR array (array 2) and the interior Delta array (array 7) after being detected at the upstream array (array 1) at Turner Cut.

Release Group	SJR Array 2	Interior Array 7
1	75	54
2	82	60
3	76	44
Total	233	158

Table 4-20 Number of steelhead tags detected for each release group at the downstream SJR array (array 3) and the interior Delta array (array 11) after being detected at the upstream array (array 2) at the Columbia Cut junction.

Release Group	SJR Array 3	Interior Array 11
1	40	17
2	47	28
3	41	24
Total	128	69

Table 4-21 Number of steelhead tags detected for each release group at the downstream SJR array (array 4) and the interior Delta array (array 13) after being detected at the upstream array (array 3) at the Middle River junction.

Release Group	SJR Array 4	Interior Array 13
1	27	9
2	45	1
3	33	5
Total	105	15

Table 4-22 Number of steelhead tags detected for each release group at the downstream SJR array (array 2) and the interior Delta array (array 7) after being detected at the upstream array (array 1) at Turner Cut. Less negative OMR flow treatments are Release Groups 1 and 2, and more negative OMR flow treatment is Release Group 3.

Release Group	SJR Array 2	Interior Array 7
Less negative OMR flows (Groups 1 and 2)	157	114
More negative OMR flows (Group 3)	76	44
Total	233	158

Table 4-23 Number of steelhead tags detected for each release group at the downstream SJR array (array 3) and the interior Delta array (array 11) after being detected at the upstream array (array 2) at the Columbia Cut junction. Less negative OMR flow treatments are Release Groups 1 and 2, and more negative OMR flow treatment is Release Group 3.

Release Group	SJR Array 3	Interior Array 11
Less negative OMR flows (Groups 1 and 2)	87	45
More negative OMR flows (Group 3)	41	24
Total	128	69

Table 4-24 Number of steelhead tags detected for each release group at the downstream SJR array (array 4) and the interior Delta array (array 13) after being detected at the upstream array (array 3) at the Middle River junction. Less negative OMR flow treatments are Release Groups 1 and 2, and more negative OMR flow treatment is Release Group 3.

Release Group	SJR Array 4	Interior Array 13
Less negative OMR flows (Groups 1 and 2)	72	10
More negative OMR flows (Group 3)	33	5
Total	105	15

The reliability of these results rests on the assumption that detection probabilities did not vary between release groups. Variability in detection probabilities at a junction across release groups would confound results because differences in steelhead tag routing could be due to differences in detection probability instead of true differences in steelhead tag movement. Previously (Section 4.2.1), we examined how detection probability varied across release groups for arrays 6 and 7 downstream of the Turner Cut junction. We found that detection probability varied across release groups for array 6, but not array 7. Therefore, we decided to use array 7 in all future analyses (including this one). This test was possible because arrays 2, 6, and 7 are dual arrays that allowed an independent probability of detection to be estimated. While this is not the case for the Middle River junction since arrays 4 and 13 were not set up as a dual array (Figure 4-23), Columbia Cut junction arrays are all dual arrays (Figure 4-24), so we could estimate release-group detection probabilities using Manly-Parr estimates (see Section 4.2.1 for detailed methods). The number and the location of receivers at the Columbia Cut junction are described in Table 4-25 and the detection probabilities for the three release groups are shown in Table 4-26.

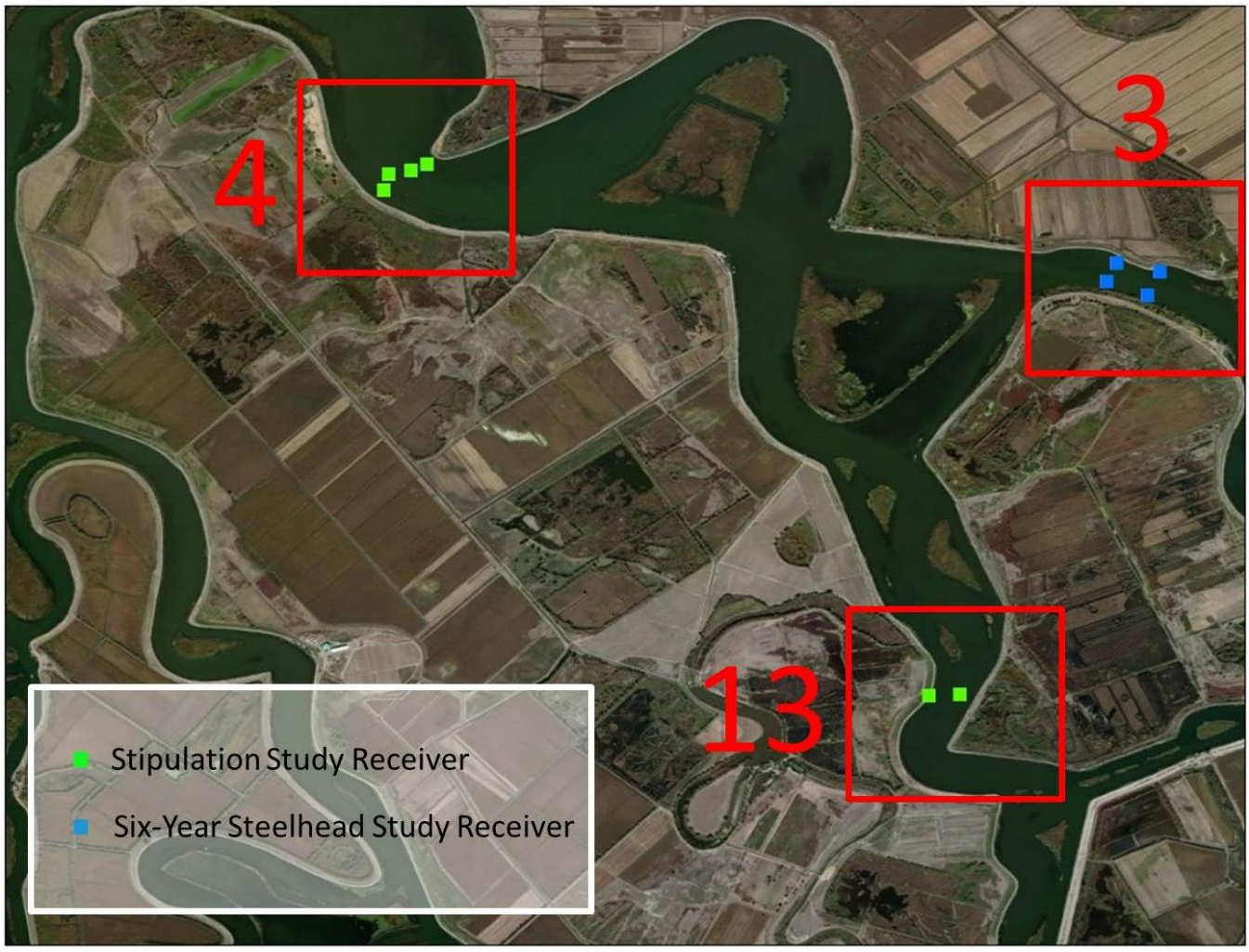

Figure 4-23 A satellite image of the Middle River junction with the placement of receiver arrays shown. Array 3 was deployed for the Six-Year Study, and arrays 4 and 13 were deployed for the Stipulation Study. Base map produced using Google Earth.

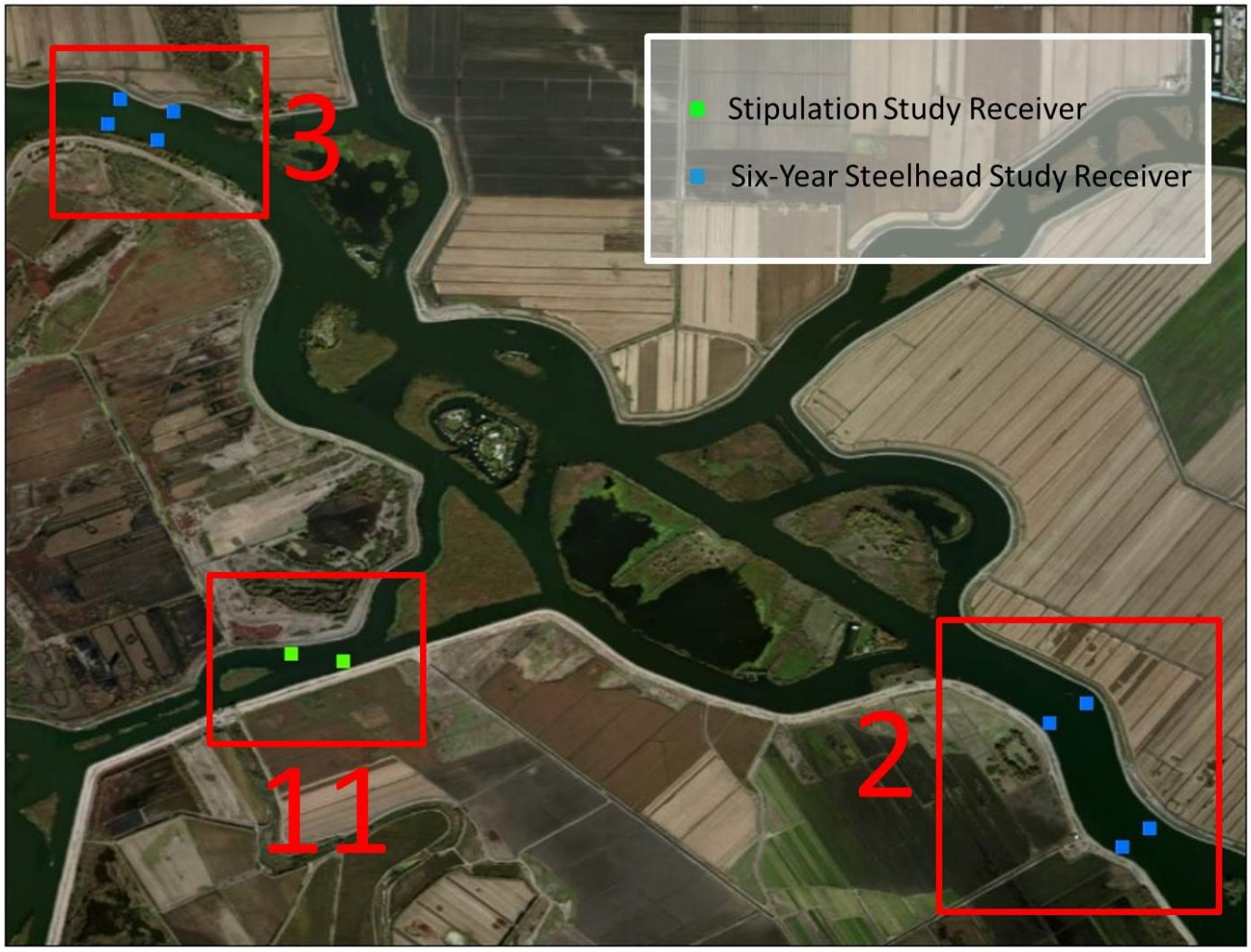

Figure 4-24 **A satellite image of Columbia Cut with the placement of receiver arrays shown.** Arrays 2 and 3 were deployed for the Six-Year Study, and array 11 was deployed for the Stipulation Study. Base map produced using Google Earth.

Table 4-25 Array number, receiver location (upstream or downstream), receiver code, station name, and latitude and longitude (decimal degrees).

Array	Upstream (A) or Downstream (B)	Receiver Code	Station Name	Latitude	Longitude
3	A	300903	MFE.1	38.0524	-121.5111
3	A	300904	MFE.2	38.0539	-121.5104
3	B	300905	MFW.1	38.0533	-121.5136
3	B	300906	MFW.2	38.0544	-121.5130
11	A	301009	8A	38.0267	-121.5020
11	B	301001	8B	38.0270	-121.5046

Table 4-26 Manly-Parr estimates of detection probabilities p for Release Groups 1, 2, and 3 for array 3 at the Columbia Cut junction. $\hat{p}1$ is the detection probability of the upstream receiver(s), $\hat{p}2$ is the detection probability of the downstream receiver(s), and $\hat{p}$ is the overall detection probability for the array. All detection probabilities are expressed as percentages.

Array 3			
Release Group	**1**	**2**	**3**
$\hat{p}_1$	100	96	100
$\hat{p}_2$	95	100	100
$\hat{p}$	100	100	100

Array 11			
Release Group	**1**	**2**	**3**
$\hat{p}_1$	81	86	75
$\hat{p}_2$	97	100	100
$\hat{p}$	100	100	100

We found that detection probabilities at the array-level were 100% across all arrays and release groups at the Columbia Cut junction (Table 4-26). Therefore, the assumption of consistent detection probabilities appears to be met for arrays 3, and 11. For this reason, we feel the findings of the analysis that the OMR flow treatments tested likely did not affect the movement of steelhead tags at Columbia Cut are valid given consistent detection probabilities.

4.3.2 MOVEMENT AT EXPORT FACILITIES

Because water is exported out of both the SWP and CVP facilities in the Delta, and mortality varies for fish entering each facility (Gingras 1997, Clark et al. 2009), understanding how pumping at each facility influences fish movement could help managers protect sensitive fish species. The relative amount of flow entering each facility may influence the relative movement of steelhead toward each facility. Therefore, we examined how the arrival of steelhead tags at each facility may have been influenced by the proportion of flow entering each facility.

Hypothesis 4.3.2: Steelhead tag arrival at each facility was not related to the proportion of total export flow entering SWP.

METHODS FOR TESTING HYPOTHESIS 4.3.2

We examined if the arrival of steelhead tags at an export facility was related to the proportion of water entering that export facility. The arrays used for analysis were arrays 20 and 21. We summed flow across all Clifton Court Forebay gates for the SWP, and measured export flow for the CVP. The proportion of total water entering each facility was quantified for 2-hour periods, which was the highest resolution flow data available for the CVP facility. Next, the steelhead tag arrival times at each facility were paired with the appropriate 2-hour flow proportion. Steelhead tags were only counted at the facility where they were first detected. Data were pooled across release groups. A steelhead tag was included only if flows were greater than zero at either or both facilities during their 2-hour arrival period. A t-test was applied to examine if the proportion of total flow entering SWP (i.e., the radial gates of Clifton Court Forebay) differed for steelhead tags arriving at the SWP versus CVP. We expected that a higher proportion of flow would be entering the SWP when steelhead tags arrived at the SWP than when steelhead tags arrived at the CVP.

RESULTS FOR HYPOTHESIS 4.3.2

While the t-test did not find a significant result, the average 2-hour proportion of flow entering the SWP was greater when a steelhead tag was first detected at array 20 (mean=0.6, SE=0.1) than when a steelhead tag was first detected at array 21 (mean=0.4, SE=0.1). Therefore, while there was great variability in the proportion of flow when a steelhead tag arrived at an export facility, on average there was a greater proportion of water arriving at an export facility when a steelhead tag was arriving at that export facility (Figure 4-25).

These results indicate that the arrival of steelhead smolts toward each export facility was not significantly related to proportional flow to a facility on a 2-hour period. Qualitatively, however, it appeared that the movement of steelhead tags might be influenced by the relative flow amount entering each facility. By coordinating the relative export levels at each facility, sensitive fish species could potentially be routed toward the facility perceived to have lower risks of fish mortality for the given time of year.

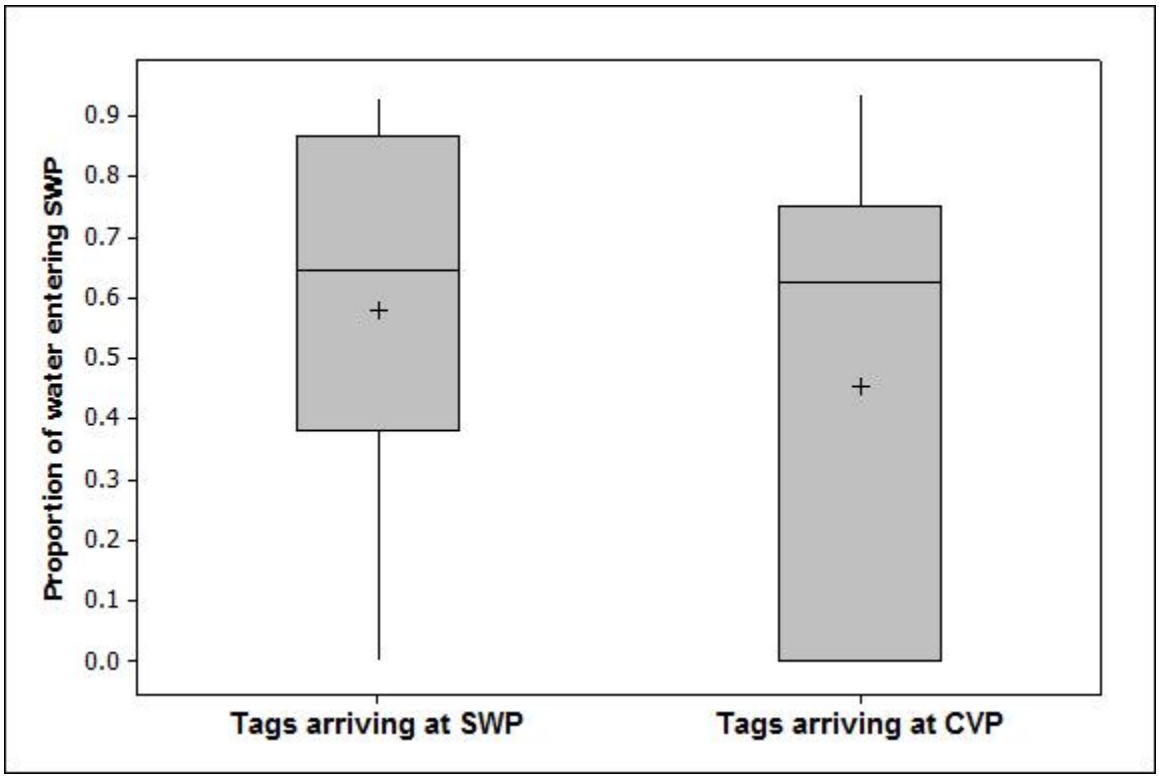

Figure 4-25 The proportion of water entering the SWP (i.e., entering the radial gates of Clifton Court Forebay) when steelhead tags arrived at the radial gates of Clifton Court Forebay (SWP) and at the CVP. The gray rectangle indicates the middle 50% (interquartile range) of the data, the horizontal line indicates the median, the "+" indicates the mean, and vertical lines extend to the highest data value within the upper limit (= Q3 + 1.5 [Q3 - Q1]) and to the lowest value within the lower limit (= Q1- 1.5 [Q3 - Q1]).

4.3.3 MOVEMENT AT RAILROAD CUT

During the Stipulation Study, steelhead tags were used as "sentinels" to identify when wild salmonids were likely approaching the export facilities to determine when more protective actions were needed for wild fish. When steelhead tag detections at Railroad Cut (array 9, Figure 4-26) exceeded a threshold (5% of fish reaching Railroad Cut), managers triggered a management option to reduce south Delta export flows in an effort to provide additional protection for ESA-listed salmonids. The trigger was meant to reduce Delta exports, leading to less negative OMR flows and less risk of smolts moving toward the export facilities and potentially becoming entrained. Therefore, we tested the effectiveness of the trigger by examining how the routing of steelhead tags toward the export facilities at Railroad Cut varied before and after the trigger and across release groups. We also examined the effect of the OMR flows tested, by examining how the proportion of tags moving toward or away from the export facilities varied with OMR flow conditions during steelhead tag routing.

Hypothesis 4.3.3: The movement patterns of steelhead tags after passing through Railroad Cut were not affected by OMR flows.

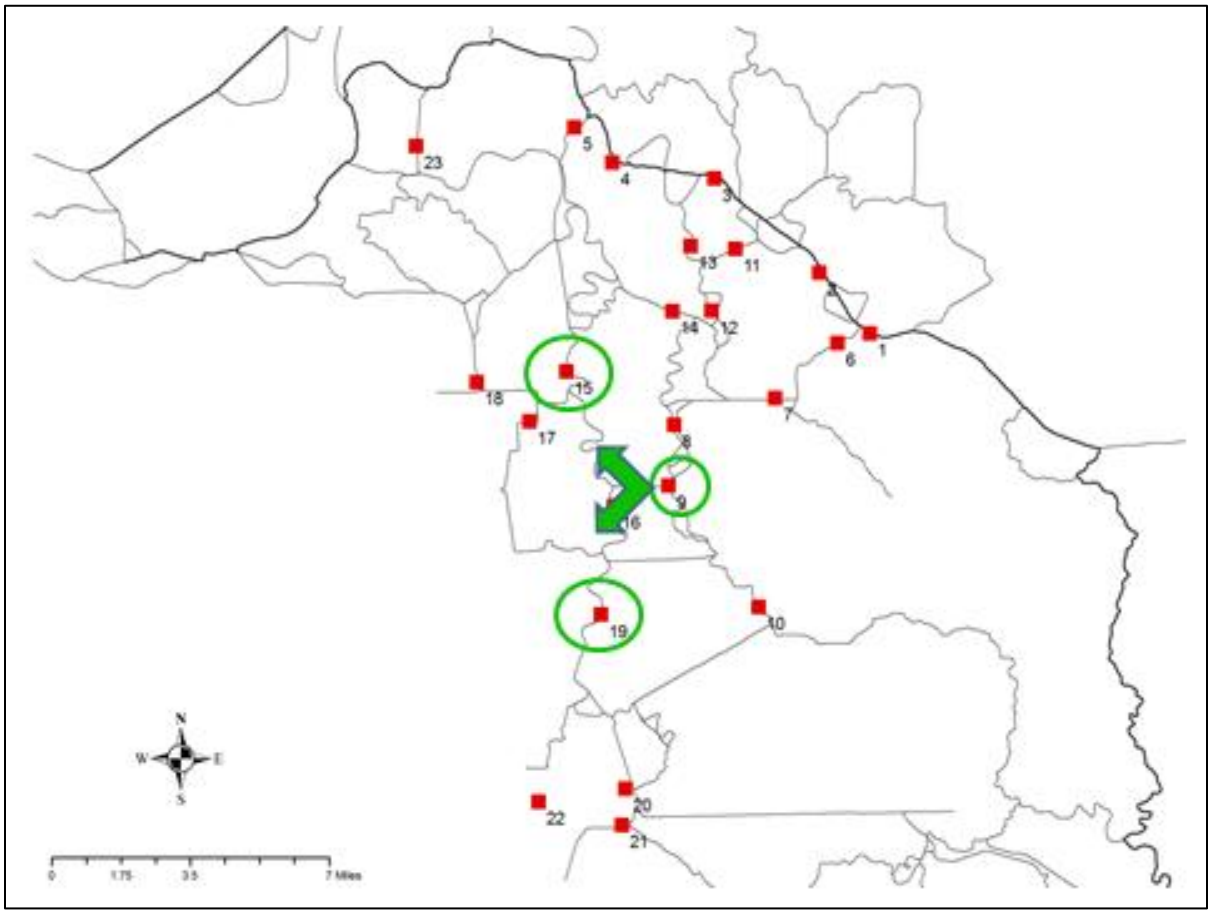

Figure 4-26 Steelhead tags arriving at Railroad Cut (array 9) were either routed away from the export facilities (array 15) or toward the facilities (array 19).

METHODS FOR TESTING HYPOTHESIS 4.3.3

We examined if a greater proportion of steelhead tags travelled away from the export facilities (array 15) than toward the facilities (array 19) before and after the trigger was implemented to reduce OMR flows and across

release groups. Therefore, we only used steelhead tags that were detected at array 9 and then detected at either or both downstream arrays (i.e., array 15 or 19). For steelhead tags detected at both downstream arrays, we used the array that detected the steelhead tag last to delineate the final route of that tag. When the day that the management option had been triggered and the less negative flows were observed to occur was identified by examining the OMR flow data (Figure 2-1) and identified as the day that the daily average OMR level was at or below -1,250 cfs. This date was determined to be April 24, May 11, and May 26 for Release Groups 1, 2, and 3, respectively. Applying similar statistical methods as Hypothesis 4.3.1, using GLMs, we examined if routing of steelhead tags differed between pre- and post-triggering of the management conditions and/or between release groups. We analyzed the data as three release groups as well as two groups, where Release Groups 1 and 2 were pooled and considered the less negative OMR flow treatment, and Release Group 3 as the more negative OMR flow treatment.

We also directly examined the effect of OMR flow on routing at Railroad Cut. We examined how routing at Railroad Cut was affected by a measurement of OMR flow while a steelhead tag was moving across Railroad Cut toward the downstream arrays of interest. Therefore, in separate GLMs, we examined if the proportion of steelhead tags moving south or north from the export facilities (i.e., last detected at array 15 or 19) was related to one or more of the following OMR flow variables:

1. Average OMR flow that the steelhead tag experienced from the day that the steelhead tag was first detected at array 9 to the day when it was first detected at the downstream array (array 15 or 19) that last detected the steelhead tag.

2. Average OMR flow that the steelhead tag experienced from the day that the steelhead tag was last detected at array 9 to the day when it was first detected at the downstream array that last detected the steelhead tag.

3. Average OMR flow that the steelhead tag experienced for the day that the steelhead tag was last detected at array 9.

4. Average minimum OMR flow that the steelhead tag experienced from the day the steelhead tag was last detected at array 9 to the day it was first detected at the downstream array that last detected the steelhead tag.

5. Average maximum OMR flow from the day that the steelhead tag was last detected at array 9 to the day it was first detected at the downstream array that last detected the steelhead tag.

6. Average OMR flow on the day that steelhead tag was last detected at the downstream array that last detected the steelhead tag.

7. Average OMR flow on the day that steelhead tag was first detected at the downstream array that last detected the steelhead tag.

8. Average OMR flow on the day that steelhead tag was last detected at the downstream array that first detected the steelhead tag.

9. Average OMR flow on the day that steelhead tag was first detected at the downstream array that first detected the steelhead tag.

RESULTS FOR HYPOTHESIS 4.3.3

We examined the detections by the upstream and downstream receivers of array 15 and 19 (Table 4-27) and found detection probabilities to be consistent between release groups at the arrays (Table 4-28). Therefore, differences in routing between release groups can be attributed to actual movement differences and not to variation in detection probability.

Table 4-27 Array number, receiver location (upstream or downstream), its receiver code, station name, and latitude and longitude (decimal degrees).

Array	Upstream (A) or Downstream (B)	Receiver Code	Station Name	Latitude	Longitude
15	A	301015	15A	37.9828	-121.5810
15	B	301053	15B	37.9844	-121.5818
19	A	300885	OR4D.2	37.8953	-121.5667
19	A	300884	OR4D.1	37.8950	-121.5661
19	B	300883	OR4U.2	37.8939	-121.5675
19	B	300882	OR4U.1	37.8938	-121.5667

Table 4-28 Manly-Parr estimates of detection probabilities p for Release Groups 1, 2, and 3 for arrays 15 and 19. $\hat{p}1$ is the detection probability of the upstream receiver(s), $\hat{p}2$ is the detection probability of the downstream receiver(s), and $\hat{p}$ is the overall detection probability for the array. Given the detection data for Release Group 1 at array 15, only the detection probabilities at the downstream receiver could be estimated. All detection probabilities are expressed as percentages.

Array 15			
Release Group	**1**	**2**	**3**
$\hat{p}_1$	N/A[a]	71	67
$\hat{p}_2$	0	100	100
$\hat{p}$	N/A[a]	100	100

Note:
[a] Detection probability not calculated because no fish were detected at both upstream and downstream receivers and the downstream receiver(s) only resulting in a division by zero error.

Array 19			
Release Group	**1**	**2**	**3**
$\hat{p}_1$	100	100	100
$\hat{p}_2$	100	100	100
$\hat{p}$	100	100	100

Other than in Release Group 1 for array 15 where we could not estimate the detection probability at the array-level, for all other periods and arrays, detection probabilities were all 100% (Table 4-28). No steelhead tags were detected at the downstream receiver at array 15 during Release Group 1, making the calculation of detection probability at the upstream receiver impossible. Given that the only estimate of detection probabilities at array 15 during Release Group 1 was 0% for the downstream receiver, and all other detection probabilities for Release Groups 2 and 3 were higher, the detection probabilities for array 15 might be confounded with release groups. To investigate detection probability at array 15 further, we calculated the array-level detection probability for Release Groups 1 and 2 combined to ensure that detection probabilities remained high between both less negative (Groups 1 and 2) and more negative (Group 3) OMR flow treatments. We estimated an array-level detection probability of 80.4% for Release Groups 1 and 2 combined, indicating that detection probability at array 15 was high (>80%) for both OMR flow treatment groups.

The observed effect caused by the triggering of reduced exports occurred after more than 90% of the steelhead tags (68/75) had already passed the east end of Railroad Cut (array 9), which provided a limited sample size (Table 4-29) to examine the effect of the management option. The majority of steelhead tags (6/7) that passed Railroad Cut after the triggering of less negative OMR flows had occurred went south (Table 4-29). Due to the limited sample sizes, we did not statistically analyze the effect of the management option, but we did examine if the release group had a significant effect. In the three release group analysis, the overall logistic regression was not significant (P=0.17). In the two release group analysis, the overall logistic regression was marginally significant (P=0.08).

Table 4-29 The number of steelhead tags detected pre- and post-triggering of the management option for the three release groups.

	Pre-Trigger Release Group 1	Post-Trigger Release Group 1	Pre-Trigger Release Group 2	Post-Trigger Release Group 2	Pre-Trigger Release Group 3	Post-Trigger Release Group 3
Northern receiver array (15)	10	1	7	0	3	0
Southern receiver array (19)	12	6	18	0	18	0

When examining the effect of OMR flows observed directly in GLMs, all of the nine independent variables were found not to be significant except for the test that examined the average OMR flow on the day that a steelhead tag was first detected at either of the downstream arrays (P=0.05, Table 4-30). The relationship showed an increasing probability of steelhead tags moving toward the export facilities as OMR flow values become more negative (Table 4-31, Figure 4-27).

Table 4-30 P-values for the logistic regression examining whether the following independent variables were significantly related to the whether a steelhead tag was last detected at array 15 or 19 after passing through Railroad Cut.

Independent Variable	P
Average OMR flow that the steelhead tag experienced from the day that the steelhead tag was first detected at array 9 to the day when it was first detected at the downstream array (array 15 or 19) that last detected the steelhead tag.	0.146
Average OMR flow that the steelhead tag experienced from the day that the steelhead tag was last detected at array 9 to the day when it was first detected at the downstream array that last detected the steelhead tag.	0.124
Average OMR flow that the steelhead tag experienced for the day that the steelhead tag was last detected at array 9.	0.157
Average minimum OMR flow that the steelhead tag experienced from the day the steelhead tag was last detected at 9 to the day it was first detected at the downstream array that last detected the steelhead tag.	0.129
Average maximum OMR flow from the day that the steelhead tag was last detected at array 9 to the day it was first detected at the downstream array that last detected the steelhead tag.	0.128
Average OMR flow on the day that steelhead tag was last detected at the downstream array that last detected the steelhead tag.	0.070
Average OMR flow on the day that steelhead tag was first detected at the downstream array that last detected the steelhead tag.	0.054
Average OMR flow on the day that steelhead tag was last detected at the downstream array that first detected the steelhead tag.	0.131
Average OMR flow on the day that steelhead tag was first detected at the downstream array that first detected the steelhead tag.	0.050

Table 4-31 Coefficient estimates, standard errors, and Z and P-values for the constant and factor of average OMR flow on the day that the steelhead tag was first detected at the downstream array that first detected it. The overall P-value for this logistic regression was 0.05.

Predictor	Coefficient	Standard Error	Z	P
Constant	0.228	0.653	0.349	0.727
OMR flow	<0.001	<0.001	1.872	0.061

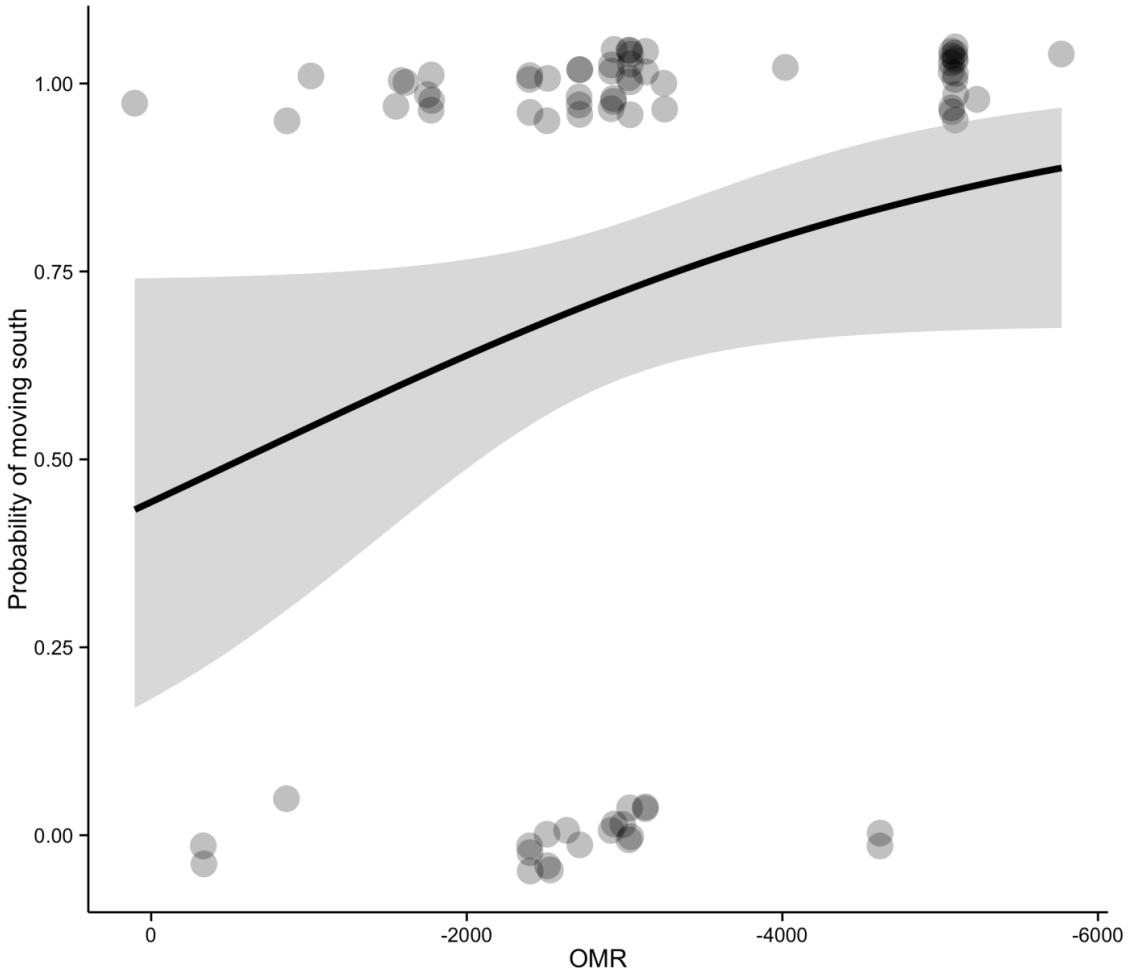

Figure 4-27 The probability of steelhead tags moving south (toward the export facilities) for the observed range of OMR flow values from a GLM with the line of best fit and the shaded area represents the 95% confidence interval. Data points for the observed OMR values were either moving south (1) or north (0). Given the overlap of data points, they were jittered so more of them can be seen in the figure.

The small sample size limited our ability to examine the effectiveness of the trigger on the movement of steelhead tags. If a trigger is implemented in the future, we recommend ensuring that a larger number of tagged fish are approaching the area before and after the management option has been observed to come into effect. We recommend that future tagging studies be conducted under a wider range of OMR flows to better understand how the range of possible OMR flows influence fish routing near the export facilities. As tidal conditions may contribute to changes in fish behavior, any future studies should also be conducted under shorter time periods with greater replication.

This page intentionally left blank.

5 DISCUSSION

CHAPTER SUMMARY:

We address the following four questions in this chapter:

1. Did OMR flows affect steelhead tag movement and survival?
2. How effective was real-time monitoring and management?
3. What were the limitations of the experimental design and how could they be improved?
4. What future experiments and methods are recommended?

Overall, under the OMR flows tested, there was little influence of OMR flows on steelhead tag movement during this study. There was limited evidence of OMR flows tested influencing steelhead tag routing at Railroad Cut in the interior Delta and arrival timing at the SWP Clifton Court Forebay radial gates. The influence of the OMR flows tested on steelhead tag behavior appears to be limited to a short distance from the SWP and CVP projects. Future studies should focus on how smolt movement and survival at Railroad Cut and south (toward the export facilities) may be influenced by a wider range of OMR flow conditions than those examined in this study. More than 90% of steelhead tags passed the real-time monitoring detection point before the effects of triggered changes to OMR flow conditions were observed (i.e., OMR flows reached -1,250 cfs). While improvements to the experimental design of any future real-time monitoring study could be completed, this study points to the inability to effectively use tagged steelhead smolts as sentinels to trigger export changes. This study also provides evidence of the challenges of managing Delta flow conditions in real-time. Because there was little evidence that altering OMR flow conditions within the range of values examined in this study would alter the movement of fish in a meaningful way, these results do not provide evidence that real-time monitoring could be used to protect salmonids.

5.1 DID OMR FLOWS AFFECT STEELHEAD TAG MOVEMENT AND SURVIVAL?

We found no evidence that the OMR flows tested affected the routing of steelhead tags along the San Joaquin River corridor. The routing of steelhead tags at Turner Cut, Columbia Cut, or where the Middle River meets the San Joaquin River was not related to release groups (and therefore the experimental OMR flow treatments evaluated in this study). The limited influence of OMR flows on steelhead tag routing along the San Joaquin River was expected due to the limited differences in modeled flow routing observed under different OMR flow treatments tested (Cavallo et al. 2012). The range of OMR flows that occurred during the study did not capture the historical operating range of flows and was conducted when the HORB was in place. Yet, the steelhead tagging results, paired with hydrodynamic modeling, indicated that OMR flows may have very limited ability to influence the migration of salmonid smolts into the interior Delta within the range of the values and conditions observed in the study.

While no evidence of an influence of OMR flow conditions on routing was found at the San Joaquin River junctions, there was some marginally significant evidence of differences in the routing of steelhead tags at Railroad Cut. This junction is closer to the export facilities and occurs along the OMR corridor. Therefore, a stronger influence of OMR flows on steelhead tag movement at Railroad Cut compared to river junctions along the San Joaquin River was not surprising. These results may be evidence of a more localized area of influence of the export facilities on salmonid smolt movement, extending as far north as Railroad Cut. However, due to sub-optimal receiver placement in the interior Delta, we were unable to precisely examine the spatial extent of influence of OMR flows on smolt movement. While this study had an elaborate deployment of telemetry equipment, we believe that more receivers, tagged fish, and release sites are needed along with different operation scenarios at CVP and SWP to better examine if OMR flows affect steelhead movement and survival.

When examining system-level steelhead tag behavior, we found no consistent pattern between release groups, suggesting that OMR flows as tested may have had minimal effect on the general movement patterns of steelhead tags during the study. In particular, we found that the "point of no return," defined as the point where steelhead tags in the interior Delta no longer arrived at Chipps Island without assistance (through salvage operations at export facilities), changed only slightly among OMR flow treatments evaluated during this study. While it was farther north for Groups 1 and 2 compared to Group 3, the difference was only two arrays (Figure 4-4 to Figure 4-6). In addition, this line being farther south for Group 3 is contradictory to what should have been expected under more negative OMR flows for Group 3, where the point of no return was expected to have been farther north if OMR flows were controlling the point of no return.

Unfortunately, we were unable to examine how OMR flows influenced survival of steelhead tags, due to the failure of the USER model to converge on individual release group models. Limited sample sizes for each individual release group likely caused the model to not converge on a solution. We recommend that future tagging studies have ample sample sizes to examine the effect of OMR flows on survival.

As part of the route-level analysis, we found no significant evidence that travel times were related to OMR flows within the ranges examined in this study, as seen in Section 4.2.3. To provide further evidence of the limited influence of OMR flow conditions on steelhead tag travel time, we examined the cumulative detections through time that occurred at many of the arrays in this study (Figure 5-1 to Figure 5-3). At most arrays, we did not see major differences in arrival timing between Group 2 (less negative OMR flows) and Group 3 (more negative OMR flows), suggesting that OMR flows had minimal effect on the general timing patterns of when steelhead tags reached an array.

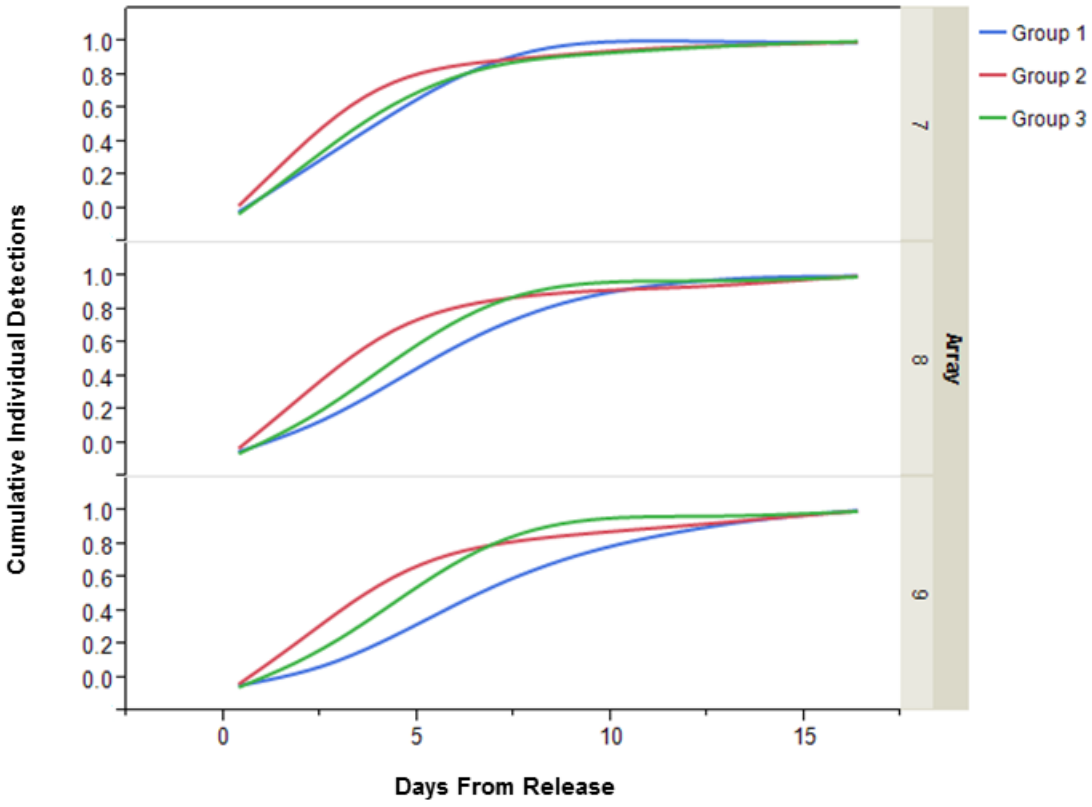

Figure 5-1 The cumulative detection curves for Groups 1, 2, and 3 at arrays 7, 8, and 9.

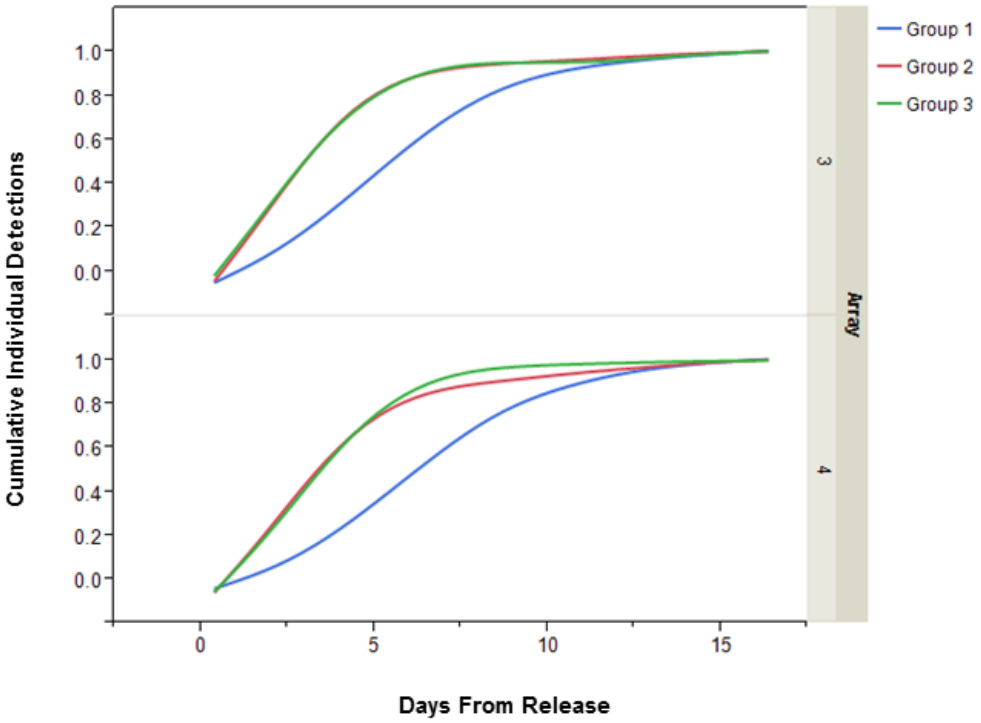

Figure 5-2 The cumulative detection curves for Groups 1, 2, and 3 at arrays 3 and 4.

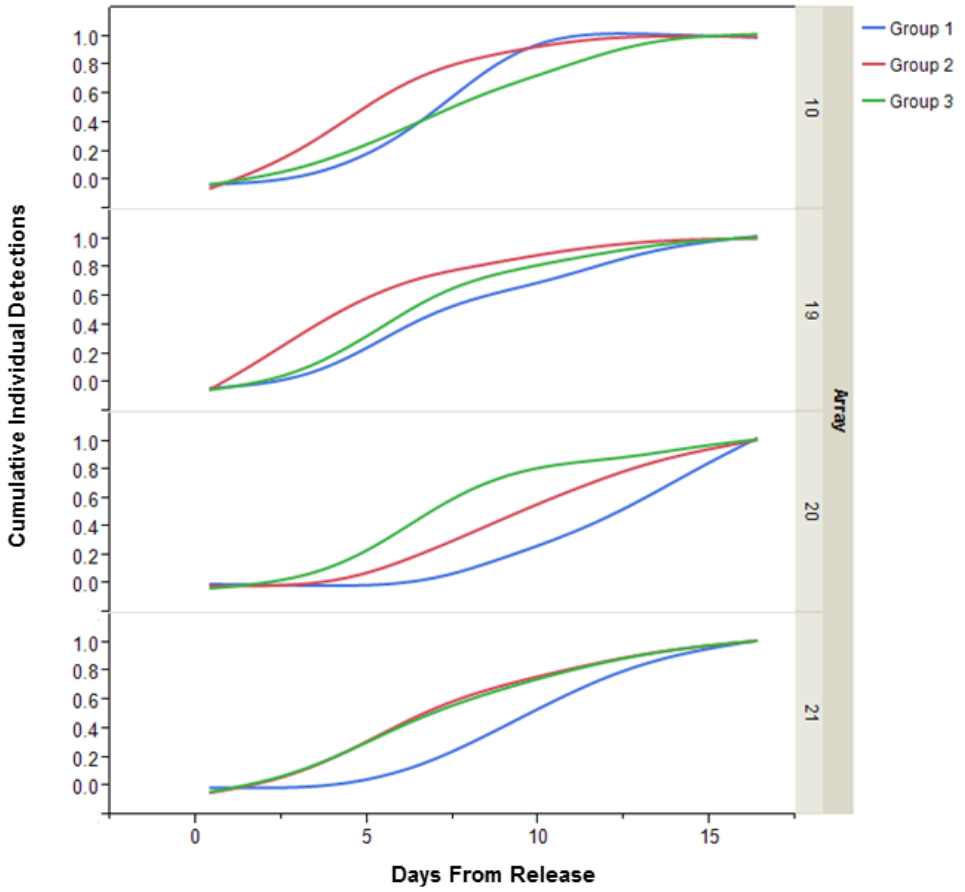

Figure 5-3 The cumulative detection curves for Groups 1, 2, and 3 at arrays 10, 19, 20, and 21.

For arrays 7, 8, 9, 3, and 4, we found that nearly all steelhead tags that reached an array did so by day 7 or 8, with the exception of Release Group 1. Also, there was little difference in the timing of steelhead tags arriving at these arrays between the Groups 2 and 3. The first group showed the largest difference in arrival timing, with slower accumulation of steelhead tag detections; the reasons for this slower rate of accumulation are unknown.

For the array at the CVP facility (array 21), a similar pattern was observed with steelhead tags from Release Groups 2 and 3 reaching this location faster than Group 1 (Figure 5-3). However, for the array at the SWP Clifton Court Forebay radial gates (20), arrival timing was fastest during the more negative OMR flow conditions of Group 3. This result may be due to radial gate operations, with radial gates possibly being opened for longer durations or opened wider during Group 3 when pumping rates were highest. In either case, this appears to be a more localized effect of OMR flows influencing the arrival timing of steelhead tags that was not observed at arrays farther from the export facilities. At Chipps Island (array 24), steelhead tags from Group 2 reached array 24 before those of Groups 1 and 3, which were slower to exit the system and would have been exposed to predators for a longer time and may have reduced survival. Further, if travel time and exposure to predators govern survival, we would expect the highest survival in Group 2, which reached Chipps Islands faster (Figure 5-4 and Section 4.2.3). While we do not have individual survival estimates for the individual release groups (Section 4.2) we do provide evidence in Figure 4-4 to Figure 4-6 that the number of steelhead tags reaching Chipps Island was higher in Group 2 than in Groups 1 and 3.

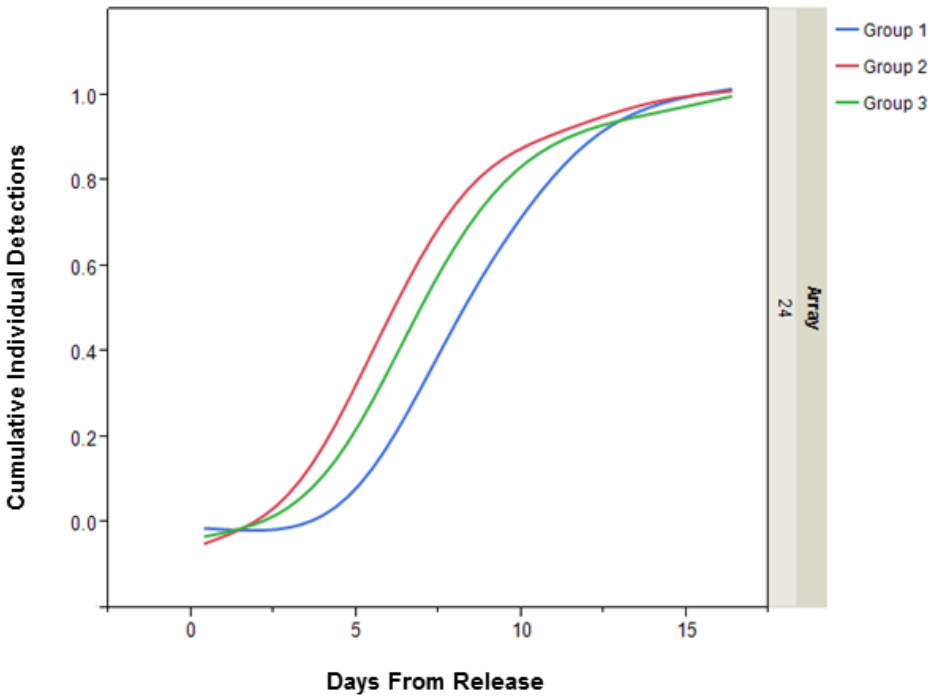

Figure 5-4 The cumulative detection curves for Groups 1, 2, and 3 at array 24.

In summary, OMR flows evaluated here appeared to have had little influence on steelhead tag movement during the study, except for limited evidence of an influence on steelhead tag routing at Railroad Cut in the interior Delta, and arrival timing at the SWP radial gates. Future studies should focus on how smolt movement and survival at Railroad Cut and southward (toward the export facilities) may be influenced by changing OMR flow conditions. In addition, future studies should be conducted under the entire range of possible OMR flow conditions to capture the range of possible effects on smolt movement and survival. As tidal conditions may also contribute to changes in fish behavior, any future studies should also be condcuted under shorter time periods with greater replication.

5.2 HOW EFFECTIVE WAS REAL-TIME MONITORING AND MANAGEMENT?

One of the project goals was to determine if real-time monitoring of steelhead smolt movement is feasible, and could it be conducted in a way to adaptively manage Delta exports to alter the routing and survival of steelhead in a timely and beneficial way. During the Stipulation Study, steelhead tags were used as "sentinels" to identify when wild salmonids were likely approaching the export facilities. Steelhead tag data were downloaded daily from the arrays near Railroad Cut (arrays 9 and 16) to track movement. When steelhead tag detections at Railroad Cut exceeded a threshold (5% of the release group detected at Railroad Cut; NMFS 2012), managers triggered a management option that reduced south Delta exports to provide additional protection for ESA-listed salmonids.

Given how quickly steelhead tags moved through the study system, most steelhead tags had already moved through the system before the triggered management option took effect. More than 90% of the steelhead tags had already left array 9 and passed by Railroad Cut before the effect of the management action was observed (OMR flows reached -1,250 cfs). Therefore, we cannot evaluate if reducing exports had the intended effect, given the small sample size of steelhead tags at Railroad Cut after the management action was implemented. While improvements to the experimental design of any future real-time monitoring study could be completed, this study points to the inability to effectively use tagged steelhead smolts as sentinels to trigger export changes. This study also provides evidence of the challenges of managing Delta flow conditions in real-time. Although the ability to manage flows is possible, the question of when and how to do this is not answered or supported from the data in this study.

In order to rapidly detect sentinel fish, receiver arrays would need to be downloaded more often than daily and ideally provide detections in real-time. True real-time detections would likely be necessary to be able to alter flow conditions quickly enough to influence fish movements. Even in real-time, monitoring stations may need to be placed farther north to allow the needed time for the presence of the focal species to be detected and the management option to be implemented and take effect before the majority of fish exit the area of influence.

The observed limited influence of OMR flows on steelhead tag behavior argues against the usefulness of real-time monitoring for protecting salmonids. Even if real-time monitoring could be conducted effectively, there is little evidence from this study to show that altering the OMR flow conditions would alter fish behavior in a meaningful way. We recommend that additional studies be conducted under a larger range of OMR flows to examine if and at what levels OMR flows affect the routing of steelhead. Flow conditions will need to be established for minimum time periods before changes are made as changing flow conditions during the study can limit the extent of analysis that can be performed.

5.3 WHAT WERE THE LIMITATIONS OF THE EXPERIMENTAL DESIGN AND HOW COULD THEY BE IMPROVED?

As with all field work and data analyses, this study faced some unforeseen challenges and complications. While no changes can guarantee that these do not occur in the future, these problems need to be identified so they can hopefully be avoided in future studies. In this section, we list and describe some examples.

Insufficient time to properly plan the study

This project was developed and implemented in a short time period that did not allow for certain important considerations to occur. The number of receivers, while extensive, was limited by the amount of time for acoustic receivers to be procured. Power analysis, which is useful in determining the proper sample size needed for an experiment, was not conducted as additional study fish were not available. Research requests for hatchery produced salmonids must be submitted several months in advance to allow for hatchery staff to produce the necessary study fish. Also, given the short amount of time for planning, careful consideration of the optimal

placement of acoustic receivers to address the study hypotheses was not possible, limiting the conclusions that could be made from the resulting dataset.

Limited range of OMR flow conditions

One of the shortcomings of how the experiment was conducted was that the least negative on average OMR flow treatment was not met for Group 1. Therefore, given the data from this study, we could only examine how changes in OMR flows from -2,446 to -5,038 cfs affected steelhead tag movement and survival. As also evidenced by the results, a more negative OMR flow is needed to possibly measure any effect on fish movement.

Incompatibility and discrepancies of hydrodynamic datasets

Sub-daily (15-minute) hydrodynamic influences (proportional flow movement at junctions, average flow, percent positive flow) on fine-scale steelhead tag movement were expected to be analyzed to examine how tidal influences affect fish migration into the interior Delta, and patterns of migration behavior and survival once steelhead tags enter the interior Delta. However, as statistical analyses were being completed, we consistently observed steelhead tags moving opposite the direction of flow movement at the Turner Cut junction (the only junction analyzed in this way). These unexpected movement patterns were observed for steelhead smolts, suggesting these findings likely were not a true observation of fish behavior, but rather a spurious artifact of steelhead tag timing not being in-sync with available sub-daily DSM2 flow data used to inform flow conditions (Cavallo et al. 2012).

To examine if the steelhead tag and flow timing were out of sync, we compared DSM2 output near Turner Cut with observed flow data at gauging stations. Although the daily flow magnitude was similar between datasets, the tidal cycle appeared to be off-sync by approximately 2 hours. If the CDEC data represent the true flow conditions, then by analyzing DSM2 Hydro data at Turner Cut and other locations we may be relating steelhead tag behavior with incorrect flow conditions. Therefore, our findings of steelhead tags moving against flow movement were likely a result of steelhead tag timing being paired with flow conditions opposite of what they may have actually experienced. Rapid changes in tidal flow conditions mean that small discrepancies in timing between predicted and actual flow patterns can lead to results directly the opposite of expectations.

After completing the preliminary analyses, we also examined data from the few CDEC flow gauges with paired acoustic receiver arrays. For example, we examined steelhead tag arrival timing at array 9, near Railroad Cut, which is next to CDEC flow gauge MDM. We found that steelhead tags moved south toward Railroad Cut more often when OMR flows were positive (flows moving strongly north). This discrepancy indicated that there was two-dimensional hydrodynamic complexity of the Delta channels near Railroad Cut that were not being captured by the one-dimensional CDEC flow gauge. Although this is only a single location, this further exemplified the difficulty of examining fine-scale flow and steelhead tag relationships using the hydrodynamic data currently available. Because of the strong tidal influence in the Delta, flow measurements and steelhead tag observations must be paired perfectly together to know exactly what the flow conditions a steelhead tag was experiencing when making a routing "decision." Therefore, we did not examine fine-scale (less than 2-hour increments as seen in Section 4.3.2) tag and flow relationships for the analyses. For future studies, we recommend deploying flow measurement equipment specifically for these studies, and pairing them with acoustic receiver locations in order to reliably relate tag behavior and fine-scale flow conditions.

Inability to distinguish between a predator or tagged smolt

As stated in the assumptions section (Section 2.4), we were unable to identify a free-swimming tagged steelhead smolt from a tag that had been consumed by a predator. Therefore, we refer to detections as detections of steelhead tags throughout this report, rather than detections of acoustically tagged steelhead. The development of tags that can allow researchers to distinguish between smolts and predators is critical to ensure accurate filtering of free-swimming smolt data from steelhead tags that were consumed by predators.

Spatial resolution of acoustic telemetry and hydrodynamic data

The 2012 study utilized a one-dimensional array of receivers, which limited the fine-scale fish movement questions that could be answered. The one-dimensional array of receivers provided a simplification of the three-dimensional complexity of the interior Delta junctions and channels, limiting this investigation to one-dimensional movement patterns. To better understand steelhead smolt movement behavior, particularly at junctions, future studies will need to track the fine-scale movement of tagged smolts, paired with high resolution hydrodynamic data.

Low detection probabilities

Although overall most arrays had high detection probabilities (>80%), some sites (e.g., arrays 2 and 21) had lower probability of detections. Before future studies are conducted, we recommend that strategies be examined to raise detection probability. Possible strategies include: increasing the number of receivers deployed, optimizing their arrangement, and validating their effectiveness with empirical studies. Further, we recommend examining other types and providers of equipment to determine the best equipment for future studies. For example, we recommend that equipment such as Hydroacoustic Technology Inc. (HTI) and Juvenile Salmon Acoustic Telemetry System (JSATS) are considered for use in future studies.

Complexity of the system

The complexity of the south Delta limited our ability to adequately place arrays at many junctions and channels, making it difficult to meet the stringent assumptions needed for the USER model (Lady et al. 2008). For example, Columbia Cut is such a complex junction that even with optimal placement of arrays, it may not be possible to estimate separate survival and route entrainment probabilities in the USER models. If greater spatial resolution is required for future studies (e.g., more reach survival or more route entrainment calculations at junctions), additional receivers would need to be placed at strategic locations throughout the south Delta to ensure adequate coverage.

Limited sample size and statistical power

The relatively small sample sizes across release groups (166, 167, and 168 for Groups 1, 2, and 3, respectively) limited our ability to analyze the data. The total number of fish released across all release groups was similar to the number of Chinook salmon released in a single release group during the VAMP study (SJRGA 2013). The limited sample size contributed to the inability of the multistate model to converge on individual release group models, leading to a pooled model across release groups. Future studies should conduct power analyses prior to conducting the field study to ensure adequate sample size to address study questions.

5.4 WHAT FUTURE EXPERIMENTS AND METHODS ARE RECOMMENDED?

Meta-data analyses of past studies

Meta-analysis is an approach that gathers datasets from previous studies and analyzes them to see if there are important and robust relationships across the relevant studies. The Delta is well studied and therefore is the ideal study system for this type of approach using the datasets collected by the various agencies and groups: the California Department of Fish and Wildlife (CDFW), Department, East Bay Municipal Utilities District, NMFS, San Joaquin River Group Authority (SJRGA), Sacramento Municipal Waste Water Treatment Plant, Reclamation, USGS, USFWS, University of California at Davis, and others. Data from studies by these groups could be compared and evaluated immediately and with a limited budget, given that the project would not require additional money for field work. These studies require no new permits, which can be challenging and time-

intensive to obtain. If this study is done, it would allow managers to know if results from one study or study period could be generalized to address other issues.

Similar study but more comprehensive with greater preparation, receiver coverage, larger sample size, more replication, and more extreme range of OMR flow values

Prior to any future experiment, careful deliberation of the experimental design and how resulting data will be analyzed would be crucial to providing more useful results. Primarily due to the extreme time limitations of the Stipulation Study, limited attention was given to determining an experimental design that could meet all project objectives. For example, only data from two of the Stipulation Study arrays were incorporated into the routing and survival model, causing us to rely on receivers from the Six-Year Study. This was due to limited consideration of how the study design would provide data required to answer study questions.

We recommend that future studies deploy additional receivers to provide better coverage of complex Delta junctions. Although expensive, it is easy to deploy receivers in numerous locations, thereby increasing the number of management questions that can be answered. However, the cost and location should be justifiable and add value to the study. For example, a central goal of this study was to quantify the routing and survival of steelhead. However, given the complexity of the system and assumptions of the modeling approach to conduct the analyses, we were only able to estimate routing at Turner Cut (arrays 1, 2, and 7). At other junctions, we did not feel there was enough coverage of receiver arrays to meet the assumptions of the modeling program USER so that it could estimate separate route entrainment and survival probabilities for each route. These receivers must be placed just upstream of the junction and closely downstream after the junction so that there is no overlap in the detection coverage of the receivers. For more information on this topic, see Chapter 2 of the doctoral thesis by Perry (2010).

For any future experiment, sufficient sample sizes of tagged fish should be released to provide the necessary statistical power to examine the hypotheses of interest. Small sample sizes during this study limited our ability to examine routing and survival differences between treatment groups. Therefore, before any future experiments are conducted, power analyses should be completed to determine the sample sizes needed to find significant differences.

We propose that a future experiment would only be useful and better to analyze if it were done with larger differences in OMR flow conditions and that treatment levels are replicated. Therefore, rather than implementing each OMR flow treatment only once, it would be best to replicate each of the treatments at least twice, if not more. This form of replication should be done over multiple years to examine inter-annual variability and the applicability of the results and relationships to other situations. Also, we recommend that the range of OMR flows examined be at least as extreme as initially planned for in this experiment (-1,250, -3,500, and -5,000 cfs), which was not met in the actual experiment. Preferably, we recommend replicated experiments that are conducted over a wider range of OMR flows, possibly differing by an order of magnitude or more (e.g., -1,000 to -10,000 or 1,500 to -15,000 cfs).

It is critical that the design and implementation of this experiment be given sufficient time. The design and implementation of any future study should not be conducted in 2 months but should be given the proper time and money for this critical stage to be deliberate, methodical, and not rushed. Sufficient time should be given to carefully consider the placement of acoustic receiver arrays to make sure that all study hypotheses can be properly examined. Time is also needed to conduct power analyses to determine proper sample sizes in order to detect differences in subsequent statistical tests. Sufficient time is also needed to identify and provide the essential field resources to implement increased sample sizes and additional receiver arrays.

Examining model design and selection and the effect on estimated parameters

We recommend that an analysis be conducted on how model design affects the parameter estimates generated by the multistate statistical release-recapture model. The choices of what arrays are used, how many are used, and

where they are positioned could affect survival or route entrainment estimates. For this study we allowed the model to fit all parameter values without making post-hoc adjustments to values to improve model fit. We did not change or set anything in the model that was not a priori determined except for replacing array 6 with 7 and pooling release group data due to lack of model convergence. For example, we could have adjusted the detection probabilities fit by the model by using our Manly-Parr detection probability estimates at dual arrays and then re-run the model. Because these model design decisions may have an impact on model outcomes, we recommend examining the consequences of these decisions in a future study. The dataset from this study could be an ideal example for this type of analysis.

Improvement of current models or creating new and more accurate models

The DSM2 Hydro PTM model underestimated the speed with which steelhead tags were migrating and inaccurately predicted their final location 7 days following release. Therefore, in its current form, the DSM2 Hydro PTM model did not appear to be a reliable model for simulating the movement patterns of steelhead tags. This result is important for management of this species as the DSM2 Hydro PTM model has been used in the past to manage for steelhead by examining the effect of various types of barriers and entrainment into various structures (e.g., agricultural diversion or export facilities). Therefore, we recommend that further study be conducted to better understand what causes the model to underestimate the speed of steelhead tags and inaccurately predict their locations and that future particle model runs incorporate specific fish movement behavior to better predict fish movement patterns. Important fish behaviors have yet to be identified and quantified. Until this step is taken, a coupled biological-physical model cannot be produced to accurately predict the speed of steelhead and other behaviors that are important for managing the species of concern or the operations of the SWP and CVP.

Experimental operation of export facilities

By conducting experimental operations of the export facilities, key questions could be answered about how exports influence the behavior and survival of salmonid smolts. To isolate the effect of each export facility (SWP and CVP) on fish behavior and survival, all exports could be shifted to either facility for a brief period of time during future biotelemetry studies. Eliminating exports completely during an experimental study (e.g., if both facilities have maintenance during the same period of time), along with examining the extreme high end of exports (as recommended above), would allow for an evaluation of the complete range of export effects.

Fine-scale and tidal experiments

While large-scale studies are useful, the large spatial scale and complexity of the environment being examined commonly result in study findings that are coarse and limited in their ability to answer fine-scale questions. Smaller scale experiments can provide higher resolution fish and environmental data more easily, and provide higher accuracy results. Conducting fine-scale experiments using two- or three-dimensional acoustic receiver arrays paired with fine-scale hydrodynamic data collected simultaneous with fish releases could help answer a multitude of questions. One sample experiment we recommend would examine fish routing and survival in the interior Delta near Railroad Cut. While we conducted an exploratory analysis examining routing at Railroad Cut (described in Section 4.3.3), we could only coarsely examine how broad movement patterns were affected across the narrow range of OMR flows examined. Greater receiver coverage and multi-dimensional tracking, paired with fine-scale hydrodynamic data and locally released smolts, would provide high resolution information on how fish move at this critical junction and what factors influence routing and survival in the interior Delta. While it could be argued that such a fine-scale study would only provide site-specific information, a better understanding of the mechanisms underlying fish routing and survival could be gained, to better understand steelhead smolt behavior at the junctions examined.

Although we examined if STST fish behavior occurred in a short reach in the interior Delta, a greater understanding of how steelhead smolts use the tides during migration is critical to understanding how best to

manage the Delta (Kneib et al. 2012). Many questions remain about how steelhead smolts use the tides for movement, including:

- Do steelhead use ebb tides equally for migration, or do they only "surf" tides during the daytime or nighttime?
- Do other factors influence how steelhead smolts use tides, such as habitat quality or predation?
- What level of tidal influence is needed for steelhead smolts to exhibit STST behavior?
- How does STST behavior vary spatially across the Delta?

We recommend conducting fine-scale smolt tagging studies across the Delta, while simultaneously collecting hydrodynamic data, to better understand how tides influence steelhead smolt movement, survival, and travel time. Releases of tagged fish could occur at various tidal stages (e.g., flood and ebb tides). Given that the tidal stage changes throughout the day, and the amplitudes of tides change multiple times in a lunar month, experiments could be conducted frequently and in short durations. Therefore, study replication would be easy to accomplish, which is key for any well-designed experiment.

Predation tags

A prototype acoustic tag has been developed that would distinguish between smolts and predators. This prototype tag is currently being tested by the Department and Reclamation. If the prototype is successful, all future tagging studies should use these new tags or similarly tested and successful tags to more accurately filter predators from the data set and provide more accurate data on tagged smolt movement and survival.

Additional management trigger studies

While the Stipulation Study attempted to use real-time monitoring of tagged hatchery steelhead to limit the entrainment of wild steelhead smolts at the export facilities, the experiment was largely unsuccessful. Most of the tagged steelhead had already passed Railroad Cut before the effect of the flow trigger was observed (OMR flows reached -1,250 cfs), thereby limiting the influence of triggered flow conditions on steelhead tag movement. It is unknown how well tagged hatchery steelhead provided a proxy for wild steelhead. If additional studies are warranted, we recommend that an experimental approach be first conducted that uses true "real-time" remote monitoring of receivers and examine multiple receiver locations to determine the location of where real-timing monitoring arrays would be most effective. In addition, a wider range and minimum duration of flow management alternatives should be examined to better understand if a real-time flow trigger can provide any benefit to steelhead smolt survival. Finally, the feasibility of using wild steelhead smolts during future real-time flow trigger experiments should be examined to more directly attempt to understand wild steelhead smolt movement in the Delta.

5.5 CONCLUSIONS

- Overall, under the OMR flows tested and the conditions that occurred during the field study, there was little influence of OMR flows on steelhead tag movement during the study.
- This study was limited by the amount of time for its preparation and the ranges of OMR flows tested. Future studies should be performed with adequate preparation time and with more control over the OMR flow ranges, including OMR flows beyond those allowed by both health and safety standards and by water quality and ESA protections.
- There was limited evidence of OMR flows influencing steelhead tag routing at Railroad Cut in the interior Delta and arrival timing at the SWP Clifton Court Forebay radial gates.

- The quantitative statistical analyses determined that the DSM2 Hydro PTM was not able to predict the movement of steelhead tags because it greatly underestimated steelhead tag movement through the study area.
- There was evidence that diurnal and nocturnal movement patterns of steelhead tags might be occurring, but these patterns were location-specific. Future study is needed to understand this pattern.
- There was limited evidence that altering OMR flow conditions tested within the levels observed in the study would alter fish behavior in a meaningful way. Future studies should be performed with a wider range of OMR flows and of minimum duration to provide evidence that real-time monitoring could be used to protect salmonids.
- Future studies should focus on how steelhead smolt movement and survival at Railroad Cut and south (toward the export facilities) may be influenced by a wider range of OMR flow conditions and minimum duration than examined in this study.
- Future studies, including a more comprehensive version of this experiment should be conducted with a wider range of OMR flows and of minimum duration that are replicated with more acoustic receivers and larger sample size of tagged fish.

This page intentionally left blank.

6 REFERENCES

Anderson, J. J., E. Gurarie, and R. W. Zabel. 2005. Mean free-path length theory of predator-prey interactions: Application to juvenile salmon migration. Ecological Modelling 186:196-211.

Bégout Anras, M. L., and J. P. Lagardere. 2004. Measuring cultured fish swimming behavior: first results on rainbow trout using acoustic telemetry in tanks. *Aquaculture* 240, 175-186.

Buchanan, R. A. 2013. Juvenile Salmonid Survival Through the San Joaquin Delta in the Presence of Predatory Fish, 2010-2011. PowerPoint presentation prepared by Rebecca Buchanan, Columbia Basin Research, School of Aquatic and Fishery Sciences, University of Washington, Seattle. Available at: https://nrm.dfg.ca.gov/FileHandler.ashx?DocumentID=69586. Accessed November 2013.

Buchanan, R. A., and R. Perry. 2011. Survival Analysis of Tagging Data. PowerPoint presentation by R. Buchanan, University of Washington, and R. Perry, U.S. Geological Survey, June 28-29, 2011.

Buchanan, R. A., J. R. Skalski, P. L. Brandes, and A. Fuller. 2013. Route use and survival of juvenile Chinook salmon through the San Joaquin River Delta. *North American Journal of Fisheries Management* 33:1, 216-229.

California Data Exchange Center (CDEC). 2013. Department of Water Resources, CDEC data for the Turner Cut Near Holt Station. Available at: http://cdec.water.ca.gov/cgi-progs/staMeta?station_id=TRN. Last accessed on October 15, 2013.

Cavallo, B., P. Bergman, J. Melgo, K. Jones, and P. Gaskill. 2012. Status Report for 2012 Acoustic Telemetry Stipulation Study. Series: Cramer Fish Sciences, 30 pages. Available at: http://deltacouncil.ca.gov/sites/default/files/documents/files/20121015_STIP_Status_Report.pdf. Last accessed on October 15, 2012.

Chapman, E. D., A. R. Hearn, C. J. Michel, A. J. Ammann, S. T. Lindley, M. J. Thomas, P. T. Sandstrom, G. P. Singer, M. L. Peterson, R. B. MacFarlane, A. P. Klimley. 2013. Diel movements of out-migrating Chinook salmon (*Oncorhynchus tshawytscha*) and steelhead trout (*Oncorhynchus mykiss*) smolts in the Sacramento/San Joaquin Watershed. *Environmental Biology of Fishes* 96:273–286.

Chittenden, C. M., S. Sura, K. G. Butterworth, K. F. Cubitt, N. Plantalech Manel-La, S. Balfry, F. Økland, and R. S. McKinley. 2008. Riverine, estuarine and marine migratory behavior and physiology of wild and hatchery-reared coho salmon Oncorhynchus kisutch (Walbaum) smolts descending the Campbell River, BC, Canada. Journal of Fish Biology 72:614-628.

Clark, K. W., M. D. Bowen, R. B. Mayfield, K. P. Zehfuss, J. D. Taplin, and C. H. Hanson. 2009. Quantification of Pre-Screen Loss of Juvenile Steelhead in Clifton Court Forebay. State of California, California Department of Water Resources, Sacramento, California.

Clements, S., T. Stahl, and C. B. Schreck. 2012. A comparison of the behavior and survival of juvenile coho salmon (*Oncorhynchus kisutch*) and steelhead trout *(O. mykiss*) in a small estuary system. *Aquaculture* 362-363:148-157.

Cramer Fish Sciences. 2013. Phase II Data Analysis Plan for the 2012 Acoustic Telemetry Stipulation Study. Prepared by David Delaney, Paul Bergman, Brad Cavallo, and Jenny Melgo, Cramer Fish Sciences, under the direction of Kevin Clark, California Department of Water Resources.

Delaney, D. G., P. Edwards, and B. Leung. 2012. Predicting regional spread of invasive species using oceanographic models – validation and identification of gaps. *Marine Biology* 2:269-282.

Drenner, S. M., T. D. Clark, C. K. Whitney, E. G. Martins, S. J. Cooke, and S. G. Hinch. 2012. A synthesis of tagging studies examining the behavior and survival of anadromous salmonids in marine environments. PLoS ONE 7(3): e31311. Doi: 10.1371/journal.pone.0031311.

Fox, J. 2005. The R Commander: A Basic Statistics Graphical User Interface to R. Journal of Statistical Software, 14(9): 1-42.

Gingras, M. 1997. Mark/recapture experiments at Clifton Court Forebay to estimate pre-screening losses to juvenile fishes 1976–1993. *Interagency Ecological Program Technical Report 55*.

Kahle, D., and H. Wickham. 2013. ggmap: A package for spatial visualization with Google Maps and OpenStreetMap. R package version 2.3. Available at: http://CRAN.R-project.org/package=ggmap. Last accessed on December 10, 2013.

Kimmerer, W. J., and M. L. Nobriga. 2008. Investigating particle transport and fate in the Sacramento-San Joaquin Delta using a particle tracking model. *San Francisco Estuary and Watershed Science* Vol. 6, Issue 1 (February), Article 4:1-26. Available at: http://repositories.cdlib.org/jmie/sfews/vol6/iss1/art4/. Last accessed on October 15, 2013.

Kneib, R. T., J. J. Anderson, A. Gore, M. S. Lorang, J. M. Nestler, and J. Van Sickle. 2012. Report of the 2012 Delta Science Program Independent Review Panel (IRP) on the Long-term Operations Opinions (LOO) Annual Review. Available at: http://nodeltagates.files.wordpress.com/2012/12/isb_report_2012_dspirp_looar_120112_final.pdf. Last accessed on December 15, 2012.

Lady, J. M., P. Westhagen, and J. R. Skalski. 2008. USER 4: User specified estimation routine. School of Aquatic and Fishery Sciences, University of Washington, Seattle, Washington. Available at: http://www.cbr.washington.edu/paramest/user/. Last accessed on October 15, 2013.

Manly, B. F. J., and M. J. Parr. 1968. A new method of estimating population size, survivorship, and birthrate from capture–recapture data. *Transactions of the Society for British Entomology* 18:81-89.

Martin, F., R. D. Hedger, J. J. Dodson, L. Fernandes, D., Hatin, F. Caron, and F. G. Whoriskey. 2009. Behavioural transition during the estuarine migration of wild Atlantic salmon (*Salmo salar* L.) smolt. *Ecology of Freshwater Fish* 18:406-417.

Melnychuk, M. C., D. W. Welch, and C. J. Walters. 2010. Spatio-temporal migration patterns of Pacific salmon smolts in rivers and coastal marine waters. PLoS ONE 5(9): e12916. Doi: 10.1371/journal.pone.0012916.

Metaxas, A., and M. Saunders. 2009. Quantifying the ‘‘Bio-’’ components in biophysical models of larval transport in marine benthic invertebrates: advances and pitfalls. *Biological Bulletin* 216:257-272.

Moore, A., E. C. E. Potter, N. J. Milner, and S. Bamber. 1995. The migratory behavior of wild Atlantic salmon (*Salmo salar*) smolts in the estuary of the River Conwy, North Wales. *Canadian Journal of Fisheries and Aquatic Sciences* 52:1923-1935.

National Marine Fisheries Service (NMFS). 2009 (June 4). *Biological Opinion and Conference Opinion on the Long-Term Operations of the Central Valley Project and State Water Project*. Southwest Regional Office, Long Beach, California.

National Marine Fisheries Service (NMFS). 2012. Technical memorandum to guide adaptive management of OMR during April and May 2012 for the protection of listed San Joaquin Basin steelhead. Southwest Regional Office, Long Beach, California.

Perry, R. W. 2010. Survival and migration dynamics of juvenile Chinook salmon (*Oncorhynchus tshawytscha*) in the Sacramento-San Joaquin River Delta. Dissertation, University of Washington.

Perry, R. W., J. R. Skalski, P. L. Brandes, P. T. Sandstrom, A. P. Klimley, A. Ammann, and B. MacFarlane. 2010. Estimating survival and migration route probabilities of juvenile Chinook salmon in the Sacramento-San Joaquin River Delta. *North American Journal of Fisheries Management* 30:142-156.

R Project. 2013. The R Project for Statistical Computing. Available at: http://www.r-project.org/. Last accessed on October 15, 2013.

RStudio Inc. 2013. Shiny: Web Application Framework for R. R package version 0.8.0. Available at: http://CRAN.R-project.org/package=shiny. Last accessed on December 10, 2013.

San Joaquin River Group Authority (SJRGA). 2011. 2010 Annual technical report on implementation and monitoring of the San Joaquin River agreement and the Vernalis Adaptive Management Plan (VAMP).

San Joaquin River Group Authority (SJRGA). 2013. 2011 Annual technical report on implementation and monitoring of the San Joaquin River agreement and the Vernalis Adaptive Management Plan (VAMP).

This page intentionally left blank.

APPENDIX A

Concordance Table

RECIRC2566.

Concordance table that covers how the objectives and hypotheses have changed, adapted, or stayed the same during the different stages of the study.

Concordance Table						
	Objective			Hypothesis		
Version	Number	Description	Changes from Previous	Number	Description	Changes from Previous
December 6, 2012	1	What factors influence route entrainment into the interior Delta from Turner Cut, Colombia Cut and Middle River?	N/A	1.1	The proportion of tagged fish entering the interior Delta route is not related to release group, study, junction, and time-at-large.	N/A
	2		N/A	2.1	The probability of fish returning to Mainstem SJR is not related to release group, study, junction and time-at-large.	N/A
				2.2	Residence time of fish in Delta reaches (between arrays) does not vary by release group, study, or time-at-large.	N/A
				2.3	The movement of fish in the Mainstem and in the interior Delta will be random (i.e., not related to tidal periodicity).	N/A
	3		N/A	3.1	The survival of tagged fish in the interior Delta is not different from the survival in the San Joaquin River.	N/A
				3.2	Survival through the Mainstem San Joaquin River is not significantly related to study or release group.	N/A
				3.3	Survival through the interior Delta is not significantly related to study or release group.	N/A
				3.4	Routing through the interior Delta does not differ with group or study.	N/A

Concordance Table						
	Objective			Hypothesis		
Version	Number	Description	Changes from Previous	Number	Description	Changes from Previous
February 11, 2013	1	How do group and study influence survival and routing?	Same as previous Objective 3.	1.1	Overall Delta survival and route survivals were not significantly related to study or release group.	Same as previous 3.2 and 3.3 combined.
				1.2	The survival of tagged fish in the interior Delta is not different from the survival in the San Joaquin River.	Same as previous 3.1.
				1.3	Routing at each junction (Turner Cut, Columbia/Middle, Railroad Cut) did not differ with group, study, or due to export trigger.	Same as previous 3.4 and 1.1 combined. Also, added in an examination of export trigger on routing.
	2	What factors influenced fine-scale migration behavior in the interior Delta?	Same as previous Objective 2.	2.1	The proportion of fish returning to Mainstem SJR was not related to release group, study, or junction.	Same as previous 2.1.
				2.2	The movement of fish in the Mainstem and interior Delta is random (i.e., not related to tidal periodicity or day/night).	Includes previous 2.3 examination of tidal periodicity and also new examination of diurnal effect.
				2.3	The last location of acoustically tagged fish was not significantly different than the last location of modeled particles.	New hypothesis.
				2.4	Routing through the interior Delta does not differ with group or study.	New hypothesis.

Concordance Table						
	Objective			Hypothesis		
Version	Number	Description	Changes from Previous	Number	Description	Changes from Previous
March 29, 2013	1	To examine if survival and routing probabilities vary between different release groups.	Same as previous Objective 1.	1.1	Overall Delta survival and route survivals were not significantly related to study or release group.	Same as previous 1.1.
				1.2	The survival of tagged fish in the interior Delta is not different from the survival in the San Joaquin River.	Same as previous 1.2.
				1.3	Survival to Chipps Island was not significantly different for tags going through salvage versus tags that did not go through salvage.	New hypothesis.
				1.4	Routing at Turner Cut did not differ with release group or study.	Similar to previous 1.3 except only examining Turner Cut junction. The other junctions are examined in the new 2.1.
	2	What factors influenced within-reach migration behavior in the interior Delta?	Same as previous Objective 2.	2.1	The proportion of tags that entered the interior Delta at Columbia Cut or Middle River was not related to release group.	Similar to previous 1.3 but only examines Columbia and Middle Junctions. Turner Cut is in new 1.4 and Railroad Cut is new 2.6.
				2.2	The movement of fish in the Mainstem and interior Delta is random (i.e., not related to day/night).	Examines diurnal effect on tag movement as in previous 2.2, but tidal effects are now examined differently in new 2.3.
				2.3	The acoustically tagged fish did not move using STST.	New hypothesis.
				2.4	The last location (receiver array) of tags was not significantly different than the last location of modeled particles.	Same as previous 2.3.
				2.5	The migration rate of tags was not significantly different between fish routes or between release groups.	New hypothesis.
				2.6	The movement patterns of tags after Railroad Cut were not different before and after the OMR trigger.	Previously part of hypothesis 1.3.

Concordance Table						
	Objective			Hypothesis		
Version	Number	Description	Changes from Previous	Number	Description	Changes from Previous
Data Analysis Plan (June 28, 2013)	1	To examine if survival and routing probabilities vary between different release groups.	Same as previous Objective 1.	1.1	Overall survival and route-specific transitions probabilities of tags were not significantly related to release group.	Same as previous 1.1.
				1.2	The survival of tagged fish in the interior Delta is not different from the survival in the San Joaquin River.	Same as previous 1.2.
				1.3	Routing at Turner Cut did not differ with release group or study.	Same as previous 1.4.
	2	What factors influenced reach-specific survival and routing in the interior Delta?	Same as previous Objective 2.	2.1	The proportion of tags that entered the interior Delta at Columbia Cut or Middle River was not related to release group.	Same as previous 2.1.
				2.2	The movement of fish in the Mainstem and interior Delta is random (i.e., not related to day/night).	Same as previous 2.2.
				2.3	The acoustically tagged fish did not move using STST.	Same as previous 2.3.
				2.4	The last location (receiver array) of tags was not significantly different than the last location of modeled particles.	Same as previous 2.4.
				2.5	The travel times of acoustically tagged fish were not significantly different between routes or between release groups.	Similar to previous 2.5 except examining travel time instead of migration rate.
				2.6	The movement patterns of tags after Railroad Cut were not different before and after the OMR trigger.	Same as previous 2.5.
				2.7	The daily proportion of tags at each of the export facilities is proportional to the fraction of the water entering the facilities.	New hypothesis.

Concordance Table						
	Objective			Hypothesis		
Version	Number	Description	Changes from Previous	Number	Description	Changes from Previous
Final Report (February 3, 2014)	4.1	**System**: Examine large-scale movement patterns of steelhead tags.	Comprises hypotheses from previous objective 2 that examine system-wide processes affecting tag movement and includes new descriptive analyses.	4.1.1	Examined the spatial pattern of steelhead tags detected at each array by release group.	New descriptive analysis without a predetermined hypothesis.
				4.1.2	Examined the spatial pattern of where steelhead tags were last detected by release group.	New descriptive analysis without a predetermined hypothesis.
				4.1.3	Examined the spatial pattern of residence time at each array by release group.	New descriptive analysis without a predetermined hypothesis.
				4.1.4	Examined the spatial pattern of the final fate of tags at each array by release group.	New descriptive analysis without a predetermined hypothesis.
				4.1.5	Created a web-based dissemination tool to spatially display the full detection history of individual tags.	New descriptive analysis without a predetermined hypothesis.
				4.1.6	The distance traveled by steelhead tags was not significantly different than the distance traveled by the passive particles.	Similar to the previous 2.4 except we reworded for clarity.
				4.1.7	Steelhead tags did not move using STST.	Similar to the previous 2.3 except we removed reference to fish.
				4.1.8	The movement of steelhead tags in the San Joaquin River and interior Delta was not related to day/night.	Similar to the previous 2.2 except we removed reference to fish.
	4.2	**Route**: Examine how steelhead tags move through the system using different defined routes.	Comprises previous Objective 1 and route-specific hypothesis from previous Objective 2.	4.2.1	Route-specific transition probabilities of steelhead tags were not significantly related to the route taken and/or release group.	Similar to previous 1.1 except release-specific models would not converge to examine release-specific survival. Also, overall survival was moved to Hypothesis 4.2.2.
				4.2.2	The estimated route-specific survival for the Turner Cut route was not significantly different from the Mainstem route.	Similar to the previous 1.2 except we deleted the reference to fish.

Concordance Table						
	Objective			Hypothesis		
Version	Number	Description	Changes from Previous	Number	Description	Changes from Previous
				4.2.3	The travel times of steelhead tags were not significantly different between routes or release groups.	Same as previous 2.5 except we deleted the reference to fish.
	4.3	**Junction**: Examine how steelhead tags move through junctions.	Comprises hypotheses from previous Objective 2 that examine junction-specific analyses.	4.3.1	The probability of steelhead tags entering the interior Delta at Turner Cut, Columbia Cut, and Middle River was not related to OMR flows.	Combines previous 1.3 and 2.1 and is the same except we deleted the reference to fish.
				4.3.2	Steelhead tag arrival at each facility was not related to the proportion of total export flow entering SWP.	Similar to previous 2.7 except we are working with 2-hour data and array level data that allows us to use finer temporal data.
				4.3.3	The movement patterns of steelhead tags after passing through Railroad Cut were not affected by OMR flows.	Same as previous 2.6 except we changed how we refer to tags.

APPENDIX B

Crosswalk Table of Tag and Dependent Analysis

Note: This appendix presents the data used to produce the figures and results for the analyses in this report (Chapter 4). If data from a steelhead tag were used in the figure and/or analysis for that section, a "1" was placed in that cell. For Section 4.1.6, we presented the data for tags that were detected on the third ("4.1.6 [3D]") and seventh day ("4.1.6 [7D]") after their release. For Section 4.3.1, we examined three junctions: Turner Cut ("4.3.1 [TC]"), Columbia Cut ("4.3.1 [CC]"), and Middle River ("4.3.1 [MR]")

RECIRC2566.

Crosswalk Table of Tag and Dependent Analysis												
Fish ID	4.1.1 - 4.1.5	4.1.6 [3D]	4.1.6 [7D]	4.1.7	4.1.8	4.2.1 & 4.2.2	4.2.3	4.3.1 [TC]	4.3.1 [CC]	4.3.1 [MR]	4.3.2	4.3.3
1133669	1	1			1	1		1	1		1	1
1133670	1	1			1	1		1				1
1133671	1	1			1	1		1	1	1		
1133672	1		1		1	1		1	1	1		
1133673	1		1		1	1		1	1			
1133674												
1133675												
1133677	1	1	1		1	1						
1133678	1	1		1	1	1		1				1
1133679	1	1		1	1	1	1	1				
1133680	1				1	1		1				
1133681	1	1	1		1	1	1	1	1	1		
1133682	1	1			1	1		1				
1133683	1		1	1	1	1		1			1	
1133684	1	1	1		1	1		1	1			
1133685	1				1	1		1				
1133686	1	1			1	1		1	1	1	1	1
1133687	1	1	1		1	1						
1133688	1	1			1	1		1	1			
1133689	1	1			1	1						
1133691	1	1	1	1	1	1		1				
1133692	1	1	1	1	1	1		1				1
1133693	1	1		1	1	1		1				1
1133694	1	1	1		1	1	1	1	1			
1133695	1	1	1		1	1		1			1	1
1133696	1		1	1	1	1		1				
1133697	1	1		1	1	1		1				1
1133698	1	1	1	1	1	1		1	1		1	1
1133699	1	1			1	1		1				
1133700	1	1	1		1	1	1	1				
1133701	1			1	1	1		1				
1133702	1		1		1	1		1				

Crosswalk Table of Tag and Dependent Analysis												
Fish ID	4.1.1 - 4.1.5	4.1.6 [3D]	4.1.6 [7D]	4.1.7	4.1.8	4.2.1 & 4.2.2	4.2.3	4.3.1 [TC]	4.3.1 [CC]	4.3.1 [MR]	4.3.2	4.3.3
1133703	1				1	1		1				
1133704	1				1	1		1	1	1		
1133705	1				1	1		1				
1133706	1				1	1						
1133707	1				1	1						
1133708	1	1	1		1	1		1	1			
1133709												
1133710	1	1	1		1	1						
1133711	1	1	1		1	1		1				
1133712	1	1		1	1	1	1	1				1
1133713	1	1			1	1		1				
1133714	1		1		1	1	1	1	1	1		
1133715	1	1			1	1		1	1			
1133716	1				1	1		1	1	1		
1133717	1				1	1						
1133718	1	1			1	1		1	1	1		
1133719	1	1			1	1						
1133720	1	1	1		1	1		1	1			
1133721	1	1	1		1	1		1	1	1		1
1133722												
1133723	1	1			1	1						
1133724												
1133725	1	1	1	1	1	1	1	1				1
1133726	1	1			1	1		1	1			
1133727	1	1			1	1		1				
1133728	1	1	1		1	1		1	1	1	1	1
1133729	1				1	1		1				
1133730	1		1		1	1	1	1	1	1		
1133731	1	1	1		1	1	1	1	1	1		
1133732	1			1	1	1		1				
1133733	1	1	1	1	1	1		1				1
1133734	1	1		1	1	1		1				

Crosswalk Table of Tag and Dependent Analysis												
Fish ID	4.1.1 - 4.1.5	4.1.6 [3D]	4.1.6 [7D]	4.1.7	4.1.8	4.2.1 & 4.2.2	4.2.3	4.3.1 [TC]	4.3.1 [CC]	4.3.1 [MR]	4.3.2	4.3.3
1133735	1		1		1	1		1	1	1		
1133736												
1133737	1	1	1		1	1		1	1			
1133738	1		1		1	1						
1133740	1	1			1	1		1	1			
1133741												
1133742	1	1	1		1	1		1				
1133743												
1133744	1	1	1		1	1	1	1	1			
1133745	1			1	1	1		1				
1133746	1	1	1		1	1	1	1	1	1		
1133747	1		1		1	1		1				
1133748	1	1	1		1	1		1	1		1	1
1133749	1		1		1	1		1	1	1		
1133750	1	1	1	1	1	1		1				1
1133751	1	1		1	1	1		1				
1133752	1				1	1						
1133753	1	1	1	1	1	1		1				
1133754	1				1	1		1				
1133755	1	1	1		1	1	1	1	1	1		
1133756												
1133757												
1133758	1		1		1	1		1				
1133759	1	1	1		1	1		1	1	1		
1133760	1	1			1	1		1	1			
1133761	1		1		1	1	1	1	1	1		
1133762	1	1	1		1	1	1	1	1	1		
1133763												
1133764	1			1	1	1		1				
1133765	1	1	1		1	1		1	1	1		1
1133766	1		1		1	1						
1133767	1				1	1		1				

Crosswalk Table of Tag and Dependent Analysis												
Fish ID	4.1.1 - 4.1.5	4.1.6 [3D]	4.1.6 [7D]	4.1.7	4.1.8	4.2.1 & 4.2.2	4.2.3	4.3.1 [TC]	4.3.1 [CC]	4.3.1 [MR]	4.3.2	4.3.3
1133768	1				1	1		1				
1133769	1	1		1	1	1		1				
1133770	1	1	1	1	1	1		1				
1133771	1				1	1						
1133772	1		1	1	1	1		1				
1133773	1				1	1	1	1	1	1		
1133774	1	1		1	1	1		1			1	1
1133775	1	1	1		1	1	1	1	1	1		
1133776	1				1	1						
1133777	1	1	1	1	1	1		1				1
1133778	1		1	1	1	1		1				1
1133779	1	1	1		1	1		1	1	1		
1133780	1			1	1	1		1				
1133782	1			1	1	1		1				1
1133783	1	1			1	1		1	1			1
1133784	1	1			1	1		1				
1133785	1				1	1						
1133786	1			1	1	1		1				
1133787	1				1	1		1	1			
1133788	1	1			1	1		1				
1133790	1				1	1		1				
1133791	1	1	1	1	1	1		1			1	1
1133792	1	1	1	1	1	1		1			1	1
1133793	1	1	1		1	1		1	1	1		
1133794	1		1	1	1	1		1			1	
1133795	1			1	1	1		1				1
1133796	1	1	1	1	1	1		1				
1133797												
1133798	1		1		1					1		
1133799	1	1			1	1		1	1	1		
1133800	1		1		1	1		1	1	1		
1133801	1	1		1	1	1		1				

Crosswalk Table of Tag and Dependent Analysis												
Fish ID	4.1.1 - 4.1.5	4.1.6 [3D]	4.1.6 [7D]	4.1.7	4.1.8	4.2.1 & 4.2.2	4.2.3	4.3.1 [TC]	4.3.1 [CC]	4.3.1 [MR]	4.3.2	4.3.3
1133802	1			1	1	1		1				1
1133803	1	1			1	1		1				
1133804	1	1	1	1	1	1	1	1				
1133805	1	1	1		1	1	1	1				1
1133806	1	1			1	1	1	1	1	1		
1133807	1	1			1	1	1	1	1	1		
1133808	1	1			1	1		1				
1133809	1		1		1	1		1	1	1		
1133810	1	1			1	1		1				
1133811												
1133812	1			1	1	1		1				
1133813	1				1	1		1	1			
1133814	1	1			1	1		1	1	1		
1133815	1	1	1		1	1		1				
1133816												
1133817	1	1	1		1	1		1	1			
1133818	1				1	1						
1133819	1	1	1		1	1		1				1
1133820	1	1	1	1	1	1		1				
1133821	1	1	1		1	1		1	1	1	1	1
1133822	1				1	1						
1133823	1	1			1	1		1	1	1		
1133824	1	1	1		1	1	1	1	1	1		
1133825	1		1		1				1	1		
1133826	1	1		1	1	1		1				
1133827	1		1	1	1	1	1	1				
1133828	1	1			1	1		1	1			
1133829	1		1		1	1		1	1			
1133830	1	1	1	1	1	1		1				
1133831	1	1	1	1	1	1		1			1	
1133832	1				1							
1133833	1				1	1						

Crosswalk Table of Tag and Dependent Analysis												
Fish ID	4.1.1 - 4.1.5	4.1.6 [3D]	4.1.6 [7D]	4.1.7	4.1.8	4.2.1 & 4.2.2	4.2.3	4.3.1 [TC]	4.3.1 [CC]	4.3.1 [MR]	4.3.2	4.3.3
1133834												
1133835	1		1		1	1		1	1			
1133836												
1133837	1	1		1	1	1		1				
1133838	1	1	1		1	1	1	1	1	1		
1133839	1		1		1	1	1	1				
1133840	1				1	1		1	1			
1133841	1				1	1		1	1	1		
1133842	1				1	1		1				
1133843	1			1	1	1		1				1
1133844	1				1	1		1	1			
1133845	1	1			1	1	1	1	1	1		
1133846	1				1	1						
1133847	1				1	1		1				
1133848	1	1			1	1	1	1	1	1		
1133849	1	1	1	1	1	1		1				1
1133850	1	1		1	1	1		1				
1133852	1	1			1	1	1	1	1	1		
1133853	1				1					1		
1133854	1	1		1	1	1		1				1
1133855	1	1			1	1		1	1	1		
1133856	1	1			1	1		1	1			
1133857	1				1	1		1				
1133858	1				1	1						
1133859	1	1	1		1	1	1	1	1			
1133860	1		1	1	1	1	1	1				
1133861	1	1			1	1		1	1			
1133862	1	1			1	1		1	1	1		
1133863	1				1	1		1	1			
1133864	1	1	1		1	1		1	1	1		
1133865	1				1	1	1	1	1	1		
1133866	1	1	1		1	1	1	1	1	1		

Crosswalk Table of Tag and Dependent Analysis												
Fish ID	4.1.1 - 4.1.5	4.1.6 [3D]	4.1.6 [7D]	4.1.7	4.1.8	4.2.1 & 4.2.2	4.2.3	4.3.1 [TC]	4.3.1 [CC]	4.3.1 [MR]	4.3.2	4.3.3
1133867	1	1			1	1		1	1		1	1
1133868	1	1		1	1	1		1				
1133869	1	1			1	1	1	1	1	1		
1133870	1	1	1	1	1	1		1			1	1
1133871	1	1			1	1		1				
1133872	1	1	1	1	1	1		1			1	1
1133873												
1133874	1	1		1	1	1		1				
1133875	1			1	1	1		1			1	1
1133876												
1133877	1	1	1	1	1	1		1			1	1
1133878	1	1	1		1	1	1	1	1	1		
1133879	1			1	1	1		1				
1133880	1	1		1	1	1	1	1				
1133881												
1133882	1	1			1	1						
1133883	1	1			1	1		1				
1133884	1			1	1	1		1				
1133885	1				1	1		1	1	1		
1133886	1	1		1	1	1		1				
1133887	1	1	1		1	1	1	1	1	1		
1133888	1		1		1	1		1	1			
1133889	1	1			1	1		1				
1133890	1				1	1		1	1	1		
1133891	1	1			1	1		1	1	1		
1133892	1	1		1	1	1		1				
1133893	1	1	1	1	1	1		1				
1133894	1				1	1	1	1	1			
1133895	1	1	1		1	1		1	1	1		
1133896	1	1		1	1	1		1				1
1133897	1				1	1		1	1	1		
1133898	1				1	1		1	1	1		

Crosswalk Table of Tag and Dependent Analysis												
Fish ID	4.1.1 - 4.1.5	4.1.6 [3D]	4.1.6 [7D]	4.1.7	4.1.8	4.2.1 & 4.2.2	4.2.3	4.3.1 [TC]	4.3.1 [CC]	4.3.1 [MR]	4.3.2	4.3.3
1133899	1	1			1	1		1	1	1		
1133900	1	1	1		1	1		1	1			
1133901												
1133902	1	1		1	1	1		1			1	
1133903	1		1	1	1	1		1				1
1133904	1	1		1	1	1		1			1	1
1133905	1			1	1	1		1				
1133906	1	1			1	1		1			1	1
1133907	1		1		1	1	1	1	1			
1133908	1		1		1	1	1	1	1	1		
1133909	1	1		1	1	1		1			1	1
1133910	1	1		1	1	1		1				1
1133911												
1133912	1				1	1		1	1	1		
1133913	1	1			1	1		1	1	1		
1133914	1	1			1	1		1	1	1		
1133915	1	1			1	1	1	1	1	1		
1133916	1				1	1		1	1			
1133917	1		1		1	1		1	1		1	1
1133918	1			1	1	1		1				
1133919	1	1			1	1	1	1	1	1		
1133920	1	1			1	1	1	1	1			
1133921												
1133922	1	1			1	1		1	1			
1133923	1	1			1	1	1	1	1	1		
1133924	1	1		1	1	1		1				
1133925	1	1			1	1		1	1	1		
1133926	1	1	1		1	1		1			1	
1133927	1	1		1	1	1	1	1				
1133928	1		1		1	1						
1133929	1		1		1	1		1	1			
1133930	1	1	1		1	1		1	1			

Crosswalk Table of Tag and Dependent Analysis												
Fish ID	4.1.1 - 4.1.5	4.1.6 [3D]	4.1.6 [7D]	4.1.7	4.1.8	4.2.1 & 4.2.2	4.2.3	4.3.1 [TC]	4.3.1 [CC]	4.3.1 [MR]	4.3.2	4.3.3
1133931	1	1			1	1		1	1	1		
1133932	1	1			1	1	1	1	1	1		
1133933	1		1	1	1	1		1				
1133934	1	1	1		1	1						
1133935	1	1			1							
1133936	1	1		1	1	1		1				1
1133937	1	1	1		1	1	1	1	1		1	
1133938	1				1	1		1	1	1		
1133939	1				1	1		1				
1133940	1			1	1	1		1				
1133941	1	1	1		1	1	1	1	1	1		
1133942	1				1	1		1	1	1		
1133943	1	1	1		1	1		1				
1133944	1				1	1		1				
1133945	1	1		1	1	1		1			1	1
1133946	1	1	1		1	1		1	1	1		
1133947	1			1	1	1		1				1
1133948	1	1			1	1		1			1	1
1133949												
1133950	1	1		1	1	1		1				1
1133951	1	1			1	1	1	1	1			
1133952	1			1	1	1		1				
1133953	1			1	1	1		1				
1133954	1			1	1	1		1				
1133955	1				1	1		1				
1133956	1			1	1	1		1				1
1133957	1	1	1		1	1	1	1	1			
1133958	1	1	1		1	1		1	1	1		
1133959	1	1			1	1		1	1	1		
1133960	1	1		1	1	1		1				1
1133961	1	1			1	1		1	1	1		
1133962	1				1	1		1	1			

Crosswalk Table of Tag and Dependent Analysis												
Fish ID	4.1.1 - 4.1.5	4.1.6 [3D]	4.1.6 [7D]	4.1.7	4.1.8	4.2.1 & 4.2.2	4.2.3	4.3.1 [TC]	4.3.1 [CC]	4.3.1 [MR]	4.3.2	4.3.3
1133963	1	1			1	1	1	1	1	1		
1133964	1				1	1		1				1
1133965	1			1	1	1		1				
1133966	1	1		1	1	1	1	1				
1133967	1				1	1						
1133968	1			1	1	1		1			1	
1133969	1				1	1		1	1	1		
1133970												
1133971	1	1			1	1		1	1			
1133972	1	1			1	1		1				
1133973	1			1	1	1		1				
1133974	1	1		1	1	1		1				1
1133975	1				1	1	1	1	1	1		
1133976	1		1		1	1		1	1			
1133977												
1133978	1	1			1	1						
1133979	1	1	1		1	1		1	1			
1133980	1				1	1	1	1	1	1		
1133981	1	1			1	1	1	1	1			
1133982	1	1			1	1	1	1	1	1		
1133983	1	1	1		1	1	1	1			1	
1133984	1	1		1	1	1	1	1				
1133985												
1133986	1	1			1	1	1	1	1			
1133987	1	1		1	1	1		1				1
1133988	1			1	1	1		1				
1133989	1	1			1	1	1	1	1	1		
1133990												
1133991	1	1		1	1	1		1				
1133992	1	1			1	1	1	1	1	1		
1133993												
1133994	1				1	1		1	1			

Crosswalk Table of Tag and Dependent Analysis												
Fish ID	4.1.1 - 4.1.5	4.1.6 [3D]	4.1.6 [7D]	4.1.7	4.1.8	4.2.1 & 4.2.2	4.2.3	4.3.1 [TC]	4.3.1 [CC]	4.3.1 [MR]	4.3.2	4.3.3
1133995	1	1		1	1	1		1				
1133996	1	1	1		1	1	1	1	1	1		
1133997	1				1					1		
1133998												
1133999												
1134000	1	1			1	1		1	1			
1134001	1	1		1	1	1		1				
1134002	1	1			1	1	1	1	1	1		
1134003	1	1	1		1	1		1	1			
1134004	1	1			1	1		1	1			
1134005												
1134006	1	1			1	1						
1134007	1				1	1		1	1			
1134009	1			1	1	1		1				
1134010	1	1	1	1	1	1		1			1	
1134011												
1134012	1		1		1	1	1	1	1	1		
1134013	1	1	1		1	1		1				
1134015	1	1	1		1	1	1	1	1	1		
1134016	1	1			1	1		1	1	1		
1134017	1			1	1	1		1				
1134018	1	1			1	1	1	1	1	1		
1134019	1	1		1	1	1	1	1			1	
1134020	1	1		1	1	1		1				1
1134021	1	1	1		1	1	1	1	1			1
1134022	1				1	1						
1134023	1			1	1	1		1			1	1
1134024	1	1			1	1	1	1	1			
1134025	1	1		1	1	1		1				
1134026	1		1		1	1	1	1				
1134027	1				1	1	1	1	1			
1134028	1	1	1		1	1		1	1			1

Crosswalk Table of Tag and Dependent Analysis												
Fish ID	4.1.1 - 4.1.5	4.1.6 [3D]	4.1.6 [7D]	4.1.7	4.1.8	4.2.1 & 4.2.2	4.2.3	4.3.1 [TC]	4.3.1 [CC]	4.3.1 [MR]	4.3.2	4.3.3
1134029	1	1			1	1		1	1	1		
1134030	1	1	1	1	1	1		1			1	1
1134031	1				1	1		1				
1134032												
1134033	1	1		1	1	1		1				1
1134034												
1134035												
1134036	1		1	1	1	1		1				1
1134037	1		1		1	1		1	1			
1134038	1				1	1		1	1	1		
1134039	1	1			1	1	1	1	1	1		
1134040	1	1			1	1	1	1	1	1		
1134041	1	1	1		1	1		1	1			
1134042	1	1			1	1		1	1			
1134043	1	1	1		1	1		1				
1134044												
1134045	1				1	1						
1134046	1	1	1		1	1		1	1	1		
1134047	1	1			1				1	1		
1134048	1				1	1						
1134049	1	1			1	1		1	1			
1134050	1				1	1		1				
1134051	1				1	1						
1134052	1	1		1	1	1		1			1	1
1134053	1	1		1	1	1		1			1	
1134054	1	1	1		1	1		1				
1134055												
1134056	1	1			1	1		1			1	1
1134057	1	1			1				1	1		
1134058	1	1		1	1	1		1				
1134059	1				1	1		1	1			
1134060	1				1	1						

Crosswalk Table of Tag and Dependent Analysis												
Fish ID	4.1.1 - 4.1.5	4.1.6 [3D]	4.1.6 [7D]	4.1.7	4.1.8	4.2.1 & 4.2.2	4.2.3	4.3.1 [TC]	4.3.1 [CC]	4.3.1 [MR]	4.3.2	4.3.3
1134061	1			1	1	1		1				
1134062												
1134063	1	1			1	1		1	1			
1134064	1		1	1	1	1		1				
1134065												
1134067												
1134068	1	1			1	1		1	1		1	1
1134069	1				1	1		1	1	1		
1134070												
1134071	1				1	1	1	1	1	1		
1134072	1		1	1	1	1		1			1	
1134073	1	1			1	1	1	1	1	1		
1134074	1				1	1						
1134075	1	1			1	1	1	1			1	1
1134076	1	1			1	1		1	1	1		
1134077	1				1	1						
1134078	1				1	1						
1134079	1	1		1	1	1	1	1			1	
1134080	1	1	1		1	1		1	1		1	
1134081	1			1	1	1		1				1
1134082	1				1	1		1				
1134083												
1134084	1	1			1	1		1	1	1		
1134085	1				1	1		1	1	1		
1134086	1	1			1	1	1	1	1			
1134087	1				1	1		1				
1134088												
1134089	1				1	1		1	1	1		
1134090	1	1			1	1	1	1	1			
1134091	1		1		1	1	1	1	1	1		
1134092	1				1	1						
1134093	1	1			1	1		1				

Crosswalk Table of Tag and Dependent Analysis												
Fish ID	4.1.1 - 4.1.5	4.1.6 [3D]	4.1.6 [7D]	4.1.7	4.1.8	4.2.1 & 4.2.2	4.2.3	4.3.1 [TC]	4.3.1 [CC]	4.3.1 [MR]	4.3.2	4.3.3
1134094	1	1			1	1		1				
1134095	1	1			1	1		1	1	1		
1134096	1				1	1		1	1			
1134097	1				1	1		1				
1134098	1				1	1						
1134099	1				1	1						
1134100	1	1	1	1	1	1		1				
1134102	1	1			1	1		1	1	1		
1134103	1	1			1	1		1				
1134104	1	1	1	1	1	1		1				
1134105	1	1	1		1	1	1	1	1	1		
1134106	1	1			1	1		1	1	1		
1134107	1	1			1	1		1				
1134108	1				1	1		1				
1134109	1	1	1		1						1	1
1134110	1	1	1	1	1	1		1	1			
1134111	1	1	1	1	1	1		1			1	1
1134112												
1134113	1	1			1	1		1	1			
1134114	1	1	1	1	1	1		1			1	1
1134115	1	1	1	1	1	1		1				1
1134116	1		1	1	1	1		1				
1134117	1	1			1	1	1	1				
1134118	1	1			1	1		1	1	1		
1134119												
1134120	1	1		1	1	1		1				
1134121	1				1	1						
1134122	1	1	1		1	1	1	1	1	1		
1134123												
1134124	1				1	1		1				
1134127	1				1	1						
1134128	1	1			1	1		1	1			

Crosswalk Table of Tag and Dependent Analysis												
Fish ID	4.1.1 - 4.1.5	4.1.6 [3D]	4.1.6 [7D]	4.1.7	4.1.8	4.2.1 & 4.2.2	4.2.3	4.3.1 [TC]	4.3.1 [CC]	4.3.1 [MR]	4.3.2	4.3.3
1134129	1				1	1		1	1			
1134130	1	1		1	1	1		1			1	1
1134131	1	1		1	1	1		1				
1134132	1	1			1	1	1	1	1	1		
1134133	1	1			1	1		1	1			
1134134	1			1	1	1		1				
1134135												
1134136	1		1		1	1		1				
1134137	1				1	1		1	1	1		
1134138	1	1		1	1	1		1				
1134139	1	1		1	1	1		1				
1134140	1	1			1	1	1	1	1			
1134141	1	1			1	1		1	1	1		
1134142												
1134143	1	1			1	1		1				
1134144	1	1			1	1		1	1	1		
1134145												
1134146	1	1			1	1						
1134147	1	1		1	1	1		1				
1134148												
1134149	1	1			1	1		1	1	1		
1134150	1	1			1	1		1				
1134151	1	1			1	1		1	1	1	1	1
1134152	1				1	1						
1134153	1	1		1	1	1		1				
1134154	1	1	1		1	1						
1134155	1	1			1	1	1	1	1	1		
1134156	1	1			1	1	1	1	1	1		
1134157	1	1	1		1				1	1		
1134158	1	1	1		1	1		1	1			
1134159	1				1							
1134160	1	1		1	1	1		1			1	1

Crosswalk Table of Tag and Dependent Analysis												
Fish ID	4.1.1 - 4.1.5	4.1.6 [3D]	4.1.6 [7D]	4.1.7	4.1.8	4.2.1 & 4.2.2	4.2.3	4.3.1 [TC]	4.3.1 [CC]	4.3.1 [MR]	4.3.2	4.3.3
1134161	1	1	1		1	1		1			1	
1134162	1	1			1	1		1	1	1		
1134163												
1134164	1	1			1	1		1				
1134165	1	1		1	1	1		1				
1134166	1	1			1	1						
1134167	1	1			1	1	1	1	1	1		
1134168												
1134169	1				1	1		1	1			
1134170	1	1		1	1	1		1				
1134171												
1134172												
1134173	1	1	1	1	1	1		1			1	
1134174	1				1				1			
1134175	1		1		1	1	1	1	1			1
1134176	1				1	1						
1134177	1				1	1		1	1			
1134179	1	1			1	1		1				
1134180	1				1	1	1	1	1			
1134181	1	1			1	1	1	1	1	1		
1134182	1	1		1	1	1		1			1	1
Total	447	276	144	131	447	435	89	391	197	120	50	75

Hydrol. Earth Syst. Sci., 19, 4257–4274, 2015
www.hydrol-earth-syst-sci.net/19/4257/2015/
doi:10.5194/hess-19-4257-2015

Hydrology and Earth System Sciences
Open Access
EGU

Reconstructing the natural hydrology of the San Francisco Bay–Delta watershed

P. Fox[1], **P. H. Hutton**[2], **D. J. Howes**[3], **A. J. Draper**[4], **and L. Sears**[5]

[1]Independent Consulting Engineer, Rockledge, FL, USA
[2]Metropolitan Water District of Southern California, Sacramento, CA, USA
[3]Irrigation Training and Research Center, BioResource and Agricultural Engineering Department, California Polytechnic State University, San Luis Obispo, CA, USA
[4]MWH Americas Inc., 3321 Power Inn Road, Suite 300, Sacramento, CA 95826, Sacramento, CA, USA
[5]Independent researcher, Beaverton, OR, USA

Correspondence to: D. J. Howes (djhowes@calpoly.edu)

Received: 20 March 2015 – Published in Hydrol. Earth Syst. Sci. Discuss.: 13 April 2015
Revised: 26 September 2015 – Accepted: 29 September 2015 – Published: 22 October 2015

Abstract. We evaluated the impact of landscape changes on the amount of delta outflow reaching San Francisco Bay. The natural landscape was reconstructed and water balances were used to estimate the long-term annual average delta outflow that would have occurred under natural landscape conditions if the climate from 1922 to 2009 were to repeat itself. These outflows are referred to as *natural* delta outflows and are the first published estimate of natural delta outflow. These natural delta outflows were then compared with current delta outflows for the same climate and existing landscape, including its re-engineered system of reservoirs, canals, aqueducts, and pumping plants.

This analysis shows that the long-term, annual average delta outflow under current conditions is consistent with outflow under natural landscape conditions. The amount of water currently used by farms, cities, and others is about equal to the amount of water formerly used by native vegetation. Development of water resources in California's Central Valley transferred water formerly used by native vegetation to new beneficial uses without substantially reducing the long-term annual average supply to the San Francisco Bay–Delta estuary. Based on this finding, it is unlikely that observed declines in native freshwater aquatic species are the result of annual average delta outflow reductions.

1 Introduction

The San Francisco Estuary, composed of San Francisco Bay and the Sacramento–San Joaquin River delta, is the largest estuary along the Pacific coast of the USA and the home to a rich ecosystem. The delta serves as one of the principal hubs of California's water system, which delivers 45 % of the water used statewide to 25 million residents and 16 000 km^2 of farmland.

The Central Valley in California is a 60 to 100 km wide broad flat alluvial plain, stretching over 750 km from north to south and covering about 58 000 km^2 (containing the irrigated land from south of Redding to south of Bakersfield in Fig. 1). This valley is entirely surrounded by mountains except for a narrow gap on its western edge through which the combined Sacramento and San Joaquin rivers flow to the Pacific Ocean through San Francisco Bay (Fig. 1). This valley is the agricultural heartland of the USA, producing over 360 products and more than half of the country's vegetables, fruits and nuts. It is often considered the most productive agricultural region in the world, a status achieved by significantly re-engineering the natural landscape. The tributary watersheds in the northern portion of the Central Valley, referred to in this work as the valley floor (Fig. 2), are the major sources of freshwater to the San Francisco Bay–Delta system. The Sacramento River from the north and the San Joaquin River from the south flow toward each other, joining in the delta.

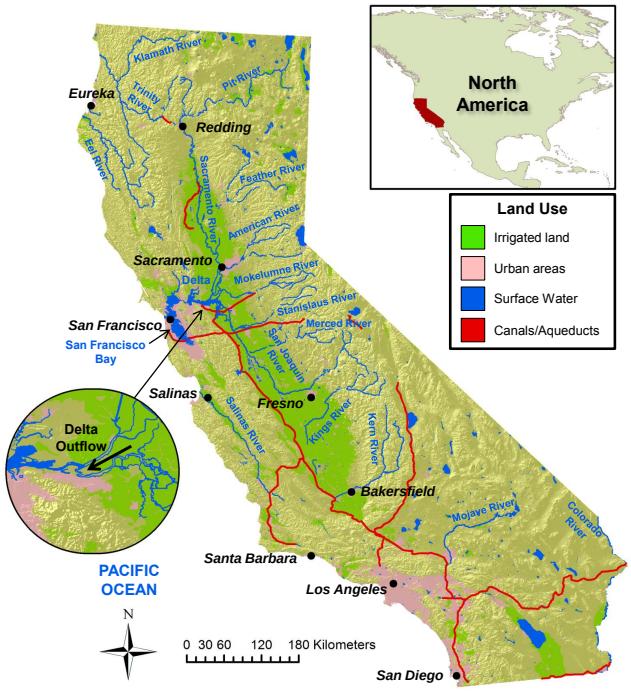

Figure 1. California, current land classifications, and major tributaries feeding into and through the Central Valley.

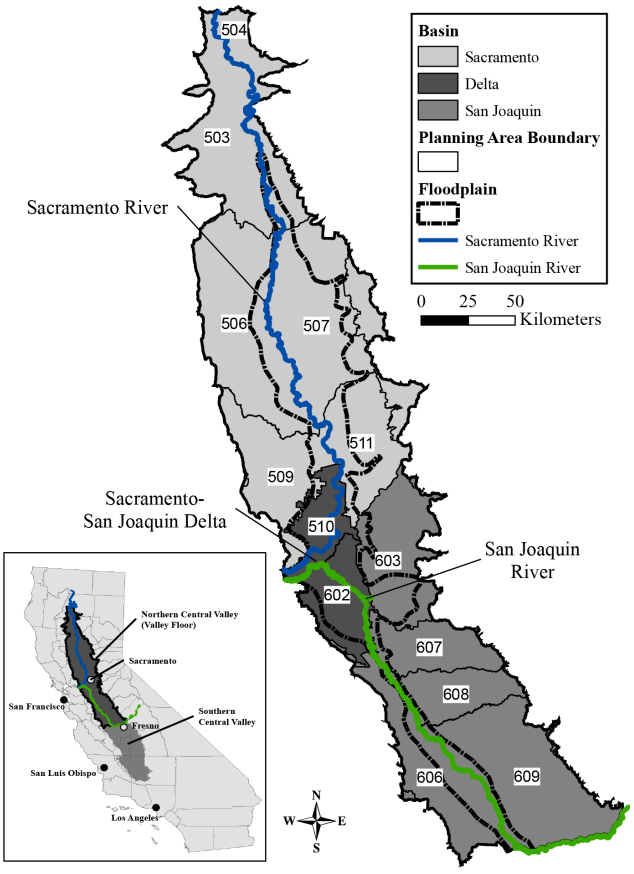

Figure 2. Valley floor study area showing the area where water use calculations were conducted by planning area and summarized by hydrologic basin. Planning areas 502, 505, 508, 601, 604, 605 and 610 within the valley floor are too small to show on this map. Planning area boundaries were defined by CDWR (2005a, b).

The development of California from small-scale human settlements that co-existed with an environment rich in native vegetation to the eighth largest economy in the world was facilitated by reconfiguring the state's water resources to serve new uses: agriculture, industry, and a burgeoning population. The redistribution of water from native vegetation to other uses was accompanied by significant declines in native aquatic species that rely on the San Francisco Bay–Delta system. Declines in native aquatic species have been documented in the San Francisco Bay–Delta system over the last several decades (Jassby et al., 1995; MacNally et al., 2010; Thomson et al., 2010). Many aquatic species have been classified as endangered, threatened, and species of concern, e.g., Sacramento River winter-run Chinook salmon, delta smelt, Sacramento splittail, longfin smelt, southern green sturgeon (Lund et al., 2007). These declines have been attributed to several factors including reduced volume and altered timing of freshwater flows from the tributary watersheds (delta outflow), decreased sediment loads, increased nutrient loads, changes in nutrient stoichiometry, contaminants, introduced species, habitat degradation and loss, and shifts in the ocean–atmosphere system (Luoma and Nichols, 1993; Jassby et al., 1995; Bennett and Moyle, 1996; MacNally et al., 2010; Glibert, 2010; Glibert et al., 2011; Miller et al., 2012; Cloern and Jassby, 2012).

The native species of concern evolved and thrived under natural landscape conditions, or those that existed prior to European settlement starting in the mid-18th century. These undisturbed conditions are referred to in this work as *natural* conditions, meaning undisturbed by western civilization. Thus, natural delta outflows are those that would have occurred with natural landscape conditions.

The natural landscape included immense inland marshes located in natural flood basins along major rivers (Alexander et al., 1874; Hall, 1887; Garone, 2011), lush riparian forests on river levees (Katibah, 1984), and vast swaths of grasslands interwoven with vernal pools and immense valley oaks in park-like savannas that extended from the floodplains to the oak- and pine-covered foothills (Holland, 1978; Burcham, 1957; Dutzi, 1978). This landscape was fed by periodic overflows of the rivers into natural flood basins along the major rivers. Figure 3 is an idealized cross section through the valley floor that illustrates the major features of this natural landscape. This landscape was dramatically altered, starting in the mid-18th century, to support new land and water uses. The native vegetation was largely replaced by cultivated crops, the flood basins were drained, the rivers were confined between levees, headwater reservoirs were built to store

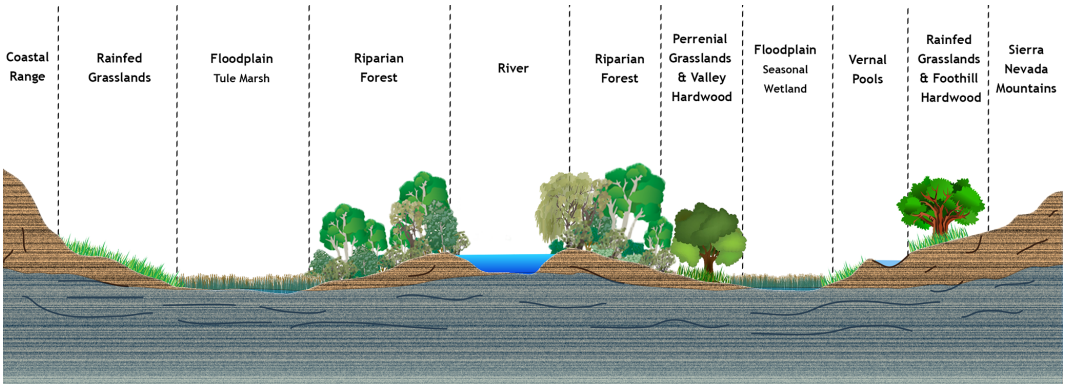

Figure 3. Idealized cross section of the valley floor under natural conditions.

floodwaters, and an extensive system of canals and aqueducts was built to move water from its point of origin to distant locations.

In this study, the hypothesis that current annual average freshwater flows are lower than natural annual average flows into the estuary is tested using a simple water balance, normalized to the contemporary climate. We then compare our natural delta outflow estimate with an estimate of delta outflow that occurs annually under current conditions. This is the first published estimate of natural delta outflow into the San Francisco Bay–Delta estuary. Others have used a surrogate, known as *unimpaired* flows in California, to estimate natural outflows. As will be demonstrated, the surrogate fails to account for evapotranspiration by native vegetation, the major consumptive use of water in the natural system, resulting in a significant overestimate of natural delta outflows.

2 Study area background

Prior to development, starting in the mid-18th century, the channels of the major rivers did not have adequate capacity to carry normal winter rainfall runoff and spring snowmelt (Grunsky, 1929; California State Engineer, 1908). The rivers overflowed their banks into vast natural flood basins flanking both sides of the Sacramento and San Joaquin rivers (Hall, 1880; Grunsky, 1929). Sediment deposited as the rivers spread out over the floodplain and built up natural levees along the river channels. These natural levees were much larger and more developed along the Sacramento River than along the San Joaquin River (Hall, 1880).

The natural levees were lined with lush riparian forest. The floodplains contained large expanses of tule marsh, seasonal wetlands, vernal pools, grasslands, lakes, sloughs, and other landforms that slowed the passage of flood waters (Whipple et al., 2012; Garone, 2011; Holmes and Eckmann, 1912). Groundwater generally moved from recharge areas along the sides of the valley towards topographically lower areas in the central part of the valley, where it was depleted through marsh, vernal pool, and riparian forest evapotranspiration (TBI, 1998; Bertoldi et al., 1991; Williamson et al., 1989; Davis et al., 1959).

Grasslands interspersed with vernal pools (seasonal wetlands) stretched from the edge of the floodplain to the foothills, generally overlying relatively impermeable hardpans and claypans that supported perched water tables. This habitat once occupied nearly all level lands between the foothills and floodplain and was the dominant vegetation under natural conditions, supplied by perched aquifers, overland runoff from the foothills, and precipitation.

This natural landscape, summarized in Fig. 4, was radically modified, starting in the mid-18th century, to make it suitable for agricultural (Smith and Verrill, 1998) and urban uses, creating the world's largest water system supporting the eighth largest economy in the world. The native vegetation was removed, river channels were dredged and rip rapped, levees were raised, the flood basins were drained, bypasses were installed to route flood waters directly into the delta, and head-stream reservoirs were built to replace side-stream storage, provide protection from floods, and generate electricity. Massive hydraulic works were built to move water from areas of relative abundance to areas of relative scarcity throughout the state, including Los Angeles and the San Francisco Bay Area. The history of these changes have been documented elsewhere (Kelley, 1959, 1989; Bain et al., 1966; Kahrl, 1979; Thompson, 1957; Hundley, 2001; Olmstead and Rhode, 2004; CDWR, 2013b).

3 Methods

Annual average delta outflow was estimated under natural landscape conditions (natural delta outflow) using a conventional water balance. The results of this calculation are compared with two estimates of delta outflow by the California Department of Water Resources (CDWR): (1) current delta outflow (CDWR, 2012) and (2) unimpaired delta outflow (CDWR, 2007). CDWR's unimpaired outflow calculation re-

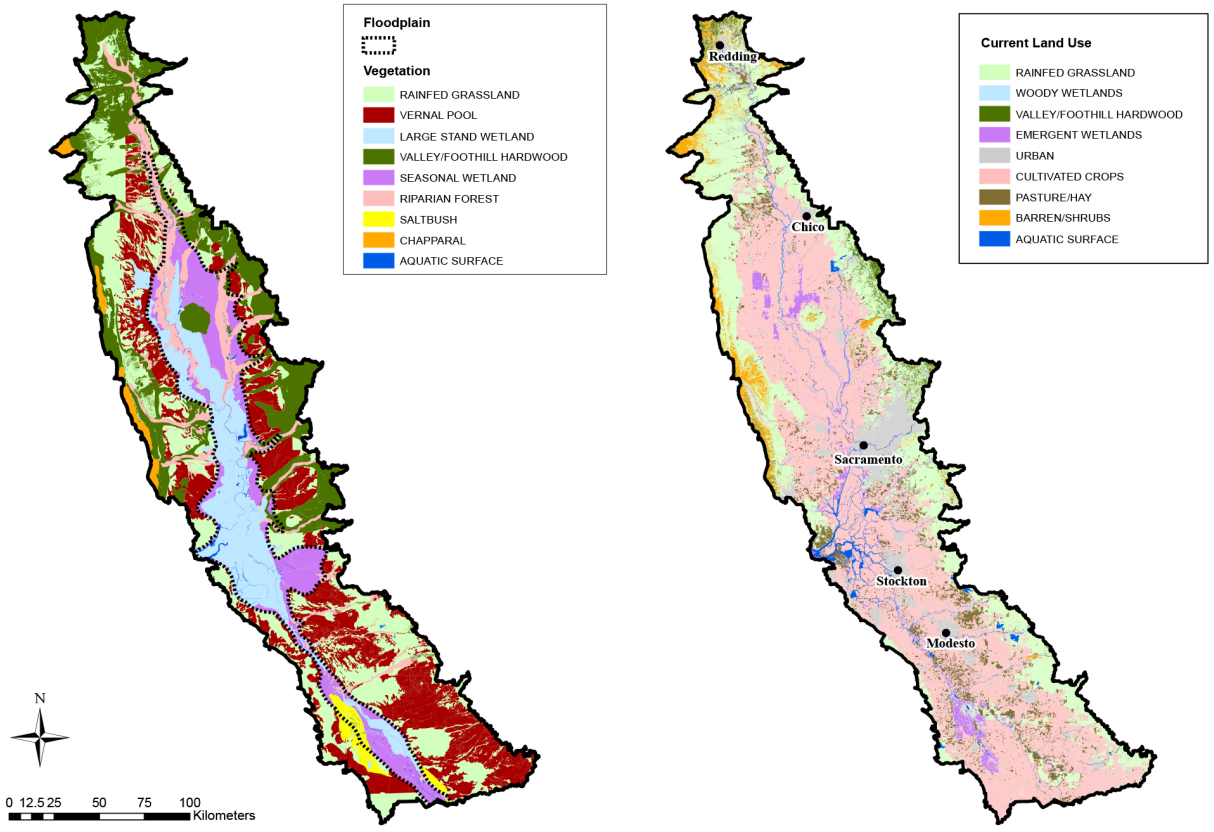

Figure 4. Natural vegetation in the valley floor map portraying the areal extent of natural vegetation based on the Case I definition of grassland composition (i.e., all grassland area outside of the floodplain was classified as either vernal pool or rainfed grassland). Although this map represents a composite of several maps, the primary source of information comes from CSU Chico's pre-1900 Historic Vegetation Map (CSU Chico, 2003) (left panel). Current land use on the valley floor (right panel).

moves the impacts of most upstream alterations from the observed hydrologic record. However, the calculation does not remove alterations such as channel improvements, levees, and flood bypasses. As a result, the calculation assumes that rim inflows from the surrounding mountain ranges are routed through the existing system of channels and bypasses in the delta with little or no interaction with the natural landscape (CDWR, 2007). These unimpaired outflows are frequently misused as a surrogate for natural delta outflow (Cloern and Jassby, 2012; Dynesius and Nilsson, 1994). All three of these estimates are based on the level of development methodology and the climate over the period 1922 to 2009 to facilitate direct comparisons.

3.1 Level of development methodology

These three estimates of delta outflow – natural, current and unimpaired – were estimated using a synthetic multi-year hydrologic sequence utilizing a level of development approach (Draper et al., 2004). This method routes the same amount of water (rim inflows plus precipitation) over a defined historical period assuming *frozen* conditions such as land use, flood control and water supply facility operations, and environmental regulations. In other words, this method simulates river flows under a repeat of historical climate, but holding land use and facility operations constant.

A historical hydrologic sequence may be generated to represent development as it existed in a particular year (i.e., 1990 level of development), as it exists today (i.e., current level of development), or as it may exist under a projected scenario (i.e., future level of development). This approach allows us to estimate the impact of anthropogenic changes on natural delta outflow by comparing a natural level of development with a current level of development.

Thus, our estimate of natural outflow is not an estimate of actual flows that occurred under Paleolithic or more recent conditions prior to European settlement (Ingram et al., 1996; Malamud-Roam et al., 2006; Meko et al., 2001). Rather, our natural delta outflow calculation is an estimate that assumes the contemporary precipitation and inflow pattern to the valley floor with the valley floor in a natural or undeveloped state: before flood control facilities, levees, land reclamation, irrigation projects, imports, etc.

Natural outflow calculations were performed on a monthly basis assuming long-term climatic conditions observed over an 88-year period (1922 to 2009). The calculations assume a conventional California October through September water year. Water balances were calculated around the portion of the Central Valley that drains into San Francisco Bay (referred to as the valley floor) as shown in Fig. 2.

3.2 Natural delta outflow

Natural delta outflow was calculated using a conventional water balance as the difference between water supply and water use:

$$\text{natural delta outflow} = \text{water supply} - \text{water use}. \quad (1)$$

Natural delta outflows are the outflows that would result if the climate for the period 1922 to 2009 were to occur under natural landscape conditions. Natural landscape conditions are those that existed prior to the advent of European settlement, starting in the mid-18th century, including native vegetation (Fig. 4) and natural landforms such as stream-side flood basins and low levees.

The water supply is the sum of rim inflows from the surrounding mountain ranges into the valley floor plus precipitation on the valley floor, adjusted to remove impairments such as diversions. The only losses of water under natural conditions were evaporation from water surfaces and evapotranspiration by native vegetation. Water that is not evaporated or evapotranspired flows out of the delta into San Francisco Bay and is referred to here as delta outflow.

Equation (1) assumes that the long-term, annual average change in groundwater storage would have been zero under pre-development conditions. This assumption would not significantly affect long-term annual average calculations as the year-to-year fluctuations of groundwater exchanges are insignificant compared to average surface water flows. However, it would affect seasonal flow patterns, which is the subject of ongoing work. Net groundwater depletions under pre-development conditions are approximately zero and unimportant to the overall annual water balance (Gleick, 1987).

Water balances are reported for three hydrologic regions that comprise the valley floor: the Sacramento Basin, the San Joaquin Basin, and the delta (Fig. 2). Water balances were calculated at a finer resolution for 16 subsets of the valley floor, referred to as "planning areas" (CDWR, 2005a, b) shown on Fig. 2.

The results of these conventional water balance calculations are compared with current delta outflow (CDWR, 2012) and a surrogate for natural outflow, unimpaired outflow (CDWR, 2007), estimated based on the level of development methodology.

3.3 Natural water supply

The water supply used in the natural water balances was estimated as the sum of rim inflows around the periphery of the valley floor plus precipitation that falls on the valley floor. The long-term annual average natural water supply is 50.1 billion $m^3\,yr^{-1}$, comprising 34.2 billion $m^3\,yr^{-1}$ from rim inflows and 15.9 billion $m^3\,yr^{-1}$ from precipitation over the valley floor.

The valley floor boundary is defined by the drainage basins of the gages used to determine valley rim inflows, adjusted (i.e., unimpaired) to remove the effects of upstream storage regulation, imports, and exports. Rim inflows are defined as the natural water supply from the surrounding mountains and other watersheds to the valley floor. The rim inflows were compiled for undeveloped and developed watersheds from several sources that cover different portions of the study area.

Rim inflows have been affected by changes in land use and forest management and by loss of natural meadows. Agricultural and urban development represents a relatively small portion (about five percent) of the rim watersheds. While low elevation hardwoods and chaparral have been lost and annual grassland areas have increased (Thorne et al., 2008), much of the rim watersheds remain characterized by conifer forest. Forest management practices, which have resulted in denser forest stands compared to pre-development conditions, may significantly affect runoff timing and volume (Bales et al., 2011; CDWR, 2013b). Denser forest canopy prevents snow from reaching the ground and leads to greater evapotranspiration and earlier snowmelt (CDWR, 2013b). However, scientific evidence necessary to quantify relationships between forest management and water supply has been inconclusive. Therefore, our work assumes natural inflows from the rim watersheds are equal to historical inflows adjusted to remove the effects of upstream storage regulation, imports, and exports (i.e., unimpaired inflows).

Historical flow records were generated from US Geological Survey (USGS) and California Department of Water Resources (CDWR) gage data and extended through linear correlation with gaged flows in nearby watersheds. Rim inflows from ungaged watersheds were estimated from adjacent gaged watersheds based on relative drainage area and average annual precipitation.

Unimpaired flows (CDWR, 2013a) from developed rim watersheds in the Sacramento and San Joaquin hydrologic regions were assumed to equal natural inflows. Similarly, unimpaired flows from the rim watershed south of the valley floor (i.e., the Tulare Lake hydrologic region) were assumed to be equal to natural inflows (CDWR, 2012). Minimal groundwater flow from the Sierra Nevada and Coastal Range to the valley floor is assumed, due to the presence of bedrock and high surface slopes (Armstrong and Stidd, 1967; Gleick, 1987; Williamson et al., 1989).

In addition to rim inflows from surrounding mountain watersheds, precipitation falling directly on the valley floor con-

tributes to the water supply. Precipitation was calculated for each planning area within the valley floor using distributed grids obtained from the PRISM Climate Group at Oregon State University (Daly et al., 2000; Daly and Bryant, 2013; PRISM Climate Group, 2013).

3.4 Natural water use

The pre-development valley floor was a diverse ecosystem of immense inland marshes, lush riparian forests, and vast swaths of grasslands interwoven with vernal pools and immense valley oaks in park-like savannas that extended from the floodplains to the oak- and pine-covered foothills (Bryan, 1923; Davis et al., 1959; Thompson, 1961, 1977; Roberts et al., 1977; Dutzi, 1978; Warner and Hendrix, 1985; TBI, 1998; Cunningham, 2010; Garone, 2011; Whipple et al., 2012).

Under natural conditions, the only water use was evapotranspiration by natural vegetation and evaporation from water surfaces such as lakes, rivers, and sloughs. We estimated the amount of water used by natural vegetation from the areal extent and evapotranspiration rate for each type of vegetation. We also estimated evaporation from lakes, rivers, and sloughs based on the area and evaporation rates from these bodies of water.

Estimating the water used by natural vegetation (ET) requires information on the vegetation evapotranspiration rate (ET_v) and the areal extent of vegetation (A_v). The volume of water used by natural vegetation is then estimated in Eq. (2) as the product of ET_v and A_v summed over all planning areas i and vegetation types j:

$$ET = \sum_{i,j} (ET_v \times A_v). \quad (2)$$

The same method was applied to evapotranspiration from free water surfaces such as lakes, ponds, sloughs, and river channels. The remainder of the section discusses how ET_v and A_v were estimated.

3.4.1 Evapotranspiration

The reference crop method was used to estimate evapotranspiration by natural vegetation (Howes and Pasquet, 2013; Howes et al., 2015). As shown in Eq. (3), the evapotranspiration rate is related to the grass reference evapotranspiration (ET_o) for a standardized grass reference crop grown under idealized conditions multiplied by a vegetation coefficient (K_v) that accounts for canopy/plant characteristics:

$$ET_v = ET_o \times K_v. \quad (3)$$

Two methods were used to estimate K_v, depending upon the available water supply used by various vegetation categories. The methods used to develop the K_v and ET_v used in this study are discussed in detail in Howes et al. (2015). The methods are briefly summarized in the following sections.

For non-stressed vegetation with a continuous water supply throughout the growing season, K_v was estimated from published studies of actual monthly (or more frequent) ET_v using a grass reference evapotranspiration (ET_o) (Howes et al., 2015). The ET_o used to derive the K_v values for this study was computed using the Standardized Penman–Monteith equation (Allen et al., 2005) when a full set of meteorological data were available; otherwise, the Hargreaves equation was used. The accuracy of this method was confirmed for permanent wetlands and riparian forest using actual evapotranspiration measured using remote sensing at two sites in central California (Howes et al., 2015).

For vegetation depending solely on precipitation (chaparral and a portion of the grasslands and valley/foothill hardwood), a daily soil water balance using the dual-crop coefficient method (Allen et al., 1998) was used to estimate ET_v and K_v over the 88-year study period (Howes et al., 2015). The ET_v values directly from the daily soil water balance were used in Eq. (2) for vegetation types reliant solely on precipitation. Since the daily soil water balance accounts for variable precipitation, the ET_v from vegetation reliant on precipitation varies from year to year. As a reference, the long-term annual average K_v values for these vegetation types were calculated from daily soil water balances for each planning area and are summarized in Table 1.

The K_v values summarized in Table 1 for non-water stressed vegetation were used in Eq. (3) to estimate monthly average ET_v for vegetation types that had access to full year-round water supply by planning area. Long-term average ET_v values for all vegetation types are shown in Table 2 (Howes et al., 2015).

3.4.2 Vegetation areas

The vegetation present on the valley floor under natural conditions included rainfed and perennial grasslands, vernal pools, permanent and seasonal wetlands, valley/foothill hardwood, riparian forest, saltbush, and chaparral (Howes et al., 2015; Barbour et al., 1993; Garone, 2011; Küchler, 1977). The areal extent of each type of vegetation was estimated from historic maps and contemporary estimates based on historic sources (Hall, 1887; Burcham, 1957; Küchler, 1977; Roberts et al., 1977; Dutzi, 1978; Fox, 1987; TBI, 1998; CSU Chico, 2003; Garone, 2011; Whipple et al., 2012; Fox and Sears, 2014), supplemented by early soil surveys for vernal pools (Holmes et al., 1915; Nelson et al., 1918; Strahorn et al., 1911; Lapham et al., 1904, 1909; Sweet et al., 1909; Holmes and Eckmann, 1912; Mann et al., 1911; Lapham and Holmes, 1908; Watson et al., 1929).

Most of these vegetation maps focused on a single type of vegetation, so we were unable to use them as our primary source. Further, we were unable to piece the more limited coverage maps together in any meaningful way as they used different vegetation classification systems and different study areas; even this collection of maps did not cover the entire

Table 1. Monthly vegetation coefficients (K_v) for non-water stressed and rainfed vegetation (Howes et al., 2015).

	Month											
Vegetation	Jan	Feb	Mar	Apr	May	Jun	Jul	Aug	Sep	Oct	Nov	Dec
Rainfed grassland*	0.78	0.72	0.64	0.58	0.35	0.06	0.00	0.00	0.03	0.16	0.47	0.73
Perennial grassland	0.55	0.55	0.60	0.95	1.00	1.05	1.10	1.15	1.10	1.00	0.85	0.85
Vernal pool	0.65	0.70	0.80	1.00	1.05	0.85	0.50	0.15	0.10	0.10	0.25	0.60
Large stand wetland	0.70	0.70	0.80	1.00	1.05	1.20	1.20	1.20	1.05	1.10	1.00	0.75
Small stand wetland	1.00	1.10	1.50	1.50	1.60	1.70	1.90	1.60	1.50	1.20	1.15	1.00
Foothill hardwood*	0.80	0.77	0.69	0.61	0.52	0.20	0.01	0.01	0.03	0.15	0.46	0.71
Valley oak savanna*	0.80	0.77	0.69	0.62	0.54	0.40	0.40	0.40	0.40	0.41	0.55	0.71
Seasonal wetland	0.70	0.70	0.80	1.00	1.05	1.10	1.10	1.15	0.75	0.80	0.80	0.75
Riparian forest	0.80	0.80	0.80	0.80	0.90	1.00	1.10	1.20	1.20	1.15	1.00	0.85
Saltbush	0.30	0.30	0.30	0.35	0.45	0.50	0.60	0.55	0.45	0.35	0.40	0.35
Chaparral*	0.55	0.61	0.54	0.40	0.22	0.03	0.01	0.01	0.03	0.14	0.40	0.57
Aquatic surface	0.65	0.70	0.75	0.80	1.05	1.05	1.05	1.05	1.05	1.00	0.80	0.60

* Evapotranspiration from rainfed vegetation was estimated from a daily soil water balance. Valley oak savanna K_v during the summer and fall was estimated to be 0.4 to account for groundwater contribution. The vegetation coefficients shown are averages over the 88-year period and all valley floor planning areas.

Table 2. Annual average evapotranspiration rates ET_v (cm yr^{-1}).

Basin	Planning area	Rainfed grassland	Perennial grassland	Vernal pool	Large stand wetland	Small stand wetland	Seasonal wetland	Foothill hardwood	Valley oak savanna	Riparian forest	Saltbush	Chaparral	Aquatic surface
Sacramento	502	39.1	130.1	75.3	139.5	204.3	131.1	45.1	67.1	134.1	60.2	29.5	127.4
	503	39.1	130.1	75.3	139.5	204.3	131.1	45.1	67.1	134.1	60.2	29.5	127.4
	504	34.0	128.9	73.9	137.8	201.7	129.4	40.2	64.0	132.5	59.6	28.8	125.8
	505	32.8	135.9	77.9	145.1	212.5	136.2	40.2	67.1	139.6	62.7	24.7	132.5
	506	32.4	135.0	77.7	144.2	211.3	135.5	39.8	67.1	138.7	62.3	25.0	131.7
	507	35.2	139.2	80.1	148.7	217.9	139.7	42.7	70.1	143.0	64.3	26.9	135.8
	508	36.6	143.3	82.3	152.4	222.5	140.2	42.7	73.2	146.3	67.1	27.4	140.2
	509	32.8	135.9	77.9	145.1	212.5	136.2	40.2	67.1	139.6	62.7	24.7	132.5
Delta	510	31.2	136.8	78.5	146.0	213.8	137.0	38.6	67.1	140.4	63.1	23.2	133.3
	602	27.2	121.3	70.3	129.5	189.8	121.8	33.3	57.9	124.6	55.9	19.3	118.3
San Joaquin	511	34.8	143.3	81.8	153.0	224.1	143.5	42.6	73.2	147.1	66.2	26.4	139.7
	601	27.4	113.5	65.5	121.1	177.4	113.9	32.3	54.9	116.6	52.3	19.0	110.6
	603	33.7	142.7	81.9	152.3	223.3	143.0	41.5	70.1	146.4	65.9	25.5	139.1
	604	30.5	137.2	79.2	149.4	213.4	134.1	39.6	67.1	140.2	64.0	24.4	134.1
	605	24.4	134.1	79.2	146.3	213.4	134.1	30.5	61.0	140.2	64.0	18.3	131.1
	606	24.0	135.6	78.4	144.7	212.1	136.1	31.2	61.0	139.2	62.6	17.4	132.2
	607	29.3	140.2	80.9	149.6	219.5	140.6	36.8	67.1	143.8	64.7	21.6	136.7
	608	28.9	144.6	83.8	154.3	226.4	145.0	36.6	70.1	148.2	66.7	21.5	141.0
	609	29.0	152.1	87.5	162.2	238.0	152.2	37.2	70.1	155.8	70.2	22.0	148.2
	610	29.0	152.1	87.5	162.2	238.0	152.2	37.2	70.1	155.8	70.2	22.0	148.2

valley floor study area. Thus, we based our natural vegetation estimates on the California State University at Chico (CSU Chico) pre-1900 map, which covered most of the valley floor.

The CSU Chico study reviewed and digitized approximately 700 historic maps from numerous collections in public libraries. These sources were pulled together in a series of maps, including a "pre-1900 historic vegetation map". We used the pre-1900 historic vegetation map as our base map, modified to cover the entire valley floor using Küchler (1977) and to further subdivide some of its vegetation classifications to match available evapotranspiration information.

CSU Chico characterized its pre-1900 map as "the best available historical vegetation information for the pre-1900 period" noting it provided "a snapshot of the most likely pre Euro-American vegetation cover" (CSU Chico, 2003). This map has been cited by others as representing natural vegetation (Bolger et al., 2011; Vaghti and Greco, 2007). It is based on a patchwork of sources, scales, and dates, with the earliest source map dating to 1874.

The accuracy of the CSU Chico pre-1900 map was confirmed to the extent feasible using GIS overlays with other available natural vegetation maps (Hall, 1887; Roberts et al., 1977; Dutzi, 1978; Fox, 1987; TBI, 1998; Garone, 2011;

Table 3. Area of natural vegetation (A_V) by planning area within the valley floor, Case I (ha).

Valley	Planning area	Rainfed grasslands	Vernal pool	Permanent wetland	Seasonal wetland	Valley/ foothill hardwood	Riparian forest	Saltbush	Chaparral	Aquatic surface	Total
Sacramento	502	0	0	0	0	692	0	0	0	0	692
	503	114 308	25 046	7	2	130 205	33 271	0	7478	1253	311 570
	504	52 570	433	96	977	78 027	34 720	0	39	807	167 667
	505	0	0	0	0	31	0	0	2170	0	2201
	506	140 301	94 683	50 395	19 679	71 054	43 383	0	9541	2429	431 466
	507	19 523	33 515	60 751	102 700	75 491	80 467	0	0	3274	375 721
	508	7289	3712	0	0	86 369	5407	0	0	590	103 368
	509	65 863	42 392	27 454	5395	58 148	25 913	0	22 000	610	247 775
	511	18 066	74 895	20 989	25 425	51 101	17 408	0	0	3116	211 000
Delta	510	718	4263	91 810	10 550	21	760	0	0	5240	113 361
	602	25 265	8533	115 385	9128	34	594	0	0	2858	161 798
San Joaquin	601	3885	3874	0	2	0	1	0	0	274	8037
	603	47 777	59 435	5117	55 734	80 998	16 614	0	157	629	266 461
	604	1098	0	0	0	741	311	0	0	0	2149
	605	4924	406	0	0	0	0	0	0	0	5331
	606	83 099	70 915	12 084	57 570	0	1281	41 405	32	1136	267 523
	607	69 411	64 097	3295	9099	1355	10 574	0	0	820	158 651
	608	66 786	51 142	3037	4945	1689	12 797	0	0	478	140 873
	609	123 728	242 041	17 323	18 450	501	8462	8099	0	1258	419 863
	610	6547	376	0	0	67	4	0	0	0	6995
Total		*851 158*	*779 758*	*407 744*	*319 657*	*636 525*	*291 966*	*49 505*	*41 416*	*24 771*	*3 402 501*

Note: Case I assumes (1) no perennial grasslands, (2) all permanent wetlands are large stand, and (3) all valley/foothill hardwoods are foothill hardwoods.

Whipple et al., 2012). Original shapefiles were used where available (Whipple et al., 2012; TBI, 1998; Küchler, 1977; CSU Chico, 2003). Other maps were scanned (400 dpi full color scanner), the scanned versions were georeferenced using various data layers (e.g., county, township), and the map features were digitized by hand using editing features in ArcMap. ArcMap (ArcGIS 10.1, ESRI, Redlands, CA) geoprocessing tools were used to determine vegetation areas (Fox and Sears, 2014).

The natural vegetation areas estimated using these methods were also compared with those estimated by others. This work estimated about 0.40 million ha of permanent wetlands. Others have estimated 0.40 (Fox 1987) to 0.53 million ha (Hilgard, 1884; Shelton, 1987) for slightly different valley floor boundaries. This work estimated about 1.62 million hectares of grasslands. Others have estimated 2.02 (TBI, 1998) to 2.18 (Fox, 1987; Shelton, 1987) million ha for slightly different valley floor boundaries. The current study estimated approximately 0.77 million ha of vernal pool habitat in the valley floor outside of the floodplain. Others have estimated about 0.97 million ha of vernal pool habitat (Holland, 1978, 1998, 2013; Holland and Hollander, 2007) for slightly different valley floor boundaries. This work also estimated 0.29 million ha of riparian forest based on CSU Chico's map, which is low compared to estimates by others including 0.35, 0.38, 0.37, 0.58, and 0.65 million ha estimated by Shelton (1987), Roberts et al. (1977), Katibah (1984), Fox (1987), and Warner and Hendrix (1985), respectively, for slightly different valley floor boundaries.

However, as the CSU Chico maps and other sources were based on maps prepared after significant modifications to the landscape had already occurred, they may underestimate some types of natural vegetation (Thompson, 1957; Whipple et al., 2012; CSG, 1862). It follows that reliance on these maps may underestimate evapotranspiration and thereby overestimate natural delta outflow. Riparian forests, for example, were cleared early to make way for cities and farms and harvested to supply fuel for steamboats traversing the rivers in support of the gold rush (Whipple et al., 2012). Widespread conversion of wetlands into agricultural uses began in the 1850s when they were leveed, drained, cleared, leveled, or filled; water entering them was impounded, diverted, or drained; and sloughs and crevasses closed to dry out the land (Whipple et al., 2012; Frayer et al., 1989; CSG, 1862). The great wheat bonanza that transformed much of the Central Valley into farmland was well underway by 1874, the date of the earliest historic map in the collection considered by CSU Chico.

The results of our natural vegetation area analysis, based on available historic maps and soil surveys, are summarized in Fig. 4 and Table 3. These areas represent the starting

point for our natural flow estimate. We call this starting point Case I.

Case I represents long-term annual average conditions. These areas are not representative of individual years due to climate-driven variations, which primarily affected grasslands and wetlands. Area size, especially of rainfed grasslands and vernal pools, likely varied from year to year with the amount of precipitation falling on the valley floor and surrounding mountains.

3.4.3 Sensitivity analysis

A sensitivity analysis was performed to address the uncertainty in both natural vegetation areas and evapotranspiration rates. The areal extent of most types of vegetation was not measured or even observed by botanists in its natural state. Further, the water used by some classes of natural vegetation, such as vernal pools and valley oak savannas, has never been measured in the valley floor while the natural water supply is largely based on measurements of rim watershed stream flows or impairments thereof and precipitation. Thus, we formulated a series of cases, in which land use was varied, to explore the range in natural vegetation water use. The cases were selected to address key uncertainties associated with classifying vegetation areas. The eight cases we studied are summarized in Table 4.

As grasslands (including vernal pools) and valley/foothill hardwood classifications represent the greatest portions of the valley floor (see Table 3), our cases focus on these two vegetation classifications. The extent of permanent wetlands, the next largest vegetation classification in the valley floor, was extensively surveyed in the 1850s (CSG, 1856, 1862; Anonymous, 1861; Flushman, 2002; Thompson, 1957) and is considered to be accurately estimated in Case I (Table 3). Further, the evapotranspiration from these wetlands has been well studied (Howes et al., 2015). Thus, we have confidence in our estimates of water use by permanent wetlands.

Grasslands occupied about half of the valley floor area or about 16 000 km^2 out of 34 000 km^2 (Table 3). The composition of these grasslands (e.g., the fraction that was perennial, rainfed, and vernal pool) is unknown, as rapid and widespread modifications occurred before any botanical study (Heady et al., 1992; Holmes and Rice, 1996; Holstein, 2001; Burcham, 1957; Garone, 2011). Some have attempted to estimate vernal pool area (Holland, 1978, 1998; Holland and Hollander, 2007), but we are not aware of any attempts to estimate the area of perennial and rainfed grasslands.

There is significant controversy over the original composition of grasslands. Some argue pristine grasslands were perennial bunchgrasses (Heady, 1988; Küchler, 1977; Bartolome et al., 2007), while others argue they were dominated by annual forbs (Schiffman, 2007; Holstein, 2001). A discussion of this controversy is provided in Garone (2011). Finally, large expanses of lands classified as *grasslands* by others (Küchler, 1977; Fox, 1987; TBI, 1998; CSU Chico, 2003) were probably vernal pool seasonal wetlands supported by perched aquifers (Zedler, 2003; Holland and Hollander, 2007; Fox and Sears, 2014). Due to these unknowns and controversies, we used six cases to explore the effect of grassland composition on natural water use, the base case compared to five variants.

In Case I, all grassland areas outside of the floodplain were classified as either vernal pool (based on soil surveys) or rainfed grassland, as shown in Fig. 4 and Table 3. We then varied the rainfed portion to assume it was vernal pool (Case II) and perennial grassland (Case III) to bound the likely range.

These three constant-area grassland cases resulted in many negative San Joaquin Basin annual outflows, mostly in dry and critical years. One explanation for this outcome is that the grasslands may have been predominately rainfed in the San Joaquin Basin since this basin is much drier than the other two. Another explanation is that our water balance model assumed the net change in groundwater storage was zero on a long-term basis, which may not be valid on a yearly and basin-wide basis.

Groundwater that was recharged in wet and above-normal years could have supplied the water needs of natural vegetation in subsequent years. Failure to account for these potential inter-annual sources of water could bias individual year water balances and could result in negative basin outflows for individual years (particularly critical and dry years that follow very wet years). Negative basin annual outflows were primarily limited to the San Joaquin Basin.

Thus, in Case IV, all grasslands in the San Joaquin Basin were classified as rainfed grasslands in an attempt to address this possibility, while grasslands in the Sacramento and delta basins were classified as a mix of vernal pool and perennial as in Case III. A similar consideration led to the classification of seasonal wetlands in the San Joaquin Basin as rainfed grasslands (Case VIII, discussed later).

We also discounted the scenario of grasslands being rainfed valley-wide as unlikely, given that our work and the work of Holland and Hollander (2007) established that a significant fraction of the valley floor was vernal pool habitat. Some of these grassland areas, particularly within the flood basins, were likely seasonal wetlands or lakes and ponds (Whipple et al., 2012) with higher water uses, but we had no basis for estimating these areas.

It was generally assumed that vegetation areas are constant from year to year in cases I to IV, which is reasonable for a long-term annual average. However, this assumption is an oversimplification when applied to individual years because vegetation area likely varied in response to climate, especially the amount and timing of precipitation and resulting riverbank overflow. The floodplain boundary, for example, would have varied significantly depending on the amount and timing of runoff, which would have affected vegetation both inside and outside of the floodplain. In July 1853, for example, engineers surveying a route for a railroad in the San Joaquin Valley reported: “The river [San Joaquin] had

Table 4. Water balance cases.

Case	Grassland assumptions		Hardwood assumptions
	Sacramento and Delta Basins	San Joaquin Basin	
Grasslands – constant area			
I	Mix of rainfed grassland and Vernal pools	Mix of rainfed grassland and Vernal pools	Foothill
II	Vernal pools	Vernal pools	Foothill
III	Mix of perennial grassland and Vernal pools	Mix of perennial grassland and Vernal pools	Foothill
IV	Mix of perennial grassland and Vernal pools	Rainfed grassland	Foothill
Grasslands – variable area			
V	Mix of rainfed and perennial grassland and Vernal pools[1]	Mix of rainfed and perennial grassland and Vernal pools[1]	Foothill
VI	Mix of rainfed and perennial grassland[2]	Mix of rainfed and perennial grassland[2]	Foothill
Other			
VII	Mix of rainfed grassland and Vernal pools	Mix of rainfed grassland and Vernal pools	Valley oak savanna
VIII	Mix of perennial grassland and Vernal pools	Rainfed grassland[3]	Foothill

[1] Vegetation areas are identical to Case I, except grassland areas not classified as vernal pools are assumed to be a mix of rainfed and perennial grassland that varies from year to year based on the annual runoff volume as measured by the Eight River Index (CDWR, 2013a). Grassland areas are assumed to be perennial in the wettest year, rainfed in the driest year, and for all other years, the mix is assumed to vary linearly with annual runoff volume between the wettest year and driest year. [2] Vegetation areas are identical to Case I, except vernal pools are assumed to be a mix of rainfed and perennial grassland. Aggregate grasslands are assumed to be perennial in the wettest year, rainfed in the driest year, and for all other years, the mix is assumed to vary linearly with annual runoff volume between the wettest year and driest year. [3] Vegetation areas are identical to Case IV, except seasonal wetlands within the floodplain are assumed to be rainfed grasslands.

overflowed its banks, and the valley was one vast sheet of water, from 25 to 30 miles broad, and approaching within four to five miles of the hills" (Williamson, 1853). The average floodplain boundary (CDPW, 1931a, b) was typically over 20 miles from these hills. We used the average floodplain boundary to estimate some vegetation types, such as seasonal wetlands within "other floodplain habitat", which would yield inaccuracies when used for individual years.

Grasslands are the vegetation type most likely to respond significantly to climate. Thus, in Cases V and VI, the mix of rainfed and perennial grasslands was varied based on the volume of rim inflow to the Sacramento and San Joaquin basins. Vegetation areas in Case V are identical to Case I, except grassland areas not classified as vernal pools are assumed to be a mix of rainfed and perennial grasslands that vary from year to year based on the annual runoff volume as measured by the eight-river index (CDWR, 2013a). Grassland areas are assumed to be perennial in the wettest year, rainfed in the driest year, and for all other years, the mix is assumed to vary linearly with annual runoff volume between the wettest year and the driest year.

Vegetation areas in Case VI are identical to Case I, except vernal pools are assumed to be a mix of rainfed and perennial grassland. Aggregate grasslands are assumed to be perennial in the wettest year, rainfed in the driest year, and for all other years, the mix is assumed to vary linearly with annual runoff volume between the wettest year and the driest year.

We believe Cases V and VI most closely represent water use under natural conditions as it is likely that vegetation varied in this fashion. It is likely that seasonal wetlands varied in a similar fashion, extending further outside of the flood basins in wet years than in dry or critical (Whipple et al., 2012). However, we did not have sufficient data to evaluate this case.

We defined two additional vegetation area cases to explore the uncertainty of natural delta outflow due to evapotranspiration and areal extent of valley foothill hardwoods (Case VII) and wetlands (Case VIII).

Case VII was included to explore the effect of valley/foothill hardwoods composition on natural delta outflow. This case primarily affects Sacramento Basin outflow as 86 % of the hardwood vegetation, or 5300 km^2, is in this basin. This vegetation class was subdivided into foothill hardwood, present at higher elevations with deeper water tables, and valley oak savannas, present in the valley floor where water tables were shallow, for purposes of estimating

evapotranspiration (Howes et al., 2015). Foothill hardwoods likely relied on soil moisture as the water table was generally deeper at these higher elevation areas than on the valley floor. Valley oak savannas, on the other hand, had deep root systems (Howes et al., 2015) that tapped the shallower groundwater at lower elevations (Bertoldi et al., 1991; Bryan, 1915; Kooser et al., 1861).

We had no basis for reliably subdividing valley/foothill hardwood land areas into subclasses. Küchler (1977) suggests that about 65 % was foothill hardwoods. Thus, we evaluated a range. In Case I, we assumed that 100 % of valley/foothill hardwood was foothill hardwood. In Case VII, we assumed 100 % was valley oak savanna, holding all other land areas constant as in Table 3.

Case VIII classifies San Joaquin Basin seasonal wetlands as rainfed grasslands. The San Joaquin Basin was modeled differently based on our annual water balances, as discussed above, supplemented by soil surveys, eyewitness accounts, and the basin's relatively dry hydrology which suggest that rainfed grasslands (rather than seasonal wetland) is a plausible alternate vegetation classification for seasonal wetlands.

4 Results

The water balance methodology described previously was used to estimate annual average delta outflow under natural conditions for each year of the 88-year hydrologic sequence (1922–2009). A long-term annual average was computed from individual yearly results and compared with CDWR's (2007, 2012) estimates of long-term annual average delta outflow under current conditions and unimpaired conditions for a similar period of record.

The results of our natural delta outflow water balances for eight land use cases are summarized in Table 5 and illustrated in Fig. 5. Under natural conditions, native vegetation used 27.1 to 36.1 billion $m^3\,yr^{-1}$ of the natural water supply, falling as precipitation in the mountain ranges surrounding the valley floor and on the valley floor itself. This amounts to 54 to 72 % of the total supply of 50.1 billion $m^3\,yr^{-1}$. The water that was not evapotranspired or evaporated, ranging from 14.0 to 23.0 billion $m^3\,yr^{-1}$, flowed into the delta and San Francisco Bay. These results are consistent with those reported by others (Shelton, 1987; Bolger et al., 2011; Fox, 1987).

The resulting evapotranspiration-to-precipitation (ET / P) ratios, 0.54 to 0.72 are estimated as total water use from Table 5 divided by the sum of valley floor precipitation (15.9 billion $m^3\,yr^{-1}$) and rim inflows (34.2 billion $m^3\,yr^{-1}$), and are consistent with ET / P ratios reported by others (Sanford and Selnick, 2014). The valley floor vegetation described in this work was not sustained by precipitation falling on the valley floor. The valley floor also used large quantities of runoff from surrounding watersheds that was not consumed in those watersheds but was made available for consumptive use through the seasonal flooding cycle. Therefore, rim inflows supplement precipitation as a water supply to the valley floor.

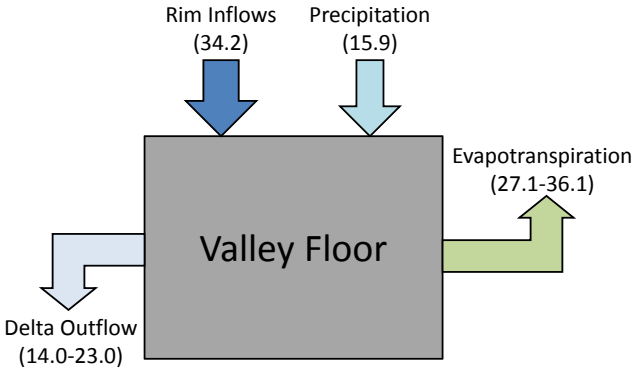

Figure 5. Schematic showing the average (1922–2009) natural water balance results (billion $m^3\,yr^{-1}$).

In sum, we believe that Cases V and VI, in which the mix of rainfed and perennial grasslands was varied based on the volume of rim inflow to the Sacramento and San Joaquin basins, most closely represent water consumed under natural conditions. In these cases, native vegetation consumed 30.4 to 29.7 billion $m^3\,yr^{-1}$ or about 60 % of the natural supply. About 41 % of the native vegetation water use in these two cases was consumed by the grassland–vernal pool complex occupying the area between the foothills and the floodplain. About 34 % of the native vegetation water use was consumed by permanent and seasonal wetlands, largely within the floodplain. The balance of the native vegetation water use was consumed by riparian vegetation (13 %), foothill hardwoods (9 %), and saltbush, chaparral, and open water surfaces (3 %).

In comparison, the current-level, long-term annual average delta outflow is 19.5 billion $m^3\,yr^{-1}$ (CDWR, 2012). This estimate was developed using a reservoir system operations model (Draper et al., 2004) and assumes a 2011 level of development for an 82-year hydrologic sequence (1922 to 2003). The current long-term annual average water supply of 51.6 billion $m^3\,yr^{-1}$ estimated by CDWR (2012) exceeds the natural water supply in our analysis by 1.5 billion $m^3\,yr^{-1}$ due to (1) groundwater overdraft of 0.9 billion $m^3\,yr^{-1}$ in the Sacramento and San Joaquin basins and (2) Sacramento River Basin imports of 0.6 billion $m^3\,yr^{-1}$ from the US Bureau of Reclamation Trinity River Diversion Project, a project that transfers water from Lewiston Reservoir through the Clear Creek Tunnel to the Sacramento River (CDWR, 2012).

The long-term annual average current-level delta outflow of 19.5 billion $m^3\,yr^{-1}$ falls within the range of estimated natural outflows as shown in Fig. 6 for the same period of record (14.0 to 23.0 billion $m^3\,yr^{-1}$). The current-level water balance indicates that 62 % of the water supply is currently

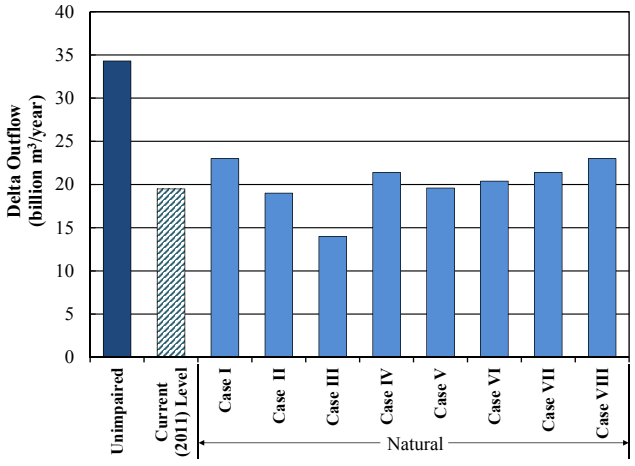

Figure 6. Comparison of long-term (1922–2009) average annual delta outflow estimated based on unimpaired, current (2011) level, and the natural scenarios (Cases I–VII) examined in this study.

consumed by irrigation, municipal, industrial, and other uses, based on the 2011 level of development (CDWR, 2013b). This estimate is roughly the midpoint of the range of estimated natural water use (54 to 72 %).

Thus, current and natural delta outflows, when reported for the same climatic conditions, are very similar because natural vegetation used nearly as much water (27.1 to 36.1 billion $m^3\,yr^{-1}$) as is consumed currently (31.9 billion $m^3\,yr^{-1}$) for agriculture, municipal, industrial, and other uses. Further, the current and natural delta outflow estimates are statistically indistinguishable due to uncertainties described elsewhere.

In sum, reconfiguring the natural water supply to accommodate new land uses (e.g., see Fig. 4), mitigate flooding, and redistribute the water supply in time and space has not substantially changed the annual average amount of freshwater reaching San Francisco Bay from the Central Valley, when controlled for climate. This is the case because natural vegetation consumed about as much water as is currently used by the new land uses within the valley floor as well as outside of it.

We believe our natural delta outflow estimates were based on conservative assumptions that will tend to underestimate evapotranspiration and thus overestimate natural delta outflows. Noteworthy conservative assumptions include (1) all of the permanent wetlands are assumed to be large stand, thereby ignoring higher water-using small stand wetlands and (2) the maps and soil surveys used to estimate natural vegetation underestimate the extent of some types of natural vegetation, such as wetlands and vernal pools, because significant modifications had been made to the landscape prior to the date of its earliest source (1874).

5 Discussion

This study shows that long-term annual average current and natural outflows fall within the same range, when controlled for climatic conditions. This occurs as the amount of water currently used from valley floor watersheds for agriculture, domestic, industrial, and other uses is about equal to the amount of water that would be used if the existing engineered system were replaced by natural vegetation.

An estimate of natural delta outflows is important as reduction in the volume of freshwater reaching the San Francisco Bay–Delta estuary due to the current level of development has frequently been advanced as one of the causes for the decline in abundance of native species. Further, estimates of hypothetical natural outflow (so-called unimpaired outflows) have been proposed to regulate current delta outflows in an effort to restore ecological health of the estuary. This work indicates that restoring flows to annual average natural outflows are unlikely to restore ecosystem health because they are indistinguishable from annual average current outflows.

The reduced outflow hypothesis advanced by some as a cause of declines in native fish abundance is typically based on unimpaired flows of 34.3 billion $m^3\,yr^{-1}$ published by CDWR (2007). These unimpaired flows are hypothetical flows that never existed. CDWR (2007) differentiates unimpaired delta outflow from natural delta outflow by characterizing them as "runoff that would have occurred had water flow remained unaltered in rivers and streams instead of stored in reservoir, imported, exported, or diverted. The data are a measure of the total water supply available for all uses after removing the impacts of most upstream alterations as they occurred over the years. Alterations such as channel improvements, levees, and flood bypasses are assumed to exist."

The long-term annual average unimpaired delta outflow estimate of 34.3 billion $m^3\,yr^{-1}$ assumes the same rim inflows and valley floor precipitation used in our natural water balances in Table 5. However, rather than reducing water supply to account for water use associated with the full extent of natural vegetation in the valley floor, the unimpaired outflow calculation assumes that water use upstream of the delta is limited to only valley floor precipitation (CDWR, 2007). In other words, the unimpaired outflow calculation assumes the only vegetation present outside of the delta was perennial grasslands with no access to groundwater. It ignores the presence of perennial grasslands, vernal pools, wetlands, riparian forest, and valley oak savannahs.

Thus, the unimpaired outflow calculation effectively assumes rim inflows pass through the valley floor and arrive in the delta in the current system of channel improvements, levees, and flood bypasses (i.e., the difference between the natural water supply of 50.1 billion $m^3\,yr^{-1}$ and valley floor precipitation of 15.9 billion $m^3\,yr^{-1}$ is 34.2 billion $m^3\,yr^{-1}$). Thus, by definition, unimpaired delta outflow calculations provide a high estimate when used as a surrogate for natural delta outflow.

Table 5. Natural water balance 1922–2009 valley floor (billion m^3 yr^{-1}).

Water supply		Water use (billion m^3 yr^{-1})							
Inflow	34.2	Grasslands – constant area				Grasslands – variable area		Other vegetation	
Precipitation	15.9								
Total water supply	50.1	Case I	Case II	Case III	Case IV	Case V	Case VI	Case VII	Case VIII
		Sacramento Basin							
Rainfed grasslands		1.5	0.0	0.0	0.0	0.9	1.5	1.5	0.0
Perennial grasslands		0.0	0.0	5.6	5.6	2.1	3.6	0.0	5.6
Vernal pool		2.2	5.4	2.2	2.2	2.2	0.0	2.2	2.2
Large stand wetland		2.3	2.3	2.3	2.3	2.3	2.3	2.3	2.3
Seasonal wetland		2.2	2.2	2.2	2.2	2.2	2.2	2.2	2.2
Foothill hardwood		2.3	2.3	2.3	2.3	2.3	2.3	0.0	2.3
Valley oak savanna		0.0	0.0	0.0	0.0	0.0	0.0	3.7	0.0
Riparian forest		3.3	3.3	3.3	3.3	3.3	3.3	3.3	3.3
Saltbush		0.0	0.0	0.0	0.0	0.0	0.0	0.0	0.0
Chaparral		0.1	0.1	0.1	0.1	0.1	0.1	0.1	0.1
Aquatic surface		0.1	0.1	0.1	0.1	0.1	0.1	0.1	0.1
		14.2	*15.9*	*18.2*	*18.2*	*15.7*	*15.5*	*15.5*	*18.2*
		Delta							
Rainfed grassland		0.1	0.0	0.0	0.0	0.0	0.1	0.1	0.0
Perennial grassland		0.0	0.0	0.4	0.4	0.1	0.1	0.0	0.4
Vernal pool		0.1	0.3	0.1	0.1	0.1	0.0	0.1	0.1
Large stand wetland		2.8	2.8	2.8	2.8	2.8	2.8	2.8	2.8
Seasonal wetland		0.3	0.3	0.3	0.3	0.3	0.3	0.3	0.3
Foothill hardwood		0.0	0.0	0.0	0.0	0.0	0.0	0.0	0.0
Valley oak savanna		0.0	0.0	0.0	0.0	0.0	0.0	0.0	0.0
Riparian forest		0.0	0.0	0.0	0.0	0.0	0.0	0.0	0.0
Saltbush		0.0	0.0	0.0	0.0	0.0	0.0	0.0	0.0
Chaparral		0.0	0.0	0.0	0.0	0.0	0.0	0.0	0.0
Aquatic surface		0.1	0.1	0.1	0.1	0.1	0.1	0.1	0.1
		3.5	*3.5*	*3.7*	*3.7*	*3.5*	*3.5*	*3.5*	*3.7*
		San Joaquin Basin							
Rainfed grasslands		1.1	0.0	0.0	2.6	0.7	1.5	1.1	3.0
Perennial grasslands		0.0	0.0	5.8	0.0	2.2	5.1	0.0	0.0
Vernal pools		4.2	7.5	4.2	0.0	4.2	0.0	4.2	0.0
Large stand wetlands		0.6	0.6	0.6	0.6	0.6	0.6	0.6	0.6
Seasonal wetland		2.0	2.0	2.0	2.0	2.0	2.0	2.0	0.0
Foothill hardwoods		0.4	0.4	0.4	0.4	0.4	0.4	0.0	0.4
Valley oak savanna		0.0	0.0	0.0	0.0	0.0	0.0	0.6	0.0
Riparian forest		0.7	0.7	0.7	0.7	0.7	0.7	0.7	0.7
Saltbush		0.4	0.4	0.4	0.4	0.4	0.4	0.4	0.4
Chaparral		0.0	0.0	0.0	0.0	0.0	0.0	0.0	0.0
Aquatic surface		0.1	0.1	0.1	0.1	0.1	0.1	0.1	0.1
		9.5	*11.7*	*14.2*	*6.8*	*11.3*	*10.7*	*9.7*	*5.2*
Total water use		*27.1*	*31.1*	*36.1*	*28.7*	*30.4*	*29.7*	*28.7*	*27.1*
delta outflow = total water supply − total water use		*23.0*	*19.0*	*14.0*	*21.4*	*19.6*	*20.4*	*21.4*	*23.0*

In spite of CDWR's caveats of its theoretical calculation of unimpaired delta outflow from natural delta outflow, unimpaired outflows have frequently been used as a surrogate measure of natural conditions, presumably because no estimate of natural delta outflow was published prior to this work. For example, Dynesius and Nilsson (1994) argue that the bay–delta watershed is strongly affected by fragmentation due to the difference between current delta outflow and the delta's reported virgin mean annual discharge of 34.8 billion $m^3\,yr^{-1}$, a quantity roughly equivalent to CDWR's long-term annual average unimpaired delta outflow calculation published by CDWR at the time of this work. More recently, the California State Water Resources Control Board (CSWRCB, 2010) submitted a report to the state legislature suggesting a flow criterion of 75 % of unimpaired delta outflow from January through June "in order to preserve the attributes of the natural variable system to which native fish species are adapted." This suggested criterion was based on fishery protection alone and did not consider other beneficial uses of water in the estuary.

Native aquatic species evolved under natural landscape conditions. Figure 4 demonstrates that very little of the natural landscape remains. Thus, habitat restoration may be an important ingredient in restoring these species. Understanding natural delta outflow and how it interacts with the natural landscape will be important to guide future restoration planning activities. The Comprehensive Everglades Restoration Plan (CERP), for example, used natural system modeling to gain a better understanding of south Florida's hydrology prior to drainage and development. CERP, which was designed to restore the Everglades ecosystem while maintaining adequate flood protection and water supply for south Florida, is using insights gained by this modeling effort, in combination with other adaptive management tools, to formulate restoration plans and set targets (SFWMD, 2014).

California's Bay Delta Conservation Plan, another such planning activity, envisions a reversal of the delta's ecosystem decline through protection and creation of approximately 590 km^2 of aquatic and terrestrial habitat (CDWR and USBR, 2013). By reconnecting floodplains, developing new marshes, and returning riverbanks to a more natural state, the plan is designed to boost food supplies and provide greater protection for native fisheries.

6 Conclusions and recommendations

This study found that the amount of water from the valley floor watershed currently consumed for agriculture, domestic, industrial, and other uses is roughly equal to the amount of water formerly used by native vegetation in this same watershed. Thus, delta outflow, or the amount of freshwater reaching San Francisco Bay, is about the same under current conditions as under natural conditions, when controlled for climate.

This finding, which used a conventional water balance methodology and assumed contemporary climatic conditions for both natural and current landscapes, suggests that human disturbances to the landscape and hydrologic cycle have not significantly reduced the annual average volume of freshwater flows entering San Francisco Bay through the delta. Rather, development has simply redistributed flows from natural vegetation to other beneficial uses. Thus, it is unlikely that observed declines in native freshwater aquatic species are due to reduction in annual average delta outflow.

Another key finding of this study is that unimpaired delta outflow calculations significantly overestimate natural delta outflow as they fail to include consumptive use by natural vegetation in the valley floor other than rainfed grasslands. Therefore, unimpaired delta outflow calculations should not be used as a surrogate measure of natural conditions or to set flow standards to restore ecosystem health.

Several limitations associated with this work point to areas for future research. The simple water balance methodology utilized in this paper is an appropriate reconnaissance-level step in reconstructing the natural hydrology of a complex system. However, this simple approach is unable to explore several important and relevant questions.

First, our analysis only considers long-term annual averages and does not evaluate inter- and intra-annual variability of natural delta outflow. Ecosystems respond to flows at timescales much shorter than annual. Thus, future work should consider these shorter timescales.

Second, our analysis does not account for complex interactions between groundwater and surface water. These interactions would place important limits on water availability to vegetation in a natural landscape on a shorter timescale.

Third, many vegetation land areas likely varied with the wetness of the year. We attempted to address this using a sensitivity analysis in which grassland–vernal pool areas were varied as a function of rim inflows and other assumptions.

Finally, we assumed natural evapotranspiration rates for vegetation types with a continuous water supply, e.g., permanent wetlands, are constant over the period of record. They likely varied as a function of climate. Future work should include a sensitivity analysis of vegetation coefficient ranges such as those shown in Howes et al. (2015).

We recommend future research in several areas of historical landscape ecology, hydrology, and estuarine hydrodynamics to address these limitations to support ongoing regulatory and habitat restoration activities in the San Francisco Bay–Delta watershed, including

- refined natural vegetation mapping in the Sacramento and San Joaquin basins, following work in the delta reported by Whipple et al. (2012);
- evapotranspiration from vernal pools and seasonal wetlands;

- interactions between groundwater and surface water under natural conditions;
- inter- and intra-annual variability of natural delta outflows;
- natural watershed geomorphology;
- natural estuarine salinity transport.

We recommend that integrated groundwater–surface water models, digital elevation models and hydrodynamic models be developed to support this research. Several collaborative efforts are currently underway to develop such models (Draper, 2014; Kadir and Huang, 2014; Grossinger et al., 2014; Fleenor et al., 2014; DeGeorge and Andrews, 2014). Finally, we recommend future research be conducted to compare the evolution of the San Francisco Bay–Delta watershed with other watersheds around the world.

Acknowledgements. This work was partially funded by San Luis Delta Mendota Water Authority and the State Water Contractors and voluntary contributions of the authors. This work benefited greatly from discussion with and information provided by Robert F. Holland (unpublished vernal pool GIS shape files), as well as Rusty Griffin, US Fish & Wildlife Service (historic wetlands map). The model used for sensitivity analysis and case definition was developed by Louis Nuyens, Peter Louie (Metropolitan Water District), and Gomathishankar (Shankar) Parvathinathan (MWH).

Edited by: M. Sivapalan

References

Alexander, B. S., Mendell, G. H., and Davidson, G.: Report of the Board of Commissioners on the Irrigation of the San Joaquin, Tulare, and Sacramento Valleys of the State of California, 43rd Congress, 1st Session, House of Representation, Ex. Doc. No. 290, Government Printing Office, Washington, 1874.

Allen, R. G., Pereira, L. S., Raes, D., and Smith, M.: Crop Evapotranspiration: guidelines for computing crop water requirements, FAO Irrigation and Drainage Paper No. 56, Food and Agricultural Organization of the United Nations, Rome, Italy, 1998.

Allen, R. G., Walter, I. A., Elliott, R. L., Howell, T. A., Itenfisu, D., Jensen, M. E., and Snyder, R. L. (Eds.): The ASCE Standardized Reference Evapotranspiration Equation, ASCE, Reston, Virginia, 2005.

Anonymous: Commissioners and Surveyor-General's Instructions to the County Surveyors of California, California State Printing Office, Sacramento, CA, USA, 1861.

Armstrong, C. F. and Stidd, C. K.: A moisture–balance profile on the Sierra Nevada, J. Hydrol., 5, 258–268, 1967.

Bain, J. S., Caves, R. E., and Margolis, J.: Northern California's Water Industry: The Comparative Efficiency of Public Enterprise in Developing a Scarce Natural Resource, Published for Resources for the Future, Inc., The Johns Hopkins Press, Baltimore, MD, 1966.

Bales, R. C., Battles, J. J., Chen, Y., Conklin, M. H., Holst, E., O'Hara, K. L., Saksa, P., and Stewart, W.: Forests and Water in the Sierra Nevada: Sierra Nevada Watershed Ecosystem Enhancement Project, report number 11.1, Sierra Nevada Research Institute, 2011.

Barbour, M. G., Pavlik, B., Drysdale, F., and Lindstrom, S.: California's changing landscapes, Diversity and Conservation of California Vegetation, California Native Plant Society, Sacramento, CA, 1993.

Bartolome, J. W., Barry, W. J., Griggs, T., and Hopkinson, P.: Valley grasslands, in: Chapter 14, Terrestrial Vegetation of California, edited by: Barbour, M. G., Keeler-Wolf, T., and Schoenheer, A. A., University of California Press, Berkeley, 367–393, 2007.

Bennett, W. A. and Moyle, P. B.: Where have all the fishes gone? Interactive factors producing fish declines in the Sacramento–San Joaquin estuary, in: San Francisco Bay: The Ecosystem, edited by: Hollibaugh, J. T., Pacific Division of the American Association for the Advancement of Science, San Francisco, CA, 519–542, 1996.

Bertoldi, G. L., Johnston, R. J., and Evenson, K. D.: Ground Water in the Central Valley, California – A Summary Report, US Geological Survey Professional Paper 1401-A, United States Government Printing Office, Washington, D.C., USA, 1991.

Bolger, B. L., Park, Y.-J., Unger, A. J. A., and Sudicky, E. A.: Simulating the pre-development hydrologic conditions in the San Joaquin Valley, California, J. Hydrol., 411, 322–330, 2011.

Bryan, K.: Groundwater for Irrigation in the Sacramento Valley, California, US Geological Survey Water-Supply Paper 375-A, United States Government Printing Office, Washington, D.C., USA, 1915.

Bryan, K.: Geology and Ground-Water Resources of the Sacramento Valley, California, US Geological Survey Water-Supply Paper 495, United States Government Printing Office, Washington, D.C., USA, 1923.

Burcham, L. T.: California Range Land: An Historical–Ecological Study of the Range Resource of California, CA, Department of Natural Resources, Division of Forestry, Sacramento, CA, 1957.

California State Engineer: Report of the State Engineer of the State of California, Sacramento, CA, USA, 11 May 1907 to 30 November 1908.

CDPW – California Department of Public Works: Sacramento River Basin, Bulletin No. 26, Sacramento, CA, USA, 1931a.

CDPW – California Department of Public Works: San Joaquin River Basin, Bulletin No. 29, Sacramento, CA, USA, 1931b.

CDWR – California Department of Water Resources: California Planning Areas, Prepared by Scott Hayes, 31 October 2005, available at: http://www.waterplan.water.ca.gov/docs/maps/pa-web.pdf (last access: 15 January 2015), 2005a.

CDWR – California Department of Water Resources: California Detailed Analysis Units, Prepared by Scott Hayes, 31 October 2005, available at: http://www.waterplan.water.ca.gov/docs/maps/dau-web.pdf (last access: 15 January 2015), 2005b.

CDWR – California Department of Water Resources: California Central Valley Unimpaired Flow Data, 4th Edn., Draft, Bay-Delta Office, California Department of Water Resources, Sacramento, CA, May 2007.

CDWR – California Department of Water Resources: The State Water Project Final Delivery Reliability Report 2011, available

at: http://baydeltaoffice.water.ca.gov/swpreliability/FINAL_2011_DRR.pdf (last access: 1 March 2015), 2012.

CDWR – California Department of Water Resources: California Data Exchange Center, Chronological Reconstructed Sacramento and San Joaquin Valley Water Year Hydrologic Classification Indices, available at: http://cdec.water.ca.gov/cgi-progs/iodir/WSIHIST (last access: 8 April 2015), 2013a.

CDWR – California Department of Water Resources: California Water Plan, Update 2013, Bulletin 160-13, Sacramento, CA, USA, 2013b.

CDWR and USBR – California Department of Water Resources and US Department of the Interior, Bureau of Reclamation: Bay Delta Conservation Plan, Public Draft, November 2013, available at: http://baydeltaconservationplan.com (last access: 3 February 2015), 2013.

Cloern, J. E. and Jassby, A. D.: Drivers of change in estuarine-coastal ecosystems: discoveries from four decades of study in San Francisco Bay, Rev. Geophys., 50, 1–33, 2012.

CSG – California Surveyor-General: Annual Report of the Surveyor-General of the State of California. Document No. 5, in: Senate, Session of 1856, Sacramento, available at: http://www.slc.ca.gov/Reports/Surveyors_General/reports/Marlette1855.pdf (last access: 7 April 2015), 1856.

CSG – California Surveyor-General: Annual Report of the Surveyor-General of California for the Year 1862, Sacramento, available at: http://www.slc.ca.gov/Reports/surveyors_general/reports/houghton1862.pdf (last access: 7 April 2015), 1862.

CSU Chico – California State University: The Central Valley Historic Mapping Project, Chico, CA, USA, April 2003.

CSWRCB – California State Water Resources Control Board: Development of Flow Criteria for the Sacramento–San Joaquin Delta Ecosystem, Prepared Pursuant to the Sacramento–San Joaquin Delta Reform Act of 2009, Sacramento, CA, USA, August 2010.

Cunningham, L.: A State of Change: Forgotten Landscapes of California, Heyday, Berkeley, CA, 2010.

Daly, C. and Bryant, K.: The PRISM climate and weather system – an introduction, PRISM Climate Group, Northwest Alliance for Computational Science and Engineering, Oregon State University, Corvallis, OR, USA, available at: http://www.prism.oregonstate.edu/documents/PRISM_historyjun2013.pdf (last access: 7 April 2015), 2013.

Daly, C., Taylor, G. H., Gibson, W. P., Parzybok, T. W., Johnson, G. L., and Pasteris, P. A.: High-quality spatial climate data sets for the United States and beyond, Trans. ASAE, 6, 1957–1962, 2000.

Davis, G. H., Green, J. H., Olmsted, F. H., and Brown, D. W.: Ground-water conditions and storage capacity in the San Joaquin Valley, California, US Geological Survey Water Supply Paper 1469, United States Government Printing Office, Washington, D.C., USA, 1959.

DeGeorge, J. and Andrews, S.: Natural Delta Hydrodynamic Model Development, Presented at the 8th Biennial Bay-Delta Science Conference, 28–30 October, Sacramento, CA, p. 38, available at: http://scienceconf2014.deltacouncil.ca.gov/sites/default/files/uploads/OralAbstractsFull.pdf (last access: 7 April 2015), 2014.

Draper, A. J.: Natural flow monthly routing model, Presented at the California Water and Environmental Modeling Forum Annual Meeting, 24–26 February, Folsom, CA, p. 36, available at: http://www.cwemf.org/AnnualMeeting/2014Abstracts.pdf (last access: 7 April 2015), 2014.

Draper, A. J., Munevar, A., Arora, S. K., Reyes, E., Parker, N. L., Chung, F. I., and Peterson, L. E.: CalSim: generalized model for reservoir system analysis, J. Water Res. Pl. ASCE, 6, 480–489, 2004.

Dutzi, E. J.: Valley Oaks in the Sacramento Valley: Past and Present Distribution, Master of Arts Thesis in Geography, University of California, Davis, 1978.

Dynesius, M. and Nilsson, C.: Fragmentation and flow regulation of river systems in the northern third of the world, Science, 266, 753–762, 1994.

Fleenor, W., Whipple, A., Bell, A., Lay, M., Grossinger, R., Safran, S., and Beagle, J.: Generating a historical Delta bathymetric-topographical digital elevation model (Part II) Data Interpolation, 24–26 February, Folsom, CA, p. 39, available at: http://www.cwemf.org/ (last access: 7 April 2015), 2014.

Flushman, B. S.: Water Boundaries: Demystifying Land Boundaries Adjacent to Tidal or Navigable Waters, John Wiley & Sons, Inc., New York, NY, USA, 2002.

Fox, J. P.: Freshwater Inflow to San Francisco Bay Under Natural Conditions, Appendix 2, SWC Exhibit No. 262, Calif. State Water Resources Hearings on the Bay-Delta, December 1987, Sacramento, CA, USA, 1987.

Fox, J. P. and Sears, L.: Natural Vegetation in the Central Valley of California, Project Report Prepared for San Luis Delta Mendota Water Authority and the State Water Contractors, San Luis Delta Mendota Water Authority and State Water Contractors, Sacramento, CA, USA, 2014.

Frayer, W. E., Peters, D. D., and Pywell, H. R.: Wetlands of the California Central Valley, Status and Trends – 1939 to mid-1980s, US Fish and Wildlife Service Report, US Fish and Wildlife Service, Region 1, Portland, OR, USA, June 1989.

Garone, P.: The Fall and Rise of the Wetlands of California's Great Central Valley, University of California Press, Berkeley, 2011.

Gleick, P. H.: The development and testing of a water balance model for climate impact assessment: modeling the Sacramento Basin, Water Resour. Res., 6, 1049–1061, 1987.

Glibert, P. M.: Long-term changes in nutrient loading and stoichiometry and their relationships with changes in the food web and dominant Pelagic fish species in the San Francisco Estuary,California, Rev. Fish. Sci., 18, 211–232, 2010.

Glibert, P. M., Fullerton, D., Burkholder, J. M., Cornwell, J. C., and Kana, T. M.: Ecological stoichiometry, biogeochemical cycling, invasive species, and aquatic food webs: San Francisco estuary and comparative systems, Rev. Fish. Sci., 4, 358–417, 2011.

Grossinger, R., Safran, S., Beagle, J., DeGeorge, J., Fleenor, W., Whipple, A., Bell, A., and Lay, M.: Generating a historical Delta bathymetric-topographical digital elevation model (Part I) data collection and development, Presented at the California Water and Environmental Modeling Forum Annual Meeting, 24–26 February, Folsom, CA, available at: http://www.cwemf.org/AnnualMeeting/2014Abstracts.pdf (last access: 7 April 2015), 2014.

Grunsky, C. E.: The relief outlets and by-passes of the Sacramento Valley flood-control project, Trans. ASCE, 93, 791–811, 1929.

Hall, W. H.: Report of the State Engineer to the Legislature of California, Session of 1880, Part 2, California State Printer, Sacramento, CA, USA, 1880.

Hall, W. H.: Topographical and Irrigation Map of the Great Central Valley of California Embracing the Sacramento, San Joaquin, Tulare and Kern Valleys and the Bordering Foothills, California State Engineering Department, Sacramento, CA, USA, 1887.

Heady, H. E., Bartolome, J. W., and Pitt, M. D.: California prairie, in: Natural Grasslands, edited by: Copland, R. T., Elsevier, New York, 313–332, 1992.

Heady, H. F.: Valley grasslands, in: Chapter 14, Terrestrial Vegetation of California, edited by: Barbour, M. G. and Major, J., John Wiley & Sons Inc., New York, NY, USA, 491–513, 1988.

Hilgard, E. W.: Report on the Physical and Agricultural Features of the State of California, Vol. 6, Tenth Census, US Census Office, Government Printing Office, Washington, D.C., 649–796, 1884.

Holland, R. F.: The Geographic and Edaphic Distribution of Vernal Pools in the Great Central Valley, California, California Native Plant Society Special Publications No. 4, California Native Plant Society, Fair Oaks, CA, USA, 1978.

Holland, R. F.: Changes in Great Valley Vernal Pool Distribution from 1989 to 1997, available at: http://www.dfg.ca.gov/biogeodata/wetlands/pdfs/Holland_ChangesInGreatValleyVernalPoolDistribution.pdf last access: 9 April 2015, California Department of Fish and Game, Sacramento, CA, 1998.

Holland, R. F.: GIS shape files for Holland vernal pool map, email from Holland, R. to Sears, L., 4 December 2013.

Holland, R. F. and Hollander, A. D.: Hogwallow biogeography before gracias, in: Vernal Pool Landscapes, Studies from the Herbarium, Number 14, edited by: Schlising, R. A. and Alexander, D. G., California State University, Chico, 2007.

Holmes, L. C. and Eckmann, E. C.: Soil Survey of the Red Bluff Area, California, US Department of Agriculture, Bureau of Soils, Washington, D.C., 1912.

Holmes, L. C., Nelson, J. W., and Party: Reconnaissance Soil Survey of the Sacramento Valley, California, US Department of Agriculture, Bureau of Soils, Washington, D.C., 1915.

Holmes, T. H. and Rice, K. J.: Patterns of growth and soil-water utilization in some exotic annuals and native perennial bunchgrasses of California, Ann. Bot., 78, 233–243, 1996.

Holstein, G.: Pre-agricultural grassland in Central California, Madroño, 4, 253–264, 2001.

Howes, D. J. and Pasquet, M.: Grass reference based vegetation coefficients for estimating evapotranspiration for a variety of natural vegetation, US Committee on Irrigation and Drainage, Proc. of October 2013 Conference, 22–25 October, Denver, CO, 181–194, 2013.

Howes, D. J., Fox, J. P., and Hutton, P.: Evapotranspiration from Natural Vegetation in the Central Valley of California: Monthly Grass Reference-Based Vegetation Coefficients and the Dual Crop Coefficient Approach, J. Hydrol. Eng., 20, 04015004, doi:10.1061/(ASCE)HE.1943-5584.0001162, 2015.

Hundley Jr., N.: The Great Thirst, University of California Press, Berkeley, 2001.

Ingram, B. L., Conrad, M. E., and Ingle, J. C.: Stable isotope record of late Holocene salinity and river discharge in San Francisco Bay, California, Earth Planet. Sc. Lett., 141, 237–247, 1996.

Jassby, A. D., Kimmerer, W. J., Monismith, S. G., Armor, C., Cloern, J. E., Powell, T. M., Schubel, J. R., and Vendlinski, T. J.: Isohaline position as a habitat indicator for estuary populations, Ecol. Appl., 1, 272–289, 1995.

Kadir, K. and Huang, G.: Simulated 1922–2009 daily inflows to the Sacramento–San Joaquin Delta under predevelopment conditions using precipitation-runoff models and C2VSIM: preliminary results, Presented at the California Water and Environmental Modeling Forum Annual Meeting, 24–26 February, Folsom, CA, p. 38, available at: http://www.cwemf.org/AnnualMeeting/2014Abstracts.pdf (last access: 7 April 2015), 2014.

Kahrl, W. L.: The California Water Atlas, State of California, Prepared by the Governor's Office of Planning and Research in Cooperation with the CA DWR, Sacramento, CA, USA, 1979.

Katibah, E. F.: A brief history of riparian forests in the Central Valley of California, in: California Riparian Forests, edited by: Warner, R. E. and Hendrix, K. M., University of California Press, Berkeley, 23–29, 1984.

Kelley, R. L.: Gold vs. grain: The hydraulic mining controversy in California's Sacramento Valley: a chapter in the decline of the concept of laissez faire, Arthur H. Clark Company, Glendale, CA, USA, 327 pp., 1959.

Kelley, R. L.: Battling the Inland Sea: Flood, Public Policy and the Sacramento Valley, University of California Press, Berkeley, CA, 1989.

Kooser, B. P., Seabough, S., and Sargent, F. L.: Notes of trips of the San Joaquin Valley Agricultural Society's visiting committee on orchards and vineyards, Reports of Committees, Committees Nos. 1 and 2 on Farms and Orchards, Trans. S. J. V. Agr. Soc., Sacramento, 258–298, 1861.

Küchler, A. W.: Natural vegetation of California, pocket map, in: Terrestrial Vegetation of California, edited by: Barbour, M. G. and Major, J., John Wiley & Sons, Inc., New York, NY, USA, 909–938, 1977.

Lapham, M. H. and Holmes, L. C.: Soil Survey of the Redding Area, California, US Department of Agriculture, Bureau of Soils, Washington, D.C., 1908.

Lapham, M. H., Root, A. S., and Mackie, W. W.: Soil Survey of the Sacramento Area, California, US Department of Agricultural Field Operations Bureau of Soils, United States Government Printing Office, Washington, D.C., USA, 1904.

Lapham, M. H., Sweet, A. T., Strahorn, A. T., and Holmes, L. C.: Soil Survey of the Colusa Area, California, US Department of Agriculture, Bureau of Soils, US Department of Agricultural Field Operations Bureau of Soils, United States Government Printing Office, Washington, D.C., USA, 1909.

Lund, J., Hanak, E., Fleenor, W., Howitt, R., Mount, J., and Moyle, P.: Envisioning Futures for the Sacramento–San Joaquin Delta, Public Policy Institute of California, San Francisco, CA, 2007.

Luoma, S. N. and Nichols, F. H.: Challenges in detecting contaminant effects on an estuarine ecosystem affected by many different disturbances: San Francisco Bay, Water–Resources Investigations Report 94-4015, US Geological Survey Toxic Substances Hydrology Program, Proc. Tech. Mtng., 20–24 September 1993, Colorado Springs, Colorado, 1993.

MacNally, R., Thomson, J. R., Kimmerer, W. J., Feyrer, F., Newman, K. B., Sih, A., Bennett, W. A., Brown, L., Fleishman, E., Culberson, S. D., and Castillo, G.: Analysis of pelagic species decline in the upper San Francisco Estuary using multivariate autoregressive modeling (MAR), Ecol. Appl., 20, 1417–1430, 2010.

Malamud-Roam, F. P., Ingram, B. L., Hughes, M., and Florsheim, J. L.: Holocen paleoclimate records from a large California estu-

arine system and its watershed region: linking watershed climate and bay conditions, Quarternary Sci. Rev., 13–14, 1570–1598, 2006.

Mann, C. W., Warner, J. F., Westover, H. L., and Ferguson, J. E.: Soil Survey of the Woodland Area, California, US Department of Agriculture, Bureau of Soils, Washington, D.C., 1911.

Meko, D. M., Therrell, M. D., Baisan, C. H., and Hughes, M. K.: Sacramento River flow reconstructed to A.D. 869 from tree rings, J. Am. Water Res. As., 4, 1029–1038, 2001.

Miller, W. J., Bryan, F. J., Manly, D., Murphy, D., Fullerton, D., and Ramey, R. R.: An investigation of factors affecting the decline of Delta Smelt (Hypomesus transpacificus) in the Sacramento–San Joaquin Estuary, Rev. Fish. Sci., 1, 1–19, 2012.

Nelson, J. W., Guernsey, J. E., Holmes, L. C., and Eckmann, E. C.: Reconnaissance Soil Survey of the Lower San Joaquin Valley, California, US Department of Agriculture, Bureau of Soils, Washington, D.C., 1918.

Olmstead, A. L. and Rhode, P. W.: The evolution of California agriculture 1850–2000, in: California Agriculture: Dimensions and Issues, edited by: Siebert, J. B., University of California Press, available at: http://giannini.ucop.edu/CalAgBook/Chap1.pdf (last access: 8 April 2015), 2004.

PRISM Climate Group: Descriptions of PRISM Spatial Climate Datasets for the Conterminous United States, available at: http://www.prism.oregonstate.edu/documents/PRISM_datasetsaug2013.pdf (last access: 9 April 2015), 2013.

Roberts, W. G., Howe, J. G., and Major, J.: A survey of riparian forest flora and fauna in California, in: Riparian Forests in California: their Ecology and Conservation, Publication No. 15, edited by: Sands, A., A Symposium Sponsored by Institute of Ecology, University of California, Davis and Davis Audubon Society Institute of Ecology, Davis, 14 May 1977.

Sanford, W. E. and Selnick, D. L.: Estimation of evapotranspiration across the conterminous United States using a regression with climate and land cover data, J. Am. Water Resour. Assoc., 49, 217–230, 2014.

Schiffman, P. M.: Species composition at the time of first European settlement, in: California Grasslands: Ecology and Management, edited by: Stromberg, M. R., Corbin, J. D., and D'Antonio, C. M., University of California Press, Berkeley, 52–56, 2007.

SFWMD – South Florida Water Management District: Natural System Regional Simulation Model (NSRSM) Fact Sheet, available at: http://sfwmd.gov, last access: 5 February 2015, West Palm Beach, Florida, USA, 2014.

Shelton, M. L.: Irrigation induced change in fegetation and evapotranspiration in the Central Valley of California, Landscape Ecol., 2, 95–105, 1987.

Smith, D. W. and Verrill, W. L.: Vernal pool-soil–landform relationships in the Central Valley, California, in: Ecology, Conservation, and Management of Vernal Pool Ecosystems, edited by: Witham, C. W., Bauder, E. T., Belk, D., Ferren Jr., W. R., and Ornduff, R., Proc. from a 1996 Conference, California Native Plant Society, 19–21 June, Sacramento, CA, 15–23, 1998.

Strahorn, A. T., Mackie, W. W., Westover, H. L., Holmes, L. C., and Van Duyne, C.: Soil survey of Marysville Area, California, US Department of Agriculture, Bureau of Soils, Washington, D.C., 1911.

Sweet, A. T., Warner, J. F., and Holmes, L. C.: Soil Survey of the Modesto–Turlock Area, California, With a Brief Report on a Reconnaissance Soil Survey of the Region East of the Area, US Dept. of Agriculture, Bureau of Soils, Washington, D.C., 1909.

TBI – The Bay Institute: From the Sierra to the Sea: The Ecological History of the San Francisco Bay-Delta Watershed, The Bay Institute of San Francisco, Novato, CA, USA, 1998.

Thompson, K.: The settlement geography of the Sacramento–San Joaquin Delta, California, PhD Dissertation, Stanford University, 1957.

Thompson, K.: Riparian forests of the Sacramento Valley, California, Ann. Assoc. Am. Geogr., 3, 294–315, 1961.

Thompson, K.: Riparian forests of the Sacramento Valley, California, in: Riparian Forests in California: Their Ecology and Conservation, No. 15, edited by: Sands, A., A Symposium Sponsored by Institute of Ecology, University of California, Davis and Davis Audubon Society, Institute of Ecology Publication, Davis, 1977.

Thomson, J. R., Kimmerer, W. J., Brown, L., Newman, K. B., MacNally, R., Bennett, W. A., Feyrer, F., and Fleishman, E.: Bayesian change-point analysis of abundance trends for pelagic fishes in the upper San Francisco Estuary, Ecol. Appl. 20, 1431–1448, 2010.

Thorne, J. H., Morgan, B. J., and Kennedy, J. A.: Vegetation change over sixty years in the Central Sierra Nevada, California, USA, Madroño, 3, 223–237, 2008.

Vaghti, M. G. and Greco, S. E.: Riparian vegetation of the Great Valley, in: Terrestrial Vegetation of California, 3rd Edn., edited by: Barbour, M. G., Keeler-Wolf, T., and Schoenherr, A. A., University of California Press, Berkeley, 425–455, 2007.

Warner, R. E. and Hendrix, K. M.: Riparian Resources of the Central Valley and California Desert, Final Draft, Department of Fish & Game, Sacramento, 1985.

Watson, E. B., Glassey, T. W., Storie, R. E., and Cosby, S. W.: Soil survey of the Chico area, California, Series 1925, Number 4, US Department of Agriculture, Bureau of Chemistry and Soils, Washington, D.C., 1929.

Whipple, A. A., Grossinger, R. M., Rankin, D., Stanford, B., and Askevold, R. A.: Sacramento–San Joaquin Delta Historical Ecology Investigation: Exploring Pattern and Process, Publication 672, San Francisco Estuary Institute (SFEI) – Aquatic Science Center, Richmond, CA, 2012.

Williamson, A. K., Prudic, D. E., and Swain, L. A.: Ground-water flow in the Central Valley, California, US Geological Survey Professional Paper 1401-D, United States Government Printing Office, Washington, D.C., USA, 1989.

Williamson, R. S.: Report of exploration in California for railroad routes to connect with the routes near the 35th and 32d parallels of north latitude, in: Reports of Explorations and Surveys, to Ascertain the Most Practicable and Economical Route for a Railroad from the Mississippi River to the Pacific Ocean, United States War Dept., United States Army, Washington, 1853.

Zedler, P. H.: Vernal pools and the concept of "IsolatedWetlands", Wetlands, 3, 597–607, 2003.

SAN JOAQUIN RIVER SPAWNING HABITAT SUITABILITY STUDY

Elaina Gordon, Hydraulic Engineer, US Bureau of Reclamation, Denver, CO,
egordon@usbr.gov, (303)445-2550
Blair Greimann, Hydraulic Engineer, US Bureau of Reclamation, Denver, CO,
bgreimann@usbr.gov, (303)445-2563

Abstract: The availability of quality spawning habitat within the San Joaquin River downstream of Friant Dam (Reach 1A) is crucial for successful reintroduction and sustained population of Chinook salmon. Several uncertainties exist as to the suitability of existing spawning habitat within Reach 1A and how sediment transport may affect efforts aimed at improving spawning and incubation habitat. Multiple studies are currently underway or have been completed to help identify the quality of the hyporheic environment as it relates to successful spawning and fry emergence, including evaluations of water quality within the hyporheic zone (DO, water temperature, fine sediment accumulation), egg survival, mesohabitat, bed material size and mobility, scour and deposition, and channel morphology changes associated with alteration to the flow regime. In addition, bedload and suspended load monitoring have been conducted within the reach since 2010.

Critical to identification of potential spawning areas are the bed material and hydraulic conditions within the reach during probable spawning periods of spring-run and fall-run Chinook salmon. This current study combines bed material characterization efforts with two-dimensional hydraulic modeling results to identify areas considered potentially suitable spawning habitat based upon depth and velocity requirements. The suitability of the potential spawning habitat is evaluated with GIS parameterization of substrate and hydraulic conditions, and correlation of surveyed redds, substrate, and hydraulic conditions are examined and quantified.

INTRODUCTION

The San Joaquin River Restoration Program (SJRRP) aims to "restore and maintain fish populations in good condition in the main stem of the San Joaquin River below Friant Dam to the confluence of the Merced River, including naturally-reproducing and self-sustaining populations of salmon and other fish." The SJRRP Fisheries Management Plan identifies spawning and incubation as a life stage to be supported for successful completion of the salmon life cycle.

SJRRP's current understanding of the system is that sufficient availability and quality of spawning habitat within Reach 1A of the San Joaquin River is imperative to sustaining a population of Chinook salmon (*Oncorhynchus tshawytscha*). Multiple studies are currently underway or have been completed to help identify the quality of the surface water and hyporheic environments as they relate to successful spawning and fry emergence (current efforts summarized in Section 3.2 of 2014 Monitoring and Analysis Plan; SJRRP, 2013a). These include efforts to evaluate water quality within the hyporheic zone (DO [Reclamation, 2012a], water temperature effects [Reclamation, 2012a], fine sediment accumulation [SJRRP, 2010a; SJRRP, 2013b]), egg survival (SJRRP, 2012), mesohabitat characterization (SJRRP, 2010b), spawning habitat use by transported fall-run Chinook (SJRRP, 2011; SJRRP, 2013c), bed material size and mobility (Tetra Tech, 2012a,b; SJRRP, 2012; SJRRP, 2013d), scour and deposition (SJRRP, 2011), and channel morphology changes associated with alteration to the flow regime (SJRRP, 2011; SJRRP, 2012; SJRRP, 2013e). In addition, bedload and suspended load monitoring have been conducted within the reach since 2010 (Graham, Mathews & Associates, 2012; Reclamation, 2014a). Most recently, spatial characterization of hydraulic conditions within Reach 1A was completed through two-dimensional hydraulic modeling across a wide range of flows (Reclamation, 2014b), and continuous facies mapping of the bed material was completed within the low-flow channel (SJRRP, 2014b).

The purpose of this current study is to initially characterize potential spawning locations within Reach1A of the San Joaquin River from Friant Dam to Highway 99 (HW99) based upon suitable hydraulics, bed material, and surface water temperature (figure 1). These potential areas will then analyzed for patterns of correlation and compared with mapped spawning redds within the reach over the past 2 years. This effort is part of a larger study to characterize suitability of spawning and incubation habitat based on physical, biological, and chemical criteria.

POTENTIAL SPAWNING HABITAT QUANTITY

Requirements for spawning Chinook salmon evaluated in this initial assessment of potential spawning habitat area include hydraulic conditions, substrate, and surface water temperature. Multiple other aspects of spawning habitat quality may impact where a fish chooses to spawn and are only briefly discussed within this paper. However, we recognize the importance of many additional variables influencing spawning habitat quality and ultimately on the incubation habitat provided for successful emergence. These are anticipated to be incorporated into future analyses.

With respect to hydraulic conditions for spawning Chinook, water depth must be sufficient to cover the fish during spawning, and velocity must be adequate to flush finer particles downstream during the process of red construction, but not so great that eggs do not remain in the egg pocket or adults have to expend too much energy holding position in the water column (SJRRP, 2014a). The SJJRP Spawning and Incubation Subgroup reviewed habitat suitability indices (HSI) from studies on the Tuolumne, Stanislaus (Aceituno, 1990, 1993), and Merced (Gard, 1997) Rivers (all tributaries to the San Joaquin River) and suggested the criteria for suitable spawning depths for the San Joaquin River to be between 0.7 and 3.7 feet (ft) and velocities between 0.8 and 3.4 ft/s. These values correspond to the criteria from the Stanislaus River and encompass the ranges for all three rivers, thereby providing the greatest flexibility for evaluation on the San Joaquin River.

Chinook salmon generally select larger substrate to spawn in than other Pacific salmon species. Suitable spawning gravel consists of a mixture of particle sizes from sands to cobbles, with a median diameter (D50) of 2.5 to 5 cm (SJRRP, 2010c). A review of reported spawning substrate in Central Valley System suggests that the preferred substrate size ranges between 2.5 and 10 cm in diameter, and some studies indicate spawning in substrate up to 30 cm in diameter (SJRRP, 2010c). Substrate requirements for spawning are highly correlated to fish size with large fish capable of using larger substrate materials than small fish (SJRRP, 2014a) to build a redd. Moir and Pasternack (2010) found that Chinook often utilize coarser substrate when higher velocities are present. Fine sediment within the system has a large influence on the incubation habitat once the eggs are laid (Tappel and Bjornn, 1983). However, the presence and influence of fine sediment on egg survival is a topic currently under investigation, the results of which will be incorporated into future designation of suitable incubation habitat.

Chinook salmon have specific water temperature requirements before and during spawning in order to survive and deposit their eggs (SJRRP, 2014a). Surface water temperatures for successful spawning and incubation are illustrated in table 1. The critical temperature range defines the range over which a fish shows definite signs of thermal stress (Elliot, 1981).

Table 1 Temperature Requirements for Spawning and Incubation (from SJRRP, 2010).

	Spawning	**Incubation and Emergence**
Optimal	≤ 57 °F (13.9 °C)	≤ 55 °F (13 °C)
Critical	60-62.9 °F (15.6-17°C)	58-60 °F (14.4-15.6°C)
Lethal	≥62.6 °F (17 °C)	≥62.6 °F (17 °C)

Two-dimensional Hydraulic Modeling: Two-dimensional hydraulic models of Reach 1A of the San Joaquin River were developed and calibrated using SRH-2D (Reclamation, 2008) to spatially characterize hydraulic conditions throughout the reach as a tool for predicting the availability of spawning habitat (Reclamation, 2014b). For computational efficiency, the reach was modeled in two sections: the first is from Friant Dam (Mile Post (MP) 267) downstream to Highway 41 (HW41) Bridge (MP 255) and is referred to as Reach1A_01, and the second extends from HW41 downstream to Highway 99 (HW99) Bridge (MP 243) and is referred to as Reach1A_02.

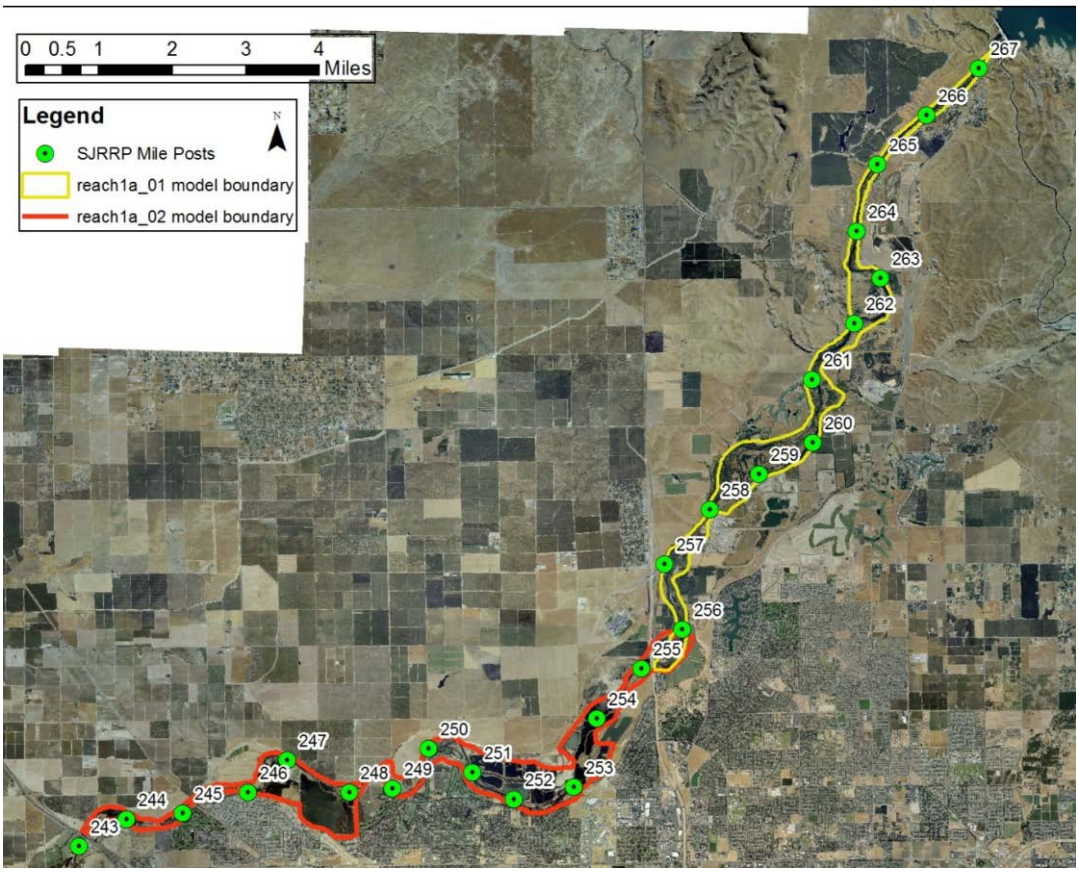

Figure 1 Map of modeled reaches. Reach 1A_01 extends from Friant Dam (MP 267.5 to HW41 (MP 255) and Reach 1A_02 extends from HW41 (MP 255) to HW99 (MP 243) for a total reach length of 24.5 river miles.

The mesh for each subreach generally consisted of rectangular cells to represent the main channel and most side channels and triangular cells to represent the floodplain. Within the channel, rectangular cell sizes ranged between 5-10 ft laterally and 20-30 ft longitudinally. The final grids were comprised of approximately 117,000 cells within the Reach 1A_01 model and 138,000 cells within the Reach 1A_02 model. Terrain data for Reach 1A are a compilation of ground-based survey points and photogrammetry collected in 1998, combined with in-channel bathymetry collected by boat using SONAR in 2009. The final topographic models for each subreach were created in State Plane CA III, NAVD88 ft. Flows modeled to date were based upon the availability of calibration data and range from 270 cfs to 7,650 cfs. Rating curves developed from measured flows and water surface elevations at HW 41 and HW 99 served as the downstream boundary conditions for each model.

Hydraulic roughness (Manning's *n*) is defined at each cell in a computational mesh. Initial roughness values were delineated based on zones of vegetation density and land use from 2007 aerial photographs (MEI, 2000; DWR, 2010). Roughness zones were modified in some areas to better reflect current conditions based upon 2011 aerial photos and to improve calibration with initial model results. Final computational meshes for model Reach 1A_01 and Reach 1A_02 consist of 8 roughness categories (table 2).

Model calibration was conducted for both subreaches using available water surface elevation and flow measurements. In-channel calibration was performed first to define roughness within the channel, and then a subsequent calibration effort was conducted to define roughness within the floodplain. Calibration was performed by varying roughness in model simulations to determine the best match to measured water surface elevations (table 2). The goal of the model calibration was to predict water surface elevations with a root mean squared error (RMSE) of less than 0.5 ft.

Table 2 Calibrated roughness values for SRH-2D hydraulic simulations.

Land Use Type	Reach1A_01	Reach1A_02
Channel Bed	0.04	0.04
Off-Channel Open Water	0.04	0.045
In-channel Riffles/Rough areas	0.065	0.065
Open /Bare Ground/ Scattered Brush	0.045	0.068
Scattered Trees	0.06	0.09
Medium Density Trees/Brush	0.08	0.12
Dense Trees/ Brush	0.1	0.15
Agriculture	0.045	0.055

Depth and velocity data were processed for 350 cfs in each reach to determine areas meeting spawning habitat hydraulic criteria. This discharge was selected as representative of the flow present during Spring-run and Fall-run Chinook spawning based upon the flow release schedule from Friant Dam into Reach 1A as specified in the Stipulation of Settlement (NRDC v. Rodgers, 2006). The spawning habitat hydraulic criteria were provided by the San Joaquin River Spawning and Incubation Subgroup and represent the depth and velocity ranges considered suitable on the Stanislaus River. Areas meeting the criteria for depths ranging between 0.7 and 3.7 feet and velocities ranging between 0.8 and 3.4 ft/s were delineated as polygons within GIS and determined as potentially suitable for spawning based on hydraulic conditions.

Bed Material Characterization: Bed material sampling has been conducted throughout Reach 1A of the San Joaquin River numerous times over the last 20 years using multiple sampling techniques to meet a variety of project goals. To most efficiently evaluate bed material for spawning habitat, a spatially continuous map of bed material was necessary. Facies maps provide an opportunity to capture spatial variability of the sediment comprising a channel bed through delineation of boundaries between notably different areas of bed material. Facies mapping was initially completed within Reach 1A in 2002, but only encompassed the first 12.3 miles downstream from Friant Dam (Stillwater Sciences, 2003), and several locations may have experienced local areas of change within the last 10 years. As such, during the summer of 2013, an effort was undertaken to update and expand upon the initial facies mapping to reflect current conditions of the river bed and to help characterize areas with suitable bed material for Chinook spawning.

In both the 2002 and 2013 mapping efforts, the Buffington and Montgomery (1999) mapping technique was adapted with slight variations between the two years. This is a hierarchical classification system of each facies according to the three most prevalent gain classes (i.e. silt, sand, gravel, cobble, and boulder) and sub-divided according to a classification based on phi-size class (very fine, fine, medium, coarse, very coarse). For example, 'sandy gravel' indicates that the most prevalent grain class is gravel but there are significant amounts of sand. Facies mapping was conducted by floating the river by kayak, delineating areas of bed material change, and visually identifying the facies classification. Simultaneously, pebble counts were performed in areas where no previous volumetric or pebble count samples had been collected. The maps and all sediment data were transferred to GIS.

An analysis was completed to associate a range of gradations with each facies category based upon pebble count data collected over the last 20 years. However, the results indicated that the pebble count data alone were not sufficient to differentiate between the coarse-scale facies categories. In addition, the pebble count data alone were incapable of differentiating between spawnable and non-spawnable facies categories because the resulting range of gradations for each facies where pebble counts were performed covered the preferred range of diameters for spawning. In other words, the results suggested that every facies category with one or multiple pebble counts contained suitable substrate for spawning. Another complication was that many facies categories, such as those over bedrock or in silt, contained no pebble count data.

Surface Water Temperature: The SJRRP has determined that water temperature is likely a limiting factor for each life history stage of Chinook salmon in the San Joaquin River, particularly in the warmest and driest years

(CDFW, 2012). As part of the SJRRP, a water temperature monitoring system was developed to better understand the longitudinal distribution of water temperature and aid in successful management of flow releases during critical salmon life-stages. With respect to salmon spawning, surface water temperature is a key factor influencing adult salmon behavior and survival during late summer and fall (August through December). Twenty water temperature monitoring locations are present within Reach 1 to help identify the spatial distribution of the potential spawning areas based upon known temperature limitations for Chinook salmon. Data collected at these sites within the last several years suggest that in general, the closer the site is to Friant Dam, the more suitable the water temperatures are during the critical spawning period. In 2011 it was observed that the closer the site was to the dam, the greater the number of days temperatures were below critical (14.4 ℃) and lethal (15.6 ℃) temperature thresholds for spawning and incubation; however, due to releases from the dam (>13℃) being greater than the optimal temperature (13℃) and cooler air temperature in late fall, more days met optimal temperature conditions further downstream than just below the dam (figure 2).

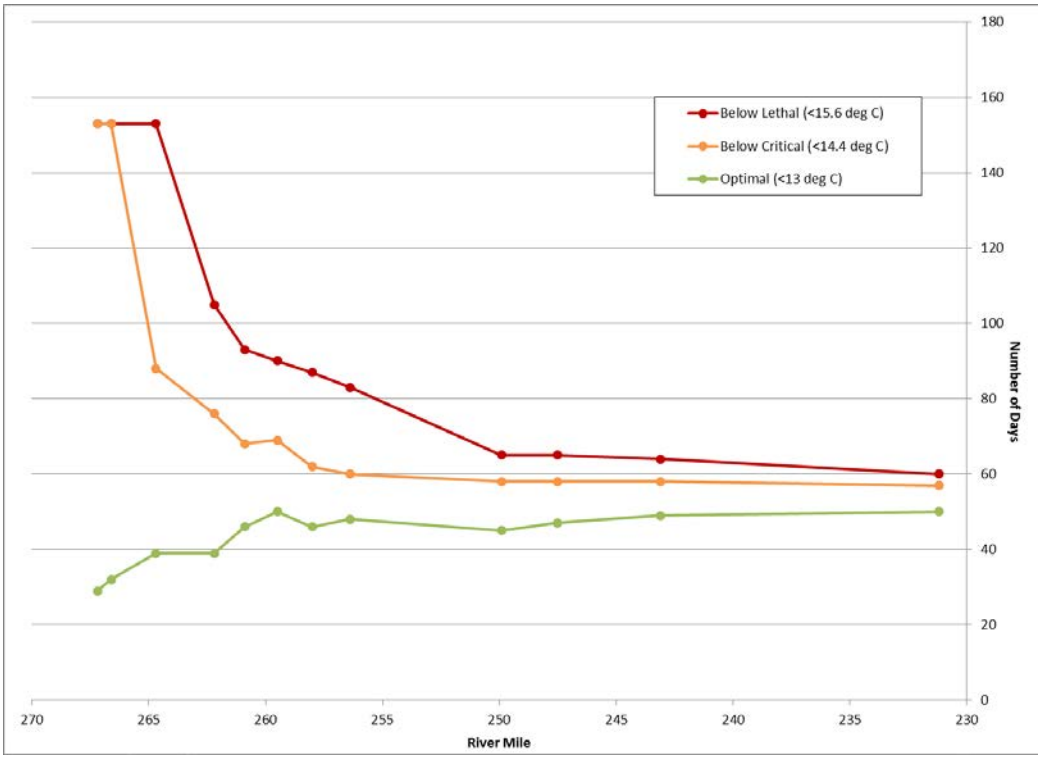

Figure 2 Number of days during expected spawning and incubation period (August through December, 2011) that water temperature was below objectives for incubation and emergence (SJRRP, 2010c).

Spring-run Chinook historically spawned in the San Joaquin River between late August and October, and Fall-run Chinook still spawn within tributaries to the San Joaquin River from October through December, peaking in early to mid-November. Based on this timing, water temperature monitoring indicates that Fall-run Chinook may not be limited by surface water temperatures during spawning within Reach 1A (figure 3). However, Spring-run spawning may be restricted to the first 10 miles downstream from Friant Dam.

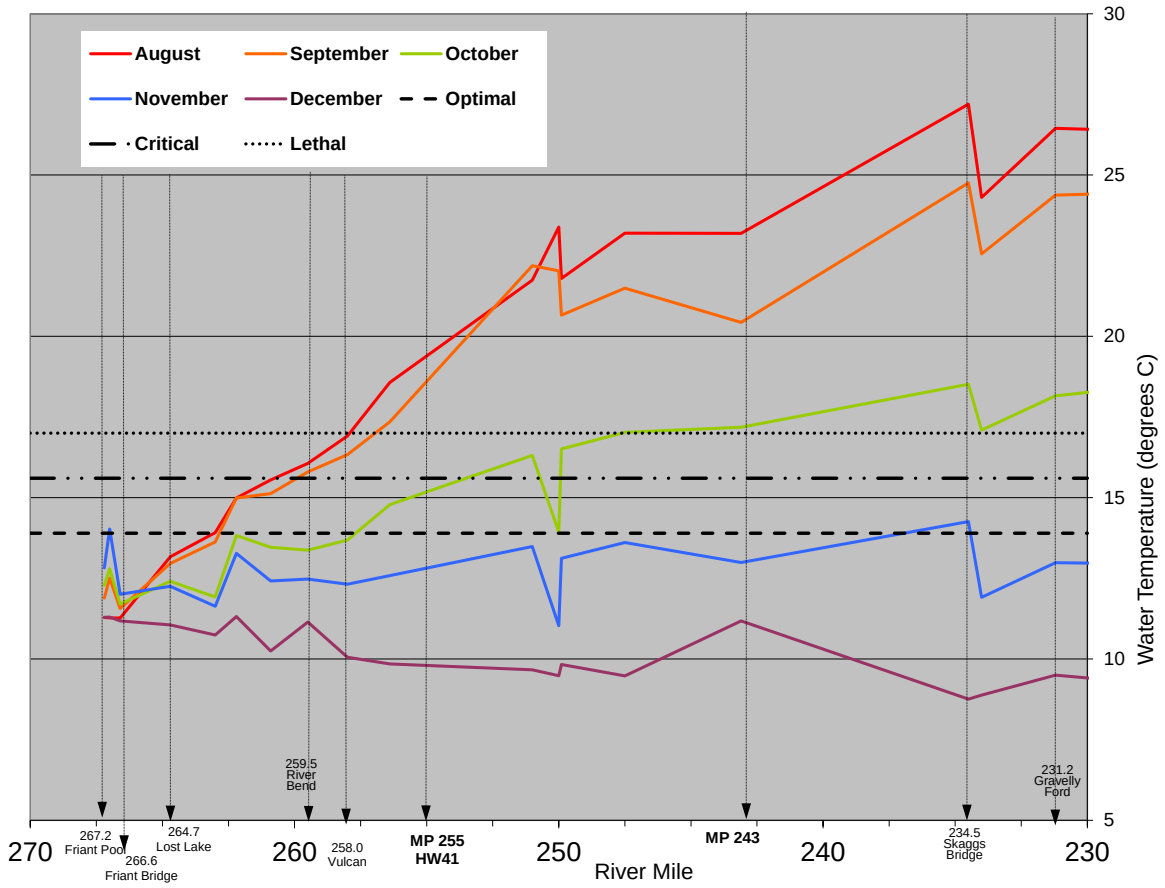

Figure 3 Monthly average stream temperatures for the period of record along with the optimal, critical, and lethal temperature ranges for spawning. The period of record differs slightly for each gage and therefore some points may represent longer time frames than others.

RESULTS OF ANALYSIS

The total modeled area encompassed over 12,000 acres (ac) (table 3). At a discharge of 350 cfs, 1,090 ac of the channel were inundated with depths greater than 0.1 feet. However, only 80 ac were determined to be potentially suitable for spawning based upon hydraulic conditions (0.7 to 3.7 ft depth and 0.8 and 3.4 ft/s velocities), indicating that only 7.4% of the total inundated area was determined to be suitable for spawning based upon hydraulic conditions alone. Inundated areas and areas of suitable hydraulic conditions were also compared with facies mapping to determine the existence of correlations between hydraulics and substrate. An example illustration of the delineation of mapped features is shown in figure 4. Inundated areas with facies designations were evaluated by dominant substrate type (figure 5). The majority of inundated area (excluding gravel pits, side channels, overbank areas, and channel margins) was comprised of sand (59%), while gravel and cobble represented a combined 36% of inundated area. The area deemed suitable based upon hydraulic conditions within each dominant substrate type is depicted in figure 6. Hydraulically suitable conditions were most common in gravel and cobble-dominated substrate, representing a total of 78% of the area (58.3 acres) identified as suitable. Twenty percent of the area with suitable hydraulic conditions was within substrate dominated by sand based upon the facies mapping.

Table 3 Modeled and inundated areas based on two-dimensional modeling results compared with the area meeting the depth and velocity criteria for spawning for each reach and also combined. Results presented are in acres.

	Area (Acres)		
	Reach1A_01	**Reach 1A_02**	**Total Combined**
Modeled Area	5,375	6,627	12,002
Inundated Area	293	797	1,090
Area Meeting Depth and Velocity Criteria for Spawning	44	36	80

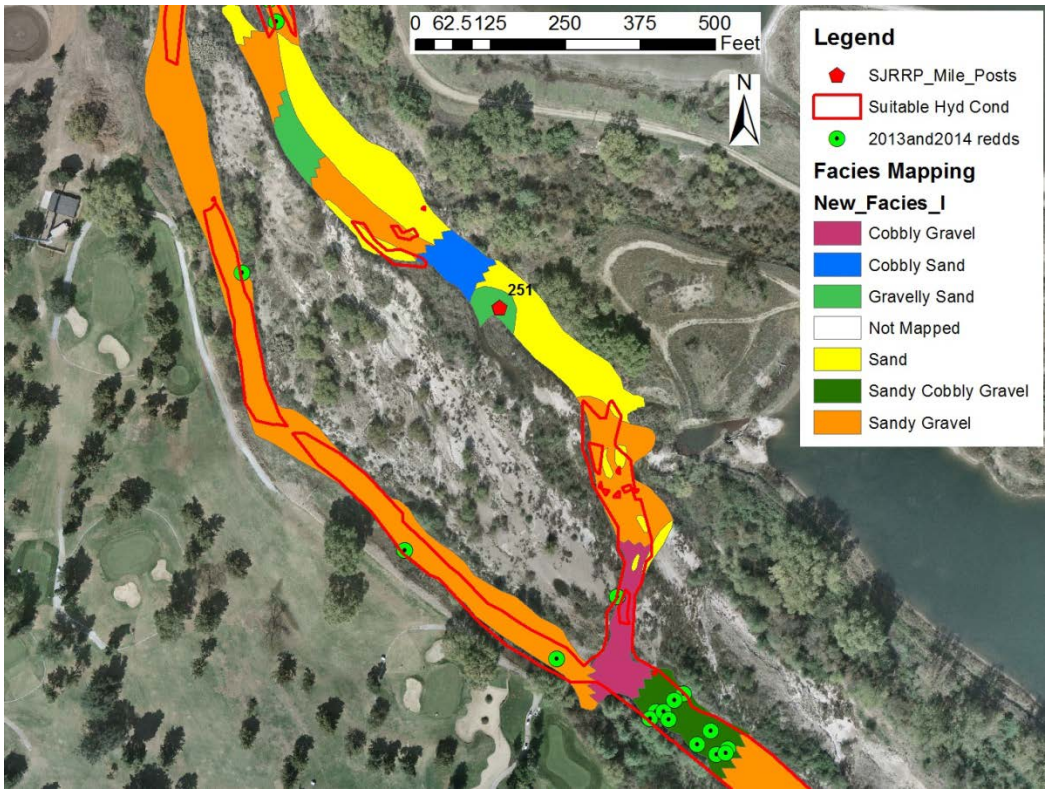

Figure 4 Example map of the delineation of redd locations, suitable hydraulic condition polygons, and facies categories near MP 251.

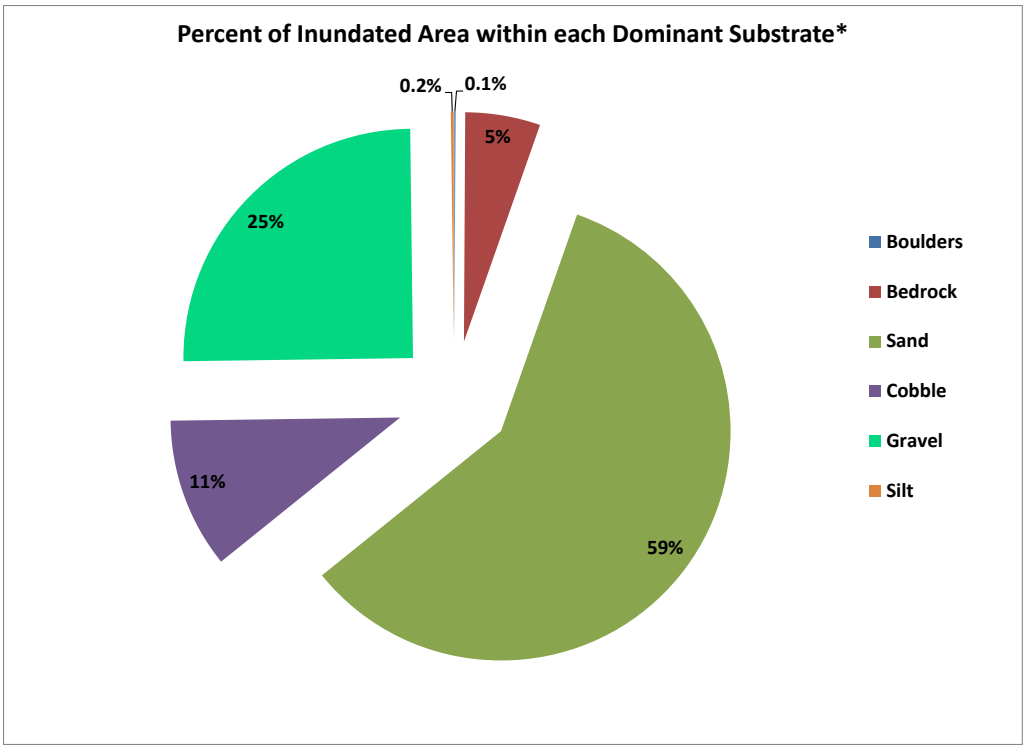

Figure 5 Percent of inundated area within each dominant substrate. *This analysis excludes inundated areas that did not have facies characterization, such as gravel pits, side channels, and channel margins.

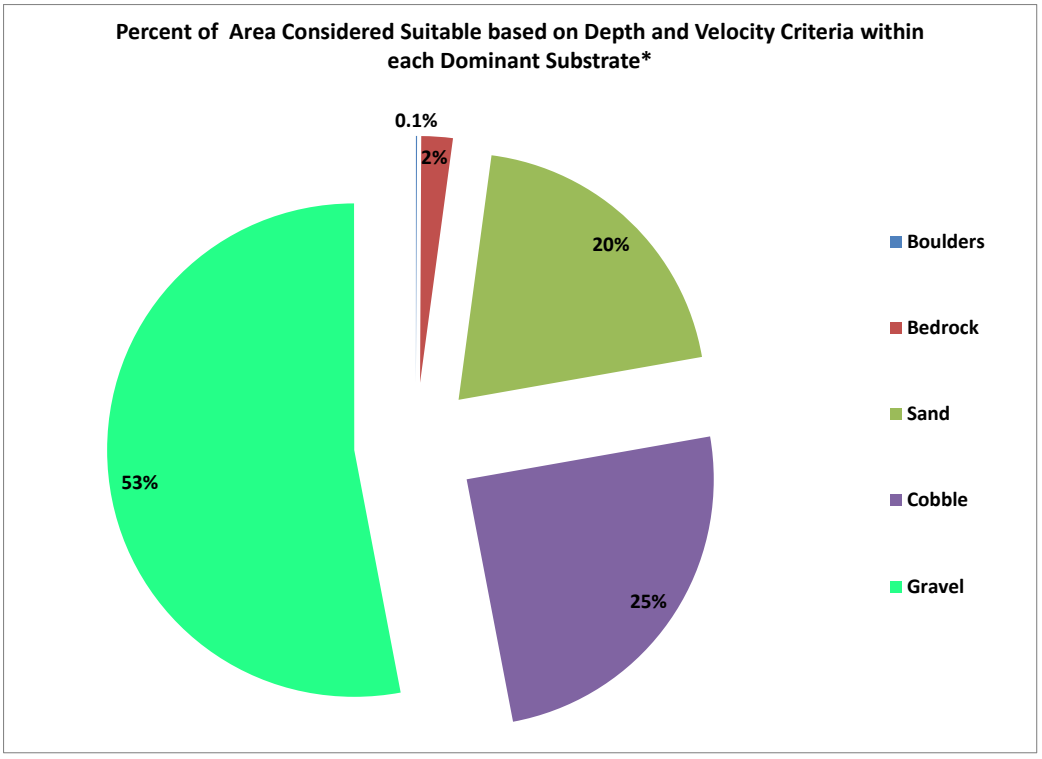

Figure 6 Percent of area with suitable hydraulic conditions within each dominant substrate type. *This analysis excludes suitable areas that did not overlap with facies characterizations, such as those in side channels and along channel margins.

There were 130 redds surveyed within the reach between Friant Dam and HW99 (figure 1) during 2013 and 2014 combined. There were an additional 22 redds surveyed just at or downstream from HW99 that were not included in the analysis because they were not located within the longitudinal extent of the mapped facies and two-dimensional modeling boundary. An analysis was done to identify which type of substrate the fish selected to spawn in based upon the facies mapping. The distribution of spawning within dominant substrate is shown in figure 7. Ten of the 130 redds were located outside of the mapped facies areas in areas identified as islands or channel margins above the low flow channel. Of the remaining 120 redds, the salmon overwhelmingly selected to spawn in facies with a gravel- (84 redds, 70%) or cobble-dominated (23 redds, 19%) substrate. However, several still chose to spawn in facies mapped as being dominated by sand or bedrock. This could be due to the presence of patches of gravel and cobble within larger generalized areas of mapped substrate.

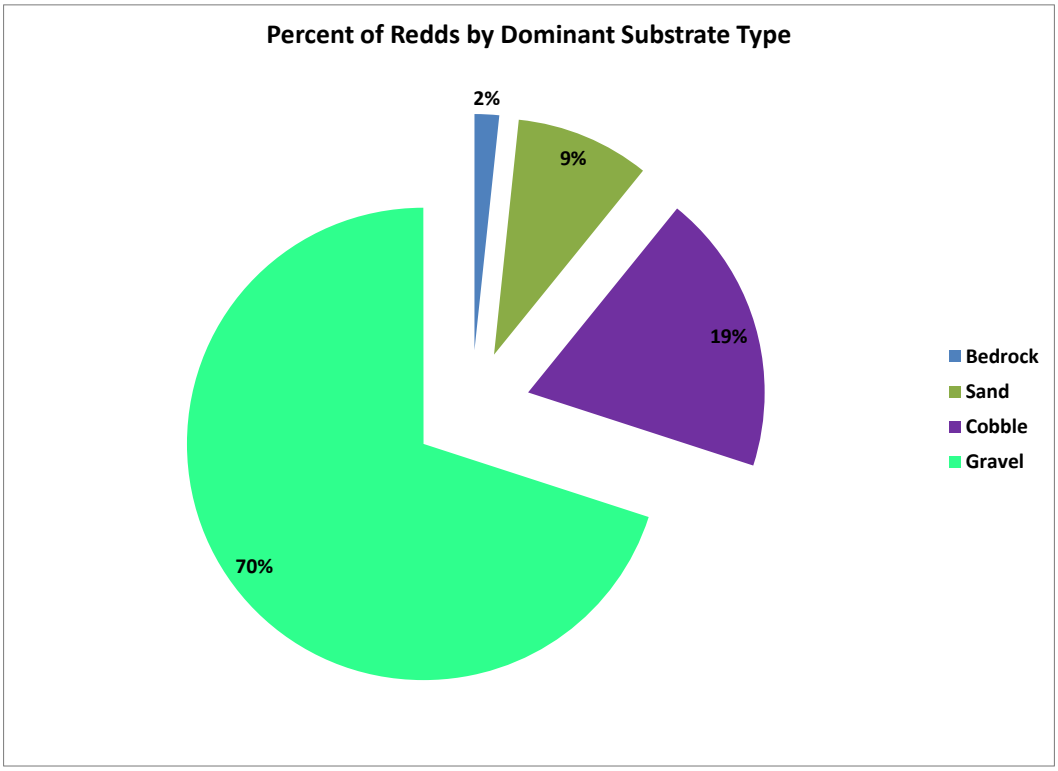

Figure 7 Percent of the occurrence of redds by dominant substrate type out of 120 redds.

Of the 130 redds within the reach, 96 of them (74%) were located within an area with suitable hydraulic conditions based upon two-dimensional modeling results; 123 (95%) were located within 15 feet of an area with suitable hydraulic conditions. It should be recalled that the numerical model grid within the channel was typically comprised of quadrilaterals ranging in size between 5-10 ft by 20-30 ft.

An investigation was completed to determine the association between those 96 redds within suitable hydraulic conditions and the dominant substrate type. Three of the redds were not located in a mapped facies as they were all constructed at the very edge of the low flow channel boundary. The results show little variation from the results of all 130 redds illustrated in figure 7, which is expected because most all the redds were located within the area defined as hydraulically suitable. A final statistical evaluation was performed using Jacob's electivity analysis to determine the preference of salmon to place redds within each dominant substrate type and within hydraulically suitable areas. Jacob's index was measured using the following formula:

$$D = (r - p)/(r + p - 2rp)$$

Where r represents the proportion of habitat used; p represents the proportion of habitat available, and D varies from -1 to 1, indicating a degree of preference for each habitat type (Hamann et al., 2014). A value of -1 indicates strong avoidance; a value of +1 indicates strong preference, and values approaching 0 suggest that the habitat is used in

proportion to its availability in the environment. The results and interpretation of the analysis are presented in table 4 and table 5.

Table 4 Results of electivity analysis indicating the degree of association of redds with hydraulic conditions.

	Jacob's Index	Interpretation
Hydraulically Suitable Area	0.9	Strong Preference
Non-hydraulically Suitable Area	-0.9	Strong Avoidance

Table 5 Results of electivity analysis indicating the degree of association of redds with dominant substrate type.

Dominant Substrate	Jacob's Index in total inundated area with mapped facies	Jacob's Index in hydraulically suitable area	Jacob's Index in non-hydraulically suitable area	Interpretation
Boulders	-1.0	-1.0	-1.0	Strong Avoidance
Bedrock	-0.5	-0.7	-0.2	Avoidance
Sand	-0.9	-0.9	-0.9	Strong Avoidance
Cobble	0.3	0.4	0.2	Mild Preference
Gravel	0.7	0.7	0.8	Preference
Silt	-1.0	-1.0	-1.0	Strong Avoidance
Cobble and Gravel	0.9	0.9	0.9	Strong Preference

CONCLUSIONS

Results of this effort provide supportive evidence for characterizing spawning habitat using hydraulic information gained from two-dimensional modeling and from substrate characterization. Based upon the hydraulic modeling effort, only 7.4% of the total inundated area was determined to be suitable for spawning. However, 74% of the redds surveyed within the last 2 years were located within these areas, and 95% were within 15 feet of these areas. These data suggest a strong correlation between the hydraulic conditions determined to be suitable for spawning using depth and velocity and between locations selected by salmon for redd construction. The results may also indicate that the current grid resolution captures the preferred spawning locations to within +/- 15 feet because the cell sizes within the channel were typically 5-10 ft wide by 20-30 ft long to limit model simulation time. A refined model at select locations may assist in further refining localized spawning preferences. However, the results also point towards the possible use of a buffer zone of approximately 15 feet around areas deemed suitable when a coarser-scale model is necessary to capture long reaches.

Redd data analyses reveal that salmon tend to spawn in gravel and cobble more frequently than other substrate. However, some fish selected to spawn in facies dominated by sand substrate. This may be partially attributed to the detail of the facies mapping. A benefit of the facies mapping is the ability to map long reaches of channel within a relatively short time frame. Patches of gravel and cobble are often present along channel margins or locally within the channel and may not be captured in the facies mapping. Refined mapping within mapped facies dominated by sands may improve the correlation between large substrate and redd construction location. Another possible explanation may be that salmon are less concerned with substrate than other factors when searching for a location to spawn, and the substrate is more important to defining incubation habitat and egg survival. Data from this effort could be used to develop preference curves for substrate for spawning salmon, in which sand and boulder substrate receive lower values than cobble and gravel substrates.

Examination of the dominant substrate within areas determined to be suitable for spawning based upon hydraulic conditions shows that even though gravel and cobble only represent a combined 36% of the total inundated area with mapped facies, 78% of the suitable hydraulic conditions are within gravel- and cobble- dominated substrate.

Similarly, the 96 redds within suitable hydraulic conditions were located in gravel- and cobble-dominated substrate 89% of the time. These data along with Jacob's electivity analysis results demonstrate a strong preference for redd sites to be located in suitable hydraulic conditions and in gravel- and cobble- dominated substrates. Clear correlations exists between substrate and suitable conditions for spawning, between redd sites and hydraulically suitable conditions, and between redd sites and gravel- and cobble-dominated substrate. From a common understanding of physical processes with the respect to the influence of hydraulic conditions on sediment transport and resultant substrate, the data from this exercise suggest that both hydraulic conditions and substrate are important in redd sites selection.

Finally, water temperature was also reviewed in this study to evaluate how it may limit the area considered suitable for spawning. Results suggest that water temperature may not limit spawning for Fall-run Chinook in most years because the temperatures, while not optimal, are below lethal in October, November, and December from Friant Dam downstream to HW 99 (~MP 243). However, the water temperatures may limit Spring-run Chinook spawning to the first 10 miles downstream from Friant Dam. These first 10 miles of the entire 24.5 mile reach encompasses 36.2 acres of suitable spawning habitat based upon depth and velocity, which represents 45% of the total suitable spawning area within Reach 1A.

STUDY DIRECTION

This current study presents a small fraction of the analysis necessary to eventually define the availability and quality of spawning and incubation habitat within Reach 1A. However, this step is important in determining that two-dimensional modeling results and substrate can indeed be used to help quantify available suitable spawning habitat. Additional analyses are planned to determine the applicability of mesohabitat maps in delineating potentially suitable spawning habitat. In addition to the reach-scale two-dimensional hydraulic modeling, finer-scale modeling of several riffles within Reach 1A is planned to identify the sensitivity of model results to refined topographic information and mesh resolution.

The quality of spawning and incubation habitat will be further distinguished through incorporation of findings from studies characterizing the hyporheic environment (DO, toxicity, temperature), vegetation and cover mapping, sediment mobility, substrate permeability, fine sediment accumulation within redds, egg survival, and escapement. One of the greatest challenges anticipated from this effort is the extrapolation of localized findings within one or several redds or riffle to the entire Reach 1A.

The ultimate goal of the larger-scale endeavor is the capability to predict the quantity and location of habitat meeting the needs of Chinook salmon to successfully complete their life cycle through spawning and incubation. Once the abundance or scarcity of suitable spawning and incubation habitat is determined based upon the anticipated fish use of the system, the limiting factors can be identified, and any means necessary to improve those conditions and the locations in need of improvement will be definable.

ACKNOWLEDGEMENTS

The authors of the paper express gratitude to all SJRRP members for their efforts in collecting and analyzing data related to spawning and incubation habitat that was used for this study. Erica Meyers was responsible for maintaining and evaluating the water temperature data as it relates to spawning and incubation, and Andy Shriver significantly contributed to the collection and GIS translation of the facies characterization. We are grateful to the SJRRP for continuing to support spawning habitat investigations, and appreciate the continued input by members of the Spawning and Incubation Subgroup.

REFERENCES

Aceituno, M. (1990). Habitat Preference Criteria for Fall-run Chinook Salmon Holding, Spawning, and Rearing in the Stanislaus River, California, U.S. Fish and Wildlife Service, Fish and Wildlife Enhancement, 27pp.

Aceituno, M. (1993). The Relationship between Instream Flow and Physical Habitat Availability for Chinook Salmon in The Stanislaus River, California, U.S. Fish and Wildlife Service, Sacramento, CA.

Buffington, J. M., and D. R. Montgomery (1999), A Procedure for classifying textural facies in gravel-bed rivers, Water Resour. Res., 35(6), 1903–1914

California Department of Fish and Wildlife (CDFW; 2012). San Joaquin River Restoration Program Stream Temperature Monitoring Study Water Year 2012 Annual Report.

California Department of Water Resources (DWR; 2010) DRAFT Two-dimensional hydraulic model of the San Joaquin River: Reach 1A, March 2010.

Elliott, J.M. (1981). Some aspects of thermal stress on freshwater teleosts. Chapter 10, in A.D. Pickering, ed. Fish and Stress. Freshwater Biological Association. Cumbria, England. Academic Press, London.

Gard, M. (1997). Technique for adjusting spawning depth habitat utilization curves for salmon, US Fish and Wildlife Service, Rivers 6(2):94-102.

Graham Matthews and Associates (2011). "San Joaquin near Ledger Island Water Year 2011 Bedload Sampling, Technical Memorandum dated June 13,2011. In Appendix D Sediment of 2011 Final Annual Technical Report San Joaquin River Restoration Program.

Hamann, E.J., Kennnedy, B.P., Whited, D.C, and J.A. Stanford (2014). Spatial variability in spawning habitat selection by Chinook salmon (*Oncorhynchus Tshawytscha*) in a wilderness river. River Res.Applic. 30:1099-1109.

MEI (2000). Hydraulic and Sediment Continuity Modeling of the San Joaquin River from Friant Dam to Mendota Dam, California.

Moir, H. J. and Pasternack, G. B. (2010). Substrate requirements of spawning Chinook salmon (Oncorhynchus tshawytscha) are dependent on local channel hydraulics. River Research and Applications 26:456-468.

NRDC v. Rodgers et al. (2006). Notice of Lodgment of Stipulation of Settlement, United States District Court, Eastern District of California, Sacramento Division, filed 09/13/2006.

Reclamation (2008). SRH-2D version 2: Theory and User's Manual, Sedimentation and River Hydraulics Group, Technical Service Center, Denver, CO. November, 2008.

Reclamation (2012a). Hyporheic water quality and salmonid egg survival in the San Joaquin River. Technical Memorandum No. 86-68220-12-03. Prepared for the San Joaquin River Restoration Project, Mid-Pacific Region, US Bureau of Reclamation.

Reclamation (2012b). Hydraulic Studies for Fish Habitat Analysis. Technical Report No. SRH-2012-15. Prepared for San Joaquin River Restoration Project, Mid-Pacific Region, US Bureau of Reclamation, Technical Service Center, Denver, CO.

Reclamation (2014a). Sediment Budget Analysis of the San Joaquin River for Water Years 2010 through 2012, Technical Report No. SRH-2015-18. Prepared for San Joaquin River Restoration Program, Mid-Pacific Region.

Reclamation (2014b). Two-dimensional modeling of Reach 1A of the San Joaquin River between Friant Dam and Highway 99. Technical Report No. SRH-2014-14, Prepared for the San Joaquin River Restoration Program, Mid-Pacific Region.

SJRRP (2010a). Final 2011 Agency Plan, Appendix A. November 2010.

SJRRP (2010b). Draft Annual Technical Report, Appendix G, Meso-Habitat Surveys. March 2010.

SJRRP (2010c). Fisheries Management Plan.

SJRRP (2011). Final 2011 Annual Technical Report. Appendix A. May, 2012.

SJRRP (2012). 2012 Mid-Year Technical Report, July 2012.

SJRRP (2013a). Final 2014 Monitoring and Analysis Plan. November 2013.

SJRRP (2013b). Artificial Redd Fine Sediment Accumulation Study, 2012 Final ATR Summary. Available online: http://restoresjr.net/flows/data-reporting/index.html

SJRRP (2013c). Fall-run Captive Rearing Study Update. February 2013. Available online: http://restoresjr.net/flows/data-reporting/index.html

SJRRP (2013d). Draft SJRRP Sediment Gradation Atlas - 1995 to 2012, version 2. July, 2013.

SJRRP (2013e). Effect of Altered Flow Regime on Channel Morphology in Reach 1A. August 2013.

SJRRP (2014a). 2014 Monitoring and Analysis Plan.

SJRRP (2014b). Draft 2013 Facies Mapping Geodatabase from Friant Dam to Highway 99. Last updated October 10, 2014.

Stillwater Sciences (2003). Draft Restoration Strategies for the San Joaquin River. Prepared by Stillwater Sciences, Berkeley, California for Natural Resources Defense Council, San Francisco, California and Friant Water Users Authority, Lindsay, California.

Tappel, Paul D. and Bjornn, Ted C. (1983). A new method of relating size of spawning gravel to salmonid embryo survival. North American Journal of Fisheries Management 3: 123-135.

TetraTech (2012a). San Joaquin River: Evaluation of sand supply, storage, and transport in reaches 1A and 1B.

TetraTech (2012b). 2011 San Joaquin River Sand Storage Evaluation.

Sampling Uncharted Waters: Examining Longfin Smelt (*Spirinchus thaleichthys*) Rearing Habitat in Fringe Marshes of the Low Salinity Zone

Lenny Grimaldo (ICF)
Fred Feyrer (USGS)
Jillian Burns (ICF)
Donna Maniscalco (ICF)

ICF INTERNATIONAL

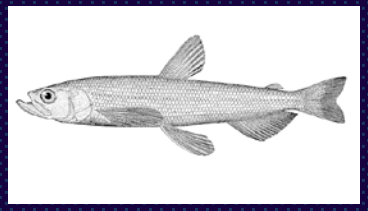

USGS science for a changing world

Basic Longfin Smelt Biology

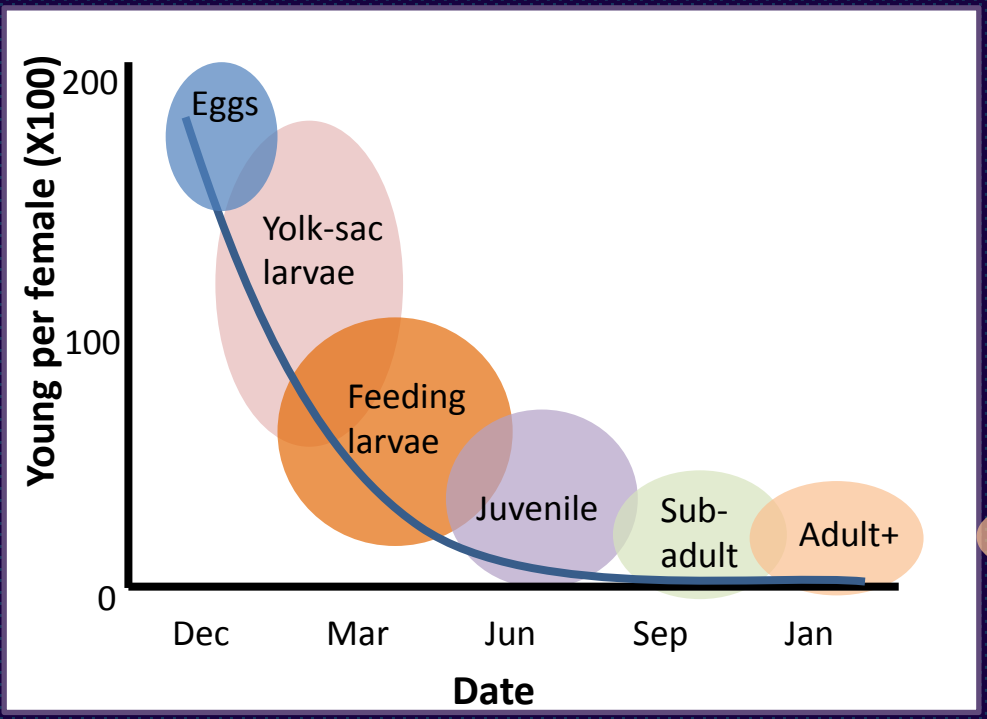

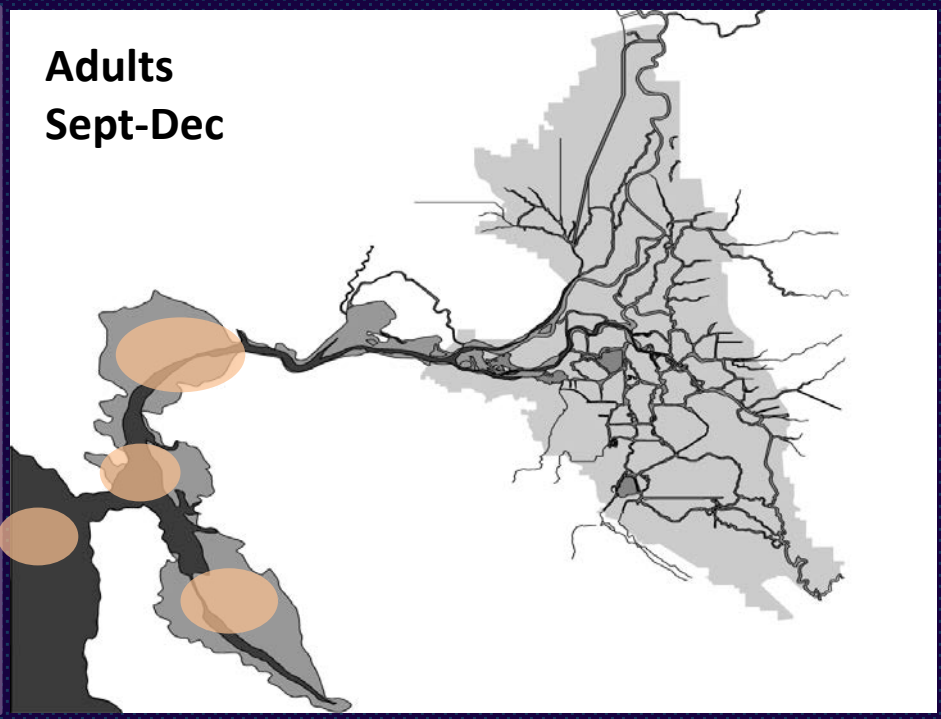

See DRERIP 2010, Rosenfield and Baxter 2011,, Merz et al. 2013

Basic Longfin Smelt Biology

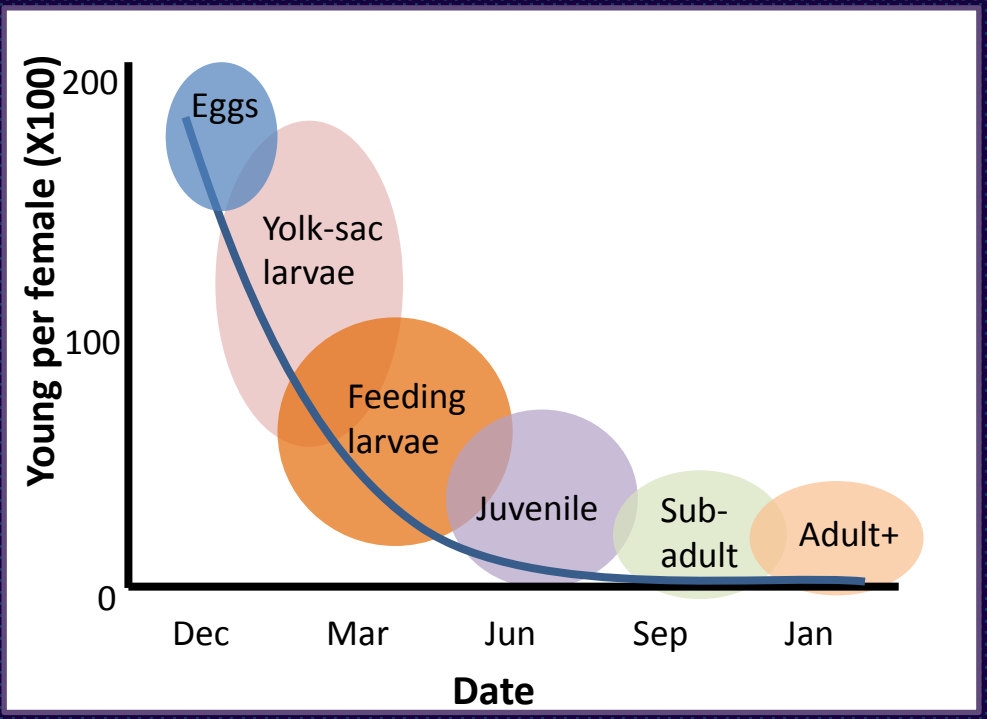

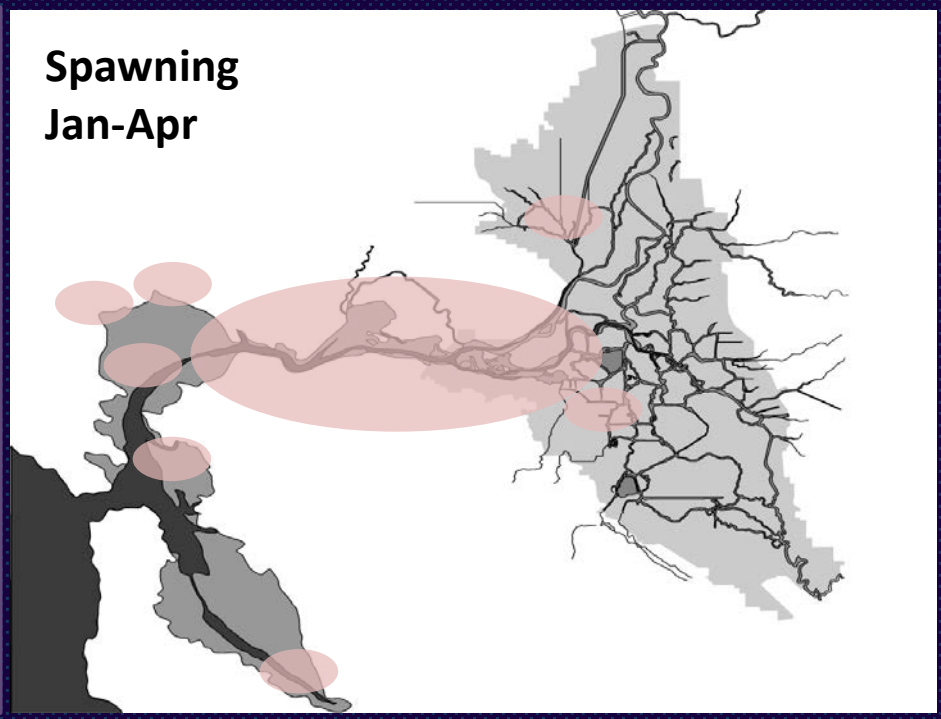

See DRERIP 2010, Rosenfield and Baxter 2011,, Merz et al. 2013

Spawning habitats?

Basic Longfin Smelt Biology

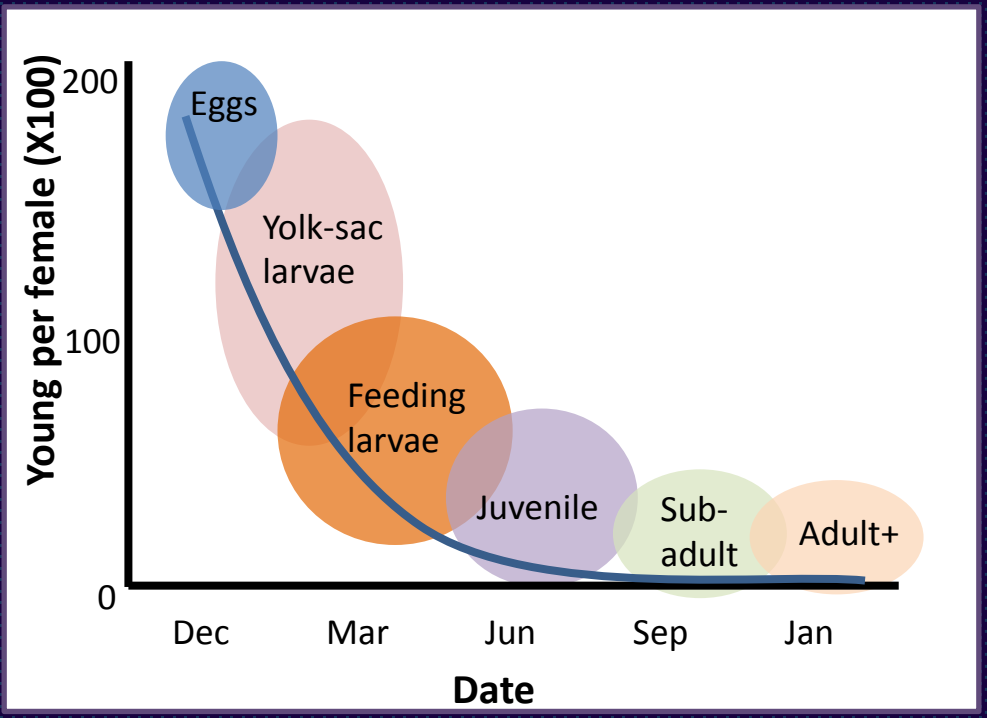

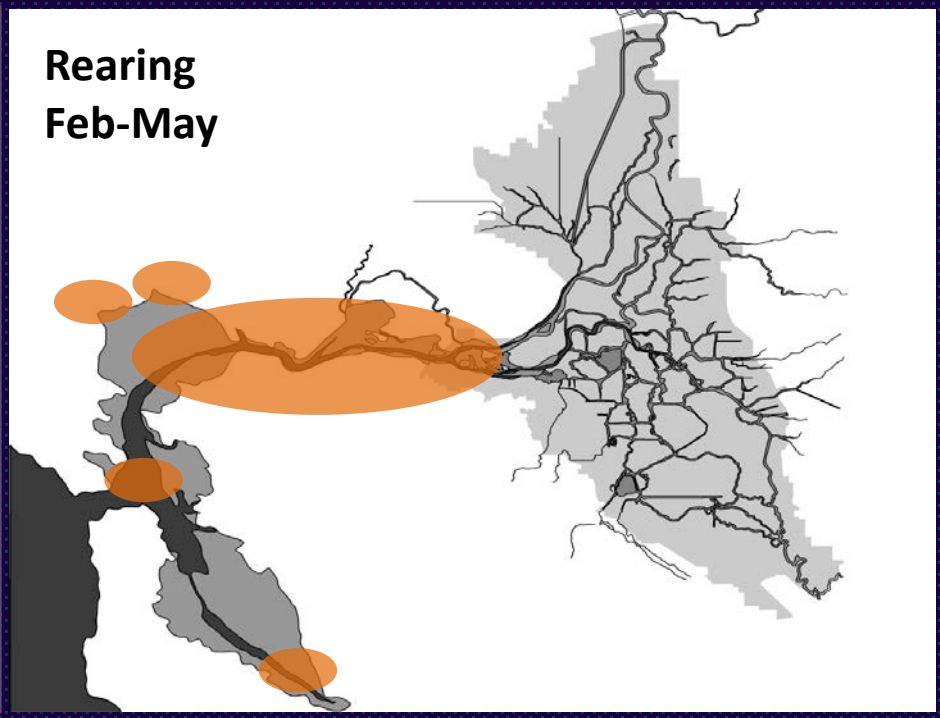

See DRERIP 2010, Rosenfield and Baxter 2011,, Merz et al. 2013

Basic Longfin Smelt Biology

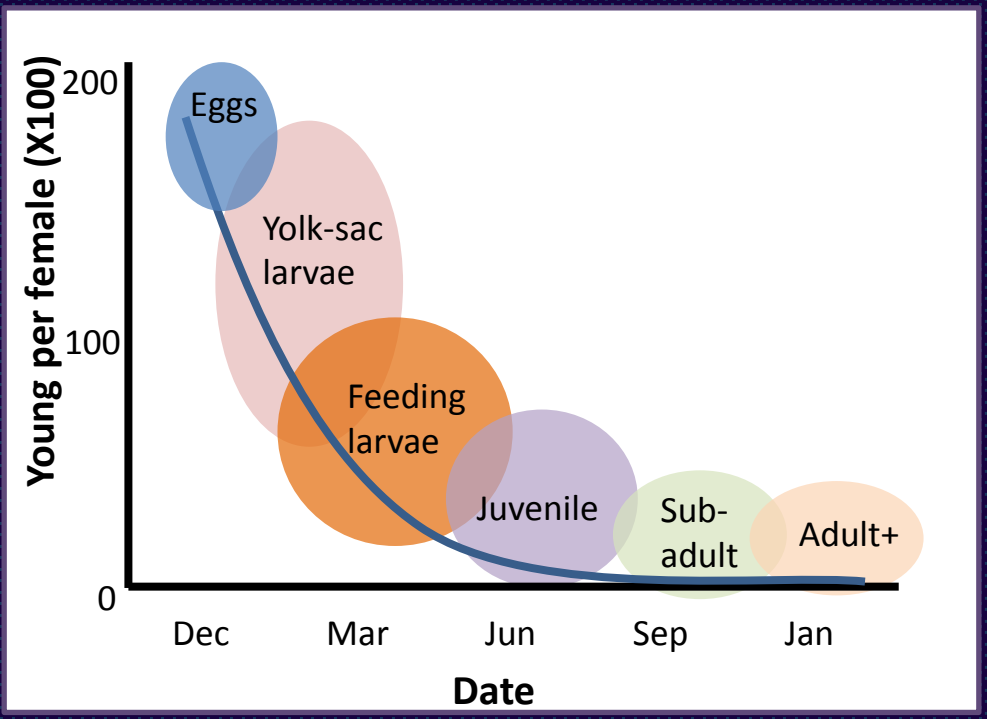

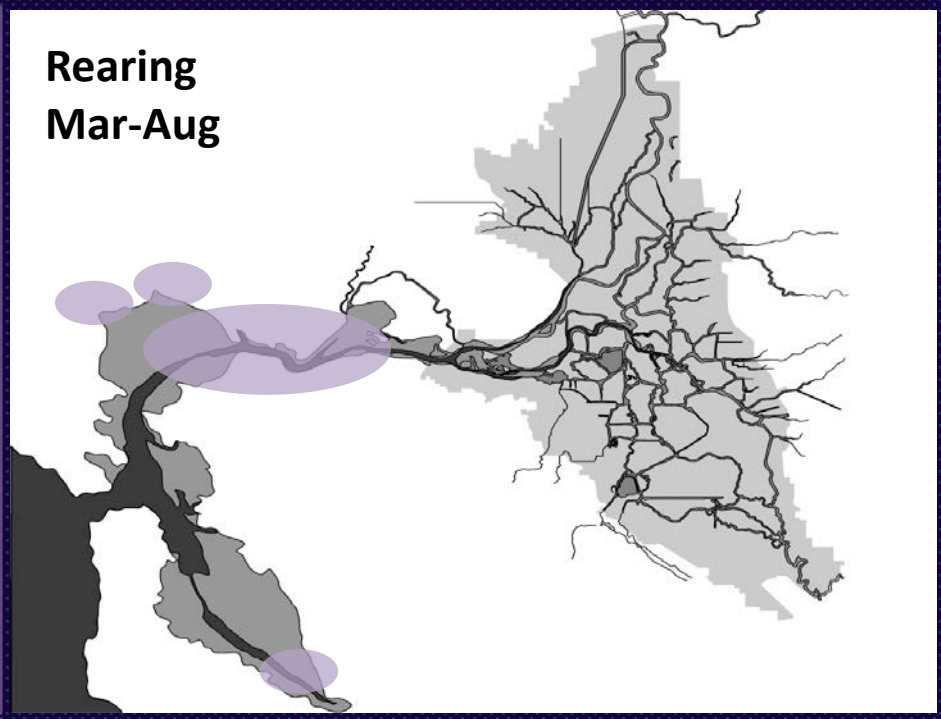

See DRERIP 2010, Rosenfield and Baxter 2011,, Merz et al. 2013

Basic Longfin Smelt Biology

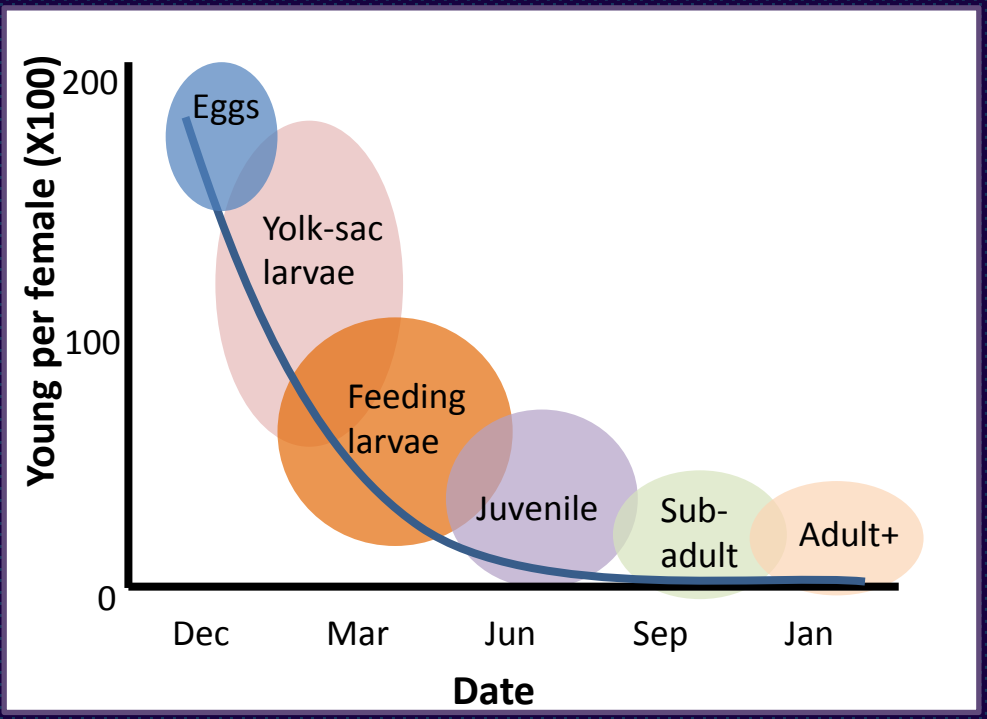

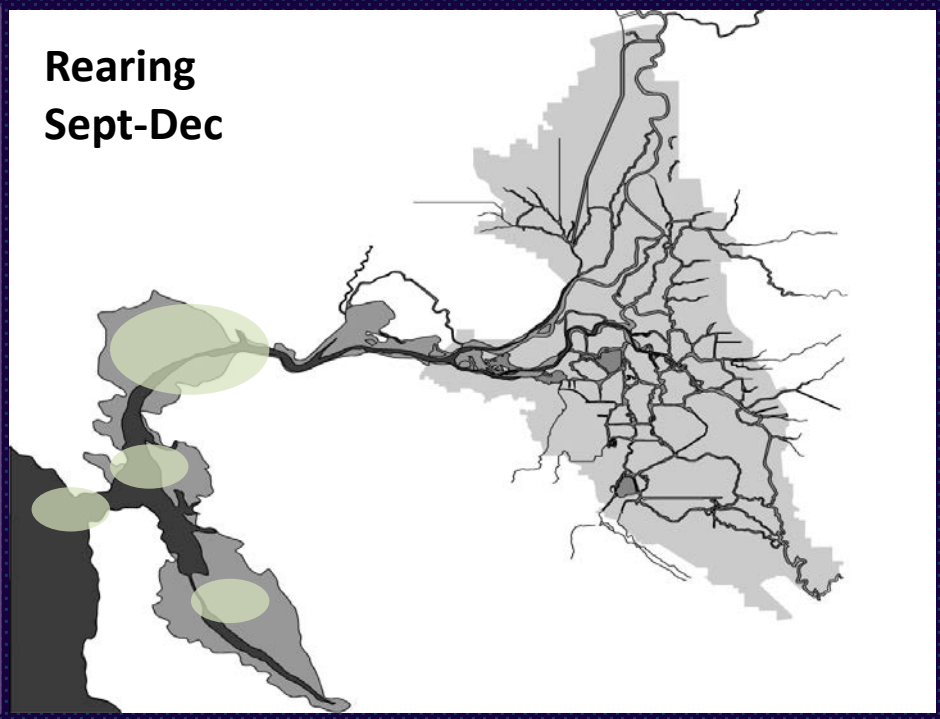

See DRERIP 2010, Rosenfield and Baxter 2011,, Merz et al. 2013

Larval longfin smelt centered near low salinity zone

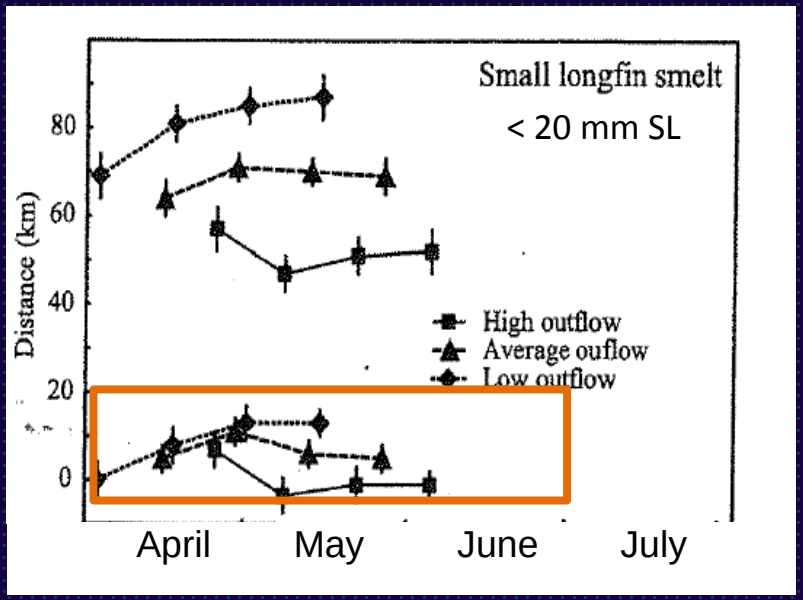

Dege and Brown 2004

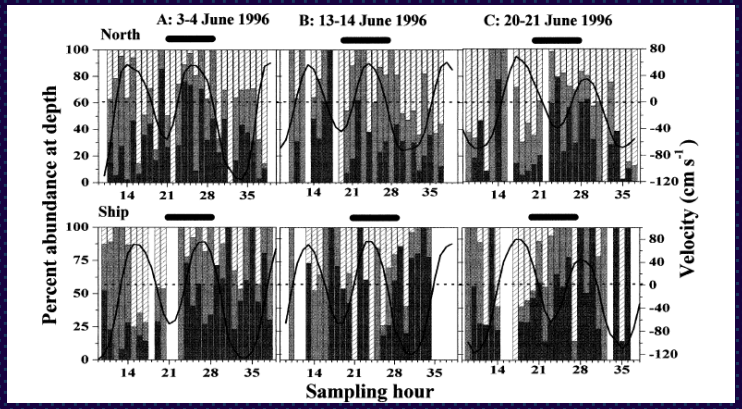

Bennett et al. 2002

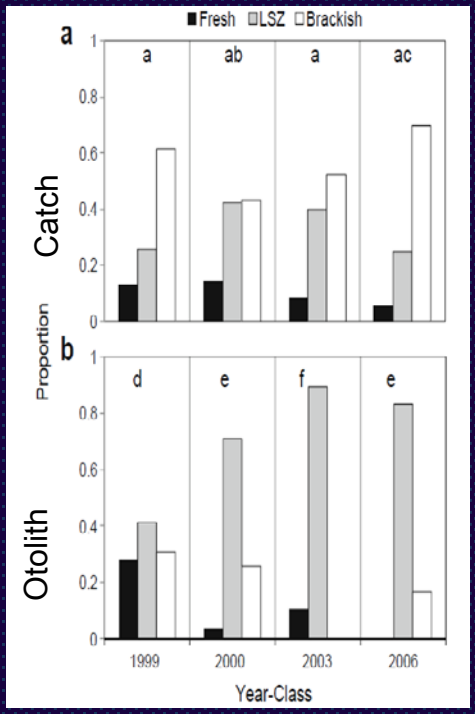

Hobbs et al. 2006

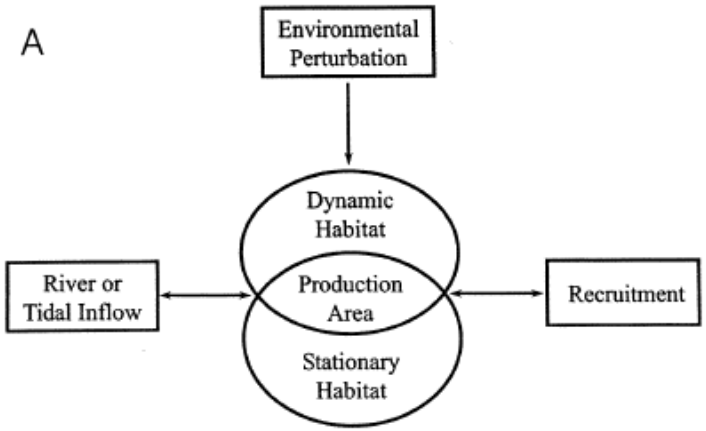

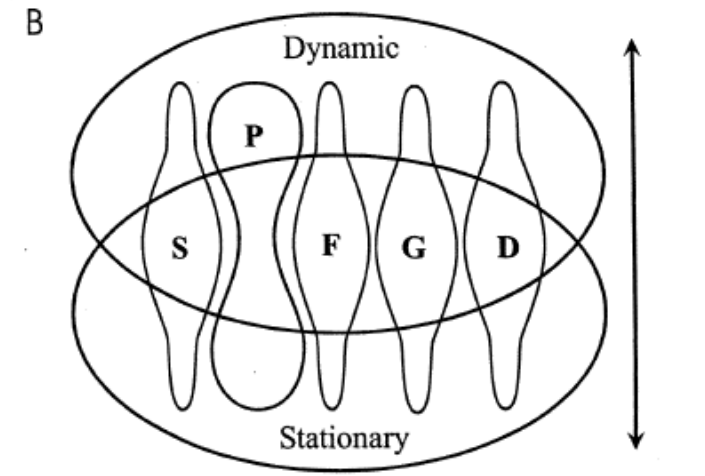

S = Survival, P = Predator, F = Foraging, G = Growth, D = Density

Peterson 2003

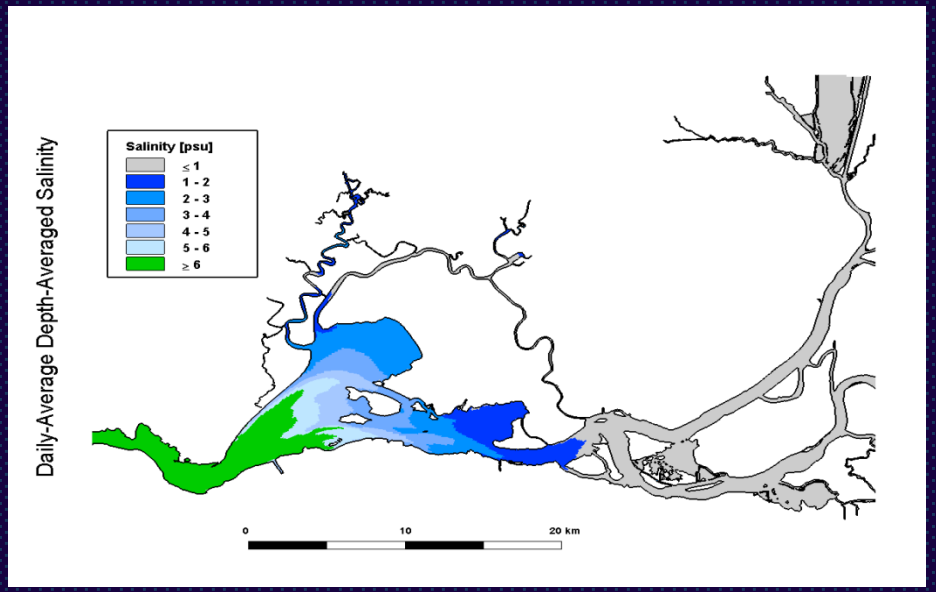

Courtesy Michael McWilliams

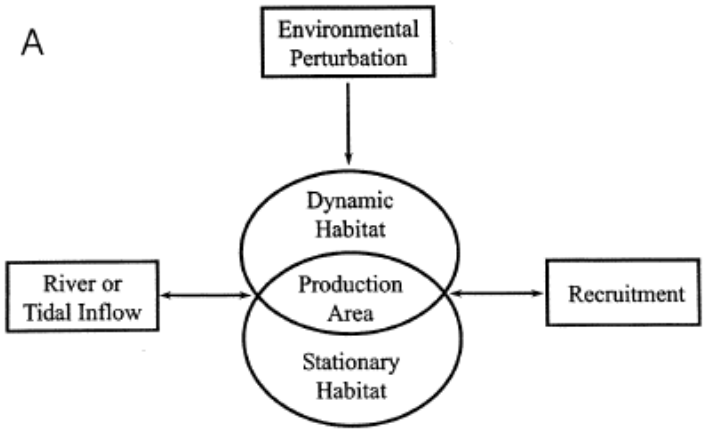

S = Survival, P = Predator, F = Foraging, G = Growth, D = Density

Peterson 2003

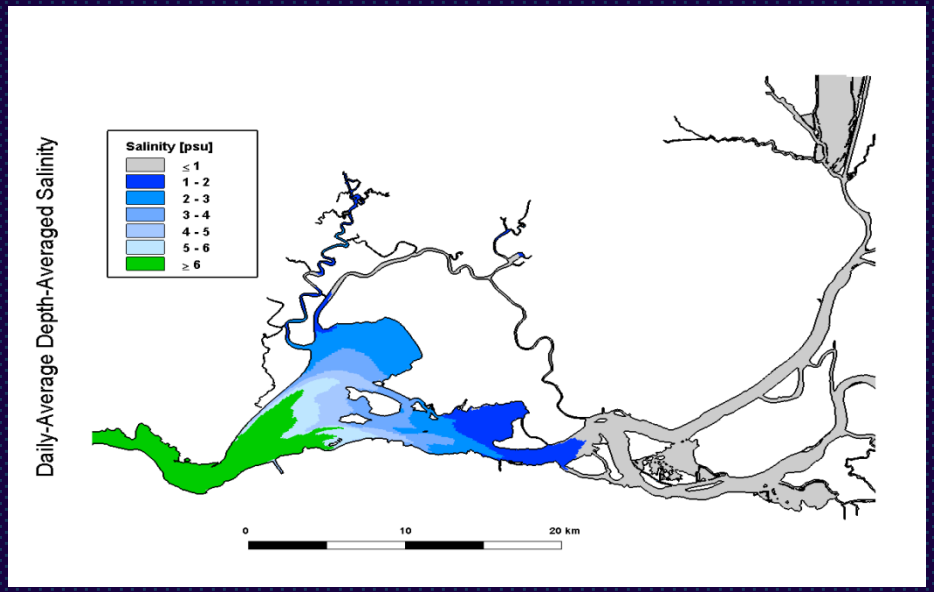

Courtesy Michael McWilliams

Larval Longfin studies 2013 (IEP) and 2014 (MWD)

Key Study Questions:

I. Do longfin smelt spawn and rear in tidal marsh and shallow open-water habitats of the low salinity zone?

II. Do larval longfin smelt densities vary between tidal marsh and shallow open-water habitat? Why?

III. How do larval longfin smelt densities in tidal marsh and shallow open water habitats in this study compare with DFW SLS densities?

IV. What are the feeding habitats of larval longfin smelt in tidal marsh and shallow open water habitats?

V. Does zooplankton abundance vary between tidal marsh and shallow open-water habitats?

Larval Longfin studies 2013 (IEP) and 2014 (MWD)

Key Study Questions:

I. Do longfin smelt spawn and rear in tidal marsh and shallow open-water habitats of the low salinity zone?

II. Do larval longfin smelt densities vary between tidal marsh and shallow open-water habitat? Why?

III. How do larval longfin smelt densities in tidal marsh and shallow open water habitats in this study compare with DFW SLS densities?

IV. What are the feeding habitats of larval longfin smelt in tidal marsh and shallow open water habitats?

V. Does zooplankton abundance vary between tidal marsh and shallow open-water habitats?

Study sites

I. Do longfin smelt spawn in tidal marsh habitats?

We caught lots of small larvae

RECIRC2566.

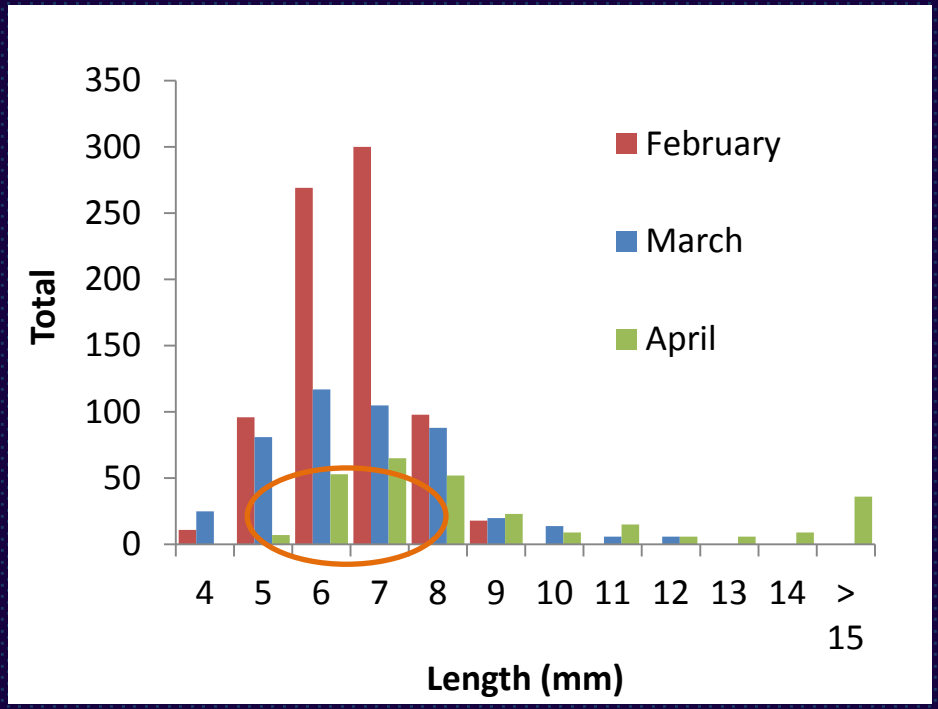

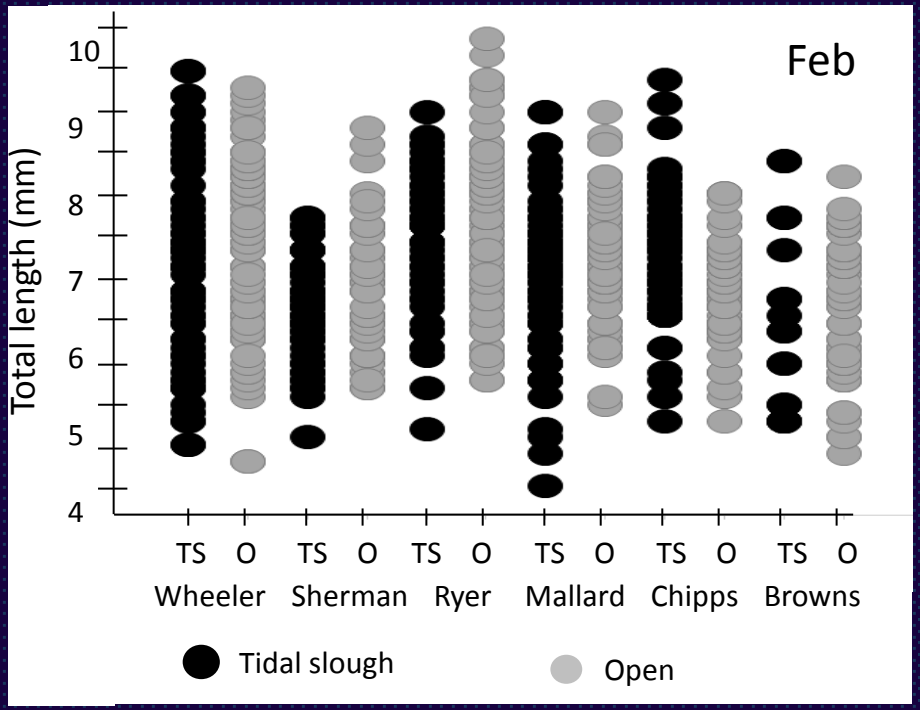

Lots of yolk-sac larvae, i.e., newly hatched fish

RECIRC2566.

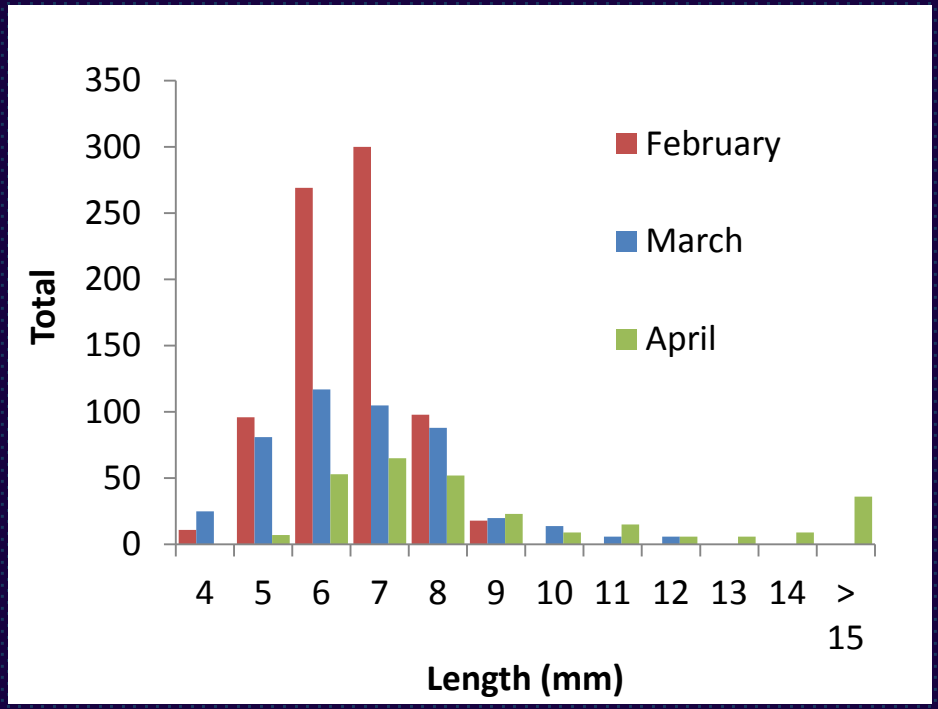

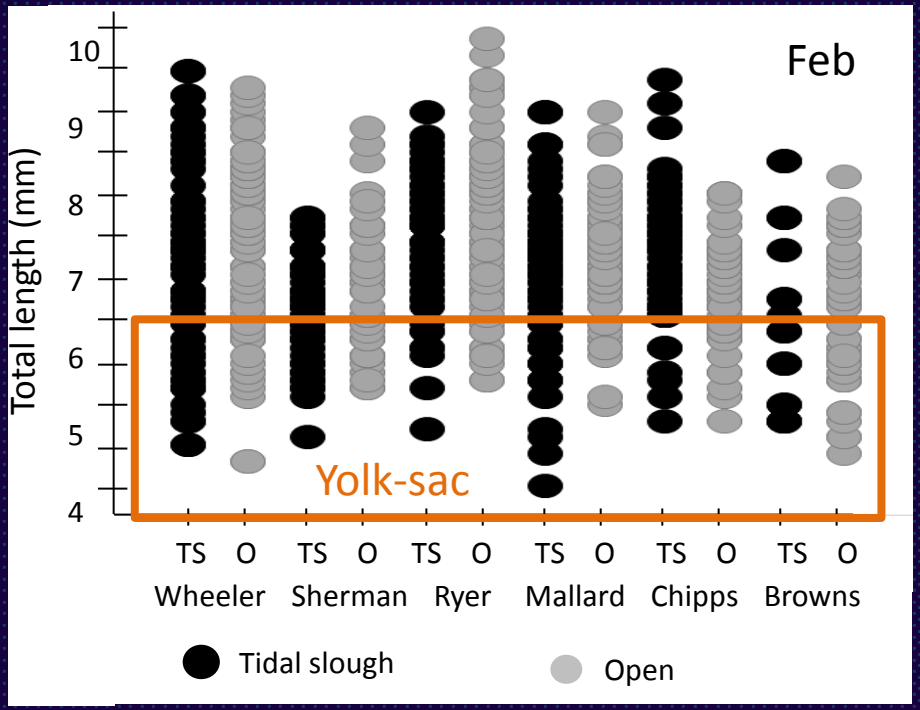

Lots of yolk-sac larvae, i.e., newly hatched fish

RECIRC2566.

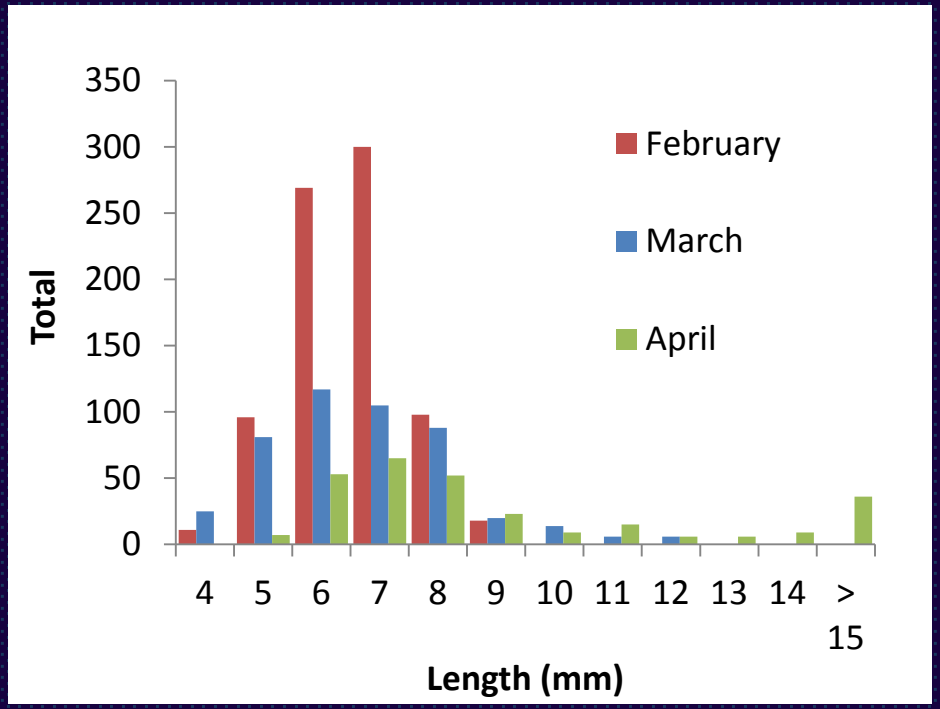

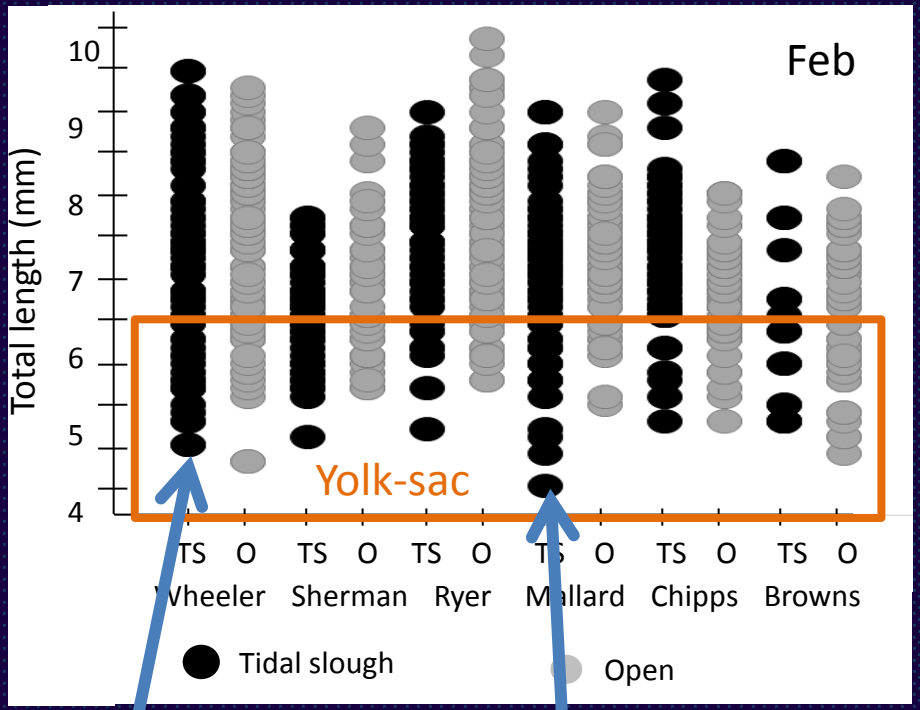

.....Especially in tidal marsh habitats

Do longfin smelt spawn in tidal marsh habitats?

RECIRC2566.

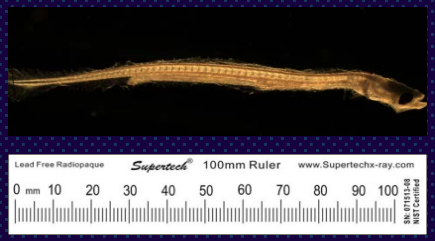

.20 mm/d
.30 mm/d
.40 mm/d

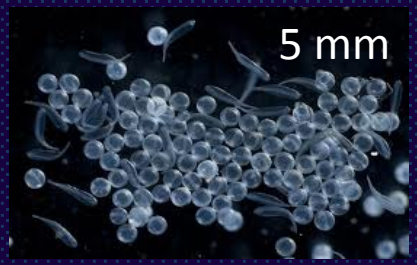

= Days to length

February

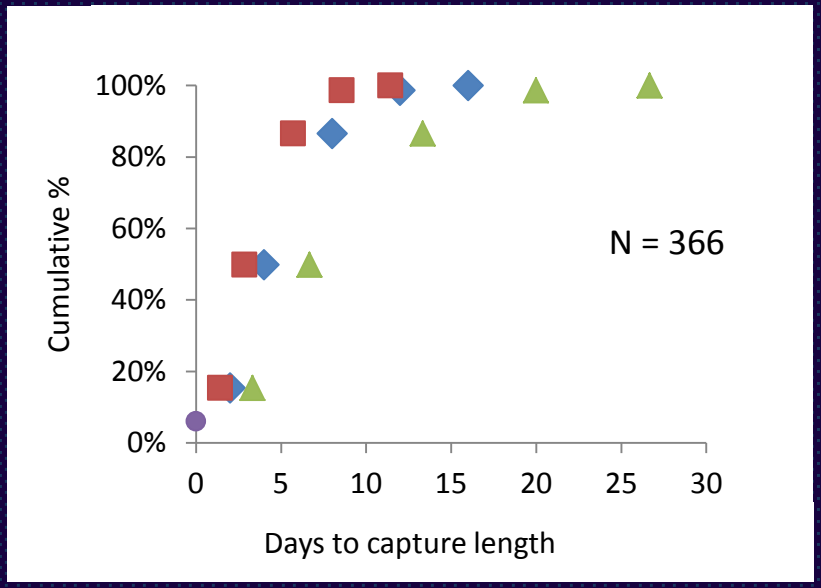

March

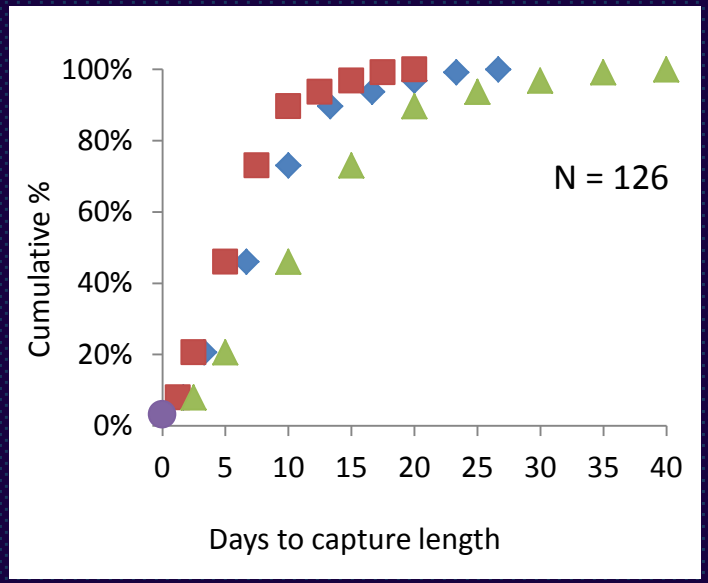

Do longfin smelt spawn in tidal marsh habitats?

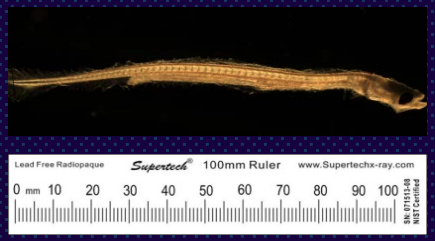

.20 mm/d
.30 mm/d
.40 mm/d

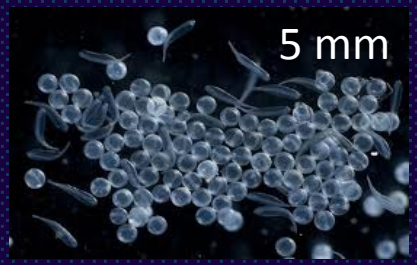

= Days to length

Evidence suggests yes

What about shallow open-water habitats?

RECIRC2566.

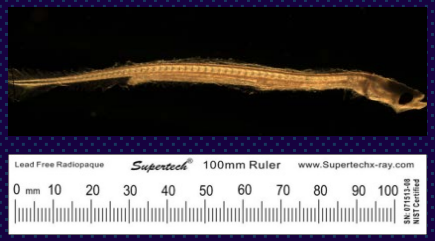

.20 mm/d
.30 mm/d
.40 mm/d

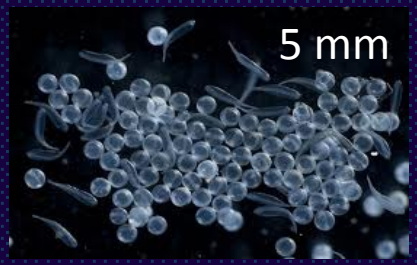

= Days to length

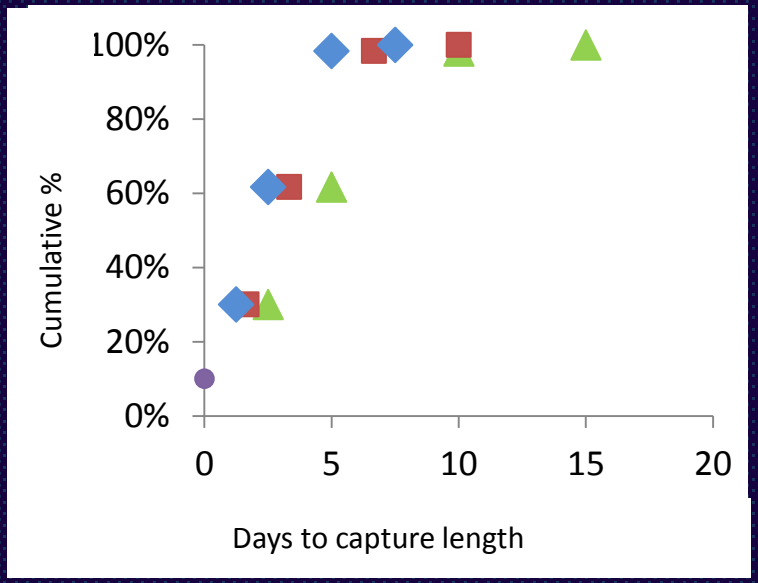

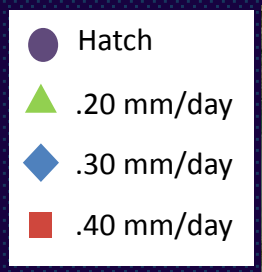

II. Do larval fish densities vary between tidal marsh and shallow open-water habitats?

Larval longfin smelt densities are higher in shallow open-water habitat

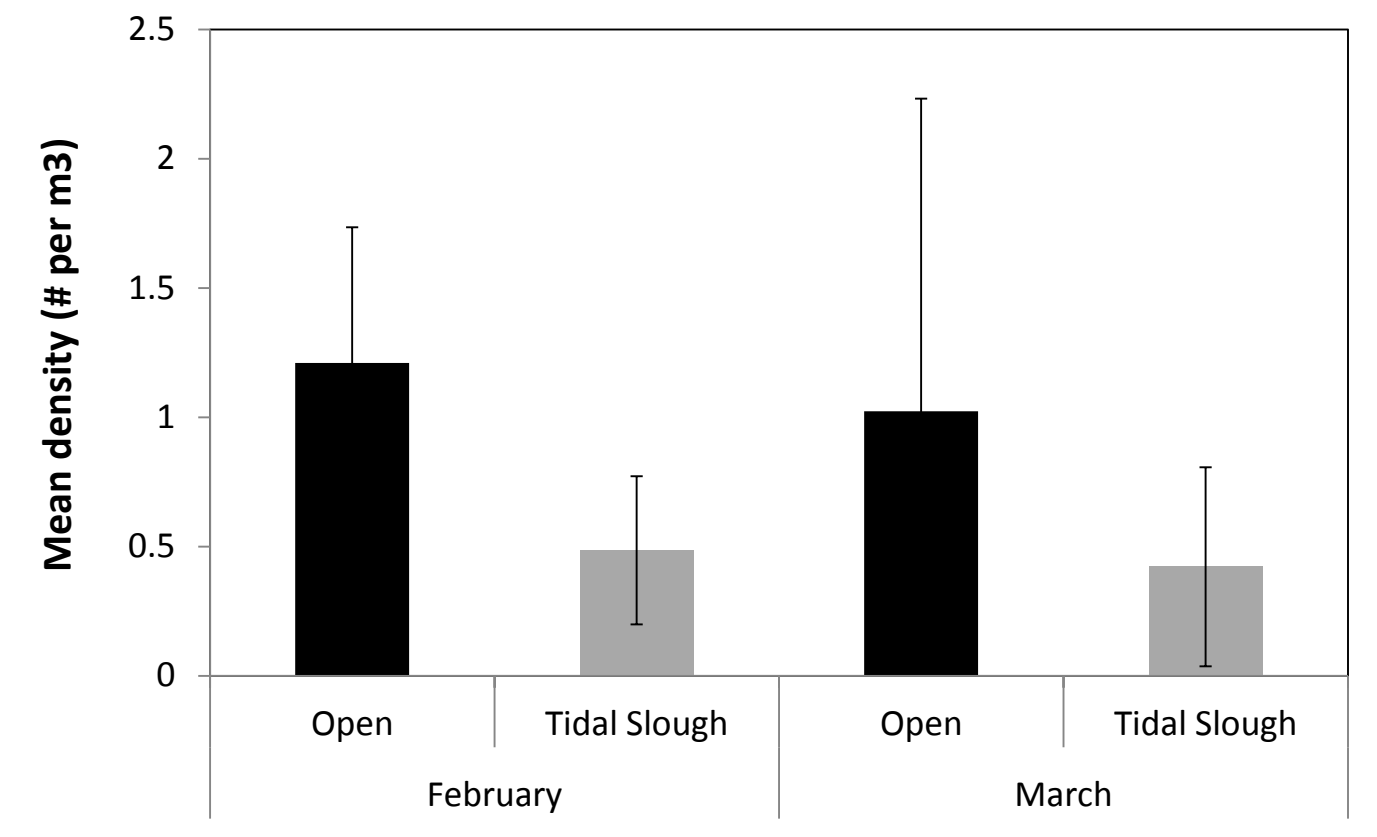

February 2013

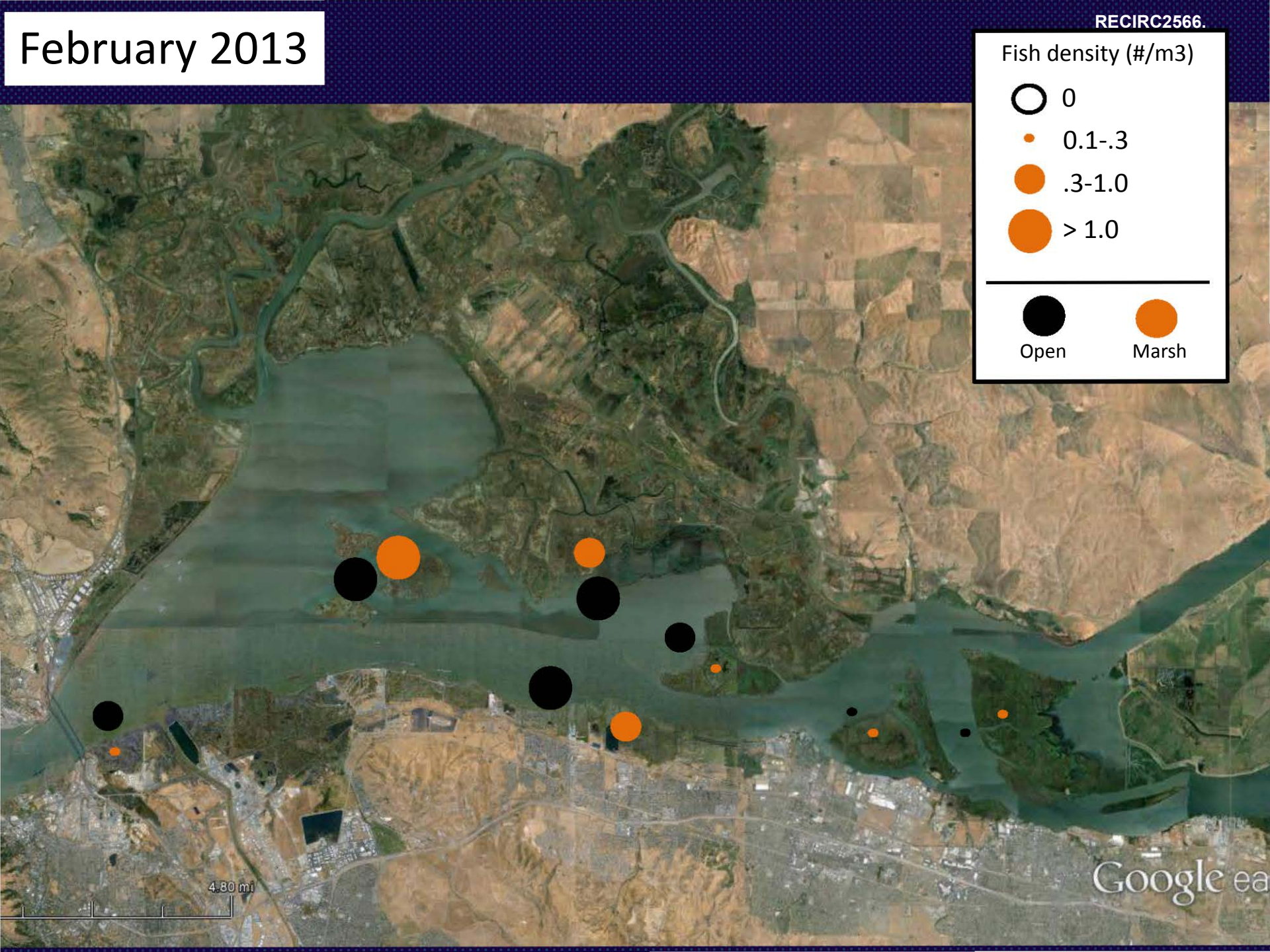

March 2013

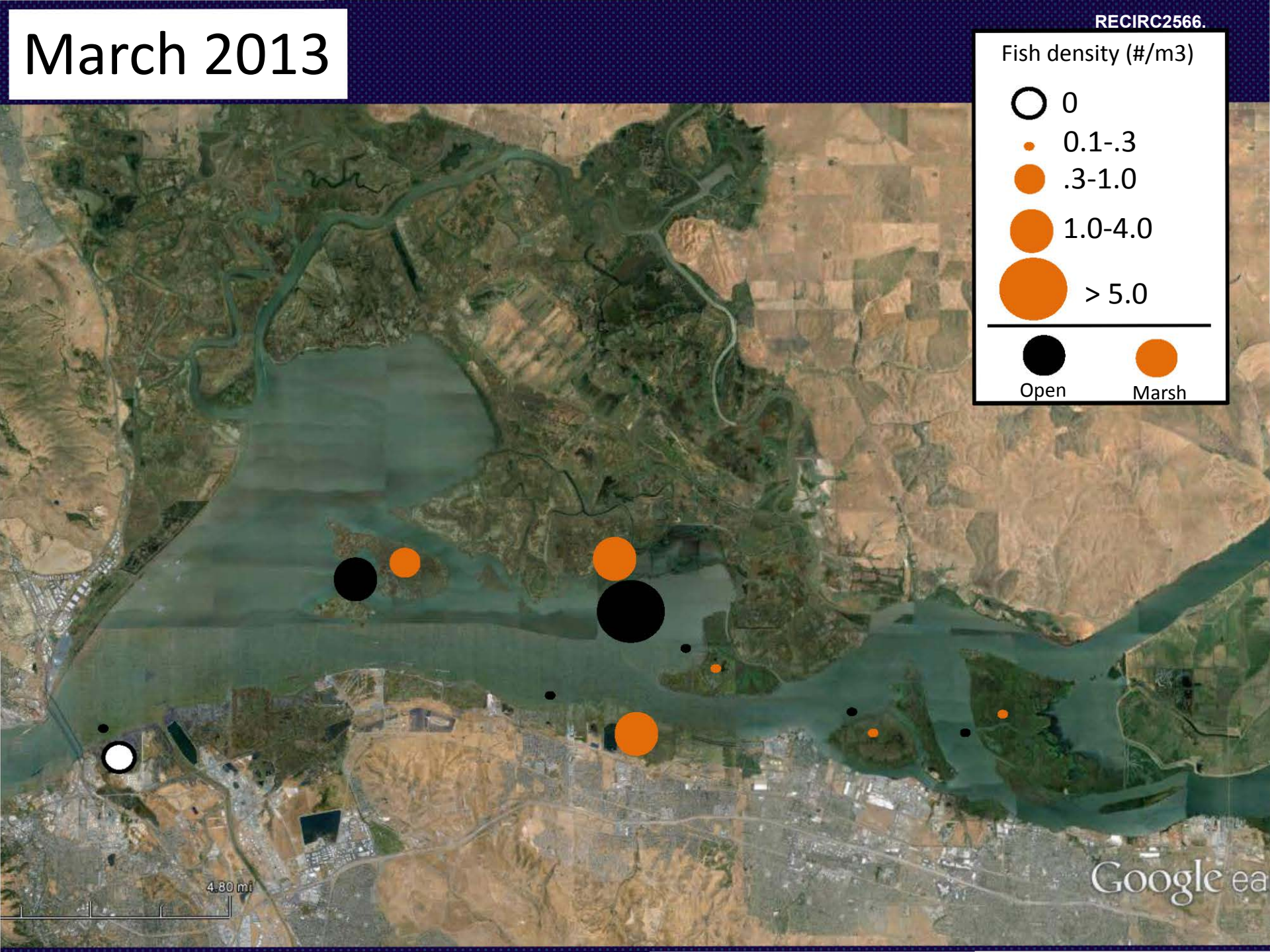
RECIRC2566.
Fish density (#/m3)
0
0.1-.3
.3-1.0
1.0-4.0
> 5.0
Open
Marsh
4.80 mi
Google ea

Water Quality Varied Between Habitats

RECIRC2566.

All sites- February and March

No wind, calm day (not common, real nice)

Windy day, bronco riding practice, (more common)

Wind or no wind, relatively calm

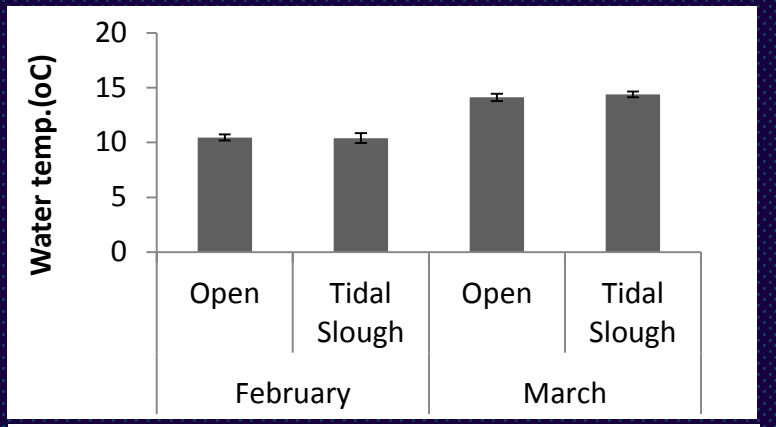

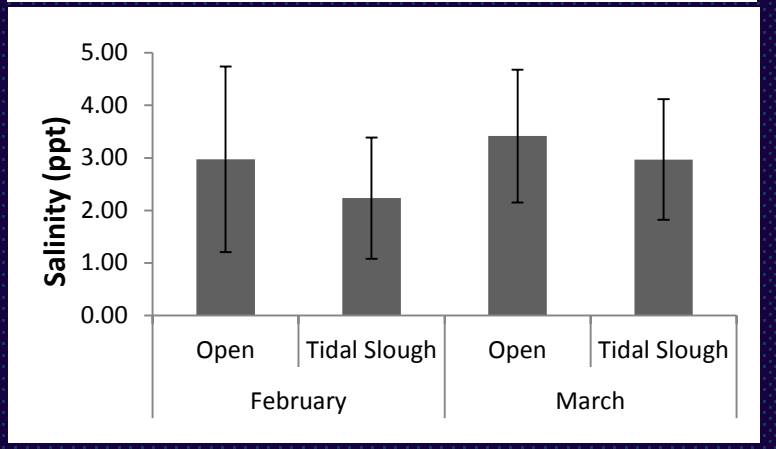

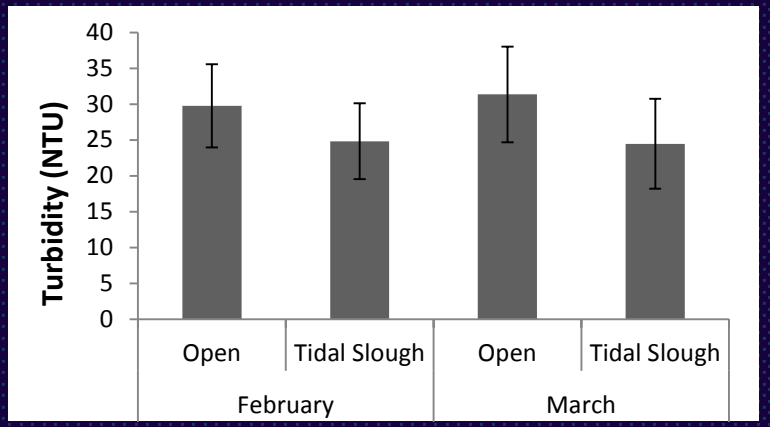

Water Quality Varied Between Habitats

RECIRC2566.

All sites- February and March

No wind, calm day (not common, real nice)

Windy day, bronco riding practice, (more common)

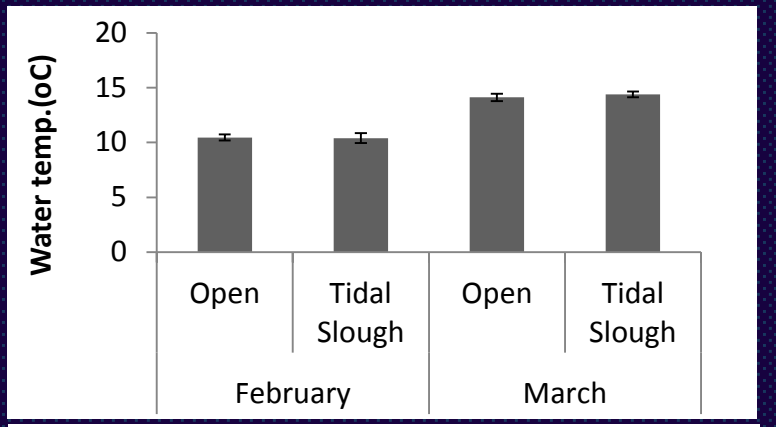

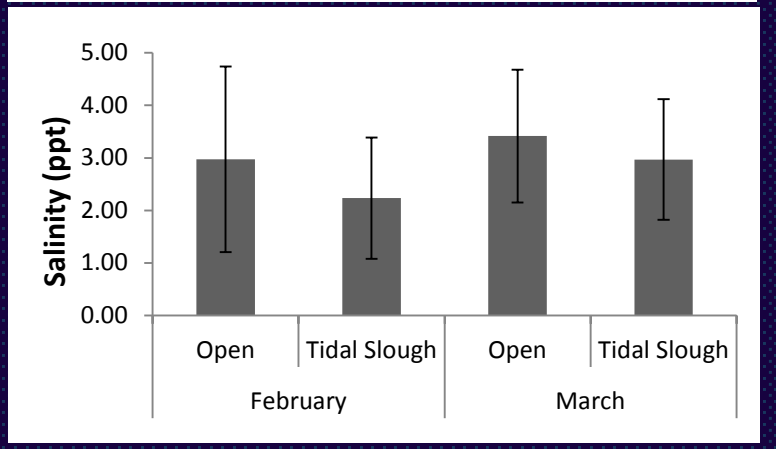

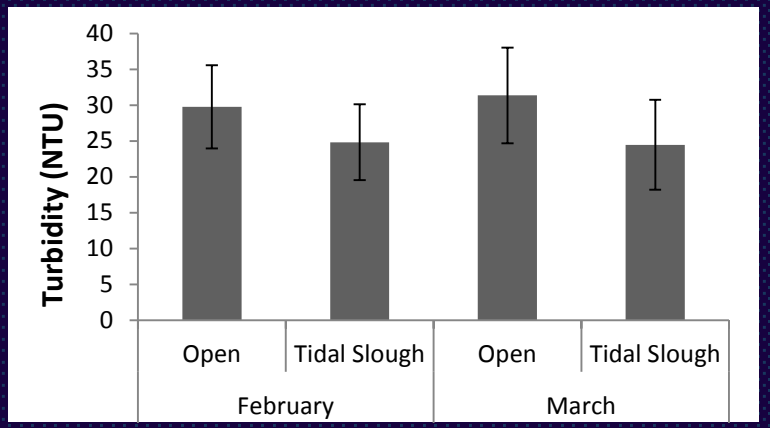

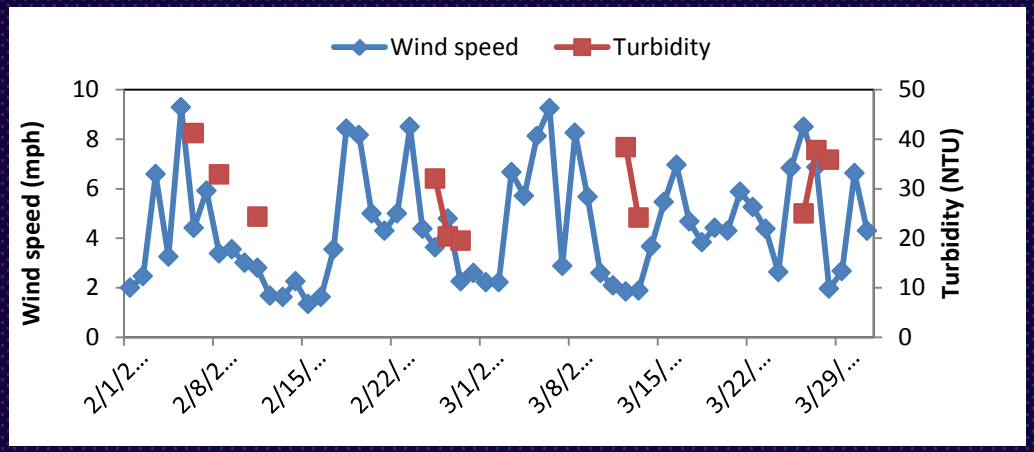

III. How do larval longfin smelt densities in tidal marsh and shallow open-water habitats in this study compare with DFW SLS densities?

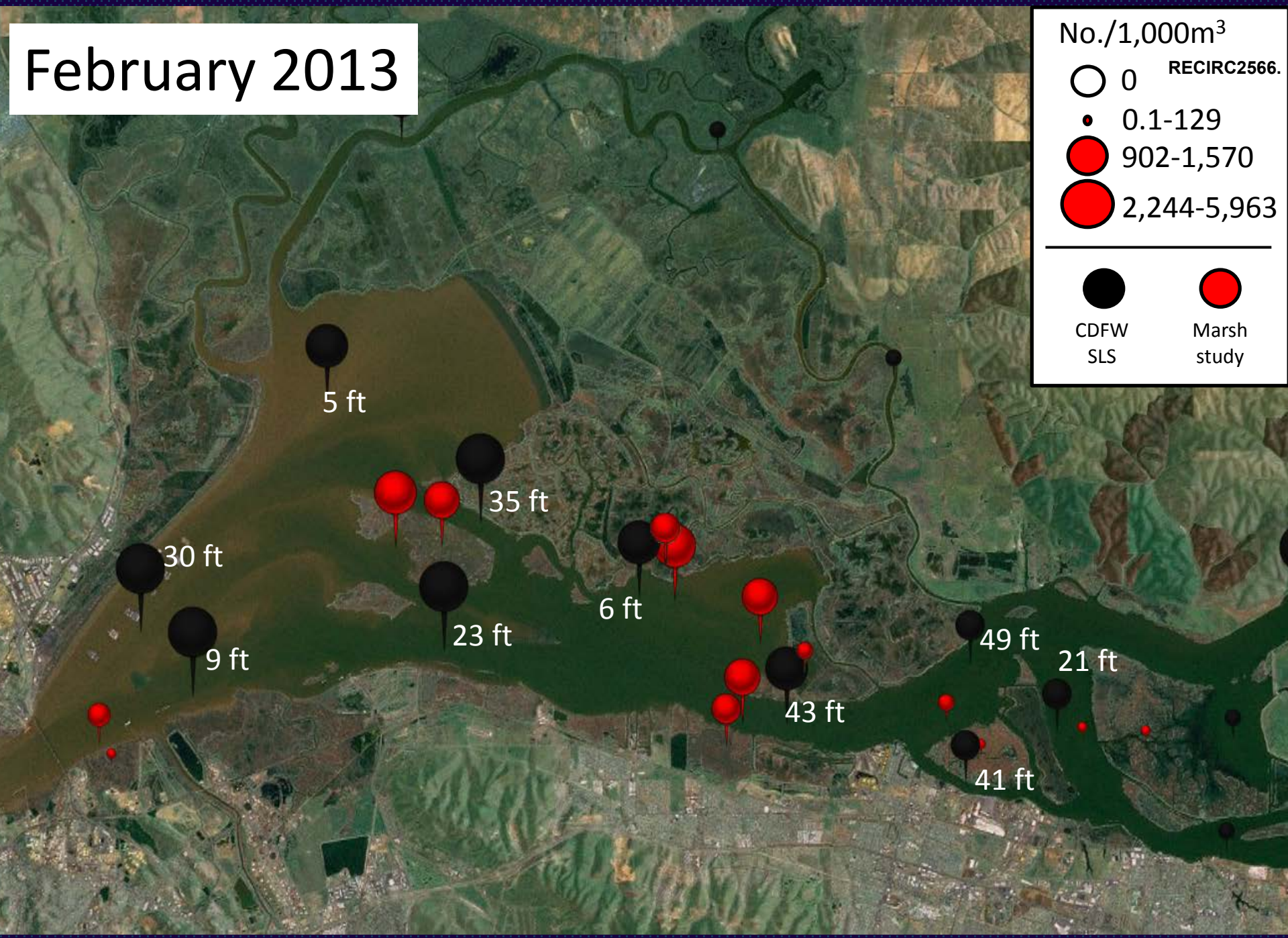
February 2013
No./1,000m3
RECIRC2566.
0
0.1-129
902-1,570
2,244-5,963
CDFW SLS
Marsh study
5 ft
35 ft
30 ft
9 ft
23 ft
6 ft
43 ft
49 ft
21 ft
41 ft

March 2013

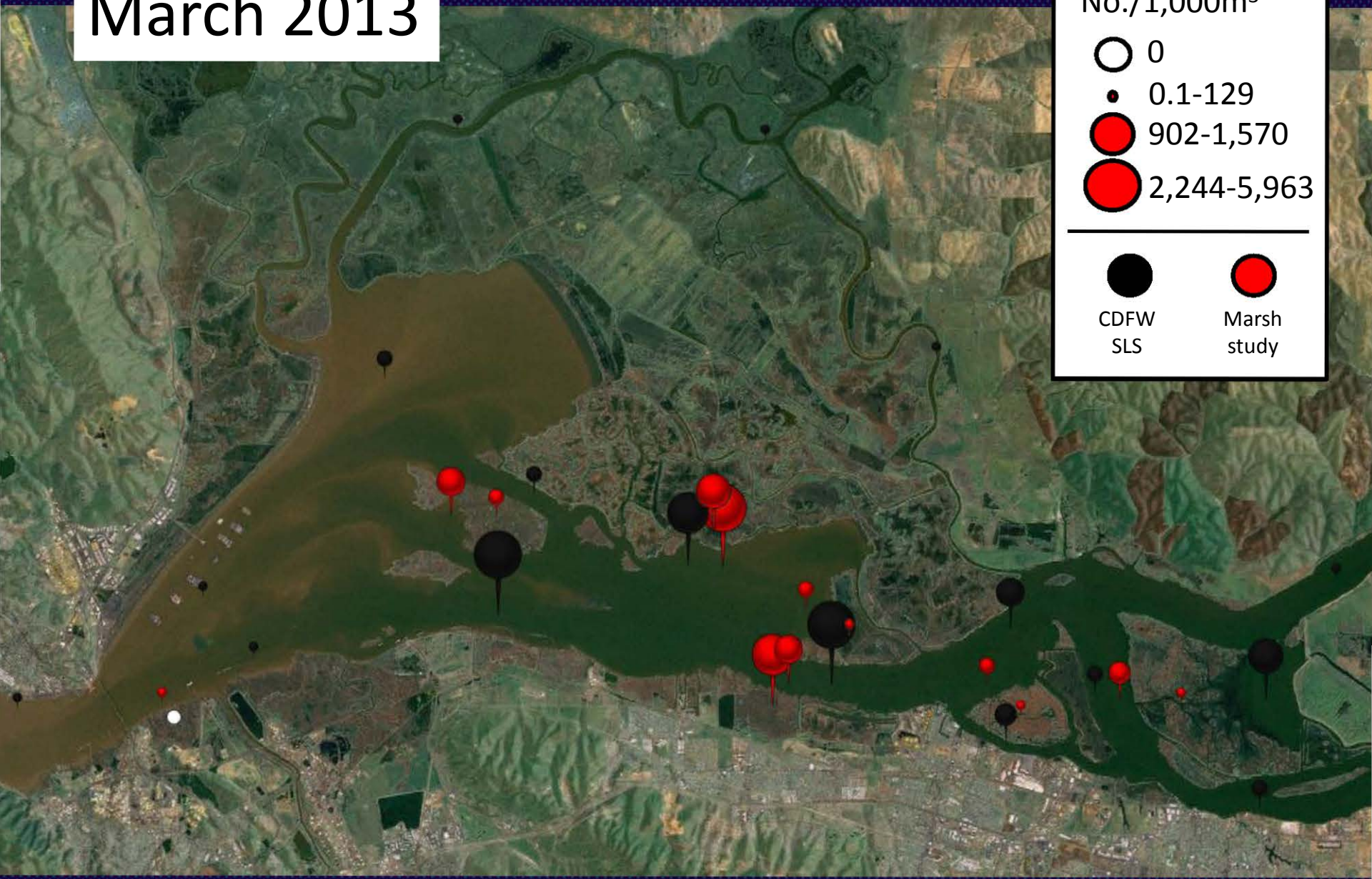

Acknowledgments

Funding

2013 IEP (Management Team)

2014 MWD (David Fullerton and Russell Ryan)

Instrumental helpers (i.e., operators, lab assistance, fish identification, permits)

Nick Sakata
Nick van Ark
Kari Ambrosia
David van Rijn
Eric Santos
Jim Starr
Jennifer Pierre
Erin Gleason

Shawn Acuna
Tenera Environmental
Colin Brennan
Dan Abbott
Eric Sommerauer
Carol Raifsnider
Dave Mayer
Johnson Wang

Folks who justed wanted to take a boat ride in the guise of helping

Dan Riordan
Gina Benigno
Rachel Johnson
Marin Greenwood
Leigh Bartoo

Carolyn Bragg
Mary Lee Knecht
Shelly Hattleburg
Maral Kasparian

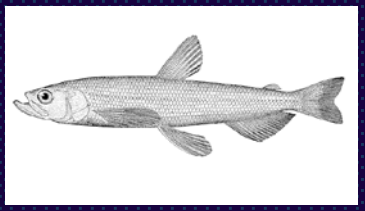

Wheeler Island

Browns Island

Mallard Island

No Name Marsh

Sherman Island

Chipps Island

North American Journal of Fisheries Management
Publication details, including instructions for authors and subscription information:
http://www.tandfonline.com/loi/ujfm20

Quantifying the Uncertainty of a Juvenile Chinook Salmon Race Identification Method for a Mixed-Race Stock

Brett N. Harvey[a], David P. Jacobson[b] & Michael A. Banks[b]

[a] California Department of Water Resources, Post Office Box 942836, Sacramento, California 94236, USA

[b] Coastal Oregon Marine Experiment Station, Hatfield Marine Science Center, Department of Fisheries and Wildlife, Oregon State University, 2030 Southeast Marine Science Drive, Newport, Oregon 97365, USA

Published online: 14 Nov 2014.

To cite this article: Brett N. Harvey, David P. Jacobson & Michael A. Banks (2014) Quantifying the Uncertainty of a Juvenile Chinook Salmon Race Identification Method for a Mixed-Race Stock, North American Journal of Fisheries Management, 34:6, 1177-1186, DOI: 10.1080/02755947.2014.951804

To link to this article: http://dx.doi.org/10.1080/02755947.2014.951804

North American Journal of Fisheries Management 34:1177–1186, 2014

ISSN: 0275-5947 print / 1548-8675 online
DOI: 10.1080/02755947.2014.951804

MANAGEMENT BRIEF

Quantifying the Uncertainty of a Juvenile Chinook Salmon Race Identification Method for a Mixed-Race Stock

Brett N. Harvey*
California Department of Water Resources, Post Office Box 942836, Sacramento, California 94236, USA

David P. Jacobson and Michael A. Banks
Coastal Oregon Marine Experiment Station, Hatfield Marine Science Center, Department of Fisheries and Wildlife, Oregon State University, 2030 Southeast Marine Science Drive, Newport, Oregon 97365, USA

Abstract

Expected daily FL ranges (length at date) of juvenile Chinook Salmon *Oncorhynchus tshawytscha* have been used throughout California's Central Valley to identify federally listed winter-run and spring-run juveniles in a mixed four-race stock. Accurate race identification is critical both to species recovery and to management of the water supply for 25 million people and a multibillion-dollar agricultural industry. We used genetic race assignment of 11,609 juveniles sampled over 6 years to characterize the accuracy of the length-at-date approach, specifically by testing two of its central assumptions: (1) juvenile FL distributions do not overlap between races on a daily basis; and (2) the growth rates that are used to project FL at date are accurate. We found that 49% of FLs for genetically identified juveniles occurred outside the expected length-at-date ranges for their respective races, and we observed a high degree of overlap in FL ranges among the four races. In addition, empirical growth rates were well below those from which length-at-date criteria were derived. Given the high degree of FL overlap between races, we conclude that modification of the length-at-date method will not substantially reduce identification error. Thus, we recommend that genetic assignment be used at least as a supplemental approach to improve Central Valley Chinook Salmon race identification, research, and management.

Management of rare species often requires decisions to be made based on inadequate data and suboptimal tools, thereby introducing uncertainty into risk assessment (Burgman 2005; Moore and Runge 2012); this uncertainty can lead to profound ecological and economic consequences (Gillespie et al. 2011; McGowan et al. 2011). Such is the case for California's Central Valley, where the monitoring of endangered Chinook Salmon *Oncorhynchus tshawytscha* populations and the legal restrictions on water exports to protect those populations depend in part on a juvenile race identification method of unknown accuracy, called the length-at-date method.

The Central Valley comprises the combined basins of California's two longest rivers, the Sacramento River and the San Joaquin River, and was once among the most productive systems for salmon on the U.S. Pacific coast. Although a 150-year history of mining, fishery exploitation, habitat loss, and water infrastructure development has led to a severe and continuing decline in Central Valley salmon (Yoshiyama et al. 1998; Katz et al. 2012), the Sacramento–San Joaquin River system remains the only river system that supports four distinct spawning races of Chinook Salmon: spring, fall, late fall, and the endemic winter run (Yoshiyama et al. 1998). While these run designations are based on a difference in the general timing of adult spawning migrations, the juvenile offspring of these races constitute a mixed population in the Central Valley basin, and there are no clear morphological or behavioral characteristics that can be used to distinguish an individual juvenile's race (Williams 2006; del Rosario et al. 2013). Winter-run Chinook Salmon were federally listed in 1990 as a threatened species under the Endangered Species Act (NMFS 1990), and the status was updated to endangered in 1994 (NMFS 1994); the spring run was subsequently listed as threatened in 1999 (NMFS 1999). After federal listing of these

*Corresponding author: brett.harvey@water.ca.gov
Received January 7, 2014; accepted July 22, 2014

races, the inability to determine the race of juveniles proved problematic for management, particularly with regard to the assessment of losses at the primary pumping facilities of the California State Water Project and federal Central Valley Project. The two pumping facilities are located in the inland delta formed by the confluence of the Sacramento and San Joaquin rivers (hereafter, Sacramento–San Joaquin Delta) and supply water to 25 million people (8% of the U.S. population: Sommer et al. 2007) and a multibillion-dollar agricultural industry that produces nearly half of the fruits, nuts, and vegetables grown in the USA (CDFA 2013). However, these pumping facilities also entrain juvenile salmon (Kimmerer 2008; Brown et al. 2009).

To monitor the status and account for take of protected Chinook Salmon, the California Department of Fish and Wildlife developed a length-at-date approach in 1989 (Fisher 1992; Harvey 2011; del Rosario et al. 2013), which continues to be used as the primary method of identifying and enumerating the take of winter-run juveniles throughout the Central Valley (e.g., NMFS 2009; del Rosario et al. 2013). The length-at-date approach originated from the observation that the spawning seasons of the four Central Valley Chinook Salmon runs are somewhat segregated in time (Fisher 1992; Harvey 2011; del Rosario et al. 2013). Based on this observation, the calendar year was divided into four adjacent, nonoverlapping time spans; the earliest and latest dates of each time span represented the earliest and latest estimated spawning dates of each run. Emergence dates (estimated from spawning intervals), a standard emergence length of 34 mm FL, and a juvenile exponential growth rate of 6.57×10^{-3} $\log_e$(mm FL)/d were then applied to project the expected minimum and maximum FLs for juveniles of each run through time. Note that throughout this document, "growth rate" refers to "apparent growth rate," a term commonly used to describe growth estimates that are potentially confounded by the influence of factors in addition to individual growth, such as immigration, emigration, and size-selective mortality (e.g., Ricker 1942; Busacker et al. 1990). Within this construct, the FL of a juvenile Chinook Salmon sampled in the Central Valley on any given day of the calendar year could be compared with a table of length-at-date criteria to designate that juvenile's race (Fisher 1992; Harvey 2011; del Rosario et al. 2013).

Although the simplicity of the length-at-date approach fulfilled an immediate need for field identification, many biologists involved with the approach's development, adoption, and subsequent use recognized that the assumptions underlying the approach were oversimplified (Williams 2006; del Rosario et al. 2013). Therefore, development of a genetic-based assignment method was initiated in 1994 to validate and potentially supplant the length-at-date identification method. Since 1996, genetic race assignment has been routine for juveniles collected at fish screens on intakes (also known as "salvaged" juveniles) at state and federal water pumping facilities, although genetic-based assignment has not been adopted for take assessment. Although salvaged fish are not counted directly toward protected species take, the number salvaged is the primary input variable for calculation of take.

An informal analysis of initial genetic test results suggested that roughly half of juveniles identified as winter run by the length-at-date method were not in fact genetic winter run; this finding led in 1997 to a doubling of the Endangered Species Act take allowance and to the adoption of modified length criteria based on a higher assumed winter-run growth rate of 8.16×10^{-3} $\log_e$(mm FL)/d, which was intended to reduce misidentification of age-0 spring-run and fall-run fish as winter run (described by Harvey 2011). Subsequently, a similar evaluation of the original length criteria also found that roughly half of the winter-run-length juveniles collected at salvage facilities were not genetic winter run (Hedgecock 2002). These prior analyses were limited in several respects. The early genetic tests used in these evaluations identified only the winter run, with all other juveniles being termed "non-winter run," and thus the length-at-date error rate could only be estimated with respect to genetic winter run (i.e., the proportion of winter-run-length fish that were not genetic winter run; and the proportion of non-winter-run-length fish that were genetic winter run). The analyses also did not correct for a bias of genetic samples toward large, early migrating juveniles in the winter-run length range for years prior to 2004, during which a variety of size-stratified sampling protocols was employed without formal documentation. Perhaps most importantly from a regulatory standpoint, the two analyses evaluated the accuracy of the original length-at-date model but did not assess the modified growth rate model currently used at the salvage facilities.

Therefore, we undertook an evaluation of the length-at-date method's accuracy, taking advantage of a greatly expanded data set, a more uniform sampling regime, improved genetic markers (Banks and Jacobson 2004), and improved analytical software (Kalinowski 2003, 2007), all of which allowed greater genetic test accuracy and race resolution. We specifically tested whether the length distributions of genetically assigned runs supported the two central assumptions of the length-at-date approach: (1) juvenile FL distributions do not overlap between races on a daily basis; and (2) the growth rates that are used to project FL at date are accurate.

METHODS

Fish that were salvaged at the state and federal pump intakes were regularly sampled (Kimmerer 2008; Grimaldo et al. 2009). The FLs of all juvenile Chinook Salmon in these samples were measured, and a subsample of juveniles was selected for nonlethal genetic analysis. Although most juveniles are salvaged between January and June in any given year, we considered a single "migration year" to encompass all juveniles that were salvaged from September of the previous year to August of the year of interest. Due to evidence of

size-biased sampling in some years, we limited most of our analyses to six migration years (2004 and 2006–2010); Kolmogorov–Smirnov and Anderson–Darling *K*-tests performed on pooled monthly FL distributions and on pooled annual sample date distributions for these migration years showed that distributions were not significantly different ($P > 0.05$ for both tests) between the subset of genetically tested juveniles and all salvaged juveniles (no more than 1 month with $P < 0.05$ for FL). However, our analysis of false-positive error rates for juveniles in the winter-run length-at-date range was extended to encompass the full 1996–2010 record because within this limited length range, unbiased sampling occurred during all years. Improper storage of tissue samples collected in 2005 precluded analysis of any samples from that year. Sampling, storage, DNA extraction, and genotyping of salvaged juveniles followed the protocol described by Banks et al. (2000). To determine genetic race assignment and to generate an estimated assignment probability (i.e., probability of correct genetic assignment) for each juvenile, we compared individual genotypes with the Central Valley Chinook Salmon HMSC16 baseline by using Genetic Mixture Analysis software (Kalinowski 2003) or its modified version, ONCOR (Kalinowski 2007).

An evaluation of genetic assignment accuracy performed on adult Chinook Salmon of known phenotypic run (Banks et al. 2014) revealed that Genetic Mixture Analysis and ONCOR software in combination with the HMSC16 baseline generated assignment probabilities that were overestimated and did not correlate well with actual misassignment rates, such that software-generated assignment probabilities were not useful for controlling genetic test error rate in our analysis. Therefore, we used all genetic assignments and qualified our conclusions based on the false-positive error rate of genetic tests for each race, as derived from Banks et al. (2014); the false-positive error rate was calculated as the number of misassigned fish divided by the total number of fish assigned to each race (Linn 2004).

Consistent with current practices at the salvage facilities, we used the modified length criteria for length-at-date assignment (Supplementary Table S.1 in the online version of this article). To visualize (1) juvenile FL conformity to ranges delineated by the length-at-date model and (2) the degree of overlap between races, we organized FL data into biweekly length frequency distributions according to sample month and day (years were combined), and we then overlaid these distributions with the length-at-date boundaries used to separate the races.

We also wanted to test whether FL distributions exhibited a more fundamental overlap between races, beyond merely an overlap in distribution tails. To accomplish this, we compared median FLs between the races within each biweekly period by using the nonparametric Kruskal–Wallis test followed by multiple comparisons with a nonparametric version of Tukey's honestly significant difference test (Siegel and Castellan 1988) as implemented in the R package "pgirmess" (R Development Core Team 2012; Giraudoux 2013). Age-0 and age-1 juveniles were visually distinguished from each other by using biweekly length frequency histograms and were compared separately. However, since early spawning for the winter run can occur soon after late spawning of the previous brood year's late-fall run and because the emigration period of age-0 winter-run juveniles coincides more with the emigration period of age-1 juveniles from the other races than with the emigration of age-0 fish from other races (Figure 1), we also compared the FLs of age-0 winter-run fish with the FLs of age-1 fish from the other races. Comparisons within each biweekly period were performed only for races with sample sizes of 10 or more FLs.

To compare empirical growth rates with the assumed growth rates of the length-at-date model, we used linear regression of $\log_e$(FL, mm) against the sample date of salvaged juveniles for each race and for each migration year; this regression approach was identical to that used in the original development of length-at-date growth rates based on juvenile Chinook Salmon raised in artificial rearing channels (Fisher 1992; Harvey 2011). For the fall, spring, and late-fall runs, which exhibited multiple migrant types, we performed separate regressions for (1) age-1 juveniles (distinguished from age-0 juveniles as previously indicated) and (2) early season fry migrants and late-season parr–smolt migrants within the age-0 class, which exhibited different growth trajectories. The transition point between the growth trajectories of fry migrants and parr–smolt migrants within the age-0 class were distinguished with segmented linear regression of $\log_e$(FL, mm) against salvage date (pooled across years for each run) using the R package "segmented" version 2.15.0 (Muggeo 2003, 2008; R Development Core Team 2012). Segmented linear regression also identified FLs in a transition period between the early season fry migrants and late-season parr–smolt migrants within the age-0 class. These FLs were not used in growth regressions because migrant type could not be distinguished. Growth rate regressions were performed only for sub-data sets containing 10 or more FLs.

The annual false-positive error rate for winter-run length-at-date assignment was calculated in similar fashion as the false-positive error rate for genetic tests. For each migration year, the false-positive error rate was the number of genetic non-winter-run fish that were within the length-at-date range for winter run divided by the total number of juveniles in the winter-run length range. This method for calculating false-positive error differs from the more common statistical approach for type I error rate but is more appropriate for expressing accuracy of the length-at-date approach as applied to the target salvage population (Linn 2004). Before calculating daily false-positive error rate, data were smoothed by averaging both the number of genetic winter-run juveniles and the number of all juveniles in the winter-run length range over the 3 d before

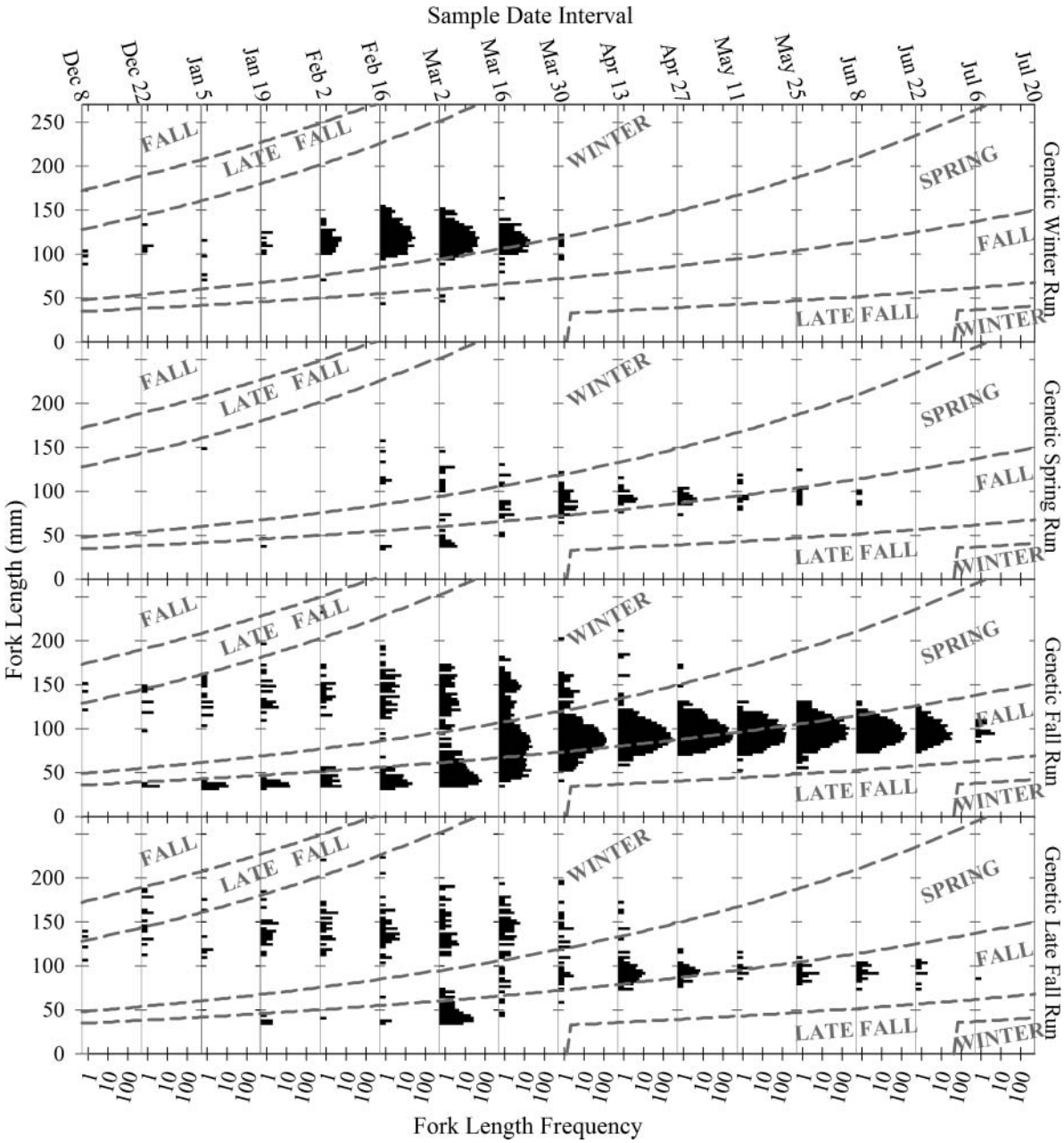

FIGURE 1. Length frequency distributions (mm FL; black bars and text), overlaid with length-at-date size criteria boundaries (gray dashed lines and text), for genetically identified winter, spring, fall, and late-fall Chinook Salmon juveniles (<270 mm) sampled over biweekly intervals at the intake canals for California State Water Project and federal Central Valley Project export facilities located in the inland Sacramento–San Joaquin Delta. Note that FL frequency is depicted on a modified $\log_{10}$ scale and that frequency distributions for most runs spread well beyond the corresponding predicted length-at-date ranges for each biweekly interval (as indicated by the intersection of dashed lines and *y*-axes).

and after each calendar day (i.e., 7-d running average). Daily rates were then averaged across years for each day of the year. All confidence intervals (CIs) for average values presented in figures and text are 95% CIs calculated from the sample from which the average was derived. All other statistical tests were performed in R (R Development Core Team 2012).

RESULTS

During our study years, 11,069 salvaged juvenile Chinook Salmon of unknown origin were assigned to race with genetic tests: 86.7% to the fall run, 7.1% to the winter run, 4.7% to the late-fall run, and 1.4% to the spring run (Table 1). There was substantial overlap of biweekly FL distributions among the

TABLE 1. Number of juvenile Chinook Salmon from each genetically assigned race that were assigned (based on FL) to each length-at-date race. Tissue was nonlethally sampled and FL was measured from fish that were collected (salvaged) at California State Water Project and federal Central Valley Project pump intakes in the Sacramento–San Joaquin Delta during 2004 and 2006–2010.

Length-at-date race assignment[a]	Genetic late-fall run	Genetic winter run	Genetic spring run	Genetic fall run
Late fall	9	0	0	3
Winter	218	749	22	287
Spring	116	56	95	4,629
Fall	193	5	45	4,915

[a] Length-at-date race was assigned using modified size criteria specific to salvage facilities (i.e., criteria were based on a higher assumed winter-run growth rate relative to the original criteria).

four genetic runs throughout the juvenile migration season. In particular, genetic fall-run, late-fall-run, and spring-run fish were broadly distributed across length ranges for all runs such that genetic assignments for nearly half (49%) of all juveniles differed from the corresponding length-at-date assignments (Figure 1). The greatest discrepancy was that 4,777 (47%) genetic fall-run juveniles fell within the spring-run length-at-date range, thus composing 95% of spring-run-length juveniles. Other large discrepancies were the 276 (3%) genetic fall-run fish and 211 (40%) genetic late-fall-run fish that fell within the winter-run length-at-date range, together constituting 39% of winter-run-length juveniles. In addition, 192 (36%) genetic late-fall-run fish fell within the fall-run length-at-date range, and 151 (44%) genetic spring-run individuals fell within either the fall-run or the winter-run length-at-date range.

The only consistent differences in the central tendency of FL distributions were between the winter run and the other runs during the four biweekly intervals from February 2 to March 29, a period in which 97% of the genetic winter-run juveniles were detected in salvage. Median FLs for the winter run were larger than median FLs for age-0 fry migrants from the other runs and were smaller than median FLs for age-1 fall-run and late-fall-run juveniles (Table 2).

Across all years and runs, we performed 12 regressions to estimate the growth rate of non-winter-run age-1 juveniles. Even when α was not corrected for multiple comparisons, only 1 of the 12 regressions exhibited a significant positive trend at $P < 0.05$ (fall run in 2007: growth rate $= 1.37 \times 10^{-3}$ $\log_e$[mm FL]/d; Figure 2). Similarly, only 5 of 15 regressions for non-winter-run parr–smolt migrants had significant FL trends at $P < 0.05$, one of which was negative (range $= -0.75 \times 10^{-3}$ to 7.47×10^{-3} $\log_e$[mm FL]/d), whereas winter-run migrants had two positive and two negative significant FL trends out of the 6 years tested (range $= -2.85 \times 10^{-3}$ to 2.13×10^{-3} $\log_e$[mm FL]/d; $P < 0.05$; Figure 2). Three of the five regressions for fry migrants had significant trends, all of which were positive (range $= 8.54 \times 10^{-3}$ to 21.05×10^{-3} $\log_e$[mm FL]/d; $P < 0.05$; Figure 2). Even among strictly the significant positive FL trends, the average rate of increase for non-winter-run age-1 migrants and age-0 parr–smolt migrants (mean $= 3.82 \times 10^{-3}$ $\log_e$[mm FL]/d; CI $= \pm 2.98 \times 10^{-3}$) was only about half the rate from which length-at-date criteria were derived (6.57×10^{-3} $\log_e$[mm FL]/d). For the winter run, the average of the positive trends (mean $= 1.98 \times 10^{-3}$ $\log_e$[mm FL]/d; CI $= \pm 1.97 \times 10^{-3}$) was less than a quarter of the winter-run growth rate assumed in the length-at-date approach (8.16×10^{-3} $\log_e$[mm FL]/d). In contrast, the average rate of increase for fry migrants (mean $= 15.61 \times 10^{-3}$ $\log_e$[mm FL]/d; CI $= \pm 15.90 \times 10^{-3}$) was more than double the length-at-date-assumed rate for non-winter-run fish (6.57×10^{-3} $\log_e$[mm FL]/d).

The yearly false-positive error rate for length-at-date winter-run assignments from 1996 to 2010 exhibited a downward trend (linear regression: $F_{2, 12} = 12.57$, $P < 0.01$; Figure 3b). Average yearly error rate over this period (mean error rate $=$ 0.56; CI $= \pm 0.11$) was higher than the single error rate (0.47) derived from data pooled across all years (not accounting for unequal distribution of sample sizes between years).

The proportion of genetic non-winter-run juveniles within the winter-run length range varied considerably over the juvenile migration season and between years as depicted by the CIs of daily false-positive error (Figure 4b). From December 1 through approximately the third week in January, the average daily false-positive error rates were highly variable, although on average they were over 0.50. Thereafter, average error rate declined, falling below 0.50 from the second week of February through the second week of March (a period of 5 weeks), and then rose rapidly to 1.0 by mid-April. However, the lower 95% confidence limit fell below 0.50 from the first week of February through the third week of March (a period of 7 weeks).

DISCUSSION

Using genetics as a validation tool, we have now characterized the uncertainty of the length-at-date method for assigning race to individual juvenile Chinook Salmon, particularly with respect to winter-run juveniles. The two central assumptions of the length-at-date approach (i.e., segregated FL ranges between races and a constant shared growth rate among races) were not supported by the FL data for genetically identified

TABLE 2. Comparison of median FL between genetically identified races of juvenile Chinook Salmon (F = fall run; L = late-fall run; W = winter run; S = spring run) sampled within the same biweekly date ranges (month and day) during 2004 and 2006–2010 at California State Water Project and federal Central Valley Project pumping plants in the Sacramento–San Joaquin Delta. Young-of-the-year (age-0) winter-run juveniles were compared with (1) age-0 juveniles of other races and (2) age-1 and older (age-1+) juveniles of other races (Kruskal–Wallis median test followed by multiple comparison tests where applicable). Races with fewer than 10 FLs in a biweekly group were not considered. Significantly different medians for races within each comparison are denoted by different lowercase letters.

Date range	Genetic race	*N*	Median FL (mm)	χ^2	df	*P*
Age-0 winter run and age-0 non-winter run						
Feb 2–15	F z	23	42	42.803	1	<0.001
	W y	39	115			
Feb 16–Mar 1	F z	74	39	168.640	1	<0.001
	W y	241	119			
Mar 2–15	F z	330	44	611.805	2	<0.001
	L z	111	42			
	W y	380	117			
Mar 16–29	F z	301	78	238.261	3	<0.001
	L z	13	77			
	W y	13	80			
	S y	126	115			
Mar 30–Apr 12	F	974	88	0.392	2	0.822
	L	12	89			
	S	33	90			
Apr 13–26	F	1,781	91	2.641	2	0.267
	L	63	92			
	S	19	92			
Apr 27–May 10	F	2,053	93	0.083	2	0.959
	L	32	93.5			
	S	18	93			
May 11–24	F	1,180	95	0.064	1	0.800
	S	10	94.5			
May 25–Jun 7	F y	1,494	98	8.751	1	0.003
	L z	21	92			
Jun 8–21	F	1,021	95	1.458	1	0.227
	L	20	92			
Age-0 winter run and age-1+ non-winter run						
Jan 19–Feb 1	F	23	135	0.0709	1	0.790
	L	24	139.5			
Feb 2–15	F y	21	142	43.770	2	<0.001
	L y	26	144			
	W z	39	115			
Feb 16–Mar 1	F y	55	145	96.739	2	<0.001
	L y	40	138			
	W z	241	119			
Mar 2–15	F y	63	135	114.574	3	<0.001
	L y	43	136			
	W z	12	117.5			
	S z	380	117			
Mar 16–29	F y	54	148	133.139	2	<0.001
	L y	49	146			
	W z	126	115			
Mar 30–Apr 12	F	32	143.5	0.885	1	0.347
	L	20	142.5			

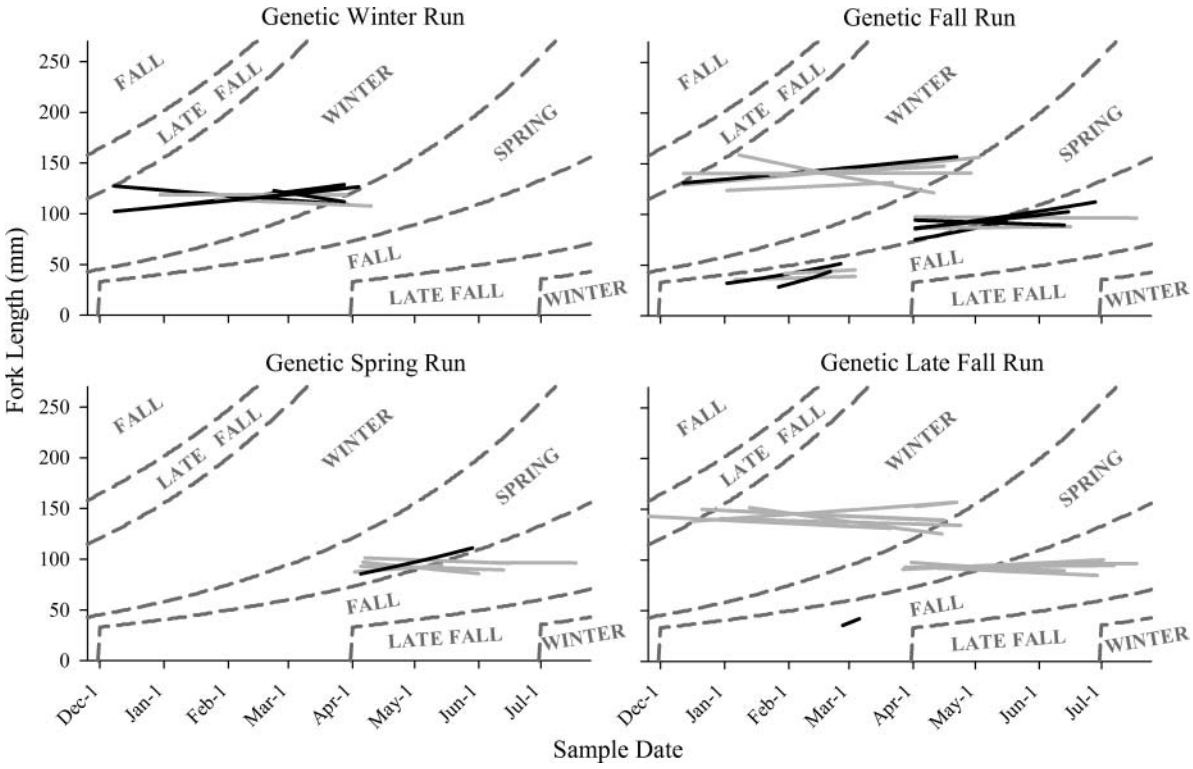

FIGURE 2. Fork length–calendar date regression lines for 2004 and 2006–2010 (solid black = $P < 0.05$; solid gray = $P > 0.05$), overlaid with length-at-date size criteria boundaries (dashed gray lines and gray text), for genetically identified Chinook Salmon juveniles (<270 mm). For the spring, fall, and late-fall runs, separate regressions were performed for age-1 juveniles (upper left in each panel), age-0 fry migrants (lower left in each panel), and age-0 parr–smolt migrants (right side of each panel) for years with 10 or more data points. Length-at-date size criteria boundaries (gray dashed lines and text) are equivalent to predicted apparent growth rates.

juveniles. Fork length ranges of the individual runs were not segregated and were widely distributed across length-at-date categories (Table 1; Figure 1), and the FL trends for all runs did not consistently exhibit the constant growth rates used to generate length-at-date criteria (Figure 2). In fact, there was so little distinction among the FL distributions of juvenile spring-run, fall-run, and late-fall-run Chinook Salmon that the median FL did not significantly differ among these runs (Table 2). The lack of distinction between FL distributions, coupled with the lack of consistent FL trend (i.e., growth rate), indicates that a simple refinement of length criteria based on modified growth rates—or even based on length ranges fitted to genetically identified races—will not produce more accurate run assignments.

Owing to the early focus on the winter run by the Central Valley salmon genetics program and because genetic tests for assigning fish to the winter run are highly accurate (genetic test error rates are <1%; Banks et al. 2014), the genetic assignment record for the winter run is the longest and most reliable among the four Central Valley races, and thus genetic validation of the length-at-date method is most robust for this race. Over the period 1996–2010, the annual proportion of genetic non-winter-run juveniles within the winter-run length range varied substantially from 23% to 89%, with a generally downward trend that was driven primarily by increasing numbers of salvaged genetic winter-run fish.

Within each year, genetic winter-run juveniles exhibited the most concentrated and segregated salvage timing of the four races. Relative to the other races, genetic winter-run fish migrated through the Sacramento–San Joaquin Delta earlier and within a shorter time frame, primarily between February 1 and April 1 (Figure 1). Although the majority of winter-run-length fish were also sampled at the salvage facilities during this time frame, the proportion of genetic non-winter run among these winter-run-length fish—and therefore the false-positive error rate—was lowest and most consistent during this period (Figure 4). However, before February 1 and after April 1, well over 50% and often closer to 80% of salvaged juveniles in the winter-run length range were not genetic winter run, thus inflating the false-positive error rate. In addition, pulses of winter-run emigrants during December and January of some years resulted in a highly variable error rate in those months.

Another dimension of management concern regarding the accuracy of race assignment is the false-negative error rate. Because the calculation of false-negative error rate relies on equal detection probability of genetic winter-run juveniles across the length-at-date ranges for all races, it was only

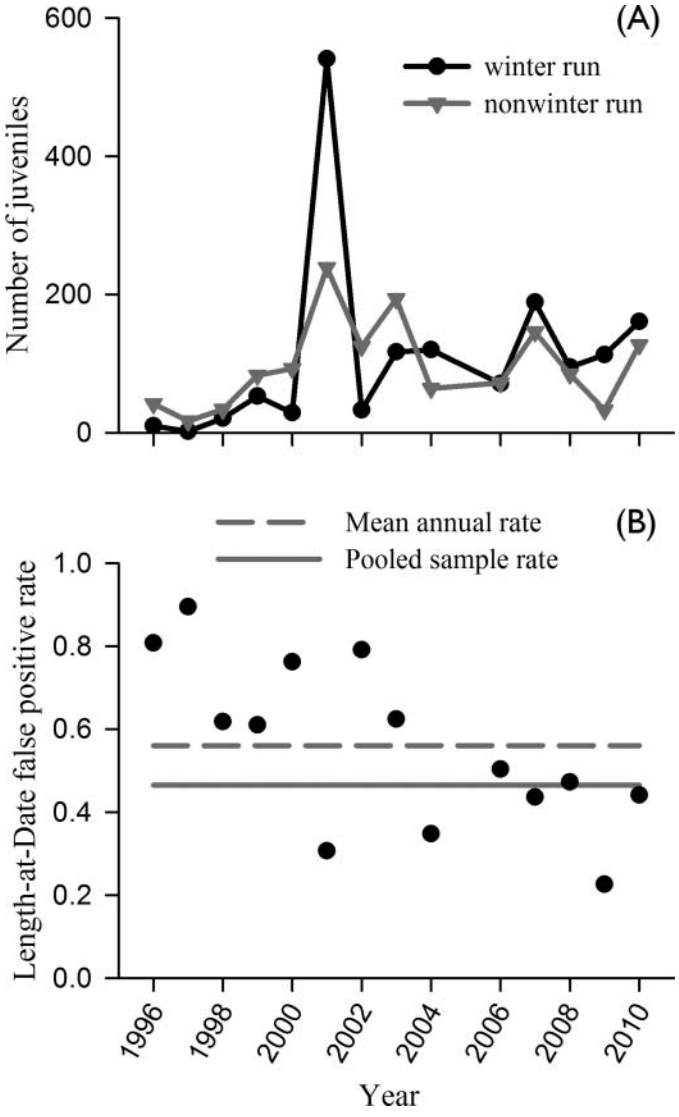

FIGURE 3. **(A)** Number of genetic winter-run fish (black) and genetic non-winter-run fish (gray) among genetically tested juveniles in the winter-run length-at-date range for Chinook Salmon salvaged at state and federal water projects; and **(B)** yearly proportion of genetic non-winter-run fish in the winter-run length-at-date range (i.e., false-positive error rate). The dashed horizontal line is the false-positive error rate calculated as an average of annual error rates (circles); the solid horizontal line is the single error rate calculated from data pooled across all years.

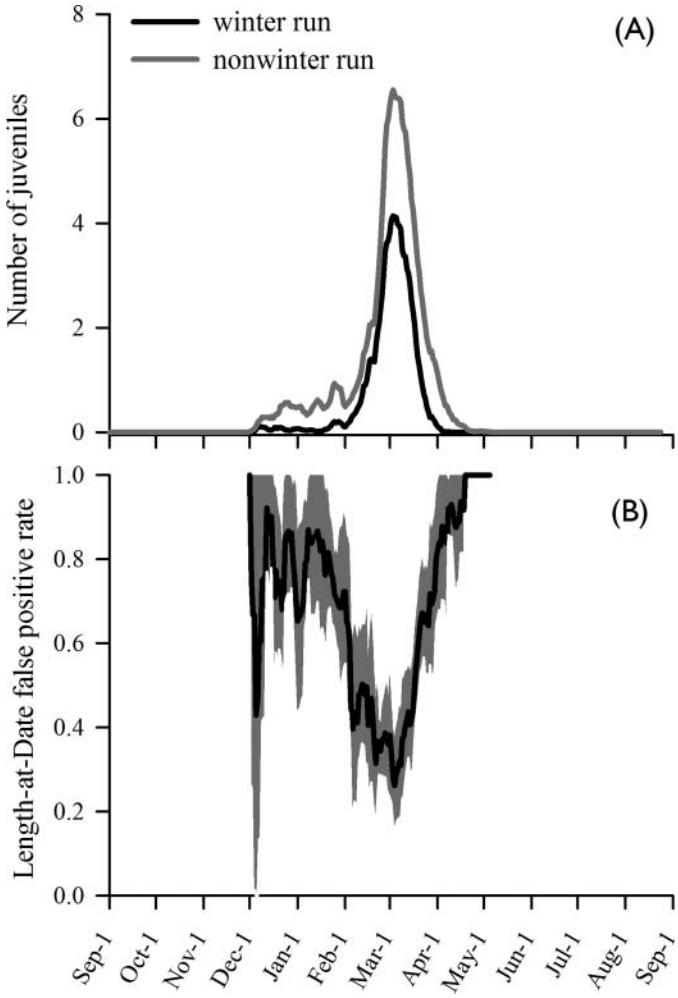

FIGURE 4. For genetically tested juvenile Chinook Salmon salvaged at state and federal water projects during 1996–2010: **(A)** average daily count of all juveniles (gray line) and genetic winter-run juveniles (black line) in the winter-run length-at-date size range; and **(B)** the average daily proportion of juveniles in the winter-run length-at-date size range that were identified as not genetic winter run (i.e., false-positive error rate). Daily count was smoothed with a 7-d running average before averaging across years. False-positive rate in panel B (black line) is shown with the 95% confidence interval (gray-shaded area).

appropriate to examine genetic assignments from 2004 and later years, when genetic samples were not biased by size-selective sampling. Although a large proportion of genetic non-winter-run fish occurred within the winter-run length range (as reflected by the false-positive rate discussed above), the majority of genetic winter-run individuals were also effectively encapsulated within the winter-run length criteria. Between 2004 and 2010, only 8% of salvaged genetic winter-run fish occurred outside the winter-run length criteria; this is double the 4% false-negative rate reported by Hedgecock (2002) but is still below 10%. The success of the length-at-date method in identifying genetic winter run did not appear to be at the cost of misidentifying large numbers of fish from the other races, as the FLs of the other genetic runs were widely distributed across the winter-run length range and broadly overlapped the genetic winter-run size distributions (Figure 1). In other words, another slight shift in the borders of the winter-run length range would probably not have substantially altered the false-negative error rate.

In a system such as the Central Valley, where protected races must be distinguishable from coexisting unprotected races and where no single tool can distinguish between them, a hybrid approach may provide the most reliable estimates for

monitoring and take assessment. A hybrid approach is currently in use at the salvage facilities, where winter-run take is based on length-at-date assignment modified by an assumed annual 50% false-positive error rate (NMFS 2009). However, incorporation of genetic analyses and updated information on the accuracy of the length-at-date method can potentially improve this hybrid system. Genetic testing could be used to monitor and assess take of the most accurately identifiable stocks (i.e., winter-run and select spring-run stocks). During the lag time between field sampling and genetic assignment, which currently varies from several days to many weeks, the interim take of winter-run fish could be estimated with a modified length-at-date approach by using a seasonally adjustable false-positive error rate (Figure 4b) and by incorporating error rate uncertainty into take assessments. Alternative genetic approaches may be applied for protected stocks that are not identifiable with current Central Valley genetic baselines, such as proportions of the spring-run population that cannot be separated from the formerly allopatric fall run due to limited recent hybridization. One such approach is parental-based genetic tests that link juveniles directly to individual spawners that have been sampled in the field (i.e., to their parents; Anderson and Garza 2006). However, parental-based genetic testing requires rigorous estimation of both juvenile production and the proportion of the adult population that is genetically analyzed—expensive and labor-intensive processes that will limit the use of this method in situations other than hatcheries.

Although the growth rates of juvenile Chinook Salmon salvaged at the fish screens were derived in the same manner as the length-at-date growth rates, it is important to note that growth was not actual growth. More accurately, the FL of salvaged fish represented juvenile length at the point of emigration from freshwater. As the most intensive program for sampling fish communities in the Sacramento–San Joaquin Delta, salvage is arguably the most comprehensive existing record of juvenile Chinook Salmon presence and FL distribution at emigration. The most marked feature of this distribution was a general convergence of fall-run, late-fall-run, and spring-run FLs to a narrow and constant range of 80–110 mm after mid-April (Figure 1). Before mid-April, winter-run juveniles and (to a lesser extent) age-1 juveniles from the other runs also exhibited narrow-range, nontrending FL distributions through time (Figures 1, 2). These distributions suggest that within the 2–4-month emigration period for each migrant type, the cues for juvenile emigration from the delta may depend more on a juvenile size or age threshold than on calendar date or environmental cues. In addition, the broad and overlapping FL ranges of the spring, fall, and late-fall runs demonstrated a diversity of juvenile emigration timing and length within all three runs. Recent analyses suggest that a portfolio of life history strategies historically existed within the Central Valley runs, lending resilience to salmon populations in California's variable and unpredictable climate (Lindley et al. 2009; Carlson and Satterthwaite 2011). Fish screen salvage data support otolith studies (Miller et al. 2010) indicating that a range of alternative emigration strategies persist despite hatchery and water management activities that strongly favor a narrowing of life history diversity (Lindley et al. 2009).

Any effort to replace the length-at-date approach will have to contend with the same issue that originally led to adoption of this method; there is no alternative approach currently available that will fulfill the requirements of expedient, nonlethal identification with low false-positive and false-negative error rates for all protected races. Genetic tests are not a panacea for problematic race assignment. Current genetic tests cannot distinguish between fall, late-fall, and spring runs at an acceptable level of accuracy, and any solution that incorporates genetic testing will need to address the lag time between sample collection and the availability of genetic test results. Nevertheless, for management of Central Valley Chinook Salmon and water resources, these genetic analyses offer a substantial improvement over historical race identification methods based on growth models, and we recommend that genetic tools be used at least as a supplemental approach to race identification and management. Based on the successful application of genetic tools to other salmon stocks and other rare fishes (e.g., Green Sturgeon *Acipenser medirostris*: Israel et al. 2004), these approaches will probably be increasingly valuable in the management of mixed stocks, both for direct identification of protected populations and as a tool to assess the uncertainty of nongenetic monitoring strategies.

ACKNOWLEDGMENTS

Funding was provided by the California Department of Water Resources (CDWR) and the Interagency Ecological Program (IEP) for the San Francisco Estuary (information at www.water.ca.gov/iep). Sheila Greene developed and managed the genetics program for CDWR from 1994 to 2011. Members of the IEP Salmon Genetics Project Work Team, two anonymous reviewers, and especially J. Louise Conrad and Ted Sommer provided guidance and valuable comments that substantially improved this manuscript.

REFERENCES

Anderson, E. C., and J. C. Garza. 2006. The power of single-nucleotide polymorphisms for large-scale parentage inference. Genetics 172:2567–2582.

Banks, M. A., and D. P. Jacobson. 2004. Which genetic markers and GSI methods are more appropriate for defining marine distribution and migration of salmon? North Pacific Anadromous Fish Commission Technical Note 5:39–42.

Banks, M. A., D. P. Jacobson, I. Meusnier, C. A. Greig, V. K. Rashbrook, W. R. Ardren, C. T. Smith, J. Bernier-Latmani, J. Van Sickle, and K. G. O'Malley. 2014. Testing advances in molecular discrimination among Chinook Salmon life histories: evidence from a blind test. Animal Genetics 45:412–420.

Banks, M. A., V. K. Rashbrook, M. J. Calavetta, C. A. Dean, and D. Hedgecock. 2000. Analysis of microsatellite DNA resolves genetic structure and diversity of Chinook Salmon (*Oncorhynchus tshawytscha*) in California's Central Valley. Canadian Journal of Fisheries and Aquatic Sciences 57:915–927.

Brown, L. R., W. Kimmerer, and R. Brown. 2009. Managing water to protect fish: a review of California's environmental water account, 2001–2005. Environmental Management 43:357–368.

Burgman, M. 2005. Risks and decisions for conservation and environmental management. Cambridge University Press, Cambridge, U.K.

Busacker, G. P., I. R. Adelman, and E. M. Goolish. 1990. Growth. Pages 363–387 *in* C. B. Schreck and P. B. Moyle, editors. Methods for fish biology. American Fisheries Society, Bethesda, Maryland.

Carlson, S. M., and W. H. Satterthwaite. 2011. Weakened portfolio effect in a collapsed salmon population complex. Canadian Journal of Fisheries and Aquatic Sciences 68:1579–1589.

CDFA (California Department of Food and Agriculture). 2013. California agricultural statistics review, 2012–2103. CDFA, Sacramento. Available: http://www.cdfa.ca.gov/statistics/. (October 2014).

del Rosario, R. B., Y. J. Redler, K. Newman, P. L. Brandes, T. Sommer, K. Reece, and R. Vincik. 2013. Migration patterns of juvenile winter-run sized Chinook Salmon (*Onchorhynchus tschawytscha*) through the Sacramento–San Joaquin delta. San Francisco Estuary and Watershed Science 11(1).

Fisher, F. W. 1992. Chinook Salmon, *Oncorhynchus tshawytscha*, growth and occurrence in the Sacramento–San Joaquin River system. California Department of Fish and Game, Inland Fisheries Division, draft office report, Redding.

Gillespie, G. R., M. P. Scroggie, J. D. Roberts, H. G. Cogger, M. J. Mahony, and K. R. McDonald. 2011. The influence of uncertainty on conservation assessments: Australian frogs as a case study. Biological Conservation 144:1516–1525.

Giraudoux, P. 2013. pgirmess: data analysis in ecology. R package version 1.5.8. Available: http://perso.orange.fr/giraudoux. (October 2014).

Grimaldo, L. F., T. Sommer, N. Van Ark, G. Jones, E. Holland, P. B. Moyle, B. Herbold, and P. Smith. 2009. Factors affecting fish entrainment into massive water diversions in a tidal freshwater estuary: can fish losses be managed? North American Journal of Fisheries Management 29:1253–1270.

Harvey, B. N. 2011. Length-at-date criteria to classify juvenile Chinook Salmon in the California Central Valley: development and implementation history. Interagency Ecological Program Newsletter 24(3). Available: http://www.water.ca.gov/iep/newsletters/2011/IEPNewsletterFinalSummer2011.pdf. (October 2014).

Hedgecock, D.. 2002. Microsatellite DNA for the management and protection of California's Central Valley Chinook Salmon (*Oncorhynchus tshawytscha*). University of California–Davis, Bodega Marine Laboratory, Final Report to the California Department of Water Resources, Amendment to Agreement B-59638, Bodega.

Israel, J. A., M. Blumberg, J. F. Cordes, and B. May. 2004. Geographic patterns of genetic differentiation among western U.S. collections of North American Green Sturgeon (*Acipenser medirostris*). North American Journal of Fisheries Management 24:922–931.

Kalinowski, S. T. 2003. Genetic mixture analysis 1.0. Montana State University, Department of Ecology, Bozeman. Available: http://www.montana.edu/kalinowski. (October 2014).

Kalinowski, S. T. 2007. ONCOR: a computer program for genetic stock identification. Montana State University, Department of Ecology, Bozeman. Available: http://www.montana.edu/kalinowski/Software/ONCOR.htm. (October 2014).

Katz, J., P. B. Moyle, R. M. Quinones, J. A. Israel, and S. Purdy. 2012. Impending extinction of salmon, steelhead, and trout (Salmonidae) in California. Environmental Biology of Fishes 96:1169–1186.

Kimmerer, W. J. 2008. Losses of Sacramento River Chinook Salmon and Delta Smelt to entrainment in water diversions in the Sacramento–San Joaquin delta. San Francisco Estuary and Watershed Science 6(2).

Lindley, S. T., C. B. Grimes, M. S. Mohr, W. Peterson, J. Stein, J. T. Anderson, L. W. Botsford, D. L. Bottom, C. A. Busack, T. K. Collier, J. Ferguson, J. C. Garza, A. M. Grover, D. G. Hankin, R. G. Kope, P. W. Lawson, A. Low, R. B. MacFarlane, K. Moore, M. Palmer-Zwahlen, F. B. Schwing, J. Smith, C. Tracy, R. Webb, B. K. Wells, and T. H. Williams. 2009. What caused the Sacramento River fall Chinook stock collapse? NOAA Technical Memorandum NMFS-SWFSC-447.

Linn, S. 2004. A new conceptual approach to teaching the interpretation of clinical tests. Journal of Statistics Education [online serial] 12(3).

McGowan, C. P., M. C. Runge, and M. A. Larson. 2011. Incorporating parametric uncertainty into population viability analysis models. Biological Conservation 144:1400–1408.

Miller, J. A., A. Gray, and J. Merz. 2010. Quantifying the contribution of juvenile migratory phenotypes in a population of Chinook Salmon *Oncorhynchus tshawytscha*. Marine Ecology Progress Series 408:227–240.

Moore, J. L., and M. C. Runge. 2012. Combining structured decision making and value-of-information analyses to identify robust management strategies. Conservation Biology 26:810–820.

Muggeo, V. M. R. 2003. Estimating regression models with unknown breakpoints. Statistics in Medicine 22:3055–3071.

Muggeo, V. M. R. 2008. segmented: an R Package to fit regression models with broken-line relationships. R News 8(1). Available: http://cran.r-project.org/doc/Rnews/. (October 2014).

NMFS (National Marine Fisheries Service). 1990. Endangered and threatened species; Sacramento River winter-run Chinook Salmon; final rule. Federal Register 55:214(5 November 1990):46515.

NMFS (National Marine Fisheries Service). 1994. Endangered and threatened species; threatened status for two Chinook Salmon evolutionarily significant units (ESUs) in California; final rule. Federal Register 59:2(4 January 1994):440, 450.

NMFS (National Marine Fisheries Service). 1999. Endangered and threatened species; threatened status for two Chinook Salmon evolutionarily significant units (ESUs) in California; final rule. Federal Register 64:179(16 September 1999):50394–50415.

NMFS (National Marine Fisheries Service). 2009. Biological opinion and conference opinion on the long-term operations of the Central Valley Project and State Water Project. Endangered Species Act Section 7 consultation. National Ocean and Atmospheric Administration, National Marine Fisheries Service, Southwest Region, Long Beach, California.

R Development Core Team. 2012. R: a language and environment for statistical computing. R Foundation for Statistical Computing, Vienna.

Ricker, W. E. 1942. The rate of growth of Bluegill sunfish in lakes of northern Indiana. Indiana University, Department of Conservation, Indianapolis.

Siegel, S., and N. J. Castellan Jr. 1988. Nonparametric statistics for the behavioral sciences, 2nd edition. McGraw-Hill, New York.

Sommer, T., C. Armor, R. Baxter, R. Breuer, L. Brown, M. Chotkowski, S. Culberson, F. Feyrer, M. Gingras, B. Herbold, W. Kimmerer, A. Mueller-Solger, M. Nobriga, and K. Souza. 2007. The collapse of pelagic fishes in the upper San Francisco Estuary. Fisheries 32:270–277.

Williams, J. G. 2006. Central Valley salmon: a perspective on Chinook and steelhead in the Central Valley of California. San Francisco Estuary and Watershed Science 4(3):Article 2.

Yoshiyama, R. M., F. W. Fisher, and P. B. Moyle. 1998. Historical abundance and decline of Chinook Salmon in the Central Valley region of California. North American Journal of Fisheries Management 18:487–521.

NOAA Technical Memorandum NMFS

JULY 2014

LIFE CYCLE MODELING FRAMEWORK FOR SACRAMENTO RIVER WINTER-RUN CHINOOK SALMON

Noble Hendrix[1]
Anne Criss[2,3]
Eric Danner[3]
Correigh M. Greene[4]
Hiroo Imaki[4]
Andrew Pike[2,3]
Steven T. Lindley[3]

[1]QEDA Consulting, LLC
4007 Densmore Ave. N
Seattle, WA 98103

[2]Institute of Marine Science
University of California, Santa Cruz
1156 High St.
Santa Cruz, CA 95064

[3]National Marine Fisheries Service
Southwest Fisheries Science Center
Fisheries Ecology Division
110 Shaffer Road
Santa Cruz, CA 95060

[4]National Marine Fisheries Service
Northwest Fisheries Science Center
2725 Montlake Blvd. East
Seattle, WA 98112-2097

NOAA-TM-NMFS-SWFSC-530

U. S. DEPARTMENT OF COMMERCE
National Oceanic and Atmospheric Administration
National Marine Fisheries Service
Southwest Fisheries Science Center

The National Oceanic and Atmospheric Administration (NOAA), organized in 1970, has evolved into an agency that establishes national policies and manages and conserves our oceanic, coastal, and atmospheric resources. An organizational element within NOAA, the Office of Fisheries, is responsible for fisheries policy and the direction of the National Marine Fisheries Service (NMFS).

In addition to its formal publications, the NMFS uses the NOAA Technical Memorandum series to issue informal scientific and technical publications when complete formal review and editorial processing are not appropriate or feasible. Documents within this series, however, reflect sound professional work and may be referenced in the formal scientific and technical literature.

NOAA Technical Memorandum NMFS
This TM series is used for documentation and timely communication of preliminary results, interim reports, or special purpose information. The TMs have not received complete formal review, editorial control, or detailed editing.

JULY 2014

LIFE CYCLE MODELING FRAMEWORK FOR SACRAMENTO RIVER WINTER-RUN CHINOOK SALMON

Noble Hendrix[1]
Anne Criss[2,3]
Eric Danner[3]
Correigh M. Greene[4]
Hiroo Imaki[4]
Andrew Pike[2,3]
Steven T. Lindley[3]

[1]QEDA Consulting, LLC
4007 Densmore Ave. N
Seattle, WA 98103

[2]Institute of Marine Science
University of California, Santa Cruz
1156 High St.
Santa Cruz, CA 95064

[3]National Marine Fisheries Service
Southwest Fisheries Science Center
Fisheries Ecology Division
110 Shaffer Road
Santa Cruz, CA 95060

[4]National Marine Fisheries Service
Northwest Fisheries Science Center
2725 Montlake Blvd. East
Seattle, WA 98112-2097

NOAA-TM-NMFS-SWFSC-530

U.S. DEPARTMENT OF COMMERCE
Penny S. Pritzker, Secretary of Commerce
National Oceanic and Atmospheric Administration
Dr. Kathryn D. Sullivan, Acting Administrator
National Marine Fisheries Service
Eileen Sobeck, Assistant Administrator for Fisheries

Abstract

In this document, we describe a strategy for quantitatively evaluating how Federal Central Valley Project (CVP) and California State Water Project (SWP) management actions affect Central Valley Chinook salmon populations. Examples of management actions include changes in water project operations, addition or removal of barriers, and a variety of habitat restoration initiatives. The analytical framework consists of linking and applying hydrological, hydraulic, water quality, and salmon population models.

The hydrological model CALSIM II describes how water resource management determines instream flows. The hydraulic models HEC-RAS and DSM2 translate these flows into depths and velocities that partly determine the capacity of riverine and estuarine habitats. Various water quality models for temperature, salinity, and potentially other parameters also determine the quantity and quality of freshwater and estuarine habitats. Finally, a stage-structured population dynamics model (also known as a life cycle model) links the habitat information to density-dependent stage transitions (describing movement, survival, and reproduction) that drive the dynamics of salmon populations.

We are developing the life cycle model in phases with the initial version focusing on winter-run Chinook. Survival in the delta will be modeled primarily relying on empirical relationships between the environment (flows, exports, and temperature) and survival of juvenile salmon. In subsequent work, salmon survival through the delta will be modeled by tracking the predicted movements of individual salmon based on DSM2's Particle Tracking Model (PTM). We will also add a hatchery component, evaluate additional winter-run management scenarios, and expand the model to evaluate spring-run and fall-run Chinook under various management scenarios.

I. Introduction

California depends on state and federal water projects that provide large scale flood control, water storage, and water transport. The Central Valley water project facilities (including reservoirs, engineered channels, flood bypasses, pumps, and canals) and their operations have radically altered the river systems upon which Chinook salmon and other anadromous fishes depend. Balancing competing desires for fisheries, flood control, water supply and other ecosystem goods and services is a durable natural resource management challenge. The ongoing efforts to develop and approve new water project operating plans and the Bay Delta Conservation Plan (BDCP) require the National Marine Fisheries Service (NMFS) to evaluate how complex and interacting management actions affect salmon populations. This document describes a salmon population dynamics model and supporting hydrological, hydraulic, and water quality models that together form a framework for analyzing the effects of complex water management, habitat restoration, and climate change scenarios on salmon populations. The models are developed for the Central Valley but could be modified for use with other salmon species and in other rivers.

II. Structure of the Analytical Framework

Overview

Our general approach is to link existing physical models to a stage-structured life cycle model through stage-transition parameters that are a function of the environment (as described by the physical models). In this section, we briefly describe the life cycle model and the supporting physical models.

Life Cycle Model

Typically, stage-structured salmon life cycle models define stages (or states) by development, e.g., egg, juvenile, adult. Transition among states reflects the possibly density-dependent processes of survival, maturation and reproduction. In the model described here, we consider both developmental stage and geographic location to define the state (e.g., fry in the mainstem river, fry in a large floodplain). Transitions among states then reflect not only survival and reproduction but also movement among habitat areas.

State transitions can be flexibly described by an extension of the Beverton-Holt stock-recruitment relationship that allows (but does not require) individuals exceeding the capacity of a habitat to move downstream, rather than die in that habitat (Greene and Beechie 2004). The three parameters describing state transitions (survival, capacity, and movement rate) are viewed as potential functions of environmental conditions, such as flow, water temperature, and the amount of suitable habitat (e.g., depth and velocities within the tolerance of the life stage in question).

Because growth prospects differ among habitats, alterations to habitats may not only change the survival of a certain developmental stage of salmon, but also patterns of rearing, migration, and size at ocean entry (i.e., life history diversity). Because size at and time of ocean entry can be important determinants of survival, effects on patterns of life history expression may have important consequences at the population level. Our model can capture such effects.

There is an important trade-off between realism and tractability when deciding how finely to divide the stages in a stage-structured model. Each stage transition requires one or more parameters, and as the dimensionality and resolution of stage variables increases, the model complexity and data requirement increase geometrically. The model needs to be complex enough to address the questions motivating its development, but no more. It is also a good strategy to start simple and add complexity only as necessary. In this work, we begin with developmental stages of eggs, fry, smolts, ocean sub-adults, and mature adults, and geographic states of the mainstem river, floodplain, delta, bays, and ocean (Figure 1).

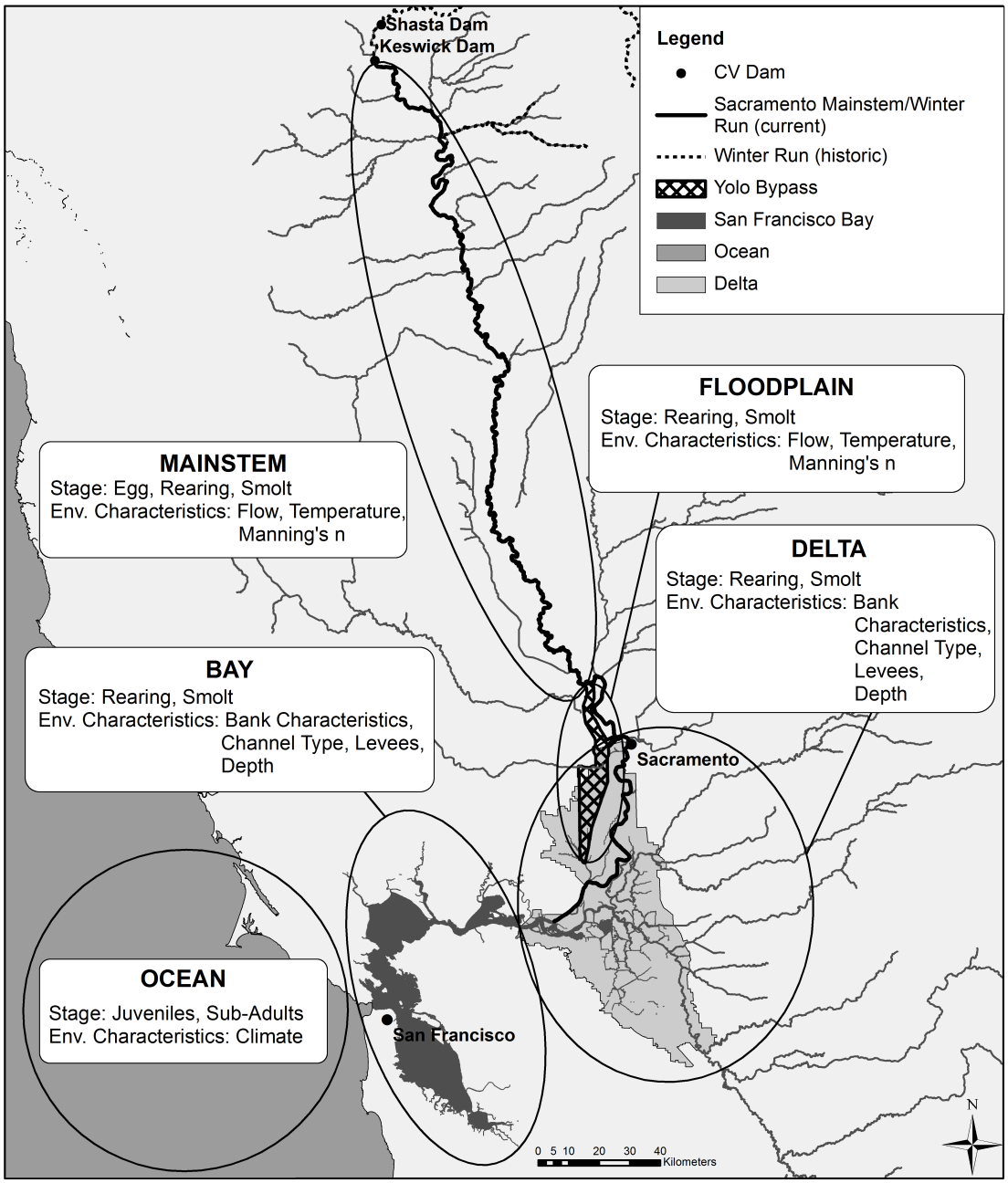

Figure 1. Geographic distribution of Chinook life stages and examples of environmental characteristics that influence survival.

Linking Management Actions to the Salmon Response

Central Valley water management goals and constraints determine the project operations (Figure 2). For example, a management goal might be to increase the water flow in a certain portion of the river to provide conditions suitable for the listed salmonids present. This goal would in turn determine a specific project operation or suite of project operations, such as releasing water from a reservoir.

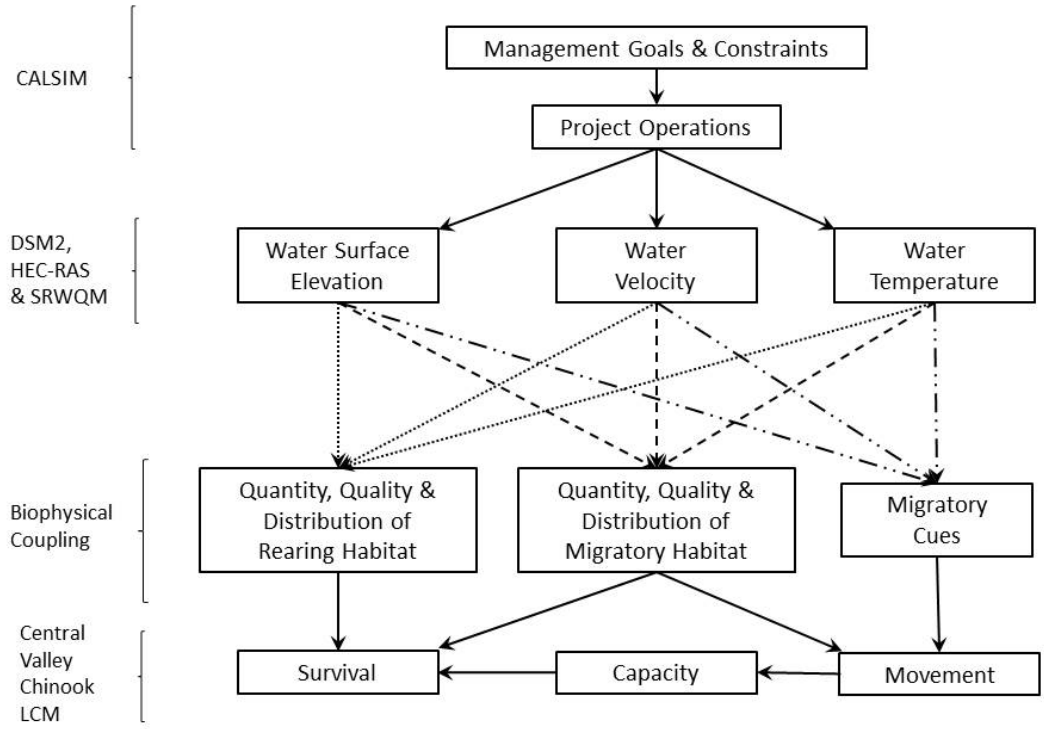

Figure 2. Conceptual model of how water project management goals and constraints influence the movement and survival of salmon through effects on hydrology, hydraulics, and water quality. The labeling along the left side of the diagram identifies corresponding model components.

The quantity and quality of rearing and migratory habitat are viewed as key drivers of reproduction, survival, and migration of freshwater life stages. Various life stages have velocity, depth, and temperature preferences and tolerances, and these factors are influenced by water project operations and climate.

Hydrology (the amount and timing of flows) will be modeled with the California Simulation Model II (CALSIM II). Hydraulics (depth and velocity) and water quality will be modeled with the Delta Simulation Model II (DSM2) and its water quality sub-model QUAL, the Hydrologic Engineering Center's River Analysis System (HEC-RAS), the U.S. Bureau of Reclamation's (USBR) Sacramento River Water Quality Model (SRWQM), and other temperature models. Many of the stage transition equations describing the salmon life cycle (detailed in Section III) are directly or indirectly functions of water quality, depth, or velocity, thereby linking management actions to the salmon life cycle. The combination of models and the linkages among them form a framework for analyzing alternative management scenarios (Figure 3). In the following section, we briefly review the physical models before describing the life cycle model in detail.

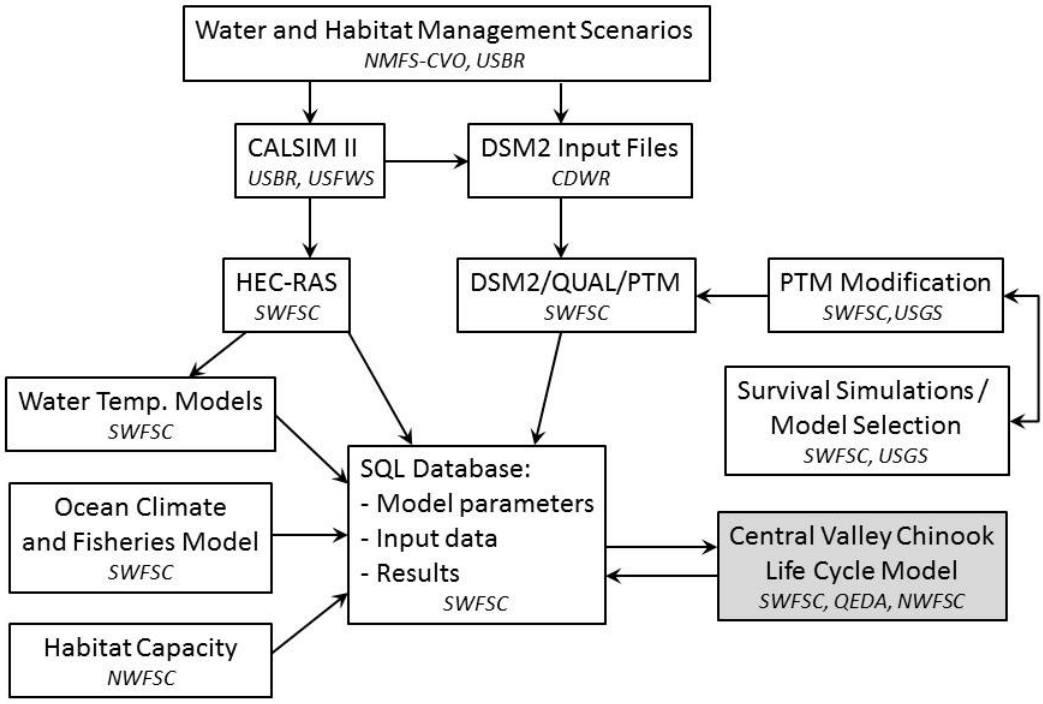

Figure 3. Schematic of the computation framework.

Submodels Used in the Life Cycle Model

CALSIM II

CALSIM II is a quantitative hydrologic planning model developed by the California Department of Water Resources (CDWR) and the USBR. It simulates the SWP and the CVP operations and flows in tributaries to the Sacramento-San Joaquin Delta. CALSIM II uses optimization techniques to route water through a CVP-SWP systems network representation. The model operates on a monthly time-step covering water years 1922 to 2003. Using historical rainfall and runoff data, the model simulates the operation of the current water resources infrastructure in the Sacramento and San Joaquin river basins on a month-to-month basis during this 82-year period. The model can also forecast future scenarios in which operational rules, climate, land use, infrastructure, and water demands are changed.

HEC-RAS

HEC-RAS is a model developed by the U.S. Army Corps of Engineers (USACE) to simulate one-dimensional hydrodynamics for riverine systems. HEC-RAS can calculate water stages, flows, and velocities for both steady and unsteady flow conditions. Inputs to the model consist of a series of river cross-sections (i.e., a bathymetric template) upon which the flow-routing and shallow water equations are solved. HEC-RAS is a widely-used, well-documented, and proven hydrodynamic model. CDWR conducted a comprehensive cross-section survey, which yielded a fully-calibrated HEC-RAS setup for the Sacramento River and major tributaries and canals for the fluvial portion of the system. We intend to downscale or disaggregate the monthly flows into a finer timescale to capture sub-

monthly flow effects, which are not apparent in monthly means. This is important for determining the degree of inundation of the Yolo Bypass.

DSM2

DSM2 is a one-dimensional mathematical model used for the simulation of hydrodynamics, water quality and particle tracking in a network of riverine or estuarine channels. It is based on the same physical principles as HEC-RAS, but unlike HEC-RAS, it is preconfigured to model the tidally-driven circulation of the Delta. DSM2 can calculate water stages, flows, velocities, and mass transport processes for conservative and non-conservative constituents (e.g., salts, water temperature, dissolved oxygen, etc.). DSM2 can also simulate the transport of neutrally buoyant individual particles. We are modifying the particle tracking portion of the model to incorporate salmon swimming behaviors so that we can model fish movement and survival within the Delta.

Water Temperature Models

SRWQM was developed to simulate mean daily reservoir and river temperatures at Shasta, Trinity, Lewiston, Whiskeytown, Keswick, and Black Butte reservoirs and the Trinity River, Clear Creek, the upper Sacramento River from Shasta Dam to Knights Landing, and Stony Creek (USBR 2008). SRWQM uses long-term operational scenarios (using CALSIM II results) and predicts mean monthly and mean daily downstream water temperatures based on CVP-SWP operations. The model employs a heat-budget approach by calculating rates of heat transfer at both the air-water interface and sediment-water interface from meteorological data.

We will use the temperature data from SRWQM in the initial version of the model. In subsequent versions, we will also model temperatures in the delta using statistical relationships between daily water temperatures and atmospheric conditions (Wagner et al. 2011). We are also compiling additional information on temperatures in the bay that we will use in future versions. Neither the bay nor delta temperatures are influenced by water operations; however, these data may be important when we evaluate climate change scenarios.

Ocean Climate and Fisheries Models

The life cycle model (LCM) uses estimates of ocean productivity to determine the survival rate of smolts transitioning from freshwater to the marine environment. These ocean productivity indicators are based on models that integrate the physical and nutrient dynamics in the coastal shelf to determine how these dynamics affect zooplankton, which are the forage food for outmigrating Chinook smolts. Ocean productivity can have important consequences for survival of Chinook smolts, driving large fluctuations in abundance. Poor ocean conditions are disproportionately bad for smaller smotls (Woodson et al. 2013).

After their first summer in the ocean, Chinook salmon from the Sacramento and San Joaquin rivers are vulnerable to the ocean commercial and recreational fisheries. Estimates of impact rates on vulnerable age classes of Chinook salmon are computed as part of the Pacific Fisheries Management Council (PFMC) annual forecast of harvest rates and review of previous years' observed catch rates. For runs that are not actively targeted, such as winter-run and spring-run Chinook, analyses of coded wire tag (CWT) groups are used to infer impact rates for these races (e.g., O'Farrell et al. 2012).

Habitat Capacity

Juvenile salmonids rear in the mainstem, delta, floodplain, and bay habitats (Figure 1). The model incorporates the dynamics of rearing by using density-dependent movement out of habitats as each habitat approaches maximum capacity for juvenile Chinook. The capacities of each of the habitats are calculated in each month using a series of habitat-specific models that relate habitat quality to a spatial capacity estimate for rearing juvenile Chinook salmon. Habitat quality is defined uniquely for each habitat type (mainstem, delta, etc.) to reflect the different habitat attributes in that specific habitat type. For example, the mainstem habitat quality is a function of velocity, depth, and bed roughness. Higher quality habitats are capable of supporting higher densities of rearing Chinook salmon, with the range of densities being determined from studies in the Central Valley and in river systems in the Pacific Northwest, where appropriate.

Defining habitat capacity. For each habitat type (mainstem, delta, and bay), capacity was calculated each month as:

$$K_i = \sum_{j=1}^{n} A_j d_j$$

where K_i is the capacity for a given habitat type i, n is the total number of categories describing habitat variation, A_j is the total habitat area for a particular category, and d_j is the maximum density attributable to a habitat of a specific category. Three variables were determined for each habitat, the ranges of each were divided into high and low quality, and all combinations were examined, resulting in a total of eight categories (2 x 2 x 2) of habitat quality for each habitat type (Table 1). Ranges of high and low habitat quality were based on published studies of habitat use by Chinook salmon fry across their range and examination of data collected by USFWS within the Sacramento-San Joaquin Delta and San Francisco Bay.

Table 1. Habitat variables influencing capacity for each habitat type.

Habitat type	Variable	Habitat quality	Variable range
Mainstem	Velocity	High	<= 0.15 m/s
		Low	> 0.15 m/s
	Depth	High	> 0.2 m, <= 1 m
		Low	<= 0.2 m, > 1 m
	Roughness	High	> 0.04
		Low	<= 0.04
Delta	Channel type	High	Blind channels
		Low	Mainstem, distributaries, open water
	Depth	High	> 0.2 m, <= 1.5 m
		Low	<= 0.2 m, > 1.5 m
	Cover	High	Vegetated
		Low	Not vegetated
Bay	Shoreline type	High	Beaches, marshes, vegetated banks, tidal flats
		Low	Riprap, structures, rocky shores, exposed habitats
	Depth	High	> 0.2 m, <= 1.5 m
		Low	<= 0.2 m, > 1.5 m
	Salinity	High	<= 10 ppt
		Low	> 10 ppt

Defining maximum densities. Determining maximum densities for each combination of habitat variables is complicated by the fact that most river systems in the Central Valley are now hatchery-dominated with fish primed for outmigration. In addition, the Central Valley river system is at historically low natural abundance levels compared to expected or potential density levels. Because of this deficiency in the Central Valley system, we used salmon fry density data from the Skagit River system, which in contrast has very low hatchery inputs, has been monitored in mainstem, delta, and bay habitats, and exhibits evidence of reaching maximum density in years of high abundance (Greene et al. 2005; Beamer et al. 2005). These data from the Skagit River were compared with Central Valley density estimates calculated by USFWS. For each of these data sets, we used the upper 90 to 95 percentile levels of density to define the maximum density levels, and assumed the highest five percentile density levels were sampling outliers.

Determining habitat areas. Two approaches were used to map the spatial extents of different combinations of habitat variables. In the mainstem and floodplain, the HEC-RAS model divides the river into units based on multiple cross-sections defining depth ranges. Each unit defined by the cross-sections has velocity and roughness parameters associated with it. Different levels of flow in a given month or year change the distribution of velocity and depth. Total habitat area in each of the eight classes is calculated by integrating over the river channels modeled by HEC-RAS.

For the delta and bay, channel type, depth, cover, salinity, and shoreline type were mapped from existing delta and bay Geographic Information Systems (GIS) products. Delta and bay polygons[1] were classified into high quality habitat types (blind tidal channels) and low quality habitat types (mainstem, distributaries, large water bodies, and bay). For the channel typing, we used several datasets as base layers, including National Wetlands Inventory (NWI) wetland polygons, San Francisco Estuary Institute's Bay Area Aquatic Resource Inventory (BAARI) stream lines and polygons, Hydro24ca channel polygons (USBR, Mid-Pacific Region GIS Service Center), aerial photos, and Google Earth. Most channel types could be mapped using these datasets except for the blind tidal channels. Instead of directly mapping blind tidal channels, we estimated these areas using allometric relationships between wetland areas and blind tidal channel areas. We tested allometric equations developed in the Skagit River by Beamer et al. (2005) and Hood (2007) to determine which equations were best suited to apply to the Central Valley and chose an allometric equation that returned conservative estimation results:

BTC (ha) = 0.0024*Wetland(ha)^1.56

where BTC is the area of blind tidal channels. We also applied the minimum area requirement (0.94 ha) to define blind tidal channels in a wetland from Hood (2007).

Salinity is another factor influencing habitat availability for juvenile Chinook salmon that can vary with water flow. The X2 position describes the distance from the Golden Gate Bridge to the 2 ppt isohaline position near the Sacramento Delta (Jassby et al. 1995). This distance predicts the amount of suitable habitat for various fish and other organisms. Based on observations of high likelihood of

[1] A closed shape used in GIS mapping that is defined by a connected sequence of x, y coordinate pairs, where the first and last coordinate pairs are the same and all other pairs are unique.

fry presence in water with salinity of up to 10 ppt in both Skagit River and San Francisco Bay fish monitoring data, we defined the low-salinity zone for Chinook as salinity < 10 ppt (i.e., habitats upstream of X10). We calculated X10 values as 75 percent of X2 values (Jassby et al. 1995), and mapped these across San Francisco Bay.

Another axis used to evaluate habitat is vegetated cover along river banks. Areas associated with vegetated cover were assumed to provide protection from predators (Semmens 2008). Such habitats in other systems are preferred by Chinook salmon (Beamer et al. 2005; Semmens 2008). The extent of these areas was estimated using Coastal Change Analysis Program (C-CAP) Land Use/Land Cover (LULC) layers. We defined sheltered habitat as forested or shrub covered areas and assumed that other areas, such as urban and bare land, did not provide sheltered habitat.

Restricting habitat areas based on connectivity. Our first analysis of habitat areas assumed all regions of the delta were equally accessible to Chinook salmon fry. This assumption may be incorrect, however, because fish monitoring has shown that fry do not inhabit certain areas in the delta. Therefore, a spatial connectivity mask, or exclusion zone, was developed to exclude certain areas from the habitat mapping. This exclusion zone was produced using month- and year-specific fish monitoring data. Poisson regression models were used to predict fish counts based on the relationships between fish counts in beach seine datasets and several covariates including river system (Sacramento or San Joaquin), distance of sampling site to its mainstem (m), physical channel depth (m), physical channel width (m), and DSM2 water stage (m). We selected these parameters based on Akaike's Information Criterion (AIC) analysis of the Poisson regression models with various combinations of the parameters. The resulting Poisson model equation was used to produce a presence-absence map for the entire delta. Restricted capacity estimates were generated by summing habitat areas with predicted fry presence.

The Chinook Salmon Life Cycle Model

The life cycle model is a stage-structured, stochastic life cycle model. Stages are defined by development and geography (Figure 1), and each stage transition is assigned a unique number (Figure 4).

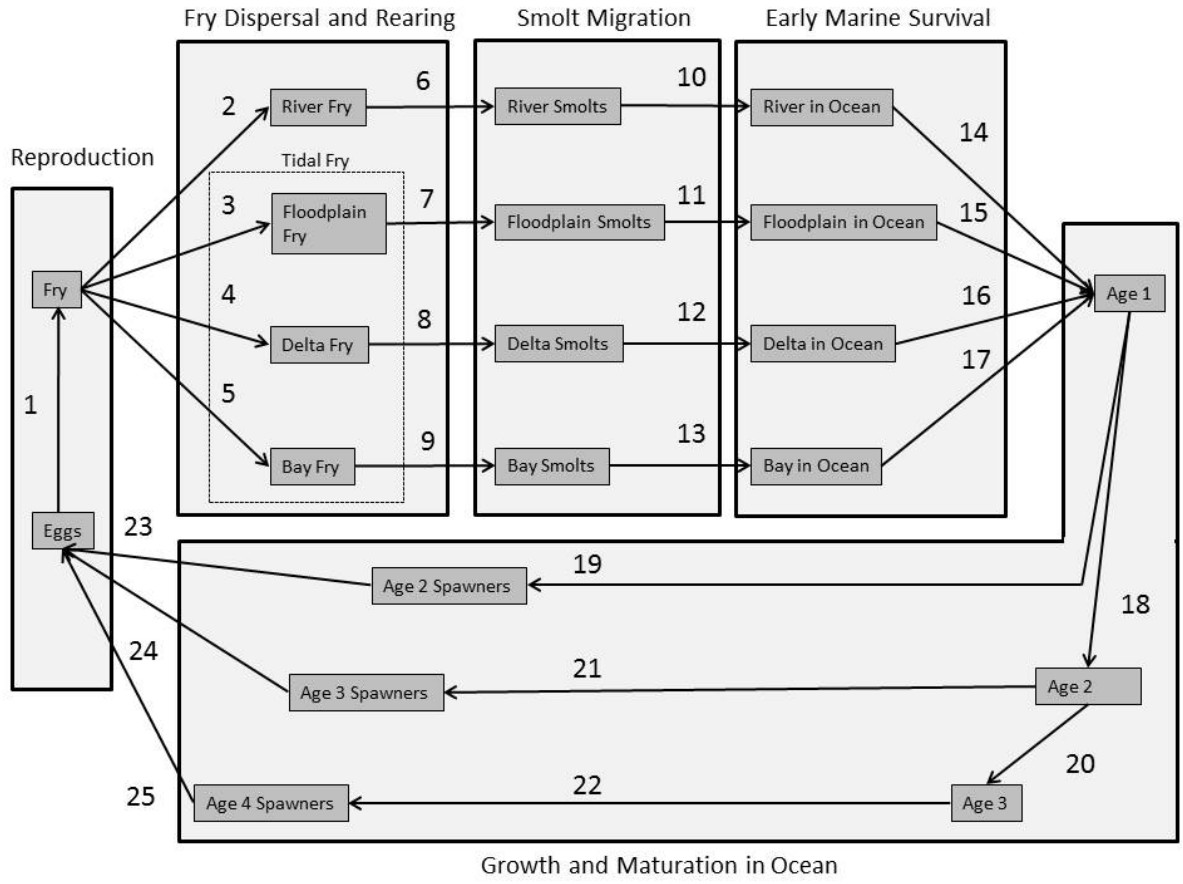

Figure 4. Central Valley Chinook transition stages. Each number represents a transition equation through which we can compute the survival probability of Chinook salmon moving from one life stage in a particular geographic area to another life stage in another geographic area. Transition equation 1 represents the survival probability for the Reproductive phase. Transition equations 2-9 represent the Fry Dispersal and Rearing phase, with transition equations 3-5 representing the Tidal Fry phase. Transition equations 10-13 represent the Smolt Migration phase. Transition equations 14-17 represent the Early Marine Survival phase. Transition equations 18-22 represent the Growth and Maturation in the Ocean phase. Transition equations 23-25 represent the survival probabilities for returning adults.

III. Transition Equations

Transition 1

Definition: Survival to Fry stage from Egg stage

Discussion: The abundance of fry is a function of the abundance of eggs and the survival rate from eggs to fry. The survival rate varies among years depending on the environmental conditions (e.g., temperature and flow) during egg incubation and fry emergence.

Equation:

Fry = Eggs $*S_{eggs}$

$\text{logit}(S_{eggs}) = \mathbf{X_1}'\boldsymbol{B_{Eggs}}$

where S_{eggs} is the survival rate of fry as a function of the coefficients, $\mathbf{X_1}$ = vector or matrix of covariate values (e.g., temperature in the natal reaches), $\boldsymbol{B_{Eggs}}$ is the vector of coefficients relating covariate effects $\mathbf{X_1}$ to survival of eggs during incubation and survival to Fry stage, and logit(x) = log(x/[1-x]) is a function that ensures that the survival rate is within the interval [0,1].

Transitions 2 - 5

Definition: Survival and dispersal from fry in the natal reaches to rearing fry in the river, floodplain, delta, and bay.

Discussion: Juvenile Chinook salmon in the Central Valley may disperse from their natal reaches shortly after emerging as fry (i.e., less than 1 month) to inhabit habitats downstream (Williams 2006). This outmigration strategy has also been observed in Chinook populations in other systems, such as the Skagit River, Washington (Greene et al. 2005). We use the term Tidal Fry (TF) to represent this life history strategy, which is consistent with Greene et al. (2005). Those fry not leaving as Tidal Fry remain in the river habitat upstream of the City of Sacramento where they stay to rear (i.e., River Fry).

Tidal Fry

To represent the Tidal Fry process in winter-run Chinook, the model can distribute Tidal Fry among habitats during the months of July to December. The majority are distributed August to November with the largest pulse in September, which is when most fry sized winter-run pass Red Bluff Diversion Dam (RBDD) (Poytress and Carillo 2012).

All habitats are not equally accessible from all other habitats. For example, we assume that the Yolo bypass or floodplain habitat is not accessible from the delta habitat (Figure 5). Furthermore, not all habitats can be accessed in all months. The entrance to the floodplain habitat is dependent upon flows that are high enough to overtop the Fremont Weir and allow access to the Yolo Bypass. Currently, flooding into the Yolo Bypass begins when Sacramento River flow exceeds 1586 m^3s^{-1} (56,000 cfs) at Verona. Entrance to the floodplain habitat is therefore dependent upon overtopping of the Fremont Weir during the month of dispersal. The model uses monthly time steps, and the monthly average flow does not adequately reflect the proportion of time in which flow overtops the Freemont Weir. Instead, the average monthly flow of 991 m^3s^{-1} (35,000 cfs) provided a better indicator of the flow into the Yolo bypass. If the Yolo bypass is accessible during the month, then a

proportion of Tidal Fry can enter during that month, otherwise Tidal Fry move to the delta and bay habitats to rear in that month.

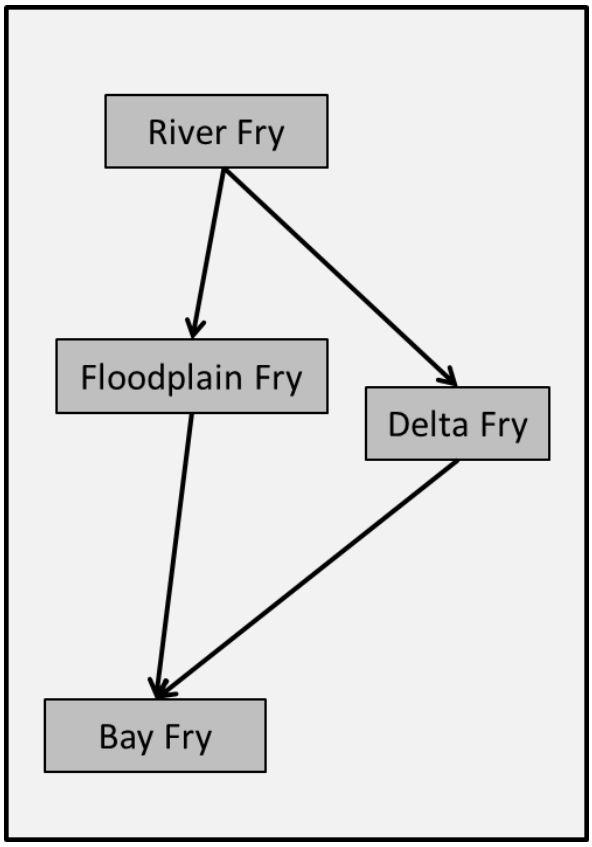

Figure 5. Connectivity among habitats for winter-run Chinook fry.

Equations:
The Tidal Fry are a function of the proportion of Tidal Fry (P_{TF}) and the total number of fry.

TidalFry = P_{TF}*Fry

The portion of fry that emigrate as Tidal Fry, P_{TF}, may vary among years as a function of flow. This process has been hypothesized to describe patterns of fry moving downstream in larger proportions in wet years versus dry years and thus captured at Chipps Island trawls and bay oriented beach seine stations (Pat Brandes, USFWS, Personal Communication, 2013).

Two possible approaches to modeling access to the floodplain habitat were developed: the first approach assumes an indicator relationship, such that whenever there are flows into the Yolo bypass, a proportion of the Tidal Fry move into the floodplain habitat; whereas, the second approach uses the proportion of flow in the Yolo bypass relative to flow in the Sacramento River with a parameter that allows the proportion of fish to be greater or less than the proportion of flow.

Alternative 1:

$$TidalFry_{FP} = S_{TF,FP} * TidalFry * P_{FP} * I(Q_{Verona} > 991.1\ m^3s^{-1})$$

where Q_{Verona} is the Sacramento River flow at Verona, I( ) is an indicator function that equates to 1 when the condition in the parenthesis is met, P_{FP} is a parameter describing the proportion of Tidal Fry that enter the floodplain habitat, and $S_{TF,FP}$ is the survival rate of Tidal Fry from the natal reach to the floodplain habitat.

Alternative 2:

$$TidalFry_{FP} = S_{TF,FP} * TidalFry * B_{FP} * Q_{Yolo}/(Q_{Verona} + Q_{Yolo})$$

where Q_{Yolo} is the flow into the Yolo bypass, Q_{Verona} is the flow at Verona on the Sacramento River, and B_{FP} is a parameter that describes the degree to which fish move with flow, $0 \leq B_{FP} * Q_{Yolo}/(Q_{Verona} + Q_{Yolo}) \leq 1$. Note that B_{FP}=1 indicates that fish move in the same proportion with flow, whereas B_{FP} > 1 would reflect more fish than flow.

Those Tidal Fry that do not enter the floodplain habitat move downstream to the delta and bay habitats to rear. For those Tidal Fry that do not enter the floodplain habitat, the positioning of the Delta Cross Channel (DCC) gate affects the values of S_{TF} to the delta and bay habitats (i.e., $S_{TF,Delta}$ and $S_{TF,Bay}$).

Those fry that do not migrate out as Tidal Fry remain in the river habitat as River Fry and are the initial abundances in the rearing portion of the life cycle.

River Fry = $S_{F,R}$*(1 - P_{TF})*Fry

where $S_{F,R}$ is the survival rate of fry remaining in the river habitat.

Rearing

Definition: Fry rear among river, floodplain, delta, and bay habitats according to density dependent movement functions.

Discussion: This transition moves juvenile salmonids among the river, floodplain, delta, and bay habitats as a function of the area-specific fry survival rates, area-specific fry capacities, and migration rate in the absence of density dependence. The transitions among habitats can be described by a schematic (Figure 6).

Winter-run sized fish pass Knights Landing in most years between November and January. The timing of passage appears to be variable, however, and depends upon the flows at Wilkinson Slough; when flows exceed 400 m^3s^{-1} at Wilkinson Slough, rotary screw trap catches of winter-run sized Chinook salmon increase at Knights Landing (del Rosario et al. 2013). Once this flow threshold has been exceeded, winter-run Chinook can move into habitats (with the exception of Tidal Fry, which have already dispersed). The life cycle model conditions the timing of the movement out of the river habitat and into downstream habitats by a flow trigger that can vary among years.

The schematic (Figure 6) shows the inputs to a monthly transition in the delta as an example. The abundance (N_{Delta}) in this month is a sum of the previous month's residents, migrants arriving from the upstream (river) habitat from the previous month, and Tidal Fry from the natal reach in the previous month. The Capacity of the habitat, the Survival rate within the habitat, the Migration rate in the absence of density dependence, and the previous month's resident abundance determine how many residents remain in the delta in the current month, and how many migrants will move downstream to the bay habitat in the following month.

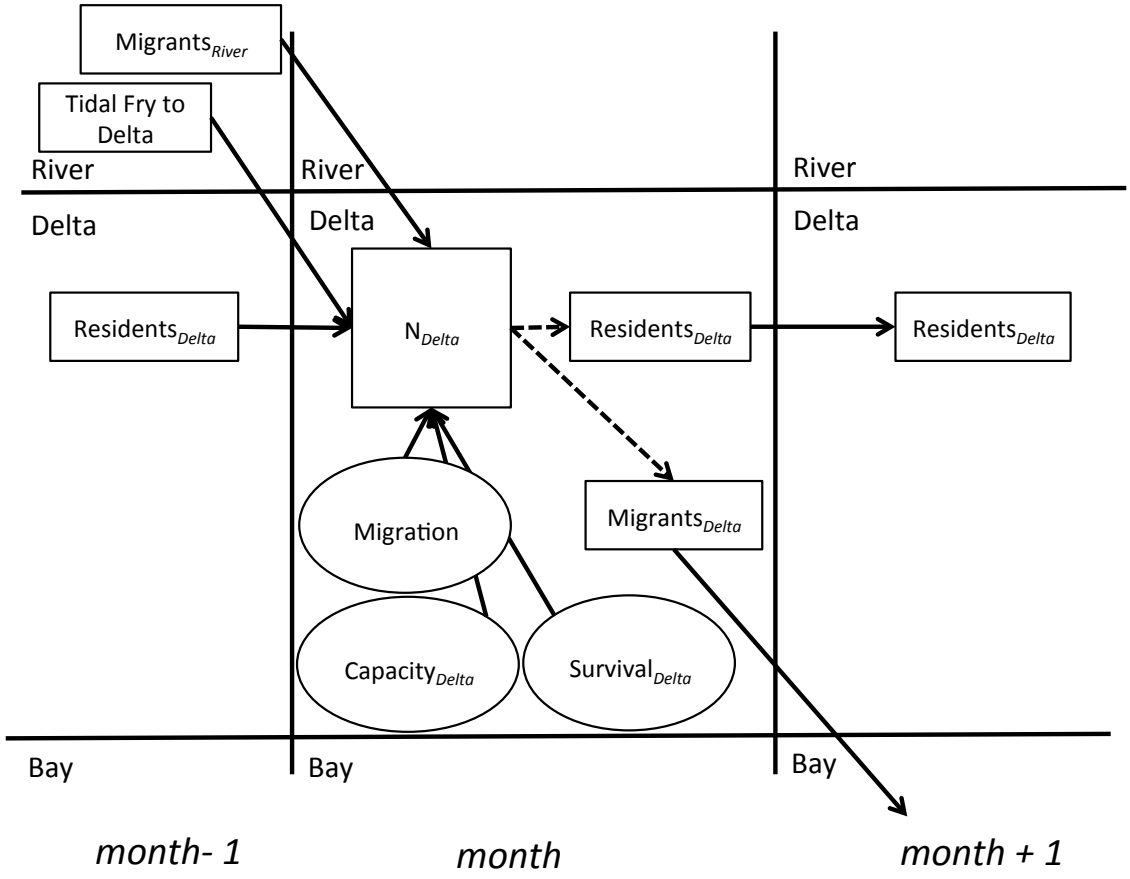

Figure 6. Schematic depicting the dynamics of Dispersers, Residents, and Migrants among habitats at the monthly time step of the model. Rectangles represent abundances of juvenile salmon, whereas ovals depict parameters of the density dependent movement function. Solid lines represent inputs to the transition function, whereas dashed lines represent outputs.

Equations:

The number of residents in the month (time subscript suppressed) is calculated from the following equation (Figure 9):

$\text{Residents}_i = S_i (1 - m) N_i / (1 + N_i/K_i)$,

where S_i is the survival rate, N_i is the pre-transition abundance, and K_i is the capacity for habitat type i = River, Floodplain, Delta, Bay, and m is the migration rate in the absence of density dependence.

The number of migrants in the month is calculated from the following equation (Figure 7):

$\text{Migrants}_i = S_i N_i - \text{Residents}_i$

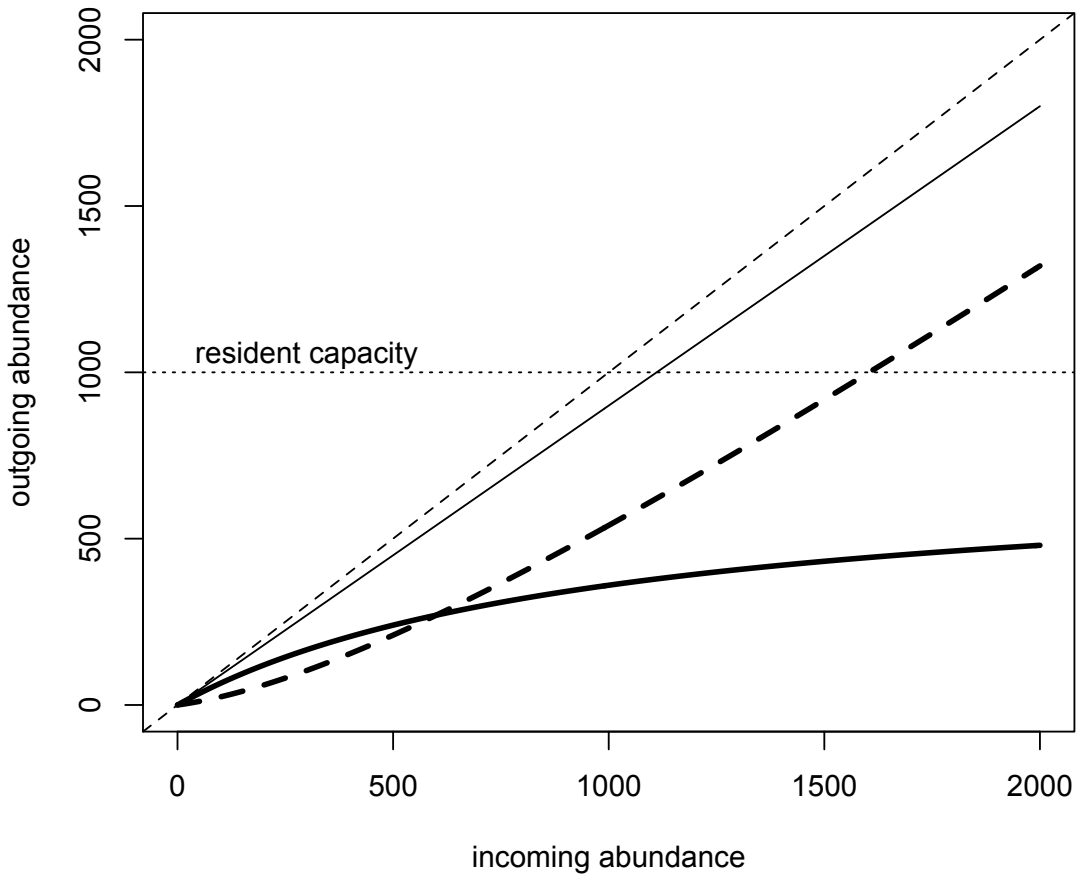

Figure 7. Example of the Beverton-Holt movement function in which the outgoing abundance (thin solid black line) is split between migrants (thick dashed line) and residents (solid dark line), that are affected by the resident capacity (thin dotted line). The 1:1 line (thin dashed line) is also plotted for reference. Parameter values used in the plotted relationship are survival, S = 0.90; migration, m = 0.2; and capacity, K= 1000.

The parameters of the density dependent movement function can be as simple as constant capacity, survival, and migration rate values over all months, habitats, and years. Alternatively, these parameter values can be dynamic and vary over year, month, and habitat to reflect the spatio-temporal dynamics in the availability of habitat for fry. We have chosen the latter approach here to incorporate these dynamics into the life cycle model.

Transitions 6 - 9

Definition: Smolting of residents in the river, floodplain, delta, and bay rearing habitats

Description: The smolting process is a complex endocrine and behavioral shift that may be affected by feeding opportunities as well as environmental drivers of photoperiod and temperature (McCormick et al. 2000; Myrick and Cech 2004; Björnsson et al. 2011). The bottom-oriented parr shift behaviorally from positioning into the flow to orienting with the flow to improve migration. Furthermore, fish that may have established stations and thus defended territories, now school to reduce the chance of predation. In addition there is a shift in the physiology to facilitate migration

and the eventual associated shift to osmoregulate in the marine environment. These physiological and behavioral processes are preceded by changes in the endocrinology of the fish that are receptive to environmental cues (Björnsson et al. 2011).

The life cycle model does not track size explicitly, so relationships between feeding and smolting may be implicitly applied via differential habitat-based smolting rates that are related to habitat quality and expected food availability. The timing of smoltification in the life cycle model is an explicit function of temperature and photoperiod, however. It is important to note that Transitions 6 – 9 are between Residents and Smolts (as opposed to Migrants and Smolts); therefore, these are not individuals that were shifted out of the habitat because of capacity limitation, but rather individuals that initiated downstream migration having reared in the habitat until they were prepared to leave.

The proportion of juveniles smolting in a given month is a function of the temperature in that month and the photoperiod. The photoperiod acts as a timer to ensure that juveniles smolt to appropriately time the downstream portion of their migration. As successive months progress, the likelihood of fish remaining in a particular habitat decreases. For example, the majority of winter-run migrate out of the habitats by May, coinciding with the peak flux of winter-run sized fish at Chipps Island (del Rosario et al. 2013).

Equations:

$Smolts_{i,k} = P_{SM,i,k} * Residents_{i,k}$

Where $P_{SM,i,k}$ is the probability of smolting in month *k* in habitat *i* (*i* = River, Floodplain, Delta or Bay) by the Residents from the previous month (*k*-1) in that habitat.

Suppressing the subscript for habitat, the probability of smolting is modeled as a proportion ordered logistic regression model (Agresti 2002) of the form:

$$\text{logit}(P_{SM,k}) = Z_k + B_{smolt}*(T_k - T_k')$$

where $-\infty < Z_1 < Z_2 \ldots < Z_k < \infty$ are the monthly rates of smoltification based on photoperiod and their ordering ensures that the probability increases over months, B_{smolt} is the effect of temperature anomalies on the photoperiod-based rate and $(T_k - T')$ is the temperature anomaly in month k over the baseline temperature T_k'.

Transition 10

Definition: Smolts that reared in the river migrate to the ocean

Discussion: Outmigrating smolts will transit the system with the goal of migrating out of the river and through the delta and bay as quickly as possible.

For winter-run Chinook, juveniles ranging in size from 100mm to 120mm pass RBDD beginning in mid-January (Poytress and Carrillo 2008; Poytress and Carrillo 2012). Because these sizes coincide with the median sizes of winter-run passing Chipps Island in March leaving the system (del Rosario et al. 2013), we assume that these are outmigrating smolts that have reared in the river and are beginning their migration to the ocean. As a result, acoustic tagged late-fall run smolts may provide useful estimates of outmigration survival (e.g., Perry et al. 2010).

Equations:

The numbers of smolts that arrive at the ocean after rearing in the river are a function of the survival rate due to migrating from the river habitat to the ocean.

River in Ocean = $S_{10}\text{Smolts}_{\text{River}}$

where River in Ocean are the smolts that migrated to the ocean from the river habitat with survival rate S_{10}.

Transition 11

Definition: Smolts that reared in the floodplain migrate to the ocean

Discussion: Outmigration of winter-run sized juveniles from the Yolo Bypass appears to occur between late February and mid-March among years when the Yolo bypass flooded (2003, 2004, and 2006) (del Rosario et al. 2013). In those years, winter-run were able to access the floodplain habitat due to the timing of flow thresholds for movement of winter-run at Wilkinson Slough and the timing of downstream access to Yolo Bypass due to overtopping of the Freemont Weir.

Equations:

The numbers of smolts that arrive at the ocean after rearing in the floodplain are a function of the survival rate due to migrating from the floodplain habitat to the ocean.

Floodplain in Ocean = $S_{11}\text{Smolts}_{\text{Floodplain}}$

where Floodplain in Ocean are the smolts that migrated to the ocean from the floodplain habitat with survival rate $S_{11.}$

Transition 12

Definition: Smolts that reared in the delta migrate to the ocean

Discussion: We assume that the winter-run that have reared in the delta are located in the interior portion of the delta habitat. Winter-run sized Chinook salmon depart the delta in March and April as indicated by the median catch rates of winter-run sized fish in the Chipps Island trawls (del Rosario et al. 2013). Sizes of winter-run during those months can vary from 100 to 140mm with median fork lengths of approximately 110mm. The survival rates from acoustic tagged late-fall run smolts may provide useful estimates of winter-run in this transition (e.g., Perry et al. 2010) in addition to the suite of covariates identified by Newman (2003) for relating survival of outmigrating smolts to environmental conditions in the delta.

Equation:

The numbers of smolts that arrive at the ocean after rearing in the delta are a function of the survival rate due to migrating from the delta habitat to the ocean.

Delta in Ocean = $S_{12}\text{Smolts}_{\text{Delta}}$

where Delta in Ocean are the smolts that migrated to the ocean from the delta habitat with survival rate S_{12}.

Transition 13

Definition: Smolts that reared in the bay migrate to the ocean

Discussion: The bay habitat represents a transition to the marine environment and it appears that migrating juvenile Chinook salmon transit the bay relatively quickly (MacFarlane and Norton 2002); yet, the survival rates of acoustically tagged late-fall Chinook may be low throughout this reach during outmigration (Sean Hayes, NMFS, personal communication, September 25, 2013).

Equation:

The numbers of smolts that arrive at the ocean after rearing in the bay are a function of the survival rate due to migrating from the bay habitat to the ocean.

Bay in Ocean = $S_{13}\text{Smolts}_{\text{Bay}}$

where Bay in Ocean are the smolts that migrated to the ocean from the bay habitat with survival rate S_{13}.

Transitions 14 - 17

Definition: Survival of smolts that reared in different habitats in the Gulf of Farallones region.

Discussion: Survival during the early ocean phase can have important effects on the overall cohort strength of the population, particularly when the nearshore ocean fails to provide a productive environment for juvenile Chinook. In the San Francisco estuary, outmigrating Chinook salmon do not use the bay habitat for feeding and arrive in the Gulf of the Farallones with relatively low lipid content (McFarlane and Norton 2002). In years where there are delays in the spring transition or upwelling has been shifted off the coast, fall-run Chinook salmon in particular, may be strongly affected by these environmental conditions (Lindley et al. 2009; Wells et al. 2007). In addition, the effects of nearshore productivity appear to be influenced by the size of the outmigrating smolts; in years of low ocean productivity the smaller sized fish appear to have substantially lower survival rates than larger sized fish, whereas in high productivity years all sizes appear to benefit equally (Woodson et al. 2013).

In the Sacramento-San Joaquin River system, several studies have found evidence for increased growth rates in juvenile Chinook rearing in favorable habitats (e.g., Kjelson et al. 1982; Sommer et al. 2001; Limm and Marchetti 2009) with favorable habitats typically defined as off-channel rearing areas. In other systems, such patterns are prevalent as well. For example in the Fraser River, British Columbia, higher growth rates were observed in off-channel marshes relative to river habitat (Levy and Northcote 1982) and in the Skagit River, Washington juvenile Chinook rearing in the estuary were larger than juvenile Chinook rearing in the river (Congleton et al. 1981). Once fish have undergone smoltification, it appears that they are unlikely to use the San Francisco Bay estuary in its current condition for compensatory growth prior to outmigration into the ocean (Kjelson et al. 1982; MacFarlane and Norton 2002). Furthermore, otolith work by Miller et al. (2010) indicated that in a sample of 100 returning Chinook adults, most fish did not spend time rearing in the bay once reaching the smolt stage.

Because the life cycle model does not track size explicitly, the influence of size is incorporated implicitly via differential survival rates to Age 1. The survival rate from each rearing habitat to Age 1

has a different sensitivity to ocean productivity: bay and delta habitats have the greatest sensitivity, whereas floodplain and river habitats are less sensitive.

Equations:

Age 1_{River} = S_{14}River in Ocean

Age $1_{Floodplain}$ = S_{15}Floodplain in Ocean

Age 1_{Delta} = S_{16}Delta in Ocean

Age 1_{Bay} = S_{17}Bay in Ocean

where the abundances in the Age 1 stage are a function of the number of smolts arriving in the ocean and the habitat-specific survival rate. The habitat-specific survival rate reflects the potential for individuals to rear to a larger size (e.g., floodplain rearing) relative to other habitats such as the delta or bay (Sommer et al. 2001).

The total number of Age 1 winter-run in the Gulf of the Farallones is obtained by summing over the different rearing habitats.

Age 1 = Age 1_{River} + Age $1_{Floodplain}$ + Age 1_{Delta} + Age 1_{Bay}

The proportion of migrants that reared in each of the habitat types (i.e., Age 1_{River} /Age 1) is also an important model component as information on otolith microchemistry (e.g., Barnett-Johnson et al. 2008) and may provide estimates of the habitats used by winter-run Chinook fry.

Transition 18

Definition: Survival in the ocean from Age 1 to Age 2

Discussion: During their ocean residence, winter-run Chinook are located in the coastal waters south of Point Arena as estimated by Coded Wire Tag (CWT) recaptures in fisheries in those areas (Grover et al. 2004; O'Farrell et al. 2012).

Equation:

Age 2 = Age 1 * (1-M_2)* S_{18}

where S_{18} is the survival rate of Age 1 fish in the ocean and M_2 is the maturation rate that leads to 2 year old spawners. The fishery for Central Valley Chinook is composed of a commercial and recreational component; however, Age 1 winter-run are not contacted in the fishery (O'Farrell et al. 2012).

Transition 19

Definition: Maturation for Age 2

Discussion: A very small proportion of winter-run Chinook return as 2-year olds (O'Farrell et al. 2012; Grover et al. 2004), with the predominant year of return as Age 3. Yet, the small proportion of returning 2 and 4 year olds has a significant effect on the cohort dynamics of winter-run Chinook (Botsford and Brittnacher 1998). The fishery for Central Valley Chinook is composed of a commercial

and recreational component; however, 2-year old winter-run are not contacted in the fishery (O'Farrell et al. 2012).

*Equation*s:

Age 2 Spawners = Age 1*M_2*S_{19}

Where M_2 is the maturation rate that leads to Age 2 spawners and S_{19} is the natural survival rate of Age 1 to the spawning grounds.

Transition 20

Definition: Survival in the ocean from Age 2 to Age 3

Discussion: As in Winship et al. (In Review), we assume that the Age 3 survival rate was constant over time, and a function of the Age 3 fishery impact rate (I_3) and the natural survival rate. Furthermore, we assume that fishery impacts occurred prior to natural mortality during a given age.

Equations:

Age 3 = Age 2 *(1-M_2) * (1- I_3)*S_{20}

where S_{20} is the survival rate for Age 2 and I_3 is the impact rate for Age 3 fish.

Transition 21

Definition: Maturation for Age 3

Discussion: As in Winship et al. (In Review), we assume that the Age 3 survival rate was constant over time, and a function of the Age 3 fishery impact rate (I_3) and the natural mortality rate (NM_3). Furthermore, we assume that fishery impacts occurred prior to natural mortality during a given age.

Equations:

Age 3 Spawners = Age 2 * (1- I_3) *M_3*S_{21}

where I_3 is the Age 3 impact rate, M_3 is the Age 3 maturation rate, and S_{21} is the Age 3 survival rate to the spawning grounds.

Transition 22

Definition: Survival and maturation rate for Age 4

Discussion: All remaining winter-run return as 4-year olds, after surviving the fishery. We assumed that the instantaneous Age 4 fishery impact rate was twice the instantaneous Age 3 fishery impact rate (O'Farrell et al., 2012).

Equations:

Age 4 Spawners = Age 3 * (1- I_4) * S_{22}

where I_4 is the Age 4 impact rate and S_{22} is the survival rate from the end of Age 3 to the spawning grounds.

Transitions 23 - 25

Definition: Number of eggs produced by spawners of Ages 2 – 4

Description: Due to the potential for spatial limitations in the spawning reach at high winter-run spawner abundances, density dependence was incorporated into the production of eggs by spawners. Spawning occurs as a mixture of Age 2, 3, and 4, although the majority of winter-run Chinook return to spawn at Age 3.

Equation:

$$Eggs = \frac{\sum_{j=2}^{4} Sp_j * V_{eggs,j}}{1 + \frac{\sum_{j=2}^{4} Sp_j * V_{eggs,j}}{K_{Sp}}}$$

where Sp_j are the number of spawners of age j = 2, 3, 4, V_{Eggs} is the production of eggs per spawner in the absence of density dependence, and K_{Sp} is the capacity of eggs in the spawning grounds as a function of spawners. The production of eggs varies by age of return with larger Age 3 and 4 females producing more eggs than Age 2 (Newman and Lindley 2006). The capacity of the spawning reach is affected by the amount of gravel (TNC et al. 2008) and the location of the temperature compliance point set in the spring for spawning adult winter-run. The capacity for a given year is a function of the areal extent of the gravel upstream of the compliance point, the average redd size, and the number of eggs produced per spawner.

IV. Conclusion

This report outlines the general framework for modeling the effects of water project operations on a population of winter-run Chinook salmon, and details the equations governing the transitions among life stages and geographic areas that describe the life cycle and dynamics of the population.

Additional work is needed before the model can be applied:

1. Development of prior distributions for parameter values from the literature and available datasets.
2. Estimation of posterior distributions or plausible ranges of parameters, based on fitting the LCM to historical data.
3. Possible adjustment of the model structure if the fit to historical data is poor.
4. Development of management scenarios for analysis.

We anticipate preparing further documentation describing the methods and results of these four activities.

We also are working on modifications to the analytic framework that will support more detailed investigations of the effects of delta operations on winter-run Chinook salmon, and similar investigations of spring- and fall-run Chinook salmon. The most significant modification planned is replacing the empirical survival functions for fry and smolts in the delta with an agent-based simulation model of juvenile salmon rearing and migration, using DSM2 HYDRO, QUAL, and a modified PTM. We are adding behaviors (swimming, holding position, route choice), environmental behavioral cues (flow direction, velocity, salinity, tidal phase), and other biological processes

(predation-driven mortality) to the PTM. Behavioral and predation models will be selected, and model parameters estimated, from statistical comparison of simulation results to CWT- and acoustic tag-based survival experiments. Because the resulting model has a theoretical and mechanistic basis, it will allow us to more reliably model survival under conditions outside of the range of data supporting the empirical relationships in the current model version.

It is fairly straightforward to modify the model structure for other populations of Central Valley Chinook (and for any salmon population where similar hydrologic and hydraulic models are available). We are working on a multi-population model for spring-run Chinook with a focus on summer water temperatures in adult holding areas. We are also developing a multi-population fall-run Chinook model that will include hatchery populations and interactions, and San Joaquin River as well as Sacramento River populations, allowing exploration of likely tradeoffs between such populations that will be affected by modifications to delta hydrodynamics.

V. References

Agresti, A. 2002. Categorical data analysis. 2nd edition. Wiley-Interscience.

Barnett-Johnson, R., T. Pearson, F. C. Ramos, C. B. Grimes, and R. B. MacFarlane. 2008. Tracking natal origins of salmon using isotopes, otoliths, and landscape geology. Limnology and Oceanography 53(4):1633-1642.

Beamer, E., A. McBride, C. Greene, R. Henderson, G. Hood, K. Wolf, K. Larsen, C. Rice, and K. Fresh. 2005. Delta and nearshore restoration for the recovery of wild Skagit River Chinook salmon: Linking estuary restoration to wild Chinook salmon populations. Appendix D of the Skagit Chinook Recovery Plan, Skagit River System Cooperative, LaConner, WA. Available at: www.skagitcoop.org.

Björnsson, B. T., S. 0. Stefansson, and S. D. McCormick. 2011. Environmental endocrinology of salmon smoltification. General and Comparative Endocrinology 170(2):290-298.

Botsford, L. W. and J. G. Brittnacher. 1998. Viability of Sacramento River winter-run Chinook salmon. Conservation Biology 12(1):65-79.

Congleton, J. L., S. K. Davis, and S. R. Foley. 1981. Distribution, abundance, and outmigration timing of chum and Chinook salmon fry in the Skagit salt marsh. Pages 153-163 in: E. L. Brannon and E. O. Salo, eds. Proceedings of the Salmon and Trout Migratory Behavior Symposium. School of Fisheries, University of Washington, Seattle, Washington.

del Rosario, R. B., Y. J.Redler., K. Newman, P. L. Brandes, T. Sommer, K. Reece, and R. Vincik. 2013. Migration patterns of juvenile winter-run-sized Chinook salmon (*Oncorhynchus tshawytscha*) through the Sacramento–San Joaquin Delta. San Francisco Estuary and Watershed Science 11(1).

Greene, C. M. and T. J. Beechie. 2004. Consequences of potential density-dependent mechanisms on recovery of ocean-type Chinook salmon (*Oncorhynchus tshawytscha*). Canadian Journal of Fisheries and Aquatic Sciences 61(4):590-602.

Greene, C. M., D. W. Jensen, G. R. Pess, E. A. Steel, and E. Beamer. 2005. Effects of environmental conditions during stream, estuary, and ocean residency on Chinook salmon return rates in the Skagit River, Washington. Transactions of the American Fisheries Society 134(6):1562-1581.

Grover, A., A. Lowe, P. Ward, J. Smith, M. Mohr, D. Viele, and C. Tracy. 2004. Recommendations for developing fishery management plan conservation objectives for Sacramento River winter Chinook and Sacramento River spring Chinook. Interagency Workgroup Progress Report. February 2004.

Hood, W.G. 2007. Landscape allometry and prediction in estuarine ecology: Linking landform scaling to ecological patterns and processes. Estuaries and Coasts 30:895-900.

Jassby, A. D., W. J. Kimmerer, S. G. Monismith, C. Armor, J. E. Cloern, T. M. Powell, J. R. Schubel, and T. J. Vendlinski. 1995. Isohaline position as a habitat indicator for estuarine populations. Ecological Applications 5(1):272-289.

Kjelson, M. A., P. F. Raquel, and F. W. Fisher. 1982. Life history of fall-run juvenile Chinook salmon, *Oncorhynchus tshawytscha*, in the Sacramento-San Joaquin estuary, California. In Estuarine Comparisons, edited by V. S. Kennedy. Academic Press, New York, New York. pp. 393-411.

Levy, D. A. and T. G. Northcote. 1982. Juvenile salmon residency in a marsh area of the Fraser River estuary. Canadian Journal of Fisheries and Aquatic Sciences 39:270-276.

Limm, M. P. and M. P. Marchetti. 2009. Juvenile Chinook salmon (*Oncorhynchus tshawytscha*) growth in off-channel and main-channel habitats on the Sacramento River, CA using otolith increment widths. Environmental Biology of Fishes 85(2):141-151.

Lindley, S. T., M. S. Mohr, W. T. Peterson, C. B. Grimes, J. Stein, J. J. Anderson, L. W. Botsford, D. L. Bottom, C. A. Busack, T. K. Collier, J. Ferguson, J. C. Garza, A. M. Grover, D. G. Hankin, R. G. Kope, P. W. Lawson, A. Low, R. B. MacFarlane, K. Moore, M. Palmer-Zwahlen, F. B. Schwing, J. Smith, C. Tracy, R. Webb, B. K. Wells, and T. H. Williams. 2009. What caused the Sacramento River fall Chinook stock collapse? NOAA Technical Memorandum NOAA-TM-NMFS-SWFSC-447.

MacFarlane, R. B. and E. C. Norton. 2002. Physiological ecology of juvenile Chinook salmon (*Oncorhynchus tshawytscha*) at the southern end of their distribution, the San Francisco Estuary and Gulf of the Farallones, California. Fishery Bulletin 100(2):244-257.

McCormick, S. D., S. Moriyama, and B. T. Björnsson. 2000. Low temperature limits photoperiod control of smolting in Atlantic salmon through endocrine mechanisms. American Journal of Physiology-Regulatory, Integrative and Comparative Physiology 278(5): R1352-R1361.

Miller, J. A., A. Gray, and J. Merz. 2010. Quantifying the contribution of juvenile migratory phenotypes in a population of Chinook salmon *Oncorhynchus tshawytscha*. Marine Ecology Progress Series 408:227-240.

Myrick, C. A. and J. J. Cech Jr. 2004. Temperature effects on juvenile anadromous salmonids in California's central valley: what don't we know?. Reviews in Fish Biology and Fisheries 14(1):113-123.

The Nature Conservancy (TNC), Stillwater Sciences, and ESSA Technologies Ltd. 2008. Sacramento River Ecological Flows Study: Final Report. Prepared for CALFED Ecosystem Restoration Program. Sacramento, California.

Newman, K. B. 2003. Modeling paired release-recovery data in the presence of survival and capture heterogeneity with application to marked juvenile salmon. Statistical Modelling 3(3):157-177.

Newman, K. B. and S. T. Lindley. 2006. Accounting for demographic and environmental stochasticity, observation error, and parameter uncertainty in fish population dynamics models. North American Journal of Fisheries Management 26(3):685-701.

O'Farrell, M. R., M. S. Mohr, A. M. Grover, and W. H. Satterthwaite. 2012. Sacramento River winter Chinook cohort reconstruction: analysis of ocean fishery impacts. NOAA Technical Memorandum NOAA-TM-NMFS-SWFSC-491.

Perry, R. W., J. R. Skalski, P. L. Brandes, P. T. Sandstrom, A. P. Klimley, A. Ammann and B. MacFarlane. 2010. Estimating survival and migration route probabilities of juvenile Chinook salmon in the Sacramento–San Joaquin River Delta. North American Journal of Fisheries Management 30(1):142-156.

Poytress, W. R. and F. D. Carrillo. 2008. Brood-year 2006 winter Chinook juvenile production indices with comparisons to juvenile production estimates derived from adult escapement. U. S. Fish and Wildlife Service, Red Bluff, California.

Poytress, W. R. and F. D. Carrillo. 2012. Brood-year 2010 winter Chinook juvenile production indices with comparisons to juvenile production estimates derived from adult escapement. U. S. Fish and Wildlife Service, Red Bluff, California.

Semmens, B. X. 2008. Acoustically derived fine-scale behaviors of juvenile Chinook salmon (*Oncorhynchus tshawytscha*) associated with intertidal benthic habitats in an estuary. Canadian Journal of Fisheries and Aquatic Sciences 65: 2053-2062.

Sommer, T. R., M. L. Nobriga, W. C. Harrell, W. Batham, and W. J. Kimmerer. 2001. Floodplain rearing of juvenile Chinook salmon: evidence of enhanced growth and survival. Canadian Journal of Fisheries and Aquatic Sciences 58(2):325-333.

U. S. Bureau of Reclamatoin (USBR). 2008. Biological assessment on the continued long-term operations of the Central Valley Project and the State Water Project. U. S. Department of the Interior, Sacramento, California. *http://www.usbr.gov/mp/cvo/ocap_page.html*

Wagner, R. W., M. Stacey, L. R. Brown, and M. Dettinger. 2011. Statistical models of temperature in the Sacramento-San Joaquin delta under climate-change scenarios and ecological implications. Estuaries and Coasts 34(3):544-556.

Wells, B. K., C. B. Grimes, and J. B. Waldvogel. 2007. Quantifying the effects of wind, upwelling, curl, sea surface temperature and sea level height on growth and maturation of a California Chinook salmon (*Oncorhynchus tshawytscha*) population. Fisheries Oceanography 16(4):363-382.

Williams, J. G. 2006. Central Valley salmon: a perspective on Chinook and steelhead in the Central Valley of California. San Francisco Estuary and Watershed Scienc, 4(3).

Winship, A. J., M. R. O'Farrell, and M. S. Mohr. In Review. Fishery and hatchery effects on an endangered salmon population with low productivity. Submitted to Transactions of the American Fisheries Society.

Woodson, L., B. K. Wells, P. K. Weber, R. B. MacFarlane, G. E. Whitman, and R. C. Johnson. 2013. Size, growth, and origin-dependent mortality of juvenile Chinook salmon *Oncorhynchus tshawytscha* during early ocean residence. Marine Ecology Progress Series 487:163-175. *Marine Ecology Progress Series, 487: 163-175.*

Appendix A. Acronyms

AIC	Akaike Information Criterion
BAARI	Bay Area Aquatic Resource Inventory
BDCP	Bay Delta Conservation Plan
BTC	Blind Tidal Channel
CALSIM II	California Simulation Model II
C-CAP	Coastal Change Analysis Program
CFS	Cubic Feet per Second
CVO	Central Valley Office
CVP	Central Valley Project
CDWR	California Department of Water Resources
CWT	Coded Wire Tag
DCC	Delta Cross Channel
DSM2	Delta Simulation Model II
DWR	Department of Water Resources
GIS	Geographic Information Systems
Ha	Hectare
HEC-RAS	Hydrologic Engineering Centers River Analysis System
LCM	Life Cycle Model
LULC	Land Use/Land Cover
NMFS	National Marine Fisheries Service
NMFS-CVO	National Marine Fisheries Service – Central Valley Office
NWFSC	Northwest Fisheries Science Center
NWI	National Wetlands Inventory
PFMC	Pacific Fisheries Marine Council
ppt	parts per thousand
PTM	Particle Tracking Model
QEDA	Quantitative Ecology and Decision Analysis
QUAL	Quality (module in DSM2)
RBDD	Red Bluff Diversion Dam
SQL Database	Structured Query Language
SRWQM	Sacramento River Water Quality Model
SWFSC	Southwest Fisheries Science Center
SWP	State Water Project
TF	Tidal Fry
USACE	United States Army Corps of Engineers
USBR	United States Bureau of Reclamation
USFWS	United States Fish and Wildlife Service
USGS	United States Geological Survey

RECENT TECHNICAL MEMORANDUMS

SWFSC Technical Memorandums are accessible online at the SWFSC web site (http://swfsc.noaa.gov). Copies are also available from the National Technical Information Service, 5285 Port Royal Road, Springfield, VA 22161 (http://www.ntis.gov). Recent issues of NOAA Technical Memorandums from the NMFS Southwest Fisheries Science Center are listed below:

NOAA-TM-NMFS-SWFSC-520 A fishery-independent survey of cowcod (*SEBASTES LEVIS*) in the Southern CA bight using a remotely operated vehicle (ROV).
STIERHOFF, K. L., S. A. MAU, and D. W. MURFIN
(September 2013)

521 Abundance and biomass estimates of demersal fishes at the footprint and piggy bank from optical surveys using a remotely operated vehicle (ROV).
STIERHOFF, K. L., J. L. BUTLER, S. A. MAU, and D. W. MURFIN
(September 2013)

522 Klamath-Trinity basin fall run chinook salmon scale age analysis evaluation.
SATTERTHWAITE, W. H., M. R. O'FARRELL, and M. S. MOHR
(September 2013)

523 Status review of the Northeastern Pacific population of white sharks *(CARCHARODON CARCHARIAS)* under the endangered species act.
DEWAR, H., T. EGUCHI, J. HYDE, D. KINZEY, S. KOHIN, J. MOORE, B. L. TAYLOR, and R. VETTER
(December 2013)

524 AMLR 2010-2011 field season report.
WALSH, J. G., ed.
(February 2014)

525 The Sacramento harvest model (SHM).
MOHR, M. S., and M. R. O'FARRELL
(February 2014)

526 Marine mammal, sea turtle and seabird bycatch in California gillnet fisheries in 2012.
CARRETTA, J. V., L. ENRIQUEZ, and C. VILLAFANA
(February 2014)

527 White abalone at San Clemente Island: population estimates and management recommendations.
STIERHOFF, K. L., M. NEUMANN, S. A. MAU and D. W. MURFIN
(May 2014)

528 Recommendations for pooling annual bycatch estimates when events are rare.
CARRETTA, J. V. and J. E. MOORE
(May 2014)

529 Documentation of a relational database for the California recreational fisheries survey onboard observer sampling program,1999-2011.
MONK, M., E. J. DICK and D. PEARSON
(July, 2014)

Evapotranspiration from Natural Vegetation in the Central Valley of California: Monthly Grass Reference-Based Vegetation Coefficients and the Dual Crop Coefficient Approach

Daniel J. Howes, P.E., M.ASCE[1]; Phyllis Fox, P.E.[2]; and Paul H. Hutton, P.E.[3]

Abstract: Restoration activities in the Central Valley of California and elsewhere require accurate evapotranspiration information, which can then be used for a wide variety of surface and subsurface hydrologic evaluations. However, directly measuring evapotranspiration can be difficult or impossible depending on the evaluation's time frame. Transferability of measured evapotranspiration in time and space is also necessary but typically requires a weather-based reference. For nonagricultural vegetation, there is at present time no standard reference, which makes the evaluation of a variety of vegetation types from different sources difficult and time-consuming. This paper examines several methods used to estimate evapotranspiration from native vegetation, including the use of vegetation coefficients (K_v). Vegetation coefficients are based on a standardized reference and are computed as the ratio of vegetation evapotranspiration (ET_v) to the grass reference evapotranspiration (ET_o). These monthly K_v values are used to compute the long-term (for this study, 1922–2009) average ET_v for vegetation types documented to exist in California's Central Valley prior to the arrival of the first European settlers in the mid-18th century. For vegetation that relies on precipitation and soil moisture storage, a calibrated daily soil–water balance with a dual crop coefficient approach was used to compute evapotranspiration regionally over the time frame. **DOI: 10.1061/(ASCE)HE.1943-5584.0001162.**

Author keywords: Water use; Evapotranspiration; Natural vegetation; Coefficients; Soil water.

Introduction

As competition for fresh water supplies intensifies, it becomes increasingly important to accurately track fresh water supply destinations through hydrologic evaluations. In many cases, these groundwater and surface water hydrologic evaluations are used to create models to estimate water distribution under historical conditions or to predict future conditions based on assumed changes in landscape, climate, management, etc. For the hydrologic evaluations to be accurate, however, the assumptions and measurements of inflows and outflows upon which they are based must also be accurate. In arid and semiarid environments, the largest percentage of fresh water is generally expended by evapotranspiration, which is notoriously difficult to measure directly. Therefore, it is crucial that procedures be developed that can accurately estimate evapotranspiration (Milly and Dunne 2010; Zhao et al. 2013).

The current trend of restoring native vegetation and habitats requires a good understanding of these habitats' water demands. For example, the current Bay Delta Conservation Plan includes over 85,000 acres of natural habitat restoration in the California Central Valley over the next 40 years (BDCP 2013). Planners require accurate estimates of evapotranspiration demands from vegetation throughout the year to properly design the habitats so as not to exceed available water supplies. Evapotranspiration demands are also needed by engineers to design new infrastructure to distribute water to these areas or examine if existing infrastructure can supply the additional habitat.

In this study, evapotranspiration estimates from vegetation that existed in the Central Valley of California are developed using standard procedures similar to those used for agriculture. For non-water-stressed vegetation such as riparian forests and permanent wetlands, monthly vegetation coefficients were generated from a detailed review of literature. These coefficients were developed to be used with a reference evapotranspiration computed from regional climate data. Alternative procedures are described for vegetation that relies primarily on rainfall, where evapotranspiration rates are dependent on moisture availability in the soil.

Current Measurement and Estimation Techniques

Techniques to measure and estimate evapotranspiration directly are available but have limitations. Common measurement techniques for actual evapotranspiration include weighing lysimeters, inflow–outflow tanks, Bowen ratio, eddy covariance, surface renewal, and remote sensing using a surface energy balance. There is consensus among researchers that if measurements are made using a localized measurement technique (techniques other than remote sensing using a surface energy balance), the measurement locations should be surrounded by vegetation of the same type, health, and size of the reference vegetation (i.e., "fetch") (Allen et al. 2011). Without the

[1]Assistant Professor/Senior Engineer, Irrigation Training and Research Center, BioResource and Agricultural Engineering Dept., California Polytechnic State Univ., San Luis Obispo, CA 93407 (corresponding author). E-mail: djhowes@calpoly.edu

[2]Consulting Engineer, 745 White Pine Ave., Rockledge, FL 32955. E-mail: phyllisfox@gmail.com

[3]Principal Engineer, Bay-Delta Initiatives, Metropolitan Water District of Southern California, 1121 L St., Suite 900, Sacramento, CA 95814-3974. E-mail: phutton@mwdh2o.com

Note. This manuscript was submitted on March 11, 2014; approved on December 2, 2014; published online on January 20, 2015. Discussion period open until June 20, 2015; separate discussions must be submitted for individual papers. This paper is part of the ***Journal of Hydrologic Engineering***, © ASCE, ISSN 1084-0699/04015004(17)/$25.00.

proper fetch, warmer, dryer air can move more easily through the vegetation, causing what is termed the clothesline effect, whereby the resulting evapotranspiration estimates are unreasonably high (Blaney et al. 1933; Allen et al. 1998, 2011). Care must be taken when setting up the studies and when examining the results, because published data still exist that report these unusually high values.

Direct measurements of evapotranspiration are often not feasible in hydrologic evaluations. Using remote sensing to compute actual evapotranspiration [Surface Energy Balance Algorithm for Land (SEBAL), Mapping of Evapotranspiration at High Resolution with Internal Calibration (METRIC), etc.] has become popular over the last decade (Allen et al. 2007a). However, this method is time-intensive, and data may only be available for a limited period. Further, remote sensing has limitations when long-term evaluations are required, future predictions are needed, or where the vegetation types are not currently growing in the area of interest.

As a case in point, the California Central Valley has changed significantly since development began in the mid-18th century when the first European settlers arrived. Early maps and eyewitness accounts indicate that the Central Valley was formerly home to vast areas of wetland, riparian forest, and grassland habitats that no longer exist (Thompson 1961; Küchler 1977; California State University Chico 2003). It is estimated that wetland acreage in the Central Valley has declined from over 4 million acres to approximately 379,000 acres (Garone 2011).

In this study, evapotranspiration occurring in a variety of aquatic and terrestrial habitats was estimated for the portion of California's Central Valley that drains to the San Francisco Bay, referred to here as the "Valley Floor." California's Central Valley has a single surface water outlet (not counting evaporation and transpiration): through the San Francisco Bay-Delta, which drains the Sacramento Basin Valley from the north and the San Joaquin Basin Valley from the south. The southern part of the San Joaquin Valley (Tulare Lake Basin) is a closed basin that rarely drains to the Delta. Water that is not consumed through evaporation or transpiration flows through the Delta and is discharged into San Francisco Bay. This is commonly referred to as Delta outflow.

Past Studies

Two studies have estimated evapotranspiration by natural vegetation within the Central Valley (Fox 1987; Shelton 1987). Fox (1987) estimated long-term annual average Delta outflow from a water balance based on unimpaired rim inflows, precipitation on the Valley Floor, and evapotranspiration from native vegetation. Shelton (1987) compared predevelopment evapotranspiration within the Central Valley with current agricultural evapotranspiration. Fox (1987) and Shelton (1987) relied on annual estimates of natural vegetation evapotranspiration from studies throughout the western United States. In some cases, these evapotranspiration measurements were conducted in the early to mid-1900s.

Bolger et al. (2011) used a 3D numerical model (HydroGeoSphere) to assess the hydraulic and hydrologic conditions in the northern San Joaquin Valley from the Kings River (south of Fresno) to Sacramento. Evapotranspiration was estimated within the model based on computed root zone soil moisture along with input information on leaf-area index, soil properties, and potential evapotranspiration (ET) (which was assumed to equal the grass reference evapotranspiration for that study). The potential ET was estimated from long-term averaged data and did not vary from year to year. Bolger acknowledges that ET was a major outflow component; however, he did not report actual evapotranspiration for each vegetation type.

With all of the past studies, a major issue in estimating evapotranspiration from natural vegetation stems from somewhat limited research of varying quality and a lack of standardization on transferability in these measurements to different locations and time frames.

K_v and Water Balance Approaches

In this study, evapotranspiration estimates were made by native vegetation type within each Planning Area [California Department of Water Resources (CDWR) 2005] in the portion of the Valley Floor that historically drained to the San Francisco Bay (Fig. 1).

The new estimation approach presented in this paper is based on studies that measured evapotranspiration from vegetation similar to that found in the predeveloped Central Valley of California. Measured evapotranspiration was used to develop transferable grass reference-based vegetation coefficients (K_v's). These K_v values were used to compute local evapotranspiration on a monthly or daily basis using a standardized approach assuming similar conditions. Two methods were employed to estimate evapotranspiration: (1) K_v method for vegetation with a continuous water supply throughout the growing season, and (2) water balance method for vegetation that depends solely on precipitation. Some estimated vegetation K_v values (for permanent wetlands and riparian forest) are compared to actual evapotranspiration measured using remote sensing. Meteorological conditions of water years 1922 through 2009 (an 88-year period) were used to compute annual average evapotranspiration (depth) for vegetation types in predeveloped California. Studies, currently underway, to simulate hydrologic conditions in predeveloped California (based on the 1922–2009 meteorological conditions) will use the monthly and annual evapotranspiration values developed in this study. The long-term average ET depths by region could be used for planning and design of restoration activities for similar vegetation. The K_v values and soil water balance procedures could be used with local climatic data from other regions around the world for a variety of ET evaluations.

Methods

Several studies have examined the composition of the vegetation in the Central Valley prior to development or early in the development of the region (Thompson 1957, 1961; Küchler 1977; Fox 1987; TBI 1998; California State University Chico 2003). This study relied on the California State University Chico (2003) research, supplemented by Küchler (1977) as discussed in Fox and Sears (2014). A more comprehensive list of historical studies can be found in the reference section of CSU Chico (2003) which is, for the most part, information compiled from many earlier sources used to create a spatial distribution of vegetation categories. The vegetation habitat types in the study area (Fig. 1) include wetlands, riparian forest, grasslands, valley oak/foothill hardwoods, chaparral, and other floodplain habitats. The latter category was subdivided based on the work of Küchler (1977).

The general categories identified in CSU Chico would likely have included vegetation within different ecosystems. Grassland habitat would include perennial grasses with access to moisture in the high water table as well as perennial and annual grasses that relied on precipitation stored in the root zone through winter rains. The other floodplain habitat category was stated as a mixture of riparian, wetland, and grassland vegetation (California State University Chico 2003), which was classified using the technique of Küchler (1977).

The water table in predeveloped California was at or less than 10 feet below ground surface throughout much of the Valley Floor,

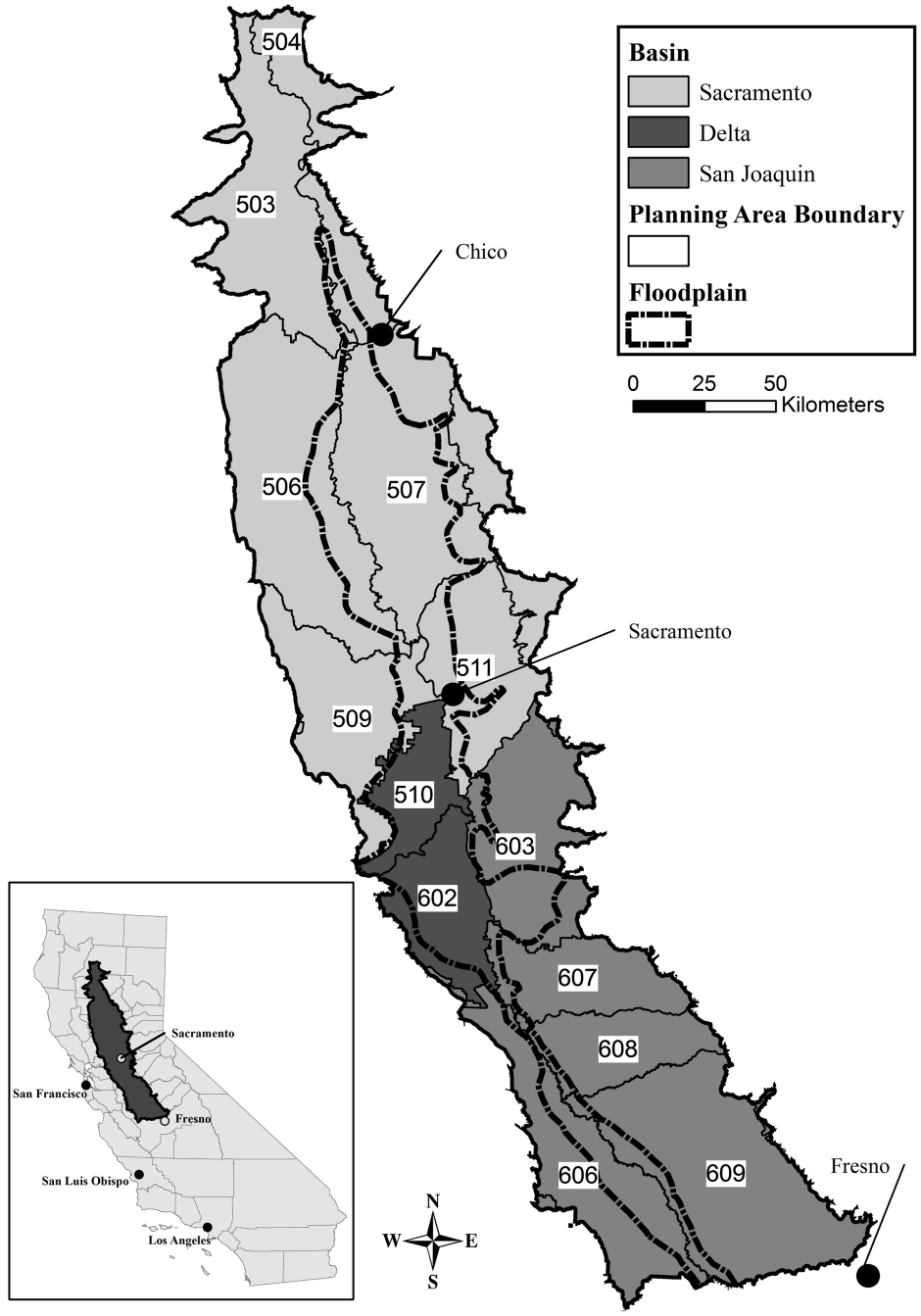

Fig. 1. Planning Areas shown with the Valley Floor and floodplain areas used for this evaluation; Planning Area 601 within the Valley Floor is too small to show on this map

and artesian conditions were widespread (Williamson et al. 1989). This shallow groundwater extended from Sutter Butte to south of the Stanislaus River, covering approximately 8,000 mi^2. In this region, grasslands were likely made up of perennial bunchgrass with year-round access to water from the water table (Küchler 1977; Heady 1988; Bartolome et al. 2007). As the depth to the groundwater table increased away from this region, the grasslands were likely more seasonal, relying on precipitation stored in the root zone. However, in some locations, a perched water table caused by a shallow clay layer or impermeable subsoil layers caused vernal pools to form. In these regions, some of the grasses and other vegetation would have access to water for a longer timeframe compared to the rainfed grasslands.

Similarly, some of the wetland habitat around the periphery of the floodplains, away from areas with high water tables would have relied on seasonal rainfall and flooding as the primary source of moisture. Once the floodwaters receded and the winter and spring precipitation ended, some of the wetlands would dry down until the next fall and winter when rainfalls and floods again occurred. Seasonal wetlands are another wetland classification within the Central Valley along with permanent wetlands and vernal pool wetlands (Garone 2011). The permanent and some vernal pool wetlands would have access to water for a majority of or the entire year.

The determination of K_v and ultimately the evapotranspiration rate from natural vegetation was split into two categories:

evapotranspiration without water deficit (nonstressed), which comprises permanent wetlands, riparian forest, and permanent perennial grasslands; and evapotranspiration under water-stressed conditions once the source water was no longer available (e.g., rainfed grasslands, valley oak/hardwoods split into foothill hardwoods and valley oak savannas, and seasonal wetlands). Vernal pools were examined differently because of the lack of reported evapotranspiration. Once the K_v values were determined for each category, the long-term average ET_v was computed for each Planning Area shown in Fig. 1.

Monthly Non-Water-Stressed K_v

An intensive review of natural vegetation evapotranspiration literature was conducted to examine studies that investigated wetland, riparian, open water evaporation, and native grasslands that had access to water throughout the growing period. There have been several reviews conducted for different native vegetation types (Johns 1989; Drexler et al. 2004; Moore et al. 2004) and it is not the intent to repeat that information here. The available reviews provided information such as who conducted the study, the vegetation type, etc. In most cases, actual results were limited to annual depth of evapotranspiration, if any results were discussed at all.

Specific information was sought for this study to develop useful, reliable K_v values. A main criterion for selection was that the study had to include at least monthly data. The authors only examined data from investigations that measured evapotranspiration from vegetation (ET_v) surrounded by similar vegetation on all sides (i.e., with sufficient fetch) using a lysimeter/tank, Bowen ratio, eddy correlation, surface renewal, or remote sensing of actual evapotranspiration using an energy balance. In one case, estimates of ET_v using porometer measurements were included because of the lack of alternative estimates. ET_v estimates using a larger scale (field or watershed) water balance were avoided due to the inaccuracies associated with measuring inflows, outflows, and changes in internal water storage. ET_v assessments using vegetative indices with empirical coefficients were also avoided since this is not an actual measurement. Several early studies were found in which ET_v was measured without proper fetch, which caused significant overestimation ET_v due to the aforementioned clothesline effect. The data gathered from the literature review focused on ET_v investigations after 1945 unless the site conditions and experimental methods were explained in sufficient detail and the researcher had sufficient experience to provide confidence in the measurements. A majority of the studies used in this paper were conducted in the western United States, although some information from Florida was used.

Computation of Non-Water-Stressed K_v

Transferring and adjusting evapotranspiration estimates made during a specific time frame in one location to a different location during a different time frame is commonly done using a reference based on local weather conditions and an adjustment coefficient based on the vegetation and growth stage (Allen et al. 1998). Weather Bureau Class A Pan evaporation was originally used as the reference for natural vegetation. Starting in the early 1970s, the Priestley-Taylor method became popular for estimating natural vegetation ET because it required less input data. The Jensen-Haise and Blaney-Criddle methods have also been used as references (Jensen et al. 1990). However, without a standard reference, different adjustment coefficients are needed for each reference equation. Attempting to compare coefficients based on different references can be challenging and has been identified as a major drawback of reference-based computations for natural vegetation (Drexler et al. 2004).

The standard approach for agricultural crops is to use a reference crop evapotranspiration (ET_o) computed from specialized weather station networks along with a crop coefficient (K_c) that was developed through research for specific stages of the crop cycle. Crop evapotranspiration (ET_c) can be computed using Eq. (1)

$$ET_c = ET_o \times K_c \tag{1}$$

The reference crop used is generally grass (short crop) or alfalfa (tall crop). The 2005 ASCE Standardized Penman-Monteith (ASCE ET_o) equation is the current standard for computation for either a grass or alfalfa reference evapotranspiration (Allen et al. 2005a). Over the past several decades, specialized reference evapotranspiration weather stations have been installed throughout the western United States. This provides a great resource for weather data and reference evapotranspiration at high temporal resolution (hourly and daily values).

This study applied this standard approach to the type of natural vegetation found in California's Central Valley predevelopment. As natural vegetation is of interest, the term crop coefficient is replaced in this work by a more general vegetation coefficient (K_v), and crop evapotranspiration (ET_c) is replaced with vegetation evapotranspiration (ET_v). There is debate on which reference crop, grass or alfalfa, is more appropriate. However, the authors believe that it is more important to define which reference crop was used to develop K_v or K_c values. Generally, regional decisions are made to use a particular reference crop with weather station networks. In California, grass reference evapotranspiration is used in the California Irrigation Management Information System (CIMIS) weather station network. Spatial, long-term daily ET_o information from locations throughout California has also been developed by the California Department of Water Resources (CDWR) CalSIMETAW program (Orang et al. 2013). For these reasons, grass reference evapotranspiration (ET_o) was selected for this study.

The grass reference is a hypothetical green surface with an assumed height, and fixed surface resistance and albedo (Allen et al. 1998). The reference crop is not intended to mimic the vegetation for which ET_v is to be estimated. The properties of the hypothetical reference crop are used in the ASCE ET_o equation along with weather information to account for regional climatic variability. The K_v values incorporate vegetation characteristics that influence evapotranspiration such as development, canopy properties, aerodynamic resistances, water availability, and ground cover. For natural vegetation, Eq. (1) can be rewritten as Eq. (2)

$$ET_v = ET_o \times K_v \tag{2}$$

Using Eq. (2), the monthly K_v values were developed from the monthly ET_v measurements obtained from the literature review and documented or estimated ET_o using Eq. (3)

$$K_v = \frac{ET_v}{ET_{o\_Study}} \tag{3}$$

Data from some studies were rejected based on methodological issues or conditions that were not representative of the vegetation conditions within the predeveloped Central Valley. Drexler et al. (2004), for example, points out that for wetlands, a drawback to the K_v approach stems from inaccurate methodologies employed during the measurement of ET_v. As previously mentioned, studies conducted without appropriate fetch (isolated stands creating a clothesline effect) were not used in this study. However, elevated ET_v values for vegetation reported to be small stand (as opposed to

isolated stands) are valid. As small-stand wetland areas were present along numerous sloughs and lakes within the floodplain, separate K_v values were developed for small-stand wetlands.

Grass Reference ET_{o_Study} to Compute K_v

In several recent studies, K_v was computed based on a Penman-Monteith equation for ET_o (grass reference) or ET_r (alfalfa reference). Some of these studies were conducted prior to the publication of the ASCE Standardized Reference Evapotranspiration Equation, but used similar equations and standards. If the K_v was developed using a grass reference, it is reported here without modification. If the K_v was based on an alfalfa reference, it was modified to convert it to a grass-reference-based K_v. These modifications will be discussed.

In some cases, the standard grass-reference equation could not be used to compute K_v. The ET_{o_Study}, for example, had to be estimated on a monthly basis for the time frame and the location that the study was conducted. As most ET_o weather stations were not installed in the western United States until the 1980s or later, it was not possible to use the standardized reference evapotranspiration equation for some datasets. Alternatively, the Hargreaves ET_o equation was used in cases where the full set of weather parameters was not available. The Hargreaves equation has been shown to provide relatively accurate ET_o estimates with limited data (maximum and minimum temperature only) in arid regions (Jensen et al. 1990; Allen et al. 1998). Hargreaves ET_o is computed based on temperature and extraterrestrial radiation (R_a) as Eq. (4)

$$\text{Hargreaves\_ET}_o = 0.0023(T_{\text{mean}} + 17.8)(T_{\text{max}} - T_{\text{min}})^{0.5} R_a \quad (4)$$

where temperatures are in degrees Celsius, and R_a and ET_o are in millimeters per unit time. The Hargreaves equation does not include direct information on wind speed or relative humidity, which can cause inaccuracies associated with the Hargreaves ET_o. Allen et al. (1998) discusses a calibration method to improve the accuracy of the Hargreaves ET_o estimate on a monthly or annual basis by comparing it to the standardized Penman-Monteith ET_o for years with overlapping data.

ET_{o_Study} was determined for each study site depending on the data availability. The list below is used to identify the method used to compute ET_o for each study summarized in the results section. The methods used for determining ET_o were as follows:

1. In cases where the vegetation coefficient was provided and ET_{o_Study} was not needed, if the K_v provided was based on an alfalfa reference crop (ET_r), these alfalfa-reference-based K_v values were multiplied by 1.15 (estimated ratio of ET_r/ET_o) to estimate K_v based on a grass reference. However, when possible, a conversion factor was computed on a monthly basis as actual ET_r/ET_o over a period of two or more years. The ratio of ET_r/ET_o was then averaged by month to account for seasonal variability improving the accuracy of the monthly grass-reference-based K_v;
2. If an ET_o weather station existed near the study location during the study period, ASCE ET_o was used;
3. If an ET_o weather station was placed near the location (within 10–20 mi depending on the climate variability and terrain) of the study site after the study was conducted, a monthly calibrated Hargreaves ET_o was used. Calibration was conducted based on years when weather station ET_o was available;
4. If no ET_o weather station was near the study location but monthly temperature data were provided with the study data, Hargreaves ET_o was used based on these temperature data; and
5. If no ET_o weather station was near the study location and monthly temperature data for the study period were not provided, Hargreaves ET_o was used based on PRISM data for the location and time frame of the study.

If methods (4) or (5) were used to estimate ET_{o_Study}, these ET_o values were checked against the long-term (10-year) average ASCE ET_o on an annual basis. The long-term average ASCE ET_o used for the check was either from weather stations within 20–30 miles with similar climate conditions or, for studies in California, from Spatial CIMIS data for the location of the study site (Hart et al. 2009). The difference between the annual ET_o values was set at a threshold of $\pm 15\%$. This reality check ensured that gross errors in the ET_{o_Study} were avoided. If the Hargreaves ET_o was outside of this threshold, alternative means of computing ET_o were attempted or the dataset was abandoned. The alternative method for computing ET_o was to find a nearby NCDC weather station with temperature data for the study's time frame and use the Hargreaves equation to compute the ET_o based on these data.

The PRISM (Parameter-elevation Regressions on Independent Slopes Model) system maintained by Oregon State University provides a grid of monthly temperatures (minimum and maximum) from 1895 to the present covering the United States (Daly et al. 2002, 2008). PRISM temperature data are computed based on surface weather station data and are interpolated based on factors such as location, coastal proximity, elevation, and topography (Daly et al. 2000).

Comparison of Nonstressed K_v Values from Previous Studies to Measured Values from Remote Sensing

As part of an unrelated, D. J. Howes, unpublished data, 2013, the primary author measured actual evapotranspiration from riparian and wetland habitats in Kern County, CA using a surface energy balance with remote sensing data. Monthly K_v values were computed based on computed ET_o in these investigations and compared to the monthly K_v values from literature. To develop the actual evapotranspiration from the riparian and wetland vegetation, LandSAT 5 images were processed over a two-year period for each site using modified METRIC procedures (Allen et al. 2007a). The primary author has modified the original METRIC procedure to use a grass-reference evapotranspiration and use a semiautomated internal calibration procedure. The values obtained from this separate study proved useful to the research discussed here, and a comparison of the data appears in the "Results and Discussion" section of this paper.

The wetland area that was examined for the comparison is within Kern Wildlife Refuge in northern Kern County, California. The wetland vegetation consists of tules, timothy, and cattails. LandSAT 5 images (Path 42/Row 35) were processed from March through October 2011, which was an unusually wet year that resulted in a portion of the wetland within the refuge having water all season. Because of limited water supplies during the summer, in most years the Kern Wildlife Refuge wetlands are seasonal with limited water supplies during the summer months.

K_v values were computed for each image processed (one per month) using Eq. (2) where the ET_v was the instantaneous value at the time of image acquisition computed with METRIC and ET_o was the instantaneous grass-reference evapotranspiration. The instantaneous ET_o was interpolated from hourly data collected at the CIMIS weather station near Lost Hills, California (Belridge Station, Number 146).

Riparian vegetation in the Central Valley no longer exists in large quantities. However, one of the most significant remaining cottonwood–willow forests in California is located along the Kern River east of Lake Isabella, California in the southern Sierra Nevada mountain range. LandSAT 5 images (Path 41/Row 35) from March through September 2011 and October and

November 2010 were used to compute actual evapotranspiration for the riparian forest near Lake Isabella. At least one image per month was used for the evaluation. K_v values were computed as previously described; however, the instantaneous ET_o was computed using the 2005 ASCE Standardized ET_o equation with weather data collected at a Remote Automatic Weather Station (RAWS) near Kernville, California (MesoWest Station KRNC1). Weather data were quality controlled prior to computing ET_o based on procedures of Allen et al. (1998).

Evapotranspiration from Rainfed Vegetation

A portion of the grasslands and valley/foothill hardwood habitats and all of the chaparral along the perimeter of the predeveloped Valley Floor would have relied on precipitation because the water table was generally deeper along the higher elevation areas. The native grasslands contained primarily perennial bunchgrasses that have deeper roots than the current annual grasses and in some cases would have had access to groundwater from the high water table (Reever Morghan et al. 2007). Grasslands that have access to groundwater would not have been water stressed, and the K_v would therefore be represented by the natural grass K_v discussed in the previous section. Special consideration was given to oak savannas that had access to groundwater (termed "valley oak savannas") as will be discussed later. However, a portion of the grasslands and valley/foothill hardwoods identified by the CSU Chico study would have relied principally on precipitation (termed "rainfed grassland" and "foothill hardwoods," respectively).

The standard relationship shown in Eqs. (1) and (2) assumes a full water supply. Thus, it cannot be used for vegetation that depends on precipitation as the only water supply. K_v values measured during a particular year would not necessarily be representative of K_v values for a different year with different precipitation rates or in areas with different soil types. Accounting for variable precipitation both from year to year and spatially requires examining root-zone soil moisture and the plant development over the period of interest. For this evaluation, a daily soil–water balance using the dual-crop coefficient method (Allen et al. 1998) was used for the 88-year period for rainfed vegetation.

The ET_v for rainfed grasslands and foothill hardwoods was estimated for this study using the soil water balance approach calibrated using data measured near Ione, CA using the eddy covariance technique (Baldocchi et al. 2004). The subject study area is within managed ranches in which brush has been removed and cattle graze the grasses and herbs. Furthermore, it no longer contains native perennial bunchgrasses believed to have once been dominant. In this oak savanna ecosystem, trees covered about 40% of the landscape, predominately blue oaks (*Quercus douglasii*) with occasional grey pines (*Pinus sabiniana*) (Miller et al. 2010). This ecosystem is used to represent "foothill hardwoods," a subset of Chico's (2003) "valley foothill/hardwood." The perennial blue oaks that dominate the site have limited access to groundwater, unlike the deciduous valley oaks that dominated the Central Valley Floor prior to development. Finally, its soils and elevation are not representative of the Valley Floor study area (Fig. 1). Thus, the soil–water balance approach based on Ione data likely underestimates the evapotranspiration that would have occurred from grassland and foothill hardwood areas under natural conditions. However, it is currently the best source of data available.

The following sections discuss soil–water balance model calibration and the use of the calibrated model to examine rainfed vegetation throughout the Valley Floor. Once the soil–water balance model was calibrated, soil type and root-zone depth (for the oaks) were modified to be more representative of conditions on the Valley Floor, as will be discussed. The third section discusses special consideration for the valley oaks that had access to groundwater but were in rainfed grasslands.

Soil–Water Balance Model Calibration

The soil–water balance model requires inputs related to plant development, soil-available water-holding capacity, root-zone depth, daily grass reference evapotranspiration, daily precipitation, and basal K_v (K_v for vegetation that is nonstressed with no surface evaporation) during different development periods. While many inputs into the model could be estimated for the Valley Floor based on weather measurements and soil reports, vegetation parameters including basal K_v and plant development timing are unknown. To estimate the vegetation parameters for the grasslands and foothill hardwoods, these parameters were adjusted manually until the modeled ET_v matched the measured ET_v. Because only two parameters were modified during the calibration, namely vegetation development and basal K_v, manual calibration was used. However, this was a time-consuming process and in the future, an automated calibration tool may be more appropriate.

Daily grass reference evapotranspiration data were obtained from CDWR Cal-SIMETAW program for the Planning Area that included Ione, California based on the spatially averaged ET_o (Orang et al. 2013). Estimated daily precipitation was also provided with ET_o. However, the annual precipitation in Valley Floor Planning Area was significantly lower during that year than reported by Baldocchi et al. (2004). This is likely due to the fact that Ione, California is at a higher elevation along the Sierra Nevada foothills and receives more precipitation than other portions of the Planning Area (Planning Area #603). However, daily precipitation data from the original study were not available. To make the adjustment, on days of precipitation in the dataset, the precipitation was increased until the annual precipitation amounts matched those of Baldocchi et al. (2004). In this way, the seasonal precipitation variability was maintained.

For model calibration, the soil-available water-holding capacity (AWHC) was based on the soil retention curves measured by Baldocchi et al. (2004). The reported soil textures were silt loam to rocky silt loam (Miller et al. 2010). The AWHC was computed to be 350 mm/m for the oak savanna and 190 mm/m for the grassland based on the soil–water retention curves. The maximum root-zone depth used for the annual grassland was 0.6 m (Reever Morghan et al. 2007).

For the foothill oak savanna, used as a surrogate for foothill hardwoods, the depth of the root zone was assumed to be 1 m, which is equivalent to the depth of the surface soil (Miller et al. 2010). Both Baldocchi et al. (2004) and Miller et al. (2010) reported that the oaks used groundwater in the summer and fall when soil moisture was limited. While the overall ET_v was significantly lower when soil moisture levels were low, a high percentage of ET_v during this time can be attributed to groundwater (Miller et al. 2010). Oak roots can extend through fractured rock to depths in excess of 24 m (Lewis and Burgy 1964). The lower ET_v during the summer and fall is due to the fact that a relatively shallow soil layer overlaid a fractured rock aquifer that was accessible to a smaller portion of roots. Miller et al. (2012) estimates that groundwater supplies account for approximately 20% of the annual evapotranspiration in the foothill oak savanna. The soil–water balance model did not include contributions from the groundwater in the summer and fall, thus underestimating evapotranspiration for foothill oak savanna. Therefore, the summer evapotranspiration comparison shown in Fig. 2(a) is higher for the measured values than the modeled values. In July and August 2002, the difference between measured and modeled ET was 14 mm and 16 mm,

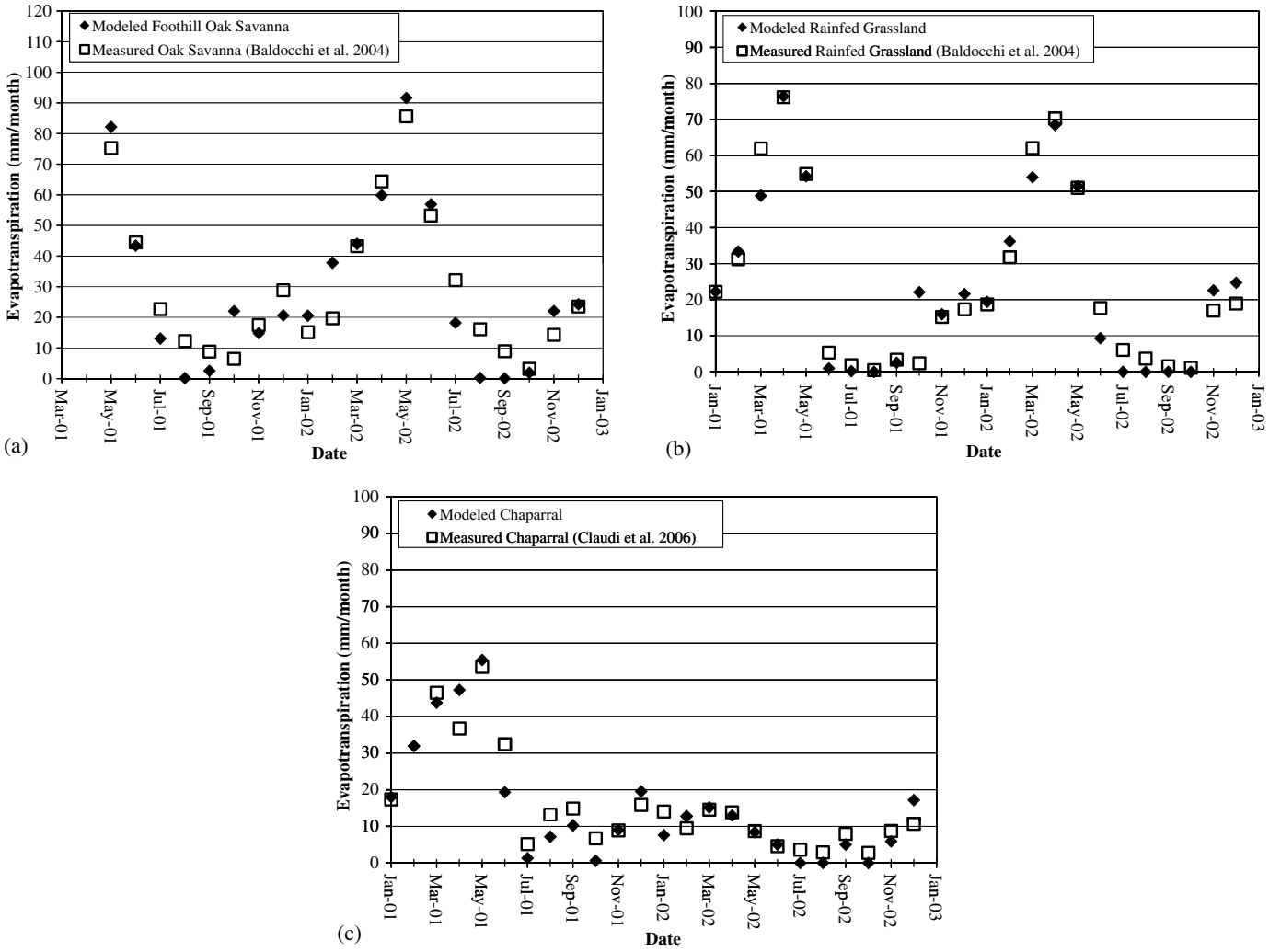

Fig. 2. Measured evapotranspiration from eddy covariance compared to calibrated soil–water balance model results for foothill oak savanna and rainfed grasslands with measured values from Baldocchi et al. (2004) and chaparral with measured values from Claudi et al. (2006)

respectively. For the valley oak savanna category, groundwater availability during the summer was assumed.

Vegetation development and basal K_v were calibrated by comparing reported ET_v data from the eddy covariance stations (Baldocchi et al. 2004) to modeled ET_v. The processed data for the years reported in the study were obtained from FLUXNET (ORNL DAAC 2013). The development stages and basal K_v were manually adjusted until the modeled and measured monthly average ET_v followed similar patterns and had similar magnitudes, as will be discussed in more detail. The basal K_v is the potential transpiration without water stress and is generally a function of leaf area and vegetation type. The actual K_v is computed using the dual-crop coefficient method in the soil–water balance model, which accounts for vegetation stress due to limited water availability and soil evaporation from a wet soil surface. This is because basal K_v values are not available for these vegetation types and would be dependent on the vegetation cover and health. Vegetation development could be predicted initially through visual examination of the ET_v from the covariance stations. Initial adjustments to the vegetation development were made until the early year trends (not magnitude) in monthly ET_v agreed. The basal K_v required more adjustment during the calibration procedure and were adjusted until the magnitude of monthly modeled and measured ET_v correlated. Additional fine tuning adjustments were made to the vegetative development timing but basal K_v seemed to be the most important for calibration. The root mean square error (RMSE) and normalized RMSE (NRMSE) for rainfed grassland were 6.1 mm and 8%, respectively. The RMSE and NRMSE for foothill oak savanna were 9.1 mm and 11%, respectively. The higher RMSE and NRMSE for the foothill oak savanna is in part due to the model underpredicting ET_v because it was conservatively assumed that the vegetation type did not have access to groundwater. Calibrated values used for the long-term modeling are shown in Table 1. A comparison between the measured and calibration results are shown in Fig. 2.

Evapotranspiration from chaparral vegetation was calibrated using a similar procedure previously discussed based on data used by Claudio et al. (2006). The chaparral leaf area and height were assumed constant throughout the year and therefore the only calibration parameter was basal K_v. This assumption, which simplified the calibration procedure, resulted in a best fit between modeled and measured data with a constant basal K_v throughout the year. This indicates that chaparral vegetation is capable of utilizing water if it becomes available and regulates its use as soil moisture depletion increases. Processed eddy covariance data from 2001 through 2002 obtained from FLUXNET (ORNL DAAC 2013) at the Sky Oaks field station located in northern San Diego County were used for the calibration. Grass reference ET_o was obtained

Table 1. Final Calibrated Parameters for the Dual Crop Coefficient Modeling of Grassland and Foothill Oak Savanna Vegetation

Parameter	Rainfed grasslands	Foothill oak savanna	Chaparral
Basal K_v initial	0.1	0.1	0.25
Basal K_v full	0.65	0.5	0.25
Initial period length (days)	70	75	n/a
Development period length (days)	75	90	n/a
Date for start of initial period	December 1	December 1	January 1
Soil moisture depletion at onset of stress (%)	55	55	55

from the CIMIS Station #137 near Temecula, California (CIMIS 2013). Calibrated values used for the long-term modeling of chaparral are shown in Table 1. The RMSE and NRMSE for chaparral modeled values were 4.9 mm and 10%, respectively. A comparison between measured and calibrated-modeled ET_v for chaparral is shown in Fig. 2(c).

Soil–Water Balance Model for Valley Floor ET_v Computations

Once the vegetation parameters were calibrated, the other model inputs were modified to represent average conditions on the Valley Floor (as opposed to the upper foothills). The calibrated model for the rainfed grasslands, chaparral, and foothill hardwoods was used as the basis of the long-term modeling of these vegetative types for the Valley Floor. However, modifications were made to the rooting depth and soil AWHC to account for differing characteristics near the Valley Floor. A root-zone depth of 1.5 m was used for the foothill hardwood, which coincides with the measured root-zone depth of older blue oaks (Millikin and Bledsoe 1999). Oak roots in the Valley Floor can be much deeper to tap into the groundwater, but because the grassland and foothill hardwoods oaks are modeled as a system (as opposed to independently), a deeper root zone would lead to overestimation of ET from the grasslands within the foothill hardwood, while underestimating ET from the hardwood themselves. In the foothill regions on the edge of the Valley Floor, Millikin and Bledsoe (1999) found that the majority of the blue oak root biomass was in the top 0.5 to 1 m of soil, and a smaller percentage below that reached to a depth of 1.5 m. However, Miller et al. (2010) found that blue oaks reach and rely on stores of groundwater more than 10 m below the surface. Thus, the approach used here would underestimate ET_v from foothill hardwoods.

The rainfed grasslands' root zone was maintained at 0.6 m based on field studies of annual and perennial bunchgrass on the Valley Floor (Holmes and Rice 1996). Major soil types covering the grassland and valley/foothill hardwood habitat were examined in GIS by overlaying the vegetation types with a large-scale soils map of California (Soil Survey Staff 2006). The major soil texture in both vegetative categories was silt loam, covering 28% of the valley/foothill hardwood and 18% of the grassland areas. Other major soil textures in these regions included gravelly loam, sandy loam, loam, and clay loam. General published values of AWHC for these soil types range from 110 to 200 mm/m (Allen et al. 1998). An average value of 150 mm/m was used for the modeling of both vegetation types.

Soil–Water Balance Model for Valley Oak Savanna ET_v with Contribution from Groundwater

Urbanization and agriculture have replaced the valley oak savannas that once covered a significant area within the Central Valley. Unlike the blue oaks that make up the majority of the foothill hardwood savannas, valley oaks are not as drought tolerant and studies have indicated that they have deep roots that tap into groundwater reserves (Griffin 1973; Knops and Koenig 1994). Valley oaks tend to grow in bottomlands where groundwater is available. Because the water table was much higher predevelopment, it is reasonable to assume that the valley oaks had unrestricted access to groundwater in a significant portion of the Valley Floor. However, no information on evapotranspiration for natural valley oak savannas was found during this investigation. Valley oaks are dormant from December to approximately March in California (Pavlik et al. 1991). During this time frame, the grass and scrub understory would continue to use water (rainfed). It was assumed that the evapotranspiration on the Valley Floor would be similar to the foothill hardwoods during the winter and spring until the soil moisture was depleted in the primary understory root zone. After this period, a K_v value of 0.4 was used throughout the summer and fall to account for groundwater use by the valley oaks. The value of 0.4 was selected to account for a medium density overstory with a shallower rooted understory that either senesces or has significantly reduced evapotranspiration during the summer and early fall. The tree density of the valley oaks during predevelopment was likely mixed, as it is today (Pavlik et al. 1991), having higher densities on the fringe of the riparian forests to wider spacing towards the foothills on the edge of the Valley Floor. An estimated minimum summer and fall K_v of 0.4 represents an average tree density that would underestimate the evapotranspiration in the dense oak forests. However, the distribution of valley oak tree densities throughout the Valley Floor predevelopment is currently unknown so an average density was assumed.

Seasonal Wetlands and Vernal Pools

In contrast to permanent wetlands, seasonal wetlands undergo periods of high water availability starting in late fall with the first precipitation events, through midsummer when the flooding ceases and the water table drops below the ground surface (Garone 2011). The seasonal wetland habitat would have been found in some vernal pools and between permanent wetlands and the margin of the floodplain along the rivers in the Central Valley (Whipple et al. 2012).

The U.S. Geological Survey examined the evapotranspiration from seasonal wetlands near Upper Klamath Lake, Oregon from 2008 through 2010 using eddy covariance (Stannard 2013). In this study, the water table dropped below the soil surface between mid-July and early August each year and returned to standing water conditions in late winter/early spring. On average, the water table dropped approximately 0.5 m below the ground surface for each year and each site by late September to mid-October. On the Valley Floor of California prior to development, the standing water and water table in seasonal wetlands would likely begin to drop as the river and stream flows began to recede in the late spring and summer. The standing water and water table recession in the Upper Klamath Lake coincides with the long-term average drop-off in estimated valley historical rim inflows from the peak flow occurring generally in May (Tanaka et al. 2006). The combination of surface and subsurface outflow and evapotranspiration from the seasonal wetlands would cause a drop in the water table, resulting in reduced ET_v due to water stress.

Because vernal pools are found nestled within grassland areas, they have historically been classified as grasslands. However, vernal pools are functionally similar to seasonal wetlands. The literature review revealed no information on measurement of actual evapotranspiration from vernal pools. Rains et al. (2006) and Williamson et al. (2005) used potential evapotranspiration

(equal to grass reference ET_o) to evaluate the likelihood of seepage from vernal pools. With the lack of monthly (or annual) or more frequent evapotranspiration measurements for vernal pools, estimates were made for K_v values based on typical conditions found in existing vernal pools in California. Vernal pools have a hardpan or low permeability layer at a relatively shallow depth below the ground surface. Rainfall from within the watershed as well as streams and overland runoff feed these vernal pools through surface and subsurface flows. The pools generally fill during the rainy season and in most cases, the pools fill before the vegetation emerges. A variety of vegetation grows within and around the vernal pools. During the summer, evapotranspiration and subsurface outflow drains the pools and some of the vegetation likely senesces. The water available to the plant during the rainy season is similar to wetlands or perennial grasses with access to a high water table. During the summer, evapotranspiration would likely drop significantly because of the lack of available water. This is similar to what occurs with rainfed grasslands, but later into the summer.

Due to the lack of evapotranspiration estimates and a variety of conditions that would be inherently difficult to estimate on a daily basis, it was infeasible to use the daily soil–water balance to estimate evapotranspiration. Estimates for monthly vernal pool K_v values were made based upon reported values from Williamson et al. (2005) on pool stage and soil moisture for vernal pools in California. Williamson et al. (2005) examined the conditions at three vernal pool sites from November through May for a single year. By April–May, the pool levels were dropping. Soil moisture measurements showed further reduction in soil moisture after the pool levels declined to surface. While the soil moisture measurements in the study ended in early June, the soil moisture was still declining, indicating continued evapotranspiration.

The vernal pool K_v was estimated based on aquatic (open water) areas in the winter (December through February) and large-stand wetlands in the spring (March through May). The K_v values in early summer to midsummer during the pool and soil moisture drydown period were estimated based on data collected by Williamson et al. (2005) and photos taken over a period of several years of vernal pool filling to vegetation senescence (Chester 2003). The K_v is assumed to drop to 0.1–0.15 in late summer and early fall until the next rainy season.

Long-Term Average ET_v

The ET_v for vegetation types other than rainfed grasslands, foothill hardwoods, and valley oak savannas were computed on a monthly basis using K_v values found in or computed from published studies and monthly ET_o by Planning Area (Fig. 1). Thirteen Planning Areas (CDWR 2005) were examined covering the Valley Floor from the westward San Joaquin River in the south to Shasta Lake in the north. Because the majority of Planning Area 504 lies outside of the Valley Floor, ET_o and precipitation from detailed analysis Units 143 and 144 (areas within 504 and the Valley Floor) were used for this area. Daily ET_o data for each planning area were averaged by month for each year from January 1922 through December 2009. The ET_v was computed using Eq. (2) for each month during this time period.

The ET_v for rainfed grasslands, foothill hardwood, and valley oak savannas was computed on a daily basis using a daily soil–water balance model from 1922 through 2009. Daily ET_o and precipitation data were developed from the CDWR CalSIMETAW program on a daily basis by Planning Area using procedures described in Orang et al. (2013).

Results and Discussion

Table 2 summarizes key information from the studies used to compute K_v, including occurrence of long-term winter freeze events, water table depth, location, and ET_v measurement method. Table 3 shows the K_v values from each study by month, the average monthly K_v from all studies for each vegetation type, and the K_v used to compute ET_v in this study. The K_v values used to compute ET_v were adjusted to account for conditions that are not representative of the study area. Thus, K_v used to compute ET_v differs from the average of the studies summarized in Table 3 for the reasons explained below.

First, some measurements were taken in climate conditions that were different than those in California. For example, long-term events where average temperatures are below freezing are not common in the Central Valley of California. The criteria for long-term winter freeze generally refer to multiple consecutive days with temperatures below freezing, which could result in severely reduced transpiration even into the early spring because of vegetation dormancy. K_v values from studies that did not have long-term winter freeze were used to compute ET_v in this study during the winter and spring time frames. This was the case for all wetland categories and was a consideration with large-stand riparian forest. For large-stand riparian forest, more weight was given to the Young and Blaney (1942) study results during the spring and summer (through August) because the other study was conducted in New Mexico with long-term winter freeze events.

Second, for permanent grass, measurements taken where the water table was greater than 0.6 m were not used to compute ET_v for this study. The perennial grasses in predeveloped California had deeper roots than the annual grasses examined in these studies. Therefore, inclusion of K_v values for studies with deeper groundwater levels would underestimate evapotranspiration. For other vegetation categories, no other adjustments were made based on water table depth. Water table depth in Table 2 is referenced from the ground surface where reported and is provided for informational purposes. A water table depth identified as "variable" was used for large-scale evapotranspiration assessments using remote sensing (surface energy balance using satellites). A water table depth referred to as "high" indicates that the actual depth was not provided but it was noted that there was the existence of a high water table.

Finally, special cases were considered that only apply to a subset of the measurements (e.g., monthly K_v values with outliers). If a study differed significantly from other studies, it was not used as significantly in the development of the K_v used to compute ET_v. For example, small-stand wetland K_v values in October and November from Young and Blaney (1942) were unusually high compared to other months and studies. In addition, more recent research from reputable sources was often weighted more heavily when deciding what monthly K_v values should be used. However, the factors previously discussed, such as water table depth and absence of long-term freeze events, were given preference when applicable.

Clarification on terminology in the measurement method category is necessary. Many of the earlier studies used inflow/outflow tanks placed within vegetation. These are sometimes referred to as "lysimeters" in literature, but that term was not used here, to differentiate tank measurements with weighing lysimeters often used for measurement of evapotranspiration. The SEB/METRIC measurement method refers to a surface energy balance using remotely sensed data that were processed using the Mapping of Evapotranspiration at High Resolution with Internal Calibration procedure (Allen et al. 2007b).

Table 2. Studies Where Monthly ET_v Data was Obtained for Different Vegetation Types under a Variety of Conditions

Category	Identifier	Vegetation	Long-term winter freeze	Water table depth	Location	Measurement method	ET_o method	Source
Large-stand wetland	1	Cattails	No	Standing	Fort Drum, Florida	Tank within vegetation	1	Mao et al. (2002)
	2	Cattails	No	Standing	Southern Florida	Tank within vegetation	1	Abtew and Obeysekera (1995)[a]
	3	Tules and Cattails	No	Standing	Twitchell Island, California	Surface renewal	1	Drexler et al. (2008)
	4	Tules/Bulrush	No	Standing	Bonsall, California	Tank within vegetation	5	Muckel and Blaney (1945)
	5	Cattails	Yes	Standing	Logan, Utah	Bowen ratio	1	Allen (1998)
Seasonal large-stand wetland	6	Tules, Cattails, Wocus Lilly	Yes	Standing to 0.8 m	Upper Klamath NWR, Oregon	Eddy covariance	1	Stannard (2013)
	7	Tules/Bulrush	Yes	Standing to 0.8 m	Upper Klamath NWR, Oregon	Eddy covariance	1	Stannard (2013)
Small-stand wetland	8	Cattails	No	Standing	King Island, California	Tank within vegetation	5	Young and Blaney (1942)
	9	Tules/Bulrush	No	Standing	King Island, California	Tank within vegetation	5	Young and Blaney (1942)
	10	Tules/Bulrush	No	Standing	Victorville, California	Tank within vegetation	5	Young and Blaney (1942)
	11	Cattails	Yes	Standing	Logan, Utah	Bowen Ratio	1	Allen (1998)
	12	Tules/Bulrush	Yes	Standing	Logan, Utah	Bowen Ratio	1	Allen (1998)
Large-stand riparian	13	Willow	No	High	Santa Ana, California	Tank within vegetation	4	Young and Blaney (1942)
	14	Cottonwood	Yes	Variable	Middle Rio Grande, New Mexico	SEB/METRIC	1	Allen et al. (2005b)
	15	R.Olive	Yes	Variable	Middle Rio Grande, New Mexico	SEB/METRIC	1	Allen et al. (2005b)
	16	Willow	Yes	Variable	Middle Rio Grande, New Mexico	SEB/METRIC	1	Allen et al. (2005b)
Smaller-stand riparian (508 m by 120 m)	17	Reed, Willow, Cottonwood	Yes	0.9 m	Central City, Nebraska	Bowen ratio	1	Irmak et al. (2013)
Large-stand perennial grassland	18	Native pasture	Yes	High	Alturas, California	Tank within vegetation	5	MacGillivray (1975)
	19	Native pasture	Yes	High	Shasta County, California	Tank within vegetation	5	MacGillivray (1975)
	20	Irrigated pasture	Yes	0-0.6 m	Carson Valley, Nevada	Eddy covariance	5	Maurer et al. (2006)
	21	Irrigated pasture	Yes	0.6-1.5 m	Carson Valley, Nevada	Bowen ratio	5	Maurer et al. (2006)
	22	Meadow pasture	Yes	0.3-1.2 m	Upper Green River, Wyoming	Tank within vegetation	1	Pochop and Burman (1987)
Large-stand saltbush	23	Saltbush	Minor	.2-.8 m	Owens Valley, California	Stomatal conductance	1	Steinwand et al. (2001)
	24	Saltbush	Minor	0.4-0.7 m	Owens Valley, California	Eddy covariance	2	Duell (1990)
	25	Saltbush	No	1.6 m	Yuma, Arizona	Tank within vegetation	4	McDonald and Hughes (1968)
	26	Saltbush	No	1.1 m	Yuma, Arizona	Tank within vegetation	4	McDonald and Hughes (1968)
Aquatic surface	27	Shallow open water	No		Fort Drum, Florida	Tank	1	Mao et al. (2002)
	28	Shallow open water	No		Delta Region, California	Tank	5	Matthew (1931)
	29	Shallow open water	No		Lake Elsinore, California	Water balance	5	Young (1947)
Rainfed vegetation	30	Oak-grass savanna	No	No	Near Iona, California	Eddy covariance	2	Baldocchi et al. (2004)
	31	Chaparral—old stand	No	N/A	Near Warner Springs, California	Eddy covariance	2	Claudio et al. (2006)
	32	Chaparral—young stand	No	N/A	Near Warner Springs, California	Eddy covariance	2	Ichii et al. (2009)
	33	Chaparral	Yes	N/A	Sierra Ancha Forest, Arizona	Tank within vegetation	5	Rich (1951)

[a]Presented in (Allen 1998).

Table 3. Monthly K_v (for Grass Reference Evapotranspiration) from Monthly Measured ET_v for Different Vegetation Types and Site Conditions

			K_v for grass reference ET_o											
Category	Identifier	Vegetation	January	February	March	April	May	June	July	August	September	October	November	December
Large-stand permanent wetland	1	Cattails	0.51	0.61	0.64	0.73	0.87	0.87	0.78	0.76	0.86	0.78	0.65	0.56
	2	Cattails		0.69	0.73	1.00	1.15	1.15	1.15	1.15	1.09			
	3	Mixed					0.80	0.92	1.02	1.09	1.01	0.90		
	4	Tules/Bulrush	0.36	0.61	0.76	1.09	1.21	1.20	1.21	1.16	1.15	1.33	0.98	0.78
	4	Tules/Bulrush	0.83	0.61	0.94	1.11	1.24	1.24	1.14	1.14	1.12	1.06	0.78	0.97
	4	Tules/Bulrush	0.98	0.77	0.66	0.83	0.99	1.22	1.27	1.37	1.25	1.23	1.20	0.70
	5	Cattails				0.35[a]	0.75	1.27	1.30	1.30	0.73			
		Average	0.67	0.66	0.75	0.85	1.00	1.12	1.12	1.14	1.03	1.06	0.90	0.75
		Non-Florida average	0.73	0.66	0.79	0.84	1.00	1.17	1.19	1.21	1.05	1.13	0.99	0.82
		Used to compute ET_v	0.70	0.70	0.80	1.00	1.05	1.20	1.20	1.20	1.05	1.10	1.00	0.75
Large-stand seasonal wetland	6	Mixed					0.92	1.06	1.10	1.12	0.72	0.80		
	7	Tules/Bulrush					0.97	1.08	1.09	1.20	0.83	0.85		
		Average					0.94	1.07	1.09	1.16	0.78	0.83		
		Used to compute ET_v[b]	0.70	0.70	0.80	1.00	1.05	1.10	1.10	1.15	0.75	0.80	0.80	0.75
Small-stand permanent wetland	8	Cattails	1.28	1.47	1.61	1.18	1.79	1.46	1.87	1.43	1.52	1.70	1.97	1.36
	9	Tules/Bulrush	0.75	1.09	1.80	1.96	2.64	1.85	1.88	1.40	1.59	2.38	1.97	0.60
	10	Tules/Bulrush	0.46	0.56	0.75	0.81	1.08	1.33	1.39	1.42	1.58	1.26	0.89	0.73
	11	Cattails				0.35	0.96	1.76	1.81	1.81	0.97			
	12	Tules/Bulrush				0.35	0.82	1.60	2.03	1.54	0.52			
		Average	1.02	1.28	1.70	0.96	1.55	1.67	1.90	1.54	1.15	2.04	1.97	0.98
		Used to compute ET_v[c]	1.00	1.10	1.50	1.50	1.60	1.70	1.90	1.60	1.50	1.20	1.15	1.00
Large-stand riparian	13	Willow		0.68	0.78	1.05	0.82	0.90	1.13	1.20	1.43	1.21	1.09	0.80
	14	Cottonwood	0.81	0.72	0.61	0.66	0.82	0.94	1.02	1.02	1.07	1.08	0.88	0.89
	15	R.Olive	0.83	0.74	0.64	0.70	0.86	0.99	1.06	1.06	1.12	1.12	0.92	0.92
	16	Willow	0.81	0.67	0.55	0.59	0.74	0.86	0.93	0.95	1.07	1.05	0.86	0.89
		Average	0.82	0.70	0.65	0.75	0.81	0.93	1.03	1.06	1.17	1.11	0.94	0.87
		Used to compute ET_v[d]	0.80	0.80	0.80	0.80	0.90	1.00	1.10	1.20	1.20	1.15	1.00	0.85
Smaller-stand riparian (508 m by 120 m)	17	Reed, Willow, Cottonwood					0.80	1.24	1.40	1.50	1.13	0.91		
	17	Reed, Willow, Cottonwood					1.00	1.69	1.75	1.79	1.97	1.66		
		Average[e]					0.90	1.46	1.57	1.64	1.55	1.28		
Perennial grassland	18	Native Pasture	0.46	0.43	0.51	0.97	0.97	1.13	1.21	1.28	1.20	1.07	0.69	
	19	Native Pasture	0.29	0.29	0.38	0.90	0.95	1.02	1.09	1.12	1.10	0.99	0.93	0.86
	20	Irrigated Pasture	0.82	0.82	0.90	1.23	1.17	0.93	0.99	0.98	1.09	0.86		
	21	Irrigated Pasture	0.75	0.70	0.63	0.76	1.00	0.84	0.77	0.56	0.50	0.48		
	22	Meadow Pasture					0.63	0.92	0.97	0.78	0.62			
		Average	0.58	0.56	0.60	0.96	0.94	0.97	1.01	0.94	0.90	0.85	0.81	0.86
		Used to compute ET_v[f]	0.55	0.55	0.60	0.95	1.00	1.05	1.10	1.15	1.10	1.00	0.85	0.85
Large-stand saltbush	23	Saltbush			0.04	0.13	0.25	0.35	0.34	0.22	0.10	0.03		
	24	Saltbush	0.39	0.45	0.36	0.41	0.54	0.62	0.75	0.82	0.55	0.32	0.62	0.69
	25	Saltbush	0.20	0.27	0.21	0.42	0.49	0.38	0.49	0.46	0.39	0.35	0.50	0.19
	26	Saltbush		0.50	0.40	0.28	0.61	0.46	0.68	0.69	0.56	0.44	0.42	
	26	Saltbush		0.09	0.20	0.43	0.58	0.60	0.70	0.72	0.64	0.46	0.68	0.72
		Average	0.29	0.33	0.24	0.33	0.49	0.48	0.59	0.58	0.45	0.32	0.56	0.53
		Used to compute ET_v	0.30	0.30	0.30	0.35	0.45	0.50	0.60	0.55	0.45	0.35	0.40	0.35

Table 3. (*Continued.*)

Category	Identifier	Vegetation	K_v for grass reference ET_o										
			January	February	March	April	May	June	July	August	September	October	November	December
Aquatic surface	27	Shallow Water	0.68	0.74	0.78	0.77	0.85	0.85	0.76	0.79	0.70	0.79	0.57	0.53
	28	Shallow Water	0.60	0.71	0.75	0.80	1.05	1.17	1.16	1.20	1.27	0.98	0.79	0.60
	29	Shallow Water	0.70	0.72	0.86	0.79	0.97	1.01	1.12	1.09	1.11	1.20	0.95	0.80
		Average	0.66	0.72	0.80	0.79	0.96	1.01	1.02	1.03	1.03	0.99	0.77	0.64
		Used to compute ET_v	0.65	0.70	0.75	0.80	1.05	1.05	1.05	1.05	1.05	1.00	0.80	0.60
Rainfed vegetation[g]	30	Oak-Grass	0.54	0.39	0.49	0.59	0.55	0.30	0.18	0.11	0.07	0.04	0.36	1.06
	31	Grassland	0.66	0.64	0.70	0.64	0.33	0.10	0.03	0.02	0.01	0.01	0.43	0.86
	31	Chaparral	0.31		0.45	0.28	0.29	0.16	0.03	0.07	0.10	0.06	0.14	0.32
	31	Chaparral	0.23	0.10	0.13	0.11	0.05	0.02	0.02	0.02	0.06	0.03	0.11	0.22
	31	Chaparral	0.19	0.32	0.27	0.25	0.30	0.31						
	32	Chaparral—Young			0.12	0.16	0.17	0.06	0.04	0.04	0.05	0.03	0.14	0.35
	32	Chaparral—Young	0.23	0.35	0.35	0.29	0.37	0.40	0.22					
	32	Chaparral—Young	0.98	0.51	0.55	0.42	0.32	0.20	0.15	0.08	0.21	0.38	0.22	0.18
	32	Chaparral—Young	0.44	0.27	0.59	0.46	0.37	0.30	0.23	0.11	0.10	0.09	0.14	0.34
	33	Chaparral	0.30	0.32	0.26	0.34	0.35	0.04	0.21	0.33	0.30	0.21	0.34	0.40
	Est[h]	Vernal pools	0.65	0.70	0.80	1.00	1.05	0.85	0.50	0.15	0.10	0.10	0.25	0.60

[a]Low K_v value was likely due to low evapotranspiration from postdormant vegetation after significant winter freezing, which is typical in Utah. This value was not used to compute ET_v in this study.
[b]The authors noted errors in measured winter ET_v. Data from permanent wetlands was used for December through January K_v values to compute ET_v for seasonal wetlands in this study. It was assumed that the November K_v was the same as the October K_v for seasonal wetlands.
[c]Low K_v values in April and September for the studies in Utah were likely due to colder temperatures later in the spring and earlier in the fall in addition to the significant winter freeze events causing vegetation dormancy. There was a significant amount of variability in ET_v and K_v from January through May and September through December. The K_v values used to compute ET_v for this study were assumed to increase and decrease relatively smoothly from January to July and July to December, respectively.
[d]Greater weight was given to the K_v values developed for the Young and Blaney (1942) study when developing the K_v values used to compute ET_v in this study especially from January through June and November and December. The other studies examined large-stand riparian forests in New Mexico, which experiences more significant winter freeze than the Central Valley of California.
[e]It was assumed that all riparian forests on the predeveloped Valley Floor were large stand. Therefore, there are no K_v values used to compute ET_v for smaller-stand riparian forests.
[f]K_v values used to compute ET_v for this study were based on studies that examined shallow water table depths within 0.6 m from the surface, as previously described.
[g]K_v values for rainfed vegetation, other than those for vernal pools, were not used to compute ET_v. They are provided here as a reference.
[h]Vernal pool K_v used to compute ET_v in this study was estimated assuming open water from December through February, permanent wetlands from March through May, and decreasing K_v from June through August as the vernal pools soil moisture dries. In November, K_v begins to increase as the rainy season begins.

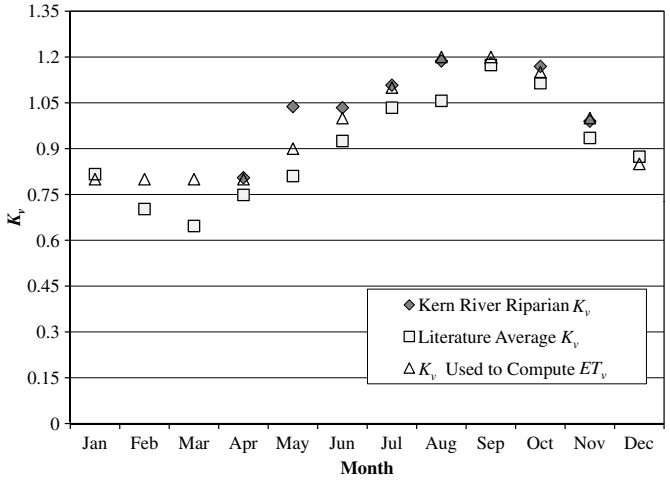

Fig. 3. Comparison of large-stand riparian forest K_v from literature and computed using surface energy balance (METRIC) with LandSAT 5 images for an area along the Kern River near Lake Isabella (March through September 2011 and October and November 2010)

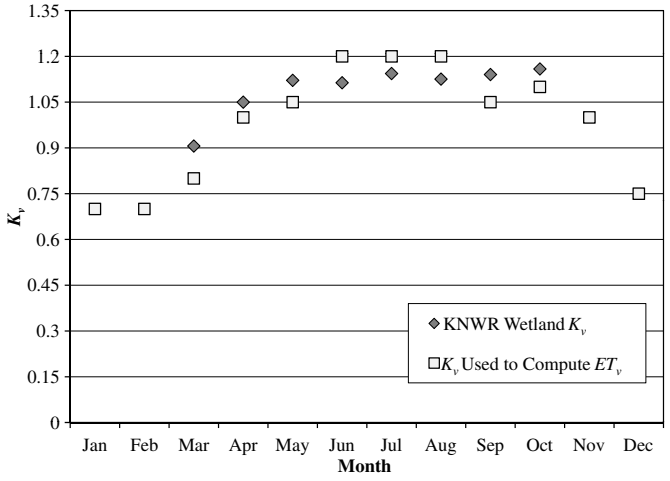

Fig. 4. Comparison of large-stand wetland vegetation K_v from literature and computed using the surface energy balance (METRIC) with LandSAT 5 images for wetlands within Kern National Wildlife Refuge from March 2011 through October 2011

Validation of Large Stand Wetland and Riparian K_v Values

Monthly K_v values for large-stand riparian forest and wetlands from Table 3 were compared to measured values using a surface energy balance (METRIC) with LandSAT 5 for similar vegetation types in California. Figs. 3 and 4 show the comparison of monthly K_v values for riparian forest and wetland vegetation, respectively.

In Figure 3, the average literature K_v values for riparian forest in Table 3 (□) were lower than those measured along the Kern River (◆) from April through August. The majority of the investigations in this category were from the Middle Rio Grande region in New Mexico (Allen et al. 2005b), which experiences winter freezes and thus are not representative of Central Valley riparian forest. Thus, more weight was given to K_v values developed in California, which does not experience winter freezes. The K_v values measured along the Kern River for this comparison were well within the variability seen in Allen et al. (2005b). The K_v used to compute ET_v in this study (Δ) closely matched the values measured at the Kern River site for the April through November analysis period except for May, when the measured K_v was higher.

A comparison of large-stand wetland habitat in Fig. 4 shows the K_v values used in this study (□) were below the measured values at Kern National Wildlife Refuge during the spring and fall (◆). In the summer, the K_v values used in the study were slightly higher than the measured. The lower values measured in the summer months could be due to various issues impacting vegetation health including existing soil conditions such as salinity and alkalinity.

Long-Term Average ET_v of Predevelopment Native Vegetation

The mean annual evapotranspiration (mm/year) from 1922 through 2009 for each vegetation category by Planning Area is shown in Table 4. The coefficient of variation (standard deviation divided by the mean) between years is shown below the annual average ET_v (in italics and parentheses). As expected, the coefficient of variation is similar for vegetation categories where the same set of K_v values were used each year. This would indicate variability due only to ET_o variation. These are not exactly the same for all vegetation types that use the same set of monthly K_v values (e.g., non-water-stressed) due to the fact that the K_v values were not the same each month for different vegetation types. If a K_v is higher in a month that tends to have higher variability in monthly ET_o, the annual coefficient of variation would be slightly higher. An increase in the coefficient of variation, for the vegetation categories that used the daily soil–water balance to determine ET_v, can be attributed to the variability in precipitation as well as ET_o.

The K_v variability within each vegetation category in Table 3 is evident. If one was to select a different set of K_v values to compute ET_v on the predeveloped Valley Floor, the resulting evapotranspiration depth would be different. To examine this, the lowest and highest reported K_v values (on an annual basis) from Table 3 were used to compute the long-term average ET_v over the Valley Floor. The ratios of Valley Floor average ET_v to the Valley Floor average ET_o are shown in Fig. 5. This evaluation was focused on the K_v values that remained constant from year to year (i.e., vegetation with full access to water) since K_v is automatically adjusted on a daily basis for the rainfed vegetation. Therefore, the rainfed vegetation categories that were modeled on a daily basis were not included in Fig. 5. These averages have not been weighted based on the size of the Planning Areas.

Fig. 5 shows that the K_v values used to compute ET_v from Table 4 were between the highest and lowest K_v values, as expected. In some cases, the difference between the ET_v/ET_o for the K_v used in this study and the lowest K_v was greater than the difference with the highest K_v. This can be attributed to several factors. For perennial grasslands, the K_v used in this evaluation was selected for water table depths that did not exceed 0.6 m below ground surface. In other cases, one set of measurements was significantly lower than others (not normally distributed). For example, the K_v used for saltbush was an average; McDonald and Hughes (1968) examined ET_v with the water table reaching 1.6 m in depth below the soil surface (lowest K_v). Therefore, the average ET_v/ET_o was skewed to the higher end because the majority of the studies had water tables closer to the soil surface. Similarly, in other cases such as large-stand riparian, wetlands, and open water evaporation, the studies resulting in the lowest K_v values over the year were outnumbered by higher values, resulting in a higher K_v used to compute ET_v in this study.

Table 4. Results of the Long-Term (1922–2009) Mean Annual Evapotranspiration (mm/year) and Coefficient of Variation between Years (Shown in Parenthesis and Italics) for Each Vegetation Category

Planning area[a]	Rainfed grassland	Perennial grasses	Vernal pools	Large-stand riparian	Large-stand wetland	Small-stand wetland	Seasonal wetland	Foothill hardwood	Valley oak savanna	Saltbush	Chaparral	Aquatic surface
503	391	1,305	755	1,341	1,413	2,043	1,288	451	685	602	295	1,274
	(0.19)	*(0.03)*	*(0.04)*	*(0.03)*	*(0.03)*	*(0.03)*	*(0.03)*	*(0.13)*	*(0.06)*	*(0.03)*	*(0.17)*	*(0.03)*
504[b]	340	1,289	741	1,325	1,395	2,017	1,271	402	640	596	288	1,258
	(0.17)	*(0.04)*	*(0.05)*	*(0.03)*	*(0.04)*	*(0.04)*	*(0.04)*	*(0.11)*	*(0.04)*	*(0.03)*	*(0.17)*	*(0.04)*
506	324	1,350	779	1,387	1,461	2,113	1,331	398	672	623	250	1,317
	(0.21)	*(0.03)*	*(0.04)*	*(0.03)*	*(0.03)*	*(0.03)*	*(0.03)*	*(0.16)*	*(0.06)*	*(0.03)*	*(0.20)*	*(0.03)*
507	352	1,392	803	1,430	1,506	2,179	1,373	427	702	643	269	1,358
	(0.19)	*(0.03)*	*(0.04)*	*(0.03)*	*(0.03)*	*(0.03)*	*(0.03)*	*(0.14)*	*(0.05)*	*(0.03)*	*(0.19)*	*(0.03)*
509	328	1,359	781	1,396	1,469	2,125	1,339	402	679	627	247	1,325
	(0.19)	*(0.03)*	*(0.04)*	*(0.03)*	*(0.03)*	*(0.03)*	*(0.03)*	*(0.14)*	*(0.06)*	*(0.03)*	*(0.20)*	*(0.03)*
510	312	1,368	787	1,404	1,478	2,138	1,347	386	673	631	232	1,333
	(0.20)	*(0.03)*	*(0.04)*	*(0.03)*	*(0.03)*	*(0.03)*	*(0.03)*	*(0.15)*	*(0.06)*	*(0.03)*	*(0.22)*	*(0.03)*
511	348	1,433	820	1,471	1,549	2,241	1,412	426	717	662	264	1,397
	(0.18)	*(0.03)*	*(0.04)*	*(0.03)*	*(0.03)*	*(0.03)*	*(0.03)*	*(0.14)*	*(0.05)*	*(0.03)*	*(0.18)*	*(0.03)*
601	274	1,135	657	1,166	1,227	1,774	1,118	323	560	523	190	1,106
	(0.20)	*(0.03)*	*(0.04)*	*(0.03)*	*(0.03)*	*(0.03)*	*(0.04)*	*(0.14)*	*(0.05)*	*(0.03)*	*(0.21)*	*(0.03)*
602	272	1,213	705	1,246	1,312	1,898	1,196	333	590	559	193	1,183
	(0.22)	*(0.03)*	*(0.04)*	*(0.03)*	*(0.03)*	*(0.03)*	*(0.03)*	*(0.16)*	*(0.06)*	*(0.03)*	*(0.24)*	*(0.03)*
603	337	1,427	821	1,464	1,543	2,233	1,407	415	710	659	255	1,391
	(0.20)	*(0.03)*	*(0.04)*	*(0.03)*	*(0.03)*	*(0.03)*	*(0.03)*	*(0.15)*	*(0.06)*	*(0.03)*	*(0.21)*	*(0.03)*
606	240	1,356	786	1,392	1,466	2,121	1,337	312	625	626	174	1,322
	(0.26)	*(0.03)*	*(0.04)*	*(0.03)*	*(0.03)*	*(0.03)*	*(0.03)*	*(0.19)*	*(0.07)*	*(0.03)*	*(0.29)*	*(0.03)*
607	293	1,402	812	1,438	1,516	2,195	1,383	368	673	647	216	1,367
	(0.23)	*(0.03)*	*(0.04)*	*(0.03)*	*(0.03)*	*(0.03)*	*(0.03)*	*(0.18)*	*(0.07)*	*(0.03)*	*(0.26)*	*(0.03)*
608	289	1,446	841	1,482	1,564	2,264	1,427	366	686	667	215	1,410
	(0.24)	*(0.03)*	*(0.04)*	*(0.03)*	*(0.03)*	*(0.03)*	*(0.03)*	*(0.19)*	*(0.07)*	*(0.03)*	*(0.28)*	*(0.03)*
609	290	1,521	879	1,558	1,644	2,380	1,499	372	715	702	220	1,482
	(0.25)	*(0.04)*	*(0.04)*	*(0.03)*	*(0.04)*	*(0.04)*	*(0.04)*	*(0.20)*	*(0.07)*	*(0.04)*	*(0.28)*	*(0.04)*

[a]Small portions of additional planning areas fell within the Valley Floor and are not shown in this table. Since the majority of those planning areas fell outside of the Valley Floor, the average ET_o and precipitation would not have been representative of the areas within our investigation boundaries. As a surrogate, ET_v from a neighboring planning area was used. Planning Areas 502, 505, 508, 604, and 610 were assumed to have the same depth of ET_v as 503, 509, 511, 510, and 609, respectively.

[b]Grass reference evapotranspiration and precipitation for Detailed Analysis Unit (DAU) 143 and 144 was used in place of Planning Area 504 since a significant portion of 504 lies outside of the Central Valley Floor. DAU 143 and 144 cover the Valley Floor portion of Planning Area 504.

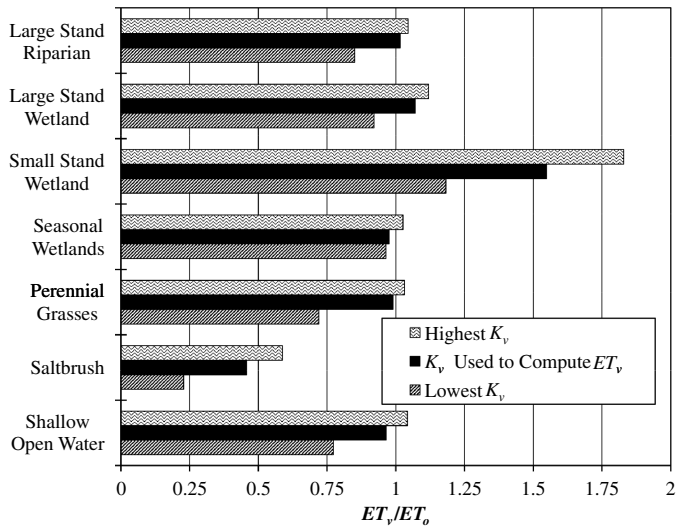

Fig. 5. Comparison of average annual ET_v/ET_o using the highest and lowest K_v to the K_v used to compute ET_v in this study for each vegetation category. The large-stand wetland habitat only considers non-Florida studies from Table 3

The evaporation from shallow open water using the highest K_v matches closely, on an annual basis, with the standard value of 1.05 (grass reference based) for this category reported by Allen et al. (1998). The ET_v/ET_o for K_v used to compute the evaporation from shallow open water was closer to 0.95, which indicates that there may be a slight underestimation in evaporation. However, in some cases the open water (termed "aquatic" in the land use classifications) could be deeper than the 2 m reported for the high ET_v/ET_o; therefore, the lower K_v value is justified.

The most significant variation in ET_v/ET_o was for small-stand wetlands. This also has the highest ratio because of the clothesline effect discussed previously. It is not unexpected that there would be a significant difference in the ET_v/ET_o for this vegetation category since variable stand size will influence ET_v due to the ability of air to move through the vegetation.

It is important to note that the annual ET_v/ET_o ratios shown in Fig. 5 are not transferable. Because the K_v varies by month, the annual ET_v/ET_o ratio will vary in regions that have higher or lower differences between winter and summer ET_o than in the Central Valley of California. Monthly K_v values are generally transferable to other regions as long as vegetative conditions are similar (i.e., no water stress, similar water table depths, similar vegetation characteristics, etc.).

Conclusion

Grass reference evapotranspiration-based vegetation coefficients, K_v, for a variety of natural vegetation categories reported to exist in the Central Valley of California prior to its development have been computed. Two methods were developed to estimate K_v, depending upon the available water supply. For nonstressed vegetation, K_v was estimated assuming a full year-round water supply (e.g., root systems that accessed groundwater). This method was used for permanent wetlands, riparian forest, perennial grassland, saltbush, and shallow open water. For stressed vegetation that relied on available soil moisture, the vegetation coefficients were reduced using a root-zone water balance or estimated based on vegetation characteristics to reduce ET_v below the potential rate due to lack of soil moisture. This method was used for foothill hardwoods, valley oak savanna, rainfed grasslands, vernal pools, seasonal grassland, and chaparral.

The resulting K_v values can be extrapolated to other climates and geographic areas by incorporating locally measured weather parameters to compute the ASCE standardized grass reference ET_o (or equivalent) using Eq. (2). These K_v values are being used by the authors as input to water balances and hydraulic models to estimate natural flows from the Valley Floor (Fig. 1). The K_v values reported here could also be used to estimate evapotranspiration demands in other applications including: to evaluate the impact of climate change on water resources; to determine the effect of vegetation harvesting on stream flows; and to estimate water supplies for habitat restoration activities, just to name a few. As restoration of native vegetation and habitat continue, planners need to be able to estimate water demands from this vegetation. Planners, managers, and policy makers should be aware of the implications of increased water demands associated with potential restoration efforts in areas that may already experience water shortages. Having accurate water consumption estimates can provide insights into which type of vegetation may be most appropriate for restoration efforts. The methods developed in this work could also be extended to other types of vegetation.

This study also highlighted the importance of data made available through networks maintained by local researchers around the world such as FLUXNET. This type of information can be a great benefit to professionals as well as researchers, provided that the data are accurate, well-maintained, and presented in a useable format. Increasing this network of evapotranspiration measurement will be of considerable benefit into the future.

This work highlights areas requiring additional research. This includes: (1) field measurements of evapotranspiration of vernal pools, valley oak savannas, and woodlands, similar to the work reported by Baldocchi et al. (2004) and Miller et al. (2010); (2) validation of small-scale measurements (such as most summarized in Table 3) using surface-energy balance methods with remote-sensing data such as LandSAT; (3) field evaluations of evapotranspiration from similar vegetation but with variable density (riparian and hardwood forests) to develop relationships between density and evapotranspiration; and (4) additional measurements of open water evaporation under variable depths and climate conditions to improve estimates using remote sensing data.

Acknowledgments

This research and evaluation was supported by the San Luis and Delta Mendota Water Authority and the State Water Contractors. The authors would like to thank Morteza Orang, Water Use Unit Chief, California Department of Water Resources, for providing the ET_o and precipitation data for the Planning Areas examined in this study. We would also like to thank Mariana Pascuet, from the Irrigation Training and Research Center, for her assistance with gathering, reviewing, and summarizing a portion of the studies reviewed during this evaluation.

References

Abtew, W., and Obeysekera, J. (1995). "Lysimeter study of evapotranspiration of cattails and comparison of three estimation methods." *Trans. ASAE*, 38(1), 121–129.

Allen, R. (1998). "Predicting evapotranspiration demands for wetlands." *ASCE Wetlands Engineering and River Restoration Conf.*, ASCE, Reston, VA, 1–13.

Allen, R. G., et al., eds. (2005a). *The ASCE standardized reference evapotranspiration equation*, ASCE, Reston, VA.

Allen, R. G., et al. (2007a). "Satellite-based energy balance for mapping evapotranspiration with internalized calibration (METRIC)-applications." *J. Irrig. Drain. Eng.*, 10.1061/(ASCE)0733-9437(2007)133:4(395), 395–406.

Allen, R. G., Pereira, L. S., Howell, T. A., and Jensen, M. E. (2011). "Evapotranspiration information reporting: I. Factors governing measurement accuracy." *Agric. Water Manage.*, 98(6), 899–920.

Allen, R. G., Pereira, L. S., Raes, D., and Smith, M. (1998). "Crop evapotranspiration: Guidelines for computing crop water requirements." *FAO Irrigation and Drainage Paper No. 56*, Food and Agricultural Organization of the United Nations, Rome.

Allen, R. G., Tasumi, M., and Morse, A. (2005b). "Satellite-based evapotranspiration by METRIC and Landsat for western states water management." *U.S. Bureau of Reclamation Evapotranspiration Workshop*, International Center for Water Resources Management at Central State Univ., Wilberforce, OH, 8–10.

Allen, R. G., Trezza, R., and Tasumi, M. (2007b). "Satellite-based energy balance for mapping evapotranspiration with internalized calibration (METRIC)-model." *J. Irrig. Drain. Eng.*, 10.1061/(ASCE)0733-9437(2007)133:4(380), 380–394.

Baldocchi, D. D., Xu, L., and Kiang, N. (2004). "How plant functional-type, weather, seasonal drought, and soil physical properties alter water and energy fluxes of an oak–grass savanna and an annual grassland." *Agric. Forest Meteorol.*, 123(1), 13–39.

Bartolome, J. W., Barry, W. J., Griggs, T., and Hopkinson, P. (2007). "Valley Grasslands." *Terrestrial vegetation in California*, M. G. Barbour, T. Keeler-Wolf, and A. A. Schoenherr, ed., University of California Press, Berkeley, CA, 712.

BDCP. (2013). *Bay delta conservation plan highlights*, California Dept. of Water Resources and California Natural Resources Agency, Sacramento, CA, 61.

Blaney, H. F., Taylor, C. A., Nickle, H. G., and Young, A. (1933). *Consumptive use of water by native plants growing in moist areas in southern California*, California Dept. Public Works, Sacramento, CA, 65–74.

Bolger, B. L., Park, Y.-J., Unger, A. J. A., and Sudicky, E. A. (2011). "Simulating the pre-development hydrologic conditions in the San Joaquin Valley, California." *J. Hydrol.*, 411(3–4), 322–330.

California State University Chico. (2003). *The central valley historic mapping project*, Dept. of Geography and Planning and Geographic Information Center, California State Univ., Chico, CA.

CDWR (California Department of Water Resources). (2005). "California Planning Areas [ESRI Shapefile]." ⟨www.waterplan.water.ca.gov/maps/⟩ (Aug. 13, 2013).

Chester, T. (2003). "Vernal pools of the Santa Rosa Plateau." ⟨tchester.org/srp/vp/⟩ (Nov. 5, 2013).

CIMIS (California Irrigation Management Information System). (2013). ⟨www.cimis.water.ca.gov⟩ (Sep. 27, 2013).

Claudio, H. C., et al. (2006). "Monitoring drought effects on vegetation water content and fluxes in chaparral with the 970 nm water band index." *Remote Sens. Environ.*, 103(3), 304–311.

Daly, C., et al. (2008). "Physiographically sensitive mapping of climatological temperature and precipitation across the conterminous United States." *Int. J. Climatol.*, 28(15), 2031–2064.

Daly, C., Taylor, G., Kittel, T., Schimel, D., and McNab, A. (2002). *Development of a 103-year high-resolution climate data set for the conterminous United States*, Oregon State Univ., Corvallis, OR.

Daly, C., Taylor, G. H., Gibson, W. P., Parzybok, T. W., Johnson, G. L., and Pasteris, P. A. (2000). "High-quality spatial climate data sets for the United States and beyond." *Trans. ASAE*, 43(6), 1957–1962.

Drexler, J. Z., Anderson, F. E., and Snyder, R. L. (2008). "Evapotranspiration rates and crop coefficients for a restored marsh in the Sacramento–San Joaquin Delta, California, USA." *Hydrol. Processes*, 22(6), 725–735.

Drexler, J. Z., Snyder, R. L., Spano, D., Paw, U., and Tha, K. (2004). "A review of models and micrometeorological methods used to estimate wetland evapotranspiration." *Hydrol. Processes*, 18(11), 2071–2101.

Duell, L. F. (1990). "Estimates of evapotranspiration in alkaline scrub and meadow communities of Owens Valley, California, using the Bowen-ratio, eddy-correlation, and Penman-combination methods." *Water Supply Paper 2370-E*, U.S. Geological Survey, Reston, VA.

Fox, P. (1987). "Report on the San Francisco Bay: Freshwater inflow to San Francisco Bay under natural conditions." *State Water Contractors Exhibit Number 262*, Bay Delta Hearings, Sacramento, CA.

Fox, P., and Sears, L. (2014). *Natural vegetation in the central valley of California*, *Technical Rep.*, State Water Contractors and San Luis and Delta-Mendota Water Authority, Los Baños, CA.

Garone, P. (2011). *The fall and rise of the wetlands of California's great central valley*, University of California Press, Berkeley, CA.

Griffin, J. R. (1973). "Xylem sap tension in three woodland oaks of central California." *Ecology*, 54(1), 152–159.

Hart, Q. J., Brugnach, M., Temesgen, B., Rueda, C., Ustin, S. L., and Frame, K. (2009). "Daily reference evapotranspiration for California using satellite imagery and weather station measurement interpolation." *Civ. Eng. Environ. Syst.*, 26(1), 19–33.

Heady, H. F. (1988). "Valley Grasslands." *Terrestrial vegetation of California*, M. G. Barbour and J. Major, eds., Wiley, New York.

Holmes, T. H., and Rice, K. J. (1996). "Patterns of growth and soil-water utilization in some exotic annuals and native perennial bunchgrasses of California." *Ann. Bot.*, 78(2), 233–243.

Ichii, K., et al. (2009). "Refinement of rooting depths using satellite-based evapotranspiration seasonality for ecosystem modeling in California." *Agric. Forest Meteorol.*, 149(11), 1907–1918.

Irmak, S., Kabenge, I., Rudnick, D., Knezevic, S., Woodward, D., and Moravek, M. (2013). "Evapotranspiration crop coefficients for mixed riparian plant community and transpiration crop coefficients for Common reed, Cottonwood and Peach-leaf willow in the Platte River Basin, Nebraska-USA." *J. Hydrol.*, 481, 177–190.

Jensen, M. E., Burman, R. D., and Allen, R. G. (1990). "Evapotranspiration and irrigation water requirements." *Manual of Practice No. 70*, ASCE, New York, NY.

Johns, E. L., ed., (1989). *Water use by naturally occurring vegetation including an annotated bibliography*, ASCE, New York.

Knops, J. M., and Koenig, W. D. (1994). "Water use strategies of five sympatric species of Quercus in central coastal California." *Madrono*, 41(4), 290–301.

Küchler, A. W. (1977). "Natural vegetation of California." *Terrestrial vegetation of California*, J. Major and M. G. Barbour, eds., Wiley, New York.

Lewis, D. C., and Burgy, R. H. (1964). "The Relationship between oak tree roots and groundwater in fractured rock as determined by tritium tracing." *J. Geophys. Res.*, 69(12), 2579–2588.

MacGillivray, N. A. (1975). "Vegetation Use in California, 1974." *Bulletin 113-3*, California Dept. of Water Resources, Sacramento, CA.

Mao, L., Bergman, M., and Tai, C. (2002). "Evapotranspiration measurement and estimation of three wetland environments in the upper St. Johns River basin, Florida." *J. Am. Water Resour. Assoc.*, 38(5), 1271–1285.

Matthew, R. (1931). *Variation and control of salinity in Sacramento-San Joaquin Delta and Upper San Francisco Bay*, California Dept. of Public Works, Sacramento, CA.

Maurer, D. K., Berger, D. L., Tumbusch, M. L., and Johnson, M. J. (2006). "Rates of evapotranspiration, recharge from precipitation beneath selected areas of native vegetation, and streamflow gain and loss in Carson Valley, Douglas County, Nevada, and Alpine County, California." *Scientific Investigations Rep. 2005-5288*, U.S. Geological Survey, Reston, VA, 70.

McDonald, C. C., and Hughes, G. H. (1968). "Studies of consumptive use of water by phreatophytes and hydrophytes near Yuma, Arizona." *Professional Paper 486-F*, U.S. Geological Survey, Washington, DC, 29.

Miller, G. R., et al. (2012). "Understanding ecohydrological connectivity in savannas: a system dynamics modelling approach." *Ecohydrology*, 5(2), 200–220.

Miller, G. R., Chen, X., Rubin, Y., Ma, S., and Baldocchi, D. D. (2010). "Groundwater uptake by woody vegetation in a semiarid oak savanna." *Water Resour. Res.*, 46(10), W10503.

Millikin, C., and Bledsoe, C. (1999). "Biomass and distribution of fine and coarse roots from blue oak (Quercus douglasii) trees in the northern Sierra Nevada foothills of California." *Plant Soil*, 214(1–2), 27–38.

Milly, P. C. D., and Dunne, K. A. (2010). "On the hydrologic adjustment of climate-model projections: The potential pitfall of potential evapotranspiration." *Earth Interact.*, 15(1), 1–14.

Moore, J. L., King, J. P., Bawazir, A. S., and Sammis, T. W. (2004). *A bibliography of evapotranspiration with special emphasis on riparian vegetation*, New Mexico Water Resources Research Institute, Las Cruces, NM.

Muckel, D. C., and Blaney, H. F. (1945). *Utilization of the waters of lower San Luis Rey Valley, San Diego County, California*, U.S. Dept. of Agriculture, Los Angeles.

Orang, M. N., et al. (2013). "California simulation of evapotranspiration of applied water and agricultural energy use in California." *J. Integr. Agric.*, 12(8), 1371–1388.

ORNL DAAC (Oak Ridge National Laboratory Distributed Active Archive Center). (2013). "Oak Ridge national laboratory distributed active archive center FLUXNET web page." ⟨fluxnet.ornl.gov⟩ (Aug. 15, 2013).

Pavlik, B. M., Muick, P. C., Johnson, S. G., and Popper, M. (1991). *Oaks of California*, Cachuma Press, California Oak Foundation, Los Olivos, CA.

Pochop, L., and Burman, Z. (1987). "Development of evapotranspiration crop coefficients, climatological data, and evapotranspiration models for the Upper Green River Basin." *Project Completion Rep., Project 59-6986-13*, Wyoming Water Research Center, Laramie, WY.

Rains, M. C., Fogg, G. E., Harter, T., Dahlgren, R. A., and Williamson, R. J. (2006). "The role of perched aquifers in hydrological connectivity and biogeochemical processes in vernal pool landscapes, Central Valley, California." *Hydrol. Processes*, 20(5), 1157–1175.

Reever Morghan, K. J., Corbin, J. D., and Gerlach, J. (2007). "Water relations." *California Grasslands: Ecology and management*, M. R. Stromberg, J. D. Corbin, and C. M. D'Antonio, eds., University of California Press, Berkeley, CA, 87–93.

Rich, L. R. (1951). "Consumptive use of water by forest and range vegetation." *Proc. Am. Soc. Civ. Eng.*, 77(90), 1–14.

Shelton, M. (1987). "Irrigation induced change in vegetation and evapotranspiration in the Central Valley of California." *Landscape Ecol.*, 1(2), 95–105.

Soil Survey Staff. (2006). "Digital general soil map of the U.S. [ESRI Shapefile]." ⟨datagateway.nrcs.usda.gov⟩ (Sep. 11, 2013).

Stannard, D. I., Gannett, M. W., Polette, D. J., Cameron, J. M., Waibel, M. S., and Spears, J. M. (2013). "Evapotranspiration from marsh and open-water sites at Upper Klamath Lake, Oregon, 2008–2010." *Scientific Investigations Rep. 2013-5014*, U.S. Geological Survey, Reston, VA.

Steinwand, A. L., Harrington, R. F., and Groeneveld, D. P. (2001). "Transpiration coefficients for three Great Basin shrubs." *J. Arid Environ.*, 49(3), 555–567.

Tanaka, S., et al. (2006). "Climate warming and water management adaptation for California." *Clim. Change*, 76(3–4), 361–387.

TBI. (1998). *From the Sierra to the Sea: The ecological history of the San Francisco Bay-Delta Watershed*, Bay Institute of San Francisco, San Francisco.

Thompson, J. (1957). "The settlement geography of the Sacramento-San Joaquin Delta, California." Ph.D. thesis, Stanford Univ., Stanford, CA.

Thompson, K. (1961). "Riparian forests of the Sacramento Valley, California." *Ann. Assoc. Am. Geog.*, 51(3), 294–315.

Whipple, A. A., Grossinger, R. M., Rankin, D., Stanford, B., and Askevold, R. A. (2012). "Sacramento-San Joaquin delta historical ecology investigation: Exploring pattern and process." *Publication 672*, San Fransisco Estuary Institute (SFEI)-Aquatic Science Center, Richmond, CA.

Williamson, A. K., Prudic, D. E., and Swain, L. A. (1989). "Ground-water flow in the Central Valley, California." *Profesional Paper 1401-D*, U.S. Geological Survey, Reston, VA.

Williamson, R. J., Fogg, G. E., Rains, M. C., and Harter, T. H. (2005). *Hydrology of vernal pools at three sites, Southern Sacramento Valley*, Dept. of Land, Air, Water Resources, Univ. of California, Davis.

Young, A. A. (1947). "Evaporation from water surfaces in California." *Bulletin No. 54*, California Dept. of Public Works, Div. of Water Resources and USDA SCS, Sacramento, CA.

Young, A. A., and Blaney, H. F. (1942). "Use of water by native vegetation." *Bulletin No. 50*, California Dept. of Public Works, Sacramento, CA.

Zhao, L., Xia, J., Xu, C.-y., Wang, Z., Sobkowiak, L., and Long, C. (2013). "Evapotranspiration estimation methods in hydrological models." *J. Geog. Sci.*, 23(2), 359–369.

Draft Manuscript for Submission to: ASCE Journal of Water Resources Planning and Management

August 19, 2015 Version

Nine Decades of Salinity Observations in the San Francisco Bay and Delta: Modeling and Trend Evaluation

Paul H. Hutton[1], John S. Rath[2], Limin Chen[3], Michael J. Ungs[4], and Sujoy B. Roy[5]

[1] Principal Engineer, Bay Delta Initiatives, Metropolitan Water District of Southern California, Sacramento, California
[2] Environmental Scientist, Tetra Tech Research and Development, Lafayette, California
[3] Principal Engineer, Tetra Tech Research and Development, Lafayette, California
[4] Principal Scientist, Tetra Tech Research and Development, Lafayette, California
[5] Director, Tetra Tech Research and Development, Lafayette, California

Abstract

The position of the low salinity zone in the San Francisco Bay-Delta—given its correlation with the abundance of several estuarine species—is used for water management in a system that supplies water to more than 20 million people and contains one of the most diverse ecosystems on the Pacific Coast. This work consolidates legacy and modern salinity data to develop a reasonably complete daily record spanning nine decades. The position of the low salinity zone, which is effectively characterized by an empirical model that was developed to support data cleaning and filling, reveals statistically significant trends consistent with increasing water demands and introduction of upstream reservoirs, e.g. increasing salinity trends in wet months and decreasing salinity trends in dry months. Reservoir effects are particularly apparent in drier years, with greater seasonal variability in the early part of the record before major reservoirs operated in the watershed. These data provide a basis for further analysis of how and why the position of the estuary's low salinity zone has changed over time.

Introduction

Freshwater inflows have a direct influence on the salinity structure in estuaries. In San Francisco Bay, the salinity structure has been related to the health of estuarine species in the Suisun Bay and western Delta (Figure 1). In particular, the location or position of two parts per thousand bottom salinity – hereafter referred to as "X2" – has been correlated with the abundance of several species (Jassby et al., 1995). Using data collected over different time periods, the low salinity zone in general and the X2 position in particular have been associated with the greatest abundance of pelagic organisms, including the protected longfin smelt (*Spirinchus thaleichthys*) (Jassby et al., 1995) and delta smelt (*Hypomesus transpacificus*) (Feyrer et. al., 2010). The X2 position has also been associated with the abundance of undesirable species such as the invasive Asian clam (*Corbula amurensis*). The relationship between the low salinity zone and the responses of individual species are a topic of continued research interest (Feyrer et al., 2007, 2010; Kimmerer et al., 2009; Moyle et al., 2010), and the broader science underlying the driving mechanisms between water quality, habitat quality, and species abundance continues to evolve (Reed et al., 2014).

The position of the X2 isohaline (defined as the distance from Golden Gate in kilometers, see Figure 1) during the months of February through June is currently used as the basis of flow management in San Francisco Bay (CSWRCB, 1999). Estuarine flows can be

managed through upstream reservoir releases as well as exports of water from the Delta. The recent biological opinion on Delta smelt (USFWS, 2008) regulates X2 position in fall months (September through November) following wet and above normal water years. Much of the published literature on X2 and its relationship to various biological indicators is based on data collected over limited periods, typically spanning the mid-1960s to the present.

Although X2 is defined in terms of bottom salinity, much of the published analysis is based on surface salinity measurements, including the seminal work on X2 (Jassby et al., 1995). Use of surface salinity as a surrogate for bottom salinity is largely motivated by the abundance of surface salinity measurements throughout the estuary, due in part to historical precedent and to the operational challenges of maintaining salinity sensors at depth. However, the estuary is known to be vertically stratified, with increasing stratification at greater river flows (Monismith et al., 2002). Stratification has been addressed by using a constant factor to relate the bottom salinity to surface salinity, i.e. 2 ppt bottom salinity is assumed to correspond to 1.76 ppt surface salinity (Jassby et al., 1995). Current regulations assume 2 ppt bottom salinity corresponds to 2.64 mS/cm surface specific conductance (CSWRCB, 1999).

Given the importance of the low salinity zone for estuarine species, and of X2 in the management of water in the estuary, the present analysis builds on past work by extending the readily available surface salinity data. The earliest salinity data incorporated in this work are based on technical reports published by the California Department of Public Works (CDPW) and its successor agency, the Department of Water Resources (CDWR), beginning in the 1920s. This work also extends previously published salinity trend evaluations in the Bay-Delta, which have focused on more limited time periods or on station-specific salinity rather than isohaline position (Fox et al., 1991; Shellenbarger and Schoellhamer, 2011; Enright and Culberson, 2009; Moyle et al., 2010). Although the data used here do not represent pre-development conditions such as those obtained through analysis of paleoclimatic signals (Stahle et al., 2001), they do represent a wide range of hydrologic conditions and watershed development activities, including reservoir construction, water exports, and land use changes (Fox et al., 1990).

The major objectives of this work were to (i) develop a cleaned database for salinity across Suisun Bay and the western Delta for the longest observational record possible and compute isohaline positions at each point in time, (ii) develop and calibrate an empirical salinity

model that could be used for additional diagnostic evaluation of the data, and (iii) evaluate changes in the isohaline position over the 91-year period of record from water year 1922 to 2012. Water years in California begin on October 1 of the preceding calendar year. By extending the starting point from the mid-1960s to the early 1920s, the readily available data set now incorporates a period of record prior to the construction of major water storage and diversion projects (completed between 1944 and 1967) as well as a period of severe drought that occurred between 1928 and 1934.

Not surprising given the extensive period of record, the data compiled in this work are not noise- and error-free, arising in part from variations in sampling and analytical methodology. A significant effort was expended to "clean" the data to remove values that appeared to be inconsistent with other values. These data were then used to develop daily salinity estimates at each station, and gaps were filled through interpolation and comparison with neighboring stations. The empirical salinity model, based on a formulation accounting only for flow inputs, was calibrated using these cleaned data. Finally, statistical analyses were performed on the individual station salinity and interpolated isohaline positions to detect changes over time and across different water year classes.

Methods

Salinity Data Sources and Cleaning

Data incorporated in this work include historical grab sample data and modern conductivity sensor data. The historical grab sample data record, hereafter referred to as the Bulletin 23 data record, is based on legacy reports spanning the period October 1921 to June 1971 (CDPW, 1924-55; CDWR 1956-62; CDWR 1963-71). Scanned paper copies of these reports were used to develop an electronic database of salinity throughout the Delta and portions of San Francisco Bay. An important salinity data set that pre-dates the Bulletin 23 data (but was not employed in this study) is based on records by the California Hawaiian Sugar Refining Corporation (C&H). C&H, which obtained most of its fresh water supply in the early 20th century by transporting water to its refinery in Crockett, maintained a record on the distance its barges traveled to obtain fresh water (typically less than 50 mg/l chloride) and the quality of water obtained (CDPW, 1931; Lund et al., 2007). While the C&H records are of great historical interest and demonstrate the seasonal variability in the salinity field prior to extensive upstream development, the nominal isohaline position of 50 mg/l chloride

was not reported with commensurate tidal cycle information and was too low (i.e. too fresh) to accurately characterize the general salinity gradient.

Modern databases were queried from several sources to supplement the Bulletin 23 data, including: 1) the California Data Exchange Center (CDEC, 2013); 2) the Interagency Ecological Program; and 3) USEPA's STORET. These modern data, hereafter referred to collectively as CDEC data, were further supplemented by U.S. Geological Survey data (USGS, 2013) to represent high outflow periods when the low salinity zone extended far downstream into San Francisco Bay. The combined data gathering effort resulted in a master database containing salinity records from October 1921 to September 2012, i.e., water years 1922–2012. The locations of key salinity stations used in this analysis are shown in Figure 1. Additional information on data sources, stations, and time periods are provided in the Supplementary Information (SI) section, Tables S1 through S3.

The raw data contained errors associated in part with variations in sampling and analytical methodology. The Bulletin 23 data report salinity as chloride concentrations. The CDEC data report salinity as specific conductance, or electrical conductivity (EC) standardized to 25 °C. All data were converted to specific conductance in units of milliSiemens (mS/cm) using regression relationships developed from co-located chloride and specific conductance data in the estuary (Denton, 2015).

The CDEC data are collected by continuous EC sensors that report every 15 minutes, and daily averages were computed directly using these sub-daily values. Given that the original sub-daily data were frequently unavailable, averages were computed over 24 hours rather than a tidal day (25 hours). Monismith et al. (2002) reported that the errors associated with this approximation were "very slight". The Bulletin 23 data were collected nominally every four days at higher high tide or low high tide. Because estuarine salinity can vary significantly over the course of a day, these grab sample data were converted to approximately equivalent daily averages using simulation output from a hydrodynamic and water quality transport model, DSM2 (for Delta Simulation Model version 2), a linked-node model that is widely used for studying Delta flow, stage, and water quality (CDWR, 2015). This tidal correction was successfully validated by comparing the resulting daily average estimates with co-occurring CDEC data (see details in Roy et al., 2014). Enright and Culberson (2010), when confronted with the same problem, tidally corrected Bulletin 23 grab sample chloride data through linear correlations with co-occurring CDEC specific

conductance data to produce long-term salinity time series records for three stations in the estuary.

Additional data cleaning and filling was performed by comparing daily average specific conductance at pairs of stations and assuming that under conditions of moderately high salinity reflecting strong ocean influence, salinity decreases monotonically downstream to upstream. When data at a pair of stations are inconsistent with this behavior, i.e., an eastern (upstream) station has a higher salinity than a western (downstream) station, a procedure was required to determine which of the two salinity values was erroneous, acknowledging there is no *a priori* way to make this determination. To perform the data cleaning step, we correlated data for nearby stations using least-squares regressions. Measured values that differed greatly (by more than four standard errors) or too frequently (by more than two standard errors multiple times) from regression predictions were removed from the dataset. This step is considered an approximate way to remove potentially erroneous values from the dataset and it is possible that some true data values are excluded in the process. However, because this analysis is not focused on the behavior of extreme values, this approach is unlikely to affect the conclusions.

The method used to calculate isohaline position, discussed in the next section, requires a reasonably complete salinity record. We filled missing values based on the salinity data of nearby stations using the correlations discussed in the previous paragraph. Filling missing downstream station values from upstream station data was found to be particularly challenging when upstream conditions were fresh, as downstream salinity can vary across orders of magnitude for the same low (or fresh) upstream salinity. After this step was completed, we filled any remaining short gaps (up to eight days) through linear interpolation. When there was an overlap of the Bulletin 23 and CDEC data (i.e., the 1964 to 1971 period), the latter were used in preference.

Isohaline Calculations

Isohaline position was calculated through interpolation of the cleaned and filled salinity record. Theoretically, different interpolation approaches may be used to calculate X2 position. The longitudinal salinity gradient changes with flow and with distance along the estuary (among other factors); thus the estimated isohaline position is somewhat dependent on the interpolation approach and stations used. We estimated daily X2 position assuming a log-linear relationship between surface salinity and distance, interpolating across two

stations that bound a specific conductance of 2.64 mS/cm (which under current regulations is assumed to correspond to a bottom salinity of 2 ppt). In a limited number of cases a weighting approach over additional stations was used if the data exhibited non-monotonic behavior near a salinity value of interest. If the bounding stations were further apart than 25 km on any given day, X2 position was not estimated due to uncertainty about interpolation accuracy. This condition resulted in X2 position not being estimated for 3.2% of the days over the study period that had one or more salinity data points. This interpolation method was used to calculate unique isohaline positions along the Sacramento and San Joaquin River branches upstream of their confluence (see Figure 1).

Monthly X2 values were estimated from the daily interpolated isohaline values. Monthly X2 position was defined as the mean value of all non-missing daily X2 values for months where at least 14 daily values were computed. Using similar methods, additional surface salinity isohalines (e.g., 6 ppt surface salinity isohaline) were estimated on daily and monthly time steps to more fully characterize the estuary's low salinity zone.

Modeling Approach

Denton (1993) developed an approach to estimate salinity at fixed locations in the estuary, based on a modification of the steady-state solution of the tidally-averaged advection-dispersion equation for salinity transport in a one-dimensional estuary. His empirical approach utilizes boundary conditions representative of the downstream ocean and upstream riverine environments, and a concept called antecedent outflow, representing flow time-history in the estuary. The equation can be represented as:

$$S(t) = (S_o - S_b) * \exp\big(-\alpha * G(t)\big) + S_b \quad \ldots\ldots\ldots\ldots\ldots\ldots\ldots\ldots\ldots\ldots\ldots\ldots\ldots (1)$$

where S(t) is the salinity at a given location, S_o and S_b are downstream (i.e. ocean) and upstream (i.e. riverine) salinity boundaries respectively, α is an empirically determined location-specific constant (units of flow^{-1}), and G(t) is a measure of the antecedent outflow. Antecedent outflow is defined by the following routing function similar to one proposed by Harder (1977):

$$\frac{\partial G}{\partial t} = \frac{\big(Q(t) - G(t)\big) * G(t)}{\beta} \ldots\ldots\ldots\ldots\ldots\ldots\ldots\ldots\ldots\ldots\ldots\ldots\ldots\ldots\ldots\ldots\ldots\ldots\ldots\ldots\ldots\ldots (2)$$

where Q is Delta outflow and β is an empirically determined constant (units of flow•time). Denton (1993) observed that the term β/G is a time constant governing the rate at which G approaches steady state. These equations can be calibrated to predict site-specific salinity.

In reference to an autoregressive empirical model for calculating the X2 position proposed by Jassby et al. (1995), Monismith et al. (2002) argues on theoretical grounds that power-law relationships with flow are preferable over logarithmic relationships and proposed an autoregressive X2 function of the following form:

$$X2(t) = \omega_1 * Q(t)^{\omega_2} + \omega_3 * X2(t-1) \quad \ldots\ldots\ldots\ldots\ldots\ldots\ldots\ldots\ldots\ldots\ldots\ldots (3)$$

where ω_1 , ω_2 and ω_3 are empirically determined constants.

Jassby et al. (1995) observed that the entire mean salinity field can be predicted if the X2 position is known, i.e., the salinity field is "self-similar" and can be predicted as a function of the longitudinal distance from Golden Gate (X) when normalized by X2. Thus, salinity as a function of X/X2 is relatively uniform for a wide range of flows. Following this observation, we integrated the Eulerian modeling approach of Denton (1993)—focused on a fixed station—and the Lagrangian modeling approach of Monismith et al. (2002)—focused on a fixed salinity—to develop a tool for diagnostic applications in the salinity data cleaning and filling process. The resulting empirical model, which is capable of estimating salinity at variable locations as well as X2 and other isohaline positions, is termed the Delta Salinity Gradient (DSG) model. Formulation of the DSG model is described briefly in the remainder of this section. Details on model formulation are provided elsewhere (Hutton 2013, 2014).

The steady state solution to Equation (3) can be derived by setting $X2(t) = X2(t-1)$ to obtain $\overline{X2} = \frac{\omega_1}{1-\omega_3} * \bar{Q}^{\omega_2}$, where $\overline{X2}$ and $\bar{Q}$ denote steady state conditions. Substituting antecedent flow G(t) for steady state flow $\bar{Q}$ gives an approximation to the unsteady response of X2 to flow variations if G(t) does not vary too rapidly. This substitution of antecedent flow is similar in concept to, and motivated by, Denton's (1993) derivation of the empirical Equation (1), where he proposed using the G flow instead of $\bar{Q}$ in a steady state analytical solution of salinity transport. Reparametrizing the constants as $\phi_1 = \frac{\omega_1}{1-\omega_3}$ and $\phi_2 = \omega_2$ gives a new empirical relationship between X2(t) and G(t) where ϕ_1 and ϕ_2 are independently calibrated to X2 from observed data:

$$X2(t) = \Phi_1 * G(t)^{\Phi_2} \ \ldots\ldots\ldots\ldots\ldots\ldots\ldots\ldots\ldots\ldots\ldots\ldots\ldots\ldots\ldots\ldots\ldots\ldots\ldots\ldots\ldots\ldots\ldots (4)$$

This empirical formulation, in contrast to those proposed by Jassby et al. (1995) and Monismith et al. (2002), is capable of estimating X2 during the early period of record when daily (and even monthly) Delta outflows frequently turned negative. Redefining the location-specific constant α as a function of X and scaling distance to the X2 isohaline (S = 2.64 mS/cm) results in the following relationship:

$$S(X,t) = (S_o - S_b) * \exp\left[\tau * \left(\frac{X}{X2(t)}\right)^{-\frac{1}{\Phi_2}}\right] + S_b \ \ldots\ldots\ldots\ldots\ldots\ldots\ldots\ldots\ldots\ldots\ldots\ldots (5)$$

where $\tau = \ln[\frac{2.64 - S_b}{S_o - S_b}]$ and salinity is reported as specific conductance in units of mS/cm. Equation (5) implicitly assumes that the estuary's salinity structure is self-similar under all flow conditions. However, Monismith et al. (2002) showed that the structure changes under high flow conditions. To address this response to flow, the downstream boundary condition S_o is assumed to vary with X2 as a sigmoidal function:

$$S_o(t) = \hat{S} + \left(2.64 - \hat{S}\right) * \exp\left(-\gamma * X2(t)^{\delta}\right) \ldots\ldots\ldots\ldots\ldots\ldots\ldots\ldots\ldots\ldots\ldots\ldots (6)$$

where $\hat{S}$ is ocean salinity (≈ 53 mS/cm) and γ and δ are empirically determined constants. Equation (5) can be used to determine salinity at any longitudinal distance from Golden Gate given X2 position and Φ_2 and assuming a reasonable value for S_b. If appropriate salinity observations are unavailable, X2 can be estimated from antecedent outflow using Equation (4). Note that Equation (5) can be rearranged to predict surface salinity isohaline positions as a function of X2:

$$X(S,t) = X2(t) * \left[\frac{\ln\left(\frac{S - S_b}{S_o(t) - S_b}\right)}{\tau}\right]^{-\Phi_2} \ \ldots\ldots\ldots\ldots\ldots\ldots\ldots\ldots\ldots\ldots\ldots\ldots\ldots\ldots\ldots (7)$$

Statistical Analyses

Sen's non-parametric estimate of slope (Gilbert, 1987 and references therein) was used to perform a trend analysis of the monthly X2 estimates over the entire period of record as well as two additional intervals: Water Years 1922 to 1967 and 1968 to 2012. These intervals were selected to coincide with Enright and Culberson's (2010) "pre" and "post" water

project periods. The significance of the breakpoint between periods is that, although the Central Valley and State Water Projects began pumping water from the Delta in 1940 and 1967, respectively, they did not begin year-round pumping operations until 1968 when the San Luis Reservoir was completed to store water south of the Delta. The Sen slope is the median of all slopes between all possible unique pairs of individual data points in the time period being analyzed. If there are n time points or periods of time, then there are a total of $n(n\text{-}1)/2$ possible pairs of time points one could use to calculate a slope, and Sen's slope is the median of these values. The method is robust and fairly insensitive to the presence of a small fraction of outliers, non-detect, or extreme data values; thus, trend estimates based on Sen slope are not biased by the occurrence of drought in the early part of the record.

The Mann-Kendall test was performed on the Sen slope at the 95% confidence level (Gilbert, 1987 and references therein), with results identified as either an upward trend (↑), a downward trend (↓) or no trend (↔). The trend slope was computed using the median value of the Sen slope. Non-zero slopes may or may not be found to be statistically significant using the Mann-Kendall test. The non-parametric Wilcoxon Rank Sum test was used for the comparison of isohaline values for specific water year classes (i.e. wet, above normal, below normal, dry, and critically dry). The Mann-Kendall test was also performed on monthly average specific conductance values over the entire period of record at five locations. Details of the implementation of the statistical procedures are presented in the SI, Appendix A.

Results

Cleaned and Filled Salinity Data

Summary statistics for the resulting cleaned and filled daily average surface specific conductance data based on the Bulletin 23 grab samples are shown in Table 1. While the filling process provides a fairly complete record for key stations downstream of approximately 100 km, substantial gaps remain in upstream station records that were used exclusively to characterize extreme drought conditions in the 1920s and 1930s. Statistics for these salinity stations are not provided in Table 1. Similar statistics for the CDEC data are presented in Table 2. The cleaned and filled CDEC data show a more complete record than the Bulletin 23 data across all stations. These data are provided electronically in the SI.

Given our goal to interpolate X2 position and other isohaline positions in the low salinity zone, the available data provide an adequate basis for the calculation.

Interpolated & Model-Predicted X2 Position

Daily and monthly X2 positions were estimated for the period of record using the previously described approach. Daily X2 position was also predicted from the DSG model for the same period following the procedure below:

- Antecedent outflow was calculated from Equation (2) assuming a nominal value for β of 475 cfs-years and assuming daily Delta outflows (Q) from the DAYFLOW model (CDWR, 2014). As detailed elsewhere (Hutton, 2014), daily outflows prior to October 1929 were estimated from monthly outflow volumes (CDWR, 1957) and daily inflow volumes (CDWP, 1924-55). Note that the same Delta flow time series is used for calibrating the model for both the Sacramento and San Joaquin River branches, and the channel-specific responses are embedded in the fitted model parameters.

- Interpolated daily X2 values for the Sacramento River branch, spanning Water Years 2000 through 2009, were used to calibrate model parameters Φ_1 and Φ_2 from Equation (4) through least-squares minimization. Best fit parameter values $\Phi_1 = 456 \pm 3.93$ (mean ± 1 SE) and $\Phi_2 = -0.193 \pm 0.001$ resulted after data points representing extremely high outflow events (X2 < 38 km) were removed from the analysis. The coefficient of determination $R^2 = 0.92$ and the standard error of estimate is 3.2 km. Our parameter estimates, when estimated using antecedent outflow in comparable units (m^3/sec), are similar to those reported by Gross et al. (2010) for various steady fit models. Differences in parameter estimates are attributed primarily to the use of a different calibration period. The autoregressive X2 function proposed by Monismith et al. (2002) (Equation 3) was calibrated to the same data set using a non-linear least squares fitting procedure and resulted in a coefficient of determination $R^2 = 0.89$ and a 3.8 km standard error of estimate, when applied with modeled data, i.e., at each timestep, the antecedent X2 in the equation was based on the modeled value.

- Best fit parameter values were also calibrated for the San Joaquin River branch, resulting in $\Phi_1 = 502 \pm 4.63$ and $\Phi_2 = -0.203 \pm 0.001$ with $R^2 = 0.92$ and a 3.6 km standard error of estimate. X2 values along the San Joaquin River branch are typically higher (i.e. further upstream) than those along the Sacramento River branch, due in large part to

smaller freshwater inflow volumes from the San Joaquin River available to repel salinity. Equation 3 was calibrated to the same data set, as reported above, and resulted in a coefficient of determination $R^2 = 0.89$ and a 4.1 km standard error of estimate. For both river channels, therefore, the DSG fits are slightly better than obtained from Equation 3.

A time series of the daily X2 position along the Sacramento River branch is shown in Figures 2a through 2d over the full 91-year period of record. The time series reveals a wide range in daily X2 position from approximately 20 km to greater than 100 km. At the lower extreme, the X2 falls in a broad region of the estuary (San Pablo Bay), where the one-dimensional approach may be limiting and there may be significant lateral gradients in salinity. The X2 position is generally more upstream (i.e. higher) in dry and critically dry years, corresponding to sustained periods of low Delta outflow. The trace in Figure 2(a), representing a period before Shasta Dam and other large upstream reservoirs were constructed, is visually distinct from the remaining time series. X2 values calculated from Equation (4) are superimposed on the interpolated X2 values for comparison. The DSG model fits the time series reasonably well, with some exceptions in the pre-Shasta period corresponding to extreme salinity incursions during major drought periods that were well beyond the model's calibration range. The generally slow rate of change in the salinity field and the use of an antecedent outflow term appear to justify the steady state approximation under most non-extreme flow conditions. The DSG model predictions show some seasonal bias when compared with interpolated X2 values (Roy et al., 2014). This bias is hypothesized to be related to inaccuracies associated with estimating net water use by agriculture in the Delta, particularly during low flow periods when this water use is a significant fraction of the Delta outflow water balance.

The interpolated monthly X2 time series was evaluated by grouping individual values into water year classes. Figure 3 shows the monthly X2 position for the Sacramento River branch averaged by water year class for the previously defined "pre-project" and "post-project" periods. The difference between pre-project X2 and post-project X2 is greatest in critically dry years and diminishes with wetter conditions (plot panels from left to right). The post-project period exhibits a dramatically reduced X2 range, relative to the pre-project period, during dry and critically dry water years. This reduced range is characterized by higher values in winter and lower values in summer. Water project operations, which typically

store runoff in the winter and spring and release storage in summer months to maintain in-basin water quality standards, clearly have a strong influence on the estuary's intra-annual salinity pattern except under wet hydrologic conditions. However, the differences between pre- and post-project conditions shown in Figure 3 cannot be fully attributed to operations of the Central Valley and State Water Projects. Intensified upstream agricultural and urban water use and associated water projects for in-basin and out-of-basin water uses, as well as changes in estuarine geometry, mean sea level and watershed snowmelt patterns have also contributed to changes in salinity patterns. A similar figure for the San Joaquin River branch is shown in the SI, Figure S1.

Other Model Predictions

Equations (5) and (6) of the DSG model were applied to predict daily specific conductance at Collinsville over the six-year drought period Water Years 1928-34 using a subset of the model-predicted X2 time series illustrated in Figure 2. Collinsville (X = 81 km) was selected to illustrate the model's predictive capability as this station plays a critical role in X2 management during spring and fall. To conduct the illustrative simulation, the following model constants were assumed: Φ_2 = -0.193; S_b = 0.2 mS/cm; γ = 2.29 x 10^{-4}; δ = 1.83. Figure 4(a) compares the DSG-predicted time series with the cleaned and filled specific conductance data. The time series is also compared with predictions from a site-specific calibration of Equation (1) reported by Denton and Sullivan (1993). The DSG model effectively represents the observed salinity variation at Collinsville over two orders of magnitude, although the extreme event in 1931 is over-predicted. Furthermore, the DSG model provides salinity estimates comparable to those provided by the site-specific empirical model.

To further illustrate the utility of the DSG model, Equation (7) was applied with the same model constants to predict low salinity zone position (bounded by surface salinities of 1-6 ppt) for Water Years 1928-34. Figure 4(b) compares the DSG-predicted time series with the interpolated isohaline data. Again, the data provide a reasonable validation of the DSG model except for the extreme event in 1931.

Isohaline Position Trend Analysis

Statistical analyses were performed on the interpolated X2 values to characterize behavior over time and in response to different hydrologic conditions. Results from the trend analysis are shown in Tables 3 and 4 with the analysis focusing on the Sacramento River branch.

Similar analyses for the San Joaquin River branch are shown in the SI (Tables S4 and S5). Key results for the Sacramento River branch are summarized below:

- The monthly trend evaluation for the entire period of record (1922–2012) shows statistically significant increases in X2 from November through June. Statistically significant decreases in X2 occur in August and September.

- Over the pre-Project period (1922–1967), there is no significant change in X2 from January through July and a statistically significant decrease in X2 from August through December. The trend directions are identical for both river branches.

- Over the post-Project period (1968–2012), there is a nearly inverse response in trends, with a statistically significant increase in X2 from September through December. Again, the trend directions are identical for both river branches.

The non-parametric Wilcoxon Rank Sum test was used for inter-period comparison of X2 position by month and water year class. The results of the Wilcoxon Rank Sum test, assuming a 95% confidence level, are summarized for the Sacramento River branch in Table 4. In general, post-Project X2 positions during dry and critically dry water years were statistically significantly higher (i.e. upstream) in December through May and lower (i.e. downstream) in August and September. Although the test shows fewer statistically significant trends under wetter conditions, the trend of lower August and September X2 during the post-Project X2 held. These statistical tests add more detail to the visual patterns displayed in Figures 2 and 3.

To further evaluate the isohaline trend analysis results, the Mann-Kendall test was performed on observed and DSG-predicted monthly average specific conductance values over the entire period of record at five locations: Martinez, Port Chicago, Mallard Island (represented by the O&A Ferry location in the Bulletin 23 data), Collinsville and Emmaton. Location-specific trends are compared with X2 trends (both derived from DSG predictions) in Table 5. Although observed data trends generally matched predicted data trends, the latter are presented to avoid bias that may be introduced by gaps in the observed salinity record. When a trend was detected in both the salinity and X2 time series, the trends are uniformly consistent. When a trend was not detected in the X2 time series, the salinity trends are

generally consistent, with exceptions in January (Mallard Island and Collinsville) and March (Mallard Island).

Discussion

Although the underlying data presented in this work were available in different documents or electronic sources, the cleaning of the raw data and integration into a single data set of daily average salinity in San Francisco Bay provides a unique perspective on the changes that have occurred over the past nine decades. This period has seen unprecedented anthropogenic change (e.g. land-use, water diversions, and reservoir construction) and significant hydrologic variability, including major floods and multi-year droughts. Additional drivers over the 20th and early 21st centuries include sea level rise as well as shifts in precipitation, snow accumulation, and runoff patterns. Understanding salinity behavior in this region is of general significance because of the ecological importance of the San Francisco Estuary on the Pacific coast and because of the economic significance of the water withdrawals from the Delta that are the single largest source of California's water supply. These data allow direct examination of the salinity responses to historical events and provide a basis for (1) relating salinity conditions in the current severe California drought to similar conditions that occurred in the past and (2) refining existing models and exploring future responses in the combined human-hydrologic system, as society adapts to changing natural dynamics and environmental requirements (embodied in the new science of sociohydrology, Sivapalan et al., 2012). Improved understanding of processes affecting the salinity in the western Delta will enhance future management of the upstream reservoirs, withdrawals, and estuarine habitat quality. Key observations from the data evaluation follow.

The construction of upstream water storage and increased in-basin and out-of-basin water use has affected the isohaline positions in different ways, depending on season and water year class. For example, X2 position exhibits less intra-annual variability in the post-project period than it did in the pre-project period. Post-project X2 position is typically further upstream (i.e. higher) in wet months (February through May) of dry and critically dry years and further downstream (i.e. lower) in the dry months of August and September. This reduction in dry year variability is a straightforward result of reservoirs being operated to store water in wet periods and to release water during dry periods, thus damping the variation in Delta salinity. At the other hydrologic extreme, in wet years, flows are

sufficiently high that reservoir operations have less impact on the Delta salinity gradient, resulting in great similarity between pre- and post-project X2 position.

The monthly trend evaluation for the entire period of record shows statistically significant increases in X2 position from November through June and statistically significant decreases in August and September. When the pre- and post-project periods are evaluated separately, important differences emerge. The pre-project period is characterized by a statistically significant decreasing trend in X2 position from August through December, reflecting project objectives to maintain freshwater conditions in the Delta during the irrigation season and to evacuate reservoir storage in the fall for winter flood control operations. The post-project period is characterized by a statistically significant increase in X2 position from September through December, reflecting increasing in-basin use and Delta exports. These observations make clear the value of utilizing data from the entire period of record to assess changes in the salinity regime of the estuary. Much of the published literature on X2 and its relationship to various biological indicators is based on data collected over limited periods, typically spanning the mid-1960s to the present. While it is recognized that such analyses are limited by lack of available biological data prior to the 1960s, conclusions drawn from this partial time interval should be evaluated in light of the more comprehensive description of the estuary's salinity regime provided herein.

Salinity trends, as measured by specific conductance at fixed locations, are broadly consistent with detected trends in X2 position and the conceptual model of increasing salinity with decreasing freshwater flows and with greater proximity to Golden Gate. However, salinity response to flow trends is not uniform along the estuary: flow trends in high flow months are more likely to translate into detectable salinity trends at downstream (higher salinity) locations and flow trends in low flow months are more likely to translate into detectable salinity trends at upstream (lower salinity) locations. For example, detection of statistically significant long-term salinity trends was limited to three months at Emmaton (an upstream location – see Table 5), compared with ten months of statistically significant long-term X2 trends (interpolated – see Table 3, trends for 1922-2012). Antecedent outflows are often sufficiently high that, at upstream locations such as Emmaton, salinity is not sensitive to modest changes in outflow, i.e. $\partial S/\partial G$ is small. The foregoing observation demonstrates the limitations of using a single location for evaluating salinity trends in the

estuary and argues for the use of a Lagrangian approach, i.e. evaluating isohaline trends derived from multiple stations.

The X2 time series reported here integrates the effects of multiple drivers, some of which act over decades, and thus affirms the importance of considering longer-term records in defining baselines or targets for defining environmental goals and assessing changes. The periods and statistical analyses presented here are illustrative, and alternative periods or seasons could be considered to examine the response of the system to specific drivers that have the potential to impact isohaline position in the estuary. The data integration presented through this work serves as a foundation for the continuing analysis of salinity behavior in the San Francisco Bay and Delta, anticipating continued interest in the health of the Delta ecosystem in response to anthropogenic and other stressors. The findings presented in this paper are influenced by the data and the cleaning procedure employed, all of which are made available electronically in the SI. Future work will consider alternative modeling approaches and statistical analyses to expand on the evaluation of how and why salinity trends in the San Francisco Bay and the Delta have changed over time.

Acknowledgements

This work was made possible through funding from the San Luis and Delta Mendota Water Authority and the State Water Contractors. We thank the California Department of Water Resources (specifically Tara Smith, Eli Ateljevich and Joey Zhou) for supporting this study through developing an independent data cleaning procedure for the CDEC salinity data and conducting a Delta hydrodynamic and water quality transport simulation to allow computation of daily ratios between higher high tide salinity and daily average salinity. We also thank three anonymous reviewers for their constructive comments.

References

California Data Exchange Center (CDEC) (2013). Salinity data available online at: *http://cdec.water.ca.gov*

California Department of Public Works (CDPW) (1924-55). Report of the Sacramento-San Joaquin Water Supervisor for the Period 1924-1954, Bulletin 23.

California Department of Public Works (CDPW) (1931). Variation and Control of Salinity in Sacramento-San Joaquin Delta and Upper San Francisco Bay, Bulletin 27.

California Department of Water Resources (CDWR) (1956-62). Report of the Sacramento-San Joaquin Water Supervisor for the Period 1955-1961, Bulletin 23.

California Department of Water Resources (CDWR) (1957). Joint Hydrology Study: Sacramento River and Sacramento-San Joaquin River Delta, Division of Planning, July.

California Department of Water Resources (CDWR) (1962). Hydrologic Data for 1962, Bulletin 65.

California Department of Water Resources (CDWR) (1963-71). Hydrologic Data for the Period 1963-1971, Bulletin 130.

California Department of Water Resources (CDWR) (2014). DAYFLOW model data available online at: *http://www.water.ca.gov/dayflow/*

California Department of Water Resources (CDWR) (2015). DSM2 documentation, available online at:

http://baydeltaoffice.water.ca.gov/modeling/deltamodeling/models/dsm2v6/documentation.cfm

California State Water Resources Control Board (CSWRCB) (1999). Water Right Decision 1641, December, available online at: *http://www.swrcb.ca.gov/waterrights/board_decisions/*

Denton, R.A. (1993). Accounting for Antecedent Conditions in Seawater Intrusion Modeling – Applications for the San Francisco Bay-Delta, Proceedings of the 1993 Hydraulic Division National Conference, American Society of Civil Engineers, San Francisco, Calif., H.W. Shen, Ed. 821-826.

Denton, R.A. and Sullivan, G.D. (1993). Antecedent Flow-Salinity Relations: Application to Delta Planning Models, CCWD Technical Memorandum, December.

Denton, R.A. (2015). Delta Salinity Constituent Analysis, Report Prepared for the State Water Project Contractors Authority, February, available online at: http://www.water.ca.gov/waterquality/drinkingwater/mwqi_reports.cfm

Enright, C., and Culberson, S.D. (2010). Salinity Trends, Variability, and Control in the Northern Reach of the San Francisco Estuary, San Francisco Estuary and Watershed Science, 7(2).

Feyrer, F., Nobriga, M. L., and Sommer, T. R. (2007). Multidecadal Trends for Three Declining Fish Species: Habitat Patterns and Mechanisms in the San Francisco Estuary, California, USA. Canadian Journal of Fisheries and Aquatic Sciences, 64(4), 723–734.

Feyrer, F., Newman, K., Nobriga, M., and Sommer, T. (2010). Modeling the Effects of Future Outflow on the Abiotic Habitat of an Imperiled Estuarine Fish. Estuaries and Coasts, 34(1), 120–128.

Finch, R. and Sandhu, N. (1995). Artificial Neural Networks with Application to the Sacramento – San Joaquin Delta. California Department of Water Resources, Delta Modeling Section, Division of Planning.

Fox, J. P., Mongan, T. R., and Miller, W. J. (1990). Trends in Freshwater Inflow to San Francisco Bay from the Sacramento–San Joaquin Delta, Journal of the American Water Resources Association, 26(1), 101–116.

Fox, J. P., Mongan, T. R., and Miller, W. J. (1991). Long-term Annual and Seasonal Trends in Surface Salinity of San Francisco Bay. Journal of Hydrology, 122(1), 93-117.

Gilbert, R. 1987. Statistical Methods For Environmental Pollution Monitoring, Van Nostrand Reinhold Co., NY. 320 pp.

Gross, E.S., MacWilliams, M.L. & Kimmerer, W.J. (2010). Three-Dimensional Modeling of Tidal Hydrodynamics in the San Francisco Estuary, San Francisco Estuary and Watershed Science, 7(2).

Harder, J.A. (1977). Predicting Estuarine Salinity from River Inflows, Journal of the Hydraulics Division, Proceedings of the American Society of Civil Engineers, Vol. 103, No. HY8, August, pp. 877-888.

Hill, K., Dauphinee, T., and Woods, D. (1986). The Extension of the Practical Salinity Scale 1978 to Low Salinities. Oceanic Engineering, IEEE Journal, 11(1), 109–112.

Hutton, P. (2013). A New Empirical Bay-Delta Salinity Model, Presented at the California Water & Environmental Modeling Forum Annual Meeting, Folsom, CA, April 24, available online at: *http://www.cwemf.org/*.

Hutton, P. (2014). Delta Salinity Gradient (DSG) Model, Version 1.0 Model Documentation, Metropolitan Water District of Southern California, Technical Memorandum, September.

Jassby, A.D., Kimmerer, W.J., Monismith, S.G., Armor, C., Cloern, J.E., Powell, T.M., Schubel, J.R., and Vendlinski, T.J. (1995). Isohaline Position as a Habitat Indicator for Estuarine Populations. Ecological Applications, 5: 272–289.

Kimmerer, W. and Monismith, S. (1992). An Estimate of the Historical Position of 2PPT Salinity in the San Francisco Bay Estuary. Issue Paper Prepared for the Fourth Technical Workshop on Salinity, Flows, and Living Resources of the San Francisco Bay/Delta Estuary. August 1992. Available online at: *http://www.calwater.ca.gov/Admin_Record/C047938.pdf.*

Kimmerer, W. J., Gross, E. S., and MacWilliams, M. L. (2009). Is the Response of Estuarine Nekton to Freshwater Flow in the San Francisco Estuary Explained by Variation in Habitat Volume? Estuaries and Coasts, 32(2), 375–389.

Lund, J., Hanak, E., Fleenor, W., Howitt, R., Mount, J., and Moyle, P. (2007). Envisioning Futures for the Sacramento-San Joaquin Delta, Public Policy Institute of California, San Francisco, Chapter 2.

Monismith, S. G., Kimmerer, W., Burau, J. R., and Stacey, M. T. (2002). Structure and Flow-Induced Variability of the Subtidal Salinity Field in Northern San Francisco Bay. Journal of Physical Oceanography, 32(11), 3003–3019.

Moyle, P. B., Lund, J. R., Bennett, W. A., and Fleenor, W. E. (2010). Habitat Variability and Complexity in the Upper San Francisco Estuary. San Francisco Estuary and Watershed Science, 8(3).

Reed, D., Hollibaugh, J., Korman, J., Peebles, E., Rose, K., Smith, P., and Montagna, P. (2014). Workshop on Delta Outflows and Related Stressors: Panel Summary Report, Delta Science Program, available online at: *http://deltacouncil.ca.gov/docs/workshopsworkgroups/2014-05-14/*

Roy, S.B., Rath, J., Chen, L., Ungs, M.J., and Guerrero, M. (2014). Salinity Trends in Suisun Bay and the Western Delta (October 1921 – September 2012), Prepared for the San Luis and Delta Mendota Water Authority and State Water Contractors, January.

Shellenbarger, G. G., and Schoellhamer, D. H. (2011). Continuous Salinity and Temperature Data from San Francisco Estuary, 1982–2002: Trends and the Salinity-Freshwater Inflow Relationship. Journal of Coastal Research, 27(6), 1191–1201.

Sivapalan, M., Savenije, H. H., & Blöschl, G. (2012). Socio-hydrology: A new science of people and water. Hydrological Processes, 26(8), 1270-1276.

Stahle, D. W., Therrell, M. D., Cleaveland, M. K., Cayan, D. R., Dettinger, M. D., and Knowles, N. (2001). Ancient Blue Oaks Reveal Human Impact on San Francisco Bay Salinity. Eos, Transactions American Geophysical Union, 82(12), 141–145.

U.S. Environmental Protection Agency (USEPA) (2012). Water Quality Challenges in the San Francisco Bay/Sacramento–San Joaquin Delta Estuary: EPA's Action Plan.

U.S. Fish and Wildlife Service (USFWS) (2008). Formal Endangered Species Act Consultation on the Proposed Coordinated Operations of the Central Valley Project (CVP) and State Water Project (SWP), available online at: *http://www.fws.gov/sfbaydelta/*

U.S. Geological Survey (USGS) (2013). Salinity data available online at: *http://ca.water.usgs.gov/projects/baydelta/*

Figure Captions

Figure 1. Key salinity stations are identified in Suisun Bay and the western Delta. Salinity data from these and other locations were used to develop a long-term record of X2, the

position of two parts per thousand bottom salinity in the estuary. X2 position is reported as the distance in kilometers from Golden Gate along the axis of the estuary, following the original definition of the term (Jassby et al., 1995). The Sacramento and San Joaquin River branches are identified on the map.

Figures 2(a) through 2(d). Time series of interpolated and DSG-predicted daily X2 values on the Sacramento River branch (Water Years 1922-2012). X2 position is generally more upstream (i.e. higher) in dry and critically dry years, corresponding to sustained periods of low Delta outflow. Figure 2(a), representing a period prior to large reservoir construction in the Sacramento Valley, is visually distinct from the remaining time series. Figures 2(a) and (b) represent the "pre-project" period and Figures 2(c) and (d) represent the "post-project" period.

Figure 3. Average monthly X2 position is shown by water year class on the Sacramento River branch under pre-project (Water Years 1922-1967) and post-project (Water Years 1968-2012) conditions, with lines connecting the seasonal medians. Symbols show individual year values (red = pre-Project; blue = post-Project), with lines connecting the seasonal medians. In all but wet years, post-project X2 position tends to be further downstream (i.e. lower) in summer months and further upstream (i.e. higher) in other months. X2 position in October and November is generally more closely associated with the previous water year; thus the x-axis spans the months December through November.

Figures 4(a) and 4(b). These figures illustrate predictive capability of the DSG model during a six-year drought in the early part of the record, Water Years 1928-34. Figure 4(a) shows a time series of observed and DSG-predicted salinity - see Equations (5) and (6) - for a representative station, Collinsville (X = 81km), following the data cleaning and filling procedures described in the text. Predictions from a site-specific empirical model (Denton & Sullivan, 1993) are provided for comparison. Figure 4(b) shows a time series of observed and DSG-predicted surface isohalines - see Equation (7) - that bound the estuary's low salinity zone (1-6 ppt).

Table Captions

Table 1. Bulletin 23 Data Summary. Statistics for the resulting cleaned and filled daily average Bulletin 23 specific conductance data are shown for key locations by river branch.

Table 2. CDEC Data Summary. Statistics for the resulting cleaned and filled daily average CDEC specific conductance data are shown for key locations by river branch.

Table 3. Mann-Kendall Test Results: Sacramento River Branch X2. Over the entire period of record, the test shows (1) statistically significant increases in X2 from November through June and (2) statistically significant decreases in X2 for August and September. Over the pre-Project period (1922–1967), there is no significant change in X2 from January through July and a statistically significant decrease in X2 from August through December. Over the post-Project period (1968–2012), there is a nearly inverse response in trends, with a statistically significant increase in X2 from September through December. Results are reported as an upward trend (↑), a downward trend (↓) or no trend (↔).

Table 4. Wilcoxon Rank Sum Test Results: Sacramento River Branch X2. In general, dry and critical year post-Project X2 was statistically significantly higher (i.e. upstream) in December through May and lower (i.e. downstream) in August and September. Wet year post-Project X2 was statistically significantly higher in May and June and lower in August and September. Results are reported as a nonparametric estimate of the median of the difference (km) between a post-Project X2 and a pre-Project X2; significance is reported as an upward trend (↑), a downward trend (↓) or no trend (↔).

Table 5. Mann-Kendall Test Results for DSG-Predicted Salinity and X2 at Selected Locations for the Entire Period of Record (1922-2012). Detected salinity and X2 trends are generally consistent. When a trend was detected in both the salinity and X2 time series, the trends are uniformly consistent. When a trend was not detected in the X2 time series, the salinity trends are generally consistent, with exceptions in January (Mallard Island and Collinsville) and March (Mallard Island). Results are reported as an upward trend (↑), a downward trend (↓) or no trend (↔).

Supplementary Information Content

Figure S1. X2 Position by Month on the San Joaquin River Branch (1922-2012) Grouped by Water Year Classification

Table S1. DWR Document Sources

Table S2. Bulletin 23 Summary of Data Used

654 Table S3. CDEC Summary of Data Used

655 Table S4. Trend Analysis on X2 for the San Joaquin River Branch (a) over 1922-1967, (b)
656 1968-2012, and (c) 1922-2012

657 Table S5. X2 on San Joaquin River Branch Wilcoxon Rank Sum Test Results (Comparison
658 of 1968–2012 Values Against 1922–1967 Values)

659 Appendix A: Statistical Analysis Methodology

660 Electronic data files of salinity and interpolated X2 value (Microsoft Excel files)

661

662 **Table 1**

Station Name	Distance from Golden Gate (km)	Approximate Period of Record	Cleaned & Filled Data Completeness		Specific Conductance Percentiles (mS/cm)		
			Count (days)	Missing (%)	10%	50%	90%
Bay Stations							
Point Orient	19.8	Feb 1926–Jun 1971	13976	16%	20.	27.	29.
Point Davis	40.6	Feb 1926–Jun 1971	14802	11%	7.0	20.	27.
Crockett	44.6	Feb 1926–Jun 1971	13685	17%	5.7	19.	26.
Benicia	52.3	Feb 1926–Jun 1971	13706	17%	3.6	16.	24.
Martinez	52.6	Feb 1926–Jun 1971	13760	17%	1.9	13.	22.
Bulls Head Point	54.7	Feb 1926–Aug 1957	9007	22%	1.9	15.	25.
West Suisun	59.5	Oct 1921–Jun 1971	13410	26%	0.7	9.7	21.
Bay Point	64.2	Oct 1921–Dec 1968	11174	35%	0.5	9.3	22.
Port Chicago	66.0	Oct 1921–Jun 1971	14745	19%	0.3	8.3	21.
O & A Ferry	74.8	Oct 1921–Jun 1971	15522	14%	0.3	1.7	14.
Lower Sacramento River Stations							
Collinsville	81.8	Oct 1921–Jun 1971	15751	13%	0.2	0.4	8.9
Emmaton	92.9	Oct 1921–Jun 1971	15185	16%	0.2	0.3	2.0
Three Mile Slough Bridge	96.6	Oct 1921–Jun 1971	15178	16%	0.2	0.3	0.8
Rio Vista	102.2	Sep 1922–Jun 1971	14408	19%	0.1	0.2	0.3
Lower San Joaquin River Stations							
Antioch	88.4	Oct 1921–Jun 1971	15451	15%	0.2	0.4	6.0
Antioch Bridge	93.7	Oct 1921–Jun 1971	14760	19%	0.3	0.3	1.8
Jersey Point	98.8	Oct 1921–Jun 1971	15380	15%	0.2	0.3	1.6
False River	101.2	Oct 1921–Jun 1971	13883	24%	0.2	0.2	0.8
Oulton Point	108.1	Sep 1952–Jun 1971	5395	21%	0.1	0.2	0.4
San Andreas Landing	113.1	Sep 1952–Jun 1971	5395	21%	0.1	0.2	0.3

663 **Table 2**

Station Name	Distance from Golden Gate (km)	Approximate Period of Record	Cleaned & Filled Data Completeness		Specific Conductance Range (mS/cm)		
			Count (days)	Missing (%)	10%	50%	90%
Bay Stations							
Point San Pablo	22	Jan 1965–Sep 2012	16839	3%	25.	38.	44.
Carquinez	45.5	Jan 1965–Sep 2012	17010	2%	12.	27.	36.
Martinez	54	Sep 1995–Sep 2012	6033	3%	2.7	18.	26.
Martinez (USBR)	55	Jan 1965–Apr 1996	11345	1%	2.2	16.	27.
Port Chicago	64	Jan 1965–Sep 2012	17389	0%	0.3	9.3	20.
Mallard Island	75	Jul 1964–Sep 2012	17505	1%	0.2	3.0	12.
Lower Sacramento River Stations							
Collinsville	81	Jul 1964–Sep 2012	16985	4%	0.2	1.0	7.7
Emmaton	92	Jul 1964–Sep 2012	17420	1%	0.1	0.2	2.2
Rio Vista	101	Jul 1964–Sep 2012	17420	1%	0.1	0.2	0.3
Lower San Joaquin River Stations							
Pittsburg	77	Jan 1965–Sep 2012	17405	0%	0.2	2.3	10.
Antioch	85.8	Jul 1964–Sep 2012	17561	0%	0.2	0.7	4.8
Blind Point	92.9	Jul 1964–Sep 2012	17540	0%	0.2	0.4	2.4
Jersey Point	95.8	Jul 1964–Sep 2012	17388	1%	0.2	0.3	1.7
Three Mile Slough @ SJR	100.4	Jul 1964–Sep 2012	17320	2%	0.1	0.3	1.1
San Andreas Landing	109.2	Jul 1964–Sep 2012	17526	0%	0.1	0.2	0.3

664 **Table 3**

Month	Full Period 1922-2012			Pre-Project Period 1922-1967			Post-Project Period 1968-2012		
	Sample Size	Sen's Slope Median (km/year)	Test Decision	Sample Size	Sen's Slope Median (km/year)	Test Decision	Sample Size	Sen's Slope Median (km/year)	Test Decision
Jan	83	0.10	↑	39	-0.11	↔	44	0.23	↔
Feb	82	0.09	↑	39	-0.03	↔	43	0.10	↔
Mar	83	0.08	↑	40	0.09	↔	43	0.02	↔
Apr	82	0.15	↑	39	0.19	↔	43	0.01	↔
May	85	0.13	↑	40	0.13	↔	45	-0.18	↔
Jun	85	0.10	↑	40	0.01	↔	45	-0.08	↔
Jul	87	-0.04	↔	42	-0.04	↔	45	-0.06	↔
Aug	86	-0.13	↓	41	-0.2	↓	45	0.06	↔
Sep	88	-0.12	↓	43	-0.43	↓	45	0.20	↑
Oct	88	0.00	↔	43	-0.31	↓	45	0.28	↑
Nov	86	0.11	↑	41	-0.2	↓	45	0.37	↑
Dec	85	0.13	↑	40	-0.19	↓	45	0.37	↑

665

666 **Table 4**

667

Month	Year Type				
	Critical	Dry	Below Normal	Above Normal	Wet
Jan	7.6 (↔)	9.1 (↑)	6.4 (↔)	-1.1 (↔)	3.7 (↔)
Feb	16.3 (↑)	10.4 (↑)	4.4 (↑)	0.7 (↔)	5.8 (↑)
Mar	14.2 (↑)	7.4 (↑)	3.2 (↔)	0.9 (↔)	1.7 (↔)
Apr	13.9 (↑)	9.1 (↑)	9.0 (↑)	7.2 (↔)	4.5 (↔)
May	12.8 (↑)	9.1 (↑)	12.9 (↑)	2.4 (↔)	6.3 (↑)
Jun	2.0 (↔)	5.5 (↔)	15.5 (↑)	1.0 (↔)	6.8 (↑)
Jul	-10.6 (↔)	-3.2 (↓)	6.1 (↑)	-7.3 (↓)	1.7 (↔)
Aug	-12.0 (↓)	-7.2 (↓)	-2.8 (↔)	-9.8 (↓)	-3.1 (↓)
Sep	-15.6 (↓)	-3.8 (↔)	-0.8 (↔)	-6.6 (↓)	-5.4 (↓)
Oct	1.9 (↔)	0.6 (↔)	-5.5 (↔)	6.1 (↔)	0.0 (↔)
Nov	9.4 (↑)	6.9 (↔)	2.7 (↔)	15.4 (↔)	3.8 (↔)
Dec	9.2 (↑)	8.6 (↑)	4.2 (↔)	11.8 (↔)	3.0 (↔)

668
669

670 **Table 5**

671

Month	Salinity Trend: 1922-2012					X2 Trend: 1922-2012
	Martinez	Port Chicago	Mallard Island	Collinsville	Emmaton	
Jan	↔	↔	↑	↑	↔	↔
Feb	↑	↑	↔	↔	↔	↑
Mar	↔	↔	↑	↔	↔	↔
Apr	↑	↑	↑	↑	↔	↑
May	↑	↑	↑	↑	↔	↑
Jun	↑	↑	↑	↑	↔	↑
Jul	↔	↔	↔	↔	↔	↔
Aug	↓	↓	↓	↓	↓	↓
Sep	↓	↓	↓	↓	↓	↓
Oct	↔	↔	↔	↔	↔	↔
Nov	↔	↔	↔	↔	↔	↔
Dec	↑	↑	↑	↑	↑	↑

672
673

Figure 1

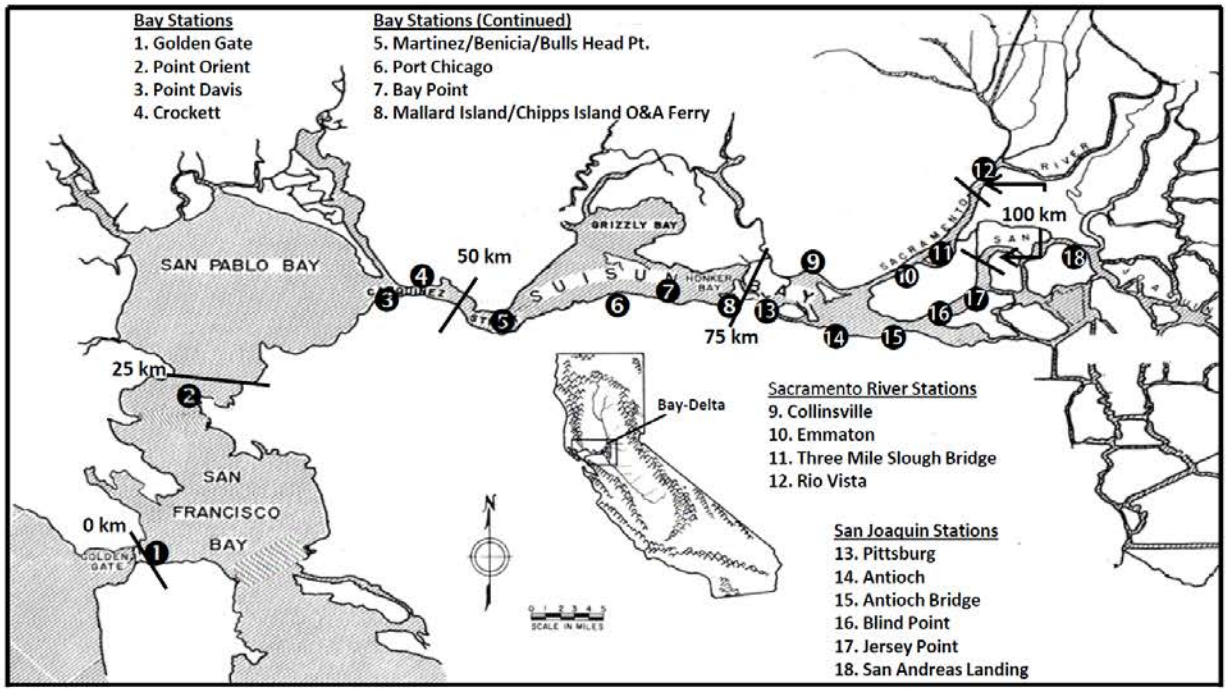
Bay Stations
1. Golden Gate
2. Point Orient
3. Point Davis
4. Crockett
Bay Stations (Continued)
5. Martinez/Benicia/Bulls Head Pt.
6. Port Chicago
7. Bay Point
8. Mallard Island/Chipps Island O&A Ferry
SAN PABLO BAY
SUISUN BAY
GRIZZLY BAY
HONKER BAY
50 km
75 km
25 km
0 km
100 km
SAN FRANCISCO BAY
GOLDEN GATE
Bay-Delta
Sacramento River Stations
9. Collinsville
10. Emmaton
11. Three Mile Slough Bridge
12. Rio Vista
San Joaquin Stations
13. Pittsburg
14. Antioch
15. Antioch Bridge
16. Blind Point
17. Jersey Point
18. San Andreas Landing
SCALE IN MILES

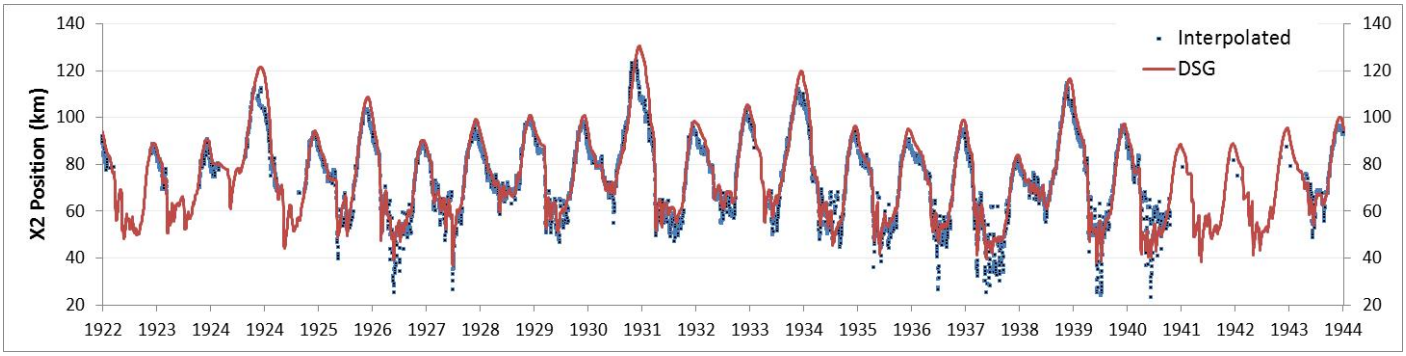

Figure 2a

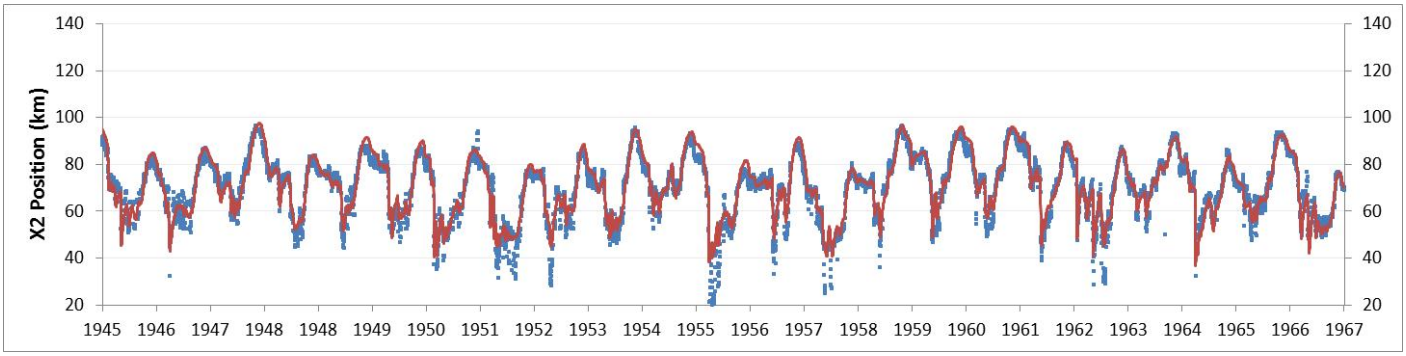

Figure 2(b)

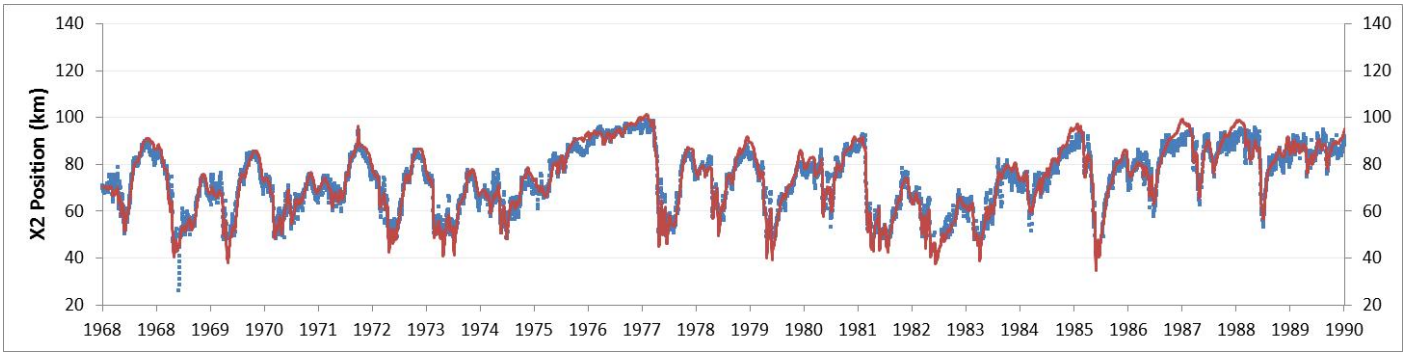

Figure 2(c)

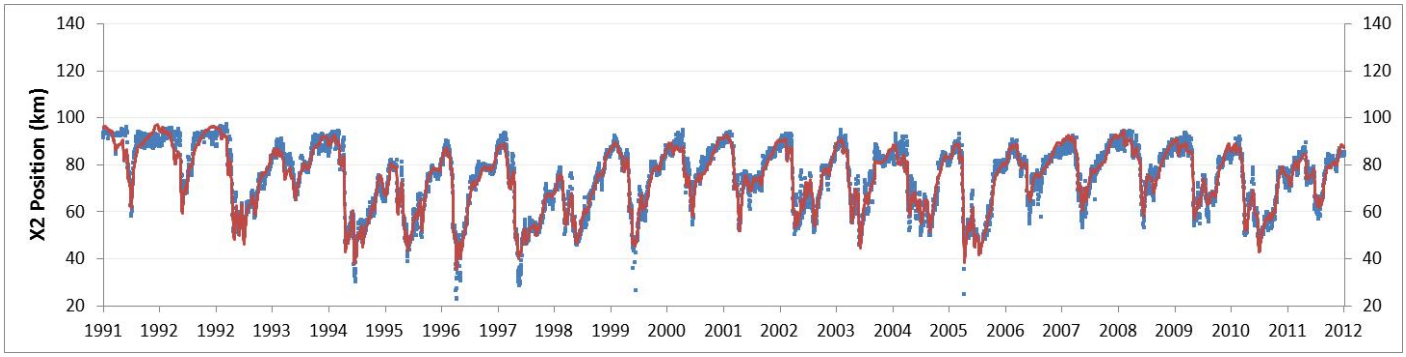

Figure 2(d)

704
705

Figure 3

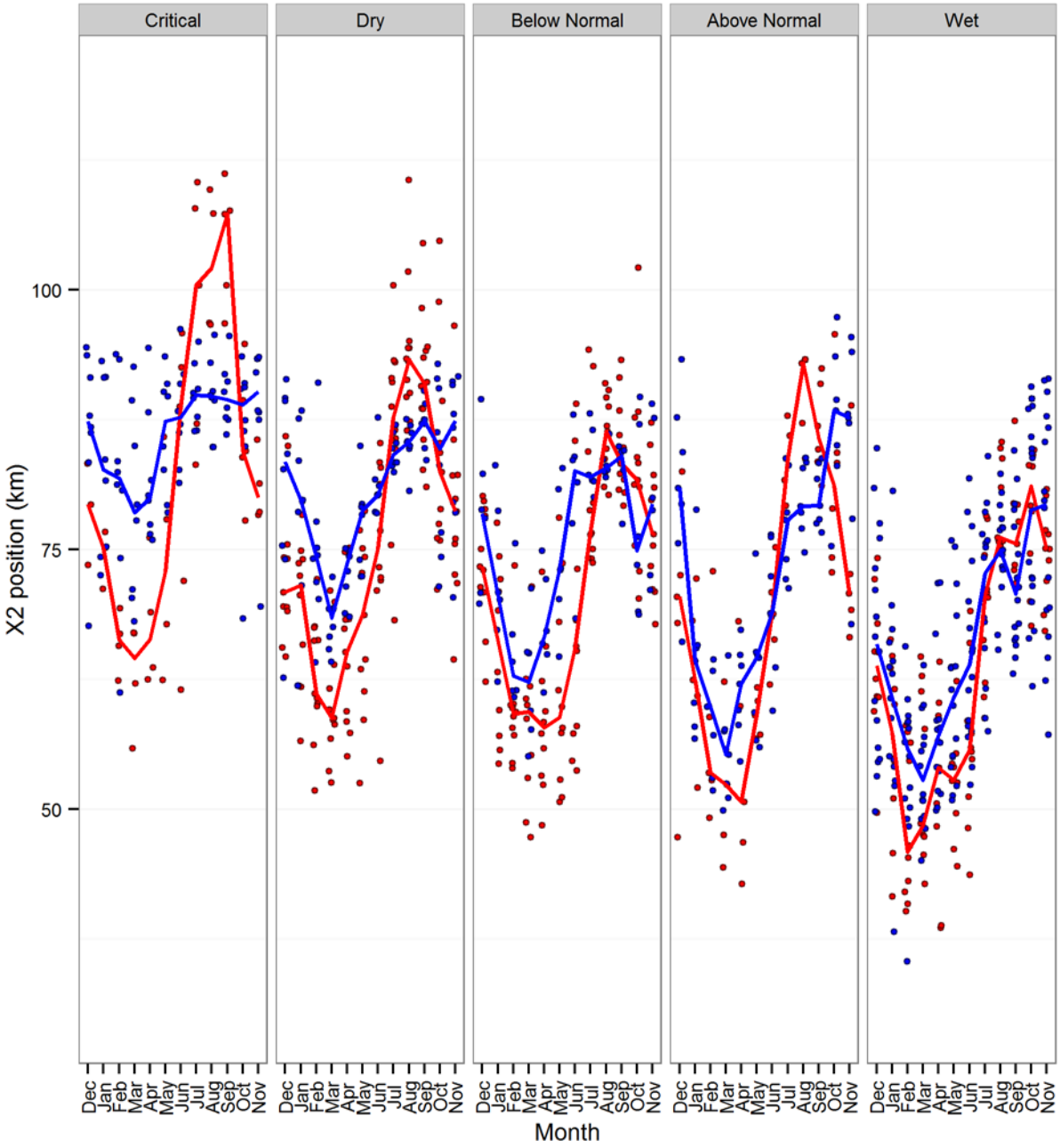

706
707
708

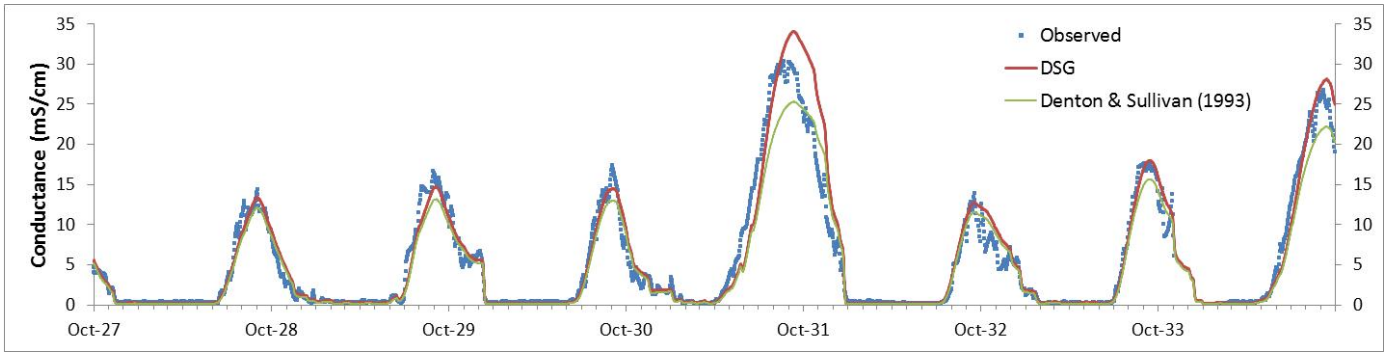

Figure 4(a)

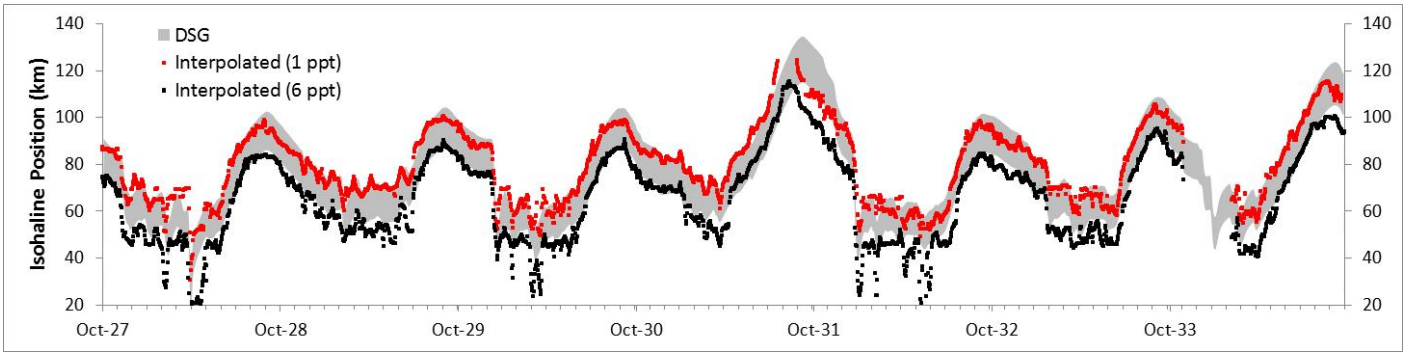

Figure 4(b)

Estuaries and Coasts
DOI 10.1007/s12237-015-9968-9

Explaining Patterns of Pelagic Fish Abundance in the Sacramento-San Joaquin Delta

Robert J. Latour [1]

Received: 30 April 2014 / Revised: 13 February 2015 / Accepted: 24 March 2015

Abstract Investigating the effects of environmental, biological, and anthropogenic covariates on fish populations can aid interpretation of abundance and distribution patterns, contribute to understanding ecosystem functioning, and assist with management. Studies have documented declines in survey catch per unit effort (CPUE) of several fishes in the Sacramento-San Joaquin Delta, a highly altered estuary on the US west coast. This paper extends previous research by applying statistical models to 45 years (1967–2012) of trawl survey data to quantify the effects of covariates measured at different temporal scales on the CPUE of four species (delta smelt, *Hypomesus transpacificus*; longfin smelt, *Spirinchus thaleichthys*; age-0 striped bass, *Morone saxatilis*; and threadfin shad, *Dorosoma petenense*). Model comparisons showed that along with year, the covariates month, region, and Secchi depth measured synoptically with sampling were all statistically important, particularly in explaining patterns in zero observations. Secchi depth and predicted CPUE were inversely related for all species indicating that water clarity mediates CPUE. Model comparisons when the year covariate was replaced with annualized biotic and abiotic covariates indicated total suspended solids (TSS) best explained CPUE trends for all species, which extends the importance of water clarity on CPUE to an annual timescale. Comparatively, there was no empirical support for any other annualized covariates, which included metrics of prey abundance, other water quality parameters, and water flow. Top-down and bottom-up forcing remain important issues for understanding delta ecosystem functioning; however, the results of this study raise new questions about the effects of changing survey catchability in explaining patterns in pelagic fish CPUE.

Keywords Delta and longfin smelt · Sacramento-San Joaquin Delta · Zero-inflated generalized linear models · Water flow · Zooplankton · Water quality

Communicated by Karin Limburg

✉ Robert J. Latour
latour@vims.edu

[1] Virginia Institute of Marine Science, College of William & Mary, P.O. Box 1346, Gloucester Point, VA 23062, USA

Introduction

The dynamics of fish populations involve a complex suite of biological processes operating at different temporal and spatial scales. Abiotic and biotic variables modulate the intrinsic biological properties of individual fish species and structure the diversity and abundances of species within ecosystems. Such variables can be ecological, environmental, climatic, and anthropogenic, and they synthetically influence ecosystem dynamics. Ecological variables are often described in the context of bottom-up (Chavez et al. 2003; Frederiksen et al. 2006) or top-down (Cury and Shannon 2004; Hunt and McKinnell 2006) control of food webs, while environmental variables such as temperature, dissolved oxygen, and others have been shown to influence early life history (Norcross and Austin 1988) and the distribution of fishes within ecosystems (Breitburg 2002; Craig 2012; Buchheister et al. 2013). Climate variability can have a multipronged impact, exerting influence on specific life stages, such as the formation of new year classes (Houde 2009), or at the level of individual species (Hare et al. 2010) or whole ecosystems (Winder and Schindler 2004; Drinkwater et al. 2009). Numerous anthropogenic stressors such as pollution, nutrient enrichment and eutrophication, introduction of nonnative species, and perhaps most notably, overexploitation have been documented to influence

ecosystem structure and fish abundance (Islam and Tanaka 2004; Molnar et al. 2008; Diaz and Rosenberg 2008;Worm et al. 2009).

Globally, centuries of anthropogenic change have transformed estuarine and coastal waters into systems with reduced biodiversity and ecological resilience (Jackson et al. 2001; Lotze et al. 2006). Given the importance of these areas to marine life, efforts to remediate the cascading effects of anthropogenic stressors will undoubtedly require deep consideration of principles inherent to ecosystem-based management (EBM; Link 2010). However, before strategic and tactical management policies can be effectively implemented, EBM rooted or otherwise, the relative roles of natural and anthropogenic factors that affect ecosystem structure and associated species abundances must be well understood.

San Francisco Bay is a tectonically created estuary located on the US Pacific coast that has experienced considerable anthropogenic change (Nichols et al. 1986). The bay and its watershed occupies 1.63×10^7 ha and drains 40 % of California's land area (Jassby and Cloern 2000). Freshwater is supplied to the estuary primarily from the Sacramento and San Joaquin rivers, which converge to form a complex mosaic of tidal freshwater areas known collectively as the Sacramento-San Joaquin Delta (referred herein as the delta). Most naturally occurring wetlands in the estuary have been lost due to morphological changes to the system for agriculture, flood control, navigation, and water reclamation activities (Atwater et al. 1979). Other notable changes include modifications to the volume of freshwater entering the delta and thus the natural delivery of land-based sediment (Arthur et al. 1996), massive sediment loading resulting from large-scale hydraulic mining activities (Schoellhamer 2011), introduction and invasion of nonindigenous species (Cohen and Carlton 1998), input of contaminants (Connor et al. 2007), and reported decreases in chlorophyll-*a* (Alpine and Cloern 1992), zooplankton (Orsi and Mecum 1996), and fish catch per unit effort (CPUE; Sommer et al. 2007).

A variety of tools can be used to understand how specific changes to ecosystem components influence fish population dynamics. These include directed field studies, statistical analyses, and multidimensional mechanistic modeling activities, with all often being required to develop a robust understanding of ecosystem dynamics. In the delta, there has been a considerable focus on empirical analyses designed to examine how temporal trends in CPUE statistically relate to various abiotic and biotic variables. Researchers have described freshwater flow within the delta as a key structuring variable of fish CPUE (Turner and Chadwick 1972; Stevens and Miller 1983; Sommer et al. 2007) along with the salinity variable X_2, which is defined as the horizontal distance up the axis of the estuary where the tidally averaged near-bottom salinity is 2 psu (Jassby et al. 1995; Kimmerer 2002; Kimmerer et al. 2009; MacNally et al. 2010). However, the evidence supporting these inferences was based on relationships between annual CPUE indices and metrics of water flow and/or X_2, which can be limiting since collapsing many raw field observations of CPUE into annual indices leads to a sizable loss of potentially valuable information. Feyrer et al. (2007, 2011) applied statistical models to raw survey data collected from the delta to quantify fish occurrences in relation to water quality variables; however, they did not examine CPUE or consider variables at broader temporal scales.

This study builds on previous empirical analyses by examining how measures of CPUE in the delta statistically relate to a broad suite of abiotic and biotic variables across multiple temporal scales and exclusively from the perspective of raw field observations. The analyses presented here follow a two-step procedure that reflects the specific objectives of this study, (1) investigate the role of covariates measured synoptically at the time of fish sampling to elucidate their effects on CPUE and (2) modify the analytical framework used for the first objective to examine the relative role of various abiotic and biotic covariates hypothesized to influence CPUE at an annual timescale. For the second objective, the covariates considered were annualized metrics of zooplankton density, chl-*a* concentration, water quality, and water flow. These analyses contribute to the understanding of ecosystem dynamics within the delta and thus aid the formulation of EBM strategies by providing foundational information of fish population responses to natural and anthropogenically modified system attributes.

Methods

Focal Fish Species

Reported declines of fish CPUE in the delta have revolved primarily around four species: delta smelt, *Hypomesus transpacificus*, longfin smelt, *Spirinchus thaleichthys*, age-0 striped bass, *Morone saxatilis*, and threadfin shad, *Dorosoma petenense*. Accordingly, these species are the focus this study. The delta smelt is a relatively small (60–70 mm standard length (SL)), endemic, annual, spring spawning, planktivorous fish that is distributed primarily in the delta and surrounding areas (Moyle et al. 1992). Delta smelt were listed as threatened under the US Endangered Species Act (ESA) in 1993 and endangered under the California Endangered Species Act (CESA) in 2010. The endemic longfin smelt is also a relatively small (90–100 mm SL), anadromous, semelparous, spring spawning fish with an approximate 2-year life cycle that is broadly distributed throughout the estuary (Rosenfield and Baxter 2007). Longfin smelt were listed as threatened under the CESA in 2010. Striped bass is a larger (>1 m SL), relatively long-lived, anadromous, late-spring spawning species deliberately introduced to the San

Francisco Estuary from the US east coast in 1879 (Stevens et al. 1985). Although subadult and adult fish reside primarily in estuarine and coastal waters, age-0 fish can be found in lower salinity areas where they feed on zooplankton and macroinvertebrates. Threadfin shad was discovered in the delta during the early 1960s (Feyrer et al. 2009) and is a relative small (<100 mm SL), summer spawning planktivorous fish that primarily inhabits freshwater areas of the estuary.

Field Sampling

The California Department of Fish and Wildlife (CDFW) has been conducting the Fall Midwater Trawl (FMWT) survey in the delta nearly continuously since 1967 (Stevens and Miller 1983; see http://www.dfg.ca.gov/delta/projects.asp?ProjectID=FMWT for additional details). The survey was initiated to measure the relative abundance of age-0 striped bass; however, survey data have been used to infer patterns in relative abundance of a variety of species inhabiting the delta (Kimmerer 2002; Sommer et al. 2007). Monthly cruises are conducted from September through December, and the number of tows each month has increased from approximately 75–80 during the early years of the program to >100 in more recent years. The survey follows a stratified fixed station design such that sampling occurs at approximately the same location within predefined regional strata (17 areas excluding areas 2, 6, and 9 per the CDFW's protocol). Sampling intensity is related to water volume in each regional stratum such that samples are taken every 10,000 acre ft for areas 1–11 and every 20,000 acre ft for areas 12–17; Fig. 1). At each sampling location, a 12-min oblique tow is made from near bottom to the surface using a 3.7 m×3.7 m square midwater trawl with variable mesh in the body and a 1.3-cm stretch mesh cod end. Vessel speed over ground during tows can be variable since sampling procedures are designed to maintain a constant cable angle throughout the tow. Each catch is sorted and enumerated by species and station-specific measurements of surface water temperature, electrical conductivity (specific conductance), and Secchi depth are recorded. CPUE is defined as number of fish collected per trawl tow.

Sampling Covariates

Generalized linear models (GLMs; McCullagh and Nelder 1989) were used to evaluate the effects of sampling covariates on CPUE of the four focal fish species. GLMs are defined by the underlying statistical distribution for the response variable and how a set of linearly related explanatory variables correspond to the expected value of the response variable. The relationship between explanatory variables and the expected value of the response variable is defined by a link function, which must be differentiable and monotonic.

Since CPUE was defined as fish count per trawl, the Poisson and negative binomial distributions were considered. Plots of the proportion of FMWT tows where at least one target animal was captured across the time series for each species showed low values for many years, which gave rise to the possibility that these data were zero-inflated (Fig. 2). In general, zero-inflated count data imply that the response variable contains a higher proportion of zero observations than expected based on a Poisson or negative binomial count process. Ignoring zero inflation can lead to overdispersion and biased parameter and standard error estimates (Zuur et al. 2009).

Zero-inflated distributions are a mixture of two distributions, one that can only generate zero counts and another that includes zeros and positive counts. In effect, the data are divided into two groups, where the first group contains only zeros (termed false zeros) and the second group contains the count data which may include zeros (true zeros) along with positive values (Zuur et al. 2009, 2012). To identify the appropriate model structure (zero-inflated versus standard GLM) and distribution of the count data (negative binomial versus Poisson), a variety of preliminary models were fitted to the FMWT data. Diagnostic plots, evaluation of overdispersion, and model comparisons using likelihood ratio tests and Akaike's information criterion (AIC; Akaike 1973; Burnham and Anderson 2002) all strongly supported application of a zero-inflated negative binomial distribution, which can be expressed as (Brodziak and Walsh 2013):

$$\Pr(y_i) = \begin{cases} \pi_i + (1-\pi_i)\cdot\left(\frac{k}{\mu_i + k}\right)^k & y_i = 0 \\ (1-\pi_i)\cdot\frac{\Gamma(y_i + k)}{\Gamma(k)\cdot\Gamma(y_i + 1)}\cdot\left(\frac{k}{\mu_i + k}\right)^k\cdot\left(\frac{\mu_i}{\mu_i + k}\right)^{y_i} & \text{otherwise} \end{cases} \quad (1)$$

where y_i is the i^{th} CPUE observation, π_i is the probability of a false zero, and μ_i and k are the mean and overdispersion parameters of the negative binomial distribution, respectively. The top equation represents the probability of obtaining a zero CPUE value, which is a binomial process that can occur either as a false zero or a true zero adjusted by the probability of not obtaining a false zero. The bottom equation is the familiar negative binomial mass function adjusted by the probability of not obtaining a false zero. GLMs were specified to mode π_i and μ_i as linear combinations of covariates with logit and log link functions, respectively.

The covariates measured synoptically with sampling that were considered included year, month, area (all categorical), and the continuous covariate Secchi depth, which was rescaled by subtracting the mean and dividing by its standard deviation. Inclusion of levels of categorical covariates with very few positive CPUE values caused model convergence and estimation problems, so levels with <5 % of the total

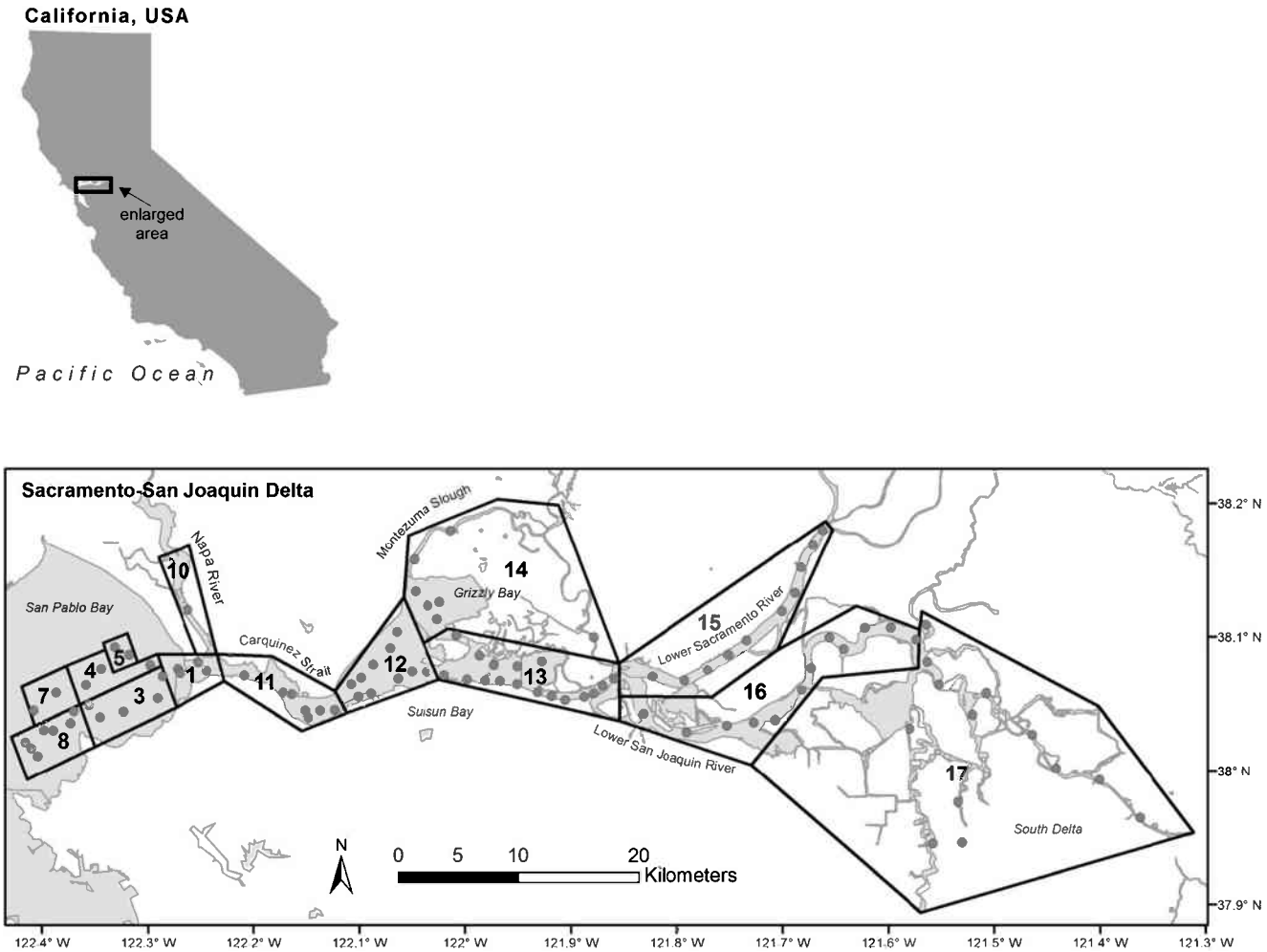

Fig. 1 Aerial stratification (*polygons*) and sampling locations (*circles*) for the Fall Midwater Trawl survey within the Sacramento-San Joaquin Delta, 1967–2012. Areas 2, 6, and 9 are not shown because they have not been consistently sampled and thus are not used by the California Department of Fish and Wildlife for estimation of catch per unit effort indices. No sampling occurred in 1974, September 1976, December 1976, and 1979. Figure adapted from Newman (2008)

survey catch of each species were deemed uninformative and excluded from the analysis. The covariates surface water temperature and surface salinity were also considered; however, variance inflation factors indicated that month/temperature and area/salinity were collinear. Month and area were chosen over temperature and salinity because an appreciable number of catch records did not have associated measures of temperature and/or salinity, and it was desirable to base analyses on the most available information. Also, the variables month and area arguably have the potential to be more useful in a management context. Interaction terms were excluded because the high proportion of zeros in the data lead to many year/area and month/area combinations for which there were no positive CPUE observations. Model parameterizations for each species ranged from inclusion of only a year covariate for the count and probability of false zero models to the saturated model with all four covariates specified for both components, including the possible combinations of unbalanced covariate specifications. AIC was used for model selection, and predictions were generated from the most supported model using estimated marginal means (Searle et al. 1980). Coefficients of variation for yearly predicted CPUE values were estimated from standard deviations of 1000 nonparametric bootstrapped samples (Efron and Tibshirani 1993). Models were fitted to data from 1967 to 2012 with the exception of 1974, September 1976, December 1976, and 1979 when no sampling occurred.

Annual Covariates

The covariate year is included in models when the goal is to develop a time series of estimated CPUE indices. However, the year covariate is simply a proxy for the ecosystem conditions over an annual timescale and thus has no direct relation to the vital rates of fish populations. Therefore, to more directly investigate factors potentially underlying interannual patterns in CPUE for each fish species, the aforementioned zero-inflated GLM structure was modified in two ways: (1) the year covariate was replaced by several hypothesized biotic and abiotic

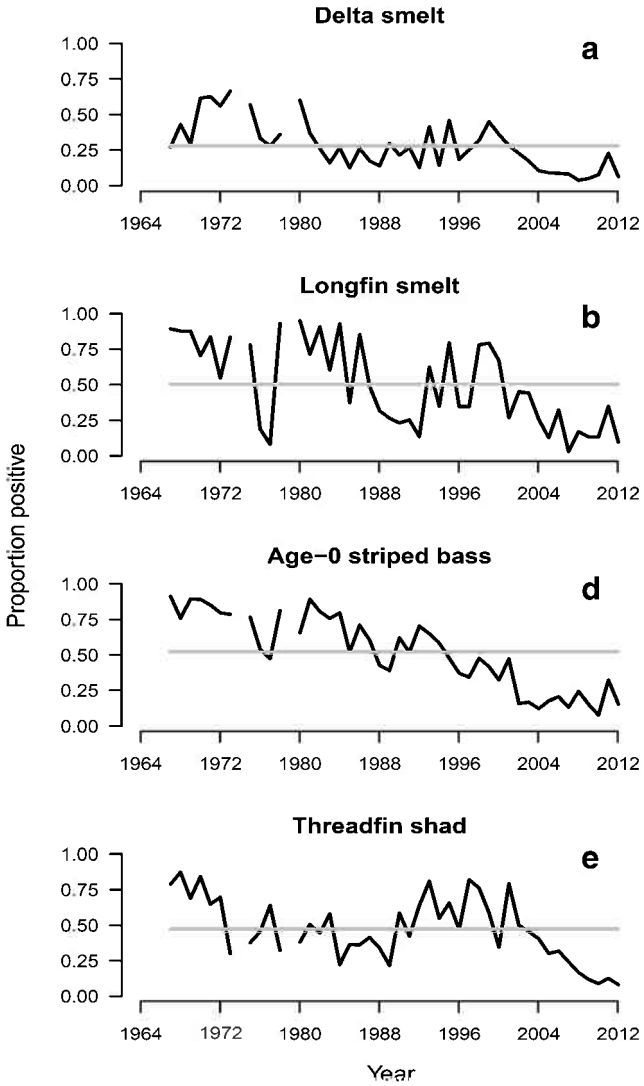

Fig. 2 Yearly proportions of positive tows (at least one target animal captured) based on the Fall Midwater Trawl survey, 1967–2012, for **a** delta smelt, **b** longfin smelt, **c** age-0 striped bass, and **d** threadfin shad. No sampling occurred in 1974, September 1976, December 1976, and 1979. *Horizontal line* is the time series mean

annualized continuous covariates, which operationally implied that the yearly value of each annualized covariate was assigned to each observed CPUE corresponding to the same year and (2) a single parameterization that included the annualized covariate along with month and area was fitted to isolate the effect of each annualized covariate on CPUE. Broad categories of the annualized covariates were zooplankton density (several taxa), chl-*a* concentration as a proxy for phytoplankton biomass, water quality metrics, and water flow (a total of 26). The years analyzed were 1976–2010, which was due to availability of chl-*a* data (began in 1976) and water flow measures (obtained through 2010). AIC was used to compare among competing annualized covariates for each fish species.

In terms of biotic covariates, the California Department of Water Resources (DWR) in collaboration with the CDFW have been compiling data on zooplankton density in the delta since 1968 (see http://www.water.ca.gov/bdma/meta/zooplankton.cfm for additional details, including specific sampling locations). The zooplankton monitoring program was initiated to investigate the population trends of pelagic organisms consumed by young fishes, particularly age-0 striped bass. Although the initial focus was to evaluate seasonal patterns in mysid abundance, the program expanded shortly after its inception to assess population levels of other key zooplankton taxa. Sampling occurs monthly at approximately 20 fixed stations. The zooplankton sampling gear consists of a Clarke-Bumpus net mounted directly above a mysid net, and the unit is deployed in an oblique fashion from near bottom to the surface. Each net is equipped with a flow meter, and all samples are preserved for sorting in the laboratory. For each station, zooplankton taxa are expressed as the total number per cubic meter of water sampled. Starting in 1976, chl-*a* concentration was recorded synoptically with zooplankton sampling.

The zooplankton taxa examined were adult calanoid copepods, adult cyclopoids, a combination of the two, and mysids. Annual estimated mean densities of zooplankton and chl-*a* were based on lognormal GLMs fitted to data from the core sampling locations and first replicate sample. The categorical covariates considered were year, survey (which is approximately equivalent to month), and area along with the continuous variable Secchi depth, which was again rescaled. Levels of categorical variables with <5 % of the total zooplankton density of each group again caused estimation problems and excluded from the analysis. Collinearity was assessed using variance inflation factors, and bias-corrected predicted (Lo et al. 1992) time series were generated from the most supported model using estimated marginal means.

In terms of abiotic covariates, the DWR has been monitoring water quality parameters at discrete sampling locations in the delta since 1970 (see http://www.water.ca.gov/bdma/meta/discrete.cfm for additional details, including sampling locations). The program was established to provide information for compliance with flow-related water quality standards for the delta set forth in the series of regulatory water right decisions and to provide abiotic data that could aid the interpretation of results from concurrent biological monitoring programs. Samples are taken at approximately 1 m depth and roughly within a 1-h window of the expected occurrence of high tide from 19 fixed stations. Sampling frequency is bimonthly during the rainy season (October/November to February/March) and monthly during the dry season (March/April to September/October).

Annual water quality metrics considered were mean summer (Jul–Sep) and winter (Jan–Mar) water temperature, total suspended solids (TSS) or filterable solids, volatile suspended solids (VSS) as a measure of the organic component of TSS, and turbidity. The annual mean water temperatures were

estimated from a multiple linear regression model while annual mean TSS, VSS, and turbidity estimates were obtained from bias-corrected lognormal GLMs. The covariates considered were categorically defined year, month, and area. Variance inflation factors were again used to assess collinearity, and predicted mean values for each year were based on estimated marginal means from the most supported model.

The water flow covariates considered were classified into two groups, "historical", which refers to measured flows taken from monitoring equipment located at various points in the delta, and "unimpaired", which is an estimated reference quantity intended to represent broader watershed-level hydrology in the absence of man-made facilities that affect flow. For each group, monthly inflow and outflow time series were assembled. Historical inflow included combined measurements from the Sacramento River, Yolo Bypass, and Eastern Delta (San Joaquin River and adjacent areas; Fig. 1), while historical outflow is a net quantity of inflow and an estimate of delta precipitation less total delta exports and diversions. All historical flow time series were based on DAYFLOW, which is a computer program designed to estimate daily average delta outflow (see http://www.water.ca.gov/dayflow/ for more details). Unimpaired inflow is an estimate of water entering the delta from the expansive watershed while unimpaired outflow is a net value adjusted for natural losses (e.g., evaporation and vegetation uptake). Flow data were provided courtesy of W. Bourez (MBK Engineers, Sacramento, CA).

For each flow covariate, a single value was calculated by averaging monthly flow values in four different ways: (i) from Jan–Jun within the year of sampling, (ii) from Mar–May within the year of sampling, (iii) from Jan–Jun of the preceding sampling year, and (iv) from Mar–May of the preceding sampling year. This approach gave rise to 16 annual flow covariates. Lagged flow covariates were considered to investigate possible delayed effects of flow on CPUE. For the most supported annualized covariate, 95 % prediction intervals of CPUE and probabilities of false zeros were based on 1000 nonparametric bootstrapped model fits (Efron and Tibshirani 1993). All statistical analyses were performed with the software package R (version 2.15.1, R Development Core Team 2012), and zero-inflated GLMs were fitted by accessing the "pscl" library.

Results

Field Sampling

Complete tow, month, area, and Secchi depth information was available for 15,273 stations sampled during monthly fall cruises from 1967 to 2012 (excluding 1974, Sep 1976, Dec 1976, and 1979 when no sampling occurred). Application of the 5 % cutoff rule for levels of categorical covariates indicated that all levels of month contained adequate nonzero CPUEs for inclusion in analyses. However, spatial data summaries showed that CPUEs were quite low in some areas, and the 5 % rule led to the inclusion of only areas 12–16 for delta smelt, 11–14 for longfin smelt, 12–16 for YOY striped bass, and 15–17 for threadfin shad (Fig. 1). Total numbers of tows analyzed for each species were 8802 for delta smelt (max. CPUE of 156 animals in December 1982), 6582 for longfin smelt (max. CPUE of 3358 animals in September 1969), 8733 for age-0 striped bass (max. CPUE of 1100 animals in September 1967), and 5019 for threadfin shad (max. CPUE of 4012 animals in December 2001). Although high CPUE values did occasionally occur, the data for each species were strongly skewed toward zero and very low CPUE values. The average percent of nonzero catches across all years analyzed was 28.1 % for delta smelt, 50.2 % for longfin smelt, 52.1 % for age-0 striped bass, and 47.1 % for threadfin shad (Fig. 2).

Sampling Covariates

Based on AIC statistics, the full zero-inflated negative binomial GLM (model M_4) received the most empirical support for each species (Table 1). For delta smelt, model M_5 received modest empirical support (ΔAIC=5.9), and for the other three species, no other parameterizations were comparatively supported. The superior performance of model M_4 suggested that all covariates were statistically important for each species and that CPUE and the probabilities of false zeros varied considerably by year, month, area within the delta, and across the domain of observed Secchi depths.

The model predicted yearly CPUE indices showed differing patterns for each species (Fig. 3). For delta smelt, higher predicted CPUE generally occurred in the early 1970s, 1980, and also for various years during the 1990s. The highest value occurred in 1991, and low CPUE was predicted for much of the 1980s and 2000s. Longfin smelt predicted CPUE was variable and high during the late 1960s, early 1970s, and for a few years during the early 1980s. Since 2000, predicted CPUE was consistently low with 2007 marking the lowest index value on record. Age-0 striped bass predicted CPUE consistently declined through time. The first year in the survey (1967) marked the highest age-0 striped bass predicted CPUE value on record while 2002 marked the lowest value. Threadfin shad predicted CPUE declined in the late 1960s, rebounded to higher but variable levels from the mid-1980s to early 2000s, and declined to the lowest value on record in 2012. Average species-specific CPUE across the time series was as follows: 1.24 fish/tow for delta smelt, 13.4 fish/tow for longfin smelt, 5.34 fish/tow for age-0 striped bass, and 22.9 fish/tow for threadfin shad. The precision of the estimated indices for all species was fairly low as bootstraped estimated

Table 1 Model selection statistics associated with the zero-inflated generalized linear models used to analyze catch-per-unit-effort data from the Fall Midwater Trawl survey for delta smelt, longfin smelt, age-0 striped bass, and threadfin shad, 1967–2012. Covariate abbreviations: *Y* year, *M* month, *A* area, *S* Secchi depth; and *nc* indicates model failed to converge successfully. No sampling occurred in 1974, September 1976, December 1976, and 1979

Model	Count covariates	False zero covariates	No. par.	Delta smelt		Longfin smelt		Age-0 striped bass		Threadfin shad	
				AIC	ΔAIC	AIC	ΔAIC	AIC	ΔAIC	AIC	ΔAIC
M_1	Y	Y	89	*nc*	*nc*	30,253.0	944.1	36,708.6	1299.4	24,364.7	1334.3
M_2	Y+M	Y+M	95	20,844.2	1348.6	29,751.4	442.5	36,630.4	1221.2	24,319.7	1289.4
M_3	Y+M+A	Y+M+A	103	19,872.9	377.3	29,602.4	293.6	36,038.7	629.5	23,336.2	305.8
M_4	Y+M+A+S	Y+M+A+S	105	19,495.6	0.0	29,308.9	0.0	35,409.2	0.0	23,030.3	0.0
M_5	Y+M+A+S	Y+M+A	104	19,501.5	5.9	29,323.0	14.1	35,423.5	14.3	23,246.9	216.7
M_6	Y+M+A+S	Y+M	100	19,795.0	299.4	29,356.0	47.1	35,537.2	128.0	*nc*	*nc*
M_7	Y+M+A+S	Y	97	19,801.9	306.3	29,690.6	381.7	*nc*	*nc*	23,332.8	302.3
M_8	Y+M+A	Y+M+A+S	104	19,635.3	139.7	29,497.7	188.8	35,677.2	268.0	23,045.0	14.6
M_9	Y+M	Y+M+A+S	100	19,795.2	299.6	29,588.6	279.7	35,988.1	578.9	23,956.3	926.0
M_{10}	Y	Y+M+A+S	97	19,834.8	339.2	29,601.4	292.5	36,137.9	728.7	23,993.2	962.8

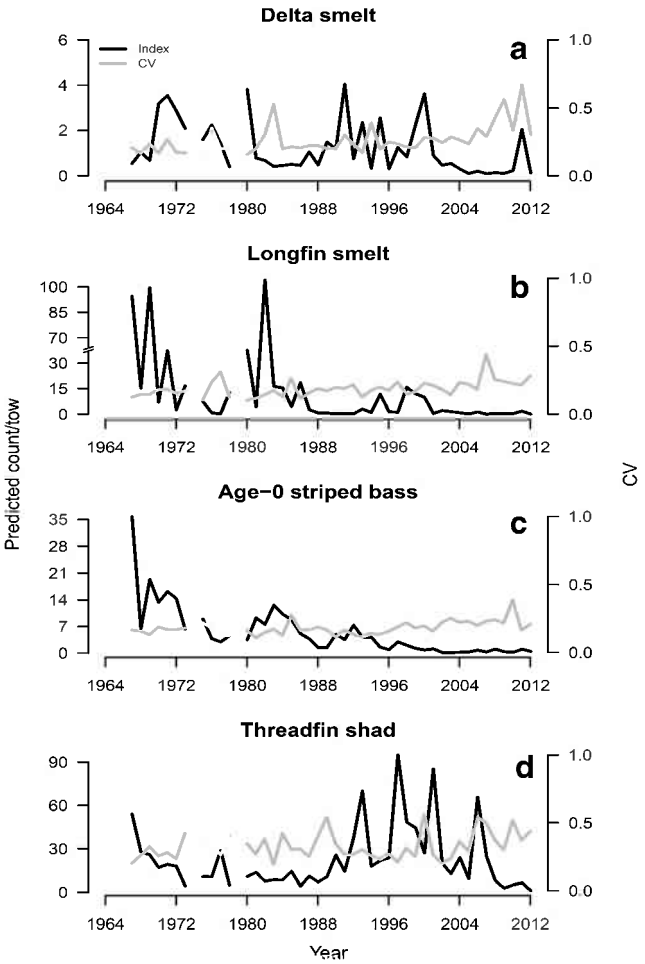

Fig. 3 Predicted yearly catch per unit effort (mean count per tow) and associated coefficients of variation (CV) based on zero-inflated generalized linear models applied to Fall Midwater Trawl survey data, 1967–2012, for **a** delta smelt, **b** longfin smelt, **c** age-0 striped bass, and **d** threadfin shad. No sampling occurred in 1974, September 1976, December 1976, and 1979. Note break in left *y*-axis for longfin smelt

yearly CVs predominately ranged between 0.15 and 0.45 with occasional values greater than 0.5.

Peak predicted monthly CPUE occurred in October for delta smelt, December for longfin smelt, September for age-0 striped bass, and November for threadfin shad (Fig. 4). Delta smelt predicted CPUE indices for November and December did not differ considerably from its peak month nor did the threadfin shad predicted December CPUE when compared to its peak. Spatially, highest predicted CPUE occurred in area 15 for delta smelt, area 12 for longfin smelt, area 15 for age-0 striped bass, and area 17 for threadfin shad. Age-0 striped bass predicted CPUE for areas 12 and 14 were comparably similar in magnitude to its peak.

The response in predicted CPUE across the range of observed standardized Secchi depths was strong and consistent across each species, as higher predicted CPUE values corresponded to low observed Secchi depths. This result emerged because the estimated Secchi depth coefficients associated with the count component of model M_4 were consistently negative across species. Related were the consistently positive estimated coefficients for the false zero model component of each species. Therefore, predicted CPUE declined with increased water clarity (higher Secchi depth) and the probabilities of false zeros increased with water clarity. In terms of actual water clarity conditions in the delta, the minimum observed Secchi depths for delta smelt, longfin smelt, age-0 striped bass, and threadfin shad were 0, 0, 0, and 0.12 m, respectively, while the maximum were 2, 1.6, 2, and 2.09 m. Relative to the maximum predicted CPUE for each species, the observed Secchi depth at which estimated CPUE decreased by 25, 50, and 75 %, respectively, was approximately 0.07, 0.17, and 0.35 m for delta smelt, 0.10, 0.25, and 0.50 m for longfin smelt, 0.11, 0.23, and 0.53 m for age-0 striped bass, and 0.4,

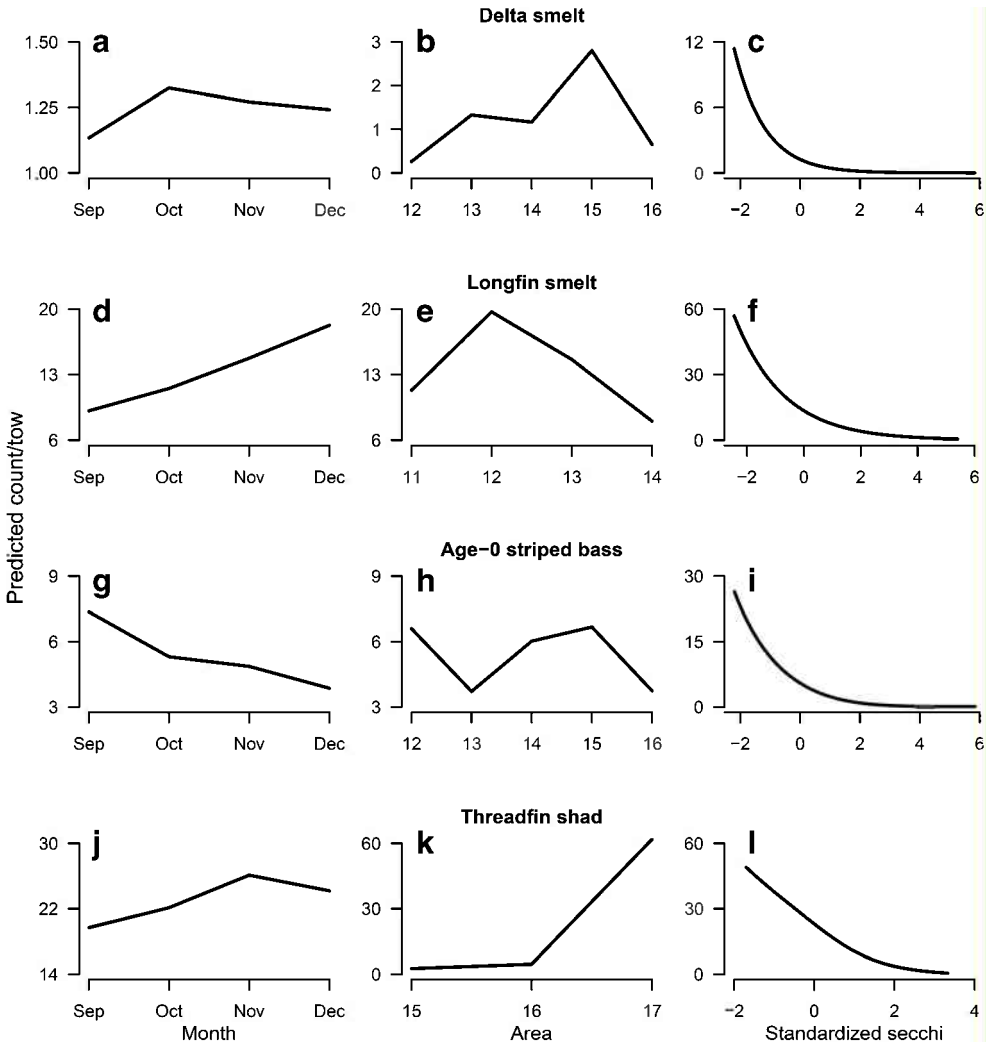

Fig. 4 Predicted catch per unit effort (mean count per tow) by sampling month, area, and across the range of observed standardized Secchi depths, respectively, based on zero-inflated generalized linear models applied to Fall Midwater Trawl survey data, 1967–2012, for (**a**–**c**) delta smelt, (**d**–**f**) longfin smelt, (**g**–**i**) age-0 striped bass, and (j–l) threadfin shad. No sampling occurred in 1974, September 1976, December 1976, and 1979

0.74, and 1.12 m for threadfin shad. Collectively, these results suggest that an increase from virtually no water clarity to roughly 0.5 to 1 m of water clarity corresponded to a 75 % or greater reduction in predicted CPUE for all species.

Annual Covariates

Predicted trends of the annualized biotic and abiotic variables showed differing patterns through time. Adult copepod density (calanoid, cyclopoid combined) has been variable but generally decreasing in the delta, with this trend being largely driven by taxa within the calanoid group (Fig. 5a–e). In contrast, the predicted trend in cyclopoid copepod density has been increasing since the mid-1990s; however, the comparably low density of cyclopoid copepods marginalized the impact of this group on the combined copepod trend. Estimated mysid density has been fairly stable since 1990 but much reduced from peak and moderate levels in the mid-1980s and late 1970s, respectively. The predicted trend of chl-*a* was relatively high and variable in the early part of the time series but considerably lower and more stable since 1987, which is when the lower trophic level food web of the delta changed in response to impacts by the introduced clam *Cobubula amurensis* (Kimmerer 2002).

Trends in predicted mean summer and winter water temperatures were generally stable over time, with estimated mean winter temperatures being slightly more variable than mean summer temperatures (Fig. 5f–j). Predicted trends of TSS, VSS, and turbidity in the delta were similar in that they showed considerable declines since the mid-1970s. Patterns in the various water flow variables showed distinct periods of "wet" and "dry" delta hydrology over time. Peak flow events occurred in 1983, the mid-1990s, and more recently in 2006, while low flows were observed in mid-1970s, early 1990s and late 2000s (Fig. 6). As expected, comparisons of type-specific (historical, unimpaired) patterns of inflows and outflows were generally the same qualitatively, with the latter simply reflecting reductions in water volume due to utilization. For the historical inflows and outflows, the two chosen averaging periods yielded virtually the same yearly volumes; however,

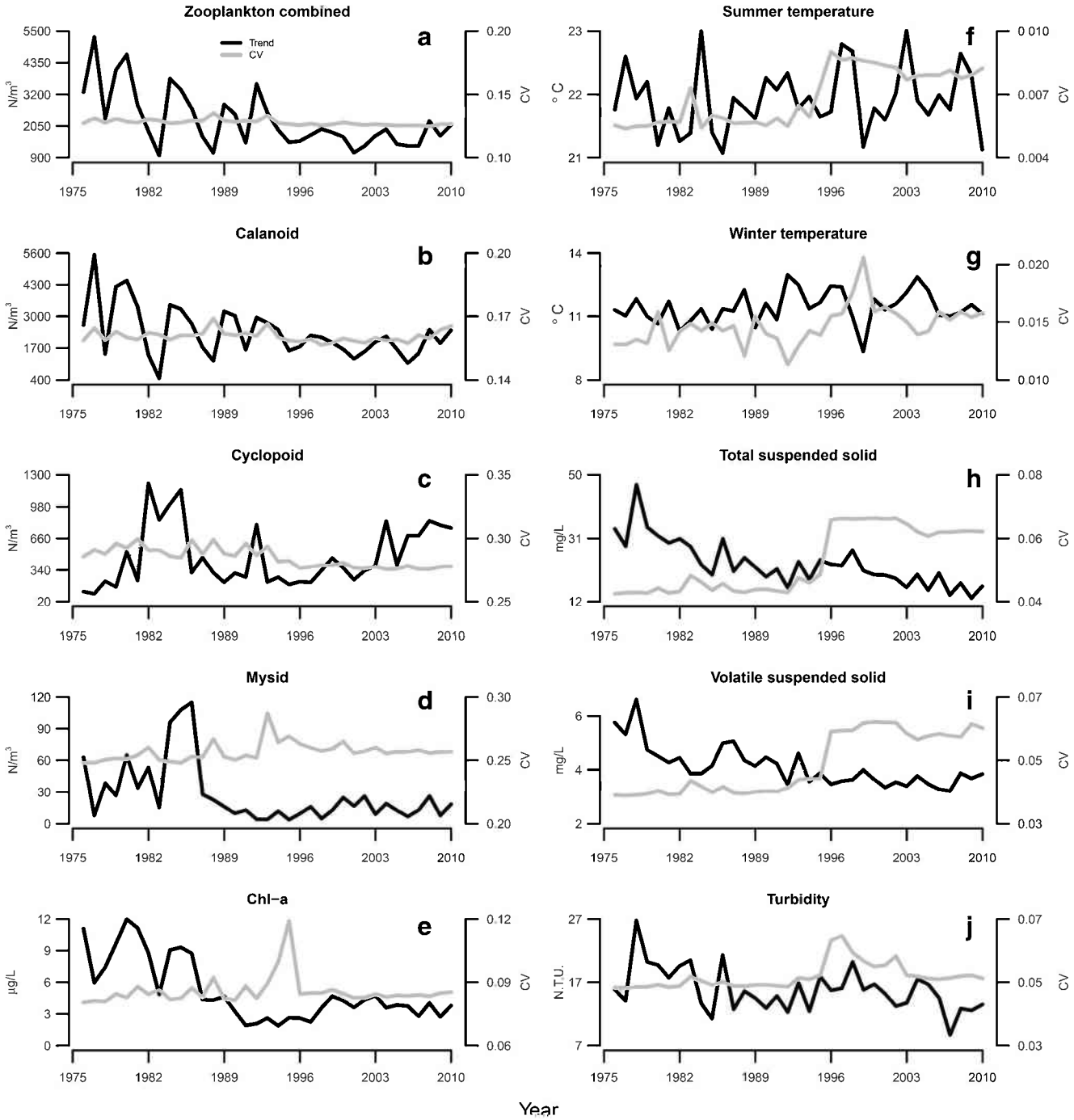

Fig. 5 Annualized mean trends and associated coefficients of variation (CV) based on various linear and generalized linear models fitted to zooplankton and discrete water quality data, 1976–2010, for **a** zooplankton combined (adult calanoid copepod and adult cyclopoid), **b** adult calanoid, **c** adult cyclopoid, **d** mysid, **e** chl-*a*, **f** summer water temperature (Jul–Sep), **g** winter water temperature (Jan–Mar), **h** total suspended solid, **i** volatile suspended solid, and **j** turbidity

there were notable differences in yearly volumes of unimpaired inflow and outflow depending on the monthly averaging period. The precision of all estimated biotic and abiotic covariates was very good as evidenced by consistently low CVs.

Based on AIC statistics, the annualized variable TSS received the most empirical support for all species (Table 2). Comparatively, there was no empirical support for any other annualized prey, water quality, or flow covariates. Predicted CPUE and probabilities of false zeros across the range of TSS were similar for three of the four species, with the exception being the predicted CPUE for threadfin shad (Fig. 7). Over the range of TSS, predicted delta smelt, longfin smelt, and age-0 striped bass CPUE increased, while the CPUE trend for

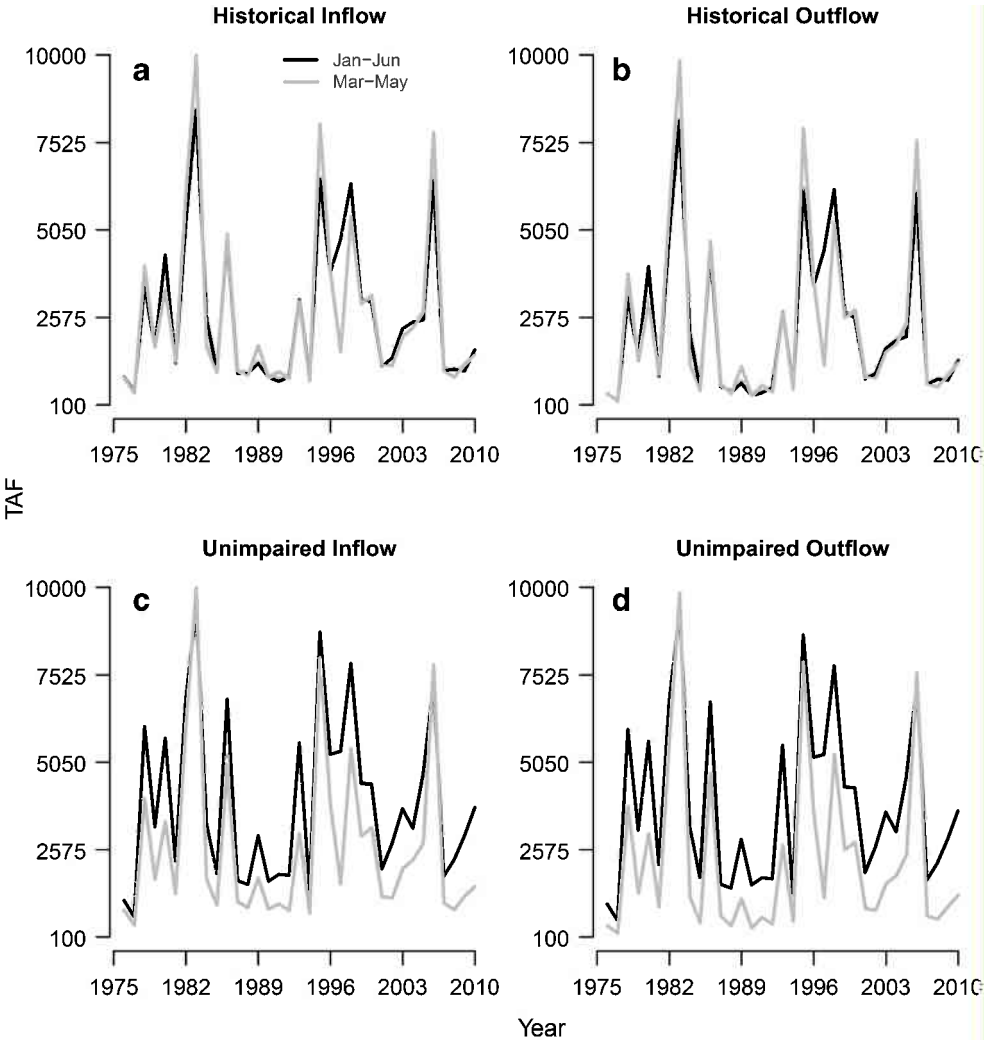

Fig. 6 Annualized trends in flow averaged monthly from January–June and March–May for **a** historical inflow, **b** historical outflow, **c** unimpaired inflow, and **d** unimpaired outflow. Flow variables lagged by 1-year are not shown

threadfin shad showed an inverse relationship. For all species, the predicted trends in probabilities of false zeros were fairly pronounced and decreasing with TSS. In terms of precision, the bootstrapped prediction intervals for both model components were generally narrow for all species.

Discussion

Sampling Covariates

Use of statistical models to quantify the importance of spatio-temporal and environmental covariates on survey CPUE can aid in understanding the dynamics of fish populations. For all species, the covariates year, month, region, and Secchi depth were important in explaining patterns in the observed CPUE data, particularly the zeros. However, relability of the results presented herein directly depends on satisfying the underlying modeling assumptions. For each species, plots of residuals for the count and false zero model components across the observed domains of the covariates showed no distinct patterns, and overdispersion was adequately handled by the zero-inflated model structure. Therefore, from a model diagnostics perspective, the means of the negative binomial and binomial distributions appear to be well estimated. In terms of precision, bootstrapped CVs of the predicted yearly CPUEs were fairly lowfor all species and likely due to the relatively high sampling intensity of the FMWT survey and the high proportion of consistently low observed CPUE values. However, the CV estimates do depend on the assumption that gear catchability (defined as q in the equation $CPUE_y=qN_y$) has remained constant over time and space, so it is possible that they are optimistic. Since the inception of the FMWT survey, the number of monthly sampling locations has grown considerably (~25 %), yet accompanying studies of potential gains/losses in bias and precision of predicted CPUE are absent from the literature. In general, model-based approaches can be useful in the design of fishery-independent surveys (Peel et al. 2013), and the methods in this study could support optimization studies to evaluate design elements, appropriate

Table 2 Model selection statistics associated with the zero-inflated generalized linear models used to evaluate the biotic and abiotic annualized covariates for delta smelt, longfin smelt, age-0 striped bass, and threadfin shad, 1976–2010

Model	Annual covariate	Delta smelt		Longfin smelt		Age-0 striped bass		Threadfin shad	
		AIC	ΔAIC	AIC	ΔAIC	AIC	ΔAIC	AIC	ΔAIC
A_1	Adult calanoid copepods	15,122.3	304.1	24,968.2	1642.2	27,545.5	691.4	19,325.6	263.8
A_2	Adult cyclopoid copepods	15,080.4	262.2	24,419.8	1093.8	27,420.7	566.6	19,247.5	185.7
A_3	Adult calanoid, adult cyclopoid combined	15,105.3	287.1	24,896.4	1570.3	27,433.2	579.1	19,310.9	249.1
A_4	Mysids	15,164.8	346.6	24,145.5	819.4	27,125.5	271.4	19,322.2	260.4
A_5	Chl-*a*	15,070.8	252.5	23,758.9	432.9	26,932.9	78.7	19,326.7	264.9
A_6	Summer temperature	15,113.2	295.0	24,633.0	1306.9	27,536.3	682.2	19,311.5	249.7
A_7	Winter temperature	15,095.2	277.0	24,282.6	956.5	27,472.6	618.5	19,325.3	263.5
A_8	Total suspended solids	14,818.2	0.0	23,326.1	0.0	26,854.1	0.0	19,061.8	0.0
A_9	Volatile suspended solids	15,074.5	256.3	24,612.9	1286.8	27,106.2	252.1	19,213.2	151.3
A_{10}	Turbidity	14,853.1	34.8	23,449.7	123.6	27,493.2	639.0	19,196.7	134.9
A_{11}	Historical outflow Jan–Jun	14,974.3	156.0	23,509.0	183.0	27,390.9	536.8	19,288.4	226.6
A_{12}	Historical outflow Mar–May	15,067.4	249.1	23,766.1	440.0	27,396.4	542.3	19,318.2	256.4
A_{13}	Historical outflow Jan–Jun, 1-year lag	15,164.2	346.0	24,872.2	1546.1	27,521.8	667.7	19,316.3	254.5
A_{14}	Historical outflow Mar–May, 1-year lag	15,158.5	340.3	24,925.1	1599.0	27,536.0	681.8	19,330.4	268.6
A_{15}	Historical inflow Jan–Jun	14,975.6	157.3	23,497.8	171.8	27,394.6	540.5	19,290.8	229.0
A_{16}	Historical inflow Mar–May	15,065.6	247.4	23,707.9	381.9	27,387.8	533.6	19,317.2	255.3
A_{17}	Historical inflow Jan–Jun, 1-year lag	15,162.8	344.6	24,879.9	1553.8	27,524.4	670.2	19,315.9	254.1
A_{18}	Historical inflow Mar–May, 1-year lag	15,158.4	340.1	24,929.6	1603.5	27,531.7	677.6	19,329.0	267.2
A_{19}	Unimpaired outflow Jan–Jun	14,989.8	171.6	23,615.2	289.1	27,436.2	582.1	19,315.2	253.3
A_{20}	Unimpaired outflow Mar–May	15,025.4	207.2	23,968.6	642.5	27,451.5	597.4	19,331.6	269.8
A_{21}	Unimpaired outflow Jan–Jun, 1-year lag	15,167.2	349.0	24,899.4	1573.3	27,549.8	695.7	19,317.4	255.5
A_{22}	Unimpaired outflow Mar–May, 1-year lag	15,152.6	334.4	24,944.6	1618.5	27,557.8	703.7	19,329.1	267.3
A_{23}	Unimpaired inflow Jan–Jun	14,989.9	171.7	23,613.4	287.3	27,436.7	582.6	19,315.4	253.5
A_{24}	Unimpaired inflow Mar–May	15,025.5	207.2	23,969.1	643.0	27,452.3	598.1	19,331.6	269.8
A_{25}	Unimpaired inflow Jan–Jun, 1-year lag	15,167.1	348.9	24,899.4	1573.3	27,550.0	695.9	19,317.4	255.6
A_{26}	Unimpaired inflow Mar–May, 1-year lag	15,152.7	334.5	24,944.3	1618.2	27,558.3	704.2	19,329.0	267.2

sample sizes, and allocation of resources for future FMWT surveys. The estimated monthly, regional, and Secchi depth effects generated relatively unique predicted CPUE patterns for each species, which can, in turn, be used as important foundational information for future hypothesis-driven field studies and mechanistic modeling activities.

The annual frequency of zero CPUE observations over the course of the entire FMWT survey was appreciably high for all species (Fig. 2). As a means of coarsely evaluating the temporal pattern of zero inflation in the FMWT data, model M_4 and its nonzero-inflated counterpart (intercept only parameterization for the false zero component) were sequentially fitted to subsets of the FMWT data set truncated by decade for each species. That is, the two models were applied to only 1960s data, then to 1960s–1970s data, then to 1960s–1980s data, and so on through the full time series. With the exception of the 1960s data for longfin smelt, AIC statistics strongly supported the zero-inflated parameterization for all species and time periods. Therefore, it appears that the FMWT survey data have almost always contained more zero CPUE observations than would otherwise be expected given a negative binomial count process, which raises the question, why?

Failing to successfully encounter target populations can arise because they are rare, samples are taken in suboptimal habitats (true zeros), or because samples are taken in optimal habitats but reduced survey catchability across time, space, and/or ecosystem conditions prevent successful collections (false zeros). For delta smelt, rarity may be a plausible explanation, especially given that the highest predicted yearly CPUE was only 4.04 fish per tow and the 45-year average was just 1.24 fish per tow. However, species rarity does not seem likely for the other three fishes given that predicted yearly longfin smelt CPUE values early in the time series were very high (>70 fish per tow), estimated adult striped bass abundance exceeded 1 million fish in the early 1970s (Stevens et al. 1985) thus requiring considerable age-0 production, and threadfin shad have been viewed as highly abundant since appearing in the delta (Feyrer et al. 2009).

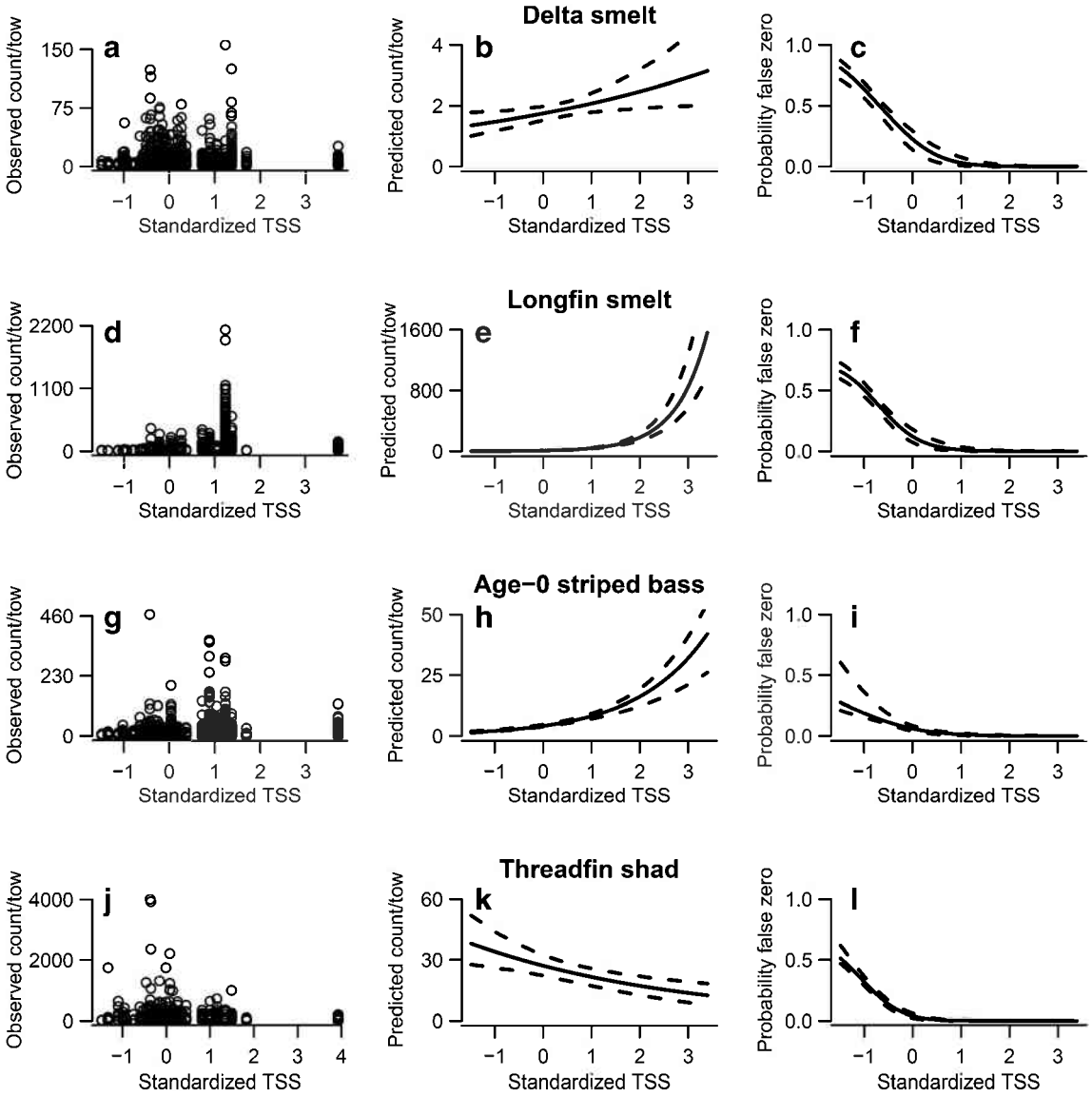

Fig. 7 Observed catch per unit effort (CPUE, mean count per tow, *left panels*), predicted CPUE (*middle panels*), and predicted probabilities of false zeros (*right panels*) with 95 % prediction intervals across observed standardized TSS for (**a**–**c**) delta smelt, (**d**–**f**) longfin smelt, (**g**–**i**) age-0 striped bass, and (**j**–**l**) threadfin shad

The FMWT survey does follow a fixed station sampling design, which raises the possibility that samples are consistently taken at locations that do not support high localized fish abundance. Additionally, if habitat utilization of fishes in the delta has systematically changed over time in response to morphological alterations of the estuary and/or sustained regimes of ecosystem conditions, differences in CPUE and distribution become confounded. The relatively high spatiotemporal sampling intensity of the FMWT survey may somewhat mitigate these concerns, but the four focal species are schooling pelagic fishes, and thus, variable distributions through time and space should be expected.

The consistency of the model prediction to Secchi depth for all species warrants deeper consideration, especially in the context of false zeros. Feyrer et al. (2007) analyzed raw FMWT survey data to evaluate fish occurrences (presence/absence of delta smelt, age-0 striped bass, and threadfin shad) in relation to various environmental variables and documented an inverse response with Secchi depth. Feyrer et al. (2011) updated that analysis and extended it to derive habitat index values for delta smelt (but see comments provided Manly et al. (2015)). The results of this study generalize the importance of Secchi depth to include CPUE. Feyrer et al. (2007) noted that higher presence/absence of delta smelt at lower Secchi depths could be due to required turbidity for feeding and/or turbidity mediated top-down predation impacts. A third potential explanation is that catchability of the FMWT survey sampling gear changes with Secchi depth. In general, Secchi depth is a coarse measurement of water clarity, and it is not possible to

distinguish among constituent groups causing low measurements. If those constituent groups are largely organic material, then a positive fish CPUE response to food availability is possible. Conversely, if those constituent groups are not largely organic, then higher CPUE at lower Secchi depths could be due to compromised foraging impacts of visually oriented piscivores such as larger striped bass (Horodysky et al. 2010). However, all of the fishes in this study are pelagic, planktivorous feeders, and thus, it is reasonable to assume that vision plays a central role in their sensory ecology. Animals could be more effective at gear avoidance under higher Secchi depths than at lower Secchi depths simply because of a larger field of visibility for gear detection.

Although experimentally testing the variable catchability hypothesis is challenging, flume trials to assess gear behavior under various hydrographic conditions, video equipment attached to sampling gear, and coordinated field studies using multiple survey gears designed to quantify relative catchabilities could be informative. Additional modeling efforts may also assist in identifying and quantifying covariate effects on relative catchability. In terms of the bottom-up hypothesis, characterization of water column constituents synoptic with fish stomach content analysis could assist in understanding trophic interactions and prey selectivity, which could aid in determining if the inverse relationship of CPUE and Secchi depth is a response to food availability. Regarding top-down impacts, results of striped bass and other fish predator diet composition studies in the delta have shown very little consumption of delta smelt and longfin smelt, and modest consumption of age-0 striped bass and threadfin shad (Nobriga and Feyrer 2007; Nobriga and Feyrer 2008). However, these studies were temporally abbreviated, and each acknowledged potential biases due to spatial limitation of predator stomach collections. Therefore, systematic temporal and spatial diet composition studies of piscivorous fishes could be helpful in more fully understanding predation impacts of larger fishes.

Annual Covariates

The annualized covariates considered were chosen in an effort to evaluate the effects of hypothesized covariates on fish CPUE that were potentially operating at an annual timescale. The choice to focus on the annual timescale was motivated from the notion that yearly environmental conditions have the potential to impact early life history and thus new year class formation. However, the analytical approach taken here to evaluate annual covariates can be used for variables aggregated across other potentially meaningful scales. For example, biotic or abiotic variables summarized monthly or seasonally could be used to more directly explore drivers of within-year CPUE patterns, and variables could be aggregated spatially to investigated rivers of fish distribution within the delta. Studies of this type represent fruitful areas of future research.

The strong empirical evidence supporting TSS as the best annualized covariate for all species is consistent with the importance of Secchi depth documented in the analysis of sampling covariates. Trends in the model predicted CPUEs and probabilities of false zeros across TSS were analogous to those associated with Secchi depth, with the exception of predicted threadfin shad CPUE which showed a modest decline with TSS. Inspection of the raw threadfin shad CPUE data in relation to TSS showed relatively high frequencies of both zero (>50 % of the tows analyzed) and large CPUE values (>100 fish per tow, 3.9 % of the tows analyzed) at low TSS values when compared to high TSS values. The collective presence of these relatively infrequent large observed CPUEs and numerous observed zero CPUE values likely created the declining predicted CPUE and probability of false zero relationships with TSS (Fig. 7k). The results for the other three species strongly confirm the effect that more turbid water yields higher predicted CPUE and demonstrates that it is also detectable at an annual timescale. As a stand-alone result, the concept that water clarity mediates CPUE keeps the bottom-up, top-down, and variable gear catchability hypotheses in play; however, the strong support for the annualized TSS covariate combined with the lack of empirical support for any of the annualized prey covariates and the aforementioned relative absence of the focal fish species in predator diets may favor the variable catchability hypothesis.

Much of the contemporary understanding regarding covariate effects on fish CPUE in the delta has revolved around flow, particularly outflow and the location of X_2. In this study, X_2 was not considered largely because it is highly variable, often moving significant distances within a single tidal cycle (pers. com., W. Bourez, MBK Engineers, Sacramento, CA) and because it is a proxy covariate directly influenced by flow. Thus, inclusion of the various flow covariates constitutes a more direct evaluation of delta hydrology. CPUE indices of pelagic fishes in the delta have been showed to be positively related to delta outflow (Kimmerer 2002; Sommer et al. 2007), but it is important to note that higher flow regimes lead to higher TSS concentrations. For the data in this study, the historical outflow January–June and March–May time series are each positively correlated with TSS and signficant at the $\alpha=0.07$ level (Pearson's product moment correlations, $\rho_{JJ}=0.32$ [$p=0.058$], $\rho_{MM}=0.31$ [$p=0.067$]). Therefore, higher delta outflow leads to poorer water clarity, which, in turn, could increase survey gear catchability and lead to higher estimated yearly CPUE indices.

If the annualized covariates analysis is restricted to only include the flow covariates, the results indicated that historical outflow averaged January–June received the most support for delta smelt and threadfin shad, and historical inflow averaged January–June and averaged March–May were best supported

for longfin smelt and age-0 striped bass, respectively (Table 2). However, there was competing empirical support for historical inflow averaged January–June for delta smelt (ΔAIC=1.3) and for historical outflow averaged January–June (ΔAIC=3.1) for age-0 striped bass. Collectively, these results fail to confirm the effect of a single dominant flow covariate on fish CPUE in the delta, which is arguably not surprising since the underlying dynamics of the focal fish species are likely shaped by intersections of a complex suite of biological, ecological, and environmental processes.

Acknowledgments The significant efforts of the many field and lab personnel responsible for populating the high-quality fish, plankton, water quality, and flow databases for the delta are outstanding. Discussions with D. Fullerton (Metropolitan Water District) about delta fish ecology and W. Bourez (MBK Engineers, Sacramento, CA) about delta hydrology and DAYFLOW data were appreciated. Funding was provided by the Northern California Water Association, and constructive comments were offered by two anonymous reviewers. This is VIMS contribution number 3456.

References

Akaike, H. 1973. Information theory as an extension of the maximum likelihood principle. In *Second international symposium on information theory*, ed. B.N. Petrov and F. Csaki, 267–281. Budapest: Akademiai Kiado.

Alpine, A.E., and J.E. Cloern. 1992. Trophic interactions and direct physical effects control phytoplankton biomass and production in an estuary. *Limnology and Oceanography* 37: 946–955.

Arthur, J.F., M.D. Ball, and S.Y. Baughman. 1996. Summary of federal and state water project environmental impacts in the San Francisco Bay-Delta Estuary, California. In *San Francisco Bay: The Ecosystem*, ed. J.T. Hollibaugh, 445–495. San Francisco: Pacific Division American Association for the Advancement of Science.

Atwater, B.F., S.G. Conrad, J.N. Dowden, C.W. Hedel, R.L. MacDonald, and W. Savage. 1979. History, landforms andvegetation of the estuary's tidal marshes. In *San Francisco Bay: The Urbanized Estuary*, ed. T.J. Conomos, 347–385. San Francisco: Pacific Division American Association for the Advancement of Science.

Breitburg, D. 2002. Effects of hypoxia, and the balance between hypoxia and enrichment, on coastal fishes and fisheries. *Estuaries* 25: 767–781.

Brodziak, J., and W.A. Walsh. 2013. Model selection and multimodel inference for standardizing catch rates of bycatch species: a case study of oceanic whitetip shark in the Hawaii-based longline fishery. *Canadian Journal of Fisheries and Aquatic Sciences* 70: 1723–1740.

Buchheister, A., C.F. Bonzek, J. Gartland, and R.J. Latour. 2013. Patterns and drivers of the demersal fishcommunity in Chesapeake Bay. *Marine Ecology Progress Series* 481: 161–180.

Burnham, K.P., and D.R. Anderson. 2002. *Model selection and multimodel inference: a practical information-theoretic approach*. New York: Springer.

Chavez, F.P., J. Ryan, S.E. Lluch-Cota, and M. Niquen. 2003. From anchovies to sardines and back: multidecadal change in the Pacific Ocean. *Science* 299: 217–221.

Cohen, A.N., and J.T. Carlton. 1998. Accelerating invasion rate in a highly invaded estuary. *Science* 279: 555–558.

Connor, M.S., J.A. Davis, J. Leatherbarrow, B.K. Greenfield, A. Gunther, D. Hardin, T. Mumley, J.J. Oram, and C. Werme. 2007. The slow recovery of San Francisco Bay from the legacy of organochlorine pesticides. *Environmental Research* 105: 87–100.

Craig, J.K. 2012. Aggregation on the edge: effects of hypoxia avoidance on the spatial distribution of brown shrimp and demersal fishes in the Northern Gulf of Mexico. *Marine Ecology Progress Series* 445: 75–95.

Cury, P., and L. Shannon. 2004. Regime shifts in upwelling ecosystems: observed changes and possible mechanisms in the northern and southern Benguela. *Progress in Oceanography* 60: 223–243.

Diaz, R.J., and R. Rosenberg. 2008. Spreading dead zones and consequences for marine ecosystems. *Science* 321: 926–929.

Drinkwater, K.F., G. Beaugrand, M. Kaeriyama, S. Kim, G. Ottersen, R.I. Perry, H. Pörtner, J.J. Polovina, and A. Takasuka. 2009. On the processes linkingclimate to ecosystem changes. *Journal of Marine Systems* 79: 374–388.

Efron, B., and R.J. Tibshirani. 1993. *An introduction to the bootstrap*, vol. 57. London: Chapman and Hall.

Feyrer, F., K. Newman, M. Nobriga, and T. Sommer. 2011. Modeling the effects of future outflow on the abiotic habitat of an imperiled estuarine fish. *Estuaries and Coasts* 34: 120–128.

Feyrer, F., M.L. Nobriga, and T. Sommer. 2007. Multidecadal trends for three declining fish species: habitat patterns and mechanisms in the San Francisco Estuary, California, USA. *Canadian Journal of Fisheries and Aquatic Sciences* 64: 723–734.

Feyrer, F., T. Sommer, and S.B. Slater. 2009. Old school vs. new school: status of threadfin shad (*Dorosoma petenense*) five decade after its introduction to the Sacramento-San Joaquin Delta. *San Francisco Estuary & Watershed Science* 7(1).

Frederiksen, M., M. Edwards, A.J. Richardson, N.C. Halliday, and S. Wanless. 2006. From plankton to top predators: bottom-up control of a marine food web across four trophic levels. *Journal of AnimalEcology* 75: 1259–1268.

Hare, J.A., M.A. Alexander, M.J. Fogarty, E.H. Williams, and J.D. Scott. 2010. Forecasting the dynamics of acoastal fishery species using a coupled climate-population model. *Ecological Applications* 20: 452–464.

Horodysky, A.Z., R.W. Brill, E.J. Warrant, J.A. Musick, and R.J. Latour. 2010. Comparative visualfunction infour piscivorous fishes inhabiting Chesapeake Bay. *Journal of Experimental Biology* 213: 1751–1761.

Houde, E.D. 2009. Recruitment variability. In *Fish Reproductive Biology: Implications for Assessment and Management*, ed. T. Jakobsen, M. Fogarty, B.A. Megrey, and E. Moksness, 91–171. Malaysia: Wiley-Blackwell Publishing.

Hunt, G.L., and S. McKinnell. 2006. Interplay between top-down, bottom-up, and wasp-waist controlin marine ecosystems. *Progress in Oceanography* 68: 115–124.

Islam, M.S., and M. Tanaka. 2004. Impacts of pollution on coastal and marine ecosystems including coast and marine fisheries and approach for management: a review and synthesis. *Marine Pollution Bulletin* 48: 624–649.

Jackson, J.B.C., M.X. Kirby, W.H. Berger, K.A. Bjorndal, L.W. Botsford, B.J. Bourque, R.H. Bradbury, R. Cooke, J. Erlandson, J.A. Estes, T.P. Hughes, S. Kidwell, C.B. Lange, H.S. Lenihan, J.M. Pandolfi, C.H. Peterson, R.S. Steneck, M.J. Tegner, and R.R. Warner. 2001. Historical overfishing and therecent collapse of coastal ecosystems. *Science* 293: 629–637.

Jassby, A.D., and J.E. Cloern. 2000. Organic matter sources and rehabilitation of the Sacramento-San Joaquin Delta (California, USA). *Aquatic Conservation: Marine and Freshwater Ecosystems* 10: 323–352.

Jassby, A.D., W.J. Kimmerer, S.G. Monismith, C. Armor, J.E. Cloern, T.M. Powell, J.R. Schubel, and T.J. Vendlinski. 1995. Isohaline position as ahabitat indicator for estuarine populations. *Ecological Applications* 5: 272–289.

Kimmerer, W.J. 2002. Effects of freshwater flow on abundance of estuarine organisms: physical effects or trophic linkages? *Marine Ecology Progress Series* 243: 39–55.

Kimmerer, W.J., E.S. Gross, and M.L. MacWilliams. 2009. Is the response of estuarine nekton to freshwater flow in the San Francisco estuary explained by variation in habitat volume? *Estuaries and Coasts* 32: 375–389.

Lo, N.C.H., L.D. Jacobson, and J.L. Squire. 1992. Indices of relative abundance from fish spotter databased on delta-lognormal models. *Canadian Journal of Fisheries and Aquatic Sciences* 49: 2515–2526.

Lotze, H.K., H.S. Lenihan, B.J. Bourque, R.H. Bradbury, R.G. Cooke, M.C. Kay, S.M. Kidwell, M.X. Kirby, C.H. Peterson, and J.B.C. Jackson. 2006. Depletion, degradation andrecovery potential of estuaries and coastal seas. *Science* 312: 1806–1809.

MacNally, R., J.R. Thomson, W.J. Kimmerer, F. Feyrer, K.B. Newman, A. Sih, W.A. Bennett, L. Brown, E. Fleishman, S.D. Culberson, and G. Castillo. 2010. Analysis of pelagic speciesdecline in the upper San Francisco Estuary using multivariate autoregressive modeling (MAR). *Ecological Applications* 20: 1417–1430.

Manly, B.F.J., D. Fullerton, A.N. Hendrix, and K.P. Burnham. 2015. Comments on Feyrer et al. "Modeling the effects of future outflow on the abiotic habitat of an imperiled estuarine fish". *Estuaries and Coasts Online First Articles.*

McCullagh, P., and J.A. Nelder. 1989. *Generalized linear models*, 2nd ed. London: Chapman and Hall.

Molnar, J.L., R.L. Gamboa, C. Revenga, and M.D. Spalding. 2008. Assessing the global threat of invasive species to marine biodiversity. *Frontiers in Ecology and the Environment* 6:485:492.

Moyle, P.B., B. Herbold, D.E. Stevens, and L.W. Miller. 1992. Life history and status of delta smelt in the Sacramento-San Joaquin Estuary, California. *Transactions of the American Fisheries Society* 121: 67–77.

Newman, K. 2008. Sample design-based methodology for estimating delta smelt abundance. *San Francisco Estuary & Watershed Science* 6(3).

Nichols, F.H., J.E. Cloern, S.M. Luoma, and D.H. Peterson. 1986. The modification of an estuary. *Science* 231: 567–573.

Nobriga, M.L., and F. Feyrer. 2007. Shallow-water piscivore-prey dynamics in California's Sacramento-San Joaquin Delta. *San Francisco Estuary & Watershed Science* 5(2).

Nobriga, M.L., and F. Feyrer. 2008. Diet composition in San Francisco Estuary striped bass: does trophic adaptability have its limits. *Environmental Biology of Fishes* 83: 495–503.

Norcross, B.L., and H.M. Austin. 1988. Middle Atlantic Bight meridional wind component effect on bottom water temperatures and spawning of Atlantic croaker. *Continental Shelf Research* 8: 69–88.

Orsi, J.J., and W.L. Mecum. 1996. Food limitation as the probable cause of a long-term decline in the abundance of *Neomysis mercedis* the opossum shrimp in the Sacramento-San Joaquin Estuary. In *San Francisco Bay: The Ecosystem*, ed. J.T. Hollibaugh, 375–401. San Francisco: Pacific Division American Association for the Advancement of Science.

Peel, D., M.V. Bravington, N. Kelly, S.N. Wood, and I. Knuckey. 2013. A model-based approach to designing a fishery-independent survey. *Journal of Agricultural, Biological, and Environmental Statistics* 18: 1–21.

Rosenfield, J.A., and R.D. Baxter. 2007. Population dynamics and distribution patterns of longfin smelt in the San Francisco Estuary. *Transactions of the American Fisheries Society* 136: 1577–1592.

Schoellhamer, D.H. 2011. Sudden clearing of estuarine waters upon crossing the threshold from transport to supply regulation of sediment transport as an erodible sediment pool is depleted: San Francisco Bay, 1999. *Estuaries and Coasts* 34: 885–899.

Searle, S., F. Speed, and G. Milliken. 1980. Population marginal means in the linear model: An alternative to least squares means. *American Statistician* 34: 216–221.

Sommer, T., C. Armor, R. Baxter, R. Breuer, L. Brown, M. Chotkowski, S. Culberson, F. Feyrer, M. Gingras, B. Herbold, W. Kimmerer, A. Mueller-Solger, M. Nobriga, and K. Souza. 2007. The collapse of pelagic fishes in theupper San Francisco Estuary. *Fisheries* 32: 270–277.

Stevens, D.E., and L.W. Miller. 1983. Effects of river flow on abundance of young Chinook salmon, American shad, longfin smelt, and delta smelt in the Sacramento-San Joaquin River system. *North American Journal of Fisheries Management* 3: 425–437.

Stevens, D.E., D.W. Kohlhorst, L.W. Miller, and D.W. Kelley. 1985. The decline of striped bass in the Sacramento-San Joaquin Estuary, California. *Transactions of the American FisheriesSociety* 114: 12–30.

Turner, J.L., and H.K. Chadwick. 1972. Distribution and abundance of young-of-the-year striped bass, *Morone saxatilis*, in relation to river flow in the Sacramento-San Joaquin Estuary. *Transactions of the American Fisheries Society* 101: 442–452.

Winder, M., and D.E. Schindler. 2004. Climate change uncouples trophic interactions in an aquatic ecosystem. *Ecology* 85: 2100–2106.

Worm, B., R. Hilborn, J.K. Baum, T.A. Branch, J.S. Collie, C. Costello, M.J. Fogarty, E.A. Fulton, J.A. Hutchings, S. Jennings, O.P. Jensen, H.K. Lotze, P.M. Mace, T.R. McClanahan, C. Minto, S.R. Palumbi, A.M. Parma, D. Ricard, A.A. Rosenberg, R. Watson, and D. Zeller. 2009. Rebuilding global fisheries. *Science* 325: 578–585.

Zuur, A.F., E.N. Ieno, N.J. Walker, A.A. Saveliev, and G.M. Smith. 2009. *Mixed effects models andextensions in ecology with R*. New York: Springer.

Zuur, A.F., A.A. Saveliev, and E.N. Ieno. 2012. *Zero inflated models and generalized linear mixedmodels with R*. Newburgh: Highland Statistics Ltd.

Fisheries Research 164 (2015) 102–111

Contents lists available at ScienceDirect

Fisheries Research

journal homepage: www.elsevier.com/locate/fishres

Use of state-space population dynamics models in hypothesis testing: advantages over simple log-linear regressions for modeling survival, illustrated with application to longfin smelt (*Spirinchus thaleichthys*)

Mark N. Maunder[a,b,*], Richard B. Deriso[b], Charles H. Hanson[c]

[a] *Quantitative Resource Assessment LLC, San Diego, CA 92129, USA*
[b] *Inter-American Tropical Tuna Commission, 8901 La Jolla Shores Drive, La Jolla, CA 92037-1508, USA*
[c] *Hanson Environmental, Inc., 446 Green View Court, Walnut Creek, CA 94596, USA*

ARTICLE INFO

Article history:
Received 28 April 2014
Received in revised form 22 October 2014
Accepted 27 October 2014
Handling Editor A.E. Punt

Keywords:
Data assimilation
Longfin smelt
Population dynamics
Random effects
State-space model
Survival

ABSTRACT

Factors impacting the survival of individuals between two life stages have traditionally been evaluated using log-linear regression of the ratio of abundance estimates for the two stages. These analyses require simplifying assumptions that may impact the results of hypothesis tests and subsequent conclusions about the factors impacting survival. Modern statistical methods can reduce the dependence of analyses on these simplifying assumptions. State-space models and the related concept of random effects allow the modeling of both process and observation error. Nonlinear models and associated estimation techniques allow for flexibility in the system model, including density dependence, and in error structure. Population dynamics models link information from one stage to the next and over multiple time periods and automatically accommodate missing observations. We investigate the impact of observation error, density dependence, population dynamics, and data for multiple stages on hypothesis testing using data for longfin smelt in the San Francisco Bay-Delta.

1. Introduction

Estimation of survival, and the factors influencing survival, are vital in the research, and to the management, of natural resources. Survival is a critical component of methods used to determine sustainable yields of harvested resources (Quinn and Deriso, 1999). Managers need to know the most influential factors affecting the survival of endangered species to focus limited financial resources on research and management actions that obtain the most benefit. Anthropogenic effects have to be separated from natural impacts to determine the relative importance of restricting human activities (e.g. Deriso et al., 2008).

Survival can be estimated using a number of approaches ranging from field studies such as following individuals using radio tracking and determining their fate (White and Garrott, 1990; Skalski et al., 2010) to sophisticated statistical state-space population dynamics models that integrate multiple data types (Besbeas et al., 2003; Maunder, 2004; Schaub and Abadi, 2010). Facilitated by the availability of time series of relative abundance, log-linear modeling of the ratio of relative abundance in two life stages is a common approach to estimate relative survival and evaluate the support for different hypotheses about the factors influencing survival (e.g. Miller et al., 2012). Log-linear modeling is used because it is conveniently implemented in traditional software packages as a linear equation. However, it restricts the analysis to a subset of models that are not necessarily the most appropriate for the particular application. Log-linear modeling also aggregates process and observation error into a single term, limiting the ability to fully characterize uncertainty. Modern nonlinear modeling software such as BUGS (Lunn et al., 2009) and AD Model Builder (Fournier et al., 2012) expand the modeling options outside those covered by "fixed effects" log-linear models, allowing flexibility in model and error structure (Bolker et al., 2013).

Correctly dealing with both observation and process error is important for hypothesis testing and evaluating the data-based support for alternative hypotheses (Maunder and Watters, 2003; Deriso et al., 2008). Process error (also known as process noise or

* Corresponding author at: Inter-American Tropical Tuna Commission, 8901 La JollaShores Drive, La Jolla, CA 92037-1508, USA. Tel.: +1 858 546 7027..
E-mail addresses: mmaunder@iattc.org (M.N. Maunder), rderiso@iattc.org (R.B. Deriso), chanson@hansonenv.com (C.H. Hanson).

http://dx.doi.org/10.1016/j.fishres.2014.10.017

process variability) generally refers to stochasticity in population dynamics (but can also relate to model structure misspecification) and is hence parameterized as "random effects", and observation error refers to inaccuracy in observations (de Valpine, 2003).

One approach for dealing with both observation and process error is to ignore one or the other entirely. Polacheck et al. (1993) found that ignoring process error (an observation error estimator) was superior to ignoring observation error (a process error estimator) when estimating the parameters of a simple population dynamics model, but they did not evaluate which choice was best for hypothesis testing. Ignoring process error biases likelihood ratio and Akaike information criterion (AIC; Akaike, 1973) based tests towards incorrectly accepting covariates (Maunder and Watters, 2003). Other tests such as analysis of deviance (Skalski, 1996) or randomization tests (Edgington, 1987; Deriso et al., 2008) can be used, but they are less elegant and impractical in some situations. An alternative approach is to include both process and observation error, but assume the ratio of the variances between these two sources of variation is known (e.g. Walters and Ludwig, 1981) or that one of the variances is known (e.g. Maunder and Watters, 2003). Incorrectly specifying the variance terms can bias hypothesis tests (Deriso et al., 2007).

The preferred approach is to use state-space models (e.g. Schnute, 1994; Newman, 1998; de Valpine, 2002; Buckland et al., 2004, 2007; Maunder and Deriso, 2011) that allow the estimation of the both observation and process error variances. It should be noted that state-space models are often described as random effect, hierarchical, or Bayesian models. de Valpine and Hastings (2002) found that state-space models led to lower bias and often lower variance estimates than least squares estimators that ignore either process noise or observation error. Traditionally, state-space models have been used to model demographic variability such as the binomial probability of individuals surviving given an average survival rate (Dupont, 1983; Besbeas et al., 2002). However, demographic variability is typically overwhelmed by environmental variability (Buckland et al., 2007), so environmental variability is often modeled instead of demographic variability or in addition to demographic variability (e.g. Rivot et al., 2004; Newman and Lindley, 2006). Nonlinear, non-Gaussian state-space models generally require computationally intensive high dimensional integrals that have no closed form solution (de Valpine, 2003). The implementation of state-space models in a Bayesian framework has been facilitated by the development of Markov chain Monte Carlo (MCMC) methods (Punt and Hilborn, 1997; Newman et al., 2009; Lunn et al., 2009). MCMC methods have also been adapted to implement state-space models in a classical framework (Lele et al., 2007). Alternatively, the Laplace approximation (Skaug, 2002; Skaug and Fournier, 2006) or importance sampling (Maunder and Deriso, 2003) can be used to implement the integration in a classical framework. Modern nonlinear modeling software packages such as BUGS and AD Model Builder have made state-space models practical for many applications (Bolker et al., 2013).

Log-linear models, such as generalized linear models, analysis of variance (ANOVA), and related statistical methods, do not incorporate demographic relationships between abundances through time (de Valpine, 2003). In contrast, lifecycle models link life-stages and time periods using population dynamics propagating information and uncertainty (Buckland et al., 2007; Maunder and Deriso, 2011). This link allows information related to one life-stage to inform processes influencing other life-stages and is particularly important when data are not available for all life stages for all time periods. Hypotheses that are difficult to consider with ANOVA and related methods can be simple to express using a population dynamics model (de Valpine, 2003). de Valpine (2003) found that a population dynamics model had much higher statistical power than ANOVA, and provided greater biological insight. Even approximately correct population dynamics models had higher power than omitting demographic structure, but the rate at which Type I error occurs may increase, or the power might be reduced as the model structure becomes more incorrect (de Valpine, 2003).

Hypothesis testing is an essential part of statistical analysis and is particularly important when evaluating factors that are impacting survival. When we refer to hypothesis testing, we are more generally referring to the evaluation of the data based support for alternative configurations of a model, where each configuration could represent an alternative hypothesis. This approach is often termed model selection to differentiate it from traditional hypothesis testing that involves the rejection of a null hypothesis (Johnson and Omland, 2004). Hypothesis testing can easily become complex when analysing population dynamics because of the many factors operating on different stages under the presence of density dependence. Deriso et al. (2008) present a framework for evaluating alternative factors influencing survival, and Maunder and Deriso (2011) extended the framework to include density dependence in survival. The first step is to identify the factors to be considered, including the life stages that are impacted by each factor and where density dependence occurs. Next, a model should be developed to include these factors. Then hypothesis tests should be conducted to determine which factors are important. Finally, impact analysis (Wang et al., 2009; Maunder and Deriso, 2011) should be conducted to determine the impact of the factors on quantities useful for management.

Density dependence is an important factor in the dynamics of many populations (Brook and Bradshaw, 2006) and can occur in multiple life stages (e.g. Ciannelli et al., 2004). It is important to consider density dependence when carrying out model selection because it can modify the impact of factors (Rose et al., 2001; Maunder and Deriso, 2011). Environmental conditions can also have a large impact on population dynamics. Environmental factors can directly affect survival through processes such as temperature tolerance or can interact with density dependence through affecting density limiting processes such as habitat or prey availability. Environmental factors and density dependence have been identified as impacting population dynamics in numerous studies either independently or in combination (e.g. Sæther, 1997; Brook and Bradshaw, 2006; Ciannelli et al., 2004; Deriso et al., 2008; Maunder and Deriso, 2011). Density dependence can easily be integrated into state-space models (e.g. de Valpine and Hastings, 2002; Maunder and Deriso, 2011).

Data from longfin smelt (*Spirinchus thaleichthys*) in the San Francisco Bay-Delta are used to illustrate the development and advantages of using state-space population dynamics models over simple log-linear regressions for modeling survival. The models are implemented in AD Model Builder using the Laplace approximation for random effects (Skaug and Fournier, 2006) under a classical (frequentist) framework. Longfin smelt is of conservation concern because it is exposed to a variety of anthropogenic factors (e.g. habitat modification, sewage outflow, farm runoff, and water diversions) and survey data have shown a decline in abundance. Longfin smelt was listed as threatened under the California Endangered Species Act in 2009. The U.S. Fish and Wildlife Service also evaluated the status of the Bay-Delta longfin smelt population and concluded in 2012 that although the species warranted protection under the federal Endangered Species Act, staff limitations precluded listing the species as of that time. Several other species in the San Francisco Estuary have also experienced declines (e.g., Bennett, 2005; Sommer et al., 2007; Mac Nally et al., 2010; Thomson et al., 2010; Maunder and Deriso, 2011), but the declines have yet to be fully explained.

2. Theory

State-space models appropriately accommodate both observation and process error. de Valpine (2002, 2003) provides a useful description of state-space models in the context of population dynamics models. Here we illustrate state-space models using a simple population dynamics model where the abundance in the next time period is simply those that survive from the previous time period:

$$E[X_{t+1}|X_t] = \mu_s X_t \quad (1)$$

where X_t is the number of individuals at time t, which are the states; and μ_s is the mean survival rate. The observations of the population are estimates of absolute abundance and the sampling variation in these estimates is assumed to be normally distributed:

$$Y_t \sim N(X_t, \sigma^2) \quad (2)$$

where Y_t is the estimate of absolute abundance at time t and σ^2 is the sampling variance.

State-space population dynamics models have three main components: (1) states ($\boldsymbol{X}$), (2) parameters ($\boldsymbol{\theta}$), and (3) observations ($\boldsymbol{Y}$). The states represent the population such as the abundance in a life stage at a given time. The parameters describe the average (or sometimes the exact) relationship (transition) between the states (e.g. the average survival rate), but also include the initial state (e.g. X_1) and the variance parameters (e.g. σ). The observations are measurements of the states, or some function of the states. The states and parameters are unknown and they, or a function of them, are the quantities of interest. The observations, which are known, are used to provide information about the states and parameters. Observations are generally not a census of the population, but a sample of the population and therefore contain sampling error (e.g. if a line transect or trawl survey is used to estimate the abundance of a population). This sampling error is the observation error and is generally represented by the likelihood function. In other words, the observation is known, but there is uncertainty in how the observation relates to the true abundance. There may also be additional observation error over and above the sampling variability, but for illustrative purposes we ignore this.

In traditional maximum likelihood estimation, the parameters of the model are estimated by finding the parameter values that, conditional on these values, give the highest probability (likelihood) that the observations came from the model. Since the states ($\boldsymbol{X}$) are a direct function of the parameters ($\boldsymbol{\theta}$), for known observations and given parameter values, the probability function described in Eq. (2) can be evaluated and maximized. To better illustrate state-space models, let

$$f(\boldsymbol{\theta}, \boldsymbol{Y}) = f(\boldsymbol{X}, \boldsymbol{Y}) \quad (3)$$

be the joint distribution of the data and parameters, since the parameters determine the states, and

$$f_\theta(\boldsymbol{Y}), \quad (4)$$

be the likelihood function evaluated at the parameter values $\boldsymbol{\theta}$. Traditional maximum likelihood assumes that there is a single true value for each parameter. State-space population dynamics models implicitly assume that the values of the parameters representing some population processes may change over time. This is the process error. Before describing state-space models, consider the survival in each time period as a separate model parameter s_t:

$$E[X_{t+1}|X_t] = s_t X_t \quad (5)$$

In this case, the likelihood function can be denoted $f_{\theta,s}(\boldsymbol{Y})$, and traditional maximum likelihood assumes that there is a single true value for survival probability in each time period and for the other model parameters (note that the average survival parameter is replaced with a set of survival parameters, one for each time period) and the survival parameters are estimated along with the other model parameters by maximizing the likelihood function. However, there is now one survival parameter for each observation and each survival will be estimated to exactly match the observation. No other parameters can be estimated (e.g. the observation error variance), and the process error cannot be separated from the observation error.

Intuitively, the estimation procedure could be improved by adding information based on the form of the process error probability distribution (e.g. if the temporal variability in survival is known to be low, a survival parameter in one time period that is very different from the survival in the other time periods is unlikely) and can be conceptualized as placing an informative prior, in the Bayesian sense, on the process error (except that the mean and variance of the prior are unknown) (e.g. $s_t = \mu_s \exp(\varepsilon_t)$, where $\varepsilon_t \sim N(0, \nu^2)$, which parallels the random effects approach in generalized linear mixed models (GLMMs), or in alternative notation $\ln(X_{t+1}) \sim N(\ln(\mu_s X_t), \nu^2)$). In this case, $f_{\boldsymbol{\theta},\boldsymbol{s}}(\boldsymbol{Y}) = f(\boldsymbol{Y}|\boldsymbol{s}, \boldsymbol{\theta}) f(\boldsymbol{s}|\boldsymbol{\theta}) = f(\boldsymbol{Y}|\boldsymbol{\varepsilon}, \boldsymbol{\theta}) f(\boldsymbol{\varepsilon}|\boldsymbol{\theta})$, where $f(\boldsymbol{\varepsilon}|\boldsymbol{\theta})$ is the process error probability distribution, and the resulting likelihood is often referred to as a penalized likelihood. The penalized likelihood combines the sampling probability distribution of the observations with the probability distribution of the states (recall that the parameters determine the state and similarly the process error probability distribution also defines the state probability distribution). These methods estimate the process errors (or states) along with the other model parameters while maximizing the joint probability distribution of the process error and the observations. However, the MLE of the process error variance is not statistically consistent (Seber and Wild, 1989) and the likelihood function is degenerative towards zero variance (Maunder and Deriso, 2003). There is often a negatively biased local maximum that has been used for inference, but the global maximum is at zero process error variance (Maunder and Deriso, 2003).

The process error variance will decrease as covariates are added and therefore the process variance should be reduced, which can only be practically achieved if the process variance is estimated. In contrast to penalized maximum likelihood, state-space models treat the process error (or states) as random variables rather than as parameters and when the process error is integrated out they produce a marginal likelihood or "true likelihood" function that is used for inference (e.g. Eq. (4) becomes $\int f_{\boldsymbol{\theta}}(\boldsymbol{Y}, \boldsymbol{\varepsilon}) d\boldsymbol{\varepsilon}$ or equivalently $\int f_{\boldsymbol{\theta}}(\boldsymbol{Y}, \boldsymbol{X}) d\boldsymbol{X}$). Intuitively, this can be thought of as summing up the likelihood of the observations for each possible state weighted by the probability of that state (conditioned on the parameter values). Each possible survival will lead to different population abundance (state). Hence, the derivation of "state-space", which refers to the whole range of possible trajectories through time of the population states (de Valpine, 2002). Integrating out the process error takes advantage of properties of random variables (e.g. the marginal distribution), which has the advantage that it provides a consistent non-degenerative MLE for the process error variance.

Pawitan (2003) appropriately summarizes state-space models/random effects as a convenient way to deal with many parameters. In a Bayesian framework (Punt and Hilborn, 1997), parameters are also treated as random variables and integrated out (e.g. Eq. (4) becomes $\int\int f(\boldsymbol{Y}, \boldsymbol{\theta}, \boldsymbol{\varepsilon}) d\boldsymbol{\varepsilon} d\boldsymbol{\varphi}$ or equivalently $\int\int f(\boldsymbol{Y}, \boldsymbol{\theta}, \boldsymbol{X}) d\boldsymbol{X} d\boldsymbol{\varphi}$, where $\boldsymbol{\varphi}$ are the parameters that are not of interest) and the probability distribution is used for inference rather than the likelihood function. One advantage of the state-space modeling approach over penalized maximum likelihood is that the marginal likelihood is consistent with AIC theory, which can be used for hypothesis testing and model selection.

3. Methods

3.1. Models

3.1.1. Log-linear regression

A common approach to model survival from one life-stage to the next as a function of explanatory variables is a log-linear regression (Christensen, 1997) of the numbers in the second stage as a ratio of those in the first stage (e.g. Miller et al., 2012). A typical analysis models the reproductive output from adults (A_t) to the surviving juveniles in the next year (J_{t+1}) as:

$$\ln(J_{t+1}/A_t) \sim N(\alpha + \boldsymbol{\beta} I_t, \sigma^2) \quad (6)$$

or equivalently in a different notation (the former notation is commonly used to describe state-space models and the latter notation commonly used to describe random effect models and can be a more useful description (de Valpine, 2003)).

$$\ln(J_{t+1}/A_t) = \alpha + \boldsymbol{\beta I_t} + \varepsilon_t \quad (7)$$

where $\varepsilon_t \sim N(0, \sigma^2)$, N represents a normal distribution, α and $\boldsymbol{\beta}$ are parameters of the linear model, $\boldsymbol{I}_t$ is a matrix of covariates (forcing functions), and σ^2 is the variance of the error. The observations are often only an index of relative abundance related to the absolute abundance by a constant q, often called catchability in the fisheries literature, such that

$$\ln(q_J J_{t+1}/q_A A_t) = \alpha + \boldsymbol{\beta I_t} + \varepsilon_t \quad (8)$$

so unless $q_J = q_A$, α no longer relates to survival (it also includes reproductive output in our example), but a combination of survival and differences in catchability. However, this does not influence hypothesis tests related to the covariates as long as the q's are constant through time or their temporal variation is random and independent of the covariates.

The parameters can be estimated by maximizing the likelihood based on the assumed error distribution (Eq. (8)). The likelihood function is typically used to represent observation error. However, ε in Eq. (8) includes both process and observation error and ε describes the unexplained variation (process error) in the modeled relationship if J and A are known without error. If J and A are known with error (multiplicative and log-normal):

$$\ln\left(\left(J_{t+1}\exp(\varepsilon_{J,t+1})\right) / \left(A_t \exp(\varepsilon_{A,t})\right)\right) = \alpha + \boldsymbol{\beta I_t} + \varepsilon_t \quad (9)$$

where $\varepsilon_{A,t} \sim N(0, \sigma^2_{A,t})$, $\varepsilon_{J,t+1} \sim N\left(0, \sigma^2_{J,t+1}\right)$, such that

$$\ln(J_{t+1}/A_t) = \alpha + \boldsymbol{\beta I_t} + \varepsilon_t - \varepsilon_{J,t+1} + \varepsilon_{A,t} \quad (10)$$

illustrating that Eqs. (6) and (7) combine process error and observation error from both measures of abundance into a single error term $\varepsilon_t \sim N(0, \sigma^2_{J,t} + \sigma^2_{A,t+1} + \sigma^2_{\varepsilon})$.

Often an estimate of the sampling precision of each observation is available (hence the time subscript on the variance terms), which eliminates the need to estimate the observation error variance, but this is generally not the case for the process error. Ignoring observation error may bias the results if the observation error variance differs substantially among observations.

3.1.2. Alternative formulation

The log-linear regression is deterministically equivalent and, depending on assumptions, stochastically equivalent to an exponential growth model. The log-linear model assumes that the unexplained variation in the log of the abundance ratios is normally distributed while the exponential growth model assumes that the unexplained variation in the abundance in the second stage is log-normally distributed

$$J_{t+1} = \alpha' A_t \exp(\boldsymbol{\beta I_t} + \varepsilon_t) \quad (11)$$

where $\alpha' = \exp(\alpha)$

3.1.3. State-space model

State-space models can be used to include both observation and process error. Non-linear state-space models are flexible in representing process and observation error. Eq. (6) assumes log-normal multiplicative error for both the observation and process error with constant variance. The log-normal assumption as implemented in Eq. (6) will provide an unbiased estimate of α, but the quantity of interest $\alpha' = \exp(\alpha)$ will be biased such that the expected value of $E[\alpha'] = \exp(\alpha + 0.5\sigma^2)$ (Maunder and Deriso, 2011). Eq. (11) could be modified to account for the bias

$$J_{t+1} = \alpha' A_t \exp(\boldsymbol{\beta I_t} + \varepsilon_t - 0.5\sigma^2) \quad (12)$$

Similarly, the likelihood and random effects can be modified to deal with the log-normal bias correction. This may be particularly important when the observations have different variances, resulting in different bias correction factors for each time period. The distribution for the process and observation error need not be normal. For example, the process error may be log-normal, while the observation error might be normal.

3.1.4. Density dependence

Population regulation is controlled by both density-independent and density-dependent factors. The log-linear regression typically includes covariates representing density-independent factors (e.g. the environment). Density dependence can be included in the log-linear regression by adding additional terms related to abundance into the regression. The Ricker model (Ricker, 1954)

$$J_{t+1} = \alpha' A_t \exp(-bA_t + \boldsymbol{\beta I_t} + \varepsilon_t) \quad (13)$$

is often used because it can be linearized by taking the natural logarithm and implemented using multiple linear regression.

$$\ln(J_{t+1}) = \alpha + \ln(A_t) - bA_t + \boldsymbol{\beta I_t} + \varepsilon_t \quad (14)$$

where $\alpha = \ln(\alpha')$. However, the Beverton–Holt model (Beverton and Holt, 1957) may be applicable for some populations, but is non-linear:

$$J_{t+1} = \frac{\alpha' A_t}{1 + bA_t} \exp(\boldsymbol{\beta I_t} + \varepsilon_t) \quad (15)$$

The models are derived based on solving the differential equation for abundance where mortality is a linear function of the cohort abundance and initial abundance for the Beverton–Holt and Ricker models, respectively. The Beverton–Holt model has asymptotic properties, which represent processes such intra-cohort competition, while the Ricker model produces lower abundance from high initial abundance, which represents processes such as cannibalism when used in a stock-recruitment context.

3.1.5. State-space population dynamics (life cycle) model

The log-linear regression only models survival from one stage to the next. A sequence of separate log-linear regressions can be used to model the survival between each stage. However this does not link information among stages, which can be useful particularly if there is substantial error in the estimates of abundance or if there are missing abundance estimates. In the case where adults are a

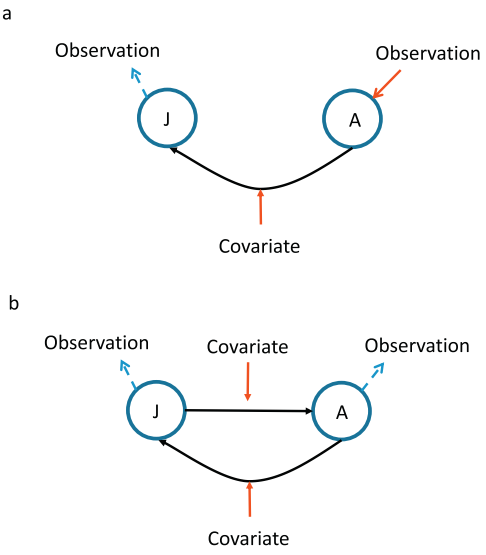

Fig. 1. Conceptual diagram illustrating the differences between (a) the exponential model representation of the log-linear regression and (b) the full state-space population dynamics model. The shaded (red) solid arrows represent forcing functions and the dashed arrows represent predictions of the observations used in the likelihood functions. (For interpretation of the references to color in this figure legend, the reader is referred to the web version of this article.)

year older than juveniles and the juveniles are measured the year after spawning:

$$J_{t+1} = \frac{\acute{\alpha}_J A_t}{1 + b_J A_t} \exp(\boldsymbol{\beta_J I_t} + \varepsilon_{J,t}) \quad (16)$$

$$A_{t+1} = \frac{\acute{\alpha}_A J_t}{1 + b_A J_t} \exp(\boldsymbol{\beta_A I_t} + \varepsilon_{A,t}) \quad (17)$$

where the process errors $\varepsilon_A \sim N(0, \sigma^2_{\in,A})$ and $\varepsilon_J \sim N(0, \sigma^2_{\in,J})$ are treated as random effects and the observation errors $N(\ln(J), \sigma^2_J)$ and $N(\ln(A), \sigma^2_A)$ are implemented using likelihoods.

The initial condition for the population dynamics model, which are the abundances in the first time period for juveniles, J_1, and adults, A_1, have to be estimated as parameters in addition to the parameters of the two Beverton–Holt models, the covariate coefficients, and the standard deviations of the random effects. Fig. 1 illustrates the difference between the exponential model representation of the log-linear regression and the state-space population dynamics model.

3.2. Hypothesis testing and model selection

Various methods can be used for hypothesis testing and evaluating the data-based evidence of support for alternative hypotheses, or, perhaps more accurately, evaluating the measure of evidence from data about alternative models (Hilborn and Mangel, 1997; Hobbs and Hilborn, 2006). The influence of a covariate can be eliminated from the model by fixing its value at zero. This produces a nested model, and model selection can be conducted using likelihood ratio tests. The likelihood ratio test is not appropriate for non-nested models. For example, when comparing between two models that include different covariates or two different density dependence assumptions. In this case, information theory-based methods such as the Akaike information criterion (AIC; Akaike, 1973) are appropriate. They are also appropriate for nested models. We use the AIC adjusted for small sample size (AIC_c) (Burnham and Anderson, 2002)

$$AIC_c = -2\ln L + 2K + \frac{2K(K+1)}{n-K-1} \quad (18)$$

where L is the likelihood function evaluated at its maximum, K is the number of estimated parameters, and n is the number of observations. The difference between a given model and the model with the lowest AIC_C value, Δ, is used for comparing models. For model comparison, Burnham and Anderson (1998) recommend: "For any model with $\Delta \leq 2$ there is no credible evidence that the model should be ruled out ... For a model with $2 \leq \Delta \leq 4$ there is weak evidence that the model is not the K–L [Kullback–Leibler] best model. If a model has $4 \leq \Delta \leq 7$ there is definite evidence that the model is not the K–L best model, and if $7 \leq \Delta \leq 10$, there is strong evidence that the model is not the K–L best model. Finally, if $\Delta > 10$, there is very strong evidence that the model is not the K–L best model."

3.3. Application

Data from longfin smelt in the San Francisco Bay-Delta from 1980 to 2009 are used to show the development and advantages of using state-space population dynamics models over simple log-linear regressions for modeling survival. We implement a range of models to determine the difference between the modeling approaches (Table 1). A conceptual model of the San Francisco Bay longfin smelt population (e.g., Rosenfield and Baxter, 2007; Baxter et al., 2008) [1] was used as a basis for identifying potential environmental covariates considered in the models. The covariates reflected various geographic regions of the estuary and seasonal periods based on the life history and seasonality of each lifestage of longfin smelt. A total of 36 potential covariates were identified in the initial selection process (Supplemental Table 1). The covariates included various flow variables (e.g., spring X2 location (a measure of the spatial extent of salinity: position of the 2% isohaline), winter-spring Delta outflow, winter-spring Napa River flow, spring outflow thresholds of 34,500 cfs and 44,500 cfs, spring Sacramento River inflow in addition to various variations of Sacramento and San Joaquin River runoff), zooplankton (prey) densities (e.g., mysid, *Eurytemora*, and *Pseudodiaptomus* densities over various seasonal time periods), predators and competitors (e.g., juvenile Chinook salmon densities in the spring, predators in various regions, and the Asian overbite clam *Potamocorbula*), and a variety of abiotic environmental variables (e.g., Secchi depth as an index of turbidity, water temperature, ammonium loading to various regions of the estuary, and the ratio of ammonium loading to Delta inflow). Based on the conceptual model, the expected sign (positive or negative) in the relationship between each covariate and an expected longfin smelt population response was also assigned to each covariate. All of the environmental covariates were then entered into two formulations of the longfin smelt lifecycle model (a model in which spawners are the adult lifestage (November–March) ages 1 and 2 and an alternative model in which pre-adults (October–March) ages 0 and 1 and adults (November–March) ages 1 and 2 were equally weighted in the model as spawners) and a series of statistical analyses were performed to identify the best model. The models were fit to indices of juvenile and adult longfin smelt abundance created using Bay study otter and mid-water trawl surveys[2]. The covariates that explained the most variation from

[1] Rosenfield, J.A. 2010. Life History Conceptual Model and Sub-Models for Longfin Smelt, San Francisco Estuary Population. Unpublished Report. Available at: http://www.dfg.ca.gov/erp/cm_list.asp. Hanson, C. H. 2014. Covariates for Consideration in Developing a Lifecycle Model for the San Francisco Bay-Delta Population of Longfin Smelt. Hanson Environmental, Inc. Unpublished contract report. 93pp. http://new.baydeltalive.com/projects/7012

[2] Maunder, M.N. and Deriso, R.B. 2013. Empirical estimates of abundance indices and standard deviation for longfin smelt from the bay study otter and mid-water trawl surveys. Unpublished QRA contract report. 13pp. http://new.baydeltalive.com/projects/7012

Table 1
Description of modeling scenarios. The symbol under the "Analysis type" column is based on the entries in the other columns with symbols: juvenile = "J", adult = "A", juvenile divided by adult = "J/A", both juvenile and adult = "J+A" None = "-", likelihood = "L", random effects = "re", Beverton–Holt = "BH", Ricker = "R".

Name	Analysis type	Dependent variable	Adult observation error	Juvenile observation error	Process error	Density dependence	Equation
Log-linear	J/A- -L-	Juvenile divided by Adult	None	None	Likelihood	None	7
Exponential	J- -L-	Juvenile	None	None	Likelihood	None	11
Log-linear with observation error	J/ArereL-	Juvenile divided by Adult	Random effect	Random effect	Likelihood	None	7
Exponential with juvenile observation error only	J-L- -	Juvenile	None	Likelihood	None	None	11
Exponential with juvenile observation error and process error	J-Lre-	Juvenile	None	Likelihood	Random effect	None	11
Exponential with observation an process error	JreLre-	Juvenile	Random effect	Likelihood	Random effect	None	11
Ricker	JreLreR	Juvenile	Random effect	Likelihood	Random effect	Ricker	13
Beverton–Holt	JreLreBH	Juvenile	Random effect	Likelihood	Random effect	Beverton–Holt	15
Population dynamics (Life cycle)	J+ALLreBH	Juvenile and Adult	Likelihood	Likelihood	Random effect for both A and J	Beverton–Holt	16 and 17

each category of covariate[3] (e.g. flow, prey, predators, environmental conditions) were then used in the application below that illustrates the benefits of state-space models.

AIC_C was used to conduct forward stepwise covariate selection. The covariates were normalized (mean subtracted and divided by the standard deviation) to improve model performance. Several covariates were chosen as candidates for the model selection procedure (Table 2 and Supplemental 2). These covariates were chosen based on initial analysis of the wider range of factors in supplemental Table 1. Many of the factors in the larger set were highly correlated and so were eliminated. We kept two flow variables that were highly correlated to illustrate some of the difficulties in hypothesis testing. The model is fit to relative abundance indices for each stage (Supplemental Table 3), as appropriate. The models were implemented using AD Model builder and the Laplace approximation was used for random effects. The observation error in Eq. (10) was implemented by treating the true population abundance as a random effect and using the sampling distribution as the likelihood for abundance. The true abundance was then used in the calculation of the regression model and the likelihoods for the observations were combined with the likelihood for the regression equation. The lognormal bias correction is not used since α is not of interest and the temporal variation in the observation error is low.

4. Results

In general, all scenarios support the two flow-related covariates (Sacramento and Napa river runoff) when a single covariate is tested (Fig. 2) followed closely by the prey species *Eurytemora*. However, after including a flow covariate, support for *Eurytemora* is lost and it is not selected in any of the final models. In all models, ammonia is the second covariate selected and temperature is the third covariate selected (Table 3). Adding density dependence (models JreLreR and JreLreBH) results in more support for Sacramento River runoff over Napa River runoff, and over the other covariates in general, when comparing single covariate models. Using observation error only for juveniles and no process error (model J-L- -; Table 1) creates greater differences in the likelihood between covariates and gives increased relative support to temperature and ammonia.

The likelihood values from the log-linear model (model J/A- -L-) and the exponential model (model J- -L-) are identical as expected (Table 3). The results from the log-linear model with observation error (model J/ArereL-), which implies both observation and process error, and the exponential model with both observation and process error (model JreLre-) are identical despite the likelihood and random effects representing different error components.

Adding observation error (e.g. compare model J- -L- with model JreLre-) makes little difference in relative likelihoods (Table 3), but changes the variables selected (Table 3). Sacramento River runoff is selected in the first stage of the stepwise regression in place of Napa River runoff when allowance is made for observation error. This is in part because Napa River runoff and Sacramento River runoff are highly correlated. The stepwise procedure also selects Napa River runoff as a fourth covariate. However, if Sacramento River runoff is dropped from the final model (that is the model chosen by the stepwise procedure that includes both flow variables) the AICc drops by 2.58 units. The AIC_C for the model which only includes Napa River runoff as the flow variable is 5.39 units lower than the model which only includes Sacramento River run off as the flow variable (Fig. 3) providing "definite" evidence of Napa River runoff over Sacramento River runoff in models that do not include density-dependence; evidence favors Napa River runoff over Sacramento River runoff in all the various model configurations, but not as definitive as the ones above (Table 3).

Ignoring process error and including observation error only for the juvenile abundance (model J-L- -) leads to much greater changes in the likelihood causing all covariates to be selected except for those that are rejected because the coefficient has the wrong sign.

The Ricker (model JreLreR) and Beverton–Holt (model JreLreBH) forms of density dependence lead to different results, with the Beverton–Holt model including Napa River runoff as a fourth covariate resulting in a better AIC_C, but it is only 1.65 units lower than the Ricker model providing "no credible" evidence to differentiate between the two forms of density dependence. The AIC_C for the Beverton–Holt model is 4.19 units less than the exponential model with observation error providing "definite" evidence for density dependence. If the Sacramento outflow is discarded from the Beverton–Holt model, the AIC_C is only 0.25 units less than the final model, and is only 1.21 units lower than if Napa River runoff is not included and Sacramento runoff is

[3] Maunder, M.N. and Deriso, R.B. 2013. Evaluation of factors impacting longfin smelt – summary analysis. Unpublished QRA contract report. 9 pp. http://new.baydeltalive.com/projects/7012

Table 2
Covariates used in the longfin smelt application (Hanson, C.H. 2014. Selection of Environmental Covariates for Consideration in Developing a Lifecycle Model for the San Francisco Bay-Delta Population of Longfin Smelt. Hanson Environmental, Inc. Unpublished contract report. 93pp. http://new.baydeltalive.com/projects/7012).

Factor	Time	Stage	Sign of coefficient
Mysid	May–June	Adult to Juveniles	+
Secchi depth	April–June	Adult to Juveniles	–
Eurytemera	April–May	Adult to Juveniles	+
Napa River flow	January–March	Adult to Juveniles	+
Predators central + San Pablo	Annual	Adult to Juveniles	–
Average temperature	April–June	Adult to Juveniles	–
San Pablo ammonium	April–June	Adult to Juveniles	–
Sacramento River runoff	Previous October–July	Adult to Juveniles	+
Overbite clam presence	Year round	Adult to Juveniles	–
Mysid	July–September	Juveniles to pre-adult	+

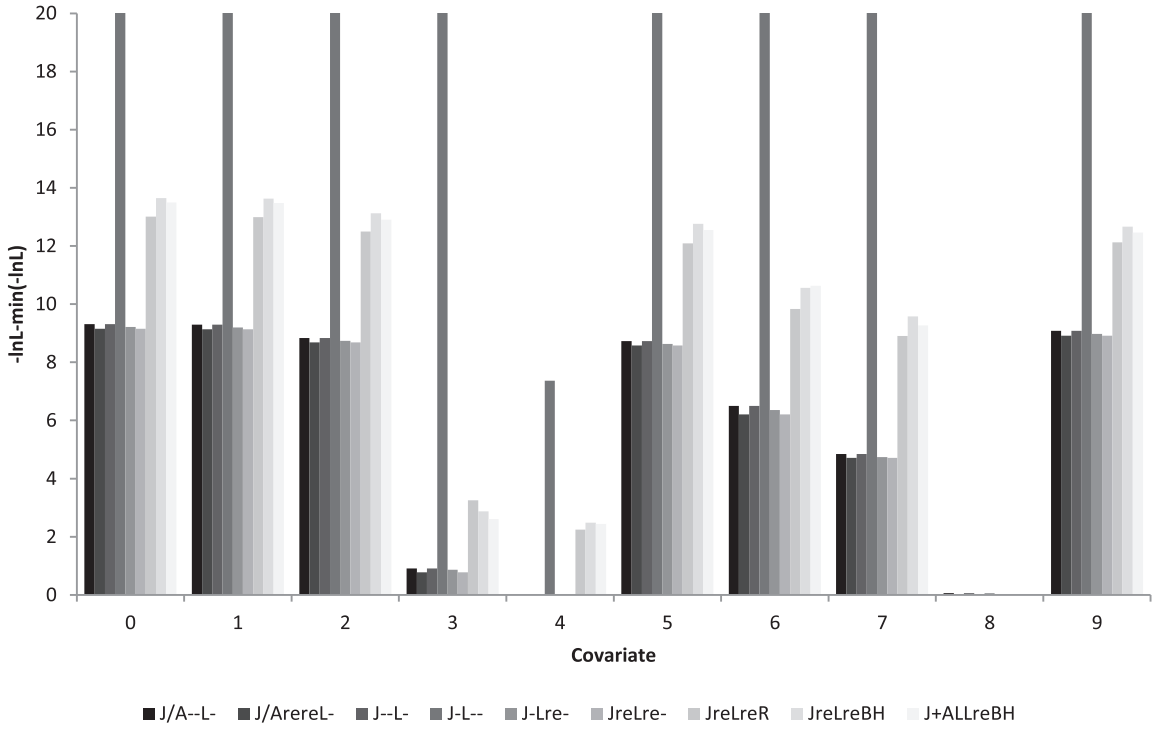

Fig. 2. Difference in negative log-likelihood from the model with the covariate minus the lowest negative log-likelihood for a scenario with any covariate [$-\ln L - \min(-\ln L)$]. A smaller value represents more support for that covariate compared to the other covariates in that scenario. The value for Model J-L- - is truncated. The covariates are presented in the same order as they are defined in Table 2, with the exception that "0" represents no covariates.

Table 3
AIC_C values for the steps (step order given in parenthesis) in the forward stepwise selection procedure and for models with no covariates and with different combinations of flow variables (temperature and ammonia included). AICc scores cannot be compared among some models because the data used to fit the model differs. Models with observation error in both abundance time series fit to both abundance time series are comparable (indicated by "b") but cannot be compared to models that fit to only the juvenile abundance time series (indicated by "a"). The two stage model (J+ALLreBH) includes two random effects and due to the method used to model random effects cannot be compared to the other models. The row labeled "Delta AICc" is the absolute difference in AICc from the selected model compared to the model without covariates for each scenario.

Covariates	Analysis type								
	J/A–L- (a)	J/ArereL- (b)	J–L- (a)	J-L– (a)	J-Lre- (a)	JreLre- (b)	JreLreR (b)	JreLreBH (b)	J+ALLreBH (c)
Mysid May–June									
Secchi depth									
Eurytemera									
Napa River flow	105.14 (1)	−19.46 (4)	105.14 (1)	359.95 (4)	50.32 (1)	−19.46 (4)		−23.64 (4)	41.33 (5)
Predators central +San Pablo				351.12 (5)					
Average temperature	88.53 (3)	−16.65 (3)	88.53 (3)	405.73 (3)	33.44 (3)	−16.65 (3)	−21.99 (3)	−22.68 (3)	44.52 (3)
San Pablo ammonium	95.23 (2)	−13.10 (2)	95.23 (2)	650.94 (2)	40.28 (2)	−13.10 (2)	−17.39 (2)	−18.98 (2)	47.62 (2)
Sacramento River runoff		−4.72 (1)		1006.95 (1)		−4.72 (1)	−10.84 (1)	−12.17 (1)	55.11 (1)
Overbite clam presence									
Mysid July–Sept									42.16 (4)
Delta AICc	32.76	30.57	32.76	1222.22	32.83	27.77	34.48	36.09	38.02
No covariates	121.29	11.11	121.29	1573.34	66.27	11.11	12.49	12.45	79.35
Napa River runoff	88.53	−22.04	88.53	365.05	33.44	−22.04	−23.59	−23.89	43.76
Sacramento River runoff	94.07	−16.65	94.07	405.73	38.89	−16.65	−21.99	−22.68	44.52
Both flow variables	91.23	−19.46	91.23	359.95	36.10	−19.46	−23.01	−23.64	43.55
Best forward stepwise	88.53	−19.46	88.53	351.12	33.44	−19.46	−21.99	−23.64	41.33

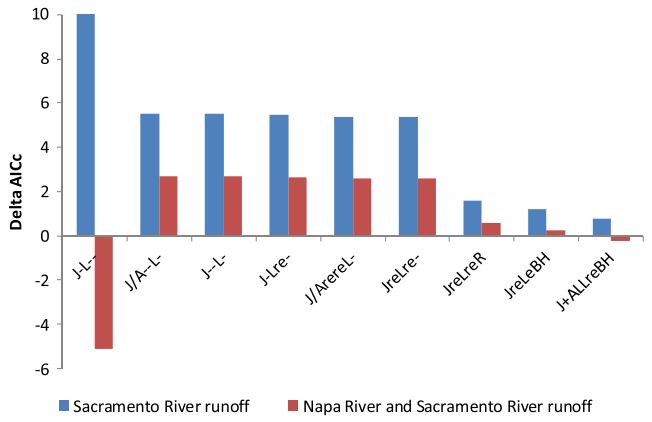

Fig. 3. Difference in AICC between the models with different flow variables. The blue histogram includes only Sacramento River runoff and the red histogram includes both Napa River and Sacramento River runoff. The ΔAICc values are the AICc values for these models minus the AICc values for the model with only Napa River runoff. The Sacramento River runoff value for model J-L-- is truncated. The models are ordered by ΔAIC_C. (For interpretation of the references to color in this figure legend, the reader is referred to the web version of this article.)

included (Fig. 3). Consequently, there is "no credible" evidence supporting one runoff covariate over the other in the presence of density dependence. This differs from the result without density dependence, which shows "definite" evidence of Napa River runoff over Sacramento River runoff.

Using a population dynamics model by linking both stages using a Beverton–Holt relationship (model J+ALLreBH) produces nearly identical support for the covariates compared to the Beverton–Holt model when evaluating single covariate models. The final selected model adds the additional prey covariate for survival from juveniles to adults.

5. Discussion

We have illustrated the progression from traditional log-linear models for estimating the factors influencing survival to state-space population dynamics life-cycle models. State-space models accommodate both observation and process error, which can be vital to avoid bias in parameter estimates, confidence intervals, and hypothesis tests (de Valpine and Hastings, 2002; Maunder and Watters, 2003; Deriso et al., 2007). Our model that ignored process error selected prey as an additional covariate, which was not selected by any other model, and would have selected additional covariates if they had not been discarded because the coefficient was the wrong sign. In our application, ignoring observation error did not have a large impact on the relative support for the various covariates. However, it did change which covariates were selected because the two flow covariates were highly correlated. In other applications, the influence of including observation error is likely to be greater where observation error is larger and particularly if it varies among data points. Explicitly modeling process error and separating it from observation error is also important in estimating the probability of future events such as extinction (Maunder, 2004) and evaluating the uncertainty in the relationships between survival and covariates so this uncertainty can be included in management advice (Maunder and Deriso, 2011).

5.1. Observation error

The observation error standard deviations used in our application, calculated from bootstrap analysis of the survey data, were assumed known and were used to represent the random sampling error. They do not include variation due to other factors such as annual changes in survey catchability. This additional observation error may influence hypothesis testing. The standard deviation representing additional variation in the observation process could be estimated analytically (Maunder and Starr, 2003; Deriso et al., 2007) or covariates could be added to the observation model, perhaps using finer scale data (e.g. Maunder, 2001; Besbeas and Freeman, 2006). Estimating the additional observation error variance adds one more parameter, which will increase the variance of parameter estimates and will probably reduce the statistical significance of covariates.

5.2. Process error

The estimated observation (sampling) error variance often incorporates the process error in models such as the log-linear and simple exponential models. They do not explicitly model the process error, but accommodate it by ignoring the observation error variances in the likelihood and estimating the variance of the likelihood function. However, it is important to understand that the variance estimates from these models represent a combination of process error and observation error. In more complex population dynamics models, such as those used in fisheries stock assessment (Maunder and Punt, 2013; Punt et al., 2013, Methot and Wetzel, 2013), which model many processes, only one type of process error is typically modeled (e.g. annual recruitment variability) and estimation of the observation error variance for a variety of data types or the modeled process error is implicitly assumed to accommodate the unmodeled process error.

Contemporary fisheries stock assessment models are often too complicated to model in a state-space framework, although some success has been achieved (McAllister and Ianelli, 1997; Maunder and Deriso, 2003; Nielsen and Berg, 2014), particularly in a Bayesian context (Punt and Hilborn, 1997). The standard approach is to use penalized likelihood, with the variance of the process error for annual recruitment fixed at a pre-determined value (Maunder and Deriso, 2003). Misspecified process error variance will bias confidence intervals and hypothesis tests. Adding covariates to explain process error will reduce the process error variance, and the variance needs to be adjusted for this. Hopefully, fisheries stock assessment models can be implemented in the state-space framework as computers and estimation algorithms get more efficient, so the process error variance can be estimated. In the meantime, it might be prudent to estimate the parameters and conduct hypothesis tests under different assumptions about the process error variance to ensure that results are consistent.

We found that modeling either process error or observation error as random effects or likelihood functions gave the same results. This was an interesting result and it is not clear if this is a general phenomenon or if it is a consequence of comparing linear Gaussian models. Further research is needed.

5.3. Model selection

Our results corroborate other studies that have found that evaluating factors in isolation can lead to different results than evaluating them in combination (e.g. Deriso et al., 2008; Maunder and Deriso, 2011). Similarly, our results parallel those of Maunder and Deriso (2011) who found that some final models had a coefficient with confidence intervals that cover zero, and removing that covariate improved the AIC_c. As with Maunder and Deriso's (2011) study, the covariate in question (Sacramento River flow) was highly correlated with another covariate (Napa River flow) included in the model.

Maunder and Deriso (2011) recommend that all possible combinations of covariates and density dependent factors should be evaluated because some factors may only be detected in

combination with other factors or in the presence of density dependence. However, conducting analyses of all possible combinations can be computationally demanding. To reduce the computational time, Maunder and Deriso (2011) applied a strategy that evaluates two covariates at a time and uses AIC_c summed over all possible one and two covariate combinations to select a covariate that has general support. In contrast, Anderson et al. (2000) warn against testing all possible combinations unless model averaging is used. Practical advice is to ensure that covariates included in the model have *a priori* support and that the framework of Maunder and Deriso (2011) is followed to identify the life stage and the relationship to density dependence before conducting an all combinations analysis. Results should be used to rank models and provide an idea of the data based evidence for alternative hypotheses rather than strict acceptance–rejection hypothesis testing (Maunder and Deriso, 2011).

5.4. Integrated analysis

We illustrated how multiple life stages of a species, each with their own data sets, can be integrated into a population dynamics model. This is an elementary form of the contemporary integrated analysis (also known as data assimilation), which attempts to include all relevant data into a single analysis (e.g. Maunder, 2003; Buckland et al., 2007; Schaub and Abadi, 2010; Maunder and Punt, 2013). Integrated analysis facilitates the propagation of information and uncertainty, particularly when states are linked from one time period to the next in a population dynamics model. For example, one life stage in the analysis of Maunder and Deriso (2011) did not have an abundance index until partway through the modeling time frame and the processes related to this stage were informed by the indices of abundance for other stages. However, the years that the index was available for were enough to help determine which stages the covariates influenced. Similarly, Tenan et al. (2012) showed how integrating different types of data allowed for the estimation of population processes not directly measured in the field. We found that adding data and a covariate for survival from juveniles to adults did not influence the support for the covariates of survival from adults to juveniles. This is somewhat reassuring since the application had good data for all time periods and therefore it would not be desirable for the results of one stage to influence those of another. If process error was not modeled, the added data may have inadvertently influenced the covariate selection. If the data were poor or missing for some time periods, then it would be reasonable and desirable for data for one stage to influence the other stages.

5.5. Model structure

The models we used to illustrate state-space models were simple compared to those used in many real applications. Alternative functions could be used to model the transition among stages. For example, Maunder and Deriso (2011) used the three-parameter Deriso–Schnute stock-recruitment model (Deriso, 1980; Schnute, 1985) and also allowed the flexibility to implement covariates before or after density dependence. The covariates were included as simple log linear terms and there may be more appropriate relationships between survival and covariates. For example there may be a dome shaped relationship between survival and temperature, with lower survival at lower and higher temperature or temperature may interact with prey availability.

5.6. Longfin smelt application

We found that multiple factors and density dependence influenced the survival of longfin smelt. The AIC_c was over four units higher for the Beverton–Holt model compared to the exponential model suggesting there is "definite" evidence for density dependence. The level of evidence is less if the models with Napa River flow are used. We also found that flow, ammonia, and temperature were consistently supported by the data for longfin smelt. Thomson et al. (2010) found that X2, which is related to flow, and water clarity explained longfin abundance. Mac Nally et al. (2010) also found that X2 explained longfin abundance, but in addition found a correlation with prey species. Among candidate flow variables, we did not find X2, OMR flow, or the two outflow threshold variables in supplemental Table 1 to be important covariates in our initial screening after the inclusion of flow variables that had higher support in the data.

Acknowledgements

Richard Deriso and Charles Hanson were funded by the State Water Contractors. Mark Maunder was funded by San Luis & Delta-Mendota Water Authority. Ken Burnham provided useful comments on the manuscript. Comments from André Punt and two anonymous reviewers improved the manuscript. Survey data was from California Department of Fish and Wildlife's San Francisco Bay Study and the Interagency Ecological Program for the San Francisco Estuary.

Appendix A. Supplementary data

Supplementary data associated with this article can be found, in the online version, at http://dx.doi.org/10.1016/j.fishres.2014.10.017.

References

Akaike, H., 1973. Information theory and an extension of the maximum likelihood principle. In: Petrov, B.N., Csaki, F. (Eds.), Proceedings of the 2nd International Symposium on Information Theory. Publishing house of the Hungarian Academy of Sciences, Budapest, pp. 268–281.

Anderson, D.R., Burnham, K.P., Thompson, W.L., 2000. Null hypothesis testing: problems, prevalence, and an alternative. J. Wildl. Manag. 64 (4), 912–923, http://dx.doi.org/10.2307/3803199.

Baxter, R., Breuer, R., Brown, L., Chotkowski, M., Feyrer, F., Gingras, M., Herbold, B., Mueller-Solger, A., Nobriga, M., Sommer, T., Souza, K., 2008. Pelagic Organism Decline Progress Report: 2007 Synthesis of Results. California Department of Water Resources, Sacramento, USA (Interagency Ecological Program Technical Report 227).

Bennett, W.A., 2005. Critical assessment of the delta smelt population in the San Francisco estuary, California. San Franc. Estuary Watershed Sci. 3 (2), 1–71.

Besbeas, P., Freeman, S.N., Morgan, B.J.T., Catchpole, E.A., 2002. Integrating mark—recapture—recovery and census data to estimate animal abundance and demographic parameters. Biometrics 58 (3), 540–547.

Besbeas, P., Lebreton, J.D., Morgan, B.J.T., 2003. The efficient integration of abundance and demographic data. Appl. Stat. 52, 95–102.

Besbeas, P., Freeman, S.N., 2006. Methods for joint inference from panel survey and demographic data. Ecology 87, 1138–1145.

Beverton, R.J.H., Holt, S.J., 1957. On the Dynamics of Exploited Fish Populations, Fisheries Investigations Series 2, 19. Ministry of Agriculture, London, U.K.

Bolker, B.M., Gardner, B., Maunder, M., Berg, C.W., Brooks, M., Comita, L., Crone, E., Cubaynes, S., Davies, T., deValpine, P., Ford, J., Gimenez, O., Kery, M., Kim, E.J., Lennert-Cody, C., Magnusson, A., Martell, S., Nash, J., Nielsen, A., Regetz, J., Skaug, H., Zipkin, E., 2013. Strategies for fitting nonlinear ecological models in R, AD Model Builder, and BUGS. Methods Ecol. Evol. 4, 501–512.

Brook, B.W., Bradshaw, C.J.A., 2006. Strength of evidence for density dependence in abundance time series of 1198 species. Ecology 87 (6), 1445–1451.

Buckland, S.T., Newman, K.B., Thomas, L., Koesters, N.B., 2004. State-space models for the dynamics of wild animal populations. Ecol. Model. 171 (1–2), 157–175.

Buckland, S.T., Newman, K.B., Fernandez, C., Thomas, L., Harwood, J., 2007. Embedding population dynamics models in inference. Stat. Sci. 22 (1), 44–58.

Burnham, K.P., Anderson, D.R., 1998. Model Selection and Inference: A Practical Information-theoretical Approach. Springer Verlag, New York.

Burnham, K.P., Anderson, D.R., 2002. Model selection and multimodel inference: a practical information-theoretic approach, 2nd ed. Springer, New York.

Christensen, R., 1997. Log-Linear Models and Logistic Regression, 2nd ed. Springer.

Ciannelli, L., Chan, K.-S., Bailey, K.M., Stenseth, N.C., 2004. Nonadditive effects of the environment on the survival of a large marine fish population. Ecology 85 (12), 3418–3427.

Deriso, R.B., 1980. Harvesting strategies and parameter estimation for an age-structured model. Can. J. Fish. Aquat. Sci. 37 (2), 268–282.
Deriso, R.B., Maunder, M.N., Skalski, J.R., 2007. Variance estimation in integrated assessment models and its importance for hypothesis testing. Can. J. Fish. Aquat. Sci. 64, 187–197.
Deriso, R.B., Maunder, M.N., Pearson, W.H., 2008. Incorporating covariates into fisheries stock assessment models with application to Pacific herring. Ecol. Appl. 18 (5), 1270–1286.
de Valpine, P., 2002. Review of methods for fitting time-series models with process and observation error and likelihood calculations for nonlinear, non-Gaussian state-space models. Bull. Mar. Sci. 70, 455–471.
de Valpine, P., 2003. Better inferences from population dynamics experiments using Monte Carlo state-space likelihood methods. Ecology 84, 3064–3077.
de Valpine, P., Hastings, A., 2002. Fitting population models with process noise and observation error. Ecol. Monogr. 72, 57–76.
Dupont, W.D., 1983. A stochastic catch-effort method for estimating animal abundance. Biometrics 39 (4), 1021–1033.
Edgington, E.S., 1987. Randomization Tests. Marcel Dekker, New York, New York, USA.
Fournier, D.A., Skaug, H.J., Ancheta, J., Ianelli, J., Magnusson, A., Maunder, M.N., Nielsen, A., Sibert, J., 2012. AD Model Builder: using automatic differentiation for statistical inference of highly parameterized complex nonlinear models. Opt. Met. SOFT 27, 233–249.
Hilborn, R., Mangel, M., 1997. The Ecological Detective: Confronting Models with Data. Princeton University Press, Princeton, N.J.
Hobbs, N.T., Hilborn, R., 2006. Alternatives to statistical hypothesis testing in ecology: a guide to self teaching. Ecol. Appl. 16 (1), 5–19.
Johnson, J.B., Omland, K.S., 2004. Model selection in ecology and evolution. Trends Ecol. Evolut. 19 (2), 101–108.
Lele, S.R., Dennis, B., Lutscher, F., 2007. Data cloning: easy maximum likelihood estimation for complex ecological models using Bayesian Markov chain Monte Carlo methods. Ecol. Lett. 10, 551–563.
Lunn, D., Spiegelhalter, D., Thomas, A., Best, N., 2009. The BUGS project: evolution, critique and future directions. Stat. Med. 28 (25), 3049–3067.
Mac Nally, R., Thomson, J.R., Kimmerer, W., Feyrer, F., Newman, K.B., Sih, A., Bennett, W., Brown, L., Fleishman, E., Culberson, S.D., Castillo, G., 2010. Analysis of pelagic species decline in the upper San Francisco Estuary using multivariate autoregressive modeling (MAR). Ecol. Appl. 20 (5), 1417–1430.
Maunder, M.N., 2001. A general framework for integrating the standardization of catch-per-unit-of-effort into stock assessment models. Can. J. Fish. Aquat. Sci. 58, 795–803.
Maunder, M.N., 2003. Paradigm shifts in fisheries stock assessment: from integrated analysis to Bayesian analysis and back again. Nat. Resour. Model. 16 (4), 465–475.
Maunder, M.N., 2004. Population viability analysis, based on combining integrated, Bayesian, and hierarchical analyses. Acta Oecol. 26, 85–94.
Maunder, M.N., Deriso, R.B., 2003. Estimation of recruitment in catch-at-age models. Can. J. Fish. Aquat. Sci. 60, 1204–1216.
Maunder, M.N., Deriso, R.B., 2011. A state-space multistage life cycle model to evaluate population impacts in the presence of density dependence: illustrated with application to delta smelt (*Hyposmesus transpacificus*). Can. J. Fish. Aquat. Sci. 68, 1285–1306.
Maunder, M.N., Punt, A.E., 2013. A review of integrated analysis in fisheries stock assessment. Fish. Res. 142, 61–74.
Maunder, M.N., Starr, P.J., 2003. Fitting fisheries models to standardised CPUE abundance indices. Fish. Res. 63, 43–50.
Maunder, M.N., Watters, G.M., 2003. A general framework for integrating environmental time series into stock assessment models: model description, simulation testing, and examples. Fish. Bull. 101, 89–99.
McAllister, M.K., Ianelli, J.N., 1997. Bayesian stock assessment using catch-age data and the sampling/importance resampling algorithm. Can. J. Fish. Aquat. Sci. 54, 284–300.
Methot, R.D., Wetzel, C.R., 2013. Stock synthesis: a biological and statistical framework for fish stock assessment and fishery management. Fish. Res. 142, 86–99.
Miller, W.J., Manly, B.F.J., Murphy, D.D., Fullerton, D., Ramey, R.R., 2012. An investigation of factors affecting the decline of delta smelt (*Hypomesus transpacificus*) in the Sacraento-San Joaquin Estuary. Rev. Fish. Sci. 20, 1–19.
Nielsen, A., Berg, C.W., 2014. Estimation of time-varying selectivity in stock assessments using state-space models. Fish. Res. 158, 96–101.
Newman, K.B., 1998. State-space modeling of animal movement and mortality with application to salmon. Biometrics 54 (4), 1290–1314.
Newman, K.B., Lindley, S.T., 2006. Accounting for demographic and environmental stochasticity, observation error and parameter uncertainty in fish population dynamics models. N. Am. J. Fish. Manag. 26 (3), 685–701.
Newman, K.B., Fernandez, C., Thomas, L., Buckland, S.T., 2009. Monte Carlo inference for state-space models of wild animal populations. Biometrics 65 (2), 572–583.
Pawitan, Y., 2003. In All Likelihood: Statistical Modeling and Inference using Likelihood. Oxford University Press, Oxford, UK.
Polacheck, T., Hilborn, R., Punt, A.E., 1993. Fitting surplus production models: comparing methods and measuring uncertainty. Can. J. Fish. Aquat. Sci. 50, 2597–2607.
Punt, A.E., Hilborn, R., 1997. Fisheries stock assessment and decision analysis: the Bayesian approach. Rev. Fish. Biol. Fish. 7, 35–63.
Punt, A.E., Huang, T.-C., Maunder, M.N., 2013. Review of integrated size-structured models for stock assessment of hard-to-age crustacean and mollusc species. ICES J. Mar. Sci. 70 (1), 16–33.
Quinn II, T.J., Deriso, R.B., 1999. Quantitative Fish Dynamics. Oxford University Press, New York.
Ricker, W.E., 1954. Stock and recuitment. J. Fish. Res. Board Can. 11, 559–623.
Rivot, E., Prevost, E., Parent, E., Bagliniere, J.L., 2004. A Bayesian state-space modelling framework for fitting a salmon stage-structured population dynamic model to multiple time series of field data. Ecol. Model. 179 (4), 463–485.
Rose, K.A., Cowan Jr., J.H., Winemiller, K.O., Myers, R.A., Hilborn, R., 2001. Compensatory density dependence in fish populations: importance, controversy, understanding and prognosis. Fish Fish. 2, 293–327.
Rosenfield, J.A., Baxter, R.D., 2007. Population dynamics and distribution patterns of longfin smelt in the San Francisco Estuary. Trans Am. Fish. Soc. 136, 1577–1592.
Sæther, B.E., 1997. Environmental stochasticity and population dynamics of large herbivores: a search for mechanisms. Trends Ecol. Evol. 12 (4), 143–149.
Schaub, M., Abadi, F., 2010. Integrated population models: a novel analysis framework for deeper insights into population dynamics. J. Ornithol. 152, 227–237.
Schnute, J., 1985. A general theory for the analysis of catch and effort data. Can. J. Fish. Aquat. Sci. 42 (3), 414–429.
Schnute, J.T., 1994. A general framework for developing sequential fisheries models. Can. J. Fish. Aquat. Sci. 51, 1676–1688.
Seber, G.A., Wild, C.J., 1989. Nonlinear Regression. John Wiley and Sons, New York.
Skalski, J.R., 1996. Regression of abundance estimates from mark—recapture surveys against environmental covariates. Can. J. Fish. Aquat. Sci. 53, 196–204.
Skalski, J.R., Townsend, R.L., Steig, T.W., Hemstrom, S., 2010. Comparison of two alternative approaches for estimating dam passage survival using acoustic-tagged sockeye salmon smolts. N. Am. J. Fish. Manag. 30, 831–839.
Skaug, H.J., 2002. Automatic differentiation to facilitate maximum likelihood estimation in nonlinear random effects models. J. Comput. Graph. Stat. 11 (2), 458–470.
Skaug, H., Fournier, D., 2006. Automatic approximation of the marginal likelihood in non-Gaussian hierarchical models. Comput. Stat. Data Anal. 51 (2), 699–709.
Sommer, T., Armor, C., Baxter, R., Breuer, R., Brown, L., Chotkowski, M., Culberson, S., Feyrer, F., Gingras, M., Herbold, B., Kimmerer, W., Mueller-Solger, A., Nobriga, M., Souz, K., 2007. The collapse of pelagic fishes in the upper San Francisco Estuary: El colapso de los peces pelagicos en la cabecera del Estuario San Francisco. Fisheries 32, 270–277.
Tenan, S., Adrover, J., Navarro, A.M., Sergio, F., Tavecchia, G., 2012. Demographic consequences of poison-related mortality in a threatened bird of prey. PLOS One 7 (11), 1–11.
Thomson, J.R., Kimmerer, W.J., Brown, L.R., Newman, K.B., Mac Nally, R., Bennett, W.A., Feyrer, F., Fleishman, E., 2010. Bayesian change point analysis of abundance trends for pelagic fishes in the upper San Francisco Estuary. Ecol. Appl. 20 (5), 1431–1448.
Walters, C.J., Ludwig, D., 1981. Effect of measurement errors on the assessment of stock-recruitment relationships. Can. J. Fish. Aquat. Sci. 38, 704–710.
Wang, S.-P., Maunder, M.N., Aires-da-Silva, A., Bayliff, W.H., 2009. Evaluating fishery impacts: application to bigeye tuna (*Thunnus obesus*) in the eastern Pacific Ocean. Fish. Res. 99 (2), 106–111.
White, G.C., Garrott, R.A., 1990. Analysis of Wildlife Radio-Tracking Data. Academic Press, San Diego.

RECIRC2566.

Longfin Smelt Distribution, Abundance and Evidence of Spawning in San Francisco Bay Tributaries

Christina Parker[1], James Hobbs[1], Jon Cook[1], Patrick Crain[1,2], Emily Trites[1], and Micah Bisson[1]
[1]Wildlife, Fish and Conservation Biology, University of California, Davis
[2]ICF-International

Which additional areas are adult Longfin Smelt spawning?

- Sampled in Napa River, Sonoma Creek, Petaluma River, & Coyote Creek tributaries every other week starting in January 2015.
- Adults sampled with otter trawl, larvae sampled with CDFW's smelt larval sled.

North bay tributaries, larval catch per 1,000 Cubic Meters

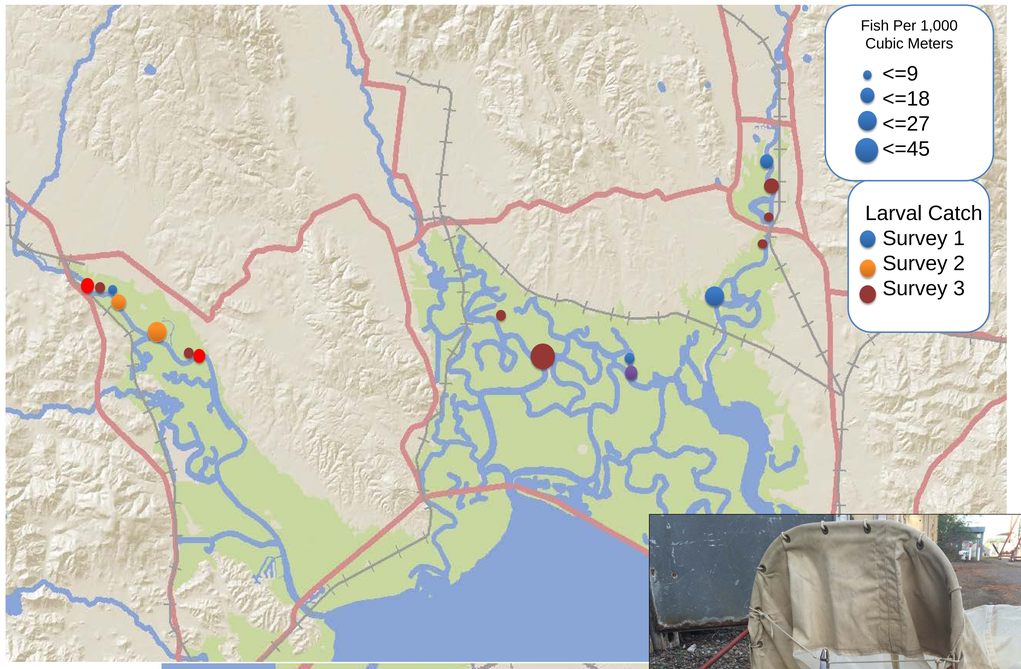

Adult Longfin catch per minute of tow time

Adult CPUE:

North Bay	South Bay
0.4	5.6

Adult Longfin Length-Frequency

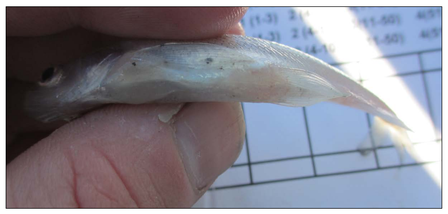

Larval Species from SLS Net

Common Name	Number Caught	% of Catch
Yellowfin Goby	89489	72%
Pacific Herring	18930	15%
Prickly Sculpin	11945	10%
Longjaw Mudsucker	2305	2%
Arrow Goby	916	1%
Pacific Staghorn Sculpin	274	0%
Longfin Smelt	34	0%
Northern Anchovy	3	0%
Shokihaze Goby	1	0%
White Croaker	1	0%
Total:	123898	

Future Studies

- Future studies will include developing otolith chemical fingerprints of SF Bay tributaries to determine proportions of the adult population originating from different natal areas of the estuary.

Acknowledgements:

- CA Dept of Water Resources
  Louise Conrad and Karen Gehrts
- Tenera Environmental
  Carol Raifsnider, Colin Brennan, Eric Sommerauer
- California Department of Fish and Wildlife
  Randy Baxter and Kathy Hieb

RECIRC2566.

USGS
science for a changing world

Effect of a Floating Fish Guidance Structure on Entrainment of Juvenile Salmon into Georgiana Slough

Russell W. Perry

Western Fisheries Research Center

and

J.G. Romine, A.C. Pope, N.S. Adams, A. Blake, J.R. Burau, S. Johnston, and T. Liedtke

Bay-Delta Science Conference
29 October 2104

U. S. Department of the Interior
U. S. Geological Survey

Overview

- Background on guidance structures
- Rationale for floating fish guidance structure
- 2014 Study using Acoustic Telemetry
- ***Preliminary*** results

USGS

Background

- Low survival in interior Delta

- Salmon entrained in interior Delta via
  - Delta Cross Channel
  - Georgiana Slough

- Increase survival by:
  1) Closing Delta Cross Channel
  2) Guiding fish away from Georgiana Slough

USGS

Background

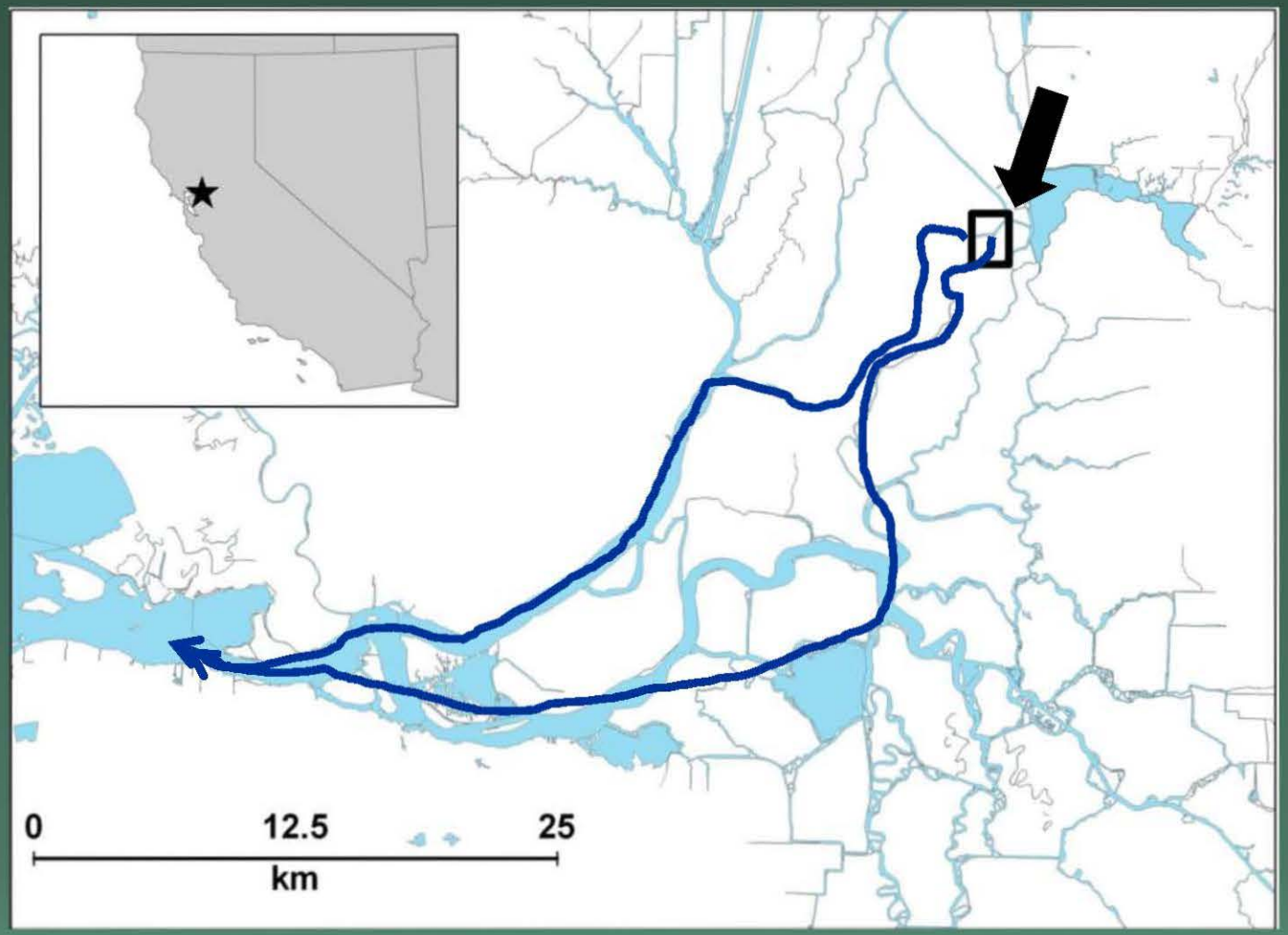

USGS

Bioacoustic Fish Fence (BAFF)

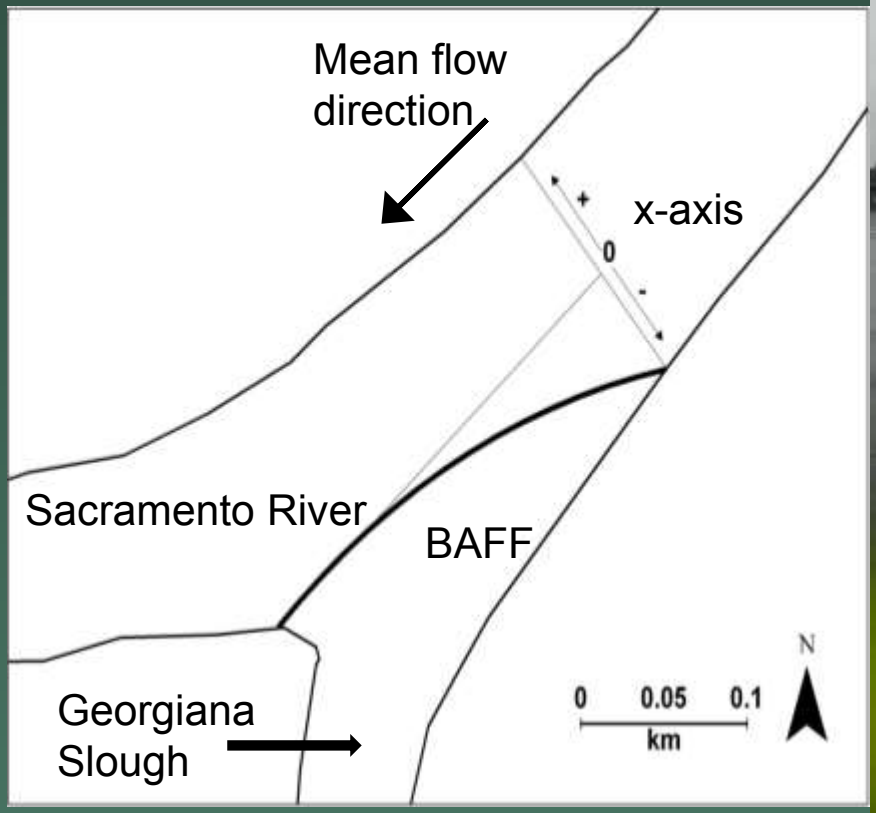

Entraintment into Georgiana Slough:
from 22.3% to 7.7% in 2011
from 24.1% to 11.4% in 2012

USGS

Bio-acoustic Fish Fence

- Drawbacks:
  - Expensive
  - Complex – many moving parts
  - Lots of maintenance
- Alternative guidance structures?
- Examine findings from BAFF study

Location, location, location

Georgiana Slough → Sacramento River

Georgiana Slough entrainment probability

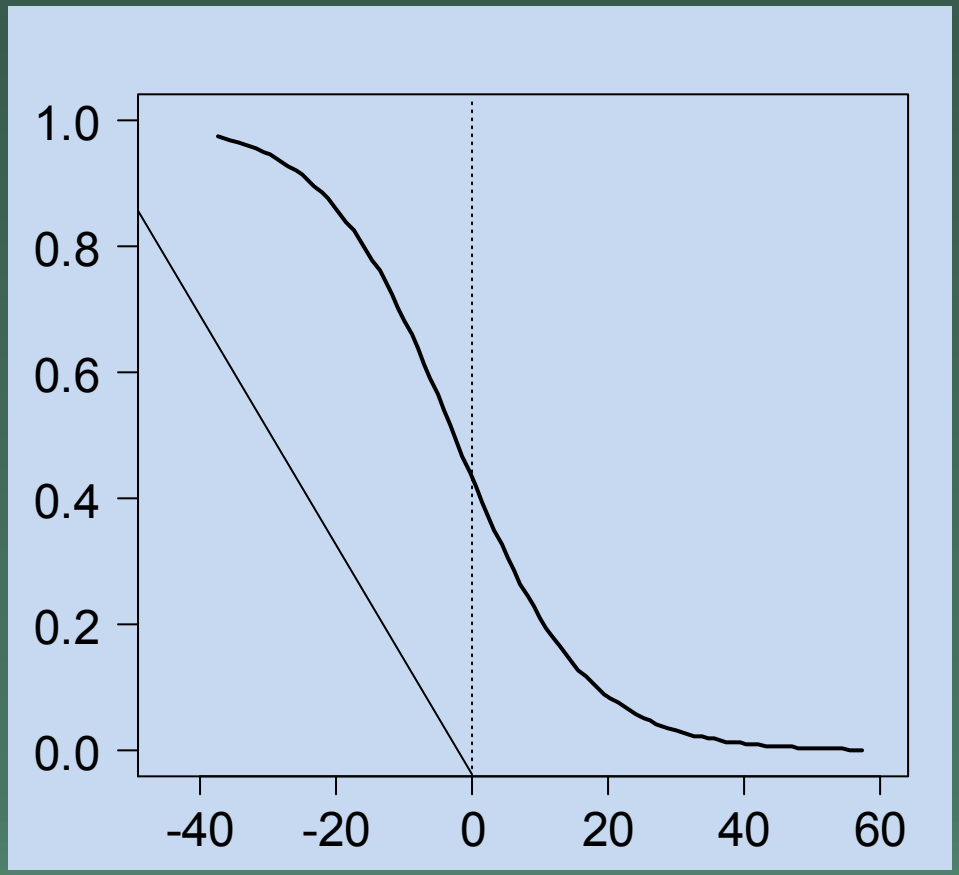

USGS

Location, location, location

Georgiana Slough → Sacramento River

Georgiana Slough entrainment probability

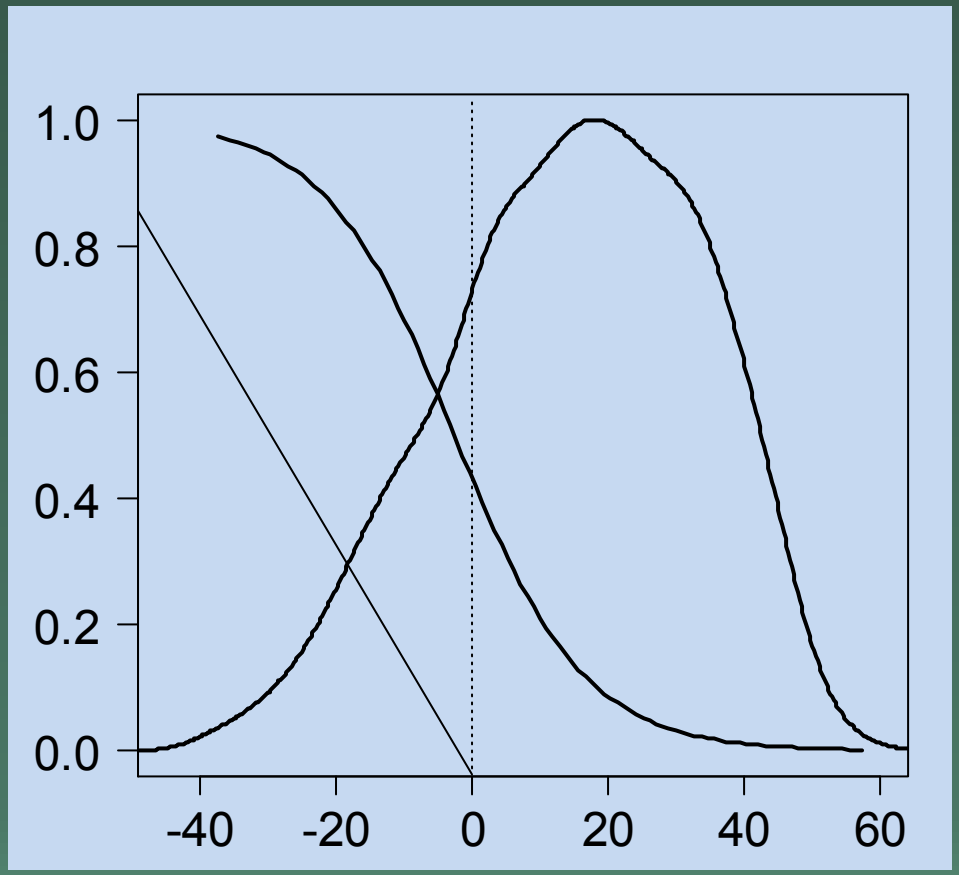

USGS

Shifting the spatial distribution

Georgiana Slough → Sacramento River

Georgiana Slough entrainment probability

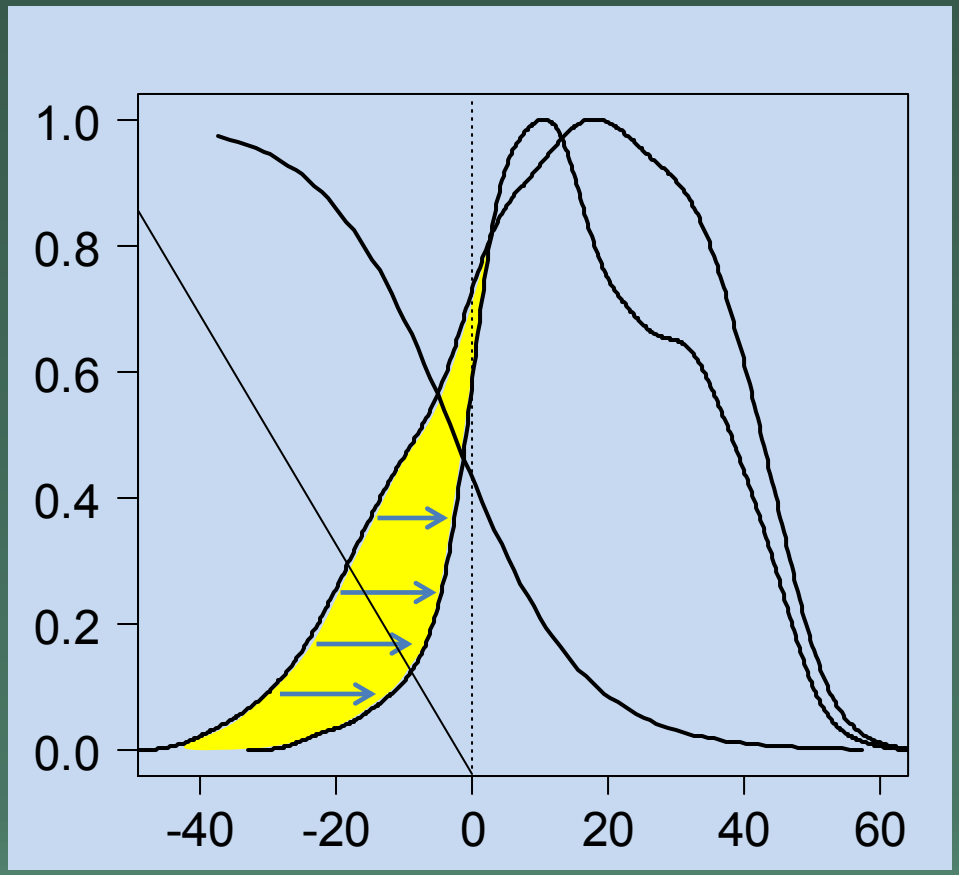

USGS

Floating Fish Guidance Structure (FFGS)

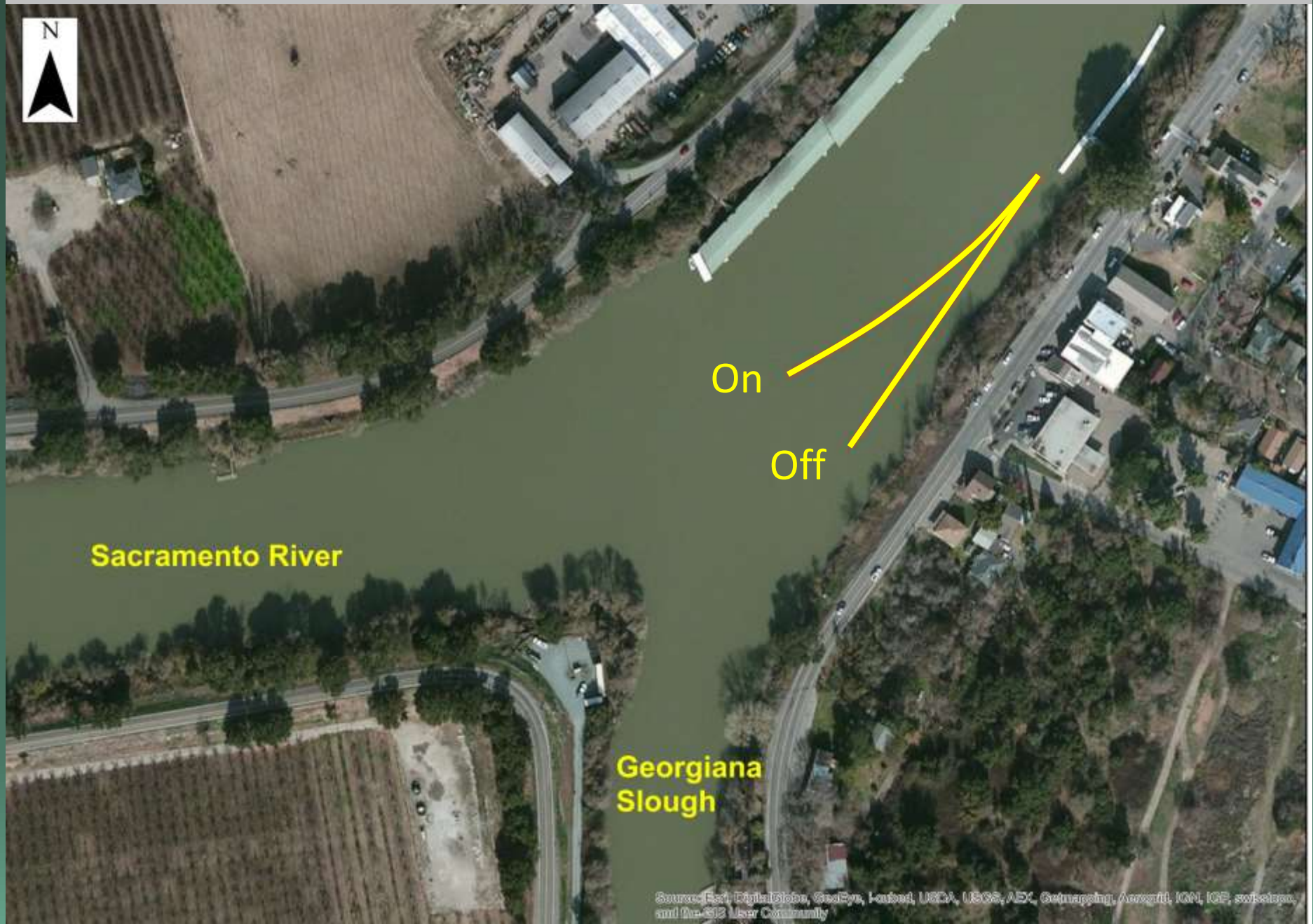

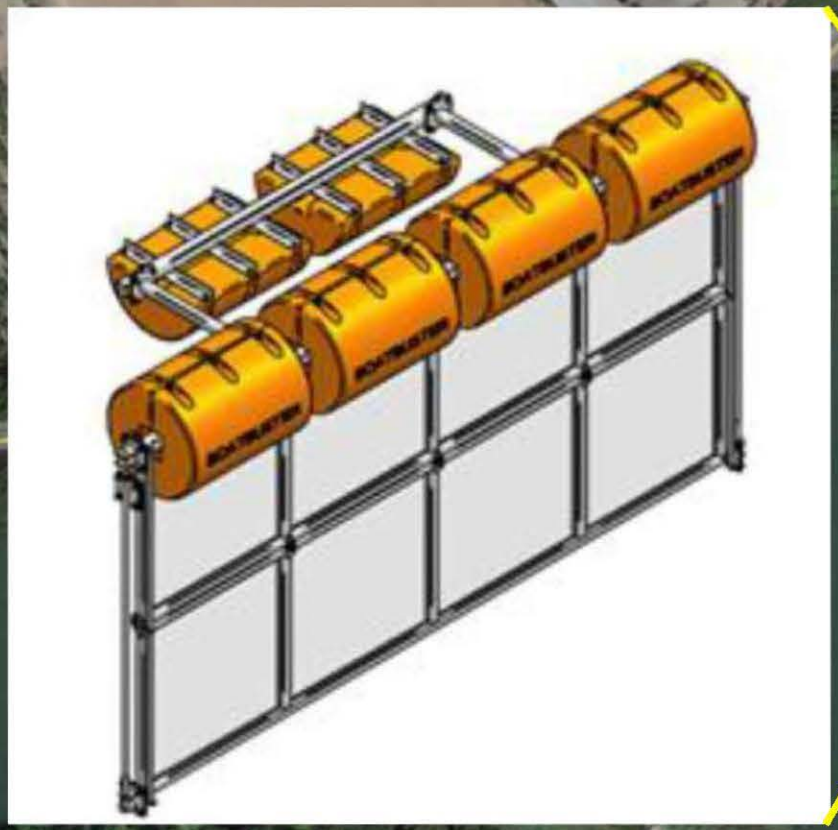

Methods

- 3,303 Late-Fall Chinook Salmon smolts
  - Acoustic tags
  - Released at Sacramento
  - Released March 1 – April 15 2014
- 1,684 arrived at FFGS
- Barrier operated
  - ~25 hours on, ~25 hrs off
  - based on tide cycle
- Discharge above Walnut Grove
  - 4,350 to 21,090 cfs

USGS

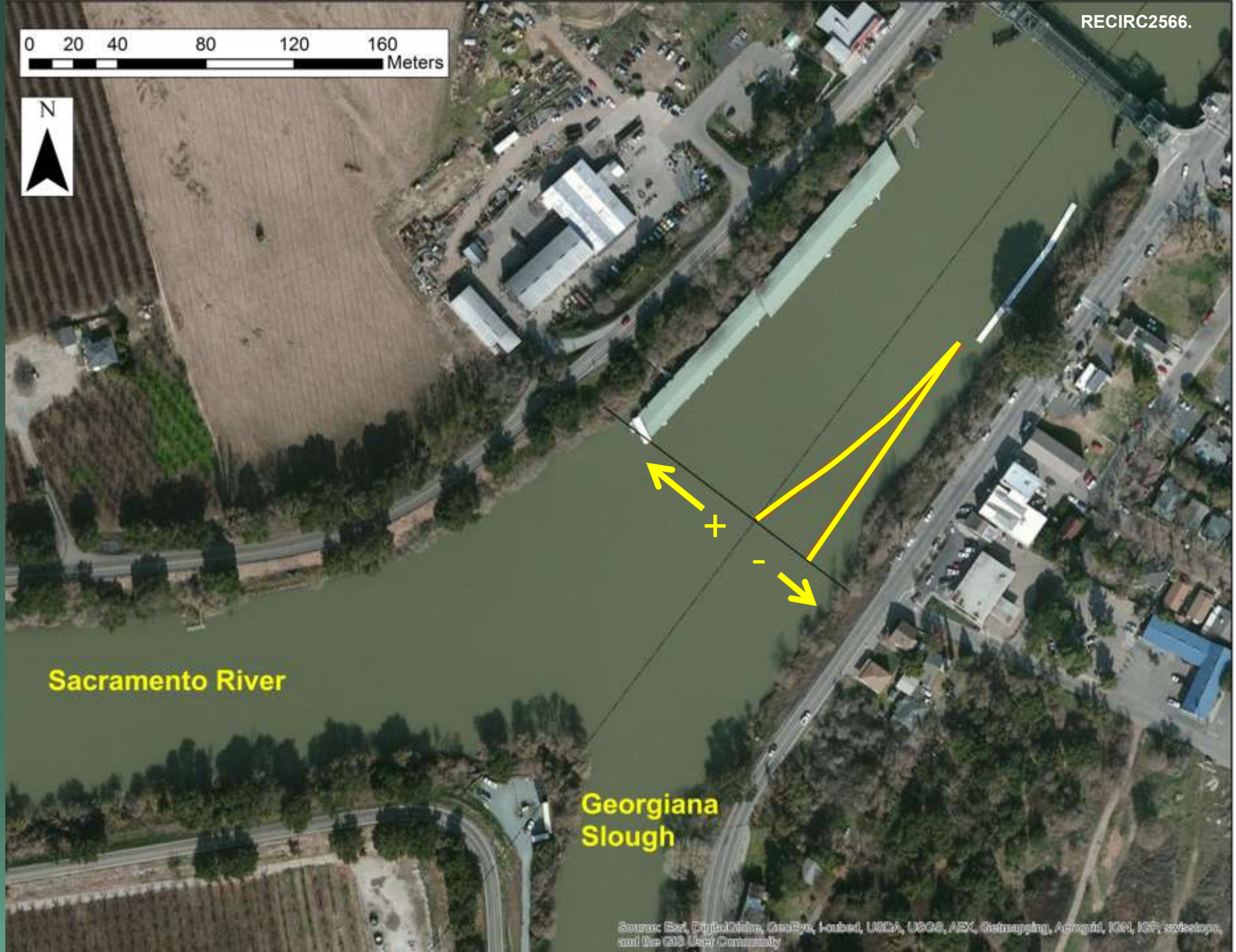
RECIRC2566.
0 20 40 80 120 160
Meters
N
+
-
Sacramento River
Georgiana
Slough

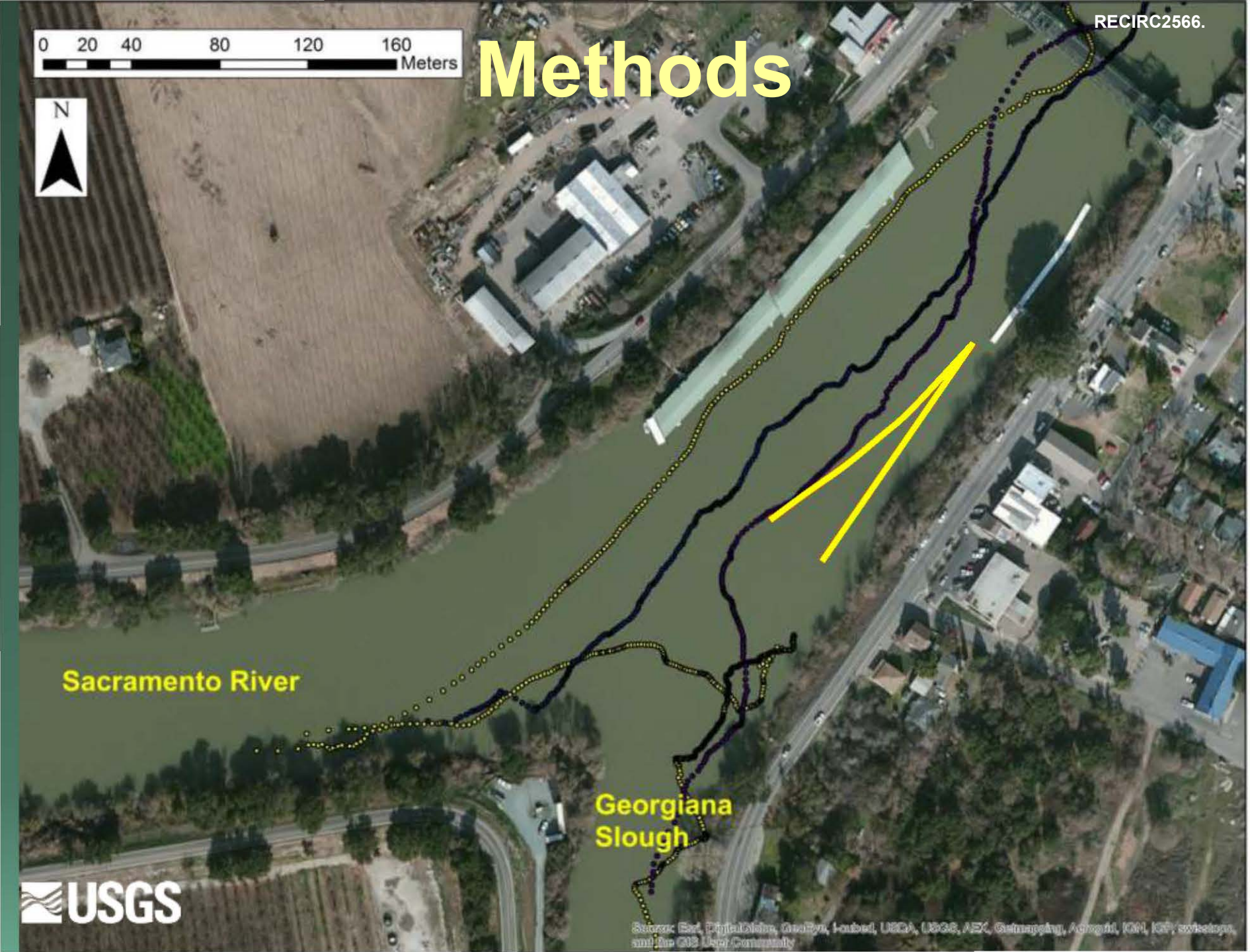
RECIRC2566.
0 20 40 80 120 160
Meters
N
Methods
Sacramento River
Georgiana Slough
USGS

Statistical Analysis

- Logistic regression
- Probability of entering Georgiana Slough
  - Georgiana Slough = 1
  - Sacramento River = 0
- Covariates
  - Cross-stream position of fish
  - Streak line location
  - Discharge
  - FFGS position, On or Off

USGS

FFGS effect on spatial distribution

Probability density

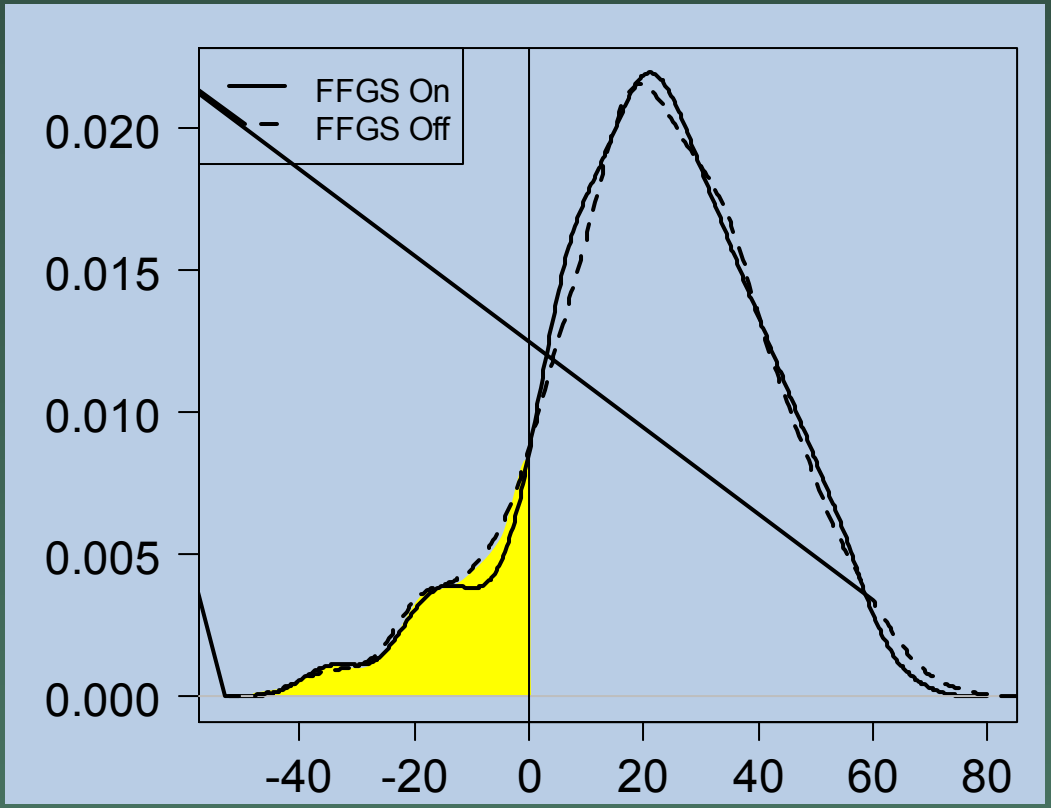

Percentage < 0:
Off = 12.4%
On = 10.6%

USGS

Compared to BAFF 2011

Probability density

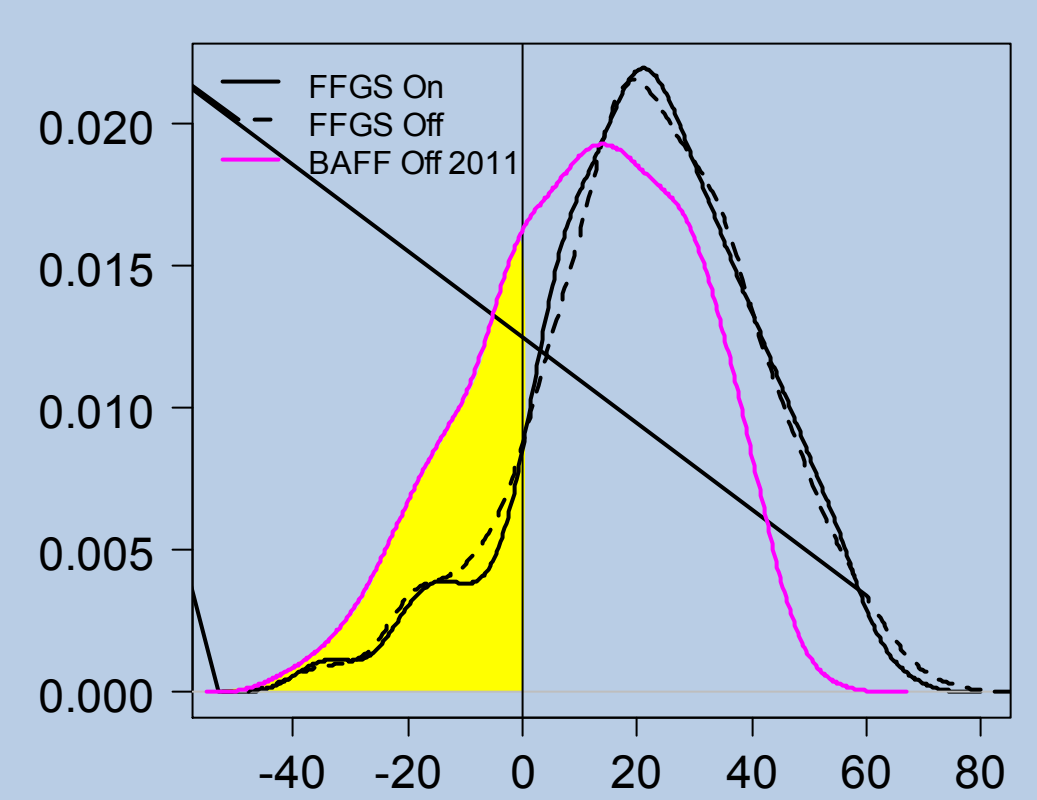

Percentage < 0:
BAFF Off 2011 = 29.1%

Mean flow:
2011: ~29,000 cfs
2014: ~11,000 cfs

USGS

Model selection

Single parameter models

Variable	Number of parameters	AIC	ΔAIC	Significant?
Cross-stream location	2	1638.7	-186.0	Yes
Streak line	2	1671.3	-153.4	Yes
Discharge	2	1743.9	-80.8	Yes
Null	1	1824.7	0	--
FFGS	2	1826.7	2.0	No

USGS

Model selection

Single parameter models

Variable	Number of parameters	AIC	ΔAIC	Significant?
Cross-stream location	2	1638.7	-186.0	Yes
Streak line	2	1671.3	-153.4	Yes
Discharge	2	1743.9	-80.8	Yes
Null	1	1824.7	0	--
FFGS	2	1826.7	2.0	No

Model selection

Single parameter models

Variable	Number of parameters	AIC	ΔAIC	Significant?
Cross-stream location	2	1638.7	-186.0	Yes
Streak line	2	1671.3	-153.4	Yes
Discharge	2	1743.9	-80.8	Yes
Null	1	1824.7	0	--
FFGS	2	1826.7	2.0	No

USGS

Percentage entering Georgiana Slough

FFGS Off: 23.3%
FFGS On: 23.0%

BAFF Off 2011: 22.3%
BAFF Off 2012: 24.1%

USGS

Summary of Preliminary Results

- No change in spatial distribution
- Low percentage interacted with FFGS
- No effect on routing

Many Questions to Be Answered

- Behavioral response?
  - Detailed analysis of 2D data awaits
- Implementation problem?
  - Location, length, angle, depth
- Confounded by support structures?
  - fixed pilings and buoys may have guided fish
- Jury is still out…

Acknowledgements

DEPARTMENT OF WATER RESOURCES
STATE OF CALIFORNIA

HTI

AECOM

USGS

Thank you
Questions?

USGS

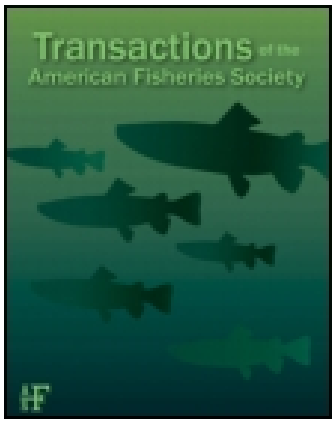

Transactions of the American Fisheries Society
Publication details, including instructions for authors and subscription information:
http://www.tandfonline.com/loi/utaf20

Effect of Tides, River Flow, and Gate Operations on Entrainment of Juvenile Salmon into the Interior Sacramento-San Joaquin River Delta

Russell W. Perry[a], Patricia L. Brandes[b], Jon R. Burau[c], Philip T. Sandstrom[df] & John R. Skalski[e]

[a] U.S. Geological Survey, Western Fisheries Research Center, 5501A Cook-Underwood Road, Cook, Washington 98605, USA

[b] Stockton Fish and Wildlife Office, 850 Guild Avenue, Suite 105, Lodi, California 95240, USA

[c] U.S. Geological Survey, California Water Science Center, 6000 J Street, Placer Hall, Sacramento, California 95819, USA

[d] Biotelemetry Laboratory, Department of Wildlife, Fish, and Conservation Biology, University of California, 1334 Academic Surge, Davis, California 95616, USA

[e] School of Aquatic and Fishery Sciences, University of Washington, 1325 Fourth Avenue, Suite 1820, Seattle, Washington 98101-2509, USA

[f] Present address: Washington Department of Fish and Wildlife, 1111 Washington Street Southeast, Olympia, Washington 98501, USA.

Published online: 08 Apr 2015.

To cite this article: Russell W. Perry, Patricia L. Brandes, Jon R. Burau, Philip T. Sandstrom & John R. Skalski (2015) Effect of Tides, River Flow, and Gate Operations on Entrainment of Juvenile Salmon into the Interior Sacramento-San Joaquin River Delta, Transactions of the American Fisheries Society, 144:3, 445-455, DOI: 10.1080/00028487.2014.1001038

To link to this article: http://dx.doi.org/10.1080/00028487.2014.1001038

Transactions of the American Fisheries Society 144:445–455, 2015

ISSN: 0002-8487 print / 1548-8659 online
DOI: 10.1080/00028487.2014.1001038

ARTICLE

Effect of Tides, River Flow, and Gate Operations on Entrainment of Juvenile Salmon into the Interior Sacramento–San Joaquin River Delta

Russell W. Perry*
U.S. Geological Survey, Western Fisheries Research Center, 5501A Cook-Underwood Road, Cook, Washington 98605, USA

Patricia L. Brandes
Stockton Fish and Wildlife Office, 850 Guild Avenue, Suite 105, Lodi, California 95240, USA

Jon R. Burau
U.S. Geological Survey, California Water Science Center, 6000 J Street, Placer Hall, Sacramento, California 95819, USA

Philip T. Sandstrom[1]
Biotelemetry Laboratory, Department of Wildlife, Fish, and Conservation Biology, University of California, 1334 Academic Surge, Davis, California 95616, USA

John R. Skalski
School of Aquatic and Fishery Sciences, University of Washington, 1325 Fourth Avenue, Suite 1820, Seattle, Washington 98101-2509, USA

Abstract

Juvenile Chinook Salmon *Oncorhynchus tshawytscha* emigrating from natal tributaries of the Sacramento River, California, must negotiate the Sacramento–San Joaquin River Delta (hereafter, the Delta), a complex network of natural and man-made channels linking the Sacramento River with San Francisco Bay. Fish that enter the interior and southern Delta—the region to the south of the Sacramento River where water pumping stations are located—survive at a lower rate than fish that use alternative migration routes. Consequently, total survival decreases as the fraction of the population entering the interior Delta increases, thus spurring management actions to reduce the proportion of fish that are entrained into the interior Delta. To better inform management actions, we modeled entrainment probability as a function of hydrodynamic variables. We fitted alternative entrainment models to telemetry data that identified when tagged fish in the Sacramento River entered two river channels leading to the interior Delta (Georgiana Slough and the gated Delta Cross Channel). We found that the probability of entrainment into the interior Delta through both channels depended strongly on the river flow and tidal stage at the time of fish arrival at the river junction. Fish that arrived during ebb tides had a low entrainment probability, whereas fish that arrived during flood tides (i.e., when the river's flow was reversed) had a high probability of entering the interior Delta. We coupled our entrainment model with a flow simulation model to evaluate the effect of nighttime closures of the Delta Cross Channel gates on the daily probability of fish entrainment into the interior Delta. Relative to 24-h gate closures, nighttime closures increased daily entrainment probability by 3 percentage points on average if fish arrived at the river junction uniformly throughout the day and by only 1.3 percentage points if 85% of fish arrived at night. We illustrate how our model can be used to evaluate the effects of alternative water management actions on fish entrainment into the interior Delta.

*Corresponding author: rperry@usgs.gov
[1]Present address: Washington Department of Fish and Wildlife, 1111 Washington Street Southeast, Olympia, Washington 98501, USA.
Received May 9, 2014; accepted December 10, 2014

Regulated rivers are managed to balance human demands (e.g., electricity generation and water withdrawal) with the maintenance of functioning aquatic ecosystems. In rivers supporting depressed populations of anadromous salmonids, this balance often involves assessing water management actions that can improve the survival of seaward-migrating juvenile salmon at the expense of using water for human benefits (Williams 2006). For example, passing water over spillways at dams increases the total survival of juvenile salmon by diverting fish away from high-mortality turbines, but this comes at the cost of foregone electricity generation (Williams 2008). Although such tradeoffs are fundamental to the management of natural resources, understanding how fish behave in response to their environment can aid in developing water management actions that provide ecosystem services while reducing negative effects on fish populations.

The Sacramento–San Joaquin River Delta (hereafter, the Delta) in California is a complex network of channels that has been highly altered to convey water for domestic and agricultural uses via two large pumping stations in the interior Delta (Nichols et al. 1986; Figure 1). Threatened populations of juvenile salmonids emigrating from the Sacramento River distribute among these channels and use multiple migration routes on their seaward journey (Perry et al. 2010). Migration routes vary in width and length as well as in biotic and abiotic factors, all of which influence the survival of juvenile salmon. For instance, juvenile Chinook Salmon *Oncorhynchus tshawytscha* that migrate through the interior Delta survive at lower rates than fish that migrate within the Sacramento River (Figure 1), likely due to high predation rates, longer migration times, and entrainment into water pumping stations (Newman and Brandes 2010; Perry et al. 2010, 2013). Because the survival of juvenile salmon in the interior Delta is lower than that in other routes, the total survival of smolts decreases as the fraction of the smolt population entering the interior Delta increases (Perry et al. 2013).

Juvenile Chinook Salmon enter the interior Delta via two channels that diverge from the Sacramento River (Figure 1). Fish first migrate past the Delta Cross Channel, a man-made, gated channel that is used to divert water into the interior Delta to reduce salinities at the pumping stations. Fish that remain in the Sacramento River then encounter Georgiana Slough, a natural channel that is located 1 km downstream from the entrance to the Delta Cross Channel. Up to 50% of juvenile Chinook Salmon encountering these two channels may be entrained into the interior Delta, exposing a substantial fraction of the population to low survival probabilities (Perry 2010). Consequently, the Delta Cross Channel is operated in a precautionary manner by closing the gates during the emigration period of endangered winter-run juvenile Chinook Salmon; this strategy is employed under the assumption that fish entrainment into the Delta Cross Channel is directly proportional to the mean fraction of river flow that is diverted to the interior Delta (SWRCB 1995; Low et al. 2006). However, the validity of this assumption is unclear,

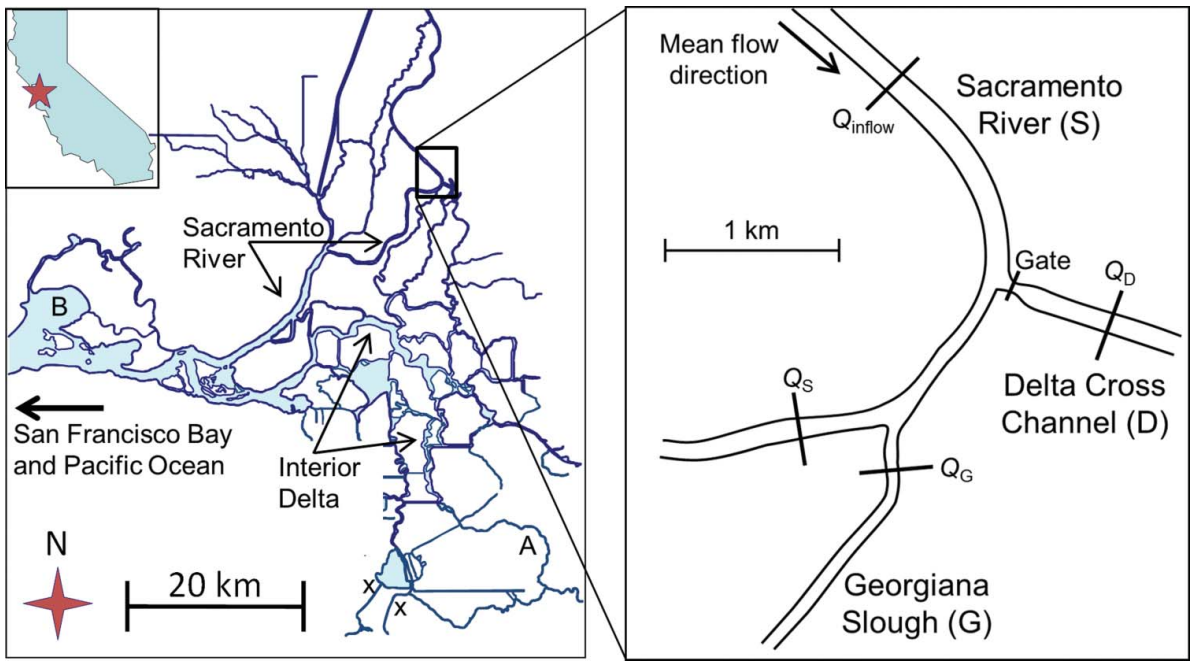

FIGURE 1. Map of the Sacramento–San Joaquin River Delta, with exploded view showing the junction of the Sacramento River with the Delta Cross Channel and Georgiana Slough. Discharge gauging stations in each channel are labeled as Q_j (Q_S = Sacramento River gauging station; Q_D = Delta Cross Channel gauging station; Q_G = Georgiana Slough gauging station). Other labels as follows: A = San Joaquin River; B = Suisun Bay; Gate = Delta Cross Channel gate; and X = water pumping stations in the southern Delta. [Figure available online in color.]

as fish passing the Delta Cross Channel may be subsequently entrained into Georgiana Slough.

Quantifying the factors that affect migration routing at this river junction is challenging because fish behavior and complex physical processes may interact to cause the entrained fraction of fish to deviate from the mean fraction of flow entering the interior Delta. Tidal forcing causes the Sacramento River to reverse direction twice daily at river flows less than about 566 m^3/s (as measured at Freeport, U.S. Geological Survey station number 11447650). This tidal forcing causes the relative distribution of flows among the three channels to vary over hourly time scales. For example, nearly all of the river's flow is diverted into the Delta Cross Channel and Georgiana Slough during reverse-flow flood tides, whereas little discharge enters the Delta Cross Channel during ebb tides. Given this hourly variation, the probability of fish entry into a given channel (i.e., entrainment probability) will depend on the hydraulic conditions that the fish encounter when migrating past each channel's entrance (Steel et al. 2013). In addition, late-fall Chinook Salmon smolts have been shown to exhibit nocturnal migration behavior in the Sacramento River (Chapman et al. 2013), and spring–neap cycles during winter cause larger-magnitude flood tides during the day and smaller tides at night. Consequently, the diel activity patterns of juvenile salmon may interact with tidal cycles to decouple the mean fraction of fish entering the interior Delta from the mean proportion of flow diverted into the interior Delta.

These complex interactions between behavioral and physical processes pose challenges for understanding the response of fish populations to management actions. Therefore, our objective was to develop a model that could be used to quantify the effects of various water management actions on entrainment of juvenile salmon into the interior Delta. First, we developed an entrainment model that was fitted to a multiyear telemetry data set describing tagged juvenile late-fall Chinook Salmon. This model estimated individual probabilities of entrainment into the Delta Cross Channel and Georgiana Slough as a function of time-dependent hydraulic conditions in each river channel. We illustrate how this model can be used to inform management actions by simulating fish entrainment into the interior Delta under alternative scenarios of gate operations and diel migration patterns. For this application, we hypothesized that opening the Delta Cross Channel gates during the daytime but closing them at night would allow water to be diverted while minimizing the risk of juvenile salmon entrainment. By simulating alternative management actions, we were able to gain insights into the potential effects of management actions for which outcomes would be highly uncertain and costly to implement in practice.

METHODS

Telemetry data.—To model entrainment probabilities at the Delta Cross Channel and Georgiana Slough, we compiled telemetry data on late-fall Chinook Salmon smolts from three acoustic telemetry studies. Detailed methods about telemetry systems, data processing, and tagging procedures for these studies are provided by Vogel (2008), Perry et al. (2010, 2013), and Singer et al. (2013). In total, 1,873 acoustic-tagged smolts were released in 13 discrete groups during the winters of 2007–2009 (Table 1). All fish were released into the Sacramento River a minimum of 40 km upstream of the Delta Cross Channel. To detect tagged fish as they entered each route, detection arrays consisting of one or more hydrophones were situated just downstream of the entrances to the Delta Cross Channel, Georgiana Slough, and the Sacramento River. The

TABLE 1. Sample sizes for release groups of juvenile late-fall Chinook Salmon that received acoustic tags during the winters of 2007–2009 (DCC = Delta Cross Channel). "Number detected with DCC open" indicates the number of fish that were detected at the river junction while the DCC gates were open.

Release group	Source	Year	Release dates	Number released	Number detected at junction	Number detected with DCC open
1	Perry et al. (2010, 2013)	2006	Dec 5–6	64	36	32
2	Vogel (2008)		Dec 11–12	96	57	49
3	Perry et al. (2010, 2013)	2007	Jan 17–18	80	39	0
4	Vogel (2008)		Jan 12–23	166	55	0
5	Singer et al. (2013)		Jan 16–Feb 2	200	11	0
6	Perry et al. (2010, 2013)		Dec 4–5	149	76	73
7	Singer et al. (2013)		Dec 7	150	36	3
8	Perry et al. (2010, 2013)	2008	Jan 15–16	130	85	0
9	Singer et al. (2013)		Jan 17	154	49	0
10	Perry et al. (2010, 2013)		Nov 30–Dec 4	192	91	47
11	Singer et al. (2013)		Dec 13	149	57	1
12	Singer et al. (2013)	2009	Jan 11	151	30	0
13	Perry et al. (2010, 2013)		Jan 13–17	192	92	0
All groups				1,873	714	205

fate of each tagged fish was assigned to one of the three river channels based on the time series of detections. Owing to migration through alternative routes and mortality between release sites and the study area, 38% (714 fish) of all released fish were detected at the river junction (Table 1). Of the 714 fish that were detected at the junction, 29% passed the Delta Cross Channel when its gates were open, and the remainder passed the junction after the gates were closed (Table 1).

Entrainment model.—Entrainment probability—the probability that a fish will enter one of the three alternative migration routes—was modeled as a multivariate Bernoulli random variable with the probability distribution

$$\pi_{i\mathrm{D}}^{I_{i\mathrm{D}}}\pi_{i\mathrm{G}}^{I_{i\mathrm{G}}}\pi_{i\mathrm{S}}^{(1-I_{i\mathrm{D}})(1-I_{i\mathrm{G}})}, \quad (1)$$

where

$\pi_{i\mathrm{D}}$ = the probability that the ith fish ($i = 1,\ldots, n$) entered the Delta Cross Channel (D);

$\pi_{i\mathrm{G}}$ = the probability that the ith fish entered Georgiana Slough (G);

$\pi_{i\mathrm{S}} = 1 - \pi_{i\mathrm{D}} - \pi_{i\mathrm{G}}$ = the probability that the ith fish entered the Sacramento River (S);

$$I_{i\mathrm{D}} = \begin{cases} 1 \text{ if the } i\text{th fish entered the Delta Cross Channel} \\ 0 \text{ otherwise; and} \end{cases}$$

$$I_{i\mathrm{G}} = \begin{cases} 1 \text{ if the } i\text{th fish entered Georgiana Slough} \\ 0 \text{ otherwise.} \end{cases}$$

When the Delta Cross Channel was closed, $\pi_{i\mathrm{D}}$ was equal to zero, and the probability distribution for an individual fish was reduced to $\pi_{i\mathrm{G}}^{I_{i\mathrm{G}}}\pi_{i\mathrm{S}}^{(1-I_{i\mathrm{G}})}$.

To model entrainment probabilities as a function of explanatory variables, we used a generalized linear models framework with a logit link function that was measured relative to a baseline category. The baseline category was selected to be the Sacramento River route such that

$$g(\pi_{ij}) = \log_e\left(\frac{\pi_{ij}}{\pi_{i\mathrm{S}}}\right) = \beta_{j0} + \beta_{j1}x_{ij1} + \ldots + \beta_{jp}x_{ijp} = \boldsymbol{\beta}_{ij}'\mathbf{x}_{ij}, \quad (2)$$

where x_{ijp} is the pth covariate for the ith fish entering the jth channel (j = D or G); and β_{jp} is the slope coefficient for the jth channel and the pth covariate. Entrainment probabilities were expressed as a function of covariates by using the inverse logit function, and the joint likelihood was the product of equation (1) over all observed fish (Agresti 2002). This formulation allowed $\pi_{i\mathrm{D}}$ and $\pi_{i\mathrm{G}}$ to be modeled by a separate set of explanatory variables. The regression coefficients were estimated by maximum likelihood estimation using optimization routines in R (R Development Core Team 2013). Variances were estimated by using the diagonal elements of the inverse Hessian matrix.

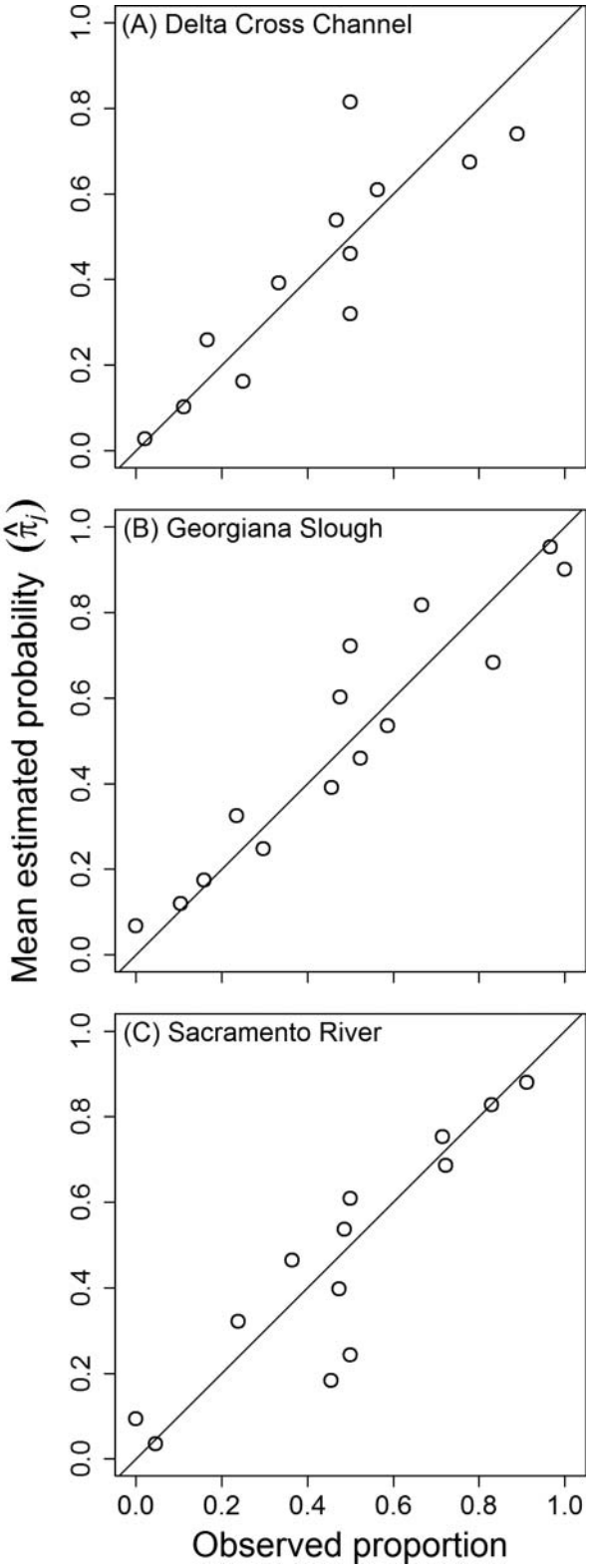

FIGURE 2. Observed proportions of juvenile Chinook Salmon entering **(A)** the Delta Cross Channel, **(B)** Georgiana Slough, and **(C)** the Sacramento River compared with the mean predicted probability of fish entry into each route. Groups were formed by discretizing the predicted probabilities into 14 intervals of equal-probability width.

Hydraulic variables.—We hypothesized that entrainment probabilities for each channel could be explained by the hydraulic conditions that were present when fish were detected as entering a given river channel. River discharge in each channel (Q_j) was the primary variable used to explain variation in entrainment probabilities (where j = S for the Sacramento River, D for the Delta Cross Channel, or G for Georgiana Slough). U.S. Geological Survey gauging stations were located just downstream of the entrance to the Delta Cross Channel (station number 11336600), Georgiana Slough (station number 11447903), and the Sacramento River (station number 11447905; Figure 1). Total discharge entering the river junction was measured by a gauging station situated just upstream of the junction (Q_{inflow} in Figure 1; station number 11447890). These gauging stations recorded discharge and water velocity every 15 min, providing detailed information about the hydraulic conditions experienced by tagged fish when they migrated through the river junction.

The effect of tidal fluctuations on hydraulic conditions at the river junction was captured by two variables. First, an indicator variable (U) was set to 1.0 when flood tides caused river flow in the Sacramento River to be reversed (i.e., $U = 1$ when $Q_S < 0$; $U = 0$ otherwise). Second, the rate of change in discharge of the Sacramento River was measured as $\Delta Q_S(t) = Q_S(t+1) - Q_S(t)$, where t is measured in units of 15 min. This variable accounted for hydraulic conditions that may be quite different on a flood-to-ebb transition compared with an ebb-to-flood transition, even though total discharge may be similar during each transition. When ΔQ_S was negative, discharge was decreasing, typical of the transition from an ebb tide to a flood tide. In contrast, when ΔQ_S was positive, discharge was increasing, as typical of the transition from a flood tide to an ebb tide.

Diel variation in the spatial distribution of juvenile salmon in the river's cross section could also influence entrainment probabilities. For example, if fish are distributed close to shore during the day but near the center of the channel at night, then this type of diel variation could influence entrainment probabilities. To assess whether entrainment probabilities varied between day and night, we included time of day as a binary covariate in the model (time of day = 1 for fish detected during the day; time of day = 0 for fish detected at night). Day and night were defined based on daily times of sunrise and sunset. Lastly, all continuous covariates were standardized by subtracting the mean from each observation and then dividing by the SD (Table 2).

Model selection and goodness of fit.—To identify the variables that best described the entrainment probabilities, stepwise deletion procedures were used. The full model included all possible explanatory variables for both π_D and π_G; the exception was Q_D, which was excluded from this model because it was highly correlated with Q_S ($r = -0.84$). Variables with the largest P-values were then dropped one at a time from $g(\pi_D)$ and $g(\pi_G)$, and the model was refitted. This process was repeated until no further variables could be dropped at $\alpha = 0.05$. Two-way interactions were then formed from the variables remaining in the reduced model and were re-examined using the same stepwise deletion procedures. Tests of significance were based on likelihood ratio tests, but for comparison we also present Akaike's information criterion for each model (Burnham and Anderson 2002).

TABLE 2. Summary of river discharge (Q_j; m^3/s) experienced by juvenile Chinook Salmon that were detected at the junction of the Sacramento River (j = S) with the Delta Cross Channel (j = D) and Georgiana Slough (j = G). Discharge at Freeport is the mean daily discharge of the Sacramento River upstream of the Delta on dates during which fish were detected at the river junction; Q_{inflow} is the total discharge just upstream of the river junction; and ΔQ_S is the change in Q_S from time t to time $t + 1$.

Flow variable	Mean	SD	Range
Q at Freeport	390.8	183.6	192.6 to 1,152.5
Q_{inflow}	293.1	126.9	−61.4 to +798.5
Q_S	177.1	139.3	−173.3 to +577.5
Q_G	86.2	32.4	30.3 to 228.6
Q_D	31.2	63.6	−38.8 to +258.8
ΔQ_S	−2.1	13.5	−47.0 to +38.5

Goodness of fit was assessed using the Hosmer–Lemeshow test by grouping the observed data into discrete classes and comparing observed and predicted probabilities of occurrence (Hosmer and Lemeshow 2000). The area under the receiver operating curve (AUC) was used to quantify the overall predictive performance of the selected model. The receiver operating curve plots the true-positive rate against the false-positive rate for all possible cutoff values that are used to classify the predicted probability into binary outcomes. An AUC of 0.5 indicates no prediction ability, and a value of 1.0 indicates perfect prediction ability. In practice, AUC values between 0.7 and 0.8 are considered "acceptable," and values between 0.8 and 0.9 are considered "excellent" (Hosmer and Lemeshow 2000).

Simulation of alternative gate operations.—To illustrate how the entrainment model can be used to evaluate the potential effects of water management actions on fish entrainment into the interior Delta, we simulated entrainment probabilities under two management scenarios: (1) a historical scenario in which the Delta Cross Channel gates were open until December 15 and closed thereafter; and (2) an alternative scenario wherein the Delta Cross Channel gates were open during the day but closed at night for the entire simulation period. The premise of this latter management action is that most of the water enters the interior Delta during large, daytime flood tides, whereas most of the late-fall Chinook Salmon smolts migrate at night (Chapman et al. 2013). The rationale is that closing the gates at night will minimize the risk of entrainment for most of the fish population, while opening the gates during the day still allows for substantial water diversion to the interior Delta.

To implement the simulation, we used the Delta Simulation Model II (DSM2; CH2MHILL 2009; CADWR 2013) to simulate river flows at a 15-min time step. The DSM2 is a hydrographic model for simulating one-dimensional, unsteady, open-channel flow in the Delta in response to river inflows, tidal forcing, and water management actions. We used historical simulations of Delta hydrodynamics from November 1, 2006, to January 31, 2007, a period during which the Delta Cross Channel gates were open until December 15, 2006, and closed thereafter. We focused on this period because historically, 45 d of discretionary gate closures were allowed for fisheries protection, thereby providing flexibility to managers in operating the Delta Cross Channel (SWRCB 1995). Our alternative management scenario was the same as the historical simulation except that the Delta Cross Channel gates were opened at sunrise and closed at sunset for the entire simulation period (hereafter, the "closed-at-night" operation). Hence, for the period November 1–December 15, 2006, simulated gate operations were switched from open 24 h/d (historical) to closed at night (alternative); and for the period December 15, 2006, to January 31, 2007, gate operations were switched from closed 24 h/d (historical) to closed at night (alternative).

Given the flow data simulated under these scenarios, we used our entrainment model to predict entrainment probabilities for each 15-min flow observation. To assess the effect of different diel activity patterns, we calculated the mean daily probability of fish entry into the interior Delta,

$$\overline{\pi}_{ID,d} = A_{\text{Day}}\overline{\pi}_{ID,d,\text{Day}} + (1 - A_{\text{Day}})\overline{\pi}_{ID,d,\text{Night}},$$

where A_{Day} is the probability of fish arrival at the junction during daylight hours; $\overline{\pi}_{ID,d,\text{Day}}$ is the mean probability of fish entry into the interior Delta during daylight hours on day d; and $\overline{\pi}_{ID,d,\text{Night}}$ is the mean probability of fish entry into the interior Delta during the night. The probability of entering the interior Delta is the sum of the probabilities of entering the Delta Cross Channel and Georgiana Slough. We compared daily entrainment probabilities between alternative gate operations for two scenarios of diel activity: (1) nocturnal migration behavior, wherein 85% of fish arrived at night; and (2) a uniform diel distribution, in which fish displayed no bias toward nocturnal or diurnal migration. These scenarios were chosen to bracket the range of diel activity patterns observed in our study, as the percentage of fish arriving at night varied from 55% to 86% among release groups.

RESULTS

Model Selection and Goodness of Fit

Although the full model consisted of 16 parameters, many variables failed to improve model fit (Table 3), thus yielding a final model comprising seven parameters and four explanatory variables (Table 4). Time of day was eliminated from the model because likelihood ratio tests showed that it did not significantly improve model fit. Upstream flow in the Sacramento River (U) and Q_{G} did not affect entrainment probability for the Delta Cross Channel (π_{D}), whereas the ΔQ_{S} did not influence the probability of fish entry into Georgiana Slough (π_{G}; Table 3). None of the remaining variables could be eliminated without significantly increasing the negative log-likelihood ($\chi^2_1 \geq 10$, $P \leq 0.002$), and none of the two-way interactions among the remaining variables was significant (Table 3).

We found little evidence of systematic departures of predicted values from observed values. The Hosmer–Lemeshow goodness-of-fit tests ($\hat{C}$) were not significant (π_{D}: $\hat{C} = 4.84$, $P = 0.775$; π_{G}: $\hat{C} = 5.19$, $P = 0.737$). Plots of observed

TABLE 3. Model selection results for the effects of hydraulic variables on the probability of late-fall Chinook Salmon entering Georgiana Slough (π_{G}) and the Delta Cross Channel (π_{D}). Shown are the likelihood ratio (LR) test and associated statistics for the model with the given variable dropped relative to the preceding model with one additional variable (AIC = Akaike's information criterion; NLL = negative log-likelihood).

Variable dropped[a]	Response	Number of parameters	AIC	NLL	LR	P-value
None (full model)		12	794.7	385.3		
Time of day	π_{G}	11	792.7	385.4	0.03	0.863
U	π_{D}	10	790.8	385.4	0.10	0.752
Time of day	π_{D}	9	789.1	385.6	0.30	0.584
Q_{G}	π_{D}	8	787.6	385.8	0.54	0.462
ΔQ_{S}	π_{G}	7	787.6	386.8	1.98	0.159
None (all interactions)		11	790.3	384.2		
$Q_{\text{S}} \times U$	π_{G}	10	788.3	384.4	0.03	0.863
$Q_{\text{S}} \times Q_{\text{G}}$	π_{G}	9	786.9	384.5	0.57	0.450
$Q_{\text{G}} \times U$	π_{G}	8	786.5	385.3	1.63	0.202
$Q_{\text{S}} \times \Delta Q_{\text{S}}$	π_{D}	7	787.6	386.8	3.08	0.079

[a] Q_j = standardized discharge of channel j (j = S for the Sacramento River or G for Georgiana Slough); ΔQ_{S} = change in Q_{S} from time t to time $t + 1$; and U = indicator of reverse flow in the Sacramento River ($U = 1$ for $Q_{\text{S}} < 0$; $U = 0$ otherwise). Time of day is coded as 1 for daytime and 0 for nighttime.

TABLE 4. Maximum likelihood parameter estimates for the best-fit model relating the probabilities of juvenile Chinook Salmon entrainment into Georgiana Slough (π_G) and the Delta Cross Channel (π_D) to hydraulic variables (Q_S = standardized discharge of the Sacramento River; Q_G = standardized discharge of Georgiana Slough; ΔQ_S = change in Q_S from time t to time $t + 1$; U = indicator of reverse flow in the Sacramento River).

Response	Variable	Parameter estimate	SE
π_G	Intercept	−0.900	0.106
	Q_S	−1.163	0.154
	Q_G	0.852	0.107
	U	1.595	0.512
π_D	Intercept	−2.337	0.391
	Q_S	−2.694	0.337
	ΔQ_S	−0.474	0.158

proportions versus mean predicted probabilities supported the statistical tests, showing no evidence of systematic deviations (Figure 2). We found that AUC was 0.785 for $\hat{\pi}_{iG}$, 0.873 for $\hat{\pi}_{iD}$, and 0.841 for $\hat{\pi}_{iS}$, indicating that the model had an excellent ability to predict the ultimate fates of fish. Taken together, the goodness-of-fit measures suggested little evidence of lack of fit, a close agreement between predicted and observed values, and a good ability to predict the likelihood of fish entering migration routes in response to hydraulic dynamics.

Under the best-fit model, Q_S, Q_G, and U significantly affected π_G, whereas Q_S and ΔQ_S affected π_D (Table 4). Parameter estimates indicated both the direction and magnitude of these variables' effects on entrainment probabilities when the remaining variables were held constant. For π_G, the slope parameter for Q_S was negative, indicating that increases in Q_S produced decreases in π_G. In contrast, the positive slope estimate for Q_G indicated that π_G increased with Q_G. Slope estimates for Q_G and Q_S were of similar magnitude, showing that a 1-SD change in either variable affected π_G by a similar magnitude but in opposite directions. The positive parameter estimate for U indicated that water flowing upstream from the Sacramento River into the river junction increased π_G over and above the effect of Q_G and Q_S. For the Delta Cross Channel, decreases in both Q_S and ΔQ_S generated increases in π_D, but the slope estimate for Q_S was five times that for ΔQ_S, indicating that Q_S was the dominant factor driving the probability of entrainment into the Delta Cross Channel (Table 4).

Response of Entrainment Probabilities to Fluctuating River Flows

At the mean river flows observed during our study (Table 2), flood tides caused the Sacramento River to reverse direction twice daily (Figures 3A, 4A). Under these conditions, Q_S varied substantially from −142 m^3/s during the full flood tide to 283 m^3/s during the full ebb tide only a few hours later. Flow into the Delta Cross Channel was inversely related to Q_S, increasing rapidly during the transition from ebb tide to flood tide as Q_S decreased (i.e., when $\Delta Q_S < 0$). Relative to Q_S and Q_D, Q_G exhibited much less variability regardless of whether the Delta Cross Channel gates were open or closed.

In response to fluctuating river flows driven by the tides, entrainment probabilities varied substantially throughout the day. For the Delta Cross Channel, π_D closely tracked Q_D and was inversely related to Q_S (Figure 3B). Thus, π_D was close to zero during the full ebb tide, when the Sacramento River flow was at its maximum and when cross channel flow was minimal. As the tide transitioned from ebb to flood, Q_S decreased and π_D increased to a maximum of about 75% just as the Sacramento River reached full flood tide. The value of π_D was nearly always less than the fraction of total discharge entering the Delta Cross Channel. After the peak of the flood tide, however, π_D declined despite the fact that the proportion of flow entering the cross channel remained relatively constant through the flood tide. This pattern was driven by the relative contributions of Q_S and ΔQ_S in the equation for π_D (Table 4). The negative slope for ΔQ_S indicated that π_D increased when Q_S declined during ebb-to-flood transitions, whereas π_D

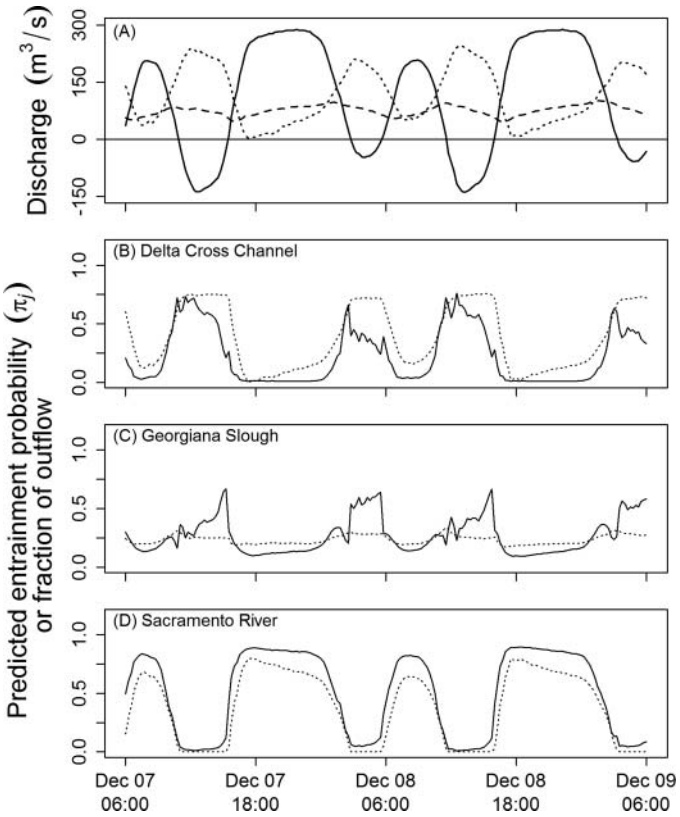

FIGURE 3. Predicted probability of juvenile Chinook Salmon entrainment into route j as a function of river flow entering each channel for 2 d in December 2007 under average flow conditions, with the Delta Cross Channel gates open. Panel **(A)** shows discharge just downstream of the river junction in the Sacramento River (Q_S; solid line), the Delta Cross Channel (Q_D; dotted line), and Georgiana Slough (Q_G; dashed line). Panels **(B)–(D)** show the predicted probability of fish entry into each channel (π_j; solid line) and the fraction of total outflow entering each channel (dotted line).

decreased when Q_S increased during flood-to-ebb transitions (Figure 3B).

The Q_G was relatively constant throughout the tidal cycle, yet π_G varied substantially over the day (Figures 3C, 4B). When the Delta Cross Channel gates were open and Q_S was positive, π_G tended to track the fraction of discharge entering Georgiana Slough (Figures 3C, 4C). However, during reverse-flow flood tides, π_G considerably exceeded the fraction of discharge entering Georgiana Slough (Figure 3C). In contrast, when the Delta Cross Channel gates were closed, the fraction of discharge entering Georgiana Slough varied between 20% and 100% as Q_S cycled between negative and positive flows about a relatively constant Q_G (Figure 4C). Therefore, when the Delta Cross Channel was closed, π_G closely tracked the fraction of flow entering Georgiana Slough, ranging from approximately 0.10 during the full ebb tide to 0.95 during the flood tide. During flood tides, π_G was higher when the cross channel gates were closed than when the gates were open (Figures 3C, 4C), illustrating that closure of the gates increased the probability of fish entry into Georgiana Slough.

Since π_G increased when the cross channel gates were closed, thereby entraining fish that would have otherwise entered the Delta Cross Channel, entrainment probability for the Sacramento River (π_S) followed a similar pattern regardless of the whether the cross channel gates were open or closed (Figures 3D, 4D). In general, π_S followed a step function, switching quickly from a high probability that fish would remain in the Sacramento River during an ebb tide to a very low probability during a flood tide (Figures 3D, 4C). During the full ebb tide, π_S remained at about 0.90 regardless of cross channel gate position. However, when the cross channel gates were open during a flood tide, π_S was near zero, indicating that fish migrating through the river junction during this tidal stage would almost certainly enter either the Delta Cross Channel or Georgiana Slough (Figure 3D). When the cross channel gates were closed, although π_S remained low during flood tides, the fish still had a 5–10% chance of remaining in the Sacramento River (Figure 4D).

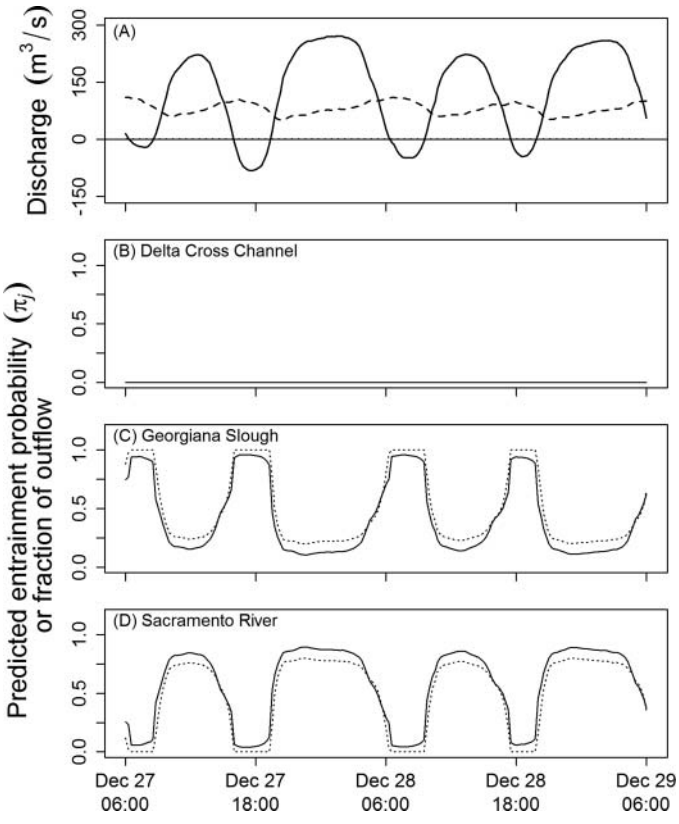

FIGURE 4. Predicted probability of juvenile Chinook Salmon entrainment into route *j* as a function of river flow entering each channel for 2 d in December 2007 under average flow conditions, with the Delta Cross Channel gates closed. Panel **(A)** shows discharge just downstream of the river junction in the Sacramento River (Q_S; solid line), the Delta Cross Channel (Q_D; dotted line), and Georgiana Slough (Q_G; dashed line). Panels **(B)–(D)** show the predicted probability of fish entry into each channel (π_j; solid line) and the fraction of total outflow entering each channel (dotted line).

Simulation of Alternative Gate Operations

Relative to the historical gate operations, closure of the Delta Cross Channel at night had a large influence on the fraction of discharge entering the interior Delta but exerted much less of an effect on the expected daily entrainment into the interior Delta (Figure 5). Sensitivity to gate closure was much lower for daily entrainment probabilities than for the fraction of discharge entering the interior Delta because the instantaneous probability of entrainment in Georgiana Slough increased when the cross channel gates were closed (Figures 3C, 4C). When the Delta Cross Channel was open 24 h/d (i.e., prior to December 15), switching to the closed-at-night operation reduced the fraction of discharge entering the interior Delta by an average of 15 percentage points (Figure 5). However, daily entrainment probabilities decreased by only 5 percentage points on average for a uniform diel arrival distribution and decreased by 7 percentage points if 85% of fish arrived at night. When the gates were closed for 24 h/d (i.e., after December 15), switching to the closed-at-night operation increased the interior Delta flow proportion by 11 percentage points on average. In this case, daily entrainment probabilities increased by 3.0 percentage points on average for the uniform arrival distribution and by 1.3 percentage points for the scenario in which 85% of fish arrived at night. Thus, relative to a fully closed gate position, opening the gates during the day was expected to have little effect on entrainment, particularly if most of the migration occurred at night. Regardless of diel activity pattern, however, the change in daily entrainment probabilities was considerably less than the change in the fraction of discharge because closure of the Delta Cross Channel increased π_G. These findings illustrate how our entrainment model can be used to understand the

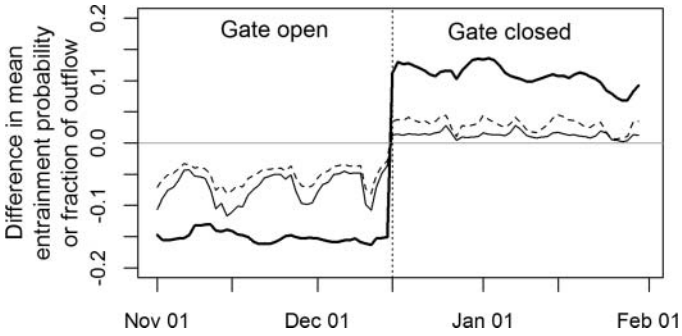

FIGURE 5. Mean daily difference between gate operation scenarios for fraction of discharge and juvenile Chinook Salmon entrainment into the interior Sacramento–San Joaquin River Delta. The vertical dotted line indicates the historical gate operations scenario in which the Delta Cross Channel gates were open until December 15, 2006, and closed thereafter. For the alternative scenario, the Delta Cross Channel gates were closed at night but open during the day for the entire simulation period. The bold solid line shows the difference in the fraction of junction inflow entering the interior Delta (closed-at-night scenario minus historical operations scenario). Also shown is the difference in mean daily fish entrainment probability between scenarios assuming either a uniform diel arrival of fish at the junction (dashed line) or 85% of fish arriving at night (thin solid line).

effect of management actions on the routing of fish in the Delta.

DISCUSSION

Prior to this study, fisheries managers had little mechanistic information with which to guide water management actions for minimizing fish entrainment into the interior Delta. Uncertainty about the driving mechanisms has forced fisheries managers to act in a precautionary manner, implementing actions that are least likely to harm endangered populations but at the expense of consumptive water use. Tagging studies have indicated that juvenile salmon entering the interior Delta via the Delta Cross Channel and Georgiana Slough survive at a lower rate than fish migrating within the Sacramento River (Newman and Brandes 2010; Perry et al. 2010, 2013). Consequently, the Delta Cross Channel has been prescriptively closed after December 15 each year under the rationale that fish distribution among the alternative migration routes is proportional to discharge (Low et al. 2006). However, our analysis suggests that the mechanisms governing route selection are more complex, and this relationship needs to be considered in managing water resources for the benefit of both fish and human use.

Our analysis revealed the strong influence of tidal forcing on the probability of fish entrainment into the interior Delta. The probability of entrainment into both Georgiana Slough and the Delta Cross Channel was highest during reverse-flow flood tides, and the probability of fish remaining in the Sacramento River was near zero during flow reversals. The magnitude and duration of reverse flows at this river junction decrease as inflow of the Sacramento River increases, ceasing at inflows greater than about 566 m^3/s at Freeport ($Q_{inflow} \approx$ 360 m^3/s). Consequently, reduced Sacramento River inflow increases the frequency of reverse flows at this junction, thereby increasing the proportion of fish that are entrained into the interior Delta, where mortality is high (Perry 2010). In the future, Sacramento River inflows may decrease through climate change (Hayhoe et al. 2004; Maurer 2007; Cloern et al. 2011) or through water management actions that reduce discharge of the Sacramento River (BDCP 2013).

Owing to hourly variation in river flows driven by tidal forcing, migration routing among channels in the Delta will be strongly dependent on fish arrival timing at river junctions. If fish actively migrate during both day and night, we would expect the mean daily entrainment into the interior Delta to be proportional to the mean fraction of discharge entering the interior Delta. However, diel activity patterns that shift migration toward nocturnal, diurnal, or crepuscular migration may decouple the mean entrainment probabilities from the mean fraction of discharge entering a particular route, shifting entrainment more toward the time-specific conditions experienced by the bulk of the population. Under these circumstances, the realized outcome of management actions based on distribution of mean flow may deviate considerably from expectations. Since diel activity patterns are observed in many fish species (Reebs 2002), our study highlights the need for understanding fish behavior in the context of water management actions. We have shown how detailed information about the response of individuals to hydraulic conditions can inform models that allow managers to develop management actions to minimize impacts on fish populations while maximizing human benefits. Our simulation analysis demonstrated how operation of the cross channel at hourly time scales (nighttime gate closures) allowed water to be diverted for human uses while having little effect on entrainment into a low-survival migration route, particularly if most of the fish migration occurred at night.

Factors that drive the diel movement patterns of juvenile salmon in the Delta are poorly understood but may vary with season, environment, life stage, and life history strategy. In our study, the proportion of juvenile Chinook Salmon that were detected at night averaged 75% even though nighttime comprised about 60% of the 24-h period. More importantly, nighttime arrival varied from 55% to 86% among release groups, ranging from diel arrival that was proportional to the availability of daylight hours to substantial nocturnal migration. Chapman et al. (2013) also found considerable variation in diel activity patterns of juvenile salmonids (Chinook Salmon and steelhead *O. mykiss*) in the Sacramento River and San Francisco Bay. Such variation is unsurprising given that diel activity patterns can switch from day to night in response to trade-offs among predation risk, physiological state, and environmental cues (Metcalfe et al. 1998, 1999). For example, an increase in nighttime activity with decreasing temperature is hypothesized as a behavioral response to lower metabolic

requirements, reducing the need for juvenile salmon to feed during the day, when predation risk is high. In our study, some preference for nocturnal migration was expected given that the study occurred during winter at water temperatures ranging from 6°C to 12°C. Evidence suggests that at higher temperatures, juvenile salmon in the Delta migrate preferentially during the day (Wilder and Ingram 2006). Although we have illustrated how gate operations can be managed to minimize entrainment by accounting for the behavior of hatchery-origin late-fall Chinook Salmon, management actions must also account for variation in behavior among species, life history strategies, life stages, and environmental conditions.

Our modeling approach may be applied more broadly both within and outside of the Delta. Within the Delta, a suite of management actions known as the Bay Delta Conservation Plan (BDCP) is currently being considered for implementation. Specifically, one BDCP scenario proposes to divert up to 255 m^3/s from the Sacramento River upstream of the Delta and convey this water through tunnels to pumping stations in the southern Delta (BDCP 2013). Similar to our simulation example, our entrainment model could be coupled with hydrodynamic simulations to quantify the effect of this management action on the proportion of the population entrained into the interior Delta. Although the Delta and related management issues are somewhat unique, our analytical approach may also be applicable to other systems. For example, hydroelectric dams typically have alternative routes of fish passage, some of which cause higher mortality (e.g., turbines) than others (e.g., spillways; Bickford and Skalski 2000). Our analytical approach could be used to understand how dam operations influence routing probabilities and, ultimately, total dam passage survival. Moreover, because we were able to link fine-scale variation in the river environment with the fates of individual fish, our modeling approach provides a basis for understanding the underlying mechanisms that give rise to population-level outcomes of management actions. Tools such as this are critically needed to help inform management actions that are intended to recover endangered fish populations while maintaining ecosystem services for human benefit.

ACKNOWLEDGMENTS

Funding for R.W.P.'s involvement with this project was provided by the U.S. Bureau of Reclamation and a CALFED Science Fellowship (Agreement U-04-SC-005 with the California Bay–Delta Authority). Tagging of juvenile salmon, ultrasonic station deployment and interrogation, and tag detection database maintenance were supported by a grant from the California Bay–Delta Authority (Agreement U-05-SC-047). We thank Kevin Niemela, Kurtis Brown, and Scott Hamelburg of the U.S. Fish and Wildlife Service (USFWS) and the staff of Coleman National Fish Hatchery for providing the late-fall Chinook Salmon and logistical support for this study. We are grateful to the staff of the USFWS in Stockton, California, for assisting with transport, holding, and release of tagged fish. Reference to trade names does not imply endorsement by the U.S. Government. We thank four anonymous reviewers whose comments improved the manuscript.

REFERENCES

Agresti, A. 2002. Categorical data analysis. Wiley, Hoboken, New Jersey.

BDCP (Bay Delta Conservation Plan). 2013. 2013 BDCP draft chapters available for review. Available: http://baydeltaconservationplan.com/Library/DocumentsLandingPage/BDCPDocuments.aspx. (November 2013).

Bickford, S. A., and J. R. Skalski. 2000. Reanalysis and interpretation of 25 years of Snake–Columbia river juvenile salmonid survival studies. North American Journal of Fisheries Management 20:52–68.

Burnham, K. P., and D. R. Anderson. 2002. Model selection and multimodel inference: a practical information-theoretic approach. Springer, New York.

CADWR (California Department of Water Resources). 2013. Delta simulation model II (DSM2). Available: http://baydeltaoffice.water.ca.gov/modeling/deltamodeling/dsm2usersgroup.cfm. (November 2013).

CH2MHILL. 2009. Delta simulation model II (DSM2) recalibration. Prepared for the California Department of Water Resources, Sacramento.

Chapman, E. D., A. R. Hearn, C. J. Michel, A. J. Ammann, S. T. Lindley, M. J. Thomas, P. T. Sandstrom, G. P. Singer, M. L. Peterson, R. B. MacFarlane, and A. P. Klimley. 2013. Diel movements of out-migrating Chinook Salmon (*Oncorhynchus tshawytscha*) and steelhead trout (*Oncorhynchus mykiss*) smolts in the Sacramento/San Joaquin watershed. Environmental Biology of Fishes 96:273–286.

Cloern, J. E., N. Knowles, L. R. Brown, D. Cayan, M. D. Dettinger, T. L. Morgan, D. H. Schoellhamer, M. T. Stacey, M. van der Wegen, R. W. Wagner, and A. D. Jassby. 2011. Projected evolution of California's San Francisco Bay–Delta River system in a century of climate change. PLoS (Public Library of Science) ONE [online serial] 6(9):e24465.

Hayhoe, K., D. Cayan, C. B. Field, P. C. Frumhoff, E. P. Maurer, N. L. Miller, S. C. Moser, S. H. Schneider, K. N. Cahill, E. E. Cleland, L. Dale, R. Drapek, R. M. Hanemann, L. S. Kalkstein, J. Lenihan, C. K. Lunch, R. P. Neilson, S. C. Sheridan, and J. H. Verville. 2004. Emission pathways, climate change, and impacts on California. Proceedings of the National Academy of Sciences of the USA 101:12422–12427.

Hosmer, D. W., and S. Lemeshow. 2000. Applied logistic regression. Wiley, New York.

Low, A. F., J. White, and E. Chappel. 2006. Relationship of Delta Cross Channel gate operations to loss of juvenile winter-run Chinook Salmon at the CVP/SWP delta facilities. California Department of Fish and Game. Available: http://science.calwater.ca.gov/pdf/ewa/EWA_delta_cross_channel_closures_06_111406.pdf. (November 2013).

Maurer, E. P. 2007. Uncertainty in hydrologic impacts of climate change in the Sierra Nevada, California, under two emissions scenarios. Climatic Change 82:309–325.

Metcalfe, N. B., N. H. C. Fraser, and M. D. Burns. 1998. State-dependent shifts between nocturnal and diurnal activity in salmon. Proceedings of the Royal Society of London B 265:1503–1507.

Metcalfe, N. B., N. H. C. Fraser, and M. D. Burns. 1999. Food availability and the nocturnal vs. diurnal foraging trade-off in juvenile salmon. Journal of Animal Ecology 68:371–381.

Newman, K. B., and P. L. Brandes. 2010. Hierarchical modeling of juvenile Chinook Salmon survival as a function of Sacramento–San Joaquin Delta water exports. North American Journal of Fisheries Management 30:157–169.

Nichols, F. H., J. E. Cloern, S. N. Luoma, and D. H. Peterson. 1986. The modification of an estuary. Science 4738:567–573.

Perry, R. W. 2010. Survival and migration dynamics of juvenile Chinook Salmon (*Oncorhynchus tshawytscha*) in the Sacramento–San Joaquin River Delta. Doctoral dissertation. University of Washington, Seattle.

Perry, R. W., P. L. Brandes, J. R. Burau, A. P. Klimley, B. MacFarlane, C. Michel, and J. R. Skalski. 2013. Sensitivity of survival to migration routes

used by juvenile Chinook Salmon to negotiate the Sacramento–San Joaquin River Delta. Environmental Biology of Fishes 96:381–392.

Perry, R. W., P. L. Brandes, P. T. Sandstrom, A. Ammann, B. MacFarlane, A. P. Klimley, and J. R. Skalski. 2010. Estimating survival and migration route probabilities of juvenile Chinook Salmon in the Sacramento–San Joaquin River Delta. North American Journal of Fisheries Management 30:142–156.

R Development Core Team. 2013. R: a language and environment for statistical computing. R Foundation for Statistical Computing, Vienna. Available: http://www.R-project.org/. (November 2013).

Reebs, S. G. 2002. Plasticity of diel and circadian activity rhythms in fishes. Reviews in Fish Biology and Fisheries 12:349–371.

Singer, G. P., A. R. Hearn, E. D. Chapman, M. L. Peterson, P. E. LaCivita, W. N. Brostoff, A. Bremner, and A. P. Klimley. 2013. Interannual variation of reach specific migratory success for Sacramento River hatchery yearling late-fall-run Chinook Salmon (*Oncorhynchus tshawytscha*) and steelhead trout (*Oncorhynchus mykiss*). Environmental Biology of Fishes 96: 363–379.

Steel, A. E., P. T. Sandstrom, P. L. Brandes, and A. P. Klimley. 2013. Migration route selection of juvenile Chinook Salmon at the Delta Cross Channel, and the role of water velocity and individual movement patterns. Environmental Biology of Fishes 96:215–224.

SWRCB (State Water Resources Control Board). 1995. Water quality control plan for the San Francisco Bay/Sacramento–San Joaquin Delta estuary. Available: http://www.waterboards.ca.gov/waterrights/water_issues/programs/bay_delta/wq_control_plans/1995wqcp/docs/1995wqcpb.pdf. (November 2013).

Vogel, D. A. 2008. Pilot study to evaluate acoustic-tagged juvenile Chinook Salmon smolt migration in the northern Sacramento–San Joaquin Delta 2006–2007. Prepared for the California Depart of Water Resources, Sacramento.

Wilder, R. M., and J. F. Ingram. 2006. Temporal patterns in catch rates of juvenile Chinook Salmon and trawl net efficiencies in the lower Sacramento River. IEP (Interagency Ecological Program) Newsletter 19(1): 18–28.

Williams, J. G. 2008. Mitigating the effects of high-head dams on the Columbia River, USA: experience from the trenches. Hydrobiologia 609:241–251.

Williams, R. N. 2006. Return to the river: restoring salmon to the Columbia River. Elsevier, San Diego, California.

Romine et al. Animal Biotelemetry 2014, 2:3
http://www.animalbiotelemetry.com/content/2/1/3

Animal Biotelemetry

RESEARCH Open Access

Identifying when tagged fishes have been consumed by piscivorous predators: application of multivariate mixture models to movement parameters of telemetered fishes

Jason G Romine[1*], Russell W Perry[1], Samuel V Johnston[2], Christopher W Fitzer[3], Stephen W Pagliughi[4] and Aaron R Blake[5]

Abstract

Background: Consumption of telemetered fishes by piscivores is problematic for telemetry studies because tag detections from the piscivore could introduce bias into the analysis of telemetry data. We illustrate the use of multivariate mixture models to estimate group membership (smolt or predator) of telemetered juvenile Chinook salmon (*Oncorhynchus tshawytscha*), juvenile steelhead trout (*O. mykiss*), striped bass (*Morone saxatilis*), smallmouth bass (*Micropterus dolomieu*) and spotted bass (*M. punctulatus*) in the Sacramento River, CA, USA. First, we estimated two types of track statistics from spatially explicit two-dimensional movement tracks of telemetered fishes: the Lévy exponent (b) and tortuosity (τ). Second, we hypothesized that the distribution of each track statistic would differ between predators and smolts. To estimate the distribution of track statistics for putative predators and smolts, we fitted a bivariate normal mixture model to the mixed distribution of track statistics. Lastly, we classified each track as a smolt or predator using parameter estimates from the mixture model to estimate the probability that each track was that of a predator or smolt.

Results: Tracks classified as predators exhibited movement that was tortuous and consistent with prey searching tactics, whereas tracks classified as smolts were characterized by directed, linear downstream movement. The estimated mean tortuosity was 0.565 (SD = 0.07) for predators and 0.944 (SD = 0.001) for smolts. The estimated mean Lévy exponent was 1.84 (SD = 1.23) for predators and −0.304 (SD = 1.46) for smolts. We correctly classified 90% of the *Micropterus* species and 72% of the striped bass as predators. For tagged smolts, 80% of Chinook salmon and 74% of steelhead trout were not classified as predators.

Conclusions: Mixture models proved valuable as a means to differentiate between salmonid smolts and predators that consumed salmonid smolts. However, successful application of this method requires that telemetered fishes and their predators exhibit measurable differences in movement behavior. Our approach is flexible, allows inclusion of multiple track statistics and improves upon rule-based manual classification methods.

Keywords: Telemetry, Predation, Survival, Chinook salmon smolt, Steelhead trout smolt, Striped bass, Smallmouth bass, Spotted bass, Sacramento River Delta

* Correspondence: jromine@usgs.gov
[1]US Geological Survey, Western Fisheries Research Center, Columbia River Research Laboratory, Cook, WA, USA
Full list of author information is available at the end of the article

Background

An inherent issue with telemetry of fishes is that they may be preyed upon during the course of telemetry studies [1-4] potentially leading to incorrect conclusions about movement, behavior or survival. This problem is especially acute in western rivers of the United States where telemetered migrating juvenile salmonids may experience high mortality rates due to predation from piscivorous fishes [5-7]. More specifically, our concern is with predation of telemetered emigrating juvenile salmonids by non-native striped bass (*Morone saxatilis*) and two species of non-native black basses, smallmouth bass (*Micropterus dolomieu*) and spotted bass (*Micropterus punctulatus*), in the Sacramento-San Joaquin River Delta (Figure 1). Here, telemetry-based survival studies (for example, [6]) assume that tag detections are from live juvenile salmonids, rather than tagged salmonids consumed by predatory fishes (hereafter, consumed smolts). Consumed smolts subsequently detected at downstream locations may lead to inflated survival estimates. Thus, in this example, it is important to differentiate between detections of live tagged smolts and consumed smolts to avoid bias in survival estimates.

Few quantitative methods have been developed to distinguish between telemetry detections of live study fishes and consumed fishes in situations where recapture of the study species is infeasible. Several studies have taken different approaches to resolving this issue, but most rely on subjective classification rules based on expert opinion rather than objective quantitative methods. For example, Vogel [8] proposed that tag detections be examined at three scales of resolution to classify an acoustic tag as a live or consumed smolt: 1) examining the acoustic pattern of a tag as it passes a hydrophone, 2) comparing movement direction relative to flow direction (typically, emigrating smolts move with the flow) and 3) comparing the movement rate of a given tag against the movement rates of the entire tagged population. Friedl *et al*. [9] used three criteria for determining natural mortality of telemetered juvenile spot (*Leiostomus xanthurus*) in estuarine creeks. Tagged fish were considered moribund or consumed if: 1) the tag ceased to move, 2) swim speeds were not within the normal range for the study fish or 3) the fish failed to emigrate from the rearing habitat. Thorstad *et al*. [2] examined depth profiles produced by pressure tags to identify Atlantic salmon (*Salmo salar*) smolts thought to have been consumed by predators. They hypothesized that sudden changes in the vertical distribution of the tag indicated predation events. Kawabata *et al*. [3] used atypical behavior based on detection patterns of telemetered black-spot tuskfish (*Choerodon schoenleinii*) to predict predation events.

The aforementioned studies relied on subjective opinion to some degree to classify predation manually based on the expected behavior of the tagged fish species. Because such methods are based on expert opinion, they could introduce bias or systematic variation among individual observers examining the detection histories. Furthermore, manual classification methods can be prohibitively laborious for large telemetry studies using thousands of tags because they require visual inspection of the entire detection history of each tag.

In contrast to user-defined classification rules, statistical classification methods can objectively classify different patterns in telemetry data. Specifically, when spatially explicit two-dimensional telemetry data are collected, mathematical characteristics of the time series of *x-y* positions (hereafter, fish tracks) may be useful in identifying behaviors indicative of tagged fish and their predators. For example, Morales *et al*. [10] used turning angles and daily movement rates to classify movement patterns of telemetered elk (*Cervus elaphus*) into two behaviors: encamped and exploratory. The encamped behavior was characterized by short movements between relocations and somewhat randomly distributed turning angles, whereas the exploratory behavior was characterized by longer, more consistent unidirectional movement.

As with the elk example, if tagged fish and predators exhibit different movement behaviors, then track statistics such as movement rate and turning angle would likely differ between the two groups [5,11,12]. For example, to maximize efficiency of their seaward migration, emigrating smolts will likely exhibit linear movement that is oriented with the direction of flow [12]. This movement would be characterized by shallow turning angles [13,14] and is similar to the exploratory behavior found by Morales *et al*. [10]. In contrast, the track of a foraging predator would likely exhibit steep turning angles and a non-linear trajectory, consistent with patrolling or prey-searching tactics or an encamped behavior characteristic of a fish holding in feeding lanes or eddies. These differences in track characteristics present are an opportunity to use quantitative methods to classify tracks as being from a smolt or predator.

While turning angles provide information about track complexity, other movement statistics may capture different aspects of behavior, which can be used to inform track classification. For example, in areas where prey are patchily distributed or in low abundance, predators often exhibit Lévy walk-type behavior [15], which may increase prey encounter rates compared to using a simple correlated random walk search [16,17]. Lévy walks are characterized by clusters of short, seemingly random steps followed by less frequent and longer directed steps [17,18]. Thus piscivorous predators constrained by abiotic conditions such as flow, may exhibit similar behavior, choosing to hold in optimal feeding lanes, moving small

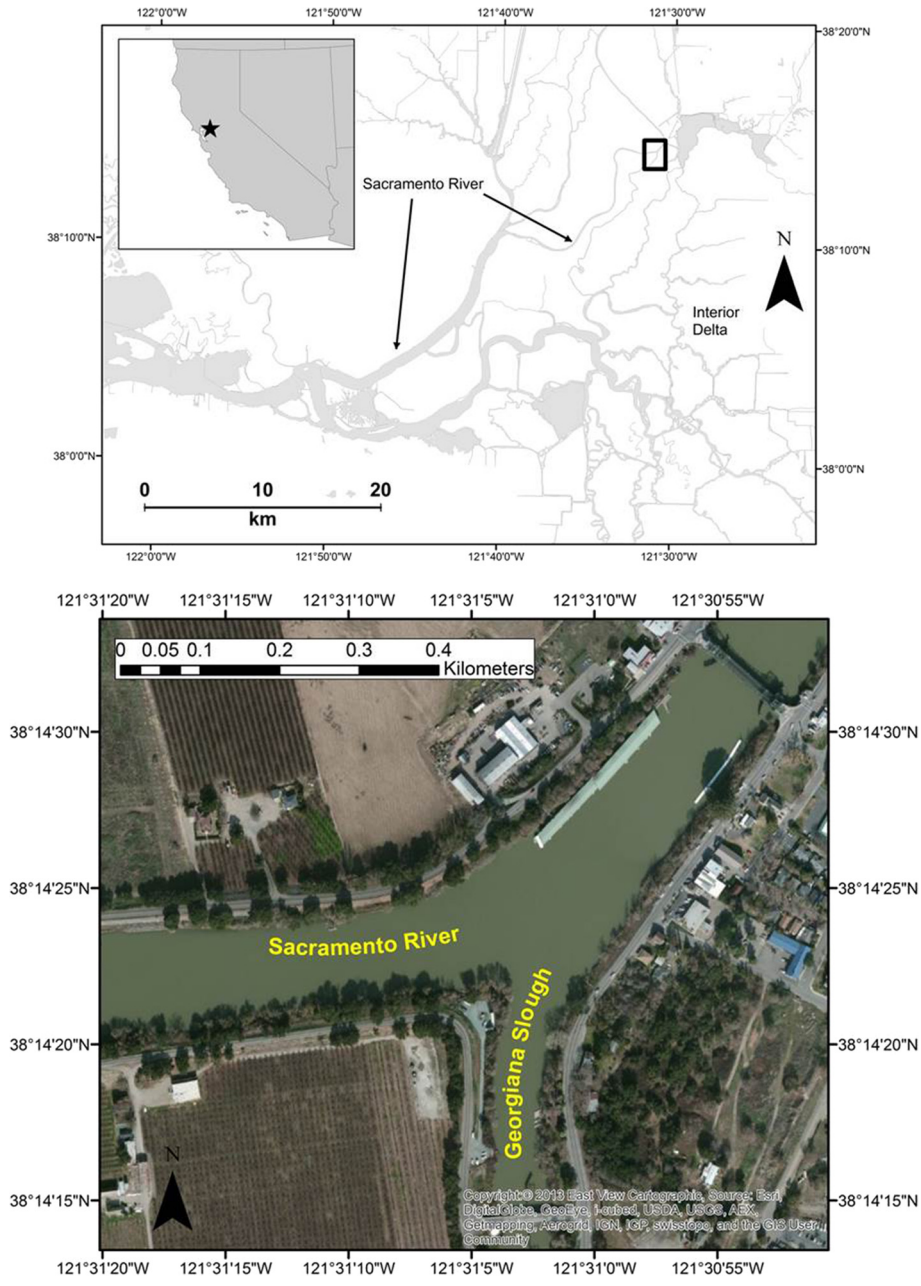

Figure 1 Map showing location of the study area. The box in the top panel shows the location of the study area in the Sacramento-San Joaquin River Delta. The bottom panel shows the detail of the study area.

distances and only making periodic directed forays to other feeding areas (for example, in response to changing hydrodynamics caused by the tides). In contrast, we would expect the distribution of step lengths of a smolt emigrating through a telemetry array to be normally distributed [12] and unrepresentative of a Lévy walk.

The work presented here was motivated by a larger study designed to evaluate whether a non-physical barrier reduced entrainment of juvenile salmonids into a low-survival migration route (see [19] for the experimental design and description). However, prior to analysis of the telemetry data, it was necessary to identify and remove the telemetry tracks of tagged smolts that may have been consumed by predators, as tracks of consumed smolts could bias the results. In Perry *et al.* [19], predators were identified through manual examination of the telemetry tracks using a rule-based classification. To reduce the amount of manual labor and eliminate the subjective nature of rule-based classification, we developed a statistical approach to identify consumed smolts, which were then removed from

the dataset used for analyses in the larger study. To differentiate tracks of live tagged smolts from tagged smolts consumed by predators, we fitted multivariate mixture models to track statistics from a telemetry study conducted in the Sacramento-San Joaquin River Delta. We first estimated the Lévy exponent and tortuosity for each track. We then fitted a bivariate normal mixture model to these statistics to estimate the parameters of the smolt- and predator-specific distributions from the combined bivariate distribution of the track statistics. Given these distributions, we then quantified the probability that any given track exhibited characteristics that were consistent with predator- or smolt-like movement and used this information to classify the track as due to a predator or smolt.

Results

In total, 1,413 Chinook salmon (*Oncorhynchus tshawytscha*), 259 steelhead trout (*O. mykiss*), 14 smallmouth bass (*Micropterus dolomieu*), 6 spotted bass (*M. punctulatus*) and 29 striped bass (*Morone saxatilis*) tracks were analyzed. Of these, 155 chinook salmon, 41 steelhead trout, 13 smallmouth bass, 6 spotted bass and 20 striped bass tracks consisted of multiple segments (the fish departed the study area and then returned). In total, 1,852 Chinook salmon, 356 steelhead trout, 443 smallmouth bass, 232 spotted bass and 129 striped bass track segments were pooled and analyzed. Our *a priori* hypotheses about the distributions of track statistics were supported by the estimated distributions from the mixture model and the observed distribution of track statistics for known predators (Figure 2). The mixture model classified 50.6% and 49.4% of the track segments as predators (λ_P) and smolts (λ_S), respectively. The fitted distributions for the Lévy parameter were centered at −0.304 (SD = 1.46) for smolt-like and 1.84 (SD = 1.23; Table 1) for predator-like behavior, which is consistent with our expectations of smolt-like and predator-like behavior. The distribution of Lévy coefficients for known predators (mean = 2.10, SD = 1.12) was similar to that estimated by the mixture model, lending further support to this approach. Examples of tracks for putative predators and smolts show how the step length distributions for predators typically followed a power function, characterized by a greater frequency of short steps than longer steps (Figure 3). In contrast, step lengths of smolt-like tracks were approximately normally distributed with a slope close to zero (Figure 3).

The fitted distributions for tortuosity were centered at 0.944 (SD = 0.001) and 0.565 (SD = 0.070), with an order of magnitude difference in the standard deviation of these distributions (Table 1). The distribution of tortuosity for known predators (mean = 0.523, SD = 0.281) was similar to the distribution estimated for predators by the mixture model. These findings support our *a priori* hypothesis that smolts would have more linear, less tortuous tracks than predators.

Our approach using the mixture model accurately classified 72% of the striped bass, 86% of the smallmouth bass and 100% of the spotted bass as predators (Table 2). Of the 1,413 Chinook salmon tracks analyzed, our approach classified 281 (20%) tracks as being predators and 1,131 (80%) tracks as being smolts. Of the 259 steelhead trout tracks analyzed, 68 (26%) tracks were classified as predators and 191 (74%) were classified as smolts. Unlike known predator tags, we were not able to validate the classification of tags implanted in smolts because tagged smolts could not be recaptured.

The total probability for tracks consisting of multiple segments was estimated as:

$$P_{\text{total},k} = 1-\left(1-p_{i,j,k}\right) \times \left(1-p_{i+1,j,k}\right) \times \ldots \times \left(1-p_{n,j,k}\right)$$

where $p_{i,j,k}$ is the probability of the ith segment $(i = 1, \ldots, n)$ of track j belonging to group k (smolt or predator).

The distribution of probabilities of being a predator was bimodal with distinct modes near zero and one (Figure 4). These findings show that most tracks could be assigned as predator or smolt with little uncertainty in the classification. In contrast, a few track segments had probabilities in the range 0.3 to 0.7 where uncertainty about classification is greater. The majority of salmonid tags that moved through the telemetry array multiple times were classified as predators, which was consistent with the movement pattern of tags known to be implanted to predators (see the example of a multiple-pass track in Figure 5). Of the 154 Chinook salmon tracks that consisted of multiple track segments, 106 (68.8%) were classified as predators. Of the 259 steelhead trout tags, 41 tracks consisted of multiple segments, 31 (75.6%) of which were classified as predators. Consistent with these findings, tagged predators made many forays through the array. The 49 tagged predators (49 tracks) produced 809 track segments, of which 13.3% of these track segments were misclassified as smolts. Most tracks consisting of more than four segments were classified as predators.

Discussion

In telemetry studies of fishes, predation by piscivores may result in erroneous conclusions because the tracks reflect the predator movements rather than the fish originally tagged. Researchers will seldom have information to verify whether detections from tags actually arise from movements of a predator that has consumed a tagged fish. Our mixture model approach explicitly accounts for the unknown state of tags (predator or smolt,

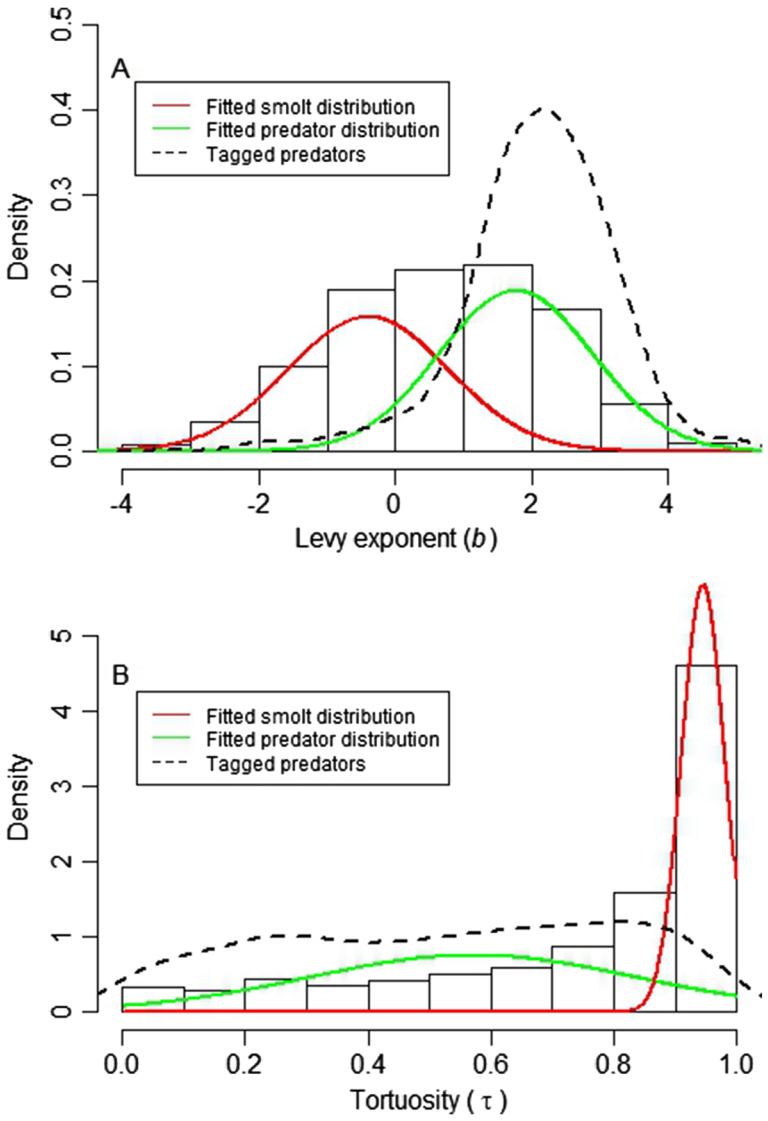

Figure 2 Distributions of the Lévy exponent (A) and tortuosity (B) for smolt (red line) and predator (green line) populations estimated using a bivariate mixture model of normal distributions. The histogram shows the mixed empirical distribution of track statistics for which the true population assignment is unknown (that is, predator or smolt). The black dashed line shows the distribution of track statistics for known predators.

Table 1 Parameter estimates from the mixture model

Parameter	Mean	Estimate[a]	Standard deviation	Estimate[a]
Lévy exponent, predators	$\mu_{P,b}$	1.84 (0.033)	$\sigma_{P,b}$	1.23 (0.048)
Lévy exponent, smolts	$\mu_{S,b}$	−0.304 (0.008)	$\sigma_{S,b}$	1.46 (0.003)
Tortuosity, predators	$\mu_{P,\tau}$	0.565 (0.037)	$\sigma_{P,\tau}$	0.070 (0.048)
Tortuosity, smolts	$\mu_{S,\tau}$	0.944 (0.001)	$\sigma_{S,\tau}$	0.001 (0.0001)

[a]The parameters were estimated from the entire population of track segments (tagged salmonids and tagged predators). Values in parentheses are standard errors estimated from 500 bootstrap simulations.

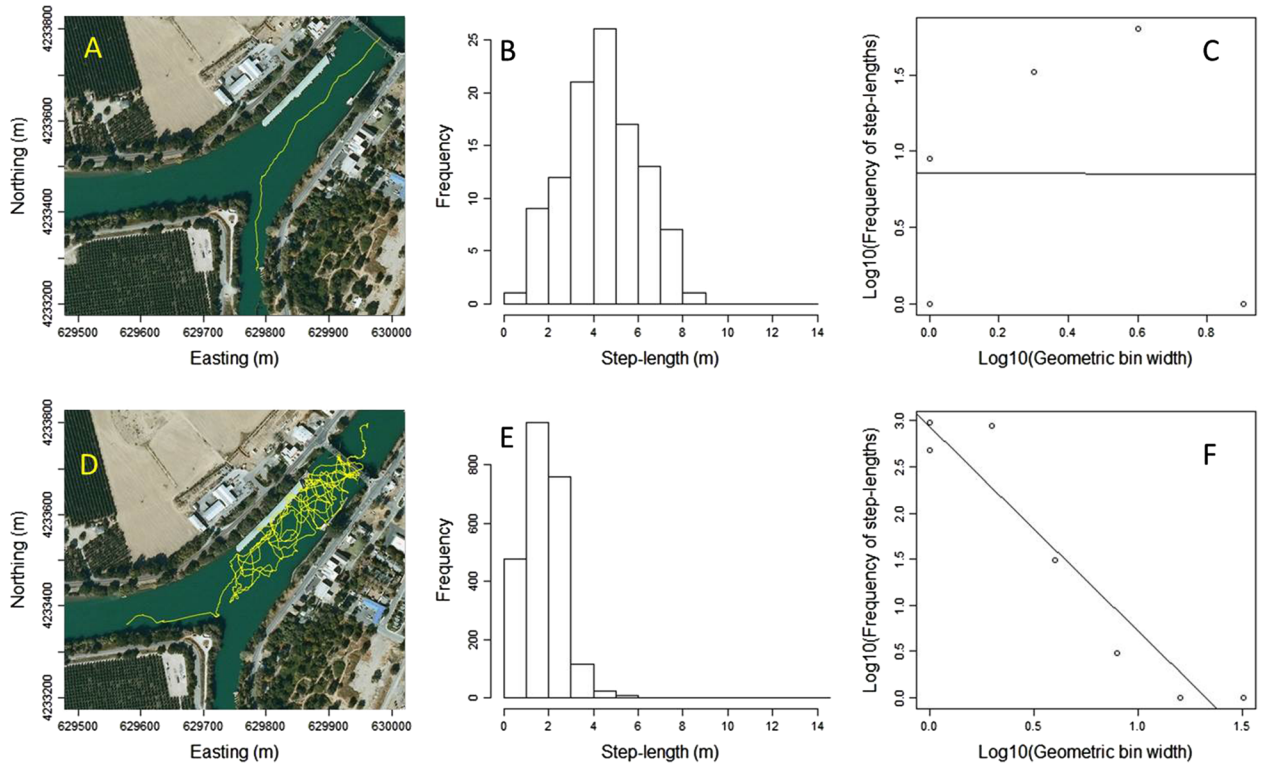

Figure 3 Comparison of tracks between an assumed smolt and assumed predator. Panels **(A,B,C)** are for the smolt and **(D,E,F)** for the predator. **(A,D)** Two-dimensional tracks. **(B,E)** Distribution of step-length frequencies. **(C,F)** $\log_{10}$-transformed step lengths versus $\log_{10}$-transformed frequency of step lengths. Solid lines in **(**C**)** and **(F)** are the linear regression fit to the log-transformed data. The slope of the regression line is the estimate of the Lévy exponent.

in this case) by using behavioral characteristics of movement paths to segregate smolt-like versus predator-like behavior. The mixture model was able to separate clearly distributions of track statistics that were consistent with hypothesized smolt and predator behavior. The mixture model also provides a probabilistic estimate of whether a given track segment arises from a predator or smolt. Furthermore, relative to the manual review of tracks, which requires considerable labor, the processing time for the mixture model is of the scale of hours.

We believe the mixture model approach is a sound alternative to the manual review of each track, but our approach need not eliminate classification schemes that include some level of manual review. Because the mixture model yields a probabilistic estimate of a track's source population, there will be regions of high certainty where a track's characteristics are consistent with those for a smolt or predator, and regions of relative uncertainty where manual review may still provide a useful "second opinion" for a track's classification (Figure 4). For example, one approach would be to divide the probability space into three equal-size regions (that is, 0 to 0.33, 0.33 to 0.66 and 0.66 to 1). Tracks falling in the central region, where the classification is less certain, could be manually reviewed and auxiliary information (for example, movement against the flow) could help inform the classification. Such an approach would provide a more systematic, quantitative method for classifying tracks while still retaining some level of manual review.

It is important to recognize that any classification method, whether statistical or manual, will be unlikely to classify tracks with 100% accuracy because both predators and smolts may exhibit multiple behavioral modes that lead to misclassification. That is, sometimes a predator track may look like a smolt track and sometimes a smolt may act like a predator. This aspect of fish behavior is

Table 2 Final classification of tags moving through the acoustic array

	Model classification	
	Smolt	**Predator**
Striped bass	8	21
Smallmouth bass	2	12
Spotted bass	0	6
Chinook salmon	1,131	281
Steelhead trout	191	68

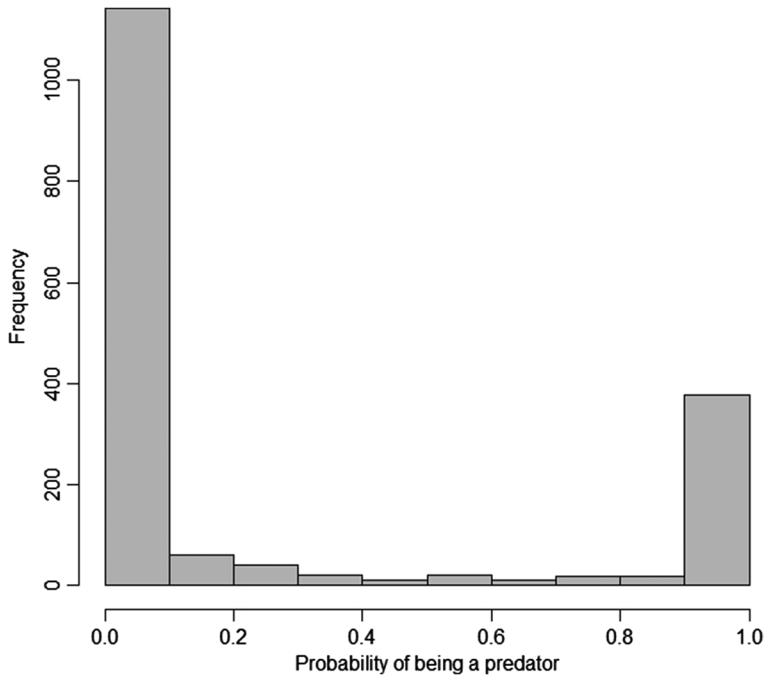

Figure 4 Results from the mixture model illustrating the probability of tracks being classified as predators.

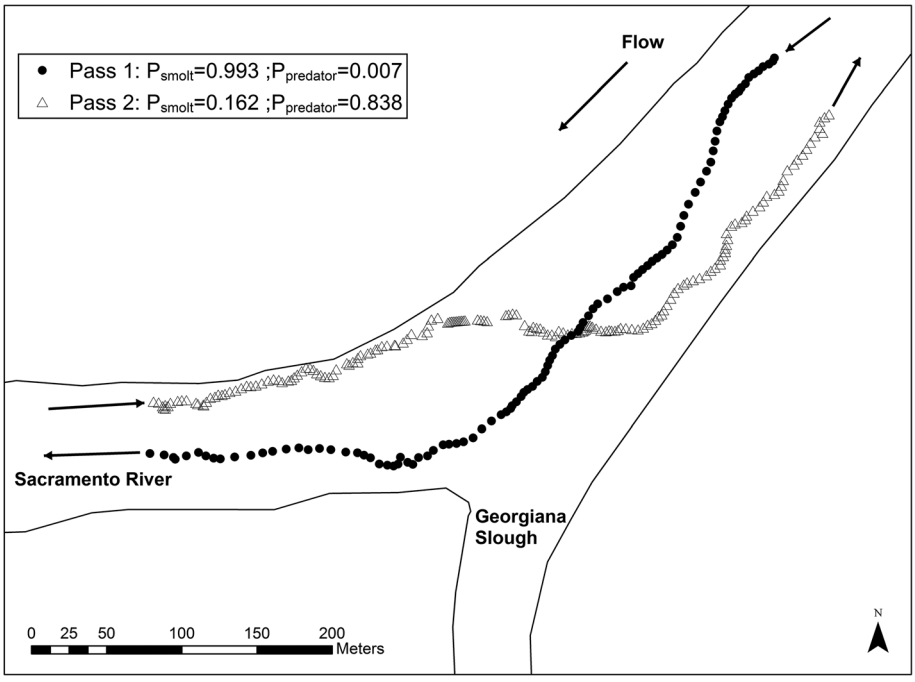

Figure 5 Example of a multiple segment track (acoustic tag 2007.01) in the study area. The first segment (solid circles) had a higher probability of being a smolt ($P_{smolt} = 0.986$) and the second segment with an upstream movement (triangles) had a greater probability of being a predator ($P_{predator} = 0.738$).

captured in our mixing model as the overlap in the distributions of track statistics for predator and prey (Figure 2). Specifically, the predator distribution overlaps the smolt distribution, indicating that predator tracks sometimes resemble a smolt track. For example, one striped bass had four distinct track segments and each track segment had different characteristics leading to its classification as both a smolt and predator (Figure 6). The first two track segments were classified as a predator with near certainty, and the third was also classified as a predator but with less certainty. In contrast, the final track was classified as a smolt because the striped bass moved quickly through the array in a linear fashion. In practice, tracks from known tagged predators would always be classified as predators despite their similarity to smolt tracks. However, including tagged predators in the analysis was important for informing parameter estimates of predator tracks and validating our classification methods for known predators.

Likewise, it is possible for smolts to exhibit movement behavior that may be mistaken for a predator. For example, under low river flows, Chinook salmon smolts may hold in areas of suitable habitat along migration pathways, a behavior similar to predator holding behavior [20,21]. In addition, predator avoidance behavior could cause the tracks of smolts to be classified as those of predators. Chapman *et al.* [22] found significant differences in migration rates during the day and night for Chinook salmon smolts in the Sacramento River. Chinook salmon migrated further during the night than during daytime hours, suggesting some smolts in our study may have exhibited holding behavior similar to predators during the day when migration may have slowed. Bradford and Higgins [23] also reported lower activity levels for both juvenile Chinook salmon and steelhead trout during the day. Furthermore, Atlantic salmon have also been shown to have a preference for migrating during the nighttime hours rather than during the day [24]. Notwithstanding multiple modes of behavior that would pose difficulty for any classification scheme, our mixture model approach provides a quantitative method for classifying behaviors that are most commonly associated with the movement of predators and smolts.

As previously stated, our approach does not eliminate the misclassification of smolts as predators, but does provide a quantitative probabilistic technique to reduce this error. Nevertheless, misclassification can introduce bias into survival estimates when this method is applied for large survival studies. For example, Buchanan *et al.* [25] provided two estimates of survival for out-migrating Chinook salmon smolts in the Sacramento-San Joaquin River Delta in 2010: one estimate was calculated where the data for putative predators was removed and the other included data for putative predators. Survival estimated

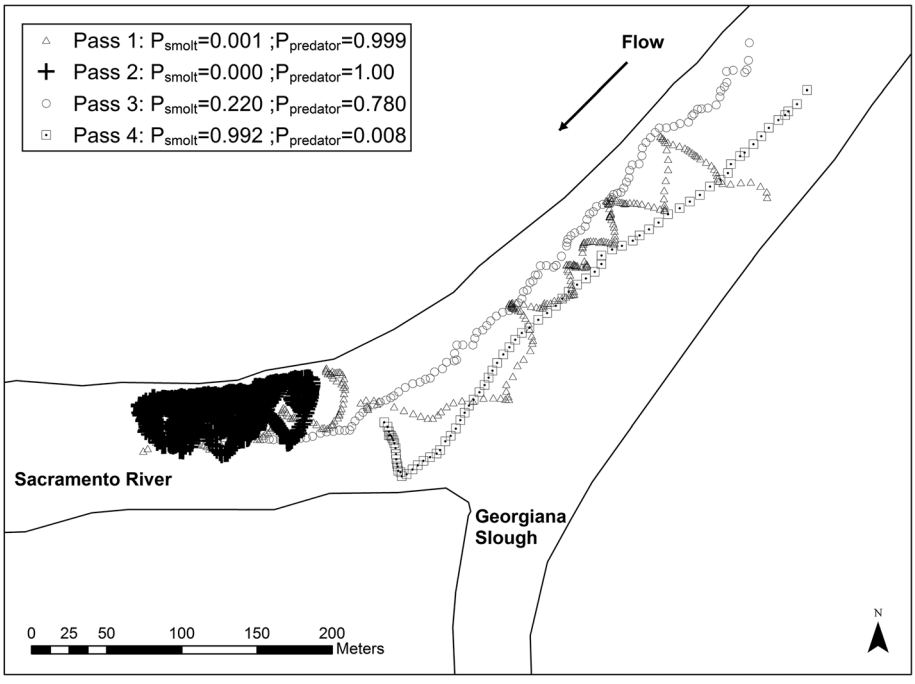

Figure 6 Track of tag 2952.15, a tagged striped bass in the study area. The figure illustrates the different behaviors of a striped bass. Segment four had a higher probability of being a smolt ($P_{smolt} = 0.971$) than a predator ($P_{predator} = 0.029$), whereas all other segments had higher probabilities of being a predator ($P_{predator} > P_{smolt}$).

for the dataset without predators was 0.05, whereas survival estimated from the dataset with predators was 0.11. The excessive misclassification of smolts as predators could result in negatively biased survival estimates, whereas failure to remove predators may result in positive bias. Given that no method can completely eliminate uncertainty associated with identifying predators, short of recapture, researchers should present the sensitivity of their results to the classification methods used.

We used two statistics to characterize movement behavior in our analysis, but our approach can be easily extended to incorporate more than two track statistics. In our case, the use of both tortuosity and the Lévy exponent in the multivariate mixture model led to high certainty in the classification of predator- or smolt-like behavior (Figure 4). We considered additional types of movement statistics (for example, swimming speed and turning angle), but they failed to improve the analysis because they were highly correlated with the other track statistics. Including additional types of track statistic should improve the analysis when the distribution of the statistic differs between the tagged fish and its predator, and the candidate statistic has a low correlation with the other track statistics in the analysis.

Although our approach provides a sound basis for estimating predation on juvenile salmonids from two-dimensional movement tracks, we had no mechanism to verify whether after tagging smolts, the tracks classified as smolts or predators were indeed from smolts or predators. In contrast, Svendsen *et al*. [14] utilized a trap below a water diversion to verify that after tagging Atlantic salmon smolts, the fish tracks were indeed from tagged smolts. Given the dynamics of our study area, the recapture of tagged fishes was impractical. Although recapture of study fish in most cases will likely be impossible, our classification methods could be further tested in studies where tagged fish can be recaptured. However, we did observe 12 smolt tags that appeared to have been defecated within the array, suggesting the fish may have been consumed. These tags initially showed the expected movement then ceased forward movement for the duration of the tag's battery life. The mixture model classified these tags as predators. These tags do provide some support for our methods, but we could not rule out other explanations. Lab studies have shown gut evacuation rates of consumed tagged smolts to be of the order of days to weeks (SVJ, unpublished data). Other possible causes include tag shedding or mortality from other causes. However, tag shedding would be highly unlikely (Liedtke, unpublished data). Other approaches for verification of our methods might include the coupling of an intensive acoustic array and single hydrophones in adjacent areas. This would provide insights into the migratory behavior of the tag, which could be used to support or refute classifications assigned by the mixture model.

Conclusion

The approach we have presented here provides the researcher with a flexible and quantitative method to distinguish between behavioral modes of prey and predator as observed through two-dimensional telemetry tracks. This is an improvement upon previous subjective smolt and consumed smolt classification schemes and should be considered when examining two-dimensional telemetry data from small-bodied fishes. In addition to providing a quantitative means to classifying telemetry tracks, the approach includes a measure of uncertainty through the estimation of group membership probabilities. As seen in Figure 4, the distribution of predator probabilities was skewed to zero or one, suggesting smolt- and predator-like behavior could be identified with little uncertainty using the multivariate mixture model approach. Furthermore, the method is flexible and allows for multiple track statistics or behavioral estimates to be used in the model fitting. In our analysis, we only used two statistics, tortuosity and the Lévy exponent. However, more metrics could be used. This study takes an important step in furthering the methods of telemetry data analysis where predation of telemetered fishes is a concern.

Methods

Study area

The study area was located 36 km south of Sacramento, CA, where the Georgiana Slough branches off the Sacramento River (Figure 1). The average water depth within the study area was 6.3 m and the width of the channel was 100 m. Discharge in this area ranges from negative (an upstream flow caused by tidal forcing) to 1,132 $m^3.s^{-1}$ during spring floods. During the study flows ranged from −127 $m^3.s^{-1}$ to 849 $m^3.s^{-1}$. This area is a critical junction for out-migrating juvenile salmonids because emigrating smolts that are entrained into the Georgiana Slough have much lower survival rates than those that remain in the Sacramento River [6].

Acoustic telemetry

Juvenile salmonids were telemetered with acoustic tags that operated at 307 kHz (Hydroacoustic Technology Inc (HTI), Seattle, WA). The tags were 6.5 mm in diameter and 16.3 mm in length and averaged 0.67 g in air. The expected battery life was 15 days (HTI Model 795 Lm). Predators were telemetered using tags that operated at 307 kHz, were 11.0 mm in diameter, 25.0 mm in length and averaged 4.5 g in air. The expected battery life was 105 days (HTI Model 795 Lg). Each tag emitted a unique acoustic signal composed of a primary and secondary pulse. The pulse rate of tags ranged from 2.003 s

to 3.474 s and the pulse length of the transmitted signal was 0.003 s.

The acoustic array consisted of 34 hydrophones (HTI, Model 590) installed throughout the study site. Hydrophones were installed near the surface and bed of the river and were arranged to enable three-dimensional positioning of the acoustic transmitters (hereafter referred to as tags) as fish moved through the study area. Hydrophones were connected via cable to receivers (HTI Model 290 Acoustic Tag Receivers) located on shore. Two receivers were used to collect and store acoustic data from the 34 hydrophones. Telemetry data were processed using vendor-supplied software to acquire, store and identify the acoustic signals.

Positions of tags were identified by calculating the differences in arrival times of tag transmissions at individual hydrophones in the array. Positioning required transmissions to be recorded by a minimum of four hydrophones. Successive locations formed tracks of individual tags.

Fish tagging and release

The salmonid fishes used in the study were juvenile late fall-run Chinook salmon and steelhead trout smolts obtained from the Coleman National Fish Hatchery operated by the US Fish and Wildlife Service (USFWS). The fork length of fishes selected for tagging ranged from 110 mm to 140 mm. The tag burden (tag weight relative to fish weight) for fishes in this size range was less than 5%. The fishes used in the study were transported daily from the hatchery to the tagging and release site located 9 km upstream of the study site. At the release site, the fishes were placed in flow-through containers submerged in the Sacramento River and held there for 18 hr to 24 hr prior to tagging. Following tagging, the fishes were returned to the flow-through containers and held for another 18 hr to 30 hr prior to release.

The fish-tagging protocols were based on Liedtke and Wargo-Rub [26]. Fish were anesthetized using buffered tricaine methanesulfonate (MS-222, 50 to 70 $mg.L^{-1}$) until loss of equilibrium. The fish were then weighed, measured and placed ventral side up on a submerged surgical platform for 5 min or until non-responsive. Their gills were irrigated with MS-222 (20 $mg\ L^{-1}$) during the 2-to-3-min surgical procedure. A small incision was made anterior to the pelvic girdle and a disinfected transmitter was placed within the body cavity. The incision was then closed using two interrupted sutures with Vicryl + 5–0 absorbable suture material. Following surgery, the fish were moved to a recovery container until they had regained equilibrium. After the fish had recovered, they were placed in flow-through containers at a density of four to five fish per container. Tagging operations were conducted twice daily and fish were released approximately every 3 hr during the study period. Fish releases started on 6 March 2012 and continued until 2 May 2012.

Smallmouth bass, spotted bass and striped bass were captured using a hook-and-line. Sampling for predators was confined to a 1.6 km radius from the divergence of the Georgiana Slough and the Sacramento River. However, capture efforts were focused within the immediate study area to avoid transporting and introducing more predators into the study area. Only *Micropterus* species greater than 300 mm in total length and striped bass greater than 360 mm in total length were retained for the study. Fish deemed fit for tagging were immediately placed in an aerated livewell and transported to in-river flow-through containers at the tagging location.

Bass were anesthetized using diffused carbon dioxide in a surgery station livewell. The oxygen level within the surgery station livewell was maintained near saturation via a diffuser and approximately 7 to 10 g of salt was added per liter of water to reduce gill irritation and help control blood hematology and chemistry [27]. The fish became unresponsive within 3 to 5 min following immersion in the carbon dioxide bath and were removed from the immersion bath and inspected for anomalies (for example, general condition of eyes, scales and fins) and general health; unfit individuals were rejected for tagging.

Tags were implanted by making a 10 mm to 12 mm incision parallel to and 2 mm perpendicular to the ventral midline anterior to the pelvic girdle. A sterilized tag was inserted into the peritoneal cavity of the fish and the incision was closed with two simple interrupted sutures using a 26 mm (FS-1) reverse cutting, 9.5 mm circle needle with 3/0 monofilament suture material. Immediately after completion of surgery, the fish were placed in recovery tubes submerged in post-surgery livewells containing freshwater saturated with oxygen. The fish were removed from the recovery tubes after approximately 10 min, but kept in the post-surgery recovery livewell for an additional 20 min. During this time, the fish were observed closely for recovery progress and behavior. After 30 min, if it was determined a fish was fully recovered and exhibiting normal behavior it was moved to an in-river livewell. After 2 hr in the in-river livewell, if it was determined the fish was fully recovered and exhibiting normal behavior it was released into the Sacramento River and the release time noted. Individuals that did not recover or exhibited impaired behavior were euthanized and the tag was retrieved for reuse.

Data analysis

Fish tracks encompassing the entire detection history of Chinook salmon smolts, steelhead trout smolts, striped bass, smallmouth bass and spotted bass were used in the analysis. Tracks were broken into discrete track

segments if the time between successive detections was greater than 30 min. Each track segment was analyzed separately. In other words, a tag that moved through the array, out of the study area, and then returned after 30 min or more was treated as two separate track segments. This resulted in some tracks consisting of multiple track segments. Tracks with fewer than 60 two-dimensional positions were omitted from the analyses. The ping rates of tags varied from 2 to 4 s. Therefore, we discretized track segments at a time step of 8 s using the adehabitatLT package in R [28] to normalize telemetry data and avoid potential bias in track statistics that might arise due to different ping rates between tags [29]. Discretizing uses linear interpolation to estimate a tag's location based on the measured locations occurring prior to and after the 'missing' location. Track segments that had an average speed of less than 0.0009 $m.s^{-1}$ over the span of 4 days were also removed from the analyses as these were motionless tags that were likely defecated by predators or were post-release mortalities.

Two statistics were estimated for each track segment for each fish, tortuosity (τ) and the Lévy exponent (b). Tortuosity (τ) was calculated as a function of the turning angle (θ):

$$\tau = \sqrt{\bar{x}^2 + \bar{y}^2}$$

where

$$\bar{x} = \frac{1}{n}\Sigma_{i=1}^{n}\cos(\theta_i)$$

and

$$\bar{y} = \frac{1}{n}\Sigma_{i=1}^{n}\sin(\theta_i)$$

Here n is the number of relocations and the turning angle (θ) is the change in direction between three successive relocations. A track with tortuosity close to one is considered linear whereas a track with tortuosity near 0.5 is more tortuous or complex.

In Lévy walks, the relation between step length (l) and the frequency of occurrence of a step length follows a power function, $f(l) = al^{-b}$, where a is an intercept parameter and b is the Lévy exponent. Lévy exponents were estimated using the logarithmic binning method following Sims *et al.* [30]. The Lévy exponent was estimated from the slope of the linear regression between log-transformed geometric bin widths and log-transformed bin frequencies of step lengths. A step length is the distance between two successive locations, and the frequency is the number of occurrences of each step length.

After track statistics were estimated for tagged smolts and predators, finite mixture models were fitted to the distributions of track statistics using the mixtools package for R [31]. Finite mixture models are a form of model-based clustering, which uses the expectation maximization algorithm to maximize the likelihood function and estimate parameters of mixed distributions for observations with unknown group membership. In our case, the bivariate distribution of track statistics (the tortuosity τ and the Lévy exponent b) was formed from a mixture of two underlying bivariate normal distributions — one for predators and one for smolts. Our goal was to use the finite mixture model to estimate the parameters of each assumed Gaussian component of the distribution, which then allowed us to estimate the probability that a track segment came from a predator or smolt from the posterior probability distribution.

A priori we assumed that predators would exhibit the encamped behavior described by Morales *et al.* [10], which has larger turning angles resulting in more tortuous tracks and Lévy exponents in the range of one to three (Table 3). In contrast, we hypothesized that smolts would exhibit a more directed path of movement or exploratory behavior, resulting in turning angles close to zero and a resulting tortuosity estimate close to one, which is indicative of a linear path. Furthermore, a lower estimate of the Lévy exponent is indicative of a smolt swimming at a constant speed through the telemetry array.

We used a mixture model and assumed that the distribution was a mixture of two bivariate normal distributions, each with an associated mean (μ) and standard deviation (σ). Thus, the mixture model estimated the parameters of a normal distribution for smolt- and predator-specific tortuosity and the Lévy exponents, resulting in eight parameters: $\mu_{S,b}$, $\sigma_{S,b}$, $\mu_{P,b}$, $\sigma_{P,b}$, $\mu_{S,\tau}$, $\sigma_{S,\tau}$, $\mu_{P,\tau}$ and $\sigma_{P,\tau}$. Here, $\mu_{j,k}$ and $\sigma_{j,k}$ are the mean and standard deviation of a normal distribution for population j (for the predator (P) or smolt (S)) and for track statistic k (the Lévy exponent b or tortuosity τ). In addition, the model also estimates λ_P, the proportion of track segments that are from predators ($1 - \lambda_P = \lambda_S$ is the proportion of track segments that are from smolts). To classify track segments as from a predator or smolt, we used the estimated parameters and the observed track statistics of each track segment to estimate p_{ik}, the probability that track segment (i) could have been produced by a smolt (k = S) or predator (k = P, see Equation two in [29]). Track segments were then classified as from a

Table 3 *A priori* assumptions for track statistics for smolts and predators

Track statistic	Smolt	Predator
Tortuosity (τ)	Higher	Lower
Lévy exponent (b)	Lower	Higher

predator if $p_{i,\mathrm{P}} > p_{i,\mathrm{S}}$ or from a smolt if $p_{i,\mathrm{P}} \leq p_{i,\mathrm{S}}$. The standard errors for the parameter estimates were estimated from 500 parametric bootstrap runs. Each bootstrap sample was randomly drawn from the distributions described by the maximum likelihood estimates. The model was then then fitted to each bootstrap sample. This was repeated 500 times to generate estimates of the standard error for the parameter estimates [31]. This algorithm was implemented using the boot.se function in the mixtools package for R. We were able to validate our methods via the misclassification of tagged predators as smolts. For tagged predators, we simply calculated the percentage of segments that were correctly identified as from predators. However, we were unable to validate the classification for tagged smolts since it was impossible to recapture tagged smolts to verify their status.

Competing interests

The authors declare that they have no competing interests.

Authors' contributions

JR performed the analyses and wrote the initial drafts of the manuscript. RP contributed to the analyses and writing of the initial drafts of the manuscript. SJ performed fieldwork, processed the acoustic data and provided comments on the initial drafts. CF and SP performed fieldwork and contributed to the initial drafts. AB conducted fieldwork, processed acoustic data and provided critical comments on the initial drafts. All authors read and approved the final manuscript.

Acknowledgements

We would like to acknowledge the numerous individuals who made this project possible. We would like to thank Nick Swyers and Scott Brewer for their expertise in post-processing the telemetry data. We would like to thank the California Department of Water Resources for providing funding for this study. Comments and suggestions from Mike Parsley, David Welch and two anonymous reviewers greatly improved the manuscript and we thank them for that. Any use of trade, product or firm names is for descriptive purposes only and does not imply endorsement by the US Government.

Author details

[1]US Geological Survey, Western Fisheries Research Center, Columbia River Research Laboratory, Cook, WA, USA. [2]Hydroacoustic Technology, Inc, Seattle, WA, USA. [3]Environmental Science Associates, Inc, Sacramento, CA, USA. [4]AECOM, Sacramento, CA, USA. [5]US Geological Survey, California Water Science Center, Sacramento, CA, USA.

Received: 20 September 2013 Accepted: 16 January 2014
Published: 10 February 2014

References

1. Kerstetter DW, Polovina J, Graves JE: **Evidence of shark predation and scavenging on fishes equipped with pop-up satellite archival tags.** *Fish Bull* 2004, **102:**750–756.
2. Thorstad EB, Uglem I, Arechavala-Lopez P, Økland F, Finstad B: **Low survival of hatchery-released Atlantic Salmon smolts during initial river and fjord migration.** *Boreal Environ Res* 2011, **16:**115–120.
3. Kawabata Y, Asami K, Kobayashi M, Sato T, Okuzawa K, Yamada H, Yoseda K, Arai N: **Effect of shelter acclimation on the post-release movement and putative predation mortality of hatchery-reared black-spot tuskfish *Choerodon schoenleinii*, determined by acoustic telemetry.** *Fish Sci* 2011, **77:**345–355.
4. Jepsen N, Aarestrup K, Akland F, Rasmussen G: **Survival of radiotagged Atlantic salmon (Salmo salar L.) and trout (Salmo trutta L.) smolts passing a reservoir during seaward migration.** *Hydrobiologia* 1998, **371–372:**347–353.
5. Fayram AH, Sibley TH: **Impact of predation by smallmouth bass on sockeye salmon in Lake Washington, Washington.** *North Am J Fish Manage* 2000, **20:**81–89.
6. Perry RW, Skalski JR, Brandes PL, Sandstrom PT, Klimley AP, Ammann A, MacFarlane B: **Estimating survival and migration route probabilities of juvenile Chinook salmon in the Sacramento-San Joaquin River Delta.** *North Am J Fish Manage* 2010, **30:**142–156.
7. Rieman BE, Beamesderfer RC, Vigg S, Poe TP: **Estimated loss of juvenile salmonids to predation by northern squawfish, walleyes, and smallmouth bass in John Day Reservoir, Columbia River.** *Trans Am Fish Soc* 1991, **120:**448–458.
8. Vogel DA: **Evaluation of acoustic-tagged juvenile Chinook Salmon movements in the Sacramento-San Joaquin Delta during the 2009 Vernalis adaptive management program.** *Prepared Vernalis Adapt Manage Program, Nat Resour Sci, Inc* 2010:63.
9. Friedl SE, Buckel JA, Hightower JE, Scharf FS, Pollock KH: **Telemetry-based mortality estimates of juvenile spot in two North Carolina estuarine creeks.** *Trans Am Fish Soc* 2013, **142:**399–415.
10. Morales JM, Haydon DT, Frair J, Holsinger KE, Fryxell JM: **Extracting more out of relocation data: building movement models as mixtures of random walks.** *Ecology* 2004, **85:**2436–2445.
11. Tabor RA, Sanders ST, Celedonia MT, Lantz DW, Damm S, Lee TM, Li Z, Price BE: *Spring/Summer Habitat Use and Seasonal Movement Patterns of Predatory Fishes in the Lake Washington Ship Canal.* Lacey, WA: US Fish and Wildlife Service, Western Washington Fish and Wildlife Office; 2010.
12. Melnychuk MC, Welch DW, Walters CJ: **Spatio-temporal migration patterns of Pacific salmon smolts in rivers and coastal marine waters.** *PLoS ONE* 2010, **5:**e12916.
13. Benhamou S: **How to reliably estimate the tortuosity of an animal's path: straightness, sinuosity, or fractal dimension?** *J Theor Biol* 2004, **229:**209–220.
14. Svendsen JC, Aarestrup K, Malte H, Thygesen UH, Baktoft H, Koed A, Deacon MG, Cubitt KF, McKinley RS: **Linking individual behaviour and migration success in *Salmo salar* smolts approaching a water withdrawal site: implications for management.** *Aquat Livin Resour* 2011, **24:**201–209.
15. Humphries NE, Weimerskirch H, Queiroz N, Southall EJ, Sims DW: **Foraging success of biological Lévy flights recorded *in situ*.** *Proc Natl Acad Sci USA* 2012, **109:**7169–7174.
16. Sims DW, Southall EJ, Humphries NE, Hays GC, Bradshaw CJA, Pitchford JW, James A, Ahmed MZ, Brierley AS, Hindell MA, Morritt D, Musyl MK, Righton D, Shepard EL, Wearmouth VJ, Wilson RP, Witt MJ, Metcalfe JD: **Scaling laws of marine predator search behaviour.** *Nature* 2008, **451:**1098–1102.
17. Bartumeus F, da Luz MGE, Viswanathan GM, Catalan J: **Animal search strategies: a quantitative random walk analysis.** *Ecology* 2005, **86:**3078–3087.
18. Viswanathan GM, Afanasyev V, Buldyrev SV, Havlin S, da Luz MGE, Raposo EP, Stanley HE: **Lévy flights in random searches.** *Physica A* 2000, **282:**1–12.
19. Perry RW, Romine JG, Adams NS, Blake AR, Burau JR, Johnston SV, Liedtke TL: **Using a non-physical behavioural barrier to alter migration routing of juvenile Chinook salmon in the Sacramento-San Joaquin River Delta.** *River Res Appl* 2012. online.
20. Zajanc D, Kramer S, Nur N, Nelson P: **Holding behavior of Chinook salmon (*Oncorhynchus tshawytscha*) and steelhead (*O. mykiss*) smolts, as influenced by habitat features of levee banks, in the highly modified lower Sacramento River, California.** *Environl Biol of Fish* 2013, **96:**245–256.
21. Todd BL, Rabeni CF: **Movement and habitat use by stream-dwelling smallmouth bass.** *Trans Am Fish Soc* 1989, **118:**229–242.
22. Chapman E, Hearn A, Michel C, Ammann A, Lindley S, Thomas M, Sandstrom P, Singer G, Peterson M, MacFarlane RB, Klimley AP: **Diel movements of out-migrating Chinook salmon (*Oncorhynchus tshawytscha*) and steelhead trout (*Oncorhynchus mykiss*) smolts in the Sacramento/San Joaquin watershed.** *Envir Biol Fish* 2013, **96:**273–286.
23. Bradford MJ, Higgins PS: **Habitat-, season-, and size-specific variation in diel activity patterns of juvenile Chinook salmon (*Oncorhynchus tshawytscha*) and steelhead trout (*Oncorhynchus mykiss*).** *Can J Fish Aquat Sci* 2001, **58:**365–374.
24. Ibbotson AT, Beaumont WRC, Pinder A, Welton S, Ladle M: **Diel migration patterns of Atlantic salmon smolts with particular reference to the absence of crepuscular migration.** *Ecol Freshwater Fish* 2006, **15:**544–551.
25. Buchanan RA, Skalski JR, Brandes PL, Fuller A: **Route use and survival of juvenile chinook salmon through the San Joaquin River Delta.** *North Am J Fish Manage* 2013, **33:**216–229.

26. Liedtke TL, Wargo-Rub MA: **Techniques for telemetry transmitter attachment and evaluation of transmitter effects on fish performance**. In *Telemetry Techniques: A User's Guide for Fisheries Research*. Edited by Adams NH, Beeman JW, Eiler JH. Bethesda, MD: American Fisheries Society; 2012:45–87.
27. Iwama GK, Ackerman PA: **Anesthesia**. In *Biochemistry and Molecular Biology of Fishes. Volume 3*. Edited by Hochachka PW, Mommsen TP. Amsterdam: Elsevier Science BV; 1994:1–15.
28. R Development Core Team: *R: A Language and Environment for Statistical Computing*. Vienna, Austria: R Foundation for Statistical Computing; 2011.
29. Laube P, Purves RS: **How fast is a cow? Cross-scale analysis of movement data.** *Trans GIS* 2011, **15:**401–418.
30. Sims DW, Righton D, Pitchford JW: **Minimizing errors in identifying Lévy flight behaviors of organisms.** *J Anim Ecol* 2007, **76:**222–229.
31. Benaglia T, Chauveau D, Hunter DR, Young DS: **mixtools: An R package for analyzing finite mixture models.** *J Stat Software* 2009, **32:**1–29.

doi:10.1186/2050-3385-2-3
Cite this article as: Romine *et al.*: Identifying when tagged fishes have been consumed by piscivorous predators: application of multivariate mixture models to movement parameters of telemetered fishes. *Animal Biotelemetry* 2014 **2**:3.

Title:
Interactive Effects Of Non-Native Predators And Anthropogenic Habitat Alterations On Native Juvenile Salmon

Author:
Sabal, Megan Christine

Acceptance Date:
2014

Series:
UC Santa Cruz Electronic Theses and Dissertations

Degree:
M.A., Ecology and Evolutionary BiologyUC Santa Cruz

Advisor(s):
Carr, Mark

Committee:
Raimondi, Pete, Palkovacs, Eric, Hayes, Sean, Merz, Joe

Permalink:
https://escholarship.org/uc/item/06m1z3kz

Abstract:

UNIVERSITY OF CALIFORNIA

SANTA CRUZ

INTERACTIVE EFFECTS OF NON-NATIVE PREDATORS AND ANTHROPOGENIC HABITAT ALTERATIONS ON NATIVE JUVENILE SALMON

A thesis submitted in partial satisfaction

of the requirements for the degree of

MASTER OF ARTS

in

ECOLOGY AND EVOLUTIONARY BIOLOGY

by

Megan Sabal

March 2014

The Thesis of Megan Sabal is

approved:

_____
Professor Mark Carr, chair

_____
Professor Pete Raimondi

_____
Professor Eric Palkovacs

_____
Sean Hayes, Ph.D.

_____
Joe Merz, Ph.D.

_____
Tyrus Miller
Vice Provost and Dean of Graduate Studies

Table of Contents

Abstract

INTERACTIVE EFFECTS OF NON-NATIVE PREDATORS AND ANTHROPOGENIC HABITAT ALTERATIONS ON NATIVE JUVENILE SALMON

by

Megan Sabal

Multiple human stressors including non-native species and habitat alterations can interact with complex consequences on native species. Human-modified habitats can change non-native predator functional and aggregative responses with additive impacts on native prey species. I assessed how the non-native predator, striped bass (*Morone saxatilis*), and habitat alterations (small diversion dam and other altered habitats) interact to influence mortality on native juvenile Chinook salmon (*Oncorhynchus tshawytscha*) migrating to sea on the lower Mokelumne River, CA (USA). Relative abundance and diet surveys across natural and human-altered habitats assessed functional and aggregative responses of striped bass. Striped bass showed elevated per capita consumption of juvenile salmon and behavioral aggregation (estimated as catch per unit effort – CPUE) at a small diversion dam site (Woodbridge Irrigation District Dam: per capita consumption= 3.54 juvenile salmon per striped bass and CPUE= 0.189) over other altered (0 juvenile salmon per striped bass; CPUE= 0.0024) and natural habitats (N/A; CPUE= 0.0003) creating a localized area of heightened predation. At this predation hotspot, experimental predator removals, diet energetic analysis, and before-after impact assessment estimated

striped bass consumption of the population of out-migrating juvenile salmon to be between 10-29%. Striped bass per capita consumption rates among the three approaches were 0.92%, 1.01-1.11%, and 0.96-1.11% respectively. This study highlights how interactions between multiple stressors can exacerbate consequences for native species and are important to examine when predicting ecological impacts from stressors and planning local management strategies.

Acknowledgements

I would like to thank my committee members Dr. Mark Carr, Dr. Sean Hayes, Dr. Joe Merz, Dr. Pete Raimondi, and Dr. Eric Palkovacs for providing support through the entire scientific process and encouraging me to think broadly about ecology. Furthermore, I am hugely grateful to the entire fisheries and wildlife staff of East Bay Municipal District (EBMUD) for taking me along on field days and providing significant extra effort helping conduct predator removal experiments. Their generosity in sharing equipment, field help, data, and advice was critical to the success of this project. Special thanks go to Casey Del Real, Robyn Bilski, and Jose Sekta for helping coordinate large parts of my experiments. Thank you to all the volunteers who devoted time helping me in the field. I am also grateful to both the RC and NMFS salmon ocean ecology labs, and EEB cohort 2012 for supporting me through various aspects of graduate school. Finally, thanks to my friends and family for their continued love and support.

Introduction

Human stressors are leading causes of declines in species and biodiversity, and wholesale changes in ecosystem structure, functions, and services (Dudgeon et al. 2006, Halpern et al. 2008b, Sanderson et al. 2009, Barnosky et al. 2012, Dodds et al. 2013). Typically, impacts of human stressors on species are studied independently, although evidence suggests that multiple stressors interact and exacerbate or ameliorate their consequences (Schindler 2001, Didham et al. 2007). Furthermore, different ecological mechanisms can cause interactions to be non-additive producing an even greater net impact on species (Crain et al. 2008). Human stressors are ubiquitous across ecosystems, and therefore it is important to examine interactive effects of multiple stressors to understand their ecological consequences, potentially predict impacts in altered systems, and design appropriate management strategies to maintain healthy populations of species (Halpern et al. 2008a).

Two significant human stressors driving global change are the establishment of non-native species and habitat alterations. Non-native species may compete with or prey upon native species or interact indirectly and change prey behavior or cause apparent competition (DeCesare et al. 2009, Sorte et al. 2010). Habitat alterations change the physical environment with direct physiological consequences for native fishes or indirect effects such as reduced growth (Schindler et al. 2000, Hojesjo et al. 2004) or reproductive success (Halfwerk et al. 2011). Habitat changes can alter predator-prey overlap (Peters et al. 2013, Kempf et al. 2013), success of invading species (Marchetti et al. 2004), prey vulnerability (Weber and Brown 2012), or

predator foraging success (Bartholomew et al. 2000), and thereby interact with non-native predators to change the magnitude of predation by modifying predator responses (Vucic-Pestic et al. 2010, Alexander et al. 2012). Locally, an aggregation of predators exerts greater net mortality on a prey population, while an increase in predator functional response, specifically per capita consumption of prey relative to prey density, results in higher net predation despite constant predator abundances (Holling 1959, Murdoch and Stewart-Oaten 1989). An increase in both predator responses results in an exponential increase in consumption of native prey also referred to as synergistic or functionally-moderated interaction. Synergistic interactions occur commonly in nature-for example, as predators aggregate at habitats where feeding is profitable (Anderson 2001b, Didham et al. 2007). Additive impacts from multiple stressors may intensify negative consequences on native species and create hotspots of artificially-inflated predation, yet also may allow for spatially-focused management strategies.

Native California salmon populations are in decline and are an integral ecological link between terrestrial, freshwater, and marine ecosystems as well as economically and culturally significant recreational and commercial resources. In the Sacramento-San Joaquin Delta in California (USA), native juvenile Chinook salmon (*Oncorhynchus tshawytscha*) populations experience high mortality during their outmigration to sea (Michel 2010). During outmigration juvenile salmon pass through various anthropogenically-altered habitats such as dams, diversions, marinas, and rip-rap channels, and also encounter multiple non-native predators. Striped bass

(*Morone saxatilis*), introduced from the east coast in 1879, are recognized as a potential threat to juvenile salmon due to their reputation as a voracious fish predator despite inconclusive predation and diet studies (Lindley and Mohr 2002, Nobriga and Feyrer 2008, Loboschefsky et al. 2012). Significant uncertainty exists in the relative and absolute importance of various stressors on salmon mortality, and this challenges management efforts aiming to restore salmon populations. Scientific studies need to assess impacts of human stressors and their interactive effects including, but not limited to habitat alterations and non-native predators (Grossman et al. 2013). A mechanistic understanding of how stressors impact juvenile salmon and context dependence of interactions will allow for more ecologically-aware and effective management strategies.

This study examines how the combined effects of habitat alterations and a non-native predator, striped bass, influence mortality on native, migrating juvenile salmon. I ask if striped bass consumption of juvenile salmon is greater at anthropogenically-altered habitats, if striped bass aggregate at these habitats, and what is the population-level impact on an out-migrating salmon population at an area of high predation. Answers to these questions are fundamental to our understanding of how and to what extent human-modified riverine habitat and introduced predators influence survival of juvenile as salmon as they migrate to sea. I used data on diet and the fish community to estimate per capita consumption and aggregative responses of striped bass. I combined predator removal experiments, diet energetic analysis, and a

before-after impact assessment to generate three separate estimates of striped bass' impact on the population of out-migrating juvenile salmon.

Methods

To address the combined effects of habitat alterations and predation by introduced striped bass on juvenile Chinook salmon, I used a combination of field observations, experiments, and laboratory analysis to ask (1) is the per capita rate of juvenile salmon consumption by introduced striped bass greater at human-modified habitats than natural habitat elsewhere in the same river? (2) If so, are predators more likely to aggregate at these sites of greatest per capita salmon consumption? And (3) what is the consumption of juvenile salmon population by striped bass at the altered habitat?

Study system

I address these questions in the lower Mokelumne River in the eastern Sacramento-San Joaquin Delta that drains approximately 1,624 km^2 of central Sierra Nevada and extends 54 km between Comanche Dam and the confluence of the San Joaquin River. River flows are highly regulated with peak flows occurring typically between November and April. My study sites lie below the Woodbridge Irrigation District Dam (WIDD) (Figure 1), which is approximately 50 m across and creates a relatively deeper pool of water immediately downstream and is distinct from other habitats, which include glides and pools bordered by natural vegetation, levees, and

rip-rap banks (Merz and Setka 2004). The river is tidally-influenced, average river gradient is 0.0003, and substrate is comprised of sand and mud. Over 38 fish species inhabit the Mokelumne River including anadromous, non-native striped bass and native Chinook salmon that spawn naturally without the aid of fish hatcheries. Juvenile Chinook salmon migrate annually from headwaters downstream passing WIDD in two pulses from February-March (approximate fork length (FL) 30-40 mm) and May-June (approximate FL 80-110 mm) (Merz and Workman 2013). The Mokelumne River Fish Hatchery plants juvenile salmon into the river downstream of my study sites, so they are not a pertinent part of the fish community in this study reach. East Bay Municipal Utility District (EBMUD) has been estimating populations of juvenile salmon emigration using rotary screw traps (2.4 meter diameter, E.G. Solutions Inc.) to record juvenile salmon catches, and is operated daily from December-July since 1990 (Volkhardt et al. 2007). Estimates of emigrating juvenile salmon populations vary annually, but ranges on the order of 60,000-280,000 fish passing WIDD. Adult striped bass migrate upstream April-July, and therefore predator and prey overlap during the peak juvenile salmon outmigration in May and June (Le Doux-Bloom 2012).

Striped bass per capita consumption of juvenile salmon by habitat

To test the hypothesis that habitat alterations affect consumption rates by striped bass, I combined relative abundance surveys with diet analysis to compare predation rates of salmon across different habitat types. Because structures, especially

dams and diversions, may disorient salmon and increase predator foraging efficiency (Davis et al. 2012), I predicted that striped bass will have the highest per capita consumption of juvenile salmon at WIDD, followed by other altered, and natural habitats. I surveyed 10 total sites and categorized them into three habitat categories: diversion dam (WIDD) (n=1), other altered (n=7), and natural (n=2). The diversion dam, WIDD, described above significantly alters the physical and hydrodynamic environment and is distinct from all other sites. Other altered habitats included sites with rip-rap channels and sites with man-made structures like docks and bridges. These hardened structures modify the river, but to a lesser extent than WIDD. Natural sites lack hardened structures and are bordered by natural vegetation. Striped bass were captured from the lower Mokelumne River using single-pass boat electrofishing (Smith Root Model SR-18EH) following the methods of Meador et al. (1993) at fixed transects parallel to each shoreline and one in the mid channel at 10 sites between April 23 and May 24, 2013 during peak fall-run Chinook salmon outmigration. I used an automatic timer to record the number of seconds electrofished at each site and used this to calculate striped bass relative abundance: number of striped bass caught per seconds electrofished (CPUE= catch per unit effort). I counted, measured (FL in mm), weighed (g), and took diet samples using non-lethal gastric lavage which were preserved in 95% ethanol (Hakala and Johnson 2004). Striped bass are gape-limited and switch to piscivory around 250 mm FL, therefore striped bass <250 mm FL were not considered as potential juvenile salmon predators (Nobriga and Feyrer 2007).

Diet samples were processed in the lab to quantify relative and absolute consumption of juvenile salmon. I identified prey items to lowest taxonomic level, and enumerated, measured, and weighed each prey group. I used diagnostic bones to distinguish between common digested prey species (Hansel et al. 1988, Frost 2000). If only one fish prey category was present in a stomach, unidentified fish tissue was included in that group weight, if more than one category was present, unidentified fish tissue was divided equally and added to each fish prey category, and non-food items were excluded from diet calculations (Poe et al. 1991). To determine if consumption of juvenile salmon increases with striped bass size or peaks at a middle size, I compared striped bass FL (mm) and number of juvenile salmon found in each diet using both a linear and second degree polynomial relationship. Multivariate methods using PRIMER v.6 were used to compare striped bass diet composition between habitat types (WIDD and other altered). Only 1 striped bass was caught at natural sites and its diet was empty, therefore the natural habitat category is not included in this analysis. I computed a similarity matrix using Bray-Curtis distance on square root transformed weights (g) of prey categories for each fish. Distance-based permutation multivariate analysis of variance PERMANOVA; (Anderson 2001a) was used to test (significance level $\alpha=0.05$) the null hypothesis of no difference of diet composition between habitat types. Analyses were based on 999 unrestricted permutations of raw data. Non-metric multidimensional scaling (nMDS) with diet vector overlay plot was used to visualize multivariate patterns. I also

analyzed diet composition by percent by weight and percent by number for each prey category, and calculated per capita consumption of salmon by habitats.

Striped bass aggregation by habitat

I tested the hypothesis that if there is a greater per capita consumption of juvenile salmon at one or more habitat(s) relative to others, then predators will also aggregate at that habitat(s) with highest rates of salmon consumption. I predicted striped bass will aggregate at man-made structures, seeing the largest aggregation at WIDD followed by other altered habitats, and lowest at natural habitats because structure may increase prey vulnerability and predator foraging success creating profitable feeding locations. I compared catch per unit effort (CPUE), a measure of relative abundance of striped bass (FL >250 mm) from sites in habitat categories: WIDD (diversion dam), other altered, and natural. CPUE data were taken from EBMUD's long-term spring fish community surveys from 1998 to 2013. These data were collected using the same single-pass electrofishing methods described in the previous section. I used one-way ANOVA and Tukey's HSD test to compare mean striped bass CPUE, a measure of aggregation, among WIDD, other altered, and natural habitats. I tested assumptions for these analyses and performed a square root transformation on CPUE data to meet these assumptions. Pearson's chi-squared test was used to compare differences in frequency of striped bass caught across sampling events for each habitat.

Impact on the population of out-migrating juvenile salmon

To further assess the impact of striped bass predation on the population of emigrating juvenile salmon at an area of high predation (WIDD), I used three independent approaches: 1) striped bass removal/salmon survival experiment, 2) diet energetic analysis, and 3) before-after impact assessment.

Striped bass removal/salmon survival experiment

I evaluated how striped bass removal affects juvenile salmon survival by marking and recapturing paired releases of juvenile Chinook salmon before and after striped bass removal. By comparing before and after releases, I hypothesize there will be greater percent of recaptures (i.e. survival) of experimental fish after striped bass removal. This experiment was conducted twice during the peak juvenile salmon migration period in 2013; from May 6 to May 10, and from May 20 to May 24. To remove striped bass I conducted four sequential passes of electrofishing, cumulatively depleting predators at WIDD. To satisfy the assumption of a closed population, required for applying the recapture method of estimating predator abundance, a block net enclosed the study area to prevent predator escapement. I concluded that depletion was complete when the catch-per-pass declined by 75% or more between successive passes (Peterson et al. 2004). To ensure equal capture efficiency between passes I used a pulsed current and kept the total seconds electrofished consistent between passes (Raleigh and Short 1981). Captured fish were held in a live well and transferred to holding tanks until I achieved depletion. I counted, weighed (g),

measured (FL; mm), and collected diet samples using gastric lavage from striped bass >250 mm FL. To assess the relative contribution of an alternative predator to patterns of juvenile salmon mortality, I also collected diet samples from black bass (includes largemouth bass-*Micropterus samoides* and spotted bass-*Micropterus punctulatus*) to compare striped bass salmon consumption with an alternate non-native predator. After depletion passes were completed, striped bass were transported and released at an alternative location (King's Island) while all other fish species collected were released back into the study area.

To estimate survival of juvenile Chinook salmon, I marked juvenile salmon obtained from the Mokelumne River Fish Hatchery with unique external visible implant elastomer tags. These tags have high retention rates, are easily detected, have no observed effect on survival and growth of juvenile fish (Hale and Gray 1998, Bilski et al. 2011, Leblanc and Noakes 2012). Therefore I did not account for tag loss in our estimates of survival. The first release (before removal treatment, n=1000) was performed at the base of WIDD in the evening two days prior to striped bass removal. A rotary screw trap (2.4 meter diameter, E.G. Solutions Inc.) approximately 200 meters downstream of WIDD was checked every morning and juvenile salmon recaptures were recorded (Volkhardt et al. 2007). The second release (after predator removal treatment, n=1000) was performed in the evening after striped bass removal. Recapture rate was calculated from the number of tagged fish recaptured in the screw trap extrapolated to the total river by volume divided by total number of tagged fish released. Both release and recapture estimates were divided by corresponding daily

flow (EBMUD's Golf gauging station) to standardize recaptures by volume of water sampled. We examined the difference between proportion of recaptures before and after striped bass removal. After final salmon recaptures were recorded, I conducted a single-pass of electrofishing to assess if striped bass remained removed over the duration of the experiment and if other fish species remained roughly consistent to what I caught on the first pass on day of removal. Changes in the fish community occurring throughout the experiments, could confound my treatment making it difficult to attribute change in salmon survival to striped bass removal.

Diet energetic analysis

To determine if the change in survival found in the first striped bass removal/salmon survival experiment was due to predation, I also calculated percent salmon consumed using diet analysis from the same predators. I calculated the average number of salmon consumed per striped bass removed from the first removal experiment, and because fish predators frequently digest prey under 24 hours, I used a range of fast (10 hours; 0.416 days) and slow (15 hours; 0.625 days) gastric evacuation rates to extrapolate to daily individual consumption (Elliott and Persson 1978, TID/MID 1992). Individual daily consumption rates were multiplied by the number of striped bass removed (11) to calculate daily population-level consumption. I used the known number of experimental fish released at WIDD and ratio of known number of recaptures of experimental fish to natural fish caught in the screw trap to estimate the number of natural fish passing WIDD. I then assumed a constant ratio of

natural fish caught in the trap to total number passing WIDD to calculate juvenile salmon populations at WIDD for the day striped bass were removed. I calculated the percent of juvenile salmon consumed by striped bass using the daily population-level consumption rate.

A black bass population estimate at WIDD was determined from multiple-pass depletion electrofishing, using least squares linear regression of black bass catch per effort (CPUE) against cumulative catch, lagged for one unit of effort (Maceina et al. 1995, Cavallo et al. 2012). Using the same methods, I also calculated population-level consumption of black bass on juvenile salmon for both first and second removal experiments.

Before-after impact assessment

I used existing data from EBMUD to retrospectively determine whether striped bass removal affects juvenile emigration survival in Mokelumne River natural Chinook salmon populations, and if the magnitude of impact is related to number of striped bass removed. The rotary screw trap below WIDD captures migrating juvenile salmon daily and because catches are highly auto-correlated, I hypothesize that juvenile salmon catch will increase the day following a predator removal and the magnitude will increase with increasing numbers of striped bass removed. I tested this prediction by calculating percent change in salmon survival (After – Before / After + Before)*100 using juvenile salmon catches in the screw trap the day before and day after an impact (predator removal) and control (no predator removal). This

value scales from 100% to -100% where 0 indicates catches before and after are identical, positive values indicate an increase, and negative values a decrease in juvenile salmon catch.

EBMUD conducted predator removals in 2009 and 2010; they used boat electrofishing to catch, deplete, and remove both striped bass and black bass from WIDD, multiple passes were not separated, and there was no block net in place. Ten total predator removal events from 2009 (n=4), 2010, (n=4), and 2013 (n=2) were included in the impact treatment. Electrofishing during predator removal can injure or cause mortality to Chinook salmon, which may diminish salmon catch in the screw trap the first day following removal (Schreer et al. 2004). For this reason, I calculated percent change in salmon survival between both the day before and the first day after removal and the second day after removal. For the control treatment I calculated percent change in salmon survival before and after all pairs of days in 2009, 2010, and 2013 excluding the day before and two days after predator removals and days there was debris in the screw trap preventing it from fishing properly (n=139). I used Welch two-sample t-tests to compare mean percent change in salmon survival between control and each impact treatment and estimate the impact of striped bass removal on juvenile salmon survival. To assess if percent change in salmon survival correlated with numbers of striped bass removed, I conducted a linear mixed regression analysis where percent change in salmon survival was the response variable, striped bass number removed was the predictor variable, and period (first or second day after removal) was a random effect.

Results

Striped bass per capita consumption of juvenile salmon by habitat

Striped bass diet composition including juvenile Chinook salmon consumption differed markedly between WIDD and other altered habitats (Figure 2; Appendix 1 and 2). Striped bass ranged from 225 to 925 mm FL with an average size of 530 mm at WIDD (n=22) and an average size of 424 mm at all other sites (n=30). Diet data showed striped bass consumption of juvenile salmon was not significantly size dependent using either linear (R^2= - 0.033, p = 0.572) or second degree polynomial (R^2= 0.057, p = 0.219; Appendix 3) relationships, and therefore diets were not separated into size classes of striped bass for energetic analysis. Multivariate PERMANOVA showed significant differences in striped bass diets between WIDD and other altered habitats (p= 0.001, df= 1, psuedo-F= 17.3). nMDS plot indicated strong grouping of striped bass diet samples by location and diet vector overlay shows the presence of juvenile salmon primarily drives diet differences (Figure 2). Juvenile Chinook salmon was the predominant prey item from striped bass caught at WIDD (56.52% number, 94.82% weight) while there was no occurrence of salmon in diets from any other locations. Striped bass consumed primarily crayfish at other locations (18.18% number, 90.87% weight; Appendix 1 and 2). Striped bass per capita consumption of juvenile salmon was 3.54 at WIDD and 0 at other altered habitats.

Striped bass aggregation by habitat

Striped bass aggregated at WIDD with an eight-fold increase in CPUE (WIDD mean= 0.0189) relative to other altered (mean= 0.0024) and sixty-fold increase relative to natural habitats (mean= 0.0003) (Figure 3). One-way ANOVA and Tukey's HSD tests indicated significant differences between all pair combinations: WIDD and other altered ($p< 0.001$), WIDD and natural ($p< 0.001$), and other altered and natural ($p= 0.03$). Striped bass were caught in 13/15 (86.6%) surveys at WIDD, 37/100 (37.0%) surveys at other altered, and 6/21 (28.6%) surveys at natural habitats (Chi-squared test: df=4, $p= 0.0048$). Striped bass ranged from 204 to 904 mm FL with an average size of 526 mm at WIDD (n= 132), ranged from 201 to 705 mm FL with an average size of 391 mm at other altered habitats (n= 90), and ranged from 225 to 510 mm FL with an average size of 363 mm at natural habitats (n=18).

Impact on the population of out-migrating juvenile salmon

Striped bass removal/salmon survival experiment

Estimated Chinook salmon survival increased 10.21% after first removal of 11 striped bass (0.92% per capita impact), and decreased 2.06% after second removal of 1 striped bass. Majority of striped bass caught in the first experiment were >400 mm FL, and although I did see re-colonization of WIDD during the 12 days between experiments all but one striped bass was <250 mm FL in the second removal experiment (Appendix 4). I depleted 78.4% and 89.9% of the total striped bass

populations including all size ranges (Appendix 5), but only removed 11 and 1 predatory striped bass capable of consuming juvenile salmon in first and second removal experiments respectively. Environmental conditions were similar between both experiments: water temperature (17.0˚C, 17.7˚C) and water flow (4.56 cms, 4.51 cms). Release groups of experimental salmon were similar in size between first and second removal experiments (mean FL= 78.95 mm and 82.31 mm, respectively) and slightly smaller than natural fish populations (mean FL= 87.3 mm and 92.11 mm, respectively). Greater than 99% of experimentally tagged fish were recaptured in the screw trap the morning following the release suggesting fish are migrating through the basin immediately, and the first release group is out of the system by the time the second group is released. After the removal experiments were completed, single-passes of electrofishing indicated I maintained removal of striped bass in the first experiment, but did not maintain removal in the second experiment (Appendix 6). Because I removed 1 predatory striped bass and caught 1 after the end of the second experiment, there was approximately no change in striped bass predation impact between tagged salmon releases. The remaining fish community had variable responses with some species increasing and others decreasing in abundance (Appendix 6).

Diet energetic analysis

Diet samples from striped bass caught in the first removal experiment contained an average of 4.75 juvenile salmon per striped bass. Gastric evacuation

rates (slow and fast range) generated individual daily consumption rates of 7.60-11.40 juvenile salmon per day. Using the 11 striped bass that I removed in the first experiment, I scaled individual consumption to daily population-level consumption of 86.9-125.4 juvenile salmon per day. Mark and recapture estimates of salmon population size were 770 salmon and 796 salmon for the first and second days of removal respectively. During the first removal experiment, the 11 striped bass removed would have consumed between 11.2% (slow) and 16.2% (fast) (1.01%-1.47% per capita impact) of the migrating juvenile salmon population passing WIDD. Despite having introduced tagged hatchery salmon into the system for my removal experiments two days before, striped bass diets were likely comprised only of natural fish because >99% of experimentally tagged fish migrated through the reach within 12 hours of release and would have been absent when diet samples were taken.

The same methods showed black bass consumed an average of 0.08 juvenile salmon and individual daily consumption rates of 0.13-0.19 juvenile salmon per day. Depletion regression estimated a population of 16.5 (R^2= 0.6209, p= 0.0708) and 38.0 (R^2= 0.9987, p= 0.0004; Appendix 7) black bass at WIDD during first and second removals respectively, which scales population level consumption to (2.08-3.13) and (4.80-7.2) juvenile salmon per day. Black bass consumed between 0.27-0.41% (0.01%-0.18% per capita impact) of the migrating juvenile salmon population passing WIDD during the first removal experiment and 0.60-0.90% (0.01%-0.02% per capita impact) during the second removal experiment.

Before-after impact assessment

The before-after impact assessment indicated a mean increase in natural salmon survival of 25-29% after predator removal. Ten removal events from 2009, 2010, and 2013 occurred in the range of May 7th to June 16th and between 1 and 68 striped bass (average 26.3) were removed. For the control, the mean percent change in salmon survival between pairs of days with no predator removal was 0.3%. For the impact treatments, percent change in salmon survival between day before and first day after predator removal was 25.9% (t= -2.02, df= 10.52, p= 0.06), and for day before and second day after predator removal was 29.2% (t= -2.61, df= 11.05, p= 0.024). Welch two-sample t-tests indicated both predator treatments showed an increase in salmon caught compared to control treatment (Figure 4). The average number of striped bass removed among all removal events was 26 striped bass; therefore, the striped bass per capita impacts are 0.96% and 1.11% for first day after removal and second day after removal respectively. Mixed linear regression indicated increasing proportional change with increasing number of striped bass removed (t= 2.43, df= 17, p= 0.026; Figure 5).

Discussion

Multiple stressors can interact with complex consequences on native species. In this example, habitat alterations, likely through an increase in foraging efficiency, increase the magnitude of predation by a non-native predator. This interaction is synergistic as habitat increases both functional and aggregative responses of a

predator. A local predation hotspot, WIDD, was associated with increased striped bass per capita salmon consumption and attracted larger numbers of striped bass decreasing migrating juvenile salmon survival by 10-29%.

I found that striped bass diets from WIDD consisted primarily of juvenile salmon, and the per capita impact of striped bass on salmon was higher at WIDD than other altered locations. Alterations at WIDD may create profitable feeding conditions by concentrating prey density because of shortened river width or upstream location before salmon experience additional downstream mortality, or disorienting migrating salmon coming over the dam with sudden changes in water velocity (Deng et al. 2010), or favoring visual predators because of reduced turbidity (Gregory and Levings 1998, Horodysky et al. 2010). Increased juvenile salmon consumption behind dam-like structures has also been observed by Sacramento pikeminnow (*Ptychocheilus grandis*) and striped bass on the Sacramento River (Tucker et al. 1998), by Northern pikeminnow (*Ptychocheilus oregonensis*), walleye (*Sander vitreus*), and small mouth bass (*Micropterus dolomieu*) on the Columbia River (Rieman et al. 1991), and on the U.S. East Coast by striped bass on the Merrimack River (Blackwell and Juanes 1998). These studies attribute increased juvenile salmon predation to disoriented prey, increased transit time through study reaches, and aggregations of predators. I cannot truly distinguish a functional response because I lack data on prey density of juvenile salmon at sites during diet sampling. I conclude there was a large difference in per capita consumption of juvenile salmon between

WIDD and other altered locations potentially due to increased foraging efficiency at WIDD.

Striped bass did aggregate at WIDD with an eight-fold increase in CPUE compared to other altered locations and sixty-fold increase compared to natural locations. This aggregation corresponds to where per capita consumption of juvenile salmon was also greatest suggesting striped bass may aggregate to areas of profitable feeding. Feeding aggregations are common in nature and include striped bass aggregating behind dams on the U.S. East Coast to feed on migrating blueback herring (*Alosa aestivalis*) (Davis et al. 2012). Alternatively, spawning aggregations or blocked upstream migration could account for the observed aggregation at WIDD, however there are no documented striped bass spawning areas on the Mokelumne River and I observed very few ripe male fish. Aggregation at other altered over natural habitats may still be due to hardened structures increasing foraging efficiency despite absence of juvenile salmon in striped bass diets. Regardless of the reason for aggregation, I saw an increase in striped bass, which increases predation on juvenile salmon relative to other locations. The habitat alteration, WIDD, interacts with the non-native predator, striped bass at WIDD, to increase both functional and aggregative predator responses. This creates a local hotspot of juvenile salmon mortality, which is artificially inflated above natural levels.

I used three separate approaches to assess striped bass impact on the population of out-migrating juvenile salmon and generated a range of 10-29% of the juvenile salmon population consumed by striped bass at WIDD. These population-

level impact values were generated for different numbers of striped bass at WIDD, but are comparable through striped bass per capita impacts which ranged from 0.92%, 1.01-1.11%, and 0.96-1.11% for striped bass removal/salmon survival experiments, diet analysis, and before-after impact assessment respectively. Despite limitations in each approach, these findings point in the same direction and similar magnitude. The first approach was the striped bass removal/salmon survival experiments which showed a 10.2% increase in salmon survival after 11 striped bass were removed and a 2% decrease in survival after 1 striped bass was removed. The 10.2% increase in survival supports my hypothesis that survival would increase after I removed striped bass. The 2% decrease suggests there was minimal change in salmon survival when only 1 striped bass was removed, which is logical given I was unsuccessful keeping striped bass removed in the second experiment. Possible other effects are electrofishing and handling stress on other fish predators that were not removed could have caused them to migrate out of the study area (Appendix 4), reduce feeding, or change other behaviors, which could confound the effect of striped bass removal on juvenile salmon survival. However, if stressing of other predators was responsible for some of the observed increase in salmon survival in the first removal experiment, I would have expected to see an increase in survival during the second removal experiment when there was minimal change in predation impact. Salmon survival minimally decreased in the second experiment suggesting striped bass are the primary influence on salmon survival in this reach.

The second approach to estimate striped bass impact on population of out-migrating juvenile salmon included a diet energetic analysis from striped bass removed during first removal experiment which showed 11-16% of the juvenile salmon population consumed. This estimate is relatively similar to the 10% increase from the first removal experiment. It is important to note that uncertainty exists in these diet estimates. Even though gastric evacuation rates I used came from the nearby Delta, using similar temperature and based on consumption of juvenile Chinook salmon, they are from a largemouth bass study (TID/MID 1992). This magnitude of consumption estimate is only for one sampling instance (population of 11 striped bass), and it is important to note that surveys at WIDD in other years have shown populations of striped bass to be upwards of 60 fish and magnitude of predation could have been even higher. The relatively low numbers of striped bass at WIDD in May 2013 may be due to basin-wide low flow conditions. Diet energetic analysis provides an alternative method to validate the magnitude of striped bass predation found in the striped bass removal/salmon survival experiment. Comparative predator analysis indicated black bass consumed <1% of the population of juvenile salmon at WIDD, suggesting WIDD may not create heightened salmon predation for all predatory fish species.

The third and most robust approach to population-level impact is the before-after impact assessment which estimated 26% or 29% increase in salmon survival after removal of striped bass populations from WIDD. This analysis included 10 replicate removal events spanning three years, differences in timing throughout the

Chinook salmon emigration period, and variation in environmental conditions. Therefore I am confident that observed increases in juvenile salmon survival is due to striped bass predation and not a correlated alternate variable. I do not know the percentage of striped bass population removed from all events, but I do know the numbers of fish removed. For eight removal events both striped bass and black bass were removed from the basin. However, diet data from black bass at WIDD showed <1% consumption of juvenile salmon, and I feel confident the increase in survival is driven primarily by striped bass. Collectively, these three approaches estimate 10-29% juvenile salmon mortality from striped bass predation at WIDD. In comparison, on the Columbia River the McNary Dam is approximately 15 times longer than WIDD and average population-level consumption of juvenile salmon by three predators (small mouth bass, walleye, and Northern pikeminnow) was 14% in the John Day Reservoir (123 km), of which 21% of loss occurred in the area immediately after the McNary Dam (0.5 km) (Rieman et al. 1991).

In the Sacramento-San Joaquin Delta there is debate about the relative importance of the major drivers of juvenile salmon mortality: water exports, habitat loss, water pollution, and non-native predators. Management decisions depend on these relative rankings to designate effort to the most significant stressor. With so much uncertainty, it is critical to assess the relative and population-level impact on juvenile salmon, and the interactive effects of these different anthropogenic stressors. There is value in local studies to assess population-level impact, and test feasibility for management strategies such as predator removals to understand mechanistic

interactions and context-dependent attributes of predator-prey interactions (Hunsicker et al. 2011, Grossman et al. 2013). My project focuses on the non-native predator, striped bass, its relative importance and interaction with habitat alterations, and local impact on population of emigrating juvenile salmon at a predation hotspot. Future studies need to assess basin-wide migration survival after predator removal because delayed downstream compensatory mortality may eliminate long term survival increases. I also examined one predation hotspot at WIDD. There are many man-made structures throughout the Sacramento-San Joaquin Delta and it is important to compare these findings to more sites and determine which common characteristics create this synergistic interaction. My findings highlight that habitat, especially large man-made structures, can create predation hotspots through modifying predator functional and aggregative responses. Therefore it is important to consider habitat alterations and interactive effects when estimating large-scale predation impacts and when planning local management strategies.

Impacts of multiple anthropogenic stressors on native populations are often studied independently despite the fact that they can interact (Didham et al. 2007, Crain et al. 2008). Interactions can be complex and further studies are necessary to examine the context-dependent nature of interactions. This study illustrates how certain habitat alterations can change both functional and aggregative predator responses with additive consequences on native prey populations. On a larger scale, widespread global change including habitat alterations and introduction of non-native species across ecosystems and taxa increases the probability of interactive effects

influencing native prey populations and heightens the importance of studies focusing on these interactions.

Figures

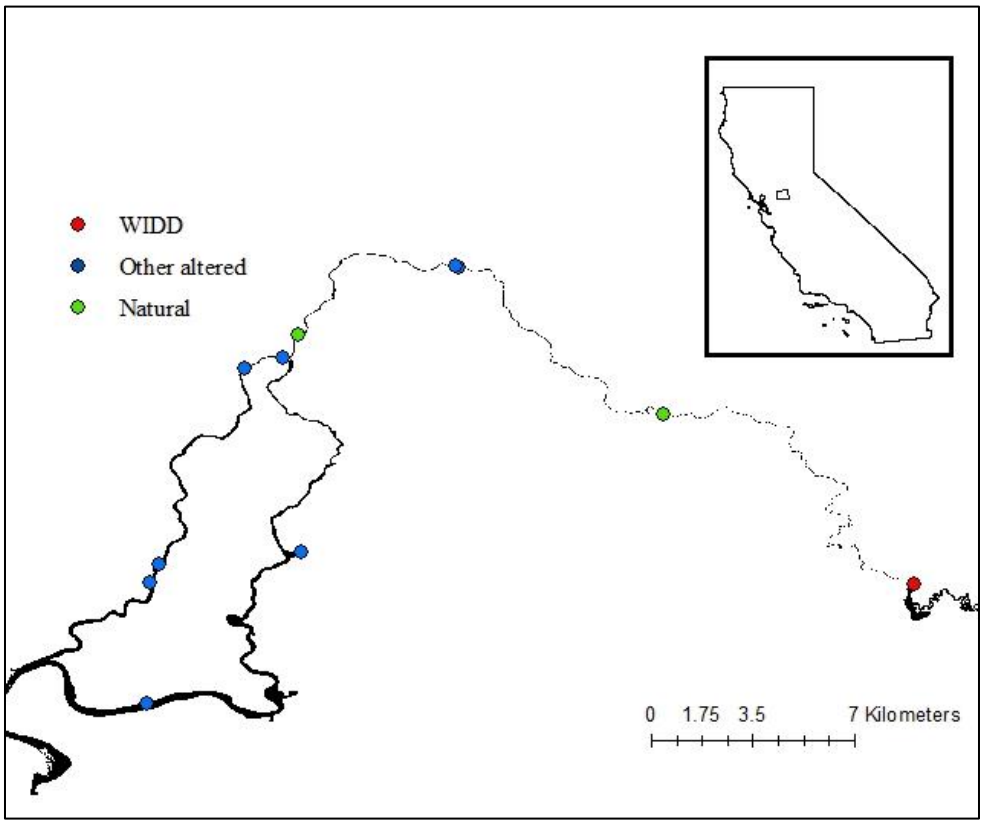

Figure 1. Map of electrofishing study sites on the Lower Mokelumne River, CA. Red circle is WIDD, blue circles are other altered habitats, and green circles are natural sites. Inset demonstrates study location in relationship to California and the San Francisco Bay.

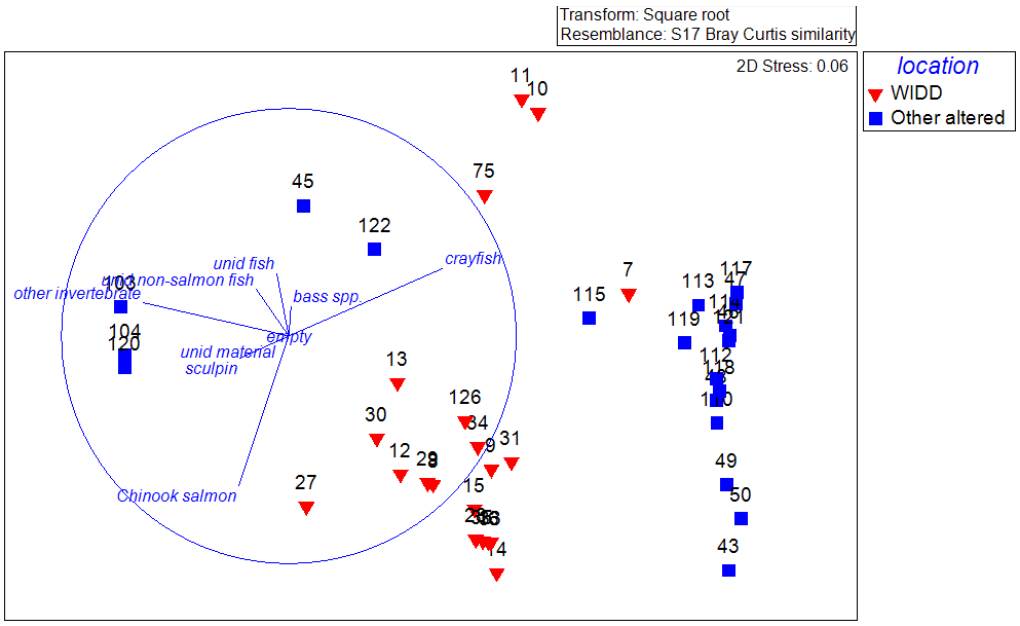

Figure 2: Non-metric multi-dimensional scaling plot with diet vector overlay. Striped bass individual relationships grouped by habitat type (WIDD and other altered) (p=0.001).

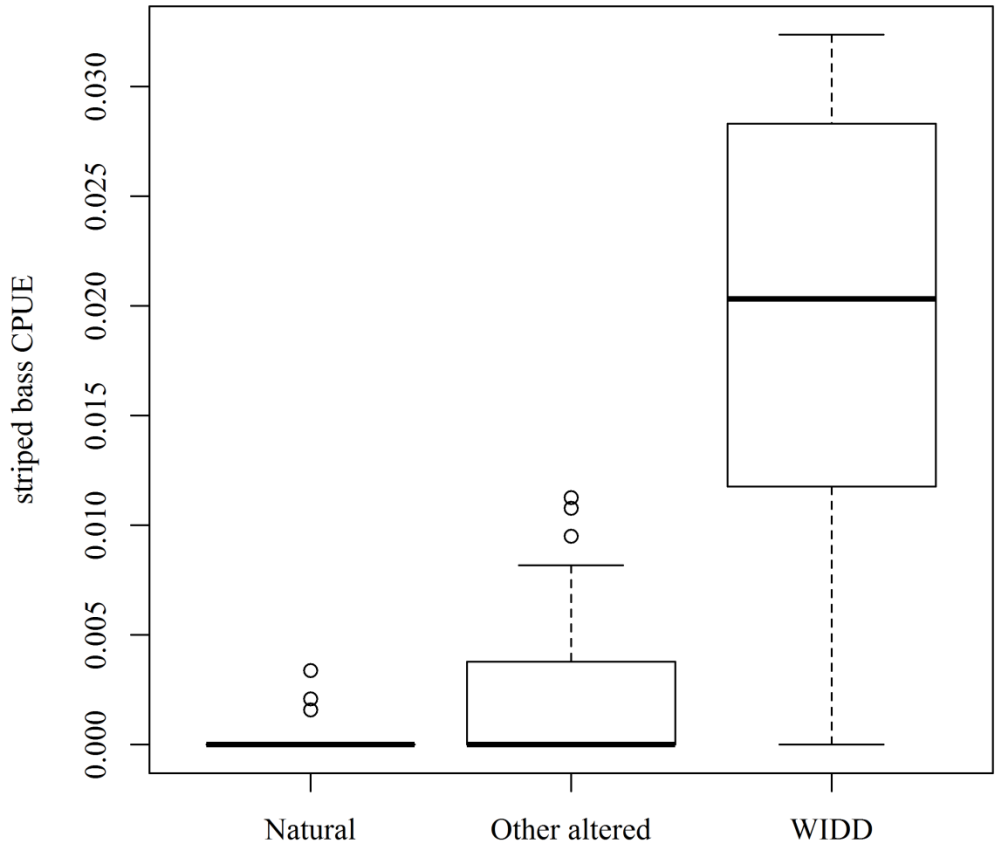

Figure 3. Striped bass (<250 mm FL) CPUE from electrofishing surveys 1998-2013 at other locations combined and WIDD. One-way ANOVA and Tukey's HSD tests indicate significant differences between WIDD and natural ($p < 0.001$), WIDD and other altered sites ($p < 0.001$), and other altered and natural habitats ($p = 0.03$).

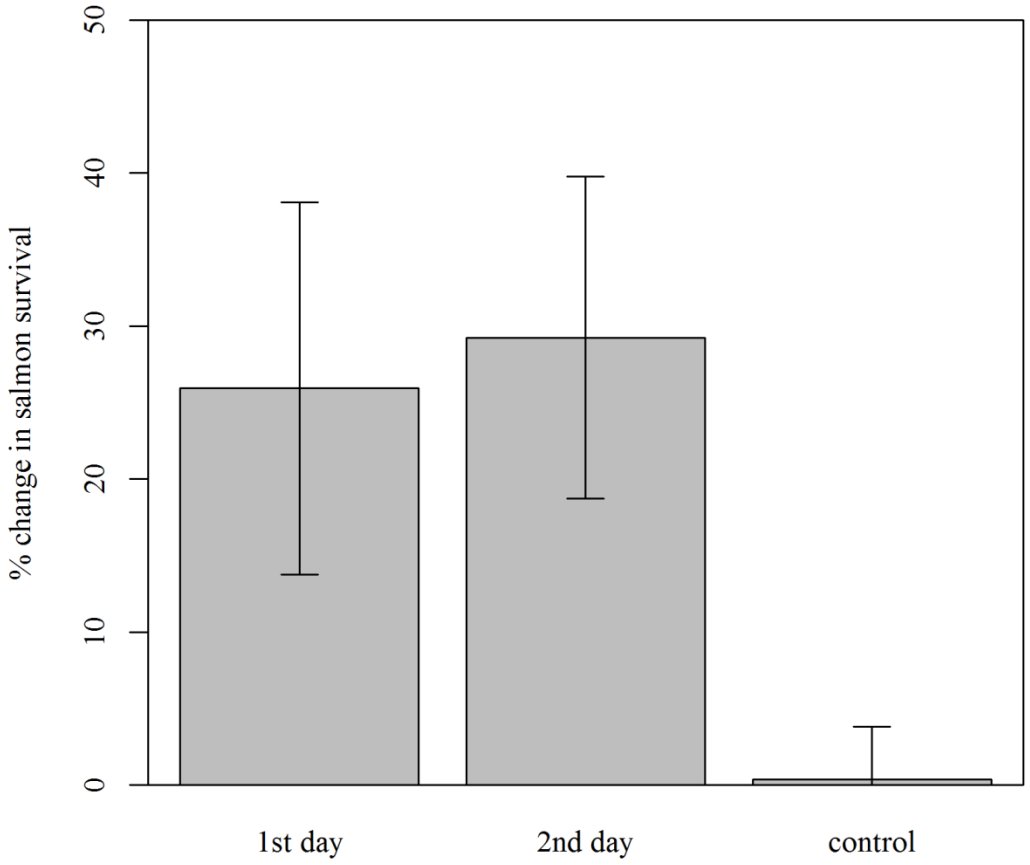

Figure 4. BACI metrics for predator removal treatments, using both 1st and 2nd day after removal and control treatment. + or – 1 SE. Two sample t test comparing treatments with control: 1st day (mean= 25.9%, t= -2.022, df= 10.52, p= 0.069), 2nd day (mean=29.2%, t= -2.605, df= 11.05, p= 0.024).

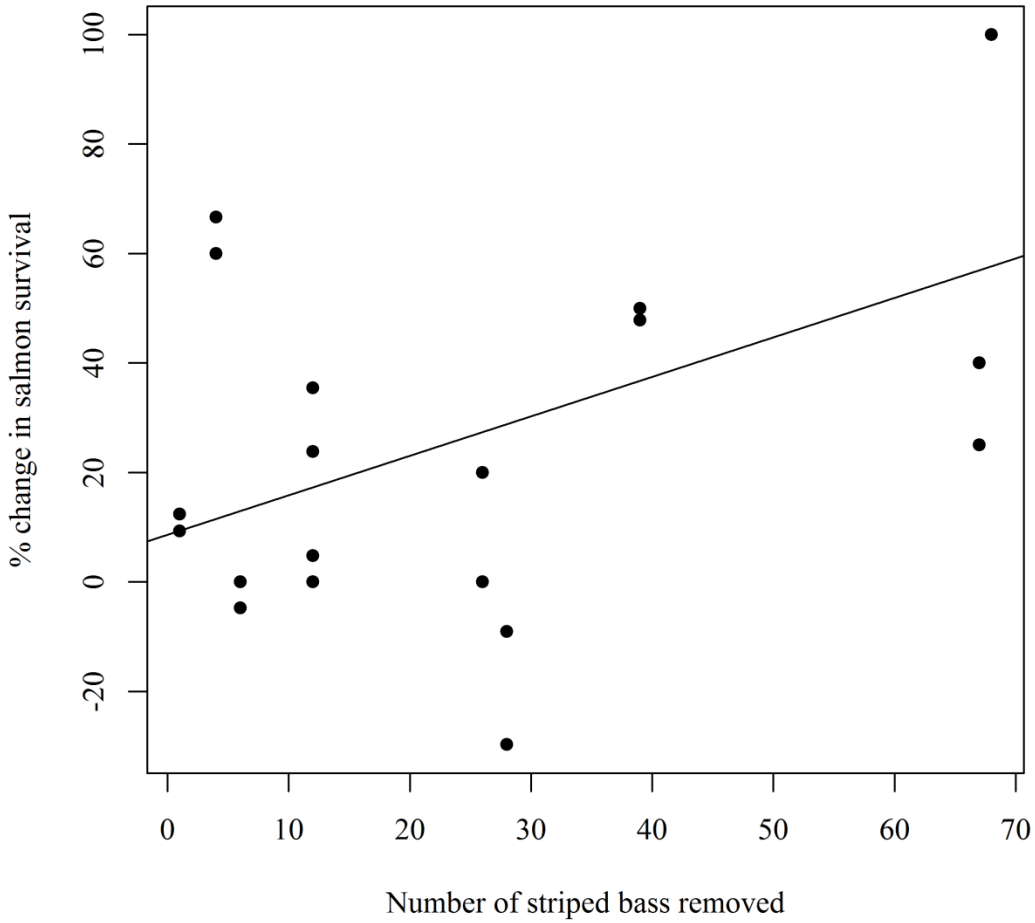

Figure 5. Mixed linear regression. BACI metric increases with increasing number of striped bass removed (t= 2.426, df= 17, p= 0.026).

Appendices

prey category	Striped bass Other altered n=30			Striped bass WIDD n=22			Black bass WIDD n=42		
	% FO	% number	% weight	% FO	% number	% weight	% FO	% number	% weight
Chinook salmon	0.00	0.00	0.00	72.73	56.52	94.82	7.14	9.68	48.70
Bass spp.	10.00	16.88	2.33	9.09	4.35	1.83	2.38	3.23	3.41
sculpin	0.00	0.00	0.00	13.64	2.90	0.16	7.14	22.58	13.01
Fish non-salmon	3.33	1.30	2.20	13.64	16.67	0.56	11.90	22.58	6.84
Un-id fish	3.33	0.00	0.43	22.73	3.62	0.94	11.90	12.90	5.98
crayfish	50.00	18.18	90.87	13.64	1.45	1.48	21.43	16.13	19.59
Other invertebrate	13.33	63.64	2.86	18.18	4.35	0.00	7.14	9.68	0.04
Un-id material	3.33	0.00	1.32	18.18	10.14	0.20	9.52	3.23	2.43

Appendix 1. Total table of diet composition including percent frequency of occurrence (FO), percent number and percent weight.

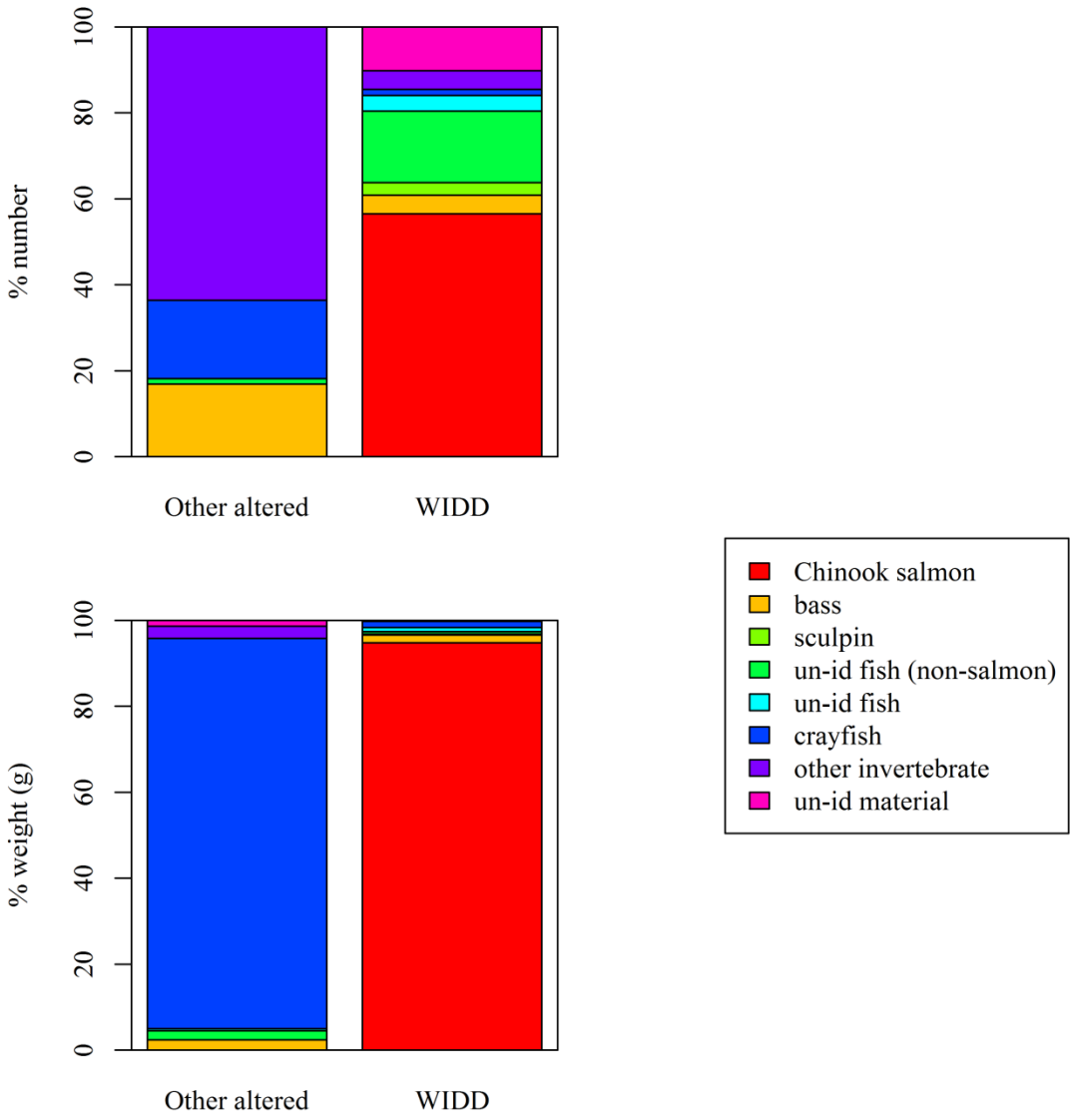

Appendix 2. Percent number and percent weight of diet items from striped bass caught at other altered sites and WIDD. Only one striped bass was caught at natural sites and it was empty, so is not shown in this figure.

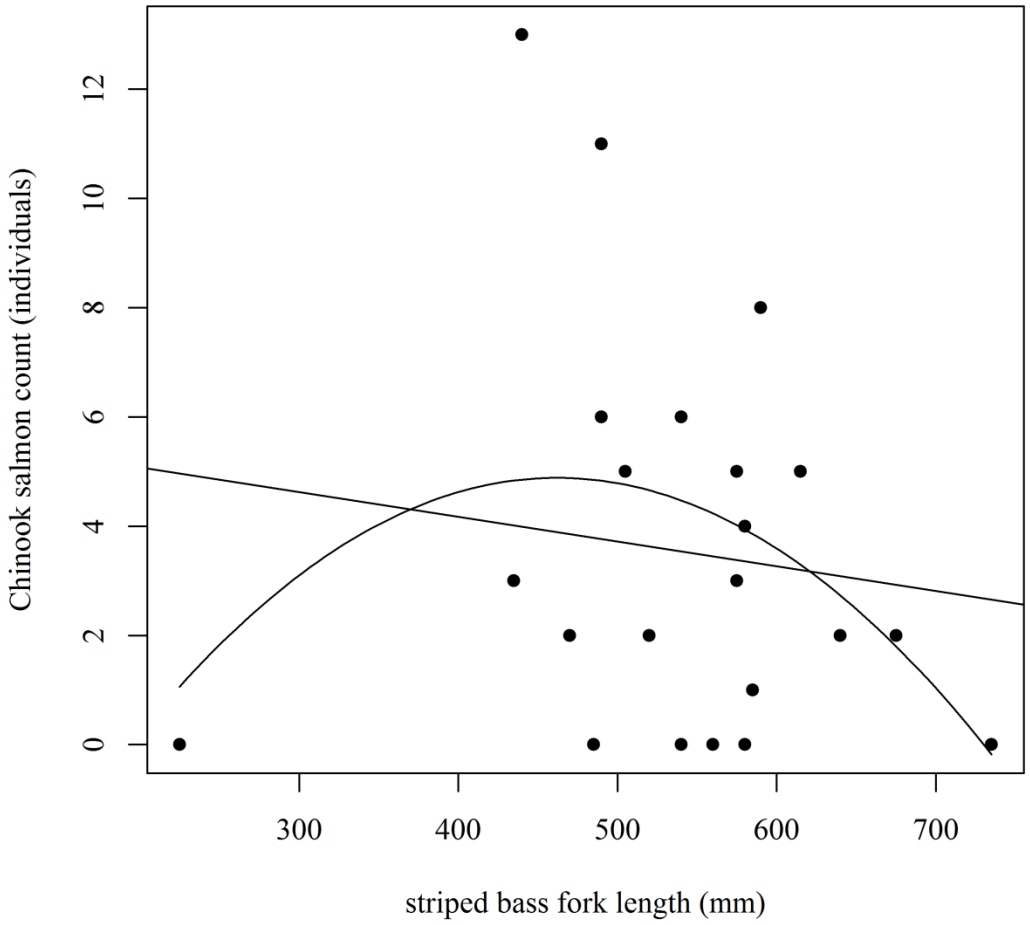

Appendix 3. Striped bass consumption of juvenile salmon by striped bass length. Linear regression (R^2= - 0.033, p = 0.572). 2^{nd} degree polynomial (R^2= 0.057, p = 0.219).

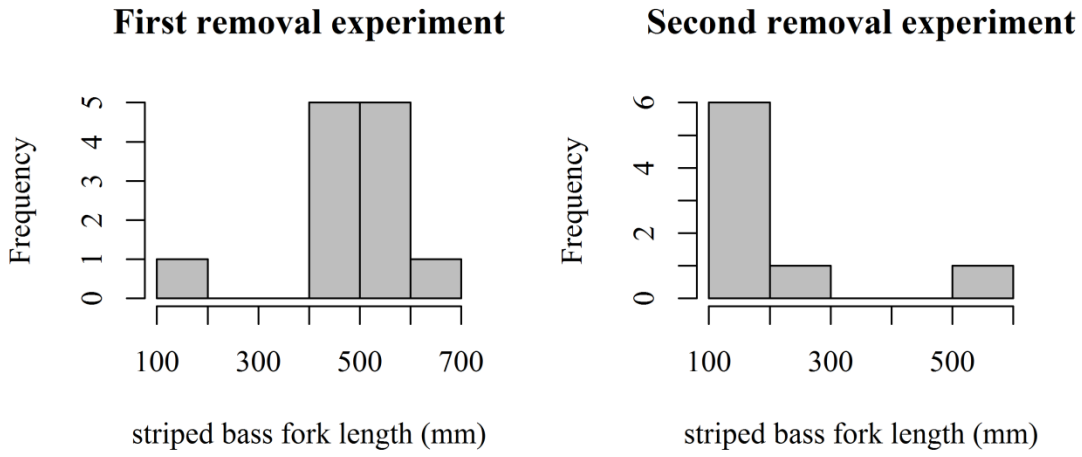

Appendix 4. Length histograms of striped bass removed in first (left) and second (right) removal experiments.

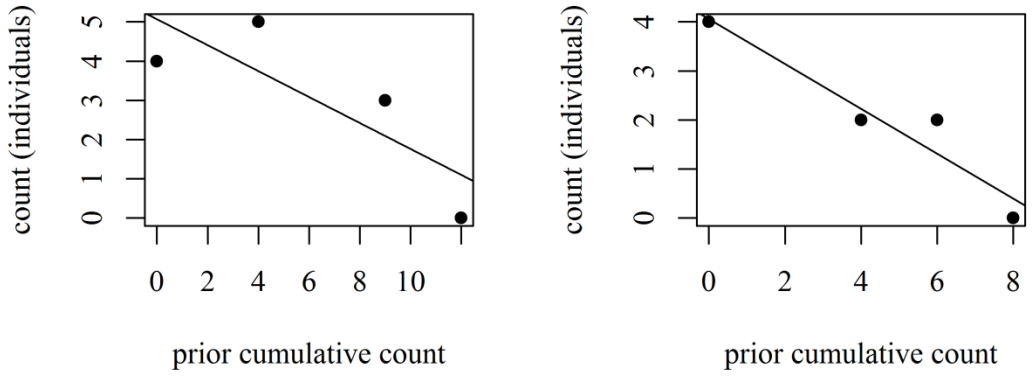

Appendix 5. Logistic regressions estimating striped bass population estimates for first removal experiment (p= 0.187, R^2= 0.491, N_0= 15.3, 78.4% depletion) and second removal experiment (p= 0.0438, R^2= 0.871, N_0= 8.87, 89.9% depletion).

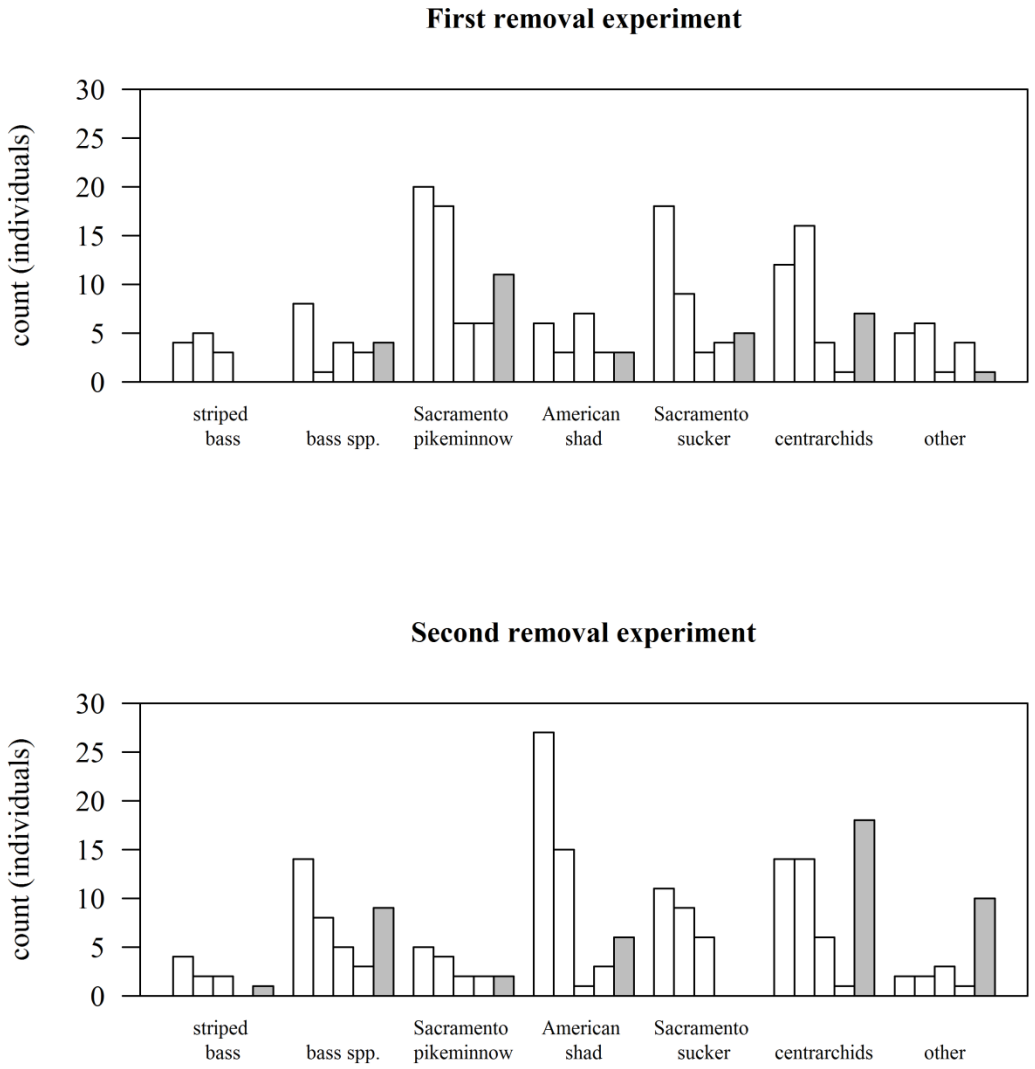

Appendix 6. White bars left to right are depletion passes 1, 2, 3, and 4 respectively. Gray bars are single pass conducted two days after depletion after experiment was complete. Bass spp. (*Micropterus* spp.), Sacramento pikeminnow (*Ptychocheilus grandis*), American shad (*Alosa sapidissima*), and Sacramento sucker (*Catostomus occidentalis*). Counts include fish of all sizes.

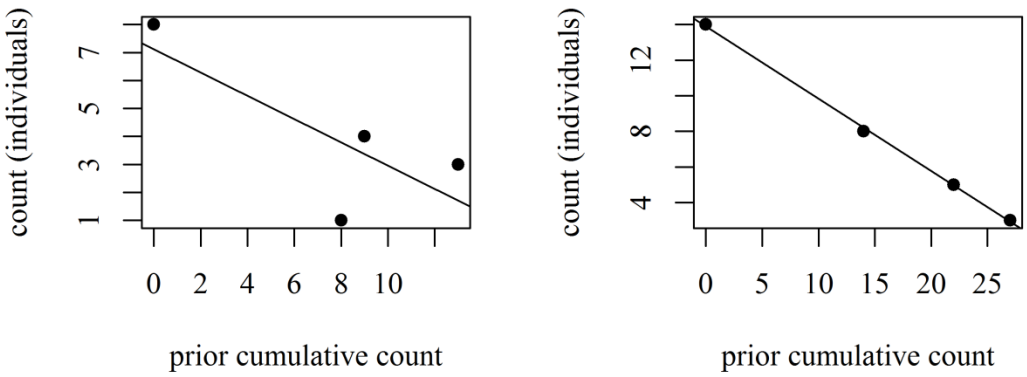

Appendix 7. Logistic regressions estimating black bass population estimates for first removal experiment (p= 0.07, R^2= 0.6209, N_0= 16.54, 96.9% depletion) and second removal experiment (p= 0.0004, R^2= 0.9987, N_0= 34.19, 80.0% depletion).

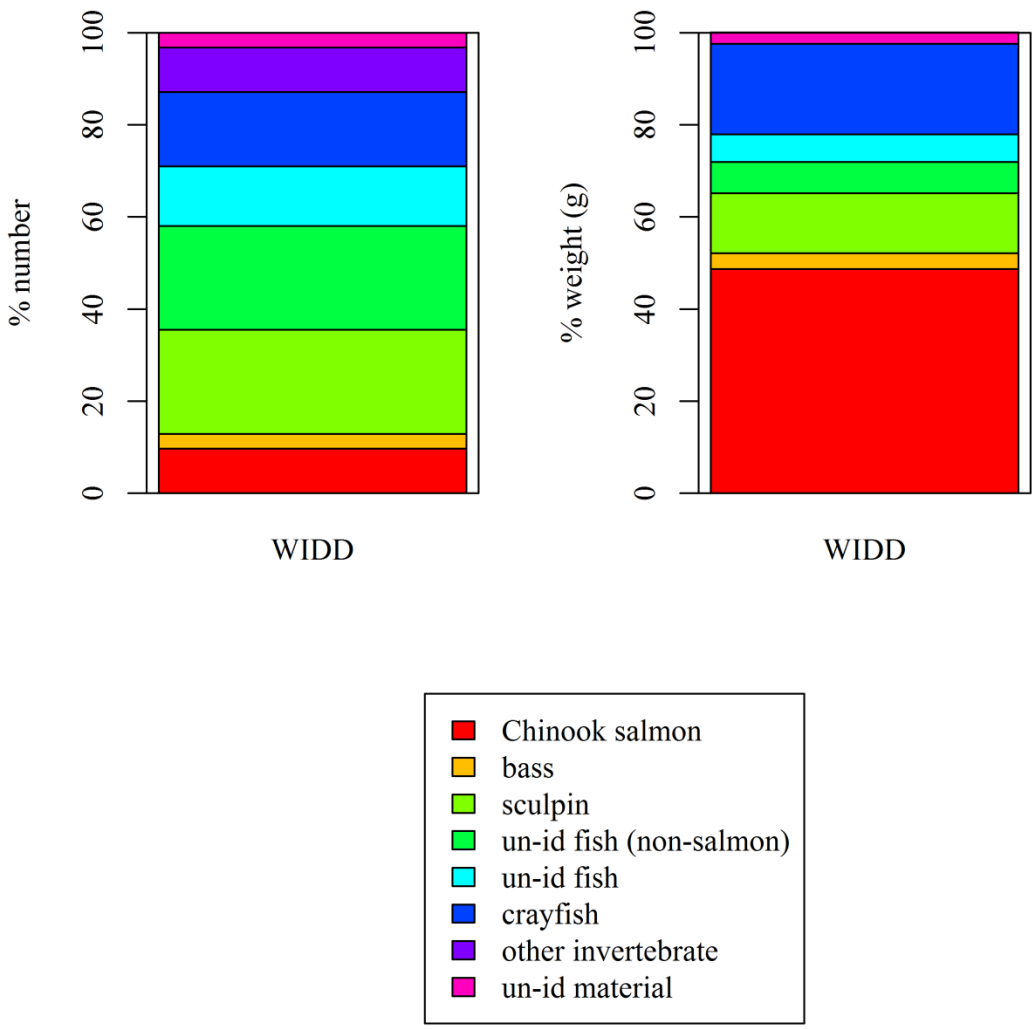

Appendix 8. Percent number and percent weight of diet items from black bass caught at WIDD.

Bibliography

Alexander, M., Dick, J., O'Connor, N., Haddaway, N., and Farnsworth, K. 2012. Functional responses of the intertidal amphipod Echinogammarus marinus: effects of prey supply, model selection and habitat complexity. Mar. Ecol. Prog. Ser. **468**: 191–202.

Anderson, M. 2001a. A new method for non-parametric multivariate analysis of variance. Austral Ecol. **26**: 32–46.

Anderson, T. 2001b. Predator responses, prey refuges, and density-dependent mortality of a marine fish. Ecology **82**: 245–257.

Barnosky, A.D., Hadly, E. a, Bascompte, J., Berlow, E.L., Brown, J.H., Fortelius, M., Getz, W.M., Harte, J., Hastings, A., Marquet, P. a, Martinez, N.D., Mooers, A., Roopnarine, P., Vermeij, G., Williams, J.W., Gillespie, R., Kitzes, J., Marshall, C., Matzke, N., Mindell, D.P., Revilla, E., and Smith, A.B. 2012. Approaching a state shift in Earth's biosphere. Nature **486**: 52–8. Nature Publishing Group.

Bartholomew, A., Diaz, R.J., and Cicchetti, G. 2000. New dimensionless indices of structural habitat complexity : predicted and actual effects on a predator ' s foraging success. **206**: 45–58.

Bilski, R., Shillam, J., Hunter, C., Saldate, M., and Rible, E. 2011. Emigration of Juvenile Chinook Salmon (Oncorhynchus tschawytscha) and Steelhead (Oncorhynchus mykiss) in the Lower Mokelumne River, December 2010 through July 2011.

Blackwell, B.F., and Juanes, F. 1998. Predation on Atlantic Salmon Smolts by Striped Bass after Dam Passage. North Am. J. Fish. Manag. **18**: 936–939.

Cavallo, B., Merz, J., and Setka, J. 2012. Effects of predator and flow manipulation on Chinook salmon (Oncorhynchus tshawytscha) survival in an imperiled estuary. Environ. Biol. Fishes.

Crain, C., Kroeker, K., and Halpern, B. 2008. Interactive and cumulative effects of multiple human stressors in marine systems. Ecol. Lett.: 1304–1315.

Davis, J.P., Schultz, E.T., and Vokoun, J.C. 2012. Striped Bass Consumption of Blueback Herring during Vernal Riverine Migrations: Does Relaxing Harvest Restrictions on a Predator Help Conserve a Prey Species of Concern? Mar. Coast. Fish. **4**: 239–251.

DeCesare, N.J., Hebblewhite, M., Robinson, H.S., and Musiani, M. 2009. Endangered, apparently: the role of apparent competition in endangered species conservation. Anim. Conserv. **13**: 353–362.

Deng, Z., Mueller, R.P., Richmond, M.C., and Johnson, G.E. 2010. Injury and Mortality of Juvenile Salmon Entrained in a Submerged Jet Entering Still Water. North Am. J. Fish. Manag. **30**: 623–628.

Didham, R.K., Tylianakis, J.M., Gemmell, N.J., Rand, T. a, and Ewers, R.M. 2007. Interactive effects of habitat modification and species invasion on native species decline. Trends Ecol. Evol. **22**: 489–96.

Dodds, W.K., Perkin, J.S., and Gerken, J.E. 2013. Human impact on freshwater ecosystem services: a global perspective. Environ. Sci. Technol. **47**: 9061–8.

Le Doux-Bloom, C.M. 2012. Distribution, habitat use, and movement patterns of sub-adult striped bass.

Dudgeon, D., Arthington, A.H., Gessner, M.O., Kawabata, Z.-I., Knowler, D.J., Lévêque, C., Naiman, R.J., Prieur-Richard, A.-H., Soto, D., Stiassny, M.L.J., and Sullivan, C. a. 2006. Freshwater biodiversity: importance, threats, status and conservation challenges. Biol. Rev. Camb. Philos. Soc. **81**: 163–82.

Elliott, J., and Persson, L. 1978. The estimation of daily rates of food consumption for fish. J. Anim. Ecol. **47**: 977–991.

Frost, C.N. (USGS). 2000. A key for identifying preyfish in the Columbia River Based on Diagnostic Bones. Cook, WA.

Gregory, R., and Levings, C. 1998. Turbidity reduces predation on migrating juvenile Pacific salmon. Trans. Am. Fish. … **127**: 275–285.

Grossman, G.D., Essington, T., Johnson, B., Miller, J., Monsen, N.E., and Pearsons, T.N. 2013. Effects of Fish Predation on Salmonids in the Sacramento River - San Joaquin Delta and Associated Ecosystems. : 1–71.

Hakala, J., and Johnson, F. 2004. Evaluation of a gastric lavage method for use on largemouth bass. North Am. J. Fish. … **24**: 1398–1403.

Hale, R., and Gray, J. 1998. Retention and detection of coded wire tags and elastomer tags in trout. North Am. J. Fish. … **18**: 197–201.

Halfwerk, W., Holleman, L.J.M., Lessells, Ck.M., and Slabbekoorn, H. 2011. Negative impact of traffic noise on avian reproductive success. J. Appl. Ecol. **48**: 210–219.

Halpern, B.S., McLeod, K.L., Rosenberg, A. a., and Crowder, L.B. 2008a. Managing for cumulative impacts in ecosystem-based management through ocean zoning. Ocean Coast. Manag. **51**: 203–211.

Halpern, B.S., Walbridge, S., Selkoe, K. a, Kappel, C. V, Micheli, F., D'Agrosa, C., Bruno, J.F., Casey, K.S., Ebert, C., Fox, H.E., Fujita, R., Heinemann, D., Lenihan, H.S., Madin, E.M.P., Perry, M.T., Selig, E.R., Spalding, M., Steneck, R., and Watson, R. 2008b. A global map of human impact on marine ecosystems. Science **319**: 948–52.

Hansel, H.C., Duke, S.D., Lofy, P.T., Gray, A., and Gray, G.A. 1988. Use of Diagnostic Bones to Identify and Estimate Original Lengths of Ingested Prey Fishes Original Lengths of Ingested Prey Fishes. Trans. Am. Fish. Soc. **117**: 55–62.

Hojesjo, J., Johnsson, J., and Bohlin, T. 2004. Habitat complexity reduces the growth of aggressive and dominant brown trout (Salmo trutta) relative to subordinates. Behav. Ecol. Sociobiol. **56**: 286–289.

Holling, C. 1959. The components of predation as revealed by a study of small-mammal predation of the European pine sawfly. Can. Entomol. **91**: 293–320.

Horodysky, A.Z., Brill, R.W., Warrant, E.J., Musick, J. a, and Latour, R.J. 2010. Comparative visual function in four piscivorous fishes inhabiting Chesapeake Bay. J. Exp. Biol. **213**: 1751–61.

Hunsicker, M.E., Ciannelli, L., Bailey, K.M., Buckel, J. a, Wilson White, J., Link, J.S., Essington, T.E., Gaichas, S., Anderson, T.W., Brodeur, R.D., Chan, K.-S., Chen, K., Englund, G., Frank, K.T., Freitas, V., Hixon, M. a, Hurst, T., Johnson, D.W., Kitchell, J.F., Reese, D., Rose, G. a, Sjodin, H., Sydeman, W.J., van der Veer, H.W., Vollset, K., and Zador, S. 2011. Functional responses and scaling in predator-prey interactions of marine fishes: contemporary issues and emerging concepts. Ecol. Lett. **14**: 1288–99.

Kempf, A., Stelzenmüller, V., Akimova, a., and Floeter, J. 2013. Spatial assessment of predator-prey relationships in the North Sea: the influence of abiotic habitat properties on the spatial overlap between 0-group cod and grey gurnard. Fish. Oceanogr. **22**: 174–192.

Leblanc, C. a., and Noakes, D.L. 2012. Visible Implant Elastomer (VIE) Tags for Marking Small Rainbow Trout. North Am. J. Fish. Manag. **32**: 716–719.

Lindley, S.T., and Mohr, M.S. 2002. Modeling the effect of striped bass (Morone saxatilis) on the population viability of Sacramento River winter-run chinook salmon (Oncorhynchus tshawytscha). Fish. Bull. **101**: 321–331.

Loboschefsky, E., Benigno, G., Sommer, T.R., Rose, K., Ginn, T., Massoudieh, A., and Loge, F. 2012. Individual-level and Population-level Historical Prey Demand of San Francisco Estuary Striped Bass Using a Bioenergetics Model. San Fr. Estuary Watershed … **10**.

Maceina, M., Wrenn, W., and Lowery, D. 1995. Estimating harvestable largemouth bass abundance in a reservoir with an electrofishing catch depletion technique. North Am. J. … **15**: 103–109.

Marchetti, M.P., Moyle, P.B., and Levine, R. 2004. Alien Fishes in California Watersheds : Characteristics of Successful and Failed Invaders. Ecol. Appl. **14**: 587–596.

Meador, M.R., Cuffney, T.F., and Gurtz, M.E. 1993. Methods for sampling fish assemblages as part of the National Water-Quality Assessment Program. *In* U.S. Geological Survey. Raleigh, NC.

Merz, J., and Workman, M. 2013. Salmon Lifecycle Considerations to Guide Stream Management: Examples from California's Central Valley. San Fr. Estuary … **11**: 1–26.

Merz, J.E., and Setka, J.D. 2004. Riverine Habitat Characterization of the Lower Mokelumne River, California. Lodi, CA.

Michel, C.J. 2010. River and estuarine survival and migration of yearling Sacramento river chinook salmon (Oncorhynchus tshawytscha) smolts and the influence of environment. University of California Santa Cruz.

Murdoch, W., and Stewart-Oaten, A. 1989. Aggregation by parasitoids and predators: effects on equilibrium and stability. Am. Nat. **134**: 288–310.

Nobriga, M., and Feyrer, F. 2007. Shallow-Water Piscivore-Prey Dynamics in California's Sacramento-San Joaquin Delta. San Fr. Estuary Watershed ….

Nobriga, M.L., and Feyrer, F. 2008. Diet composition in San Francisco Estuary striped bass: does trophic adaptability have its limits? Environ. Biol. Fishes **83**: 495–503.

Peters, W., Hebblewhite, M., DeCesare, N., Cagnacci, F., and Musiani, M. 2013. Resource separation analysis with moose indicates threats to caribou in human altered landscapes. Ecography (Cop.). **36**: 487–498.

Peterson, J., Thurow, R., and Guzevich, J. 2004. An evaluation of multipass electrofishing for estimating the abundance of stream-dwelling salmonids. Trans. Am. Fish. Soc. **133**: 462–475.

Poe, T.P., Hansel, H.C., Vigg, S., Palmer, D.E., and Prendergast, L.A. 1991. Feeding of predaceous fishes on out-migrating juvenile salmonids in John Day Reservoir, Columbia River. Trans. …: 405–420.

Raleigh, R., and Short, C. 1981. Depletion sampling in stream ecosystems: assumptions and techniques. Progress. Fish-Culturist **43**: 115–120.

Rieman, B.E., Beamesderfer, R.C., Vigg, S., and Poe, T.P. 1991. Estimated loss of juvenile salmonids to predation by northern squawfish, walleyes, and smallmouth bass in John Day Reservoir, Columbia River. Trans. …: 448–458.

Sanderson, B.L., Barnas, K. a., and Rub, a. M.W. 2009. Nonindigenous Species of the Pacific Northwest: An Overlooked Risk to Endangered Salmon? Bioscience **59**: 245–256.

Schindler, D.E., Geib, S.I., and Williams, M.R. 2000. Patterns of Fish Growth along a Residential Development Gradient in North Temperate Lakes. Ecosystems **3**: 229–237.

Schindler, D.W. 2001. The cumulative effects of climate warming and other human stresses on Canadian freshwaters in the new millennium. Can. J. Fish. Aquat. Sci. **58**: 18–29.

Schreer, J.F., Cooke, S.J., and Connors, K.B. 2004. Electrofishing-induced cardiac disturbance and injury in rainbow trout. J. Fish Biol. **64**: 996–1014.

Sorte, C.J.B., Williams, S.L., and Carlton, J.T. 2010. Marine range shifts and species introductions: comparative spread rates and community impacts. Glob. Ecol. Biogeogr. **19**: 303–316.

TID/MID. 1992. Lower Tuolumne River Predation Study Report.

Tucker, M.E., Williams, C.M., and Johnson, R.R. 1998. Abundance, Food Habits and Life History Aspects of Sacramento Squawfish and Striped Bass at the Red Bluff Diversion Complex, Including the Research Pumping Plant, Sacramento River, California, 1994-1996.

Volkhardt, G.C., Johnson, S.L., Miller, B.A., Nickelson, T.E., and Seiler, D.E. 2007. Rotary Screw Traps and Inclined Plane Screen Traps. *In* Salmonid field protocols handbook: techniques for assessing status and trends in salmon and trout populations. Bethesda, Maryland. pp. 235–266.

Vucic-Pestic, O., Birkhofer, K., Rall, B.C., Scheu, S., and Brose, U. 2010. Habitat structure and prey aggregation determine the functional response in a soil predator–prey interaction. Pedobiologia (Jena). **53**: 307–312.

Weber, M.J., and Brown, M.L. 2012. Effects of predator species, vegetation and prey assemblage on prey preferences of predators with emphasis on vulnerability of age-0 common carp. Fish. Manag. Ecol. **19**: 293–300.

OPEN ACCESS Freely available online

PLOS ONE

Controls on the Entrainment of Juvenile Chinook Salmon (*Oncorhynchus tshawytscha*) into Large Water Diversions and Estimates of Population-Level Loss

Steven C. Zeug*, Bradley J. Cavallo

Cramer Fish Sciences, Auburn, California, United States of America

Abstract

Diversion of freshwater can cause significant changes in hydrologic dynamics and this can have negative consequences for fish populations. Additionally, fishes can be directly entrained into diversion infrastructure (e.g. canals, reservoirs, pumps) where they may become lost to the population. However, the effect of diversion losses on fish population dynamics remains unclear. We used 15 years of release and recovery data from coded-wire-tagged juvenile Chinook Salmon (*Oncorhynchus tshawytscha*) to model the physical, hydrological and biological predictors of salvage at two large water diversions in the San Francisco Estuary. Additionally, entrainment rates were combined with estimates of mortality during migration to quantify the proportion of total mortality that could be attributed to diversions. Statistical modeling revealed a strong positive relationship between diversion rate and fish entrainment at both diversions and all release locations. Other significant relationships were specific to the rivers where the fish were released, and the specific diversion facility. Although significant relationships were identified in statistical models, entrainment loss and the mean contribution of entrainment to total migration mortality were low. The greatest entrainment mortality occurred for fish released along routes that passed closest to the diversions and certain runs of Chinook Salmon released in the Sacramento River suffered greater mortality but only at the highest diversion rates observed during the study. These results suggest losses at diversions should be put into a population context in order to best inform effective management of Chinook Salmon populations.

Citation: Zeug SC, Cavallo BJ (2014) Controls on the Entrainment of Juvenile Chinook Salmon (*Oncorhynchus tshawytscha*) into Large Water Diversions and Estimates of Population-Level Loss. PLoS ONE 9(7): e101479. doi:10.1371/journal.pone.0101479

Editor: João Miguel Dias, University of Aveiro, Portugal

Received November 12, 2013; **Accepted** June 9, 2014; **Published** July 14, 2014

Funding: This study was funded by the California Department of Water Resources. The funders had no role in study design, data analysis, decision to publish, or preparation of the manuscript. Staff from the funding agency participated in data collection in coordination with other state and federal resource agencies.

Competing Interests: The authors have declared that no competing interests exist.

* Email: stevez@fishsciences.net

Introduction

Diversion of freshwater for urban, industrial and agricultural use is a common practice around the world and is likely to become more frequent as demand increases [1]. There are numerous changes that take place in aquatic ecosystems as a result of flow reduction that can negatively affect fish including: alteration of sediment budgets, reduction or elimination of floodplain connectivity and altered cues for migration and reproduction [2,3]. Additionally, fish may be lost through direct impingement on intake screens or entrainment into water storage facilities and canals [4]. Although many studies have documented responses of fish populations to altered flow regimes, ecological correlates of the entrainment process and population effects of direct loss at diversions are insufficiently documented and poorly understood [5].

Impingement and entrainment of large numbers of fishes have been reported in water diversions from rivers [6,7], lakes [8] and estuaries [9,10]. Most entrained fish are early life stages (age 0+) and species composition generally reflects habitat adjacent to the diversion [10]. Estimation of population impacts of diversion losses have been more difficult to quantify, although some such studies have been performed [11,12]. Migratory fish species are unique in that their exposure to entrainment is primarily during periods of migration between habitats whereas resident species may be susceptible to entrainment until they leave the diversion vicinity or attain a less susceptible size [13].

Entrainment of juvenile anadromous salmonids (*Oncorhynchus spp.*) into two large water diversions in the San Francisco Estuary, California, USA has frequently been implicated in the decline of these species [14]. A portion of entrained salmon are salvaged and returned to the estuary however, mortality associated with the diversions is thought to impact these populations [15]. Loss densities (fish loss•volume of water diverted^{-1}) at these diversions are currently used as triggers to restrict the volume of water diverted in an effort to protect endangered winter Chinook Salmon (*O. tshawytscha*), spring Chinook Salmon, and steelhead trout (*O. mykiss*). Loss density triggers can be problematic because they are not scaled for population abundance. Thus, triggers may be reached due to abundance fluctuations that do not represent an increase in the proportion of the population lost. In general, the physical and hydrological conditions associated with entrainment remain unclear and population-level effects of fish loss at the diversions are not known.

Our goals for this study were to elucidate these physical, biological and hydrologic conditions and to put entrainment losses in a population context. We assumed that salvage (the metric that can be measured) is proportional to total entrainment at the two diversions. To accomplish these goals we constructed statistical

models of salvage and estimated total loss using 15 years of release and recovery data for coded wire tagged salmon raised at hatcheries throughout the Central Valley of California. The use of coded wire tagged fish is important relative to previous work because it allows loss to be scaled by the number of fish released; comparable analyses of raw salvage would be confounded by uncertainty in stock identity and population abundance. The results provide essential information for resource managers charged with recovering salmon stocks and implications for diversion losses in river systems worldwide.

Methods

All data used in this study had previously been collected by state and federal resource agencies. The authors had no role in the handling of organisms.

Study site

The Sacramento and San Joaquin Rivers drain approximately 40% of California' surface area including most of the western slope of the Sierra Nevada Mountains, the eastern slope of the Coast Range and portions of the southern Cascades. The two rivers converge in a tidal freshwater estuary known as the Sacramento-San Joaquin Delta (hereafter referred to as the "Delta") before entering San Francisco Bay (Figure 1). Both rivers have been subjected to intense water development beginning in the late 19th century associated with urban and agricultural development in the Central Valley of California. Dam construction, channelization, levee construction and pollution have been prominent in both systems. Water diverted from these rivers provides water for millions of Californians and supports economically valuable agriculture throughout the Central Valley. Both rivers supported robust populations of Chinook Salmon in the past. However, 48% of historic habitat has been lost [16] and drastic reductions in the number of returning adults have triggered restrictions and even total closures of commercial and recreational fisheries in some years.

Freshwater is extracted in the tidal Delta at two large diversions that divert up to 60% of total flow in some years. Both diversions contain facilities where fish are salvaged and then released in the western Delta, away from the pumps. Fish entering the salvage facilities are subsampled at regular intervals (10–20 minutes$\bullet h^{-1}$) and total salvage is estimated based on the volume diverted and time since the previous sub-sample. Although salvage occurs at both diversions, there are significant differences in facility design that may affect the number of fish collected. The Central Valley Project (CVP) diverts water directly from a tidal channel in the Delta and fish are directed by a series of louvers into the salvage facility (Figure 2). The State Water Project (SWP) diverts water from a forebay filled by operable gates located on a tidal channel of the Delta (Figure 2). Thus, fish salvaged at the SWP have first been drawn into the forebay where they are exposed to resident predators before they are directed by louvers into the salvage facility as water is pumped out of the forebay. Additionally, the origin of salmon collected at the diversions is likely to have an influence on salvage. Fish released in the San Joaquin River are likely to first encounter the CVP whereas fish released in the Sacramento are likely to encounter the SWP first.

Salmon releases

Chinook Salmon are raised at several hatcheries in the Sacramento-San Joaquin system and released at various locations as mitigation for habitat lost through dam construction, and as part of studies conducted by state and federal resource agencies. A portion of these hatchery fish have coded wire tags (CWTs) inserted for identification when recaptured. These tags are short lengths of steel wire with a numeric code that identifies a specific release group. Fish receiving a CWT also have their adipose fin clipped so tagged fish can be visually identified at capture. The tagging rate and number of fish released can vary considerably among runs. All hatchery winter run and late-fall run are tagged whereas the percentage of fall run tagged and released has varied between years. Spring run are raised at one hatchery; however, only 16 spring run release groups were identified within the study area and few of these fish ever arrived at salvage. Thus, spring run were not included in the analysis. Fish released into tributaries of the Sacramento River including: Battle Creek and Feather River are hereafter referred to as Sacramento River releases. Similarly, fish released into tributaries of the San Joaquin River including the Stanislaus River, Tuolumne River, and Merced River are hereafter referred to as San Joaquin River releases.

Juvenile salmon with an adipose clip collected at the diversions are retained, the coded wire tag is read, and the number of fish salvaged from that release group is estimated. Juvenile salmon exiting the Delta downstream of the diversions are sampled by a mid-water trawl at Chipps Island operated by the United States Fish and Wildlife Service (Figure 1). Trawling effort is variable among and within years and capture probability is low; however, some trawling occurs during all months of the year. Tagged salmon also are recovered from the commercial and recreational ocean fishery for several years after release.

Release data for juvenile salmon were obtained from the Regional Mark Processing Center coded wire tag database maintained by the Pacific States Marine Fisheries Commission (http://www.rmpc.org/). Data from release years 1993–2007 were queried from the database. We chose these years to represent current water management in the Delta which changed in the mid-1990's in response to the Bay-Delta Accord (California State Water Resources Control Board Ruling D-1641). Additionally, we excluded releases under 1000 individuals and releases made downstream of the last entrance to the interior Delta from the Sacramento River at Threemile Slough (Figure 1). The data queried included: release site, release size, date of release, mean fork length at release and age specific recoveries in the ocean. The number of salmon recovered in the ocean was expanded prior to analysis using the method described in Zeug and Cavallo [17]. Ocean recovery information was limited for later release years because the ocean fishery was restricted in 2007 and closed in 2008 in response to the collapse of the fall run. Recovery information was obtained from the United States Fish and Wildlife Service Chipps Island Survival table (http://www.fws.gov/stockton/jfmp/datamanagement.asp). These data included: number of tagged salmon recovered in the Chipps Island trawl, the expanded number of tagged salmon collected at the CVP and SWP salvage facilities, and the range of dates over which fish from each release group were captured in the trawl.

Environmental data

Juvenile salmon are released in the Sacramento and San Joaquin rivers and tributaries (from <30 to >600 km from the diversions); however, they are not vulnerable to entrainment until they enter the tidal Delta. A study of salmon migration with acoustic telemetry indicated juvenile salmon migrated through the Delta in 6.4 days on average [18]. To capture the conditions experienced during Delta migration, hydrologic variables were averaged over 7 days after salmon entered the Delta. To estimate the date when each release group arrived at the Delta, we calculated the median date between the first and last capture in the

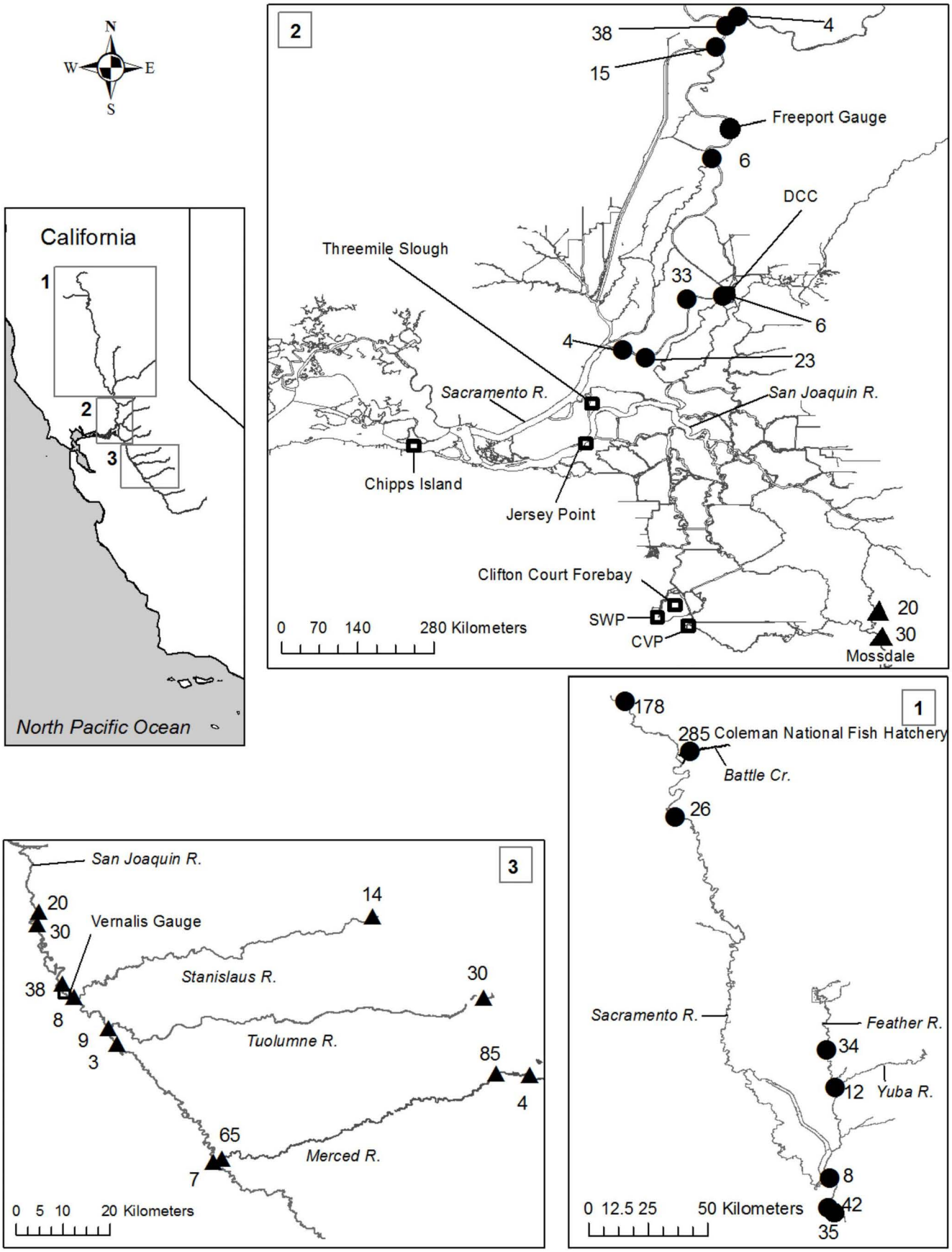
N
W
E
S
California
1
2
3
North Pacific Ocean
2
38
4
15
Freeport Gauge
6
DCC
Threemile Slough
33
6
4
23
Sacramento R.
San Joaquin R.
Chipps Island
Jersey Point
Clifton Court Forebay
SWP
CVP
20
30
Mossdale
0 70 140 280 Kilometers
1
178
285 Coleman National Fish Hatchery
Battle Cr.
26
Sacramento R.
Feather R.
34
12
Yuba R.
8
42
35
0 12.5 25 50 Kilometers
3
San Joaquin R.
20
30
Vernalis Gauge
14
Stanislaus R.
30
38
8
9
3
Tuolumne R.
85
4
65
Merced R.
7
0 5 10 20 Kilometers

Figure 1. Map depicting the location of the study region within California and relevant locations within the study region. Release locations in the Sacramento River are indicated by closed circles and release locations in the San Joaquin River are indicated by closed triangles. The number of releases that occurred at each that location appears next to the marker. Abbreviations: SWP = State Water Project, CVP = Central Valley Project.
doi:10.1371/journal.pone.0101479.g001

Chipps Island trawl at the exit of the Delta. The 7 days prior to the median capture date was the time period over which hydrologic conditions were averaged.

Mean daily flow (hereafter "flow") for the Sacramento River was obtained from the United States Geological Survey (USGS) gauge 11447650 at Freeport, California (Figure 1). San Joaquin River flow was obtained from USGS gauge 11303500 at Vernalis, California (Figure 1). Daily water diversion rates from the CVP and SWP were obtained from the DAYFLOW online data archive maintained by the California Department of Water Resources. An additional variable in the Sacramento River was the position of the Delta Cross Channel (DCC). The DCC is a large gate that diverts water from the main stem Sacramento River into interior portions of the Delta (Figure 1). When the gate is open, there is a greater probability of fish migrating down the Sacramento River will enter routes leading to the diversions [19].

Data analysis

The response variable in all statistical models was the number of fish salvaged. The number of fish released was included as an offset variable to account for differences in release group size. Models were constructed separately for each diversion facility to determine if different independent variables affected salvage at diversions that extract water directly from a tidal channel (CVP) vs. a forebay (SWP). Models were also constructed separately for releases in the Sacramento and San Joaquin Rivers.

Independent variables in statistical models were selected based on hypothesized relationships with salvage. These variables could potentially affect the process of salvage or the exposure of fish to salvage. For example, zero salvage could occur because most fish were not exposed to entrainment or died prior to entering the Delta. Hypothesized relationships between independent variables and salvage are summarized in Table 1. To account for mortality prior to salvage, fork length at release and the shortest distance from release site to the nearest salvage facility were included. We expected survival would be negatively associated with distance [20] and positively associated with mean fork length [21]. For fish in the Delta we hypothesized that salvage would increase as flows decreased and as diversion increased. Previous analyses of fish entrainment have utilized a ratio of diversion to flow as a predictor of entrainment risk instead of using these variables as separate independent predictors. However, analyses of survival in the Delta have suggested diversion rate, and flow alone may have similar predictive capability without conflating these two variables [22]. To determine if a diversion-to-flow ratio was superior to modeling these effects separately, statistical models were constructed using

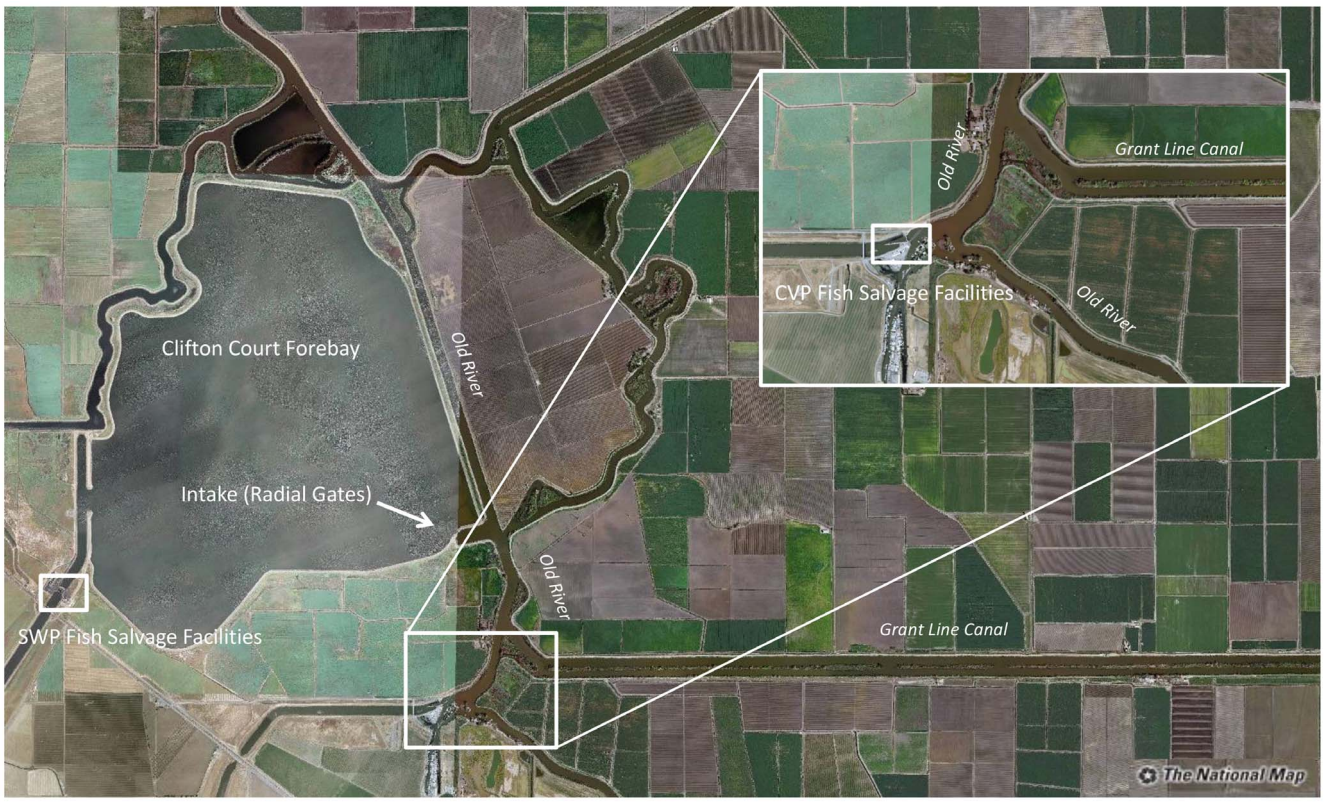

Figure 2. Aerial view of the layout of the two water diversion and fish salvage facilities. The State Water Project (SWP) diverts from Clifton Court Forebay that is filled from radial gates located on Old River; a distributary of the San Joaquin River. The Central Valley Project (CVP) diverts water directly from Old River. Image was downloaded from The National Map: http://nationalmap.gov/.
doi:10.1371/journal.pone.0101479.g002

Table 1. Predicted relationships between independent variables and salvage (count model) and independent variables and zero salvage (zero-inflation model).

Parameter	Count model	Zero-inflation model
Flow	−	+
Water diversion	+	−
DCC position	+	−
Fork length	−	+
Distance from salvage facilities	−	+
Chipps Island recoveries	−	+
Ocean recoveries	−	+

doi:10.1371/journal.pone.0101479.t001

both methods and then compared using Akaike's corrected information criteria (AIC_c). When the difference between AIC_c values (ΔAIC_c) for a pair of models was greater than 2.0, the model with the lower AIC_c values was considered to have the best support in the data.

To account for fish that survived the Delta and avoided salvage, catch-per-unit effort in the Chipps Island trawl (number•min^{-1}), and expanded ocean recoveries for each release were included in each model. We predicted that salvage would be negatively associated with recoveries at Chipps and in the ocean (i.e. when fewer fish are entrained at the diversion, more are available to be caught later in the trawl). Sacramento models also included a dummy variable for the position of the DCC where 1 = open and 0 = closed. All continuous variables were transformed into z-scores so results could be interpreted in units of standard deviations. A correlation analysis was performed to determine if multicollinearity existed among independent variables however, no strong correlations were identified.

Screening of the response variable indicated that many releases in both rivers resulted in zero salvage. Thus, zero-inflated negative binomial regression was employed. These models are composed of two parts; a count model that explains salvage as a function of covariates and a zero-inflation model that accounts for the processes that result in zero salvage as a function of covariates. The predicted sign of coefficients in the count model are listed in Table 1. Coefficients for the zero-inflation model would be predicted to have a sign that is opposite of the count model. Zero-inflated Poisson regression was explored but model diagnostics indicated over-dispersion. To determine if a zero-inflated model was necessary, a negative binomial regression model was constructed with the same independent variables and a Vuong non-nested hypothesis test was performed to determine if the zero-inflated model provided an improved representation of the data [23]. Once a model was identified, overall model fit was determined with a likelihood ratio test comparing an intercept-only model with the model containing independent variables. All modeling was performed with the R statistical program and the packages "pscl" and "MASS" [24].

To estimate a population-level effect of fish loss at the diversions, the contribution of loss relative to the total mortality rate during migration (hereafter referred to as relative loss) was estimated [11,12]. Loss is defined as the fish that were entrained into the diversion and did not survive to release after salvage and trucking. To estimate loss for each release group, we first estimated the number of fish that encountered the louvers at each facility:

$$F_L = \frac{S}{0.90}$$

where F_L is the number of fish that encountered the louvers, S is estimated salvage and louver efficiency is assumed to be 90% [15]. Total entrainment was then estimated as:

$$E = \frac{F_L}{S_{PL}}$$

where E is total entrainment and S_{PL} is the pre-louver survival. The pre-louver survival at the SWP was assumed to be 15%; the mean rate reported in a study by [25]. No data on pre-screen survival is available for the CVP so we assumed 85% following the methods of [15]. Total loss at each facility was then estimated as:

$$L = E - (S \times 0.96)$$

where L is total loss and survival during trucking and handling was 96% [15]. Loss estimates were summed for each facility and divided by the release group size to estimate the proportion of fish from each release group lost at the diversion.

To bracket the range of relative loss at the diversions, the highest and lowest observed mortality values during migration were used. Because published mortality estimates were not available for all release locations, only releases (n = 285) from Coleman National Fish Hatchery (CNFH) and directly into the tidal Delta (Sacramento River = 129, San Joaquin River = 88) were used. Separate estimates were calculated for each run. Though winter run were released upstream of the CNFH, we assumed that migration mortality of this run was similar to fish released directly from CNFH. Mortality estimates of Sacramento River releases during migration through the Delta were obtained from acoustic tagging experiments [19]. The highest through-Delta (Freeport to Chipps Island) mortality estimate from this study was 64.9% and the lowest was 45.7%. A single mean mortality estimate during migration from CNFH to Chipps Island (88%) was obtained from Michel [18] and San Joaquin estimates were obtained from Newman [26] and Buchanan et al. [27] where the highest through-Delta (Mossdale to Chipps Island) mortality estimate was 95.0% and the lowest was 79% (Mossdale to Jersey Point). The relative loss for each release was estimated as:

$$M_L = \left(\frac{R_L}{M_T}\right) \times 100$$

where M_L is relative loss at the diversions, R_L is the proportion of each release group lost at the diversions and M_T is the total mortality during migration.

To quantify how uncertainty in the estimates of louver efficiency and pre-louver survival at both diversions influenced relative loss, a sensitivity analysis for the estimates of M_L was performed using Monte Carlo methods. A distribution was constructed for each of the three estimates and they were allowed to vary one at a time while the other two were held constant. One hundred resamples were drawn, M_L calculated, and the mean and standard deviation of the 100 resamples was estimated. The mean and standard deviation for pre-louver mortality at SWP [25] was used to inform a normal distribution. No data are available to inform a normal distribution for CVP pre-louver mortality so a uniform distribution was used where mortality ranged from 5–70%. A uniform distribution was also used for louver efficiency where values ranged from 50–95%.

There is considerable interest by resource managers in understanding how losses of salmon are related to diversion rate thus, the M_L value for each release group was plotted against water diversion rate for each run of Chinook Salmon released from CNFH, and directly into the tidal Delta. These M_L estimates were calculated with the lowest M_T estimates to provide an estimate of the maximum mortality that could be accounted for by loss at the diversions. Additionally, relative loss was calculated assuming that no entrained fish were salvaged to estimate the effect of salvage facilities on loss estimates.

Results

Salvage of Sacramento River releases

A total of 749 releases comprised of $>28{\bullet}10^6$ fish were used to model salvage of Sacramento River Chinook Salmon. Fall run accounted for 419 releases, winter run 178 releases and late-fall run 152 releases. Only 16 release groups for tagged spring run Chinook Salmon were available and very few of these fish ever arrived at salvage; spring run Chinook Salmon were not included in further analyses. Across all Sacramento River releases an estimated 19281 CWT salmon were salvaged which represented 0.068% of the tagged fish released. Among the three runs of Chinook Salmon released, late-fall run fish were salvaged more frequently (0.2%) than winter and fall run (0.05 and 0.01% respectively). Average total loss (expanded for louver efficiency and pre-louver mortality) was greatest for late-fall run releases (0.84%) and lowest for fall run (0.03%) with an intermediate value for winter run (0.2%, Table 2).

A zero-inflated negative binomial model was a superior fit to the CVP salvage data for Sacramento River releases ($V = 8.11$, $P < 0.001$), and the model fit the data well (likelihood ratio test, $P < 0.001$). Similarly, salvage of Sacramento River releases at the SWP also was best described by a zero-inflated model ($V = 7.66$, $P < 0.001$) and it was a good fit to the data (likelihood ratio test, $P < 0.001$). The models that included flow and diversion as separate variables were a better fit to the CVP and SWP data than models using a ratio of diversion to flow with ΔAIC_c values of 23.4 and 76.9 respectively. The count models at both diversions revealed that there was a significant increase in salvage as diversion rate increased (Table 3). Contrary to expectations, salvage increased at both diversions when the DCC was closed. The DCC was only open for 48 of the 749 releases (6%) and given the large number of zeros in the data set, there was a lower probability of a large salvage event occurring when the DCC was open. Other significant relationships were specific to each facility. There was a significant negative relationship between flow and salvage, and a positive relationship between distance and salvage at the CVP facility. Fork length and Chipps Island recoveries had significant positive relationships with salvage at the SWP. There was also a significant negative relationship between ocean recoveries and salvage at the SWP (Table 3).

The zero-inflation part of the analysis produced coefficients to estimate when salvage is zero versus any non-zero number. The zero-inflation models for Sacramento releases revealed consistent patterns between SWP and CVP. Specifically, there was a significantly greater likelihood of zero salvage when flows were higher, when water diversion was lower and when fish were released at a smaller size (Table 3). There were no significant relationships with DCC position in this portion of the model.

Salvage of San Joaquin River releases

In the San Joaquin River there were 313 releases comprised of $>7{\bullet}10^6$ juvenile Chinook Salmon (Table 2). Only fall run were released in the San Joaquin River. A greater percentage of salmon released in the San Joaquin Basin were salvaged (0.6%) relative to any run of Sacramento River-origin fish. Mean total loss was also greater for releases in the San Joaquin River (1.4%, Table 2) relative to any run released in the Sacramento River. Similar to the Sacramento River releases, models that used diversion and flow as separate predictors were superior to models that used the diversion-flow ratio for the CVP and SWP ($\Delta AIC_c = 57.5$ and 82.5 respectively).

A Vuong test indicated that a zero-inflated negative binomial model was the best description of San Joaquin releases salvaged at the CVP facility ($V = 7.72$, $P<0.001$). This model was a good fit to the data (likelihood ratio test, $P<0.001$). Additionally, a zero-inflated negative binomial model best represented the SWP salvage data ($V = 6.22$, $P<0.001$) and fit the data well (likelihood ratio test, $P<0.001$). The count models at both facilities yielded a significant increase in salvage as diversion rate increased (Table 4). The only other significant relationship in the count models at either facility was a positive coefficient for ocean recoveries in the SWP model.

The zero-inflation models for both facilities yielded significant negative relationships between the probability of zero salvage and diversion rate and ocean recoveries (Table 4). At the CVP, there was also a significant negative relationship between zero salvage and flow, and a significant positive relationship with recoveries at Chipps Island. For the SWP, fork length was found to have a significant positive relationship with zero salvage.

Contribution to total migration mortality

Relative loss at the diversions was low for Sacramento River fish released at CNFH and directly into the Delta (Table 5). For CNFH releases, relative loss was greater at the SWP facility relative to the CVP facility although both values were $<0.4\%$. A similar pattern was observed for Sacramento River fish released directly into the tidal Delta regardless of the migration mortality estimate. However, relative loss at the CVP was similar for fish released at CNFH and in the Delta whereas relative loss at the SWP was greater for fish released in the Delta. Mean relative loss of San Joaquin River releases was more than double that of Sacramento River releases at both facilities (Table 5). The pattern among the facilities was similar where relative loss was greater at the SWP relative to the CVP.

The sensitivity analysis indicated that incorporating uncertainty in louver efficiency resulted in higher estimates of relative loss. Uncertainty in pre-louver survival at the CVP resulted in lower estimates relative to the baseline and uncertainty in pre-louver survival at the SWP produced similar estimates. The largest

Table 2. Means and coefficients of variation for variables used in models of salvage.

	Sacramento River			San Joaquin River
Parameter	**Late-fall**	**Winter**	**Fall**	**Fall**
Release size	58,365 (0.38)	6,354 (1.02)	43,936 (2.17)	24,917 (0.21)
Total salvage•release^{-1}	118.5 (1.80)	2.7 (2.12)	1.9 (2.89)	149.6 (1.66)
Proportion salvaged	0.002 (1.64)	0.0005 (2.42)	0.0001 (2.96)	0.0058 (1.64)
Proportional loss	0.008 (1.65)	0.002 (2.57)	0.0003 (3.23)	0.014 (2.05)
Distance from salvage (km)	452 (0.47)	623 (0)	348 (0.61)	152 (0.56)
Flow $m^3 \cdot s^{-1}$	941 (0.83)	782 (0.55)	919 (0.69)	255 (0.90)
Water diversion $m^3 \cdot s^{-1}$	213 (0.50)	226 (0.30)	121 (0.74)	74 (0.56)
Salvage at CVP	44.4 (1.91)	1.1 (3.54)	0.5 (5.29)	102.5 (1.66)
Water diversion from CVP $m^3 \cdot s^{-1}$	97 (0.45)	105 (0.19)	54 (0.68)	40 (0.57)
Salvage at SWP	74.1 (1.84)	1.6 (2.34)	1.5 (3.26)	48.2 (2.14)
Water diversion from SWP $m^3 \cdot s^{-1}$	115 (0.59)	116 (0.31)	60 (0.93)	33 (0.75)
Length at release (mm)	128 (0.09)	78 (0.09)	67 (0.19)	82 (0.06)
Expanded ocean recoveries	593 (0.94)	16 (1.74)	365 (1.46)	85 (1.62)
Chipps trawl cpue	9.64 (0.98)	0.49 (1.40)	3.20 (1.57)	7.42 (1.38)

Variables were separated by run for Sacramento releases. Currently the San Joaquin only supports fall run Chinook Salmon.

doi:10.1371/journal.pone.0101479.t002

difference resulting from incorporation of parameter uncertainty was for San Joaquin River-origin fall run where mean estimates incorporating uncertainty in louver efficiency were 2.9% relative to the baseline value of 1.7%. All other differences were <1% (Figure 3).

For Sacramento River fall run Chinook Salmon, combined loss at the diversions (CVP + SWP) was always less than 1% of total migration mortality (relative loss) regardless of the diversion rate or release location (Figure 4). A small percentage of relative loss was observed for late-fall run released from CNFH until the diversion rate exceeded approximately 275 $m^3 \cdot s^{-1}$. Once this level of water diversion was reached, relative loss increased, although the variation also increased (Figure 4). Most late-fall Chinook Salmon released into the Delta experienced relative losses less than 2.5%. However, nine releases had relative losses that ranged between 3.0% and 10.5%. Seven of these releases occurred within days of each other in 2007 when the diversion rate was approximately 187 $m^3 \cdot s^{-1}$. Relative losses of winter run releases were variable throughout the range of observed diversion levels but were less than 2% for most releases and never exceeded 5.5% (Figure 4). Fall run Chinook Salmon released into the San Joaquin River experienced a greater relative loss at the diversions than any run released in the Sacramento River (Figure 4). Water diversion was less than 100 $m^3 \cdot s^{-1}$ during most San Joaquin River releases and although relative loss was less than 5% for most releases; this value ranged as high as 17.5%. Three releases occurred when the diversion rate was greater than 100 $m^3 \cdot s^{-1}$ and relative loss was less than 1% of total mortality for all three (Figure 4).

Salvage reduced relative loss by 19% for late-fall and winter run Chinook Salmon and 15% for fall run released at CNFH (Table 6). Salmon released in the Sacramento River received the greatest benefit from salvage with a reduction in relative loss of 42% and 41% for fall run and late-fall run respectively. Relative loss of fall run Chinook Salmon released in the San Joaquin River was reduced by 24% due to the presence of salvage facilities.

Discussion

During the study period, over 1000 releases of $>35 \cdot 10^6$ juvenile Chinook Salmon were performed. For releases in both rivers and among both diversions, there was a significant positive relationship between water diversion rate and salvage. The salvage facilities at these diversions have been likened to giant sampling devices [13]. Thus, it is not surprising that more fish are encountered as more water is sampled per-unit-time. Kimmerer [15] also found strong effects of water diversion on entrainment of salmon in this system and positive relationships between diversion volume and fish entrainment have been reported in other systems [7–9]. In contrast, the relationship between salvage and flow could not be generalized among rivers. For Sacramento River releases, there was a significant increase in salvage at the CVP facilities with decreasing flow. Supporting the same trend, greater flows significantly increased the probability of zero salvage of Sacramento River releases at both facilities. The lack of strong relationships between salvage and flow and the consistent strong relationships with salvage and diversion rate likely explain why using a ratio of diversion rate to flow where these two variables are conflated was a poor predictor relative to modeling these variables separately.

Perry [28] found that when discharge is low in the Sacramento River, flow changes direction with the tide at the junction of routes leading to the diversions and upstream flow increases the probability of salmon entering these junctions. Several releases of late-fall run in the Delta that were released within days of each other experienced unusually high rates of salvage. The timing of fish arrival at junctions leading to the diversions and tides were unmeasured here but may be important predictors of salvage and may have influenced these anomalous points in the late-fall Delta releases. For San Joaquin River releases, relationships with flow were less clear and the only significant relationship was between zero salvage at the CVP and flow. Salvage of San Joaquin River releases may only occur when fish are abundant near the diversion regardless of flow conditions. Other studies of fish entrainment at

Table 3. Parameter estimates for zero-inflated negative binomial regression describing salvage of coded wire tagged juvenile salmon at the Central Valley Project and State Water Project facilities.

	Central Valley Project				State Water Project			
	Count model		Zero-inflation model		Count model		Zero-inflation model	
Parameter	**estimate**	***p*-value**	**estimate**	***p*-value**	**estimate**	***p*-value**	**estimate**	***p*-value**
Flow $m^3 \cdot s^{-1}$	**−0.651**	**<0.001**	**0.427**	**0.026**	**−0.208**	**0.227**	**0.521**	**<0.001**
Diversion $m^3 \cdot s^{-1}$	**0.663**	**<0.001**	**−0.443**	**0.004**	**0.29**	**0.005**	**−1.296**	**<0.001**
DCC open	**−0.800**	**0.001**	−0.134	0.751	**−0.917**	**<0.001**	−0.293	0.634
Fork length (mm)	0.008	0.944	**−1.497**	**<0.001**	**0.614**	**<0.001**	**−0.977**	**<0.001**
Distance from salvage facilities (km)	**0.331**	**0.001**	−0.246	0.116	0.149	0.085	0.144	0.270
Chipps Island recoveries (number$\cdot$min^{-1})	0.194	0.067	−0.014	0.928	**0.345**	**0.011**	0.206	0.243
Ocean recoveries	0.020	0.827	−0.186	0.190	**−0.297**	**0.032**	−0.187	0.233

The count model describes the salvage process whereas the zero-inflated model describes the process resulting in zero salvage. All releases were in the Sacramento River.

doi:10.1371/journal.pone.0101479.t003

Table 4. Parameter estimates for zero-inflated negative binomial regression describing salvage of coded wire tagged juvenile salmon at the Central Valley Project and State Water project facilities.

	Central Valley Project				State Water Project			
	Count model		Zero-inflation model		Count model		Zero-inflation model	
Parameter	**estimate**	***p*-value**	**estimate**	***p*-value**	**estimate**	***p*-value**	**estimate**	***p*-value**
Flow $m^3 \cdot s^{-1}$	0.098	0.247	−0.781	0.002	−0.019	0.874	−0.017	0.919
Diversion $m^3 \cdot s^{-1}$	0.453	<0.001	−0.791	<0.001	1.000	<0.001	−0.517	0.003
Fork length (mm)	0.030	0.692	−0.127	0.392	0.104	0.285	0.468	0.006
Distance from salvage facilities (km)	−0.060	0.505	0.091	0.567	−0.158	0.075	0.019	0.896
Chipps Island recoveries (number$\cdot$min^{-1})	0.161	0.153	0.651	0.042	−0.295	0.054	0.171	0.503
Ocean recoveries	0.084	0.361	−1.996	<0.001	0.666	<0.001	−1.252	<0.001

The count model describes the salvage process whereas the zero-inflated model describes the process resulting in zero salvage. All releases were in the San Joaquin River.

doi:10.1371/journal.pone.0101479.t004

Table 5. Estimates of the % of total migration mortality accounted for by loss at each diversion (relative loss) for releases in the Sacramento and San Joaquin Rivers.

River	Release location	Facility	Migration mortality estimate (%)	Relative loss (%)	Confidence interval
Sacramento	CNFH	CVP	88.0	0.013	0.008–0.017
Sacramento	CNFH	SWP	88.0	0.372	0.328–0.416
Sacramento	Delta	CVP	64.9	0.009	0.004–0.013
Sacramento	Delta	CVP	45.7	0.012	0.006–0.018
Sacramento	Delta	SWP	64.9	0.449	0.237–0.661
Sacramento	Delta	SWP	45.7	0.614	0.324–0.905
San Joaquin	Delta	CVP	95.0	0.091	0.050–0.131
San Joaquin	Delta	CVP	79.0	0.109	0.060–0.157
San Joaquin	Delta	SWP	95.0	1.334	0.739–1.930
San Joaquin	Delta	SWP	79.0	1.596	0.884–2.309

Estimates were generated for Sacramento River fish released at Coleman National Fish Hatchery (CNFH) and directly into the tidal Delta. San Joaquin River estimates were only made for fish released into the tidal Delta.

doi:10.1371/journal.pone.0101479.t005

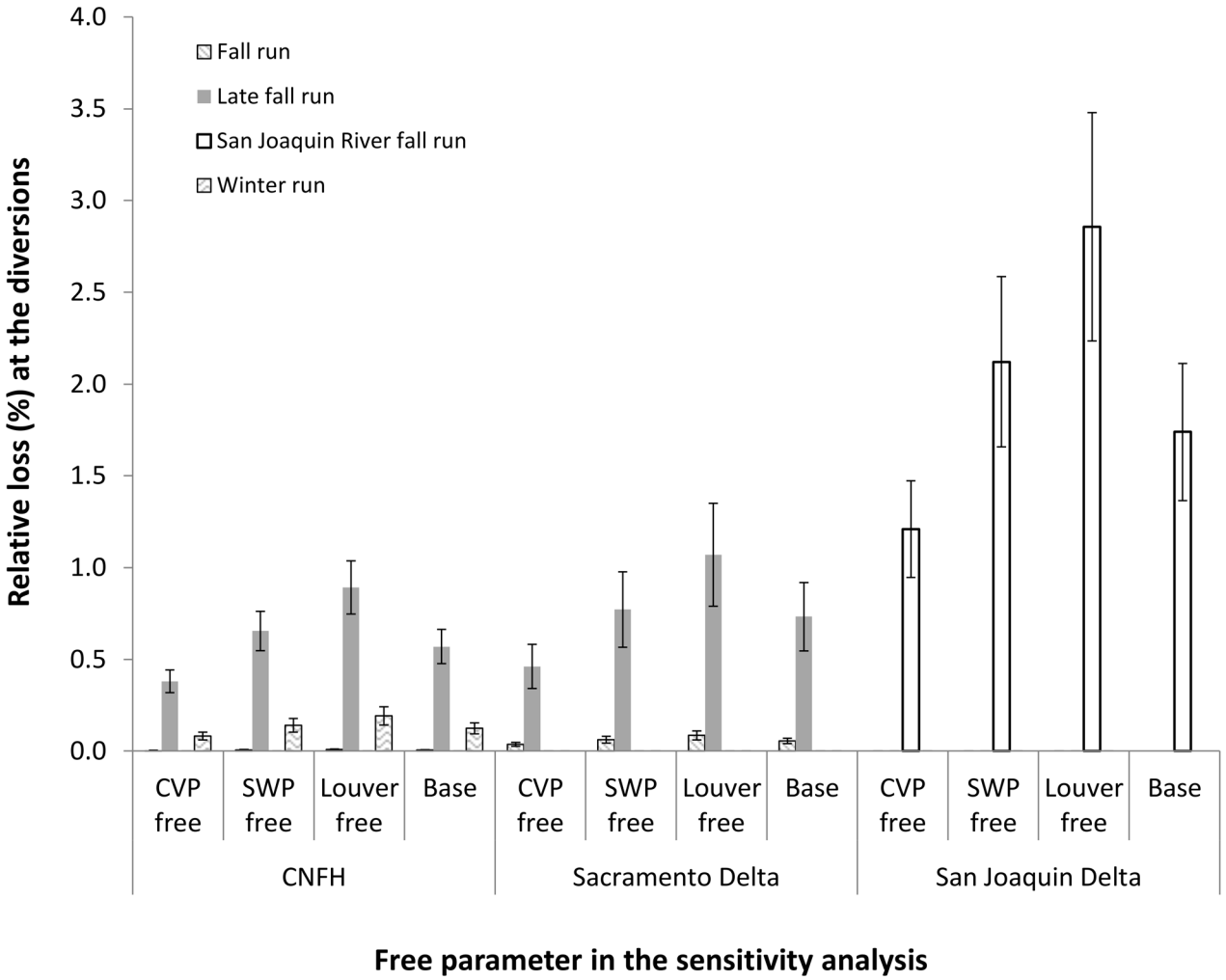

Figure 3. Results of the sensitivity analysis for the calculation of relative loss at the diversions as a function of uncertainty in the parameters used for the calculation. Three parameters (CVP pre-louver mortality, SWP pre-louver mortality and louver efficiency) were modeled as distributions and one parameter at a time was allowed to vary while the others were held constant. 100 re-samples were performed and the means and standard deviations are reported here.

doi:10.1371/journal.pone.0101479.g003

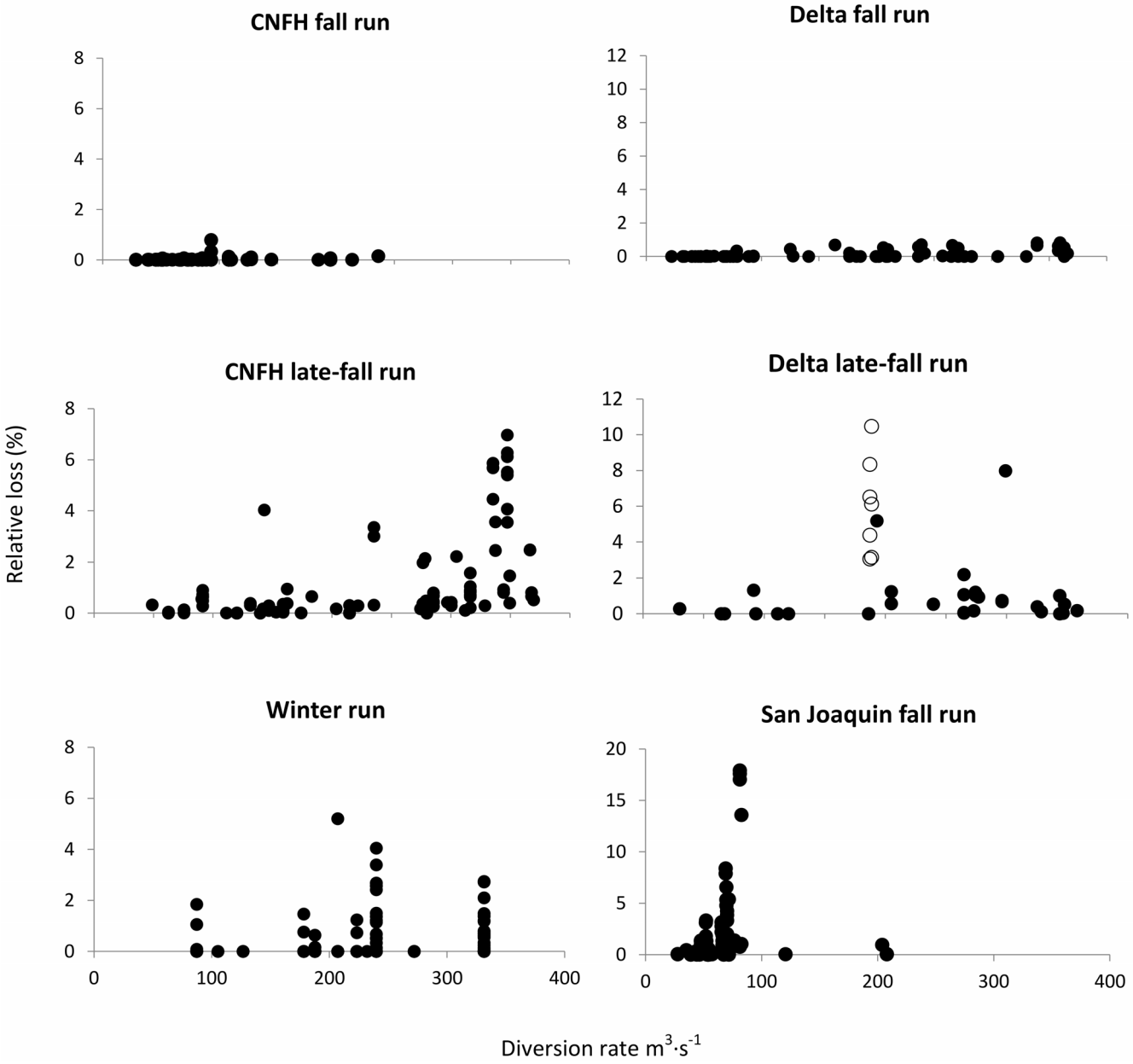

Figure 4. Plot of the percentage of migration mortality accounted for by loss at the two diversions (relative loss) as a function of diversion rate for three runs of Chinook Salmon released from the Coleman National Fish Hatchery (CNFH) or directly into the Delta. Open circles in the Delta late-fall run plot represent a set of releases that occurred within days of each other in 2007 and experienced unusually high loss. Note that the range of the y-axis changes among release locations.
doi:10.1371/journal.pone.0101479.g004

Table 6. Percent of migration mortality accounted for by loss at the diversions (relative loss) with and without accounting for salvage.

		Coleman Releases	Sacramento Delta Releases	San Joaquin Delta Releases
Fall	Salvage	0.017 (0.007)	0.076 (0.024)	1.704 (0.373)
	No salvage	0.020 (0.008)	0.132 (0.029)	2.242 (0.475)
Late-fall	Salvage	0.953 (0.153)	1.339 (0.430)	N/A
	No salvage	1.178 (0.189)	2.279 (0.535)	N/A
Winter	Salvage	0.222 (0.043)	N/A	N/A
	No salvage	0.273 (0.051)	N/A	N/A

doi:10.1371/journal.pone.0101479.t006

water diversions have found that catch is largely proportional to abundance in the channel being diverted from [6,11].

Prior to constructing salvage models, we hypothesized that fish size at release and the distance of release sites from the diversions would influence how many fish would be susceptible to salvage through the effect of these variables on survival [20,21]. However, both fish size and distance from the diversions were only strong predictors of zero salvage for releases in the Sacramento River. Zero salvage was more likely when fish were released at a smaller size and salvage of larger fish was greater at the SWP. Most potential predators of salmon smolts are gape-limited fishes such as striped bass (*Morone saxatilis*) and larger size may confer a survival advantage especially at the SWP where fish are exposed to high predation rates in the forebay prior to salvage [25]. Size effects were mostly insignificant for San Joaquin releases (although zero salvage was positively related to size at the SWP); however, fish were released at a wider range of sizes in the Sacramento River relative to the San Joaquin River. In particular, late-fall run Chinook Salmon were salvaged more frequently than any other run from the Sacramento River and this run was released at larger sizes than any other run.

The distance of release sites from the diversions also was important only for Sacramento River releases however the relationship was opposite of our expectation (positive coefficient). Large, late-fall run Chinook Salmon were salvaged more than any other run and these fish were primarily released at CNFH that was located 577 rkm from the closest salvage facility. There were no significant relationships between distance and salvage of San Joaquin River releases. The maximum distance of a release site in the San Joaquin was 262 rkm, which was less than half of the maximum distance of Sacramento releases (624 rkm) and may have masked distance effects in the San Joaquin River.

Relationships between salvage and recoveries downstream of the facilities were inconsistent and conflicting without any clear patterns. Previous studies in the Delta have attempted to link recovery rates at downstream locations with the water diversion rate from the Delta and have not produced strong evidence of an effect [26,29,30]. Additionally, Zeug and Cavallo [17] failed to find a relationship between salvage at these facilities and recovery rates in the ocean. Unlike many water diversions, these allow for a fraction of entrained fish to be returned to the channel alive and our results suggest that salvage reduced migration mortality due to entrainment by 15–42%.

Although several strong relationships were identified between salvage and predictor variables, total loss and the contribution of juvenile salmon loss at the diversions to total mortality (relative loss) during migration was low. This may partially explain the poor and inconsistent relationships between salvage and recovery of tagged fish in Chipps trawl and the ocean. Although diversion-related entrainment is frequently invoked as a threat to fish populations, few studies have evaluated population-level effects of fish loss at diversions [5]. Several studies of entrainment loss relative to population mortality have reported relatively small contributions of entrainment similar to the estimates reported here [9,11,12]. The location of the diversions may also contribute to low relative loss. Both diversions are located on a distributary of the San Joaquin River thus, only salmon migrating through that route are susceptible to entrainment. In general, less than half of the juvenile salmon migrating down the San Joaquin River are likely to enter channels leading to the diversions [27] and even fewer Sacramento River-origin salmon are likely to enter this channel [19].

Although the results presented here suggest the total effect of loss at these diversions on migrating juvenile salmon is small, caution should be used when applying these results to other systems or even to the Sacramento-San Joaquin Delta generally. First, these diversions include salvage facilities that allow some fish to be returned alive. In many systems, fish that are entrained in diversions cannot return and are lost. Although it is largely unknown how these losses affect populations, Roberts and Rahel [4] suggested these diversions can function as sink habitats. Second, there are a large number of small diversions in the Delta that do not contain fish screens or salvage mechanisms and the aggregate effect of these diversions could be significant [31]. The calculation of entrainment loss includes estimates for louver efficiency and pre-louver survival that have low certainty and better quantitative estimates for these parameters could reveal greater estimates of total loss. Finally, all fish in this study (and in the acoustic studies used to calculate migration mortality) were hatchery reared fish. Thus, we are making the assumption that the behavior and survival of hatchery Chinook Salmon is similar to naturally produced fish in both rivers.

The data presented here indicated that a variety of hydrologic (diversion rate and flow), physical (distance from facilities) and biological (fish size) factors influence the salvage of CWT juvenile Chinook Salmon at two large water diversions. However, the relative importance of these factors varied among the two river systems where fish were released and among the two diversions which differed in the configuration of water diversion. Attempts to increase survival of juvenile salmon migrating through the Delta have largely focused on restriction of water diversion [14]. Yet the total contribution of loss at these facilities was small relative to total migration mortality and relationships between salvage and recoveries downstream were inconsistent and conflicting. The ability of fish to be salvaged and the physical location of the pumps off of the main stem rivers likely reduced the total population-level effect of these diversions. As water development continues worldwide, the inclusion of effective salvage facilities in diversion designs, and careful selection of diversion locations could help mitigate fish losses.

Acknowledgments

We thank Annie Brodsky for assisting in the preparation of data for analysis and creating maps of the study area. Steve Cramer, David Delaney and Tommy Garrison provided insights that significantly improved the statistical analyses. Staff from the California Department of Water Resources and the United States Fish and Wildlife Service staff provided necessary data.

Author Contributions

Conceived and designed the experiments: SZ BC. Analyzed the data: SZ. Wrote the paper: SZ BC.

References

1. Dudgeon D, Arthington AH, Gessner MO, Kawabata ZI, Knowler DJ, et al. (2006) Freshwater biodiversity: importance, threats, status and conservation challenges. Biol Rev 81: 163–182.
2. Poff NL, Allan JD, Bain MB, Karr JR, Prestegaard KL, et al. (1997) The natural flow regime. BioScience 47: 769783.
3. Bunn SE, Arthington AH (2002) Basic principles and ecological consequences of altered flow regimes for aquatic biodiversity. Environ Manage 30: 492–507.
4. Roberts JJ, Rahel FJ (2008) Irrigation canals as sink habitat for trout and other fishes in Wyoming drainage. T Am Fish Soc 137: 951–961.
5. Moyle PB, Israel JA (2005) Untested assumptions: effectiveness of screening diversions for conservation of fish populations. Fisheries 30: 20–28.

6. Carter KL, Reader JP (2000) Patterns of drift and power station entrainment of 0+ fish in the River Trent, England. Fish Manage and Ecol 7: 447–464.
7. Baumgartner LJ, Reynoldson NK, Cameron L, Stanger JG (2009) Effects of irrigation pumps on riverine fish. Fisheries Manag Ecol 16: 429–437.
8. Kelso JRM, Milburn GS (1979) Entrainment and impingement of fish by power plants in the Great Lakes which use the once-through cooling process. J Great Lakes Res 5: 182–194.
9. Hadderingh RH, Jager Z (2002) Comparison of fish impingement by a thermal power station with fish populations in the Ems Estuary. J Fish Biol 61: 105–124.
10. Nobriga ML, Matica Z, Hymanson ZP (2004) Evaluating entrainment vulnerability to agricultural irrigation diversions: a comparison among open-water fishes. In Feyrer F, Brown LR, Brown RL and Orsi JJ, editors. Early Life History of Fishes in the San Francisco Estuary and Watershed. American Fisheries Society Symposium 39: 281–295.
11. Post JR, Van Poorten BT, Rhodes T, Askey P, Paul A (2006) Fish entrainment into irrigation canals: an analytical approach and application to the Bow River, Alberta, Canada. N Am J Fish Manage 26: 875–887.
12. Carlson AJ, Rahel FJ (2007) A basinwide perspective on entrainment of fish in irrigation canals. T Am Fish Soc 136: 1335–1343.
13. Grimaldo LF, Sommer T, Van Ark N, Jones G, Holland E, et al. (2009) Factors affecting fish entrainment into massive water diversions in a tidal freshwater estuary: can fish losses be managed? N Am J Fish Manage 29: 1253–1270.
14. National Marine Fisheries Service (2009) NMFS Final 2009 Biological Opinion on the Long-Term Central Valley Project and State Water Project Operation, Criteria, and Plan. June 4, 2009. Available: http://swr.nmfs.noaa.gov/sac/myweb8/BiOpFiles/2009/Draft_OCAP_Opinion.pdf/. Accessed 2012 Mar.
15. Kimmerer WJ (2008) Losses of Sacramento River Chinook salmon and Delta smelt to entrainment in water diversions in the Sacramento-San Joaquin Delta. San Francisco Estuary and Watershed Science 6(2).Available: http://www.escholarship.org/uc/item/7v92h6fs/. Accessed 2010 Aug.
16. Yoshiyama RM, Gerstung ER, Fisher FW, Moyle PB (2001) Historical and present distribution of Chinook salmon in the Central Valley of California. Calif Depart Fish Game Bull 179: 71–176.
17. Zeug SC, Cavallo BJ (2013) Influence of estuary conditions on the recovery rate of coded-wire-tagged Chinook salmon (*Oncorhynchus tshawytscha*) in an ocean fishery. Ecol Freshw Fish 22: 157–168.
18. Michel CJ (2010) River and estuarine survival and migration of yearling Sacramento River Chinook salmon (*Oncorhynchus tshawytscha*) smolts and the influence of environment. Master's thesis, University of California, Santa Cruz.
19. Perry RW, Skalski JR, Brandes PL, Sandstrom PT, Klimley, et al. (2010) Estimating survival and migration route probabilities of juvenile Chinook salmon in the Sacramento-San Joaquin River Delta. N Am J Fish Manage 30: 142–156.
20. Zabel RW, Faulkner J, Smith SG, Anderson JJ, Van Holmes C, et al. (2008) Comprehensive passage (COMPASS) model: a model of downstream migration and survival of juvenile salmonids through a hydropower system. Hydrobiologia 609: 289–300.
21. Zabel RW, Achord S (2004) Relating size of juveniles to survival within and among populations of Chinook salmon. Ecology 85: 795–806.
22. Newman KB (2003) Modelling paired release-recovery data in the presence of survival and capture heterogeneity with application to marked juvenile salmon. Stat Model 3: 145–177.
23. Vuong QH (1989) Likelihood ratio tests for model selection and non-nested hypotheses. Econometrica 57: 307–333.
24. R Core Team (2012) R: a language and environment for statistical computing. R foundation for statistical computing, Vienna, Austria. Available: http://www.R-project.org/. Accessed 2012 July.
25. Gingras M (1997) Mark-recapture experiments at Clifton Court Forebay to estimate pre-screening losses to juvenile fishes 1976–1993. Interagency Ecological Program Technical Report 55, 26 p. Available: http://science.calwater.ca.gov/pdf/workshops/SP_workshop_predation_M.Gingra.pdf/. Accessed 2012 July.
26. Newman KB (2008) An evaluation of four Sacramento-San Joaquin river Delta juvenile salmon survival studies. United States Fish and Wildlife Service, Stockton, California. 182p. Available: http://www.science.calwater.ca.gov/pdf/psp/PSP_2004_final/PSP_CalFed_FWS_salmon_studies_final_033108.pdf/. Accessed 2010 June.
27. Buchanan RA, Skalski JR, Brandes PL, Fuller A (2013) Route use and survival of juvenile Chinook salmon through the San Joaquin River Delta. N Am J Fish Manage 33: 216–229.
28. Perry RW (2010) Survival and migration dynamics of juvenile Chinook salmon (*Oncorhynchus tshawytscha*) in the Sacramento-San Joaquin river Delta. Doctoral dissertation, University of Washington.
29. Newman KB, Rice J (2002) Modeling the survival of Chinook salmon smolts outmigrating through the lower Sacramento River system. J Am Stat Assoc 97: 983–993.
30. Newman KB, Brandes PL (2010) Hierarchical modeling of juvenile Chinook salmon survival as a function of Sacramento-San Joaquin Delta water exports. N Am J Fish Manage 30: 157–169.
31. Walters AK, Holzer DM, Faulkner JR, Warren CD, Murphy PD, et al. (2012) Quantifying cumulative entrainment effects for Chinook salmon in a heavily irrigated watershed. T Am Fish Soc 141: 1180–1190.